sitc

Society for Immunotherapy of Cancer

Abstracts

SITC 2018

WASHINGTON, D.C.

Walter E. Washington Convention Center

sitcancer.org/2018

TABLE OF CONTENTS

Abstract and Poster Information **2**
Author Index **4**
Keyword Index **75**
Regular Oral Abstract Presentations **84**
Regular Poster Abstract Presentations **138**
Late-Breaking Abstract Oral Presentations **904**
Late-Breaking Abstract Poster Presentations **909**

ABSTRACT AND POSTER INFORMATION

Publication
Regular abstracts submitted in conjunction with the 33rd Annual Meeting are published in the November 6, 2018 issue of the *Journal for ImmunoTherapy of Cancer* (JITC), SITC's official journal. Late-Breaking abstracts will be published in the December 6, 2018 issue of JITC. All abstracts are available on the SITC website and in this electronic Abstract Book. An abstract listing is available beginning on page 84 of this abstract book.

Oral Abstracts
SITC Leadership has selected the highest scoring abstract submissions for oral presentations. Oral presentations during regular sessions are ten minutes long. Oral presentations during the Rapid Oral Presentation Sessions are five minutes long.

Late-Breaking Abstracts
To fulfill SITC's commitment to the most cutting-edge science, late-breaking abstract submission was offered from August 24-September 13, 2018. Only those who submitted applications by the August 1, 2018 deadline were eligible to submit during this period. The highest scoring submissions were selected for oral presentation during the late-breaking abstract sessions within the 33rd Annual Meeting.

Poster Abstracts
Accepted posters for the 33rd Annual Meeting are on display in the Exhibit and Poster Hall in Hall E. Posters are available for viewing on Friday and Saturday of the Annual Meeting. For a full listing of displayed posters, please see the listing starting on page 84. Reulgar and late-breaking abstracts that are accepted for oral and poster presentations can display their abstract as a poster. During the poster display staffing hours listed below, designated posters are staffed by respective authors, allowing for information exchange and interaction between researchers and attendees.

Exhibit and Poster Hall Location
Hall E

Exhbit and Poster Hall Hours
Friday, Nov. 9 from 8 a.m. – 8 p.m.
Saturday, Nov. 10 from 8 a.m. – 8:30 p.m.

Poster Presentation Hours (*based on abstract poster number):*

Odd Numbered Posters (Poster Authors are Present)
Friday, Nov. 9, from 12:45 – 2:15 p.m.
Friday, Nov. 9 from 6:30 – 8 p.m.

Even Numbered Posters (Poster Authors are Present)
Saturday, Nov. 10 from 12:20 – 1:50 p.m.
Saturday, Nov. 10 from 7:00 – 8:30 p.m.

Travel Award Recipients

This image denotes the 2018 Travel Award recipients.

Presidential Travel Award Recipients
See abstracts O9, O15, O33, O39

Abstract Travel Award Recipients
See abstracts O5, O10, O13, O32, O36, O47, P6, P43, P207, P269, P281, P338, P424, P464, P493, P518, P531, P546, P547, P556, P557, P564, P572, P588, P589, P616, P649, P679

Poster Numbers

Regular Oral Abstract Posters O1-O47

Regular Abstract Posters
ADCC/CDC P1-P11
Best Practices for Improving Cancer Immunotherapy P12
Biomarkers and Immune Monitoring P13-P147
Cancer Vaccines, Personal Vaccines and Technology ..... P148 – P190
Case Studies P191-P194
Cellular Metabolism and Antitumor Immunity P195-P209
Cellular Therapy Approaches P210-P286
Clinical Trials (Completed) P287-P302
Clinical Trials (In Progress) P303-P343
Combination Therapy P344-P396
Co-Stimulatory Ligand-Receptor Interactions P397-P409
Cytokines in Anti-Tumor Immunity P410-P425
Emerging Models and Imaging P426-P446
Immune Effect of Chemotherapy P447-P475
Immunosuppressive Cells in the Tumor Microenvironment P476-P503
Impact of Diet, Exercise, and/or Stress on Antitumor Immunity P504-P508
Innate Anti-Tumor Immunity P509-P532
irAE Mangement P533-P540

Mechanisms of Resistance to Immunotherapy P541-P561
Mechanisms of Toxicity P562-P568
Microbiome and Anti-Tumor Immunity or I-O Agent Toxicity P570-P575
Micro-RNA, Epigenetics and Tumor/ Immune-cell Signaling Pathways in Anti-Tumor Immunity P576-P579
Oncogenetics and Immunogenomics P580-P596
Oncolytic Viruses and Intratumoral Therapies P597-P624
Other P625-P641
Patient Experience P643
T cell Checkpoints and Checkpoint Inhibitors P644-P705

Late-Breaking Oral Abstract Posters O48-O52

Late-Breaking Abstract Posters P706-P721

AUTHOR INDEX

Author A Abstract Number

Aaboe Jørgensen, Mia P175
Aaron, Wade P608
Abate-Daga, Daniel P263, P264
Abbott, Charles P13
Abbott, Derek P30
Abbott, Sandra P404
Abdallah, Rehab P338
Abdelfattah, Nouran P156
Abdelrahim, Maen P644
Abdel-Wahab, Noha P644
Abdel-Wahab, Omar P156
Abdullah, Shaad P14
Abelson, Michelle P210
Aberg, Ida P656
Åberg, Ida P683
Abolhalaj, Milad P195
Abraham, Anson O26
Abraham, Pranav P692
Abrams, Scott O42
Abril-Rodriguez, Gabriel O39, P557
Abrol, Srishti P430, P431
Abu-Akeel, Moshen P143
Abudayyeh, Ala P644
Abu-Sbeih, Hamzah P194, P533, P534, P535, P536, P537, P538, P645
Accolla, Roberto P711
Acharya, Rajesh P48, P65
Achour, Ikbel P14, P308
Acs, Balazs P88
Acuna, Gonzalo P413
Adamow, Matthew P297
Adams, Bruce P211
Adams, Lisa P341
Adams, Sarah P303, P496
Adams, Stephen P458
Adams, Sylvia P468
Adamstein, Nicholas P36
Adamus, Agnieszka P204, P515
Addala, Venkateswar P580
Addepalli, Murali P418
Adeniran, Adebowale P84
Adjei, Alex O24
Adler, Adam P646
Admon, Arie O8
Adurthi, Sreenivas P694
Adusumilli, Lavanya P202
Advani, Ranjana P240
Advani, Sunil P458
Aerni, Hans P417
Afar, Daniel P72, P690
Agarwal, Maria P189
Agarwal, Veena P368
Agaugué, Sophie P213, P218, P220, P221, P231, P232, P274, P275, P626
Ager, Casey P299, P546
Aggarwal, Charu O24, P319
Aggen, David P719
Agnello, Giulia P345
Agorku, David P45
Aguilar, Ethan P508
Aguilera, Joesph P458
Ahmad, Gulzar P227
Ahmadzadeh, Elaheh P445, P509
Ahn, Myung-Ju P139, P308, P341
Ahsan, Sama P329
Ai, Midan P546
Ai, Weiyun P327
Ailawadhi, Sikander P5, P6
Aithal, Kiran P529
Aitken, Malinda P382
Aivado, Manuel P450
Ajami, Nadim P572
Akbay, Esra O35
Akce, Mehmet P506, P507
Akimova, Tatiana P494
Akram, Muzaffar P598
Aksoy, Bulent O40
Aksoy, Murat P106
Alatrash, Gheath P644
Al-banna, Nadia P91
Albayrak, Adem P109

AUTHOR INDEX

Albershardt, Tina.....P607
Albert, Jennifer.....P416
Albrengues, Jean P521
Albu, Diana.....P598
Alcoba, Diego PP711
Aldeghaither, Dalal.....P561
Alderson, Ralph P304, P305, P366
Alese, Olatunji P506, P507
Alessandrini, Gabriele P97
Alexander, Richard.....P339
Alfaro-Munoz, Kristin P431, P432
Alfonso Calvo, Felipe Manuel P466
Ali, Faisal P534, P536, P537, P538
Ali, Waleed P408
Aliabadi-Wahle, Shaghayegh O31
Alici, Evren.....P522
Alilou, Mehdi.....P426
Alison, Andrew P30
Aljumaily, Raid.....P409
Allaf, Mohamad.....P338
Allen, Clint O20
Allen, Jeff.....O48
Allen, Melanie P279
Allison, James.....O5, P352
Allison, Patrick.....P700
Almåsbak, Hilde.....P256
Al-Masri, Hytham P107
Alpaugh, R. P396
Alpert, Amir.....P246
Alsaadi, Dana.....P447, P538
Al-Saleem, Essel P396
Alten, Leoni P246
Altintas, Isil.....P402, P647
Altiok, Soner.....P67, P439
Altmann, Heidi P113
Altura, Rachel.....P532
Alvarado, Diego.....P510
Alvarez de Lacerda-Landry, Lara P233
Alvarez, Juan P123, P423
Amado, Rafael.....O18, P276
Amani, Vladimir P497
Amaravadi, Ravi..... O40, P108
Amaria, Rodabe O5, P505, P572, P710
Ambrose, Christine P267
Ameratunga, Malaka P287
Amir, Eitan P698
Amonkar, Mayur..... P585
Amsalem, Nofar..... P197
An, Annie P368
An, Jeongshin..... P569
An, W. Frank P398
Anadon, Carmen..... O9
Anagnostou, Theodora P648
Anagnostou, Valsamo..... O47, P589
Anand, Neel P364
Anandakumar, Ponni P196
Anceriz, Nadia..... P4
Anders, Robert..... P128, P541, P703
Andersen, Mads..... P175, P177, P478
Andersen, Mark P83, P256
Anderson, Amy P35, P697
Anderson, Bart..... P344
Anderson, James..... P329
Anderson, Kristin O15, P719
Anderson, Mark..... P501
André, Pascale O51
Andreas, Jonathan..... P75, P77, P549
Andrejeva, Gabriella P206
Andresen, Thomas..... P215, P226, P227, P272
Andrews, David..... P161, P198
Andrews, Lawrence P649
Andrews, Miles P505, P572
Andtbacka, Robert..... P53, P295, P717
Angelo, Michael..... P20
Angra, Natasha P14
Anker, Jonathan..... P98
Annamalai, Anand P713
Annels, Nicola P597
Annis, D. Allen..... P450
ANP-BC, PhD P643

AUTHOR INDEX

Ansell, Stephen P648
Antonarakis, Emmanuel P338
Antonia, Scott O24
Antoniani, Barbara P640
Antonoff, Mara P233
Aoki, Hiroyasu P300
Apodaca, Minjun P93
Appah, Ebenezer P141
Appel, Lena P103
Applegate, Allison P108
Appleman, Leonard P294, P298
Aran, Dvir P687
Aranda Orgilles, Beatriz P214
Archer, Kristina P678
Ardeshna, Kirit P240
Ardila, Connie P411
Ardito, Matthew P180
Arepally, Aravind P456
Argiris, Athanassios P85, P328
Ariel, Yuval P197
Arif, Mehreen P597
Ariizumi, Hirotsugu P51
Arima, Hideki P334
Arkenau, Hendrik-Tobias P87
Armand, Philippe P315
Armenio, Vincent P318
Arnold, Cody P438
Arora, Reetakshi P572
Arriola, Edume P715
Ascierto, Maria P14
Ascierto, Paolo P329, P711
Ashkin, Emily P555
Ashok, Devika P15, P35, P320, P321, P322, P323, P673
Askmyr, Maria P7
Asmellash, Senait P66
Aspeslagh, Sandrine P255
Astsaturov, Igor P396
Atabakhsh, Elnaz P44
Atarashi, Koji P574
Athanassios, Argiris P342, P343
Atkins, James P361
Atkins, Michael P380, P447, P548
Atkinson, Victoria O24, O28, P717
Atmaca, Akin P248, P251
Au, Qingyan P487
August, David P339
Aulakh, Sonikpreet P6
Aulukh, Sonikpreet P5
Aung, Sandra O4
Aurellano, Jerald P1
Austin, Richard P608
Austin, Wayne P44
Authie, Pierre P445
Autio, Karen P87, P297
Au-Young, Janice P27, P571
Avalle, Lidia P184
Avallone, Antonio P711
Avalos, Christian P43
Avery, Kendra P411, P664
Awad, Mark P109, P174, P314
Awada, Ahmad P255
Axelrod, Rita P328, P342, P343
Ayanoglu, Gulesi P532
Aydin, Iraz P1
Ayers, Mark P31
Azad, Nilofer P622
Aziz, Omar P681
Azpilicueta, arantza P466

Author B Abstract Number

Baars, Arnold P293
Bacac, Marina P413
Baccei, Chris P209
Bacchiocchi, Antonella P721
Badeaux, Mark P345, P363
Bader, Robert P7
Badri, Tayf P133
Bagarazzi, Mark P171
Bagnardi, Vincenzo P374
Bagwell, C. Bruce P111
Baharom, Faezzah P164, P172
Bahary, Nathan P706

AUTHOR INDEX

Bai, Xue P16
Bailey, Kelly P476
Bailey, Lucas P485
Bailey, Shannon P581
Bailey, Stefanie P284
Baird, Andrew P73
Baird, Jason P410, P471
Baird, Stuart P73
Bajaj, Anshika P17
Bakhshi, Sameer P714
Balakumaran, Arun P315
Balar, Arjun P625
Balasubramanian, Wesley P529
Balasubramanyam, Aarthi P60
Balasubramanyam, Sadhana P546
Balch, Leslie O20
Baldini, Capucine O30
BALIGA, RAMESH P405
Ballerini, Andrea P152
Ballesteros Merino, Carmen P18, P59, P429, P440, P578
Ballinger, Marcus O1, P66
Balmanoukian, Ani P409
Balyasnikova, Irina P277
Bambina, Shelly P455, P471
Banas, Dana P524
Banaszak, Katarzyna P515
Banavali, Shripad P714
Banchereau, Jacques P445
Banchereau, Romain P19
Banerjee, Hridesh P397
Banerji, Udai P287, P669
Bang, Yung-Jue P139, P335, P662
Bang, Yung-Lue P308, P341
Baniel, Claire P459
Banik, Debarati P576
Bankoti, Jaishree P72
Bannink, Jeannette P7
Bao, Riyue P48, P65, P371, P584
Bao, Xingfeng P598
Bao, Xuhui P551
Bao, Yangyi P285
Bar-Ad, Voichita P343
Barakat, David P234
Baras, Alexander P588
Barath, Manasi P608
Barber, Glen P601
Barberi, Theresa P234
Barbes, benigno P466
Barcelos-Hoff, Mary Helen P466
Barchan, Karin P656
Bardwell, Philip P215
Bares, Amanda P38, P627
Barker, Christopher P347
Barker, Kristi P428
Barman, Ishita P685
Barnhart, Bryan P685
Barretina-Ginesta, Maria-Pilar P326
Barrett, J. Carl P134
Barrett, John P682
Barron, Luke P216
Barsin, Sophie P637
Bartha, Gabor P78, P151
Barthels, Christian P375
Bartkowiak, Todd P546, P719
Bartlett, David P603
Bartlett, Nancy P327
Barton, Debora O22
Barzi, Afsaneh P592
Bask, Michael P592
Basu, Samik P276
Bata, Adam P524
Batelli, Sara P442
Bates, Breanna O15
Batey, Sarah O44, P631
Bath, Natalie P276
Battaglia, Sebastiano P188
Bauer, Todd O25, O26, P295
Baughman, Jan O24, P304, P305, P306
Bauman, Jessica P302, O51
Bauman, Lynne P339
Baumann, Matthias P299

AUTHOR INDEX

Bayle, Joseph.....P217
Bazarna, Anna P349
Bazhenova, Lyudmila P701
Beal, Dominic P185
Bear, Harry..... .....P491
Beatty, Gregory.....P706
Beatty, Matthew O16, P224, P241
Beaty, Melissa P576
Beaumont, Maribel P532
Beavis, Paul O46
Becher, Burkhard P68
Beck, Michael P661
Becker, Annette P697
Becker, Juergen.....P337
Becker, Oren P197
Beckermann, Katy P206
Bedard, Philippe.....P651, P698
Bednarik, Daniel.....P262
Bednarz, Bryan P464
Bedognetti, Davide.....P110, P468, P587
Bee, Christine P684
Beechem, Joseph P113, P131, P389, P428, P429
Beeler, Kristina P628
Behar, Vered P197
Behera, Deepak.....O49
Behren, Andreas.....P324
Behrens, Carmen.....P490
Bekaii-Saab, Tanios P290
Bel Aiba, Rachida.....P375
Bell, Bryan P562
Bell, David P570
Belldegrun, Arie P47
Bello, Akintunde.....P636
Belouali, Anas.....P548
Belt, Brian.....P498
Beltran, Antonio.....P200, P236, P251, P252
Beltran, Himisha.....P193, P591
Beltran, Mariana P501
Beltran, Pedro P599
Benchaaben, Assil..... P492
Bendall, Sean P20
Bendell, Johanna P87, P289, P305, P306, P316
Bender, Lewis P622
Bender, Steve P351
Bendjama, Kaidre P148
Bendjama, Kaïdre P181
Benhadji, Karim O30
Benjamin, Joel..... P614
Benjamin, Jonathan P1
Bennett, Gavin..... P398
Bentebibel, Salah Eddine..... O4, P424, P564, P710
Bentzen, Soren P302
Benz, Steve P311
Benzaid, Ismahene..... P263
Bera, Kaustav..... P104, P426
Berchadsky, Julia..... P362
Berdugo, Gad..... P180
Berent-Maoz, Beata..... O39, P47, P557
Berger, Alan P541
Berglund, Peter..... P17, P607
Berman, Abigail P319
Berman, Mark..... P609
Bernard, Hether..... P476
Bernardo, Marie P621
Bernatchez, Chantale..... O4, P233, P268, P424, P542, P710
Bernett, Matthew..... P411, P664
Bernstein, Howard..... P219
Berraondo, Pedro P466
Berry, Sneha P128
Berry, Wade..... P320, P321, P322, P323, P673
Berry, William P496
Bertan, Claudia P287
Bertelli, Francois..... P11
Bertheloot, Damien P524
Berthelot, Maud O44
Bertino, Erin..... P79
Bertozzi, Carolyn..... O37, P676

AUTHOR INDEX

Berz, David P385
Berzofsky, Jay P173
Besada, Rana P49
Besharati, Sepideh P541
Besneux, Matthieu P479
Bessell, Catherine P570
Betancur, Alec P367
Betof, Allison P521
Betts, Gareth P276
Betts, Keith P350, P355
Beuron, Fabienne P55
Bhandary, Lekhana P260
Bharadwaj, Uddalak P424
Bhardwaj, Nina O7, P149, P150, P182, P330, P403
Bhatia, Shilpa P448
Bhatt, Kamal P171
Bhatt, Rupal P123
Bhatta, Ankit P233
Bhosale, Priya P299
Bhumireddy, Archana P529
Bifulco, Carlo P18, P429
Bigley, Alison P501
Bigner, Darell P612
Bignone, Veronica P184
Biike, Sven P590
Bilen, Mehmet O4, P506, P507
Bilic, Sanela P215
Binder, Gwendolyn P276
Bindra, Ranjit P33
Bingham, Jim P678
Binns, Oliver P549
Birnbaum, Ariel O24
Birt, Alyssa P267
Bissonnette, Reid P346
Biswas, Manjusha P718
Bitting, Rhonda P298
Bivalacqua, Trinity P338
Black, Lora O50
Blackburn, Matthew P548
Blagovic, Katarina P219
Blahnik-Fagan, Gabriele P7
Blakely, Collin P385
Blanc, Véronique P375
Blanchard, Miran O50
Blando, Jorge O5
Blank, Christian O5, P389
Blank, Stephanie P182
Blanusa, Milan P375, P532
Blayney, Douglas P495
Blazquez, Ana P149, P150
Bleeker, Maaike P693
Blery, Mathieu P4
Blum, Steven P566
Blumenschein, Wendy P532
Boasberg, Peter O21
Bobowska, Aneta P204
Boczkowski, David P612
Bodo, Veronique P666, P667
Bogaert, Liz P411
Bogman, Katrijn O23
Bohana-Kashtan, Osnat P356
Boisvert, Heike P627
Boku, Narikazu P636
Boland, Genevieve P16, P92
Boland, Kathryn P86
Bolanos, Elisabeth P466
Bollard, Catherine O17, P240
Bollini, Sangetha P340
Bolsée, Jennifer P218, P274, P275
Bommireddy, Ramireddy P266
Bond, Catherine P580
Bondarenko, Riva O24
Bongiorno, Emily P161
Boni, Valentina P87
Bonilla, Luisa P225
Bonneau, Pierre P442
Bonner-Ferraby, Phoebe P32
Bonvini, Ezio O24, P304, P305, P306, P366
Bonzom, Emilie P492
Bonzon, Christine P411, P664
Bookhardt, Sam P162

AUTHOR INDEX

Boomer, Ryan....P216
Booty, Matthew....P219
Bordeaux, Jennifer....P127
Borghaei, Hossein....P396
Boriello, Frank....P502
Bornhauser, Martin....P113
Bornschein, Simon P220, P221
Borodovsky, Alexandra....P665
Boross-Harmer, Sarah....P225
Borowsky, Jennifer....P580
Borrebaeck, Carl....P195
Borrello, Ivan....P86
Bose, Nandita....P527, P708
Bosenberg, Marcus....O32
Bosse, Marc....P20
Boston, Christopher....P550
Bot, Adrian....P47, P212
Boto, Agedi....P678
Boudadi, Karim....P338
Bourgogne, Agathe....P246
Bourgon, Richard....P19
Boussahmain, Chakib....P39, P654
Bowers, Jacob....P250
Boyd-Kirkup, Jerome....P477
Boyer, Eric....P685
Boyer-Chammard, Agnès....O51
Boyle, Sean....P13, P78, P151
Bradford, Delia....P202
Bradley, Jeffrey....P319
Brahmer, Julie....O47, P12, P589
Brail, Les....P307
Brammer, Jonathan....P240
Brandely-Talbot, Maud....P148
Braun, Nathalie....P255
Bregeon, Delphine....P4
Breij, Esther....P402, P647
Breman, Eytan....P213, P218, P220, P231, P232, P255, P626
Brenner, Malcolm....O17
Brewis, Neil....O44, P631
Bridgeman, John....P222, P223, P243, P261
Brieschke, Brigitte....P9
Brieu, Nicolas....P21
Brignone, Chrystelle....O28, P387
Briones, Javier....P327
Brioschi, Matteo....P482
Briskin, Michael....P271
Brisson, Ryan....P48
Britten, Cedrik....O8, O18
Brittsan, Christine....P178
Brix, Liselotte....P56, P129
Brixner, Diana....P137
Broadhead, Alex....P209
Brockstedt, Dirk....P202
Brockwell, Natasha....P22
Broderick, Jim....O37
Brodkin, Heather....P404
Brody, Joshua....O45, P139, P205, P330, P341
Brohl, Andrew....P346
Brookes, Hannah....P445
Broom, Wendy....P154, P166
Brose, Marcia....P392
Brossart, Peter....P333
Brouwer, Margreet....P666, P667
Brovarney, Martin....P202
Brown, Alice....P479
Brown, Anthony....P115, P715
Brown, Bob....P287
Brown, Elisabeth....P272
Brown, Jeff....O37
Brown, Jennifer....P306, P525
Brown, Michael....P612
Brown, Ryan....P464
Brown, Tommy....P159
Bruce, Jeffrey....P437
Bruderer, Roland....P42
Brunkhorst, Beatrice....P291
Bruno, Tullia....O36, P70, P556, P583, P649, P679
Brunsvig, Paal....P715

AUTHOR INDEX

Bruun, Jonas....P226, P272
Bryan, Locke....P327
Brzozka, Krzysztof....P204, P515
Bu, Luke....P600, P606, P610
Buatois, Vanessa....P650
Bucci, Vanni....P574
Buchbinder, Elizabeth....P108, P566
Buchi, Melanie....P486
Buchkovich, Martin....P120
Buckler, Alan....P550
Budach, Wilfried....P332
Budco, Alexei....P429
Budde, Lihua....P240
Budhani, Pratha....P546
Budhu, Sadna....P143, P347, P521
Buechler, Markus....P103
Buell, Jamie....P40
Buell, Jennifer....P189
Buffet, Delphine....O44
Buffo, Mary Jo....P294
Buggy, Joseph....P54, P205
Bukur, Juergen....P554
Bukur, Valesca....O8
Bulliard, Yannick....P246
Bunch, Brittany....P224
Bunk, Sebastian....P246
Buonaguro, Luigi....P711
Buqué, Aitziber....P473, P504
Buren, Luxuan....P511
Burge, Matthew E....P580
Burgher, Blake....P75, P77, P549, P707
Burkart, Jarred....P79
Burke, James....P524
Burm, Saskia....P402, P647
Burnett, Madison....O15
Burns, Robert....P366
Burra, Arun....P687
Burton, Elizabeth....O5, P505, P564, P572
Burtness, Barbara....O51
Bushway, Meghan....P49
Busser, Brian....P283
Bussler, Holm....O20
Butler, Brian....P152
Butler, Marcus....P225, P662, P698
Butterfield, Lisa....O5, P176, P294, P528, P559, P709
Byers, Lauren....P452, P470
Bykowski, Juli....O50
Byrne, Ann....O46
Byun, Jiyun....P69

Author C Abstract Number

Cabral, Crystal....P154, P166
Cabrales, Pedro....P99
Cabrera, Paula....P47
Caffaro, Carolina....P417
Cahoon, Jason....P37
Cai, Haiying....P364
Calabro, Valérie....P637
Caldara, Jenifer....P90
Calderon, Florencio....P137
Calhoun, Susan....P405
Callahan, Margaret....P143
Callejas-Valera, Juan....P465
Callihan, Evan....P608
Calme, Griffin....P130
Calmels, Franceline....O51
Calvo, Emiliano....O23
Calvo, Katherine....P61
Camargo, Maria....P458
Camilleri, Matt....P44
Campan, Mihaela....P592
Campbell, Jean....P53
Campbell, Kerry....P396
Campesato, Luis....P347
Campf, Jessica....P159
Camphausen, Kevin....P61
Campisi, Anthony....O2
Campo, Giulia....P97
Candia, Albert....P25
Canestrari, Emanuele....P282
Cann, Jennifer....P409, P638

AUTHOR INDEX

Canoll, Peter....P437
Canon, Jean-Luc....P255
Canon, Jude....P599
Canter, Robert....P508
Canton, David....P717
Cao, Hui....P621
Cao, Lizhi....O37
Cao, Pengpeng....P226, P272
Cao, Yu....O9
Capili, Allan....P550
Capitini, Christian....P434
Capoccia, Ben....P512
Capoccia, Benjamin....P512
Capper, David....O8
Carabulea, Gabriel....P609
Caramia, Franco....O46
Carbone, David....P79
Carcereny, Enric....P715
Cardenas, Luis....P68
Cardia, James....P258
Cardnell, Robert....P452
Carey, Shawn....P226, P272
Carlino, Matteo....P329
Carlson, Peter....P464
Carman, Julie....P524
Carman, Lori....P87
Carmer, Scott....P262
Carnaz Simoes, Ana Micaela....P478
Carnaz Simões, Ana Micaela....P478
Carpizo, Darren....P339
Carrasco, Javier....P255
Carreira, Suzanne....P287
Carrillo, Caroline....P605
Carroll, Chantia....P1
Carroll, Pamela....P154, P166
Carroll, Sean....P1
Carter, Alun....P512
Carter, Corey....P99, P372
Carter, Erik....P166
Carter, Kenneth....P262
Carter, Laura....P358
Carthon, Bradley....P506, P507
Caruso, Santina....P215
Carvajal, Luis....P450
Carvajal-Hausdorf, Daniel....P133
Carvalho, Carlos....P200, P236, P251, P252, P253, P257
Carven, Gregory....P550
Cascone, Tina....P233
Castillo-Martin, Mireia....P150, P251, P252, P253, P257
Castle, John....O8, P189
Catanese, Maria Teresa....P184
Catlett, Melissa....P336
Cattaruzza, Fiore....O4, P364
Caushi, Justina....O47
Cavallo, Federica....P413
Cavet, Guy....O3, P1
Cebon, Jonathan....P324
Ceccarelli, Michele....P587
Cecco, Loris....P110
Cecere, Fabiana....P97
Cecil-Taylor, Madelyn....P550
Cedano-Hilton, Angel....P210
Celentano, Lorne....P550
Celestino, May....P233
Cesano, Alessandra....P113, P136
Cescon, David....P698
Cetz, Janet....P364
Chae, Young Kwang....P98, P568, P582, P586
Chaft, Jamie....O47
Chagin, Karen....O18, P276
Chain, David....P442
Chambers, Andrea....P513, P523, P531
Chamie, Karim....P47, P712
Champhekar, Ameya....P557
Champion, Brian....P479
Chan, Anissa....P527, P708
Chan, Hok Yee....O47, P589
Chan, Ivan....P297
Chan, Timothy....P156, P570
Chanan-Khan, Asher....P5, P6

AUTHOR INDEX

Chand, Dhan....P659
Chandhok, Namrata....P719
Chandra, Abhinav....P385
Chandra, Dinesh....P598
Chandramohan, Vidyalakshmi ...P612
Chang Lee, Rachael....P324
Chang, Alfred....P285
Chang, De-Kuan....P215, P227
Chang, Esther....P457
Chang, Hua-Chen....P700
Chang, Sangmin....P568, P586
Chang, Wei-Chun....P217
Chang, Wen-Chung....P259
Changelian, Armen....P38
Chao, Joseph....P26
Chao, Yee....P191
Chaparro, Rodolfo....P185
Chapman, Carolyn....P338
Chappel, Scott....P666
Chapron, Christopher....P550
Charabaty, Aline....P447, P538
Charo, Jehad....O23, P413
Chartash, Elliot....O25, O26
Chartier, Cecile....P210
Charych, Deborah....P348, P368, P378, P419
Chatel, Laurence....P650
Chatterjee, Anindya....P662
Chatterjee, Gourab....P38
Chau, Ian....P327
Chauchet, Xavier....P650
Chaudhary, Ruchi....P27
Chaumette, Tanguy....P711
Chaussabel, Damien....P110
Chaves, Jorge....P327
Chavez, Brandy....P516
Cheever, Martin....P298
Chen, Aimei....P3
Chen, Austin....P209
Chen, Chao-Hsien....P427
Chen, Chuanben....P544
Chen, David....P417
Chen, Emily....P640
Chen, Francine....P304
Chen, Georgia....P444
Chen, Helen....P26
Chen, Hui....P362
Chen, I-Ju....P163
Chen, Isan....O27
Chen, Jian....P228, P325, P514
Chen, Jonathan....P721
Chen, Lieping....P133, P678
Chen, Limo....P354, P470
Chen, Li-Tzong....P636
Chen, Liuhong....P398
Chen, Peiling....P494
Chen, Richard....P13, P78, P151
Chen, San-chi....P191
Chen, Shu-Jen....O48
Chen, Shuming....P652
Chen, Wangjuh (Sting)....O48
Chen, Wei....O33, P481, P583
Chen, Weizao....P270
Chen, Xiaomu....O3, P1
Chen, Xueying....P651
Chen, Yao....P494
Chen, Yi....P532
Chen, Yi-Jen....P26
Chen, Yu....P544
Chénard-Poirier, Maxime....P287
Cheng, Zhi-jie....P661
Cheou, Pamela....P482
Cherwinski, Holly....P532
Chesney, Jason....O22
Chesson, Brent....P424
Chesson, Charles....P613
Cheung, Phyllis....P349
Cheung-Lau, Gardenia....P47, P557
Chian, David....P202
Chiang, Veronica....P84
Chiec, Lauren....P586
Chikina, Maria....O33
Chin, Renee....P427

AUTHOR INDEX

Chintakuntlawar, Ashish P186, P409
Chiou, Victoria P699
Chiriboga, Luis P468
Chisamore, Michael P708, P715
Chitguppi, Chandala P85
Chittenden, Thomas P29
Chiu, Edison O15
Chiu, Vi P361
Chmielewski, Stefan P515
Chmielowski, Bartosz P716
Cho, Charles P351
Cho, Daniel O4, P87, P423
Cho, Hearn P149
Cho, May P336
Chodon, Tinle P47
Choi, HyeongWook P598
Choi, Kati P194
Choi, Lydia P130
Chomas, James P456
Choueiri, Toni O45, P54, P350, P355
Chouljenko, Dmitry P600, P606, P610
Chow, Eric P687
Chow, Laura P64, P335, P340
Choy, Gavin P377
Christensen, James O27, P385
Christine, Thioudellet P181
Christmas, Rudy P624
Chu, Chia Lin P384
Chu, Christina P396
Chu, Felix O3, P1
Chu, Jaemi P155
Chu, Lulu P359, P563, P665
Chu, Seung P411
Chu, Shaoyou P9
Chua, Ying Xuan P152
Chuang, Jeffrey P582
Chuckran, Chuckran O36
Chung, Hyun Cheol P662
Chung, Hyun-Cheo P308
Church, Deanna P129
Church, Sarah P113, P428, P429, P719
Ciboddo, Michele P156
Cilfone, Nicholas P29
Ciliberto, Gennaro P97
Cillo, Anthony O36, P556, P583, P649
Cimen Bozkus, Cansu P182
Citrin, Deborah P61
Clark, Ryan P209
Clarke, Jeffrey P146, P503, P549, P596
Claudepierre, Marie-Christine P181
Clavijo, Paul O20
Claxton, David P381
Cleary, James P304
Cleary, Lisa P49, P307, P314
Clemens, Wendy O4
Clemente, Jose P494
Clifton, Guy P159
Clump, David P462
Clyde, Karen P571
Coble, Vincent P164, P172
Cocorocchio, Emilia P374
Coffman, Robert P25
Cogdill, Alexandria O5, P505, P572
Cognetti, David P85, P328, P343, P489
Cohen, Adi P453
Cohen, Ezra O50, P25, P333, P716
Cohen, Justine P16, P92, P108
Cohen, Lorenzo P505
Cohen, Roger O24, P174, O51
Cohn, Allen P391, P393
Colas, Christophe P202
Colcher, David P259
Coleman, Kevin P365
Colen, Rivka P430, P431, P432
Colevas, Dimitrios O51
Collaku, Agron O19, P361
Collignon, Aurélie P492

AUTHOR INDEX

Collins, Hannah P506, P507
Colloca, Stefano P184
Colombetti, Sara P413
Colon, Eugenia P522
Coltharp, Carla P18, P144, P433
Comacho, Mark P225
Combs, Katherin P240
Comfort, Laurie P550
Comin-Anduix, Begoña P557
Comin-Anduix, Begonya O39, P47
Concha-Benavente, Fernando ... P480
Conejo-Garcia, Jose O9
Conforti, Fabio P374
Cong, Mei P661
Conlin, Alison O31
Conlon, Kevin P61, P416
Conrad, Daniel P491
Conroy, Jeffrey P75, P76, P77, P549, P707
Cons, Laura P650
Contessa, Joseph P84
Cook, David P572
Cooke, Keegan P599
Cooper, Sara P278
Cooper, Zachary P14
Copeland, Ron P678
Cordes, Nicole P229
Cordon-Cardo, Carlos P257
Cornax, Ingrid O43
Cornfeld, Mark P669
Corrales, Leticia P351, P412
Cortes Gomez, Eduardo O42
Cortez, Czrina P521
Cosgrove, Cormac P57, P153
Cossette, Daniel P278
Costa, Matthew P659
Costales, Cristina P592
Costello, Kimberly P396
Cote, Gregory P305
Cottrell, Tricia P128, P589
Cotugno, Gabriella P184
Couey, Marcus P562
Coughlin, Zoe P246
Cougot, Delphine P88
Coukos, George P482
Coupet, Tiffany P8
Couto, Nuno P251
Cova, Agata P110
Coventry, Brendon P30
Cowan, Scott P342
Cowey, C. Lance P291
Cox, Joanna P708
Crabill, George P652
Craig, Sandra P189
Crawford, Alison P438
Crawley, Simon P63
Creasy, Caitlin P542
Cremin, Michael P608
Crespo, Mateus P287
Cripe, Timothy O52
Cristea, Mihaela P259
Cristescu, Razvan P31
Critchlow, Susan P388
Crittenden, Marka P410, P455, P471, P562
Crocker, Andrea P510
Croll, Mariya P154
Crook, Kenneth P4
Crosignani, Stefano P667
Croteau, Josh P705
Cruz, Hans P316
Csiki, Ildiko P171
Cua, Daniel P532
Cubillos-Ruiz, Juan O9
Cuende, Julia P666
Cui, Feifei P653
Cui, Lei P362
Cukierman, Edna P396
Cull, Elizabeth P327
Cullen, Kevin P302
Cummings, Christine P407
Cummings, Craig P19
Cummings, Kara P178

AUTHOR INDEX

Curran, Michael.....P157, P299, P427, P546
Curran, Riley.....P49
Currence, Scott.....O24
Curry, Jonathan.....P564
Curry, Joseph.....P85, P328, P343, P489
Curti, Brendan.....O4, O22, P562
Cutler, Gene.....P202
Cwiertnia, Grzegorz.....P515
Cyanam, Dinesh.....O48, P27, P707
Czupalla, Cathrin.....P1

Author D Abstract Number

Dadey, Becky.....P481
Daehling, Angelika.....P337
Dagbay, Kevin.....P550
Daginakatte, Girish.....P529
Dahlberg, Suzanne.....P109
Dahlman, Anna.....P7, P656, P683
Dai, Hong.....P167
Dai, Wenjie.....O9
Daige, Christopher.....P345
Daine-Matsuoka, Barbara.....P205
Dakappagari, Naveen.....P65, P126, P127
Dakhova, Olga.....O17
Daley, Laura.....P634
Dalgleish, Angus.....P288
D'Alise, Anna Morena.....P184
Daly, Thomas.....P407
Dama, Paola.....P451
Daman, Andrew.....O15
D'Amico, Leonard.....P298
Damien, Kee.....P324
Damsky, William.....O32
Danaee, Hadi.....P326
D'Andrea, Daniel.....P640
Danehy, Francis.....P550
Danese, Mark.....P692
D'Angelo, Sandra.....O18
Daniel-MacDougall, Carrie.....P505
Daniels, Gregory.....O4, P58, P717
Danielson, Mike.....P708
Danilova, Ludmila.....O6
Dann, Christina.....P282
Danton, Makenzie.....P438
D'Antonio, Marc.....P235
Dao-Pick, Trang.....P205
Dar, Henia.....P279
Darcy, Phillip.....O46
D'Argio, Kenneth.....P210
Darmon, Audrey.....P463
Daro, Dorothée.....P220, P221, P274
Darvishian, Farbod.....P468
Das, Amritava.....P434
Daszkiewicz, Lidia.....P435
Datar, Ila.....P33
Datta, Abhishek.....P550
Daud, Adil.....P139, P341
Davar, Diwakar.....O21, O22
Davidson-Moncada, Jan.....P304, P338
Davies, Angela.....P443, P444
Davies, John.....O34
Davies, Michael.....O5, O44, P505, P572, P631, P710
Davis, Meredith.....P566
Dawes, Joanna.....P287
Dawson, Keith.....P408
Dayao, Maria Rosalyn.....P608
De Bono, Johann.....P287
de Groot, Anne.....P180
de Gruijl, Tanja.....P293, P577, P693
De Henau, Olivier.....P347, P521, P666
de la Cruz Merino Sr., Luis.....P327
de la Cruz-Merino, Luis.....P549
De Lucia, Maria.....P184
de Miranda, Noel.....P256
de Oliveira, Catarina.....P253, P257
De Pas, Tommaso.....P374
de Silva, Suresh.....P519, P657, P658
De Smidt, Elien.....P604
de Souza, Paul.....P320, P321, P322, P673

AUTHOR INDEX

de Vries, Elisabeth.....P87
Dean, Dennis.....P524
Debarge, Rachel.....P169
DeCillis, Arthur.....P174
Decker, Brennan.....P164, P172
Decker, Roy.....P319
Declerck, Paul.....P604
Decock, Julie.....P230
DeFalco, Jeff.....O3, P1
Defor, Todd.....P573
deGroot, John.....P431, P432
Dekker, Allison.....P48
Delbeau, Daniela.....P625
Delgoffe, Greg O11, O13, P207, P208, P528, P616
Della Corte, Carminia.....P452
Dellacecca, Emilia.....P153
Delman, Devora.....P706
Delwar, Zahid.....P600, P606, P610
Demaria, Sandra.....P170, P469, P623
Demarzo, Angelo.....P338
Demberg, Thorsten.....P246
Dembrow, Daniel.....P262
Demols, Anne.....P336
Demonte, Daniel.....P400
DeMora, Thomas.....P302
Demoulin, Benjamin.....P231, P274, P626
Deng, Andy.....P684
Deng, BoLiang.....P364
Deng, Weiwen.....P351
deng, youping.....P301
Denies, Sofie.....P666
Denlinger, Crystal.....P396, P409
Dennis, Melissa.....P239
DeOlivera, Elizabeth.....P86
DePeaux, Kristin.....P616
DePietro, Paul.....P549
depil, Stephane.....P214, P283
Dequeant, Mary Lee.....P279
Deregnaucourt, Theo.....P667
DeRenzo, Christopher.....O17
Derhovanessian, Evelyna..... O8
Desai, Ami..... P584
Desai, Shruti..... P33
Desbien, Anthony..... P351
Deshmukh, Chetan..... P714
Deshpande, Rahul..... O13
Desjarlais, John..... P411, P664
Desnoyers, Luc R..... P87
d'Esposito, Angela..... P237
Detheux, Michel..... P666, P667
Devarajan, Karthik..... P396
Devi, Gayathri..... P551
DeVito, Nicholas..... P545
DeWaele, Peter..... P626
Dewan, Anna..... P691
Dey, Joyoti..... P618
Dey, Souvik..... P177
DeYulia, Garrett..... P563
Dhandapani, Sripriya..... P532
Dhawan, Ish..... P1
Dhudashia, Amit..... P694
Dhudashiya, Amit..... P529
Di Carlo, Anna..... P640
di Genova, Gianfranco..... P479
Di Matteo, Elena..... P184
Di Modugno, Francesca..... P640
Di Simone, Christopher..... P392, P393
Diab, Adi..... O4, P424, P505, P537, P564, P565, P644, P710
Diao, Lixia..... P452, P470
Diaz, Luis..... P703
Diaz, Rosa..... O52
Dicker, Adam..... P630
Dickey, Jennifer..... O48
Diekmann, Jan..... P621
Dietrich, Pierre-Yves..... O8
Dietsch, Gregory..... P410
Diken, Mustafa..... P402, P621, P647
Dillon, Stacey..... P400, P406
Dilworth, Ryan..... P144, P433
Dimitrov, Dimiter..... P270
Dinavahi, Saketh..... P381

AUTHOR INDEX

Ding, Jeffrey P34
Ding, Jun P600, P606, P610
Diodoro, Maria Grazia P640
DiRenzo, Daniel P35, P320, P321, P322, P323, P673, P697
Dispersyn, Gerrit P258
Dittamore, Ryan P69
Diwanji, Tejan P302
Dixit, Vaishali P598
Do, Khanh P295
Doan, Matthew P458
Doberstein, Stephen P364
Dobrzanska, Monika P515
Dobson, Jason P154, P166
Dodoo, Ernest P248
Doener, Fatma P337
Doi, Shun P334
Doi, Toshihiko P300
Dolan, Jillian P73
Dolata, Izabela P515
Dolinski, Brian P238, P271
Dolling, David P287
Domankevich-Bachar, Vered P453
Dominah, Gifty P36
Dómine Gómez, Manuel P715
Dominguez, George O2
Dominici, Massimo P237
Dong, Haidong P394
Dong, Shilan P37
Dong, Wen P577
Dong, Yi P160, P245
Donio, Michael P512
Donis, Erick P154, P166
Donovan, Michael P149, P150
Donson, Andrew P497
Doody, Jacqueline O44, P631
Dooley, Kevin P618
Doolittle-Hall, Janet P575
Dorner, Sonja O8
Dor-On, Eyal P197
Dorraki, Mohsen P30
Dose, Christian P45
Doshi, Kshama P454
Dostalek, Mirek P309
Dotan, Efrat P396
Dotti, Gianpietro O17
Dottino, Peter P149
Dougan, Michael P467
Dougan, Stephanie P467
Dougherty, Janna P675
Dovedi, Simon P359
Dow, Edward P189
Downing, Sean P38, P39, P40, P627, P654
Doyle, Laura P340
Drabick, Joseph P381
Draganov, Dobrin P609, P617
Draghi, Monia P530
Dragnev, Konstantin P549, P715
Dragovich, Tomislav P361
Drakaki, Alexandra P47
Drake, Charles P338
Dranoff, Glenn O35
Dressman, Devin P76, P549
Driescher, Caroline O38
Driessens, Gregory P666, P667
Dronca, Roxana P394
Dropulic, Boro P270
Drouin, Elise P189
Druta, Mihaela O18
Dry, Jonathan P594
Dryer-Minnerly, Rebecca P276
Du, Ella P350, P355
Du, Lihua P495
Du, Xiaoyan P532
Dubeau, Louis P592
Dubensky, Jr., Thomas P351
Dubois, Sigrid P416
Duchateau, Philippe P214, P283
Duckworth, Victoria P144
Dudek, Liesel P339
Dudek, Marcelina P204
Duffy, Colm P352

AUTHOR INDEX

Dufort, Fay P267
Dugo, Matteo P110
Dummer, Reinhard P68
Dunai, Cordelia P508
Duncan, Alex P178
Dunlap, Steven P326
Dunn, Steven P482
Duong, Ellen P518
DuPage, Amy P87
Duperret, Elizabeth P155
Dupis, Edouard P331
DuPont, Hebert P194
Dupuis, Nicholas P41, P42, P628
Duran, Adrienne P572
Durham, Nicholas P409
Dusek, Rachel P348
Dushyanthen, Sathana O46
Dutcus, Corina P391, P392, P393
Dutoit, Valérie O8
Duval, Matthieu P492
Duvvuri, Umamaheswar P583
Dwyer, Connor P250, P273, P284
Dy, Grace P146, P503, P549, P595, P596
Dyalram, Donita P302
Dziedzic, Katarzyna P204

Author E Abstract Number

Early, Amy P77
Eastgate, Melissa O28
Eaton, Keith O27
Eck, Steven P699
Eckert, Andrea O43
Economides, Kyriakos P618
Edeline, Julien P475
Edwards, Nancy P36
Edwards, Robert O36
Efrati, Margalit P453
Egan, James O31
Egeblad, Mikala P468, P521
Egelston, Colt P43
Eggermont, Alexander P329
Ehrich, Mathias P58
Eisel, Sarah P630
El Asmar, Margueritta O47
El Salek, Kamel P430, P431
Elakkad, Ahmed P431
El-Difrawy, Sameh P63
Elf, Shannon P156
Elhmouzi-Younes, Jamila P375
Elias, Rawad P566, P567
Elist, James P167
El-Khoueiry, Anthony P87, P622
Elkord, Eyad P230
Elliott, Robert P483
Ellison, Christie O50
Ellison, Christopher P58
Ellmark, Peter P7, P195, P656, P683
Elpek, Kutlu P271
El-Rayes, Bassel P266, P290, P506, P507
El-Sawada, Jack P126
Elser, Christine P698
Elshafeey, Nabil P430, P431, P432
Elshafeey, Nancy P432
Elston, Sawako P225
Emens, Leisha O45
Emerling, Daniel O3, P1
Encarnacion, Carlos P392, P393
Endo, Atsushi P598
Enell Smith, Karin P656
Engelhardt, Benjamin P690
Engelman, Alexander P302
England, Lee P173
Engle, Elizabeth P128, P541
Englert, Stefan P72
Enhinger, Gerhard P113
Enstrom, Amanda P209
Enzler, Danlee P345
Ephrame, Sophiya P203
Erbe, Amy P10, P419, P459, P485

AUTHOR INDEX

Erbs, Philippe.....P181
Erickson, Loren.....P493
Ericson, Nolan P132
Erminia, Massarelli.....P385
Ernest, Dodoo P252
Ernst, Ulrich.....P187
Ernstoff, Marc O22, P294, P423
Eroglu, Zeynep O21, P346
Erps, Timothy P44
Ertunc, Onur.....P338
Escher, Claudia.....P41, P628
Eskander, Ramez.....P76
Eskiocak, Ugur.....P386, P407
Espat, N. Joseph P318, P456
Espiritu Santo, Gregg.....P1
Essman, Matthew O12
Estes, Scott.....P618
Estrada, Juan.....P599
Estrem, Shawn O30
Eswarappa, Rajesh P529
Ettenberg, Seth P216
Ettinger, David.....P12
Etxeberria, Inaki P466
Evans, Elizabeth.....O20
Evans, Kathy P545
Evans, Lawrence.....P400
Evans, Myron P551
Evans, Natathiel P342
Evans, Thomas P608
Evaristo, Cesar.....P45
Even, Caroline O51
Evensen, Erik.....P54
Everett, Katy.....O44
Evers, Stefan.....P413
Eves, Taylor P325
Ezell, Tucker P271

Author F Abstract Number

F. Sanmamed, Miguel P466
Fa'ak, Faisal P424
Fabian, Kellsye.....P353
Fabritius, Charles-Henry P515
Fabrizio, David O48
Facciolo, Francesco..... P97, P640
Fachin, Fabio..... P226, P272
Fadden, Riley P16
Fadul, Camilo P493
Faggioni, Raffaella P308
Fahl, Shawn..... P100
Faiena, Izak P47
Faitg, Thomas P276
Fakih, Marwan P26, P305, P336
Falahat, Rana P601
Falchook, Gerald..... O21, P139, P297, P341
Faltaos, Demiana O27
Fan, Frank P661
Fan, Rong P721
Fan, Xuejun P370
Fan, Youhong P470
Fan, You-Hong P452
Fang, Bin P264
Fang, Frank P598
Fang, Jie P524
Fang, Jun P487
Fang, Lei..... P653, P671
Fang, Victoria..... P675
Fanning, Philip P335, P340
Fanta, Paul P76
Fanton, Christie O4, P364
Faoro, Leonardo P289
Fardis, Maria..... O22
Farrar, Michael O43
Farren, Matthew..... P290
Farwell, Michael O49
Fayette, Jerome O51
Fayngerts, Svetlana..... P276
Feau, Sonia P553
Fedele, Stefania P479
Federico, Lorenzo P233
Fehlings, Michael..... O1
Feigenberg, Steven P319
Feist, Mathilde..... P603

AUTHOR INDEX

Feldstein, Eric P437
Feliciano, Josephine P12
Felip, Enriqueta P715
Feller, John P609
Feng, Lei P157
Feng, Yan P351, P636
Ferber, Kyle P154, P166
Ferlin, Walter P650
Ferlini, Cristiano O23
Fernandez, Sheila P1
Fernandez Banet, Julio P385
Fernandez-Penas, Pablo P717
Ferraresi, Virginia P97
Ferrarotto, Renata P157
Ferreira, Ana P287
Ferris, Robert O24, O36, P70, P332, P462, P480, P556, P583, P649
Ferrucci, Pier Francesco P374
Ferte, Charles P308
Fertig, Elana P561
Fiander, Michelle P137
Fichera, Imma P184
Fidai, Shafique P415
Fieschi, Jacques P492
Fife, Brian P280
Figueiredo, Ines P287
Figueroa, Nathania P498
Filgueira, Carly P152
Finck, Rachel P106
Findeis, Mark P178, P189
Fink, Brian P525
Finley, Michaela P708
Finn, Jessica P106
Finnigan, John P149
Fioretos, Thoas P195
Firouznia, Marjan P426
Fischer, Christopher O50
Fischer, Nicolas P650
Fischer, Paul P382
Fischer, Suzanne O32
Fisher, Adam P624
Fisher, Andrew P442
Fisher, Kerry P479
Fisher, Terrence O20
Fishman, Mayer P224, P423
Fitzgerald, Jonathan P215, P226, P272
Fitzgerald, Kerry P58
Fjallskog, Marie- Louise P716
Flaherty, Keith P16, P307
Flament, Anne P255
Flechtner, Jessica P154, P166
Fleisher, Thomas P416
Fleury, Michelle P271
Flick, Heather P425
Flies, Dallas P678
Fling, Steven P298
Flohr, Christian P711
Flohr, Penny P287
Flood, Blake P412
Flores-Borja, Fabian P55
Florio, Vincent P410
Florou, Vaia P586, P719
Flossdorf, Michael P103
Flowers, Christopher P327
Flynn, Brianna P8, P266, P721
Flynn, Susan O1, P60, P101
Folci, Marco P152
Folgori, Antonella P184
Foloppe, Johann P181
Fong, Lawrence O45, P54, P82, P298, P687
Fontaine, Martina P232, P274
Foo, Wai Chin P564
Ford, Laurie Ann O42
Forde, Patrick O47, P12, P361, P589
Foreman, Nicholas P497
Forget, Marie-Andrée P233, P542
Forghani, Parvin P390
Forman, Stephen P259
Forster, Martin P387
Forsyth, Peter P263
Foster, Aaron P217

AUTHOR INDEX

Foster, Corey P48
Foti, Jamie P166
Fouladzadeh, Anahita P30
Foulk, Brad P707
Fox, Bernard P18, P59, P162, P429, P440, P578
Fox, Floyd O19, P361
Fox, Stephen O46
Fradette, Jared P354
Francese, Kaitlyn P625
Franchi, Luigi P524
Franchini, Genoveffa P61
Francica, Brian P351, P516, P517
Francis, Julie-Ann P460
Francque, Sven P711
Frank, Ian P210
Fransen, Signe P137
Franzese, Ornella P97
Fraser, Jonathan P198
Fray, Michael P216
Frazier, Victoria P612
Frederick, Joshua P102, P295
Frederix, Kim P667
Freedman, Christine P16
Freedman, Joshua P479
Freeman, Daniel P308
Freimark, Bruce P614
Freimoser-Grundschober, Anne P413
Frendeus, Bjorn P602
Frenzel, Katrin O8
Frey, Alan P675
Fridman, Wolf Herman O5
Friedland, David P294
Friedlander, Philip P149, P150
Friedlander, Terence O7, P687
Friedman, Alan P234
Friedman, Claire P108
Friedman, David P455
Fritsche, Jens O8, P246
Fritzell, Sara P7
Fromm, George P519, P657, P658
Fu, Siqing P299
Fuchs, Charles P33
Fueyo, Juan P370, P605
Fuhrman, Kit P719
Fujii, Rika P353
Fujimoto, Junya P470
Fuller, Steven P167
Funari, Vincent O48
Fung, Eileen P199
Fung, Leslie P111
Furebring, Christina P656, P683
Furqan, Fateeha P73
Futreal, Phillip Andrew P233
Fyrsta, Michael P225

Author G Abstract Number

Gaber, Ahmed P644
Gabrilovich, Dmitry O2
Gadi, Vijayakrishna P64
Gainor, Justin O21
Gajewski, Thomas P124, P412, P558, P584, P704
Galand, Claire P659
Galetto, Roman P214
Galezowski, Michal P204
Galioto, Michele P643
Gallant, Carey P624
Gallatin, Michael P410
Galli, Veronica P61
Galligan, Carole P362
Galluzzi, Lorenzo P170, P473, P504, P623
Galsky, Matthew P149
Galtlin, Wayne O37
Gameiro, Sofia P660
Gameiro, Steven P682
Gamelin, Erick P25
Gamez-Guerrero, Maria P608
Gan, Lu P53
Gandhi, Anita P475
Ganguli, Arunima P681
Ganju, Vinod O24, P22

AUTHOR INDEX

Gao, Jianjun O5, P536
Gao, Quanli P286, P395
García Carcedo, Ines P55
Garcia, Bradley P459
Garcia, Nicolas O15
Garcia, Samantha P161
Garcia Campelo, Maria Rosario P715
Garcia-Corbacho, Javier P87, P139, P341
Garcia-Manero, Guillermo P565
Gardner, Kellie P548
Gardner, Mark P75, P76, P549, P707
Gargano, Maria P566
Gargano, Michele P708
Gargosky, Sharron P717
Garman, Bradley P155
Garnero, Lucile P666
Garon, Edward O27, P297
Garralda, Elena O23, P669
Garrido-Laguna, Ignacio P289
Garrus, Jennifer O25
Gartner, Jared P543
Gartung, Allison P209
Garvin, Denise P661
Gasmi, Billel P521
Gaspar, Miguel O44
Gassama, Awa P693
Gates, Matthew P638
Gates, Samantha P49
Gaudreau, Pierre-Olivier O5, P354, P572
Gaule, Patricia P88, P295
Gaur, Pankaj P356, P357, P358
Gavai, Ashvinikumar P524
Gay, Carl P452
Gaynor, Richard O7, P49, P169, P307, P314
Ge, Tingting P174
Gedrich, Richard P510
Gee, Adrian O17
Gee, Kayla P245
Gelber, Richard P374
Genden, Eric P149
Geng, Wanping P291
George, Daniel P71, P146, P503
George, Joshy P445
George, Saby O45, P54, P350, P355
George, Tad P132
George, Thomas P331
Gerding, Kelly P71
Geretti, Elena P215
Gerken, Claudia O17
Gershenwald, Jeffrey O5, P329, P572
Gettinger, Scott P116, P147, P319
Geukens, Nick P604
Geulen, Lars P435
Geva, Ravit P651
Geyer, Julia P193
Geynisman, Daniel P396
Ghanbari, Hossein P167
Gharavi, Robert P341
Ghasemi, Farhad P682
Ghobadi, Armin P212
Ghosh, Shomir P524
Ghosh, Srimoyee P325, P365, P677
Giambalvo, Raffaella P631
Giamo, Vincent P75, P77, P549
Giannakis, Marios P54
Gibas, Agnieszka P515
Gibbons, Don P233, P354, P452, P470, P565
Gibney, Geoffrey P313, P548
Gibson, Laura P354
Gieffers, Christian O29
Giehl, Esther P603
Giese, Rachel P347
Gieseke, Friederike P402, P621, P647
Gigoux, Mathieu P156
Gilbert, Madaline P216
Gilbert, Mark P265
Gilden, Julia P661
Giles, Amber P265
Gilham, David P213, P218, P220, P221, P231, P232, P274, P275, P626

AUTHOR INDEX

Gilkeson, Robert.....P426
Gillies, Stephen P10
Gillings, Mireille P346
Gillison, Maura.....P332
Gimotty, Phyllis P303
Giobbie-Hurder, Anita.....P566, P567
Giordano, Sharon P644
Giraldo, Nicolas P128
Giranda, Vincent P553
Girgis, Natasha P185
Giri, Sanjeev P529
Gitau, Mark O50
Gittelman, Rachel.....P86
Giurleo, Jason.....P438
Glaser, Bryan.....P485
Gleeson, Michelle.....P692
Glenn, Sean P75, P76, P77, P146, P503, P549, P596, P707
Glick, Gary P524
Glickman, Laura.....P235, P351
Gliddon, Dan P631
Glisson, Bonnie.....P157, P470, P699, P710
Glitza, Isabella P505, P572
Gluza, Karolina P515
Gnad-Vogt, Ulrike.....P337, P711
Gnjatic, Sacha.....P149, P150, P330
Go, William.....P212
Godbersen, Claire.....P8
Gogna, Rajan P200, P201, P236
Golan, Talia O25
Golas, Aniela P204
Gold, David.....P107
Gold, Kathryn O50, P701
Goldberg, Sarah P84
Goldberg, Stacie O24, P305
Goldhirsch, Aron P374
Goldman, Aaron P718
Goldman, Richard.....P343
Goldstein, Joel.....P510
Goldstein, Matthew..... O7, P49, P169, P307, P314
Golinelli, Giulia..... P237
Gombos, Randi P659
Gomez-Manzano, Candelaria P370, P605
Gomez-Martin, Carlos P475
Gonda, Kenji P118
Gong, Zimu P538
Gonzalez, Ana P189
Gonzalo, Maria P629
Goodman, Aaron P58
Goodman, Emma..... P631
Goodwin, Neal P443, P444
Goodwin, Rachel..... O45
Goodwin, Ria P681
Gopalakrishnan, Vancheswaran O5, P194, P505, P572
Gopichand, M. P714
Gopinath, Kodaganur..... P718
Gorden, Keith..... P527
Gordon, Judi P87
Gordon, Michael..... O49, P174, P307, P403, P409
Gordy, James P158
Gori, Jennifer P238, P271
Gostissa, Monica..... P455
Gottardo, Raphael P269
Gottimukkala, Rajesh..... P571
Gottschalk, Stephen O17, P277
Gouble, Agnes..... P214
Gough, Michael..... P410, P455, P471
Gouttefangeas, Cecile..... O8, P711
Goverse, Gera..... P435
Govindan, Ramaswamy O7, P49, P314
Gowda, Nagaraj P694
Gowda, Nagesh..... P694
Gowda, Raghavendra P381
Gradinaru, Cristian..... P631
Graff, Jeremy P708
Graham, Garrett P561
Graham, Laura P491
Grahn, Amy..... P396

AUTHOR INDEX

Grailer, Jamison.....P661
Grand, Celine.....P375
Grandclaudon, Maximilien.....P375
Grandhi, Miral.....P339
Grassi, Paolo.....P110
Grasso, Catherine.....O39, P557
Grattoni, Alessandro.....P152
Graves, Alexander.....P239
Graves, Jonathan.....P524
Gray, Diana.....P225
Gray, Melissa Anne.....P676
Grazi, Gian Luca.....P640
Green, Benjamin.....P128
Green, Roland.....P485
Greenbaum, Benjamin.....P182
Greenbaum, Jason.....P148
Greenberg, Norman.....O3, P1
Greenberg, Philip.....O15
Greengard, Emily.....O20
Greenwood, Bernadette.....P609
GREGOIRE, Anne.....P298
Gregoire, Vincent.....P332
Gregory, Gareth.....P315
Greshock, Joel.....O7, P49
Gribbin, Matthew.....P699
Griesinger, Andrea.....P497
Griffiths, Elizabeth.....O42
Grignani, Giovanni.....O4
Grilley, Bambi.....O17
Grisendi, Giulia.....P237
Grivas, Petros.....P64
Grob, Jean-Jacques.....P329
Groh, Eric.....P543
Gromeier, Matthias.....P612
Grossenbacher, Steven.....P508
Grosser, Rachel.....P434
Grosso, Joseph.....P718
Grosu, Daniel.....P58
Grover, Shilpa.....P566
Grudzinski, Joseph.....P464
Grunwitz, Christian.....P402, P621, P647
Grycuk, Karolina.....P204
Gu, Chunyan.....P54, P205
Gu, Xuesong.....P92
Guan, Siyu.....P477
Gucalp, Ayca.....P651
Gudgeon, Chelsea.....P406
Gueorguieva, Ivelina.....O30
Guerlavais, Vincent.....P450
Guerriero, Jennifer.....P719
Guest, Ryan.....P222, P223, P243
Gugenberger, Romana.....P2
Guglietta, Silvia.....P68
Guha, Prajna.....P318, P456
Guiducci, Cristiana.....P25
Gulcher, Jeffrey.....P29, P581
Gulley, James.....P61
Gundala, Chennakrishnareddy.....P529, P694
Gunter, Kurt.....P240
Guo, Ge.....P190
Guo, Haidan.....O47, P589
Guo, Lingling.....P544
Guo, Matthew.....P391, P392, P393
Guo, Ming.....P157
Guo, Taylor.....P653, P671
Guo, Wei.....P326
Guo, Zong Sheng.....P603
Gupta, Aayush.....P349
Gupta, Abha.....P225
Gupta, Aditi.....P347
Gupta, Rajan.....P71
Gupta, Richa.....P84
Gupta, Seema.....P356, P357, P358
Gupta, Shilpa.....P295
Gupta, Snigdha.....P368
Gupta, Sudeep.....P714
Gupta, Swati.....P138
Gupta, Vikas.....O48
Gupte-Singh, Komal.....P380
Gurel, Bora.....P287
Gustin, jason.....P633
Gutierrez, Dario.....P553
Gutierrez, Leah.....P420

AUTHOR INDEX

Gutzmer, Ralf P337
Guzman, Wilson P386, P407
Gwee, Jia P271

Author H Abstract Number

Haake, Markus O41
Haanen, John P389
Haas, Mike P474
Haaser, Nicole P1
Haber, Lauric P438
Hackett, Amy P591
Hackett, Maria P185
Hacohen, Nir O5
Haddad, Robert P333
Hadley, Melissa P203
Hagen, Jacob P75, P549, P707
Hagerbrand, Karin P683
Hägerbrand, Karin P195
Hagiya, Ashley P592
Hagner, Patrick P475
Hailemichael, Yared P424
Haimes, Josh P50
Hakgor, Sevan P225
Hakimi, Kevin P547
Halaban, Ruth P108, P721
Hale, Diane P159
Haley, Jeremy P381
Hall, Clinton P631
Hall, Emma P287
Hall, MacLean P224, P241
Halle, Joern-Peter P383, P384
Halmos, Balazs O27
Halwani, Ahmad P327
Hamada, Kazuyuki P51
Hamid, Omid O19, P87, P291, P307
Hamilton, Erika O21, P139, P341
Hamilton, Michael P685
Hammer, Bonnie P485
Hammerbacher, Jeffrey O40, P149
Hammerich, Linda P205, P330
Hammerman, Peter O35
Hammond, Russell P510
Hammond, Scott P699
Han, Guangchun O5
Han, Lu P286, P395
Han, Minhua P684
Hanafi, Laila-Aicha P663
Hance, Kenneth P384
Hancock, Wayne P494
Handy, John P429
Hank, Jacquelyn P10, P419, P459, P485
Hanks, Brent P545
Hann, Christine P12
Hanna, Diana P622
Hannah, Alison O4
Hansbauer, Eva-Maria P375
Hansen, Aaron O23, P225, P698
Hanson, Amanda P52
Hao, Minghong P598
Haond, Christophe P492
Haq, Rizwan P566
Harbell, Michael P1
Harbell, Mike O3
Hardaway, John P318, P456
Harding, Fiona P72
Harding, James O49
Harding, Thomas P348
Hardt, Olaf P45
Hare, Jennifer P388
Harford, Joe P457
Hargreaves, Adam P274
Hariri, Robert P247
Harrington, Kevin P333, P597
Harris, Angela P572
Harris, David P550
Harris, Jaryse P303
Harris, Jason P151
Harrison, Ben P527, P708
Harrison, Rane P618
Harshman, Lauren P298

AUTHOR INDEX

Harshyne, Larry P85, P198, P328, P342, P343, P489
Hart, Courtney P52
Hartberg, Reidun P256
Harting, Jorien P293
Hartley, Genevieve P427
Hartmann, Karen O32
Hartnett, Jim P661
Harui, Airi P721
Harvey, Christopher P52, P455
Harvey, R. Donald P506, P507
Haryutyunan, Karine O14
Hasan, Aisha O18
Haserlat, Sara P530
Hassan, Ahmed P430, P431
Hassan, Islam P430, P431, P432
Hassan, Raffit P360
Hassanzadeh-Kiabi, Nargess P411
Hassel, Jessica P103
Hasser, Nicole O3
Hatogai, Ken P124
Hatten, Kyle P302
Hattori, Masahira P574
Hauke, Ralph O24
Haura, Eric P264
Hauschild, Axel P329
Hauther, Christine P114
Havel, Jonathan P570
Havenith, Karin P11
Hawkins, Julie P681
Hawkins, Robert P222, P223, P243
Haydock, Mark P185
Haydon, Andrew O28, P717
Haydu, Lauren O5, P505
Hayes, Melissa P154
Hayes, Sandy P520
Haymaker, Cara O4, P233, P268, P424, P542, P564, P710
Hazama, Shoichi P334
He, AIwu P105
He, Kai P79, P385
He, Li-Zhen P510
He, Philip P704
He, Shuyang P247
He, Yi P403
Healy, Jane O25, O26, P315
Heath, Elisabeth P171
Heath, James P721
Heather, Heidi P474
Hebert, Andrew P621
Hebert, Courtney P40
Hebert, Valerie P663
Hecht, J. Randolph O21
Hedvat, Michael P664
Heeren, Marijne P693
Heery, Christopher P339
Heesch, Sandra O8
Heffernan, Timothy P572
Hegde, Priti O1, P19, P60, P101
Hegde, Shweta P422
Heguy, Adriana P468
Heidenreich, Regina P337, P711
Heimberger, Amy P446
Heinonen, Karl O29
Heinrich, Bianca P44
Heinze, Clinton P459
Heinzerling, Lucie P337
Heinzmann, Daniel P41
Heist, Rebecca O45
Helke, Simone P362
Heller, Kevin P678
Heller, Scott P238, P271
Hellmann, Matthew O6, O7, O45, O47, O49
Helm, Klaus P381
Helmink, Beth O5, P194, P505, P572
Helmlinger, Gabriel P359, P563, P665
Hemmati, Golzar P608
Henderson, Dan P279
Hendlisz, Alain P255
Hendrickx, Wouter P468, P587
Henick, Brian P116, P133, P147

AUTHOR INDEX

Hennek, Stephanie P39, P654
Hennessy, Marlene P364
Henning, Steven P153
Henry, Verlene P605
Hensing, Thomas O27
Henson, Michael O43
Hepburne-Scott, Henry P32
Hepp, Julia P408
Heras-Murillo, Ignacio P103
Herbert, Garth P159
Herbst, Jörg P408
Herbst, Ronald P632
Herbst, Roy P102, P116, P133, P147
Herlyn, Meenhard P639
Herman, James P556
Herman, Robert P417
Hermant, Annelise P667
Hernandez, Reinier P464
Hernandez-Aya, Leonel O45
Hernandez-Hoyos, Gabriela P7
Hernendez, Maria P576
Herner, Alexander P349
Herrera, Alex P327
Herrmann, Amanda P539
Herz, Thomas P429, P436
Heslop, Helen O17, P240
Hess, Bruce P298
Heuchel, Rainer O38
Hew, Kinjal P72
Hewes, Becker P215, P226, P272
Heymach, John P233, P452, P470, P490
Hickeron, Annelies P159
Hickerson, Annelies P159
Hickey, Carlos P438
Hickey, John P160, P245
Hicking, Christine P291
Hicklin, Daniel P404
Hicks, Kristin P660
Hiebsch, Ronald P512
Higgins, Jack P9
Higgins, Wayne P276
Higgs, Brandon P14, P699
Higgs, Emily P584
Hilf, Norbert O8
Hill, Craig P205
Hill, Oliver O29
Hill, Wendy P174
Hille, Darcy P31
Hilton, Traci P162
Hinerfeld, Douglas P428, P429
Hingorani, Dina P458
Hinrichs, Christian O34
Hinterwimmer, Lisa P486, P488
Hinton, Marlene P553
Hippely, Sarah O3
Hirano, Naoto P225
Hirasawa, Yuya P51
Hirschhorn-Cymerman, Daniel P521
Hlavaty, Kelan P219
Ho, Ching-Ping P525
Ho, Jeremy P152
Ho, Thai P346
Ho, William P484
Hoch, Ute O4, P424
Hochster, Howard P339
Hodge, James P353
Hodi, F. Stephen P108, P309, P566
Hoe, Nicholas P487
Hoefges, Anna P459, P485
Hoffgaard, Franziska O8
Hoffmann, Chantal P148
Hofmeister, Hans P251, P252
Hogg, David P225
Hohl, Raymond P381
Hoimes, Chris P423
Holl, Eda P612
Hollebecque, Antoine P475, P662
Hollen, Heather P629
Hollevoet, Kevin P604
Hollmann, Tracvis P521
Holmes, Jarrod P159

AUTHOR INDEX

Holmkvist, Petra....P602
Holström, Morten....P478
Holt, John....P149
Holt, Robert....P115, P715
Holtzhausen, Alisha....P545
Honda, Kenya....P574
Hong, Christina....P371
Hong, David....O19, P299, P361, P385, P427, P619
Hoofd, Chaterine....P666
Hoogland, Aasha....P630
Hooijberg, Erik....P293
Hooper, D. Craig....P161, P198, P342, P343
Hooper, Ellen....P52
Hopkins, Alex....P86
Hopson, Kristen....P295
Horak, Christine....P108
Horn, Leora....P385
Horton, Brendan....P704
Horvai, Andrew....P117
Hossain, Ausmeema....P225
Hotson, Andrew....P54, P205
Hotson, Drew....O45
Hotz, Christian....P621
Hou, Wanqiu....P26
Houee, Marine....O44
Houghton, Sean....P521
Houke, Haley....P277
Houot, Roch....P327
Housseau, Franck....P589
Houthuys, Erica....P666, P667
Howard, Melissa....P575
Howard, Rachel....P719
Howell, Alan....O20
Howng, Bruce....P87
Hoyt, Clifford....O6, P18, P433, P638
Hsieh, Edward....P532
Hsu, David....P545
Hsu, Frank....P327
Hsu, Karl....P621
Hsu, Miles....P625
Hsu, Ruby....P17
Hu, Hong-Ming....P162
Hu, Jian....P427
Hu, Leijun....P662
Hu, Peirong....P270
Hu, Qiang....P595
Hu, Xiao....P358
Hu, Yi-Zhen....P3
Hua, Fei....P411
Huang, Chiun-Sheng....P163
Huang, Elaine....P279
Huang, Emily....P202
Huang, Fei....P401
Huang, Kuan-Chun....P598
Huang, Lan....P495
Huang, Ruea-Yea....P188
Huang, Shaoyan....P190
Huang, Yuting....P49
Hubbard, Antony....P703
Huber, Christoph....O8
Huber, Veronica....P110
Huberty, Fanny....P220, P626
Hudgens, Courtney....O5, P539
Huels, Vanessa....P87
Hughes, Brett....O45
Hu-Lieskovan, Siwen....O7, O20, O39, P307, P557
Hulot, Sandrine....P185
Humeau, Laurent....P155
Hung, Annie....P297
Hung, Jung-Tung....P163
Hung, Tsai-Hsien....P163
Hunt, Donald....P178
Hunt, Gayle....P178
Hunt, John....P524, P525
Hurban, Patrick....P120, P122, P575
Hurd, Mark....P268
Hurov, Kristen....P398
Hurst, Katie....O12
Hurwitz, Albert....P178
Hurwitz, Arthur....P178

AUTHOR INDEX

Hurwitz, Michael O4
Husain, Marium P79
Huseni, Mahrukh P19
Hutz, Janna P598
Hwang, Kevin P38
Hwang, Shelley P612
Hwu, Patrick O5, P505, P555, P565, P572, P710
Hwu, Wen-Jen P505, P572, P710
Hyland, Fiona P27, P81, P571

Author I Abstract Number

Iaccucci, Ernesto O4
Iberg, Aimee P9
Ibrahim, Mohamed P551
Ibrahim, Nageatte P329
Idan, Amanda P320, P321, P322, P673
Idorn, Manja O8
Idris, Tagwa P431
Igarashi, Yuka P183
Iida, Michihisa P334
Iizumi, Susumu P183
Illingworth, Sam P479
Im, Ellie P326
Imatani, James O31
Imperiale, Michael O4
Iñarrairaegui Bastarrica, Mercedes P711
Infante, Jeffrey P297, P409
Ingersoll, Christy P598
Ingram, Piers P477
Inman, Shannon P240
Innamarato, Patrick P244
Inniss, Mara P238, P271
Inokuchi, Go P462
Inokuma, Margaret P111
Irie, Hanna P149
Irshad, Sheeba P55
Irvine, Darrell P649
Ishida, Hiroo P51
Ishida, Wataru P437
Ishizuka, Andrew P164, P172
Ishizuka, Jeffrey P566
Isser, Ariel P245, P570
Isufi, Iris P327
Italiano, Antoine P662
Ito, Satoru P300
Ivey, Richard P269
Iwai, Toshiki P472
Iwamoto, Noriko P119
Iyengar, Malini P276

Author J Abstract Number

Jabbour, Salma P319
Jablonski, Sandra P561
Jaccard, Arnaud P240
Jackson, Jeffrey P202
Jackson, Jennifer P71
Jackson, Justin P550
Jackson, Katherine P498
Jacob, Robin P549
Jacobs, Liesl P604
Jacobsen, Eric P240
Jacobsen, Kivin P56, P129
Jacobson, Caron P212
Jacobson, Scott P202
Jacobson, Steve P61
Jacques-Hespel, Céline P220, P274, P626
Jaeger, Elke P248
Jaen, Juan P668
Jafari, Omid P713
Jaffe, Kim P520
Jäger, Elke P251, P252
Jain, Angela P396
Jain, Priya P152
Jain, Sharad P392
Jaishankar, Dinesh P57
Jaiswal, Ashvin P546
Jajja, Mohammad Raheel P266
Jalali, Shahrzad P648
James, Michael P624
Janardhanan, Sathya P678
Jang, Sekwon O4, P13

AUTHOR INDEX

Jang, Su Chul P618
Janiga, Anita P204
Janku, Filip P651
Janssen, Louise P424
Janssen, Robert P25
Janssen, Wout P517
Janssens, Holden P94, P95
Jaquish, Abigail P464
Jaroch, David P456
Jaschinski, Frank O9, P486, P488
Jasinski, Daniel P217
Javaid, Sarah P553
Javle, Milind P268
Jayaprakash, Priyamvada P546
Jayaprakash, Vijayvel P332, P333
Jayaraman, Lata P572
Jeff, Grein P532
Jeffery, Erin P178
Jeffrey, Jenna P35
Jenkins, David P326, P365, P677, P696
Jenkins, Molly P383, P384
Jennings, Joseph P538
Jenq, Robert P194, P505, P572
Jensen, Ash O50
Jensen, Shawn P18, P59, P429, P440, P578
Jensen, Taylor P58
Jensen, Vanessa P572
Jesernig, Brenda P281
Jhunjhunwala, Suchit O1
Jhunjhunwala, Sushit P19
Ji, Hong P408
Ji, Hongkai O47
Ji, Zhicheng O47
Jia, Shidong P28
Jia, William P600, P606, P610
Jiang, Hong P370, P605
Jiang, Qun P360
Jiang, Rongrong P598
Jiang, Shuwei O3
Jiang, Wenqing P671
Jiang, Xian P483
Jiang, Yizhou P212
Jiang, Yuqiu P60, P101
Jiang, Zhi-Dong P194
Jianjun, Zhang P233
Jilaveanu, Lucia P84
Jim, Heather P630
Jimeno, Antonio O25, P295, O51
Jin, Feng P340
Jin, Lixia P320, P321, P322, P323, P673
Jin, Ping P176
Jizzini, Mazen P540
Jo, Jasmin P493
Joe, Andrew P31
Joerger, Autumn O16, P224, P241
Johansen, Jennifer P355
Johansen, Lisa P295
Johansson, Maria P683
Johnson, Daniel P484, P564, P644, P710
Johnson, David P646
Johnson, Douglas P108, P691
Johnson, Erin P420
Johnson, Faye P157
Johnson, Jennifer P85, P186, P328, P342, P343, P489
Johnson, Laura P50
Johnson, Lisa P362
Johnson, Melissa O27, P174
Johnson, Sherra P202
Johnson, Syd P304, P305, P366
Johnson, Tyler P216
Jonas, Adria P527, P708
Jones, Daniel P631
Jones, Douglas P227
Jones, Frank P310, P713
Jones, Greg P141
Jones, James P87
Jones, Jeff P520
Jones, Jennifer P61

AUTHOR INDEX

Jones, Kristi P262
Jones, W P205
Jones, Wendell P62
Jordan, Kimberly P318
Jordanova, Ekaterina P693
Joseph, Ingrid P417
Joshi, Bishnu P178, P189
Joshi, Shilvi P635
Joshua, Anthony O24, P306, P669
Jotte, Robert P385
Joyce-Shaikh, Barbara P532
Juglair, Laurent P408
juillerat, Alexandre P283
Julian, Claire P476
Jun, H. Toni P672
Juncker-Jensen, Anna P487
Junghans, Richard P318
Jure-Kunkel, Maria P14, P699
Jurisica, Igor P91

Author K Abstract Number

Kabinnavar, Fairooz P47
Kaczanowska, Sabrina P719
Kadara, Humam P490
Kadel, Edward P19
Kagey, Mike P474
Kai, Xin P530
Kaiser, Andrew P229
Kaiser, Judith P298
Kakrecha, Bijal P382
Kalaitzidis, Demetrios P279
Kalathil, Aravind P33
Kalbasi, Anusha P547
Kaldjian, Eric P132
Kalinka-Warzocha, Ewa O4
Kallert, Sandra P488
Kalra, Ashish P550
Kalra, Mamta O17, P246
Kamat, Asha P63, P81
Kamiya Matsuoka, Carlos P432
Kamiyama, Toshiya P580
Kanchev, Ivan P429
Kandimalla, Ekambar P344
Kane, Lawrence P397, P674
Kane, Marissa P497
Kane, Michael P339
Kanekal, Sarath P377
Kanekiyo, Sinsuke P334
Kanetsky, Peter P108
Kang, Hye Jin P240
Kang, Hyunseok P302
Kang, Lin P247
Kang, Richard P344
Kang, Yoon-Koo P636
Kang, Yubin P545
Kanne, David P351
Kapil, Ansh P21
Kaplan-Lezco, Paula P47
Kapoun, Ann P289
Kapp, Kerstin P399
Karakousis, Giorgos O40
Karakunnel, Joyson P320, P321, P322, P323, P673
Karam, Sana P448, P449
Karbach, Julia P248, P251, P252
Kariko, Katalin P621
Karki, Binisha P424
Karlsson, Mikael O38
Karnik, Sushant P279
Karpinets, Tatiana P233
Karr, Robert P512
Karras, Jenna O40
Karyampudi, Lavakumar O22
Karzai, Fatima P61
Kashanchi, Fatah P61
Kashyap, Abhishek P486
Kashyap, Seema P121
Kasichayanula, Sreeneeranj P690
Kasiewicz, Melissa P363
Kassner, Paul P202, P484
Kastelein, Robert P532
Kasturi, Vijay P291
Kasumova, Gyulnara P16
Katabathula, Ramachandra P135

AUTHOR INDEX

Kataoka, Shunsuke P674
Kato, Daiki P249
Kato, Shumei P58, P76, P707
Katopodi, Tania P222, P223
Katz, Steven P318, P456
Kauder, Steven P340
Kaufman, Howard P291
Kaufmann, Daniel P91
Kaufmann, Johanna P365, P696
Kavanaugh, W. Michael P87
Kawahara, Mamoru P183
Kawakami, Yutaka P249, P560, P574
Kawamata, Futoshi P580
Kays, Sarah-Katharina P337
Kayyal, Talal P336
Kazakoff, Stephen P580
Kean, Rhonda P161
Keen, Nicholas P398
Keisari, Yona P453
Keler, Tibor P403, P510
Keller, Carter P646
Kelley, Robin Kate P475
Kelly, Kimberly P58
Kelly, Marcus P438
Kelly, Ronan P12
Kelly, William P548
Kelson, Itzhak P453
Kemmer-Brueck, Alexandra O8
Kendra, Kari P79
Kennealey, Gerard P336
Kennedy, Eugene P142, P331, P706
Kennedy, Jacob P269
Kennedy, Laura P64
Kennedy, Timothy P339
Kennedy, Tobin P172
Kennedy, William P144
Kenter, Gemma P693
Kepley, Julia P61
Keren, Leeat P20
Kesari, Santosh P609
Keung, Emily O5
Keyt, Bruce P405
Khalil, Maya P595
Khan, Abdul Wadud P572
Khan, Amir P506, P507
Khan, Md P505
Khattak, Adnan O28
Khattri, Arun P48, P65
Khemka, Vivek P289
Khiabany, Atousa P55
Khleif, Samir P356, P357, P358, P567
Khojasteh, Mehrnoush P703
Khong, Hiep P424
Khorasani, Hooman P149
Khorrami, Mohammadhadi P104, P292
Khuat, Lam P508
Khunger, Arjun P126, P127
Khushalani, Nikhil P263, P346
Kidd, Michael P224, P244
Kiecker, Felix P337
Kiesel, Katharina O8
Kiessling, Rolf P695
Kikuchi, Masahiro P462
Kilinc, Mehmet P609
Kilinc, Okyay P617
Killian, Marisela P465
Kim, Andrea P202
Kim, Dae-Shik P598
Kim, Danny P124
Kim, Debora P370
Kim, Dongkyoon O3, P1
Kim, Eun-Hae P71
Kim, Hyo Jin P648
Kim, HyunGoo P569
Kim, Jennifer P203
Kim, Jessica P199
Kim, JIN SEOK P240
Kim, Jong Bin P569
Kim, Jong-kyu P569
Kim, Ju Young P65, P127
Kim, Ju-hyun P74
Kim, Kendrick P608

AUTHOR INDEX

Kim, Kyung P445
Kim, Kyu-Pyo P139, P341
Kim, Leesun O1
Kim, Lisa P58
Kim, Michelle P16
Kim, Namyong P23, P24
Kim, Richard P304
Kim, Sang P565
Kim, Sang-Soo P457
Kim, Sang-We P308
Kim, Sojung P262
Kim, Soo-Jung P74
Kim, Ted P502
Kim, Won Seog P240
Kim, Yong-Man P74
Kim, Yoon P411
Kim, Yoon-Keun P569
Kim, Young Uk P233
King, Matthew P388
King, Tom P311
Kirillova, Natallia P243
Kirksey, Yolanda P364
Kirkwood, John O11, O22, O36, P108, P176, P329, P556, P559, P709
Kirouac, Daniel P411
Kirschmeier, Paul O35, P166
Kirshner, Jessica P438
Kis, Bela P327
Kiselicki, Dragan P248, P251, P252
Kissick, Haydn P506, P507
Kistler, Mira P310, P713
Kitano, Shigehisa P300
Kitanovic, Ana P524
Kivimae, Saul P364
Kivimäe, Saul P378
Klar, Richard O9, P486, P488
Klaski, Rachel P272
Kleffel, Sonja P404
Klein, Christian P413
Klein, Oliver P324
Klema, Elaine P48
Kline, Justin P451
Klinghoffer, Ariel P476
Klinkhardt, Ute P337
Kloch Bendtsen, Simone P175
Kluger, Harriet O22, P84, P131, P138
Kluger, Yuval P133
Knight, Robert P318
Knochelmann, Hannah P250, P273, P284
Knoedler, Alice P548
Knops, Alexander P489
Knox, Clayton P410
Knudsen, Anne P631
Knudson, Karin P660
ko, Taeyeong P568
Kochanny, Sara P48, P65
Kodumudi, Krithika P241, P244
Kodysh, Julia P149
Koenig, Anna-Katharina P103
Koenigsrainer, Alfred P711
Koers, Alexander O44, P631
Koguchi, Yoshinobu P18
Kohle, Ravindra P142
Kohler, Jessica P169
Kohler, Victoria P49
Kokate, Rutika P396
Kokolus, Kathleen P381
Kolbe, Carolin P229
Kolber-Simonds, Donna P598
Kolhe, Ravindra P706
Kolodziej, Starsha P624
Kolonias, Despina P136
Komanduri, Krishna P136
Kondoh, Osamu P472
Koneru, Mythili P662
Kong, Eric P71
Kono, Koji P118
Konopleva, Marina O14
Konstorum, Anna P188
Koomen, John P264
Koon, Henry P143
Kopit, Justin P332, P333

AUTHOR INDEX

Kopp, Katharina.....P177
Koriazova, Lilia P417
Korkut, Anil.....P555
Korman, Alan.....P684, P685
Korn, Rene.....P436
Korn, Ronald.....O49
Kornacki, Deanna P669
Koropatnick, James P682
Korytowsky, Beata P137, P692
Kosaka, Yoko P401
Kosco-Vilbois, Marie P650
Kosinsky, Yuri P359, P563, P665
Kosoff, Rachelle.....P520
Koster, Bas.....P293
Kothambawala, Tasnim.....P405
Koti, Madhuri P460
Kotrotsou, Aikaterini.....P430, P431, P432
Koubek, Emily.....P381
Kouki, Yasunari.....P334
Kouro, Taku P183
Kovacina, Kristina.....P409
Kowanetz, Marcin O1, P19, P60, P66, P101
Koya, Richard P188
Koyama, Shohei.....O35, P688
Kozbial, Andrew P260
Kozlowska, Anna P259
Kradjian, Giorgio P384
Kraemer, Lauren.....P185
kraiem, Manel P4
Kraitcheva, Annie P63
Kramer, Gwen P471
Krauss, Juergen P337
Kravets, Sasha P109
Kraynyak, Kimberly P171, P186
Kreahling, Jenny P67, P439
Krebs, Matthew.....P715
Kreiter, Sebastian.....O8, P402, P621, P647
Kremer, Sarah P547
Kremer, Veronika P522
Krenciute, Giedre..... P277
Krepler, Clemens P717
Krieg, Carsten P68
Krieg, Jennifer..... P637
Krigsfeld, Gabriel P107
Krijgsman, Oscar..... O5
Kristensson, Julia P398
Kroemer, Guido P504
Kroep, Judith..... O8
Krogsgaard, Michelle P675
Krueger, Joseph P90
Kruglyak, Kristina P590
Krupa, Rachel..... P69
Kublin, Jessica P398
Kubota, Yutaro..... P51
Kucuk, Omer P298
Kudchadkar, Ragini P506, P507
Kuhn, Andreas P621
Kuijper, Joe P406
Kujawa, Maciej P515
Kulkarni, Abhishek P238, P271
Kulkarni, Amit P573
Kumanogoh, Atsushi..... P688
Kumar, Akhil P714
Kumar, Amit..... O2
Kumar, Ayan P489
Kumar, Rakesh P409, P699
Kumar, Sujatha P365
Kummar, Shivaani..... O45, P54, P316
Kundu, Samrat P354
Kuo, James P308
Kuo, Judy..... P487
Kuo, Peiwen P418
Kuppen, Peter P587
Kurland, Brenda P649
Kurman, Michael P346
Kuroda, Sakiko P300
Kürten, Cornelius..... P70
Kurzrock, Razelle..... P58, P76, P707
Kuseryk, Skye P520
Kutok, Jeffery..... P716
Kutscher, Sarah..... P711

AUTHOR INDEX

Kuttruff-Coqui, Sabrina O8
Kwant, Kathryn P608
Kwei, Long O45, P54
Kwek, Serena P687
Kwon, Deukwoo P136
Kwon, Hyungju P569

Author L Abstract Number

La Motte-Mohs, Ross P305
Labiano, Tania P466
Labit, Delphine P663
Labriola, Matthew P71, P146, P503, P596
Lacey, Sean P52
Lacroix, Andreanne P298
Lacuoture, Mario P521
Lafyatis, Robert P481, P583
Lager, Joanne P621
Lahdenranta, Johanna P398
Lahm, Armin P184
Lai, Zhongwu P594
Laing, Christian P126
Lajoie, Jason P407
Lakeman, Kelsey P216
Lakhani, Nehal O24, O26, P306, P335, P340, P669
Lakins, Matthew P631
Lakshmaiah, KC P714
Lala, Mallika O25
Lam, Hubert P166
Lamb, April P49
Lambert, Stacie P72, P690
Lambertini, Chiara O23
Lamble, Adam P401
Lambolez, Florence P666
Lan, Yan P383, P384
Lanchantin, Matthew P166
Lander, Elliot P609
Landers, Mark P69
Lang, Frederick P370, P605
Lang, Joshua P385
Langan, Russell P339
Lange, Zach P187
Langer, Corey P319
Langermann, Sol P678
Langley, Meghan P271
Langone, Francesca P184
Langsdorf, Chris P3
Lani, Rachid P398
Lanista, Janice P215
Lanka, Arunasree P418
Lapointe, Rejean P91
Laport, Ginna O45, P54, P205
Larkin, James O4
Larson, Christopher P372
Larson, Ryan P278
Larson, Timothy P385
Lassen, Ulrik O8
Lattime, Edmund P339
Lattouf, Jean-Baptiste P91
Latz, Eicke P524
Lau, Kah Weng P140
Laubli, Heinz O37
Läubli, Heinz P676
LaVallee, Theresa P572
Law, Che-Leung P608
Law, Deborah P52
Law, Meng P430, P431
Law, Vincent P263
Lawlor, Rita Teresa P640
Lawrence, Donald P16, P92
Lawrence, Kiley O12
Lawson, David P291, P506, P507
Lawson, Mark P718
Lazar, Alexander O5, P539
Le Brocq, Michelle P222, P223, P243
Le Poole, Caroline P57
Le Poole, I Caroline P153
Le, Catherine P508
Le, Michael P225
Le, Quynh Thu P332
Le, William O49
Le, Xiuning P490

AUTHOR INDEX

Leach, Craig P494
Leal, Ticiana P385
Lebowitz, Michael P167
LeBrun, Aurore P161
Lecagoonporn, Srisuda P710
Leddy, Lee O12
Lederer, James P502
LeDuc, David P630
Lee, Aileen P591
Lee, Allison P635
Lee, Boon Heng O1
Lee, Catherine P209
Lee, Chee Khoon P320, P321, P322, P673
Lee, Daewoo P168
Lee, Daniel P240
Lee, Eileen P72
Lee, Erica P600, P606, P610
Lee, Gloria P346
Lee, HongBum P502
Lee, Howard P367
Lee, Hun Ju P240
Lee, J Jack P157
Lee, Jacqueline P500
Lee, James O25, P139, P341
Lee, Jeffrey O5
Lee, Jessica P171
Lee, Joey P185
Lee, John O50, P310, P353, P660, P712, P713
Lee, Josephine P129
Lee, Jun Woo P569
Lee, Lucy P716
Lee, Peter P26, P43
Lee, Sangyun P570
Lee, Seongwon P73
Lee, Shin Wha P74
Lee, Sung-Hyung P411
Lee, Sungjong P168
Lee, Sunyoung P73
Lee, Susan P320, P321, P322, P323, P673, P697
Lee, Suzanna P76
Lee, Sylvia P281
Lee, Won-Chul P490
Lee, Won-Hee P569
Lee, Young P14
Leen, Ann P282
Lefebvre, Gautier O51
Leger, Paul P202
Leggett, Barbara P580
Lehmann, Frédéric P255
Lei, Xiudong P644
Leiby, Benjamin P328, P342, P343
Leidner, Rom P48, P65, P361, P562
Leis, Dayna P625
Lekakis, Lazaros P212
Leleti, Manmohan P35
Leleux, Jardin P607
Lemaillet, Guy P408
LeMar, Sara P9
Lemech, Charlotte P308
Lemiashkova, Darya P225
Lemon, Bryan P608
Leng, Ning P19, P66
Lenger, Steven P220, P221
Lenkala, Divya P169
Lenzo, Felicia P75, P76, P77, P549, P707
Leonard, Conrad P580
Leonard, John O20
Leones, Eric P487
Leong, Justin P351
Leong, Meredith P351, P516, P517
Leoni, Guido P184
Lerias, Joana P251
Lérias, Joana P251, P252, P253, P257
Leroy, Xavier P666, P667
Les, Marcin P515
Lesinski, Gregory O20, P290, P371, P376

AUTHOR INDEX

Leung, Irene P411
Leung, Yvonne P1
Leuzzi, Adriano P184
Leventhal, Daniel P624
Leveque, Joseph P297
Levesque, Mitchell P68
Levey, Alicia P209
Levey, Daniel P178, P189
Levin, Maren O3
Levin, Steven P400, P406
Levit, Mikhail P621
Levitsky, Katie P279
Levitsky, Victor P408, P637
Levy, Eric P13, P78, P151
Levy, Ronald P25
Lewandowska, Natalia P204
Lewis, Colleen P506, P507
Lewis, Jason O49
Lewis, Karl O4, P291, P307
Lewis, Katherine P400, P406
Lewis, Nancy P309
Lewis, Nuruddeen P618
Lewis-Tuffin, Laura P5, P6
Lewtak, April P362
Lhospice, Florence P4
Lhuillier, Claire P170, P469
Li, Adrienne P166
Li, Bin P285
Li, Dan Jun P238, P271
Li, Gen P125
Li, Hanying P459
Li, Henry P368
Li, Jacky P687
Li, Jessica O1
Li, Jia P409
Li, Joey P706
Li, Jonathan P366
Li, Kaitao P675
Li, Meng P291
Li, Mingjia P79
Li, Mingyao P108
Li, Nan P546
Li, Ning P624
Li, Qiao P285
Li, Robin P78
Li, Tan P285
Li, Tiepeng P286, P395
Li, Tony P687
Li, Wei P286, P395
Li, Yanmin P190
Li, Yanyun P143, P521
Li, Yiwen P376, P390
Li, Yong O21, P543
Li, Yunmin P211
Li, Yvonne O35
Liadi, Ivan P675
Liang, Xiaoyan P215
Liang, Xue P553
Liang, Yan P113
Lianoglou, Steve P19
Liaw, Kai-Li P31, P585
Libermann, Towia P92
Licitra, Lisa P333
Liebner, David O18
Lienlaf, Maritza P263
Liffers, Sven-Thorsten P349
Ligeiro, Dario P253
Ligeiro, Dário P251, P252, P253, P257
Ligon, Gwenda P510
Lilljebjörn, Henrik P195
Lillquist, Jay P510
Lim, James P254
Lim, Kiat Hon (Tony) P140
Lim, Michael P437
Lim, Min P659
Lim, Min Hui P43
Lim, Sherlly P140
Lim, Woosung P569
Lin, Chia-Chi P662
Lin, Hongwei P286, P395
Lin, Huang P649
Lin, Jessica O7

AUTHOR INDEX

Lin, S. Jack P608
Lin, Susan P550
Lin, Tayson P130
Lin, Yan P709
Lin, Ya-Wei P133
Lin, Yi P240
Lin, Yong P319
Linch, Elizabeth P83
Lind, Evan P401
Lindner, Katharina P103
Linehan, David P498
Linghu, Bolan P594
Lininger, Nicole P643
Link, Alexander P408
Link, Charles P142, P331, P706
Linn, Douglas P379
Linton, Kim P327
Littlefield, Christopher P550
Litton, Jennifer P159
Liu, Arthur P546
Liu, Cailian P143, P521
Liu, Chang P649, P679
Liu, Dai P114
Liu, Dan P125
Liu, Daorong P366
Liu, Diane P225
Liu, Guoyu P600, P606, P610
Liu, Hao O17
Liu, Hongtao P451
Liu, Ke P411
Liu, Li P171
Liu, Liang P205
Liu, Linda P678
Liu, Linying P144, P433
Liu, Liqin P304, P305, P366
Liu, Liu P285
Liu, Lucy P407, P530
Liu, Qin O40
Liu, Sandy P47
Liu, Song P595
Liu, Stephen P548
Liu, Wenbin O5
Liu, Will P606, P610
Liu, Xikui P358
Liu, Xu P409
Liu, Yuan P506, P507
Liu, Yuting P116, P147
Liu, Zhaoping P80
Liu, Ziuye P290
Li-Wang, Bifang P525
Lizee, Gregory P233
Ljung, Lill P7
Llosa, Nicolas P589
Lloyd, Julia P681
Lo, Charlotte P225
Lo, Fei-Yun P163
Lo, Kin-Ming P383, P384
Lo, Sheng-fu P437
Lobb, Roy P267
Loboda, Andrey P31, P553
Locke, Frederick P212
Lodge, Anne P196
Loeffler, Markus P711
Logan, Theodore P294
Loh, Christina P111
Loh, Jie Hua, Josh P140
Lohmueller, Jason P208
Lohr, Joanna P304, P306
Lohr, Michele PO50
Löhr, Matthias O38
Loi, Sherene O46
Loiacono, Kara P598
Loibner, Hans P2, P10
Loizeaux, James P154, P166
Lolkema, Martijn O23
Lonberg, Nikhil P18, P59, P440
Lonez, Caroline P255
Long, Georgina P329
Long, Tiffany P592
Long, Vatana P366
Loo, Deryk P306
Loomis, Cynthia P468

AUTHOR INDEX

Looney, Timothy P81, P82, P83, P256, P709
Lopes, Gilberto P586
Lopes, Jared P425
Lopes, Maria-Beatriz P493
Lopez Gonzalez, Marta P577
Lopez, Juanita P287
Lopez-Casas, Pedro P547
Lora, Jose P624
Lorens, James P115, P715
Lorenzi, Maria P585
Lorigan, Paul O4, P243
Lorrain, Dan P209
LoRusso, Patricia O21, P33, P316, P335, P340
Losey, Heather P123, P423, P425
Lott, Steven P111
Lotze, Michael P294
Lou, Yanyan O24, P361
Loughhead, Scott P219
Low, Simon P185
Lowe, Ashley P305
Lowe, Jamie P708
Löwer, Martin O8
Lowman, Geoffrey P81, P83, P256, P707
Lowther, Daniel P276
Lozinska, Iwona P204
Lu, Ann P211, P254
Lu, Benjamin P84
Lu, Bo P342
Lu, Dan P414
Lu, David P69
Lu, Emily P262
Lu, Hailing P327, P367
Lu, Huifang P565
Lu, Shanhong P70
Lu, Sharon O21, P326
Lu, Steve O6
Lu, Xiaokang P524
Lu, Yang P537
Lubeck, Deborah P692
Lubek, Josh P302
Lucido, Christopher P465
Luddy, John O26
Ludwig, Jörg O8, P711
Luen, Stephen O46
Luginbuhl, Adam P85, P328, P343, P489
Lugowska, Iwona P669
Lukas, Jason P159
Luke, Jason O21, O45, P54, P309, P329, P558
Luker, Andrea P491
Lulu, Amanda P178
Lum, Lawrence P130
Luna, Jesus P508
Luna, Xenia P414
Lund, Jim P581
Lundberg, Kristina P195
Lundqvist, Andreas P522
Lung, Peter P304
Luo, Shujun P78
Luo, Wenyi P192, P534, P535, P538, P702
Lupo, Kyle P523
Lupo, Kyle B. P513, P523, P531
Lutgen-Dunckley, Linda O42
Lutje Hulsik, David P517
Lutz, Eric P86
Lutzky, Jose O22, P291
Lu-Yao, Grace P342, P343
Lye, Melvin P23, P24
Lyman, Susan K. P87
Lynch, Mark P332, P333
Lynch, Miranda O42
Lynes, John P36
Lynn, Geoffrey P164, P172
Lyons, Jesse P215
Lyster, Dawn P501

Author M Abstract Number

Ma, Anna P135, P139, P341
Ma, Barbara P548

AUTHOR INDEX

Ma, Dangshe P438
Ma, Junfeng P561
Ma, Lina P417
Ma, Yuk P711
Macabali, Mignonette P47
MacDonald, Katherine (Kate) P685
MacDougall, John P368
Mace, Thomas P290
Macfarlane, Alexander P396
Mach, Linh P178
Machado, Hidevaldo P220, P221
Machiels, Jean-Pascal P255, P662
Mackay, Laura O46
Mackay, Sean P8, P721
MacKinnon, Alexander P549
Madabhushi, Anant P104, P292, P426
Madakamutil, Loui P364, P418
Madan, Esha P200, P201, P236
Madhavan, Subha P548
Madriaga, Antonett P205
Maeng, Hoyoung P173
Maeng, Kelly P279
Maeurer, Markus P248, P251, P252, P253, P257
Mahabhashyam, Suresh P716
Mahadevan, Daruka O45
Mahajan, Aayushi P437
Mahajan, Millind P149
Mahajan, Tushar P515
Mahmood, Hibah P1
Maia, Andreia P251, P252, P253, P257
Mailloux, Adam P601
Maio, Michele O4
Maiti, Mekhala P418
Maitra, Anirban P268, P555
Majeed, Habeeb P225
Majumder, Biswanath P718
Majzoub, Imad P540
Makarova, Anastasia P235
Makielski, Kelly O43
Makonnen, Sosina P438
Malamas, Anthony P353
Maleki Vareki, Saman P682
Malhotra, Deepali P632
Malhotra, Jyoti P319
Malhotra, Kanam P167
Malhotra, Usha P339
Malkova, Natalia P621
Mallow, Crystal O20
Malone, Kelly P185
Maloveste, Karla P678
Malyapa, Robert P302
Mamchak, Alusha O3
Man, Michael O30
Mancao, Christoph O23
Mancini, Champions Oncology c/o P443
Mandavia, Divyesh P714
Mandavilli, Bhaskar P3
Mandeli, John P149, P150
Manesse, Mael P38, P627
Mangadu, Ruban P553
Mangarin, Levi P521
Mangold, Susanne P637
Mangul, Serghei P687
Manhas, Namratta P203
Manna, Alak P5, P6
Manning, Pamela P512
Manning-Bog, Amy O3, P1
Mansson Kvarnhammar, Anne .. P683
Manuchakian, Rami P5, P6
Manzo, Teresa O10
Mao, Hai-Quan P160
Marabelle, Aurélien P325
Maranchie, Jodi P294
Marchand, Celine P626
Marchand, Jean-Baptiste P148, P602, P615
Marchante, Joao P667
Marches, Florentina P445, P509
Marcinowicz, Agnieszka P331
Mardekian, Stacey P85, P343
Marelli, Bo P383, P384
Margolin, Kim O7

AUTHOR INDEX

Margolis, Claire P719
Maria S Kahn, Laura P424
Mariathasan, Sanjeev..... P19
Marijsse, Jérôme P221, P626
Marillier, Reece P667
Marin, Daniele..... P146, P503
Marincola, Francesco P587
Marine, Jeffrey P313
Marino, Joseph..... P494
Marino, Nalini P479
Marino, Rose P423
Markham, Richard..... P158
Markman, Ben..... O45, P324
Markovic, Svetomir P394
Marle, Sjoerd van P484
Marnellos, George P572
Maron, Steven..... P718
Marron, Thomas..... P149, P330, P719
Marrone, Kristen O47, P12, P589
Marschall, Viola..... O29
Marsh, Henry P510
Marshall, Lisa P202
Marshall, Margaret O19, P361
Marshall, Netonia..... P330
Marshall, Sylwia P631
Marte, Jennifer..... P61
Martel, Maritza O31
Martens, Brandon O42
Mårtensson, Linda P602
Martin, Constance..... P550
Martin, Lainie P396
Martin, Linsey..... P572
Martin, Marta Gil P139, P341
Martin, William P180
Martinek, Jan P445, P509
Martinenaite, Evelina..... P175
Martinez-Garcia, Maria O23
Martinez-Morilla, Sandra P88
Martinez-Outschoom, Ubaldo ... P489
Martínez-Ricarte, Francisco O8
Martin-Fernandez, Javier..... P251, P252, P253, P257
Martini, Dylan P506, P507
Martin-Liberal, Juan..... P651
Martinoli, Chiara..... P667
Martirosyan, Anna P492
Martomo, Stella..... P414
Marwitz, Sebastian P18, P59, P578
Masabanda, Julio P641
Masciari, Serena P621
Maser, Rick P445
Masison, Cynthia P61
Mason, Jennifer P120
Masouris, Ilias..... P552
Masque Soler, Neus..... P631
Massard, Christophe..... O30
Massarelli, Erminia P157
Massilamany, Chandirasegaran. P279
Master, Viraj P506, P507
Masternak, Krzysztof P650
Mata, Melinda O17
Mataraza, Jennifer..... P651
Matatia, Peri P166
Matijevich, Karen..... P558
Matos, Ignacio O23
Matosevic, Sandro P513, P523, P531
Matsui, Hiroto..... P334
Matsushima, Kouji P300
Matthews, Michael..... P107
Mattson, Paulette..... P708
Matvienko, Victor P436
Matzner, Mirela P408
Mauen, Sebastien..... P213, P626
Mauldin, Ileana..... P493
Maurer, Deena..... P176
Maurer, Dominik O8, P246
Maurer, Mark P406
Mau-Soerensen, Morten O23
Mautino, Mario..... P331
Maxwell, Melissa P258
May, Stuart P609
Mayer-Mokler, Andrea P711

AUTHOR INDEX

Mayo, Michele O37
Mayorga, Lina P466
Mazloom, Amin P58
Mazurek, Jolanta P515
McAllister, Andres P602
McAllister-Lucas, Linda P476
McCaffery, Ian P54
McCaffrey, Joanne P222, P223
McCall, Shannon P71, P146, P503
McCann, Katy O8
McCarthy, Brian P169
McCarthy, Erin P58
McCarthy, Timothy O27
McCauley, Scott P297, P369
McClay, Edward P609
Mcclellan, Merriam P72
McClory, Rena P13, P78, P151
McClure, Ty P52
McComb, Scott P179
McConnell, Emma O44
McCormick, Kyle P437
McCoy, Christine P618
McCracken, Kevin P414
McDaniel, Amanda P614
McDermott, David P294, P380, P423
McDevitt, Jennifer P209
McDonnell, Kevin P398
McEachern, Kristen O21, P677
McEwen, Robert P134
McGeehan, Andrew P235
McGinness, Kathleen P216
McGowan, Thomas P396
McGraw, Steven O50
McGuire, Alison P678
McGuire, John P88
Mcilwain, Sean P459
McInnis, Christine P226, P272
McKann, Katy P148
McKenna, Jeffrey P351
McKinnon, Katherine P61
McLachlan, Sandra P721
McLennan, Graham P58
McMahan, Catherine P7
McMichael, Elizabeth P462
McMiller, Tracee P541, P652
McMullan, Trevor P171
McNeil, Lisa P174
McQuade, Jennifer P505, P572
McQuinn, Christopher P290
McRee, Autumn P186
McShane, Lisa O48
McWhirter, Sarah P309, P351
Meadows, Danielle P550
Medcalf, Melanie O44
Mediavilla-Varela, Melanie P67, P439
Medina, Jan P217
Medrikova, Dasa P429
Meehan, Robert P295
Mehanna, Hisham P48, P65
Mehmi, Inderjit P313
Mehnert, Janice P669
Mehra, Navi P90
Mehra, Ranee P302
Mehrotra, Shikhar O9
Mehta, Shivani P585
Mei, Zhuyong O17
Meinel, Jorn P113
Melby, Drew P459
Melcher, Alan P597
Melchionna, Roberta P640
Melchiori, Luca P276
Melero, Ignacio P466
Melief, Cornelis P157
Mell, Loren P333
Menard, Laurence P382
Mendler, Anna P552
Mendrzyk, Regina O8
Meng, Martin P299
Meng, Maxwell P687
Menk, Ashley O11, O13, P207, P528
Menon, Rajeev P690
Menon, Siddharth P324

AUTHOR INDEX

Mensing, Sven P690
Merazga, Zohra P185
Merchan, Jaime O52
Merchant, Fahar P415
Merchant, Melinda P665
Mercier, Marjorie P666
Merghoub, Taha O47, P143, P156, P347, P521
Meric-Bernstam, Funda P139, P299, P309, P341, P542, P619
Merino, Diana O48
Merritt, Chris P131, P428
Merz, Christian O29
Meseck, Marcia P149, P150
Messersmith, Wells P309, P335, P340
Messmer, Davorka P209
Metang, Patrick P445
Metchette, Ken P351
Mettu, Niharika P289
Metz, Clara P637
Metzger, Derek P209
Meyer, Krista P66
Meyer, Miriam O8
Michalik, Kinga P515
Michaloglou, Chrysiis P388
Michaux, Alexandre P213, P220, P626
Michaux, Anne-Catherine P667
Michel, Kyle P708
Michel, Sven O9, P486, P488
Mick, Courtney P696
Micklem, David P115, P715
Mier, James P393
Migliorini, Denis O8
Mikesell, Glen P205
Mikkelsen, Tarjei P129
Miklos, David P212
Milani, Pamela P78
Milella, Michele P640
Mileo, Anna Maria P640
Miles, Brett P149
Milhem, Mohammed P25, P53
Miljkovic, Milos P61, P416
Milla, Marcos P417
Millar, Mike P501
Millard, Frederick P298
Millare, Beatriz O3, P1
Miller, Lance P587
Miller, Lauren P83, P256, P709
Miller, Paul P624
Miller, Peter P144, P433
Miller, Richard O45, P54, P205
Miller, William P18
Milling, Lauren P407
Mills, Lauren O43
Mills-Chen, Laura P510
Minchom, Anna P287
Minev, Boris P609, P617
Minev, Ivelina P609, P617
Minnar, Christine P508
Mintoff, Chris O46
Miret, Juan O35
Mirsoian, Annie P508
Misher, Lynda P7
Misiukiewicz, Krysztof P149
Mitchell, Danielle P7
Mitchell, Jason P280
Mitchell, Petia P599
Mitchell, Tara O40, P108, O49
Mithra, Sanjena P287
Mittal, Payal P494
Mittal, Vinay P27
Mittendorf, Elizabeth P159
Miyauchi, Tsubasa P560
Miyazaki, Takahiro P418, P422
Mizrahi, Rena P646
Mocci, Simonetta P60
Modiano, Jaime O43
Modugno, Francesmary O36
Moghe, Manish P457
Moh, Shizen P703
Mohamed, Ali P246
Mohamed, Eslam O9
Mohamed, Jamal P572

AUTHOR INDEX

Mohammed, Abdul P38
Mohankumar, Gayathri P442
Mohanlal, Ramon P495
Mohindra, Nisha O27, P586
Mohr, Peter P329, P337
Moise, Leonard P180
Mok, Stephen P352
Mola, Natalie P593
Moles, Melissa O7, P49, P307, P314
Molina, Ana P193, P591
Molinero, Luciana P19
Moller, Mecker P717
Molloy, Tim P22
Mom, Stijn P693
Monette, Anne P91
Moniz, Raymond P618
Monjazeb, Arta P508
Monk, Paul P298
Montano, Mauricio P211
Montbel, Adeline P4
Monté, Marc P692
Montgomery, Ruth P133
Moody, Ashley P318
Moody, Gordon P632
Moogk, Duane P675
Moon, Byung-In P569
Mooradian, Meghan P92
Moore, Brittni P173
Moore, Dirk P339
Moore, Gregory P411, P664
Moore, Jonathan P220, P221
Moore, Kathleen P289
Moore, Lauren P88
Moore, Paul P304, P305, P366
Morales, Robert P302
Morehouse, Christopher P409
Morel, Ariane P4
Morel, Yannis P4
Moreno, Victor P326
Morgado, Ester P4
Morgado, Micaela P102
Mori, Masahide P688
Morii, Kenji P249, P560
Morikawa, Naoto P470
Morilla, Ricardo P287
Morin, Benjamin P178, P189, P659
Morishima, Chihiro P93
Morisot, Nadege P94, P95
Morita, Satoru P574
Moron, Fanny P430, P431
Morou, Antigoni P91
Morre, Michel P298
Morris, Clive P141
Morris, John P173
Morris, Katherine P303, P496
Morris, Scott P96
Morris, Zachary P2, P10, P419, P459, P464
Morrison, Brett O13
Morrison, Carl P75, P76, P77, P146, P503, P549, P596, P707
Morrow, Matthew P171, P186
Morrow, Michelle O44, P631
Morse, Jennifer P224, P244
Morse, Kevin P8, P721
Morse, Michael P551
Moskalev, Igor P600
Moskovitz, Jessica O36, P649
Motz, Greg P216
Moudgil, Tarsem P18, P162
Moxon, Nicole O31
Moynihan, Kelly P649
Mroczkowska, Magdalena P515
Mu, Dakai P279
Muchhal, Umesh P411, P664
Mudd, Gemma P398
Mudri, Sherri P406
Mueller, Christian O28, P387
Mugundu, Ganesh P563, P665
Muik, Alexander P402, P647
Muise, Eric P532
Mukhopadhyay, Pamela P580
Mulcahy Levy, Jean P497

AUTHOR INDEX

Mulé, James P601
Mullally, Ann P156
Muller, Alexander P177
Muller, Carolyn P303
Mullinax, John O16
Mumm, John P297, P632
Munir Ahmad, Shamaila P175
Munn, David O9, P142, P706
Munoz-Olaya, Jose P631
Muñoz-Rodríguez, José P703
Muntel, Jan P42
Murad, John P259
Murad, Yanal P600, P606, P610
Murakami, Kiichi P225
Murkar, Amol P418
Murphy, Erin P425
Murphy, Joseph P498
Murphy, Michael P38, P627
Murphy, Mike P510
Murphy, William P508
Murray, James P44
Murray, Joseph P561
Murray, Maryann P240
Murtaza, Anwar P524, P525
Murthy, Rashmi P159
Murthy, Ravi P619
Murthy, Shashi P260
Mutschlechner, Oliver P2
Muzaffar, Mahvish P686
Myers, III, John P159
Myers, Paisley P178
Myhill, Natasha P261
Myint, Melissa P219
Mylavarapu, Apoorva P96
Mymryk, Joe P682

Author N Abstract Number

Nabeel, Sarah P339
Nabel, Gary P621
Nadler, Steven P382
Nag, Shona P714
Nagane, Masaki P200
Nagano, Hiroaki P334
Nagarajan, Priyadharsini P539
Nagy, Mate P487
Naidoo, Jarushka O47, P12, P589
Naik, Shruthi O43
Naing, Aung O7, P87, P297, P299, P409, P542
Nair, Namitha P50
Nair, Smita P612
Nair, Sujit P149
Naito, Yujiro P688
Najjar, Yana O11
Naka, Tetsuji P249
Nakagawa, Takayuki P249
Nakajima, Masao P334
Nakajima, Takahiro P118
Nakashe, Prachi P58
Nakatsura, Tetsuya P300
Nakayama, Takayuki P300
Nallagatla, SubbaRao P344
Nam, Daeun P168
Nanda, Shivani P662
Nandre, Rahul P356, P357, P358
Nangia, Chaitali P310
Nania, Salvatore O38
Nanjappa, Puru P407
Nanus, David P193, P591
Naqash, Abdul Rafeh P686, P719
Narasimhan, Narayana P450
Nardin, Alessandra O1
Nardozzi, Jonathan P227
Naremaddepalli, Sudarshan P529, P694
Narushima, Seiko P574
Nasrullah, Yusuf P169
Nathanson, Katherine P108
Navas, Chris P406
Navin, Nicholas P268
Nayak, Asha O19, P361
Ndubaku, Chudi P351
Nduom, Edjah P36
Neander, Christian P349

AUTHOR INDEX

Neblett, Katherine.....P141
Neelapu, Sattva.....P533
Neeson, Paul O46
Negrao, Marcelo P490
Neighbors, Jeffrey P381
Nellan, Anandani.....P497
Nelles, Megan P225
Nellore, Kavitha.....P694
Nelson, Allison.....P216, P530
Nelson, Alyssa P185
Nelson, Kelly.....P505, P539
Nelson, Michael P169
Nelson, Michelle P7, P250, P273, P284
Nemeth, Michael.....O42
Nersesian, Sarah P460
Neskorik, Tavette O27
Nesline, Mary P75, P76, P77, P549, P707
Neuner, Russell P44
Newell, Evan.....O1, P140
Newell, Felicity P580
Newman, Jenna.....P613
Newman, Lane P474
Newman, Walter.....P143, P474
Ng, Tony P55
Nghiem, Paul P636
Nguyen, Andrew P311
Nguyen, Christine.....P547
Nguyen, Duong.....P609, P617
Nguyen, Linh P225
Nguyen, Ly.....P299
Nguyen, Minh.....P348
Nguyen, Ngan.....O3, P1
Nguyen, Peter P128
Nguyen, Rosa P719
Nguyen, Teresa P370, P605
Nguyen, Thao P279
Nguyen, Thuy P218
Nguyen, Tina P179
Niazi, Kayvan P311
Nicholas, Courtney.....P546
Nichols, Anthony P682
Nickles, Dorothee P19
Nicolini, Valeria..... P413
Nicosia, Alfredo P184
Nie, Jessica..... P225
Nie, Xinxin..... P678
Nielsen, Finn P148
Nielson, Nels..... P404
Nieves, Jeffery P396
Nieves, Wildaliz..... P364
Nieves-Rosado, Héctor P397
Nikanjam, Mina P58, P76
Nikiforov, Anastasia..... P550
Niland, Katie P53
Nilsson, Anneli P7
Ning, Jing P546
Nirschl, Christopher..... P404
Nishimura, Ryohei P249
Nisperos, Sean P69
Nisthal, Alex..... P664
Nistico', Paola P97, P640
Niu, Jiaxin..... O25
Noessner, Elfriede P552
Nofchissey, Robert..... P496
Noland, Thomas..... P598
Nomura, Shogo..... P300
Nones, Katia..... P580
Noonan, Anne..... P290
Noonan, Kimberly..... P86
Noonepalle, Satish..... P203, P576
Nordquist, Luke P167
Norlen, Per..... P683
Norman, Jason..... P574
Normington, Karl O37
Normolle, Daniel..... P294
Norry, Elliot..... O18
Novak, Anne P648
Novotny Jr, James..... P107
Nowak, Mateusz..... P204
Nowak, Ryan..... O50
Nowicki, Theodore..... O39
Nowogrodzki, Marcin P204

AUTHOR INDEX

Nuccitelli, Richard P614
Nunez, Daniel P276
Nurieva, Roza P565
Nutakki, Ravikumar P418
Nwajei, Felix O14, P446
Nyawame, Florence P666
Nyawouame, Florence P667

Author O Abstract Number

Obalapur, Palakshi P418
Obara, Alicja P204
Obeid, Elias P396
Oberkovitz, Galia P356
Obot, Tete P678
O'Brien, Erin O40
Obungu, Arnold P36
Ochoa, Sebastian P548
O'Connell, Allison P526, P561
O'Connell, Brenda P716
O'Connor, Samantha P1
Oda, Shannon O15
Odingo, Joshua P410
O'Donnell, Rebekah P404
O'Donnell, Timothy P149
O'Donoghue, Joseph O49
Odunsi, Kunle P255
Oelke, Mathias P262
Offringa, Rienk P103
Oft, Martin P297, P369, P421
Ogenstad, Stephan P495
Ogiwara, Haru P300
O'Gorman, Bill O1
Ogurtsova, Aleksandra P128
Oh, Aaron P69
Oh, David P82, P687
Oh, Michael P98
Oh, Sean P362
Oh, William P149
O'Hara, Mark P403
Ohashi, Pamela P225
Ohkuma, Ryotaro P51
Ohri, Rachit P37
Ohtake, Junya P183
Okada, Craig P327
Okada, Hideho O8
Okada, Hisatake P51
Okal, Abood P202, P484
Okamura, Ryosuke P76, P707
Okano, Akinori P202
O'Keeffe, Michael P154, P166
Oki, Yasuhiro P240
Okimoto, Ross P117
Olafson, Traci P209
Old, Matthew O52
Olencki, Thomas P294
Olhava, Edward P524
Olinger, Grace P271
Oliphant, Amanda P530
Oliveira, Carlos P66
Olle, Bernat P574
Ols, Michelle P238, P271
Olson, Brian O20, P371
Olson, Daniel P719
Olson, Julie P629
Olson, Peter O27, P385
Olson, William P438
Olszanski, Anthony P361, P622
Oluwole, Olalekan P212
Olwill, Shane P375
Omelchenko, Andrey P563
O'Neal, Tanya P338
O'Neil, Bert P290
O'Neil, Vincent P502
O'Neill, Allison P189
O'Neill, John P396
O'Neill, Thomas P510
O'Neill, Tom P678
O'Neill, Vincent P368
Ong, Giang P131, P428
Ong, Irene P459
Ong, SuFey P136
Ontiveros, Priscilla P69
Onyshchenko, Mykola P557

AUTHOR INDEX

Opyrchal, Mateusz P255
Ord, Robert P302
Ordentlich, Peter P357
Orentas, Rimas P270
Orlowski, Robert P315
Oronsky, Bryan P99, P372
O'Rourke, Martin P681
Osa, Akio P688
O'Shaughnessy, Joyce O3
Osman, Iman P675
Ostertag, Derek P620
Osterwalder, Bruno P708
Ostrowski, Dana P330
O'Sullivan, Gerard O43
O'Sullivan, Roderick P207
Oswald, Detlef P399
O'Toole, Sandra P22
Ott, Patrick O7, P87, P297, P307, P566
Ottensmeier, Christian O8, P148
Otterson, Greg P79
Ottinger, Samantha P407
Ottoson, Nadine P527, P708
Ouellette, Marc P225
Overacre-Delgoffe, Abigail P481, P719
Overwijk, Willem P424
Owen, Dwight P79
Owens, Gemma P222
Owera, Rami O27
Owonikoko, Taofeek P506, P507
Ozawa, Yohei P660

Author P Abstract Number

Pabla, Sarabjot P75, P76, P77, P146, P503, P549, P596, P707
Paces, Will P90
Pacey, Simon P139, P341
Pachter, Jonathan P373
Pachynski, Russell P298, P579
Paczkowski, Patrick P8, P721
Padalia, Zinkal P279
Padget, Michelle P353
Padmanabhan, RaghavKrishna .. P487
Paek, Se Hyun P569
Page, David O31
Page, Melba Marie P67, P439
Pai, Chien-Chun P687
Pai, Sara P587
Pai, Tapasya P216
Paik, Nam Sun P569
Painter, Jeane P542
Pala, Laura P374
Paladino, Maria P637
Palakurthi, Sangeetha P500
Palcza, John O26, P315
Palermo, Belinda P97
Palma, John P60, P101
Palmer, Erica P203, P576
Palmer, Jodie P324
Palucka, A. Karolina P445, P509
Pan, Fan P652
Pan, Shu P320, P321, P322, P673
Panageas, Katherine P521
Pandha, Hardev P597
Pandit-Taskar, Neeta O49
Panetta, Mariangela P97, P640
Pang, Jia P47
Panigrahy, Dipak P209
Panizo, Carlos P327
Pankove, Rebecca P376, P390
Pant, Shubham P297
Pantuck, Allan P47
Papadatos-Pastos, Dionysis P287
Papadimitriou, John P302
Papadopoulos, Kyri P297, P316
Papanicolau-Sengos, Antonios .. P75, P76, P77, P549, P596, P707
Papp, Eniko P71
Pappalardo, Zachary P211
Paradé, Marc P517
Paraschoudi, Georgia P251, P252, P253, P257
Parasuraman, Sudha P53

AUTHOR INDEX

Pardoll, Drew.....O47, P128, P338, P588, P589, P652
Parekh, Hiral.....P336
Parekh, Samir.....P149
Parente, Phillip.....P717
Parikh, Apurvasena.....P72, P690
Parikh, Rahul.....P294
Paris, Sébastien.....P463
Parisi, Giulia.....P547, P557
Park, Adam.....P320, P321, P322, P323, P673
Park, Jong Chul.....P325
Park, Lee Chun.....P568, P582, P586
Park, Peter.....P398
Park, Shinyoung.....P73
Park, Wungki.....P586
Park, Yoon.....P685
Parker, Belinda.....P22
Parker, Jefferson.....P135
Parker, Taylor.....P200, P201, P236
Parmar, Mona.....P287
Parra, Edwin.....P490
Pastan, Ira.....P360
Paszkiewicz, Konrad.....P477
Patch, Ann-Marie.....P580
Patel, Anisha.....P539
Patel, Ashish.....P562
Patel, Aysha.....P222, P223
Patel, Jeegar.....P414
Patel, Jigar.....P459
Patel, Katir.....P38, P39, P40, P116, P627, P654
Patel, Ketan.....P134
Patel, Manish.....O27, P139, P297, P341, P385, P573, P635, O52
Patel, Maulik.....P96
Patel, Naina.....P287
Patel, Pranalee.....P551
Patel, Priyanka.....P591
Patel, Ravi.....P10, P464, P719
Patel, Sandip.....P79, P96, P699, P701
Patel, Sapna.....P505, P537, P572, P619, P710
Patil, Namrata.....P60, P101
Patil, Pradnya.....P104, P426
Patil, Sandeep.....P529, P694
Patnaik, Akash.....P371
Patnaik, Amita.....O26, P325, P716
Patsalidou, Marilena.....P479
Patsenker, Jonathan.....P133
Pattarini, Lucia.....P375
Patterson, Colleen.....P510
Patterson, Ethan.....P633, P634
Paulos, Chrystal.....P250, P273, P284
Paulovich, Amanda.....P269
Paulus, Aneel.....P5, P6
Paustian, Christopher.....P162
Pavlicek, Adam.....O27, P385
Pavlick, Anna.....O22, P150
Pavlidou, Marina.....P375
Pavlova, Yelena.....P417
Pavlovich, Christian.....P338
Pawar, Vinay.....P442
Pawlowski, Nina.....O8
Pawlowski, Traci.....P590, P707
Paz-are, Luis.....P715
Pazdrak, Barbara.....P424
Peace, Kaitlin.....P159
Pearce, Beth.....P226
Pearce, Tillman.....P187
Pearson, Alexander.....P48, P124
Pearson, John.....P580
Pease, Daniel.....P635
Pechouckova, Sarka.....P631
Pecot, Chad.....O35
Pedersen, Ayako.....P177
Peeper, Daniel.....O5
Peeters, Marc.....P662
Pei, Fen.....P672
Peled, Amnon.....P356
Pelham, Christopher.....P200, P201, P236
Pena, Michael.....P417
Pena, Rhoneil.....P364

AUTHOR INDEX

Pencheva, Pepi P306
Peng, David P354
Peng, Kah Whye O52
Peng, Li O37, P676
Peng, Linda O24
Peng, Stanford P400, P406
Pennacchioli, Elisabetta P374
Peoples, George P159
Peper, Janet P375
Peralta, Ronal O13, P207
Perea, Amy P44
Pereira, Daniel P512
Pereira, Rita P287
Perera, Ayesh P308, P409
Perets, Ruth O25
Perez-Garcia, Arianne P675
Perez-Gracia, Jose Luis P466
Perez-Lanzon, Maria P504
Perez-Villarroel, Patricio P601
Perkins, Padma P685
Perry, James P154
Peskov, Kirill P359, P563, P665
Pestic-Dragovich, Lidija P703
Peter, Senaka P31
Peters, Eric P60, P101
Petersen, Christopher P266
Peterson, Maureen P60, P101
Peterson, Nichole P460
Petit, Robert P520
Petitprez, Florent O5
Petrone, Adam O37, P676
Petrosino, Joseph P572
Pettersson, Jonas P592
Pettit, Lauren P520
Peyton, Charles P224
Pfeiffer, Katherine P129
Pham, Anthony P385
Phan, Giao O22
Phan, Linda P342, P343
Phillips, Bonnie P38, P39, P40, P627, P654
Philp, Nancy P489
Piccione, Emily P205
Piemonti, Lorenzo P640
Pienta, Kenneth P185, P234
Pieper, Alexander P419
Pierce, Robert P53
Pierzchala, Olga P204
Piha-Paul, Sarina P299
Pikiel, Joanna P326
Pilataxi, Fernanda P699
Pillai, Manon P243
Pilon-Thomas, Shari O16, P224, P241, P244, P601
Pimentel, Helly Xiao Yan P17
Pimentel, Rodrigo P563
Pinapati, Richard P459
Pinheiro, Elaine P553
Piovesan, Dana P15, P320, P321, P322, P323, P673
Piro, Jordi O8
Pirollo, Kathleen P457
Pirson, Romain P667
Pishvaian, Michael O21
Plagnol, Vincent P141
Platten, Michael O8
Plautz, Greg P636
Plescia, Christopher P624
Plichta, Damian P574
Plimack, Elizabeth P396
Plumb, Darren P479
Pluta, John P108
Plyte, Simon P637
Poch, Michael P224
Pocorni, Noëlle P693
Poczkaj, Aleksandra P515
Podyminogin, Rebecca P132
Poholek, Amanda P207, P481
Poirot, Laurent P214, P283
Poklepovic, Andrew P329
Poli, Valeria P184
Pollard, Jack P621
Poller, Dawn P342, P343

AUTHOR INDEX

Polo, Alex O2
Polonskaya, Zhanna P414
Polson, Craig P510
Ponce Aix, Santiago P139, P341
Ponce Kiess, Ana P302
Pons, Jaume P335, P340
Ponsati, Berta O8
Ponz-Sarvise, Mariano P466
Pookot, Deepa P202
Poplin, Elizabeth P339
Popova, Irina K. P87
Porciuncula, Angelo P50, P102
Porcu, Pierluigi P240
Porras, Ashley P279
Port, Elisa P149
Portal, Daniella P339
Porten, Sima P687
Porter, Roderick P204
Posada, Eliza P505
Poschke, Isabel P103
Posner, Marhsall O51
Postow, Michael O49, P143, P716
Potvin, Diane O27
Poulet, Heïdi P408
Poulin, Jean-Francpos P663
Poulin, Michelle P111
Pouliot, Philippe P663
Poulsen, Hans O8
Pourdehnad, Michael P475
Pourpe, Stephane P156
Pouyet, Laurent P4
Powderly, John O45, P54, P139, P304, P306, P341, P669, P699
Powell, Steven O50, O52, P465
Powers, Jason P120, P575
Powers, Jay P35, P668
Powles, Thomas P19
Prabhash, Kumar P714
Pramanik, Preeti P87
Prapa, Malvina P237
Prasad, Shruthi P666
Prasanna, Prateek P104, P292
Prasit, Peppi P209
Pravin, John O44
Pregibon, Daniel P44
Preillon, Julie P666, P667
Presley, Carolyn P79
Prestat, Emmanuel P492
Price, Leo P435
Priceman, Saul P259
Price-Troska, Tammy P648
Prickett, Todd P543
Priddy, Leslie P345
Prieto, Peter P498
Primack, Benjamin P271
Prince, Ethan P318
Princiotta, Michael P520
Prins, Petra P105
Prinz, Petra P552
Pritchard, Theresa P652
Privezentzev, Cyril O44
Procopio, Giuseppe P110
Proffitt, Andrew P510
Proscurshim, Igor P189
Prosniac, Mikhail P198
Prostak, Naseem P186
Prout, Toby P287
Pruitt, Scott P31
Ptacek, Jason P106
Ptacin, Jerod P417
Pucilowska, Joanna O31
Puerta-Martinez, Francisco P370
Pufky, John P120
Punt, Simone P555
Puro, Robyn P512
Purvis, Norman P114
Puthiamadathil, Jeevan P548
Putiri, Emily P423
Putta, Santosh P114
Puzanov, Igor O4, P313, P316, P717

Author Q Abstract Number

AUTHOR INDEX

Qazi, Taha.....P566
Qdaisat, Aiham.....P540
Qi, Huilin.....P524
Qi, Jin.....P383, P384
Qi, Jingjing.....P143
Qi, Zengbiao.....P583
Qian, Lu.....P108
Qiao, Wei.....P534, P535, P537
Qin, Guozhong.....P383, P384
Qin, Maochun.....P75, P549
Qing, Jing.....P599
Qiu, Hongchen.....P525
Qiu, Xiaohong.....P527, P708
Qu, Hui.....P621
Quach, Henry.....P691
Quach, Phi.....P364, P418
Quan, Francine.....P420
Quan, Walter.....P420
Quayle, Steven.....P185
Quemeneur, Eric.....P148, P181, P602, P615
Quinn, Katie.....O48
Quintero, Marisol.....P547
Quon, Harry.....P302

Author R Abstract Number

Rabizadeh, Shahrooz.....P311, P660
Rabolli, Virginie.....P666
Radford, John.....P240
Radhakrishnan, Vivek.....P714
Radzimierski, Adam.....P515
Rae, Chris.....P235
Rafferty, Conor.....P44
Rahbaek, Lisa.....P209
Rahbari, Ashkon.....P586
Rahma, E.....O24, P305, P566, P567
Rahman, Sachi.....P405
Rahmati, Sara.....P91
Rainbolt, Elizabeth.....P550
Rait, Antonina.....P457
Raitano, Susanna.....P220, P221
Raithatha, Sheetal.....P239
Raja, Rajiv.....P14
Rajamanickam, Venkatesh.....O31, P162
Rajan, Anusha.....P269
Rajapakshe, Kimal.....P157
Rajiah, Prabhakar.....P426
Rajopadhye, Milind.....P144
Raju, Gottumukkala.....P534
Raju, Siddharth.....P687
Rakestraw, Andy.....P226, P272
Rakhmilevich, Alexander.....P10, P419, P459, P485
Ramachandra, Murali.....P529, P694, P714
Ramachandra, Raghuveer.....P694
Ramachandran, Indu.....P276
Ramachandran, Umesh.....P239
Ramaekers, Ryan.....P385
Ramalingam, Suresh.....P506, P507
Ramamurthy, Maya.....P259
Raman, Pichai.....P550
Ramaswamy, Sridhar.....P365, P677
Ramchandren, Radhakrishnan..P139, P341
Ramchurren, Nirasha.....P298
Ramello, Maria.....P263, P264
Ramelot, Nancy.....P232
Ramirez-Valdez, Andrei.....P164
Ramirez-Valdez, Ramiro.....P172
Ramkumar, Kavya.....P452
Rammensee, Hans Georg.....P453, P711
Rammensee, Hans-Georg.....O8
Ramos, Carlos.....O17
Ramos, Hilario.....P9
Ramos, Kimberly.....P520
Ranade, Koustubh.....P699
Rancan, Chiara.....P687
Randolph, Sophia.....P335, P340
Randolph, William.....P295
Rao, Martin.....P248, P251, P252, P253, P257
Rao, Sheela.....P336
Rao, Shruti.....P548

AUTHOR INDEX

Rao, Sumati P350, P355, P380
Rapisuwon, Suthee P548
Rasco, Drew O25, P391, P392, P393, P669
Rashid, Naureen P591
Rashid, Rumana P411, P664
Rasmussen, Kayla P10
Rassoulpour, Arash P94, P95
Rastelli, Luca P368
Rathkey, Daniel P360
Rathman, Blaine P708
Rathmell, Jeffrey P206
Rathmell, W P206
Ratnam, Nivedita P265
Ratta, Raffaele P110
Ratti, Navneet P297, P421
Rautela, Jai P22
Ravelli, Andrea P233
Ravindranathan, Sruthi P266, P376, P390
Ravishankar, Buvana P202
Ravishankar, Rathna P247
Rawls, Tracey P403
Ray, Anita P496
Ray, Karina P468
Rayavarapu, Vijaysai P529
Razak, Albiruni P225, P698
Reagan, Patrick P212
Reardon, Christopher P238, P271
Rebelatto, Marlon P21
Reddy, Anita P72
Reddy, Mamatha P377
Reddy, Sangeetha O5, P719
Redkar, Sanjeev P377
Redmond, William P18, P363, P378, P696
Redondo Müller, Mauricio O29
Reduta, Allan P304
Regan, Meredith P380
Regine, William P302
Reichen, Christian P408
Reid, Tony P99, P372
Reilley, Matthew P299
Reiner, Gabrielle P351
Reinfeld, Bradley P206
Reinhardt, Carsten O8, P246, P711
Reinieren-Beeren, Inge P517
Reiter, Lukas P42
Rekdal, Oystein P623
Remark, Romain P4
Remy-Ziller, Christelle P181
Ren, Jian-Guo P450
Ren, Zhongxu P364
Rennert, Paul P267
Rennie, Paul P600
Rennier, Keith P579
Renouf, Daniel O45
Rens, Joost P517
Reshef, Dan P636
Restifo, Nicholas O34, P675
Reu, Frederic P524
Reuben, Alexandre O5, P233, P490, P564
Reus, Jacek P204
Reuss, Joshua P567
Reyes, Cielito P540
Reynolds, John O50
Rezazadeh Kalebasty, Arash O24
Rha, Sun Young P31, P139, P341
Rhee, Ji Hyun P568
Rhee, Kyunghoon P568
Rhoades, Martyn O44
Rhode, Peter P712
Rhudy, Jessica P152
Ribas, Antoni O20, O21, O39, P25, P547, P557, P716
Ribeiro, Matthew P84
Ricca, Jacob P521
Ricciuti, Biagio P109
Rich, Jeani P241
Richard, Guilhem P180
Richards, Allison P241
Richards, David O29, P533, P535, P538

AUTHOR INDEX

Richards, Donald P385, P392, P393
Richardson, Celeste P238, P271
Richardson, Jennifer P87
Richardson, Robin P69
Richter, Anne P45
Rickel, Erika P400
Riddell, Stanley P269, P281
Ridge, John P302
Rieger, Aimee P320, P321, P322, P323, P673
Riese, Matthew O45
Rigamonti, Nicolo P637
Riggins, Angela P93
Riisnaes, Ruth P287
Rimm, David O6, P88, P116, P131, P133, P138, P147
Rinchai, Darawan P110, P587
Ring, Aaron O32, P415
Rini, Brian O45, P54
Riordan, Christina P659
Ritchings, Corey P380
Rittase, William P675
Rittenhouse, Natalie P207, P481
Ritter, Gerd P482
Ritthipichai, Krit P210
Rittner, Karola P181
Rivadeneira, Dayana P208, P616
Rivas, Sarai P422
Rivera-Molina, Yisel P370, P605
Rivière, Matthieu P375
Rivoltini, Licia P110
Rixe, Olivier P303, P331, P361
Rizvi, Moshahid P121
Rizvi, Naiyer O48, P87, P409
Rizwan, Ahsan O4
Roarty, Emily P233
Robbins, Paul P543
Roberson, Brenda P173
Robert, Caroline P329
Roberts, Bruce P574
Roberts, Charles P128
Roberts, Jennifer P716
Roberts, Morgan P600
Robertson, Catherine O17
Robertson, Gavin P381
Robillard, Liliane P348
Robinson, Garrett P9
Robinson, Mark P68
Robinson, Tanya P422
Robinson, William O3, P1, P108
Roblyer, Darren P454
Rocha, Sony P608
Rock, Amy P712
Roda Perez, Desamparados P326
Rodeck, Ulrich P85, P328, P489
Roder, Heinrich P66, P294
Roder, Joanna P66, P294
Rodolfo, Monica P110
Rodon, Jordi O8, P299
Rodrigues Mantuano, Natalia P676
Rodrigues, Leonor O44
Rodriguez Ehrenfried, Aaron P103
Rodriguez, Bertha Leticia P354, P470
Rodriguez, Inmaculada P466
Rodriguez, Nicole P411
Rodriguez, Paulo O9
Rodriguez-Canales, Jaime P157, P442, P632, P638
Rodriguez-Ruiz, Maria P466, P719
Roehle, Kevin P467
Roelands, Jessica P110, P587
Roeser, Julien P94, P95
Rogacki, Maciej P204
Rogers, Clare P111
Rognoni, Lorenz P442
Rojo, Bianca P297
Rolig, Annah P363, P378
Roman, Kristin P18, P433
Roman, Shilina P681
Romano, Alfredo P475
Rooney, Center Director P240, P277
Rooney, Cliona O17
Roop, John O2

AUTHOR INDEX

Roque, Tammy P385
Ros, Willeke O23
Roscoe, Nathan P65
Rose, Daniel P378
Rosen, Anna P683
Rosén, Anna P656
Rosenberg, Andrew P136
Rosenberg, Steven O34, P543
Rosencranz, Samantha P171
Rosenzweig, Michael P532, P553
Rosner, Dalya P405
Ross, Ashley P338
Ross, Helen P409
Ross, John P185
Ross, Kendra P225
Ross, Merrick P53, P329
Ross, Nikki P618
Rossi, Gabriela P142, P706
Rossi, John P212
Rossi, Sean P123, P423
Rossignoli, Filippo P237
Rössler, Bernhard O8
Roszik, Jason P233, P555
Roth, Jack P233
Roth, Michael P721
Rothe, Christine P375
Rotman, Jossie P693
Rottey, Sylvie P255
Roudko, Vladimir P182
Roush, William P524
Rousseau, Louise P91
Rousseva, Valentina P247
Routy, Jean-pierre P91
Rowe, Valerie P12
Rowlinson, Scott P345, P363
Roy, Amit P636
Roy, Amitesh O28
Roy, Dhruvajyoti P125
Rozeman, Elisa O5
Rozeman, Lisette P389
Rozenblit, Mariya P468
Ruan, Alex P566
Ruan, Jia P240
Rubas, Werner P364, P378
Rubin, Krista P16
Rubinstein, Mark O40, P68
Rubinstein, Max P39, P654
Rubinsteyn, Alexander P149
Rucevic, Marijana P112
Ruck, Rebecca P553
Rudnick, Jennifer P205
Rudqvist, Nils-Petter P170, P469
Rudraraju, Lakshmi P86
Ruffolo, Luis P498
Rugo, Hope P163
Ruidera, Robert P185
Ruiz, Iván Victoria P87
Rusch, Elisa O8
Rusk, Jennifer P700
Russell, Stephen O43, O52
Rutella, Sergio P113
Ruth, Karen P396
Rutledge, Teresa P303
Ryabin, Jessica P185
Ryall, Karen P90
Ryan, Aideen P719
Ryan, David P304
Rybkin, Igor P385
Rybstein, Marissa P473
Rytelewski, Mateusz O14

Author S Abstract Number

Saada-Bouzid, Esma O51
Saba, Nabil P444
Sabado, Rachel P149, P150
Sabitha, K.S. P718
Sacchetta, Brian P171
Sachadeva, Ankush P47
Sachdev, Esha P719
Sacher, Adrian P225
Sachsenmeier, Kris P134, P665
Sade-Feldman, Moshe O5
Sadis, Seth P27

AUTHOR INDEX

Saeidi, Navid.....P302
Saerens, Laura.....P220
Safa, Houssein.....P644, P710
Safanov, Anton.....P108
Safonov, Anton.....P108
Sage, Julien.....P470
Sagert, Jason P279
Saggu, Gurpanna.....P185
Sagorsky, Sarah P12
Saha, Krishanu.....P434
Sahafi, Flora.....P487
Sahebjam, Solmaz O19, P255, P325
Sahin, Ugur.....O8, P103, P402, P621, P647
Sahuquillo, Juan O8
Saibil, Sam P225
Said, Jonathan P47
Sait, Sheila.....O42
Sakellariou-Thompson, Donastas.....P233, P268
Salas, Sebastien.....O51
Salathe, Sebastian P245
Salcedo, Theodora P647
Salgado, Roberto.....O46
Salim, Agus.....O46
Salini, Avneesh P405
Salles, Gilles.....P240
Salmeron, Andreas.....P404
Salmon, Gary.....P681
Salojin, Konstantin P114
Saloura, Vassiliki.....P48
Salter, Alexander.....P269
Samant, Manoj.....P450
Samarkina, Anastasia P639
Samavedam, Siva P276
Samberg, Nancy O22
Samiulla, Dodheri.....P529, P694
Sampath, Padmavathi P616
Samuels, Sanne P693
San Jose, Kristine.....P417
Sanborn, Rachel P87, P162, P403, P429
Sanborn, Zach P311
Sancenon, Vicente P477
Sanchez, Brian P524
Sanchez, Jerick..... P202
Sanchez, Katherine O31
Sanchez, Victoria P36
Sanchez-Salazar, Jorge..... P618
Sandanayaka, Vincent P203
Sandén, Carl..... P195
Sander, Cindy..... O11, P559
Sane, Ramola P524
Sangro, Bruno P711
Sanjuan, Miguel P524
Sanmamed, Miguel..... P133
Sansas, Benoit..... P181
Sanseviero, Emilio..... O40
Santegoets, Saskia P293
Santiago, Solimar..... P450
Santidrian, Antonio..... P609, P617
Santino, Salvatore..... P685
Santopietro, Ariana P548
Santoro, Armando P475
Santos, Patricia P176, P528
Sanzari, Jenine P692
Sapida, Jerald..... P129
Saravia, Diana P586
Sarhan, Dhifaf O38
Sarikonda, Ghanashyam P126
Sarkar, Saumendra P616
Sarlis, Nicholas..... P159
Sarnaik, Amod..... O16, O22, P224, P241, P244, P263
Sarver, Aaron O43
Sasada, Tetsuro P183
Sasaki, Yasutsuna..... P51
Sasikumar, Pottayil P529, P694
Satala, Grzegorz..... P204
Sathyanarayanan, Sriram P618
Satijn, David..... P402, P647
Sato, Ai..... P473
Sato, Akihiro P300
Satoh, Etsuko P51

AUTHOR INDEX

Sauer, Scott P551
Sauer, Tim P277
Sautes-Fridman, Catherine O5
Savage, Alison P385
Savage, Jason P61
Savas, Peter O46
Savelyeva, Natalia P148
Savitsky, David P659
Savvatakis, Konstantinos P349
Sawant, Anandi P379
Sawant, Deepali O33
Sawka, Dariusz O4
Saxena, Neetu P600
Saxton, Claire P629
Scafe, Charles P27
Scarpa, Aldo P640
Scarselli, Elisa P184
Sceneay, Jaclyn P572
Schachner, Ben P241
Schachner, Benjamin O16
Schad, Sara P347
Schadt, Eric P149
Schaefer, Rachel P144, P433
Schaer, David P143
Schafer, Jamie P530
Schaible, Doris P408
Schalck, Aislyn P268
Schalk, Dana P130
Schalper, Kurt P33, P50, P84, P102, P116, P133, P147, P295
Scharping, Nicole O13, P207, P616
Schaser, Thomas P229
Schebesta, Michael P271
Schebye, Xiao Min P684
Scheel, Birgit P337
Schehr, Jennifer P385
Scheid, Elizabeth P225
Schell, Monika P486, P488
Schell, Todd P381
Schellenberger, Volker P187
Schellens, Jan O23
Scheper, Rik P293
Scherer, Julian P49
Scherman Plogell, Ann-Helen P522
Schieven, Gary P525
Schildknecht, Patricia P408
Schindler, Ulrike P668
Schlegel, Anja P637
Schlereth, Julia P621
Schlom, Jeffrey P353, P660
Schluns, Kimberly P422
Schmidt, Emmett P391, P392, P393
Schmidt, Guenter P21
Schmidt, Manuel P299, P399
Schmidt, Michael P407, P453, P530
Schmidt, Shelly O30
Schmitz, Marc P113
Schneck, Jonathan P160, P245, P570
Schneider, Dina P270
Schoen, Robert O36
Scholer-Dahirel, Alix P375
Scholz, Alexander P1
Schönborn-Kellenberger, Oliver P337
Schonemann, Wojciech P515
Schonhoft, Joseph P69
Schoor, Oliver O8, P246
Schreiber, Taylor P519, P657, P658
Schroeder, Matthias O29
Schubbert, Suzanne P411
Schuchter, Lynn O40, O49, P108
Schueler, Julia P681
Schuetze, Scott O18
Schulick, Richard P318
Schultz, Huguette P148
Schumacher, Ton O5
Schürpf, Thomas P550
Schürpf-Huber, Franziska P474
Schuster, Cornelia P115
Schuurhuis, Danita P402, P647
Schwartz, Jacob P202
Schwestermann, Jonas P637
Sciarra, Laura P39, P654
Scolyer, Richard P329

AUTHOR INDEX

Scott, Ellen O16, P241
Scott, Milcah O43
Scribner, Katherine P592
Scrivens, Maria O20
Seder, Robert P164, P172
Seery, Tara P713
Seetharam, Mahesh O24
Sefrin, Julian O29
Segerer, Felix P442
Seibel, Tobias P337
Seidel, Ronald P185
Seidel-Dugan, Cynthia P404
Seigna, John P298
Seitz, Christina P522
Seitz, Lisa P15, P35, P320, P321, P322, P323, P668, P673, P697
Seiwert, Tanguy O51, P48, P65, P718
Sekhavati, Farzad P699
Selby, Mark P684
Seliger, Barbara P499, P554, P695
Selmi, Abderaouf P621
Selvanantham, Thiru P111
Selvaraj, Periasamy P266
Semmrich, Monika P602
Sen, Seema P121
Sen, Triparna P452, P470
Sender, Leonard P310, P713
Sender, Matthew P494
Sentman, Charles P8
Sepesi, Boris P233
Serada, Satoshi P249
Serafini, Tito P1
Serna, Carylinda O34
Serzan, Michael P548
Sethi, Aisha P303
Setogawa, Takeshi P51
Seu, Lillian P382
Seymour, Len P479
Sgouroudis, Vicky P663
Shaath, Hibah P230
Shabaneh, Tamer O40
Shabanowitz, Jeffrey P178
Shabbir, Fahad P116, P147
Shabto, Julie P506, P507
Shah, Krishna P546
Shah, Mohsin P540
Shah, Monil O31
Shah, Neel P549
Shah, Neil P447, P548
Shahda, Safi P290
Shahlaee, Amir P167
Shaib, Walid P290, P506, P507
Shamah, Steven P238, P271
Shames, David P66, P101
Shang, Limin P650
Shang, Yiman P286
Shankar, Sadhna P313
Shanmugasundaram, Meenakshi P446
Shao, Wenlin P665
Shapiro, Geoffrey P295, P325, P716
Sharei, Armon P219
Sharma, Arati P381
Sharma, Geeta P365, P677
Sharma, Meenu P424
Sharma, Padmanee O5
Sharma, Sunil P289
Sharova, Tatyana P16, P92
Shaw, Amy P226, P272
Shaw, Sandra P630
Shaw, Stephen P356
Shawver, Laura P417
Shaza, Leila P255
Sheehan, Mike P699
Sheffer, Michal P719
Sheikh, Muhammad Mubbashir P582, P586
Shen, Cong P297
Shenderov, Eugene P338
Sheng, Jennifer P636
Sheng, Jie P546
Shepherd, Deneuve P625
Sher, Taimur P5, P6
Sheridan, James P72
Sheridan, Joseph P117

AUTHOR INDEX

Sherman, Jeffrey P396
Sherry, Lorcan P501
Sheth, Rahul P619
Shi, Jian P528, P559
Shi, Yuankai P495
Shibata, Masahiko P118
Shibuya, Grant P202
Shichino, Shigeyuki P300
Shields, Anthony P186
Shields, Peter P79
Shimada, Takashi P119
Shimomura, Manami P300
Shimura, Tatsuo P118
Shin, Dong Ho P605
Shin, John P216
Shin, Woo Jae P579
Shinde, Arvind P713
Shindo, Yoshitaro P334
Shingu, Takashi P427
Shiota, Atsushi P574
Shitara, Kohei P300
Shively, John P259
Shnitzer, Tal P133
Shoda, Kayoko P300
Shoja E Razavi, Ghazaleh P567
Sholl, Lynette P109
Shore, Neal P167, P171
Shraibman, Bracha O8
Shulgin, Boris P563
Shumaker, Robert P391, P392, P393
Shyne, Michael P635
Si, Han P699
Sia, Christine P618
Sidders, Benjamin P594
Sidhom, John-William P588
Sidransky, David P443
Siegartel, Lisa P137
Sieling, Peter P311
Siemer, Ramona P45
Sieprawska-Lupa, Magdalena P515
Sierra, Rosa O9
Siggelkow, Sara P72
Silk, Jonathan P276
Silva, Abraham P21
Silverman, Deborah P555
Silvestre, Nathalie P148, P602
Sim, Bee-Cheng P187
Simcox, Mary P185
Simeone, Ester P711
Simmons, Andrew P348
Simmons, John P71
Simone, Charles P319
Simone, Peter P71
Simoni, Yannick P140
Simons, Diana P43
Simpson, Allison P550
Simpson, Guy P597
Sims, Jennifer P120, P122, P469, P575
Sinclair, Angus P405
Sinelnikov, Evgueni P248, P251, P252
Singh, Bhavana P105
Singh, Gopal P542
Singh, Harpreet O8, P246
Singh, Hema P15, P697
Singh, Lata P121
Singh, Manisha P424
Singh, Mithalesh P121
Singh, Prashant O42
Singh, Salendra P135
Singh, Shailbala P152
Singh-Jasuja, Harpreet P711
Singson, Victoria P87
Sirard, Cynthia P143
Sirmans, Elizabeth P505, P572
Siska, Peter P206
Siu, Lillian P622, P698
Siveke, Jens P349
Sivick Gauthier, Kelsey P351
Sjoquist, Katrin P320, P321, P322, P673
Skardelly, Marco O8
Skelly, Ashwin P574

AUTHOR INDEX

Skoble, Justin.....P235
Skolnik, Jeffrey P186
Skrahina, Tatsiana P387
Slansky, Jill.....P318
Slater, Lorna P479
Slichenmyer, William P123, P423
Slingluff, Craig P493
Slowinski, Jacob.....P10, P419
Smalley, Inna P263
Smalley, Keiran.....P263
Smalley, Munisha P718
Smedenfors, Kristine P683
Smirnov, Denis P707
Smith, Aubrey.....P250, P273, P284
Smith, Darren P226
Smith, David P692
Smith, Eric P438
Smith, Ernest.....O20
Smith, Julianne P214
Smith, Karen.....P178
Smith, Kellie O47, P589
Smith, Steven P484
Smithy, James.....P131, P138
Snell, Dan P408
Snider, James P302
Snyder, Christopher P328, P489
Snyder, Megan P216
Snykers, Sarah P255
So, Alex.....P590
Soares, Heloisa P331
Sohn, Silke O38
Sokolovska, Anna P624
Solanki, Anisha P388
Solomides, Charalambos.....P342, P343
Somasekharan, Syam P600
Somasundaram, Ashwin.....O36, P556, P649, P679
Somasundaram, Rajasekharan...P639
Sondak, Vernon.....P329
Sondel, Paul.....P2, P10, P419, P459, P464, P485
Song, Chang P678
Song, Colette O8
Soni, Abha..... P128
Sonnemann, Heather..... P265
Sood, Jessica P614
Soon-Shiong, Patrick..... P310, P660, P712, P713
Soose, Ryan..... P583
Sorani, Ella P356
Soriano, Jonathan P185
Sosman, Jeffrey..... P108, P139, P341
Sotiropoulou, Panagiota P231, P232, P255
Soto, Ricardo P189
Sotov, Valentin P225
Soukou, Foteini P204
Soulières, Dennis P333
Sourdive, David..... P214
Souteyrand, Edouard..... O44
spada, sheila P640
Spakowicz, Dan P79
Spaner, David..... P209
Spano, Carlotta P237
Spanos, William O50, P465
Spaulding, Emily..... P185
Speed, Terence O46
Spencer, Christine..... O5, P505, P572
Spencer, David P217
Spencer, Kristen..... P339
Spencer, Sarah P279
Sperduti, Isabella P640
Spicer, James P139, P341, P715
Spigel, David P307, P314
Spijkers, Sanne..... P517
Spira, Alexander..... O4, P87, P305, P306, P385
Spitzer, Matthew P687
Spranger, Stefani P518, P558
Spreafico, Anna..... P225, P698
Springuel, Lorraine P274, P275, P626
Squarcina, Paola P110
Sridar, Janani P169
Sridhar, Sriram..... P14

AUTHOR INDEX

Srinivasan, Lakshmi O7, P49
Sriramaneni, Raghava P464
Srivastava, Pragya O42
Stam, Anita P577, P693
Stanczak, Michal O37, P676
Standarski, Lindsey P700
Standifer, Nathan P409
Stanski, Donald P359
Stanton, Rick P697
Stark, Valerie P241
Starobinets, Hanna P166
Statkiewicz, Grzegorz P204
Stav-Noraas, Tor Espen P256
Stebbins, Karin P209
Stecha, Pete P661
Steele, Keith P21, P436, P442, P699
Steenwinckel, Valérie P274, P626
Steffin, David P277
Stein, Julie P128
Stein, Kevin P629
Stein, Robert P178, P189, P532
Stein, Stacey P304
Steinberg, Amir P330
Steinberg, Gary P124, P180
Steinbrueck, Philipp P45
Steiner, Philipp P404
Steiniche, Torben P31
Steinman, Lawrence P1
Stelzer, Greg P111
Stenehjem, David P137
Stepan, Daniel P391, P392, P393
Stephens, Geoffrey P246
Stern, Martin O23
Steuer, Conor P506, P507, P716
Stevanovic, Stefan O8
Stewart, mark O48
Stewart, Tyler P84
Stickler, Marcia P72
Stieglbauer, Monika O8
Stock, Nick P209
Stockhausen, Marie O8
Stoffel, Kevin P508
Stokes, Brittany P219
Stone, Erica O40
Storkus, Walter P709
Stout, Bhavani P247
Strack, Tanja P337
Straten, Per Thor O8
Stratford, Jeran P122
Stratton, Kelly P325
Straume, Oddbjørn P115
Strauss, James O27, O52, P305
Streicher, Katie P409, P699
Strobel, Oliver P103
Stroh, Mark P87
Strome, Scott P302
Stromko, Caitlyn P525
Stroncek, David P173, P176
Strop, Pavel P685
Stubbington, Michael P129
Stuebner, Kathleen O43
Stumpp, Michael P408, P637
Sturgill, Elizabeth P363, P696
Sturgill, Ian P508
Stutz, Andrea P524
Su, Lihe P267
Su, Wu-Chou P662
Suarez Gutierrez, Magdalia O15
Suarez, Felipe P240
Suarez, Lauren P262
Suarez-Almazor, Maria P565, P644
Subbiah, Vivek P539
Subegdjo, Safiya P109
Subramaniam, Deepa P548
Subramanian, Janakiraman P326
Subramanian, Kulandayan P651
Succaria, Farah P128
Suda, Wataru P574
Sudol, Sylwia P515
Sugimoto, Masamichi P472
Suh, Cheolwon P240
Sukhadia, Bhoomika P582, P586

AUTHOR INDEX

Sulkowski, Parker P33
Sullivan, Ryan P16, P92, P294, P295, P716
Sumatoh, Hermi O1
Sumi, May P1
Sumrow, Bradley P669
Sun, Debin P34
Sun, Dexue P238, P271
Sun, Fangxian P621
Sun, Huadong P525
Sun, Jichao P306
Sun, Jingwei P678
Sun, Lei P123, P423, P425
Sun, Peng P332
Sun, Tao O33
Sun, Weijing P186
Sun, Yang P687
Sun, Yanqiu P546
Sun, Yao P64
Sun, Zhe O33, P481
Sundaram, Ranjini P33
Suntharalingam, Mohan P302
Surace, Michael P442, P632, P638
Suresh, Rahul P234
Surh, Natalie P351
Suri, Anish P185
Suri, Prerna O47
Suri, Vipin P238, P271
Susmilch, Kayla P406
Susnjar, Antonia P152
Sutanto-Ward, Erika P177
Suteja, Lisda P140
Suthram, Silpa P202
Sutton, David P450
Suzuki, Nobuaki P334
Suzuki, Sam O22
Suzuki, Toshihiro P300
Svane, Inge Marie P175
Sveinbjornsson, Baldur P623
Swanson, Jesse P525
Swanson, Ryan P400, P406
Sweis, Randy P124, P180
Swendseid, Brian P489
Swiderek, Kristine P400, P406
Swiercz, Jakub P667
Swirski, Mateusz P204
Swisher, Stephen P233
Sykora, Jaromir O29
Sykorova, Martina P223
Syrigos, Kostas P102
Szalay, Aladar P609, P617
Szeremeta-Spisak, Joanna P204
Szmulewitz, Russell P298
Sznol, Mario O4, O19, O45, P54, P108, P721
Szpurka, Anna P662
Szymczak-Workman, Andrea P649

Author T Abstract Number

Tabaran, Alexander-Flaviu O43
Tabatabai, Ghazaleh O8
Tabib, Tracy P481, P583
Tacha, David P641
Tafe, Laura P549
Tagawa, Scott P193, P591
Taggart, David P125
Tagliaferri, Mary O4
Tagliamonte, Maria P711
Tahara, Makoto P332
Tajon, Michael P26
Takahashi, Masaru P51
Takahashi, Shuichi P225
Takahashi, Shunji P651
Takahashi, Takehiro P51
Takamura, Toshimi O22
Takano, Angela P140
Takeda, Shigeru P334
Takenoshita, Seiichi P118
Taketomi, Akinobu P580
Talay, Oezcan P202
Talluto, Craig P309
Talmon, Ronen P133
Tam, Alda P619

AUTHOR INDEX

Tam, Miguel P705
Tamada, Koji P334
Tan, Chin Leng P103
Tan, David P651
Tan, Eng Huat P140
Tan, Joanne P35, P320, P321, P322, P323, P668, P673, P697
Tan, S. W. Daniel P140
Tan, Seng-Lai P500
Tan, Tira P698
Tan, Tze Heng P442
Tan, Yi-Hung Carol P48, P65
Tanaka, Shinya P225
Tang, Alice P382
Tang, Lei P703
Tang, Tenglong P533, P535, P645
Tang, Wei-Chien P163
Tang, Xiaobin O3
Tangela, Saikrishna P694
Tanne, Antoine P178, P189
Tannir, Nizar P297
Tanoue, Takeshi P574
Tao, Aiyang P309
Tap, William O18
Tapia, Coya P542
Tarasiewicz, Zoe P271
Tarhini, Ahmad P126, P127, P176, P380, P709
Tarolli, Jay P106
Tassa, Carlos P215
Tassell, Vanessa P385
Taube, Janis O6, O47, P128, P541, P589
Tavaré, Richard P438
Tawbi, Hussein O5, P176, P505, P572, P709, P710
Tayar, Jean P565
Taylor, Jennifer P709
Taylor, Joanna P408
Taylor, Matthew P391, P392, P393
Taylor, rodney P302
Taylor, Sarah P129
Teichgraeber, Volker P413
Teige, Ingrid P602
Temburni-Blake, Sonal P283
Tendyke, Karen P598
Teo, Zhi Ling O46
Teoh, Jeffrey P278
Ter Meulen, Jan P17, P367, P607
Terheyden, Patrick P337
Terrell, Andrew O50
Terrett, Jonathan P279
Tetteh, Paul P279
Tetzlaff, Michael O5, P194, P539
Tewari, Ashutosh P149
Thagesson, Mia P656, P683
Thakkar, Dipti P477, P719
Thakur, Archana P130
Thambi, Nithya P520
Thanos, Christopher P235
Thapa, Dharma P185
Thaxton, Jessica O12, P719
Thayer, Desiree P187
Thelemann, Tamara P486, P488
Theofano, Orfanelli P182
Thiemann, Meinolf O29
Thievanthiran, Bala P545
Thin, Tin Htwe P150, P257
Thistlethwaite, Fiona P87
Thiyagaragan, Saravanan P718
Thomas, Charlene P591
Thomas, Christopher P404
Thomas, Jacob P622
Thomas, John-michael P137
Thomas, Lawrence P510
Thomas, Remy P230
Thomas, Sajeve O22, P717
Thompson, Jonathan P715
Thompson, Paul O50
Thor Straten, Per P478
Thorne, Stephen P616
Thurston, Gavin P438
Thyagarajan, Shweta P1

AUTHOR INDEX

Tian, Chuan P313, P336, P669
Tiersten, Amy P149
Tighe, Robert P386, P407, P530
Tillmann, Bodo P621
Ting, Ying Sonia P49
Tipping, Alex P276
Titz, Alexander P408
Tivitmahaisoon, Parcharee P202
Tjoa, Benjamin P196
TMB Harmonization Team, Friends of Cancer Research O48
To, Long P44
Tobin, Kennedy P164
Tokar, Tomas P91
Toki, Maria P102, P131
Tokumitsu, Yukio P334
Tolcher, Anthony O24
Tolstykh, Tatiana P621
Tom, Warren P27
Tomaszewska-Kiecana, Monika P669
Tomochika, Shinobu P334
Toms, Laurence P333
Tong, Pan P452
Tong, Yan P290
Toor, Salman P230
Topacio-Hall, Denise P82, P83, P709
Topalian, Suzanne P541, P652
Topchy, Elena P239
Topolnicki, Grzegorz P515
Tormoen, Garth P471
Tornberg, Ulla-Carin P602
Torno, Sebold O20
Torrejon, Davis O39, P547, P557
Torres Chavez, Alejandro P282
Tosch, Caroline P181
Tosevski, Ivana P408
Tovey, Holly P287
Towfic, Fadi P475
Townsley, Danielle P699
Trager, James P511
Trajkovic-Arsic, Marija P349
Trampont, Paul P700
Tran, Ben P308
Tran, Cynthia P192
Tran, Dao P137
Tran, Eric P162
Tran, Hai P157
Tran, Karen P238, P271
Trautz, Aspen P155
Treat, Joseph P396
Trehu, Elizabeth P52
Treiber, Tobias P628
Trent, Jonathan P136
Triebel, Frederic O28, P387
Trifan, Ovid P710
Trigo, José P326, P715
Trillo-Tinoco, Jimena O9
Trindade, Hélder P253
Trinh, Van P644
Trivedi, Trupti O18, P276
Troise, Fulvia P184
Troxel, Andrea P625
Trujillo, Damian P309
Trujillo, Jonathan P558
Truong, Hong-An P684
Tsai, Frank O49
Tsimberidou, Apostolia P299
Tsoi, Jennifer P557
Tsung, Allan P528
Tsunoda, Takuya P51
Tucci, Fabio P184
Tuck, David P135, P139, P341
Tucker, Christopher P280
Tuluc, Madalina P85, P328, P343
Tuna, Mihriban O44, P631
Tunariu, Nina P287
Tureci, Ozlem P402, P647
Turk, Mary Jo O40
Turner, Alison P287
Turner, Michelle P12
Turunen, Brandon P494
Tuting, Thomas P25
Tutt, Andrew P55

AUTHOR INDEX

Tweardy, David P424
Twitty, Christopher P717
Tyer, Tiffani P302
Tykodi, Scott O4
Tzetzo, Stephanie O42

Author U Abstract Number

Uboha, Nataliya P87
Udaka, Keiko P334
Uddajjara Shanthappa, Basavaraja P718
Uduman, Mohamed P189
Uecker, Darrin P614
Ueha, Satoshi P300
Uematsu, Toshinari P334
Uenami, Takeshi P688
Ueng, Shir-Hwa P163
Ueno, Tomio P334
Uger, Bob P362
Uhlenbroich, Sandra O44
Uhlik, Mark P708
Ulahannan, Susanna P289
Ulges, Alexander O8
Ulrich, Brian P692
Umana, Pablo P413
Umeton, Renato P109
Underwood, Dennis P178, P532
Unfricht, Darryn P144
Ung, Johnson P130
Upadhyaya, Punit P398
Urba, Walter P162
U'Ren, Lance P64, P132
Ursic, Lauren P700
Uyeki, James P385
Uyttenhove, Catherine P482

Author V Abstract Number

Vadakekolathu, Jayakumar P113
Vadde, Sri P530
Vagnali, Dario P679
Vahanian, Nicholas P142, P331, P706
Vainstein-Haras, Abi P356
Vaishampayan, Ulka P423
Valentini, Davide P251
Valge-Archer, Viia P388
Valmori, Danila P711
Valton, julien P283
Van As, Brendan P225
van Berkel, Patrick P11
van Beusechem, Victor P577
Van Buuren, Marit P169
van de Ven, Rieneke P577
van den Eertwegh, Alfons P293
Van den Eynde, Marc P255
van der Burg, Sjoerd O8, P157, P256
van der Touw, William P247
van Eenennaam, Hans P516, P517
van Elsas, Andrea P351, P516, P517
Van Hagen, Tom P717
van Ham, Marieke P293
van Hoogdalem, Ewoud-Jan P484
van Rietschoten, Katerine P398
Van Snick, Jacques P482
Van Tine, Brian O18
Van Vlasselaer, Peter P297
Van Winkle, Erin P276
Van, Trieu My P389
VandenHeuvel, Sabrina P10
VanderVeen, Laurie P418
Vangerow, Burkhard P662
Vaporciyan, Ara P233
Varadan, Vinay P135
Varadarajan, Navin P675
Varadhachary, Gauri P268
Varela, Juan P262
Vargas, Joe P641
Varma, Rajat P411
Vasiljeva, Olga P87
Vasselli, Jim P338
Vaupel, Christine P65, P126, P127
Veatch, Joshua P281
Veitonmaki, Niina P656
Veitonmäki, Niina P683
Velazquez Albino, Ambar P434

AUTHOR INDEX

Velcheti, Vamsidhar P102, P104, P143, P292, P423, P426
Velculescu, Victor O47, P589
Velghe, Amélie P275
Vembu, Prathima P576
Venkatraman, Vignesh P659
Vera, Juan P282
Verbel, David P598
Verburg, Mark P133
Verdegaal, Elizabeth (Els) P256
Verdugo, Patrick O16, P244
Vergato, Cameron P454
Verma, Bhavana P443, P444
Verma, Bikash P255
Verma, Rakesh P369, P421
Verma, Vivek P356, P357, P358
Vermeer, Daniel P465
Vermeer, Paola P465
Verschraegen, Claire P79
Verzoni, Elena P110
Viale, Giuseppe P374
Vianden, Christina P424
Viaud, Sophie P620
Viboch, Elena P113
vicencio, Jose P55
Vicente-Suarez, Ildefonso P219
Vicini, Paolo P409
Vidal, Igor P338
Vieira, Ana P251, P252
Vieira, Ana Isabel P257
Vieito, Maria O30
Vignali, Dario O33, O36, P481, P556, P583, P649
Vignali, Paolo O13, P207
Vijayakrishnan, Balakumar P11
Vijayvergia, Namrata P396
Vile, Richard P597
Villaflor, Victoria P586
Villagra, Alejandro P203, P576
Villarroel-Espindola, Franz P133
Villasboas, Jose P648
Villiger-Oberbek, Agata P618
Vink, Paul P435, P517
Vinogradov, Sergei O14
Vinolas Segarra, Nuria P715
Virassamy, Balaji O46
Virdi, Gurpal P579
Visca, Paolo P640
Vitale, Laura P510
Vitale, Rosa P184
Viveiros, Pedro P582, P586
Vivier, Eric P4
Vlachostergios, Panagiotis P193, P591
Vo, Thao P31
Voeller, Julie P10
Voets, Erik P516, P517
Vogelzang, Nicholas O24, P391, P392, P393
Voillet, Valentin P269
Vokes, Everett P48
Volkmuth, Wayne P1
Volz, Barbara P399
Vom Baur, Elmar P408
von Deimling, Andreas O8
von Keudell, Gottfried P327
Von Moltke, Lisa P423
Vonderheide, Robert P186
Vonghia, Luisa P711
Vora, Kruti P566
Voronova, Veronika P359, P665
Vosganian, Gregory P72
Voskoboynik, Mark P308
Vowinckel, Jakob P41, P628
Vreeland, Timothy P159
Vujanovic, Lazar P559
Vuppugalla, Ragini P524

Author W Abstract Number

Wada, Satoshi P51
Waddell, Ian P681
Waddell, Nic P580
Wadsworth, Angela P202
Wagenaar, Timothy P621

AUTHOR INDEX

Wages, Nolan P493
Wagner, Claudia O8, P246
Wakabayashi, Masashi P300
Wakita, Daiko P472
Wald, Noemie P666, P667
Waldhauer, Inja P413
Waldmann, Thomas P61, P416
Waldner, Hanspeter P279
Walia, Rohit P396
Walker, M P167
Walker, Nigel P697
Walker, Paul P141, P686
Waller, Edmund P266, P376, P390, P444
Walmacq, Celine P262
Walsh, Garret P233
Walsh, Richard P708
Walter, Steffen P246
Walters, Ian P622
Walters, Jewell P155
Walters, Matthew P15, P35, P320, P321, P322, P323, P668, P673, P697
Wan, Hong P335, P340
Wang, Amy P28
Wang, Beatrice P405
Wang, Betty P72
Wang, Chichung P18, P433
Wang, Chuan P148
Wang, Daphne P128
Wang, Ding P295
Wang, Guocan P546
Wang, Hao P338
Wang, Hongwei P139, P341
Wang, Hua P357
Wang, Huifen P134
Wang, Jennifer P565
Wang, Jianmin O42
Wang, Jiao P513, P523, P531
Wang, Jing P157, P452, P470
Wang, Jixin P14
Wang, John P598
Wang, Judy O21
Wang, Jun P661, P678
Wang, Lei P357
Wang, Lilli P276
Wang, Ling P405
Wang, Linghua O5
Wang, Liqing P494
Wang, Lisa P698
Wang, Ming P672
Wang, Ruoxi P276
Wang, Shangzi P526
Wang, Shuhua P376, P390
wang, shuiming P301
Wang, Si P586
Wang, Ting P481, P583
Wang, Xiang P36
Wang, Xiangxue P703
Wang, Xianzhe P407
Wang, Xiaomei P217
Wang, Xiaoyan P47
Wang, Yan P53
Wang, Yi P285
Wang, Ying O21, P325, P573
Wang, Yinghong P192, P194, P533, P534, P535, P536, P537, P538, P564, P645, P702, P719
Wang, Yipeng P69
Wang, Yirong P75, P77, P549, P707
Wang, Yiyang P208
Wang, Yu P301
Wang, Yun P553
Wang, Zhengyi P653, P671
Wang, Ziming P508
Wani, Khalida P539, P564
Want, Muzamil P188
Ward, Pamela P592
Ward, Rebecca P659
Ward, Stacey P633
Ware, Yvonne P49
Wargo, Jennifer O5, P194, P354, P505, P539, P564, P572
Warr, David P698

AUTHOR INDEX

Warren, Christopher P154
Warren, Sarah P113, P131, P136, P389, P428, P429
Wasiuk, Anna P510
Waszak, Angela O21
Watanabe, Norihiro P282
Watkins, Amanda P553
Watkins-Yoon, Jennifer P530
Watson, McLane O13, P208
Wawersik, Stefan P550
Waxman, David P454
Weathers, Shiao-Pei P431
Weaver, David P373
Webb, Santhana P173
Weber, Amy P241, P244
Weber, Jeffrey P262, P675
Weber, Wolfgang O49
Weeratna, Risini P179
Wegrzyn, Paulina P204
Wei, Wei P138
Weichert, Jamey P464
Weickhardt, Andrew O24
Weide, Benjamin P337
Weidlick, Jeffrey P510
Weigel, Kelsey P90
Weigman, Victor P120, P122, P575, P593
Weiner, David P155
Weiner, Doris P244
Weiner, Louis P526, P561
Weingartner, Elizabeth P71
Weinschenk, Toni O8, P711
Weinschenk, Tony P246
Weis-Banke, Stine Emilie P175
Weise, Amy O45
Weishaupt, Carsten P337
Weiss, Ido P86
Weissferdt, Annikka P233
Welsh, Joshua P61
Welters, Marij O8
Wen, Zhifa P162
Wendell, Stacy O13
Wennerberg, Erik P469, P623
Werchau, Doreen P7, P656, P683
Werner, Lillian P380
Werner, Theresa P309
Werner-Wasik, Marie P342
Wesa, Amy P443, P444
Wesche, Holger P608
Wesolowski, Robert P189
West, John P78, P151
West, Katy P479
West, Kip P624
West, Robert P20
Westfall, Matt P114
Westin, Jason P533
Weyandt, Jamie P206
Whang, Sung P342
Wheeler, Eloise P38
Wheler, Jennifer P651
Whetstone, Ryan O13
Whidden, Mark P1
White, Andrew P428, P429
White, James P71, P107, P692
White, Jonathan P681
Whiteaker, Jeffrey P269
Whitehall, Vicki P580
Whiteman, Kathleen P216
Whiting, Chan P209
Whitman, Eric O22
Whitney, Duncan P135
Wiatrowska, Karolina P204, P515
Wiatrowski, Kyle O42
Wicha, Max P285
Wichroski, Michael P524
Wick, Wolfgang O8
Wicke, Lena P621
Wickenhauser, Claudia P499
Wickett, Marcy P3
Widger, Jenifer P510
Widmaier, Moritz P429
Wieder, Eric P136
Wiederschain, Dmitri P621

AUTHOR INDEX

Wiener, Doris P241
Wiesnoski, Diana P194
Wiestler, Tobias P436
Wiggins, Jason P345
Wigginton, Jon O24, P304, P305, P306, P338
Wiley, Kathleen P643
Wilkinson, Brandy P700
Wilky, Breelyn P136, P189
Will, Matthias P87
Willert, Erin P9
William, Josette P487
William, William P157
Williams, Alan P283
Williams, Leila P555
Williams, Milton P506, P507
Williams, Richard P29, P581
Williams, Shuntae P107
Williamson, Caitlin P465
Williamson, Kevin O3, P1
Willingham, Stephen O45, P54
Willis, Connor P137
Wilson, Douglas P532
Wilson, Ian O49
Wilson, Melissa O22
Wilson, Nicholas P659
Wilson, Nick P254
Wilson, W. Casey P512
Wind-Rotolo, Megan P108
Winkler, David P524
Winn, Jennifer P396
Winston, William P404
Winter, Michael B. P87
Wischhusen, Jörg O41
Wise, Aaron P590
Wistuba, Ignacio P157, P233, P470, P490
Witt, Davis P497
Witt, Luke P185
Wittig, Burghardt P399
Witzel, Sonja P621
Woessner, Richard P665
Wohlwender, Tom P557
Wojcik-Jaszczynska, Katarzyna .. P515
Wolchok, Jedd O49, P108, P143, P156, P347, P521, P716
Wolf, Andrea P149
Wolf, Benjamin P407
Wolf, Jeffrey P302
Wolf, Melissa P206
Wolfson, Martin P400, P406
Wollerton, Francisca O44, P631
Wong, Albert P254
Wong, Alexis P39, P654
Wong, Deborah P297
Wong, Felix P55
Wong, Kenneth P87
Wong, Kwok-Kin O35
Wong, Michael O4, P505, P572, P710
Wong, Phillip P143, P297
Wong, Pok Fai P131, P138
Wong, Steve P202
Woo, Joohyun P569
Wood, Edgar P681
Wood, Lauren P173
Wood, Scott P580
Woodman, Scott O5
Workman, Creg O33, P481, P649, P679
Worth, Amy P305
Wortman, Jennifer P572
Wortmann, Philip P442
Woyciechowski, Jakub P204
Wrangle, John P68
Wright, Amy P93
Wright, Kevin P608
Wronowski, Marek P204
Wu, Anna O49
Wu, Christina O20, P290, P506, P507
Wu, Darong P270
Wu, Jiayi P598

AUTHOR INDEX

Wu, Johnny P60, P101
Wu, Kevin P590
Wu, Lan P267
Wu, Meng-Fen O17
Wu, Song P699
Wu, Te-Chia P445
Wu, Tony O24, P305
Wu, Yuling P409
Wuerthner, Jens P316
Wustrack, Rosanna P117
Wustrow, David P202, P484
Wyant, Timothy P135, P139
Wyatt, Hailey P84
Wyatt, Megan P250, P273, P284
Wydro, Mateusz O44, P631

Author X Abstract Number

Xavier, Ramnik P574
Xia, Julie P38
Xia, Leiming P285
Xia, Xiaofeng P228, P514
Xia, Yuhe P625
Xiao, Christine P545
Xiao, Feng P308
Xiao, Yinghua P608
Xiao, Zhilan P424
Xie, Chen P28
Xie, Mingchao O48, P594
Xiong, Ying P270
Xu, Chunxiao P383, P384
Xu, David P701
Xu, Guangxin P341
Xu, Haiying P128
Xu, Ke P618
Xu, Lihui O37
Xu, Qihong P366
Xu, Qinying P580
Xu, Wei O40
Xu, Wenxin P123
Xu, Xiaowei O40

Author Y Abstract Number

Yada, Erika P183
Yadav, Mahesh O1
Yaguchi, Tomonori P249, P560
Yam, Jennifer P225
Yamamoto, Shigeru P334
Yamane, Hide P164, P172
Yamashita, Makiko P300
Yamazaki, Takahiro P170, P473, P504, P623
Yan, Dingxue P258
Yan, Jian P155
Yan, Kuan P435
Yan, Li P409
Yan, Yiyi P394
Yanagawa, Jane P199
Yang, Fan P187
Yang, Hushan P342, P343
Yang, Jinho P569
Yang, Li P686
Yang, Lily P266
Yang, Lin P285
Yang, Min P474
Yang, Muh-Hwa P191
Yang, Shuo P350, P355
Yang, Wenqing P368
Yang, Xia P143
Yang, Yeun-yeoul P569
Yang, Yinhua P366
Yang, Yonghao P286, P395
Yang, Yuanquan P595, P719
Yang, Zhi Zhang P648
Yano, Hiroshi O33
Yao, Joyee P590
Yap, Timothy O30, P299
Yarar, Defne P219
Yarchoan, Mark P541
Yau, Edwin P146, P503, P596
Yaung, Stephanie P60, P101
Yazaki, Paul P259
Ye, Chengzhong O46
Ye, Chun Jimmie P687
Yeckes-Rodin, Heather P346

AUTHOR INDEX

Yee, Cassian.....P152, P710
Yellin, Michael.....P403
Yeong, Joe.....P140
Yerigeri, Keval.....P12
Yeung, Bertrand.....P129
Yeung, Sai-Ching.....P540
Ying, Tianlei.....P270
Yizhak, Keren.....O5
Yogarajah, Meera.....P141
Yoo, Sanghee.....P502
Yoon, Dok Hyun.....P240
Yosef, Reut.....P197
Yoshida, Shin.....P334
Yoshida, Tatsuya.....P262
Yoshikawa, Toshiaki.....P300
Yoshimura, Kiyoshi.....P51
Yoshino, Shigefumi.....P334
Young, Kirsten.....P206
Young, Samuel.....P493
Young, Steve.....P15, P35, P668
Younis, Rania.....P719
Yourstone, Scott.....P575
Yu Jen, Kai.....P326
Yu, Alice.....P163
Yu, Binbing.....P134
Yu, Chun.....P445, P509
Yu, Danni.....P662
Yu, Evan.....P298
Yu, Guangjie.....P162
Yu, Huakui.....P383, P384
Yu, Jiayi.....P142, P706
Yu, Jovian.....P133
Yu, Qunyan.....P621
Yu, Sheng.....P606
Yu, Stephen.....P608
Yu, Timothy.....P608
Yu, Wanfeng.....P581
Yu, Zhiya.....O34, P675
Yu, Zhongjie.....P45
Yuan, Jianda.....P31
Yuan, Wei.....P287
Yuan, Zhou.....P675
Yushak, Melinda.....P53
Yusko, Erik.....P86

Author Z Abstract Number

Zacharek, Sima.....P102, P295
Zahavi, David.....P561
Zaidi, Mohammad.....P376
Zakharia, Yousef.....P142
Zaks, Tal.....P295
Zal, Anna.....O14, P446, P546
Zal, Tomasz.....O14, P446, P546
Zalevsky, Jonathan.....O4, P364, P368, P378, P418, P424
Zamarin, Dmitriy.....O19
Zammarchi, Francesca.....P11, P316
Zandberg, Dan.....O24, P302
Zang, Jingwu.....P653, P671
Zangl, Luke.....P464
Zappasodi, Roberta.....P143, P156, P347, P521
Zaretsky, Jesse.....O39
Zarr, Melissa.....P678
Zastawna, Magdalena.....P204
Zauderer, Maurice.....O20
Zawadzka, Magdalena.....P515
Zaynagetdinov, Rinat.....P384
Zecchini Barrese, Tomas.....P157
Zehir, Ahmet.....O48
Zeldis, Jerry.....P318
Zeng, Zhen.....O25
Zerba, Kim.....P107
Zerbib, Robert.....O48
Zha, Yuanyuan.....P124, P558
Zhai, Shuyan.....P294
Zhan, Jinghui.....P599
Zhang, Amy.....P39, P654
Zhang, Bingqing.....P17
Zhang, Chi.....P598
Zhang, Danhui.....O3, P1
Zhang, Hao Chi.....P702
Zhang, Hong.....P61

AUTHOR INDEX

Zhang, Huimin O17
Zhang, Jacky P585
Zhang, Jiajia O47, P12, P589, P719
Zhang, Jianjun P490
Zhang, Jianzhong P190
Zhang, Jing P285
Zhang, Jingli P360
Zhang, Kang P125
Zhang, Li P82
Zhang, Ling O34
Zhang, Minying P555
Zhang, Pei P594
Zhang, Ping P418, P463
Zhang, Qianxia O33
Zhang, Rong P481
Zhang, Rosemary P525
Zhang, Shaojun O5
Zhang, Shile P590
Zhang, Shuli P532
Zhang, Simo P28
Zhang, Tian P71, P146, P503, P549, P596
Zhang, Tuo P170
Zhang, Wen P364
Zhang, Wenjun P703
Zhang, Xiaokui P247
Zhang, Yanping P384
Zhang, Yong P286, P395
Zhang, Yong-Wei P561
Zhang, Yu-An P621
Zhao, Chen O48
Zhao, Hao O5
Zhao, Hui P644
Zhao, Lingdi P286, P395
Zhao, Ni O47
Zhao, Ronghua P600, P606, P610
Zhao, Sharon P15, P697
Zhao, Steven P239
Zhao, Xinfang P129
Zhao, Yonggang P335
Zhao, Yumin O30, P662
Zheng, Alice P63, P83
Zheng, Beiyao P87
Zheng, Gang P621
Zheng, Jianping P571
Zheng, Lianghong P125
Zheng, Lianqing P212
Zheng, Lianxing P351
Zheng, Yanan P699
Zheng, Yi P144, P433
Zhong, Hong P143
Zhong, Shi P675
Zhong, Wangjian P385
Zhou, Jing P8, P721
Zhou, Juhua P190
Zhou, Ruhong P570
Zhou, Shouhao P446
Zhou, Ting O32
Zhou, Xueyuan P398
Zhu, Cheng P675
Zhu, Genyuan P601
Zhu, Jason P71, P146, P503, P596
Zhu, Jian P145
Zhu, Qingfeng P541, P703
Zhu, Rebecca P145
Zhu, Yaling P164, P172
Zhu, Zhongyu P270
Zibelman, Matthew P396, P549
Zibinsky, Mikhail P202
Ziblat, Andrea P704
Ziembik, Magdalena P204
Zigo, Liliana P629
Zijlmans, Henry P693
Zill, Oliver P19
Zinn, Pascal P430, P432
Zinner, Ralph P85, P328, P342, P343
Zinzani, Pier P315
Ziolkowska, Martha O49
Zippelius, Alfred P486, P488, P676
Zitt, Christof P408

AUTHOR INDEX

Zizlsperger, Nora P407, P530
Zloza, Andrew P319, P613
Zocca, Mai-Britt.....P177
Zollinger, Dan P428
Zomorodian, Nazy.....P47
Zou, Hui P672
Zou, Wei P60, P101
Zugazagoitia, Jon.....P116, P133, P147
Zuniga, Luis.....P532
Zuraw, Aleksandra.....P21
Zwirtes, Ricardo P636
Zyczynski, Teresa.....P137

KEYWORD INDEX

Adoptive immunotherapy.....O9, O10, O15, O16, O17, O18, O22, O34, P3, P9, P17, P37, P56, P80, P86, P103, P134, P140, P160, P169, P188, P196, P200, P210, P211, P212, P213, P214, P215, P216, P217, P218, P219, P220, P221, P222, P223, P225, P226, P227, P229, P230, P234, P238, P239, P240, P241, P243, P244, P245, P246, P247, P248, P249, P250, P251, P252, P253, P254, P255, P256, P257, P258, P262, P263, P264, P266, P269, P270, P272, P273, P275, P276, P278, P279, P280, P282, P283, P284, P285, P286, P298, P310, P330, P369, P395, P420, P434, P446, P459, P491, P513, P514, P533, P543, P547, P552, P555, P570, P600, P601, P603, P607, P629, P714

Angiogenesis.....O23, P136, P155, P198, P391, P392, P393, P639

Antibody O3, O19, O20, O21, O23, O24, O25, O26, O29, O37, O41, O44, O51, P1, P2, P3, P4, P7, P8, P10, P11, P32, P36, P38, P39, P40, P57, P67, P87, P88, P95, P107, P116, P119, P122, P133, P152, P153, P163, P187, P193, P200, P205, P236, P257, P270, P289, P291, P306, P308, P316, P320, P321, P322, P323, P325, P326, P329, P338, P350, P361, P366, P372, P375, P377, P386, P389, P390, P391, P392, P393, P398, P402, P403, P404, P405, P407, P413, P414, P415, P416, P437, P438, P451, P459, P466, P474, P477, P482, P485, P487, P500, P510, P512, P516, P517, P525, P530, P531, P532, P550, P556, P561, P579, P604, P608, P627, P631, P641, P646, P647, P650, P651, P653, P654, P656, P659, P661, P662, P664, P666, P672, P673, P678, P681, P683, P684, P685, P686, P690, P696, P703, P705, P710

Antigen presenting cells.....O20, O23, O28, P5, P39, P49, P53, P56, P65, P108, P124, P129, P154, P156, P159, P160, P166, P169, P173, P174, P176, P180, P196, P201, P209, P219, P262, P272, P298, P309, P335, P340, P364, P367, P372, P375, P387, P390, P400, P402, P403, P406, P435, P491, P499, P510, P515, P516, P517, P518, P519, P528, P532, P555, P557, P577, P580, P586, P588, P598, P618, P622, P623, P624, P632, P637, P641, P658, P665, P674, P695, P710, P712, P718

Autoimmunity..... P56, P81, P108, P153, P175, P397, P447, P489, P535, P538, P540, P562, P564, P565, P568, P635, P691

B cell O3, O5, P1, P5, P6, P14, P24, P62, P91, P100, P111, P122, P167, P205, P253, P327, P397, P459, P493, P590, P637, P639, P641, P646

Bioinformatics..... O2, O3, O33, O47, O48, P1, P8, P13, P20, P21, P27, P28, P29, P30, P42, P44, P56, P58, P60, P63, P78, P81, P82, P91, P108, P110, P111, P122, P135, P145, P148, P164, P169, P180, P182, P188, P190, P207, P426, P429, P430, P431, P432, P436, P440, P452, P459, P469, P555, P571, P580, P581, P583, P584, P586, P587, P591, P593, P594, P595, P628, P682, P687, P719, P721

Biomarkers O1, O2, O3, O6, O19, O31, O41, O43, O48, O49, O51, O52, P8, P13, P14, P15, P16, P17, P18, P19, P20, P21, P22, P24, P25, P26, P27, P28, P29, P30, P31, P32, P33, P34, P35, P36, P37, P38, P39, P40, P41, P42, P44, P48, P49, P51, P52, P53, P54, P56, P58, P59, P60, P62, P63, P64, P65, P66, P67, P68, P69, P70, P71, P72, P75, P76, P77, P78, P79, P80, P81, P82, P83, P86, P87, P88, P90, P91, P92, P93, P94, P95, P96, P99, P100, P101, P104, P105, P106, P107, P108, P109, P111, P112, P114, P115, P116, P118, P119, P120, P122, P123, P124, P125, P126, P127, P128, P130, P131, P132, P133, P134, P135, P136, P137, P138, P139, P140, P142, P143, P144, P145, P146, P147, P148, P157, P180, P182, P193, P195, P196, P201, P225, P230, P257, P278, P289, P290, P291,

KEYWORD INDEX

Biomarkers (continued)..... P292, P295, P297, P326, P327, P342, P343, P348, P361, P371, P377, P379, P385, P389, P394, P397, P407, P408, P423, P425, P426, P428, P429, P430, P431, P432, P433, P439, P440, P451, P452, P455, P459, P475, P487, P492, P493, P501, P503, P506, P507, P541, P544, P549, P556, P557, P571, P578, P579, P581, P582, P586, P588, P590, P591, P594, P596, P614, P627, P628, P641, P654, P662, P675, P682, P687, P693, P703, P707, P708, P709, P710, P718, P719, P721

CAR T cells.....P23, P24, P80, P111, P179, P196, P208, P212, P213, P214, P216, P217, P218, P220, P221, P228, P229, P231, P232, P237, P238, P249, P254, P255, P256, P259, P262, P263, P264, P267, P269, P270, P271, P274, P275, P277, P278, P279, P282, P283, P318, P369, P397, P434, P456, P497, P511, P533, P626, P633, P634, P643

Carcinogenesis.....P56, P200, P236, P389, P510, P578

Checkpoint blockade.....O1, O3, O4, O5, O6, O11, O12, O19, O20, O21, O24, O25, O26, O27, O28, O32, O36, O38, O39, O40, O41, O45, O47, O50, O51, P9, P11, P12, P14, P15, P16, P19, P20, P21, P22, P25, P26, P27, P32, P33, P36, P48, P51, P53, P58, P60, P64, P65, P66, P67, P68, P69, P70, P71, P72, P79, P80, P81, P82, P85, P87, P88, P90, P95, P97, P99, P107, P108, P109, P112, P115, P116, P124, P126, P127, P128, P131, P133, P135, P136, P137, P138, P139, P140, P141, P142, P143, P146, P147, P155, P157, P174, P176, P184, P191, P192, P193, P194, P199, P203, P209, P235, P249, P258, P280, P286, P287, P289, P290, P297, P299, P300, P302, P303, P304, P305, P306, P307, P308, P310, P312, P313, P315, P319, P320, P321, P322, P323, P324, P325, P326, P328, P329, P330, P335, P336, P337, P338, P339, P340, P341, P342, P343, P344, P345, P346, P347, P350, P351, P352, P353, P354, P355, P359, P360, P361, P362, P363, P365, P366, P367, P368, P371, P372, P373, P374, P375, P377, P379, P380, P381, P382, P383, P384, P385, P386, P387, P388, P389, P390, P394, P395, P396, P397, P401, P406, P413, P414, P424, P426, P427, P432, P435, P437, P443, P447, P450, P451, P455, P457, P459, P462, P464, P465, P467, P469, P470, P472, P473, P474, P475, P477, P484, P498, P503, P504, P505, P506, P507, P508, P510, P512, P516, P517, P519, P521, P524, P525, P526, P527, P529, P532, P534, P535, P536, P537, P538, P540, P541, P545, P546, P548, P550, P556, P557, P558, P562, P563, P564, P565, P566, P567, P568, P571, P573, P574, P576, P579, P582, P586, P590, P596, P597, P599, P600, P602, P603, P604, P606, P612, P613, P621, P625, P631, P635, P636, P643, P644, P645, P646, P648, P649, P650, P651, P652, P653, P657, P658, P660, P661, P663, P664, P665, P666, P667, P668, P669, P671, P672, P673, P675, P676, P677, P678, P679, P681, P682, P683, P684, P685, P686, P688, P690, P691, P692, P693, P694, P695, P696, P697, P698, P700, P701, P702, P703, P704, P707, P708, P710, P713, P714, P715, P717, P718, P719, P720, P721

Chemokine..... O31, P8, P44, P53, P115, P158, P168, P181, P196, P198, P231, P265, P348, P352, P397, P446, P454, P460, P468, P479, P484, P500, P510, P527, P545, P553, P556, P576, P579, P708, P716, P721

Chemotherapy..... O3, O50, P22, P36, P60, P105, P121, P193, P200, P201, P209, P236, P244, P288, P290, P306, P310, P314, P319, P320, P321, P322, P332, P339, P342, P343, P353, P374, P384, P394, P421, P451, P452, P454, P460, P465, P472, P559, P591, P620, P622, P698, P706, P713

Clinical study O1, O2, O19, O22, O23, O28, O31, O45, O50, O51, P15, P16, P25, P32, P34, P53, P58, P64, P66, P87, P110, P115, P125, P126, P138, P142,

KEYWORD INDEX

Clinical study (continued)..... P167, P171, P174, P186, P189, P193, P194, P210, P212, P225, P240, P251, P255, P287, P289, P290, P291, P293, P294, P295, P299, P300, P308, P310, P311, P313, P314, P316, P320, P321, P322, P323, P325, P327, P329, P331, P336, P337, P341, P342, P343, P346, P350, P354, P355, P361, P380, P387, P389, P394, P396, P408, P416, P423, P430, P432, P451, P465, P475, P484, P495, P534, P535, P536, P537, P538, P539, P573, P586, P591, P619, P625, P636, P645, P662, P669, P673, P686, P690, P692, P698, P706, P708, P710, P712, P713, P714, P715, P716, P718

Clinical trial.....O4, O7, O8, O17, O18, O19, O21, O23, O24, O25, O26, O27, O28, O30, O31, O45, O47, O49, O50, O52, P15, P19, P26, P32, P47, P49, P54, P66, P68, P72, P85, P87, P90, P101, P115, P126, P136, P139, P142, P149, P150, P157, P159, P163, P173, P205, P212, P225, P240, P244, P246, P255, P272, P276, P285, P287, P288, P289, P290, P291, P293, P294, P295, P298, P299, P300, P302, P303, P304, P305, P306, P307, P309, P310, P311, P312, P313, P315, P318, P319, P320, P321, P322, P323, P324, P325, P326, P327, P328, P329, P330, P331, P332, P333, P334, P335, P336, P337, P338, P339, P340, P341, P342, P343, P346, P350, P355, P377, P387, P389, P391, P392, P393, P396, P397, P403, P408, P409, P416, P432, P451, P465, P484, P495, P507, P532, P542, P563, P572, P593, P609, P622, P651, P668, P669, P673, P690, P699, P706, P708, P709, P710, P711, P712, P713, P714, P715, P717, P719

Coinhibition.....O21, O36, O41, P97, P115, P286, P308, P349, P363, P365, P375, P376, P386, P397, P406, P450, P470, P477, P526, P541, P602, P646, P647, P661, P664, P671, P672, P676, P677, P678, P691, P694, P697, P715

Costimulation..... O15, O29, O32, O36, O44, P7, P37, P52, P97, P102, P143, P160, P176, P185, P203, P205, P216, P218, P236, P259, P275, P288, P295, P334, P356, P357, P358, P363, P364, P370, P373, P375, P382, P386, P390, P397, P398, P400, P402, P404, P405, P406, P407, P408, P409, P455, P491, P519, P521, P552, P562, P605, P631, P637, P646, P647, P656, P657, P658, P659, P661, P664, P674, P678, P682, P683, P704, P710

Cytokine..... O4, O22, O30, O31, O32, O33, O34, O36, O41, O52, P2, P8, P37, P44, P67, P68, P80, P99, P115, P118, P123, P126, P158, P174, P181, P185, P190, P196, P198, P203, P209, P211, P215, P225, P226, P227, P239, P241, P246, P247, P251, P252, P253, P257, P265, P271, P272, P277, P280, P285, P291, P294, P297, P298, P310, P312, P325, P348, P352, P364, P369, P383, P396, P397, P398, P405, P409, P410, P411, P412, P413, P414, P415, P416, P417, P418, P419, P420, P421, P422, P423, P424, P425, P437, P454, P460, P464, P468, P470, P482, P496, P500, P510, P513, P515, P519, P524, P527, P531, P541, P554, P556, P559, P564, P576, P600, P601, P609, P618, P621, P626, P647, P652, P657, P658, P660, P681, P705, P712, P713, P717, P721

Dendritic cell..... O28, O42, P14, P17, P25, P47, P124, P150, P153, P154, P158, P161, P166, P169, P173, P175, P176, P209, P260, P262, P272, P293, P335, P387, P390, P403, P406, P435, P446, P467, P509, P510, P515, P517, P518, P519, P520, P524, P528, P577, P597, P618, P622, P623, P632, P637, P682, P704, P709, P710, P713

Epidemiology.....P178, P397, P505, P585, P644

KEYWORD INDEX

Gene expression O5, O6, O9, O31, O32, P13, P14, P17, P19, P25, P35, P42, P48, P54, P62, P73, P76, P87, P91, P96, P98, P102, P110, P113, P129, P135, P136, P157, P158, P195, P198, P200, P201, P209, P220, P221, P228, P229, P236, P238, P239, P258, P265, P268, P284, P327, P348, P372, P379, P397, P406, P412, P428, P452, P454, P457, P460, P468, P475, P504, P520, P541, P555, P564, P579, P581, P582, P583, P584, P587, P591, P594, P596, P600, P605, P614, P618, P633, P634, P697, P708, P709, P718

Genetic polymorphism.....P81, P108, P598

Granulocyte O2, O35, P32, P223, P468, P495, P498, P517, P527, P532, P545

Immune adjuvant O8, O28, O44, P6, P148, P149, P150, P158, P161, P164, P166, P172, P200, P219, P235, P236, P293, P298, P309, P329, P334, P339, P342, P343, P344, P353, P387, P397, P410, P453, P460, P473, P485, P489, P601, P612, P619, P681, P712

Immune contexture.....O20, O35, O39, O49, P14, P18, P22, P38, P39, P40, P59, P61, P70, P74, P82, P90, P94, P95, P103, P113, P124, P132, P133, P157, P177, P233, P248, P268, P276, P294, P324, P377, P400, P401, P428, P429, P442, P492, P495, P496, P501, P522, P552, P559, P577, P578, P587, P592, P594, P595, P596, P605, P615, P627, P632, P654, P687, P703, P718

Immune monitoring O1, O2, O3, O4, O5, O7, O8, O16, O22, O43, O49, O51, O52, P4, P13, P15, P18, P22, P23, P24, P25, P26, P30, P32, P36, P37, P38, P39, P40, P41, P45, P48, P49, P50, P52, P56, P57, P59, P61, P64, P65, P66, P67, P68, P69, P70, P73, P77, P78, P79, P80, P81, P82, P83, P84, P85, P86, P87, P91, P92, P93, P94, P95, P97, P99, P103, P104, P106, P110, P111, P112, P114, P116, P117, P119, P120, P122, P124, P126, P127, P129, P132, P133, P139, P140, P141, P142, P143, P149, P150, P151, P162, P163, P225, P233, P248, P254, P256, P276, P290, P292, P293, P297, P298, P299, P307, P324, P342, P343, P348, P356, P357, P358, P388, P394, P397, P403, P408, P418, P429, P439, P451, P459, P463, P465, P467, P485, P489, P492, P494, P527, P531, P556, P558, P559, P588, P600, P609, P614, P641, P654, P663, P681, P682, P687, P688, P693, P695, P697, P705, P706, P708, P709, P710, P717, P718, P719, P721

Immune suppression O13, O14, O15, O22, O33, O35, O36, O37, O38, P5, P6, P16, P36, P37, P39, P53, P66, P70, P80, P84, P90, P99, P106, P110, P113, P118, P135, P139, P143, P145, P168, P175, P194, P197, P198, P201, P202, P203, P204, P205, P206, P209, P235, P244, P288, P300, P320, P321, P322, P323, P331, P334, P346, P352, P354, P359, P370, P371, P372, P377, P385, P390, P397, P401, P415, P429, P433, P435, P450, P466, P477, P478, P479, P480, P481, P482, P484, P485, P486, P487, P488, P489, P490, P491, P492, P493, P495, P498, P500, P502, P504, P510, P519, P522, P523, P528, P531, P532, P534, P535, P536, P537, P538, P541, P545, P546, P550, P551, P553, P555, P556, P560, P577, P580, P584, P587, P602, P607, P615, P617, P645, P652, P653, P654, P657, P663, P667, P668, P672, P673, P675, P678, P679, P685, P691, P696, P703, P705, P716, P719

Immune tolerance..... O9, O22, O41, P6, P20, P24, P55, P80, P90, P113, P118, P155, P167, P175, P180, P202, P206, P236, P316, P325, P397, P437, P450, P457, P478, P532, P533, P537, P544, P556, P587, P668, P672, P718, P719

Immune toxicity P6, P12, P16, P24, P81, P92, P108, P109, P187, P192, P194, P215, P303, P397, P407, P415, P447, P451, P457, P512, P521, P533, P534, P535, P536, P537, P538, P539, P540, P562, P563, P564, P566, P567,

KEYWORD INDEX

Immune toxicity (continued).....P568, P608, P618, P629, P630, P635, P643, P644, P645, P691, P702, P714, P720

Immunoscore.....O48, P18, P22, P59, P66, P74, P85, P114, P130, P439, P592, P638, P719

Inflammation.....O30, P30, P41, P44, P55, P66, P68, P79, P84, P118, P124, P175, P194, P209, P210, P234, P235, P368, P390, P397, P400, P406, P442, P447, P460, P468, P487, P494, P498, P510, P515, P521, P524, P525, P534, P559, P562, P564, P565, P578, P612, P613, P621, P639, P681, P691, P702, P718

Leukemia/Lymphoma.....O42, P5, P6, P61, P87, P111, P113, P195, P201, P212, P214, P231, P238, P240, P256, P262, P267, P270, P278, P279, P283, P285, P315, P327, P330, P369, P373, P401, P451, P475, P530, P609, P650, P656, P714

MDSC.....O2, O20, O38, P32, P93, P114, P118, P126, P127, P145, P175, P201, P202, P209, P244, P373, P390, P435, P453, P457, P465, P477, P486, P488, P491, P492, P494, P495, P498, P500, P502, P532, P545, P546, P553, P609, P632, P689, P714, P718

Metabolism.....O10, O11, O12, O13, O14, O35, P161, P176, P177, P196, P197, P198, P202, P203, P204, P205, P206, P207, P208, P209, P216, P254, P345, P370, P381, P397, P473, P488, P502, P504, P506, P507, P508, P513, P528, P531, P546, P605, P616, P719

Microbiome.....P194, P239, P505, P570, P571, P572, P573, P574, P575, P719

Monocyte/Macrophage.....O38, P6, P26, P32, P38, P40, P48, P62, P68, P99, P106, P111, P113, P114, P116, P161, P166, P175, P181, P197, P198, P209, P234, P235, P260, P335, P340, P352, P362, P368, P372, P373, P378, P406, P427, P429, P435, P446, P448, P458, P463, P468, P471, P487, P489, P494, P495, P496, P498, P500, P501, P509, P510, P512, P517, P519, P524, P529, P532, P541, P552, P576, P577, P580, P618, P628, P634, P637, P650, P652, P678, P681, P716

Myeloid cells.....O2, O20, O35, P32, P68, P93, P100, P111, P118, P175, P198, P202, P209, P234, P235, P244, P335, P340, P352, P373, P381, P401, P427, P435, P443, P444, P445, P446, P477, P486, P487, P488, P489, P491, P492, P494, P495, P498, P500, P509, P516, P517, P518, P524, P528, P532, P545, P546, P553, P577, P618, P632, P637, P650, P700, P706, P708, P716, P718

Neoantigens.....O1, O7, O8, O22, O47, O48, P13, P33, P49, P56, P65, P101, P129, P148, P151, P154, P156, P160, P164, P166, P169, P170, P174, P178, P180, P182, P183, P184, P188, P190, P210, P233, P239, P241, P252, P260, P262, P281, P307, P311, P314, P459, P469, P543, P570, P580, P582, P586, P587, P588, P589, P599, P622

NK/NK T cell.....O28, O32, O38, O40, O51, P3, P7, P14, P62, P68, P100, P123, P145, P167, P203, P217, P247, P254, P257, P258, P285, P288, P310, P348, P387, P398, P407, P411, P414, P415, P416, P417, P418, P419, P422, P423, P425, P457, P468, P474, P480, P483, P504, P511, P513, P514, P520, P522, P523, P525, P526, P530, P531, P544, P557, P561, P578, P597, P609, P617, P623, P628, P632, P656, P659, P666, P697, P712, P713

Pediatric tumors.....O20, O43, P2, P10, P121, P236, P237, P270, P459, P497, P584

KEYWORD INDEX

Proteomics.....P8, P20, P37, P38, P39, P40, P41, P42, P44, P66, P92, P106, P111, P112, P151, P269, P311, P389, P452, P459, P628, P675, P719, P721

Radiotherapy.....O50, P10, P26, P61, P170, P291, P302, P319, P332, P333, P347, P359, P362, P378, P384, P389, P410, P437, P449, P453, P455, P458, P459, P462, P463, P464, P465, P466, P469, P471, P473, P623, P713

Regulatory T cell (Treg cell).....O13, O19, O22, O29, O33, O36, O40, O44, O52, P11, P36, P62, P70, P99, P114, P123, P126, P127, P143, P144, P145, P154, P166, P180, P195, P252, P291, P316, P334, P346, P354, P361, P373, P388, P404, P405, P409, P415, P423, P424, P425, P427, P439, P448, P449, P453, P463, P481, P484, P485, P486, P487, P500, P501, P502, P600, P602, P609, P615, P641, P649, P653, P654, P666, P683, P693, P696, P697, P699, P700, P712, P718, P719

Solid tumors.....O2, O3, O4, O5, O6, O7, O8, O14, O15, O17, O18, O19, O20, O21, O24, O25, O26, O28, O30, O32, O35, O38, O41, O45, O47, O49, O51, O52, P2, P3, P9, P10, P11, P12, P14, P15, P17, P22, P26, P30, P33, P42, P43, P45, P48, P49, P53, P54, P58, P60, P62, P63, P66, P67, P70, P71, P72, P73, P75, P76, P77, P84, P85, P87, P91, P92, P94, P95, P97, P100, P102, P103, P105, P106, P107, P117, P123, P125, P126, P127, P128, P131, P133, P136, P137, P138, P140, P142, P143, P144, P146, P149, P150, P151, P152, P155, P157, P159, P161, P163, P167, P170, P173, P174, P178, P180, P183, P185, P186, P187, P189, P190, P191, P193, P197, P198, P199, P200, P203, P205, P206, P207, P210, P213, P214, P215, P216, P219, P222, P223, P224, P225, P226, P227, P233, P234, P235, P236, P237, P239, P241, P244, P246, P247, P249, P250, P251, P252, P253, P254, P255, P257, P259, P261, P263, P264, P266, P267, P268, P271, P272, P273, P274, P276, P277, P279, P288, P289, P290, P291, P292, P293, P294, P295, P298, P299, P302, P305, P306, P308, P312, P313, P316, P318, P319, P320, P321, P322, P323, P324, P326, P328, P329, P331, P332, P333, P335, P336, P337, P339, P340, P342, P343, P344, P346, P350, P353, P354, P361, P362, P363, P364, P376, P380, P386, P387, P388, P390, P391, P392, P393, P396, P399, P404, P407, P408, P409, P411, P415, P416, P417, P419, P421, P423, P426, P430, P431, P432, P433, P436, P437, P440, P442, P443, P446, P450, P453, P454, P456, P457, P458, P459, P463, P470, P471, P473, P475, P476, P479, P480, P482, P487, P491, P494, P497, P498, P500, P503, P504, P506, P507, P513, P516, P521, P522, P524, P526, P531, P542, P543, P545, P548, P549, P552, P555, P558, P559, P563, P573, P576, P577, P578, P579, P581, P582, P583, P585, P586, P589, P590, P591, P592, P594, P597, P600, P601, P602, P605, P608, P609, P612, P617, P618, P619, P622, P623, P626, P630, P631, P632, P635, P636, P637, P650, P651, P656, P660, P662, P664, P669, P673, P678, P682, P687, P690, P691, P692, P693, P698, P699, P700, P703, P707, P709, P710, P711, P713, P714, P715, P716, P718, P719, P721

Stem cell/cancer-initiating cell.....P201, P254, P444, P523, P600, P639, P681

Surgery..... P85, P117, P301, P303, P328, P339, P342, P343, P469, P562, P682

Systems biology..... P19, P20, P23, P29, P30, P58, P61, P70, P91, P103, P106, P110, P144, P145, P428, P429, P433, P473, P477, P581, P583, P587, P594, P687

T cell..... O1, O4, O7, O8, O9, O10, O12, O14, O15, O16, O17, O18, O19, O20, O21, O23, O28, O29, O31, O32, O33, O34, O36, O38, O40, O44, O46, O47, O49, O51, O52, P3, P5, P7, P8, P9, P14, P15, P22, P23, P26, P33, P36, P37, P38, P40, P43, P45, P49, P50, P51, P56, P62,

KEYWORD INDEX

T cell (continued).....P69, P72, P73, P76, P78, P80, P81, P82, P83, P84, P87, P91, P97, P99, P100, P102, P103, P106, P111, P114, P116, P120, P123, P129, P130, P132, P133, P139, P140, P143, P144, P148, P149, P150, P153, P154, P155, P156, P158, P159, P160, P161, P162, P164, P166, P167, P168, P169, P171, P172, P174, P175, P177, P179, P180, P183, P184, P185, P186, P187, P188, P194, P195, P196, P202, P203, P207, P209, P210, P211, P214, P215, P216, P219, P220, P221, P222, P223, P224, P225, P226, P227, P229, P230, P231, P232, P233, P238, P240, P241, P243, P244, P245, P246, P249, P250, P251, P252, P253, P256, P257, P259, P261, P262, P265, P268, P269, P270, P271, P272, P273, P276, P278, P280, P281, P283, P284, P289, P293, P295, P297, P298, P299, P300, P304, P305, P309, P310, P311, P325, P327, P334, P339, P345, P349, P351, P352, P354, P356, P357, P359, P360, P361, P363, P364, P366, P367, P368, P369, P370, P372, P373, P375, P377, P381, P382, P385, P386, P387, P388, P390, P394, P398, P399, P400, P401, P402, P404, P405, P406, P407, P408, P409, P411, P413, P414, P415, P416, P417, P419, P421, P422, P423, P425, P427, P428, P429, P433, P434, P439, P442, P443, P444, P450, P455, P456, P457, P463, P465, P467, P468, P469, P470, P472, P475, P476, P478, P479, P481, P482, P484, P486, P488, P494, P495, P496, P501, P519, P521, P522, P525, P534, P535, P536, P537, P546, P547, P552, P555, P556, P557, P565, P570, P574, P576, P577, P578, P579, P580, P582, P584, P588, P589, P590, P592, P597, P598, P599, P600, P602, P603, P605, P607, P608, P609, P613, P616, P617, P618, P624, P626, P628, P631, P632, P633, P634, P641, P648, P649, P653, P654, P656, P657, P658, P659, P660, P661, P663, P664, P665, P666, P667, P668, P671, P672, P674, P675, P676, P679, P681, P683, P684, P685, P687, P688, P690, P693, P695, P696, P697, P699, P700, P703, P704, P705, P706, P708, P709, P710, P712, P714, P717, P718, P721

T cell lineages..... O40, O44, O46, P82, P84, P120, P159, P164, P177, P250, P257, P299, P405, P417, P434, P442, P443, P444, P463, P556, P557, P578, P628, P634, P687, P718

Targeted therapy..... O18, O19, O21, O24, O28, O30, O37, O38, O48, O51, P5, P7, P8, P9, P10, P11, P17, P30, P34, P67, P69, P87, P88, P90, P95, P105, P115, P116, P133, P166, P172, P173, P174, P175, P176, P178, P185, P186, P187, P197, P200, P201, P205, P212, P217, P219, P221, P226, P229, P230, P231, P232, P236, P237, P246, P259, P261, P262, P271, P272, P276, P300, P304, P305, P306, P318, P332, P333, P335, P340, P348, P352, P354, P355, P360, P361, P369, P371, P373, P375, P377, P384, P385, P386, P387, P388, P391, P392, P393, P400, P405, P408, P413, P415, P438, P448, P449, P450, P451, P456, P457, P458, P459, P464, P474, P477, P482, P486, P488, P489, P511, P513, P523, P530, P531, P554, P561, P585, P592, P596, P597, P602, P604, P605, P606, P608, P612, P619, P620, P626, P631, P634, P637, P662, P675, P691, P715, P716

TLR..... P22, P25, P150, P164, P172, P235, P273, P288, P293, P299, P327, P337, P344, P364, P367, P378, P399, P435, P453, P468, P545, P547, P557, P607, P618

Tumor antigens..... O1, O3, O7, O8, O18, O48, P1, P4, P8, P10, P17, P49, P56, P69, P82, P129, P140, P144, P148, P149, P154, P155, P156, P158, P160, P161, P163, P164, P166, P167, P172, P173, P174, P178, P180, P181, P183, P185, P186, P189, P190, P196, P200, P210, P219, P221, P225, P226, P230, P232, P233, P237, P239, P241, P246, P249, P251, P252, P253, P259, P261, P262, P267, P270, P272, P274, P276, P281, P310, P311, P351, P366, P372, P375, P386, P399, P400, P433, P438, P439, P459, P469, P472, P519, P528, P530, P588, P589, P590, P593, P599, P601, P608, P613,

KEYWORD INDEX

Tumor antigens (continued).....P622, P641, P657, P658, P678, P693, P705, P711, P713, P718

Tumor evasion.....O14, O32, O38, O39, O41, P13, P36, P55, P70, P80, P84, P99, P106, P113, P143, P187, P198, P199, P203, P204, P257, P259, P315, P320, P321, P322, P323, P325, P335, P340, P342, P346, P354, P368, P386, P401, P404, P428, P429, P435, P445, P450, P478, P482, P484, P489, P492, P494, P499, P504, P515, P522, P530, P531, P541, P544, P545, P546, P547, P551, P552, P555, P556, P557, P558, P559, P561, P576, P577, P578, P579, P580, P582, P587, P593, P600, P601, P617, P652, P654, P667, P672, P673, P676, P679, P718

Tumor infiltrating lymphocytes (TILs).....O4, O9, O12, O13, O14, O16, O22, O31, O32, O33, O36, O39, O40, O41, O46, O47, O49, O51, P4, P9, P11, P14, P22, P25, P33, P38, P39, P40, P43, P45, P51, P53, P62, P65, P67, P73, P78, P83, P84, P90, P91, P96, P97, P98, P99, P100, P102, P103, P104, P106, P114, P116, P117, P120, P124, P126, P127, P129, P130, P131, P132, P133, P139, P140, P143, P144, P145, P152, P155, P157, P158, P160, P162, P168, P170, P175, P184, P205, P206, P207, P210, P222, P223, P224, P233, P235, P236, P239, P241, P243, P244, P248, P250, P251, P252, P253, P257, P261, P268, P273, P281, P316, P325, P327, P339, P340, P345, P348, P349, P351, P352, P354, P356, P363, P364, P367, P368, P369, P370, P371, P375, P378, P379, P382, P383, P386, P388, P399, P400, P402, P404, P406, P407, P408, P414, P415, P417, P421, P428, P429, P433, P435, P436, P437, P439, P442, P443, P446, P450, P459, P462, P463, P467, P469, P470, P472, P474, P475, P477, P479, P480, P481, P485, P486, P488, P493, P494, P496, P500, P501, P520, P522, P530, P541, P542, P543, P546, P550, P553, P555, P557, P572, P574, P576, P578, P582, P584, P587, P588, P590, P594, P600, P601, P602, P605, P606, P607, P612, P613, P614, P616, P618, P622, P623, P631, P632, P638, P639, P641, P647, P649, P653, P654, P658, P660, P664, P666, P672, P676, P678, P682, P684, P685, P687, P693, P696, P700, P703, P709, P718, P719, P721

Tumor microenvironment..... O4, O5, O6, O9, O10, O11, O12, O13, O14, O15, O19, O20, O22, O27, O30, O31, O32, O33, O35, O36, O37, O38, O40, O41, O49, P3, P5, P13, P18, P20, P22, P25, P33, P35, P36, P38, P39, P40, P42, P43, P45, P48, P53, P54, P55, P59, P61, P62, P67, P69, P70, P73, P76, P77, P78, P83, P84, P85, P87, P90, P91, P94, P95, P98, P100, P102, P103, P106, P108, P113, P114, P116, P117, P120, P121, P124, P126, P127, P128, P129, P131, P132, P133, P138, P140, P142, P144, P146, P147, P151, P158, P160, P161, P170, P175, P177, P181, P187, P197, P198, P200, P201, P202, P203, P204, P205, P207, P208, P209, P210, P211, P216, P226, P233, P234, P235, P236, P237, P239, P249, P254, P255, P268, P271, P272, P276, P288, P292, P299, P316, P318, P320, P321, P322, P323, P325, P328, P335, P337, P338, P339, P340, P342, P343, P345, P346, P348, P349, P351, P352, P354, P356, P357, P358, P359, P363, P367, P368, P370, P371, P372, P373, P375, P377, P378, P381, P382, P383, P388, P389, P390, P391, P392, P393, P399, P401, P404, P407, P408, P409, P410, P412, P427, P428, P429, P433, P435, P437, P439, P440, P442, P445, P446, P448, P449, P450, P453, P455, P457, P458, P459, P460, P463, P468, P469, P474, P475, P476, P477, P479, P480, P481, P482, P483, P484, P485, P486, P487, P488, P489, P490, P491, P492, P494, P495, P496, P497, P499, P501, P502, P503, P506, P507, P509, P513, P515, P517, P518, P520, P522, P523, P525, P526, P530, P531, P541, P544, P545, P546, P549, P550, P552, P555, P556, P557, P558, P559, P560, P564, P569, P572, P576, P577, P578, P579, P580, P582, P583, P584, P587, P588, P590, P592, P594, P595, P597, P598, P600, P601, P602, P605, P607, P608, P609, P610, P612, P613, P615, P621, P622, P623, P624, P627, P631, P632,

KEYWORD INDEX

Tumor microenvironment (continued)……P637, P638, P639, P640, P641, P648, P649, P650, P652, P654, P659, P660, P664, P665, P666, P667, P668, P672, P673, P678, P681, P682, P686, P687, P693, P696, P699, P703, P709, P710, P712, P716, P717, P718, P719

Tumor stroma.....P18, P22, P39, P67, P73, P84, P90, P102, P114, P116, P121, P131, P132, P135, P138, P144, P147, P160, P198, P200, P201, P236, P349, P368, P413, P428, P429, P433, P439, P440, P442, P458, P463, P479, P482, P486, P487, P488, P489, P492, P498, P501, P515, P526, P546, P555, P578, P592, P608, P637, P639, P640, P654, P703, P719

Vaccine.....O7, O8, P2, P17, P49, P149, P150, P153, P155, P156, P157, P158, P159, P161, P162, P163, P164, P168, P170, P171, P172, P173, P174, P175, P176, P177, P178, P181, P182, P183, P184, P185, P189, P190, P219, P260, P307, P310, P311, P314, P327, P334, P339, P353, P356, P357, P358, P372, P419, P424, P453, P558, P602, P605, P614, P617, P621, P709, P711, , P712

REGULAR ORAL ABSTRACT PRESENTATIONS

Biomarkers and Immune Monitoring

O1

Identification and profiling of neoantigen-specific T cells in NSCL cancer patients treated with atezolizumab

Michael Fehlings[1], Suchit Jhunjhunwala, BS, PhD[2], Marcin Kowanetz, PhD[2], Bill O'Gorman[2], Priti Hegde, PhD[2], Jessica Li, Master of Science[2], Hermi Sumatoh[1], Boon Heng Lee[1], Alessandra Nardin, DVM[1], Mahesh Yadav, PhD[2], Leesun Kim[2], Susan Flynn[2], Marcus Ballinger, PhD[2], Evan Newell, PhD[3]

[1]immunoSCAPE, Singapore, Singapore
[2]Genentech, South San Francisco, CA, USA
[3]SiGN, Singapore, Singapore

Background
There is strong evidence that immunotherapy-mediated tumor rejection is associated with the reinvigoration of tumor-specific CD8+ T cells most likely recognizing neoantigens derived from tumor somatic mutations. However, despite a substantial number of mutations present in some tumors, only a small fraction of neoantigens have been shown to be immunogenic, partly due to the challenge in identifying rare neoantigen-specific CD8+ T cells in tumor-bearing individuals.

Methods
We employed mass cytometry and highly-multiplexed combinatorial tetramer staining together with cellular barcoding and high-dimensional phenotypic characterization to longitudinally monitor neoantigen-specific CD8+ T cells in PBMC from 14 NSCL cancer patients treated with atezolizumab. Close to 800 candidate tumor neoantigens and 73 viral-derived control peptides were screened across all patient samples; T cells were simultaneously profiled using 30 or more markers.

Results
Virus-specific T cells were detected in most patient samples at frequencies as low as 0.004% of total CD8+ T cells. T cells reactive for 13 different neoantigens were also identified with a medium to high confidence across all patients and time points. Interestingly, the majority of medium-to-high confidence hits (9/13) were detected among the 8 patients who presented an objective response to treatment, with only 4 of the 13 hits detected in the 6 patients with progressive disease. The neoantigen-specific cells differed phenotypically from bulk CD8+ T cells in the peripheral blood and displayed a diverse phenotype.

Conclusions
This study demonstrates the utility of the use of mass cytometry together with a combinatorial tetramer staining for the ex vivo identification, characterization, and longitudinal follow-up of rare tumor-specific T cells. Importantly, it suggests that the detection of neoantigen-specific T cells may be used as a predictor of response to checkpoint blockade and supports further research into this.

Trial Registration
NCT01903993

References
1. Atezolizumab versus docetaxel for patients with previously treated non-small-cell lung cancer (POPLAR): a multicentre, open-label, phase 2 randomised controlled trial The Lancet. Volume 387, No. 10030, p1837–1846, 30 April 2016

Ethics Approval
This study was performed on de-identified samples from POPLAR trial, a multicentre, randomized, open-label, allcomer, multicenter phase 2 trial. The

POPLAR trial was performed in full accordance with the guidelines for GCP and the Declaration of Helsinki. Protocol; approval was obtained from an independent ethics committee for each trial site.

Consent

All patients gave appropriate ethical approval for this analysis. Statements confirming compliance with ethical regulations, the committees that approved the POPLAR study protocol, and confirmation of informed consent from all study participants are included in the previous publications describing the POPLAR trial [1].

O2

Using artificial intelligence to distinguish subjects with prostate cancer (PCa) from benign prostate hyperplasia (BPH) through immunophenotyping of MDSCs and lymphocyte cell populations

John Roop[1], Alex Polo[1], Anthony Campisi, BS[1], Dmitry Gabrilovich, MD, PhD[2], Amit Kumar, PhD[1], George Dominguez, PhD[1*]

[1]*Anixa Biosciences, San Jose, CA, USA*
[2]*The Wistar Institute, Philadelphia, PA, USA*

Background

Myeloid-derived suppressor cells (MDSCs) are key contributors in supporting tumor progression and tumor escape through their ability to suppress anti-tumor responses mediated through T cell and natural killer (NK) cell activity [1,2]. Several studies have quantified MDSCs to detect tumor development, monitor progression, and/or predict therapeutic responses [3, 4]. The objective of this study was to determine if flow cytometry data analysis of MDSCs and other leukocytes could be incorporated with a supervised machine learning classifier to identify individuals presenting either with a prostate malignancy (PCa) or benign condition (such as benign prostate hyperplasia or BPH).

Methods

We used standard multiparametric flow cytometry techniques to immunophenotype MDSCs and other leukocytes found in the peripheral blood of 73 PCa, 48 BPH, and 73 control subjects; all prostate pathologies were confirmed with a transrectal ultrasound guided prostate (TRUSP) biopsy. Subjects were excluded if they had a previous history of cancer (not including subjects under active surveillance), had a medical intervention for prostate cancer, or were receiving a dihydrotestosterone (DHT) or alpha-1 blocker for active treatment of BPH. Next, a series of neural networks were created with inputs consisting of the numerical event counts from the flow cytometry FCS file (fluorescent or scatter intensity values). Three datasets were constructed: the training dataset – to 'teach' two output categories through backpropagation and parameter fitting; the validation dataset – to evaluate the fit to minimize overfitting; and the test dataset – to rank the trained networks against each other and estimate the classification performance. Finally, a naïve testing set (i.e. never seen by the network) was used to determine the overall performance of the top-ranking networks after voting.

Results

With this approach, we were able to distinguish PCa subjects (both high and low grade) from control subjects with 91.7% accuracy (AUROC = 0.929; 95% CI: 0.8418 to 1.016). Using the same approach, we can further identify PCa from BPH subjects with 87.5% accuracy (AUROC = 0.869; 95% CI: 0.7938 to 0.9442).

Conclusions

By pairing supervised machine learning with the immunophenotyping of MDSCs and other leukocytes using flow cytometry, we have developed a novel method for distinguishing PCa from control or BPH subjects with high levels of accuracy. We believe this methodology could be used to predict patient

responses to immunotherapies and/or to monitor tumor recurrence.

References

1. Kumar V, Patel S, Tcyganov E, Gabrilovich D. The nature of myeloid-derived suppressor cells in the tumor microenvironment. Trends Immunol. 2016; 37:208-220.
2. Marvel D, Gabrilovich D. Myeloid-derived suppressor cells in the tumor microenvironment: expect the unexpected. J Clin Invest. 2015; 125:3356-3364.
3. Elliott L, Doherty G, Sheahan K, Ryan E. Human tumor-infiltrating myeloid cells: phenotypic and functional diversity. Front Immunol. 2017; 8:86.
4. Okla K, Wertel I, Wawruszak A, Bobinski M, Kotarski J. Blood-based analyses of cancer: circulating myeloid-derived suppressor cells – is a new era coming? Crit Rev Clin Lab Sci. 2018.

Ethics Approval

The study was approved by The Wistar Institute's Institutional Review Board, protocol number 21802305.

O3

Anti-tumor immune responses in metastatic breast cancer exceptional responder patients

Alusha Mamchak, PhD[1], Ngan Nguyen, PhD[1], Danhui Zhang, MD PhD[1], Felix Chu, MS[1], Mike Harbell, BS[1], Beatriz Millare, BS[1], Kevin Williamson[1], Xiaomu Chen[1], Xiaobin Tang[1], Shuwei Jiang[1], Dongkyoon Kim, BS PhD[1], Nicole Hasser[1], Sarah Hippely[2], Maren Levin[2], Amy Manning-Bog, PhD[1], Jeff DeFalco[1], william Robinson, MD[1], Daniel Emerling, PhD[1], Norman Greenberg, PhD[1], Guy Cavet, PhD[1], Joyce O'Shaughnessy, MD[2]

[1]*Atreca Inc, Redwood City, CA, USA*
[2]*Baylor University Medical Center, Dallas, TX, USA*

Background

Analyzing anti-cancer immune responses can offer insights into the mechanisms that underlie successful cancer therapies. While the role of T cell immunity in anti-cancer responses has been well characterized, the role of the humoral immune response to cancer remains less clear. Thus, we set out to identify anti-tumor antibodies from 11 metastatic breast cancer (MBC) patients who had exceptional responses to systemic therapy with multi-year benefit, all of whom were disease-free or long-term non-progressors. The patients' breast cancers were diverse with respect to hormone receptor status, HER2 status, and treatment history.

Methods

We used flow cytometry to isolate plasmablasts, which are antibody secreting cells produced in lymphoid tissues through activation, affinity maturation, and differentiation of antigen-specific naive and memory B cells. Natively paired IgG sequences were generated from individual cells using Immune Repertoire Capture® (IRC™) technology. Similar immunoglobulin sequences were grouped into putative antibody lineages based on germline gene usage and CDR3 sequence features.

Results

A total of 9160 native pairs of expression-ready, heavy and light chain immunoglobulin sequences were generated. The antibody sequences were grouped into putative clonal lineages, with 931 of these lineages being expressed by two or more plasmablasts, providing evidence of selection and expansion. Comparison of the immunoglobulin repertoires across patients revealed several cases in which similar families of antibodies were identified in more than one patient, suggesting convergent selection. Antibodies in the putative convergent families were predominantly IgG2 (86%) which was significantly higher than the frequency of IgG2 in non-convergent lineages.By computationally selecting immunoglobulin sequences and expressing

them as recombinant proteins, patient-derived antibodies were identified that bind to human and mouse cancer cell lines, including human breast and lung cancer, and tissues derived from xenogeneic murine models of human breast and prostate cancer. In addition, several antibodies were shown by immunohistochemistry to bind specifically to non-autologous human breast cancer tissue but not to adjacent breast tissue.

Conclusions

Through the use of IRC™ technology and antibody binding assays, the humoral immune response in MCB exceptional responder patients has been quantified. Of particular interest, this study has identified patient derived-antibodies that bind specifically to non-autologous breast cancer tissue and have potential to form the basis of new cancer therapeutics.

O4

Immune monitoring after NKTR-214 plus nivolumab (PIVOT-02) in previously untreated patients with metastatic Stage IV melanoma

Adi Diab, MD[1], Scott Tykodi[2], Brendan Curti, MD[3], Daniel Cho, MD[4], Michael Wong, MD PhD FRCPC[1], Igor Puzanov, MD, MSCI, FACP[5], Karl Lewis, MD[6], Michele Maio, MD, PhD[7], Gregory Daniels, MD, PhD[8], Alexander Spira, MD, PhD, FACP[9], Mary Tagliaferri, MD[10], Alison Hannah, MD[10], Wendy Clemens, PhD[10], Michael Imperiale[10], Chantale Bernatchez[1], Cara Haymaker, PhD[1], Salah Eddine Bentebibel[11], Jonathan Zalevsky, PhD[10], Ute Hoch, PhD[10], Christie Fanton, PhD[10], Ahsan Rizwan, MPharm, PhD[10], Sandra Aung, PhD[10], Fiore Cattaruzza[10], Ernesto Iaccucci[10], Dariusz Sawka[12], Mehmet Bilen, MD[13], Paul Lorigan[14], Giovanni Grignani[15], James Larkin, MD[16], Sekwon Jang, MD[17], Ewa Kalinka-Warzocha, PhD, MD[18], Mario Sznol, MD[19], Michael Hurwitz, MD, PhD[19]

[1]The University of Texas MD Anderson Cancer Center, Houston, TX, USA
[2]University of Washington and Fred Hutchinson Cancer Research Center, Seattle, WA, USA
[3]Providence Cancer Institute and Earle A. Chiles Research Institute, Portland, OR, USA
[4]NYU Medical Oncology Associates, New York, NY, USA
[5]Roswell Park Cancer Institute, Buffalo, NY, USA
[6]University of Colorado Denver, Aurora, CO
[7]Azienda Ospedaliera Universitaria Senese, Siena, Italy
[8]Moores Cancer Center, University of California San Diego, La Jolla, CA, USA
[9]Virginia Cancer Specialists, PC, Fairfax, VA, USA
[10]Nektar Therapeutics, San Anselmo, CA, USA
[11]The University of Texas MD Anderson Canc, Houston, TX, USA
[12]Szpital Specjalistyczny w Brzozowie Podkarpacki Osrodek Onkologiczny, Brzozów, Poland
[13]Emory University Hospital (Winship Cancer Institute), Atlanta, GA, USA
[14]The Christie NHS Foundation Trust, Manchester, UK
[15]Institute for Cancer Research and Treatment (IRCC), Candiolo, Italy
[16]The Royal Marsden, London, UK
[17]Inova Schar Cancer Institute, Fairfax, VA, USA
[18]Instytut Medyczny Santa Familia, Lodz, Poland
[19]Yale School of Medicine, New Haven, CT, USA

Background

In patients with melanoma, low levels of tumor-infiltrating lymphocytes and low/absent PD-L1 expression are associated with limited response to anti-PD-1/anti-PD-L1 therapies. NKTR-214 (IL-2Rβγ-biased cytokine) monotherapy stimulates proliferation and activation of lymphocytes in blood and tumor and increases PD-1/PD-L1 expression. The impact of NKTR-214 and nivolumab on the systemic immune system and local tumor microenvironment is presented.

Methods
The melanoma cohort is closed; 41 patients were enrolled with 38 evaluable for efficacy (≥1 follow-up scan). Tumor biopsies were analyzed using multispectral IHC, gene expression, and TCR sequencing. Flow cytometry and hematology were used to evaluate blood cells. PD-L1 expression was evaluated using DAKO, 28-8 PharmDx Assay.

Results
Immune monitoring of blood revealed clear activation of the IL-2 pathway following administration of NKTR-214 plus nivolumab. Lymphocyte numbers increased 9x (N=41) from nadir reaching their peak 7 days post dose and maintained that magnitude of increase after each cycle. The proportion of proliferating (Ki67+, n=12) CD4+, CD8+, and NK cells increased 13x, 20x, and 6x over baseline, respectively. Similar immune activation was reported with NKTR-214 monotherapy (8x, 8x, and 7x over baseline, respectively). Immune cells demonstrated an antigen-experienced phenotype with an increased proportion of HLA-DR expression on CD4+, CD8+, and NK cells 3x, 2x, and 6x over baseline, respectively. ICOS levels increased 2x on CD8+ T cells. Baseline and week 3 biopsies (n=12, evaluable) showed local effects on the tumor microenvironment including elevated expression of PD-L1 on the tumor (patients converted from PD-L1 negative to positive), increased total numbers of CD8 infiltrate, and increased proportion of proliferating cells all ranging from 6-17x over baseline. Following treatment, intratumoral gene expression analyses showed elevations in networks associated with the NKTR-214 mechanism of action, including induction of an interferon-gamma gene signature. The investigator-assessed objective response rate as of 12 July 2018 was 50% (N=38), and no responder has relapsed. Deepening of response was observed over time and was associated with immune activation, consistent with the MOA of NKTR-214 plus nivolumab. The median duration of response has not been reached.

Conclusions
NKTR-214 is a robust agonist of the IL-2 pathway and together with nivolumab promotes immune activation in the periphery and tumor microenvironment for significant clinical activity. A global phase 3 trial in treatment-naïve advanced melanoma patients of NKTR-214 plus nivolumab versus nivolumab (1:1) will be open for enrollment in 2018.

Trial Registration
Clinicaltrials.gov NCT02983045 (PIVOT-02)

O5 Abstract Travel Award Recipient

B-cells and tertiary lymphoid structures (TLS) predict response to immune checkpoint blockade (ICB)

Sangeetha Reddy, MD, MSci[1], Beth Helmink, MD PhD[1], Jianjun Gao, MD PhD[1], Shaojun Zhang, PhD[1], Keren Yizhak[2], Moshe Sade-Feldman[3], Jorge Blando, DVM[1], Guangchun Han[1], Vancheswaran Gopalakrishnan, MPH, PhD[1], Hao Zhao[1], Wenbin Liu[1], Hussein Tawbi, MD, PhD[1], Rodabe Amaria, MD[1], Michael Davies, MD, PhD[1], Patrick Hwu, MD[1], Jeffrey Lee, MD[1], Jeffrey Gershenwald, MD[1], Scott Woodman[1], Elizabeth Burton[1], Lauren Haydu, MS, BChe, MIPH[1], Alexander Lazar, MD, PhD[1], Courtney Hudgens, MS[1], Alexandria Cogdill, MEng[1], Oscar Krijgsman, PhD[4], Elisa Rozeman, MD[4], Daniel Peeper, PhD[4], Christian Blank, MD[4], Ton Schumacher, PhD[4], Emily Keung[1], Pierre-Olivier Gaudreau[1], Alexandre Reuben[1], Christine Spencer, PhD[1], Lisa Butterfield, PhD[5], James Allison, PhD[1], Michael Tetzlaff, MD PhD[1], Florent Petitprez, MS[6], Wolf Herman Fridman, MD, PhD[6], Catherine Sautes-Fridman, PhD[6], Nir Hacohen, PhD[2], Padmanee Sharma, MD, PhD[1], Linghua Wang, PhD[1], Jennifer Wargo, MD, MMSc[1]

[1]MD Anderson Cancer Center, Houston, TX, USA
[2]Broad Institute, Cambridge, MA, USA

[3]*Massachusetts General Hospital, Boston, MA, USA*
[4]*The Netherlands Cancer Institute, Netherlands, Netherlands*
[5]*University of Pittsburgh Medical Center, Pittsburgh, PA, USA*
[6]*Centre de Recherche des Cordeliers, Paris, France*

Background
Mutational load, cytotoxic T-cell markers, and PD-L1 have been identified as biomarkers of response to ICB. However, there is a growing understanding of the contribution of B-cells in shaping response to ICB. We conducted a neoadjuvant ICB trial in patients with high-risk resectable melanoma ((NCT02519322), and identified B-cell signatures in responders by protein expression profiling.

Methods
To further investigate this, we performed transcriptomic profiling of longitudinal specimens in this melanoma cohort. Differentially expressed genes (DEG) were assessed in baseline samples with adequate tumor purity. Targeted immune profiling was further performed using immune deconvolution tool MCP-counter in all baseline and on-treatment samples, with additional validation from a metastatic renal cell carcinoma (RCC) trial of ICB (NCT02210117) and the melanoma TCGA dataset. Cases were dichotomized by CD8 T-cell scores to study interaction between B- and T-cells. Singlet and multiplex immunohistochemistry assessed spatial organization of the tumor infiltrating B-cells. Single cell RNA sequencing was performed in an independent cohort of metastatic melanoma patients treated with ICB.

Results
The most DEG at baseline in melanoma responders to ICB were B-cell related genes such as MZB1, BTLA, and IGLL5 (NR) ($p<0.0001$ for all). B-cell signatures were confirmed by a targeted immune gene assessment using MCP-counter, showing higher B lineage signatures among responders at baseline ($p=0.036$) and on-treatment ($p=0.038$). Among baseline cases, B-cells were more strongly predictive among CD8 T-cell low subsets ($p=0.085$) compared to T cell high ($p=0.833$). The applicability of these findings to other tumors was demonstrated in an RCC cohort, in which B lineage scores was predictive of response ($p=2.6e-03$), and differential effects were again seen between CD8 T-cell low ($p=0.008$) and high cases ($p=0.564$). In the melanoma TCGA, B-cell lineage score was correlated with improved survival ($p<0.0001$ for overall and disease-specific survival), in particular in CD8 T-cell low cases including after multivariable adjustment ($p=0.001$ for overall survival and 0.006 for disease-specific survival). Single cell sequencing in an independent melanoma cohort identified DEG within B-cells by response, providing insights into B-cell phenotypes associated with outcomes. Assessment of tissue sections from tumor samples in the neoadjuvant melanoma ICB cohort demonstrated co-localization of the B cells in TLS with CD8 and CD4 T-cells and CD21 follicular dendritic cells. The ratio of tumor area occupied by TLS was higher in responders ($p=0.037$ at baseline and 0.002 on-treatment).

Conclusions
Together, these results highlight the potential significance for B-cell signatures as prognostic and predictive factors for response to ICB.

O6

Comparison of biomarker assay modalities in anti-PD-(L)1 monotherapy: a meta-analysis

Steve Lu, BS[1], Steve Lu, BS[1], Ludmila Danilova, PhD[2], David Rimm, MD, PhD[3], Clifford Hoyt, MS[4], Matthew Hellmann, MD[5], Janis Taube, MD[1]

[1]*Johns Hopkins University School of Medicine, Baltimore, MD, USA*
[2]*Johns Hopkins Medical Institutions, Baltimore, MD, USA*

[3]*Yale University School of Medicine, New Haven, CT, USA*
[4]*PerkinElmer, Hopkinton, MA, USA*
[5]*Memorial Sloan Kettering Cancer Center, New York, NY, USA*

Background
Substantial effort is ongoing to identify predictors of response to immunotherapy. Numerous PD-L1 immunohistochemistry (IHC) assays are now FDA-approved. More recent biomarker approaches include the assessment of tumor mutational burden (TMB), gene expression profiling (GEP) and quantitative and/or spatial assessment of multiple proteins by multiplex IHC/immunofluorescence (mIHC/IF). The purpose of this project was to determine the relative sensitivity and specificity of these modalities.

Methods
We performed a meta-analysis of the association between overall response rate to anti-PD(L)1 monotherapy and PD-L1 IHC, TMB, GEP, or mIHC/IF. For PD-L1 IHC, only clinical trials that resulted in FDA-approved indications for anti-PD-(L)1 monotherapy were included. Due to the earlier development phase of TMB, GEP, and mIHC/IF, all identified publications or meeting abstracts using these modalities were included. Results were filtered to ensure that each study/data set was represented only once. Studies focused on MSI-high tumors were not included in the TMB category. For each individual study, the specificity, sensitivity, negative and positive predictive values (NPV and PPV) were determined according to each individual study's scoring algorithm of a positive vs. negative test. Summary receiver-operating characteristic (sROC) curves corresponding to each of the modalities were generated with each study 1) weighted equally (i.e. unweighted) and 2) weighted by patient specimen number tested.

Results
7454 patient specimens representing 10 different solid tumor types were assayed, and the results were correlated with anti-PD-(L)1 response. This data was derived from n=25 reports that tested PD-L1 IHC, n=11 for TMB, n=6 for GEP, and n=5 for mIHC/IF. When each modality was evaluated with sROC curves, PD-L1 had the lowest predictiveness (unweighted AUC 0.664, weighted AUC 0.659) followed by TMB (unweighted AUC 0.732, weighted AUC 0.708, Figure 1A, 1B). Although GEP and mIF/IHC had the least data available, they had the highest AUCs (unweighted AUC 0.859 and 0.821, weighted AUC 0.877 and 0.785, respectively, Figure 1A, 1B). Most modalities provide relatively high NPV, but mIHC/IF also demonstrates high PPV.

Conclusions
Several distinct biomarkers have predictive value in identifying patients most likely to respond to PD-(L)1 therapy. TMB has modestly better performance relative to PD-L1 IHC, and newer approaches such as GEP and mIHC/IF may have improved sensitivity and specificity. Further studies are needed to determine the most predictive analytes and scoring algorithms, and to assess whether biomarker performance varies by tumor type. Composite approaches including more than one of these modalities may perform better than any single modality alone.

Ethics Approval
The study was approved by the Johns Hopkins University Institutional Review Board.

Figure 1.

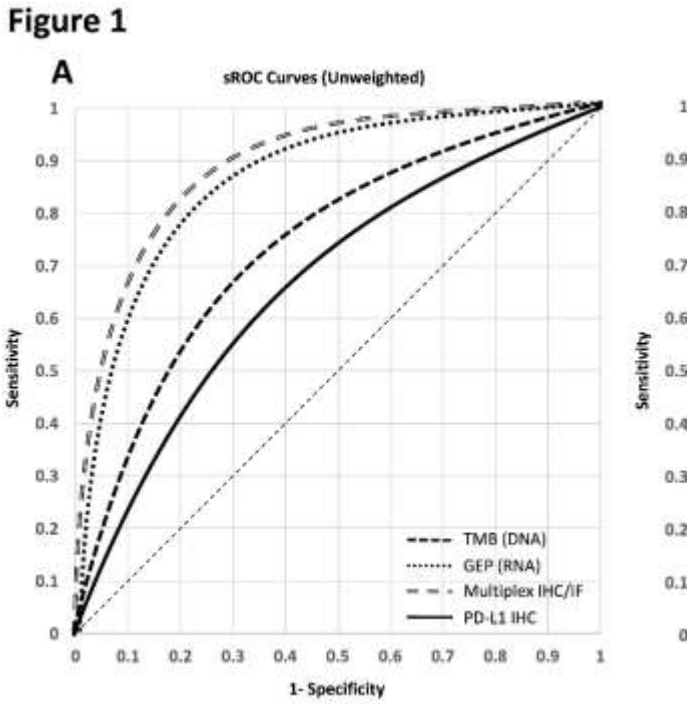

Cancer Vaccines, Personal Vaccines and Technologies/Personalized Medicine

O7

The personal vaccine, NEO-PV-01 with anti-PD1, induces neoantigen-specific de novo tumor-related immunity in patients with advanced cancer

Siwen Hu-Lieskovan, MD, PhD[2], Ramaswamy Govindan, MD[3], Aung Naing, MD, FACP[4], Terence Friedlander, MD[5], Kim Margolin, MD[6], Jessica Lin, MD[7], Nina Bhardwaj, MD, PhD[8], Matthew Hellmann, MD[9], Lakshmi Srinivasan[1], Joel Greshock[1], Melissa Moles[1], Richard Gaynor, MD[1], Matthew Goldstein, MD, PhD[1], Patrick Ott, MD, PhD[10]

[1]Neon Therapeutics, Inc, Cambridge, MA, USA
[2]Ronald Reagan UCLA Medical Center, Los Angeles, CA, USA
[3]Washington University Medical School, Saint Louis, MO, USA
[4]MD Anderson Cancer Center, Houston, TX, USA
[5]Division of Hematology/Oncology, UCSF, San Francisco, CA
[6]City of Hope, Duarte, CA, USA
[7]Massachusetts General Hospital, Boston, MA, USA
[8]Icahn School of Medicine at Mount Sinai, New York, NY, USA
[9]Memorial Sloan Kettering Cancer Center, New York, NY
[10]Dana Farber Cancer Institute, Boston, MA, USA

Background

Neoantigens arise from DNA mutations in cancer cells and are important targets for T cell mediated anti-tumor immunity. NEO-PV-01 is a personal neoantigen vaccine of up to 20 peptides designed based on a patient's neoantigen and HLA profile that is directed at inducing tumor-specific T cell responses to neoantigens. We report clinical and immune data from NT-001, a phase 1b study of NEO-PV-01 + adjuvant in combination with nivolumab in metastatic melanoma, NSCLC and bladder cancer (ClinicalTrials.gov: NCT02897765).

Methods

After 12 weeks of nivolumab treatment, patients received NEO-PV-01 vaccine plus adjuvant poly-ICLC in a prime-boost format spanning 12 weeks. The primary endpoint is safety; secondary endpoints include overall response rate (ORR) and the rate of post-vaccination responses. Comprehensive genomic and immune assessments were performed with serial biopsies and apheresis before and after vaccination to characterize treatment-related immune response in each patient.

Results

In 31 patients across tumor cohorts, all vaccine-related AE's were grade 1/2, with the most frequent being injection site reactions and fatigue. There were no vaccine-related SAEs. Among the 13 melanoma patients who received the full vaccine course at the

time of data cut, the ORR was 62% (8/13), of which two responses were seen post-vaccination. A total of 11/13 (85%) vaccinated melanoma patients remain on treatment with a median duration of 41.3 weeks (range = 29.6-62.0 weeks). ORR's were 33% (1/3) for both the NSCLC and bladder cohorts with a median time on treatment of 39.0 and 31.9 weeks respectively. Notably, one NSCLC patient who had stable disease on nivolumab alone had a partial response post-vaccination. Serial immune analysis completed on 10 melanoma patients demonstrated CD4 and CD8 T cell responses against 58% of vaccine peptides as measured by via IFNγ ELISpot. T cell responses were neoantigen-specific for 86% (12/14) of peptides tested. Most T cell responses were polyfunctional, producing multiple cytokines and were of a memory phenotype. Epitope spreading, defined by post-vaccination T cell responses to neoantigens not included in the vaccine, was observed in 4/6 (67%) melanoma patients analyzed. Multi-platform assessments of immune response, including serial exome sequencing and TCR repertoire analysis of tumor biopsies will be presented.

Conclusions
Treatment with NEO-PV-01 + adjuvant and nivolumab was well tolerated and demonstrated evidence of clinical activity. In addition, this combination induced broad de novo neoantigen-specific immune responses in metastatic cancers.

O8

The GAPVAC approach of actively personalized peptide vaccination for patients with newly diagnosed glioblastoma.

Norbert Hilf, PhD[1], Sabrina Kuttruff-Coqui, PhD[1], Katrin Frenzel[2], Valesca Bukur[2], Stefan Stevanovic[3], Cecile Gouttefangeas, PhD[3], Michael Platten, MD[4], Ghazaleh Tabatabai[5], Valérie Dutoit[6], Sjoerd van der Burg, PhD[7], Per Thor Straten[8], Francisco Martínez-Ricarte, MD[9], Berta Ponsati[10], Hideho Okada, MD, PhD[11], Ulrik Lassen[12], Arie Admon[13], Christian Ottensmeier, MD PhD FRCP[14], Alexander Ulges[1], Sebastian Kreiter, MD[2], Andreas von Deimling[4], Marco Skardelly[5], Denis Migliorini[6], Judith Kroep, MD, PhD[7], Manja Idorn, PhD[8], Jordi Rodon[15], Jordi Piro[10], Hans Poulsen[12], Bracha Shraibman[13], Katy McCann[14], Regina Mendrzyk[1], Martin Löwer[2], Monika Stieglbauer[3], Cedrik Britten, MD[16], David Capper[17], Marij Welters[7], Juan Sahuquillo[9], Marie Stockhausen[12], Katharina Kiesel[1], Evelyna Derhovanessian[2], Elisa Rusch[3], Colette Song[1], Sandra Heesch[2], Claudia Wagner[1], Alexandra Kemmer-Brueck[2], Jörg Ludwig[1], John Castle[18], Oliver Schoor, PhD[1], Jens Fritsche, PhD[1], Miriam Meyer[1], Nina Pawlowski, PhD[1], Sonja Dorner[1], Franziska Hoffgaard[1], Bernhard Rössler, Dipl INg (FH), MBA[19], Dominik Maurer, PhD[1], Toni Weinschenk, PhD[1], Carsten Reinhardt, MD, PhD[1], Christoph Huber, MD[2], Hans-Georg Rammensee, PhD[3], Harpreet Singh, PhD[1], Ugur Sahin, MD[2], Pierre-Yves Dietrich[6], Wolfgang Wick, MD[4],

[1]Immatics Biotechnologies GmbH, Tuebingen, Germany
[2]BioNTech AG, Mainz, Germany
[3]Eberhard Karls Universität Tuebingen, Tuebeingen, Germany
[4]University Hospital Heidelberg, Heidelberg, Germany
[5]University Hospital Tuebingen, Tuebingen, Germany
[6]Geneva University Hospital, Geneva, Switzerland
[7]Leiden University Medical Center, Leiden, Netherlands
[8]CCIT, University Hospital Herlev, Copenhagen, Denmark
[9]Vall d'Hebron University Hospital, Barcelona, Spain
[10]BCN Peptides S.A., Barcelona, Spain
[11]UCSF and Parker Institute, San Francisco, CA, USA
[12]Ringhospitalet, Copenhagen, Denmark
[13]Technion - Israel Institute of Technology, Haifa, Israel
[14]University of Southampton, Southampton, UK
[15]Vall d'Hebron University Hospital (present address:

MDACC, Houston), Barcelona, Spain
[16]CIMT, BioNTech AG (present address: GSK, UK), Stevenage, UK
[17]University Hospital Heidelberg (present address: Charité Berlin), Heidelberg, Germany
[18]BioNTech AG (present address: Agenus Inc., USA), Mainz, Germany
[19]Immatics biotechnologies GmbH (present address: Rigontec GmbH, Munich), Planegg, Germany

Background
The need for treatment personalization in cancer therapy is evident as every tumor is molecularly unique. Especially immunotherapy should be customized to the highly individual antigenic landscape of every tumor for optimal efficacy. Glioblastoma are immunologically regarded as resistant and "cold" with an average of 30-50 mutations per tumor resulting in very few targetable neoantigens. To fully exploit all available antigens in glioblastoma, mutation-derived neoantigens as well as non-mutated antigens that are over-presented in the individual tumor should be addressed.

Methods
The GAPVAC consortium realized an immunotherapy, in which patients with newly diagnosed glioblastoma were offered two peptide-based actively personalized vaccines (APVAC) in addition to standard chemotherapy. Personalization was based on the mutational landscape, transcriptome and immunopeptidome of the individual tumors. Analysis of the patients' immune repertoire before treatment completed the dataset. GAPVAC-101 (NCT02149225) enrolled 16 patients in a European phase I feasibility, safety and immunogenicity trial integrated into standard of care. For APVAC1, up to 7 peptides were selected from a trial-specific warehouse based on individual biomarker data. Vaccination (i.d.) with GM-CSF (i.d.) and poly-ICLC (s.c.) started with the 1st adjuvant cycle of temozolomide. For APVAC2, analyses revealed between 19 and 84 somatic, non-synonymous mutations in the patients' tumors. From the 4th TMZ cycle onwards, 11 patients received APVAC2 with usually 2 *de novo* antigens per patient (preferentially neoantigens).

Results
Personalized APVAC vaccines could be designed and manufactured for all patients demonstrating the feasibility of the complex personalization approach. Adverse events were largely reversible injection site reactions but also 2 anaphylactic reactions and one increase in cerebral edema. All immune evaluable patients developed at least one APVAC-specific immune response. Short, non-mutated APVAC1 antigens induced sustained CD8+ T-cell responses, in most cases with induction of a memory phenotype. 51% of vaccinated APVAC1 class I peptides were immunogenic (*ex vivo* readout). 84.7% of the mutated APVAC2 peptides induced predominantly multi-functional CD4+ T-cell responses of favorable TH1 type; 45% of APVAC2 peptides induced also CD8+ T-cell responses against nested HLA class I neoantigens. Median OS was 29 months from diagnosis in patients that received APVAC vaccination (N = 15). For one patient, a broad APVAC-specific immune response in periphery and tumor was paralleled with a favorable clinical course.

Conclusions
Overall, the GAPVAC approach displayed expected safety profiles and high biological activity warranting further development. This concept may be extrapolated to future developments of personalized medicines.

Trial Registration
NCT02149225

Ethics Approval
The GAPVAC-101 trial was approved by ethics committees in the following countries:- Germany: Ethikkommission der Medizinischen Fakultät Heidelberg; Zeichen: AFmo-126/2014- Netherlands:

Centrale Commissie Mensgebonden Onderzoek; EC No: NL51127.000.14- Denmark: De Videnskabsetiske Komiteer Region Hovedstaden; Protocol-Nr: H-4-2014-121- Spain: Comité Ético de Investigación Clínica del Hospital Universitari Vall d'Hebron (CEIC)- Switzerland: Commission cantonale d'ethique de la recherche (CCER); No. CER 14-189

Cellular Metabolism and Antitumor Immunity

O9 Presidential Travel Award Recipient

Endoplasmic reticulum stress-induced transcription factor C/EBP homologous protein (Chop) thwarts effector T cell activity in tumors through repression of T-bet

Yu Cao, PhD[1], Rosa Sierra[1], Jimena Trillo-Tinoco[1], Carmen Anadon[1], Wenjie Dai[1], Eslam Mohamed[1], Richard Klar, PhD[2], Sven Michel[2], Frank Jaschinski, PhD[2], Shikhar Mehrotra, PhD[3], Juan Cubillos-Ruiz[4], David Munn, MD[5], Jose Conejo-Garcia, MD, PhD[1], Paulo Rodriguez[1]

[1]H. Lee Moffitt Cancer Center & Research Institute, TAMPA, FL, USA
[2]Secarna Pharmaceuticals GmbH & Co. KG, Planegg/Martinsried, Germany
[3]Medical University of South Carolina, Charleston, SC, USA
[4]Weill Cornell Medicine, New York, NY, USA
[5]Augusta University, Augusta, GA, USA

Background
The inhibited T cell function present in most patients and experimental animals with cancer represents a key obstacle in the development of promising immunotherapies. Several suppressive mechanisms including starvation of nutrients, exposure to high levels of reactive species, and acidosis impair T cell responses and are characterized by the induction of cellular stress pathways. However, the molecular targets that render tumor-infiltrating T cells dysfunctional remain practically unknown. Here, we aimed to determine the role of the C/EBP-homologous protein (Chop, encoded by Ddit3 gene), a downstream sensor of severe endoplasmic reticulum (ER) stress, in the functional regulation of tumor-exposed T cells.

Methods
For in vitro analysis, tumor-exposed activated T cells were collected for real-time PCR, Western Blot, Fluorescence-Activated Cell Sorting (FACS), RNA-seq, and Chromatin Immunoprecipitation assays. For T cell adoptive transfer, CD8+ T cells were isolated from control or Chop (Ddit3) null Pmel mice, stimulated with gp100 peptide, and transferred into mice bearing established B16 melanoma tumors. Next, transferred T cells were detected by FACS and the production of IFN-gamma examined through ELISpot and FACS. For in vivo tumor growth, T cell-conditional Chop null (Ddit3 T cell-KO) mice were generated and injected with s.c. tumors. In some experiments, CD8+ T cells were eliminated from tumor-bearing mice after treatment i.p. with a depleting anti-CD8 antibody every 3 days.

Results
Our results show that Chop is upregulated in tumor-infiltrating CD8+ T cells from tumor-bearing mice and patients with advanced ovarian carcinoma. Chop upregulation in tumor-infiltrating CD8+ T cells correlated with poor clinical outcome. The induction of Chop in tumor-exposed T cells was mediated by an increase in reactive oxygen species and a subsequent activation of the ER stress-associated kinase Perk. Deletion of Chop in CD8+ T cells enhanced effector/cytotoxic pathways, promoted significant anti-tumor effects, and overcame tumor-induced T cell tolerance. Mechanistically, Chop intrinsically repressed the transcription of the master regulator of effector T cell function, T-bet, and therefore enhanced anti-tumor effector mediators. Moreover, therapeutic inhibition of Chop in CD8+ T

cells, through specific anti-sense oligonucleotides, dramatically augmented the anti-tumor effectiveness of T cell-based adoptive transfer therapies.

Conclusions
Our study reveals for the first time the significant regulatory role of the ER stress-driven Chop in the T cell dysfunction occurring in tumors and suggests the therapeutic potential of inhibiting Chop in T cells as a strategy to overcome tumor-induced T cell tolerance and enhance the effect of T cell-based immunotherapy.

O10 Abstract Travel Award Recipient

Lipid accumulation in the pancreatic tumor microenvironment drives metabolic exhaustion of CD8+ T cells

Teresa Manzo, PhD[1]

[1]*IEO, Milan, Italy*

Background
The advent of immunotherapy has revolutionised cancer treatment by inducing, providing, and/or reactivating anti-tumuor T cells. Complete and durable clinical responses have been achieved in patients whose cancers were resistant to available standard treatments. Yet it has still met with limited success in most patients with solid tumours, including pancreatic ductal adenocarcinoma (PDAC). Several studies both in murine models of pancreatic cancer and PDAC patients have demonstrated that CD8+ T cells were often scarce and, if present, dysfunctional. However, our knowledge of the mechanisms that regulate their function in the context of the tumour microenvironment (TME) is still limited. We designed a study to fill this gap, aiming to enhance the clinical efficacy of immunotherapy.

Methods
To identify the sequence of events leading to CD8+ T cell dysfunction in the context of PDAC, first we conducted a longitudinal analysis of the T cell infiltration in a mouse model that recapitulates the progression of the human disease. Second, we employed MALDI-FT-ICR imaging mass spectrometry (IMS) to reveal the compositional changes in the regions of the murine and human TMEs infiltrated by CD8+ T cells. Thus, we profiled metabolically and transcriptionally both murine flow-sorted and patient-derived intra-pancreatic CD8+ T cells to gain mechanistic insights on their dysfunction. Finally, we performed adoptive T cell therapy in an engineered mouse model of PDAC to provide preclinical evidence that metabolic reprogramming of tumour-specific T cells might represent an effective strategy to enhance outcomes of immunotherapy in PDAC.

Results
We describe high levels of lipid accumulation in the TME areas of PDAC populated by infiltrating CD8+ T cells. In this lipid-rich TME, transcriptional deregulation in CD8+ T cells of pathways involved in lipid metabolism prevented engagement of fatty acid catabolism, leading to mitochondrial dysfunction and ultimately impairing their effector functions during PDAC progression. Intra-pancreatic CD8+ T cells from both murine and human tumours showed down-regulation of the very-long-chain acyl-CoA dehydrogenase (ACADVL) enzyme. Metabolic reprogramming of tumour-specific T cells through enforced expression of ACADVL enabled enhanced intra-tumoral T cell persistence in an engineered mouse model of PDAC.

Conclusions
CD8+ T cells penetrate into PDAC TME and persist until late stages, but eventually become functionally impaired. Our comprehensive understanding of the metabolic state of PDAC TME offers novel insights in the dynamic of PDAC immunity and we harnessed

this information to generate an innovative immunotherapy strategy based on metabolic reprogramming of tumour-specific T cells.

O11

Tumor cell oxidative metabolism as a barrier to PD-1 blockade immunotherapy in melanoma

Ashley Menk, BS[1], Yana Najjar, MD[2], John Kirkwood, MD[2], Cindy Sander, BS[2], Greg Delgoffe, PhD[1]

[1]University of Pittsburgh, Pittsburgh, PA, USA
[2]UPMC Hillman Cancer Center, Pittsburgh, PA, USA

Background
PD-1 blockade therapy has been paradigm-shifting for melanoma, but durable responses only occur in a subset of patients. While we have previously shown that tumor-infiltrating T cells have repressed metabolic machinery, the environment itself is nutrient poor due to the deregulated metabolism of tumor cells. While recent studies have suggested that T cells compete with tumor cells for glucose, our studies suggest it is the oxidative metabolism that may be limiting in tumor immunity. We hypothesize resistance to immunotherapy may be due to deficiencies in the metabolic makeup of the tumor microenvironment, and that we can infer that environment's metabolism in patients by metabolically profiling tumor cells.

Methods
Melanoma patient samples were profiled by Seahorse analysis in parallel to flow cytometric analysis of tumor infiltrating lymphocytes (TIL). Murine melanoma cells were generated including RNAi constructs to specific metabolic pathways. Response to PD-1 blockade immunotherapy was monitored and lymph node or TIL T cells were tested for effector function, metabolism, and localization by flow cytometry and immunofluorescence.

Results
Analysis of melanoma patient biopsies showed striking heterogeneity in the metabolism of tumor cells. Patients with more metabolically active tumors have more dysfunctional TIL, while tumors that were metabolically quiescent contained T cells with superior effector function. Profiling of patient tumor cells prior to PD-1 blockade therapy revealed that patients with metabolically oxidative tumors had poorer responses while patients with quiescent tumors experienced long-term response. To confirm the role of oxidative metabolism, we generated murine melanoma lines in which glucose or oxidative metabolism was inhibited. Tumor cells in which oxidative (but not glucose) metabolism was inhibited created a less hypoxic microenvironment, had improved T cell function, and an increased response to PD-1 blockade immunotherapy.

Conclusions
Our data suggest that the degree of tumor hypoxia, driven through deregulated oxidative metabolism of the tumor cell, determines whether T cells have a permissive microenvironment for effective immunotherapy, and that inhibiting tumor cell oxidative metabolism may be an attractive strategy to improve the efficacy of immunotherapy.

O12

Chronic endoplasmic reticulum stress drives mitochondrial exhaustion of CD8 TILs

Jessica Thaxton, PhD, MSCR[1], Kiley Lawrence[1], Katie Hurst[1], Lee Leddy[1], Matthew Essman[1]

[1]Medical University of South Carolina, Charleston, SC, USA

Background
Tumor antigen-specific T cells rapidly lose energy and effector function in tumors. The cellular mechanisms by which energy loss and inhibition of effector

function occur in tumor infiltrating lymphocytes (TILs) are ill-defined. Processes upstream of the mitochondria guide cell-intrinsic energy depletion. We hypothesized that a mechanism of T cell-intrinsic energy consumption that may affect exhausted CD8+ TILs was the process of oxidative protein folding that takes place in the endoplasmic reticulum (ER) guided by protein kinase R-like endoplasmic reticulum kinase (PERK) and its downstream target ER oxidoreductase ERO1a.

Methods
To test our hypothesis, we created TCR transgenic mice with a T cell-specific PERK gene deletion (OT-1-Lckcre-PERKf/f, PERK KO) to determine how the PERK axis shapes T cell energetics and oxidative stress. We used proteomics, small molecule inhibitors, and quantification of PERK axis gene activation in CD8 TILs to measure how this axis impacts T cell bioenergetics.

Results
We found that, through PERK, ERO1a drives energy consumption and oxidative stress in T cells. Proteomics analysis revealed that ERO1a induced a protein profile in T cells associated with increased translation, energy production and consumption, and extraction of misfolded proteins. We identified a biomarker of PERK-ERO1a-mediated metabolic exhaustion and oxidative stress in T cells as mitochondrial reactive oxygen species (mtROS), and we found that PD-1+ CD8+ TILs express mtROS and high levels of ERO1a. In vivo treatment with a PERK inhibitor abrogated mtROS and boosted viability and effector function of PD-1+ CD8 TILs. Combination therapy was effective compared to control conditions in a sarcoma mouse model.

Conclusions
Our data identify the ER as a regulator of T cell energetics and indicate that ER elements are effective targets to improve cancer immunotherapy.

O13 **Abstract Travel Award Recipient**

Lactic acid metabolically supports the high suppressive function of tumor infiltrating regulatory T cells

McLane Watson, BS[1], McLane Watson, BS[1], McLane Watson, BS[1], Paolo Vignali, BA[1], Ryan Whetstone, MS, PhD[1], Ronal Peralta[1], Rahul Deshpande, PhD[1], Ashley Menk, BS[1], Nicole Scharping, BS[1], Brett Morrison, MD, PhD[2], Stacy Wendell, PhD[1], Greg Delgoffe, PhD[1]

[1]*University Of Pittsburgh, Pittsburgh, PA, USA*
[2]*Johns Hopkins, Baltimore, MD*

Background
Cancer immunotherapy fails for a majority of patients due a number of resistance mechanisms including the recruitment, activation, and differentiation of regulatory T cells (Treg). While metabolically harsh conditions in the tumor microenvironment (TME) starve infiltrating effector T cells, it has been shown that Treg cells have a distinct metabolic profile potentially providing them metabolic flexibility to utilize metabolites rich in the TME. Therefore, we hypothesized that the TME is metabolically supporting Treg cells.

Methods
Methods: B16, a mouse model of melanoma, was used. From tumor bearing mice conventional effector T cells and Treg cells were transcriptionally and metabolically profiled using flow cytometry, proliferation assays, suppression assays, and isotopic flux analysis. A mouse with a Treg specific deletion of MCT1, a predominant lactate transporter, was generated. A pharmacological inhibitor of MCT1 was used to prevent lactate uptake.

Results
Results: In vitro, Treg cells conditioned in no or low

glucose media were superior suppressors to those conditioned in high glucose. Similarly, sorting Treg cells based on glucose uptake revealed low glucose Treg cells to be superior suppressors. Transcriptional and metabolic profiling revealed intratumoral Treg cells upregulate a distinct metabolic profile utilizing the glycolytic end-product, lactic acid. Lactic acid has been known to be immunosuppressive, and indeed, it curbed the function of conventional effector cells in vitro. However, lactic acid had no effect on Treg cell function. Isotopic flux analysis revealed lactate is utilized by Treg cells to generate glycolytic intermediates, in part through gluconeogenic pathways. Inhibition of gluconeogenesis in vivo resulted in decreased proliferation of tumor infiltrating Treg cells. Preventing lactate transport in Treg cells through a conditional knockout of MCT1 resulted in mice with normal immune homeostasis, but superior anti-tumor immunity when implanted with melanoma. This coincided with increased IFN-γ production by intratumoral CD8, Treg, and Tconv cells leading to dramatically slowed tumor growth.

Conclusions

Conclusions: These data suggest that lactic acid supports Treg cells in the TME and that targeting lactate metabolism to weaken Treg cells may increase efficacy of cancer immunotherapy.

O14

Reinvigorating TILs by hyper-oxygenation

Mateusz Rytelewski, PhD[2], Karine Haryutyunan[2], Felix Nwajei, PhD[2], Sergei Vinogradov, PhD[3], Marina Konopleva, MD, PhD[2], Tomasz Zal, PhD[2], Anna Zal[2]

[1]University of Texas MD Anderson Cancer C, Houston, TX, USA
[2]MD Anderson Cancer Center, Houston, TX, USA
[3]University of Pennsylvania, Philadelphia, PA, USA

Background

Active migration of lymphocytes within tumors is pre-requisite to immune therapies. Both solid tumors as well as bone marrow malignancies develop regions of low oxygen partial pressures, i.e. below 5 mmHg, known as tumor hypoxia. Tumor hypoxia plays multiple roles in tumor immune suppression including tissue expression of checkpoint molecules, decreased antigen presentation and deactivation of various tumor-infiltrating lymphocytes (TILs). However, the relationship of intratumoral oxygen distribution to the motility of TILs remains undefined, largely owing to the lack of a suitable method for contextual imaging of oxygen gradients and cell dynamics in vivo.

Methods

Using PtP-C343 oxygen probe, we developed a regimen of intravital 2-photon microscopy that combines TIL motility recording with oxygen imaging based on phosphorescence lifetimes. We applied this method, termed 2-photon pre-pulse phosphorescence lifetime imaging microscopy (2PreP-PLIM) to relate the dynamic behavior of T cells to the local oxygen gradients that develop inside solid lung tumors and leukemic bone marrow in pre-clinical mouse models.

Results

We found that tumor infiltrating T-lymphocytes traversed regions of varying oxygen concentrations, including regions of hypoxia that developed within the solid tumor cores and in bone marrow with advanced-stage B-cell acute lymphocytic leukemia (B-ALL). T cell motilities were markedly decreased in hypoxic regions compared to the neighboring normoxia, and many of the TILs experiencing hypoxia appeared stalled. Remarkably, breathing 100% oxygen, which alleviated hypoxia inside solid lung tumors, rapidly increased the migratory behavior of otherwise stalled T cells.

Conclusions
The devised technique for intravital oxygen and cell dynamics co-imaging reveals a role of oxygen supply in promoting intratumoral T cell migration. Our results reveal reinvigoration of TIL motility as a new mechanistic benefit of oxygen and, possibly, other hypoxia countermeasures in counteracting tumor immune suppression.

Acknowledgements
This work is supported by grants NCI R01CA155056 and CPRIT MIRA 160683 to TZ and MK and grants EB018464 and NS092986 from the National Institutes of Health (USA) to SV. MR is the recipient of a post-doctoral fellowship from the Canadian Institutes of Health Research (CIHR).

Ethics Approval
The study was approved by the University of Texas MD Anderson Cancer Center Institutional Animal Care and Use Committee under protocol number 00000878-RN01.

Cellular Therapy Approaches

O15 Presidential Travel Award Recipient

Engineering adoptive T cell therapy to co-opt Fas ligand-mediated death signaling in solid tumors

Kristin Anderson, PhD[1], Shannon Oda[1], Breanna Bates, BS[1], Madison Burnett[1], Edison Chiu, BS[2], Magdalia Suarez Gutierrez[1], Nicolas Garcia, BS[1], Andrew Daman[1], Philip Greenberg, MD[1]

[1]*Fred Hutchinson Cancer Research Center, Seattle, WA, USA*
[2]*University of Washington, Seattle, WA, USA*

Background
Over 20,000 women are diagnosed with ovarian cancer annually, and over half will die within 5 years. This rate has changed little in the last 20 years, highlighting the need for therapy innovation [1]. One especially promising new strategy employs immune T cells engineered to target proteins uniquely overexpressed in tumors, with the potential to limit tumor growth without toxicity to healthy tissues. Mesothelin (Msln) is a rational target for ovarian cancer immunotherapy [2] - it contributes to the malignant and invasive phenotype in these tumors and has limited expression in healthy cells [3,4,5].

Methods
Deep transcriptome profiling of whole tumor tissue was used to confirm the expression of similar gene signatures in human cancers and in the preclinical ID8 mouse model, including comparable expression of immunosuppressive pathways. For example, RNA sequencing, flow cytometry and immunohistochemistry analysis revealed consistently high expression of the immunomodulatory protein Fas ligand (FasL). Human/mouse T cells were engineered to express a human/mouse Msln-specific high-affinity T cell receptor (TCR-Msln)[6] and tested for cytotoxic activity against human patient-derived or ID8 mouse ovarian cancer cell lines *in vitro* and *in vivo*.

Results
In a disseminated ID8 tumor model, adoptively transferred TCR-Msln T cells preferentially accumulated within established tumors, delayed ovarian tumor growth, and significantly prolonged mouse survival. However, our data also revealed that elements in the tumor microenvironment (TME) limit engineered T cell persistence and anti-cancer activity. We and others previously detected FasL in the tumor vasculature [7] and TME of human and murine ovarian cancers. FasL can induce apoptosis in infiltrating lymphocytes expressing Fas receptor (Fas)[8]. To overcome this potential T cell evasion mechanism, we generated a panel of immunomodulatory fusion proteins (IFP) containing the Fas extracellular binding domain fused to a CD28

or 4-1BB co-stimulatory domain, rather than the natural death domain. Relative to T cells modified with only TCR-Msln, T cells engineered to express both TCR-Msln and a Fas IFP preferentially infiltrate tumors, expand/persist and retain function in the TME of tumor-bearing mice. Moreover, adoptive immunotherapy with IFP+ T cells significantly prolonged survival in tumor-bearing mice, relative to TCR-Msln T cells lacking an IFP.

Conclusions

Fas/FasL signaling can mediate T cell death, including activation-induced cell death, an apoptotic mechanism responsible for regulating T cell expansion. Thus, tumor cells may upregulate FasL for protection from tumor-infiltrating lymphocytes. As many solid tumors overexpress FasL, IFPs may provide an opportunity to enhance engineered adoptive T cell therapy against many malignancies.

Acknowledgements

The authors thank Matthias Stephan for the ID8-VEGF cell line, Sunni Farley, Robert Pierce, Savanh Chanthaphavong, Brian Johnson and Megan Larmore for histopathology assistance, Ingunn Stromnes and Tom Schmitt for MSLN TCR development, and the Fred Hutchinson Cancer Research Center Flow Cytometry Core for technical support.

References

1. Vaughan S, Coward JI, Bast RC, Berchuck A, Berek JS, Brenton JD, Coukos G, Crum CC, Drapkin R, Etemadmoghadam D, Friedlander M, Gabra H, Kaye SB, Lord CJ, Lengyel E, Levine DA, McNeish IA, Menon U, Mills GB, Nephew KP, Oza AM, Sood AK, Stronach EA, Walczak H, Bowtell DD, Balkwill FR. Rethinking ovarian cancer: recommendations for improving outcomes. Nat. Rev. Cancer. 2011;11(10):719–725.
2. Cheever MA, Allison JP, Ferris AS, Finn OJ, Hastings BM, Hecht TT, Mellman I, Prindiville SA, Viner JL, Weiner LM, Matrisian LM. The Prioritization of Cancer Antigens: A National Cancer Institute Pilot Project for the Acceleration of Translational Research. Clin. Cancer Res. 2009;15:5323–5337.
3. Chang K, Pastan I, and Willingham MC. Isolation and characterization of a monoclonal antibody, K1, reactive with ovarian cancers and normal mesothelium. Int. J. Cancer. 1992;50: 373–381.
4. Chang K, and Pastan I. Molecular cloning of mesothelin, a differentiation antigen present on mesothelium, mesotheliomas, and ovarian cancers. Proc. Natl. Acad. Sci. USA. 1996;93:136–140.
5. Gubbels JAA, Belisle J, Onda M, Rancourt C, Migneault M, Ho M, Bera TK, Connor J, Sathyanarayana BK, Lee B, Pastan I, Patankar MS. Mesothelin-MUC16 binding is a high affinity, N-glycan dependent interaction that facilitates peritoneal metastasis of ovarian tumors. Mol. Cancer. 2006;5:50.
6. Stromnes IM, Schmitt TM, Hulbert A, Brockenbrough JS, Nguyen HN, Cuevas C, Dotson AM, Tan X, Hotes JL, Greenberg PD, Hingorani SR. T Cells Engineered against a Native Antigen Can Surmount Immunologic and Physical Barriers to Treat Pancreatic Ductal Adenocarcinoma. Cancer Cell. 2015;28:638–652.
7. Motz GT, Santoro SP, Wang LP, Garrabrant T, Lastra RR, Hagemann IS, Lal P, Feldman MD, Benencia F, Coukos G. Tumor endothelium FasL establishes a selective immune barrier promoting tolerance in tumors. Nat. Med. 2014;20(6):607-615.
8. Waring P, and Mullbacher A. Cell death induced by the Fas/Fas ligand pathway and its role in pathology. Immunology and Cell Biology. 1999;77:312-317.

Ethics Approval

The Institutional Animal Care and Use Committees of the University of Washington and the Fred Hutchinson Cancer Research Center approved all animal studies.

O16

Tscm-like CD8+ T-cells are associated with adoptive TIL therapy response and survival

Matthew Beatty, PhD[1], Benjamin Schachner[1], Autumn Joerger[1], Ellen Scott[1], Patrick Verdugo[1], John Mullinax, MD[1], Amod Sarnaik, MD[1], Shari Pilon-Thomas, PhD[1]

[1]*Moffitt Cancer Center, Tampa, FL, USA*

Background

Adoptive Cell Transfer (ACT) using Tumor Infiltrating Lymphocytes (TIL) for unresectable metastatic melanoma results in a median progression free survival of 6 months and median overall survival of 33 months at our institution. The purpose of this study is to analyze the phenotype and function of patient infused TIL and identify TIL phenotypes associated with response and progression free survival.

Methods

Patient-derived and infused TIL samples were phenotyped for composition of CD4+ and CD8+ T-cells, expression of co-stimulatory and co-inhibitory markers (4-1BB, PD-1, OX-40, BTLA, LAG3, TIM3, TIGIT), and Tregs (CD4+ CD25hi CD127-). Additionally, T-cell memory markers were used to analyze the proportion of naïve (CD45RA+ CCR7+ CD62L+ CD95-), T stem cell memory (Tscm) (CD45RA+ CCR7+ CD62L+ CD95+), central memory (CD45RA- CCR7+ CD62L+ CD95+), effector memory (CD45RA- CCR7- CCR7- CD62L- CD95+), and terminal effector (CD45RA+ CCR7- CD62L- CD95+). Samples was co-cultured with HLA-matched melanoma cell lines and analyzed for IFNγ production.

Results

Forty one infused TIL samples were analyzed. We observed an increased CD8+:CD4+ T-cell ratio in patients who were partial or complete responders (responders) compared to stable disease and progressive disease (non-responders) by RECIST criteria. No differences in expression of co-stimulatory or co-inhibitory markers on CD8+ or CD4+ T-cells were found. An overall increase in Treg percentage was found in non-responders, though there was no increase in Tregs as a percentage of CD4+ T-cells. Among memory T-cell populations, responders had enrichment for CD8+ Tscm cells as a percentage of total TIL compared to non-responders. Additionally, patients with greater than 12% CD8+ Tscm in the TIL product have not met their median 5 year progression free survival compared to 6 months for patients with 12% of less CD8+ Tscm. Of 37 samples, 20 were reactive in an MHC class I dependent manner against at least one HLA-matched melanoma cell line. Additionally, reactivity was associated with an increased progression free survival of 35 months compared to 5 months for non-reactive samples.

Conclusions

In this study we show that CD8+ Tscm T-cells within the ACT TIL therapy product as well as reactivity to HLA-matched cell lines is associated with patient response to therapy as well as progression free survival. Tscm cells have been of great interest in cellular therapies due to their increased persistence. These data form the rationale for enriching CD8+ Tscm cells in TIL ACT products and could lead to better clinical outcomes.

O17

Infusion of TGFβ-resistant EBV-specific T-cells post cytoreductive chemotherapy is safe and associated with clinical benefit in patients with recurrent/metastatic NPC

Christopher DeRenzo, MD[1], Mamta Kalra[2], Carlos Ramos[2], Catherine Robertson[2], Huimin Zhang[2], Claudia Gerken[2], Olga Dakhova[2], Melinda Mata[2], Meng-Fen Wu[2], Hao Liu[2], Catherine Bollard[2],

Zhuyong Mei[2], Adrian Gee[2], Bambi Grilley[2], Gianpietro Dotti, MD[2], Helen Heslop, MD[2], Malcolm Brenner[2], Cliona Rooney[2], Stephen Gottschalk[1]

[1]Center for Cell and Gene Therapy (Houston, TX); St. Jude Children's Research Hospital (Memphis, TN), Memphis, TN, USA
[2]Center for Cell and Gene Therapy (Houston, TX), Houston, TX, USA

Background
Outcomes for patients with recurrent/metastatic Epstein-Barr virus positive (EBV+) nasopharyngeal carcinoma (NPC) are poor and treatment options are limited. Previously, systemic administration of up to 3x10^8/m2 autologous EBV-specific T-cells was safe, however antitumor activity was limited. Lack of efficacy was likely due to i) limited specificity of the infused T-cell products to EBV antigens expressed in NPC, ii) lack of T-cell expansion, and iii) the immunosuppressive tumor microenvironment. To address these limitations, we developed a product enriched in LMP1-, LMP2-, EBNA1-, and BARF1-specific T-cells. T-cells were also modified to resist TGFβ mediated immunosuppression by introducing a dominant-negative TGFβ receptor (DNR.NPC T-cells). We evaluated the safety and antitumor activity of these DNR.NPC T-cells in patients with recurrent/metastatic NPC.

Methods
In a phase 1 trial, NCT02065362, we administered 0.4-1x10^8/m2 autologous DNR.NPC T-cells to patients with recurrent/metastatic EBV+ NPC with or without cytoreductive chemotherapy. Post-infusion we evaluated safety, T-cell expansion, and antitumor activity.

Results
Four patients received two doses of 2x10^7/m2 DNR.NPC T-cells 14 days apart. Without cytoreduction, T-cell expansion was limited as judged by DNR-qPCR (mean peak: 80.2 copies/µg DNA; range: 10.4-133.6 copies/µg DNA). The protocol was therefore modified to include cytoreductive chemotherapy with cyclophosphamide (Cy; 500mg/m2/day) and fludarabine (Flu; 30mg/m2/day) on days -4 to -2 prior to T-cell infusion. Cy/Flu and T-cell infusions were well tolerated without dose limiting toxicities in 4 patients who received either 4x10^7 cells/m2 (n=2) or 1x10^8 cells/m2 (n=2). There was a 128-fold greater DNR.NPC T-cell expansion ($p<0.05$) in patients who received cytoreduction compared to those who did not. T-cell expansion occurred at a median 7 days post infusion (range: 4-7 days) with a peak DNR-qPCR level of 10,305 copies/µg DNA (range: 1,016-31,765 copies/µg DNA). Antitumor activity was assessed 6 weeks post T-cell infusion. Without cytoreduction, 2/4 patients had progressive disease, 1 had stable disease (SD), and 1 was not evaluable. Of the 4 patients who received cytoreduction followed by T-cells, 3/4 had SD, and 1, who had imaging findings of unknown significance (recovering marrow vs metastatic disease), had a complete response. With a median follow up of 19.5 months (range: 18.2-27.7 months), 3/3 patients who received T-cells only died from disease progression. In contrast, 4/4 patients who received T-cells preceded by cytoreduction are alive; 2 with SD, and 2 in remission.

Conclusions
Infusion of DNR.NPC-specific T-cells after cytoreductive chemotherapy is safe, results in robust T-cell expansion, and is associated with objective clinical benefit in patients with recurrent/metastatic NPC.

Ethics Approval
This study (ClinicalTrials.gov identifier: NCT02065362) was approved by the institutional review board at Baylor College of Medicine (Houston, TX) and by the US Food and Drug Administration.

O18

Preliminary clinical data from a pilot study of NY-ESO-1c259T-cells in advanced myxoid/round cell liposarcoma

Sandra D'Angelo[2], Justina Stadanlick[1], Mihaela Druta[3], David Liebner, MD[4], Scott Schuetze[5], Brian Van Tine[6], William Tap[2], Cedrik Britten, MD[7], Karen Chagin, MD[1], Aisha Hasan, MBBS MD[7], Elliot Norry, MD[1], Trupti Trivedi, MS[1]

[1]*Adaptimmune, Philadelphia, PA, USA*
[2]*Memorial Sloan Kettering Cancer Center &, New York, NY, USA*
[3]*Moffit Cancer Center, Tampa, FL, USA*
[4]*Ohio State University Medical Center, Columbus, OH, USA*
[5]*University of Michigan, Ann Abror, USA*
[6]*Washington University St.Louis, St. Louis, USA*
[7]*GlaxoSmithKline, Stevenage, UK*

Background
Metastatic myxoid/round cell liposarcoma (MRCLS) has a poor prognosis. NY-ESO-1 is expressed in 80-90% of MRCLS tumors, making it an attractive target for adoptive T-cell immunotherapy. This study evaluates affinity enhanced autologous NY-ESO-1c259T-cells (SPEAR T-cells) recognizing an NY-ESO-1-derived peptide complexed with HLA-A*02 in MRCLS (NCT02992743).

Methods
This open label phase I/II single arm pilot study evaluates efficacy, safety, and translational research endpoints. The protocol was approved by each center's Institutional Review Board, and all patients signed informed consent forms. Eligible patients are ≥ 18 years old; HLA-A*02:01+, *02:05+ or *02:06+; have advanced MRCLS expressing NY-ESO-1 at 2+/3+ intensity in ≥30% of tumor cells by immunohistochemistry; have measurable disease; received anthracycline therapy; ECOG status 0 or 1; and have adequate organ function. Following apheresis, T-cells are isolated, expanded, transduced with a lentiviral vector containing the NY-ESO-1c259TCR, and 1– 8 × 109 transduced T-cells are infused on day 1 after lymphodepletion with fludarabine 30 μg/m2/d and cyclophosphamide 600 μg/m2/d on d -7 to -5. Response is assessed at 4, 8, 12, and 24 weeks and then every 3 months until disease progression.

Results
Thirty-nine patients were screened: 20 had the requisite HLAs, and 17 of these had NY-ESO-1 present at required levels. Thirteen patients were enrolled, and 10 received the TCR therapy between 04 October 2017 and 27 June 2018 (as of 12 July 2018). The patients received 1.0-5.7 × 109 transduced T-cells. Two patients were recently treated, and tumor lesion assessment at week 8 is still pending. There are post-infusion tumor lesion assessments for 8 patients: 3 females, 5 males, with a median age of 48, and median 4 lines of prior systemic therapies. At the time of the data cut-off, 4 of the 8 patients (50%) have achieved a confirmed partial response (PR) and 50% have stable disease (SD) as the best overall response. The duration of responses varies from 4 weeks to greater than 5 months; 2 of the patients have ongoing PRs as of 12 July 2018. AEs ≥ grade 3 in these 8 patients include lymphopenia (6), neutropenia (5), leukopenia (5), thrombocytopenia (3), hypophosphatemia (2), anemia (1), cytokine release syndrome (1; SAE), pyrexia (1) and leukocytosis (1). None required study discontinuation.

Conclusions
These preliminary data indicate that treatment with NY-ESO-1c259T-cells in MRCLS appears to have an acceptable safety profile consistent with other NY-ESO-1c259T-cell studies, with potential for anti-tumor effects. We will report updated results.

Trial Registration
NCT02992743

Clinical Trials (Completed)

O19

Phase 1 study using mogamulizumab (KW-0761) to deplete regulatory T cells in combination with checkpoint inhibitors durvalumab (MEDI4736) or tremelimumab in subjects with advanced solid tumors

Dmitriy Zamarin, MD, PhD[2], Omid Hamid, MD[3], Asha Nayak, MD[4], Solmaz Sahebjam, MD[5], Mario Sznol, MD[6], Agron Collaku, PhD[1], Floyd Fox, PhD[1], Margaret Marshall, MD[1], David Hong, MD[7]

[1]*Kyowa Kirin Pharmaceutical Development, Inc., Princeton, NJ, USA*
[2]*Memorial Sloan-Kettering Cancer Center, New York, NY, USA*
[3]*The Angeles Clinic and Research Institute, Los Angeles, CA, USA*
[4]*Georgia Cancer Center, MARTINEZ, GA, USA*
[5]*H. Lee Moffitt Cancer Center, Tampa, FL, USA*
[6]*Yale Cancer Center, New Haven, CT, USA*
[7]*MD Anderson Cancer Center, Houston, TX, USA*

Background
Regulatory T cells (Tregs) play a pivotal role in maintaining immunological tolerance, which can inhibit antitumor immune responses and may mediate resistance to immunomodulatory therapy targeting CTLA-4 or PD-1/PD-L1. Mogamulizumab (Moga) is a humanized IgG1 monoclonal antibody (mAb) targeting anti-CC-chemokine receptor 4 (CCR4), which is highly expressed on Tregs. This study sought to evaluate whether Treg depletion by Moga enhanced antitumor response in combination with PD L1 blockade by Durvalumab (Durva) or CTLA-4 blockade by Tremelimumab (Treme).

Methods
Study 0761 012 was a multicenter, Phase 1, open-label, dose escalation/cohort expansion study of Moga in combination with either Durva (Treatment A; TrA) or Treme (Treatment B; TrB) in adult subjects with advanced solid tumors. Dose escalation (Part 1) included 4 dose cohorts for each combination (Table 1). There was one tumor-specific expansion cohort (Part 2). The primary objective was to assess safety and tolerability; the secondary objectives were to evaluate antitumor effect (RECIST 1.1 and irRECIST 1.1), pharmacokinetics, and immunogenicity. Exploratory objectives were to examine biomarkers/pharmacodynamics.

Results
A total of 64 subjects were enrolled and treated: n=40 in Part 1 (Table 1) and n=24 in Part 2. Dose escalations were completed in Part 1 without any dose-limiting toxicities, and combinations of 1 mg/kg Moga with 10 mg/kg of either Durva (TrA) or Treme (TrB) were used to treat an expansion cohort with pancreatic cancer in Part 2. Treatment-emergent adverse event (TEAE) rates and most common TEAEs for each treatment combination are shown in Table 2 (Table 2). Moga showed pharmacologic activity by reduction in number of peripheral blood CCR4+ effector Tregs (eTregs) in both TrA and TrB; however, other important effector cell types were also depleted. One TrA subject with ASPS and one TrB subject with prostate cancer had partial responses, with a duration of response of 10.6 months and 3.7 months, respectively. Five (26.3%) TrA subjects and 7 (36.8%) TrB subjects showed disease stability. No subjects with pancreatic cancer responded. There was no correlation between the degree of peripheral blood eTreg depletion and response.

Conclusions
Combining Moga with either Durva or Treme in solid tumors was tolerable and effectively decreased eTregs in peripheral blood. There was no efficacy beyond what was anticipated from the individual

monotherapy with Durva or Treme. Concomitant depletion of non eTreg effector T cell populations may have been responsible for the apparent lack of therapeutic enhancement.

Trial Registration
NCT02301130

Ethics Approval
This study was approved by an Institutional Review Board at each investigative site.

Table 1.

Treatment A				Treatment B			
Cohort	Moga	Durva	Subject Tumor Type (n)	Cohort	Moga	Treme	Subject Tumor Type (n)
1A	0.3 mg/kg	3 mg/kg	Breast (1) Head & Neck (1) Prostate (1) Sarcoma (1)	1B	0.3 mg/kg	3 mg/kg	Colorectal (1) Head & Neck (1) NSCLC, non-squamous(1)
2A	1 mg/kg	3 mg/kg	Pancreatic (1) Sarcoma (2)	2B	1 mg/kg	3 mg/kg	Colorectal (1) Head & Neck (1) Other[c] (1)
3A	1 mg/kg	10 mg/kg	Colorectal (1) NSCLC, squamous (1) Ovarian (2) Sarcoma (2) Other[a] (1)	3B	1 mg/kg	10 mg/kg	Anal (1) Head & Neck (1) Ovarian (1) Prostate (3) Renal Cell (3)
4A	3 mg/kg	10 mg/kg	Colorectal (4) NSCLC, non-squamous (3) Renal Cell (1) Other[b] (2)	4B	3 mg/kg	10 mg/kg	Colorectal (2) Pancreatic (2) Other[d] (1)

a: Other: Cholangiocarcinoma
b: Other: Adenocarcinoma of Unknown Primary
c: Other: Thymus
d: Other: Acinic Cell Carcinoma of the Parotid Gland
Moga=mogamulizumab, Durva=durvalumab, NSCLC=non-small cell lung cancer, Treme=tremelimumab

Table 2.

	Treatment A[a] (Moga+Durva)	Treatment B[a] (Moga+Treme)
Part 1 (Dose escalation) All dose cohorts	N=21	N=19
Any TEAE[b] (n, %) ≥Grade 3 (n, %) ≥Grade 3, related to either IMP (n, %) SAE(n, %) SAE, related to either IMP (n, %) Most common TEAEs (preferred term, %)	21 (100.0) 15 (71.4) 6 (28.6) 12 (57.1) 4 (19.0) Fatigue 12 (57.1) Diarrhea 9 (42.9)	19 (100.0) 15 (78.9 9 (47.4) 9 (47.4) 5 (26.3) Diarrhea 10 (52.6) Fatigue 9 (47.4) Decr appetite 8 (42.1)
Part 2 (Dose expansion) Pancreatic cancer	N=12	N=12
Any TEAE[b] (n, %) ≥Grade 3 (n, %) ≥Grade 3, related to either IMP (n, %) SAE (n, %) SAE, related to either IMP (n, %) Most common TEAEs (preferred term, %)	12 (100.0) 10 (83.3) 4 (33.3) 10 (83.3) 3 (25.0) Fatigue 11 (91.7) Abdominal pain 9 (75.0) Constipation 6 (50.0) Nausea 6 (50.0)	12 (100.0) 10 (83.3) 4 (33.3) 8 (66.7) 1 (8.3) Edema peripheral 8 (66.0) IRR 6 (50.0) Hypomagnesemia 6 (50.0)

a: In Part 2, Treatment A = 1 mg/kg Moga + 10 mg/kg Durva; Treatment B = 1mg/kg Moga + 10mg/kg Treme.
b: TEAEs during any cycle
Decr=decreased; IMP=investigational medicinal product; IRR=infusion related reaction; Moga=mogamulizumab; SAE=serious adverse event; Treme=tremelimumab

Clinical Trials (In Progress)

O20

Reprogramming suppressive myeloid cells in tumor microenvironment with pepinemab, first-in-class Semaphorin 4D Mab, enhances combination immunotherapy

Terrence Fisher, PhD[2], John Leonard, MD PhD[1], Crystal Mallow, BS[1], Holm Bussler, PhD[1], Sebold Torno, BS[1], Maria Scrivens[2], Alan Howell, MS[2], Leslie Balch, BS[2], Clint Allen, MD[3], Paul Clavijo, PhD[3], Gregory Lesinski, PhD, MPH[4], Christina Wu, MD[4], Brian Olson, PhD[4], Siwen Hu-Lieskovan, MD, PhD[5], Antoni Ribas, MD, PhD[5], Emily Greengard, MD[6], Ernest Smith, PhD[2], Maurice Zauderer, PhD[2], Elizabeth Evans, PhD[1], Elizabeth Evans, PhD[1]

[1]*Vaccinex, Rochester, NY, USA*
[2]*Vaccinex Inc, Rochester, NY, USA*
[3]*NIH/NIDCD Head and Neck Surgery Branch, Bethesda, MD, USA*
[4]*Winship Cancer Institute of Emory Univer, Atlanta, GA, USA*
[5]*David Geffen School of Medicine at UCLA, Los Angeles, CA, USA*
[6]*University of Minnesota Masonic Children, Minneapolis, MN, USA*

Background
Tumor growth inhibition by anti-semaphorin 4D (SEMA4D, CD100) blocking antibody is enhanced when combined with various immunotherapies in preclinical animal models. Immune checkpoint combinations with pepinemab (VX15/2503), humanized anti-SEMA4D antibody, are currently being evaluated in several clinical trials.

Methods
Mechanistic studies in syngeneic preclinical models investigated the effects of SEMA4D blockade on anti-tumor activity and immune responses, both as a

single agent and in combination with various immunotherapy agents. Pepinemab (VX15/2503) is currently being evaluated as single agent or in combination with other immunotherapies in four clinical trials: (i) a Phase 1b/2a combination trial of pepinemab with avelumab in NSCLC (CLASSICAL-Lung) (NCT03268057); (ii) a phase 1 combination trial of pepinemab with nivolumab or ipilimumab in melanoma patients who have progressed on any anti-PD-1/PD-L1 (NCT03425461); (iii) a neoadjuvant integrated biomarker trial in patients with metastatic colorectal and pancreatic cancers treated with pepinemab in combination with nivolumab or ipilimumab (NCT03373188); and (iv) a Phase 1/2 trial of pepinemab in children with solid tumors and children and young adults with osteosarcoma (NCT03320330).

Results

SEMA4D exerts multi-faceted effects within the tumor microenvironment by creating a barrier at the tumor-stroma margin to restrict immune cell infiltration and promoting immunosuppressive activity of myeloid-derived cells. Blocking antibody to SEMA4D directly enhanced M1/M2 ratio, and both reduced expression of chemokines that recruit MDSC and the ability of MDSC to suppress T cell proliferation. In preclinical models, anti-SEMA4D reduced the function of MDSC and Treg in the TME while simultaneously restoring the ability of dendritic cells and cytotoxic T cells to migrate into the tumor. Importantly, anti-SEMA4D MAb enhanced the activity of co-administered immunotherapies in murine colon, head and neck (HNSCC), and melanoma models. For example, anti-SEMA4D plus anti-CTLA-4 resulted in 90% complete tumor rejection (CR) ($p<0.0001$) in an HNSCC model representative of a T cell inflamed tumor with high MDSC suppression. Combination treatment of anti-SEMA4D with anti-LAG3 or epigenetic modulator entinostat resulted in maximal tumor growth delay and 90% CR ($p<0.0001$).Pepinemab treatment was well tolerated in a Phase I trial in patients with advanced refractory solid tumors (NCT01313065). Several clinical trials are in progress to evaluate safety, tolerability, efficacy, and biological endpoints, including immunophenotyping tumors and blood of patients treated with pepinemab in combination with immunomodulatory agents. Trial design will be reported and enrollment updates are expected.

Conclusions

SEMA4D blockade represents a novel approach to promote functional immune infiltration into the tumor, reduce mesenchymal suppression, and enhance immunotherapy effects.

Trial Registration

NCT01313065NCT03268057NCT03425461NCT03373188NCT03320330

References

1. Evans, EE et al. Cancer Immunol Res. 2015 Jun;3(6):689-701.
2. Patnaik A et al. Clin Cancer Res. 2016 Feb 15;22(4):827-363. Adusumilli PS et al. J Immunother Cancer. 2016 Jun 20; 5:50.

O21

A phase 1 study of TSR-022, an anti-TIM-3 monoclonal antibody, in combination with TSR-042 (anti-PD-1) in patients with colorectal cancer and post-PD-1 NSCLC and melanoma

Diwakar Davar, MD[1], Peter Boasberg, MD, FACP[2], Zeynep Eroglu, MD[3], Gerald Falchook, MD[4], Justin Gainor, MD[5], Erika Hamilton, MD[6], J. Randolph Hecht, MD[7], Jason Luke, MD, FACP[8], Michael Pishvaian[9], Antoni Ribas, MD, PhD[7], Judy Wang, MD[10], Kristen McEachern, PhD[11], Angela Waszak[11], Sharon Lu[11], Yong Li[11], Ying Wang[11], Patricia LoRusso, DO[12]

[1]University of Pittsburgh Department of Medicine, Pittsburgh, PA, USA

[2]*The Angeles Clinic and Research Institute, Santa Monica, CA, USA*
[3]*Moffitt Cancer Center, Tampa, FL, USA*
[4]*Sarah Cannon Research Institute at HealthONE, Denver, CO, USA*
[5]*Massachusetts General Hospital, Boston, MA, USA*
[6]*Sarah Cannon Research Institute at Tennessee Oncology, Nashville, TN, USA*
[7]*Ronald Reagan UCLA Medical Center, Los Angeles, CA, USA*
[8]*The University of Chicago Medicine, Chicago, IL, USA*
[9]*MedStar Georgetown University Hospital, Washington, DC, USA*
[10]*Sarah Cannon Research Institute, Sarasota, FL, USA*
[11]*TESARO, Inc., Waltham, MA, USA*
[12]*Yale Cancer Center, New Haven, CT, USA*

Background

T cell immunoglobulin and mucin-domain containing-3 (TIM-3) is a key immune checkpoint that is often co-expressed with programmed cell death protein (PD)-1 and has been implicated in both effector T cell exhaustion and immune suppression mediated by myeloid cells. TIM-3 expression on effector T cells is associated with reduced cell proliferation and cytokine production, while TIM-3 expression on dendritic and other myeloid cells may prevent recruitment and priming of T cells. In combination with PD-1 blockade, anti-TIM-3 enhances the activation of T cells and demonstrates greater anti-tumor activity than anti-PD-1 alone in preclinical models. TSR-022 is a potent, selective anti-TIM-3 antibody that is being developed in combination with PD-1 blockade.

Methods

TSR-022 is being investigated in a multicenter, open-label, first-in-human phase 1 trial that is enrolling patients with advanced or metastatic solid tumors that have progressed after treatment with available therapies or are intolerant to standard treatment. Part 1 includes an evaluation of dose escalation of TSR-022 as a monotherapy, as well as in combination with TSR-042, an anti-PD-1 antibody, also including immuno-oncology–naïve patients. Patients received IV infusion of TSR-022 alone and in combination with 500 mg TSR-042 in escalating, fixed doses. The primary objective of the part 1 study is to determine the recommended phase 2 dose (RP2D) and to evaluate the safety and tolerability of TSR-022 alone and in combination with TSR-042. In part 2 of the study, the anti-tumor activity of TSR-022 in combination with TSR-042 is being evaluated in colorectal cancer, post-PD-1 melanoma, and post-PD-1 NSCLC.

Results

As of July 13, 2018, 98 patients have been treated in part 1 of this study and 104 patients have been treated in part 2. Of these 202 patients, 52 received TSR-022 monotherapy and 150 received combination therapy of TSR-022 and TSR-042. The incidence of grade ≥3 treatment-related adverse events in combination therapy was 6.7%. The grade ≥3 treatment-related adverse events in combination therapy that occurred in >1.0% of patients were lipase increased (1.3%) and rash maculo-papular (1.3%). There was a dose-proportional increase in TSR-022 exposure and receptor occupancy. Objective responses were observed in patients with post-PD1 NSCLC and melanoma and will be reported.

Conclusions

TSR-022 in combination with TSR-042 was well tolerated across multiple dose levels. Adverse events were manageable and consistent with the safety profiles of other checkpoint inhibitors. Clinical activity was observed and warrants continued exploration.

Trial Registration

clinicaltrials.gov NCT02817633

O22

Safety and efficacy of cryopreserved autologous tumor infiltrating lymphocyte therapy (LN-144, lifileucel) in advanced metastatic melanoma patients following progression on checkpoint inhibitors

Amod Sarnaik, MD[1], Sajeve Thomas[2], Diwakar Davar, MD[3], John Kirkwood, MD[4], Harriet Kluger, MD[5], Jose Lutzky, MD, FACP[6], Melissa Wilson[7], Anna Pavlick, MD, MBA[8], Brendan Curti, MD[9], Eric Whitman, MD, FACS[10], Giao Phan, MD[11], Marc Ernstoff, MD[12], Jason Chesney, MD[13], Toshimi Takamura, BS[14], Debora Barton, MD[14], Sam Suzuki, MS[14], Lavakumar Karyampudi[14], Nancy Samberg, PhD[14], Maria Fardis, PhD, MBA[14]

[1]*H. Lee Moffitt Cancer Center, Tampa, FL, USA*
[2]*Univ. of Florida Health Cancer Center, Orlando, FL, USA*
[3]*Univ. Pittsburgh Hillman Cancer Center, Pittsburgh, PA, USA*
[4]*Univ Pittsburgh Hillman Cancer Center, Pittsburgh, PA, USA*
[5]*Yale Cancer Center, New Haven, CT, USA*
[6]*Mount Sinai Comprehensive Cancer Center, Miami Beach, FL, USA*
[7]*Thomas Jefferson Kimmel Cancer Center, Philadelphia, PA, USA*
[8]*NYU Perlmutter Cancer Center - Langone, New York, NY, USA*
[9]*Chiles Research Inst. Providence Cancer, Portland, OR, USA*
[10]*Atlantic Health System Cancer Care, Morristown, NJ, USA*
[11]*Virginia Commonwealth University, Richmond, VA, USA*
[12]*Roswell Park Comprehensive Cancer Center, Buffalo, NY, USA*
[13]*James Graham Brown Cancer Center, Louisville, KY, USA*
[14]*Iovance Biotherapeutics, Inc., San Carlos, CA, USA*

Background

While immunotherapy including checkpoint inhibitors and targeted therapies (BRAF/MEK inhibitors) are options for patients with metastatic melanoma, many patients experience progression. Patients progressed after multiple checkpoints and targeted therapy have few treatment options available including high dose IL-2 and chemotherapy. Response rates of 4-10% have been reported for investigator's choice of these second line agents. Adoptive cell therapy utilizing tumor-infiltrating lymphocytes (TIL) is recognized as an effective treatment in metastatic melanoma and other solid tumors eliciting durable and complete responses, even in heavily pretreated patients. We provide preliminary data of responses to lifileucel and biomarkers in heavily pre-treated metastatic melanoma patients who have progressed on multiple checkpoint and BRAF/MEK inhibitors (if BRAF mutated).

Methods

C-144-01 is a global phase 2, open-label, multicenter study of efficacy and safety of lifileucel in patients with unresectable metastatic melanoma. We report on Cohort 2 (N=30) patients who received cryopreserved Gen-2 lifileucel. Tumors resected at local institutions are processed at central GMP facilities in a 22-day manufacturing process. The final product is cryopreserved and shipped to the sites. Patients receive one week of a preconditioning cyclophosphamide/fludarabine lymphodepletion regimen, followed by a single infusion of lifileucel, plus up to 6 doses of intravenous IL-2 (600,000 IU/kg).

Results

Cohort 2 patients with Stage IIIC/IV melanoma had a median of 3 prior therapies. Concomitantly administered treatment regimens containing multiple agents, such as ipilimumab and nivolumab,

were counted as a single prior therapy if the therapies were started within 28 days of one another. Preliminary results from this ongoing study indicate efficacy in Cohort 2: ORR=33% (1 uCR, 7 PR, 2 uPR), DCR=73%, median follow-up of all patients was 6 months, median time to initial response 1.7 months (range: 1.6-4.4 months), and median DOR not reached (8 ongoing responders out of 10). Median follow up for all responders was 4.5 months. A longer follow-up led to improving responses in some patients including the CR. Per investigator assessment, none of the grade 5 SAEs were due to any of the study treatment. Lifileucel-induced in vitro IFNγ response to antibody coated beads (anti-CD3, anti-CD28, anti-CD137) and serum IP-10 levels post-treatment, correlates with reduction in tumor (Sum of Diameter of target lesions) and/or overall response.

Conclusions

These preliminary data support TIL therapy with lifileucel as an efficacious and well tolerated therapeutic option for patient with metastatic melanoma who have failed multiple lines of prior therapies including checkpoint inhibitors and BRAF/MEK inhibitors (if BRAF mutated).

Trial Registration

NCT02360579

Ethics Approval

The C-144-01 study was approved by Western Institutional Review Board, approval number 20160198, along with additional approvals by applicable institutional Ethics/Review Boards.

Table 1.

Table 1. Demographics & Baseline Characteristics

	Cohort 2 (N=30)		Cohort 2 (N=30)
Gender, n (%)		Baseline LDH (U/L)	
Male	17 (57)	Median	254
Female	13 (43)		
Age		Target Lesion Sum of Diameter (mm)	
Median	57	Median	110.0
Min, Max	35, 70	Min, Max	17, 343
Baseline ECOG score, n (%)		# Baseline Target and Non-Target Lesions	
0	15 (50)	Median	5
1	15 (50)	Min, Max	2, 14
Prior therapies, n (%)		BRAF Status, n (%)	
IL-2	3 (10)	Mutated (V600E or V600K)	10 (33)
Anti-CTLA-4[1]	27 (90)	Wild Type or other mutants	20 (67)
Anti-PD-1[2]	30 (100)		
BRAF and MEK Inhibitor[3]	8 (27)		

[1] Ipilimumab (MDX-010)
[2] Pembrolizumab, Nivolumab, Durvalumab
[3] Two of 10 patients with V600E or V600K BRAF mutations had not received prior BRAF inhibitor due to enrollment under an earlier version of the protocol.

O23

Combination of subcutaneous selicrelumab (CD40 agonist) and vanucizumab (anti-Ang2/VEGF) in patients with solid tumors demonstrates early clinical activity and a favorable safety profile

Emiliano Calvo, MD PhD[1], Jan Schellens[2], Ignacio Matos[3], Elena Garralda[3], Morten Mau-Soerensen[4], Aaron Hansen[5], Maria Martinez-Garcia[6], Martijn Lolkema[7], Jehad Charo, PhD[8], Chiara Lambertini[8], Christoph Mancao[8], Katrijn Bogman[8], Cristiano Ferlini, MD[8], Martin Sern, MD[9], Willeke Ros, MSc[2]

[1]*START Madrid, Madrid, Spain*
[2]*The Netherlands Cancer Institute, Amsterdam, Netherlands*
[3]*Vall d'Hebron University Hospital, Barcelona, Spain*
[4]*Rigshospitalet, Copenhagen, Denmark*
[5]*Princess Margaret Hospital, Toronto, Canada*
[6]*Hospital del Mar, Barcelona, Spain*
[7]*Erasmus Medical Center, Rotterdam, Netherlands*
[8]*Roche pRED, Schlieren, Switzerland*
[9]*Roche Innovation Center Zurich, Schlieren, Switzerland*

Background
Selicrelumab is a fully human agonistic IgG2 monoclonal antibody to CD40, a member of the TNF-receptor superfamily expressed on antigen-presenting cells (APC), endothelial cells and some tumors. CD40 activation of APCs primes T-cells, whereas vanucizumab (anti-Ang2/VEGF bispecific antibody) - on top of anti-angiogenic effects - supports dendritic cell maturation and inhibits immunosuppressive signals. Here, results of the dose escalation study exploring selicrelumab administered subcutaneously (SC) combined with vanucizumab are reported.

Methods
This is an ongoing study in patients with advanced/metastatic solid tumors not amenable to standard therapy (NCT02665416) assessing safety, PK/PD, and antitumor activity by RECIST and irRC.

Results
Fifty-nine patients received intravenous vanucizumab (2g; q2w) followed by SC selicrelumab at doses of 1-72mg (q4w). Selicrelumab serum concentrations were below the limit of quantification at doses up to 14mg, higher doses resulted in measurable serum levels with high inter-subject variability. Dose-limiting toxicity occurred in 1 patient with injection site reaction (ISR) G3 in the 8mg selicrelumab cohort. The most frequent observed AEs were ISR (91.5%), pyrexia (54.2%), nausea (49.2%), fatigue and hypertension (44.1% each). No selicrelumab-related G4/G5 AEs were reported, vanucizumab toxicity was as expected for a VEGF inhibitor. Best response by RECIST in 54 efficacy-evaluable pts was 1 CR (bladder cancer, 32mg) + 1 PR (ovarian cancer, 24mg), and 29 SD. SD patients included 3 patients with unconfirmed PR and one irPR (medullary thyroid, head and neck, esophageal, and adrenal carcinoma; at 8, 12, 14, and 14mg, respectively); two of these patients stopped treatment due to wound healing complications after rapid and deep response.Exploratory biomarker analyses showed selicrelumab-dose dependent peripheral B-cell depletion, despite non-detectable serum drug levels, followed by activation/proliferation of CD8+ T-cells - most prominently observed at intermediate selicrelumab dose levels (8-32mg). Furthermore, tumor infiltration of activated/proliferating T-cells was generally higher at these dose levels. Baseline B-cell counts in tumor and periphery and post-treatment activation of peripheral CD8 T-cells potentially correlate with radiological response. Immune modulation is being investigated by comparing gene expression patterns of paired baseline vs. on-treatment biopsies.

Conclusions
Selicrelumab with vanucizumab shows pharmacodynamic and early clinical activity in patients with advanced solid tumors. Correlative analyses suggest a contribution of CD40 agonism to the activity observed. The combination demonstrated a favorable safety profile with no evidence for systemic autoimmune toxicity. The results triggered an expansion of the study in selected tumor indications with 16mg SC selicrelumab in combination with bevacizumab (anti-VEGF).

Trial Registration
This study is registered on Clinicaltrials.gov: NCT02665416

Ethics Approval
This study was approved by the local IRB at each participating study site.

Combination Therapy

O24

A phase 1, open-label, dose-escalation study of enoblituzumab in combination with pembrolizumab in patients with select solid tumors

Charu Aggarwal, MD MPH[1], Anthony Joshua, MD[2], Robert Ferris, MD, PhD[3], Scott Antonia, MD, PhD[4], E E. Rahma, MD[5], Anthony Tolcher, MD, FRCP(C)[6], Roger Cohen[1], Yanyan Lou, MD[7], Ralph Hauke, MD[8], Nicholas Vogelzang, MD[9], Dan Zandberg, MD[10], Arash Rezazadeh Kalebasty, MD[11], Victoria Atkinson, MD[12], Alex Adjei, MD PhD[7], Mahesh Seetharam[7], Ariel Birnbaum, MD[13], Andrew Weickhardt, MBBS, FRACP, DMedSc[14], Vinod Ganju, MBBS, FRACP[15], Riva Bondarenko, PhD[16], Linda Peng, MS[16], Tony Wu, PhD[16], Scott Currence[16], Jan Baughman, MPH[16], Ezio Bonvini[16], Stacie Goldberg, MD[16], Jon Wigginton, MD[16], Nehal Lakhani, MD, PhD[17]

[1]University of Pennsylvania, Philadelphia, PA, USA
[2]St. Vincent's Hospital, Syndey, Australia
[3]University of Pittsburgh, Pittsburgh, PA, USA
[4]Moffitt Cancer Center, Tampa, FL, USA
[5]Dana Farber Cancer Institute, Boston, MA, USA
[6]START, San Antonio, TX, USA
[7]Mayo Clinic, Jacksonville, FL, USA
[8]Nebraska Cancer Specialists, Omaha, NE, USA
[9]Comprehensive Cancer Centers of Nevada, Las Vegas, NV, USA
[10]University of Maryland, Baltimore, MD, USA
[11]Norton Cancer Institute, Louisville, KY, USA
[12]University of Queensland, Woolloongabba, Australia
[13]Rhode Island Hospital, Providence, RI, USA
[14]Olivia Newton-John Cancer Research Inst., Melbourne, VT, Australia
[15]Peninsula and Southeast Oncology, Frankston, Australia
[16]MacroGenics, Inc., Rockville, MD, USA
[17]Start Midwest, Grand Rapids, MI, USA

Background
Enoblituzumab is a humanized IgG1 monoclonal antibody (mAb) targeting B7-H3 (CD276), and is Fc-engineered to enhance antibody-dependent cell-mediated cytotoxicity. B7-H3 has limited normal tissue expression, but is highly expressed in many solid tumors. Enoblituzumab monotherapy has demonstrated antitumor activity with an acceptable safety profile in patients with selected solid tumors. Pembrolizumab is a humanized IgG4 anti-PD-1 mAb and is FDA approved for multiple solid tumor indications. It is hypothesized that coordinate engagement of both innate and adaptive immunity via targeting of two distinct members of the B7 family, the combination of enoblituzumab and pembrolizumab could achieve greater antitumor activity than either agent alone.

Methods
Patients with advanced/metastatic solid tumors received weekly (qwk) enoblituzumab (doses 3-15 mg/kg) IV plus pembrolizumab (2 mg/kg) IV q3wk during dose-escalation (3+3 design) and cohort expansion. Tumor B7-H3 and PD-L1 expression was assessed via immunohistochemical staining. Disease assessment occurred after 6 weeks, then q9wks thereafter. Expansion cohorts included non-small cell lung cancer (NSCLC; checkpoint-inhibitor naïve, PD-L1 <1%) NSCLC (post checkpoint inhibitor), squamous cell carcinoma of the head and neck (SCCHN; checkpoint-inhibitor naïve), SCCHN (post checkpoint inhibitor), and urothelial cancer (UC) and melanoma (post checkpoint inhibitor).

Results
The combination demonstrated acceptable tolerability in the overall population (N=133) at doses up to enoblituzumab 15 mg/kg+pembrolizumab (2 mg/kg), with no maximum tolerated dose defined. Treatment-related adverse events (AE, all grade) occurred in 85% of patients, with > G3 in 28%. Infusion-related reaction and elevated lipase (6%) were the only Grade > 3 AE

occurring in > 5% of patients. One treatment-related death due to pneumonitis occurred. The combination demonstrated antitumor activity in checkpoint-inhibitor-naïve SCCHN patients, and also induced objective responses in patients anticipated to have relatively limited responsiveness to pembrolizumab alone, including NSCLC with tumor PD-L1 expression <1% and checkpoint-inhibitor-refractory UC. To date, objective responses have occurred in 6/18 (33%) response-evaluable, checkpoint-inhibitor-naïve SCCHN patients, including 4 confirmed and 2 unconfirmed PR, with stable disease in 6/18 (33%). Among SCCHN patients with tumor B7-H3 expression >10%, the ORR was 40% (6/15). In NSCLC patients (PD-1 naïve, tumor PD-L1 <1%), there were 4/14 PR (29%; 2 confirmed and 2 unconfirmed) and 9 SD (64%). Two of 16 post-checkpoint-inhibitor UC patients achieved a PR and unconfirmed CR, respectively.

Conclusions
The enoblituzumab+pembrolizumab combination demonstrated an acceptable safety profile, encouraging initial antitumor activity in patients with checkpoint-inhibitor-naïve SCCHN, and the ability to induce partial responses in patients anticipated to be poorly responsive to checkpoint inhibitor alone.

Trial Registration
NCT02475213

Ethics Approval
This study was approved by each Institution's Ethics Board prior to enrolling.

O25

Phase 1 dose-finding study of the anti–TIGIT antibody MK-7684 as monotherapy and in combination with pembrolizumab in patients with advanced solid tumors

Talia Golan[1], Todd Bauer, MD[2], Antonio Jimeno, MD, PhD[3], Ruth Perets[4], Jiaxin Niu[5], James Lee, MD, PhD[6], Mallika Lala[7], Jennifer Garrus[7], Zhen Zeng[7], Elliot Chartash[7], Jane Healy[7], Drew Rasco, MD[8]

[1]Sheba Medical Center, Ramat Gan, Israel
[2]Sarah Cannon Research Institute/TN Oncol, Nashville, TN, USA
[3]University of Colorado, Denver, CO, USA
[4]Rambam Medical Center, Haifa, Israel
[5]Banner MD Anderson Cancer Center, Gilbert, AZ, USA
[6]University of Pittsburgh Medical Center, Pittsburgh, PA, USA
[7]Merck & Co., Inc., Kenilworth, NJ, USA
[8]START, San Antonio, TX, USA

Background
TIGIT (T-cell immunoreceptor with Ig and ITIM domains) is an immunomodulatory receptor that functions as a negative immune checkpoint. In preclinical models, TIGIT inhibition provided antitumor activity, with an enhanced effect observed when combined with PD-1 inhibition. MK-7684 is a humanized, IgG1 monoclonal antibody that binds TIGIT and blocks its interaction with its ligands, CD112 and CD155. We present the dose escalation portion of the first-in-human study of MK-7684 as monotherapy or in combination with pembrolizumab in patients with advanced solid tumors.

Methods
Eligible patients had metastatic solid tumors that failed standard treatment options, measurable disease, and ECOG PS 0-1. MK-7684 dose escalation followed a modified toxicity probability interval design with a target DLT rate during cycle 1 of ~30% and planned doses of 2.1, 7, 21, 70, and 210 mg Q3W. MK-7684 and pembrolizumab 200 mg Q3W were given for up to 35 cycles or until progression, intolerable toxicity, or investigator or patient decision. Study objectives included evaluation of safety and tolerability, pharmacokinetics, and ORR of MK-7684 monotherapy and MK-7684 plus

pembrolizumab. Data cutoff date was July 16, 2018.

Results

68 patients were treated. 34 patients received MK-7684 monotherapy; median age was 67.5 years, 50% had ECOG PS 1, and 50% received ≥3 prior therapies. 34 patients received MK-7684 plus pembrolizumab; median age was 62.5 years, 65% had ECOG PS 1, and 32% received ≥3 prior therapies. There were no DLTs. Across doses, treatment-related AEs occurred in 53% of monotherapy and 65% of combination therapy recipients (grade 3-5, 6% and 12%); no patients died or discontinued because of treatment-related AEs. The most common treatment-related AEs were fatigue (15%) and pruritus (12%) with MK-7684 and pruritus (21%) and rash (15%) with MK-7684 plus pembrolizumab. The pharmacokinetic profile of MK-7684 was generally consistent with that of a typical monoclonal antibody. Exposure increased with increasing dose, and target-mediated drug disposition was observed at low doses. Clearance was linear at a dose of 210 mg. ORR (confirmed+unconfirmed) was 3% with monotherapy (1 PR) and 18% with combination therapy (6 PRs). DCR was 35% and 48%, respectively.

Conclusions

MK-7684 as monotherapy and in combination with pembrolizumab 200 mg Q3W was well tolerated and had an acceptable safety profile across all dose levels. Promising antitumor activity was seen, especially for the combination. Dose confirmation and evaluation of efficacy for monotherapy and combination therapy is ongoing in patients with select advanced solid tumors.

Trial Registration

ClinicalTrials.gov, NCT02964013

O26

The anti–LAG-3 antibody MK-4280 as monotherapy and in combination with pembrolizumab for advanced solid tumors: first-in-human phase 1 dose-finding study

Nehal Lakhani, MD, PhD[1], Todd Bauer, MD[2], Anson Abraham, PhD[3], John Luddy[3], John Palcza, MS[3], Elliot Chartash[3], Jane Healy[3], Amita Patnaik, MD FRCP(C)[4]

[1]*START-Midwest, Grand Rapids, MI, USA*
[2]*Sarah Cannon Research Institute/TN Oncol, Nashville, TN, USA*
[3]*Merck & Co., Inc., Kenilworth, NJ, USA*
[4]*START, San Antonio, TX, USA*

Background

LAG-3 (lymphocyte-activation gene 3) is an immunomodulatory receptor that regulates T_{eff} homeostasis, proliferation, and activation and has a role in T_{reg} suppressor activity. Preclinical data suggest that dual LAG-3/PD-1 blockade synergistically reverses tumor-specific anergy. MK-4280 is a humanized, IgG4, anti–LAG-3 monoclonal antibody that prevents LAG-3 from binding its ligand, MHC class II. We present dose-escalation results of the first-in-human study of MK-4280 as monotherapy or in combination with pembrolizumab for patients with advanced solid tumors.

Methods

Adults with metastatic solid tumors without clinically effective treatment, measurable disease, and ECOG PS of 0-1 were eligible. Dose finding for monotherapy and combination therapy followed standard 3+3 dose escalation using MK-4280 doses of 7, 21, 70, 210, and 700 mg Q3W. MK-4280 and pembrolizumab 200 mg Q3W were given for 35 cycles or until progression, intolerable toxicity, or investigator or patient decision. The DLT evaluation period was cycle 1. Study objectives included evaluation of the safety and tolerability, pharmacokinetics, and ORR of MK-4280 as monotherapy and in combination with pembrolizumab. Data cutoff date was June 12, 2018.

Results
18 patients received MK-4280 monotherapy; 15 received MK-4280 plus pembrolizumab. Median age was 60 years, 67% of patients had ECOG PS 1, and 48% received ≥3 prior therapies. MK-4280 dose escalation proceeded to 700 mg Q3W for both monotherapy and combination therapy without any DLTs. Treatment-related AEs occurred in 61% of monotherapy and 53% of combination therapy recipients, were of grade 3-4 toxicity in 6% and 20%, and led to discontinuation in 6% and 13%. There were no treatment-related deaths. Treatment-related AEs that occurred in ≥10% of patients were fatigue (17%) and arthralgia (11%) for monotherapy and fatigue (20%), pyrexia (20%), pruritus (13%), and maculopapular rash (13%) for combination therapy. The pharmacokinetic profile was generally consistent with that of a typical monoclonal antibody. Exposure increased with increasing dose, and target-mediated drug disposition was observed at low doses. Clearance was linear at doses of 210 mg and 700 mg. ORR was 6% with monotherapy (1 PR) and 27% with combination therapy (4 PRs). DCR was 17% and 40%, respectively.

Conclusions
MK-4280 as monotherapy and in combination with pembrolizumab was well tolerated and had an acceptable safety profile across all dose levels. Promising antitumor activity was observed, particularly for the combination. Dose confirmation and efficacy evaluation of MK-4280 alone and in combination with pembrolizumab is ongoing in patients with select advanced solid tumors.

Trial Registration
ClinicalTrials.gov, NCT02720068

O27

Phase 2 trial of mocetinostat in combination with durvalumab in NSCLC patients with progression on prior checkpoint inhibitor therapy

Melissa L. Johnson, MD[1], Keith Eaton, MD[2], Balazs Halmos, MD[3], Edward Garon, MD[4], Thomas Hensing, MD[5], Nisha Mohindra, MD[6], James Strauss, MD[7], Timothy McCarthy[8], Rami Owera[9], Isan Chen, MD[10], Peter Olson[10], Demiana Faltaos, PharmD, PhD[10], James Christensen[10], Diane Potvin[10], Tavette Neskorik[10], Adam Pavlicek[11], Manish Patel, DO[12]

[1]Sarah Cannon Research Institute, Nashville, TN, USA
[2]Seattle Cancer Care Alliance, Seattle, WA, USA
[3]Montefiore Medical Center, White Plains, NY, USA
[4]University of California-Los Angeles, Santa Monica, CA, USA
[5]NorthShore University Health System, Evanston, IL, USA
[6]Northwestern University, Chicago, IL,USA
[7]Mary Crowley Cancer Research Center, Dallas, TX, USA
[8]Virginia Cancer Specialists, Fairfax, VA, USA
[9]Woodlands Medical Specialists, Pensacola, FL, USA
[10]Mirati Therapeutics, San Diego, CA, USA
[11]Monoceros Biosystems Inc., San Diego, CA, USA
[12]University of Minnesota Masonic Cancer, Minneapolis, MN, USA

Background
Mocetinostat, a spectrum-selective class I histone deacetylase inhibitor, has multiple potential immunomodulatory features including: 1) induction of major histocompatibility complex Class I and Class II expression on tumor cells, 2) enhanced function of T effector cells, and 3) decreased function of immunosuppressive cell subsets including regulatory T cells and myeloid derived suppressor cells. Given these pleiotropic immune activating effects, the combination of mocetinostat and the PD-L1 blocking mAb durvalumab was tested in NSCLC patients (pts) with checkpoint inhibitor therapy (CIT) naïve disease or had progressive disease after prior CIT.

Methods
Phase 1 of the study explored increased doses of

mocetinostat administered orally (50, 70, 90 mg three times weekly [TIW]) in combination with durvalumab in patients with advanced solid tumors. Review of all safety data supported a recommended Phase 2 dose of mocetinostat 70 mg TIW with durvalumab (1500 mg) on day 1 of each 28-day cycle. Study objectives include evaluation of safety and Objective Response Rate (ORR) in pts with NSCLC who have progression of disease (PD) on or after treatment with CIT or are CIT-naïve. Two CIT-experienced cohorts enrolled pts based on prior clinical benefit with CIT. A predictive probability design is used for assessment of enrollment expansion in each stage and treatment arm. Other objectives include tolerability, pharmacokinetics, incidence of anti-drug antibody and multiple correlative endpoints.

Results

Enrollment in Stage 1 of the CIT-experienced cohorts is complete. As of July 13, 2018, 37 patients who received at least one dose of mocetinostat and durvalumab were included in the assessment. Six of the 37 pts achieved a partial response (PR); 4 confirmed and 2 unconfirmed (2/24 PRs in Prior Clinical Benefit; 2 PRs/2 uPRs/13 in No Prior Clinical Benefit cohorts, respectively) and 11/37 pts demonstrated tumor reductions; with the longest treatment duration exceeding 55 weeks. Treatment-related AEs (>10% of pts; all grades) included fatigue, nausea, diarrhea, vomiting, and decreased appetite. Updated safety, efficacy, and correlative science data will be presented.

Conclusions

Based on preliminary data, the combination of mocetinostat with durvalumab is clinically active with manageable side effects.

Trial Registration

Clinical Trial Information: NCT02805660

Ethics Approval

This study was approved by Copernicus Group Independent Review Board; approval tracking PRA0-16-027.

Co-Stimulatory Ligand-Receptor Interactions

O28

Results from a Phase I dose escalation trial (TACTI-mel) with the soluble LAG-3 protein (IMP321, eftilagimod alpha) together with pembrolizumab in unresectable or metastatic melanoma

Frederic Triebel, MD, PhD[1,2], Christian Mueller[2], Chrystelle Brignone[2], Victoria Atkinson, MD[3], Melissa Eastgate, MD[4], Amitesh Roy, MD[5], Adnan Khattak, MD[6], Andrew Haydon, MBBS PhD[7]

[1]Prima Biomed Ltd, Orsay, France
[2]Immutep, Orsay, France
[3]Princess Alexandra Hospital, Woolloongabba, Australia
[4]Royal Brisbane Womens Hospital, Herston, Australia
[5]Flinders Centre for Innovation in Cancer, Bedfork Park, Australia
[6]Fiona Stanley Hospital, Murdoch, Australia
[7]Alfred Hospital, Melbourne, Australia

Background

Eftilagimod alpha (efti, IMP321) is a recombinant soluble LAG-3Ig fusion protein binding to MHC class II molecules and mediating antigen presenting cell (APC) activation followed by CD8 T-cell activation. The activation of the dendritic cell network and the subsequent T cell recruitment at the tumor site with efti may lead to stronger anti-tumor CD8 T cell responses. Combining an APC activator with an immune checkpoint inhibitor (ICI) aims to increase efficacy without additional toxicity. We report results of the dose escalation phase I trial (NCT02676869) with pembrolizumab and efti.

Methods

Melanoma patients (pts) on pembrolizumab (2

mg/kg i.v.) with progressive disease (irPD), stable disease (irSD) or partial response (irPR) acc. to irRC after 3 cycles received 1 mg (n=6), 6 mg (n=6) or 30 mg (n=6) s.c. injections of efti (every 2 weeks for 6 months) from cycle 5 of pembrolizumab onwards. Blood samples for pharmacokinetics were taken in cycle 1 and 9.

Results
In stage A, 18 pts (17 male, 1 female) with a median age of 66 years (range 48-85) were enrolled. Fifteen (83 %) and seven (39 %) pts had stage M1C disease and elevated LDH, respectively. Seven (39 %) pts completed the 6 months combination treatment. Reasons for discontinuation were irPD (n=7), withdrew consent (n=2) and death not related to efti or pembrolizumab (n2). The most common AEs were fatigue (44 %), rash (33 %), diarrhea (28 %), nausea (28 %), arthralgia (17 %) and colitis (11 %). One patient experienced intracranial hemorrhage grade 4, another had a colitis grade 4, both not related to efti or pembrolizumab. No dose limiting toxicity has been reported. A dose-dependent increase in serum IMP321 concentration was observed among the three dose levels with a Cmax between 4 and 24 hours. Objective response rate (ORR) taking cycle 5 of pembrolizumab as baseline was 33 % (irRC) including one patient with a confirmed irCR after progress on pembrolizumab monotherapy.

Conclusions
Up to 30 mg efti in combination with pembrolizumab are safe and well tolerated. The responses observed in pts with suboptimal response to pembrolizumab alone may point to a benefit of adding a systemic APC activator to an ICI.

Trial Registration
NCT02676869

Ethics Approval
The study was approved by Metro South Human Research Ethics Commitee (Australia), approval number HREC/15/QPAH/726

Consent
Written informed consent was obtained from the patient for publication of this abstract and any accompanying images. A copy of the written consent is available for review by the Editor of this journal.

Co-Stimulatory Ligand-Receptor Interactions

O29

Immuno-oncology tHERApy with HERA-GITRL: the novel hexavalent human GITR agonist activates T cells and promotes anti-tumor efficacy independent of Fc-functionality

Viola Marschall, PhD[1], Meinolf Thiemann[1], Jaromir Sykora[1], David Richards[1], Christian Merz[1], Julian Sefrin[1], Karl Heinonen[1], Matthias Schroeder[1], Mauricio Redondo Müller[1], Christian Gieffers[1], Oliver Hill[1]

[1]*Apogenix AG, Heidelberg, Germany*

Background
Glucocorticoid-induced TNFR-related protein (GITR, TNFRSF18, CD357), a TNFR-SF member, is a co-stimulatory receptor that increases anti-tumor T cell activation. Based on Apogenix hexavalent TNFR-SF agonist (HERA-ligand) technology platform, we created a fully human hexavalent GITR ligand fusion protein HERA-GITRL intended for T cell costimulatory approaches in immuno-oncology (IO) therapy. HERA-GITRL is composed of a trivalent single chain GITRL-receptor-binding-domain fused to an IgG1-derived silenced Fc-domain serving as dimerization scaffold. Because of the unique design of the silenced Fc-domain, HERA-GITRL allows the study of pure GITR agonism in contrast to Fc-mediated mixed modes of action. Here we report in vitro and in vivo properties of our novel HERA-GITRL construct.

Methods
N/A

Results
For functional characterization of HERA-GITRL in vitro, human immune cells isolated from healthy-donor blood were profiled by multicolor flow cytometry and real-time cell analysis (RTCA). Stimulation of unfractionated human T cells or purified naïve CD4+ T cells by anti-CD3 antibody was further augmented by HERA-GITRL. This effect was accompanied by increased proliferation, differentiation and elevated levels of TNF-α and IFN-γ. HERA-GITRL enables effector T cells proliferation even in the presence of regulatory T cells. In line with these findings, the murine surrogate mmHERA-GITRL enhanced antigen-specific clonal expansion of both CD4+ (OT-II) and CD8+ (OT-I) T cells in vivo. In a direct in vitro comparison of the anti-human GITR monoclonal antibody TRX518, trivalent GITRL and hexavalent HERA-GITRL, only HERA-GITRL showed full biological activity independent of additional crosslinking. Importantly, HERA-GITRL mediated T cell activation increases tumor cell killing by PBMCs in vitro. Finally, mmHERA-GITRL showed in vivo anti-tumor efficacy as a single agent in a subcutaneous syngeneic colon cancer model (CT26wt) in mice. The anti-tumor efficacy of mmHERA-GITRL is independent of its Fc functionality, as both mmHERA-GITRL with a functional Fc- and a silenced Fc-domain show a similar tumor growth inhibition.

Conclusions
By clustering six receptor chains in a spatially well-defined manner, HERA-GITRL induces potent agonistic activity without being dependent on additional Fc-mediated crosslinking. The anti-tumor effect of most anti-GITR antibodies is dependent on a fully functional Fc domain and is generally mediated by depletion of Treg cells. HERA-GITRL boosts antigen-specific T cell activity and shows anti-tumor efficacy while having no effect on Treg cells. This property of HERA-GITRL makes it particularly suitable for IO-combination therapies. The HERA-ligand concept has also been successfully translated to HERA-TRAIL (now in Phase I), -CD40L, -CD27L, -OX40L, -HVEML (LIGHT) and -4-1BBL.

Ethics Approval
The experimental protocols were registered by the regional board in Freiburg, Germany (Regierungspräsidium Freiburg; approval number G-15/41).

Cytokines in Anti-Tumor Immunity

O30

First-in-human phase 1 dose-escalation trial of the potent and selective next generation transforming growth factor-β receptor type 1 (TGF-βR1) inhibitor LY3200882 in patients with advanced cancers

Timothy Yap, MD[2], Capucine Baldini, MD[3], Christophe Massard, MD, PhD[3], Ivelina Gueorguieva, PhD[1], Yumin Zhao, PhD[1], Shelly Schmidt[1], Michael Man, PhD[1], Shawn Estrem, PhD[1], Karim Benhadji, MD[1], Maria Vieito, MD[4]

[1]Eli Lilly and Company, Indianapolis, IN, USA
[2]Univ. of Texas MD Anderson Cancer Center, Houston, TX, USA
[3]Gustave Roussy Cancer Campus, Villejuif, France
[4]Vall d'Hebron University Hospital & VHIO, Barcelona, Spain

Background
The TGF-β pathway is commonly deregulated in cancer and plays a pivotal role during tumorigenesis. LY3200882 is a potent and selective TGF-βR1 inhibitor. This multicenter, nonrandomized, open-label, phase 1 study assessed the recommended phase 2 dose of LY3200882 as monotherapy in patients (pts) with advanced cancers.

Methods
Pts with refractory advanced or metastatic cancer were enrolled and were required to have adequate organ function as well as ECOG PS of 0 or 1. LY3200882 tosylate salt (hereafter referred to as LY3200882) was given twice daily (BID) to 5 cohorts of patients at increasing doses (5 to 50 mg) for 14 days in a 28 day cycle. Primary endpoint was to determine the recommended phase 2 dose. Secondary objectives included safety, response assessments and pharmacokinetics (PK), and exploratory objectives included pharmacodynamics (PD).

Results
30 pts were enrolled (19 males and 11 females); median age 47 y (32 y-74 y). The most common tumors were gliomas (15 pts), of which 5 were glioblastomas. No dose-limiting toxicities were observed. All treatment-related adverse events were grade 1-2 and most frequently included thrombocytopenia (2 pts), acneiform dermatitis (2 pts), rash (2 pts, 1 maculopapular rash and 1 pustular rash), and constipation (2 pts). LY3200882 was absorbed within 2-6 hours (h) and mostly eliminated within 48 h, with mean terminal half-life of 7.4 h (*n*=15). Drug exposures increased with escalating dose levels, up to the highest planned dose in the targeted therapeutic range of 50 mg BID. Plasma exposures in patients receiving the 50 mg BID dose were comparable to efficacious exposure levels from preclinical *in vivo* target inhibition and efficacy models. Detailed PD biomarker studies are ongoing and data will be presented. A confirmed partial response per Response Assessment in Neuro-Oncology (RANO) of a 85.7% decrease was observed in a glioblastoma pt (*EGFR* mutation; *CDK4* amplification; *IDH1/2* wildtype, *MGMT* methylated) treated at 50 mg BID who remains on LY3200882 for >11 months. Tumor regression (1.3%-85.7%) was observed in 5 pts (oligoastrocytoma, glioma (2 pts), astrocytoma, and glioblastoma).

Conclusions
LY3200882 monotherapy is well tolerated, with appropriate plasma exposures observed at the recommended phase 2 dose of 50 mg BID for 14 days in 28 days cycle, where preliminary antitumor activity has been observed. An expansion cohort assessing pts with glioblastoma is ongoing.

Trial Registration
ClinicalTrials.gov NCT02937272

Ethics Approval
MD Anderson Office of Protocol Review IRB approved protocol number 2016-0582 on 25-Aug-2016; Gustave Roussy Ethic Committee (Comite de Protection des Personnes Ile de France 3) approved protocol on 15-Nov-2016 and Competent Authority (Agence Nationale de Sécurité des Médicaments et de produits de santé) approved on 27-Oct-2016; VHIO Ethic Committee (Dictamen del comite de etica de la investigacion con medicamentos) approved protocol on 30-Sep-2016 and Competent Authority (Agencia espanola de medicamentos y productos sanitarios) approved on 03-Nov-2016; the EudraCT number 2016-001431-12 is the file number indicated on all approvals in Europe

O31

Tumor infiltrating lymphocyte recruitment after peri-lymphatic IRX-2 cytokine immunotherapy in resectable breast cancer and head and neck carcinoma

Joanna Pucilowska, PhD[2], Venkatesh Rajamanickam[2], Nicole Moxon, RN[2], Katherine Sanchez, MD[1], Monil Shah, PharmD[3], James Imatani, MD[1], Shaghayegh Aliabadi-Wahle, MD[1], Maritza Martel, MD[2], Alison Conlin, MD[2], James Egan, PhD[3], David Page, MD[2]

[1]*Providence Portland Cancer Center, Portland, OR, USA*
[2]*Providence Portland Medical Center, Portland, OR,*

USA
[3]IRX Therapeutics, Skillman, NJ, USA

Background
The IRX-2 biologic is a subcutaneous injectable immunotherapy composed of IL-2 and other cytokines derived from stimulated lymphocytes. Preclinically, IRX-2 activates T cells, natural killer cells, macrophages, and dendritic cells, and facilitates maturation of antigen-presenting cells. Tumor-infiltrating lymphocytes (TILs) are associated with improved outcomes in many cancers including early stage breast cancer (ESBC) and head and neck squamous cell carcinoma (HNSCC). We report data on TIL recruitment associated with pre-operative IRX-2 in a phase Ib ESBC trial, as well as phase Ib and IIa HNSCC trials.

Methods
The pre-operative IRX-2 regimen was evaluated in both ESBC and HNSCC trials for safety and immunologic activity. Beginning 21 days prior to surgical resection, enrolled operable patients with resectable stage I-III ESBC and stage II-IVA HNSCC received single low-dose intravenous cyclophosphamide (300 mg/m2 to facilitate T-regulatory cell depletion), followed by 10 days of subcutaneous injections of IRX-2 (1mL × 2 directed to regional peri-lymphatic space, 230IU/day). Endpoints included feasibility, TIL count by H&E blinded pathology review, and Nanostring RNA analysis.

Results
In the ESBC trial, 16 patients were enrolled and evaluable for TIL analysis, whereas in the HNSCC trials, 40 patients were enrolled and 36 patients were evaluable. In both trials, all patients received all planned injections with no treatment-related surgical delays, complications, or treatment-related grade III/IV toxicities. Treatment was associated with a mean 116% relative increase in TILs (range –36% to +1275%, p = 0.02) in ESBC and a mean 58% relative increase (range -57 to +452%, p=0.01) in HNSCC. Treatment was associated with PD-L1 RNA upregulation in EBSC (mean +54%, range –53% to +185%, p=0.04) but not HNSCC, however PD-L1 was higher at baseline in HNSCC. RNA analysis in ESBC and HNSCC revealed concordant increases in cytokine gene expression, including CXCL2, CCL4, CXCR4, and CXCL12 as well as transcription factors including FOS, ETS1, NFKB, EGR1/2 which are involved in T-cell activation and differentiation. We also note augmentation of ITGAE (CD103), a known marker of memory T-cell activation in EBSC cohort.

Conclusions
Pre-operative IRX-2 was well tolerated in both tumor histologies with statistically significant TIL recruitment, as well as PD-L1 upregulation in ESBC. Future directions include an evaluation of neoadjuvant IRX-2 with anti-PD-1 and chemotherapy in stage II-III TNBC, ongoing follow-up of a randomized phase IIb trial of neoadjuvant IRX-2 regimen in HNSCC to ascertain clinical benefit, and trials evaluating efficacy of IRX-2/anti-PD-1 combination across various metastatic cancers.

Trial Registration
NCT02950259, NCT02609386

Ethics Approval
The study was approved by Providence Portland Medical Canter Institutution's Ethics Board, approval number 132055.

O32 Abstract Travel Award Recipient

Decoy-resistant Interleukin-18 overcomes the soluble immune checkpoint IL-18BP to unlock a potent immunotherapeutic cytokine pathway

Ting Zhou[1], William Damsky, MD, PhD[1], Karen Hartmann, MS[1], Suzanne Fischer, BS[1], Marcus Bosenberg, MD, PhD[1], Aaron Ring[1]

[1]Yale University School of Medicine, New Haven, CT, USA

Background

Decades before the advent of immune checkpoint inhibitors (ICIs), recombinant cytokine treatments established that the immunotherapeutic paradigm could produce durable cures in patients [1]. From single-cell RNA expression analyses of tumor-infiltrating lymphocytes [2], we found that the Interleukin-18 (IL-18) pathway is markedly upregulated in activated and dysfunctional CD8 T cells, suggesting its promise as an immunotherapeutic target. However, previous clinical trials found that IL-18 therapy is ineffective, with no objective responses seen in a phase 2 study of melanoma patients [3]. We hypothesized that the endogenous, high-affinity IL-18 antagonist, IL-18BP, acts as a "soluble immune checkpoint" that restricts the effectiveness of IL-18 immunotherapy.

Methods

Using directed evolution with yeast-surface display, we engineered a "decoy-resistant" IL-18 variant (DR-18) that is impervious to neutralization by IL-18BP. We measured DR-18's affinity for IL-18Ralpha and IL-18BP using surface plasmon resonance and its ability to stimulate downstream signaling with phosphoflow cytometry of primary lymphocytes. We assessed the anti-tumor efficacy of DR-18 in immunogenic tumor models and ICI-resistant models that lack MHC class I surface expression.

Results

DR-18 exhibits >10,000,000-fold reduced affinity for IL-18BP compared to WT IL-18 and can potently elicit MyD88 signaling despite concentrations of IL-18BP sufficient to completely neutralize WT IL-18. Similar to the clinical experience with recombinant IL-18, WT IL-18 produced no benefit alone or in combination with anti-PD-1 in the treatment of MC38, YUMMER1.7, or CT26 tumors. By contrast, DR-18 produced monotherapeutic efficacy commensurate with anti-PD-1, with robust synergism observed in combination therapy. Antibody-mediated depletion studies indicated that DR-18's efficacy in these models required CD8 and CD4 cells, but not NK cells. To determine whether DR-18 was effective in the setting of ICI-resistance, we utilized three tumor models with impaired MHC class I surface expression (RMA/S and Beta-2 microglobulin-deficient MC38 and YUMMER1.7). In these models, DR-18 treatment exhibited strong NK-cell dependent efficacy, whereas no response was observed with combined blockade of CTLA4 and PD-1.

Conclusions

We established that IL-18BP is the key barrier to IL-18 immunotherapy using an engineered cytokine variant, DR-18, that is impervious to the decoy receptor. DR-18 is a promising candidate immunotherapeutic that can augment conventional ICIs and treat ICI-refractory tumors that have lost antigen presentation through MHC class I, one of the most common mechanisms of ICI resistance [4]. These results highlight the IL-18 pathway as a powerful target for immunotherapeutic intervention and establish the value of precisely-engineered protein therapeutics to dissect complex immunoregulatory pathways.

References

1. Atkins MB, Kunkel L, Sznol M, Rosenberg SA. High-dose recombinant interleukin-2 therapy in patients with metastatic melanoma: long-term survival update. Cancer J Sci Am. 2000;6 Suppl 1:S11-4.
2. Singer M, Wang C, Cong L, Marjanovic ND, Kowalczyk MS, Zhang H, Nyman J, Sakuishi K, Kurtulus S, Gennert D, Xia J, Kwon JY, Nevin J, Herbst RH, Yanai I, Rozenblatt-Rosen O, Kuchroo VK, Regev A, Anderson AC. A Distinct Gene Module for Dysfunction Uncoupled from Activation in Tumor-Infiltrating T Cells. Cell. 2016;166(6):1500-11 e9.
3. Tarhini AA, Millward M, Mainwaring P, Kefford R, Logan T, Pavlick A, Kathman SJ, Laubscher KH, Dar

MM, Kirkwood JM. A phase 2, randomized study of SB-485232, rhIL-18, in patients with previously untreated metastatic melanoma. Cancer. 2009;115(4):859-68.
4. Zaretsky JM, Garcia-Diaz A, Shin DS, Escuin-Ordinas H, Hugo W, Hu-Lieskovan S, Torrejon DY, Abril-Rodriguez G, Sandoval S, Barthly L, Saco J, Homet Moreno B, Mezzadra R, Chmielowski B, Ruchalski K, Shintaku IP, Sanchez PJ, Puig-Saus C, Cherry G, Seja E, Kong X, Pang J, Berent-Maoz B, Comin-Anduix B, Graeber TG, Tumeh PC, Schumacher TN, Lo RS, Ribas A. Mutations Associated with Acquired Resistance to PD-1 Blockade in Melanoma. N Engl J Med. 2016;375(9):819-29.

Ethics Approval
These studies were approved by the Yale Institutional Animal Care & Use Committee (IACUC), approval number 2016-20117.

O33 Presidential Travel Award Recipient

Adaptive plasticity of IL10+ and IL35+ regulatory T cells and their cooperative regulation of anti-tumor immunity

Hiroshi Yano, BS[1], Deepali Sawant, PhD[1], Maria Chikina, PhD[1], Qianxia Zhang, PhD[1], Zhe Sun[1], Tao Sun[1], Wei Chen[1], Creg Workman, PhD[1], Dario A. Vignali, PhD[1]

[1]*University of Pittsburgh, Pittsburgh, PA, USA*

Background
Regulatory T cells (Tregs), while contributing to the maintenance of self-tolerance, are a barrier to effective cancer immunotherapy [1]. Previous studies have shown that tumor-infiltrating (TIL) Tregs substantially upregulate the expression of inhibitory cytokines, such as IL10 [2] and IL35 [3]. Although we have reported that IL35+ Tregs support tumor growth by promoting inhibitory receptor (IR) expression in CD8+ TILs [3], the underlying mechanism of IL35-mediated IR-upregulation and whether and how IL35+ Tregs and IL10+ Tregs cooperatively regulate anti-tumor immunity remain elusive. Improving our understanding of Treg functions in the tumor microenvironment (TME) will help us identify new targets and develop novel immunotherapy with greater efficacy.

Methods
To address the question, we generated Ebi3tdTomato.Il10GFP.Foxp3Cre-YFP reporter mice to assess whether there are phenotypic, functional, and transcriptomic differences between Treg subpopulations. We also utilized Foxp3Cre-YFP, Ebi3L/L-tdTom.Foxp3Cre-YFP, Il10L/L.Foxp3Cre-YFP, and Ebi3L/L.tdTom.Il10L/L.Foxp3Cre-YFP conditional knockout mice to examine the impact of inhibitory cytokine-deficient Tregs on CD8+ TILs via multi-parameter flow cytometry and global transcriptomic analyses.

Results
IL10 and IL35 were reciprocally expressed by Tregs, while inhibitory cytokine-producing Tregs were significantly enriched in the TME. However, single cell RNAseq analysis and a significant clonal overlap among TIL Tregs demonstrated by TCRseq revealed Tregs in transitional-states between IL10+, IL35+, and IL10+IL35+ Treg populations. Our observations suggest a strong developmental relationship between IL10+ and IL35+ Tregs.Interestingly, despite the distinct signaling pathways utilized by IL10 and IL35 receptors, both IL10- and IL35-deficient Treg mice presented a similar reduction of IR expression on CD8+ TILs and tumor growth, while double-deficient Treg mice did not show a notable additive phenotype. Our subsequent analyses demonstrated that Blimp1 is a common target of IL10 and IL35 signaling in CD8+ T cells, and its expression was significantly downregulated in CD8+ TILs from all the cytokine-deficient Treg mice.

Conclusions

Blimp1 has been reported as one of the key transcription factors that drive exhaustion of CD8+ T cells [4], but upstream external stimuli in the TME that trigger Blimp1 activities have not been fully understood. Here, we report the direct link between Treg-derived inhibitory cytokines, IL10 and IL35, and Blimp1-mediated CD8+ T cell exhaustion. These observations suggest that inflammatory cues in the TME induce the plasticity of IL10 and IL35 expression in Tregs that may further differentiate into functionally distinct subtypes of effector Tregs to cooperatively modulate the balance between exhausted and memory CD8+ TIL compartments.

References

1. Tanaka A, Sakaguchi S. Regulatory T cells in cancer immunotherapy. Cell Research. 2016; 27:109. 2. Stewart, CA, et al. Interferon-dependent IL-10 production by Tregs limits tumor Th17 inflammation. J Clin Invest. 2013; 123(11):4859-74. 3. Turnis, ME, et al. Interleukin-35 limits anti-tumor immunity. Immunity. 2016; 44(2):316-29. 4. Shin, H, et al. A role for the transcriptional repressor Blimp-1 in CD8(+) T cell exhaustion during chronic viral infection. Immunity. 2009; 31(2):309-20.

O34

Next-generation retroviral vector with membrane-anchored IL-12 to improve adoptive T cell immunotherapy and enhance its safety

John Davies[1], Carylinda Serna[1], Zhiya Yu[1], Nicholas Restifo, MD[1], Steven Rosenberg, MD, PhD[1], Christian Hinrichs, MD[1], Ling Zhang, PhD[1]

[1]*National Institutes of Health, Bethesda, MD, USA*

Background

IL-12 is an important regulator of cell-mediated immunity. Though antitumor activity of IL-12 has been demonstrated in mouse tumor models, its clinical application was limited by systemic toxicity. Previously, we developed an IL-12 vector with a promoter containing binding motifs for Nuclear Factor of Activated T cell (NFAT-IL12) to secret IL-12 upon T cell activation. In a phase I/II clinical study using autologous tumor infiltrating lymphocytes (TIL) engineered with NFAT-IL12 in patients with metastatic melanoma, 62.5% of patients receiving a dose above 3X108 NFAT-IL12 TILs exhibited objective responses. However, increasing cell doses resulted in high serum levels of IL-12 and IFNg and clinical toxicities, including fever, liver dysfunction and hemodynamic instability. Therefore, a safer delivery of IL-12 is needed

Methods

To avoid detrimental toxicity of secreted IL-12, we designed a next-generation retroviral vector in which IL-12 is anchored on the cell surface by B7 transmembrane domain and cytoplasmic tail (LTR-mIL12.mB7). This vector was evaluated in two different murine tumor treatment models. The Pmel or OTI-T cells were transduced with membrane-anchored IL12 (LTR-mIL12.mB7) or secreting IL-12 (NFAT.mIL12) and were used to treat mice bearing B16 melanoma or B16-OVA melanoma. To further guide IL-12 expression at the tumor sites, we constructed NFAT inducible membrane-anchored IL12 vectors (NFAT-mIL12.mB7 and NFAT-hIL12.hB7). The treatment efficacy and safety profile of these vectors were evaluated in vitro and in vivo.

Results

Our results showed that T cells engineered with LTR-mIL12.mB7 could effectively control tumor burden, and importantly with an improved safety profile compared with T secreting IL-12. No IL-12 was detected in the serum and no body weight loss was observed from mice who were treated with membrane-anchored IL-12 T cells. In contrast, a transient body weight loss and increase serum level of IL-12 and IFNg were found in mice receiving T cells

secreting IL-12. Furthermore, T cells modified with inducible membrane-anchored IL-12 vector could efficiently express IL-12 on cell surface with minimal IL-12 secretion upon T cell activation. Adoptive transfer of OT-I T cells modified by NFAT-mIL12.mB7 significantly enhanced tumor regression in a dose dependent manner without toxicity. In an NSG mice bearing human HPV positive epithelia tumor, T cells co-expression HPV16-E7 TCR and NFAT-hIL12.hB7 improved treatment efficacy without detection of IL-12 in serum.

Conclusions
Taken together, the results support a clinical application of this novel IL-12 vector for cell-based immunotherapy with controlled toxicity

Immunosuppressive Cells in the Tumor Microenvironment

O35

Suppression of myeloid cell arginase activity leads to therapeutic response in a NSCLC mouse model by activating anti-tumor immunity

Esra Akbay, PhD[7], Juan Miret[2], Paul Kirschmeier[2], Shohei Koyama[3], Yvonne Li[2], Glenn Dranoff, MD[4], Peter Hammerman[4], Chad Pecot[5], Kwok-Kin Wong, MD, PhD[6]

[1]University of Texas Southwestern Medical Center, Dallas, TX, USA
[2]Dana-Farber Cancer Institute, Boston, USA
[3]Osaka University, Osaka, Japan
[4]Novartis, Cambridge, MA, USA
[5]University of North Carolina, Chapel Hill, USA
[6]New York University, New York, NY,USA
[7]University of Texas Southwestern Medical, Dallas, TX, USA

Background
Tumor orchestrated metabolic changes in the microenvironment limit generation of anti-tumor immune responses. Availability of arginine, a semi-essential amino acid, is critical for lymphocyte proliferation and function. Levels of arginine are regulated by the enzymes arginase 1,2 and nitric oxide synthase (NOS). However, the role of arginase activity in lung tumor maintenance has not been investigated in clinically relevant orthotopic tumor models.

Methods
RNA sequencing (RNA-seq) of sorted cell populations from mouse lung adenocarcinomas derived from immunocompetent genetically engineered mouse models (GEMM)s was performed. To complement mouse studies, a patient tissue microarray consisting of 150 lung adenocarcinomas, 103 squamous, and 54 matched normal tissue were stained for arginase, CD3, and Cd66b by multiplex immunohistochemistry. Efficacy of a novel arginase inhibitor compound 9 in reversing arginase mediated T cell suppression was determined in splenocyte ex vivo assays. Additionally, the anti-tumor activity of this compound was determined in vitro and in an autochthonous immunocompetent KrasG12D GEMM of lung adenocarcinoma model.

Results
Analysis of RNA-seq of sorted myeloid cells suggested that arginase expression is elevated in myeloid cells in the tumor as compared to the normal lung tissue. Accordingly, in the patient samples arginase 1 expression was mainly localized in the granulocytic myeloid cells and significantly elevated in both lung adenocarcinoma and squamous tumors as compared to the controls. Our ex vivo analysis demonstrated that myeloid derived suppressor cell (MDSC)s cause T cell suppression by arginine depletion, and suppression of arginase activity by a novel Arg1/2 inhibitor, compound 9, led to restoration of T cell function by increasing arginine. Treatment of KrasG12D GEMM of lung cancer model with compound 9 led to a significant

tumor regression associated with increased T cell number and function, while it had no activity across several murine and human non-small cell (NSCLC) lung cancer lines in vitro.

Conclusions
We show that arginase expression is elevated in mouse and patient lung tumors. In a KRASG12D GEMM arginase inhibition diminished growth of established tumors. Our data suggest arginase as an immunomodulatory target that should further be investigated in lung or other tumors with high arginase activity.

Ethics Approval
Human tissue specimen investigations were performed after approval by an institutional review board at University of North Carolina Chapel Hill (IRB # 14-1755). Written informed consent was obtained from all patients.

O36 Abstract Travel Award Recipient

Neuropilin-1 stabilizes human Tregs in cancer patients leading to more potent suppressive function

Chuckran Chuckran, BS[1], Anthony Cillo, PhD[1], Jessica Moskovitz, MD[1], Ashwin Somasundaram, MD[1], John Kirkwood, MD[1], Francesmary Modugno, PhD[1], Robert Edwards, MD[1], Robert Schoen, MD[1], Robert Ferris, MD, PhD[1], Tullia Bruno, PhD[1], Dario A. Vignali, PhD[1]

[1]*University of Pittsburgh School of Medicine, Pittsburgh, PA, USA*

Background
Regulatory T cells (Tregs) maintain peripheral tolerance;[1] however, in cancer, Tregs dampen anti-tumor immunity, contributing to disease progression.[2,3] Neuropilin-1 (NRP1) is required for intratumoral Treg stability as Treg-specific knockout of NRP1 leads to reduced tumor growth.[4]Genome-wide transcriptional analyses in mice revealed that intratumoral NRP1-deficient Foxp3+ Tregs develop an effector phenotype, characterized by interferon-gamma (IFNγ) production and decreased suppression of conventional T cells.[5] Whereas NRP1 is constitutively expressed on mouse Tregs, expression on human Tregs is activation-driven and thus may be modulated by immune processes. Furthermore, NRP1's role in maintaining human Treg stability amidst proinflammatory signals is not known. We hypothesize that (1) surface NRP1 expression marks highly suppressive human Tregs, (2) NRP1 expression is driven by proinflammatory signals in the tumor microenvironment, and (3) NRP1 binding to its cognate ligand, Semaphorin 4A, is required for maximal suppressive function.

Methods
Phenotypic profiling of peripheral blood (PBL) and tumor infiltrating lymphocytes (TILs) from head and neck squamous cell carcinoma (HNSCC), melanoma, non-small cell lung, ovarian, and colorectal cancer patients was conducted by flow cytometry. Treg function was evaluated in vitro by a micro-scale suppression assay, which measures the ability of Tregs to suppress CD8+ T cell proliferation. Paired with our phenotyping, we cultured Tregs under various stimulatory conditions to query drivers of NRP1 expression. These included numerous cytokine conditions, T cell receptor stimulation, co-culture with antigen presenting cells, as well as blockade of specific costimulation/inhibitory receptors.

Results
NRP1+ Tregs are greatly enriched in cancer patient PBL and TIL across numerous malignancies, and high NRP1 expression on intratumoral Tregs negatively correlates with disease-free survival in HNSCC. NRP1+ Tregs upregulate several inhibitory receptors commonly found on Tregs, including TIGIT, ICOS, and TNFR2, as well as markers of proliferation and

survival. NRP1+ Tregs also suppressed cytotoxic T cell proliferation to a greater degree than their NRP1- counterparts. NRP1+ Tregs were enriched in vitro in low interleukin-2 (IL-2) conditions as well as upon T cell activation. Proinflammatory cytokines, such as IFNγ, also drove increased NRP1 expression in a subset of cancer patient samples.

Conclusions

NRP1+ Tregs constitute a more suppressive human Treg subset based on their enhanced regulatory phenotype and function. Given the increased expression of proliferation and survival markers, especially under destabilizing conditions, NRP1 confers a survival advantage to these Tregs, allowing them to persist and function amidst such signals. Therefore, destabilizing intratumoral Tregs with NRP1 blockade may compliment other T cell therapies such as anti-PD1 blockade.

References

1. Vignali DAA, Collison LW, Workman CJ. How regulatory T cells work. Nat. Rev. Immunol. 2008; 8: 523–532.
2. Tanaka A, Sakaguchi S. Regulatory T cells in cancer immunotherapy. Cell Res. 2017: 27: 109–118.
3. Liu C, Workman CJ, Vignali DAA. Targeting regulatory T cells in tumors. FEBS J. 2016; 283:2731–2748.
4. Delgoffe GM, Woo SR., Turnis ME, Gravano DM, Guy C, Overacre AE, Bettini ML, Vogel P, Finkelstein D, Bonnevier J, Workman CJ Vignali DAA. Stability and function of regulatory T cells is maintained by a neuropilin-1–semaphorin-4a axis. Nature.. 2013; 501:252–256.
5. Overacre-Delgoffe AE, Chikina M, Dadey RE, Yano H, Brunazzi EA, Shayan G, Horne W, Moskovitz JM, Kolls JK, Sander C, Shuai Y, Normolle DP, Kirkwood JM, Ferris RL, Delgoffe GM, Bruno TC, Workman CJ, Vignali DAA. Interferon-γ Drives T reg Fragility to Promote Anti-tumor Immunity. Cell. 2017; 169:1130–1141.e11.

Ethics Approval

This study was approved by the local Institutional Review Board under protocol UPCI 99-069, and patients provided informed consent.

Innate Anti-Tumor Immunity

O37

A new immunomodulatory strategy of inhibiting the glyco-immune checkpoint axis with EAGLE technology to treat cancer

Lizhi Cao[2], Adam Petrone[2], Lihui Xu, BS[1], Wayne Galtlin, MS[1], Michele Mayo[1], Michal Stanczak[3], Carolyn Bertozzi[4], Karl Normington, PhD, MBA[1], Jeff Brown[1], Heinz Laubli[3], Jim Broderick, MD[1], Li Peng, PhD[2]

[1]*Palleon Pharmaceuticals, Waltham, MA, USA*
[2]*Palleon Pharma, Waltham, MA, USA*
[3]*University Hospital Basel, Switzerland, Switzerland*
[4]*Stanford University, Stanford, CA, USA*

Background

Cancer therapy has been revolutionized by the recent developments of immune-checkpoint inhibitors to harness the power of the immune system in fighting cancer. However, the majority of patients fail to have durable responses or become resistant to immuno-oncology drugs, highlighting the need to identify new mechanisms of immune evasion in cancer and to develop new therapeutic modalities. Recently, the glyco-immune checkpoint axis (sialoglycan/Siglec pathway) has emerged as a novel mechanism of immune regulation involving both innate and adaptive immunity and an important mechanism of cancer immune escape. Upon ligation of sialylated glycans to ITIM-containing Siglecs on immune cells, this pathway plays a previously unrecognized role in regulating functions of NK cell, macrophages, dendritic cells, monocytes and T-cells

in the tumor microenvironment. It suppresses multiple facets of anti-cancer immunity, including cancer antigen release, cancer antigen presentation, priming and activation of anti-cancer T-cell immunity, which may represent a novel mechanism of resistance to current immunotherapy.

Methods
Here, we described a novel therapeutic modality, a multi-functional antibody-like molecule named EAGLE (Enzyme-Antibody Glyco-Ligand Editing), to inhibit the glyco-immune checkpoint axis in the tumor microenvironment by selectively removing the terminal sialic acids of sialoglycans on tumor cells.

Results
We demonstrated that EAGLE decreased sialic acid levels on tumor cells and led to increased immune cell infiltration and activation in vivo in syngeneic mouse tumor models. EAGLE treatment achieved 50% complete regressions in well-established tumor models as a monotherapy with no reductions in body weight, and remarkably 100% cures in combination with anti-PD1 mAb. Furthermore, re-challenge experiments in cured mice from the EAGLE monotherapy treatment group resulted in a complete rejection of tumor cells, demonstrating that EAGLE induced anti-tumor immunological memory.

Conclusions
In summary, we demonstrated EAGLE as a novel and promising immunomodulatory therapeutic modality and the great potential of inhibiting the glyco-immune checkpoints for overcoming resistance to current immunotherapies.

O38

Remodeling the tumor microenvironment – Targeting scavenger receptors

Dhifaf Sarhan, PhD[1], Caroline Driescher, MS[1], Silke Sohn, MS[1], Salvatore Nania[1], Rainer Heuchel[1], Matthias Löhr[1], Mikael Karlsson[1]

[1]*Karolinska Institutet, Solna, Sweden*

Background
Immunotherapy for cancer has revolutionized clinical practice and enabled cures for previously lethal cancers. However, the clinical responses are variable and highly influenced by immune regulatory compartments in the tumor microenvironment (TME). These include, Myeloid-derived suppressor cells (MDSC), and Tumor-associated macrophages (TAMs). We have previously shown that antibodies targeting scavenger receptors (SR) expressed on TAMs, reduces tumor growth and metastasis in murine melanoma and breast cancer models. Thus, we hypothesized that targeting these receptors will remodel the suppressive environment and relive the anti-tumor responses to increase the efficacy of immunotherapy.

Methods
To test our hypothesis, analysis of SR gene expression data from the Human Protein Atlas (HPA) project was performed investigating pancreatic tumors (n=176), as these consist of up to 80% stroma, compared with healthy pancreatic tissues (n=171). In vitro, we first cytokine-polarized macrophages from healthy blood donors towards M1 anti-tumor and M2 pro-tumor phenotype. Alternatively, macrophages were cultured with tumor cell lines under hypoxia and normoxia conditions. M1, M2, or tumor-conditioned macrophages were co-cultured with cytotoxic cells to mimic their interaction in the TME. Later, macrophages were treated with anti-SR Abs and their phenotype, metabolism, and cytokine profile were examined prior and following interaction with immune effector cells. Subsequently, T and NK cell activation was measured by cytokine production, proliferation, degranulation, and capacity to kill tumor cells.

Results
We found a 30-fold increase in SR expression in pancreatic tumors compared to healthy tissues. Also, a significant (p=0.03) correlation between high expression and decreased survival was noted in pancreatic cancer patients. Furthermore, pancreatic cancer cell lines induced SR expression on macrophages and dedifferentiated them towards MDSC. This effect was amplified by hypoxic condition. Notably, SR+ MDSC in contrast to control monocytes and M1-macrophages, suppressed cytotoxic cell anti-tumor activities, which was reversed by treatment with anti-SR Abs. In addition, targeting M2-macrophages with anti-SR Abs, abolished their anti-inflammatory phenotype and normalized their metabolism towards M1.

Conclusions
Our findings demonstrate a novel approach to specifically target M2-like TAMs and MDSC for treatment of pancreatic cancer.

Mechanisms of Resistance to Immunotherapy

O39 Presidential Travel Award Recipient

PAK4 inhibition reverses immune cell exclusion and overcomes resistance to checkpoint blockade therapy

Gabriel Abril-Rodriguez, MS[1], Antoni Ribas, MD, PhD[1], Davis Torrejon, MD[1], Jesse Zaretsky[1], Theodore Nowicki, MD, PhD[1], Siwen Hu-Lieskovan, MD, PhD[1], Beata Berent-maoz[1], Begonya Comin-Anduix, PhD[1], Catherine GrassO1

[1]UCLA, Los Angeles, CA, USA

Background
Lack of immune cell infiltration is the main mechanism of primary resistance to PD-1 blockade therapies for cancer.

Methods
Here, we performed a transcriptomic analysis of metastatic melanoma biopsies taken from patients treated with anti-PD-1 (n= 41) with biopsies pre- (n=27) and during treatment (n=33), and investigated cancer cell intrinsic mechanisms of immune evasion.

Results
We first performed RNAseq deconvolution to estimate the relative levels of the different immune cell populations and confirmed that on-treatment responding biopsies had increased levels of T-cells (p-value = 1.21e-05) and dendritic cells (p-value = 1.9e-05) compared to non-responding tumor biopsies. To elucidate potential mechanisms of immune cell exclusion, we performed differential gene expression analysis between infiltrated and non-infiltrated tumor biopsies. P21 (RAC1) Activated Kinase 4 (PAK4) was consistently enriched in tumor biopsies with low T-cell (q-value = 2.75e-07) and dendritic cell (q-value = 1.9e-05) infiltration and was validated using an independent cohort of 99 metastatic melanoma biopsies treated with anti-PD-1 published by Riaz et al. Cell 2017 (q-value= 1.59e-11). PAK4 is a kinase known to be involved in tumorigenesis that directly binds and phosphorylates β-catenin to activate Wnt signaling. In our series, PAK4 expression negatively correlated with several immune cell populations including T-cells (pcc = -0.21, p-value = 1.04e-07) and dendritic cells (pcc= -0.49, p-value = 6.60e-05). Furthermore, tumor biopsies from patients without a response to PD-1 blockade showed increased levels of PAK4 expression (p-value = 0.004). We performed a pan-cancer correlation analysis between PAK4 expression and T-cell infiltration using TCGA expression data from 32 cancer types, identifying a negative correlation in melanoma (pcc = -0.31 and p-value= 7.4e-12), prostate cancer (pcc = -0.26 and p-value=

7.9e-09) and pancreatic cancer (pcc = -0.41 and p-value= 1.6e-08) among 20 other cancer types with similar negative correlation. To study the anti-tumor efficacy of PD-1 blockade in the context of PAK4 deletion, we treated syngeneic C57BL/6 mice (n=7 each group) bearing either B16 PAK4 KO or B16 WT tumors with anti-PD-1. We observed anti-tumor efficacy in the B16 PAK4 KO anti-PD-1 treated group (p-value = 0.0006) while no significant difference was found in the B16 WT treated group (p-value = 0.11). Depletion of CD8 T-cells abrogated the anti-tumor efficacy observed in the B16 PAK4 KO group.

Conclusions

In summary, high PAK4 expression is correlated with non-responding tumor biopsies with low T and dendritic cell infiltration, and inhibition of PAK4 overcomes resistance to PD-1 blockade in a CD8 dependent manner.

References

1. Riaz, N., et al., Tumor and Microenvironment Evolution during Immunotherapy with Nivolumab. Cell, 2017. 171(4): p. 934-949 e15.

Ethics Approval

The study was approved by UCLA IRBs 11-001918 and 11-003066.Mice were used under the UCLA Animal Research Committee protocol #2004-159-23.

O40

Anti-CTLA4 activation of intratumoral NK cells may contribute to intratumoral Treg depletion

Erin O'Brien, MS[1], Emilio Sanseviero[1], Jenna Karras, PhD[1], Tamer Shabaneh[2], Bulent Aksoy, PhD[3], Wei Xu[4], Xiaowei Xu[4], Giorgos Karakousis[4], Ravi Amaravadi, MD[5], Mark Rubinstein, PhD[3], Mary Jo Turk[2], Jeffrey Hammerbacher, BA[3], Lynn Schuchter, MD[4], Tara Mitchell[4], Qin Liu[1], Erica Stone, PhD[1]

[1]*The Wistar Institute, Philadelphia, PA, USA*
[2]*Norris Cotton Cancer Center, Dartmouth, Lebanon, NH, USA*
[3]*MUSC, Charleston, SC, USA*
[4]*University of Pennsylvania, Philadelphia, PA, USA*
[5]*The University of Pennsylvania, Philadelphia, PA, USA*

Background

Antibodies targeting CTLA4 induce durable responses in some patients with melanoma and are being tested in a variety of human cancers. However, a majority of patients across tumor types fail to respond. Further understanding the mechanisms of action of these therapies will enable the development of novel strategies to overcome resistance and biomarkers to identify patients most likely to respond. In murine models anti-CTLA4 efficacy depends on interactions between the Fc region of anti-CTLA4 antibodies and Fc receptors (FcRs). Anti-CTLA4 binding to FcRs has been linked to depletion of intratumoral Tregs by myeloid cells including non-classical monocytes. However, FcR engagement can lead to Natural Killer (NK) cell activation and NK cells can mediate antibody-dependent cell mediated cytotoxicity (ADCC).

Methods

Flow cytometry was used to investigate surface CTLA4 expression on murine and patient T cell subsets, including tumor-infiltrating lymphocytes and T cells from matched patient blood. Using murine tumor models we assessed the effect of anti-CTLA4 administration on intratumoral and peripheral immune cells including NK cells. A previously published RNA-seq data set was used to investigate intratumoral CD56 expression in cutaneous melanoma patients who benefited from Ipilimumab treatment compared to those who did not.

Results

In agreement with previous studies, we found that in murine models intratumoral Tregs have the highest expression of surface CTLA4 (sCTLA4) and anti-CTLA4

leads to Fc/FcR-dependent depletion of these Tregs. Similarly, analysis of T cells infiltrating patient-derived tumor tissue showed that Tregs have the highest sCTLA4 expression, and intratumoral Tregs express significantly more sCTLA4 than circulating Tregs. Interestingly, cutaneous melanoma patients who benefited from Ipilimumab treatment had higher intratumoral expression of the NK cell marker CD56. Using murine tumor models, we found that anti-CTLA4-induced Treg depletion coincided with activation and degranulation of intratumoral NK cells.

Conclusions
Taken together, our data suggest that anti-CTLA4-induced Treg depletion may be mediated in part by NK cells. These results suggest new strategies to overcome resistance to anti-CTLA4 therapies.

Ethics Approval
Patient-derived tumor tissue specimens were collected in accordance to the Institutional Review Boards at HFGCC of Christiana Health Care System or The University ofPennsylvania.

O41

Tumor-derived GDF-15 which impairs LFA-1 dependent T cell recruitment represents a roadblock and a new target for cancer immunotherapy

Markus Haake, PhD[2], Jörg Wischhusen, PhD[1]

[1]*University of Wuerzburg, Wuerzburg, Germany*
[2]*University of Wuerzburg Medical School, Würzburg, Germany*

Background
Growth and differentiation factor 15 (GDF-15, also known as macrophage inhibitory cytokine MIC-1 or placental TGF-beta) is a divergent member of the TGF-beta superfamily characterized by a very limited tissue distribution. Elevated GDF-15 serum levels seem to be required during pregnancy to prevent miscarriage. In mice, GDF-15 improves survival after cardiac ischemia-reperfusion injury: by inhibiting LFA-1/beta2-integrin activation on polymorphonuclear granulocytes GDF-15 protects the infarcted myocardium from excessive influx of leukocytes. In solid tumors where GDF-15 is frequently overexpressed it is known to correlate with poor survival. Nevertheless, its influence on immune cell trafficking and immune escape have hardly been explored in the tumor context.

Methods
Effects of GDF-15 on LFA-1 activation, T cell adhesion, rolling and immune cell infiltration were analyzed in vitro and ex vivo, using human biomaterials and tissue microarrays. Mouse models were performed to show the impact of GDF-15 on infiltration of immune cells into tumor tissue. The ability of GDF-15 to modulate responses to immunotherapy was studied in the MC38 colon cancer model. Finally, serum samples were obtained from melanoma patients scheduled to receive PD-1 based immune checkpoint blockade. In these pre-treatment samples GDF-15 serum levels were measured and correlated with clinical responses and survival.

Results
GDF-15 impairs activation of LFA-1 on human T cells. Rolling and adhesion on activated endothelial cells are also reduced by GDF-15. In line with this finding brain metastases from human melanoma show a strong inverse correlation between CD8+ T cell infiltration and GDF-15 expression. In mouse models, infiltration of immune cells into MC38 tumors is impaired by GDF-15 overexpression. Moreover, transgenic expression of GDF-15 can even induce resistance to PD-1 based immunotherapy in MC38 colon carcinomas. Neutralization of GDF-15 improves responses to immunotherapy. Strikingly, GDF-15 serum levels can also predict failure of anti PD-1

treatment and hence poor survival in human melanoma patients treated with immune checkpoint blockade.

Conclusions
Serum GDF-15 may predict responses to current PD-1 based checkpoint blockade. GDF-15 is, however, much more than a mere biomarker. By inhibiting immune cell infiltration into tumor tissue, GDF-15 actively promotes resistance towards PD-1 based immune checkpoint blockade. Consequently, GDF-15 represents a new "vascular immune checkpoint" which may serve as a promising target for future personalized combination therapies in immunooncology.

Ethics Approval
Use of patient samples for this study had been approved by the institutional ethics committee Tübingen (ethic vote 125/2015BO2). Use of surplus sera collected in the University of Zurich Hospital (USZ) Biobank during routine blood draws from consenting metastatic melanoma patients was performed according to IRB approval (KEK.Zh-647/800) and followed the Declaration of Helsinki on Human Rights.

Consent
All patients had given written informed consent to have clinical data recorded by the Central Malignant Melanoma Registry (CMMR) database.

Micro-RNA, Epigenetics and Tumor/Immune-cell Signaling Pathways in Anti-Tumor Immunity

O42

LSD1 inhibition promotes CD141Hi dendritic cell differentiation in myelodysplastic syndromes

Pragya Srivastava, PhD[1], Pragya Srivastava, PhD[1], Kyle Wiatrowski, BS[1], Prashant Singh, PhD[1], Eduardo Cortes Gomez, MS[1], Jianmin Wang, PhD[1], Miranda Lynch, PhD[1], Sheila Sait, PhD[1], Laurie Ann Ford, BS[1], Brandon Martens, BS[1], Linda Lutgen-Dunckley, BS[1], Elizabeth Griffiths, MD[1], Michael Nemeth, PhD[1], Stephanie Tzetzo, MA[1], Scott Abrams, PhD[1]

[1]*Roswell Park Comprehensive Cancer Center, Buffalo, NY, USA*

Background
Immunotherapeutic approaches for patients with the myelodysplastic syndrome (MDS) have shown promise. Progress is limited by incomplete understanding of the immunologic milieu in MDS. We performed a phase I study of vaccination against the tumor antigen NY-ESO-1 in combination with decitabine in newly diagnosed patients with MDS (1). Response to vaccination was associated with the presence of CD141Hi conventional dendritic cells (cDCs). This population of cells is critical to effective anti-tumor immune responses in solid tumors. We confirmed a deficiency of CD141Hi cDCs in MDS patients and proceeded to identify translatable regulatory mechanisms to enhance their development.

Methods
We quantified DC populations in bone marrow from MDS patients (n = 61) using flow cytometry. RNA-seq analysis was used to assess gene expression in MDS and healthy CD34+ progenitors. We assessed CD141Hi differentiation of MDS and healthy CD34+ progenitors using an in vitro differentiation model.

Results
We binarized patients into cohorts based on detectable (n = 36) versus undetectable (i.e. below the limit of detection; n = 25) CD141Hi cDC populations. Patients with detectable numbers of CD141Hi cDCs had longer median progression-free and overall survival compared to patients with undetectable CD141Hi cDCs (416 versus 216 days and 650 versus 304 days respectively). The

transcription factor IRF8 is a master regulator of CD141Hi cDC differentiation. Expression of IRF8 in MDS progenitors (as measured by RNA-seq) was associated with detectable numbers of CD141Hi cDCs. This result suggests that increased IRF8 expression drives enhanced CD141Hi cDC differentiation. We hypothesized that inhibition of lysine-specific histone demethylase 1A (LSD1), known to enhance IRF8 expression, would induce CD141Hi cDC differentiation (2). We showed that pharmacologic LSD1 inhibition (GSK2879552; GSK) enhances IRF8 expression in KG1 AML cells. Treatment of MDS CD34+ progenitors with GSK increased the number of CD141Hi cDCs in 2/4 patients samples compared to untreated controls (by 2.7 and 25.7-fold increase respectively). Cultured cells maintained MDS associated cytogenetic abnormalities (del 5q and -7), indicating their derivation from the malignant population. LSD1 inhibition also enhanced differentiation of healthy CD34+ cells to CD141Hi cDCs. This approach can therefore drive differentiation of CD141Hi cDCs which can arise from both malignant and healthy CD34+ cells.

Conclusions

These data highlight an unrecognized and potentially reversible immune defect in patients with MDS. Since immunotherapeutic strategies, including checkpoint inhibitors and vaccinations, require functional CD141Hi cDCs, strategies to enhance this population are critical for effective immune therapy for MDS patients.

References

1. Griffiths EA et al. Clin Cancer Res. 2018;24:1019-1029.2. Maiques-Diaz A et al. Cell Rep. 2018;22:3641-3659.

Ethics Approval

The study was approved by the Roswell Park Institututional Review Board (BDR 079816 and NCT01834248).

Oncolytic Viruses and Intratumoral Therapies

O43

Characterization of anti-tumor immune responses and Effects on Survival of Neoadjuvant Oncolytic Virotherapy in spontaneous Osteosarcoma

Shruthi Naik, PhD[1], Kelly Makielski, DVM, MS[2], Michael Henson, DVM, PhD[2], Kathleen Stuebner[2], Alexander-Flaviu Tabaran, DVM, MSc, PhD[2], Ingrid Cornax, PhD[2], Gerard O'Sullivan, MVB, PhD[2], Andrea Eckert[2], Lauren Mills, PhD[2], Milcah Scott, BS[2], Aaron Sarver, PhD[2], Michael Farrar[2], Stephen Russell, MD, PhD[1], Jaime Modiano, VMD, PhD[2]

[1]Mayo Clinic, Rochester, MN, USA
[2]University of Minnesota, Minneapolis, MN, USA

Background

Development of effective therapies for osteosarcoma, an infrequent disease that primarily affects adolescents and young adults, is a critical unmet medical need. The rarity and heterogeneity of these cancers have hindered research in this field. Comparative oncology studies in naturally occurring osteosarcoma in companion dogs provide opportunities to advance development in a clinically realistic setting where the tumors resemble their human counterparts but where the barriers of rarity and cost are lowered [1]. Vesicular stomatitis virus (VSV) is a rapidly replicating, robustly immunogenic oncolytic virus platform with demonstrated cytotoxicity in canine osteosarcoma cell lines. VSV-IFNβ-NIS, a recombinant oncolytic VSV, can be safely administered intravenously (IV) to reach sites of metastatic disease and has been shown selectively replicate in and destroy tumor cells and activate an anti-tumor immune response [2]. The aim of this study is to evaluate neoadjuvant VSV-IFNβ-NIS therapy for osteosarcoma using a comparative oncology approach and characterize anti-tumor

immune responses in spontaneous canine osteosarcoma.

Methods
A veterinary clinical study was initiated. Dogs with osteosarcoma are randomized to receive neoadjuvant oncolytic VSV-IFNβ-NIS (109 TICD50/kg) or placebo followed by amputation and carboplatin chemotherapy. Pre- and post-treatment tumor biopsies and serial peripheral blood mononuclear cells are obtained to assess anti-tumor immunity by histopathology, RNA and DNA sequencing, and lymphocyte effector functions.

Results
To date 24 dogs have been enrolled, of 30 dogs planned. The VSV safety profile is excellent, with mild, transient changes in body temperature and evidence of acute cytokine responses. Preliminary analyses show survival outcomes exceed the expectation for standard-of-care alone. Focal tumor necrosis that is potentially treatment-related has been observed in osteosarcoma lesions in resected tissue. Assessment of naïve and treatment-associated gene cluster expression summary scores from RNA sequencing is ongoing, as is massive parallel sequencing of lymphocyte antigen receptors to describe clonal expansion and attrition.

Conclusions
Neoadjuvant VSV treatment is well-tolerated, and shows preliminary evidence of biological activity and clinical efficacy. Updated results describing anti-tumor immunity that is attributable to oncolytic VSV, and its effects on patient outcomes will be presented. These data will indicate if intravenous neoadjuvant VSV-IFNβ-NIS therapy improves clinical outcomes in canine osteosarcoma and inform clinical studies to evaluate this therapeutic approach as an addition to current chemotherapy protocols for osteosarcoma patients.

Consent
1. Scott, M.C., et al., Molecular subtypes of osteosarcoma identified by reducing tumor heterogeneity through an interspecies comparative approach. Bone, 2011. 49(3): p. 356-67.
2. Naik, S., et al., Curative one-shot systemic virotherapy in murine myeloma. Leukemia, 2012. 26(8): p. 1870-8.

T-cell Checkpoints and Checkpoint Inhibitors

O44

FS120 mAb^2, a dual agonist bispecific antibody targeting OX40 and CD137, activates T cells *in vitro* and induces potent, FcγR-independent anti-tumour activity

Miguel Gaspar, PhD[1], Cyril Privezentzev, PhD[1], Katy Everett, PhD[1], Sandra Uhlenbroich[1], John Pravin[1], Leonor Rodrigues, MSc[1], Delphine Buffet[1], Marine Houee[1], Francisca Wollerton[1], Melanie Medcalf[1], Edouard Souteyrand[1], Alexander Koers, PhD[1], Emma McConnell, Master in Phyhsiology and Pharmacology for Researc[1], Martyn Rhoades, miat[1], Mateusz Wydro, PhD[1], Maud Berthelot, MSc[1], Sarah Batey[1], Michael Davies[1], Jacqueline Doody, PhD[1], Michelle Morrow, PhD[1], Mihriban Tuna, PhD[1], Neil Brewis, PhD[1]

[1]*F-star Biotechnology ltd, Cambridge, UK*

Background
Following the success of checkpoint blockade, activation of the co-stimulatory Tumour Necrosis Factor Receptor (TNFR) superfamily receptors represents the next stage of cancer immunotherapy with clinical trials underway for antibodies stimulating T cell co-stimulatory pathways. Targeting OX40 and CD137 has the potential to strongly activate the immune system due to their broad

expression across CD4+ and CD8+ T cells and NK cells. However, FcγR-mediated crosslinking is often required for the activity of monoclonal antibodies, and this likely limits clinical activity, due to the inherently low affinity of Fc:FcγR interactions, as well as due to FcγR-mediated depletion of T cells through ADCC. FS120 is a novel, dual agonist bispecific antibody that does not bind to FcγR, but instead crosslinks OX40 and CD137 resulting in potent activation of both CD4+ and CD8+ T cells, independent of FcγR binding.

Methods

FS120 was generated by introducing an OX40-binding specificity into the Fc-region of a human IgG1 targeting CD137. FcγR binding was significantly decreased using the LALA mutation. A parallel approach was taken to generate a murine surrogate molecule to test *in vivo*.

Results

FS120 binds simultaneously to OX40 and CD137 with subnanomolar affinity and has strong activity in PBMC and T cell stimulation assays. Conventional OX40 and CD137 agonist antibodies require crosslinking, e.g. via anti-Fc secondary antibodies for their activity. OX40 agonist antibodies activate CD4+ T cells, but not CD8+ T cells and CD137 agonist antibodies activate CD8+ T cells but not CD4+ T cells. FS120 has subnanomolar dual agonist activity on both CD4+ and CD8+ T cells, which is independent of additional crosslinking. This activity is dependent on concurrent binding to the two receptors. An anti-mouse OX40/CD137 bispecific antibody showed greater anti-tumour activity than a combination of OX40 and CD137 agonists in a CT26 mouse tumour model, which was associated with peripheral T cell activation and proliferation. The anti-tumour activity was independent of T regulatory cell (Treg) depletion, as evidenced by similar levels of tumour infiltrating Treg cells in mice treated with the anti-mouse OX40/CD137 mAb² and isotype control. Anti-tumour activity was also demonstrated in a B16-F10 syngeneic model.

Conclusions

An OX40/CD137-specific mAb[2] can autonomously stimulate both CD4+ and CD8+ T cells *in vitro* independent of FcγR binding and mediate potent anti-tumour activity *in vivo* via an FcγR-independent mechanism of action. These data support initiation of clinical development of FS120, a first-in-class dual agonist bispecific antibody for the treatment of human cancer.

Acknowledgements

We thank the following people for their technical assistance:*In vivo* team for animal studies, Protein sciences team for protein production

Ethics Approval

Murine studies were conducted under a U.K. Home Office License in accordance with the U.K. Animal (Scientific Procedures) Act 1986 and EU Directive EU 2010/63.

O45

Refractory renal cell cancer (RCC) exhibits high adenosine A2A receptor (A2AR) expression and prolonged survival following treatment with the A2AR antagonist, CPI-444

Lawrence Fong, MD[1], Lawrence Fong, MD[1], John Powderly, MD, CPI[2], Jason Luke, MD, FACP[3], Drew Hotson, PhD[4], Mario Sznol, MD[5], Saby George, MD, FACP[6], Toni Choueiri[7], Brian Rini, MD[8], Matthew Hellmann, MD[9], Shivaani Kummar, MD[10], Leonel Hernandez-Aya, MD PhD[11], Daruka Mahadevan, MD, PhD[12], Brett Hughes, MD[13], Ben Markman[14], Matthew Riese, MD, PhD[15], Joshua Brody, MD[16], Daniel Renouf, MD[17], Rebecca Heist, MD[18], Rachel Goodwin, MD[19], Amy Weise, DO[20], Leisha Emens, MD, PhD[21], Stephen Willingham, PhD[4], Long Kwei, PhD[4], Ginna Laport, MD[4], Richard Miller, MD[4]

[1]*University of California, San Francisco, CA, USA*
[2]*Carolina BioOncology Institute, Huntersville, NC, USA*
[3]*University of Chicago, Chicago, MA, USA*
[4]*Corvus Pharmaceuticals, Burlingame, CA, USA*
[5]*Yale University, New Haven, CT, USA*
[6]*Roswell Park Cancer Institute, Buffalo, NY, USA*
[7]*Dana Farber Cancer Institute, Boston, MA, USA*
[8]*Cleveland Clinic Foundation, Cleveland, OH, USA*
[9]*Memorial Sloan Kettering Cancer Center, New York, NY, USA*
[10]*Stanford University School of Medicine, Stanford, CA, USA*
[11]*Washington University, Saint Louis, MO, USA*
[12]*University of Arizona, Tucson, AZ, USA*
[13]*Royal Brisbane Hospital, Herston, Australia*
[14]*Monash Health and Monash University, Melbourne, VIC, Australia*
[15]*Medical College of Wisconsin, Milwaukee, WI, USA*
[16]*Icahn School of Medicine at Mt Sinai, New York, NY, USA*
[17]*British Columbia Cancer Agency, Vancouver, Canada*
[18]*Massachusetts General Hospital, Boston, MA, USA*
[19]*Ottawa Hospital Cancer Center, Ottawa, Canada*
[20]*Karmanos Cancer Institute, Detroit, MI, USA*
[21]*Johns Hopkins University, Pittsburgh, PA, USA*

Background

Adenosine plays a role in blocking the function of immune cells through binding to the A2AR. CPI-444 is an oral A2AR antagonist that has been evaluated in Phase 1 trials in advanced cancer.

Methods

This Phase 1b trial was conducted at 30 centers. RCC patients (pts) with progressive disease were randomized to receive either CPI-444, 100 mg po bid monotherapy or CPI-444 in combination with atezolizumab 840 mg IV every 2 weeks and treated until progression or unacceptable toxicity. Endpoints included safety, tumor response (RR), progression free survival and overall survival (OS). Peripheral blood and tumor biopsies were obtained at baseline and on-treatment and evaluated for lymphocyte subsets and gene expression of A2AR using Nanostring. A2AR signaling was assessed by measurement of inhibition of pCREB.

Results

Results: 68 pts enrolled (N=33 monotherapy, N=35 combination); median prior therapies was 3 (range 1-5) including TKI, 84%; anti-PD(L)1 (IO), 72%; median time since last IO was 3.1 and 1.7 months for monotherapy and combination, respectively. Median treatment duration was 4.6 months. CPI-444 was well-tolerated with no Gr3/4 toxicity in monotherapy; 7 pts had reversible Gr3 toxicity in combination. CPI-444 blocked A2AR signaling based on inhibition of phosphorylation of CREB in blood lymphocytes. A2AR mRNA was measured in 31 pre-treatment RCC tumor biopsies and compared to other cancers (36 lung; 12 bladder; 5 colon; 8 prostate, 9 melanoma and 20 triple negative breast). RCC showed increase in A2AR expression compared to lung ($p<0.01$) and the other tumors ($p<0.001$). Objective clinical responses were observed in 8% of pts; another 21% had reduction of tumor not meeting criteria for response. Responses were seen in both monotherapy and combination arms and in pts who failed prior IO agents. 40% and 58% of pts experienced disease control (DC) for > 3 months (confirmed scans) in monotherapy and combination, respectively, including in pts resistant to prior IO. The OS for both monotherapy and combination exceeded 80% at 16 months. Treatment increased CD8+ T cells in tumors in pts with DC>6mo compared to DC<6mo ($p<0.02$).

Conclusions

CPI-444 is active in RCC and is associated with prolonged survival and DC in treatment refractory pts, including those who have failed prior IO. Prolonged DC was associated with treatment-induced increase in tumor infiltrating CD8+ cells. Our results compare favorably to those reported with

atezolizumab demonstrating 1 yr OS of 81% and RR of 15% in IO naïve RCC with median 2 prior therapies[1].

Acknowledgements
not applicable

Trial Registration
NCT02655822

References
1. McDermott D, Sosman J, Sznol M, Massard C, Gordon M, Hamid O, Powderly J, Infante J, Fasso M, Wang Y, Zou W, Hegde P, Fine G, Powles T. Atezolizumab, an anti-programmed death- ligand 1 antibody, in metastatic renal cell carcinoma: long-term safety, clinical activity, and immune correlates from a Phase 1a study. J Clin Oncol. 2016;34:1-10.

Ethics Approval
The protocol was approved by the institutional review board or ethics committee at each participating center.

O46

Increased tumor-resident memory T cells in breast cancer is associated with improved prognosis

Peter Savas[1], Balaji Virassamy[1], Chengzhong Ye[2], Agus Salim[3], Chris Mintoff[1], Franco Caramia[1], Roberto Salgado[4], Zhi Ling Teo[1], Sathana Dushyanthen[1], Ann Byrne[1], Stephen Luen[1], Paul Beavis, PhD[1], Stephen Fox[1], Phillip Darcy[1], Terence Speed[2], Laura Mackay[5], Paul Neeson, PhD[6], Sherene Loi, MD, PhD[6]

[1]Peter MacCallum Cancer Center, Melbourne, Australia
[2]WEHI, Melbourne, Australia
[3]La Trobe University, Melbourne, Australia
[4]GZA Ziekenhuizen, Antwerp, Belgium
[5]University of Melbourne, Melbourne, Australia
[6]Peter MacCallum Cancer Centre, Melbourne, Australia
[7]Peter Mac Callum Cancer Center, Victoria, Australia

Background
The level of tumor infiltrating lymphocytes (TIL) is a prognostic factor for improved patient survival in triple negative and HER2-overexpressing breast cancer (BC) subtypes. T cells are the main immune subset in BC tumors with a high TIL content, TIL(hi); however the influence of the T cell qualitative response on patient prognosis is unknown.

Methods
To address this issue, TILs were isolated from 129 primary and metastatic BC samples, T cells were sorted and single-cell RNA sequencing (scRNA-seq) performed to reveal the BC TIL T cell clusters present. BC TIL scRNAseq data was confirmed by multi-parameter flow cytometry (FACS). We also performed bulk RNA seq on FACS-sorted T cell populations, and interrogated BC TIL T cell receptor (TCR) sequences to compare the difference in TCR usage between clusters. We explored BC TIL functional responses (cytokines, effector proteins) following co-culture with autologous BC cells. Finally we compared the clinical outcome data for triple negative BC patients who expressed high vs low levels of the signature clusters in BC TILs.

Results
Our study showed BC T cells were heterogeneous in sub-type and functional polarization. In particular, BC TIL(hi) cases contained increased CD8+ tumor-resident memory T (TRM) cells. These cells expressed CD103 and high levels of immune checkpoint molecules (PD1, CTLA-4, TIM-3, Lag-3) and T cell effector proteins (perforin and granzyme B). Further analysis of BC TILs by multi-parameter FACS confirmed the presence of increased CD8+ TRM in TIL(hi) BC tumors, these CD8+ TRM also released granzyme B on co-culture with autologous BC cells. In two primary tumors, the BC TRM had different

TCR usage to TEM suggesting these are clonally distinct populations. Using the scRNAseq data, we developed a CD8+ TRM gene signature that was associated with improved patient disease free survival (DFS), (n=329, log-rank p=0.003) in early-stage triple negative breast cancers (TNBC) from the METABRIC data set. The CD8+ TRM gene signature also stratified patients with high vs low CD8A expression for DFS (log-rank p = 0.03).

Conclusions

In conclusion, patients with BC TIL(hi) tumours have a qualitatively different T cell response which includes CD8+ TRM differentiation. These cells express high levels of immune checkpoint molecules, plus T cell effector proteins suggesting they could be the key responders to immune checkpoint inhibitor therapy. Further studies exploring BC-associated CD8+ TRM cell development and homeostasis will be critical for creating new opportunities for BC immunotherapy.

Acknowledgements

We wish to thank H Thorne, E Niedermayr, all the kConFab research nurses and staff, the heads and staff of the Family Cancer Clinics, and the Clinical Follow Up Study (which has received funding from the NHMRC, NBCF, Cancer Australia, and the National Institute of Health (USA)) for their contributions to this resource, and the many families who contribute to kConFab. kConFab is supported by a grant from NBCF, and previously NHMRC, the Queensland Cancer Fund, the Cancer Councils of New South Wales, Victoria, Tasmania and South Australia, and the Cancer Foundation of Western Australia. We wish to thank the FACS core facility staff R Rossi, V Milovac and S Curcio, and T Tan and P Petrone for additional FACS assistance. We also thank S Ellis for assistance with confocal imaging, G Mir Arnau for facilitating RNASeq, and the Anatomical Pathology staff at the Peter MacCallum Cancer Centre. Special thanks also to J Jabbari and the Australian Genome Research Facility for making the single cell sequencing possible.

Ethics Approval

This project was approved by the Human Research Ethics Committee of the Peter MacCallum Cancer Centre (project approval number "SEGMENT" 13/123, Kathleen Cuningham Foundation Consortium for Research into Familial Breast Cancer (kConFab) project approval numbers #129 and #150).

Consent

All participating patients provided written informed consent.There is no sensitive or identifiable information in the abstract.

O47 Abstract Travel Award Recipient

Peripheral T cell dynamics in resectable NSCLC patients treated with neoadjuvant PD-1 blockade

Jiajia Zhang, MD, MPH[1], Zhicheng Ji[1], Margueritta El Asmar, MD[1], Justina Caushi[1], Valsamo Anagnostou, MD PhD[1], Hok Yee Chan, MS[1], Prerna Suri, MS[1], Haidan Guo, BS, and BA[1], Kristen Marrone, MD[1], Jarushka Naidoo, MD[1], Taha Merghoub, PhD[2], Jamie Chaft, MD[2], Matthew Hellmann, MD[2], Janis Taube, MD, MSC[1], Julie Brahmer, MD[1], Victor Velculescu, MD, PhD[1], Ni Zhao[1], Patrick Forde, MD[1], Drew Pardoll, MD, PhD[1], Hongkai Ji[1], Kellie Smith, PhD[1]

[1]Johns Hopkins University, Baltimore, MD, USA
[2]Memorial Sloan Kettering Cancer Center, New York, NY, USA

Background

Neoadjuvant PD-1 blockade has recently been shown to induce major pathologic responses (MPRs) and delay time to relapse in patients with resectable non-small cell lung cancer (NSCLC)[1]. While the role of tumor-specific T cells in facilitating tumor regression has been demonstrated in advanced NSCLC, it is unknown how neoadjuvant PD-1 blockade affects

the anti-tumor T cell repertoire and how these factors correlate with clinical outcome. The neoadjuvant setting provides a unique opportunity to evaluate T cell mobility into the tumor and other tissues after checkpoint blockade, which is challenging in studies of patients with metastatic disease.

Methods

Patients with resectable NSCLC were treated with neoadjuvant PD-1 blockade (NCT02259621). T cell receptor (TCR) sequencing was performed on pre- and post-treatment tissues, bulk serial peripheral blood samples, and pre-treatment blood sorted for PD-1 expression. Whole exome sequencing and neoantigen prediction was performed on pre-treatment tumor biopsies and matched normal lung tissue. Peripheral dynamics of intratumoral T cell clonotypes, as well as enrichment of TCR motifs were evaluated. The associations of T cell dynamics and neoantigen recognition with MPRs and recurrence-free survival were assessed.

Results

Substantial alterations in the T cell repertoire and influx of peripheral T cell clonotypes into tumor tissue, normal lung, and lymph nodes were observed following PD-1 treatment. Peripheral TCR responses were independent of MPR status. T cell clonality in the resected tumorpost-treatment tissue positively correlated with pre-treatment tumor mutational burden and negatively correlated with percent residual tumor. Tumor infiltrating clonotypes underwent dynamic peripheral remodeling on-treatment; the magnitude of clonal reshaping was significantly higher than clonotypes not found in the tumor. Tumor-infiltrating clonotypes that were also detected in the peripheral blood were of significantly higher frequency than those only present in the tumor. Notably, an anergic/monoclonal anti-tumor TCR repertoire was observed in a patient with KRAS/STK11 co-mutations and an early relapse after PD-1 blockade. Analyses of the dynamics of T cell clonotypes with differential PD-1 expression is ongoing.

Conclusions

Significant and systemic alterations exist in the peripheral anti-tumor T cell repertoire in NSCLC patients treated with neoadjuvant PD-1 blockade. The periphery represents a vital biological compartment for the anti-tumor immune response.

Trial Registration

www.clinicaltrials.gov (NCT02259621)

References

1. Forde PM, Chaft JE, Smith KN, et al. Neoadjuvant PD-1 Blockade in Resectable Lung Cancer. N Engl J Med 2018; 378: 1976–86.

Ethics Approval

The study was approved by Johns Hopkins Institutution‘s Ethics Board, approval number CIR00038778

Consent

Written informed consent was obtained from the patient for publication of this abstract and any accompanying images. A copy of the written consent is available for review by the Editor of this journal.

REGULAR POSTER ABSTRACT PRESENTATIONS

(ADCC/CDC) Direct Antibody Mediated Anti-Tumor Activity and Anti-body-Directed Conjugates

P1

The identification of potent anti-tumor antibodies for ADC therapeutics from patients undergoing immunotherapy

Alexander Scholz, PhD[1], Jerald Aurellano[1], Michael Harbell, MS PhD[1], Danhui Zhang, MD PhD[1], Samantha O'Connor[1], May Sumi, BS[1], Beatriz Millare, BS[1], Felix Chu, MS[1], Sheila Fernandez[1], Cathrin Czupalla[1], Iraz Aydin, PhD[1], Amy Manning-Bog, PhD[1], Yvonne Leung, BS, PhD[1], Kevin Williamson, BS PhD[1], Chantia Carroll[1], Dongkyoon Kim, BS PhD[1], Xiaomu Chen, MS PhD[1], Sean Carroll, BS, PhD[1], Ish Dhawan, PhD[1], Ngan Nguyen, BS PhD[1], Shweta Thyagarajan[1], Mark Whidden[1], Gregg Espiritu Santo, BS PhD[1], Nicole Haaser, MS[1], Hibah Mahmood[1], Guy Cavet, PhD[1], Lawrence Steinman, MD[2], Tito Serafini, PhD[1], Wayne Volkmuth, BS PhD[1], Jonathan Benjamin, MD, PhD[1], William Robinson, MD[2], Norman Greenberg, PhD[1], Daniel Emerling, PhD[1], Jell DeFalco[1]

[1]Atreca Inc, Redwood City, CA, USA
[2]Stanford University School of Medicine, Stanford, CA, USA

Background
Anti-tumor therapy with antibody-drug conjugates (ADCs) is predicated on the identification of antibodies that demonstrate suitable selectivity for tumor cells that are also internalized upon binding their cognate target. Remarkably, only a select number of such antibodies with the propensity to internalize have been identified, limiting the range and breadth of ADC therapeutics in the clinic. Here we show that Atreca's Immune Repertoire Capture (IRC™) technology can identify potent anti-tumor antibodies with internalization activity applicable for ADC therapeutics from patients undergoing immunotherapy.

Methods
We analyzed blood plasmablasts from patients with non-progressing metastatic cancer using IRC™ technology. Briefly, plasmablasts were collected from patients and paired heavy and light chain antibody sequences were then obtained from individual cells. Antibody sequences representing expanded clonal families were subsequently expressed and analyzed for their ability to (i) bind to human tumor and non-tumor tissues and (ii) internalize into cancer cells when labeled with a pH-sensitive dye. Those antibodies with a high internalization rate were directly conjugated with a cytotoxic agent (auristatin MMAE) and tested in an in vitro ADC assay.

Results
Patient-derived antibodies from several cancer types bound to human tumor tissue but not adjacent normal tissue and also internalized into A549 lung tumor cells. These internalizing antibodies were able to induce target cell death in vitro when conjugated directly or indirectly to a cytotoxic agent across several human tumor cell lines.

Conclusions
In this study we demonstrate that patient-derived antibodies which bind to public tumor-selective antigens and internalize into cancer cells can be identified by our IRC™ technology. Furthermore, we demonstrate that these antibodies can deliver a cytotoxic payload to target tumor cells to induce cell death.

Ethics Approval
The study was approved by Sutter Health Institutional Review Board, approval #2016.148-1

P2

Intratumoral application of hu14.18-IL2 for treatment of GD2+ pediatric malignancies: A novel immunotherapeutic approach aiming at in-situ vaccination

Romana Gugenberger, PhD[1], Zachary Morris, MD, PhD[2], Oliver Mutschlechner[1], Paul Sondel, MD, PhD[2], Hans Loibner, PhD[1]

[1]*Apeiron Biologics AG, Vienna, Austria*
[2]*University of Wisconsin, Madison, WI, USA*

Background
hu14.18-IL2 is an antibody-cytokine fusion protein that combines targeting and immune activation of a human IgG1 monoclonal antibody with the immune stimulatory function of IL2. The humanized antibody portion targets the GD2 ganglioside antigen expressed on a variety of tumors of neuroectodermal origin. Clinical efficacy of the immunocytokine by i.v. application has been shown already in several clinical trials in melanoma and neuroblastoma. Dose limiting toxicity relates to systemic IL2 toxicity. A novel approach was explored preclinically in murine tumor models to deliver hu14.18-IL2 locally by intratumoral (IT) injection aiming at induction of a systemic immune response (in-situ vaccination). We present here activity of the immunocytokine in vitro against various GD2 positive pediatric tumor cell lines. We also discuss a humanized mouse model based on patient-derived xenografts (PDX) by directly transplanting surgical material. Finally we will present the design of a clinical trial to explore safety and clinical activity of IT hu14.18-IL2 in patients with GD2+ pediatric malignancies.

Methods
Expression of the target antigen GD2 on human cell lines MG63 (osteosarcoma), TC-71 (Ewing´s sarcoma), RH41 (rhabdomyosarcoma) and Y79 (retinoblastoma) was analyzed by flow cytometry. Hu14.18-IL2 mediated ADCC and whole blood cytotoxicity (WBT) was determined by 51Cr release assays.

Results
We found expression of antigen GD2 on all cell lines derived from neuro-ectodermal pediatric malignancies. Hu14.18-IL2 was effective in mediating ADCC and WBT against all cell lines in vitro, and potency was found higher than that of the unconjugated chimeric anti-GD2 antibody ch14.18/CHO in osteosarcoma and retinoblastoma. The effects were antigen specific as addition of an anti-idiotypic antibody abrogated the cytolytic activity. A humanized mouse model (CD34+ cell engraftment and transplantation of patient derived GD2+ sarcoma tissue) with intra-tumoral application of the immunocytokine is presently set up.

Conclusions
Immunocytokine hu14.18-IL2 is effective in vitro against various GD2 positive pediatric malignancies by activation of both antibody and IL2 effector functions. Humanized mouse tumor models with GD2+ patient derived tumors may be useful to explore IT immunocytokine in vivo. A clinical phase I/II trial in several advanced pediatric GD2 positive tumors (mostly sarcomas; “basket study”) is in preparation with repeated IT administration of low doses of hu14.18-IL2 (in-situ vaccination).

P3

Evaluating antibody-mediated cellular cytotoxicity and potency of antibody-drug conjugates within three-dimensional tumor models

Chris Langsdorf, BS[1], Bhaskar Mandavilli, PhD[1], Yi-Zhen Hu[1], Aimei Chen, Bachelor of Science[1], Marcy Wickett[1]

[1]*ThermoFisher Scientific, Eugene, OR, USA*

Background

Three dimensional tumor spheroids provide biochemical conditions that closely resemble the tumor microenvironment in an intact organism. Noninvasive approaches such as fluorescence microscopy are highly advantageous as they allow for the study of these three dimensional systems. Here we investigate the penetration and potency of natural killer cells, cytotoxic T cells, and antibody-drug conjugates in three-dimensional models of breast and lung cancer.

Methods

Tumor spheroids were formed by incubating cancer cell lines overnight in Nunclon Sphera 96-well plates. Natural killer cells were isolated from human PBMCs using negative magnetic selection and expanded in culture for 16 days. Natural killer cells were added to SKBR3 breast cancer spheroids with or without trastuzumab. T cells were isolated from human PBMCs using negative magnetic selection and activated for 72 hours. Activated or resting T cells were added to lung cancer spheroids. Immune cell penetration and tumor cytotoxicity were evaluated using whole-spheroid imaging on a confocal high-content imaging system. Trastuzumab was site-specifically conjugated with monomethyl auristatin E (MMAE) and iFL pHrodo Red via SiteClick conjugation. Spheroids of HER2+ breast cancer cells were treated 48 hours with this antibody drug conjugate. ADC penetration and apoptosis were evaluated using confocal high-content imaging.

Results

Unstimulated T cells produced minimal cytotoxicity, similar to untreated spheroids. Activated T cells penetrated and produced significant cytotoxicity throughout cancer spheroids. SKBR3 breast cancer cells form a compact, viable spheroid. Addition of NK cells leads to moderate cytotoxicity, while addition of NK cells and trastuzumab results in substantial cytotoxicity and degradation of spheroid structure (Fig. 1). Trastuzumab labeled with iFL pHrodo Red becomes brightly fluorescent following specific endosomal internalization into breast cancer cells, but minimal toxicity is observed. Trastuzumab conjugated with both iFL pHrodo Red and MMAE internalizes into cells and results in cell killing (Fig. 2).

Conclusions

Fluorescence microscopy combined with novel cell and antibody labeling methods permits investigation of the penetration and potency of natural killer cells, cytotoxic T cells, and antibody-drug conjugates in three-dimensional solid tumor models.

Figure 1.

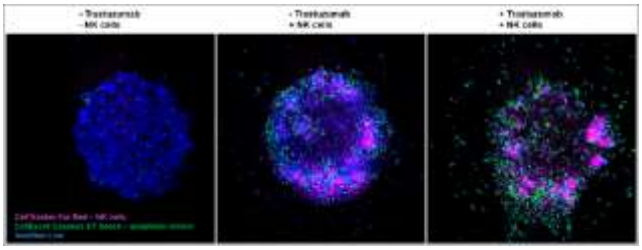

Figure 2.

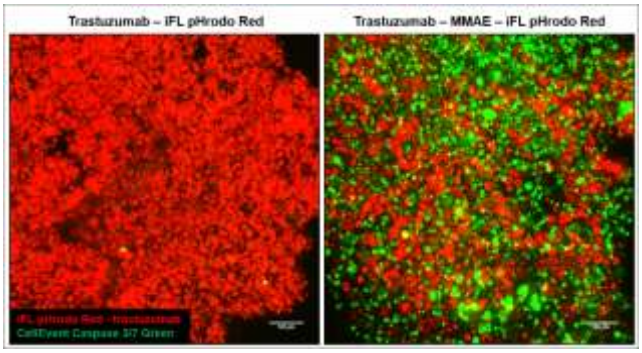

P4

PBD-based anti-MICA/B antibody drug conjugate with a dual mechanism of action: direct tumor cell killing and restoration of NKG2D-mediated immunosurveillance

Florence LHOSPICE, Pharm D[1], Laurent Pouyet, PhD[2], Ester Morgado[2], Romain Remark, PhD[1], Delphine Bregeon[1], Adeline Montbel[1], Nadia Anceriz[1], Mathieu Blery, PhD[1], Ariane Morel, PhD[1], Manel Kraiem[1], Kenneth Crook[1], Eric Vivier[1], Yannis Morel, PhD[1]

[1]*Innate Pharma, Marseille, France*
[2]*MI-mAbs, Marseille, France*

Background

MICA and MICB can be expressed at the surface of a wide variety of tumor cells upon stress, while having a very limited expression on healthy tissues. This makes MICA/B promising targets for the development of antibody drug conjugates (ADC). In addition, MICA and MICB serve as ligands for NKG2D, a potent activating receptor expressed on NK, CD8+T and γδ T cells. As a consequence, the expression of MICA and MICB promotes recognition and elimination of tumors by these lymphocytes through NKG2D engagement. However, in vitro and in vivo studies have reported that chronic engagement of NKG2D by its ligands induces NKG2D downregulation and lymphocyte dysfunction, leading to compromised immunity. We thus aimed to generate an ADC targeting MICA/B-expressing tumors with a dual function to achieve optimal therapeutic benefits: (i) killing of tumor cells and (ii) disrupting the interaction between MICA/B and NKG2D that induces impaired immunosurveillance [1] [2].

Methods

Antibodies were screened based on their binding affinity for the most frequent MICA/B alleles, as well as for their internalization, cytotoxicity and immunomodulatory properties. The MICA/MICB cross-reactive, pan-allele antibody with the highest affinity was conjugated to valine-alanine-pyrrolobenzodiazepine (PBD) dimers using bacterial transglutaminase-based site-specific conjugation to generate anti-MICA/B-PBD ADC

Results

Anti-MICA/B-PBD showed potent in vitro cytotoxicity against a variety of solid cancer cell lines as well as in vivo efficacy in both HCT116 human colon carcinoma and breast cancer patient-derived xenograft models. The immunomodulatory properties of anti-MICA/B-PBD were assessed in MICA-transgenic mice engrafted with MICA-expressing mouse melanoma B16-F10. Lastly, cell surface MICA/B expression and soluble form concentration were assessed in a large panel of samples from healthy donors and patients with various cancers in order to determine potential therapeutic indications for clinical development.

Conclusions

MICA/B molecules are attractive targets for an ADC approach based on their selective expression in a wide range of malignancies while showing restricted expression in healthy tissues along with manageable concentrations of their soluble form. The anti-MICA/B-PBD shows efficacy both in vitro and in vivo, paving the path for further evaluation towards clinical development.

References

1. Wiemann K, Mittrucker HW, Feger U, Welte SA, Yokoyama WM, Spies T, et al. Systemic NKG2D down-regulation impairs NK and CD8 T cell responses in vivo. J Immunol. 2005;175(2):720-9. PubMed PMID: 16002667.
2. Blery M, Vivier E. NKG2D-MICA Interaction: A Paradigm Shift in Innate Recognition. J Immunol. 2018;200(7):2229-30. Epub 2018/03/21. doi: 10.4049/jimmunol.1800176. PubMed PMID: 29555675.

P5

Anti-CD38 immunotherapy kills Treg (CD4+CD25+FoxP3+CD38hi) and Breg (CD19+CD24+CD38hi) cells and restores the anti-tumor T-cell repertoire in chronic lymphocytic leukemia (CLL).

Alak Manna, PhD[1], Sonikpreet Aulukh, MD[1], Laura Lewis-Tuffin, PhD[1], Taimur Sher, MD[1], Sikander Ailawadhi, MD[1], Rami Manuchakian, MD[1], Asher A. Chanan-Khan[1], Aneel Paulus, MD[1]

[1]*Mayo Clinic, Jacksonville, FL, USA*

Background

CLL is the most common adult B-cell leukemia in western hemisphere. A subset of CLL cells immunophenotypically resembles B-regulatory cells (Bregs) and produce IL-10 and TGFβ that functionally imparts to them tumor-supportive properties. These cells are known to support and maintain T-regulatory (Treg) cells. Together, CLL Bregs and Tregs suppress CD8+ cytotoxic T-cell (cTLs) fostering an immunosuppressive and tumor promoting milieu that contribute to disease progression. We observed that a large proportion of CLL-Bregs and Tregs have a high CD38 receptor expression. This led us to hypothesize that eliminating them can potentially restore anti-tumor immune-effector response and is possible through anti-CD38 immunotherapy.

Methods

Blood peripheral mononuclear cells (PBMCs) were isolated from patients with a confirmed diagnosis of CLL (n=17) or healthy donors (n=6, control) under a protocol approved by the Mayo Clinic IRB. Characterization of CLL B-cells (CD19+CD5+), CLL-Bregs (CD19+CD24+CD38+IL10+), Tregs (CD4+CD25+CD127dimFoxP3+) was performed by flow-cytometry. Anti-CD38 immunotherapeutic, Daratumumab (Dara) was used in experiments. Intracellular IL-10 and FoxP3 were measured via fix/perm protocol followed by cytokine staining. Naïve T-cell to Treg transformation was determined using a trans-well co-culture assay. Extracellular IFNγ and IL-10 were measured via ELISA. Apoptosis was determined using annexin-V/PI staining. cTL proliferation was assessed via CFSE labeling of CD8+ sorted T-cells. For in vivo studies, a CLL patient-derived-xerograph (PDX) mouse model was established. (Figure 1)

Results

We noted that compared to healthy donors, CLL patients had a significantly higher % of Tregs (55.23±6.85%) and these Tregs had high CD38 expression (MFI=616.8±36.27). Consistent with our hypothesis, ex-vivo treatment of CLL patient PBMCs with Dara (1ug/mL) was highly lethal to CD38hi Bregs and Tregs. We also noted that CD38hi CLL-Bregs promoted transformation of naïve CD4+ T cells into Tregs in an IL-10/TGFβ dependent manner and neutralization of IL-10/TGFβ prevented this process. Notably, Dara treatment of naïve CD4+ T cells elicited same effect. Overall, Dara induced CLL cell death via ADCC, CDC, ADCP and mitochondrial/FcγR-mediated apoptosis. In Dara-treated CLL PBMC+T-cell co-cultures, ex vivo, we observed decreased IL-10 but increased IFN-y, Th17 and cTL counts. Similarly, in the PDX model, Dara-treated mice showed an increase in CD8+ and Th17 cells but a decrease in Bregs and Tregs.

Conclusions

Anti-CD38 immunotherapy is lethal to immunosuppressive CD38hi Breg/Treg cells and may improve anti-tumor T-cells function via modulating CLL immune-microenvironment. The results of these analyses have led to the approval of a phase-II clinical study that will be testing Dara in relapsed/refractory CLL patients.

Acknowledgements
Acknowledgement: Daniel Foundation of Alabama and Mayo Clinic Cancer Center (CA015083; A.A.C-K.), University of Iowa and Mayo Clinic Lymphoma SPORE Developmental Research Program (P50 CA097274; A.P.) and the Predolin Foundation (A.A.C-K).

Ethics Approval
Ethics Approval: The study was approved by Mayo Clinic Institutional Research Board (IRB# 14-009163)

Figure 1. Anti-CD38 immunotherapy kills Treg and Breg

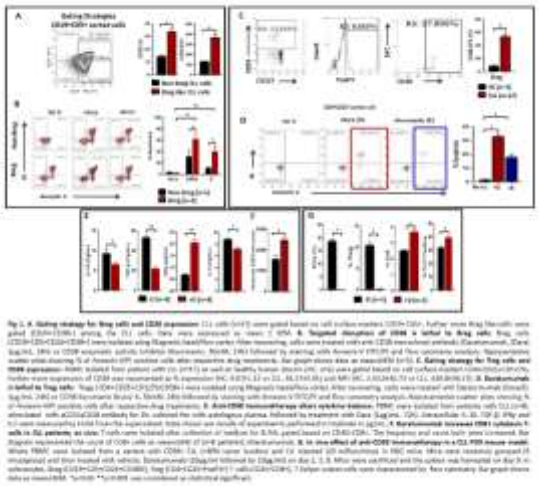

P6 ★ **Abstract Travel Award Recipient**

Anti-CD38 immunotherapy kills Treg (CD4+CD25+FoxP3+CD38hi) and Breg (CD19+CD24+CD38hi) cells and restores the anti-tumor T-cell repertoire in chronic lymphocytic leukemia (CLL).

Alak Manna, PhD[1], Sonikpreet Aulakh, MD[1], Laura Lewis-Tuffin, PhD[1], Taimur Sher, MD[1], Sikander Ailawadhi, MD[1], Rami Manuchakian, MD[1], Asher A. Chanan-Khan[1], Aneel Paulus, MD[1]

[1]*Mayo Clinic, Jacksonville, FL, USA*

Background
CLL is the most common adult B-cell leukemia in western hemisphere. A subset of CLL cells immunophenotypically resembles B-regulatory cells (Bregs) and produce IL-10 and TGFβ that functionally imparts to them tumor-supportive properties. These cells are known to support and maintain T-regulatory (Treg) cells. Together, CLL Bregs and Tregs suppress CD8+ cytotoxic T-cell (cTLs) fostering an immunosuppressive and tumor promoting milieu that contribute to disease progression. We observed that a large proportion of CLL-Bregs and Tregs have a high CD38 receptor expression. This led us to hypothesize that eliminating them can potentially restore anti-tumor immune-effector response and is possible through anti-CD38 immunotherapy.

Methods
Blood peripheral mononuclear cells (PBMCs) were isolated from patients with a confirmed diagnosis of CLL (n=17) or healthy donors (n=6, control) under a protocol approved by the Mayo Clinic IRB. Characterization of CLL B-cells (CD19+CD5+), CLL-Bregs (CD19+CD24+CD38+IL10+), Tregs (CD4+CD25+CD127dimFoxP3+) was performed by flow-cytometry. Anti-CD38 immunotherapeutic, Daratumumab (Dara) was used in experiments. Intracellular IL-10 and FoxP3 were measured via fix/perm protocol followed by cytokine staining. Naïve T-cell to Treg transformation was determined using a trans-well co-culture assay. Extracellular IFNγ and IL-10 were measured via ELISA. Apoptosis was determined using annexin-V/PI staining. cTL proliferation was assessed via CFSE labeling of CD8+ sorted T-cells. For in vivo studies, a CLL patient-derived-xerograph (PDX) mouse model was established.

Results

We noted that compared to healthy donors, CLL patients had a significantly higher % of Tregs (55.23±6.85%) and these Tregs had high CD38 expression (MFI=616.8±36.27). Consistent with our hypothesis, ex-vivo treatment of CLL patient PBMCs with Dara (1ug/mL) was highly lethal to CD38hi Bregs and Tregs (Figure 1). We also noted that CD38hi CLL-Bregs promoted transformation of naïve CD4+ T cells into Tregs in an IL-10/TGFβ dependent manner and neutralization of IL-10/TGFβ prevented this process. Notably, Dara treatment of naïve CD4+ T cells elicited same effect. Overall, Dara induced CLL cell death via ADCC, CDC, ADCP and mitochondrial/FcγR-mediated apoptosis. In Dara-treated CLL PBMC+T-cell co-cultures, ex vivo, we observed decreased IL-10 but increased IFN-γ, Th17 and cTL counts. Similarly, in the PDX model, Dara-treated mice showed an increase in CD8+ and Th17 cells but a decrease in Bregs and Tregs.

Conclusions

Anti-CD38 immunotherapy is lethal to immunosuppressive CD38hi Breg/Treg cells and may improve anti-tumor T-cells function via modulating CLL immune-microenvironment. The results of these analyses have led to the approval of a phase-II clinical study that will be testing Dara in relapsed/refractory CLL patients.

Acknowledgements

Acknowledgement: Daniel Foundation of Alabama and Mayo Clinic Cancer Center (CA015083; A.A.C-K.), University of Iowa and Mayo Clinic Lymphoma SPORE Developmental Research Program (P50 CA097274; A.P.) and the Predolin Foundation (A.A.C-K).

Ethics Approval

Ethics Approval: The study was approved by Mayo Clinic Institutional Research Board (IRB# 14-009163)

Figure 1. Anti-CD38 immunotherapy kills Treg and Breg

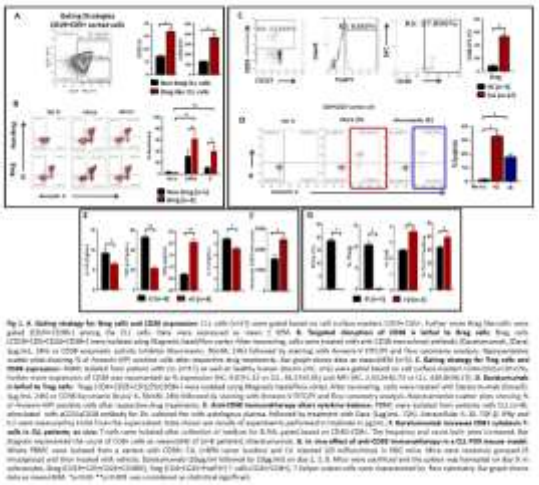

P7

Potent tumor-directed T cell activation and tumor inhibition induced by a 4-1BB x 5T4 ADAPTIR™ bispecific antibody

Michelle Nelson, PhD[1], Gabriele Blahnik-Fagan[1], Robert Bader[1], Doreen Werchau, BS[2], Anneli Nilsson[2], Lill Ljung[2], Jeannette Bannink, BS[1], Danielle Mitchell[1], Lynda Misher[1], Catherine McMahan[1], Maria Askmyr[2], Anna Dahlman[3], Peter Ellmark, PhD[2], Gabriela Hernandez-Hoyos[1], Sara Fritzell[2,4]

[1]*Aptevo Therapeutics Inc., Seattle, WA, USA*
[2]*Alligator Bioscience AB, Lund, Sweden*
[3]*Allligator Bioscience AB, Lund, Sweden*
[4]*Alligator Bioscience, Lund, Sweden*

Background

4-1BB (CD137) is an important activation-induced co-stimulatory receptor that regulates immune responses of activated CD8+ T and NK cells, by enhancing proliferation, survival, cytolytic activity and IFN-γ production. The ability to induce potent

anti-tumor activity by stimulating 4-1BB on tumor-specific cytotoxic T cells makes 4-1BB an attractive target for designing novel therapeutics for immuno-oncology. However, clinical development of a monospecific 4-1BB agonistic antibody has been hampered by dose-limiting hepatic toxicities. To minimize systemic immune toxicities, we have developed a novel 4-1BB x 5T4 bispecific antibody designed to direct tumor-specific T cell responses to the tumor microenvironment by stimulating 4-1BB function only when co-engaged with 5T4, a tumor-associated antigen.

Methods

ALG.APV-527 was built based the ADAPTIR™ platform with binding domains to 4-1BB and 5T4 generated using the ALLIGATOR-GOLD® human scFv library and subsequently optimized to increase binding affinity, function, stability and manufacturability. To assess its agonistic function, ALG.APV-527 was tested in NF-κB luciferase reporter systems and assays using primary cells in the presence or absence of cells expressing 5T4. To stimulate primary cells, enriched CD8+ T cells or unseparated PBMC were sub-optimally cultured with anti-CD3 antibody. Secretion of IFN-γ was measured at 72 hrs using ELISA or Luminex-based assays. To measure proliferation, PBMC were labelled with Cell TraceTM and CD8+ T cells were gated using multicolor flow cytometry. For tumor inhibition studies, the human colon carcinoma HCT116 xenograft model expressing endogenous levels of 5T4 was used. 5T4 expression was evaluated in normal human tissues and a range of different human tumors by immunohistochemistry (IHC).

Results

In vitro, ALG.APV-527 triggers luciferase reporter activity in the presence of 5T4-expressing cells. Using enriched T cells or whole unseparated PBMC, ALG.APV-527 induces a concentration-dependent increase of IFN-γ production when co-cultured with 5T4-expressing cells. ALG.APV-527 enhances primary CD8+ T cell proliferation preferentially over CD4+ T cells. Of significance, ALG.APV-527 is capable of inhibiting tumor growth in a human colon carcinoma xenograft model. IHC staining confirms that 5T4 is overexpressed in a range of solid tumors but not in normal tissues, indicating that ALG.APV-527 may primarily localize to the tumor improving potential for a achieving concentrations that demonstrate efficacy in a solid tumor setting.

Conclusions

ALG.APV-527 induces potent CD8+ T cell co-stimulation but only in the presence of 5T4 antigen. Based on preclinical data, ALG.APV-527 is a promising anti-cancer therapeutic for the treatment of a variety of 5T4-expressing solid tumors.

P8

Single-cell proteomic analysis of T cells stimulated by Bi-specific T-cell Engagers (BiTEs) shows robust and unique polyfunctional secretion profile

Sean Mackay, MBA[1], Patrick Paczkowski[1], Brianna Flynn, MS[1], Kevin Morse[1], Tiffany Coupet, BS[2], Claire Godbersen, BS[2], Charles Sentman[2], Jing Zhou, MD, PhD[1]

[1]IsoPlexis, Branford, CT, USA
[2]Geisel School of Medicine at Dartmouth, Lebanon, NH, USA

Background

T cell cytokines can drive anti-tumor activity and greater polyfunctionality (co-secretion of 2+ proteins per single cell) has been shown to be associated with improved clinical outcome in the study of CAR-T cell therapy and vaccine. We employed single-cell proteomics to fully evaluate the impact of BiTEs on polyfunctional T cells. BiTEs as cancer-targeting drugs link T cells with tumor by binding CD3 and a tumor antigen. Natural killer group 2, member D (NKG2D) ligand, such as MICA, expressed on more than 90%

of human tumors but limited on normal tissues has emerged as appealing targets for BiTEs. This study has explored the polyfunctional profile of T cells by two BiTEs: B2-OKT3 (MICA x CD3) and hNKG2D-OKT3 (NKG2D ligands x CD3).

Methods

Blood T cells were negatively enriched from 3 healthy donors and incubated with K562 cells at a ratio of 1:2 in the presence of 250 ng/ml of B2-OKT3, hNKG2D-OKT3 or control Tz47-2C11. After 36 hours stimulation at 37°C, 5% CO2, CD4+ and CD8+ T cells were separated with anti-CD4 or anti-CD8 microbeads. Approximately 30,000 cells were loaded on the IsoCode single-cell chip (SCBC), pre-patterned with a 32-plex antibody ELISA array per cellular microchamber. Secreted proteins were captured from ~1500 single T cells after 16-hour-on-chip incubation at 37°C, 5% CO2. The T cell polyfunctional profile was evaluated across 5 functional groups: effector (Granzyme B, IFN-γ, MIP-1α, Perforin, TNF-α, TNF-β), stimulatory (GM-CSF, IL-2, IL-5, IL-7, IL-8, IL-9, IL-12, IL-15, IL-21), regulatory (IL-4, IL-10, IL-13, IL-22, TGF-β1, sCD40L, sCD137), inflammatory (IL-1β, IL-6, IL-17A, IL-17F, MCP-1, MCP-4), and chemoattractive (CCL-11, IP-10, MIP-1β, RANTES).

Results

Both B2-OKT3 and hNKG2D-OKT3 BiTEs enhanced single-cell polyfunctionality and polyfunctional strength index (PSI) of both CD4+ and CD8+ T cells when activated by K562 tumor cells compared to the Tz47-2C11 negative control (Figure 1). The polyfunctional response was mainly driven by effector cytokines, including Granzyme B, IFN-γ, and MIP-1α, chemoattractive MIP-1β, and regulatory sCD137. hNKG2D-OKT3 elicited more robust polyfunctional response of both CD4+ and CD8+ T cells to K562 cells stimulation than B2-OKT3. Detailed polyfunctional cell subsets with unique cytokine signatures induced by each BiTE are elucidated through high-dimensional single-cell visualizations of the data.

Conclusions

Single-cell proteomic analysis reveals a significantly upregulated polyfunctional profile of T cells induced by the BiTEs against tumor cells than the negative control, providing important insights into BiTE-triggered T cell activity as well as better evaluation and understanding of BiTE therapies.

Figure 1: T Cell Polyfunctional Strength Enhanced by BiTEs

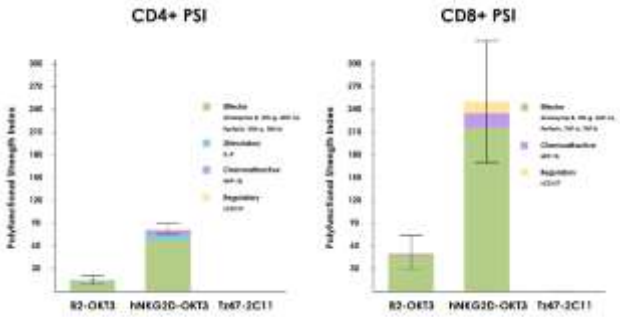

P9

Identification and functional profiling of PD-L1 targeted engineered toxin bodies for antigen seeding technology and redirection of T cell response to tumors

Brigitte Brieschke, BS[1], Sara LeMar[1], Garrett Robinson[1], Aimee Iberg, PhD[1], Shaoyou Chu, PhD[1], Jack Higgins, PhD[1], Erin Willert, PhD[1], Hilario Ramos, PhD[1]

[1]*Molecular Templates, Austin, TX, USA*

Background

Molecular Templates' Engineered Toxin Body (ETB) platform comprises recombinant immunotoxins leveraging Shiga-like Toxin A subunit (SLTA) properties of self-internalization, predictable retrograde transport, and lethal ribosomal inactivation with antibody binding domains to create targeted biologics capable of potent and specific direct killing of cancerous cells (MOA-1). Antigen

Seeding Technology (AST) addition to the ETB scaffold provides a novel approach for redirection of preexisting memory cytotoxic T lymphocytes (CTLs) to cancerous cells (MOA-2). Both MOAs are designed to be functional in patients previously treated with standard of care agents. Here we describe the development of PD-L1 targeted ETBs with AST functionality capable of promoting cytolytic activity by CTLs recognizing a common Cytomegalovirus (CMV) viral antigen (HLA:A02 restricted CMV-pp65-NLVPVMATV, A2-pp65) on targeted tumor cells. We further describe the characteristics that distinguish the complementary mechanisms of action.

Methods

ETBs comprising SLTA fused to PD-L1 scFvs were engineered with or without A2-pp65 peptide. Human tumor cell lines expressing or lacking PD-L1 and HLA:A2 were used as target cells for cytotoxicity assays. Antigen restricted CTLs were expanded from human donors and used in co-culture models as effector cells.

Results

ETBs with potent direct cell kill activity have been identified to bind PD-L1 outside of or overlapping critical contact residues for PD-1. These ETBs have checkpoint inhibitor activity in a PD-1/PD-L1 blockade assay, though significantly less than their corresponding monoclonal antibody. A2-pp65 peptide fusion to ETBs resulted in cell-surface presentation of A2-pp65 peptide in complex with MHC-I and triggered efficient lysis by A2-pp65 specific CTLs in a target and HLA-restricted fashion. SLTA mutations which cause ER retention or do not inactivate ribosomes have no direct cell kill activity (remove MOA-1) but retain the antigen presentation and CTL directed lysis (maintain MOA-2). Additionally, genetic engineering identified modifications that could enhance MOA-1 activity without limiting MOA-2 activity, thus identifying molecules with optimal activity for clinical development. The predictable routing of ETBs support both MOAs and indicates a reduced threshold and routing requirement for MOA-2 as compared to MOA-1, allowing for broader cytotoxicity.

Conclusions

We have developed ETBs which bind distinct epitopes on PD-L1 and provide two unique and complementary mechanisms of action. Coupling both mechanisms of cytotoxicity into one molecule allows for potential to increase target penetrance, expand a prolonged immune response, and overcome resistance. In vivo syngeneic and xenograft studies are ongoing in preparation for clinical development of PD-L1 targeted ETBs with AST functionality in 2019.

P10

Local radiation with intratumoral anti-disialoganglioside (anti-GD2) and interleukin-2 (IL2) induces significant tumor responses with immunologic memory in a syngeneic murine NXS2 neuroblastoma model

Julie Voeller, MD[1], Amy Erbe[1], PhD[1], Kayla Rasmussen, MS[1], Jacob Slowinski[1], Sabrina VandenHeuvel[1], Ravi Patel, MD, PhD[1], Hans Loibner, PhD[2], Stephen Gillies, PhD[3], Jacquelyn Hank, PhD[1], Alexander Rakhmilevich, MD, PhD[1], Zachary Morris, MD, PhD[1], Paul Sondel, MD, PhD[1]

[1]University of Wisconsin Madison, Madison, WI, USA
[2]HL Bioscience Research GmbH, Vienna, Austria
[3]Provenance Biopharmaceuticals, Carlisle, MA, USA

Background

Neuroblastoma is the most common extracranial solid tumor in pediatrics. Standard therapy for patients with high-risk disease includes anti-disialoganglioside (anti-GD2) monoclonal antibody (mAb), GM-CSF (granulocyte-macrophage colony stimulating factor), and IL2 (interleukin-2)—an

immunotherapeutic regimen that has significantly improved survival rates. Our lab has previously shown that local radiation therapy (RT) combined with intratumoral (IT) immunocytokine (IC; a fusion of hu14.18 anti-GD2 mAb and IL2) can cure mice with melanoma. We aimed to test and optimize this in situ vaccine approach in a murine neuroblastoma model.

Methods

Using the murine NXS2 neuroblastoma cell line, subcutaneous neuroblastoma tumors were established on the dorsal right flank of syngeneic A/J mice. Mice bearing 155mm3 tumors (engrafted about 2 weeks prior) received no RT or 12Gy RT to the tumor on treatment day 1, followed by daily intratumoral injections of either 50µg IC or PBS on treatment days 6-10. All mice with complete response were rechallenged on treatment day 90 by injecting NXS2 cells into the dorsal left flank.

Results

We observed improved tumor control (Figure A) and animal survival (Figure B; p<0.0001) when animals were treated with a combination of RT and IT-IC. Complete tumor regression was observed in 75% (9/12) of animals receiving RT and IT-IC, with 89% (8/9) of these rejecting rechallenge. Of all the other groups, only 9% (1/11) of animals receiving IT-IC alone and 33% (4/12) of animals receiving 12Gy and PBS had complete tumor regression.

Conclusions

Combined treatment with RT and intratumoral IC cures most mice bearing a single, 155mm3 NXS2 neuroblastoma tumor and induces immunologic memory. Our ongoing studies continue to investigate this immunotherapy regimen to test its effectiveness in more advanced disease as well as in other in vivo syngeneic murine neuroblastoma model systems.

Figure 1.

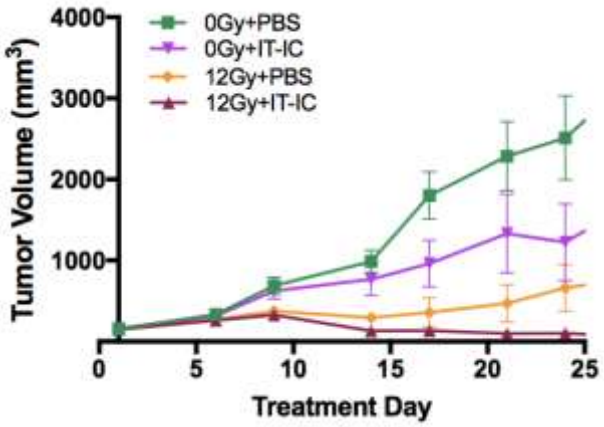

Figure 2.

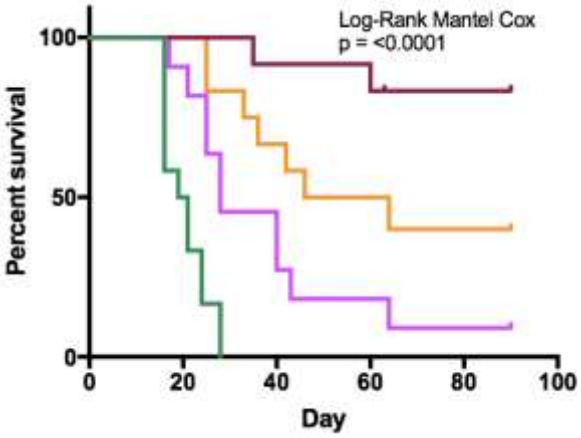

P11

A CD25-targeted pyrrolobenzodiazepine dimer-based antibody-drug conjugate shows potent anti-tumor activity in pre-clinical models of solid tumors either alone or in combination with a PD-1 inhibitor

Francesca Zammarchi, PhD[1], Karin Havenith, PhD[1], Francois Bertelli[2], Balakumar Vijayakrishnan[2], Patrick van Berkel, PhD[1]

[1]ADC Therapeutics, London, UK
[2]Spirogen/MedImmune, London, UK

Background

Regulatory T (Treg) cells infiltrate into various types of human cancers and contribute to the immunosuppressive tumor microenvironment [1]. The intratumoral balance between Tregs versus T effectors (Teffs) cells appears to impact the outcome of the immune system-mediated tumor eradication and numerous attempts are currently underway to reduce the CD25-expressing Tregs cells [2].

Methods

Sur301 is an antibody-drug conjugate (ADC) composed of PC61, a rat monoclonal antibody directed against mouse CD25, stochastically conjugated to a pyrrolobenzodiazepine (PBD) dimer via a protease-cleavable linker, with a drug-to-antibody ratio of 2.

Results

In vitro, sur301 demonstrated potent and specific cytotoxicity in a CD25-expressing mouse lymphoma cell line, while no specific cytotoxicity was observed in two CD25-negative murine colon cancer-derived cell lines, MC38 and CT26. All three cell lines were highly sensitive to SG3199, the PBD dimer toxin of sur301, irrespective of their CD25-status. In vivo, sur301 anti-tumor activity was investigated in the syngeneic MC38 and CT26 models, two immunogenic colon cancer models with tumor-infiltrating CD25-positive Treg cells [3]. Sur301 was administered either alone (0.1, 0.5 or 1 mg/kg, single dose) or in combination with an anti-PD1 antibody. A non-binding control ADC was used as negative control and tested as single dose at 1 mg/kg, either alone or in combination with an anti-PD1 antibody. Single doses of sur301 at 0.5 or 1 mg/kg induced strong and durable anti-tumor activity in both models. When tumor free survivor (TFS) animals were re-challenged with MC38 or CT26 cells, no mice developed new tumors, demonstrating tumor-specific protective immunity was generated by the single action of sur301. A single sub-optimal dose of sur301 at 0.1 mg/kg elicited limited anti-tumor activity when tested as single agent, but combination with an anti-PD1 antibody resulted in synergistic anti-tumor activity in both models. Combination of a single dose of sur301 at 0.5 or 1 mg/kg with the anti-PD1 antibody further increased the number of responders and none of the re-challenged animals developed new tumors. The non-binding control ADC showed no or significant reduced activity when tested at the same dose as sur301.

Conclusions

In conclusion, sur301 demonstrated potent in vivo activity against CD25-negative immunogenic solid tumors with infiltrating CD25-positive Treg cells. Sur301 in vivo activity was further enhanced by combination with anti-PD1 antibody. These data warrant further investigation of ADCT-301, a PBD-based ADC targeting human CD25, in patients with solid tumors, either alone or in combination with checkpoint inhibitors.

References

1. Sasidharan Nair V, Elkord E. Immune checkpoint inhibitors in cancer therapy: a focus on T-regulatory cells. Immunol Cell Biol, 2018. 96(1): p. 21-33.
2. Menetrier-Caux C, et al. Targeting regulatory T cells. Target Oncol, 2012. 7(1): p. 15-28.
3. Arce Vargas F, et al. Fc-optimized anti-CD25 depletes tumor-infiltrating regulatory T cells and synergizes with PD-1 blockade to eradicate established tumors. Immunity, 2017. 46(4): p. 577-586.

Ethics Approval

All in vivo study work was approved by the Institutional Animal Care and Use Committee at Charles River Laboratories, Morrisville, N.C..

Best Practices for Improving Cancer Immunotherapy

P12

Response and toxicity with immune checkpoint inhibition in older patients with non-small-cell lung cancer

Keval Yerigeri, BS[1], Kristen Marrone, MD[2], Jiajia Zhang, MD, MPH[2], Julie Brahmer, MD[2], Patrick Forde, MD[2], Christine Hann, MD, PhD[2], David Ettinger, MD[2], Ronan Kelly, MD MBA[2], Josephine Feliciano, MD[2], Sarah Sagorsky, PA-C[2], Michelle Turner, NP[2], Valerie Rowe, NP[2], Jarushka Naidoo, MD[2]

[1]*Northeast Ohio Medical University, Copley, OH, USA*
[2]*Johns Hopkins University School of Medicine, Sidney Kimmel Comprehensive Cancer Center, Baltimore, MD, USA*

Background
Immune checkpoint inhibition (ICI) has rapidly become standard of care in advanced or metastatic non-small-cell lung cancer (NSCLC) treatment. Initial phase III clinical trials suggest ICI may have decreased efficacy in NSCLC patients ≥ 75 years old. The relationship between age-related immune system changes and ICI treatment is poorly understood.

Methods
The Johns Hopkins Upper Aerodigestive Diseases Immunotherapy Database was queried for all patients ≥ 75 years old treated with anti-PD-1/PD-L1 agents as part of a clinical trial or standard of care, from 2007 to 2018.

Results
Thirty-one patients ≥ 75 years old receiving anti-PD-1/PD-L1 agents for locally advanced or metastatic NSCLC were identified. Eleven patients were female, median age was 80.8 years (range: 75.1-90.6) with median ECOG PS=1 (range: 0-3). Twenty-seven patients received PD-1/PD-L1 monotherapy (nivolumab=16, pembrolizumab=10, atezolizumab=1) and 4 received combination (+chemotherapy=1, +ipilimumab=2, +additional ICI=1). Ten patients received ICI in the first-line setting (1L); 21 patients in the second-line or beyond (2L+). In 1L ICI monotherapy (n=8), median doses received was 5.5 (range: 2-19), median progression-free survival (mPFS) was 7.3m, and median overall survival (mOS) was 11.3m. In 2L+ patients, median dose administration was 4 (range: 1-24), mPFS was 7m and mOS was 7.6m. Across 1L and 2L+ ICI monotherapy patients, a rate of 81.5% all-grade toxicity was seen, of which 30% were high-grade (3+). All 1L and 2L+ ICI combination patients (n=4) experienced a toxicity, with 3 patients experiencing high-grade events. Across all patients, the most common low-grade toxicities were fatigue (n=8) and dyspnea (n=8). High-grade pneumonitis was seen in two 1L ICI monotherapy patients; 2L+ ICI monotherapy high-grade toxicities included dyspnea (n=4), hypoxia (n=1; Grade 5), pneumonitis (n=1), chest pain (n=1), delirium (n=1), aspiration (n=1), heart failure (n=1), lymphadenopathy (n=1) and pleural infection (n=1). Combination ICI high grade toxicities included pneumonitis (1L=1; 2L+=1) and rash (2L+=1). Across patients, reasons for treatment discontinuation included progressive disease (31%), with double the patients stopping for toxicity (62%) and treatment ongoing for 2 patients.

Conclusions
Our results indicate increased frequency and severity of toxicity in anti-PD1/PD-L1 treated older NSCLC patients, with decreased time to off treatment compared to landmark phase III studies. Survival data comparisons are limited in the setting of the current small sample size, but show interesting trends of decreased time on therapy and decreased overall survival. Further translational evaluation of senescent remodeling's role in outcome and toxicity with ICI in older NSCLC patients is needed.

Acknowledgements
We would like to thank the patients and their families who agreed to participate in the Johns Hopkins Upper Aerodigestive Diseases Immunotherapy Database.

Ethics Approval
The study was approved by the Johns Hopkins School of Medicine's Ethics Board, IRB00087582.

Biomarkers and Immune Monitoring

P13

Molecular profiling of anti-PD-1 treated melanoma patients reveals importance of assessing neoantigen burden and tumor escape mechanisms for clinical treatment

Charles Abbott, PhD[1], Sean Boyle, PhD[1], Eric Levy, PhD[1], Rena McClory[1], Sekwon Jang, MD[2], Richard Chen[1]

[1]*Personalis, Menlo Park, CA, USA*
[2]*Inova, Fairfax, VA, USA*

Background
Despite the remarkable response of some melanoma patients to checkpoint inhibitor therapy, significant numbers of patients do not achieve complete response. It is of great interest to identify biomarkers and mechanisms that influence immunotherapy effectiveness. Here we apply a comprehensive tumor immuno-genomics platform (ACE ImmunoID) to identify potential biomarkers of response to checkpoint blockade therapy.

Methods
We characterized the immuno-genomics of tumors from 31 stage III/IV melanoma patients who have received anti-PD-1 treatments to assess potential factors influencing response. Tumor responses to the therapy were evaluated using RECIST criteria with a median follow-up of 12 months. Immuno-genomic profiling was performed using Personalis' ACE ImmunoID platform: an augmented exome/transcriptome platform and analysis pipeline. Analysis included assessment of tumor mutations, neoantigen characterization, HLA typing, gene expression quantification, and tumor micro-environment profiling. The molecular information of the tumors was then analyzed together with their corresponding clinical response.

Results
We observed a trend that higher neoantigen burden was associated with better progression free survival. Further investigation of patients with high neoantigen burden that failed to achieve complete response (3 PD, 1 PR) revealed potential resistant mechanisms to anti-PD-1 therapy. Specifically, we identified two of these patients with high expression of IDO1 or CTLA4, which may facilitate immune escape in a PD-1 independent manner. Additionally, we found two patients with mutations in their antigen presentation machinery (APM). The first patient had two independent HLA mutations in HLA-A and HLA-B (stop-gain mutation and splice site mutation, respectively), leading to the likely loss of surface expression of two classes of HLA-A and HLA-B proteins. In the second APM mutation patient we observed a frameshift deletion event detected in B2M at a very high frequency (80% AF) in their tumor. These APM mutations suggest reduced neoantigen presentation in these patients, likely underlying mechanisms for tumor escape.

Conclusions
While we observed the expected association between neoantigen burden and response to checkpoint blockade therapy, we also identified potential resistance mechanisms in patients that involve perturbations to antigen presenting machinery and high expression of non-targeted checkpoint genes. This highlights the potential importance of broad immuno-genomic profiling of

patients that are candidates for receiving immunotherapy. We are continuing to increase our cohort size to identify additional mechanisms for immune evasion.

Ethics Approval
IRB file # 16-2427

P14

Durvalumab treatment-induced transcriptional changes in the tumor microenvironment associated with longer survival in patients with late stage Non-Small Cell Lung Cancer (NSCLC)

Ikbel Achour, PhD[1], Zachary Cooper, PhD[1], Sriram Sridhar[1], Maria Ascierto, PhD[1], Jixin Wang[1], Young Lee[1], Natasha Angra[1], Shaad Abdullah, MD, FACP[1], Rajiv Raja, PhD[1], Brandon Higgs, PhD[1], Maria Jure-Kunkel[1]

[1]*Medimmune, Gaithersburg, MD, USA*

Background
Baseline biomarkers including PD-L1, IFNg signature and tumor mutational burden (TMB) have demonstrated clinical utility in predicting overall survival in patients treated with anti-PD(L)1 therapies. However, changes in the tumor microenvironment on checkpoint therapy and their relationship to survival are poorly understood. Here, we systematically analyzed tumor microenvironment transcriptional profiles before and on durvalumab treatment and explored association with survival in patients with NSCLC.

Methods
CP1108/NCT01693562 is a nonrandomized phase 1/2 trial evaluating durvalumab (10 mg/kg, Q2W) in patients with solid tumors including advanced NSCLC (squamous and non-squamous). RNA sequencing was performed on 97 baseline tumors and 29 paired baseline and on-treatment (6 weeks) tumors. Gene and pathway level analyses were performed in relation to overall survival at baseline (prolonged OS >2yrs, n=23, compared to short OS <1yrs, n=61) and following durvalumab treatment (n=11 in both OS groups); clinical data cut off was 10/16/2017

Results
Among 763 genes differentially expressed at baseline between tumors from patients with prolonged compared to short survival (FC≥ 1.5 ; p≤0.05), gene signatures of CD8, Th1, T-agonist, T-effector, B, Natural Killer cells (NK), M1 macrophages, dendritic cells (DC), chemoattractant chemokines, and IFNg were expressed at higher levels (FC≥2 ; p≤0.04). Following durvalumab-treatment, in both OS groups, CD8 and T-effector gene signatures were significantly increased (FC≥3 ; p≤0.04), and IFNg,Th1, M1 and chemoattractant chemokine gene signatures were moderately induced (FC≥1.7 ; p≤0.1). Baseline levels of Th2, M2 macrophages and MDSC gene signatures did not significantly change on durvalumab. T-agonist, B, NK and CD1c+ DC cell gene signatures were further induced (FC≥2 ; p≤0.05) only in patients with OS>2 yrs. High expression levels of T-agonist, B cell, and CD1c+ DC signatures correlated with improved OS in early stage non-squamous NSCLC in TCGA. On-treatment reduction of at least 2-fold (p≤0.04) in genes involved in angiogenic, metabolic, cell-cell adhesion and cell cycle pathways including WNT7B, VEGFA, FASN, EVPL and CDKN2B were observed specifically in patients with prolonged OS compared to no change in patients with short OS.

Conclusions
Durvalumab treatment resulted in substantial changes in gene expression in the tumor microenvironment, with notable increases in B and dendritic cell signatures associated to prolonged survival. Our results provide new insights into the anti-tumor mechanism of PD-L1 blockade.

Trial Registration
NCT01693562

P15

Development of a robust, simplified method to measure receptor occupancy in peripheral blood from patients treated with a novel anti-PD-1 agent, AB122

Devika Ashok, PhD[1], Dana Piovesan, MSc[1], Sharon Zhao[1], Hema Singh[1], Steve Young, PhD[1], Matthew Walters, PhD[1], Lisa Seitz, MSc[1]

[1]*Arcus Bio, Hayward, CA, USA*

Background
Exhausted T cells express high levels of immune checkpoint proteins, including programmed cell death-1 (PD-1) receptor. Preclinical and clinical data support the role of PD-1 and its ligand, programmed cell death ligand 1 (PD-L1), in promoting tumor evasion by curtailing immune responses. In a Phase 1 clinical trial of the anti-PD-1 monoclonal antibody AB122, we determined receptor occupancy (RO) in peripheral blood T cells using a directly conjugated competitive antibody method. We contrasted the data quality and derived RO values to previously established methodology described for nivolumab using biotinylated anti-human IgG4.

Methods
RO assays were developed using healthy donor peripheral blood mononuclear cells (PBMCs) spiked with AB122. We evaluated parameters including specimen stability, fresh vs. frozen samples, wash conditions, reagent concentrations and adapted the protocol for application to whole blood specimens to eliminate the need for PBMC isolation. Multi-color flow cytometry enabled determination of RO as well as proliferation status in individual T cell subsets using Ki67 as a functional readout of the effect of anti-PD-1 therapy. We developed the RO panel to work in conjunction with an intra-nuclear staining protocol for Ki67. This included identification of optimal clones for surface staining, blocking non-specific staining and selection of a clone for Ki67 identification. Finally, we deployed both RO determination protocols to evaluate an initial set of samples from cancer patients enrolled in the ongoing dose escalation Phase 1 study of AB122.

Results
Comparable RO data were obtained using both the AB122 competitive antibody and saturation methodologies using biotinylated anti-human IgG4 in PBMC samples from study subjects. Across all initial subjects tested, including different dose groups and time points, an average of ≥ 90% RO was observed using either method. In addition, a greater than 2-fold increase in Ki67+ T cell subsets was observed in approximately half of the patients.

Conclusions
Data from our Phase 1 dose-escalation cohorts demonstrates complete RO across a range of dosing regimens of AB122 and is consistent with data published for other anti-PD-1 antibodies. This optimized assay eliminates the need for multiple wash steps, decreases variability and enables testing with smaller numbers of cells. In addition, we have modified the direct competition method to enable direct assay of whole blood specimens allowing for a one-step staining process and preservation at a central lab to eliminate PBMC isolation.

P16

Better efficacy of PD-1 antibody predicted by immune-related adverse effects is impaired by high dose steroids

Xue Bai, MD[1], Michelle Kim[2], Gyulnara Kasumova[2], Tatyana Sharova[3], Justine Cohen, DO[4], Donald Lawrence, MD[4], Christine Freedman, RN[4], Riley Fadden, NP[4], Krista Rubin, MS, FNP-BC[4], Ryan

Sullivan, MD[4], Keith Flaherty[4], Genevieve M. Boland, MD, PhD[2]

[1]Massachusetts General Hospital Cancer Center, Harvard Medical School; Department of Renal Cancer and Melanoma, Peking University Cancer Hospital and Institute, Boston, USA
[2]Department of Surgical Oncology, Massachusetts General Hospital, Harvard Medical School; Geisel School of Medicine at Dartmouth, Hanover, USA
[3]Department of Surgical Oncology, Massachusetts General Hospital, Harvard Medical School, Boston, MA, USA
[4]Massachusetts General Hospital Cancer Center, Harvard Medical School, Boston, MA

Background
PD-1 antibody has greatly improved the prognosis of unresectable or metastatic melanoma, and is now the standard first line therapy. It also brings a spectrum of immune-related adverse effects (irAEs). However, the correlation between the presence and timing of irAEs and the efficacy of PD-1 antibody remains elusive.

Methods
We retrospectively collected clinical data of pembrolizumab or nivolumab monotherapy-treated patients in Massachusetts General Hospital from 2009 to 2017. Correlations between irAEs and clinical outcomes were statistically analyzed.

Results
Of total 147 enrolled patients, 81 (55.1%) had irAE(s) (median 1/patient), 33 (22.4%) had severe irAE(s) (grade 3,4). The presence of irAE(s) was correlated with better therapeutic efficacy, which was impaired but not entirely offset by the application of high dose steroids, i.e. irAE+/high-dose steroids(-) subgroup had the best clinical outcome (median PFS 132.1 weeks, median OS not reached), followed by irAE+/high-dose steroids(+) (median PFS 43.0 weeks, median OS 182.6 weeks), which was better than irAE- subgroup (median PFS 11.4 weeks, median OS 74.7 weeks) (P<0.001 as for both PFS and OS). In total 158 irAEs were reported, among which 37 (23.4%) affected skin, 32 (20.3%) endocrine system, 31 (19.6%) muscle and joints, 21 (13.3%) gastrointestinal, 12 (7.6%) pulmonary, 9 (5.7%) hepatic, 4 (2.5%) renal, 4 (2.5%) neural, 2 (1.3%) pancreas, and 6 (3.8%) others. Median onset time of irAEs affecting each system was significantly different (P=0.036), early onset irAEs included neuropathy (6.9 weeks), hepatitis (7.3 weeks), and late onset irAEs included musculoskeletal (32.7 weeks), and cutaneous (27.6 weeks). Within the subpopulation of patients with irAE(s), those with musculoskeletal irAEs had better therapeutic response (ORR 84.6% vs. 48.1%) (P=0.005), longer median PFS (119.6 vs. 43.4 weeks) (P=0.010), and longer median OS (not reached vs. 189.6 weeks) (P=0.013). While cutaneous irAEs in total did not correlate with outcomes, the subset of vitiligo patients (n=8) had longer median PFS (not reached vs. 60.4 weeks) (P=0.032), and the tendency towards better therapeutic response (ORR 87.5% vs. 56.9%) (P=0.186) and longer median OS (not reached vs. 229.3 weeks) (P=0.191). Interestingly, rare irAEs* requiring high dose steroids (median onset of 7.7 weeks), were correlated with shorter median PFS (28.1 vs. 90.0 weeks) (P=0.006) and shorter median OS (120.0 weeks vs. not reached) (P=0.037).

Conclusions
The presence of irAE(s) serves as a prognostic biomarker during PD-1 antibody monotherapy. Application of high dose steroids impairs PD-1 antibody efficacy, and may impact subtype-specific predictive values of different irAEs.

P17

Combined MAGE-A1,3/6,4, and 10 expression levels quantified in solid tumors by (BaseScope™) RNA in situ hybridization (ISH) identify targets for immunotherapy

Anshika Bajaj, PhD[1], Helly Xiao Yan Pimentel[2], Bingqing Zhang, PhD[2], Ruby Hsu, PhD[2], Peter Berglund, PhD[1], Jan Ter Meulen, MD, PhD[1]

[1]*Immune Design, Seattle, WA, USA*
[2]*Advanced Cell Diagnostics, Neward, CA, USA*

Background
Ongoing clinical trials of cancer vaccines and adoptive cell therapies target members of the melanoma-associated antigen (MAGE-A) family, highly prevalent in tumors. However, no multiplexed diagnostic assay is available to quantify MAGE-A expression for ideal patient selection. The homologous nature with 50-80% sequence identity between the MAGE-A genes poses significant challenges to their specific detection in tumors. Due to antibody cross-reactivity there is limited capability of protein-specific assays to detect and distinguish between the various MAGE-A antigens. Here, an RNA ISH based assay was developed to assess and quantitate *MAGEA1*, *MAGEA3/6*, *MAGEA4*, *MAGEA10* expression in normal and tumor tissue.

Methods
MAGEA (*-A1*, *-A3*, *-A4*, and *-A10*) specific probes were designed targeting sequences with minimal inter-gene identity. Tissue samples that passed quality control were evaluated for *MAGEA* expression. BaseScope™ LS Red ISH assays were performed on Leica Bond RX using the BaseScope LS kit on cell pellet arrays, tumor, and normal tissues.

Results
4 assays were developed, each designed to specifically detect RNA encoding MAGE-A1, -A3/6, -A4, or -A10. Experiments done in control cell lines (1 negative and 4 cells lines each expressing 1 of the 4 *MAGEA* genes) demonstrated that the assays were highly specific and sensitive for their respective target genes. *MAGEA* expression was assessed in 10 melanoma, head and neck, lung, and esophageal cancer biopsies. Samples were assigned dot scores based on semi-quantitative visual scoring of the number of dots (RNA molecules)/cell. Moderate-high expression of all 4 *MAGEAs* (score of 2-3) was observed in biopsies from 1/1 melanoma patients, 2/3 lung cancer patients, and 1/4 head and neck cancer patients. High *MAGEA1* and *3* expression only (score of 3) was observed in 3/4 head and neck cancer patients. As expected, analysis of normal tissue samples except for testes revealed minimal signal.

Conclusions
Specific and sensitive BaseScope assays were developed for *MAGEA1*, *MAGEA3/6*, *MAGEA4*, and *MAGEA10*. The assays demonstrate inter-gene specificity, are amenable to multiplexing, and can potentially be used as a companion diagnostic in clinical trials targeting *MAGEA* antigens. Furthermore, these preliminary results demonstrate that these 4 MAGE-A antigens are highly prevalent in cancers such as head and neck, melanoma, and lung and support the development of an active immunotherapy based on Immune Design's dendritic cell-targeting ZVex® vector platform.

P18

Preliminary evaluation of a novel whole slide multispectral assessment of seven markers: Potential to minimize bias in the characterization of the tumor immune environment

Carmen Ballesteros Merino, PhD[1], Shawn Jensen, PhD[2], Carla Coltharp, PhD[3], Kristin Roman, MS[3], Chichung Wang[3], Nikhil Lonberg, HSDG[2], Sebastian Marwitz[2], Tarsem Moudgil, MS[2], William Miller, BS[2],

William Redmond, PhD[2], Yoshinobu Koguchi, MD, PhD[2], Carlo Bifulco, MD[2], Clifford Hoyt, MS[3], Bernard A. Fox, PhD[2]

[1]Robert W Franz Cancer Center, Earle A Chiles Research Insititute, Portland, OR, USA
[2]Robert W Franz Cancer Center, Earle A Chiles Research Institute, Portland, OR, USA
[3]Perkin Elmer, Hopkinton, MA, USA

Background
PD-L1 expression and tumor-mutational burden enrich for patients that respond to checkpoint blockade, but these evaluations are only a component of the entire story. Recently, our lab reported that evaluation of specific cell-cell relationships provided a powerful biomarker for overall survival in patients with HPV- head and neck cancer (HNSCC). However, the areas selected for analysis were operator selected “hot spots”. This approach introduces the potential for unconscious bias in the selection process. To address this, we have sought to perform whole slide evaluations of sections to compare with hot spot analysis. This study is a preliminary report applying a novel set of fluorophores and filters that allow the visualization of seven colors on a whole slide.

Methods
Tissue samples included pellets of cultured lymphocytes and tumor specimens. A sample of the cultured lymphocytes that were fixed and embedded were analyzed by flow cytometry for immune markers. Formalin-fixed paraffin embedded (FFPE) sections were stained with antibodies for CD8, CD68, FoxP3, PD-1, PD-L1, cytokeratin and DAPI. PerkinElmer Opal reagents were used to identify markers and included standard and a new set of fluorophores that included Opal 480, 520, 570, 620, 690, and 780. Slides were imaged using a new scanning approach on a Vectra Polaris (PerkinElmer, Inc, Waltham, MA).

Results
Preliminary comparison of cells that were used to produce FFPE blocks by flow cytometry and multiplex IHC provided similar results for some markers. Determining optimal staining, exposure times and thresholds for analysis for this new method needs work, but the potential exists for effective evaluation of a whole slide with 7 different markers.

Conclusions
Our preliminary results provide reason to be optimistic that this approach can assess 7 colors in a whole slide. Whole sections labelled with 7 colors and spectrally unmixed supports deeper analysis of immune-biology on multiple scales, including re-analysis of spatial metrics based on emerging hypotheses about how cellular and expression distributions relate to disease progression and response to therapy.

P19

Molecular determinants of response to PD-L1 blockade across tumor types

Romain Banchereau[1], Ning Leng[1], Edward Kadel, BS[1], Dorothee Nickles, PhD[1], Steve Lianoglou, BS, MSc, PhD[1], Oliver Zill[1], Sushit Jhunjhunwala[1], Luciana Molinero, PhD[1], Mahrukh Huseni[1], Marcin Kowanetz, PhD[1], Richard Bourgon, BS, PhD[1], Craig Cummings, PhD[1], Sanjeev Mariathasan, PhD[1], Priti Hegde, PhD[1], Thomas Powles, MBBS, MD, MRCP2

[1]Genentech, South San Francisco, CA, USA
[2]BART, London, UK

Background
Immune checkpoint inhibitors targeting the PD-1/PD-L1 axis lead to durable clinical responses in subsets of cancer patients across multiple indications including non-small cell lung cancer (NSCLC), urothelial carcinoma (UC) and renal cell carcinoma

(RCC). This work aims at determining whether unifying molecular profiles can predict response across these tumor types.

Methods

379 samples from three phase II trials were investigated. PD-L1 expression on tumor-infiltrating immune cells (IC), tumor mutation burden (TMB) and bulk transcriptome measurements were obtained before treatment with atezolizumab from 218 UC (IMvigor210), 83 NSCLC (POPLAR) and 78 RCC (IMmotion150) patients. Objective response was assessed by RECIST v1.1. Patients from a phase I atezolizumab monotherapy basket study (PCD4989g) were employed as an independent validation cohort. PD-L1 IC was assessed by immunohistochemistry (Ventana SP142: >1% of IC was defined as positive). TMB was assessed by whole exome sequencing. Bulk tumor transcriptomes were assessed by RNAseq.

Results

Initial analyses focused on responder prevalence in PD-L1 IC+ and/or TMBhigh individuals. They revealed variable results across tumor types with overall sensitivity/specificity of 76.4%/34.5% and 74.5%/55.4% for PD-L1 IC and TMB respectively. Importantly, no common TMB threshold predicted response across indications. Unsupervised analysis revealed that RCC tumors cluster away from UC and NSCLCs. Supervised analysis showed that PD-L1 IC expression correlated with myeloid and lymphoid signatures across tumor groups, while few immune genes associated with TMB. Modular transcriptional analysis failed to identify a unified tumor signature associated with response, although parallels were seen between NSCLC and UC, but not RCC. Using a linear model that accounted for genes associated with PD-L1 IC levels, the CDK4/6 inhibitor CDKN2A, which is frequently mutated in UC and NSCLC tumors, was identified as the most significant correlate of response to PD-L1 inhibition, highlighting the association of non-immune pathways to checkpoint blockade outcome. Tumor-related pathways including mismatch repair and senescence were enriched in responders with low tumor immune infiltrate. Finally, machine learning identified a 42-gene signature associated with outcome, which included both immune- and tumor-related components. This signature complemented TMB and PD-L1 IC to increase responder prevalence both in training and independent validation cohorts.

Conclusions

While no unifying gene signature correlated with response across tumor types, consistent overlaps were observed between UC and NSCLC, highlighting common mechanisms of response to PD-L1 inhibition between tumors from different origins. Machine learning can integrate high-dimensional datasets across indications to identify both immune- and tumor-related determinants of response to checkpoint blockade.

P20

A structured tumor-immune microenvironment in triple negative breast cancer revealed by multiplexed ion beam imaging

Leeat Keren[1], Marc Bosse[1], Robert West[2], Sean Bendall, PhD[1], Michael Angelo, MD, PhD[1]

[1]*Stanford University, Stanford, CA, USA*
[2]*Stanford, Stanford, CA, USA*

Background

Cancer progression is a complex process that depends on the interplay between cells in the tumor, the microenvironment, and the immune system, which can act both to promote and suppress growth and invasion [1]. Triple-negative breast cancer (TNBC) is an aggressive form of invasive breast cancer lacking appreciable expression of therapeutic targets: estrogen receptor, progesterone receptor, and Her2 [2]. In terms of TNBC immunotherapy, no single biomarker has been sufficient for adequate

patient stratification [3]. Consequently, there is still much interest in its tumor immune landscape: which immune cell types are present, which immunoregulatory proteins are expressed, and how these vary between patients.

Methods

We leveraged a next-generation tissue pathology imaging platform we have developed, Multiplexed Ion Beam Imaging [4] coupled to Time of Flight (MIBI-TOF) mass analysis, to perform a retrospective study on TNBC patients from the Stanford Pathology archive. With this we simultaneously quantified in-situ expression of 36 proteins covering identity, function and immune regulation at sub-cellular resolution in 41 TNBC patients. This data enabled us to develop a multi-step analysis pipeline for standardized processing of this multiplexed imaging cohort, including deep-learning-based segmentation, cell type identification, and spatial enrichment analysis of the tumor immune microenvironment.

Results

While the composition of tumor-immune populations varied widely between individuals, this heterogeneity could be reconciled by the overall amount of immune infiltration, where there was enriched co-occurrence and ordering of specific immune populations conserved across the cohort. Monocytes were at all levels of infiltrate while B and NK cells only in patients with the greatest immune cell density. At the same time, distinct immune populations expressed checkpoint proteins (i.e. PD1, PD-L1, IDO, and LAG3) in different patients, and patients that express one immunosuppressive pathway were more likely to express another. Data-driven analysis of spatial organization revealed either immune compartmentalized or immune mixed tumors. Most interestingly, this histological organization was significantly correlated with expression of checkpoint molecules (particularly PD1, PD-L1, and IDO) in a cell-type- and location-specific manner. Here, ordered immune structures along the tumor-immune border served as a hallmark of tumor compartmentalization and were linked to overall survival with standard chemotherapy.

Conclusions

Together, these data demonstrate an organization in the tumor-immune microenvironment that is structured in cellular composition, spatial arrangement, and expression of regulatory proteins. We elucidate these organizational features creating a resource for TNBC and provide a framework to apply highly multiplexed subcellular imaging to complex immune oncology.

Acknowledgements

S.C.B. is supported by a gift from Christy and Bill Neidig, the Damon Runyon Cancer Research Foundation (DRG-2017-09), the NIH 1DP2OD022550-01, 5U19AI116484-02, and U19AIP97

*Corresponding author email: paola.nistico@ifo.gov.it9. M.A is supported by 1-DP5-OD019822. S.C.B and M.A. are jointly supported by 1R01AG056287–01, 1R01AG057915-01, and 1U24CA224309-01 from the NIH. L.K. is a Damon Runyon Fellow supported by the Damon Runyon Cancer Research Foundation (DRG-2292-17)

References

1. Chen DS, Mellman I. Elements of cancer immunity and the cancer–immune set point. Nature. 2017;541:321–330.
2. Denkert C, Liedtke C, Tutt A, von Minckwitz G. Molecular alterations in triple negative breast cancer—the road to new treatment strategies. Lancet. 2017;389:2430–2442.
3. Maleki Vareki S, Garrigós C, Duran I Biomarkers of response to PD-1/PD-L1 inhibition. Crit. Rev. Oncol. Hematol. 2017;116:116–124.
4. Angelo M, et al. Multiplexed ion beam imaging of human breast tumors. Nat. Med. 2014;20:436–42.

P21

Deep learning-based PD-L1 tumor cell (TC) scoring improves survival prediction compared to pathologists on durvalumab-treated NSCLC patients

Nicolas Brieu, PhD[1], Ansh Kapil[1], Aleksandra Zuraw, Dr[1], Abraham Silva, MD[1], Marlon Rebelatto, DVM, PhD, DACVP[2], Keith Steele, DVM, PhD[2], Guenter Schmidt, PhD[1]

[1]*Definiens, Munich, Germany*
[2]*MedImmune, Gaithersburg, MD, USA*

Background

PD-L1 expression in non-small cell lung carcinoma (NSCLC) patients is commonly quantified by the tumor cell (TC) score estimated by pathologists. An accurate score is key to identify patients that could benefit from anti-PD-L1 check point inhibitor treatment, patients with high score being more likely to respond to such therapy [1]. Recent advances in deep learning algorithms for computer vision enable an accurate alternative to pathologist scoring via the identification of positive and negative tumor regions [2]. With statistical analysis of the clinical response, we show the predictive value of the automated scoring system and evaluate it against pathologist scoring.

Methods

The dataset consists of tissue sections of NSCLC patients from subsets of NCT01693562 [1] and NCT02000947 [3] clinical trials and stained with Ventana SP263 PD-L1 assay. Using two-fold cross validation, we train a deep semi-supervised convolutional neural network [2] for the automated segmentation of PD-L1 positive and PD-L1 negative tumor cell regions. Training is based on labeled patches generated from the manual annotation of positive and negative tumor cell regions by two pathologists on a subset of images (n=20) as well as on unlabeled patches generated from the remaining non-annotated images (n=305). The dataset for network application, TC score estimation and further statistical analysis consists of the non-annotated NSCLC samples of the durvalumab monotherapy clinical trial (NCT01693562) for which overall survival (OS), progression free survival (PFS) defined by RECIST criteria, and three pathologist scores are available (n=152). The automated score is estimated from the segmented regions as the relative area of the PD-L1 positive tumor cell region. Using leave-one-out cross-validation, we finally optimize the cutpoint between low and high scores regarding log-rank test associated with overall survival and progression free survival.

Results

The deep learning-based score is strongly correlated with the consolidated pathologist score obtained by majority voting (Pearson:0.80). It yields more significant OS and PFS stratifications in terms of Cox proportional hazards regression than the pathologist score for both the standard 25% cut-off [1] and the respective optimized cut-off (Figure.1 and Table.1).

Conclusions

Our results suggest that the proposed deep learning based system for PD-L1 TC scoring enables the retrospective stratification of durvalumab-treated NSCLC patients into predictive groups. Upon further improvement of the correlation to pathologists and confirmation of the presented results in a prospective trial, we envision that the proposed model could be used in a clinical routine setting to identify patients which may benefit from anti-PD-L1 therapy.

References

1. M. Rebelatto, J. Walker et al., Development of a programmed cell death ligand-1 immunohistochemical assay validated for analysis of non-small cell lung cancer and head and neck squamous cell carcinoma, Diagnostic Pathology (2016), 11:95, DOI 10.1186/s13000-016-0545-8

2. A. Kapil, N. Brieu et al., Deep Semi Supervised Generative Learning for Automated PD-L1 Tumor Cell Scoring on NSCLC Tissue Needle Biopsies, ArXiv (2018), https://arxiv.org/abs/1806.11036
3. S. Antonia, NA. Rizni et al., Safety and antitumour activity of durvalumab plus tremelimumab in non-small cell lung cancer: a multicentre, phase 1b study, Lancet Oncol (2016), 17(3):299-308, DOI 10.1016/S1470-2045(15)00544-6

Ethics Approval

This works relies on data from NCT01693562 and NCT02000947 clinical trials (clinicaltrials.gov)

Figure 1.

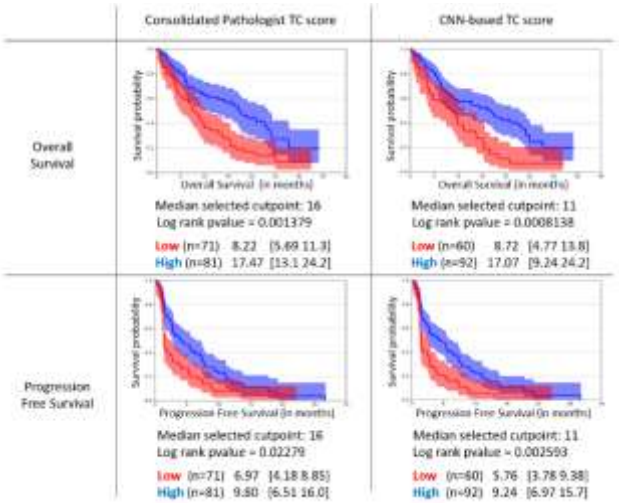

Table 1.

		Overall Survival (OS)			Progression Free Survival (PFS)		
		p value	hazard ratio exp(coef)	CI 95% [low up]	p value	hazard ratio exp(coef)	CI 95% [low up]
Standard 25% cutpoint	Consolidated Path. TC score	0.0033	0.530	[0.3472 0.8101]	0.057	0.708	[0.4963 1.01]
	CNN-based TC score	0.0024	0.519	[0.3395 0.7929]	0.0017	0.563	[0.393 0.8057]
Optimized cutpoint (LOOCV)	Consolidated Path. TC score	0.0017	0.514	[0.339 0.7782]	0.024	0.664	[0.4659 0.9469]
	CNN-based TC score	0.001	0.489	[0.3193 0.7495]	0.0029	0.571	[0.395 0.8259]

P22

Impact of tumor inherent interferons on immune reactivity and personalized therapy in triple negative breast cancer

Natasha Brockwell, BBiomed (Hons)[1], Jai Rautela[3], Tim Molloy, PhD[4], Sandra O'Toole, MD, PhD[5], Vinod Ganju, MBBS, FRACP[6], Belinda Parker[1]

[1]*La Trobe Institute for Molecular Science, Bundoora, Australia*
[2]*La Trobe Institute for Molecual Science, Bundoora, Australia*
[3]*Walter and Eliza Hall Institute, Melbourne, Australia*
[4]*St Vincents Centre for Medical Research, Sydney, Australia*
[5]*Garvan Institute for Medical Research, Sydney, Australia*
[6]*Hudson Institute for Medical Research, Frankston, Australia*

Background

Triple negative breast cancer (TNBC) is known for its ability to rapidly metastasize within the first two years and its association with tumor infiltrating lymphocytes (TILs). As immune infiltrate has been associated with a good prognosis and therapeutic response in TNBC, immunotherapy is now being trialed. However, responses have been underwhelming to date and difficult to predict, leading to an inability to accurately weigh up the benefit-to-risk ratio for their implementation. Previous work done in our laboratory demonstrated that type I IFN signalling can increase the heat of the tumor, induce a tumor specific T cell responses and sensitize mice to checkpoint inhibitors [1]. This suggested that characterization of a tumors heat is imperative in deciding which patients are most likely to benefit from immunotherapy and the type of immunotherapy they should receive.

Methods

Multiplex immunohistochemistry using the OPAL method was utilized to characterize tumor heat through assessment of T cell subsets and effector status and novel IFN biomarkers. A TNBC cohort (n = 21) where sequential biopsies were taken pre, mid

and post chemotherapy was used to assess the role of tumor heat in chemotherapeutic response and relapse. Two independent adjuvant TNBC cohorts (n = 398; n = 159) were used to validate findings. Murine TNBC cells were manipulated to have constitutive expression of the type I IFN pathway. Syngeneic mouse models were used to assess the role of inherent type I IFN signalling on chemotherapeutic response, survival and the immune landscape.

Results

We demonstrate the superior prognostic information that can be gathered from TIL characterization whereby T cell subsets and their effector function can be used to predict response to chemotherapy and relapse. Furthermore we identified a novel prognostic marker that indicates presence of an intact type I IFN signalling pathway. Patients with loss of this marker were up to eight times more likely to relapse with metastatic disease than those who retained the biomarker, this was prognostic in 3 independent TNBC cohorts. Overexpression of the type I IFN pathway in murine TNBC cells resulted in increased sensitivity to chemotherapy, decreased metastasis and promotion of a T cell inflamed tumor.

Conclusions

Our work suggests tumor inherent type I IFN signalling and TIL characterization predicts relapse. Immunotherapy aimed at increasing tumor heat may hold promise in those lacking immune activation or IFN signalling prior to chemotherapy or checkpoint inhibitors, supporting the notion of TME characterization pre-treatment to personalize therapy.

References

1. Brockwell N K, Owen K L, Zanker D, Spurling A, Rautela J, Duivenvoorden H M, Baschuk N, Caramia F, Loi S, Darcy P K, Lim E, and Parker B S, "Neoadjuvant Interferons: Critical for effective PD-1 based immunotherapy in TNBC," Cancer Immunol. Res., Aug. 2017; Vol 5:871-884.

Ethics Approval

This study was approved by the latrobe animal ethics committee, approval number AEC15-62. This study was approved by the human resources ethics committee of the Royal Prince Alfred Hospital, approval number X15-0388 [SSA/16/RPAH/397].

P23

Centrifuge-less immunostaining of suspension cells for flow cytometry analysis by DA-Cell™ washer and plate for superior data and workflow

Namyong Kim, PhD[1], Melvin Lye[1], Namyong Kim, PhD[1]

[1]*Curiox Biosystems*

Background

We describe the DA-Cell™ system, a novel wall-less plate and laminar-flow cell washer that enables the automated washing of suspension cells and retains more than 95% cells at a fraction of the time and with higher viability of cells.

Methods

The wall-less DropArray (DA) plate consists of an array of 96 hydrophilic spots separated and surrounded by a hydrophobic surface, which functions as a virtual wall. In a typical immunostaining assay, a 50 µl drop, containing cells and antibody mix, is dispensed on each spot of the DA plate. During incubation, cells settle on the surface of the spots. The plate then undergoes a laminar-flow washing process in DA-Cell washer by repeated cycles of aspiration and dispensing of buffer through two sets of nozzles. The controlled buffer flow minimizes turbulence and cell loss. The cell washing process only requires 3-4 minutes by eliminating the need of a centrifuge, which also reduces stress on the cells and possible cross-

contamination of antibodies on cell membranes, leading to better segregation of cell populations in flow cytometry. Additional incubation time of 10-20 minutes improves cell retention to more than 99%. Most importantly, cell incubation and washing on a DA-Cell system minimizes operator variability as mixing and washing steps are mechanically controlled and mostly automated, significantly improving reproducibility and consistency of flow cytometry analysis.

Results
We show a series of immunostaining assays comparing the DA-Cell system with a conventional centrifugation. Based on the staining index, absolute cell counts and additional data, we demonstrate that the DA-Cell system produces superior data while simplifying and expediting cell preparation for flow cytometry analysis.

Conclusions
The DA-Cell system produces superior data while simplifying and expediting cell preparation for flow cytometry analysis.

Acknowledgements
Singapore Immunology Network

P24

Centrifuge-less red blood cell lysis and immunostaining of whole blood for flow cytometry using DA-Cell washer and plate

Namyong Kim, PhD[1], Melvin Lye[1], Namyong Kim, PhD[1]

[1]*Curiox Biosystems, San Carlos, TX, USA*

Background
Blood cells are prime indicators of immuno-surveillance, and the ease of blood sampling makes blood analysis a key interest for clinical and research applications. While current flow cytometry methods are high-throughput and provide fine resolution in the segregation of white blood cell (WBC) populations, WBC enrichment involving red blood cell (RBC) lysis are laborious and typically performed manually, contributing to experimental variability especially as blood cells are sensitive to physical and chemical stress.

Methods
We describe RBC lysis and leukocyte immunostaining on a centrifuge-less platform DA-Cell™, using a novel wall-less plate and laminar flow washer. The DropArray (DA) plate consists of an array of 96 hydrophilic spots surrounded by hydrophobic surface, which functions as a virtual wall that separates each spot. The maximum volume of each spot can be increased to 300µL with an insert. During lysis, WBC settle to the surface of the spot, allowing the spent lysis buffer to be removed. After removal of the insert, the plate goes through a gentle 3-4min laminar-flow washing process in the DA-Cell washer, decreasing cell washing time by at least 50% while eliminating centrifugation that stresses cells and disrupts antibody binding.

Results
In studies comparing mouse whole blood lysis (1X RBC Lysis buffer, eBioscience) and antibody staining by conventional tube centrifuge and DA-Cell, DA-Cell achieved dramatically higher staining index and improved resolution of cell cluster by flow cytometry. CD45+ leukocyte recovery and viability was uncompromised compared to conventional tube centrifuge.

Conclusions
In summary, DA-Cell system provides gentle, fast and convenient blood lysis, while improving data quality with superior antibody staining.

P25

Consistent pharmacodynamics and immunological responses to the TLR9 agonist, SD-101, following intratumoral injection in multiple cancer types

Albert Candia, PhD[1], Cristiana Guiducci, PhD[1], Ezra Cohen, MD[2], Ronald Levy, MD[3], Mohammed Milhem, MBBS[4], Antoni Ribas, MD, PhD[5], Thomas Tuting, MD[6], Erick Gamelin, MD PhD[1], Robert Janssen, MD[1], Robert Coffman, PhD[1]

[1]*Dynavax Technologies, Berkeley, CA, USA*
[2]*Moores Cancer Center, La Jolla, CA, USA*
[3]*Stanford University Hospital and Clinics, Stanford, CA*
[4]*University of Iowa Health Care, Iowa City, IA, CA*
[5]*University of California at Los Angeles, Los Angeles, CA*
[6]*University Hospital Magdeburg, Magdeburg, Germany*

Background
SD-101 is a synthetic class C CpG oligonucleotide agonist of Toll-like receptor 9. SD-101 stimulates dendritic cells to release interferon-alpha and mature into antigen presenting cells that effectively activate T cell responses. SD-101 is administered intratumorally (IT) and has been evaluated in combination with radiation therapy for lymphoma, and is currently being evaluated with pembrolizumab for melanoma and HNSCC. Pharmacodynamic and biomarker assessments across these three different tumor types offer mechanistic insights into the anti-tumor activity observed in the clinic.

Methods
Peripheral blood collected before and 24 hours after dosing was analyzed with Nanostring or qPCR by a panel of IFN responsive genes as an indirect measure of target engagement. Biopsies from injected lesions were collected prior to treatment and at specific post-dose time points, and gene expression was analyzed by Nanostring to evaluate the immunophenotype of the tumor environment. Tumor responses were assessed using Cheson criteria for lymphoma and RECIST v1.1 for melanoma and HNSCC.

Results
Type 1 IFN production was demonstrated by the activation of IFN responsive genes in peripheral blood. The range of induction on an individual basis (2 to 29 fold) and maximal induction on an averaged cohort basis (approximately 10-fold) were comparable across tumor types indicating similar mechanism of dendritic cell activation. Analysis of gene expression in tumor biopsies before and after treatment across the three tumor types shows a consistent increase in immune functions and cell types expected to contribute to anti-tumor activity. These changes are also consistent with the known mechanisms of action for SD-101 and include increases in CD8+, Th1, and NK cells. Responding patients (PR/CR) had average increases of at least 2-fold and as high as 9-fold in these cell types and functions. These increases in immune functions occurred in patients with or without prior checkpoint inhibitor therapy, and in the largest data set from melanoma patients, the changes in these cell types and functions correlated significantly with reductions in size of target lesions.

Conclusions
Biomarker assessments across three different tumor types following IT administration of SD-101 demonstrate consistent pharmacodynamic and biomarker activities consistent with its mechanism of action. The results suggest that activation of the innate immune system may be a core component of combination therapies in orchestrating an anti-tumor immune response in a wide range of cancer types.

Ethics Approval
The studies described were approved at the

Institutional Review Boards of the respective clinical sites.

P26

High-dimensional flow cytometry of circulating immune cells predicts clinical responses to combination Immune Checkpoint Blockade (ICB) and Radiotherapy (RT) in Gastroesophageal Cancer (GEC)

Joseph Chao, MD[1], Wanqiu Hou[1], Yi-Jen Chen, MD, PhD[1], Helen Chen[1], Michael Tajon[1], Marwan Fakih, MD[1], Peter P. Lee, MD[1]

[1]City of Hope Comprehensive Cancer Center, Duarte, CA, USA

Background
While ICB has been promising, the majority of GEC patients do not respond to single agent anti-PD-1 therapy. Combination strategies are being explored to augment immune responses including combining ICB with RT. We are currently conducting a prospective trial testing palliative RT with pembrolizumab in patients with metastatic GEC. To study immune correlates of ICB, we employed high-dimensional flow cytometry single cell analyses to characterize blood immune profiling as predictive biomarkers of clinical response.

Methods
In this single institutional trial, patients received standard palliative RT 30 Gy over 10 fractions to a single site of disease. Pembrolizumab 200 mg was given concurrently with RT with first dose concordant with the first fraction. Cycles repeated every 3 weeks for up to 35 cycles in the absence of disease progression or unacceptable toxicity. Peripheral blood was collected at baseline prior to first fraction of RT (C1D1 pembrolizumab) and ~21 days after completion of RT (~C2D15 pembrolizumab). Blood comprehensive immune profiling was interrogated using three 15-color flow cytometry panels. Abscopal responses were assessed using RECIST1.1 of lesions out of the field of RT.

Results
In this current analysis, 5 patients were included. RECIST responses included 2 confirmed partial responses (PRs), and 3 patients with progressive disease. The 2 PRs have been durable lasting >12 months and ongoing at data cut-off. On C2D15, most patients demonstrated a decrease in CD56hi NK cells (p=0.04), CD1c+ dendritic cells (p=0.02), plasmacytoid dendritic cells (p=0.01), CD33hi myeloid-derived suppressor cells (p=0.02), and PD-1+KLRG1+ exhausted CD8 T cells (p=0.005). Comprehensive immune profiling demonstrated a strong correlation of RECIST responses with low levels of circulating follicular helper T cells (r=0.99, p=0.001), and PD-1+BTLA+ exhausted CD4 T cells (r=0.91, p=0.03) at baseline C1D1. Analysis of immune changes over time also demonstrated a strong correlation of RECIST responses with an increase in circulating T cells (r=0.94, p=0.02) and nonclassical monocytes (r=0.92, p=0.03) as well as a decrease in Th2 cells (r=0.89, p=0.04) at C2D15 vs. C1D1.

Conclusions
Palliative RT plus pembrolizumab demonstrated encouraging activity in our dataset. Durable RECIST responses correlated with changes at C2D15 in circulating innate immune (T cells and nonclassical monocytes) as well as adaptive immune signatures (follicular helper T cells, Th2, and exhausted CD4 T cells). The ability to identify blood biomarkers early in ICB therapy that may predict durable clinical benefit is of significant clinical utility in GEC and warrants study in larger prospective cohorts.

Acknowledgements
Joseph Chao and Wanqiu Hou contributed equally to this work.

Trial Registration
NCT02830594

Ethics Approval
The study was approved by the Institutional Review Board of the City of Hope, approval number 16099.

P27

Tumor mutational burden assessment on FFPE samples using a targeted next-generation sequencing assay

Ruchi Chaudhary, PhD[1], Dinesh Cyanam, PhD[2], Vinay Mittal[2], Charles Scafe[2], Warren Tom, PhD[2], Janice Au-Young[2], Seth Sadis[2], Fiona Hyland[2]

[1]Thermofisher Scientific, South San Francisco, CA
[2]Thermo Fisher Scientific, South San Francisco, CA

Background
Recently, high Tumor Mutational Burden (TMB) was associated with significantly longer progression-free survival from immune checkpoint blockade combination therapy in NSCLC. Although TMB was originally determined by whole exome sequencing (WES) of matched tumor-normal samples, the high input requirement, complex bioinformatics, and long turn-around time makes this approach impractical for routine testing. Herein, we develop a targeted amplicon-based panel for computing TMB and detecting important variants from FFPE research samples.

Methods
A targeted panel was designed that included 409 key cancer genes covering 1.7 Mb of genomic region. Utilizing Ion AmpliSeq multiplex PCR chemistry, the workflow required only 20 ng of input DNA. The assay enabled a 2.5-day turn-around time from sample to report. The workflow enabled < 60 min of hands-on time for automated library preparation and templating on a batch of 4 samples. Sequencing was performed on Ion GeneStudio S5 System at sufficient coverage depth (~1200x) to support accurate variant detection with an analysis pipeline containing optimized variant calling parameters. A tumor only informatics workflow was developed that removed germline variants present in population databases. Two cell line samples and nine FFPE samples were analyzed by the tumor only workflow. Matched tumor-normal samples were analyzed by WES and the tumor samples were independently analyzed using the targeted TMB panel.

Results
An in-silico analysis using 10,000 exomes from the TCGA MC3 project demonstrated the panel could support high sensitivity (≥85%) and PPV (≥90%) necessary to stratify high and low mutation burden samples. TMB estimates on a normal diploid cell line (NA12878) was < 1 TMB for all 8 replicates. In a cancer cell line (HCC1143; expected TMB 8.33 mutations/Mb), the average TMB for 4 replicates was 6.11 (SD 0.43). TMB estimates obtained with the tumor only workflow using the targeted panel had high concordance (r2 = 0.87) with the TMB values obtained from the matched tumor/normal analysis using WES. For two samples with highest TMB by both assays, the assay detected loss of function mutations in MSH2 and TP53 genes. The informatics pipeline identified mutation signatures consistent with specific mechanisms such as UV and tobacco damage, and detected samples impacted by FFPE processing.

Conclusions
A simple workflow has been developed on the Ion Torrent sequencing platform to estimate TMB from FFPE and fresh frozen tumor research samples. This solution will advance research in immuno-oncology.

P28

Detection and validation of cancer immunotherapy biomarkers in blood and urine-based liquid biopsy

Simo Zhang[2], Shidong Jia[2], Amy Wang[2], Chen Xie[2]

[1]*Predicine, Inc., Hayward, CA, USA*
[2]*Predicine, Hayward, CA, USA*

Background
Immunotherapy response varies widely, making it difficult for physicians to know whether immunotherapy will be effective for a given patient. Indeed, ~80% or more patients with cancer fail to respond to checkpoint inhibitor immunotherapy. In addition to PD-L1IHC staining, recent studies reported that patients with deleterious mutations in mismatch repair (MMR) genes, high tumor mutation burden (TMB) or microsatellite instability (MSI) are also associated with better clinical response. As tissue biopsy represents a practical challenge due to its insufficient quantity or lack of access, noninvasive molecular has emerged as an efficient complementary test and attracted increasing attention in clinical development of cancerimmunotherapy. With Predicine's gene RARDAR technology, we developed a blood-based PredicinePLUS NGS panel to capture genomic alterations in 180 cancer genes including tumor mutation burden (TMB) and microsatellite instability (MSI). Technical validation was performed to evaluate assay sensitivity, specificity and accuracy using reference samples with known genetic profiling. The panel has been further tested using tissue biopsy and plasma samples from cancer patients. The development of PredicinePLUS panel offer a comprehensive solution to stratify and monitor cancer patients who may benefit from cancer immunotherapy

Methods
Nucleic acids were extracted from plasma samples and tested for DNA based SNV, CNV and gene rearrangement by proprietary pipeline.

Results
Mutation detection at DNA level can go down to 0.1% AF. At 0.25% expected AF, 94.4% SNVs were detected; at 0.1% expected AF, 78.6% SNVs were detected.High linearity was observed from detected and expected copy number from spiked-in cell lines; clinical validation of HER2 amplification in breast cancerHigh correlation between panel-TMB and TMB from WES on 14 cell lines. Consistency of panel-TMB at AF =0.5% or above in a series of dilution of reference materialsHigh correlation of panel-TMB with WES in a public study (Rizvi et al. Science 2015). D. high panel-TMB showed favorable PD-1 response in the public study.

Conclusions
A non-invasive PredicinePLUS NGS test was developed to support cancer immunotherapy clinical studies. A cfRNA-based PD-L1 mRNA assay was developed to monitor PD-L1 mRNA gene expression in circulation.

P29

Ensemble computational intelligence reveals novel molecular signatures of cancer biology and pan-cancer survival

Richard Williams[1], Thomas Chittenden[1], Nicholas Cilfone, x[1], Jeffrey Gulcher[1]

[1]*Wuxi NextCODE, Cambridge, MA, USA*

Background
Next-generation sequencing has significantly advanced our understanding of cancer biology by providing a unique genomic perspective of the molecular states of human disease. However, combining multiple 'omics' measurements into biologically-relevant statistical computing

frameworks to define causal molecular underpinnings of disease remains a significant challenge.

Methods
To address these issues, we developed novel feature learning approaches that enhance quantitative assessment of annotated tissues from The Cancer Genome Atlas. Our a priori biological-knowledge and data-driven network-based approaches improve performance and interpretability of both deep learning and probabilistic programming strategies.

Results
Herein, we demonstrate the utility of collapsing molecular signals, from five different -omics platforms, into integrated metagenes that are highly informative across roughly 8,200 tumors, encompassing 22 cancer types. We identified multiple immune related genes and pathways comparing cancer sub-types (e.g. CCR1, IFNA4, CD34, IL25 – kidney renal clear cell carcinoma vs. kidney renal papillary cell carcinoma), between 22 diverse cancer types (e.g. IL-20 and tumor necrosis factor production nested in negative regulation of cellular metabolic process), and associated with overall patient survival (e.g. FCGR2A, IFNE, TGFB1, IL23A, CD80 and type I interferon signaling pathway nested in cell proliferation).

Conclusions
Our results demonstrate the potential of deep learning methodologies to help revolutionize the analysis and interpretation of multi-omics data, how to identify more complex disease etiology than previous methods, and how to hypothesize putative 'network driver genes' of disease state and progression. Taken together, these aspects allow researchers to generate better novel hypotheses of therapeutic targets or diagnostic biomarkers

P30

Tracking the cancer immune response using neural network deep learning of serial inflammatory marker data for forecasting timing of therapy

Brendon Coventry, MD PhD[1], Mohsen Dorraki, MSc, BS[1], Anahita Fouladzadeh, BSc[1], Andrew Alison[1], Derek Abbott, PhD[1]

[1]*University of Adelaide, Adelaide, SA, Australia*

Background
The immune response in advanced cancer patients is not static but fluctuates under homeostatic control around a mean level of inflammation indicative of the anti-cancer response occurring in the patient. Immunotherapy given during immune activation (as opposed to immune inhibition) might be expected to better induce stronger anti-cancer responses, therefore timing is likely to be important. In multiple studies, the key inflammatory marker C-reactive Protein (CRP) has been widely associated with cancer survival; predicting cancer risk; a bio-maker for tumour recurrence; as a marker in oncology for prognosis; and as a reliable tool for making critical treatment decisions for several cancer types. Since CRP is biomarker of immune system activity, and CRP concentrations exhibit low values in healthy subjects, the ability to forecast CRP trends might potentially guide clinical decisions in cancer therapies based on the inflammatory state existing in the patient at the precise time of treatment.

Methods
We investigated time-series analyses of our previous data sets from advanced melanoma and other ovarian cancer patient data using (i) Periodogram analysis and (ii) Recurrent Neural Networks (RNNs) using Long Short-Term Memory (LSTM)-based, approaches to predict the future state in a C-reactive protein (CRP) time-series in cancer patients. Deep learning provided CRP time-series forecasting.

Results

Using Periodogram methods, the time-series used in [1,2] did not contain enough data points in the measured time period to conclude whether the CRP data was periodic or not, particularly for the previously hypothesised period of seven days. Moreover, the study [3] provided a prescription for the minimum data sampling rate required for improved testing of a periodic CRP (or other biomarker) signal hypothesis. We abandoned this method in favour of investigating RNN approaches. The distribution of CRP was highly skewed, so a log(.) representation that is more symmetric and less skewed is recommended for CRP estimation. We challenged our data interpretation [1] and other data [4] for periodicity in either serial daily CRP measurements in melanoma patients, or in gynaecological cancer patients [2] with less frequent measurements.

Conclusions

Deep learning and other of machine learning-based approaches for biomedical signal analysis can be used to predict trends in C-reactive protein time-series, with greater accuracy than periodogram approaches. Deep LSTM RNN with 200 layers achieves the lowest prediction error. These approaches offer useful avenues for bio-marker monitoring. Forecasting CRP trends can provide potentially valuable information for guiding clinical decision-making for more accurately timing of therapies, including immunotherapies.

Acknowledgements

Australian Melanoma Research Foundation & Cancer Council SA/ SA Government/ SAHMRI for supporting the Trial Data collection and CRP monitoring,

References

1. Coventry BJ, Ashdown ML. Quinn MA, Markovic SN, Yatomi-Clarke SL, Robinson AP. CRP identifies homeostatic immune oscillations in cancer patients: a potential treatment targeting tool? J Transl Med. 2002; vol. 7, no. 102.
2. Madondo MT, Tuyaerts S, Turnbull B, Vanderstraeten A, Kohrt H, Narasimhan B, Amant F, Quinn M, and Plebanski M. Variability in CRP, regulatory T cells and effector T cells over time in gynaecological cancer patients: a study of potential oscillatory behaviour and correlation. Journal of Translational Medicine. 2014; 12:179.
3. Dorraki M, Fouladzadeh A, Salamon SJ, Allison A, Coventry BJ, and Abbott D. On detection of periodicity in C-reactive protein (CRP) levels, Sci. Rep., in press.
4. Leontovich AA, Dronca RS, Suman VJ, Ashdown ML, Nevala WK, Thompson MA, Robinson A, Kottschade LA, Kaur JS, McWilliams RR, Ivanov LV, Croghan GA, Markovic SN. Fluctuation of systemic immunity in melanoma and implications for timing of therapy. Front Biosci (Elite Ed). 2012 Jan 1;4:958-75.

P31

Prevalence of high microsatellite instability in cancer patients in the real world

Razvan Cristescu, PhD[1], Kai-Li Liaw, PhD[1], Scott Pruitt, MD, PhD[1], Mark Ayers, PhD[1], Jianda Yuan, MD, PhD[1], Thao Vo, MD[1], Senaka Peter[1], Andrew Joe, MD PhD[1], Darcy Hille[1], Sun Young Rha[2], Torben Steiniche[3], Andrey Loboda, PhD[1]

[1]Merck & Co., Inc., Kenilworth, NJ, USA
2Yonsei Cancer Center, Seoul, Korea, Republic of
[3]Aarhus University Hospital, Aarhus, Denmark

Background

High microsatellite instability (MSI-H) cancers are vulnerable to immunotherapies targeting the PD-1/PD-L1 pathway. PD-1–blocking mAb pembrolizumab was recently approved by the FDA for the treatment of MSI-H cancer, regardless of tumor histology or location. This analysis evaluated MSI-H prevalence by cancer type and stage using

several real-world observational studies to examine the potential patient populations that might benefit from treatment.

Methods
Four data sources, including 1 database and 3 retrospective observational molecular epidemiology studies, were evaluated. Microarray analysis of loss of MLH1 gene expression was used as a surrogate for MSI-H status (<2.35 on log10 scale in quantile-normalized data) to assess prevalence of MSI-H in the Moffitt Cancer Center database of ~16,000 archived tumors. Results were compared with those of 3 epidemiologic studies that evaluated MSI-H status using a PCR-based assay on archival tissue of gastric, ovarian, endometrial, cervical, and 8 rare cancers, most (72%-100%) from patients with stage III-IV disease.

Results
In the Moffitt database, for the following cancers, MSI-H prevalence by MLH1 expression loss was: endometrial (138/664, 20.8%), sarcoma (4/38, 10.5%), gastric (4/41, 9.8%), colorectal (194/2251, 8.6%), esophageal (2/49, 4.1%), kidney (2/60, 3.3%), cervical (2/72, 2.8%), melanoma (1/41, 2.4%), prostate (1/88, 1.1%), lung (22/2064, 1.1%.), ovarian (5/523, 1.0%). MSI-H prevalence was generally higher in stage I-II than in stage III-IV. In epidemiologic studies of advanced disease, MSI-H prevalence by PCR was assessed in Korean patients with gastric cancer (0/103, 0%) and in patients with ovarian (1/40, 2.5%), endometrial (7/49, 14.3%), cervical (1/44, 2.3%), and rare cancers (0/305, 0%) in Denmark.

Conclusions
Using MLH1 expression loss as a surrogate, a large database with comprehensive molecular data of cancer patients provided MSI-H prevalence estimates in many cancer types not usually tested for MSI-H. The results were generally comparable with those of epidemiologic studies that used PCR-based MSI testing. These real-world data found MSI-H tumors in multiple cancers and may help to identify patients who can potentially benefit from treatment with pembrolizumab.

Ethics Approval
The abstract is based upon 1 database and 3 retrospective observational molecular epidemiology studies; no ethics approval was required.

P32

Monitoring of M-MDSC vs. G-MDSC in clinical studies – which is more important? (monocytic versus granulocytic myeloid derived suppressor cells)

Henry Hepburne-Scott, PhD[1], Phoebe Bonner-Ferraby[1]

[1]*Serametrix, Carlsbad, CA, USA*

Background
It is now almost universal good practice to monitor MDSC during clinical trials for novel checkpoint inhibitors and combination therapies. This is because MDSC protect tumors from anti-PD-1 and other such drugs by infiltrating tumors and providing localized immunosuppression. MDSC monitoring is also increasingly important in combination studies to help assess the efficacy of putative anti-MDSC agents, such as HDAC inhibitors.However, MDSC is an elusive biomarker, a “catch-all” category of immature immune cells and immunologists rarely agree on a definitive phenotype. Even having navigated the minefield of markers there is still the question of whether monocytic or granulocytic MDSC are dominant in protecting tumors from checkpoint-mediated de-repression of cytotoxic T cells. Whilst a biomarker assay for M-MDSC is already well established and widely used, a reliable assay for G-MDSC has proved more challenging. Here we report the development and application of a novel assay for

G-MDSC for use in I-O clinical studies.

Methods
A flow cytometry panel consisting of Lineage Cocktail, CD14, CD33, CD15 and HLA-DR was developed, validated and used to identify G-MDSC in peripheral whole blood samples drawn from cancer patients. To ensure operator independent gating of the continuous HLA-DR marker a computational algorithm was used to determine sample-specific thresholds for gating. Data for G-MDSC were compared with same-sample data for M-MDSC.

Results
The assay was successful in identifying G-MDSC in peripheral Whole Blood samples collected in 5mL Cyto-Chex BCT tubes. A single blood draw yielded sufficient material to measure both M-MDSC and G-MDSC from the same sample. However, during assay validation the stability of the G-MDSC was found to be significantly less than the stability of M-MDSC (logistical implications of this will be discussed). There was poor correlation between the two cell types: samples that were rich in M-MDSC did not always have high levels of G-MDSC and vice versa.

Conclusions
Whilst MDSC monitoring is a valuable part of some immune-oncology clinical development it may not be sufficient to rely on measuring the monocytic phenotype alone for all studies. The poor correlation between M-MDSC and G-MDSC observed in this study suggests that both types should be included if a biomarker program is to be truly effective. The use of a combo-MDSC assay will enable a fuller understanding of the mechanisms of resistance to checkpoint blockade.

P33

DNA damage detected by localized γH2AX is associated with elevated TILs and PD-L1 expression in human colorectal carcinomas

Shruti Desai, PhD[1], Parker Sulkowski[1], Aravind Kalathil[1], Ranjini Sundaram[1], Ila Datar, PHD[1], Charles Fuchs, MD, MPH[1], Patricia LoRusso, DO[1], Ranjit Bindra[1], Kurt A. Schalper, MD, PhD[1]

[1]*Yale University School of Medicine, New Haven, CT, USA*

Background
Cancer cells accumulate genomic aberrations due to the frequent combination of increased DNA damage and decreased DNA repair capacity. H2AX is a histone component of nucleosomes and its phosphorylation on Serine139 (γH2AX) is the first step in recruiting repair proteins upon DNA damage. DNA alterations can produce mutant neoantigens that are recognized as non-self and presented by the HLA system to trigger anti-tumor immune responses and mediate sensitivity to immune checkpoint blockers. To date, evidence for the association between active DNA damage in cancer cells and adaptive anti-tumor immune responses in intact tumors specimens remains elusive.

Methods
Using γirradiated cell line preparations and expression controls, we standardized a multiplexed quantitative immunofluorescence (mQIF) panel for simultaneous and localized measurement of DAPI (all cells), cytokeratin for tumor epithelial cells (AE1/AE3, DAKO), γH2AX to map active DNA damage (JBW301, Millipore), CD3 for T-lymphocytes (Rabbit polyclonal, DAKO) and PD-L1 (E1L3N, CST) in formalin-fixed paraffin-embedded (FFPE) tissue samples. We then used the assay to study 265 stage I-IV colorectal carcinomas (CRCs) from Yale represented in tissue microarray format. We analyzed the level of the targets, their association and correlation with major clinicopathologic variables and survival.

Results
The levels of γH2AX (but not total H2AX) were

significantly higher in FFPE preparations of γirradiated HEK293 cells than in control/untreated cells or in morphologically normal human tissues. The radiation-induced γH2AX increase was abrogated in HAP1 cells with targeted deletion of the H2AX gene. Detectable γH2AX protein was found in 170 (64%) of CRCs with nuclear staining pattern and predominant expression in cytokeratin-positive tumor cells. Elevated tumor γH2AX was significantly associated with increased CD3+ tumor infiltrating lymphocytes (TILs) and PD-L1 protein expression ($P<0.05$). Elevated CD3, PD-L1 and γH2AX were associated with lower tumor stage and better overall survival in the cohort. No significant association was seen between the markers and age, gender or smoking status.

Conclusions

Tumor DNA damage as measured by nuclear γH2AX protein expression occurs in 64% of CRCs and is associated with increased anti-tumor immune responses and better prognosis. TILs and PD-L1 are prognostic in CRC. Our results support targeting DNA repair deficiency pathways in combination with immune stimulatory agents as therapeutic strategy in a proportion of CRCs.

Acknowledgements

Research supported by a Stand Up to Cancer Colorectal Cancer Dream Team Translational Research Grant (Grant Number SU2C-AACR-DT22-17)

P34

Clinical application of urinary cell free DNA as a marker for cancer

Jeffrey Ding[1], Debin Sun[1]

[1]*Admera Medical Technology Corp., Suzhou, China*

Background

The role of circulating cell free DNA holds great promise for individualized medicine for cancer. As it carries information on DNA from cells exfoliated in urine and from circulation, urinary cell free DNA (UcfDNA) is believed to have the potential of being a useful and ultra-noninvasive tool for cancer screening, diagnosis, prognosis, and monitoring of cancer progression and therapeutic effect [1]. However, compared with the widely studied cell-free DNA in blood, less is known about the role of UcfDNA. The presence of UcfDNA signals from tumor has remained controversial, possibly due to the lack of appropriate method and technology to robustly extract and detect the potentially highly degraded UcfDNA.

Methods

We developed and optimized UcfDNA extraction method from urine samples, and compared UcfDNA quantity and quality regarding the urine sampling time and the storage condition. As a proof of concept, we processed urine samples from pregnant women during their second trimester and used real-time quantitative PCR (qPCR) assays to successfully detect UcfDNA from fetal in maternal urine. We subsequently collected urine samples from lung cancer patients and applied the developed methods to extract UcfDNA. The qPCR assay with the blocker-based enrichment method was developed and used for EGFR mutation detection in UcfDNA (Image 1,2). We also explored the possible application of UcfDNA for the microsatellite instability(MSI) testing.

Results

We successfully detected EGFR mutations in UcfDNA which also found in the corresponding tumor tissue samples, demonstrating the UcfDNA extraction and genotyping was possible from urine samples of cancer patients (Image 3).

Conclusions

We have confirmed the existence of UcfDNA from tumor, and have shown that UcfDNA could be used for noninvasive cancer genetic test and cancer research.

References
1. Lu T, Li J. Clinical applications of urinary cell-free DNA in cancer: current insights and promising future. Am J Cancer Res. 2017 Nov 1;7(11):2318-2332.

Image 1.

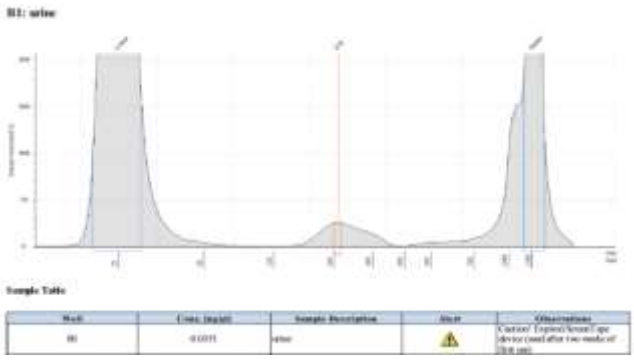

Image 2.

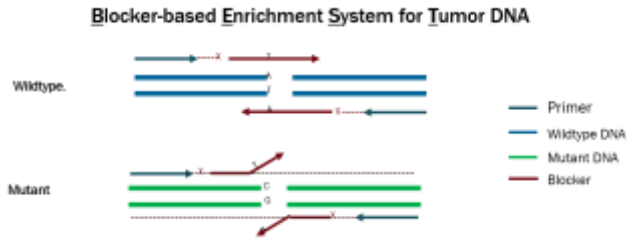

Image 3.

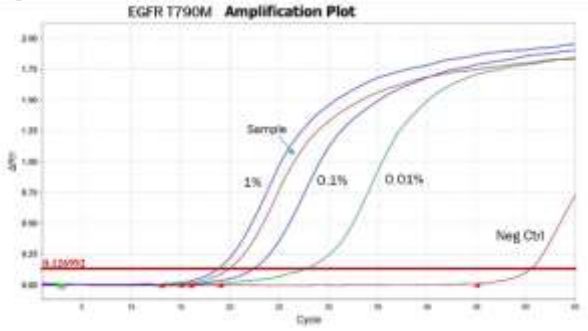

P35

Development of biomarkers to assess adenosine generation & activity in support of clinical trials conducted with the adenosine receptor antagonist AB928

Daniel DiRenzo, PhD[1], Joanne Tan, PhD[1], Devika Ashok, PhD[1], Amy Anderson, PhD[1], Jenna Jeffrey, PhD[1], Lisa Seitz, MSc[1], Manmohan Leleti, PhD[1], Steve Young, PhD[1], Jay Powers, PhD[1], Matthew J. Walters, PhD[1]

[1]*Arcus Biosciences, Hayward, CA, USA*

Background

The high levels of adenosine (ADO) found in the tumor microenvironment have been shown to inhibit immune responses through activation of the A2aR and A2bR receptors on immune cells. The extracellular enzymes ecto-5'-nucleotidase (CD73) and tissue non-specific alkaline phosphatase (TNAP) catalyze the extracellular conversion of adenosine monophosphate (AMP) into ADO. We have previously shown that AB928, a dual A2aR/ A2bR antagonist, blocks the immunosuppressive effects of ADO in human cell culture systems and in mouse syngeneic tumor models. Herein, we describe the development of assays to measure the expression and activity of adenosine-generating enzymes in human tumor samples and peripheral blood. These assays are being implemented in ongoing clinical trials with AB928, to identify tumor types and patients most sensitive to adenosine receptor antagonism.

Methods

Gene expression data were extracted from The Cancer Genome Atlas (TCGA). To correlate protein and gene expression levels, immunohistochemistry (IHC) and NanoString analyses were performed on serial sections of formalin fixed paraffin embedded (FFPE) tumor tissue. Circulating levels of CD73 were quantified with an in-house developed CD73 ELISA and total AMP-ase enzymatic activity in plasma was determined using an AMP-Glo assay.

Results
TCGA gene expression analysis identified non-small cell lung, renal clear cell, triple-negative breast, ovarian, colorectal, and gastro-esophageal cancers as tumors that express high levels of adenosine processing enzymes. Specifically, combined CD73 and TNAP levels were highest in lung adenocarcinoma (CD73 = 4.024; TNAP = 4.753) whereas colorectal (CD73 = 4.101; TNAP = 0.7493) and ovarian (CD73 = 2.173; TNAP = 5.288) cancers were heavily biased towards CD73 or TNAP, respectively. IHC on human FFPE tumor microarrays demonstrated that NSCLC had the highest CD73 protein levels with a stark contrast between adenocarcinoma (70.5 +/- 17.3 µM2) and squamous cell carcinoma (7.3 +/- 1.9 µM2). In contrast, prostate cancer had low CD73 gene expression (median TPM = 1.82) and protein levels (0.99 +/- 0.07 µM2). Overall, there was strong agreement between TCGA data and IHC (R2 = 0.793) suggesting that transcript levels of CD73 broadly predict local protein levels. In addition, we are in the process of determining the relationship between tumoral CD73 levels and, using different methodologies, peripheral CD73 protein levels and enzymatic activity.

Conclusions
Collectively, these assays provide a detailed picture of the capacity of individual human tumors to generate adenosine and should enable the correlation of this information with peripheral activity/levels of adenosine-generating enzymes and potentially the clinical benefit of AB928.

P36

Defining the expression of Programmed Death-Ligand 2 in high grade glioma tumor microenvironment

Gifty Dominah[1], Victoria Sanchez, BS[1], John Lynes, MD[1], Nicholas Adamstein[2], Arnold Obungu, BS, BA[3], Xiang Wang, MS[1], Nancy Edwards, BA[1], Edjah K. Nduom, MD[1]

[1]NINDS/NIH, Bethesda, MD, USA
[2]Columbia University College of P&S, New York, NY, USA
[3]Indiana University School of Medicine, Indianapolis, IN, USA

Background
Checkpoint blockade with anti-programmed death-1 (PD-1) therapy has been demonstrated as a promising treatment for many systemic cancers. Tumor programmed death-ligand 1 (PD-L1) expression has been shown to increase the response to anti-PD-1 immunotherapy in many tumor types. We have recently validated PD-L1 expression as a negative prognostic factor in high grade gliomas (HGG). However, PD-1 has two ligands, PD-L1 and PD-L2, and PD-L2 expression has not been characterized in HGG tissue. Accordingly, the potential prognostic and/or predictive value of PD-L2 has not yet been assessed. This study aims to establish reliable means to detect PD-L2 expression in HGG patient samples, validate this expression and define its clinical relevance.

Methods
The PD-L2 antibody clone 24F.10C12 was optimized for staining by immunofluorescence (IF) in PD-L2-plasmid transfected HEK293 cells. Further antibody validation was performed via immunohistochemistry (IHC), IF staining, and RNAscope in situ hybridization (ISH) using normal brain slides and human heart tissue as a positive control. After antibody validation, immunohistochemistry and RNAScope ISH was used to evaluate PD-L2 protein and mRNA expression in paraffin-embedded HGG slides.

Results
PD-L2 expression using clone 24F.10C12 was found in transfected HEK293 cells, but not in untransfected cells. By IHC, IF, and ISH, PD-L2 was expressed adjacent to blood vessels in normal brain and HGG

slides. There was heterogeneity between HGG patient tumor samples as some tissues also had perinuclear expression of PD-L2. Moreover, HGG tissues that expressed low grades of PD-L1 showed high PD-L2 expression grades per IHC suggesting an inverse relationship between the two.

Conclusions

PD-L2 expression in HGG has a distinct cellular pattern and distribution, separate from the expression of PD-L1. PD-L2 expression should be further characterized in these tissues to determine the potential prognostic or predictive value of this marker for immune therapy of HGG patients.

References

1. Pratt D, Dominah G, Lobel G, Obungu A, Lynes J, Sanchez V, ... Maric D. Programmed death ligand 1 ss a negative prognostic marker in recurrent isocitrate dehydrogenase-wildtype glioblastoma. neurosurgery. 2018.

P37

Multiplexed biomarker quantification to assay and characterize T-cell activation

Shilan Dong, MS[1], Jason Cahoon, BS[1], Rachit Ohri, PhD[1]

[1]*Enable Life Sciences LLC, Worcester, MA, USA*

Background

Multiplexed biomarker based characterization has proven effective for disease diagnosis and therapeutics development [1]. We adapted a similar multiplexed biomarker strategy for characterizing T-cell activation, with the goal of developing a standardized cell-culture assay for immuno-oncology applications. The panel of chosen biomarkers expressed by T-cells included: [a] IL-2, important for downstream immune activation [b] TNFα, important in acute phase immune cell activation, differentiation and migration [c] IL-10, with the role of tumor-specific immune surveillance and mitigating pathologic inflammation, and [d] IFNγ, with the role of tumor-protection through immune cell activation including dendritic cells.

Methods

Activation of T-cells was induced by ionomycin and PMA (phorbol 12-myristate 13-acetate) [2] (Sigma-Aldrich, St. Louis). Jurkat cells [UMass, Worcester at 1X106 cells/ml] and primary CD3-positive pan T cells [iXCells Biotechnologies, San Diego at 8X105 cells/ml] were cultured in 24 well plates in RPMI 1640 media (10% FBS and 1% Penn-Strep). 24 h protein-level expression (in the cell supernatant) of IL-2, IFNγ, TNFα, and IL-10 was quantified in response to a wide concentration range for both activators (250 - 2000 ng/ml for ionomycin and 10 - 100 ng/ml for PMA). For the specific combination of 2000 ng/ml ionomycin and 50 ng/ml PMA, time-course expression levels were also determined over a 0h - 56h period. Biomarker quantification was pursued using Luminex methodology.

Results

Our multiplexed biomarker data indicates significant overall consistency of expression trends comparing one biomarker to another, though minor differences does occur (eg. the optimal time point for activation), even though comparative concentration levels varied. Additionally, consistency was also observed between the activation profiles of primary CD3+ pan T-cells and the Jurkat T-cell line for [a] the most synergistic combination of ionomycin and PMA for T-cell activation [i.e. 2000 ng/ml ionomycin and 50 ng/ml PMA] (IL-2 expression levels statistically higher i.e. $p<0.05$ or equal compared to any other combinations of PMA and ionomycin) (Figures 1A, 1B), as well as [b] the time-course of T-cell activation [i.e. biomarker plateauing or high expression most commonly in the 8h - 48h window] (Figures 2A-D). Despite overall consistency, nuanced differences

were observed between primary T-cells and Jurkat cells (e.g. timing of the peaking or plateauing of individual biomarker expression), which may further vary between different sources of primary T-cells (to be evaluated).

Conclusions

In conclusion, our results provide the basis of a robust, standardized, sensitive and efficient assay for pan T-cell activation.

Acknowledgements

The authors acknowledge and thank MBI (Massachusetts Biomedical Initiatives), WPI (Worcester Polytechnic Institute), and University of Massachusetts Medical School for the use of their facilities.

References

1. Wagner JA. Strategic approach to fit-for-purpose biomarkers in drug development. Annu. Rev. Pharmacol. Toxicol. 2008; 48:631-651. 2. Manger B, Weiss A, Weyand C, Goronzy J, Stobo JD. T cell activation: differences in the signals required for IL 2 production by nonactivated and activated T cells. The Journal of Immunology. 1985; 135(6):3669-3673.

Figure 1A.

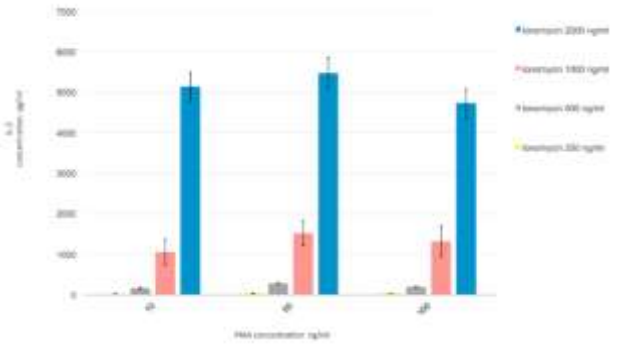

Figure 1B.

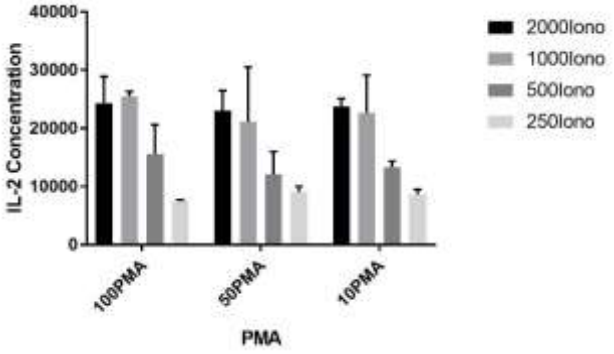

Figure 2A.

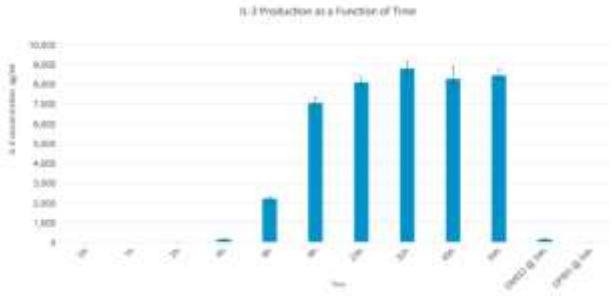

Figure 2B.

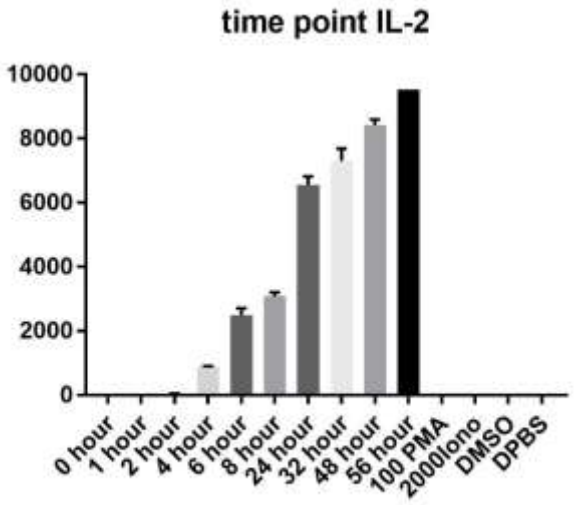

Figure 2C.

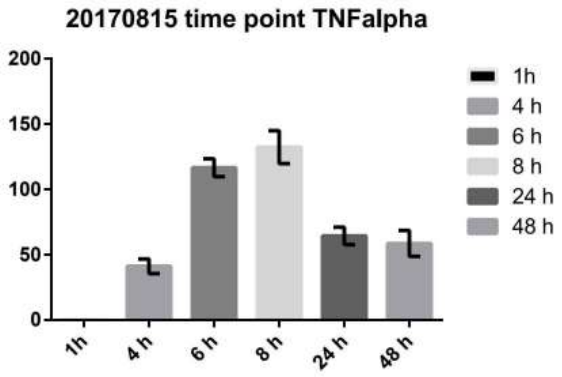

Figure 2D.

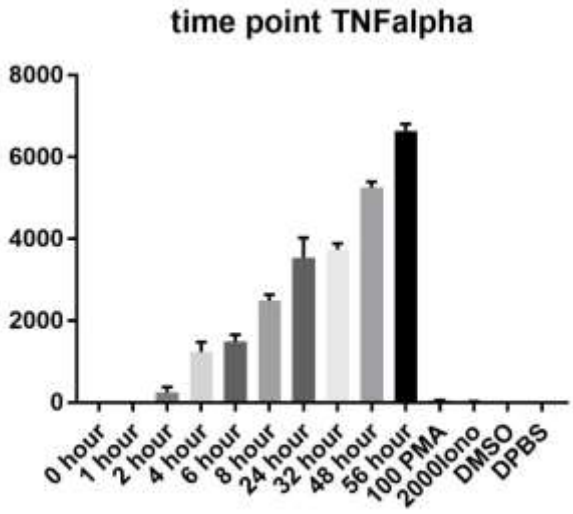

P38

Highly multiplex spatial immuno-profiling in FFPE tumor tissue with InSituPlex technology

Abdul Mohammed, PhD[1], Gourab Chatterjee, PhD[1], Kevin Hwang, PhD[1], Julie Xia[1], Amanda Bares, PhD[1], Michael Murphy[1], Eloise Wheeler[1], Armen Changelian[1], Katir Patel, PhD[1], Bonnie Phillips, PhD[1], Sean Downing, PhD[1], Mael Manesse, PhD[1]

[1]*Ultivue, Cambridge, MA, USA*

Background

Innovative and future translational research tools are key to enabling the full impact of personalized medicine. Current pathology methods rely on chromogenic and H&E staining with low multiplexing capabilities, limiting the depth of information obtained from a single tissue sample. Fluorescence-based tissue staining and analysis enable quantification and higher multiplexing; however, current multiplex immunohistochemistry (mIHC) technologies not only compromise throughput and potentially damage the sample with each round of staining, but also require post-acquisition spectral unmixing. Using InSituPlex technology, a highly multiplexed assay (8-plex) can be carried out in a single work day, with maximum tissue preservation and no spectral unmixing.

Methods

InSituPlex technology was used to carry out high-multiplexed immuno-profiling on deidentified FFPE tissue sections. Samples included human tonsil as well as multiple tumor types in skin, lung, and colon. A panel of eight different markers was developed, including CD3, CD8, CD45RO, CD68, PD-1, PD-L1, FoxP3, as well as pan-cytokeratin and Sox10 as tumor markers. Staining of the eight markers was performed in a single run on individual slides, following a manual or automated protocol on the Leica BondRX. Images were acquired using commercially available fluorescence slide scanning platforms, including the Zeiss Axio Scan.Z1, without the need for linear unmixing. All images were analyzed using IndicaLabs HALO.

Results

Images from the eight-plex assay on tonsil tissue were compared to individually stained reference samples to confirm the specificity of the markers in the multiplex assay. In tumor samples, abundance of immune and tumor cells was characterized through

cell counting. In addition, the different expression levels of PD-L1 in immune and tumor cell types were recorded over the entire section. Phenotyping and spatial distribution analysis was carried out to identify cytotoxic T-cells, memory T-cells, exhausted T-cells, regulatory T-cells, and macrophages on single sections. Reproducibility of the assay was also assessed using the data points from serial sections.

Conclusions
InSituPlex technology enables the staining of eight different immune and tumor markers on single FFPE sections, with a streamlined workflow and high reproducibility. Resulting images were then used to perform phenotyping of multiple subsets of T-cell population, macrophages, and tumor cells.

P39

PD-L1 expression on tumor versus antigen presenting cells investigated with multiplexed IHC using UltiMapper™ I/O assays

Amy Zhang, MS[1], Alexis Wong, PhD[1], Max Rubinstein[1], Laura Sciarra, PhD[1], Chakib Boussahmain, BS[1], Bonnie Phillips, PhD[1], Katir Patel, PhD[1], Sean Downing, PhD[1], Stephanie Hennek, PhD[1]

[1]*Ultivue, Cambridge, MA, USA*

Background
In the field of immuno-oncology, there is great promise for improving outcomes by identifying meaningful biomarkers within the tumor microenvironment. The TME is highly heterogeneous, requiring characterization of what cell types are present and what cellular interactions are taking place. Multiplexed IHC is a promising approach to profile cell types and map interactions to identify useful biomarkers. Ultivue has developed UltiMapper assays that provide numerous advantages over other multiplexed IHC approaches including high multiplexing in situ, sample preservation, streamlined workflows, and versatile implementation. The checkpoint marker PD-L1 has become a common marker in immune-oncology, but the usefulness of this marker in insolation has been questioned. In this study, we investigate the expression of PD-L1 on both tumor cells and antigen presenting cells to better understand which cell phenotypes may be important biomarkers.

Methods
Multiplexed immunofluorescence was carried out using UltiMapper assays on multiple deidentified FFPE tissue samples, including lung, melanoma, colon, and breast. Each sample was stained and analyzed for the UltiMapper I/O PD-L1 and APC panel using serial sections. The UltiMapper I/O PD-L1 panel included the markers CD8, CD68, PD-L1, pan-cytokeratin, and Sox10. The UltiMapper I/O APC panel included markers CD11c, CD20, CD68, CD163, and MHCII. Staining was performed manually or using the Leica Bond Rx™ autostainer. Imaging was performed on various tissue scanners including the Zeiss Axio Scan.Z1, and image analysis was performed using HALO from Indica Labs.

Results
Cell phenotyping was carried out to measure the abundance of PD-L1 co-staining on macrophages, dendritic cells, B-cells, cytotoxic T-cells, and tumor cells. In tumor samples, PD-L1 expression was observed on both immune cells and tumor cells with a range of different expression levels and percent positive cells. Spatial analysis was employed to measure the distances between immune cells of differing phenotypes and tumor cells, which could be used to classify tumor samples hot or cold.

Conclusions
Multiplexed IHC is necessary to understand complex cancer biology and the mechanisms by which the immune system is activated or suppressed. The UltiMapper approach is efficient and easy to implement to achieve high quality multiplexed data

on a range of tissue types. The UltiMapper I/O PD-L1 panel is complimented by the UltiMapper I/O APC panel to characterize PD-L1 expression on antigen presenting cells and tumor cells. The abundance and location of PD-L1 positive APCs may be a preferred biomarker over tumor cell PD-L1 expression.

P40

Intra-assay and inter-assay assessment of reproducibility and quantification of UltiMapperTM I/O PD-1 and PD-L1 immuno-oncology panels for tissue multiplexing

Bonnie Phillips, PhD[1], Katir Patel, PhD[1], Courtney Hebert[1], Jamie Buell[1], Sean Downing, PhD[1]

[1]*Ultivue, Cambridge, MA, USA*

Background
The field of immuno-oncology has enthusiastically adopted multiplex IHC techniques to establish the spatial relationships between various immune cells in tumor biology in context. Multiplexing enables researchers to gain a deeper understanding and insight into the tumor microenvironment. Unfortunately, many of the multiplexing technologies currently utilized in the immuno-oncology field face a number of challenges, specifically in generating highly robust, reproducible, and easily quantifiable data sets. Ultivue's UltiMapper I/O PD-1 and PD-L1 I/O kits that utilize InSituPlex (ISP) technology, a new method of multiplexed immunohistochemistry (IHC) that utilizes streamlined single antigen retrieval, staining, elongation, and detection steps allowing for the completion of the assay < 5hr. Here we assess these kits for intra-assay and inter-assay reproducibility and quantification.

Methods
Intra-assay reproducibility and quantification was accomplished by manually staining 5 serial sections from three different tissue types (tonsil, melanoma, NSCLC) with one set for each of the UltiMapper PD-1 (CD3, CD45RO, PD-1, CK/Sox10) and PD-L1 (CD8, CD68, PD-L1, CK/Sox10) I/O kits. Inter-assay assessment was determined by staining a single slide from a set of serial sections of each tissue type described above once a week for 5 consecutive weeks. Images were acquired using the Zeiss Axio Scan.Z1, without the need for linear unmixing allowing for direct whole slide imaging. Analysis was accomplished using IndicaLabs HALO software. Coefficient of variations (CV) were calculated based on resulting data.

Results
Analysis of intra-assay serial section images revealed that cell counts from section to section were within a CV of <10% across all markers, in all tissues, for both the UltiMapper PD-1 and PD-L1 kits. This included total cell counts, top 10% brightest cells, and all quartiles of cell counts based on fluorescence signal intensity. Similar results were seen for inter-assay comparisons over 5 weeks for both kits (<10% CV).

Conclusions
The results presented here indicate that InSituPlex technology is potentially much more reproducible than other tissue multiplexing techniques currently available, such as TSA. Histological standards for coefficient of variations in IHC based assays typically are <15%. Data presented here falls well within that standard indicating the potential for future translational applications. In conclusion, InSituPlex is a highly reproducible and quantifiable multiplexing staining technology across a variety of tissue types and markers, within a single run and over time.

P41

Characterization of circulating biomarkers in subjects with NSCLC using data independent acquisition mass spectrometry reveals host immune response mechanisms

Nicholas Dupuis, PhD[1], Jakob Vowinckel, PhD[1], Daniel Heinzmann[1], Claudia Escher[1]

[1]*Biognosys, Schlieren, Switzerland*

Background
Identification of circulating biomarkers in cancer has proven utility in applications for early detection, differential diagnosis, predicting pre-treatment response to therapy, and treatment monitoring. More recently, circulating proteomic biomarkers have been evaluated as surrogate endpoints for early indication of benefit for immunotherapies. This last application is especially relevant during immunotherapy development where the optimal endpoint, overall survival (OS), can take longer to mature. Here, we present an unbiased survey of the circulating proteome of subjects with NSCLC to identify candidate biomarkers which may have utility in multiple stages of patient care.

Methods
Unbiased, data-independent acquisition (DIA) mass spectrometry was used to analyze plasma samples from subjects with Stage III-IV non-small cell lung cancer (NSCLC, n = 15) and age matched healthy donors (n = 15), enabling simultaneous sequencing and quantification of plasma proteins. Samples were prepared for mass spectrometry and spiked with a panel of standards covering 500 plasma proteins. All samples were analyzed using 1 hour gradients on a C18 column coupled to a Thermo Scientific Q Exactive HF mass spectrometer. Data was extracted using Spectronaut (Biognosys) with a sample specific spectral library and statistical analysis was conducted to identify disease associated biomarker candidates. Pathway analysis highlights dysregulated biological functions and predicts upstream regulatory pathways.

Results
A protein library was created containing 771 unique proteins. In DIA acquisition, 462 proteins were quantified across all samples. Univariate statistical testing identified 26 dysregulated proteins (20 up-regulated and 6 down-regulated; q-value > 0.05 and log2 fold change > 0.58). Multivariate (PLS-DA) analysis identified c-reactive protein (CRP) and serum amyloid a (SAA1/SAA2), complement C9, S100A8/S100A9, and leucine rich glycoprotein 1 (LRG1) as the most significantly changed proteins across sample groups. Significantly enriched pathways include acute phase response, complement system as well as IL-12 and IL-6 signaling. Similarly, upstream activated candidate pathways included STAT3, IL-6, and EZH2.

Conclusions
26 proteins were identified as candidate biomarkers and reflect the host immune response via acute phase response signaling, innate immune response (complement system), and other proinflammatory stimuli. Several of these markers have been linked to patient outcomes and poor prognosis. Accurate monitoring these proteins offers the possibility to define surrogate, molecular based, markers with multiple modes of utility.

P42

Expanding insights into the colorectal cancer tumor proteome; unbiased protein profiling reveals multiple proteomic-based tumor subtypes

Jan Muntel[1], Roland Bruderer[1], Nicholas Dupuis, PhD[1], Lukas Reiter[1]

[1]*Biognosys, Zurich, Switzerland*

Background
Recent approvals of microsatellite instability (MSI) and PD-L1 testing, have expanded the tools available to identify tumor characteristics which predict patient responses to immunotherapies. However, even in MSI and PD-L1 positive subgroups, not all

subjects achieve a durable response and work continues to identify tumor characteristics that will further predict the likelihood of patient response. To support and advance this area of research, new tools are being developed that provide deeper and unbiased views of the tumor proteome. Here, we characterize the protein expression profiles of 95 colorectal cancer tumors (CRC) using SWATH acquisition mass spectrometry (SWATH MS) to probe tumor phenotypic characteristics.

Methods

FFPE colon tissue samples (95 cancer, 10 healthy) from subjects with colorectal cancer across seven regions of the colon: cecum (16), ascending (17), right hepatic flexor (2), left splenic flexor (5), descending (12), sigmoid (21), nonspecific (22). Proteins were extracted from the tissue, processed to peptides, and injected on a Triart C18 column (YMC) coupled to a NanoLC 425 system (SCIEX). Eluted peptides were then analyzed with a TripleTOF® 6600 system (SCIEX) operated in SWATH mode. Data were analyzed in Spectronaut Pulsar X (Biognosys) with a project specific library.

Results

Across all samples, >4,500 protein groups were quantified (approximately 3,600 per sample). Data analysis revealed a large number of proteins (~1,000) were differentially expressed in the cancer cohort, including an elevation of proteins involved in translation which is consistent with increased tumor cell proliferation. Unsupervised clustering of the data separated the healthy and the cancer cohort and revealed three main proteomic subtypes within in the cancer cohort (A, B and C) which were largely distinguished by expression of cell adhesion proteins, including neuronal growth regulator 1 (NEGR1), a potential tumor suppressor. Interestingly, hepatocyte nuclear factor 4-alpha (HNF4A), a transcription factor which is known to be elevated in CRC, was most significantly overexpressed in subtype B, which correlates with protein signatures from MSI high samples from previous studies. Additional analysis of key protein networks related to CRC and MSI high status, as well as analysis of the mismatch repair proteins MSH2 and MSH6 expression, will be presented from this work.

Conclusions

High-throughput proteomic profiling of FFPE tissues using SWATH-MS enables the deepest phenotypic characterization of tumor tissue. Through global profiling, these analyses will help improve the functional understanding of the interplay between the expression of protein networks, tumor microenvironment, and response to immune-directed therapies.

P43 Abstract Travel Award Recipient

The presence of exhausted CD8+ T cells identifies a subset of immunogenic ER+ breast cancer patient tumors

Colt Egelston, PhD[1], Christian Avalos[1], Diana Simons[1], Min Hui Lim[1], Peter Lee, MD[1]

[1]Beckman Research Institute, City of Hope, Duarte, CA, USA

Background

Estrogen receptor positive (ER+) breast cancers are generally thought to be less immunogenic and less immune infiltrated than triple negative breast cancer (TNBC). In TNBC the presence of tumor infiltrating lymphocytes (TILs) is predictive of response to chemotherapy and associates favorably with patient survival. However, in ER+ breast cancer the relationship between T cell infiltration and disease is less clear. Expression of both PD-1 and CD39 on exhausted CD8+ T cells has been described in murine models of chronic disease and recently human carcinomas. Here we profile human breast tumors for the frequency and phenotype of exhausted CD8+

T cells and their association with a unique immunogenic tumor microenvironment.

Methods
Fresh surgical tumor specimens were obtained from consented patients. Single cell suspensions were analyzed by flow cytometry for immune phenotyping and functional assessment of cytokine production by T cells. Single cell sorted T cells were subjected for whole transcriptome RNA sequencing and bulk sorted T cells were submitted for T cell receptor repertoire sequencing by Adaptive Biotechnologies. Formalin fixed tissues were then used for multispectral immunohistochemistry and RNA transcript analysis by Nanostring.

Results
Of 35 ER+ tumors assessed, 20% were found to have exhausted PD-1+ CD39+ CD8+ T cells at a significant frequency of total CD8+ TILs. On the contrary, 60% of TNBC tumors assessed contained exhausted PD-1+ CD39+ CD8+ T cells. These T cells showed a significant reduction of IFNγ, TNFα, and IL-2 production capacity. Further phenotyping of exhausted CD8+ T cells revealed a loss of expression of both the IL-7 receptor alpha (CD127) and KLRG1, suggesting terminal differentiation of these cells. Single cell and T cell receptor sequencing revealed distinct transcriptional and clonal signatures of PD-1+ CD39+ CD8+ T cells suggesting them to be a unique population in response to tumor antigen. Immunohistochemistry of tumor tissues showed that ER+ tumors with PD-1+ CD39+ CD8+ T cells were significantly more infiltrated with T cells and showed characteristics of 'hot' tumors. Finally, Nanostring analysis of RNA transcripts from tumor tissues revealed that ER+ tumors containing PD-1+ CD39+ CD8+ T cells had a significantly higher expression of gene signatures of inflammation and IFNγ signaling.

Conclusions
This work suggests that a subset of ER+ breast cancer patients have inflamed, highly lymphocyte infiltrated tumors. These tumors are associated with the presence of exhausted CD8+ T cells, suggesting a tumor antigen driven response in these tumors and that these patients may benefit from immunotherapeutic interventions.

P44

Discovery and screening of protein biomarkers with the FirePlex Technology Platform

Timothy Erps[1], Amy Perea, PhD[1], Russell Neuner, PhD[1], Bianca Heinrich, PhD[1], Wayne Austin[1], Conor Rafferty, PhD[1], Matt Camilleri[1], Long To[1], James Murray, PhD[1], Daniel Pregibon, PhD[1], Elnaz Atabakhsh, PhD[1]

[1]*Abcam, Inc, Cambridge, USA*

Background
In patients and animal models, molecular biomarkers are used as indicators of normal and pathogenic processes. In drug discovery and screening pipelines, molecular biomarkers are used to assess the mechanism of action, efficacy, and toxicity of lead compounds. To address the need for rapid and sensitive quantitation of protein biomarkers, we have developed the FirePlex® Technology Platform. Utilizing patented hydrogel particles and a three-region encoding design, FirePlex Immunoassays allow for true, in-well multiplexing, providing flexible and customizable quantification of analytes.To facilitate biomarker discovery studies, we offer our standard-throughput FirePlex Immunoassays, which enable quantitation of up to 75 protein analytes per sample, from only 12.5 µl of input. These assays demonstrate 5 logs of dynamic range and sub-picogram/ml sensitivity, allowing for highly sensitive quantitation of analytes in serum, plasma, cell culture supernatant, urine, and saliva. Assays are run in 96well plate format, with readout on standard flow cytometers.

Methods
For drug discovery and screening studies, we offer our high-throughput FirePlex (FirePlex®-HT) Immunoassays for quantitation of up to 10 protein analytes per sample from only 6.25 µl biofluid input, in 384-well plate format. FirePlex-HT assays provide 3-4 logs dynamic range, demonstrate 1-100 pg/ml sensitivity, and have been validated in serum, plasma, and cell culture supernatant. The two-step workflow, no-wash assay format, and readout on high-content imagers limit hands-on time and are amenable to automation, thus making FirePlex-HT ideally suited for high-throughput screening studies.

Results
Here we present data from studies investigating cytokine profiling in human and rodent samples using the FirePlex immunoassays, and introduce the simplified workflow of the FirePlex-HT® immunoassays with data demonstrating the performance for quantifying key cytokines in multiplex, in biological samples.

Conclusions
Together, this novel combination of multiplexed, high-sensitivity assays and bioinformatics tools enables rapid quantitation of protein biomarker signatures in biofluid specimens.

P45

Tumor infiltrating T cells: complete workflows allow faster and improved analysis

Cesar Evaristo, PhD[1], Ramona Siemer, BTA[1], Philipp Steinbrueck[1], Zhongjie Yu[1], David Agorku, BS[1], Olaf Hardt, PhD[1], Christian Dose, PhD[1], Anne Richter, PhD[1]

[1]*Miltenyi Biotec, Bergisch Gladbach, Germany*

Background
Immunotherapies engaging T cells have proven clinical efficacy and tremendous potential. However, responses are often suboptimal. Further research is required to understand tumor-infiltrating leukocytes (TILs) biology and enhance outcomes. TIL analysis is technically challenging and labor intensive. Their number can be very low and small subpopulations might escape analysis as they get lost in the background noise. Importantly, tumor-infiltrating T cells are embedded in a highly immunomodulatory environment such that unbiased cell-intrinsic functional characterization is hindered. When working with large cohort sizes, even immunophenotyping TILs by flow cytometry is time consuming and data processing is laborious. Therefore, it is fundamental to use effective tools to streamline the workflow and to generate reliable data.

Methods
We established complete workflows combining tissue storage, dissociation, T cell isolation and phenotyping of mouse and human tumors. Tissues were processed immediately or stored in a solution that was shown to maintain cell viability and phenotype up to 48h after collection (Tissue Storage Solution™). Tumor dissociation was automated and optimized for epitope preservation using a tissue dissociator (gentleMACS™ Octo). We developed new T cell-specific enrichment reagents for magnetic cell sorting, incorporating novel technology enabling the removal of both superparamagnetic beads and antibody fragments (REAlease®). We labeled TILs using recombinant antibodies engineered to eliminate Fc receptor-mediated background (REAfinity™). Finally, flow cytometric analysis was performed using an automated analyzer (MACSQuant X™ and MACSQuant 16™).

Results
Optimal enzymatic dissociation was essential for analysis of critical tumor-specific sub-populations, such as PD1hiTim3+Lag3+CD39+CD8+ T cells present in tumors. Magnetic cell sorting resulted in

enrichment of rare tumor infiltrating T cells by up to 500-fold, while maintaining activation status and phenotype. Isolation of T cells using REAlease technology allowed enrichment of subpopulations such as gamma delta T cells and Tregs with high purity. Use of REAfinity antibodies significantly diminished non-specific labeling of cells present in the tumor microenvironment. Use of MACSQuant analyzers decreased hands-on as well as total acquisition time by facilitating fast and fully automated sample processing, including sample mixing and absolute cell counting.

Conclusions

We optimized workflows that include standardized processing of tumor samples, newly developed tools for (semi-) automated magnetic isolation of tumor infiltrating T cells and automated flow cytometric analysis. These workflows greatly reduce experimental time and allow the performance of more complex experimental setups. We believe the use of these innovative tools and workflows can significantly increase the quality of the data obtained in immuno-oncology and immunotherapy research.

P47

Immune response in patients treated with autologous dendritic cells transduced with AdGMCA9 (DC-AdGMCAIX) in patients with mRCC from the phase I, open label, dose escalation and cohort expansion study

Izak Faiena, MD[1], Nazy Zomorodian[1], Beata Berent-Maoz[1], Ankush Sachadeva[1], Adrian Bot, MD, PhD[2], Fairooz Kabinnavar[1], Jonathan Said[1], Gardenia Cheung-Lau[1], Jia Pang[1], Mignonette Macabali[1], Tinle Chodon[1], Xiaoyan Wang[1], Paula Cabrera[1], Paula Kaplan-Lezco[1], Sandy Liu[1], Begonya Comin-Anduix, PhD[1], Allan Pantuck, MD[1], Arie Belldegrun, MD, FACS[1], Karim Chamie, MD[1], Alexandra Drakaki, MD,PHD[1]

[1]UCLA, Los Angeles, CA, USA
[2]Kite Pharma, Santa Monica, CA, USA

Background

Patients with metastatic RCC were treated in a phase I trial with autologous dendritic cells transduced by a replication deficient adenovirus comprised of GM-CSF+CAIX. Nine patients in three dose escalation cohorts (5, 15, and 50 X 106 cells/administration) were injected based on a 3+3 design.

Methods

An enzyme-linked immunospot (ELISpot) assay was used to determine the frequency of CAIX-specific IFN-γ producing T cells in blood. 15-mer overlapping peptides from CAIX protein, AdV5-pepton, and controls (+/-) were plated in Elispot plates pre-coated with anti-IFN-γ antibody. Subsequent to assay development, the number of T-cells responding to CAIX was calculated as above the lower limit of detection (LLD) (7 spots). After subtracting the backgrounds, fold change was calculated with respect baseline. The criterion for positive immunological response was defined as the mean fold change plus two. Further assessment included immunohistochemistry (IHC) staining of tissue from patients #4 (with PD) and #8 (with SD) for CAIX, CD4/8, Ki67, GrZ8, PD1/L1. The samples were scored based on percent positivity and staining intensity (Table 1). Tissue was obtained from the primary tumor prior to vaccination, and the target tumor at the end of the study period (18 months).

Results

ELISpot showed consistently positive responses against CAIX upon vaccination with DC vaccine, more prominently in patients in cohort 3 (high dose) as well as in those with longer time to progression (Figure 1). None of the treated patients showed an objective response. However, patient #8 who achieved stable disease (SD) lasting 18 months had more than 2-fold change in immune response over baseline on day 35 and 60 after the first vaccination

cycle. All nine patients showed different degrees of immunological reaction to AdV5 at baseline and elevation at the end of the study. IHC showed that both patients had high CAIX expression in primary tumor and on the target lesion post vaccination. Immune infiltrates were seen at baseline in both subjects, with predominant CD4/8 T-cells in patient #8 with a high PD-1 expression in infiltrating lymphocytes without PD-L1 expression in the tumor environment.

Conclusions

DC-AdGMCAIX vaccination may elicit robust immunologic response against CAIX in patients with ccRCC. The findings of high PD-1 expression in the patient with SD in both the primary tumor and target lesion warrants future efforts to explore how combination therapies with biological response modifiers may further enhance clinical responses.

Acknowledgements

Supported by NCI RAID Initiative NSC 740833 and Kite Pharma

Trial Registration

NCT01826877

Ethics Approval

The study was approved by UCLA institutional review board IRB#12-000577

Figure 1. ELispot immune response in study subjects

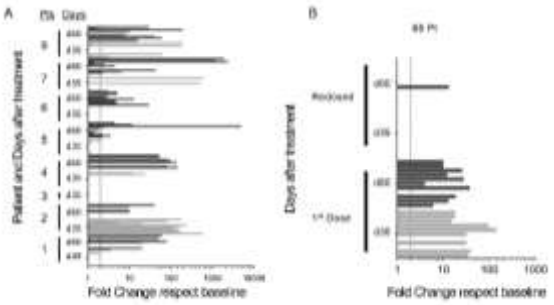

Table 1. Immunohistochemistry staining

		Non-responder #3				Stable disease #8			
		Pre		Post		Pre		Post	
		Percent	Intensity	Percent	Intensity	Percent	Intensity	Percent	Intensity
CAIX		100	3	100	3	100	3	100	3
CD4		60	3	80	3	8	3	10	3
CD8		10	1	30	1	60	3	5	1
Gzb		2	1	2	1	5	1	10	1
KI67		0	0	5	1	5	1	10	1
PD-1	Tumor cell	0	0	0	0	100	1	100	1
	Immune cell	<5	1	<5	1	60	3	80	3
PD-L1	Tumor cell	0	0	0	0	0	0	0	0
	Immune cell	0	0	0	0	<1	1	<1	1

Percent of biopsy specimen

P48

A high baseline neutrophil-to-lymphocyte ratio in patients receiving anti-PD-1 therapy for head and neck cancer associates with poor prognosis, tumor hypoxia, and tumor M2 macrophage predominance

Corey Foster, MD[1], Riyue Bao, PhD[2], Sara Kochanny, BA[1], Arun Khattri, PhD[1], Rajesh Acharya, MS[1], Allison Dekker, RN[1], Yi-Hung Carol Tan, PhD[1], Elaine Klema, BS[1], Ryan Brisson, BS[3], Vassiliki Saloura[1], Alexander Pearson, MD, PhD[1], Everett Vokes, MD[1], Rom Leidner, MD[4], Hisham Mehanna, PhD[5], Tanguy Seiwert, MD[1]

[1]*The University of Chicago Medicine, Chicago, IL, USA*
[2]*The University of Chicago, Chicago, IL, USA*
[3]*Oakland University, Rochester, MI, USA*
[4]*Providence Cancer Center, Portland, OR, USA*
[5]*University of Birmingham, Birmingham, UK*

Background
The associations among a high neutrophil-to-lymphocyte ratio (NLR), prognosis, and the tumor microenvironment for patients with head and neck (H&N) cancer receiving anti-programmed death receptor 1 (PD-1) therapy are not established.

Methods
One-hundred-fourteen patients with metastatic H&N cancer received anti-PD-1 therapy with high baseline NLR defined as >8.77 (highest quartile). Logistic regression analyzed the association with overall response rate (ORR), and Kaplan-Meier methods and Cox proportional hazards regression models were used to test the association between NLR group and progression-free survival (PFS) and overall survival (OS). Tissue was available from 60 patients for gene expression profiling and pathway analysis using RNA sequencing. Expression abundance was quantified by Kallisto and normalized using the trimmed mean of M-values normalization method. Genes differentially expressed in the high vs. low NLR group were detected using limma voom with precision weights. Pathway enrichment and upstream regulator prediction was performed through the use of IPA (QIAGEN Inc.).

Results
Median follow-up was 14.3 months. ORR was 22.3% with a trend towards lower ORR for the high NLR group (p=0.20). Median PFS was 1.7 months (95% confidence interval [CI]: 1.0-3.6) for high NLR patients and 3.7 months (95% CI: 3.2-6.2) for low NLR patients (p=0.01). Median OS was 9.6 months shorter in the high vs. low NLR group (3.8 months vs. 13.4 months, p<0.0001), and a decreased NLR 6 weeks into therapy associated with improved OS (p=0.0008). High NLR remained associated with OS (p=0.01) on multivariate analysis and trended toward independent association with PFS (p=0.07). High NLR associated with higher expression of CD163 (p=0.006) and HIF1-alpha (p=0.009), which was further supported by predicted activation of HIF1-alpha-target molecules based on experimental evidence from the Ingenuity Knowledge Base (activation z-score = 2.834, p=1.88E-04).

Conclusions
High baseline NLR associates with poor prognosis for patients with metastatic H&N cancer receiving anti-PD-1 therapy and correlates with increased expression of genes related to M2 macrophage predominance and hypoxia within the tumor microenvironment.

Ethics Approval
This study was approved by The University of Chicago Institutional Review Board.

P49

Comprehensive immune and molecular analysis of a cohort of non-small cell lung cancer (NSCLC) patients treated with a personal neoantigen vaccine, NEO-PV-01, in combination with anti-PD1

Joel Greshock[1], Ramaswamy Govindan, MD[2], Riley Curran[1], Rana Besada[1], Samantha Gates[1], Victoria Kohler[1], Meghan Bushway[1], Julian Scherer, PhD[1], Ying Sonia Ting[1], Yuting Huang, Master of Science[1], Yvonne Ware, Masters[1], April Lamb[1], Lisa D.Cleary[1], Melissa Moles[1], Richard Gaynor, MD[1], Matthew Goldstein, MD, PhD[1], Lakshmi Srinivasan[1]

[1]Neon Therapeutics, Inc
[2]Washington University Medical School, Saint Louis, MO, USA

Background
Neoantigens arise from DNA mutations and are important targets when presented on the surface of cancer cells for tumor-specific T cell responses. Vaccines targeting neoantigens have the potential to induce de novo and amplify pre-existing anti-tumor T cell responses. NEO-PV-01, a personal neoantigen vaccine, designed based on a patient's tumor-specific

mutations and are predicted to be presented by MHC molecules, is comprised of up to 20 long peptides and administered along with an immune adjuvant Poly-ICLC. Here we report comprehensive immune and molecular analysis observed in a cohort of metastatic non-small cell lung cancer (NSCLC) patients treated with NEO-PV-01 in combination with nivolumab (ClinicalTrials.gov: NCT02897765).

Methods
Tumor biopsies were scheduled for collection: i) prior to any treatment, ii) after 12 weeks of nivolumab monotherapy and iii) after completion of NEO-PV-01 vaccination. Tumor biopsies from each collection time point were analyzed for multiple immune and tumor markers by immunohistochemistry, gene expression and whole exome sequencing. Immune monitoring from peripheral blood samples was also evaluated at similar times for the presence of antigen-specific responses by IFNγ ELISPOT, intracellular cytokine staining, multi-parameter surface and functional phenotyping by FACS and the presence of cytolytic properties.

Results
IFNγ ELISPOT analysis with peripheral blood mononuclear cells (PBMCs) revealed neoantigen-specific CD4+ and CD8+ T cell responses that were only detected in the post-vaccination samples. Vaccine-induced immune responses were durable in one of the patients who reached the week 52 treatment timepoint. Neoantigen-specific T cells were of effector memory and central memory phenotype. Additionally, these cells were cytolytic and secreted IFNγ, TNFα and IL2. Assessment of serial tumor biopsies with repeat exome sequencing, gene expression, TCR repertoire analysis, immunohistochemistry and pathologic analysis will be presented.

Conclusions
NEO-PV-01 is immunogenic and leads to durable de novo neoantigen-specific immune responses in the peripheral blood of patients with metastatic NSCLC.

P50

Characterization of T cell receptor repertoire from FFPE extracted RNA from glioblastoma patients by anchored multiplex PCR and next-generation sequencing

Laura Johnson, PhD[1], Josh Haimes[1], Namitha Nair[1], Angelo Porciuncula, PhD[2], Kurt Schalper, MD, PhD[2]

[1]*ArcherDX, Boulder, CO, USA*
[2]*Yale School of Medicine, New Haven, CT, USA*

Background
The adaptive immune system is involved in various disease conditions including cancer, chronic infection, autoimmune disease and transplant rejection. Adaptive immunity is mediated by B and T lymphocytes, which are activated upon antigen binding to antigen receptors expressed on their surface. Therefore, the spectrum of these antigen receptors, or immune repertoire (IR), provides a means to monitor adaptive immune responses to disease, vaccination and therapeutic interventions. Next-generation sequencing (NGS) of antigen receptor genes is a valuable tool in the study of disease states and responses to various interventions. The Archer® Immunoverse™ TCR assay quantitatively assesses the T-cell content and clonal diversity of patient derived RNA. Here, we describe the use of an Anchored Multiplex PCR (AMP)-based NGS assay to analyze RNA extracted from FFPE samples from glioblastoma patients during an immunotherapeutic clinical trial.

Methods
In this study RNA was extracted both pre and post treatment, and the effects of the two therapeutic interventions were compared. Testing was performed by two independent labs and with both

NGS and NanoString™ based assays.

Results
The results of the two different assays showed concordance with the T cell content increasing significantly post immunotherapeutic intervention as detected by the NanoString assay (p=0.003) while the increase was not significant post standard of care treatment (p=0.438). The trend was the same with the Archer® Immunoverse™ assay where a larger increase in T cell clones was detected post immunotherapeutic treatment compared to post standard of care treatment (p=0.037 vs. 0.5275 respectively). The results we present also show that the number of detected TCR clones and clonotypes depended on sample input amount, sequencing depth and RNA quality.

Conclusions
The results of this study support the utility of the Archer® Immunoverse™ assay in the study of FFPE derived RNA from patient samples.

P51

Objective quantitative measurements of PD-L1 expression in tumor tissue by Phosphor Integrated Dots staining in patients with non-small cell lung cancer

Kazuyuki Hamada, MD, PhD[1], Ryotaro Ohkuma, MD[1], Takehiro Takahashi, MD, PhD[1], Takeshi Setogawa[2], Masaru Takahashi[2], Hisatake Okada[2], Hiroo Ishida[1], Yutaro Kubota, MD, PhD[1], Hirotsugu Ariizumi, MD PhD[1], Etsuko Satoh, MD, PhD[1], Yuya Hirasawa, MD[1], Yasutsuna Sasaki, MD, PhD[1], Kiyoshi Yoshimura, MD, PhD[1], Takuya Tsunoda, MD[1], Satoshi Wada, MD, PhD[1]

[1]*Showa University, Tokyo, Japan*
[2]*Konica Minolta, Inc., Tokyo, Japan*

Background
The PD-1/PD-L1 signal suppresses activated T cells. Anti-PD-1 antibody treatment has an anti-tumor effect by blocking the PD-1/PD-L1 signaling, thereby reactivating exhausted T cells, especially tumor antigen-specific T cells. Several clinical studies were reported that the effect of anti-PD-1 antibody was associated with the number of CD8 T cells in tumor tissue. It was also reported that the effect of anti-PD-1 antibody was associated with the expression ratio (%) of PD-L1 in tumor tissue. However, the effect was also shown in cases with low PD-L1 expression ratio (%). Thus, the expression ratio (%) of PD-L1 in tumor tissue has not yet been a clearly predictive biomarker for anti-PD-1 antibody treatment. This may be a result of the pathologist individually measuring the percentage of PD-L1 positive cells in tumor tissue by immunohistochemistry (IHC).

Methods
Phosphor Integrated Dots (PID) staining is a highly accurate measurement method that detects the expression of specific molecules with high sensitivity and can be quantified as a particle number. In this study, we performed objective quantitative measurements of PD-L1 expression per unit area of tumor tissue by PID staining (PD-L1 PID score) in five patients with non-small cell lung cancer (three responders and two non-responders) treated with anti-PD-1 antibody. In addition, double staining with PD-L1 and CD8 T cells in tumor tissue was performed by PID and IHC, respectively.

Results
PD-L1 expression per unit area of tumor tissue was quantified by PID analysis. We also established double staining of IHC for CD8 T cells and PD-L1 with PID. It was proved that the PD-L1 PID score was significantly associated with the number of tumor-infiltrating CD8 T cells. Additionally, the effective cases of anti-PD-1 antibody tended to have a higher ratio of the PD-L1 PID score and the number of CD8 T cells.

Conclusions
PID staining is might be useful for PD-L1 measurement in tumor tissue. By conducting further case analysis and clarifying the relationship between the PD-L1 PID score and immune cells, characteristics of responders treated with anti-PD-1 antibody may be clarified.

Ethics Approval
The study was approved by Showa University School of Medicine's Ethics Board, approval number 2253.

P52

Emergence of an ICOShi CD4 T cell subset correlates with tumor reductions in subjects treated with the ICOS agonist antibody JTX-2011

Amanda Hanson[1], Sean Lacey, MA Biostatistics[1], Courtney Hart[1], Ty McClure[1], Ellen Hooper, MD[1], Elizabeth Trehu, MD[1], Deborah Law, DPhil[1], Christopher Harvey, PhD[1]

[1]*Jounce Therapeutics, Cambridge, MA, USA*
[2]*Jounce Therapeutics, Inc., Cambridge, MA, USA*

Background
Inducible T cell Co-stimulator (ICOS) is a costimulatory molecule expressed primarily on T lymphocytes that is upregulated upon cell activation. ICOS was identified as a potential target of interest based on clinical data from studies with anti-CTLA-4. Sustained ICOS upregulation was associated with clinical benefit, with preclinical data confirming a role for ICOS signaling in optimal anti-tumor activity. JTX-2011 is a first-in-class ICOS agonist antibody that has been demonstrated preclinically to have a tumor-centric dual mechanism of action through stimulation of CD4 T effector cells and depletion of intratumoral T regulatory cells. Clinical and biological activity of JTX-2011 is currently being evaluated in the advanced solid tumor setting in the ongoing Phase I/II ICONIC trial (NCT02904226).

Methods
Relapsed/refractory cancer patients received escalating doses of JTX-2011 as a monotherapy or in combination with nivolumab (240mg) administered q3w. Serial collection of peripheral blood mononuclear cells (PBMCs) was performed to enable longitudinal assessment of biological activity through flow cytometry-based assays, including target engagement (TE), and immunophenotyping (IP) including a limited assessment of T cell exhaustion.

Results
At the RP2D, peripheral TE demonstrated sustained (>70%) engagement over the entire dose cycle, and IP data demonstrated no consistently significant changes in T cell populations following JTX-2011 treatment. The potential of sustained agonism to drive phenotypic T cell exhaustion was assessed, and no evidence of phenotypic T cell exhaustion was observed in subjects treated with the combination of JTX-2011 and nivolumab. No conclusions could be reached in monotherapy setting due to limited sample availability. Further analysis of peripheral T cell phenotype demonstrated the emergence of an ICOShi subset of CD4 T cells in select subjects. Interestingly, the emergence of this cell population correlated with tumor reductions in both JTX-2011 monotherapy and combination subjects. Of the evaluable subjects assessed (N=37), emergence of the ICOShi subset was detected in 7/7 subjects with a reduction of their target lesion >30%, but not in any subject with best overall response of progressive disease.

Conclusions
Analysis of longitudinal blood samples from subjects treated with JTX-2011 suggests that the emergence of a distinct ICOShi population of peripheral CD4 T cells correlates with a radiographic response to JTX-2011 treatment. The emergence of this population may serve as a surrogate biomarker of response and

may be useful in guiding future clinical development.

P53

X4P-001, an orally bioavailable CXCR4 antagonist, increases immune cell infiltration and tumor inflammatory status in the microenvironment of melanoma

Timothy Henion[1], Robert Andtbacka, MD, CM, FACS, FRCSC[2], Robert Pierce, MD[3], Jean Campbell, PhD[3], Melinda Yushak, MD, MPH[4], Mohammed Milhem, MBBS[5], Merrick Ross, MD[6], Katie Niland[7], Lu Gan, MD, PhD[7], Sudha Parasuraman, MD[7], Yan Wang, PhD[7]

[1]Acumen Medical Communications, Cambridge, MA, USA
[2]Huntsman Cancer Institute, Salt Lake City, UT, USA
[3]Fred Hutchison Cancer Research Center, San Diego, CA, USA
[4]Emory University School of Medicine, Atlanta, GA, USA
[5]University of Iowa, Iowa City, IA, USA
[6]MD Anderson Cancer Center, Houston, TX, USA
[7]X4 Pharmaceuticals, Cambridge, MA, USA

Background
The CXCR4/CXCL12 axis plays a central role in the trafficking of key immune cells in the tumor microenvironment (TME). Enhanced survival is reported in multiple syngeneic mouse models when a CXCR4 antagonist is combined with a check point inhibitor. X4P-001 is an oral, selective, allosteric inhibitor of CXCR4 that robustly inhibits the growth of murine B16-OVA melanoma. A biomarker-driven Phase 1b clinical study (NCT02823405) is on-going in melanoma patients to test the hypothesis that X4P-001 has the potential to modulate the TME in favor of an improved response to checkpoint inhibitors.

Methods
The primary objectives for this trial are to evaluate the safety and tolerability of X4P-001 alone and in combination with pembrolizumab in patients with metastatic melanoma and to characterize the effects of X4P-001 on tumor immune cell infiltrates. Serial biopsies of cutaneous or subcutaneous melanoma lesions, peripheral blood mononuclear cells, and serum samples were collected pre-dose, after three weeks of single-agent X4P-001, and after six weeks of combination treatment. Biopsies were assessed by immunohistochemistry and multiplex immunofluorescence for multiple protein markers, including CD8, FoxP3, and Granzyme B; and by NanoString analysis for changes in gene expression. Serum samples were assessed using the multi-analyte profile platform for key chemokines and cytokines.

Results
As of June 5th, 2018, 16 patients (median age 74.5 years, range 53-91) have been enrolled and all have completed treatment or are off study. X4P-001 alone increased infiltration of CD8+ T cells, granzyme B signal, antigen-processing and presentation machinery, such as HLA-DR, and both Tumor Inflammatory Signature (TIS) and IFN-gamma gene expression signature scores in the TME of select patients with paired evaluable biopsies. These biomarker responses were further enhanced when X4P-001 was combined with pembrolizumab. Adverse events related to either X4P-001 or pembrolizumab (greater than 10%) were diarrhea, fatigue, maculo-papular rash, dry eye, acute kidney injury, chills, decreased appetite, dry mouth, ocular hyperemia, oral candidiasis, and pruritus. These data, along with measurements of serum chemokines and cytokines, will be presented.

Conclusions
Treatment with single-agent X4P-001 consistently results in enhanced immune cell infiltration and activation in the TME leading to increases in TIS and IFN gamma gene expression signature scores. X4P-001 as a single-agent and in combination with

pembrolizumab has an acceptable safety profile. These data support the use of X4P-001 to potentially improve outcomes for patients with tumors that are less responsive to checkpoint inhibitors.

Trial Registration
NCT02823405

Ethics Approval
Institutional Review Board approval was obtained from each participating center.

Consent
Each patient provided consent to participate in this clinical trial.

P54

Adenosine signature genes associate with tumor regression in renal cell carcinoma (RCC) patients treated with the adenosine A2A receptor (A2AR) antagonist, CPI-444

Andrew Hotson, PhD[1], Stephen Willingham, PhD[1], Lawrence Fong, MD[2], John Powderly, MD, CPI[3], Jason Luke, MD, FACP[4], Mario Sznol, MD[5], Saby George, MD, FACP[6], Toni Choueiri[7], Marios Giannakis, MD, PhD[7], Brian Rini, MD[8], Shivaani Kummar, MD[9], Erik Evensen[10], Ian McCaffery, PhD[1], Chunyan Gu[1], Long Kwei, PhD[1], Ginna Laport[1], Joseph Buggy[1], Richard A. Miller, MD[1]

[1]*Corvus Pharmaceuticals, Burlingame, CA, USA*
[2]*University of California, San Fransisco, San Francisco, CA, USA*
[3]*Carolina BioOncology Institute, Huntersville, NC, USA*
[4]*University of Chicago, Chicago, IL, USA*
[5]*Yale University Cancer Center, New Haven, CT, USA*
[6]*Roswell Park Cancer Institute, Buffalo, NY, USA*
[7]*Dana Farber Cancer Institute, Boston, MA, USA*
[8]*Cleveland Clinic Foundation, Cleveland, OH, USA*
[9]*Stanford University School of Medicine, Stanford, CA, USA*
[10]*Basis Bioscience, Foster City, CA, USA*

Background
Adenosine in the tumor microenvironment is immunosuppressive. CPI-444, an adenosine A2A receptor (A2AR) antagonist, restores immune function and is active in preclinical tumor models. CPI-444 is being investigated as monotherapy and in combination with atezolizumab (Tecentriq®) in an ongoing Phase 1/1b trial in patients (pts) with treatment-refractory renal cell carcinoma (RCC). Biomarker objectives included identifying tumor gene expression pathways associated with tumor response.

Methods
Tumor biopsies obtained at trial screening from pts with RCC (n=30) were analyzed for gene expression profiles with the Nanostring PanCancer Immune Panel that included 770 markers of immune activity and inflammation. The gene expression correlation (Spearman) matrix was hierarchically clustered (Ward's method) to identify modules of genes that were co-expressed across tumors. Gene cluster expression intensity was compared between pts with evaluable best change in tumor size ≤0 (n=8) vs >0 (n=15). The composite adenosine gene signature score was calculated as the average of the Log2 of expression values for seven genes (CXCL1, CXCL2, CXCL3, CXCL5, IL1B, IL8, SERPINB2) shown to be induced in vitro in normal peripheral blood mononuclear cells by adenosine [1].

Results
Analysis of baseline RCC tumors revealed a cluster of correlated genes in T cell activation, IFNg-signaling, and antigen presentation pathways; this cluster was not significantly associated with tumor response to CPI-444 monotherapy or combination. However, the gene cluster containing the adenosine gene signature was associated with tumor regression (p=0.02). This cluster included 18 other genes such

as chemokines (e.g. CCL20), complement genes, and serum amyloid A1. An additional cluster contained components of the adenosine signature, CXCL3 and CXCL5, and also associated with regression (p=0.04). In contrast, a cluster enriched for growth factor response genes associated with tumor progression (p=0.01) and negatively correlated with the adenosine signature cluster. Likewise, a cluster containing CX3CL1 and complement inhibition also associated with tumor progression (p=0.04) and inversely with the adenosine signature. These data support the co-regulation of adenosine and other biological processes within the tumor microenvironment, such as a negative relationship between adenosine and both CX3CL1 and growth factor signaling.

Conclusions
CPI-444 anti-tumor activity in RCC was associated with baseline expression of adenosine responsive genes, and is consistent with the mechanism of action of CPI-444. Adenosine-mediated immunosuppression and growth factor pathway activation may represent alternative oncogenic processes that define RCC pt subsets and could provide pathway specific biomarkers for prognosis and pt selection.

Trial Registration
NCT02655822

References
1. Willingham S, et al. Identification of adenosine pathway genes associated with response to therapy with the adenosine receptor antagonist CPI-444. European Society for Medical Oncology poster presentation. Munich, Germany, 2018.

Ethics Approval
The protocol was approved by the institutional review board or ethics committee at each participating center.

P55

Within the secretome: Immunomodulatory role of extracellular vesicles in breast cancers.

Sheeba Irshad, MD, PhD[1], Atousa khiabany, Mres[1], Fabian Flores-Borja, PhD[1], Ines García Carcedo[1], Felix Wong[1], Fabienne Beuron, PhD[2], Jose vicencio[3], Andrew Tutt[1], Tony Ng[1]

[1]*Kings College London, London, UK*
[2]*Institute of Cancer Research, London, UK*
[3]*University College London, London, UK*

Background
Extra-cellular vesicles (ECVs) are heterogeneous submicron-sized vesicles that vary in size, composition and surface biomarkers. Recently, evidence suggests ECVs can have dichotomic role in the regulation of the immune system, enhancing or suppressing an immune response depending on their cell of origin and functional state. We investigated the immunomodulatory functions of breast cancer cell line and patient-derived serum ECVs.

Methods
ECVs were isolated from cell line culture media and serum of patients diagnosed with early breast cancers (BC) using ultracentrifugation and gradient column methods, respectively. Isolated ECVs were characterized by nanoparticle flow, electron microscopy and dot blot analyses. ECVs were cultured with human PBMCs with or without ECVs for upto 5 days. Cell phenotypes, and their proliferation and activation states were evaluated by flow cytometry.

Results
Breast cancer cell-line ECVs significantly improved the survival of PBMCs in vitro (p=0.005). PBMCs cultured with ECVs had significantly higher CD4+T-cells (p=0.01) but reduced number of CD8+T-cells (p=0.001) compared to unstimulated PBMCs. No

significant differences in the B-cell or NK-cell counts were observed. Assessment of the activation status demonstrated that BC cell line-derived ECV inhibited the activation of CD4+T-cells by anti-CD3/anti-CD28 activation beads (p=0.01) but no significant difference was observed in the activation status of CD8+T-cells. No differences in the proliferation rates of CD3+CD4+ or CD3+CD8+ T cells between ECV-stimulated versus no ECV stimulation was observed. Further analysis for the co-expression of CD45RO and CCR7 on CD4+ or CD8+ distinguished between naïve (CD45RO−CCR7+), central memory (CD45RO+CCR7+,Tcm), memory effector (CD45RO+CCR7−, TEM), and effector (CD45RO−CCR7−, Teff) T-cells. PBMC- ECV co-cultures significantly increased the percentage of CD4+ Tcm-cells (p=0.001) and CD8+ Tcm-cells (p=0.001), as compared to the decrease see in the frequency of the CD4+ Teff cells (p=0.001). Significant increase in T-regulatory cells populations in the PBMC-ECV co-culture conditions was observed (p=0.01). The effect of patient-derived serum ECVs on PBMCs in vitro are ongoing but have revealed differences in ECV secretion capacity within BC subtypes (TNBC, HER2+, ER+ ECVs). Functional validation of our preclinical results is awaited.

Conclusions

These results suggest that BC cells utilise ECVs to tame immune cells to promote an immunosuppressive microenvironment. The skewed maturation phenotype of T-cells following ECVs stimulation with increase in Tcm-cells suggest an accelerated maturation of naive T-cells. These reported differences in the immunomodulatory function of ECVs require further investigation.

P56

New Dextramer technology for T-cell epitope profiling, and single cell deep phenotyping using DNA barcodes, transcriptomic and genetic sequence analysis, on single cells

Kivin Jacobsen, PhD[1], Liselotte Brix, phd[1]

[1]*Immudex, Copenhagen, Denmark*
[2]*Immudex Aps, Copenhagen, Denmark*

Background

Identification of disease-specific T-cell epitopes is key to the development of many novel vaccines and immunotherapies. Profiling disease-specific T cells, emerging during a cellular immune response e.g. in tumor development or destruction, is an important aspect of personalized immunotherapy. The epitope diversity of the human population is large, and the technologies for identifying disease-specific epitopes have been inadequate.We have developed a process in which DNA barcoded Dextramer reagents are used to simultaneously screen for hundreds, or potentially thousands, of T-cell epitopes in a few milliliters of blood. Single cell deep phenotyping is quickly emerging, analyzing both cellular proteins, transcriptome and genetics of single cells by sequence analysis.DNA barcoded Dextramer reagents extend these technologies, to include simultaneous analysis of antigen specific T cells, by single cell sequencing.

Methods

We present a process in which DNA barcoded Dextramer reagents (dCODE Dextramer, can be used to simultaneously screen for hundreds, or potentially thousands, of T-cell epitopes in one small patient sample. Similar to previously reported academic methods, CITE-seq and REAP-seq, it is now possible to combine DNA barcoded MHC Dextramer technology, with single cell analysis allowing direct correlation between the specificity of the antigen specific T cell and its cognate T cell receptor protein sequence, which has not been possible with existing technologies.

Results

Profiling of antigen-specific T cells, by simultaneous

detection of a large numbers of T-cell specificities in the same small cell sample, was performed using DNA barcode MHC Dextramer analysis, followed by mass sequencing. Pools of 50 MHC Dextramer reagents was screened on PBMC samples from human donors, and the analysis could identify relevant antigen-specific T-cell populations. The results were confirmed by Dextramer analysis using conventional fluorochrome based flow cytometry.

Conclusions

DNA Barcoded Dextramer reagents in large libraries, allows for, high-throughput screening of antigen-specific T cells in limited sample material.DNA Barcoded Dextramer, together with single cell sequencing technology, can be used for deep T cell phenotyping by barcode sequencing and transcriptomic or genetic sequence analysis, on the single cell level.

P57

A rapid multi-color fluorescence imaging on frozen tissues

Dinesh Jaishankar, PhD[1], Cormac Cosgrove, PhD[2], Caroline Le Poole[2]

[1]*Northwestern University, Chicago, IL, USA*
[2]*Feinberg School of Medicine, Chicago, USA*

Background

Immunofluorescence (IF) imaging is a commonly performed routine technique. To detect >four molecules that identify different cell types in a single image, multiplex imaging techniques now exist wherein the fluorophores are spectrally separated to avoid overlap [1]. Quantitative multispectral imaging on tissues can provide a wide range of information ranging from predicting response rates of immunotherapies to immune monitoring [2]. Current techniques to perform multispectral imaging are tedious, require expensive kits, and have been developed with paraffin-embedded sections in mind. Here, using readily available fluorophore-conjugated antibodies, and a rapid IF staining protocol, we imaged up to six different colors in a frozen mouse spleen section.

Methods

8μm sections of a naïve and frozen mouse spleen were cut, acetone fixed, and stored at -20oC until the staining process. An antibody cocktail comprising of primary-labeled antibodies to CD3, CD8, CD19, CD11b and CD206 was made. For the staining, sections were blocked using the Superblock, incubated with the antibody cocktail for 1hr at RT and coverslips were added with Prolong Diamond mounting medium. The DAPI stain was used to stain the nuclei. Single color and unstained slides were also processed the same way. Image acquisition, under 20x objectives, and the multispectral imaging analysis was performed on the Vectra 3.0 from Perkin Elmer.

Results

Using the spectral library generated from the single stained and unstained slides, the multispectral imaging analysis revealed the detection of six different colors on the frozen section.

Conclusions

For the first time, we show a rapid and easy method of detecting different markers on a single frozen tissue section. This method has great potential for immune monitoring studies to measure the number and colocalization of immune and target cells.

Acknowledgements

We would like to thank Ryan Deaton, the imaging specialist at the University of Illinois at Chicago for helping with the multispectral imaging.

P58

The use of low-coverage sequencing of cell-free DNA for monitoring response to immune checkpoint inhibitors throughout treatment

Taylor Jensen, PhD[1], Aaron Goodman[2], Shumei Kato, MD[2], Mina Nikanjam[2], Christopher Ellison[1], Gregory Daniels, MD, PhD[2], Lisa Kim, MS[2], Kimberly Kelly, MS[1], Kerry Fitzgerald, PhD[1], Erin McCarthy[1], Prachi Nakashe, MS[1], Amin Mazloom[1], Graham McLennan, MS[1], Daniel Grosu, MD, MBA[1], Mathias Ehrich[1], Razelle Kurzrock, MD[2]

[1]Sequenom, a LabCorp company, San Diego, CA, USA
[2]University of California San Diego, San Diego, CA, USA

Background
Immune checkpoint inhibitors continue to revolutionize the cancer treatment paradigm. It has been observed that even some patients with advanced, refractory malignancies achieve durable responses; however, only a minority of patients benefit, demonstrating the importance of developing new biomarkers to predict and/or monitor patient outcome. While markers including PD-1/PD-L1 expression, microsatellite instability, and tumor mutational burden have been shown to have varying degrees of predictive power, they are not the ideal markers to monitor and differentiate response during treatment. Interrogating cell-free DNA (cfDNA) isolated from plasma (liquid biopsy) provides a promising noninvasive method for monitoring response.

Methods
Whole blood was collected in Streck BCT tubes and plasma subsequently separated using centrifugation. cfDNA was isolated from 4 mL of plasma using an automated process and used to prepare sequencing libraries. The total amount of cfDNA isolated from each plasma sample was quantified using droplet digital PCR. All sequencing libraries were then subjected to low-coverage, genome-wide sequencing using illumina HiSeq2500 instruments, generating a median of 35.4 million reads (~0.3X genomic coverage). A newly developed metric – the Genome Instability Number (GIN) – was utilized to measure and quantify the cumulative abundance of copy number alterations (CNAs) present in the cfDNA and additional algorithms were applied to identify the genomic loci containing CNAs.

Results
A series of 477 plasma aliquots prospectively collected at various time points throughout the treatment of 98 cancer patients receiving immunotherapy was measured in this study. These data built on previous results to further describe how the GIN can be used to discriminate clinical response from progression, differentiate progression from pseudoprogression, and identify hyperprogressive disease, as early as 4-6 weeks after treatment initiation. In addition, the cfDNA profiles of a small cohort of melanoma patients were evaluated at frequent intervals shortly after the initiation of checkpoint inhibitor therapy to better identify response kinetics. Finally, CNAs across the genome were analyzed to determine whether specific genes or genomic regions were associated with patient response to checkpoint inhibitors.

Conclusions
These data suggest that low coverage, genome-wide sequencing of cfDNA may have utility for monitoring response to immunotherapy in cancer patients.

Ethics Approval
This study was performed and consents were obtained in accordance with UCSD Institutional Review Board guidelines for specimen collection and data analysis (NCT02478931) and for any investigational treatments.

P59

Assessment of consistency of multiplex fluorescent immunohistochemistry data across multiple users utilizing different quantitative analysis strategies

Shawn Jensen, PhD[1], Carmen Ballesteros Merino, PhD[1], Sebastian Marwitz[1], Nikhil Lonberg, HSDG[1], Bernard A. Fox, PhD[1]

[1]Robert W Franz Cancer Center, Earle A Chiles Research Institute, Portland Providence Medical Center, Portland, OR, USA

Background

Tools that facilitate examination of the tumor microenvironment in cancer patients who either respond or do not respond to treatment are informative to the future design of immunotherapeutic strategies. Multiplex fluorescent immunohistochemistry (mIHC) is a technique enabling examination of the number and location of cells within the tumor microenvironment. Recently, we described the Cumulative Suppression Index (CSI), which examines the number of $CD8^+$ T cells in the invasive margin of tumor combined with the number of $FoxP3^+$ or $PD\text{-}L1^+$ cells within 30 um of $CD8^+$ T cells[1]. This CSI correlated with overall survival in a cohort of 119 patients with HPV^- oral squamous cell cancer. Future application of the CSI will require reliable analysis methods with minimal variation across studies and users to enable comparative analysis. In this current study, we systematically compared the reliability of three different methods of enumerating cellular phenotypes of mIHC images across multiple users.

Methods

Primary tumors obtained from oral squamous cell cancer patients were sectioned and stained with antibodies to CD3, CD8, FoxP3, CD163, and PD-L1. Nine representative images were collected from one patient and analyzed using either commercial phenotyping software based on machine-learning to phenotype cells (C), commercial phenotyping software coupled with a Thresholding method (C+T), or the Thresholding method alone (T). Multiple independent users analyzed the same nine images determining the number of $CD3^+$ $PD\text{-}L1^-$, $CD3^+PD\text{-}L1^+$, $CD8^+PD\text{-}L1^-$, $CD8^+PD\text{-}L1^+$, $FoxP3^+$, $CD163^+PD\text{-}L1^-$, $CD163^+PD\text{-}L1^+$, or $PD\text{-}L1^+$ cells using each of the three methods.

Results

Analysis of the variation within each user across the three different analysis methods demonstrated tight correlation for the principle phenotypes of the CSI, namely $CD8^+PD\text{-}L1^-$, $CD8^+PD\text{-}L1^+$, $FoxP3^+$, and $PD\text{-}L1^+$ cells (Spearman Rank Correlation $p<0.05$). $CD163^+PD\text{-}L1^{+/-}$ cells and $CD3PD\text{-}L1^{+/-}$ cells showed a correlation in only a fraction of the users which was partially influenced by low cell counts in a portion of those cellular phenotypes. More importantly, examining the reproducibility of data between users using the intraclass correlation coefficient demonstrated consistency across all phenotypes for all users using either the C+T or T methods ($p<0.05$).

Conclusions

Comparative analysis of mIHC data between multiple users requires confidence in a reproducible and consistent method for data analysis. These data demonstrate that C+T or T methods of analyzing data minimize inter-user variation when using the CSI mIHC panel tested in this study.

References

1. Feng Z, et al. Multiparametric immune profiling in HPV- oral squamous cell cancer. *JCI Insight.* 2017;2(14):e93652.

P60

Circulating tumor DNA assessment in plasma samples collected in Atezolizumab versus docetaxel in subjects with previously treated non-small-cell lung cancer (OAK) study

Yuqiu Jiang, PhD[1], Namrata Patil, PhD[2], Johnny Wu[1], Wei Zou[2], Stephanie Yaung[1], Aarthi Balasubramanyam[1], Susan Flynn[2], Maureen Peterson[2], Eric Peters[2], Priti Hegde, PhD[2], Simonetta Mocci[2], Marcin Kowanetz, PhD[2], John Palma[1]

[1]Roche Sequencing Solutions, Pleasanton, CA, USA
[2]Genentech, South San Francisco, CA, USA

Background
Circulating tumor DNA (ctDNA) sequencing and analysis has the potential to transform clinical management of subjects with advanced NSCLC. It has been shown that mutation(s) or molecular tumor burden assessed in plasma using NGS could potentially serve as disease monitoring tool or therapy response predictions.

Methods
In this exploratory pilot study, longitudinal plasma samples have been analyzed for presence of ctDNA in NSCLC subjects from the OAK study. 108 subjects were selected based on their clinical response profiles of early and late responders, and early and late progressors. For this preliminary report, 102 baseline samples and subsequent plasma collected at C2D1, C3D1, and C4D1 were analyzed by NGS. The AVENIO ctDNA Surveillance kit** (Roche, Branchburg, NJ) were used for sequencing analysis. The Surveillance kit (200 kb size) contains 17 cancer driver genes and additional 180 frequently mutated genes in cancer. This kit is capable of detecting four mutation classes: SNVs, fusions, CNVs and InDels. Association of survivals with ctDNA level or change was interrogated with Cox regression model. Response to treatment was assessed using RECIST v1.1.

Results
102 of the 108 (94%) baseline plasma samples were successfully sequenced. All 102 (100%) samples had somatic variants detected. The most commonly mutated genes in tumors were TP53 (59/102 subjects), KRAS (21/102), APC (21/102), and NPAP1 (15/102). The median number of variants detected per subject was 7. Mutant molecules per milliliter (MMPM) was also assessed for each baseline samples. The median MMPM was 139, ranging from 1 to 1972 for these 102 samples. Survival and therapy response in relation to ctDNA level or change at different time points will be reported at the time of presentation.

Conclusions
ctDNA testing with molecular barcoded sequencing and digital background error suppression of a 197 gene panel offers high sensitivity for tumor variant detection. The study demonstrated that tumor variants can be detected in blood in pre-treatment samples using the AVENIO kit. Subsequent analysis will be performed with plasma samples collected at C2D1, C3D1, and C4D1, and reported at the time of submission.**For Research Use only; Not for diagnostic purposes.

Acknowledgements
We would like to acknowledge Dr. Dan Klass, Ph.D., Katrina Mayol, and Nasiema Wingate-Pearse for their insightful discussions.

P61

Development of an exosome / EV analysis pipeline for tumor and immune monitoring

Joshua Welsh, PhD[1], Kevin Conlon, MD[1], Milos Miljkovic, MD, MSc[1], Julia Kepley, BS[1], Jennifer Marte, BS MD[1], Jason Savage, PhD[1], Veronica Galli, PhD[1], Katherine McKinnon, MS[1], Katherine Calvo,

MD, PhD[2], Hong Zhang[1], Cynthia Masison[1], Fatima Karzai, MD[1], Fatah Kashanchi[3], Deborah Citrin[1], Steve Jacobson[4], James Gulley, MD, PhD, FACP[1], Genoveffa Franchini, PhD[1], Thomas Waldmann, MD[1], Kevin Camphausen, MD, PhD[1], Jennifer Jones, MD, PhD[1]

[1]*National Cancer Institute, Bethesda, MD, USA*
[2]*NIH Clinical Center, Bethesda, MD*
[3]*George Mason University, Fairfax, VA, USA*
[4]*NINDS, NIH, Bethesda, MD, USA*

Background

Exosomes and other Extracellular Vesicles (EVs) carry surface receptors that are characteristic of their cells of origin. Therefore, Extracellular Vesicles (EVs) have tremendous potential as non-invasive biomarkers for immunotherapy. We have developed a first-in-class pipeline to characterize EV heterogeneity and provide high-sensitivity quantification of informative EVs in biofluids before, during, and after treatment. This pipeline combines multiplex assays with high-resolution single EV flow cytometric methods together into a Mutiplex-to-Single EV Analysis (Mt-SEA) pipeline. With this pipeline, we are able to characterize a broad range of relevant EV subsets, while also accurately measuring the concentration of specific EV populations. With clinical cases, we demonstrate the performance of Mt-SEA method by confirming strong correlations of liquid biopsy EV repertoires with tumor burden and responses to treatment, including an abscopal immune response following radiation. Furthermore, EV analysis with Mt-SEA may identify previously unrecognized prognostic epitopes or EVs subsets.

Methods

To evaluate the use of this pipeline in an exploratory clinical cohort, we evaluated EVs from plasma samples of Adult T Cell Leukemia/Lymphoma patients receiving palliative radiation. Plasma was obtained before and after treatment. Multiplex EV capture beads were used with additional detection antibodies to identify more than 40 major EV subsets. General exosome and EV detection epitopes included CD63, CD9, and CD81. Tumor-specific epitopes for each patient included CD4, CD5, and CD25, based on available histo-/cyto-pathology results. Next, high-resolution single EV analyses were performed with nanoFACS sorting and a prototype nanoFCM analyzer.

Results

ATLL-derived EVs were detected in each pre-treatment sample, with reduced specific ATLL-derived EV subsets concentrations at the end of treatment. Furthermore, ATLL-specific EVs from patients with progressive systemic disease prior to treatment were found to carry CD44 and other stemness-associated epitopes, consistent with increasing tumor aggressiveness. Responses to treatment that were clinically evident mirrored changes in the Mt-SEA EV profiles, and Mt-SEA identified new candidate prognostic EV profiles associated with clinical outcomes that would not have been predicted.

Conclusions

The use of EVs as clinical biomarkers requires a combination of methods to broadly characterize EVs and rigorously enumerate specific selected EV subsets. Therefore, we developed the Mt-SEA pipeline. Mt-SEA provides unexpected insights into tumor biology, and detection of tumor-associated and immune-associated EVs and detection of EV repertoire changes during treatment paves the way to future evaluation of the Mt-SEA pipeline for personalized, bio-adaptive therapies in a wider range of tumor types.

Ethics Approval

The study was approved by the NCI IRB, with NIH intramural protocol number 02-C-0064.

Consent

Written informed consent was obtained from the patient for publication of this abstract and any

accompanying images. A copy of the written consent is available for review by the Editor of this journal.

P62

A Pan-cancer view of the immune landscape in the tumor microenvironment via RNA and their potential for biomarkers in clinical trials

Wendell Jones[1]

[1]*EA Genomics / Q2 Solutions*

Background
Immune-based biomarkers are now commonly available when measuring the tumor microenvironment (TME), although many are based on immuno-histochemistry methods which sometimes have drawbacks: specificity, quantitation, variety. In addition, next-gen RNA sequencing and focused RNA assays are now much more accessible (for example, processing formalin-fixated material has a much higher degree of success) and are commonly employed in clinical trials to measure tumor activity and immune cell content in the TME.

Methods
Based on previous research [1-3] and pan-cancer information from TCGA, we have derived gene signatures for immune activity encompassing a dozen distinct subcomponents of the immune system and its response to tumor evolution. We have applied these immune signatures in multiple independent oncology datasets from the same indication and in multiple solid tumor indications (> 20) from TCGA and other sources to explain variation in disease-free and overall survival (DFS and OS). Using Cox multivariable analysis, we further have clarified the potential impact of these various immune components and tumor mutational burden (TMB) relative to therapy response and overall survival in the presence of multiple clinical covariates many of which are specific to each indication but which typically include patient age, tumor stage, and residual disease status. These signatures are available from a variety of RNA measurement platforms, including those that specialize in measuring difficult input material.

Results
The results include recognizing that the immune status, reflected in the expression-based signatures, play a large role (based on Hazard Ratio estimates) in explaining variation in survival in many indications, often having a larger potential impact than other biological factors or interventions. In addition, we show that there is often an interplay between cytotoxic and immune modulating cell activity in the TME (for example, cytotoxic lymphocytes vs. M2TAM cells) that explains much more variation than either factor by itself. We also show that these results are reproducible across multiple independent datasets for the same indication, implying they are robust. Further we show that while some indications have much commonality regarding the potential impact of specific immune components, other indications (such as pancreatic and kidney cancer) show more complex and sometimes counter-intuitive results regarding immune status which need to be explored further.

Conclusions
The results suggest relevant biomarkers for immune status that can be gleaned and developed from RNA measurements of the TME which can then be applied to clinical trials or converted into companion diagnostics as needed.

Acknowledgements
Some of the results presented are in part based upon data generated by the TCGA Research Network: http://cancergenome.nih.gov/

References
1. Newman AM, Liu CL, Green MR, Gentles AJ, Feng W, Xu Y, Hoang CD, Diehn M, Alizadeh AA. Robust

enumeration of cell subsets from tissue expression profiles. Nature methods. 2015 May 1;12(5):453-7.
2. Rőszer T. Understanding the mysterious M2 macrophage through activation markers and effector mechanisms. Mediators of inflammation. 2015;2015.
3. Bindea G, Mlecnik B, Tosolini M, Kirilovsky A, Waldner M, Obenauf AC, Angell H, Fredriksen T, Lafontaine L, Berger A, Bruneval P. Spatiotemporal dynamics of intratumoral immune cells reveal the immune landscape in human cancer. Immunity. 2013 Oct 17;39(4):782-95.

Ethics Approval
This study is a meta-analysis of data from other studies and thus did not require review by an institutional ethics board.

P63

Estimation of Microsatellite Instability (MSI) by next-generation sequencing using a novel MSI classification method

Asha Kamat, PhD[1], Sameh El-Difrawy[1], Annie Kraitcheva[2], Alice Zheng[1], Simon Crawley[1]

[1]*Thermofisher Scientific, South San Francisco, CA, USA*
[2]*ThermoFisher.com, Carlsbad, CA, USA*

Background
Cancer-associated instabilities at microsatellite locations throughout the genome have been shown to be predictive of response to immunotherapy treatment.Here, we describe an NGS-based method to assess Microsatellite Instability (MSI) status in tumor-only and tumor-normal samples utilizing Ion AmpliSeq™ HD technology and an Ion GeneStudio™ S5 next-generation sequencer.

Methods
We have identified optimal chemistry and developed a novel algorithm to assess MSI status of samples using a large number of markers on an Ion GeneStudio S5™ Series sequencer. The diverse marker set includes monomers that vary in length between 10 BP and 40 BP in addition to di- and tri-nucleotide STR markers. The algorithm works with tumor-only or tumor-normal samples. Each sample is assigned an MSI score based on features that measure MSI response of markers in the assay.

Results
Combining a groundbreaking AmpliSeq™ HD workflow and a novel analysis method, we developed an assay that utilizes a diverse set of MSI markers. We evaluated performance of the assay and algorithm with a set of 50 samples including CRC, Endometrial and Gastric carcinomas tumor in both MSI-High and MSS status. The resulting scores were in concordance with results from capillary electrophoresis studies.

Conclusions
A next-generation sequencing based assay using multiple markers was developed to assign MSI status to tumor samples with great precision. The accuracy of the assay was validated using an orthogonal test. MSI status can be assigned using tumor-only or tumor-normal samples.

P64

Evaluation of PD-L1 and IRF-1 expression on circulating tumor cells as a predictive biomarker of checkpoint inhibitor response

Laura Kennedy, MD PhD[1], Lance U'Ren, DVM, PhD[2], Yao Sun[2], Petros Grivas, MD, PhD[1], Laura Chow, MD[1], Vijayakrishna Gadi, MD, PhD[1]

[1]*University of Washington, Seattle, WA, USA*
[2]*Rarecyte, Inc., Seattle, WA, USA*

Background
PD-1 CPI therapy can generate durable responses

with fewer side effects compared to conventional cytotoxic chemotherapy. Unfortunately, CPI can induce an objective response in less than 15 - 20% of non-melanoma solid tumor patients [1-3]. Multiple biomarkers have been evaluated as potential factors predicting response, but none has shown reproducible clinical utility across tumor types. Higher PD-L1 expression in tumor tissue is associated with higher response rates, but a single tumor tissue sample may not reflect spatial and temporal variability in PD-L1 expression. Circulating tumor cells can be collected at multiple timepoints with minimal risk and may provide a more comprehensive and dynamic view of tumor heterogeneity. Higher IRF-1 expression in tumor tissue has been correlated with longer progression-free survival (PFS) in metastatic melanoma patients treated with CPIs [4]. We hypothesize that evaluating both PD-L1 and IRF-1 expression on CTCs may better predict patient response to PD-1 CPIs.

Methods

Patients with metastatic solid tumors receiving de novo CPI alone or in combination with other treatments are eligible. Patients undergo peripheral blood collection for CTC evaluation at 3 timepoints: prior to receiving the first dose of CPI, prior to the second dose of CPI, and 3-6 months after starting therapy or at the time of CPI discontinuation. PFS is defined as time between initiation of therapy and progression or death of any cause, with patients censored at the time of last follow up. To isolate CTCs from peripheral blood, we use the AccuCyte® kit to create slides and a Ventana Discovery Ultra autostainer to stain the slides with a pancytokeratin (CK)/EpCAM antibody cocktail, anti-CD45, and a nuclear dye. Using the CyteFinder® software, CTCs are identified by positive staining for CK/EpCAM and negative staining for CD45. PD-L1 and IRF-1 expression are determined using mean fluorescence intensity (MFI) in computationally estimated cell compartments.

Results

To optimize the assay, low and high PD-L1/IRF-1 were created by spiking A549 cells cultured with or without 10 ng/mL interferon-gamma into whole blood (Figure 1). We will present progression-free survival data and corresponding CTC data for the first set of patients enrolled. A number of these patients have tumor tissue samples with varying degrees of PD-L1 expression by IHC, which will allow correlation between tumor tissue and CTC PD-L1 expression.

Conclusions

CTC PD-L1 and IRF-1 expression may provide a more comprehensive predictive biomarker for patients starting PD-1/PD-L1 CPIs.

Acknowledgements

We would like to thank the patients and providers of the Head/Neck/Lung Oncology group, the Genitourinary Oncology group, the Gastrointestinal Oncology, and the Breast Oncology group at the Seattle Cancer Care Alliance for participating in this trial. We would like to thank Alisa Clein for assistance with clinical research coordination.

References

1. Borghaei H, et al. Nivolumab versus docetaxel in advanced nonsquamous non-small-cell lung cancer. New England Journal of Medicine. 2015;373:1627-1639. 2. Powles T, et al. Atezolizumab versus chemotherapy in patients with platinum-treated locally advanced or metastatic urothelial carcinoma (IMvigor211): A multicentre, open-label, phase 3 randomised controlled trial. Lancet. 2018;391:748-757. 3. El-Khouiery A, et al. Nivolumab in patients with advanced hepatocellular carcinoma (Checkmate 040): An open-label, non-comparative, phase 1/2 dose escalation and expansion trial. Lancet. 2017; 389:2492-2502.4. Smithy J, et al. Nuclear IRF-1 expression as a mechanism to assess “capability” to express PD-L1 and response to PD-L1 therapy in metastatic melanoma. J Immunother Cancer. 2017;5:25.

Ethics Approval
This study was approved by the Fred Hutchinson Cancer Research Center Institutional Review Board, Committee D, Protocol #10031.

Figure 1.

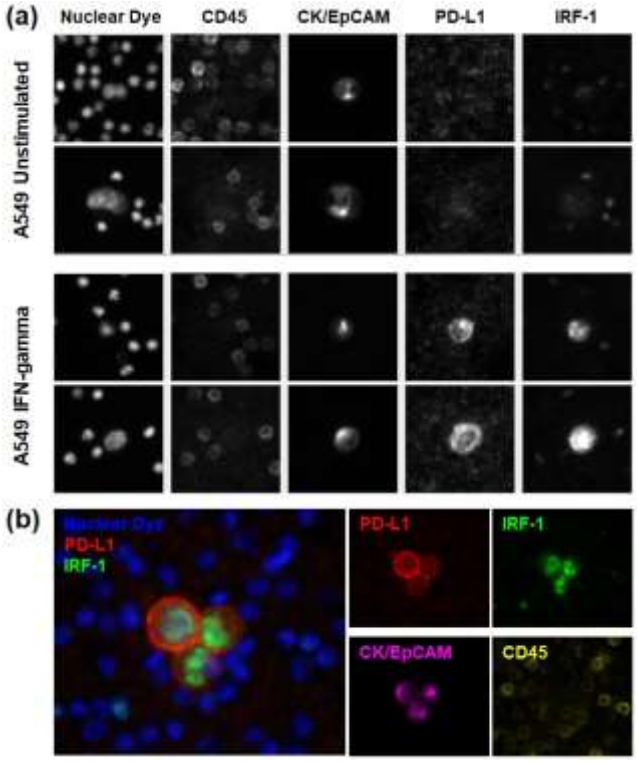

P65

IDO/HLA-DR expression and tumor mutational burden are complementary predictive biomarkers of anti-PD-1 immunotherapy in squamous cell carcinoma of the head and neck

Arun Khattri, PhD[1], Ju Young Kim[2], Riyue Bao, PhD[3], Rajesh Acharya[3], Yi-Hung Carol Tan, PhD[3], Rom Leidner, MD[4], Hisham Mehanna, PhD[5], Nathan Roscoe[6], Christine Vaupel, PhD[6], Naveen Dakappagari[6], Tanguy Seiwert, MD[3], Sara Kochanny, BA[7]

[1]*Department of Medicine, The University of Chicago, Chicago, IL, USA*
[2]*Navigate Biopharma Services, Inc., Carlsbad, CA, USA*
[3]*The University of Chicago, Chicago, IL, USA*
[4]*Providence, Portland, OR, USA*
[5]*Institute of Cancer and Genomic Sciences, Birmingham, UK*
[6]*Navigate Biopharma, Carlsbad, CA, USA*
[7]*University of Chicago, Chicago, IL, USA*

Background
Background: PD-1 checkpoint blockade is active in squamous cell carcinoma of the head and neck (SCCHN) (e.g. Seiwert et al, Lancet Oncol, 2016). Biomarkers such as PD-L1 immuno-histochemistry (IHC) and markers of the T-cell inflammation (e.g. Interferon-γ gene signature, INF-G) identify tumors more likely to benefit from treatment. However, both protein- and genomic markers have not been concurrently examined to identify an ideal combination of predictive markers in SCCHN.

Methods
Methods: Pretreatment formalin-fixed paraffin-embedded biopsies of 82 anti-PD-1 treated recurrent/metastatic SCCHN patients were studied for key immune resistance markers, namely, PD-L1 (tumor, stroma, PD-1/PD-L1 interaction), Myeloid suppressor cells (CD11b/IDO1/HLA-DR/ARG1) and regulatory T cells (CD4/CD8/CD25/FOXP3/Ki67) by combining multiplexed immunofluorescence (IF) and novel quantitative spatial imaging algorithms via AQUA® (Automated Quantitation Analysis) technology. Concurrently, INF-G gene signature was assessed by RNA-seq and tumor mutational burden (TMB) via exome sequencing (or if not available 1000-gene panel-sequencing (OncoPlus)). Correlations with overall survival (OS) and progression free survival (PFS) were performed using optimized cut points.

Results
Results: Stromal PD-L1 level was more predictive of survival than tumor PD-L1 level or PD-1/PD-L1

interaction score (OS, p=0.039; PFS p=0.019). However, tumor- IDO1/HLA-DR expression was most predictive of survival (OS, p=0.0005, HR = 0.4; PFS, p=0.0015, HR = 0.42), outperforming PD-L1 and INF-G signature. The markers remain significant after adjusting for HPV status in the multivariate model. TMB (using a previously established cutpoint of 175mt/exome=10mt/MB) was also associated with PFS in the overall population (OS, p=0.13; PFS, p=0.016), but TMB performed much better in HPV(-) SCCHN (OS, p=0.0083; PFS, p=0.043). Interestingly, IDO1/HLADR expression and TMB were only weakly correlated (r=0.20, P=0.078). Four distinct subgroups of tumors were identified using this combination with the combined IDO1/HLA-DRhi + TMBhi group having 60% OS plateau. HPV (+) patients had significantly higher levels of IDO1/HLADR expression in their tumors compared with HPV(-) patients (p<0.0001). Unique biologic characteristics of each of the four subgroups were also identified.

Conclusions

Conclusions: Our results show that IDO1/HLADR expression by tumor cells is highly predictive of outcome in SCCHN patients treated with anti-PD-1 therapy. TMB provides distinct and complementary predictive information and performs particularly well in HPV(-) tumors. The combined IDO/HLA-DR – TMB analysis identifies unique subgroups of patients, which are relevant for combination drug development as well as potential clinical care after further prospective validation.

References

1. Seiwert TY, Burtness B, Mehra R, Weiss J, Berger R, Eder JP, Heath K, McClanahan T, Lunceford J, Gause C, Cheng JD, Chow LQ. Safety and clinical activity of pembrolizumab for treatment of recurrent or metastatic squamous cell carcinoma of the head and neck (KEYNOTE-012): an open-label, multicentre, phase 1b trial. Lancet Oncol. 2016 Jul;17(7):956-965.

Ethics Approval

The study was approved by the IRB of the University of Chicago (IRB# 8980)

Consent

Written informed consent was obtained from the patient for publication of this abstract and any accompanying images. A copy of the written consent is available for review by the Editor of this journal

P66

Evaluation of Immune – related Markers in circulating proteome and their association with atezolizumab efficacy in patients with 2L+ NSCLC

Marcin Kowanetz, PhD[1], Ning Leng[1], Joanna Roder, PhD[2], Carlos Oliveira, PhD[2], Senait Asmellash, PhD[2], Krista Meyer, PhD[2], Heinrich Roder, DPhil[2], Marcus Ballinger, PhD[1], David Shames, PhD[1]

[1]*Genentech, South San Francisco, CA, USA*
[2]*Biodesix, Steamboat Springs, CO, USA*

Background

Anti-PD-L1/PD-1 therapy has become a standard of care in NSCLC. However, understanding of the biological mechanisms of treatment efficacy and resistance is still incomplete. Here we examine the role of the circulating proteome in 2L+ NSCLC patients treated with atezolizumab (anti-PD-L1).

Methods

Using expression data for the circulating proteome from mass spectrometry of pre-treatment serum samples collected from 77 patients with NSCLC treated with atezolizumab (atezo) in a single arm Phase 1a study (NCT01375842) (development cohort) and machine learning methods, a test was developed to classify patients into “Good” and “Poor” prognosis groups. Protein set enrichment analysis (PSEA) was used to compare the underlying biology of classification of Good and Poor

phenotypes. Blinded pre-treatment serum samples from 270 patients treated with atezo or docetaxel (doc) in the randomized Phase 2 study POPLAR (NCT01903993) were subsequently used for validation.

Results

The test stratified patients treated with atezo in the development cohort by overall survival (OS) (Good vs. Poor prognosis HR=0.23, p <0.001) and progression-free survival (PFS) (Good vs. Poor prognosis HR = 0.52, p = 0.012). PSEA identified trends in association of increased complement activation, acute inflammation and immune response type 2 in the Poor classification phenotype. In the blinded analysis of the validation cohort (POPLAR), 262 samples (97%) passed QC, and 134 (51%) were classified to the Good prognosis group. In the validation cohort, OS and PFS were associated with atezo efficacy compared to doc in the Good but not in the Poor prognosis group, with unadjusted classifier-treatment interaction p-value 0.005 for PFS and interaction p-value 0.001 for OS (Figure 1).

Conclusions

Patients characterized by complement activation, acute inflammation and immune response type 2 markers in their baseline serum appeared to derive less benefit from atezolizumab. The analysis of circulating-proteome-defined phenotypes may help to better understand the biological mechanisms beyond response and resistance to checkpoint inhibition in cancer patients.

Trial Registration

NCT01375842, NCT01903993

Figure 1.

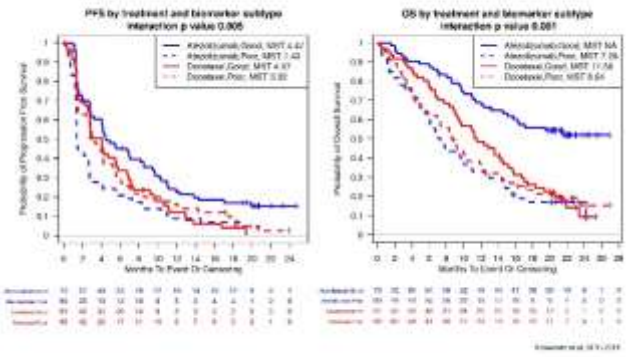

P67

Innovative combinatorial approach to characterize the immune landscape and analyze the tumor response after anti-PD-1 blockade in a 3D ex-vivo tumoroid system of non-small cell lung cancer

Melba Marie Page, PhD[1], Melanie Mediavilla-Varela, PhD[1], Jenny Kreahling, PhD[1], Soner Altiok, MD, PhD[1]

[1]*Nilogen Oncosystems, Tampa, FL, USA*

*Corresponding author email: melanie@nilogen.com

Background

Cell lines and mouse models have provided valuable information in understanding the tumor microenvironment. The overall success in translating these results to the clinic is less than 10% and lacks the full complexity of the tumor microenvironment. Understanding these greater complexities is critical to the development of immuno-oncology therapies. Nilogen Oncosystems' proprietary 3D-EXSM ex vivo drug screening platform analyzes fresh patient tumor tissue that remains embedded in its natural environment as a tumoroid. This approach includes a powerful combination of confocal image analysis, flow cytometry analysis, cytokine assays as well as

gene expression analysis. With this model, we can visualize response, phenotype the tumor microenvironment and accurately determine the response to checkpoint inhibitors in non-small cell lung cancer (NSCLC) and correlates can be found among different platforms.

Methods
For the 3D-EX vivo platform, tumoroids were shaped from procured fresh tumor tissue from NSCLC cancer patients. They were then treated with Keytruda ex-vivo and treatment-mediated changes in TIL subpopulations were analyzed using confocal analysis, flow cytometric analysis, cytokine release by Bio-Rad's 17-plex cytokine assay as well as gene expression by NanoString's 770 gene Immune Panel.

Results
Ex vivo treatment of the 3D tumoroids with Keytruda, showed significant changes in T-cell activation and immune cell populations in 26% of NSCLC tumors. This was observed by the simultaneous increase in IFN-γ and TNF-α upon cytokine analysis. Furthermore, we found a differential expression of signature genes such as CD8, CXCL10, CXCL9, EOMES, Granzyme A/B, IFN-γ, related to T-cell subpopulations via Nanostring analysis, which was accompanied by an increase in Granzyme B via flow cytometry. Confocal imaging analysis allowed detection of immune cell mediated killing of tumor cells upon ex-vivo drug treatment.

Conclusions
The positive and negative associations between expression of immune function genes, TIL activation, and cytokine production by ex-vivo treatment shows that Nilogen Oncosystems' 3D-EXSM platform can accurately recapitulate the tumor microenvironment. This comprehensive approach including the powerful visualization by confocal analysis provides profound technological advantages in analyzing the tumor immune microenvironment. With this combinatorial approach, the 3D-EXSM platform delivers a better understanding of the mechanism of action of immuno-oncology drugs that may aid in developing biomarkers that can be used for patient selection.

P68

Using high dimensional mass cytometry (CyTOF) and machine assisted analysis to detect biomarkers in the immunotherapy of cancer

Carsten Krieg, PhD[1], Silvia Guglietta[1], John Wrangle, MD[1], Luis Cardenas, BS[1], Mitchell Levesque[2], Reinhard Dummer, MD[2], Burkhard Becher[3], Mark Rubinstein, PhD[1], Mark Robinson[4]

[1]*Medical University of South Carolina (MUSC), Charleston, SC, USA*
[2]*University Hospital Zurich, Zurich, Switzerland*
[3]*University Zurich, Zurich, SC, Switzerland*
[4]*University Zurich (IMLS), Zurich, Switzerland*

Background
Immunotherapy has created a lot of enthusiasm in oncology but, as not all patients respond, it becomes evident that the strategy "one drug fits all" is not applicable to all patients and all cancers. Therefor, selection of patients benefiting from mono-immunotherapy, combination therapy or advice on which drug to use on therapy, ideally by biomarker, is in high demand.

Methods
Here we approached the problem by designing a customized workflow by using high-dimensional single cell mass cytometry combined with machine-learning bioinformatics for the in-depth characterization of single immune cells in predicting and monitoring immune responses. The analysis is data driven, can be adapted to high throughput approaches and can model arbitrary trial designs such as batch effects and paired designs. We tested our workflow on two studies:

Results

a) Predict response to anti-PD-1 immunotherapy in melanoma. In our discovery cohort peripheral blood mononuclear cells (PBMCs) from 20 patients with stage IV melanoma before and 12 weeks on anti-PD-1 therapy was analyzed. We observed a clear T cell response on therapy. The most evident difference in responders before therapy was an enhanced frequency of CD14+ CD16+HLA-DRhi classical monocytes. We validated our results using conventional flow cytometry in an independent exploratory cohort of 31 patients before therapy. Finally, we correlated enhanced monocyte frequencies before therapy initiation with clinical response and could show association with lower hazard, extended progression-free and overall survival.b) Monitoring the immune response in non small cell lung cancer patients refractory to anti-PD-1 immunotherapy treated with a novel combination immunotherapy of anti-PD-1 and an IL-15 superagonist. 21 patients with non small cell lung cancer who got refractory to anti-PD-1 treatment received a novel combination therapy of IL-15 superagonist plus anti-PD-1. A response in the CD8+ T cell compartment was observed characterized, among other factors, by expansion of TCR variety. Unexpected we observed a strong expansion of effector NK cells starting around day 4 of therapy.

Conclusions

Taken together, high throughput mass cytometry together with an unbiased artificial intelligence driven analysis workflow might support patient selection prior to therapy, select the right drug combination and identify new drugable cell populations.

Ethics Approval

These studies have been approved by the University of Zurich and Medical University of South Carolina Ethics Boards.

P69

Simultaneous quantification of activated immune cells and PD-L1 expressing circulating tumor cells (CTCs) in peripheral blood of cancer patients receiving checkpoint inhibitor therapy

Rachel Krupa, BS[1], Robin Richardson[1], Priscilla Ontiveros[1], Joseph Schonhoft[1], Yipeng Wang, PhD, MD[1], Jiyun Byun, MS[1], David Lu[1], Aaron Oh[1], Sean Nisperos[1], Mark Landers, MS[1], Ryan Dittamore, MS[1]

[1]*Epic Sciences, San Diego, CA, USA*

Background

Expression of PD-L1 on tumor and tumor infiltrating lymphocytes has been associated with improved response to PD-1 and PD-L1 checkpoint inhibitors, however clinical utility is limited. Multimodal characterization of both the tumor and host immune system is an unmet medical need for the improved prediction of response to immunotherapy. Metastatic lesions are likely to be under-sampled by biopsy given tumor heterogeneity, clonal evolution, and temporal changes in the host immune system under therapeutic pressure. Therefore, we sought to expand the existing Epic Sciences' non-invasive liquid biopsy platform to simultaneously examine expression of PD-L1 on circulating tumor cells (CTCs) as well as quantify changes in activated immune cell populations from a single sample in patients undergoing checkpoint inhibitor therapy. Examining dynamic biomarker changes both prior to and on therapy could yield novel diagnostic tools for response prediction and pharmacodynamics response for immunotherapy.

Methods

Blood samples from bladder, kidney, and prostate cancer patients undergoing checkpoint inhibitor therapy were collected at baseline and on-therapy (when available). Contrived samples were developed using cancer cell lines and healthy donor (HD) blood.

Red blood cells were lysed and nucleated cells were plated onto glass slides and stained with DAPI and immune panels including pan-CK, CD45, PD-L1, CD4, CD8, and Ki-67. Approximately 3 million cells per slide were imaged through advanced digital pathology pipelines to detect and quantify changes in immune cell populations and to assess circulating tumor burden.

Results
An immuno-panel was developed to profile activated (CD8+Ki-67+ and CD4+Ki-67+) leukocyte subpopulations and PD-L1+ CTCs from a single blood sample. Feasibility was demonstrated in cell lines, HD, and patient blood. CTCs were detected in 76% (32/42) of samples tested. Of the 25 baseline samples tested, 12% (3/25) had PD-L1+ CTCs detected. No PD-L1+ CTCs were detected in the 13 on-therapy samples tested. Of 14 patients with matched samples, 50% (7/14) patients had an increase in activated CD4+ leukocytes and 14% (2/14) patients had an increase in activated CD8+ leukocytes in on-therapy samples compared to baseline. A decrease in activated CD4+ leukocytes was observed in 7% (1/14) patients and a decrease in activated CD8+ leukocytes was also observed in 7% (1/14) patients with therapy.

Conclusions
Development of a liquid biopsy based platform that can simultaneously measure immune biomarkers in CTCs and leukocytes will allow for real time assessment and monitoring of response to immune checkpoint inhibitors and may lead to novel diagnostic tools for response prediction.

P70

CD4+FOXP3+ regulatory T cells in the periphery of HNSCC patients demonstrate high phenotypic diversity depending on Treg subtype

Cornelius Kürten, MD[1], Shanhong Lu[2], Tullia Bruno, PhD[3], Robert L. Ferris, MD, PhD[3]

[1]*University of Essen, Essen, PA, Germany*
[2]*Centre South University, Pittsburgh, PA, USA*
[3]*University of Pittsburgh, Pittsburgh, PA, USA*

Background
Regulatory T cells (Treg) promote immune escape and are a putative biomarker for response to immunotherapy. Indeed, previous data from our group demonstrated that Ki67+ Treg were elevated in head and neck cancer (HNSCC) responders to nivolumab (CheckMate-141). Importantly, phenotypic markers for different subsets of Treg have been described: naïve Treg (nTreg, CD45RA+FOXP3low), effector Treg (eTreg, CD45RA-FOXP3high) and non-suppressive Treg (nsTreg, CD45RA-FOXP3low). While these populations have been described in peripheral blood lymphocytes (PBL) and tumor-infiltrating lymphocytes (TIL) of cancer patients, the presence of suppressive eTreg in the blood is a biomarker for disease progression in HNSCC patients. Thus, a more detailed characterization of this cell population is warranted.

Methods
Multi-parameter flow cytometry (CD8, CD4, CD45RA, FOXP3, Neuropilin-1, CD39, PD-1, Tim-3, LAG-3, CTLA-4, TIGIT, CD69, pAKT, Ki67, Bcl2) was performed on PBL from HNSCC patients (n = 50). T cell function was assessed using intracellular staining for cytokine production (IFNy, TNFa) after a 4 hour stimulation with PMA/Ionomycin. Findings were correlated with patient demographics and clinical outcome.

Results
A higher percentage of eTreg express inhibitory receptors (IRs) (two-way ANOVA: PD-1: mean diff. 22%, $p < 0.0001$; Tim-3: mean diff. 15 %, $p < 0.01$; CTLA-4: mean diff. 13 %, $p < 0.05$; TIGIT: mean diff. 26 %, $p < 0.0001$; CD39: mean diff. 40 %, $p < 0.0001$) compared to naïve/non-suppressive Treg population.

IR expression correlated highly on eTreg (Spearman correlation e.g. for PD-1 with Tim-3 r2 = 0.70, PD1 with TIGIT r2 = 0.72, PD-1 with CD39 r2 = 0.82, all $p < 0.0001$), but not on the non-effector Treg. Interestingly, proliferative eTreg (measured by Ki67 expression) were strongly associated with better survival (Hazard Ratio: 0.29, $p < 0.05$).

Conclusions

eTreg are a distinct cell subtype in HNSCC, as shown by their differential expression of IRs and proliferation/activation markers. The higher IR expression suggests that eTreg are an important target of currently available immunotherapy drugs among the whole Treg population. This also underscores the putative value of this cell subset as a biomarker of response to monitor longitudinally during anti-PD-1 immunotherapy.

P71

Characterization of tumor mutational burden (TMB) and homologous recombination repair (HRR) mutations to assess correlation with immune checkpoint inhibitors (ICIs) response in renal cell carcinoma

Matthew Labriola, MD[1], Jason Zhu, MD[2], Rajan Gupta[1], Shannon McCall, MD[1], Jennifer Jackson, PhD[3], James White, PhD[3], Elizabeth Weingartner[3], Eric Kong[3], Peter Simone, PhD[4], Eniko Papp, PhD[3], Kelly Gerding, PhD[3], Eun-Hae Kim, PhD[3], John Simmons, PhD[3], Daniel George, MD[2], Tian Zhang, MD[2]

[1]*Duke University Hospital, Durha, NC, USA*
[2]*Duke Cancer Institute, Durham, NC, USA*
[3]*Personal Genome Diagnostics, Baltimore, MD, USA*
[4]*Pesronal Genome Diagnostics, Baltimore, MD, USA*

Background

The advent of immune checkpoint inhibitors (ICI) has revolutionized the treatment landscape for patients with metastatic renal cell carcinoma (mRCC) [1,2]. However, traditional biomarkers such as PD-L1 have not served as predictive markers of treatment response. Given the risk of toxicity and variable response rates, there is a need to develop more reliable predictive biomarkers to support precision immunotherapy. High tumor mutational burden (TMB) has been previously described as a robust biomarker for predicting ICI response in metastatic melanoma [3] and non-small cell lung cancer [4], but has not yet been fully explored in mRCC. Here, we describe the prediction of clinical outcomes for mRCC patients and ICI response using a solid tissue-based next-generation sequencing (NGS) assay to identify genetic correlates and tumor mutation burden.

Methods

34 patients with mRCC who had received ICI therapy at Duke Cancer Institute were identified. FFPE tumor samples from archival tissue banks were evaluated using Personal Genome Diagnostics elioTM tissue complete investigational NGS assay, screening for somatic variants across >500 genes, as well as TMB and microsatellite status. Clinical information was extracted from the medical record and tumor response was evaluated based on RECIST 1.1 criteria.

Results

16 of 34 patients displayed disease control (overall responses of: stable disease, partial response, or complete response) following ICI therapy. This patient cohort displayed a range of TMB scores from 0.4 to 12.2 mutations/Mb (predicted whole exome equivalent), with a mean TMB score of 2.8 mutations/Mb, exome equivalent. Overall, there was no significant difference in TMB scores between responders and non-responders, and no significant correlation between increased TMB score and response to ICI was found (Figure 1). Interestingly, genes related to DNA repair pathways, particularly homologous recombination (including FAM175A, RAD50, RECQL4, and SLX4), were more often found

to be mutated in the ICI responder group compared to ICI non-responders. Of the 16 responders, 9 were found to harbor somatic mutations in at least one gene associated with DNA repair (Figure 2).

Conclusions

Overall, TMB did not appear to correlate to patient outcomes or ICI response in this mRCC patient cohort. However, NGS analysis showed an increase in somatic mutations in DNA repair genes in responders compared to non-responders. Recently, hereditary RCC syndromes have been mechanistically linked to defects in homologous recombination [5]. Our findings suggest that mutations in DNA repair pathway genes may correlate with ICI response and may have potential as a predictive biomarker for treatment success.

Acknowledgements

Study supported by research funds from Personal Genome Diagnostics (PGDx).

References

1. Motzer RJ, Escudier B, McDermott DF, et al. Nivolumab versus everolimus in advanced renal-cell carcinoma. New England Journal of Medicine. 2015; 373(19): 1803-13.
2. Motzer RJ, Tannir NM, McDermott DF, et al. Nivolumab plus ipilimumab versus sunitinib in advanced renal-cell carcinoma. New England Journal of Medicine. 2018; 378(14): 1277-90.
3. Goodman AM, Kato S, Bazhenova L, et al. Tumor mutational burden as an independent predictor of response to immunotherapy in diverse cancers. Mol Cancer Ther. 2017; 16(11): 2598-608.
4. Hellmann MD, Ciuleanu TE, Pluzanski A, et al. Nivolumab plus ipilimumab in lung cancer with a high tumor mutational burden. New England Journal of Medicine. 2018; 378(22): 2093-104.
5. Sulkowski PL, Sundaram RK, Oeck S, et al. Krebs-cycle-deficient hereditary cancer syndromes are defined by defects in homologous-recombination DNA repair. Nat Genet. 2018. Epub ahead of print.

Ethics Approval

This study was approved by Duke University's Institutional Review Board, protocol number Pro00088779.

Figure 1.

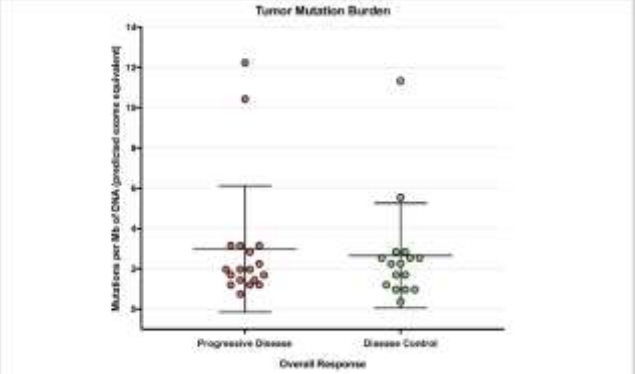

Figure 2.

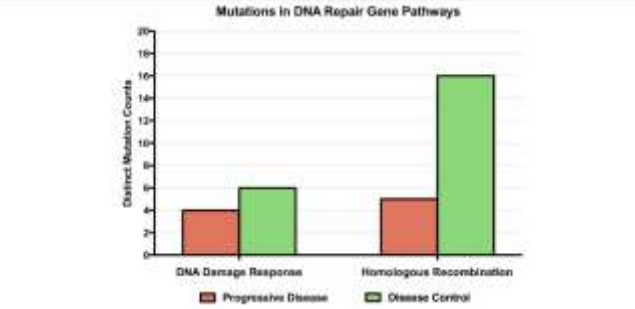

P72

Biomarker and preliminary pharmacodynamic evaluations of the PD-1 inhibitor ABBV-181 from an ongoing phase 1 clinical trial in patients with advanced solid tumors

Stacie Lambert[1], Gregory Vosganian, MD[1], Fiona Harding, PhD[1], James Sheridan[1], Stefan Englert, Dr[1],

Sara Siggelkow[1], Apurvasena Parikh, PhD[1], Betty Wang[1], Kinjal Hew[1], Jaishree Bankoti[1], Marcia Stickler[1], Eileen Lee[1], Merriam Mcclellan[1], Daniel Afar, PhD[1], Anita Reddy, PhD[1], Stacie Lambert[1]

[1]AbbVie, Inc, Redwood City, CA, USA

Background

ABBV-181 is a humanized, recombinant, modified IgG1 monoclonal antibody targeting programmed cell death 1 (PD-1). Here we present preliminary analyses of ABBV-181 pharmacodynamic (PD) data from an ongoing Phase 1 study in patients with solid tumors (NCT03000257).

Methods

Prior to initiation of clinical testing, ABBV-181 was characterized in vitro for PD-1 blocking ability and bioactivity and a PD-1 saturation assay was developed. In the ongoing Phase 1 study, patients with previously treated advanced solid tumors received ABBV-181 at 1, 3, or 10 mg/kg intravenous once every 2 weeks (Q2W) in dose escalation. Following dose finding, multi-histology, non-small cell lung cancer (NSCLC) and head and neck squamous cell cancer (HNSCC) cohorts were opened at 250 mg Q2W. PD-L1 expression was assessed on pre-treatment tumor samples (PD-L1 immunohistochemistry 28-8 pharmDx, 1% threshold). Whole blood samples were collected pre and post dosing to measure PD-1 receptor saturation and expression of Ki-67 and other biomarkers in circulating T cell populations by flow cytometry, while serum was collected pre and post dosing to measure cytokine biomarkers. Pharmacokinetic (PK) sample collections and PK-PD analyses were also conducted.

Results

In vitro characterization demonstrated that ABBV-181 blocked PD-1 binding to its ligands and increased IFNγ production in functional human and non-human primate peripheral blood mononuclear cell assays. T cells from non-human primates administered ABBV-181 showed PD-1 saturation. Preliminary clinical PD data were available for 72 patients treated with ABBV-181 (n=25 in dose escalation, n=47 in ongoing 250 mg Q2W dose expansion). PD-L1 was expressed on 32/60 (53%) available pretreatment tumor samples, with higher expression rates in the NSCLC and HNSCC cohorts compared to the multi-histology cohort. Rapid and sustained PD-1 saturation on circulating CD4 T central memory cells was observed at all ABBV-181 doses tested. A transient decrease in circulating T cell counts following dosing was also observed, consistent with prior reported clinical observations of PD-1 blocking agents. Increases in Ki-67+ CD8+ T cells within the first cycle were detected in approximately half of the tested patients. Significant increases in serum chemokines including IP-10 were also found post dosing with ABBV-181.

Conclusions

Preliminary results indicate that ABBV-181 demonstrates PD-1 receptor saturation and biological activity in peripheral blood at all clinical doses tested. PD data is consistent with the biological activities previously reported for other PD-1 blocking antibodies. Enrollment in these expansion cohorts continues at 250 mg Q2W and 500 mg once every 4 weeks as supported by ongoing PK-PD analyses.

Acknowledgements

AbbVie and the authors thank the patients participating in this clinical trial and all study investigators for their contributions.

Trial Registration

ClinicalTrials.gov, NCT03000257

Ethics Approval

This study (NCT03000257) was approved by each participating institution's Ethics Board.

P73

Analysis of survival and mRNA expressivity in the tumor microenvironment of adenocarcinoma via K-means clustering algorithm

Sunyoung Lee, MD, PhD[1], Andrew Baird, MD[3], Jillian Dolan, BS[4], Stuart Baird[5], Fateeha Furqan, MD[6], Shinyoung Park, MS[1]

[1]*Roswell Park Cancer Institute, Williamsville, NY, USA*
[2]*National Institute for Mathematical Sciences, Seoul, Korea, Republic of*
[3]*University of Pittsburgh Medical Center, Pittsburgh, PA, USA*
[4]*University at Buffalo School of Medicine, Buffalo, NY, USA*
[5]*St. Lawrence University, Canton, NY, USA*
[6]*Rochester General Hospital, Rochester, NY, USA*

Background

Stromal elements in tumor microenvironment (TME) impact the response to cytotoxic chemotherapy and immunotherapy. Advances in mRNA-sequencing have improved our understanding of TME expressivity. However, few models exist to analyze immune crosstalk between TME elements and mRNA expressivity in terms of patient survival.

Methods

mRNA-seq of 3,758 adenocarcinoma tumors and 314 non-tumor tissues (lung, breast, esophageal, gastric, colorectal, pancreatic, ovarian, endocervical, and prostate adenocarcinoma) were obtained from the Cancer Genome Atlas (TCGA) and analyzed based on mRNA expression. The mRNA expressivity of 195 genes enriched in stromal components were arranged into 26 gene groups (tables 1 and 2). Using mRNA expressivity via K-means algorithm (50 cycles of machine learning), patients were clustered into two groups (high and low mRNA expression) for each gene group. Kaplan-Meier and correlation analyses were performed to assess the significance of each gene group in survival.

Results

Genes associated with immune activation correlate with better survival until 60 (lung), 110 (breast), 50 (esophageal), and 20 months (pancreatic). There is negative correlation with survival in gastric and colorectal, no correlation in ovarian, and positive correlation in endocervical. Angiogenesis is negatively associated with survival in colorectal ($p<0.1$), lung and gastric ($p<0.05$). Genes related to desmoplasia and immunosuppressive chemokines have a significant association with poor survival in gastric, colorectal, and endocervical ($p<0.05$), as well as ovarian ($p<0.1$). Pancreatic has extensive expression of genes associated with desmoplasia and immunosuppressive chemokines, but degree of expressivity does not correlate with survival. Neutrophils are negatively associated with survival in gastric and endocervical ($p<0.05$), as well as esophageal and ovarian ($p<0.1$), but positively correlate in breast ($p<0.1$). Genes associated with cancer stem cells negatively correlate with survival in pancreatic. In prostate, expressivity of immune-related genes was low, and no correlation was found except for genes related to type II IFN, which positively correlate with survival. Patients with enhanced expression of genes associated with type I IFN and antigen presentation in tumor tissue show increased expression of these genes in their respective non-tumor tissue samples.

Conclusions

Analysis of large data was assisted by K-means (machine learning) algorithm, showing that stromal genes have varied impact on survival in adenocarcinoma. Genes associated with immune activation have temporal correlation with survival, which seems to be a result of tumor immune escape. Expressivity of type I IFN and antigen presentation in non-tumor tissues is conserved in tumor tissues. Future prospective studies in response to

chemotherapy and immunotherapy are warranted.

Table 1.

Table 1. genes associated with each gene group

Gene groups	Genes associated with gene groups
CD8+ T cells	CD8A, CD8B
B cells	CD19B, BTLA, FCRL3, BANK1, CD79A, BLK, FAIM3, FCRL1, HVCN1, BACH2
Type 1 IFN response	MX1, TNFSF10, RSAD2, IFIT1, IFIT3, IFIT2, IRF7, DDX4, MX2, ISG20
Cytolytic activity	GZMA, GZMB, GZMH, GZMK, PRF1, GNLY, SERG7, CD3E, CD247
Antigen presentation	HLA-A, HLA-B, HLA-C, B2M, TAP1, TAP2, NLRC5, PSMB8, PSMB9
IFN-stimulated cytokines	CCR5, CCL3, CCL4, CCL5, CXCL9, CXCL10, CXCL11
Th1	IFNG, IFNGR1, IFNGR2, IRF1, STAT1, IL12A, IL12B
Adhesion molecules	ICAM1, ICAM2, ICAM3, ICAM4, ICAM5, VCAM1
CD4 regulatory T cells	FOXP3, CCR4(ref3), IL2, CTLA4, IL10, GPR15, IL4
Type 2 IFN Response	GPR146, MLLP, AHR
Cancer stem cell	CD44, PROM1, EPCAM
Desmoplasia	ACTA2, COL3A1, COL1A2, PDPN, TPM1, MYH9, PDGFRA, TGFB
Immunosuppressive factors	IDO1, IDO2, DOK3, CSF2RA, CSF2RB, PDCD1, CD274, CD244, HAVCR2, LAG3, CTLA4, C1QA, C1QB, C1QC
Immunosuppressive chemokines	TGFA, PDGFA, PDGFB, MSH, FGF2, IL8, TGFB1, TGFB2, TGFB3, MDC1, HGF, FAP, VIM, LOXL2, PTGES2, HIF1A
Angiogenesis	VEGFA, VEGFB, VEGFC, MMP9
Th2	IL4, IL10, IL13, CCL17, CCL22, CCL24, AB3, CLEC7A, BTK
EMT marker	S100A4, PLAUR, TGFB1, TGFB2, TGFB3
Immune score	Geometric mean of GZMA, GZMB, PRF1, GNLY, HLA-A, HLA-B, HLA-C, HLA-E, HLA-F, HLA-G, HLA-H, HLA-DMA, HLA-DMB, HLA-DOA, HLA-DOB, HLA-DPA1, HLA-DPB1, HLA-DQA1, HLA-DQA2, HLA-DQB1, HLA-DRA, HLA-DRB1, IFNG, IFNGR1, IFNGR2, IRF1, STAT1, PSMB9, CCR5, CCL3, CCL4, CCL5, CXCL9, CXCL10, CXCL11, ICAM1, CAM2, ICAM3, ICAM4, ICAM5, VCAM1
Macrophage	FUCA1, MMP9, LGMN, HS3ST2, TM6SF19, CLEC7A, GPNMB, C11orf43, CD68, CYBB
Neutrophil	KDM6B, HSD17B11, EVI2B, MNDA, MEGF9, SELL, NLRP12, PADI4, TRAIN3, VNN3
NK cells	KLRF1, KLRC1
Plasmacytoid dendritic cells	LILRA4, CLEC4C, PLD4, P4HB, IL3RA, PTCRA, IRF8, IRF7, GZMB, CXCR3
APC co-stimulation	ICOSLG, CD70, TNFSF14, CD40, TNFSF9, TNFSF4, TNFSF11, TNFSF18, TNFSF8, SLAMF1, CD58
T cell co-stimulation	ICOS, CD28, CD27, TNFSF14, CD40LG, TNFRSF9, TNFRSF4, TNFRSF25, TNFSF18, TNFRSF8, SLAMF1, CD2, CD226
APC co-inhibition	PDCD1LG2, CD274, C10orf54, LGALS9, PVRL3
T cell co-inhibition	LAG3, CTLA4, CD274, CD160, BTLA, C10orf54, LAIR1, HAVCR2, CD244, TIGIT

Table 2.

Table 2. gene groups and association with survival in adenocarcinoma, analyzed by Kaplan-Meier analysis

Gene groups	Lung (n=513)	Breast (n=1,093)	Esophageal (n=80)	Gastric (n=415)	Colon (n=621)	Pancreatic (n=178)	Ovarian (n=101)	Endometrial (n=47)	Prostate (n=497)
CD8+ T cells	++ (60m)	++ (110m)	++ (50m)	--	-	ns	ns	ns	ns
B cells	++	ns	++ (50m)	ns	--	ns	ns	ns	ns
Type 1 IFN response	++ (60m)	++ (110m)	++ (50m)	--	ns	ns	ns	++	ns
Cytolytic activity	++ (60m)	++ (110m)	-	ns	--	ns	+	ns	ns
Antigen presentation	ns	ns	ns	ns	ns	ns	+	ns	ns
IFN-stimulated cytokines	++ (60m)	++ (110m)	--	ns	ns	ns	++	-	ns
Th1	++ (60m)	++ (110m)	ns	ns	ns	ns	ns	-	ns
Adhesion molecules	++ (60m)	++	ns	ns	-	ns	ns	ns	ns
CD4 regulatory T cells	ns	ns	++	ns	ns	ns	ns	ns	ns
Type 2 IFN Response	++ (60m)	++ (110m)	++ (50m)	--	--	++ (20m)	-	ns	++
Cancer stem cell	ns	ns	ns	ns	+	--	ns	ns	ns
Desmoplasia	ns	ns	ns	--	-	ns	-	ns	ns
Immunosuppressive factors	ns	++ (110m)	ns	ns	--	ns	ns	ns	ns
Immunosuppressive chemokines	ns	ns	ns	--	--	ns	-	--	ns
Angiogenesis	--	ns	ns	--	-	ns	ns	ns	ns
Th2	++ (60m)	ns	ns	ns	ns	ns	ns	ns	ns
EMT marker	ns	ns	ns	ns	ns	-	ns	ns	ns
Immune score	++ (60m)	++ (110m)	ns	ns	-	-	+	-	ns
Macrophage	ns	ns	ns	ns	ns	ns	ns	ns	ns
Neutrophil	ns	+	-	ns	ns	ns	ns	ns	ns
NK cells	ns	++	++ (50m)	ns	ns	ns	ns	ns	ns
Plasmacytoid dendritic cells	++	ns	ns	-	ns	ns	ns	ns	ns
APC co-stimulation	++	ns	ns	ns	ns	++ (20m)	ns	ns	ns
T cell co-stimulation	ns	ns	-	ns	-	++ (20m)	ns	ns	ns
APC co-inhibition	ns	ns	ns	ns	ns	ns	ns	ns	ns
T cell co-inhibition	ns	++	ns	ns	-	++ (20m)	ns	ns	ns
Number of non-tumor tissue	n=59	n=112		n=35	n=51	n=4			n=52

++ and --, positive and negative correlation with survival with $p < 0.05$; + and -, positive and negative correlation with $0.05 < p < 0.1$; ++ (x m), positive until x month; ns, no correlation with survival ($p > 0.1$); APC, antigen presenting cell; NK, natural killer; m, month; Th, T helper cell; IFN, interferon; EMT, epithelial-mesenchymal transition

The immune score is geographic mean of mRNA expression of genes associated with cytolytic activity, antigen presentation, IFN-stimulated chemokines, and adhesion.

P74

Validation the immune contexture as prognostic biomarkers in high-grade serous ovarian cancer

Shin Wha Lee, MD[1], Ju-hyun Kim[1], Soo-Jung Kim[2], Yong-Man Kim[1]

[1]Ulsan University, ASAN Medical Center, Seoul, Korea
[2]ASAN Institute for Life Science, Seoul, Korea, Republic of

Background

The analysis of single parameters alone may not provide sufficient insights about complex immune system–tumor interactions. This study is to validate the immune contexture as prognostic biomarkers in high-grade serous ovarian cancer (HGS-OC) and to find new era of immunoscore in HGS-OC.

Methods

We collected FFPE samples from 187 patients with HSOC and produced TMA samples. We accomplished the OPAL multiplex IHC assay for the quantitative analysis of immune markers, including CD4, CD8, CD20, FoxP3, PD-L1, and CK. Multiplex Biomarker Imaging and inForm® Image Analysis Software was used.

Results

FIGO stage III and IV patients were 84.5% (158/187). The optimal debulking surgery was done in 66.8% (125/187). The 3-year disease-free survival and 5-year overall survival were 35.1% and 50.0%, respectively. Any single marker was not related to the survival including CD8, FoxP3, and PD-L1. However, high CD8:FoxP3 and CD8:PD-L1 ratios were correlated with the good survival. In cox regression model, the risk factors for HGS-OC survival were FIGO stage (HR 1.784, 95% CI: 1.295-2.457, p<0.001) and platinum resistance (HR 4.257, 95% CI: 2.753-6.582, p<0.001). Additionally, CD8:PD-L1 ratio was a

favorable prognostic factor (HR 0.621, 95% CI: 0.042-0.917, p=0.017).

Conclusions

These findings indicate that, although any single immune marker is not related to the survival, CD8:FoxP3 and CD8:PD-L1 ratios provide the positive correlation with the prognosis in HGS-OC. Especially, CD8:PD-L1 ratio is prognostic biomarker which is comparable to clinical biomarkers. The next study for immunoscore is necessary to define immunoscore in ovarian cancer.

Acknowledgements

This study was supported by the R&D Project, Asan Institute for Life Sciences, Seoul, Korea (2016-588).

P75

Development of a next-generation sequencing-based microsatellite instability assay (MSI-NGS) for solid tumor testing

Sean Glenn, PhD[1], Sarabjot Pabla, MSc, PhD, BS[1], Jonathan Andreas, MS[1], Blake Burgher, BS, RN[1], Jacob Hagen[1], Jeffrey Conroy, BS[1], Mary Nesline, MS[1], Antonios Papanicolau-Sengos, MD[1], Vincent Giamo, BS, MS[1], Felicia Lenzo[1], Maochun Qin, MD, MS[1], Yirong Wang, MS[1], Mark Gardner[1], Carl D. Morrison, MD, DVM[1]

[1]OmniSeq, Inc., Buffalo, NY, USA

Background

Microsatellite instability (MSI) is as a screening test for Lynch syndrome (HNPCC), is FDA-approved as a companion diagnostic for checkpoint inhibition, and has demonstrated high positive predictive value for response to anti-PD1 therapy for MSI-high/dMMR patients. Typically, MSI analysis involves comparison of allelic profiles of microsatellite markers generated by amplification of DNA from matching normal and tumor samples using a fluorescent PCR-based assay. The requirement of needing matched normal DNA has limited the number of patients that can have testing performed due to the difficulty in obtaining adjacent benign tissue in the tumor specimen received. Utilizing advances in NGS technologies and bioinformatics, we have developed a targeted, multi-plexed NGS assay (MSI NGS) which robustly and accurately determines MSI status without the requirement of a matched normal DNA.

Methods

Utilizing previously published data sets, 29 highly significant loci within the genome were determined for interrogation and integration into the MSI NGS targeted assay. For each loci, the number of peaks and average indel lengths were utilized in a custom algorithm on a gold standard training set, where MSI status was previously determined by MSI PCR methods, to define cluster centroid metrics which determine MSI and MSS status. By this process cluster 1 and cluster 2 were assigned as “MSI” and cluster 3 was assigned as “MSS” with 100% PPV and 96% NPV. The Euclidean distance of each experimental sample is then calculated across all 29 loci, and the cluster centroid closest to the sample determines the MSI status.

Results

Utilizing a 100 gold-standard sample set the overall concordance of the MSI NGS assay to MSI PCR is extremely high with only two false negative calls (98% concordance). The two false negative cases can be attributed to the fact that these cases are in cluster 1 which is closer (Euclidean distance) to the centroid of cluster 3 (MSS) than the centroid of cluster 2 (MSI). To this end, the reported sensitivity and specificity of the accuracy study are 96% and 100% respectively with a PPV of 100% and an NPV of 96%.

Conclusions
The development of a MSI NGS assay, which has recently been NYS-CLEP approved for all solid tumors, allows for robust and accurate testing of MSI status without the need of matched normal tissue, a major hurdle with conventional testing.

Ethics Approval
OmniSeq's analysis utilized deidentified data that qualified as non-human subject research under IRB protocol (BDR #073166) approved by Roswell Park Comprehensive Cancer Center (Buffalo, NY).

P76

Analysis of the complex immune-cell milieu of tumors from patients treated with immunotherapy to better understand clinical response

Shumei Kato, MD[1], Ryosuke Okamura[1], Mina Nikanjam[1], Ramez Eskander, MD[1], Paul Fanta, MD[1], Suzanna Lee[1], Sean Glenn, PhD[2], Devin Dressman, PhD[2], Sarabjot Pabla, MSc, PhD, BS[2], Jeffrey Conroy, BS[2], Mary Nesline, MS[2], Antonios Papanicolau-Sengos, MD[2], Felicia Lenzo[2], Mark Gardner[2], Carl Morrison, MD, DVM[2], Razelle Kurzrock, MD[1]

[1]UC San Diego Moores Cancer Center, La Jolla, CA, USA
[2]OmniSeq, Inc., Buffalo, NY, USA

Background
Although immunotherapies, especially checkpoint inhibitors, have achieved salutary anti-cancer effect among patients with advanced cancers, most patients do not respond to immunotherapies. We comprehensively evaluated biomarkers associated with the "cancer-immunity cycle" among patients with diverse solid tumors to understand the immune landscape in metastatic cancers and the resistance mechanism for anti-PD1/PDL1 inhibitors.

Methods
Interrogation of key markers of the cancer-immunity cycle was carried out in patients (n=101) with diverse malignancies using a NYS Clinical Laboratory Evaluation Program (CLEP) approved targeted RNA sequencing assay (51 genes) developed in a Clinical Laboratory Improvement Amendments (CLIA) certified laboratory. Resultant gene expression data was QC filtered, normalized and ranked based on an assorted reference population of various tumor types. Gene signatures were determined using these ranked values with a rank value > 85th percentile considered high.

Results
The immune phenotypes of the patients' tumor milieu demonstrated overexpression of multiple checkpoint blockade markers including PD-L1 (6.9%), PD-L2 (10.9%), CTLA4 (3%), LAG-3 (8.9%), TIM-3 (9.9%) and VISTA (15.8%). Overexpression of other cancer-immunity cycle markers were also observed including myeloid suppression markers (e.g. CCL2, CCR2 and CSF1R; 10-22%), metabolic immune escape markers (e.g. ADORA2A and IDO1; 9-16%) and T-cell primed markers (e.g. CD40, GITR, ICOS and OX40; 4-26%). Each patient had a unique cancer-immunity expression pattern that was distinctive from others in this cohort. Overexpression of TIM-3 and VISTA was associated with significantly shorter progression-free survival (PFS) from anti-PD1/PDL1 based therapies (P=0.007 and P=0.001 respectively).

Conclusions
Evaluation of the gene expression levels of biomarkers associated with the cancer-immunity cycle was feasible among diverse solid tumors using targeted RNA sequencing. Checkpoint blockade markers (TIM-3 and VISTA) were associated with shorter PFS with anti-PD1/PDL1 based therapies. All patients had unique immune related expression profiles suggesting more extensive molecular profiling beyond tumor mutation burden and PD-L1 status may be essential to personalize treatment

options such as individualized combination immunotherapy.

Ethics Approval
All investigations followed the guidelines of the UCSD Institutional Review Board for data collection (Profile Related Evidence Determining Individualized Cancer Therapy, NCT02478931) and for any investigational therapies for which the patients consented. OmniSeq's analysis utilized deidentified data that qualified as non-human subject research under IRB protocol (BDR #073166) approved by Roswell Park Comprehensive Cancer Center (Buffalo, NY).

P77

Identifying major immune-related subsets of GI tumors for clinical purposes

Amy Early, MD[1], Sarabjot Pabla, MSc, PhD, BS[2], Jeffrey Conroy, BS[2], Mary Nesline, MS[2], Sean Glenn, PhD[2], Felicia Lenzo[2], Antonios Papanicolau-Sengos, MD[2], Blake Burgher, BS, RN[2], Vincent Giamo, BS, MS[2], Jonathan Andreas, MS[2], Yirong Wang, MS[2], Carl D. Morrison, MD, DVM[2]

[1]*Roswell Park Comprehensive Cancer Center, Williamsville, NY, USA*
[2]*OmniSeq, Inc., Buffalo, NY, USA*

Background
Gastrointestinal (GI) tumors, both colorectal and non-colorectal, have a low response rate to immune checkpoint inhibitors (ICIs) outside of the setting of microsatellite (MSI) unstable. Currently there is uncertainty how to evaluate microsatellite stable GI tumors for evidence of checkpoint blockade as PD-L1 IHC has minimal applications in this setting. Furthermore understanding other mechanisms of immunosuppression in GI tumors, such as myeloid or metabolic suppression and the degree of CD8+ T-cell infiltration, can have profound influence on the selection of immunotherapies in this patient population.

Methods
131 MSI stable GI tumors (82 colorectal, 41 pancreatic, 8 small bowel) from multiple institutions were evaluated for PD-L1 expression by IHC, TMB (DNA-seq), and expression of 54 immune-related genes (RNA-seq) that are the target of multiple immunomodulatory immunotherapeutics or evaluate tumor infiltrating lymphocytes (TILs) in a CLIA setting.

Results
PD-L1 IHC was positive (TPS>=1%) in 32 (24%) of cases, but with only 3 (2%) of cases strongly positive (TPS>=50%). In PD-L1 IHC negative cases (n=99; TPS<1%) the corresponding PD-L1 RNA-seq value was low in 88 (89%) and moderately high to high in 11 cases (11%). A high macrophage content was identified in 50 (31%) cases indicative of strong myeloid suppression. All of these cases over expressed one or more myeloid-related immunotherapeutic targets including CCR2, CSF1R, or TGFB1. The majority of these 50 cases (n=37; 74%) also over expressed VISTA or TIM3, or both, indicating that over expression of these two checkpoint blockade receptors are strong indicators of myeloid suppression. In a similar fashion PD-L2 was frequently over expressed in these 50 cases (n=23; 46%). While a low number of CD8+ T-cells were common in cases with strong myeloid suppression (6/50;12%) it was more common in the remaining 81 cases at 47% (38/81). This latter group of cases with few exceptions can be aptly described as immune deserts.

Conclusions
Using a more sophisticated approach to evaluating the tumor microenvironment in GI tumors 3 major groups including PD-L1 positive, myeloid suppression, and immune deserts can be identified that has major implications for the application of

precision immunotherapy for this patient population.

Ethics Approval
OmniSeq's analysis utilized deidentified data that qualified as non-human subject research under IRB protocol (BDR #080316) approved by Roswell Park Comprehensive Cancer Center (Buffalo, NY).

P78

More sensitive identification of T-cell receptor beta rearrangements with an augmented transcriptome method

Eric Levy, PhD[1], Sean Boyle, PhD[1], Gabor Bartha[1], Pamela Milani[1], Robin Li[1], Shujun Luo[1], Rena McClory[1], John West, MBA[1], Richard Chen[1]

[1]*Personalis, Inc., Menlo Park, CA, USA*

Background
With the growth of new immunotherapies, there is an increasing need for comprehensive immuno-genomic profiling of tumors to identify new potential biomarkers. This includes neoantigen identification, HLA, immuno-modulators, tumor microenvironment, and T-cell receptor (TCR) repertoire. However, limited sample amount, formalin-fixed paraffin embedded tissue (FFPE) degradation, and cost of multiple sequencing assays pose a significant barrier to comprehensive immuno-genomics biomarker characterization in clinical trials.To address these challenges, we developed an augmented, immuno-oncology optimized exome/transcriptome platform (ACE ImmunoID) that can also identify abundant TCR clones, from limited FFPE tumor biopsy samples.

Methods
We designed the next generation of our ACE ImmunoID platform to augment RNA profiling of TCR and BCR, including TCR beta. We next characterized the performance of our platform at profiling TCR beta. First, we analyze the impact of sequencing depth and input material amount on the observed repertoires of diverse PBMC samples. We test LOD by diluting well-characterized clonal T-cell line samples into PBMCs. Finally, we analyze patient-derived FFPE and FF tumors to understand the profiles of tumor-infiltrating immune repertoires and effects of FFPE damage.

Results
We observe that at our specified 400ng of fragmented input RNA and 100M cluster sequencing depth, we detect approximately 26,000 clones, enough to get a picture of the clonality of a sample. Our platform has higher sensitivity to TCR clones compared to non-augmented transcriptome methods at a comparable depth of sequencing. Furthermore, in comparison to a commercially-available deep TCR kit, we identify 93.9% of the top 1000 clones, showing that we confidently identify high-abundance clones. We also are able to reliably identify clones down 0.0004% RNA by mass in the mixture. We further tested on FFPE samples, showing our platform works well with degraded RNA.

Conclusions
Our ACE ImmunoID platform has been designed to enable sensitive detection of major TCR repertoire clones in addition to comprehensive biomarkers from exome/transcriptome results. Here we demonstrate that our platform achieves both a higher sensitivity for TCR clones compared to non-augmented transcriptome approaches and a high concordance with the top abundance clones derived from targeted TCR methods. We show our method is feasible with FFPE samples, making it practical for clinical trial use. In summary, by combining exome/transcriptome with TCR characterization into a single assay, our ACE ImmunoID platform enables comprehensive immuno-genomics characterization of a tumor sample while reducing overall sample requirements and cost.

P79

Change in neutrophil to lymphocyte ratio during treatment with immune checkpoint inhibitors predicts survival in patients with advanced cancer

Mingjia Li, MD[1], Dan Spakowicz, PhD, MS[1], Jarred Burkart[1], Sandip Patel[1], Marium Husain, MD, MPH[1], Kai He, MD, PhD[1], Carolyn Presley[1], Erin Bertino[1], Peter Shields[1], David Carbone, MD, PhD[1], Claire Verschraegen, MD[1], Greg Otterson[1], Kari Kendra[1], Mingjia Li, MD[1], Dwight Owen[1]

[1]*The Ohio State University, Columbus, OH, USA*

Background

Baseline neutrophil to lymphocyte ratio (NLR) is known to be prognostic for patients with many cancer types treated with immune checkpoint inhibitors (ICI), including non-small cell lung cancer (NSCLC). We evaluated NLR at baseline and during treatment for patients who received ICI to evaluate the prognostic value of the change in NLR over time.

Methods

A retrospective review of patients with advanced cancer who received ICIs from 2011 to 2017 at the Ohio State University was performed with IRB approval. NLR was calculated as ratio of absolute neutrophil/lymphocyte counts, and considered elevated if ≥ 5. Overall Survival (OS) was calculated from the initiation of ICI to death of date or last follow-up. Significance of Cox Proportional-Hazards models were evaluated by log-rank test at Alpha = 0.05. All calculations were performed using the survival and survminer packages in R.

Results

677 patients were included in the analysis. NLR was collected at the initiation of ICI and at least one time after (median 21, IQR 8 days, Chart 1).Patients with baseline NLR ≤5 had median OS 592 days (95% CI: 497-681) compared to median OS 224 days (95% CI: 158-269) for patients with baseline NLR >5, P<0.001 (Figure 1). Patients with on-treatment NLR ≤5 had median OS 616 days (95% CI: 532-878) compared to median OS 177 days (95% CI: 143-242, P< 0.001 for patients with on-treatment NLR >5 (Figure 2). Subgroup analysis of 121 NSCLC patients at baseline and on-treatment NLR showed similar prognostic value (Figure 3 and 4).For patients with baseline NLR >5 but where on-treatment NLR normalized to ≤5, there was improved median OS of 433 days (95% CI: 304-NA) compared to median 150 days (95% CI: 120-214) for patients when NLR remained high, P< 0.001 (Figure 5). Similar results were seen in NSCLC patient with baseline NLR >5 with on-treatment normalization of NLR (P=0.0018, Figure 6).

Conclusions

We confirmed the prognostic value of baseline NLR in patients with advanced cancer treated with ICI, including metastatic NSCLC. We demonstrated that change in NLR over time may identify patients with poor prognosis at baseline who nevertheless benefit from ICI. To our knowledge, the association between dynamic changes in NLR during treatment with ICI and survival have not previously been reported in NSCLC. This biomarker is especially attractive because NLR can be easily obtained from routine labs.

Ethics Approval

The study was approved by the Ohio State University Institutional Review Board, approval number # 2016C0070

Figure 1.

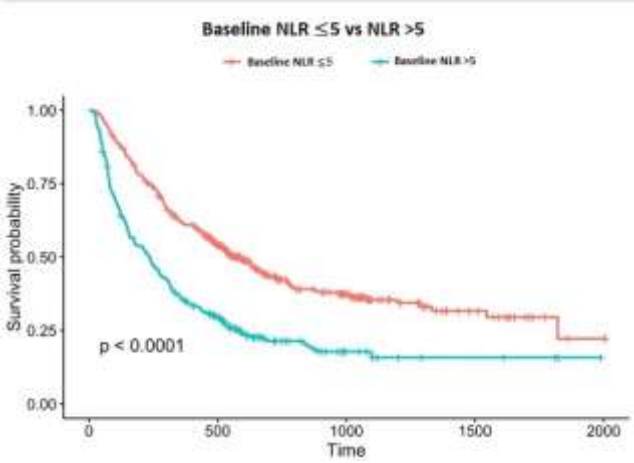

Figure 2.

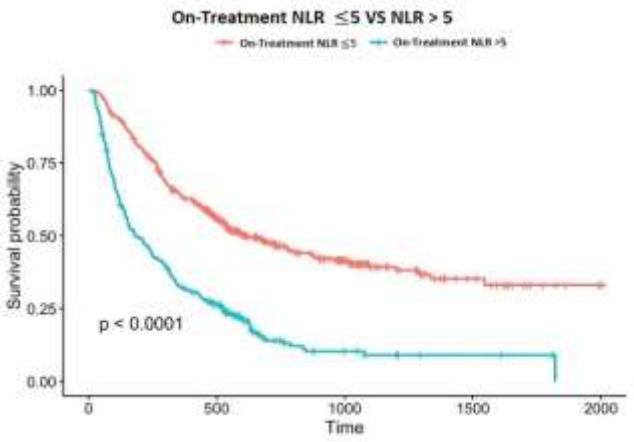

Figure 3.

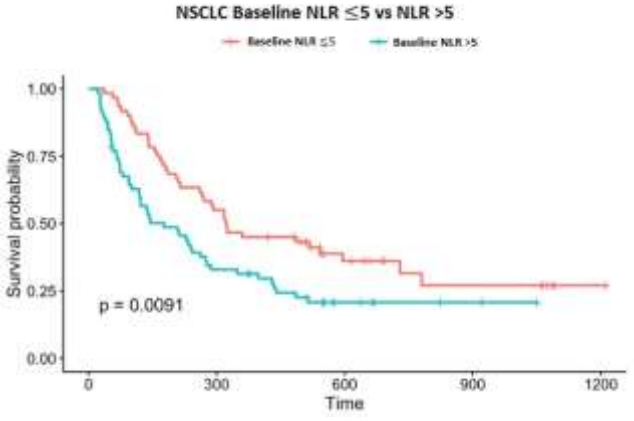

Figure 4.

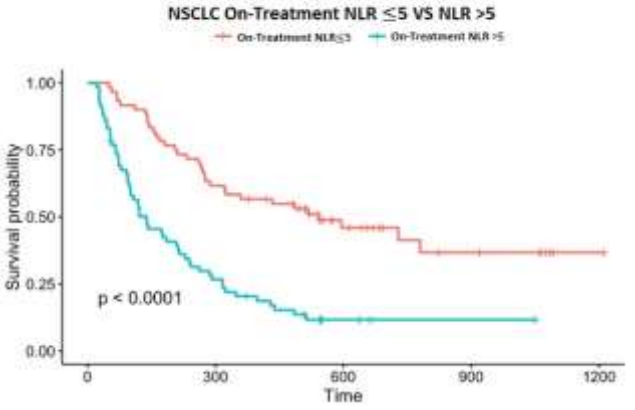

Figure 5.

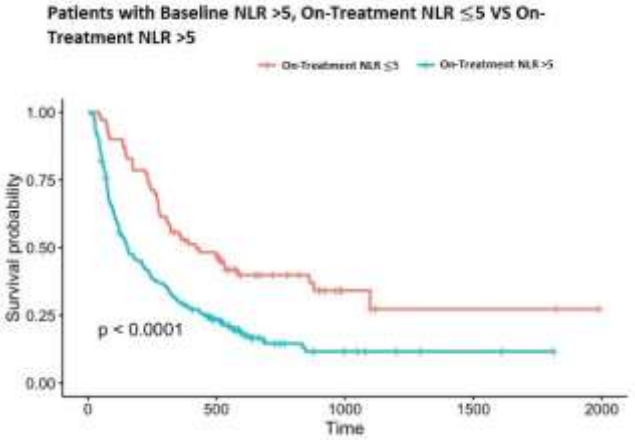

Figure 6.

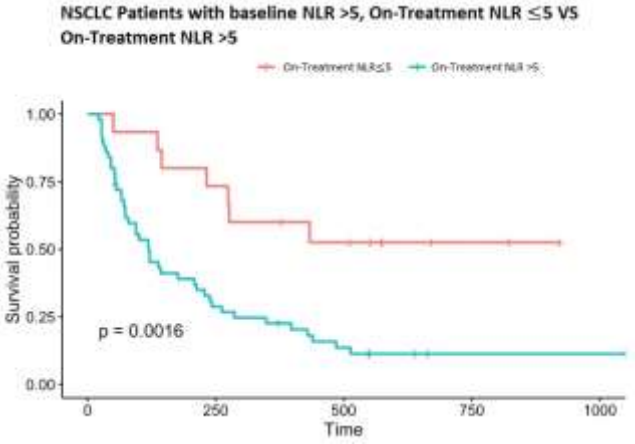

Chart 1.

Cancer Type	n	Staging	n
NSCLC	121	Stage 3	81
Melanoma	266	Stage 4	579
Renal Cell Ca	72	Other/Unknown	17
Head and Neck	48		
Other	170		
Immunotherapy	n		
Nivolumab	296		
Pembrolizumab	128		
Ipilimumab	171		
Other	82		

n = Number of Patients

P80

Day-to-day profiling of T cell activation by measuring cellular markers and secreted cytokines in a rapid multiplexed cell/bead mixture assay

Zhaoping Liu, PhD[1]

[1]*Sartorius, Albuquerque, NM, USA*

Background

Optimized adoptive cell therapy protocols, and profiling drug candidates against immuno-oncology targets such as immune checkpoint proteins requires precise monitoring of ex vivo activation of human T lymphocytes. Here we describe the development of a large scale multiplexed assay using high throughput flow cytometry to daily profile T cell activation in human PBMCs treated with different activators (Figure 1).

Methods

On Day 0, PBMCs were stained with cell proliferation tracing dye before being plated into a 96-well plate. Cells were treated and cultured with this protocol: 3 different T cell modulators—CD3/CD28magnetic beads, phytohemagglutinin (PHA), and Staphylococcal enterotoxin B (SEB)—with 12 serial titrations and duplicate wells per dose. On culture Days 1, 3, and 6, cell and supernatant mixture samples were removed from the culture plate and evaluated without dilution using a multiplex cell/bead mixture assay that combined cell phenotype, T cell activation markers, cell proliferation, cell viability measurements and secreted cytokine analysis measured by bead-based ELISA. In each sample well of the assay plates, secreted levels of 3 cytokines (IL-4, IFNg and TNFa) were quantified by the standard curves generated from the standard wells in the same assay plate. In addition, over the course of a six-day activation, we generated multiple cellular readouts identifying the presence of different T cell subpopulations expressing early and late T cell action markers CD69, CD25 and HLA-DR. Cell proliferation, cell viability and cell number for different subpopulations were also evaluated. Each plate was read on the iQue Screener Plus system in approximately 20 minutes (Figure 2).

Results

In total, we measured 16 endpoints and generated 1152 data points per 96-well assay plate and 3456 data points from 3 assay plates (days). We also acquired a total of 144 EC50s or IC50s (16-endpoint EC50/IC50s x 3 Days x 3 Activators), demonstrating the unique signature pattern of 3 different modulators on T cell activation (Figure 3).

Conclusions

These large-scale experiments with high throughput flow cytometry provide extensive T cell activation profiles with rapid assay turnaround time. The use of these assays can provide valuable information for optimizing immuno-oncology drug development such as checkpoint inhibitors and adoptive cell therapy development and manufacturing protocols.

Figure 1. Assay biochemistry

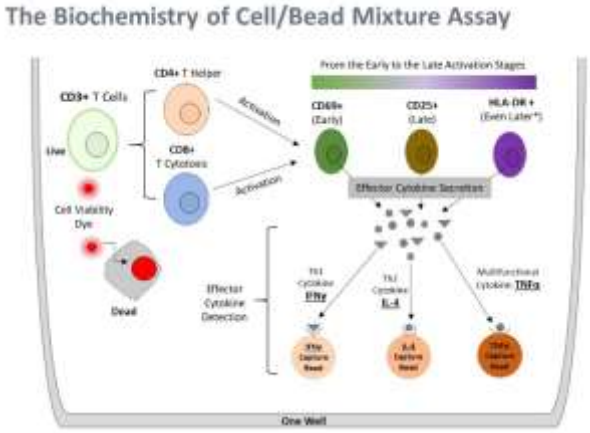

Figure 2. Gating strategy

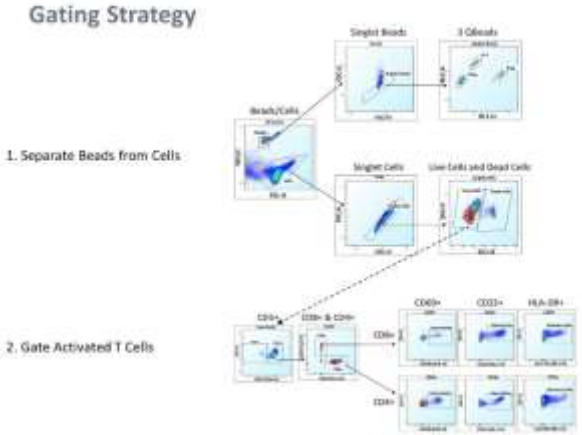

Figure 3. High content readout

P81

Germline encoded TRBV polymorphism predicts adverse events during checkpoint blockade immunotherapy

Timothy Looney, PhD[1], Geoffrey Lowman, PhD[1], Asha Kamat, PhD[1], Fiona Hyland[1]

[1]*Thermo Fisher Scientific, South San Francisco, CA, USA*

Background

Identifying predictive biomarkers for immune related adverse events (IRAEs) during immunotherapy is a key objective of current immuno-oncology research. Polymorphism within the TCRB variable gene (TRBV) has been implicated in autoimmune disease and may be mechanistically linked to IRAEs. Efforts to evaluate TRBV polymorphism by traditional approaches such as whole genome sequencing (WGS) have been hampered by the repetitive nature of the TCRB locus and incomplete genome assembly. Here we employed a novel long-amplicon TCRB repertoire sequencing approach to evaluate the link between TRBV polymorphism and adverse events in 54 Caucasians receiving checkpoint blockade immunotherapy for cancer.

Methods

To circumvent the challenge in measuring TRBV polymorphism by WGS, we instead employed next-generation sequencing of rearranged TCRB chains using RNA extracted from peripheral blood. Our strategy utilized multiplex PCR via framework 1 and constant gene primers to create ~330 bp amplicons spanning the three beta chain CDR regions including the germline-encoded framework and CDR1 and 2 regions of the receptor. Resultant amplicons were sequenced via the Ion Torrent, annotated by comparison to the gold-standard IMGT database, then mined to construct TRBV allele profiles for each individual including, where detected, novel alleles

not found in the IMGT database. Finally, we correlated TRBV allele profiles with adverse events annotations to detect alleles or sets of alleles associated with severe (grade 3 or higher) adverse events following immunotherapy.

Results
Sequencing of TCRB libraries yielded on average 29k clonotypes per individual with mean evenness (normalized Shannon entropy) of .85. Principal component analysis and k-means clustering of TRBV allele profiles revealed the presence of 4 major sets of coincident variable gene alleles which we term haplotype groups. The incidence of severe adverse events varied markedly across haplotype groups: one group, comprising approximately one fourth of the sample set, appeared completely protected against grade 3 or higher adverse events (0% incidence), while up to 57% of individuals in other haplotype groups had severe adverse events (p = 2.4E-3, Fisher's exact test).

Conclusions
These data suggest that germline-encoded TRBV polymorphism may play a mechanistic role in autoimmune toxicity during checkpoint blockade immunotherapy. We find that a subset of Caucasians appear to be at low risk of IRAEs and thus may be particularly well suited for immunotherapy regimens having elevated incidence of toxicity. Current and future studies will further explore the utility of TRBV polymorphism as a predictive biomarker for IRAEs.

P82

Peripheral blood TCRB repertoire convergence and clonal expansion predict response to anti-CTLA-4 monotherapy for cancer

Li Zhang, MD PhD[2], Timothy Looney, PhD[1], David Oh, MD, PhD[2], Denise Topacio-Hall, BS, MA[1], Lawrence Fong, MD[2]

[1]Thermo Fisher Scientific, South San Francisco, CA, USA
[2]University of California - San Francisco, San Francisco, CA, USA

Background
Tumor antigen-driven selection may expand T cells having T cell receptors (TCRs) of shared antigen specificity but different amino acid or nucleotide sequence in a process known as TCR convergence. Efforts to evaluate the biomarker utility of TCR convergence through TCRB repertoire sequencing have been hampered by the base substitution error rate of the Illumina platform, given that such errors may create artifacts resembling TCR convergence. Here we leverage the low base substitution error rate of the Ion Torrent platform to evaluate convergence as a predictive biomarker for response to anti-CTLA-4 monotherapy in a set of 22 individuals with cancer. For context, we compared convergence values obtained using this platform to those for the same samples interrogated with Illumina-based TCRB repertoire sequencing. Finally, we examined whether TCR convergence may be combined with measurements of clonal expansion to improve prediction of immunotherapy response.

Methods
Total RNA extracted from pretreatment peripheral blood leukocytes (PBL) from 22 recipients of Ipilimumab monotherapy. TCRB repertoire libraries were constructed by multiplex PCR via the Oncomine TCRB-LR assay, then sequenced using the Ion Torrent S5 to a target depth of 1.5M raw reads per library. To evaluate convergence within each repertoire we searched for instances where TCRB rearrangements were identical in amino acid space but had distinct nucleotide sequences within the CDR3. For a subset of samples, TCRB sequencing was performed in parallel via Illumina-based approaches.

Results
Sequencing of TCRB libraries yielded on average 31k clonotypes per individual with mean evenness (normalized Shannon entropy) of .82. TCR convergence was elevated in pretreatment PBL of responders compared to non-responders (mean frequency .022 vs .009; p=.03, Wilcoxon), and could discriminate responders from non-responders (AUROC = .77). Pretreatment evenness was reduced in responders vs non-responders and also predictive of response (AUROC = .74). A logistic regression model combining both features improved prediction of response (AUROC = .89).

Conclusions
These data suggest that PBL TCR convergence may serve as a predictive biomarker for response to anti-CTLA-4 monotherapy, potentially in combination with other immune repertoire features. Notably, measurements of TCR convergence appear to be sensitive to base substitution sequencing errors. These results highlight the impact of different sequencing approaches for assessing TCR repertoire.

P83

T cell receptor beta immune repertoire sequencing in several FFPE tissue types – Interrogation of the tumor microenvironment in archived tissue samples

Denise Topacio-Hall, BS, MA[1], Lauren Miller, BS[1], Elizabeth Linch, BS[1], Alice Zheng, PhD[1], Geoffrey M. Lowman, PhD[1], Timothy Looney, PhD[1], Mark Andersen, PhD[1]

[1]*ThermoFisher Scientific, Carlsbad, CA, USA*

Background
Immune repertoire sequencing is a valuable tool for studies of the tumor microenvironment and potential immune responses to cancer immunotherapy. Here we describe a T cell receptor beta (TCRβ) sequencing assay that leverages the low sample input requirements of AmpliSeq library preparation technology to extend the capability of targeted immune repertoire sequencing to include FFPE samples which can often be degraded and in short supply.

Methods
Evaluation of the highly diverse CDR3 region of TCRβ allows for T cell clone identification and frequency measurement. We demonstrate assay functionality with input of RNA or DNA samples, as well as flexibility in sequencing throughput and sample multiplexing capability. T cell repertoires were evaluated from as low as 10ng to 1ug of input material of varying repertoire diversity, such as sorted T cells, peripheral blood leukocytes, fresh-frozen tissue, and FFPE tissue from a variety of normal and cancerous tissues such as lung, colon, brain, spleen, lymph node, and thymus.

Results
Accuracy is demonstrated through the evaluation of samples comprised of known numbers of sorted T cells or spike-in experiments using well-studied lymphoma rearrangements. In order to test functionality of the assay with a range of degraded input material, RNA was controllably degraded with heat treatment at 90-95°C. In these systematically degraded samples we observe a strong correlation (r = 0.97) between the percentage of RNA molecules over 200bp in length and the amount of productive repertoire reads that the assay produces, while maintaining performance levels with samples with RIN values approaching 2. T cell richness and diversity in repertoires measured from FFPE tissue samples vary, as expected, depending on sample quality, disease state, and tissue of origin. To aid in sample input determination we present a complimentary qPCR assay, specific for T cell markers, which allows for sample T cell quantification and acts to guide optimal sample input ranges for library construction.

Conclusions
These data introduce a T cell immune repertoire sequencing solution for applications in a wide range of sample types including challenging FFPE preserved tissues. This assay is capable of profiling repertoire metrics from samples over a large range of input amounts from several tissue types. In addition, we demonstrate use of a qPCR assay for quantification of sample T cell content to guide sample input for TCRβ immune repertoire sequencing with samples with highly variable T cell content.

P84

Quantitative evaluation of tumor-infiltrating lymphocyte subsets and PD-L1 expression in lung cancer brain metastases

Benjamin Lu, MD[1], Richa Gupta[1], Hailey Wyatt[1], Matthew Ribeiro[1], Tyler Stewart[1], Veronica Chiang, MD[1], Joseph Contessa[1], Adebowale Adeniran[1], Harriet Kluger, MD[1], Lucia Jilaveanu, MD[1], Kurt Schalper, MD, PhD[1], Sarah B. Goldberg, MD, MPH[1]

[1]*Yale Cancer Center, New Haven, CT, USA*

Background
Lung cancer brain metastases (BrM) are associated with prominent morbidity and mortality. PD-1/PD-L1 inhibitors are safe and clinically active in patients with BrM in non-small cell lung cancer (NSCLC). While PD-L1 expression is associated with increased tumor infiltrating lymphocytes (TILs) and sensitivity to PD-1/PD-L1 inhibitors in extracranial tumors, the level and association between these markers in lung cancer BrM is unknown. Using spatially resolved/multiplexed tumor tissue analysis, we performed a comparative analysis of PD-L1 and major TIL subsets in primary lung cancers, BrM, and extracranial metastases (ECM).

Methods
We studied formalin-fixed paraffin-embedded tumor samples from a retrospective collection of 94 stage I-IV lung cancer patients from Yale between 2002-2013 represented in a tissue microarray. In total, 40 primary lung cancers, 63 BrM, and 15 ECM were included. Paired samples included primary-BrM from 11 patients and BrM-ECM from 12 patients. TIL density was determined by a semi-quantitative pathologist-based, scoring system using H&E preparations. Multiplexed quantitative immunofluorescence was used to evaluate PD-L1, CD4 for helper T-cells, CD8 for cytotoxic cells, and CD20 for B-lymphocytes. Signal for each marker was measured in marker-selected tissue compartments using the Automated Quantitative Analysis (AQUA) platform. We studied the association between markers and major clinicopathologic variables, including overall survival.

Results
Lung cancer histology included adenocarcinoma 62.5%, squamous cell carcinoma 11.5%, small cell 9.4%, and other NSCLC 16.7%. Only 8.5% of patients received immune checkpoint inhibitors. TIL density by pathologist read was significantly lower in BrM compared with primary lung tumors ($p<0.0001$). BrM had significantly lower levels of CD4+ T-cells ($p=0.0416$), CD8+ T-cells ($p=0.0003$), and CD20+ B-lymphocytes ($p=0.0058$) than primary lesions. Levels of tumor PD-L1 were comparable between BrM and primary lung tumors or ECMs ($p>0.05$). However, PD-L1:CD8 ratios were significantly higher in BrM compared with primary tumors ($p=0.0024$) or ECM ($p=0.0322$) without differences in PD-L1:CD4 ratios ($p>0.05$). Paired sample analyses demonstrated similar trends, though statistical significance was not achieved. There was no association observed between overall survival and TIL density, levels of TIL subsets, or PD-L1 expression.

Conclusions
Despite having lower levels of major TIL subsets, lung cancer BrM displayed similar PD-L1 expression compared with lung primary cancers and ECM. The

latter indicates differences in the adaptive immune modulation of PD-L1 in BrM compared with extracranial tumors, suggesting alternative TIL-independent mechanisms sustaining PD-L1 expression in BrM. A better understanding of how the PD-1 axis differs in the brain microenvironment may help improve anti-PD-1/PD-L1 efficacy and reveal additional therapeutic targets

Ethics Approval
The study was approved by Yale University's Institutional Review Board, HIC# 1310012801.

P85

Correlation of clinical response and pathologic treatment effect after 4 weeks of preoperative PD-1 blockade in primary head and neck squamous cell carcinoma (HNSCC)

Adam Luginbuhl, MD[1], Jennifer Johnson, MD[1], Madalina Tuluc, MD[1], Stacey Mardekian, MD[1], Chandala Chitguppi, MD[1], Larry Harshyne, PhD[1], Ralph Zinner, MD[1], Joseph Curry, MD[1], David Cognetti, MD[1], Ulrich Rodeck, MD PhD[1], Athanassios Argiris, MD, PhD[1], Adam Luginbuhl, MD[1]

[1]*Thomas Jefferson University, Philadelphia, PA, USA*

Background
Nivolumab, a PD-1 inhibitor, has been integrated into the clinical management of recurrent or metastatic HNSCC and is being evaluated in earlier stages of this disease. It is unclear whether imaging modalities, such CT and MRI, accurately reflect tumor response to immune checkpoint inhibition due to treatment-induced inflammatory changes at tumor sites. We sought to explore the relationship of imaging and pathology findings in the context of an ongoing neoadjuvant trial of preoperative nivolumab with or without tadalafil in resectable HNSCC.

Methods
Patients (n=17) with resectable primary HNSCC received nivolumab 240 mg IV Q 2 weeks for 2 doses and were randomized 1:1 to also receive tadalafil 10 mg PO for 28 days or not. Surgery was performed 4 weeks after the first nivolumab infusion. Tumor volumes were assessed pretreatment and on the day of surgery by CT scan. Resection specimens were graded histopathologically by two pathologists. Percent of treatment effect was determined by dividing the area of tumor showing changes consistent with treatment effect (fibrosis with chronic inflammation, foamy macrophage reaction and multinucleated giant cells) by total area containing treated and residual tumor. Radiographic effect was determined both by modified iRECIST and investigator assessment. Fischer exact test was performed to assess association between radiological and pathological tumor response. Percentage shrinkage of tumor was calculated in both radiological and pathological modalities and strength of association was calculated using Pearson correlation coefficient.

Results
Imaging results were used to stratify patients into response categories ranging from progression, stable disease and partial/complete response. Radiographic tumor shrinkage was observed in 11/17 (65%) patients with 16-100% volume reduction. A statistically significant relationship was noted between the radiological findings and treatment effects confirmed histopathologically ($p = 0.009$). A strong correlation was observed between these two groups (Pearson's $r = 0.7185$; $p = 0.001$). All patients with stable disease or radiographic progression (6/17) at 4 weeks had no evidence of treatment effect in pathologic specimens.

Conclusions
In this treatment naive cohort, imaging approaches accurately captured treatment responses validated by histopathologic assessment of HNSCC surgical

specimens obtained after two doses of nivolumab.

Acknowledgements
Sidney Kimmel Cancer Center at Thomas Jefferson UniversityBristol-Myers Squibb

Trial Registration
NCT03238365

Ethics Approval
The study was approved by Thomas Jefferson University Institutution's Ethics Board, approval number #17P.210

P86

T-cell receptor (TCR) repertoire features associated with disease-free survival following infusion with marrow-infiltrating lymphocytes (MILs)

Eric Lutz, PhD[1], Alex Hopkins, PhD[2], LAKSHMI RUDRARAJU, MS[1], Elizabeth DeOlivera[1], Ido Weiss, PhD[1], Rachel Gittelman, PhD[3], Erik Yusko, PhD[3], Kathryn Boland, DVM, PhD[3], Ivan Borrello, MD[2], Kimberly A. Noonan, Ph.D[1]

[1]*WindMIL Therapeutics Inc., Baltimore, MD, USA*
[2]*Johns Hopkins University, Baltimore, MD, USA*
[3]*Adaptive Biotechnologies, Seattle, WA, USA*

Background
MILs are an autologous T-cell product expanded from bone marrow (BM) being developed as a novel cell therapy for both hematological and solid malignancies. In a Phase I trial evaluating MILs in patients with advanced multiple myeloma, 6 (27.3%) of 22 patients achieved a complete remission (CR). Immune analyses demonstrated that the establishment of persistent tumor antigen-specific T cells in BM correlated with improved clinical responses [1].Herein, we sought to identify the repertoire of T cell clonotypes within MILs, including the subset that specifically recognize tumor antigens; to track and compare their frequencies in blood and BM before and after infusion; and to compare T cell repertoire characteristics, such as clonality, between clinical responders and non-responders.

Methods
The TCRb CDR3 was sequenced using Adaptive Biotechnologies' immunoSEQ Assay and used to identify and track MILs T cell clonotypes. The immunoSEQ assay was used on 11 specimens (unsorted MILs, IFNg-capture-sorted tumor antigen-specific CD4+ and CD8+ T cells, and blood and BM collected pre-treatment and 60, 180 and 360 days post-infusion) from 6 patients (3 clinical responders who achieved a CR and 3 non-responders whose disease progressed) from the Phase I study.

Results
When cumulative frequencies of MILs T-cell clonotypes were tracked in BM and blood, there were significant differences between responders and non-responders. Responders had a lower frequency of clonotypes at baseline but showed larger and more persistent increases in the frequency of clonotypes in both BM and blood. At day 360, fold-change from baseline in the frequency of MILs in both compartments segregated responders from non-responders. In general, T-cell repertoires in MILs were highly polyclonal and no specific TCRb variable genes were enriched in tumor antigen-specific T cells suggesting that multiple antigens are targeted. In all 6 patients, MILs were more polyclonal than pre-expanded BM. However, starting repertoires were more polyclonal in responders, and responders had larger and more persistent post-infusion increases in clonality. At day 360, all 3 responders maintained an increase in clonality whereas clonality returned to baseline or lower in all 3 non-responders.

Conclusions
These data provide a 1st look at the repertoire of T cell clonotypes in MILs and how the repertoire evolves after treatment. The data also demonstrate

the highly polyclonal nature of tumor antigen-specific T cells within MILs, which could provide an advantage against heterogeneous tumors.

References

1. Noonan KA, Huff CA, Davis J, Lemas M. V, Fiorino S, Bitzan J, Ferguson A, Emerling A, Borrello I. Adoptive transfer of activated marrow-infiltrating lymphocytes induces measurable antitumor immunity in the bone marrow in multiple myeloma. Sci. Transl. Med. 2015; 7: 288ra78.

Ethics Approval

The study was approved by the Johns Hopkins University IRB.

P87

Preliminary evidence of intratumoral activation and immunomodulatory effect of CX-072, a Probody therapeutic antibody prodrug targeting PD-L1, in a phase 1/2a trial

Susan K. Lyman[1], Judi Gordon[1], Amy DuPage[1], Preeti Pramanik[1], Bruce Howng[1], Michael B. Winter[1], Irina K. Popova[1], Olga Vasiljeva[1], James Jones[1], Kenneth Wong, MA[1], Victoria Singson[1], Jennifer Richardson, PhD[1], Beiyao Zheng, PhD[1], Mark Stroh, PhD[1], Lori Carman, RN[1], Vanessa Huels[1], Karen Autio, MS, MD[2], Valentina Boni[3], Daniel Cho, MD[4], Javier Garcia-Corbacho[5], Iván Victoria Ruiz[5], Omid Hamid, MD[6], Nataliya Uboha[7], Elisabeth de Vries[8], Anthony El-Khoueiry, MD[9], Alexander Spira, MD, PhD, FACP[10], Rachel Sanborn, MD[11], Fiona Thistlethwaite, MD, PhD[12], Hendrik-Tobias Arkenau[13], Johanna Bendell[14], Patrick Ott, MD, PhD[15], Naiyer Rizvi, MD[16], Matthias Will, MD[1], W. Michael Kavanaugh, MD[1], Aung Naing, MD, FACP[17], Luc R. Desnoyers, Ph D[1]

[1]CytomX Therapeutics, Inc., South San Francisco, CA, USA
[2]Memorial Sloan Kettering Cancer Center, New York, NY, USA
[3]Hospital Universitario HM Sanchinarro, Madrid, Spain
[4]Laura and Isaac Perlmutter Cancer Center, New York, NY, USA
[5]Hospital Clinic de Barcelona, Barcelona, Spain
[6]The Angeles Clinic and Research Institute, A Cedars-Sinai Affiliate, Los Angeles, CA, USA
[7]University of Wisconsin, Madison, WI, USA
[8]University Medical Center Groningen, the Netherlands, Groningen, Netherlands
[9]USC Norris Comprehensive Cancer Center, Los Angeles, CA, USA
[10]Virginia Cancer Specialists, Fairfax, VA, USA
[11]Earle A. Chiles Research Institute, Providence Cancer Center, Portland, OR, USA
[12]The Christie Hospital NHS Trust and University of Manchester, Manchester, UK
[13]Sarah Cannon Research Institute-UK, London, UK
[14]Tennessee Oncology, Nashville, TN, USA
[15]Dana Farber Cancer Institute, Boston, MA, USA
[16]Columbia University Medical Center, New York, NY, USA
[17]The University of Texas, Houston, TX, USA

Background

CX-072 is a Probody™ therapeutic antibody prodrug directed against PD-L1. Probody therapeutics are masked antibodies designed to be selectively activated within the tumor microenvironment by tumor-associated proteases. CX-072 is designed to reduce systemic immune-related toxicities of anti-PD-L1 therapy, especially in combination with other drugs, while maintaining antitumor activity. PROCLAIM-CX-072 is a first-in-human, phase 1/2, open-label dose-finding trial investigating the safety and maximum tolerated dose of CX-072 as monotherapy and in combination with ipilimumab or vemurafenib. PROCLAIM-CX-072 patients have metastatic or recurrent solid tumors or lymphomas for which approved PD-1/-L1–based therapy is not available. Here we present the initial results of the tissue-based biomarker program intended to evaluate the mechanism of action of CX-072 in

patients from PROCLAIM-CX-072.

Methods

Tumor biopsy and matched plasma samples were collected during the screening phase and after dosing of CX-072. PD-L1 and CD8 expression were analyzed using immunohistochemistry. Relevant tumor-associated protease activity was measured by tissue zymography. Intratumoral CX-072 unmasking and activation were measured using capillary immunoelectrophoresis. Gene expression was profiled by NanoString.

Results

Results of the first 13 evaluable biopsies obtained are reported here. Nine of 12 (75%) predose biopsies had detectable levels of relevant protease activity. Two of 4 (50%) biopsies from patients treated with CX-072 at 3 mg/kg and 4 of 4 (100%) biopsies from patients treated at ≥10 mg/kg had detectable intratumoral activation of CX-072, and the concentration of activated CX-072 in tumors increased with increasing dose. The preliminary calculated estimate of tumor receptor occupancy for patients receiving the 10 mg/kg dose was similar to that targeted for the PD-L1 inhibitor atezolizumab [1], and was consistent with quantitative systems pharmacology model predictions. Notably, the concentration of activated CX-072 measured in human tumor samples was similar to that associated with efficacy in a syngeneic preclinical tumor model. Consistent with the inhibition of the PD-L1 pathway by CX-072, we found an increase in CD8+ T cells and elevation of cytotoxic T-cell markers in the tumor of the one CX-072 monotherapy patient whose biopsy met evaluability criteria. These data support selection of the 10 mg/kg dose for clinical expansion cohorts.

Conclusions

These preliminary results show the presence of relevant protease activity, intratumoral Probody therapeutic activation, and biological effect of a Probody therapeutic in human subjects treated with CX-072. Taken together with previous data demonstrating stability of the masked Probody therapeutic in systemic circulation [2], these results support proof-of-mechanism for the Probody platform.

Acknowledgements

Editorial support was provided by ApotheCom (San Francisco, CA).

Trial Registration

ClinicalTrials.gov, NCT03013491

References

1. Stroh, M, Winter H, Marchand M, et al. Clinical pharmacokinetics and pharmacodynamics of atezolizumab in metastatic urothelial carcinoma. Clin Pharmacol Ther. 2017;102:305-312.
2. Autio K, Arkenau H-T, O'Neil B, et al. Preliminary results of the first-in-human, dose-finding PROCLAIM-CX-072 trial of the PD-L1 Probody therapeutic CX-072 as monotherapy in patients (pts) with advanced solid tumors. J Clin Oncol. 2018;36(suppl):abstr 3071.

Ethics Approval

The animal study was performed in accordance with the Guide for the Care and Use of Laboratory Animals under a protocol (AP203) approved by the Institutional Animal Care and Use Committee at CytomX. The CX-072 clinical study was approved by all participating sites institutional review boards as well as the overseeing Ethics Board.

P88

Quantitative assessment and standardization of the programmed death 1 ligand 1 (PD-L1) immunohistochemistry companion diagnostic assays

Sandra Martinez-Morilla, PhD[1], John McGuire[1],

Patricia Gaule, PhD[1], Lauren Moore[1], Balazs Acs[1], Delphine Cougot[2], David Rimm, MD, PhD[1]

[1]*Yale University, New Haven, CT, USA*
[2]*Horizon Discovery, Cambridge, UK*

Background
Programmed Death 1 Ligand 1 (PD-L1) Immunohistochemistry (IHC) is the only FDA approved predictive marker to identify responders to anti-PD1 axis drugs. Multiple PD-L1 IHC assays with various antibodies and cut-points have been used in clinical trials across tumor types. Comparative performance characteristics of these assays have been extensively studied qualitatively, but not quantitatively. Since PD-L1 is a continuous marker, we propose the use of a standardized PD-L1 Index TMA to objectively evaluate concordance between antibody assays for PD-L1 using quantitative image analysis.

Methods
A panel of 10 isogenic cell lines expressing various amounts of PD-L1 was developed by Horizon Dx and constructed as an Index Tissue Microarray (TMA). Identical but independent batches of isogenic cells lines were cultured to create 3 TMA batches at 3 separate timepoints to control for any batch effect that may occur. The TMAs were validated using a previously published quantitative immunofluorescence protocol (QIF-AQUA). Comparing antibodies E1L3N, SP142 and SP263, reproducibility was assessed between batches. We then compared US Food and Drug Administration (FDA)-approved 22C3, 28-8, SP142 and SP263 assays and E1L3N lab developed test (LDT). Digital image analysis was used to quantify chromogenic PD-L1 assays using the open-source QuPath platform.

Results
There was very high reproducibility between blocks (R2=0.875-0.995) with the IF assay. The IF concordance between antibodies was also extremely high (R2=0.986-0.987). The 4 FDA approved assays and the E1L3N LDT were compared on the Index TMAs using quantitative chromogenic assessment with QuPath. The assays for 22C3-FDA, 28-8-FDA, SP263-FDA and E1L3N-LDT were essentially identical. The SP-142-FDA assay failed to detect low expressing cell lines detected by the other 4 assays. Levey-Jennings analysis was done to show the value of using the index array over time as a standardization tool in the CLIA lab setting.

Conclusions
We have built a standardized Index TMA that spans the dynamic range of PD-L1 expression that shows reproducibility by QIF across independent blocks. Quantitative assessment of the 4 FDA assays and the E1L3N LDT shows the assays recognize the entire dynamic range in a reproducible manner, except for the SP-142 assay that fails to detect low PD-L1 expressers. We propose this commercial TMA as a useful standardization mechanism to compare results between institutions and to identify abnormalities while running routine clinical samples. A multi-institutional comparison study with this Index TMA with different assays and platforms is currently underway.

P90

Using artificial intelligence to predict response to immunotherapy

Anthony Milici, PhD[1], Navi Mehra[1], Jospeh S. Krueger, BS, PhD[1], Karen Ryall, PhD, BS[1], Jenifer Caldara, BS[1], Will Paces, BS[1], Kelsey Weigel, PhD[1]

[1]*Flagship Biosciences, Branford, CT, USA*

Background
PD-L1/PD-1 checkpoint blockade is the backbone for the myriads of combination therapies being developed; and thus effective PD-L1 IHC testing remains critical for predicting patient response to

these therapies. Pathological interpretations applied to PD-L1 immunohistochemistry (IHC) as a response biomarker are becoming more complex, going beyond simple Tumor Proportion Score (TPS) and requiring more complex diagnostic algorithms which evaluate the role of PD-L1 expression in 1) The tumor cells; 2) Immune cells in the Tumor Microenvironment (TME); and 3) Tumor infiltrating lymphocytes (TILs); all whose spatial relationships are critical for understanding the immune contexture. This complex matrix of several different biological cell types and spatial relationships can quickly become impossible for a pathologist to record and report successfully.

Methods

Recent advances in computer computational ability, machine learning algorithms, and data science now allow the application of Artificial Intelligence (AI) methods to create data-rich profiles from Whole Slide Images (WSI) of tissue that capture this key tissue context information about PD-L1. In this study, tissue image analysis was applied to this setting to increase objectivity and reproducibility of scoring, and AI interpretation of the results used to increase accuracy and sensitivity of the diagnostic performance of existing PD-L1 IHC testing methods. In this manner, existing FDA approved PD-L1 IHC tests can be re-evaluated by AI approaches to create this value in the clinical setting, without change to the IHC assay or significant disruption in the normal procedures performed in pathology labs.

Results

In this study, we demonstrate how our WSI AI platform captures the different attributes of PD-L1 stained slides to create a summary, singular score or output for decision making. Flagship's cTA® records the PD-L1 staining, morphological, organizational, and spatial aspects of a tissue section to create a more sophisticated scoring system and better diagnostic cutpoint in a cohort of patient tissues measured against clinical response.

Conclusions

By applying Flagship's cTA® Artificial Intelligence to existing PD-L1 IHC CDx, clinical labs can now go beyond using tissue image analysis for improving objectivity and reproducibility, and can also create entirely new scoring approaches from existing PD-L1 IHC CDx for improved clinical performance.

P91

It's pan-o'clock: Tumor and circulating lymphocytic pan-pathology targets of the failed immune response

Anne Monette, PhD[1], Antigoni Morou, PhD[2], Nadia Al-banna[3], Louise Rousseau, RT[4], Jean-Baptiste Lattouf, MD, FRCSC[2], Sara Rahmati[5], Tomas Tokar[6], Daniel Kaufmann, MD[2], Jean-pierre Routy[7], Igor Jurisica, PhD[8], Rejean Lapointe, PhD[2]

[1]University of Montreal / University of Montreal Hospital Research Centre / Lady Davis Institute for Medical Research / Jewish General Hospital, Montreal, Canada
[2]University of Montreal / University of Montreal Hospital Research Centre, Montreal, QC, Canada
[3]McGill University / University of Montreal Hospital Research Centre, Montreal, Canada
[4]University of Montreal Hospital Research Centre, Montreal, QC, Canada
[5]University of Toronto / Krembil Research Institute, Toronto, Canada
[6]Krembil Research Institute, Toronto, Canada
[7]McGill University Health Centre Chronic Viral Illnesses Service and Division of Hematology, Montreal, QUEBEC, Canada
[8]University of Toronto / Krembil Research / Toronto Western Hospital / Techna Institute, Toronto, ON, Canada

Background

Tumor infiltrating lymphocytes are widely associated

with positive outcomes, yet carry key indicators of a systemic failed immune response against unresolved cancer. Cancer immunotherapies can reverse their tolerance phenotypes, while preserving tumor-reactivity and neoantigen-specificity shared with circulating immune cells.

Methods
We performed comprehensive transcriptomic analyses to identify gene signatures common to circulating and tumor infiltrating lymphocytes in the context of clear cell renal cell carcinoma. Modulated genes also associated with disease outcome were validated in several other cancer types. Using bioinformatics, we identified practical diagnostic markers and actionable targets of the failed immune response.

Results
On circulating lymphocytes, a minimal set of genes could efficiently stratify patients from healthy control donors. From their associations with resistance to cancer immunotherapies and microbial infections, we have uncovered not only pan-cancer, but pan-pathology failed immune response profiles of effector and antigen presenting lymphocytes.

Conclusions
A prominent lymphocyte-specific cell migration pathway, is central to a panoply of diseases and tumor immunogenicity, correlates with multi-cancer recurrence in patients, and identifies a feasible, non-invasive approach to pan-pathology diagnoses.

Ethics Approval
The study was approved by the CHUM research ethics board Ethics Board, approval reference number SL07.053.

Consent
Written informed consent was obtained from the all study participants by the CHUM kidney biobank.

P92

Predictive plasma proteomic biomarkers of immunotherapy toxicity in patients (pts) with metastatic melanoma (MM)

Meghan Mooradian, MD[1], Xuesong Gu[2], Donald Lawrence, MD[1], Justine Cohen, DO[1], Tatyana Sharova[1], Genevieve Boland, MD, PhD[1], Towia Libermann[2], Ryan J. Sullivan, MD[1]

[1]Massachusetts General Hospital, Boston, MA, USA
[2]Harvard University, Boston, MA, USA

Background
Mechanisms underlying immune checkpoint inhibition (ICI) efficacy and toxicity have yet to be fully elucidated and, to date, there are no reliable biomarkers predictive of the development of immune-related adverse events (irAEs) or efficacy.

Methods
Pts with MM who developed select irAEs (colitis, hepatitis and arthritis) while receiving ICI (anti-PD-1, anti-CTLA-4 or combination anti-PD-1/CTLA-4) were identified. Using SOMAscan (SomaLogic; Boulder, CO), a proteomics platform that enables measurement of 1,305 proteins, quantitative plasma protein profiles were generated from banked plasma samples to identify candidate protein biomarkers predictive of irAEs and of progression-free survival (PFS). Comparator samples from pts without toxicity served as matched controls. Baseline protein expression was assessed and in evaluable pts, change in protein expression pre- and post-treatment was performed. PFS data was captured.

Results
36 pts were tested; 28 with confirmed irAEs and 8 controls. Baseline expression of IL-17, CXCL10 and TGFβ1 was associated with irAE development. Baseline IL-17 and CXCL10 expression was especially prominent in cases of ICI-induced arthritis, whereas

TGFβ1 was linked to both ICI-induced arthritis and colitis. Independent ELISA validation studies of the candidate biomarkers are underway and will be presented. The one-year PFS of the toxicity cohort was 54% and 65% in those treated with PD-1 inhibition +/- anti-CTLA-4, respectively. Elevated TGFβ1, as well as LGALS3 and DLL4, were associated with poorer outcomes.

Conclusions

This study demonstrates the feasibility of SOMAscan to identify potential biomarkers of toxicity and outcome. Previous literature has linked IL-17 and CXCL10 in autoimmunity, and TGFβ1 with a more pleiotropic role in immune regulation and melanoma pathogenesis. Our findings illustrate their possible role in the development of irAEs and outcome. If confirmed to be mechanistically involved in irAEs, targeted inhibitors of these proteins may serve as effective methods to abrogate or even prevent ICI-induced toxicity while minimizing effect on efficacy.

Ethics Approval

The study was performed with the approval of the MGH IRB, under research protocol 11-181

P93

Pre-analytical variables affect myeloid-derived suppressor cell quantitation by flow cytometry

Chihiro Morishima, MD[1], Amy Wright[1], Angela Riggins[1], Minjun Apodaca[1]

[1]*University of Washington, Seattle, WA, USA*

Background

Background: Myeloid-derived suppressor cells (MDSC) have been found to play an important role in limiting immune responses in many disease states including cancer. Higher circulating MDSC levels have been associated with greater tumor burden, poorer response to immunotherapy, and poorer survival. Optimal measurement of MDSC levels could provide clinicians with a useful management and/or prognostic tool.

Methods

Methods: Whole blood was obtained from healthy and diseased subjects through a University of Washington Institutional Review Board-approved study, #51834. A nine color flow cytometric assay included fluorescently-labeled antibodies against CD45, CD3, CD19, CD20, CD56, CD16, HLA-DR, CD33, CD11b, CD14 and CD15, and BD Trucount beads for quantitation. Samples were analyzed using a BD LSRFortessa and FlowJo software v9.9.5. Total MDSC were defined as CD45+CD3-CD19-CD20-CD56-CD16-HLA-DR-CD33+CD11b+ cells, while the monocytic (M-MDSC) and granulocytic (G-MDSC) subsets were defined as CD14+ or CD15+, respectively.

Results

Results: To confirm that our MDSC whole blood (WB) assay identified the same cells reported by other groups using PBMC as source material, we performed standard Ficoll density centrifugation of WB. The MDSC population identified by our assay in WB (0.32% of CD45+ cells) was found among cells from the Ficoll interface (0.28% of CD45+), but not the Ficoll pellet (0.02% of CD45+). Surprisingly, the yield of total and M-MDSC was higher with EDTA compared to heparin tubes (median 68% and 83% greater, respectively) among 5 donors with simultaneous blood collection in the two tube types, tested within 4 hours of blood draw. In addition, the duration of time that WB was kept at room temperature prior to cell labeling affected the yield of MDSC identified. For blood collected in EDTA tubes, total MDSC numbers decreased slightly by medians of 9% (N=7) and 11% (N=5) at 8 and 24 hours, respectively. M-MDSC numbers decreased somewhat more by medians of 14% (N=7) and 53% (N=5) at 8 and 24 hours, respectively. Finally, bilirubin levels as low as 1.6 mg/dL could impair the accurate identification of MDSCs. After controlling

for these pre-analytical factors, significant differences in MDSC levels were still found among patients with hepatocellular carcinoma (N=35) compared to healthy controls (N=35, p=0.001).

Conclusions

Conclusions: MDSC are a heterogenous group of cells, and their quantitation in WB can be affected by a number of pre-analytical variables. Consideration of these factors, and measurement using a material type that has not been manipulated, such as WB, is likely to yield the most accurate results.

P94

Measurement of adenosine and other immunomodulators in the tumor microenvironment by in vivo microdialysis

Nadege Morisot, PhD[1], Julien Roeser, PhD[1], Holden Janssens, PhD[1], Arash Rassoulpour, PhD[1]

[1]*Charles River Laboratories, South San Francisco, CA, USA*

Background

Understanding the tumor microenvironment is essential to gaining a better understanding of cancer biology and pathophysiology, and to date has proven to be challenging. The ability to determine the levels of adenosine and/or other molecules in the extracellular environment of tumors could provide unique insight into molecular targets for novel therapies in the treatment of cancers.

Methods

We implemented in vivo microdialysis to measure oncomodulator levels in the tumor microenvironment of freely moving mice. Microdialysis probes were implanted within 4T1 or CT26 syngeneic tumors and in the contralateral rump of the same animals. Probes were perfused with a buffered solution and dialysate samples were continuously collected for several hours. Levels of 12 metabolites (adenosine, cAMP, cGMP, arginine, ornithine, putrescine, tryptophan, kynurenine, kynurenic acid, 3-hydroxy-kynurenine, anthranilic acid, and xanthurenic acid) and lactate in the dialysates were quantified by liquid chromatography–mass spectrometry (LC-MS). Additionally, some animals received erythro-9-(2-hydroxy-3-nonyl)adenine (EHNA) through the microdialysis probe to examine the effects of adenosine deaminase inhibition on metabolite levels.

Results

We first confirmed that probe implantation did not affect the growth of 4T1 and CT26 allografts by comparing the volume of probe-implanted and -free tumor. Next, we found that adenosine levels were significantly elevated in both 4T1 and CT26 tumors, whilst the levels of cAMP and cGMP were reduced compared to non-tumor dialysis. Application of EHNA significantly increased the levels of Adenosine, cAMP, and cGMP in 4T1 tumors compared to basal levels. Additionally, we found that the levels of several kynurenine pathway metabolites were reduced within 4T1 tumors compared to the contralateral side. Interestingly, putrescine levels were elevated in CT26 but not 4T1 tumors compared to non-tumor dialysis. Finally, we observed high levels of lactate in both 4T1 and CT26 allografts.

Conclusions

Together, we have demonstrated the ability to detect levels of several signaling molecules that are believed to play a role in cancer biology. Additionally, we have been able to show that the reported levels are specific to the tumor microenvironment, and not a global circulating phenomenon within the same animal. In vivo microdialysis in murine tumor models may help in elucidating the mechanisms by which therapies such as chemotherapy and immune checkpoint inhibitors modulate the tumor microenvironment, helping identify the next-

generation of therapies in oncology.

P95

Modulation of adenosine levels in the tumor microenvironment following treatment with anti-PD1 antibodies and oxaliplatin: an in vivo microdialysis study

Arash Rassoulpour, PhD[1], Nadege Morisot, PhD[1], Julien Roeser, PhD[1], Holden Janssens, PhD[1]

[1]Charles River Laboratories, South San Francisco, CA, USA

Background
Elucidating the mechanisms by which cancer treatments modulate cellular signaling within the tumor microenvironment represents a major challenge in cancer research. In addition, the lack of reliable measurement of anti-cancer drug penetration in solid tumor may slow the development of effective systemic drug delivery strategies. We propose that microdialysis of the tumor microenvironment in syngeneic tumor models coupled to liquid chromatography–mass spectrometry may help filling in these gaps.

Methods
Mice bearing MC38 syngeneic tumors received control or anti-PD1 antibodies (5 mg/kg, i.p.) treatment on post-inoculation day 6, 9, 12 and 15. Next, animals were implanted with microdialysis probes within MC38 allografts. Dialysate samples from the tumor microenvironment were continuously collected in freely moving animal. In a separate cohort of MC38-bearing mice with microdialysis probes implanted in the tumor and contralateral subcutaneous (SC) space, baseline dialysate samples were collected, and mice received an acute systemic administration with oxaliplatin (10 mg/kg, i.p.). Dialysates were collected for two hours after treatment. Levels of adenosine, inosine and cAMP as well as the concentration of oxaliplatin in the tumoral and SC dialysates were quantified by liquid chromatography–mass spectrometry (LC-MS).

Results
We found that chronic treatment with an anti-PD1 antibody treatment reduced the levels of adenosine and inosine in MC38 allografts compared to control treated animals. Intriguingly, cAMP levels were higher in the tumor dialysates from anti PD-1 treated mice compared to controls. Moreover, oxaliplatin treatment produced a rapid and transient increase in adenosine and inosine levels in MC38 tumors. In contrast, changes in the concentration of these metabolites were much less pronounced in the SC space. From the same samples we were able to quantify the levels of oxaliplatin, and found that the levels in the core of the tumor were significantly less that in the SC of the same animal.

Conclusions
Here we bring proof-of-concept evidence that pharmacological and pharmacokinetic changes can be measured within tumor allografts in freely moving animals. Utilizing in vivo microdialysis we are able to simultaneously measure the levels of oncomodulators and anti-cancer drugs. Our experimental method may help the development of effective oncology therapeutic strategies.

P96

Assessment of RNA turbulence and PD-L1 expression on tumor-infiltrating lymphocytes in breast cancer

Apoorva Mylavarapu, BS[1], Scott Morris[2], Maulik Patel, PharmD, PhD[3], Sandip Patel, MD[4]

[1]University of California at Los Angeles, David Geffen School of Medicine, San Diego, CA, USA
[2]Paradigm Diagnostics, Phoenix, AZ, USA
[3]Abbvie Inc., Redwood City, CA, USA

[4]*University of California San Diego, Moores Cancer Center, La Jolla, CA, USA*

Background
Triple negative breast cancer (TNBC) as a subtype is generally associated with poorer outcomes compared to other breast cancer subtypes. In this study, we explore the utility of a novel tissue-based biomarker, RNA turbulence score, derived from a panel of 56 gene targets. We describe the RNA turbulence landscape and examine potential association of RNA turbulence score with PD-L1 positive tumor infiltrating lymphocytes (TILs) in breast cancer tissue samples.

Methods
Biomarkers were examined in breast cancer tissue samples (N=516). Expression of PD-L1 on tumor/tumor infiltrating lymphocytes (TILs) was assessed by immunohistochemistry with two different anti-PD-L1 clones (22C3 and E1L3N). PD-L1 positivity for this analysis was defined as staining intensity ≥ 1+ with tumor/immune cell staining of >1%. Molecular testing was conducted at Paradigm Diagnostics utilizing a 56-gene panel for RNA turbulence assessment. RNA turbulence score was calculated by assessing the number of genes with mRNA over-expression by at least 5-fold or greater with a significance of $p<0.01$.

Results
Average RNA turbulence score was higher (12.45 vs. 10.18, Mann-Whitney $p<0.001$) in patients whose tumor samples were positive for PD-L1 expression on TILs (19%, N=55) than in negative samples (N=233). A total of 40% (18/45) of TNBC samples were positive for TILs expressing PD-L1. In contrast, 11% (8/70) of estrogen receptor/progesterone receptor (ER/PR) positive tumors had evidence of PD-L1 positive TILs. The greater percentage of samples expressing PD-L1 on TILs in TNBC samples than in ER/PR-positive samples was statistically significant ($p=0.0005$; Fisher's exact test). Average RNA turbulence score was also higher in TNBC samples than in ER/PR-positive samples (11.96 vs. 9.79, Mann-Whitney $p<0.01$). ER/PR-positive samples had *ESR1* exclusively over-expressed with *AREG* and *ERBB2* relatively higher in expression in comparison to TNBC. In contrast, the top three genes exclusively over-expressed in TNBC were *VEGFA*, *BAX*, and *LRP6*.

Conclusions
RNA turbulence score is greater in breast cancer patients whose tumor samples were also positive for PD-L1 expressing TILs. Additionally, we observe greater PD-L1 positive TILs in TNBC samples in comparison to ER/PR-positive samples. These findings suggest that RNA turbulence score may in part identify an increased immune active tumor microenvironment as assessed by PD-L1 positive TILs. Studies correlating RNA turbulence with response to anti-PD(L)-1 directed therapies in TNBC are warranted.

P97

Different functionality of CD8 PD-1-positive CD28-negative T cells in the periphery and in the tumor of lung cancer patients

Belinda Palermo[1], Ornella Franzese[2], Mariangela Panetta[1], Giulia Campo[1], Fabiana Cecere[1], Virginia Ferraresi[1], Gabriele Alessandrini[1], Francesco Facciolo[1], Gennaro Ciliberto, MD[1], Paola Nistico', MD[1]

[1]*IRCCS - Regina Elena National Cancer Institute, Rome, Italy*
[2]*School of Medicine, University of Tor Vergata, Rome, Italy*

Background
The main objective of cancer immunotherapy is an efficacious control over tumor progression through the generation of a strong and persistent T-cell mediated immune response. CD8+ T cells are key

players able to recognize and kill cancer cells, which experience phenotypic and functional changes due to the constant exposure to tumor-associated antigens, frequently in association with a dysfunctional state mediated by co-inhibitory receptors, including Programmed Death 1 (PD-1). Recently CD28 has been proven to be the main downstream target of PD-1-mediated signaling [1], and accordingly we have reported that a subset of Ag-specific CD8+ T-cell clones, characterized by PD-1 expression in the absence of CD28, show high proliferative capability and an AKT-dependent anti-tumor functionality sustained by ICOS [2-4]. Whereas, the co-expression of PD-1 and CD28 confers an exhausted phenotype and a defective anti-tumor functionality, reversible by PD-1 blockade. The role of these subsets in the tumor site is still not clarified, and there is a need to determine their presence and functionality to improve current therapies.

Methods

T cells were isolated from peripheral blood, tumoral (T) and adjacent non-tumoral (NT) tissue of lung cancer patients and analyzed by multiparametric flow cytometry for phenotypic characterization and polyfunctionality. Ag-specific CD8+ T cell clones (Melan-A and gp-100) were obtained as described [2-4].

Results

To elucidate the critical role of PD-1 in regulating CD8+ T-cell functionality, we have investigated the phenotypic and functional distribution of CD8+ T cells, with respect to PD-1 and CD28 expression, in the peripheral blood of patients with different solid tumors and at the tumor site of lung cancer patients. Preliminary results indicate that distinct PD-1+CD28- and PD-1+CD28+ CD8+ subsets could be found among T cells isolated from the periphery and both NT and T tissues. In the periphery we found that the differentiation and functional pattern of these T cells is similar to that identified in Ag-specific CD8+ T-cell clones [2-4], also in terms of GrzB, IFN-gamma and TNF-alpha production, ICOS and Ki-67 expression. Differently, when we compared periphery and tissue sites, we observed a heterogeneous phenotype and functionality of CD8+ T cells, also in terms of polyfunctionality and frequency of CD103+CD69+ T-resident as well as CD39+CD127- T-cell subsets, recently described as the major tumor-reactive T cells [5, 6].

Conclusions

These results highlight the critical role of PD-1 and CD28 molecules in regulating T-cell functionality and may help in the identification of biomarkers predicting the efficacy of anti-PD-1 therapy.

Acknowledgements

§ B.P. and O.F. contributed equally to this work. This work was supported by Associazione Italiana Ricerca sul Cancro (AIRC) IG n°15224

References

1. Hui E, Cheung J, Zhu J, et al. T cell costimulatory receptor CD28 is a primary target for PD-1-mediated inhibition. Science. 2017 Mar 31;355(6332):1428-1433.
2. Palermo B, Franzese O, et al. Antigen-specificity and DTIC before peptide-vaccination differently shape immune-checkpoint expression pattern, anti-tumor functionality and TCR repertoire in melanoma patients. OncoImmunology. In Press. https://doi.org/10.1080/2162402X.2018.1465163;
3. Franzese O, Palermo B, et al. Polyfunctional Melan-A-specific tumor-reactive CD8(+) T cells elicited by dacarbazine treatment before peptide-vaccination depends on AKT activation sustained by ICOS. OncoImmunology 2016. Feb 1;5(5):eP582

*Corresponding author email: rajesh.gottimukkala@thermofisher.com03;

4. Palermo B, et al. Dacarbazine treatment before peptide vaccination enlarges T-cell repertoire diversity of melan-a-specific, tumor-reactive CTL in

melanoma patients. Cancer Res. 2010 Sep 15;70(18):7084-92.
5. Duhen T, Duhen R, Montler R et al. Co-expression of CD39 and CD103 identifies tumor-reactive CD8 T cells in human solid tumors. Nat Commun. 2018 Jul 13;9(1):2724.
6. Thommen DS, Koelzer VH, Herzig P et al. A transcriptionally and functionally distinct PD-1+ CD8+ T cell pool with predictive potential in non-small-cell lung cancer treated with PD-1 blockade. Nat Med. 2018 Jun 11.

Ethics Approval
The study was approved by Regina Elena National Cancer Institute's Ethics Board, approval number 1008/17

P98

High gene expression of estrogen and progesterone receptor is associated with increased T cell infiltration in patients with NSCLC

Michael Oh, MD[1], Jonathan Anker, MD[1], Young Kwang Chae, MD[1]

[1]*Northwestern University Feinberg School of Medicine, Chicago, USA*

Background
Recent reports have demonstrated that hormonal markers, including estrogen and progesterone receptor (ER and PR) status, may have prognostic and predictive relevance in non-small cell lung cancer (NSCLC). The precise impact of hormone signaling on clinical outcomes in NSCLC remains unclear, as initial studies have had diverging results. Here, we investigate the impact of hormone receptor status on tumor inflammation and survival in patients with NSCLC.

Methods
A dataset of NSCLC patients was obtained from The Cancer Genome Atlas (TCGA). RNA-Seq data was used to determined mRNA expression levels of ESR1 (ER-alpha), ESR2 (ER-beta), PGR (PR), and ARO (aromatase). Tumor infiltration by activated T cells was predicted using a previously-described method based on expression of immune metagenes [1]. Overall survival (OS) and progression-free survival (PFS) was assessed using Kaplan-Meier analyses with log-rank test.

Results
High levels of ESR1 was associated with significantly increased proportion of tumors infiltration by CD4+ (58% of tumors vs 19%, adjusted $p < 0.001$) and CD8+ activated T cells (55% vs 14%, adj. $p < 0.001$). Increased expression of PGR similar was associated with increased CD4+ (44% vs 18%, adj. $p = 0.001$) and CD8+ (48% vs 12%, adj $p < 0.001$) activated T cells. There were no significant differences based on ESR2 or ARO. These findings remained even after stratifying patients based on sex and histologic tumor type. In a multivariate logistic regression analysis, ESR1, PGR, and tumor mutation burden all were identified as independent factors predicting T cell infiltration. However, greater expression of ESR1, PGR, or a combined measure of both genes did not confer greater overall or progression-free survival in this cohort.

Conclusions
Increased gene expression of estrogen receptor-α and progesterone receptor was associated with increased activated T cell infiltration in patients with NSCLC. The relevance of these findings will need be validated, potentially with clinical studies using immunotherapy based on hormone receptor status.

References
1. Angelova M, et al. Characterization of the immunophenotypes and antigenomes of colorectal cancers reveals distinct tumor escape mechanisms and novel targets for immunotherapy. Genome Biol. 2015;16:64.

P99

RRx-001 is a Phase 3-Ready small molecule dual inhibitor of CD47 and SIRPalpha

Pedro Cabrales, PhD[1], Bryan Oronsky, MD, PhD[2], Tony Reid, MD PhD[2], Corey Carter, MD[2]

[1]*University of California San Diego, La Jolla, CA, USA*
[2]*EpicentRx Inc., La Jolla, CA, USA*

Background
CD47 binds to SIRPα on the surface of macrophages delivering a "do not eat" signal to suppress phagocytosis. To evade macrophage-mediated destruction, tumor cells frequently overexpress CD47. One area of intense interest is the targeting of CD47 with monoclonal antibodies (mAbs), three of which, Hu5F9-G4, CC-90002, and TTI-621, have proceeded to clinical trials [1]. However, these mAbs have been associated with severe hemolytic anemia and thrombocytopenia. RRx-001 is a minimally toxic small molecule that dually downregulates CD47 on tumor cells and SIRPα on macrophages and triggers tumor associated macrophage phagocytosis of tumor cells in vitro and in vivo. RRx-001 is entering Phase 3 trials for the treatment of multiple cancer indications.

Methods
The effect of RRx-001 on the expression of CD47 and SIRPα on macrophages was evaluated with Western blotting and flow cytometry. An in vitro phagocytotic assay was used to determine whether RRx-001 promoted engulfment of A549 tumor cells by macrophages. Transcriptional mRNA profiling in murine tumor associated macrophages (TAMs) was performed to analyze the cytokine profile of TAMs in the presence or absence of RRx-001. Finally, nude mice bearing A549 tumors were treated with RRx-001 in the presence or absence or absence of clodronate to determine the effect of macrophage depletion on RRx-001 anticancer activity.

Results
RRx-001 was shown to downregulate CD47 and SIRPα expression on tumor cells and macrophages, respectively, and to promote the phagocytosis of high-expressing CD47 A549 tumor cells. RRx-001 also stimulated the production of pro-inflammatory cytokines in TAMs. In tumor bearing mice, depletion of macrophages by clodronate reduced the antitumor effects of RRx-001.

Conclusions
RRx-001 is a Phase 3-ready small molecule innate immune checkpoint inhibitor, which triggers tumor associated macrophage phagocytosis of high-expressing CD47 tumor cells. Dual downregulation of CD47 and SIRPα by RRx-001 results in TAM repolarization and phagocytosis of tumor cells. Depletion of macrophages by clodronate in tumor-bearing mice reduced the antitumor effects of RRx-001 and further suggests that the target of RRx-001 is the macrophage.

References
Liu X, Kwon H, Li Z, Fu Y. Is CD47 an innate immune checkpoint for tumor evasion? J Hematol Oncol. 2017; 10:12. DOI: 10.1186/s13045-016-0381-z

Ethics Approval
All applicable international, national, and/or institutional guidelines for the care and use of animals were followed.

P100

Exploring dissociated human tissues as an alternative to fresh tissue for multiple downstream applications

Rebecca Parker[1], Shawn Fahl, PhD[2]

[1]*Conversant Bio, Huntsville, AL, USA*

[2]Folio Conversant, Huntsville, AL, USA

Background
The foundation of the future of biomedical research requires access to highly-annotated primary human biospecimens. The logistical barriers of acquiring fresh tissue remains an impediment to advances in medicine, requiring the coordination of not only the tissue collection but also the downstream applications in the laboratory. Dissociation and cryopreservation of solid tissue provides a solution to this problem. These single cell suspensions remain viable following cryopreservation and ease the demands on large-scale experimental assays. Furthermore, these cells provide the ability to screen new biomarkers and therapeutic targets as they are uncovered without the need to source new fresh tissue.

Methods
Using this model, we have analyzed viably cryopreserved single cell suspensions generated from over 400 unique patients across 11 oncology indications by flow cytometry. Flow cytometry allows for the identification of cell surface marker expression on the single cell level and provides in-depth characterization of the cellular composition of the tumor microenvironment. This large-scale characterization revealed indication-specific trends to the tumor composition, which are vitally important considerations as the next-generation of therapeutic interventions are developed.

Results
N/A - Results pending late breaking submission requested.

Conclusions
Viably cryopreserved single cell suspensions from solid tissues provides numerous benefits to the logistical demands of sourcing fresh tissue. Using solid tumor indications as a model, we have demonstrated the utility of cryopreserved dissociated tumor cells to understand and screen the cellular composition of the tumor microenvironment. In particular, these results highlight the patient-specific heterogeneity of the tumor microenvironment, but also demonstrates indication-specific trends that are crucial when developing future immunotherapies.

P101

Evaluation of ctDNA mutations detected in plasma as potential correlate of immunotherapy efficacy in NSCLC patients

Namrata Patil, PhD[2], Yuqiu Jiang, PhD[3], Wei Zou[2], Johnny Wu[3], Stephanie Yaung[3], Susan Flynn[2], Maureen Peterson[2], Eric Peters[2], Priti Hegde, PhD[2], John Palma3, Marcin Kowanetz, PhD[2], David Shames, PhD[2], Yuqiu Jiang, PhD[3]

[1]Genentech/ Roche, South San Francisco, CA, USA
[2]Genentech, South San Francisco, CA, USA
[3]Roche Sequencing Solutions, Pleasanton, CA, USA

Background
Multiple recent studies have shown that tumor mutation burden (TMB) may be a surrogate for the overall neoantigens likely to presented for an effective immune response. High TMB, including TMB measured in blood (Gandara et al. 2017), has been associated with clinical benefit with checkpoint inhibitors in several malignancies. The goal of this analysis was to evaluate whether the number of mutations detected in ctDNA by the AVENIO Surveillance panel (200kb) correlates with immunotherapy efficacy in NSCLC patients.

Methods
A subset of 375 baseline plasma samples from 2L+ NSCLC subjects enrolled in study OAK (NCT02008227) were analyzed using the AVENIO ctDNA Surveillance kit**, which covers 200 kb (Roche, Branchburg, NJ), from 375 pts. Data from

108 patient samples have been analyzed so far. The Surveillance kit contains 17 cancer driver genes and an additional 180 frequently mutated genes in cancer. This kit is capable of detecting four mutation classes: SNVs, fusions, CNVs and Indels. Tumor tissue samples from these patients were also analyzed for tumor mutation burden (tTMB) using the FoundationOne assay.

Results

102 samples of the 108 (94%) baseline plasma samples that passed QC metrics were successfully sequenced. All 102 samples had somatic variants detected. The median number of variants detected per patient was 7. Mutant molecules per milliliter (MMPM) was also assessed for each of the baseline samples. The median MMPM was 139, ranging from 1 to 1,972 for these 102 samples. Preliminary analysis of the number of variants detected with a limited filters algorithm was positively correlated (r=0.56) with tissue Tumor Mutation Burden (tTMB).

Conclusions

ctDNA testing with molecular barcoded sequencing and digital background error suppression of a small 197 gene panel offers high sensitivity for tumor variant detection (all 102 samples with variants detected). This study demonstrated that tumor variants can be detected in blood in pre-treatment samples using the AVENIO Surveillance kit. Preliminary analysis suggests that the number of mutations detected correlate with immunotherapy efficacy, specifically PFS. Analysis of all 375 pts as well as association with clinical benefit to atezolizumab will be presented.

Trial Registration

NCT02008227

References

1. Gandara DR, Pawel JV, Sullivan RN, Helland A, Han J, Aix SP, Rittmeyer A, Barlesi F, Kubo T, Park K, Goldschmidt JH, Gandhi M, Yun C, Yu W, Matheny C, He P, Sandler A, Ballinger M, Fehrenbacher L. Journal of Clinical Oncology. 2017; 35:15_suppl, 9001-9001.

P102

Localized measurement and clinical significance of OX40 and OX40L expression in human non-small cell lung cancer (NSCLC)

Angelo Porciuncula, PhD[1], Micaela Morgado[1], Sima Zacharek, PhD[2], Maria Toki, MD, MSc[1], Kostas Syrigos[3], Vamsidhar Velcheti, MD FACP[4], Joshua Frederick, PhD[2], Roy Herbst, MD, PhD[1], Kurt A. Schalper, MD, PhD[1]

[1]*Yale University, New Haven, CT, USA*
[2]*Moderna Therapeutics, Cambridge, MA, USA*
[3]*Athens School of Medicine, Athens, Greece*
[4]*Cleveland Clinic, Pepper Pike, OH, USA*

Background

Immunostimulatory therapies targeting co-inhibitory T-cell checkpoint pathways such as PD-1 and CTLA-4 produce lasting anti-tumor responses in a proportion of patients with diverse malignancies, including NSCLC. However, the majority of patients show primary resistance to treatment and a fraction of those initially responding have subsequent disease progression. Activation of co-stimulatory signals such as the OX40/OX40L pathway can favor anti-tumor immune responses and clinical trials modulating this pathway are currently ongoing. The expression, tissue distribution, biological associations and clinical significance of OX40/OX40L protein expression in human tumors remain largely unexplored.

Methods

Using formalin-fixed paraffin-embedded (FFPE) preparations from cell line transfectants and human tissue controls, we validated and standardized a multiplexed quantitative immunofluorescence (mQIF) assay for simultaneous and localized measurement of DAPI (all cells), cytokeratin for

epithelial tumor cells (clone-AE1/AE2), OX40 (clone-SP195) and OX40L (clone-D6K7R). We used this panel to interrogate 619 stage I-IV NSCLCs from 3 retrospective cohorts represented in tissue microarray format (cohort#1 [Yale, n=280], cohort#2 [Greece, n=207]). In addition, we analyzed a collection of lung adenocarcinomas with molecular testing for major oncogenic drivers (cohort#3 [Yale, n=132]). The targets were measured in all cells of the preparation using fluorescence co-localization with DAPI and specifically in tumor (CK-positive) and stromal (CK-negative) cells. Associations between the markers and with major clinicopathological variables, driver mutations and survival were studied.

Results

Expression of OX40 protein was seen in 90% of NSCLCs in cohort#1 and 87% of cases in cohort#2. OX40 staining was predominantly located in stromal cells with membranous staining pattern. Detectable OX40L signal was identified in 9% of cases in the first cohort and 14% of the second collection with membranous/perinuclear staining pattern and predominant expression in CK-positive tumor cells. There was no clear association between OX40 and OX40L expression in the cohorts. The levels of OX40 and OX40L were not consistently associated with major clinicopathogical variables, level of T-cell infiltration or with the presence of oncogenic mutations in EGFR/KRAS in lung adenocarcinomas (cohort#3). Elevated levels of OX40L protein (but not OX40) were significantly associated with longer 5-year overall survival in both NSCLC cohorts (log-rank P=0.03 and P=0.04, respectively).

Conclusions

Our preliminary data show that OX40 protein is expressed in the majority of NSCLCs with predominant location in stromal/immune cells and does not segregate with a specific clinicopathological variant or molecular subtype. Elevated OX40L, observed in ~15% of NSCLCs, is unrelated with OX40 levels and has favorable prognostic value.

P103

Bulk and single-cell TCR and transcriptome profiling reveals significant phenotypic, spatial and temporal heterogeneity in the TIL repertoire of pancreatic cancer and melanoma patients

Chin Leng Tan[1], Ignacio Heras-Murillo, MSc[1], Katharina Lindner[1], Aaron Rodriguez Ehrenfried[1], Lena Appel[1], Anna-Katharina Koenig[2], Markus Buechler[2], Ugur Sahin, MD[3], Jessica Hassel[2], Oliver Strobel[2], Michael Flossdorf[4], Rienk Offringa, PhD[1], Isabel Poschke, PhD[1]

[1]*German Cancer Research Center, Heidelberg, Germany*
[2]*Heidelberg University Hospital, Heidelberg, Germany*
[3]*Johannes Gutenberg University Mainz, Mainz, Germany*
[4]*Technical University of Munich, Germany, Heidelberg, Germany*

Background

Presence of tumor-infiltrating lymphocytes (TIL) is associated with good survival in many cancers, and harnessing of the T-cell response through checkpoint inhibition or infusion of ex vivo expanded TIL can result in tumor regression. While pancreatic ductal adenocarcinoma (PDA) has been considered a poorly-immunogenic tumor, we detect TIL infiltrates - and aggregates - in the majority of patients with primary resectable disease. PDA TIL phenotype and expansion capacity resemble that of melanoma TIL - our benchmark of an immunogenic tumor, and 80% of in vitro expanded PDA TIL cultures exhibit reactivity against autologous tumors.

Methods

To gain a better understanding of TIL reactivity, we performed repertoire profiling of freshly isolated TIL by T-cell receptor (TCR) deep- and high-throughput

single-cell sequencing and transcriptomics, as well as phenotypic and functional analysis of bulk and single-cell expansion cultures.

Results

Intra-tumoral and intra-patient heterogeneity is significant and highly individual: TIL repertoires from multiple regions of the same tumor show an overlap between 8.4-100%. Lesions within the same patient share between 0-70% of TCRs and tend to overlap less if biopsies are not acquired concurrently, indicating a continuous turn-over or reshaping of TIL composition. Notably, repertoire-sharing is most prominent among the largest TIL clones, possibly explained by efficient migration/re-circulation of some clones, or their maintenance by ubiquitously expressed (tumor-)antigens. Enrichment of highly frequent CDR3 sequences within the TIL repertoire suggests in situ proliferation in response to tumor-derived antigens. Droplet-based TCR- and transcriptome-analysis of >6000 PDA TIL cells revealed that dominant T-cell clones exhibit multiple distinct phenotypes, enriched for markers associated with activation, proliferation and exhaustion. Importantly, TIL in vitro expansion - with protocols established for therapeutic TIL application- induces dramatic shifts in repertoire composition, resulting in loss of dominant clones and enrichment of bystander clones with high proliferative potential.

Conclusions

Our findings call for careful sampling and optimized culture conditions for TIL infusion products and illustrate the need to probe T-cell reactivity directly ex vivo. The heterogeneous TIL response implies that therapeutic efficacy of TCR gene therapy using tumor-dominant TCRs could be more consistent than that of TIL therapy. Emerging high-throughput single cell technologies and resulting data will facilitate rapid identification of relevant TIL populations.

Ethics Approval

The study was approved by the local ethics committee at the medical faculty of Heidelberg university and conducted in accordance with the declaration of Helsinki.

P104

Radiomic features that can predict response to PD-1 inhibitors in late-stage Non-Small Cell Lung Cancer are also associated with tissue-derived measures of immune response

Prateek Prasanna, PhD[1], Mohammadhadi Khorrami, PhD[1], Pradnya Patil[2], Kaustav Bera, MBBS[1], Vamsidhar Velcheti, MD FACP[2], Anant Madabhushi, PhD[1]

[1]*Case Western Reserve University, Cleveland, OH, USA*
[2]*Cleveland Clinic, Cleveland, OH, USA*

Background

Nivolumab is a FDA approved immune checkpoint inhibitor (ICI) for treatment of patients with chemotherapy refractory advanced NSCLC. The current standard for identifying candidates who would benefit from ICIs is sub-optimal. First, the role of computer-extracted textural descriptors (radiomic features) [1] on baseline CT in predicting response to ICIs, is investigated. Secondly, since the degree of immune response is reflective of a cancer's ability to respond to ICIs, understanding the distribution of lymphocytic infiltration will help provide a morphological basis for the observed radiographic phenotypes. Towards that end, the predictive radiomic features are correlated with lymphocytic arrangement to understand their morphologic underpinning.

Methods

Non-contrast CT scans, before ICI treatment, were retrospectively acquired from 73 NSCLC patients. Patients with an objective response (complete/partial response) per RECIST after two

cycles of nivolumab were defined as “responders” and patients with progressive disease were defined as “non-responders”. 454 intra-tumoral texture, 24 shape features and 7426 features from annular rings outside the expert-annotated nodules, capturing different measures of phenotypic heterogeneity, were extracted from the baseline scans. A linear discriminant analysis (LDA) classifier was trained using the most predictive features identified on the discovery set (n=29) and validated on the test set (n=44). Digitized H&E histology scans of baseline biopsies were available for 56 cases. The nuclei were first segmented [2] and then classified into either lymphocytes or non-lymphocytes using texture, shape, and color features. 76 features quantifying density or compactness of tumor infiltrating lymphocyte (TIL) clusters were subsequently extracted. A pairwise Spearman correlation analysis was performed between the TIL compactness measures and the top discriminating radiomic features.

Results

A combination of 2 intra-tumoral, 6 peri-tumoral and 1 shape delta radiomic feature yielded an area under the receiver operating characteristic curve (AUC) of 0.85 ± 0.05 within the discovery set and an AUC=0.81 within the validation set. TIL density was found to be statistically significantly (correlation coefficient=-0.5, $p<0.05$) correlated with a peritumoral Gabor [3] feature, as illustrated in Figure 1.

Conclusions

Radiomic features extracted from baseline CT scans were predictive of objective response to ICIs. The TIL compactness features model relationships between lymphocytes and their surrounding cells. Presence of an immune infiltration is more likely to manifest via unique textural patterns in the tumor environment. The radiomic features could therefore be capturing the degree of immune response, which in turn is known to be correlated with the likelihood that the tumor will have a favorable response.

Acknowledgements

Research reported in this publication was supported by the National Cancer Institute of the National Institutes of Health under award numbers 1U24CA199374-01, R01CA202752-01A1, R01CA208236-01A1, R01 CA216579-01A1, R01 CA220581-01A1, National Center for Research Resources under award number1 C06 RR12463-01, the DOD Prostate Cancer Idea Development Award; the DOD Lung Cancer Idea Development Award; the DOD Peer Reviewed Cancer Research Program W81XWH-16-1-0329, the Ohio Third Frontier Technology Validation Fund, the Wallace H. Coulter Foundation Program in the Department of Biomedical Engineering and the Clinical and Translational Science Award Program (CTSA) at Case Western Reserve University. The content is solely the responsibility of the authors and does not necessarily represent the official views of the National Institutes of Health.

References

1. Prasanna P, Patel J, Partovi S, Madabhushi A, Tiwari P.. Radiomic features from the peritumoral brain parenchyma on treatment-naive multi-parametric MR imaging predict long versus short-term survival in glioblastoma multiforme: preliminary findings. European radiology. 2017; 27(10): 4188-4197.
2. Veta M, Van Diest PJ, Kornegoor R, Huisman A, Viergever MA, Pluim JP.. Automatic nuclei segmentation in H&E stained breast cancer histopathology images. PloS one. 2013 8(7): e70221.
3. Tuceryan M, Jain AK. Texture analysis. In Handbook of pattern recognition and computer vision (pp. 235-276).

Ethics Approval

The study protocol was approved under University Hospitals (UH) IRB 02-13-42C

Figure 1. Radiomic expression and TIL density patterns

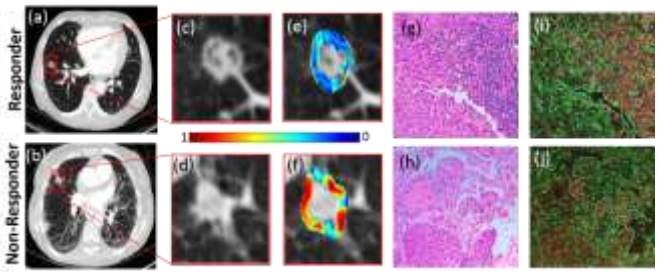

P105

Response to immunotherapy in hepatocellular carcinoma, a single-institutional analysis

Petra Prins[1], Bhavana Singh, MD[2], AIwu He[2]

[1]*Georgeotwn University, Washington, DC, USA*
[2]*Medstar Georgetown University Hospital, Washington, DC, USA*

Background
Despite advances in our understanding of the molecular pathways involved in hepatocellular carcinoma (HCC), therapeutic options remain limited and patient (pt) survival is dismal. Immunotherapy (IO) is one of the newer and more promising options for the treatment of HCC, with nivolumab being at the forefront. In the CheckMate 040 non-randomized, open-label, phase-1/2 study of nivolumab in pts with advanced liver cancer, a median overall survival (OS) of 15 months (m), an overall response rate of 15%, and a median duration of response of 16.6m was observed

Methods
In this single-institutional retrospective analysis, 30 pts with HCC received one of five different IO regimens. Thirteen pts had received sorafenib prior to initiation of IO. Patients received either atezolizumab plus bevacizumab, cemiplimab, pembrolizumab, nivolumab, or nivolumab plus ipilimumab until disease progression (PD) or unacceptable toxicity. Responses were assessed using RECIST v 1.1 criteria for stable disease (SD), partial response (PR) and PD, and blood biomarker levels, and were correlated with clinical outcomes like best response and progression free survival (PFS).

Results
Demographics for our cohort (n=30) were as follows: 73% were male and 27% female; 33% were African American, 30% Caucasian, 23% Asian, and 13% of other ethnicities. Of our cohort 33% had HBV and 30% had HCV as part of their disease etiology. A positive treatment response was observed in 90% of the pts with 67% having SD and 23% having a PR. Median OS was 20m (95%CI, 7.0-32.0) from the start of IO. A positive response to therapy significantly improved OS (20m SD versus 5m PD, p=0.005). A positive treatment response also showed clear PFS benefits: 20m (95%CI, 0-40.0) for PR, 7m (95%CI, 2.4-11.6) for SD and 3m (95%CI, 0-6.2) for PD (p=0.016). Data for circulating blood biomarkers and image biomarkers are currently being analyzed.

Conclusions
Overall, treatment with immunotherapy resulted in durable responses and favorable PFS and OS in pts with advanced HCC within our institution, making immunotherapy a valid option for the treatment of HCC. Additional correlation of IO treatment response with blood biomarkers might improve our understanding of treatment response.

P106

Multiplexed ion beam imaging (MIBI) for characterization of the tumor microenvironment (TME) across tumor types

Jason Ptacek, PhD[1], Rachel Finck[1], Murat Aksoy[1], Jay Tarolli[1], Jessica Finn[1]

[1]*Ionpath, Inc, Menlo Park, CA, USA*

Background

Cancer arises from tumor cells taking advantage of complex relationships between stromal, vascular, and immune cell subsets. To date the ability to characterize the cellular composition and spatial organization of the TME has been limited by the techniques available to image the necessary number of biomarkers for broad phenotyping at a subcellular resolution. Here we show the applicability of MIBI for cell phenotype identification and their spatial relationships across multiple tumor types.

Methods

FFPE samples from tumor biopsies were imaged for their cellular composition and architecture using multiplexed ion beam imaging. Samples were stained with a panel of 15 antibodies, each labeled with a specific metal isotope. The panel was validated by comparing to single-plex IHC and included antibodies for tumor and immune cell subsets in addition to immunotherapy targets (PD-1, PD-L1). In MIBI the stained section is scanned via secondary ion mass spectrometry to image the tissue for expression of the antibody targets. Multi-step processing, including machine-learning-based segmentation, was used to produce images of the TME and determine both the frequency of cell subsets and the distance between immune cells and tumor cells.

Results

A total of 25 tumor specimens from 8 tumor types, plus control samples, were characterized for their immune profile, spatial organization of tumor and immune cells and their expression of PD-1 and PD-L1. Tumor-associated macrophages (TAMs) and tumor infiltrating lymphocytes (TILs) were observed in breast, gastric, lung, ovarian, and head and neck cancers. Nearest-neighbor immune:tumor distances revealed the level of mixing between tumor and immune cells (Figure 1). For example, ovarian serous carcinoma samples showed large numbers of infiltrating cytotoxic T cells and macrophages amongst tumor cells. However, the TMEs differed with one showing mixing of the populations and the second showing a compartmentalized organization. In contrast, an ovarian endometrioid carcinoma specimen showed much less robust immune cell infiltrate. Similar results of mixing or compartmentalization were observed for lung and gastric adenocarcinomas. Interestingly, PD-L1 expression was detectable in all gastric adenocarcinomas with the strongest expression observed in the tumor showing the most compartmentalization.

Conclusions

The function and phenotypes of cells can only be determined through the co-expression of multiple proteins. Multiplexed imaging by MIBI reveals the complex tumor immune landscape by enabling the characterization of the spatial relationship of immune and tumor cells and the expression of immunoregulatory proteins. This work demonstrates the possibilities of MIBI for future patient stratification through characterization of the TME.

Figure 1. Spatial distribution of cells within tumor samples

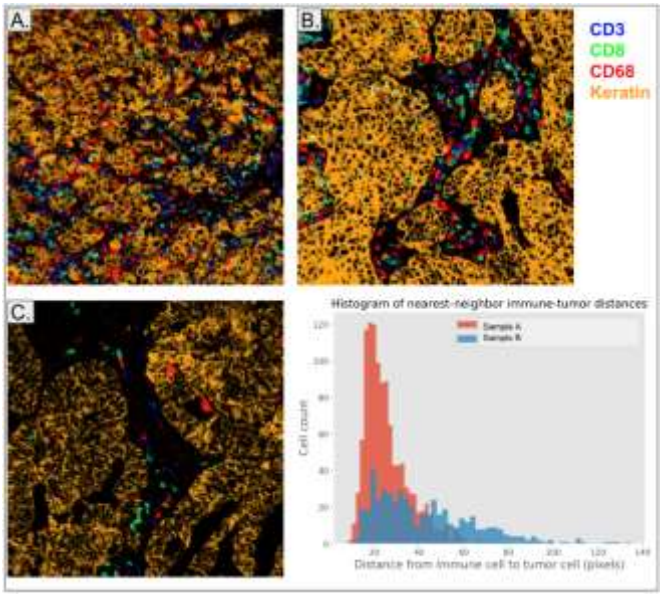

P107

A comparative study of the PD-L1 IHC 22C3 and 28-8 assays in melanoma samples

Gabriel Krigsfeld, PhD[1], Kim Zerba[1], James Novotny Jr[1], Shuntae Williams[2], Michael Matthews, MS[3], Hytham Al-Masri, PhD[2], David Gold[1], James White[1]

[1]*Bristol-Myers Squibb, Princeton, NJ, USA*
[2]*Hematogenix Laboratory Services, LLC, Tinley Park, IL, USA*
[3]*Acupath Laboratories, Inc, Plainview, NY, USA*

Background

Nivolumab is a programmed death-1 (PD-1) receptor blocking antibody approved as monotherapy or in combination with ipilimumab for patients with unresectable or metastatic melanoma. The Dako programmed death ligand 1 (PD-L1) immunohistochemistry (IHC) 28-8 pharmDx is an FDA-approved PD-L1 complementary diagnostic for melanoma. While the Dako PD-L1 IHC 22C3 pharmDx is an FDA-approved companion diagnostic for several tumor types, it is not approved for melanoma. To date, studies have compared the 2 assays in non-small cell lung cancer and urothelial carcinoma. We report a comparison of the 28-8 and 22C3 assays on real-world melanoma samples, which provide new data to address the potential interchangeable use of these assays in clinical practice.

Methods

Formalin-fixed, paraffin-embedded melanoma samples were obtained from Acupath Laboratories, Inc (Plainview, NY) with basic demographic information. Staining and scoring of slides were performed at Hematogenix (Tinley Park, IL). The 28-8 and 22C3 PD-L1 assays were used per manufacturer's protocols and evaluated using the 28-8 pharmDx tumor cell scoring algorithm [1]. Slides were randomized and pathologists were blinded to the assay at scoring, with paired 28-8 and 22C3 assay results read by the same pathologist. Samples that were heterogeneous (determined by bracket evaluation with H&E staining), had high melanin content, or failed to meet minimum criteria (≥100 tumor cells per 28-8 assay) were excluded from the final analysis.For the primary analysis, overall, positive, and negative percentage agreement (OPA, PPA, and NPA) at the ≥1% PD-L1 expression level were evaluated. Secondary analyses included agreement rates at the ≥5% expression level, Passing–Bablok regression, and Bland–Altman plots with summary statistics describing the differences between assays across the dynamic range.

Results

Of 265 samples analyzed, 202 were confirmed to contain melanoma tissue with quantifiable PD-L1 expression. Average patient age was 66.4 years. Average sample age was <2 years (657 days [range 637–678]), and samples ranged from stage I to IV melanoma. High analytical concordance was observed between the 28-8 and 22C3 assays across paired melanoma samples. OPA, PPA, and NPA for all

paired samples at the ≥1% PD-L1 expression level were 93.1%, 82.1%, and 97.3%, respectively. Identical PD-L1 expression values for the 28-8 and 22C3 assays were reported for 82.7% of samples, with a ≤10% difference in tumor cell membrane staining for 98.0% of samples.

Conclusions

These data support the potential interchangeability of the PD-L1 IHC 28-8 and 22C3 pharmDx assays for assessing tumor cell membrane PD-L1 expression on melanoma samples.

Acknowledgements

Medical writing assistance was provided by Bernard Kerr, PGDipSci, CMPP™, of Spark Medica Inc. (US), funded by Bristol-Myers Squibb. This study was funded by Bristol-Myers Squibb.

References

1. Dako. PD-L1 IHC 28-8 pharmDx SK005. Package Insert. 2017. [https://www.agilent.com/cs/library/packageinsert/public/128371004.PDF] Accessed July 30, 2018.

P108

HLA class I subtypes are associated with immune-related adverse events in patients with melanoma treated with ipilimumab

Anton Safonov, MD[1], John Pluta[1], Lu Qian[2], Ravi Amaravadi[1], Allison Applegate[3], Elizabeth Buchbinder, MD[4], Justine Cohen, DO[4], Claire Friedman, MD[5], Ruth Halaban, PhD[6], F. Stephen Hodi, MD[4], Christine Horak, PhD[7], Douglas Johnson, MD, MSCI[8], John Kirkwood, MD[9], Tara Mitchell[1], William Robinson, MD, PhD[3], Lynn Schuchter, MD[1], Jeffrey Sosman, MD[10], Mario Sznol, MD[6], Megan Wind-Rotolo, PhD[7], Jedd Wolchok, MD, PhD[5], Mingyao Li[1], Peter Kanetsky[2], Katherine L. Nathanson[1]

[1]Perelman School of Medicine, University of Pennsylvania, Philadelphia, PA, USA
[2]Moffitt Cancer Center, Tampa, FL, USA
[3]University of Colorado, Denver, CO, USA
[4]Dana Farber Cancer Institute, Boston, MA, USA
[5]Memorial Sloan Kettering Cancer Center, New York, NY, USA
[6]Yale University, New Haven, CT, USA
[7]Bristol-Myers Squibb, Lawrenceville, NJ, USA
[8]Vanderbilt Cancer Center, Nashville, TN, USA
[9]University of Pittsburgh Medical Center, Pittsburgh, PA, USA
[10]Feinburg School of Medicine, Northwestern University, Chicago, IL, USA

Background

Checkpoint immunotherapies have demonstrated substantial benefit in patients with melanoma. However, there are currently no established biomarkers to predict immune-related adverse events (irAEs). Because genetic variation at the human leukocyte antigen (HLA) locus is associated with increased risk of autoimmune disorders, we evaluated associations between irAEs and HLA subtypes.

Methods

We utilized clinical and genomic data from 269 chemotherapy and immunotherapy-naïve melanoma patients treated with ipilimumab monotherapy on the Bristol-Meyers-Squibb clinical trial CA184-169 (NCT01515189). DNA samples were genotyped on Affymetrix 6.0 and standard sample- and SNP-level quality control pipelines were conducted; only samples with high levels of European genetic ancestry (i.e. Caucasian) were further analyzed. Genotype imputation was completed using the Haplotype Reference Consortium Backbone. We used SNP2HLA to establish estimated allele dosages for each 4-digit HLA allele (n = 172), and subsequently collapsed these calls into one of nine established class I supertypes. We catalogued occurrences of immune-related adverse events by

CTCAE grade and affected organ system. Logistic regression was performed to evaluate associations of class I HLA supertype allele dosage with irAE outcomes (grade < 2 vs grade ≥ 2) adjusting for ECOG score, dosage, and number of doses.

Results

HLA-A24 was significantly associated with hepatitis (Grade > 2), with meta-analysis odds ratio 3.69 [95% CI 1.75 to 7.51, p = 0.0005]. Odds ratio was 3.54 [95% CI 1.51 to 8.31, p = 0.0036] in the BMS dataset (remaining significant after correction for multiple comparisons), and OR 3.85 [95% CI 0.96 to 15.5, p = 0.056] from the consortium data set. The frequency of HLA-A24 in our population was 9.6%.

Conclusions

Our results demonstrate that a specific HLA subtype, HLA-A24, is associated with checkpoint-inhibitor related hepatitis. HLA-A24 has been explored in its dose-dependent response to hepatitis B and C vaccination. Our results potentially demonstrate unmasking of germline-mediated immune sensitivity by checkpoint inhibitors. This data warrants further study into HLA subtypes as predictive biomarkers for immune-related adverse effects. These findings should be confirmed in additional study populations, potentially with sequence-based HLA typing.

Trial Registration

NCT00135408, NCT00261365, NCT01515189

Ethics Approval

The protocol and all amendments were approved by the institutional review board or independent ethics committee for each study center

P109

Clinical efficacy of immune checkpoint inhibitors in patients with small cell lung cancer is associated with high tumor mutational burden and development of immune-related adverse events

Biagio Ricciuti, MD[1], Suzanne Dahlberg[1], Sasha Kravets[1], Safiya Subegdjo[1], Renato Umeton[1], Adem Albayrak, MS[1], Lynette Sholl[2], Mark M. Awad[1]

[1]Dana Farber Cancer Institute, Boston, MA, USA
[2]Brigham and Women's Hospital, Boston, MA, USA

Background

Immune-checkpoint inhibitors (ICIs) have shown promising activity in only a fraction of patients with small cell lung cancer (SCLC), and factors associated with clinical benefit are not well characterized. High tumor mutational burden (TMB), quantified by whole exome sequencing, has been shown to predict response to ICIs in SCLC. However, whether targeted next generation sequencing (NGS) can be used to identify SCLC patients with high TMB who might benefit from treatment with immunotherapy is currently unknown. The relationship between the development of immune-related adverse events (irAEs) and immunotherapy response in SCLC is also unknown.

Methods

Patients with SCLC at the Dana-Farber Cancer Institute (DFCI) who received treatment with immunotherapy and/or had successful NGS were included in this study. TMB was determined using the DFCI NGS OncoPanel platform of >450 genes. The relationships between TMB, the development of irAEs, and clinical outcomes were determined among patients with SCLC treated with PD-1 inhibitors alone or in combination with a CTLA-4 inhibitor.

Results

Out of a total of 145 patients, 125 (86.2%) had

successful NGS with TMB assessment and 64 (44.1%) were treated with ICIs. The median (range) TMB was 9.29 (1.21-33.89) mutations/megabase. Among 44 TMB-evaluable patients treated with ICIs, the median progression-free survival (mPFS) was significantly longer in the 21 patients with a TMB above median ("TMB-high") compared to the 23 patients below median ("TMB-low") (4.1 vs. 1.4 months, HR: 0.39 [95%CI: 0.19-0.77], P < 0.01) (Figure 1A). The median overall survival (mOS) was significantly prolonged in the TMB-high group compared to the TMB-low group (10.5 vs. 2.7 months, HR: 0.43 [95%CI: 0.20-0.89], P = 0.02) (Figure 1B). Among 64 patients with SCLC treated with ICIs (44 TMB-evaluable), the 21 (32.8%) patients who developed at least one irAE had significantly longer mPFS (4.1 vs. 1.3 months, HR: 0.33 [95%CI: 0.19-0.56], P < 0.001) and mOS (12.5 vs. 3.2 months, HR: 0.35 [95%CI: 0.20-0.62], P < 0.01) compared to the 43 (67.2%) patients who did not develop irAEs (Figure 2 A,B). Patients with irAEs had a significantly higher mean TMB than those who did not experience any irAEs (13.09 vs. 9.41, P = 0.02).

Conclusions

Median PFS and OS on immunotherapy were significantly longer among patients with SCLC and high TMB and among those who developed at least one irAE. TMB determination by NGS may be a helpful biomarker for identifying patients who are likely to benefit from treatment with ICIs in SCLC.

Figure 1.

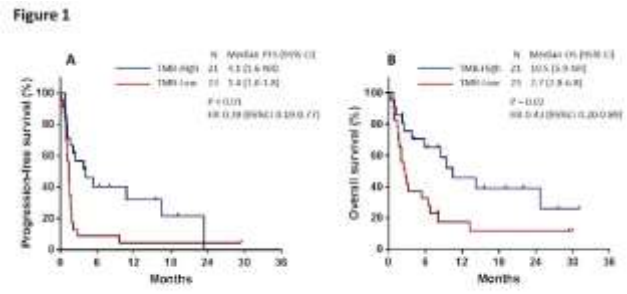

Figure 2.

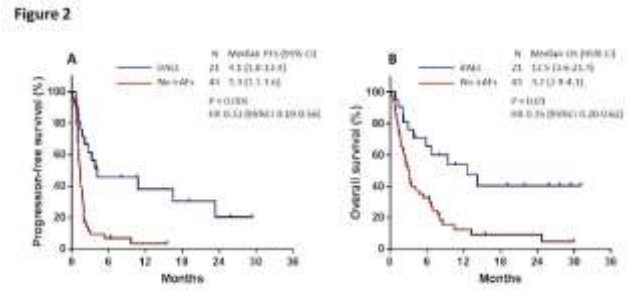

P110

Modular repertoire analysis of blood transcriptomic immune response in metastatic renal cell carcinoma patients treated with Pazopanib

Darawan Rinchai, PhD[1], Elena Verzoni[2], Agata Cova[2], Paola Squarcina[2], Loris Cecco[2], Paolo Grassi[2], Raffaele Ratta[2], Veronica Huber[2], Matteo Dugo[2], Monica Rodolfo[2], Jessica Roelands, Master[1], Damien Chaussabel[1], Giuseppe Procopio[2]. Davide Bedognetti, MD, PhD[1], Licia Rivoltini, MD[2]

[1]*Sidra Medicine, Doha, Qatar*
[2]*Fondazione IRCCS Istituto Nazionale Tumori, Milan, Italy*

Background

Transcriptional modular repertoire analysis has been developed and successfully used as a basis for the selection of biomarkers and development of multivariate transcriptional indicator of disease progression in patients with systemic lupus erythematosus or infectious diseases. In the context of cancer immunotherapy, understanding the molecular mechanisms modulated by a given drug is critical to implement more efficient therapeutic approaches. Here, we employed a modular repertoire approach to investigate immune response in metastatic renal cell carcinoma patient treated with Pazopanib (Tyrosine kinase inhibitors).

Methods

Peripheral blood mononuclear cells collected from 8 metastatic renal cell carcinoma patients (mRCC) receiving first-line Pazopanib were prospectively analyzed at baseline, 3 and 6 months for whole-genome transcriptomic perturbations using Illumina HT12v4BeadChip. As for the best response, partial response was observed in 3 patients and stable disease in 5 patients. A set of 260 transcriptional modules was used for the analysis of this dataset using a pre-defined framework (1–3). A module is considered to be "responsive" to the treatment when significant changes in abundance are observed for a proportion of its constitutive transcripts that is greater that what could be expected by chance.

Results

We first assessed changes in transcript abundance at the modular level. The percentage of responsive transcripts constitutive of a given module was determined for each time point (group comparison) or individual comparison. The group comparison analysis showed that module perturbations peaked at 3 months and decreased at 6 months. These perturbations include enrichment of modules M3.6 & M8.46 (Cytotoxic/NK), M4.11(Plasma cells), and M8.89 (Immune response) (Figure 1). In addition, individual-level analysis showed that Pazopanib administration was associated with the decreased of the immunosuppressive module M9.34 in 5 patients. Such module was up-regulated only in one patient who did not respond to treatment. Interestingly, a rapid increased of Interferon (IFN) modules (M1.2 & M3.4) was observed exclusively in responding patients (Figure 2).

Conclusions

These results suggest that Pazopanib has a strong immune modulatory effect and might reshape anti-tumor immunity by reducing immunosuppression and triggering cytotoxic mechanisms and IFN pathways. The peak of this immune modulation is observed 3 months after treatment. These data provide a strong rationale for exploring combinatorial immune-targeted therapy based on kinase inhibitors such as a Pazopanib and for implementing transcriptomic analysis of peripheral blood in the context of cancer immunotherapy.

References

1. Chaussabel D, Quinn C, Shen J, Patel P, Glaser C, Baldwin N, et al. A modular analysis framework for blood genomics studies: application to systemic lupus erythematosus. Immunity. 2008 Jul 18;29(1):150–64.
2. Obermoser G, Presnell S, Domico K, Xu H, Wang Y, Anguiano E, et al. Systems Scale Interactive Exploration Reveals Quantitative and Qualitative Differences in Response to Influenza and Pneumococcal Vaccines. Immunity. 2013 Apr 18;38(4):831–44.
3. Chaussabel D, Baldwin N. Democratizing Systems Immunology with Modular Transcriptional Repertoires Analyses. Nat Rev Immunol. 2014 Apr;14(4):271–80.

Figure 1.

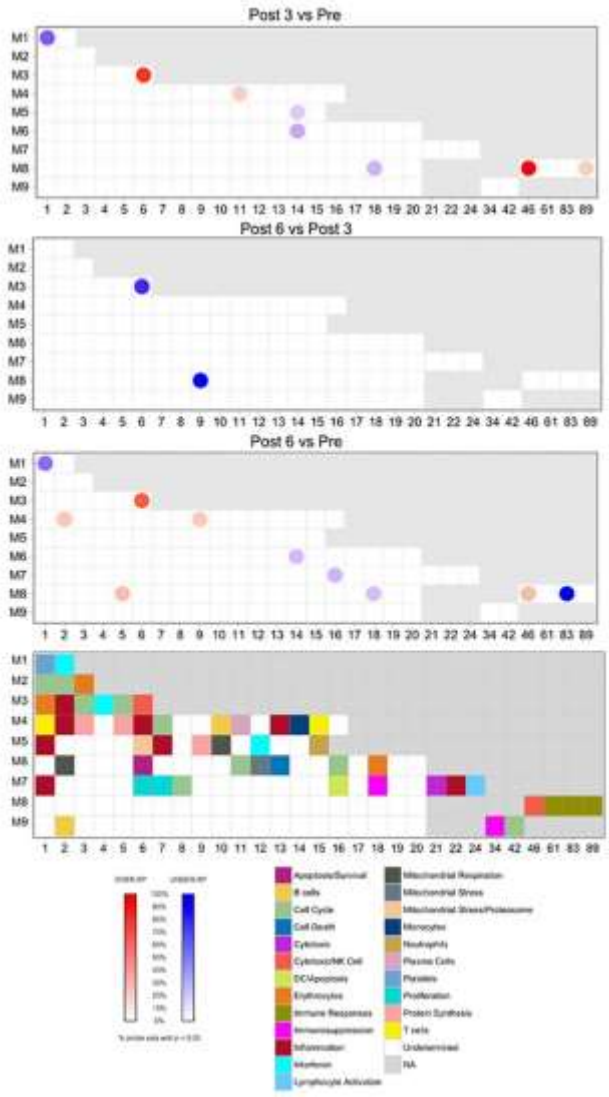

Figure 2.

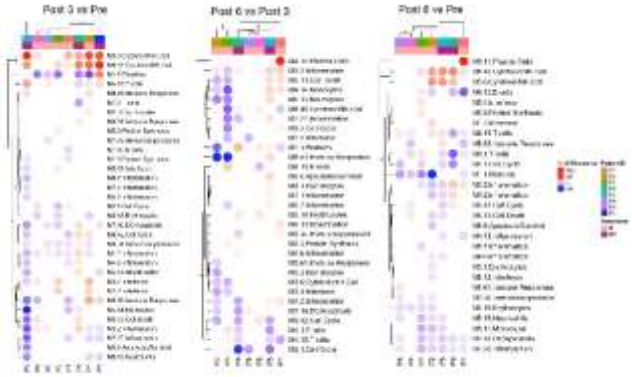

P111

Streamlined human immune monitoring with mass cytometry: 29 markers in a single tube with automated data analysis

Christina Loh, PhD[1], Thiru Selvanantham, PhD[1], Leslie Fung[1], Michelle Poulin[1], C. Bruce Bagwell[2], Margaret Inokuma[2], Clare Rogers, MS[1], Greg Stelzer, PhD[1], Steven Lott, PhD[1]

[1]*Fluidigm, South San Francisco, CA, USA*
[2]*Verity Software House, Topsham, ME, USA*

Background

Immune monitoring is an essential method for quantifying changes in immune cell populations in health and disease. The extreme heterogeneity of immune cells demands a high-parameter approach to more fully and efficiently quantify these changes. Mass cytometry is an ideal solution, enabling simultaneous detection of over 40 phenotypic and functional markers in a single tube of sample.

Methods

We developed a single-tube, 29-marker panel for mass cytometry based on the Human ImmunoPhenotyping Consortium (HIPC) consensus panel [1], expanded to allow identification of additional leukocyte subsets, particularly T cells. Automated data analysis with Verity Software House GemStone™ has been developed specifically for data collected with the panel, providing users with results in minutes, reducing time-to-answer and variability inherent in manual gating.

Results

Repeatability was tested with a single PBMC sample stained by a single technician in two technical replicates and acquired in triplicate on two Helios™ mass cytometers. SDs for percent of parent were 1% or less for 16 identified populations. Reproducibility was tested by determining the variability in

measurements of five PBMC lots stained by five technicians and collected on two Helios instruments. CVs on mean percent of all measured populations were under 20%. R2 values for agreement of percent parent populations using the full 29 marker panel compared to smaller 10-to-12-marker panels for T, B and myeloid cell populations were 0.94 or higher. In addition, comparison of cell population frequencies determined using GemStone analysis with manual gating in WinList demonstrated a high degree of concordance.

Conclusions

We conclude that this panel kit can provide consistent immune population identification and enumeration for any given lot of PBMC, and that data generated by the kit is amenable to either manual or automated data analysis.

References

1. Maecker HT, McCoy JP, Nussenblatt R, Standardizing immunophenotyping for the Human Immunology Project. Nature Reviews Immunology 2012; 12: 191-200.

P112

Proteomic profiling of biomarkers for response to checkpoint immunotherapy in melanoma patients

Marijana Rucevic, PhD[1]

[1]*Olink Proteomics, Watertown, MA, USA*

Background

Checkpoint immunotherapy has greatly improved clinical outcomes in patients with several malignancies including melanoma. However, only a subset of advanced melanoma patients generates durable responses to such immunotherapy. To date, there are no reliable methods to predict responders which urges a need to develop serological biomarkers of melanoma response to immune checkpoint therapy.

Methods

We applied an innovative and highly sensitive Proximity Extension Assay (PEA) for comprehensive profiling of ~1000 proteins in the plasma of 55 metastatic melanoma patients that received anti-PD-1 treatment whereas, 18 patients were previously treated with anti-CTLA-4 while 37 received anti-PD-1 monotherapy. Of the 55 patients, 42 were classified as having benefit from immunotherapy ('responders') and 13 had no benefit ('non-responders'). Our study included analyses of samples collected at baseline, on-treatment (~67 days from baseline) and post-treatment from these patients.

Results

Proteome wide analysis identified changes in ~100 immune response proteins over the course of treatment with different characteristic behavior across the treatment period. The dynamic response proteins included current and new exploratory checkpoint targets (PD-1, PDL-1, LAG-3, Gal-9, CD27, TNFR2) as well as, many proteins associated with the events that are hallmarks of immune response to cancer, such as cytokines/chemokines, angiogenesis, vascular cell adhesion and oncogenic signaling proteins. Importantly, 7 proteins including HER3, SAA4, NID1, ST6GAL1, OPN, TIMP1 and CXCL13 were found distinctive between responders and non-responders at the first on-treatment time point and demonstrated potential to classify responders and non-responders Thus, they may represent a protein signature that can predict treatment response or serve as surrogate markers for efficacy to immune checkpoint therapy in melanoma.

Conclusions

Our study might provide better understanding of immune system interaction with checkpoint inhibitors and demonstrates potential to improve melanoma patient's management that may have a significant impact to the field of immunotherapy.

P113

Digital spatial profiling of bone-marrow infiltrating immune cells in acute myeloid leukemia.

Sergio Rutella, MD, PhD, FRCPath[1], Jayakumar Vadakekolathu, PhD[1], Sarah Church[2], Heidi Altmann[3], Elena Viboch, MS[2], Jorn Meinel, MD[3], Yan Liang, MD PhD[2], Joseph Beechem, PhD[2], Alessandra Cesano, MD, PhD[2], Sarah Warren, PhD[2], Gerhard Enhinger, MD[4], Marc Schmitz, MD[4], Martin Bornhauser, MD[3]

[1]Nottingham Trent University, Nottingham, UK
[2]NanoString Technologies, Inc., Seattle, WA, USA
[3]University Hospital Carl Gustav Carus, Dresden, Germany
[4]Technische Universität Dresden, Dresden, Germany
[5]The John van Geest Cancer Research Centre, Nottingham, UK

Background

The therapeutic approach in patients with acute myeloid leukemia (AML) has not changed substantially in >30 years. The discovery of new treatment strategies, including immunotherapy, remains a priority [1-3]. Herein, we employed Digital Spatial Profiling (NanoString Technologies, Seattle) to characterize the expression of 31 immuno-oncology (IO) proteins in 10 bone marrow (BM) samples from adult patients with newly diagnosed AML.

Methods

FFPE BM slides were incubated with fluorescent markers (CD3 to identify T cells, CD123 to identify AML blasts, and Syto83 to stain nuclei) to establish the overall tissue morphology, followed by a cocktail of antibodies conjugated with oligo tags via a photo-cleavable linker. We then identified regions of interest (ROIs: CD3-rich and CD3-poor) with visible light-based imaging and selected them for high-resolution multiplex profiling. Oligo tags from the selected ROIs released upon exposure to UV light, were collected via a micro-capillary tube, hybridized to 6-spot optical barcodes, and digitally counted using the NanoString nCounter® platform. In parallel, we measured the expression of 770 immune-related mRNAs (including 14 molecules covered by the DSP IO panel) using the Pan-Cancer Immune Profiling Panel™ (NanoString Technologies, Seattle).

Results

We selected 24 geometric ROIs per BM sample using fluorescent anti-CD3 and anti-CD123 antibodies. Overall, T cell abundance across the 10 BM biopsies was highly variable and median CD3 barcode counts were used to classify samples into CD3-rich and CD3-poor. In the context of the six CD3-rich biopsies (Fig. 1A), ROIs were assigned to either CD3low, CD3int and CD3high categories using the 25th and 75th percentile of the area-normalized CD3 barcode counts. The expression levels of PD1, B7-H3, CD45RO, FoxP3, CD4 and CD8 were significantly higher in CD3high compared with CD3int and CD3low ROIs. The density of CD8+ T cells with an activated/exhausted CD45RO+PD1+ phenotype correlated with PD-L1 expression, consistent with the establishment of adaptive immune resistance (Fig. 1B). A similarity matrix of IO proteins allowed us to identify co-expression patterns of monocyte/macrophage markers (CD14/CD68) and negative immune checkpoints (B7-H3 [CD276] and VISTA), as well as a correlation between PD-L1, Bcl-2 and PTEN within the selected ROIs (Fig. 1C). Finally, in situ expression of mRNA and barcode counts for CD19, CD14, CD68, CD56 and Bcl-2 were also significantly correlated.

Conclusions

This proof-of-concept study provides evidence for heterogeneous immune profiles and advances our understanding of the immuno-biology of AML. DSP could support the implementation of future immunotherapy clinical trials.

Acknowledgements
Grant support: Qatar National Research Fund (#NPRP8-2297-3-494), Roger Counter Foundation (Dorset, UK) and John and Lucille van Geest Foundation to S.R.

Ethics Approval
Bio-banked tissue biopsies were collected at Technische Universität Dresden, Germany, under approval by the SAL AML Biobank's Ethics Committee.

Figure 1. Digital spatial profiling of AML

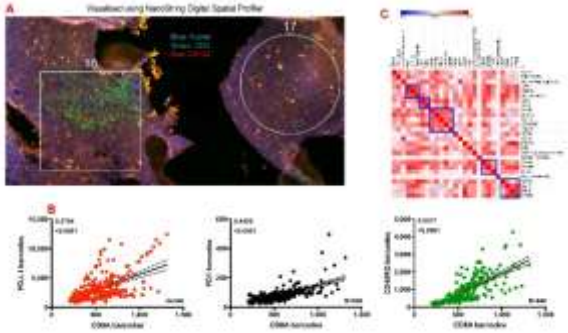

P114

ImmunoINTEL, a flow cytometry based platform that identifies and quantifies the most critical cell subsets and related functional potential in dissociated solid tumors

Konstantin Salojin, PhD[1], Christine Hauther[1], Dai Liu[1], Santosh Putta[2], Norman Purvis, PhD[1], Matt Westfall, PhD[1]

[1]Pierian Biosciences, Franklin, TN, USA
[2]Qognit,Inc., Franklin, TN, USA

Background
Standard immunohistochemistry (IHC) approaches to tumor-infiltrating leukocyte (TIL) phenotyping yield limited information, as they utilize antibody (Ab) panels not broad enough to identify and functionally characterize the complexity of TIL subsets. A flow cytometry platform was developed that delivers quantitative, clinically relevant information to support the following: 1) Phenotypic and functional analysis of TILs to characterize the immune status within the tumor microenvironment (TME), and 2) Quantification of TIL and tumor cell (co-)expression profiles of targetable immunomodulatory receptors (IMR) and ligands (IMR-L).

Methods
Standardized flow cytometry set-up, QC and sample processing procedure were established. Automated instrumentation and sample processing procedures were implemented in a barcode-based workflow utilizing Hamilton STARlet automated liquid handlers fully integrated with an SMS/LIMS and multi-dimensional flow cytometry data analysis software. Six Ab panels, ranging from 6-12 colors were designed, optimized, and validated to profile PBMC and TIL subsets.

Results
Phenotypic composition of the following cell subsets in the TME was delineated and quantified using qualified antibody panels for: (1) T, B, and NK cells; (2) T regulatory cells; (3) myeloid cell subsets (classical/nonclassical monocytes, M1/M2-macrophages); (4) myeloid cells with suppressive phenotypes (M- and G-MDSC); (5) myeloid/plasmacytoid DCs; (6) epithelial and mesenchymal cells. The relative quantities of the TIL subsets were tabulated based on tumor type. The ImmunoINTEL panels were complemented with drop-in IMR and IMR-L markers (PD1/PDL1, TIGIT/CD112-CD155, TIM-3/Galectin-9, SIRPa/CD47, LAG-3/HLADR) to profile the functional status of TILs, and to study the cytotoxic potential of tumor TILs. Reliable separation of IMR/IMR-L positive TILs from negative TILs and IMR/IMR-L positive tumor cells from negative tumor cells was observed, with notable heterogeneity, across cell and tumor types. This included the elevated expression of several IMR-Ls on TILs and IMRs on epithelial and stromal cells,

suggesting tumor- and TIL-intrinsic mechanisms modulating checkpoint interactions. Results demonstrate a highly reproducible data set with minimal variability in PBMC reference/control specimens (CVaverage < 5%; n = 30) and accurate quantitation of lymphoid, myeloid, epithelial, and mesenchymal cell subsets in tumor samples.

Conclusions
Stringent flow cytometry QC processes were developed and implemented to ensure quality and precision of phenotypic and functional analyses of dissociated TILs and tumor cells, capturing the most critical metrics of intra-tumor immune responses and providing quantitative characterization of IMR and/or IMR-L interactions for more refined selection of potential responders to immune checkpoint inhibitors.

Ethics Approval
This study was reviewed and approved by BioIVT's and iSpecimen's Ethics/Regulatory Committees, approval numbers: 0944, 0984, 0985, 01034, 01045, 01050, 01071, 01084, 01095, & 01096. All of the samples collected under the above listed approvals are in full compliance with applicable Good Clinical Practices as defined by U.S. Food and Drug Administration (FDA) and U.S. Department of Health and Human Services (HHS) regulations as well as the International Conference on Harmonization (ICH) guidelines.

P115

Predictive and pharmacodynamic biomarkers associated with treatment with the oral selective AXL Inhibitor bemcentinib in combination with pembrolizumab in patients with advanced NSCLC and Melanoma

Robert Holt, PhD[1], David Micklem, PhD[1], Anthony Brown[1], Cornelia Schuster[2], Oddbjørn Straume[2], James Lorens, PhD[1]

[1]BerGenBio ASA, Bergen, Norway
[2]Haukeland University Hospital, Bergen, Norway

Background
Bemcentinib (BGB324) is a first-in-class, oral, potent and highly selective inhibitor of the AXL tyrosine kinase currently in phase II clinical development across several cancer types. AXL over-expression has been observed in patients failing PD-1 therapy in several cancers whereas AXL inhibition via bemcentinib has shown synergistic effect with checkpoint blockade in pre-clinical models. Selective blockade of Axl by bemcentinib in combination with pembrolizumab in NSCLC and melanoma is currently being explored in two Phase 2 trials BGBC008 (NCT03184571) and BGBIL006 (NCT02872259). Here we report results of the biomarker research programmes designed to identify predictive and pharmacodynamic biomarkers associated with bemcentinib/pembrolizumab treatment.

Methods
Fresh pre-treatment tumour biopsies were mandatory for PD-L1 and AXL analysis by IHC. Plasma protein biomarker levels were measured using the DiscoveryMap v3.3 panel (Myriad RBM) at pre-dose and C2D1 to identify predictive and pharmacodynamic biomarkers associated with bemcentinib/pembrolizumab treatment. The co-localisation of AXL and PD-L1 in tumour infiltrating immune cells was determined using NeoGenomics MultiOmyx.

Results
One cycle of treatment with bemcentinib significantly altered soluble Axl protein levels in a subset of patients including those who had benefited from treatment. This observation was consistent across multiple disease indications and treatment regimes. Protein biomarkers predictive of patient benefit following bemcentinib treatment have been identified - correlations with AXL and PD-L1 IHC will

also be presented. AXL is expressed in a subset of tumour infiltrating immune cells, primarily macrophages. Inaddition, AXL and PD-L1 were found to be co-expressed.

Conclusions
Predictive biomarker candidates were identified supporting potential companion diagnostics development for bemcentinib/pembrolizumab treatment. Pharmacodynamic biomarkers indicate that bemcentinib is selective and on target. AXL is expressed on macrophages and is co-expressed with PD-L1.

Trial Registration
NCT03184571 and NCT02872259

Ethics Approval
All relevant ethical and regulatory approvals were obtained.

P116

Quantitative measurement of CD8, CD68 and PD-L1 expression in a novel multiplex assay and associations of overall survival in non-small cell lung cancer (NSCLC) patients treated with anti-PD-1 Therapy

Fahad Shabbir, MD[1], Jon Zugazagoitia, MD[1], Yuting Liu, PhD candidate[1], Katir Patel, PhD[2], Brian Henick, MD[3], Scott Gettinger, MD[1], Roy Herbst, MD, PhD[1], Kurt Schalper, MD, PhD[1], David Rimm, MD, PhD[1]

[1]Yale School of Medicine, New Haven, CT, USA
[2]Ultivue Inc, Cambridge, MA, USA
[3]Columbia University Irving MedicalCenter, New York, NY, USA

Background
While PD-1 axis therapies have dramatically changed outcomes in some lung cancer patients, many patients don't benefit from these immunotherapies. Quantitative immunofluorescence (QIF) may provide a method for selection of those that benefit. This approach has been limited by the fact that traditional fluorescent multiplexing using tyramide amplification and unique species antibodies result in complexity that would be challenging in the CLIA lab setting. Here we test a novel, single mix, multiplex approach to simultaneously assess CD8, CD68 and PD-L1 in immmuno-therapy treated NSCLC patients

Methods
A tissue microarray with 81 spots in two-fold redundancy was derived from Yale patients treated with immunotherapy between 2011and 2017. Both a traditional tyramide and species unique multiplex (DAPI, CD68, PDL1 and Cytokeratin) and a DNA-based kit (UltiMapper Kit 1: CD8, CD68, PD-L1 & Cytokeratin/SOX10 with a nuclear dye) were assessed using the PM2000 microscope and AQUA software. The UltiMapper antibody premix is a single step, antibody mix which decreases overall staining time in anticipation of CLIA lab usage. We validate this new assay by regression with conventional QIF and overall survival (OS).

Results
Reproducibility was measured using two slides from 2 different blocks on two different days and showed that they were significantly correlated for CD8 (R2 = 0.58), CD68 (R2 = 0.67) and PD-L1 (R2 = 0.71). Comparative regressions between the two different protocols for the expression of PD-L1 in both tumor and stromal compartments were excellent (R2 = 0.93, and 0.83). From a total of 81 patients, we excluded those whose samples were taken after therapy and those who received more than one immunotherapy resulting in 62 patients for outcome analysis using only the data from the Ultimapper assay. Assessment by OS showed significant relationships for high PD-L1 in tumor (21m vs 8m median OS, p=0.036) and high PD-L1 in CD68 positive macrophages (20m vs 10m median OS, p=0.012). Also, on the same slide, high CD8 was associated

with better OS (22m vs. 11m median OS, p=0.011).

Conclusions
Expression levels of PD-L1 in tumor, but also in macrophages and the presence of CD8 in tumor show OS benefit in patients treated with immune checkpoint blockade in NSCLC. Future studies are required to evaluate this approach within a CLIA certified laboratory setting.

Acknowledgements
Sponsored research agreement between Yale and Ultivue (D. Rimm - PI)

Ethics Approval
Yale Human Investigation Committee protocol #9505008219.

P117

Host immune response in undifferentiated pleomorphic sarcoma – 10-year retrospective analysis

Joseph Sheridan[1], Andrew Horvai[1], Ross Okimoto[1], Rosanna Wustrack[1]

[1]*University of California, San Francisco, San Francisco, CA, USA*

Background
Undifferentiated pleomorphic sarcoma (UPS) is an aggressive soft-tissue sarcoma (STS) characterized by high rates of local and metastatic recurrence. Due to the paucity of therapeutic options, advanced disease remains lethal in a large majority of patients. An improved understanding of how the tumor microenvironment modulates UPS progression may enhance our ability to predict therapeutic responses and improve outcomes.

Methods
Thirty-six clinically annotated UPS patients collected over 10 years at a single institution with minimum five-year follow-up and available tumor specimens were included in this retrospective study. Using primary tumor specimens, we performed a targeted immunohistochemical analysis of the UPS microenvironment. We quantified expression of lymphocyte markers (CD8, CD20, CD68) and immune checkpoint protein (PD-L1) in all 36 UPS tumors using automated image analysis. The median percentage of positive cells for each subpopulation was used to define high expression vs. low expression. The Kaplan-Meier method was used to analyze OS and DFS; the association of specific TILs with OS and DFS was analyzed using the Log Rank Test.

Results
Factors that correlated with improved overall survival in our UPS cohort included localized disease (p=0.015), and use of intraoperative radiation therapy (IORT) or adjuvant radiation therapy (p=0.01). Our immunohistochemical analysis revealed the presence of TILs (CD8, CD20, CD68) and expression of immune checkpoint protein (PD-L1) in UPS tumors. Patients with a greater population of CD8+ TILs had a 5-year OS of 66% compared to those with lower levels of 28% (p=0.003, Figure 1). CD8+ T-cell expression in UPS tumors inversely correlated with local recurrence (p=0.04), suggesting CD8+ T-cell mediated immune surveillance. Interestingly, we also observed an increase in metastatic events in patients whose tumors harbored low CD8 expression compared to high CD8 expression (59% vs. 41%).

Conclusions
Through our quantitative immunohistochemical (IHC) analysis of immune cell subsets in UPS tumors, we identified improved survival in patients with increased infiltration of CD8+ T-Cells. Our study demonstrates that patients with low levels of CD8+ TILs are at increased risk of local (and potentially metastatic) recurrence. These findings underscore

the importance of immune mediated tumor surveillance in UPS. Recent advancements in systemic immunotherapy further highlight the immunogenicity of UPS tumors and demonstrate the clinical impact of targeting the tumor microenvironment to improve outcomes for UPS patients.

Ethics Approval
Approval from the Institutional Review Board was obtained before beginning this study.

Figure 1.

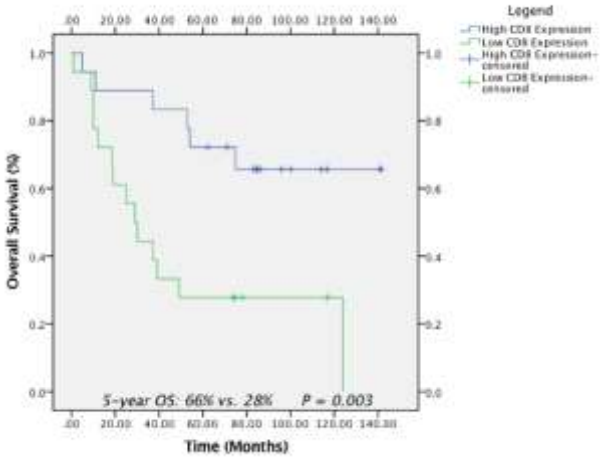

P118

Immunosuppression involving MDSC and IL-17 is associated with decreased levels of serum rapid turnover protein and shorter survival in patients with gastrointestinal cancer

Masahiko Shibata, MD[1], Kenji Gonda, MD, PhD[1], Takahiro Nakajima[1], Tatsuo Shimura[1], Koji Kono[1], Seiichi Takenoshita[1]

[1]*Fukushima Medical University, Fukushima, Japan*

Background
Although a causal relationship of inflammation and immune function of cancer patients is more widely accepted today, the precise cell mechanisms mediating this relationship have not been elucidated. Accumulating evidence suggests that myeloid-derived suppressor cells (MDSC) may contribute to the negative regulation of immune responses during cancer and inflammation. IL-17 is a pro-inflammatory cytokine that is primarily secreted by T helper (Th)17 cells and has been reported to be associated with immunosuppressive conditions in patients with cancer. We have reported that systemic inflammation is closely associated with immunosuppression, malnutrition, and poor prognosis in several types of cancer. Cancer cachexia is a multifactorial condition characterized by hypoproteinemia, and systemic inflammation is a major cause of cachexia.

Methods
Rapid turnover proteins such as prealbumin (PA), retinol binding protein (RBP) and transferrin (TF), were measured and analyzed in correlation with prognosis in 288 patients with esophageal cancer (Study 1). In order to characterize the inflammation, the production of IL-17 was measured and MDSC (CD11b+CD14-CD33+) in peripheral blood were detected by flow cytometry in 106 patients including 43 with gastric and 63 with colorectal cancer. Blastogenic response of lymphocytes with PHA (SI: stimulation index) was used as a marker of cell-mediated immunity (Study 2).

Results
(Study 1) The patients were divided according to their average levels of PA, RBP and TF. The survival of the patients with higher PA, RBP or TF levels were significantly longer than of those with lower PA, RBP or TF levels. The levels of PA, RBP and TF were significantly inversely correlated with SI. (Study 2) The IL-17 production and MDSC levels were both increased along with disease advancement, and

significantly correlated with each other. Further, they both were correlated with neutrophil/lymphocyte ratio (NLR), and CRP, inflammatory markers, and significantly inversely correlated with the levels of PA, RBP, and TF. The overall survival of the patients with higher IL-17 production or higher MDSC was shorter than of those with lower IL-17 production or lower MDSC.

Conclusions

IL-17-mediated inflammation may associate with immunosuppression involving MDSC, malnutrition and shorter survival and IL-17-targeting therapy may be effective for cancer treatment.

P119

Fab-selective proteolysis coupled with liquid chromatography-mass spectrometry for monitoring therapeutic antibodies in circulation

Takashi Shimada, PhD[1], Noriko Iwamoto, PhD[1]

[1]*Shimadzu Scientific Instruments, Bothell, WA, USA*

Background

Individual cancer treatment according to drug efficacy indicators is very important matter. The genetic background, drug surrogate biomarker, and immune cell monitoring will be potentially incorporated into the future medicine as well as the expression level of target molecule or pharmacokinetic information. For the analysis of low-MW drugs, liquid chromatography-mass spectrometry (LC-MS) are often used. This is optimal approach for the structure identification and quantitation with sequential and comprehensive manner. However, for the high-MW biopharmaceuticals, pharmacokinetic parameters are often analyzed by ligand binding assays (LBA). The LBA may have some significant limitation. Therefore, analytical innovation should be indispensable independent of a variety of antibodies. For LC-MS, it should be developed the integrated and overall optimized approaches from complex biological samples because of the issue in separation and ionization suppression. We have focused on the two features: antibody structure-indicated analysis, and complementarity-determining region (CDR)-targeting quantitation. The ideal antibody analysis is possible using the selective quantitation of somatic mutated region CDRs.

Methods

IgGs were immobilized in resin pore (100 nm) via Fc, so that Fab was oriented to reaction solution. And proteolysis was performed by immobilized trypsin on the surface of FG nanoparticles (200 nm). Owing to these diameter difference, limited proteolysis on Fab was successful with maintaining the antibody specificity while minimizing the complexity or protease contamination. We named this method nano-surface and molecular-orientation limited (nSMOL) proteolysis.[1] And the generated signature peptides from each antibody were quantified using triple quadrupole LC-MS/multiple reaction monitoring (MRM) analysis.

Results

We have performed the assay validation development for Trastuzumab, Bevacizumab, Nivolumab, and more than 25 items according to the guideline on bioanalysis method validation.[2] The quantitation range in human plasma was obtained from about 0.2 to 300 µg/ml, which is enough to cover the clinical levels. And the verification of clinical samples has also been successfully with high-reproducibility.

Conclusions

The feature of nSMOL is the breakthrough solution for the accuracy, reproducibility, cost, general-purpose, QC and stability. We have some study design for the elucidation of overall mechanism of antibody drugs to discuss the relationship between drug level and efficacy or anti-drug antibody assay.

And for practical use, we have another activity into the expanded clinical application, comparative assay of original/biosimilar, and therapeutic drug monitoring. Furthermore, the antibody profiles and distribution mechanism[3] in tumor tissues based on nSMOL may be expected to aid the acceleration of the biopharmaceuticals.

Acknowledgements
This study was partly collaboration results with Dr. Hamada A of National Cancer Center and Dr. Yonezawa A of Kyoto University.

References
1. Iwamoto N, Shimada T, Umino Y, Aoki C, Aoki Y, Sato TA, Hamada A, Nakagama H. Selective detection of complementarity-determining regions of monoclonal antibody by limiting protease access to the substrate: nano-surface and molecular-orientation limited proteolysis. Analyst. 2014;139(3):576-580.
2. Iwamoto N, Shimada T, Terakado H, Hamada A. Validated LC-MS/MS analysis of immune checkpoint inhibitor Nivolumab in human plasma using a Fab peptide-selective quantitation method: nano-surface and molecular-orientation limited (nSMOL) proteolysis. J Chromatogr B Analyt Technol Biomed Life Sci. 2016;1023-1024:9-16.
3. Terrell-Hall TB, Nounou MI, El-Amrawy F, Griffith JIG, Lockman PR. Trastuzumab distribution in an in-vivo and in-vitro model of brain metastases of breast cancer. Oncotarget. 2017 Jul 26;8(48):83734-83744.

P120

Validated next generation sequencing assay for the characterization of the T-cell repertoire from RNA

Jennifer Sims[1], Martin Buchkovich, PhD[1], Victor Weigman[1], Jason Powers[1], John Pufky[1], Jennifer Mason, PhD[1], Patrick Hurban, PhD[1]

[1]Q2 Solutions, Morrisville, NC, USA

Background
Activation of T-cells during cell-mediated immunity is initiated by the stimulation of the T- cell receptor (TCR) by major histocompatibility complex-antigen complexes. While the entire TCR chain is diverse, most of the diversity is concentrated in a hypervariable complementarity-determining region 3 (CDR3) loop, the center of the antigen-binding site for the TCR. The frequency of a specific CDR3 sequence within the T-cell repertoire is a surrogate for the abundance of its corresponding T-cell clone. Deep sequencing of the TCR CDR3 region assists with resolving T-cell diversity, and, in oncology, detects specific clones or changes in clonality associated with anti-tumor immune responses. Here, we have validated an RNA based TCRβ/γ next-generation sequencing assay for use with whole blood, peripheral blood mononuclear cells (PBMCs) and formalin-fixed paraffin-embedded (FFPE) tissues.

Methods
TCR analysis was performed using RNA or total nucleic acids derived from whole blood, PBMCs or tumor FFPE specimens. The TCRβ/γ sequencing assay entailed gene specific cDNA synthesis, preparation of sequencing libraries, TCR gene specific amplification, sample barcoding and sequencing. A 2x150 bp sequencing was performed and ≥2 million paired-end reads for each sample were obtained. Data analysis was performed using Archer Analysis software.

Results
Rarefaction analysis was used to characterize the analytical sensitivity of the assay at varying sequence depths and input amounts, using RNA from whole blood and PBMCs from healthy donors. The total number of unique TCRβ RNA fragments observed using 20-1,200 ng of RNA ranged from 2,890 to 94,969 for whole blood, and 8,433 to 174,350 for PBMCs. The assay detected 1 TCRβ RNA fragment in the background of up to 174,350 TCRβ molecules, yielding a sensitivity of 5.7 *10-6. 100% accuracy was

observed for both TCRβ and TCRγ using pre-characterized T-cell derived cell lines. FFPE tumor specimens from patients with lung and breast adenocarcinoma were used to determine TCR repertoire and its diversity. Each tumor was classified as having either high (≥15%), medium (7-14%), or low (≤7%) TILs in FFPE sections using H&E analysis. Using 400ng RNA, the number of unique TCR fragments detected in FFPE samples ranged between 53-1,632. FFPE samples were either polyclonal or highly clonal, however TCR clonality did not always correlate with TIL count.

Conclusions

We have validated an RNA-based NGS assay for the analysis of TCRβ/γ in whole blood, PBMC and FFPE specimens. The assay can support both TCR repertoire analysis and minimal residual disease monitoring in T-cell malignancies.

P121

Interaction of immune checkpoints in tumor-stromal microenvironment of primary and chemoreduced retinoblastoma

Lata Singh, PhD[1], Mithalesh Singh[2], Seema Kashyap[2], Seema Sen, MD[2], Moshahid A. Rizvi, PhD[1]

[1]*Jamia Millia Islamia, New Delhi, India*
[2]*All India Institute of Medical Sciences, New Delhi, India*

Background

Interactions between malignant and non-malignant cells create the tumor microenvironment (TME). The non-malignant cells of the TME have a dynamic and tumor-promoting function at all stages of carcinogenesis. Cytotoxic T lymphocyte-associated antigen 4 (CTLA4), programmed death-1 (PD-1) and programmed death-ligand 1 (PD-L1) are key components of the immune checkpoint pathway. They play a crucial role in the regulation of T-cell activation and their expression in TME constitutes a predictive biomarker in cancers. It has recently been shown that chemotherapeutic agents could modify tumor microenvironment. Therefore, we investigated the expression of PD-1, PD-L1 and CTLA-4 in primary and chemoreduced retinoblastoma to define their significance in the tumor microenvironment with patient prognosis.

Methods

Expression of immune markers (PD-1, PD-L1 and CTLA-4 protein) was evaluated in 75 prospective cases of primary (Group I) and 25 cases of chemoreduced (Group II) enucleated retinoblastoma specimens by immunohistochemistry. mRNA expression of genes of interest were investigated by quantitative real time PCR (qPCR) and results were finally correlated with clinicopathological parameters and patient outcome by statistical analysis.

Results

Differential expression pattern of PD-1, PD-L1 and CTLA-4 proteins was found in both group I (primary retinoblastoma) and group II (chemoreduced retinoblastoma) cases. Immunohistochemistry showed cytoplasmic/membranous staining of these immune markers using their respective antibodies. Increased expression of PD-1, PD-L1 and CTLA-4 were found in stromal/immune cells of group II as compared to Group I. Expression of these immune markers showed significant correlation with poor tumor differentiation, tumor invasion and patient outcome ($p<0.05$).

Conclusions

This is the first of its kind study investigating the role of immune markers in primary retinoblastoma and their alteration in expression after chemotherapy. Tumor microenvironment of retinoblastoma showed expression of PD-L1 in primary patients and increased expression in PD-L1, CTLA-4 and PD-1 after chemotherapy. This paves the way for development of new strategies for treatment of chemoreduced

retinoblastoma.

Acknowledgements
Dr. Lata Singh was supported by Department for Science and Technology (DST), Govt. of India, funding agency for providing National Post-Doctoral fellowship (N-PDF) and conducting this research.

Ethics Approval
This study was approved by Institute's Ethical Committee, AIIMS (Ref. No. IEC-424/RP-6/2016)

Consent
Written consent was obtained from all the patient's guardian

P122

Validated next generation sequencing RNA-based assay of the IGHV mutation status and repertoire diversity

Jeran Stratford[1], Patrick Hurban, PhD[1], Victor Weigman[1]

[1]*Q2 Solutions, Morrisville, NC, USA*

Background
High-throughput sequencing of immune repertoire is increasingly used for clinical diagnosis, monitoring of residual disease, and development of cancer immunotherapies. The load of somatic hypermutations in the rearranged immunoglobulin heavy-chain variable region gene (IGHV) is a powerful prognostic biomarkers in CLL. CLL arising from unmutated IGHV cells (≥98% identity to closest germline rearrangement) are more aggressive and associate with poor prognosis, while CLL with mutated IGHV (<98% identity) have favorable outcomes and a higher rate of durable remissions after treatment with chemoimmunotherapy combinations. Historically, IGHV mutation status has been performed using Sanger sequencing looking at a single dominant clone. However, next-generation sequencing can reveal the sample's IGHV diversity. We have developed an NGS based IGHV assay with comparable results to Sanger sequencing. The assay is certified by the European Research Initiative on CLL (ERIC) [1].

Methods
Purified RNA is used as template to produce PCR amplicons of the VH1, VH3, VH4 and combined VH2/VH5/VH6/VH3-21 subfamilies. Productive PCR reactions are analyzed, sequencing libraries are prepared and sequenced using 2x300 paired-end Illumina MiSeq method. Paired reads within each sequenced amplicons are synthetically joined and aligned using all V-region sequences of the ImMuno GeneTics reference. Following filtering, the proportion of remaining reads corresponding to each IGHV gene is determined. The NCBI's IgBlast software is used to assign a mutation status (<98% is mutated and ≥98% is unmutated) for each sequenced amplicons with ≥50% of reads aligned to a single gene. Sequenced amplicons with <50% of reads assigned to a single gene are classified "polyclonal". A sample level mutation status is then determined by reconciling the mutation status for each sequenced amplicon. If all sequenced amplicons for a sample are polyclonal, the sample is classified as "polyclonal". If the sample has any amplicons labeled as mutated and an absence of any unmutated labeled amplicons then the sample will be classified as mutated. If the sample has any amplicons with an unmutated status, the sample is classified as unmutated.

Results
For each sample we report the mutation status, percent identity to germline IGHV clonotypes, V/D/J assignment, and re-arrangement productivity. We also identify stereotype subset #2 and indicate its prognostic value.

Conclusions
Our assay has met ERIC guidelines [2] and was awarded IGHV assay certification. With its ability to characterize IGVH diversity, the utility of a certified NGS IGHV assay is critical in determining care for CLL patients now and providing a springboard for future biomarker development.

References
1. http://www.ericll.org/ighv-gene-mutational-analysis-certification/
2. Rosenquist R, Ghia P, Hadzidimitriou A, Sutton L-A, Agathangelidis A, Baliakas P, Darzentas N, Giudicelli V, Lefranc M-P, Langerak A, Belessi C, Davi F, Stamatopoulos K. Immunoglobulin gene sequence analysis in chronic lymphocytic leukemia: updated ERIC recommendations. Leukemia. 2017; 31:1477-1481.

P123

Peripheral blood lymphocyte responses in patients with renal cell carcinoma treated with high-dose interleukin-2

Rupal Bhatt, MD, PhD[1], Lei Sun, Ph.D[2], William Slichenmyer, MD[3], Sean Rossi[2], Juan Alvarez, PhD[4], Wenxin Xu, MD[1], Heather Losey, PhD[2]

[1]*Beth Israel Deaconess Medical Center, Boston, MA*
[2]*Alkermes, Inc., Waltham, MA, USA*
[3]*Alacrita Consulting, Waltham, MA, USA*
[4]*Merck & Co, Boston, MA, USA*

Background
High-dose interleukin-2 (HD IL-2) activates the expansion of immunosuppressive regulatory T cells (Tregs), cytotoxic CD8+ T cells and natural killer (NK) cells. Previous data show that immunosuppressive ICOS+ Tregs are significantly expanded after treatment with HD IL-2 [1], but no data are readily available that specifically quantify and compare the levels of expansion of cytotoxic effectors such as CD8+ T cells and NK cells relative to Tregs. This study was conducted with the primary goal to assess the pharmacodynamic effects of HD IL-2 on numbers of circulating CD8+ T cells, NK cells, and Tregs.

Methods
Whole blood samples were collected prior to the first dose and after the last dose of treatment cycles 1 and 2 from a cohort of renal cell carcinoma patients receiving treatment with HD IL-2. CD8+ T cells, NK cells, and Tregs were quantified by flow cytometry. Safety and antitumor activity were monitored throughout the study period. Response was assessed according to RECIST, and best response was recorded.

Results
Ten patients with renal cell carcinoma were enrolled: median age 55 (range 39-62), male/female 6/4, ECOG PS of 0=9/1=1, and median number of prior therapies 2 (range 1-3). All treatment emergent adverse events seen were consistent with the known adverse event profile of HD IL-2 [2]. Capillary leak syndrome was reported in 5 patients. Five of the 10 patients achieved best response of partial response, and 1 patient had mixed response. Administration of HD IL-2 resulted in robust expansion of circulating Tregs with a mean maximum expansion of ~4-fold as compared to ~2-fold expansion of circulating CD8+ T cells and NK cells.

Conclusions
The safety profile and clinical response observed in this small cohort of patients were similar to previous published data [2]. A more robust expansion of Tregs over CD8+ T cells and NK cells was observed in patients treated with HD IL-2, consistent with the known biological activities of IL-2.

Acknowledgements
This study was funded by Alkermes, Inc. The authors gratefully acknowledge the patients and their families who participated in this study.

References
1. Sim GC, et al, IL-2 therapy promotes suppressive ICOS+ Treg expansion in melanoma patients. J. Clin. Invest. 2014;124(1): 99–110.
2. Marabondo S and Kaufman HL. High-dose interleukin-2 (IL-2) for the treatment of melanoma: safety considerations and future direction. Expert Opin. Drug Saf. 2017;16(12):1347-1357

Ethics Approval
This study was approved by the Beth Israel Deaconess Medical Center IRB, protocol #06-105.

P124

Quantitative multichannel immunofluorescence imaging to assess the immune composition of the T cell-inflamed tumor microenvironment in bladder cancer

Randy Sweis, MD[1], Ken Hatogai[1], Danny Kim[1], Yuanyuan Zha, PhD[1], Alexander Pearson, MD, PhD[1], Gary Steinberg, MD[1], Thomas Gajewski, MD, PhD[1]

[1]*University of Chicago, Chicago, IL, USA*

Background
A T cell inflamed tumor microenvironment is linked to improved prognosis and response to immunotherapy in bladder cancer. This immune phenotype can be measured by the presence of tumor-infiltrating T-cells with various gene expression signatures reflective of the immune response. Tumor-infiltrating BATF3+ dendritic cells have been shown in murine models to be critical for both priming an immune response and for recruitment of effector CD8+ T cells to the tumor microenvironment. In human bladder cancer specimens, the presence and distribution of tumor-infiltrating BATF3-dendritic cells has not been previously evaluated.

Methods
We performed quantitative multiplex immunofluorescence imaging on 64 bladder cancer specimens from patients to investigate the population of immune-infiltrating cells present in the tumor such as BATF3 cells and CD8+ T cells (Figure 1). We used a previously described immune gene expression signature to determine the presence of absence of the T cell-inflamed tumor microenvironment based on RNA sequencing for a subset of these samples. Immune cells proportions were calculated relative to the tumor cell counts in 5 randomly selected regions of interest for each specimen.

Results
The proportion of BATF3+ cells per 1000 tumor cells ranged from 0 to 6.32 with an average of 0.68. There were no BATF3+ cells in 23 out of 64 specimens (36%). The proportion of CD8+ cells per 1000 tumor cells ranged from 0 to 135 with an average of 10.4. There were no CD8+ cells in 8 out of 64 specimens (13%). In a subset of 18 samples for which RNA sequencing data were available, we found a 39-fold higher proportion of BATF3+ cells in tumors that were T cell-inflamed by gene expression profiling compared with those that were non-T cell-inflamed (P=0.02). T-cell inflamed tumors also had a 2.4-fold higher CD8+ cell proportion compared with non-T-cell inflamed tumors, but this difference did not reach significance (P=0.30).

Conclusions
The presence of tumor-infiltrating BATF3+ dendritic cells correlates strongly with the presence of a T cell-inflamed tumor microenvironment by gene expression profiling. Further analyses are ongoing to assess the impact of spatial relationships of immune cells and their association with immunotherapy response and outcomes.

Ethics Approval
Specimens used in this study were obtained through a protocol approved by the University of Chicago Institutional Review Board (IRB 15550B)

Figure 1. Multichannel immunofluorescence for CD8 and Batf-3

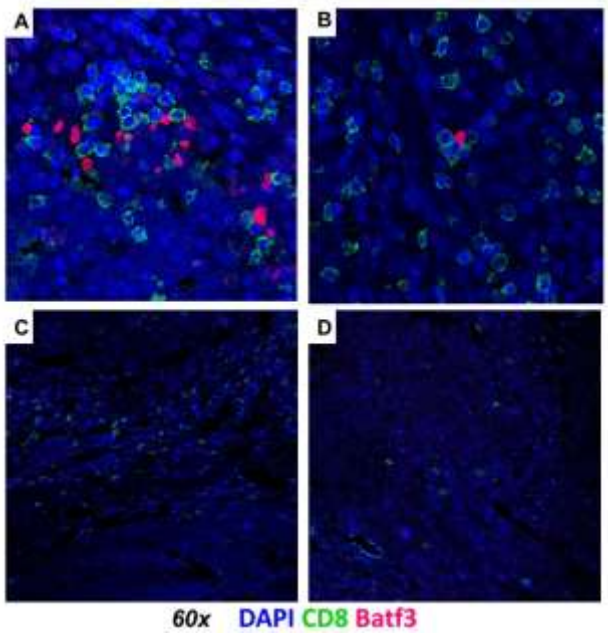

P125

DNA methylation biomarkers for noninvassive detection of hepatocellular carcinoma

David Taggart, PhD[1], Dhruvajyoti Roy, PhD[1], Gen Li[1], Dan Liu[1], Lianghong Zheng[1], Kang Zhang[2]

[1]*The Laboratory for Advanced Medicine, Inc., West Lafyette, IN, USA*
[2]*University of California San Diego, San Diego, CA, USA*

Background
The epigenetic inactivation of tumor suppressor genes by promoter hypermethylation is an important aspect of tumorigenesis. Indeed, aberrant methylation of CpG sites within genomic DNA isolated from cancer cells has been shown to correlate with clinically relevant information and has the potential to be used for cancer diagnosis and identification of the cancer tissue of origin. Malignant cells shed genomic DNA into circulation through both cell death and active release by viable cells. Therefore, investigating the methylation of cell-free DNA allows for the noninvasive detection and early diagnosis of cancers, such as hepatocellular carcinoma. Here, we identified and validated hepatocellular carcinoma-specific methylation markers for diagnosis of the disease with high sensitivity and specificity.

Methods
Banked samples were obtained for 130 subjects, including: 60 subjects diagnosed with hepatocellular carcinoma (Stage I to IV), 30 subjects without liver disease, 10 subjects diagnosed with benign liver disease and 30 subjects diagnosed with breast, colorectal or lung cancer. Samples were provided to the laboratory blinded for analysis. Cell-free DNA was then extracted from the samples, bisulfite converted, and DNA methylation was quantified by using the IvyGene® Platform. After data collection and analysis of all samples was complete, the samples were unblinded to calculate test performance.

Results
A total of 57 of the 60 samples drawn from subjects with hepatocellular carcinoma were correctly identified for an overall calculated sensitivity of 95%, with little difference between the sensitivity of detecting Stage I to Stage IV hepatocellular carcinoma (range 89% to 100%). Additionally, 29 of 30 samples drawn from subjects without liver disease and 9 of 10 samples drawn from subjects diagnosed with benign liver disease were correctly identified as non-cancer for a combined calculated specificity of 97.5%. Of the samples drawn from subjects with cancer other than liver cancer, 90% of breast cancer samples, 80% of colorectal cancer

samples and 90% of lung cancer samples were correctly identified as not liver cancer, for a total calculated analytical specificity of 87%.

Conclusions

These data demonstrate the high diagnostic potential of cfDNA methylation markers in the blood for the detection of hepatocellular carcinoma. Indeed, quantification of cfDNA methylation may be a more sensitive and specific method for the detection of hepatocellular carcinoma than ultrasound, which is the current recommended imaging method for surveillance of high-risk populations.

Ethics Approval

This project was approved by the Institutional Review Boards (IRBs) of Sun Yat-sen University Cancer Center, Xijing Hospital, and West China Hospital.

P126

Peripheral immune monitoring identifies biomarkers of response and toxicity after neoadjuvant combination immunotherapy with ipilimumab (ipi) and high dose IFNα2b (HDI) in patients with melanoma

Ahmad Tarhini, MD, PhD[1], Ghanashyam Sarikonda[2], Arjun Khunger, MD[3], Jack El-Sawada, MD[4], Christian Laing[2], Christine Vaupel, PhD[2], Naveen Dakappagari[2]

[1]Cleveland Clinic and Case Comprehensive Cancer Center, Cleveland, OH, USA
[2]Navigate BioPharma Services, Inc., A Novartis Subsidiary, Carlsbad, CA, USA
[3]Cleveland Clinic, Cleveland, OH, USA
[4]University of Pittsburgh Medical Center, Pittsburgh, PA, USA

Background

Neoadjuvant ipi-HDI given over 6 weeks for locally/regionally advanced melanoma showed preoperative radiologic response of 36% and pathologic complete response (pCR) of 32% [1]. Mechanistic studies may illuminate the underlying mechanisms of immune susceptibility and resistance and identify biomarkers of response and toxicity.

Methods

Peripheral blood mononuclear cells (PBMC) from treated patients (N=28) on this trial were tested at baseline (before initiating ipi-HDI), 6-weeks, 3-months and 12-months following neoadjuvant ipi-HDI). High complexity (14-color) flow cytometry designed to detect key immunological biomarkers such as MDSCs, regulatory T cells, PD-1 and TIM3 expression on T-cells, and differentiation of T-cells into Th1, Th2 or Th17 phenotype were used to evaluate the effects of immunological biomarkers on safety and efficacy. Statistical significance was determined using R-package employing Kruskal's test.

Results

Higher levels of Th1 cells (defined as CD45RA- CCR6- CXCR3+ CCR4-) correlated with preoperative radiological response (p=0.0070) while higher Th2 cells (defined as CD45RA- CCR6- CXCR3- CCR4+) was associated with progressive disease (0.0092). In evaluating pathologic response, a higher multimarker score consisting of Th1 cells and CD8+ central memory T-cells was associated with pCR (p=0.0406), in contrast, higher TIM3 expression on T-cells correlated with gross viable tumor (p=0.0472). Higher levels of phenotypically naive and effector memory CD8+ T-cells (p=0.0140) or lower levels of Th2 cells were associated with lower toxicity as well (p=0.0243). Finally, a multimarker score consisting of higher CD19+ and CD8+ cells was associated with lower toxicity (p=0.0013) and vice versa

Conclusions
Peripheral immune monitoring may identify predictive biomarkers of response and toxicity following combination neoadjuvant immunotherapy. Validation and long term immune monitoring studies are ongoing and will be presented.

Trial Registration
https://clinicaltrials.gov/ct2/show/NCT01608594NCT01608594

References
1. Tarhini AA, Rahman Z, Lin Y, Vallabhaneni P, Tawbi HA-A, Gnan A, et al. Neoadjuvant combination immunotherapy with ipilimumab (3 mg/kg or 10mg/kg) and high dose IFN-a2b in locally/regionally advanced melanoma. Journal of Clinical Oncology. 2016;34(15_suppl):9585-.

Ethics Approval
The study was initiated after approval from the institutional review board (IRB) and was conducted in accordance with the Declaration of Helsinki

Consent
A University of Pittsburgh IRB approved written informed consent (IRB# PRO12020161) was obtained from all patients.

P127

Characterization of changes in tumor immune microenvironment after treatment with neoadjuvant combination immunotherapy with ipilimumab (ipi) and high dose IFNα2b (HDI) in patients with melanoma

Arjun Khunger, MD[1], Jennifer Bordeaux, PhD[2], Ju Young Kim[2], Christine Vaupel, PhD[2], Naveen Dakappagari[2], Ahmad A. Tarhini, MD, PhD[3]

[1]Cleveland Clinic, Cleveland, OH, USA
[2]Navigate BioPharma Services, Inc., A Nov, Carlsbad, CA, USA
[3]Cleveland Clinic and Case Comprehensive Cancer Center, Cleveland, OH, USA

Background
Neoadjuvant ipi-HDI given over 6 weeks for locally/regionally advanced melanoma showed preoperative radiologic response of 36% and pathologic complete response (pCR) of 32% (Tarhini, et al. ASCO 2016). Mechanistic studies may reflect the underlying dynamics of tumor immune microenvironment (TME) in response to neoadjuvant treatment and offer important insights into immune mechanisms of response and resistance.

Methods
Tumor biopsy specimens of 28 patients with locally/regionally advanced melanoma, who were treated with neoadjuvant ipi-HDI were obtained at baseline and post-treatment assessment. Primary (archival) tumor samples collected at the time of diagnosis were also available. Multiplexed fluorescence immunohistochemistry combined with unique AQUA (Automated Quantitative Analysis) algorithms specifically designed to classify regulatory T cells (Tregs), Myeloid derived suppressor cells (MDSCs), CD3+ T cells, PD-1 expression, PD-L1 expression and IDO1/HLA-DR co-expression was used to assess tumor immune modulation in response to neoadjuvant immunotherapy. Statistical significance was determined using the paired t-test.

Results
Our analysis revealed that there was a significant decrease in the proportion of Tregs between pre-treatment primary and post-treatment biopsy samples (p=0.007). Also, there was a significant increase in the percentage of CD3+ T cells between pre-treatment primary and post-treatment biopsy samples (p= 0.005), supporting the hypothesis of increased generation of effector T-cells post-treatment. In correlation with pathologic response, there was a consistent trend towards a decrease in

IDO1/HLA-DR co-expressing cells post-treatment as compared to pre-treatment primary (p= 0.067) and baseline (p=0.08) biopsy samples. No significant changes in expression of PD-1 or PD-L1 were seen between pre-treatment baseline and primary samples and post-treatment samples. In addition, no significant changes were detected in the immune profiles of pre-treatment baseline versus primary tumor biopsy.

Conclusions

A significant increase in CD3+ T cells and a significant decrease in Tregs was observed following treatment with neoadjuvant immunotherapy in our study. Consistent trends towards a decrease in IDO1/HLA-DR co-expression in responding patients support a role for IDO1 in immune resistance. Comparable TME profiles between preprimary and pre-treatment baseline tumor biopsies may be useful in guiding future studies.

Trial Registration

https://clinicaltrials.gov/ct2/show/NCT01608594NCT01608594

References

1. Tarhini AA, Rahman Z, Lin Y, Vallabhaneni P, Tawbi HA-A, Gnan A, et al. Neoadjuvant combination immunotherapy with ipilimumab (3 mg/kg or 10mg/kg) and high dose IFN-a2b in locally/regionally advanced melanoma. Journal of Clinical Oncology. 2016;34(15_suppl):9585-.

Ethics Approval

The study was initiated after approval from the institutional review board (IRB) and was conducted in accordance with the Declaration of Helsinki.

Consent

A University of Pittsburgh IRB approved written informed consent (IRB# PRO12020161) was obtained from all patients.

P128

Multiplexed immunofluorescent assay development for study of the PD-1/PD-L1 checkpoint in the tumor immune microenvironment (TIME)

Sneha Berry, MS[1], Sneha Berry, MS[1], Sneha Berry, MS[1], Nicolas Giraldo, MD PhD[1], Peter Nguyen, MS[1], Benjamin Green, BS[1], Haiying Xu[1], Aleksandra Ogurtsova[1], Abha Soni, DO[1], Farah Succaria, MD[1], Daphne Wang, MS[1], Charles Roberts[1], Julie Stein, MD[1], Elizabeth Engle, MSc[1], Drew Pardoll, MD, PhD[1], Robert Anders, MD, PhD[1], Tricia Cottrell, MD, PhD[1]

[1]*Johns Hopkins University School of Medicine, Baltimore, MD, USA*

Background

Multispectral immunofluorescent (mIF) staining of formalin-fixed paraffin-embedded (FFPE) tissue allows spatially-resolved quantitative analysis of cell position and protein expression. The design and validation of mIF panels is a challenge. Our goal was to develop a 7-plex assay for characterizing PD-1 and PD-L1 expression, with high sensitivity for multiple markers and minimal bleed-through between fluorescent channels, while avoiding steric hindrance among markers occupying the same cellular compartment.

Methods

Single IF slides were stained for PD-1, PD-L1, CD8, FoxP3, CD163, and a tumor marker (e.g. Sox10/S100 for melanoma) using primary antibodies at manufacturer's recommended concentrations and visualized with an Opal kit (PerkinElmer). Positive signal was compared to chromogenic IHC (n=3 tonsil specimens). In some instances, the kit's HRP-polymer was substituted for one that provided greater amplification. Primary antibody titrations were performed, and the concentration with comparable signal to chromogenic IHC that showed the highest IF

signal to noise ratio was selected. Using the selected primary antibody concentration, TSA dilution series were performed on n=5 tumor specimens to minimize bleed-through. Finally, the optimized single IF stains were combined into multiplex format, which was again validated to ensure no positivity loss. Images were scanned with the Vectra 3.0 and processed using inForm (Ver 2.3).

Results

The percent positive pixels for CD163, CD8, and tumor marker expression by IF were comparable to chromogenic IHC with manufacturer's recommended protocols ($p>0.05$). However, PD-1, PD-L1, and FoxP3 showed ~50% loss of signal ($p<0.05$), which was recovered by replacing the Opal kit's secondary HRP polymer with PowerVision (Leica). Unbalanced fluorescence intensities between 540 to 570 Opal dyes resulted in significant bleed-thorough and led to false positive pixels. This error was minimized >2 fold (2.5% to 1.1%) by concentrating the 570 dye and ensuring that this dye pair was used to study markers in different cellular compartments (nuclear FoxP3 vs. membrane CD8), so any residual bleed-through could be discounted during image analysis. Using the optimized panel, we are able to reliably identify cell types contributing PD-L1 and PD-1 to the TIME, and even resolve populations of PD-1^{high} vs. PD-1^{low} lymphocytes.

Conclusions

We demonstrate successful optimization of a 7-color multiplex panel characterizing the PD-1/PD-L1 axis to provide high quality data sets for whole slide or regional analysis of the TIME. With the use of multiparametric assays such as this, we hope to guide improved approaches to patient selection and potentially identify additional tumor types likely to respond to anti-PD-(L)1 immunotherapy.

Ethics Approval

The study was approved by Johns Hopkins University Institutional Review Board.

P129

Simultaneous single cell analysis of multiple analytes resolves T cell populations at high resolution

Sarah Taylor, PhD[1], Katherine Pfeiffer[1], Michael Stubbington, PhD[1], Josephine Lee[1], Jerald Sapida[1], Liselotte Brix, phd[2], Kivin Jacobsen, PhD[2], Bertrand Yeung[3], Xinfang Zhao[3], Tarjei Mikkelsen[1], Deanna Church, PhD[1]

[1]10x Genomics, Pleasanton, CA, USA
[2]Immudex, Copenhagen, Denmark
[3]BioLegend, San Diego, CA, USA

Background

Characterization of lymphocyte types and understanding their antigen binding specificities are key to the development of effective therapeutics. Recent technological advancements have enabled the integration of simultaneous cell-surface protein, transcriptome, immune repertoire and antigen specificity measurements at single cell resolution, providing comprehensive, high-throughput characterization of immune cells.

Methods

Using the 10x Genomics Single Cell Immune Profiling Solution with Feature Barcoding technology in conjunction with TotalSeq™-C oligo-conjugated antibodies (BioLegend) and DNA barcoded MHC Dextramer® reagents (Immudex), we performed multi-omic characterization of PBMCs from cytomegalovirus (CMV) seropositive and seronegative donors. Next generation sequencing libraries were made following the 10x Genomics workflow, where gene expression and immune repertoire libraries are generated alongside libraries from DNA barcodes conjugated to antibodies or MHC Dextramer reagents, allowing quantification of cell surface proteins and identification of TCR specificities. Analysis was performed using the latest

version of Cell Ranger (v3.0). The TCR-dist algorithm was used to identify clusters of related TCR sequences and enriched CDR3 motifs.

Results

Combining single cell TCR assembly with barcoding of MHC Dextramer reagents allowed the identification of full length, paired alpha and beta TCR sequences with specificity for known CMV antigens. Cells were also labelled with barcoded antibody reagents to allow cell type characterization based on surface protein expression to augment the transcriptomic information provided by the gene expression portion of the assay. The combination of these single cell assays allowed the identification of CD8+ cell populations with specificity for CMV/MHC. Multiple TCRs that bound CMV/MHC were observed and we identified enriched amino acid motifs within the TCR sequences. We analyzed the distribution of CMV-binding TCRs with similar sequences shared across individual donors and compared the observed CMV-binding TCR sequences with those previously reported in TCR-antigen databases.

Conclusions

The analytical approaches outlined here provide a systematic and scalable method for deciphering TCR-peptide MHC specificity, with clear implications in understanding the complexity of the tumor microenvironment. The multi-omic combination of gene expression, paired adaptive immune receptor repertoire, antibody-based detection of cell surface proteins and Dextramer-based analysis of antigen binding specificity for the same single lymphocytes allows the comprehensive characterization of immune cell populations at unprecedented resolution and throughput. Identifying discrete cellular phenotypes that underlie immune receptor specificity and antigen binding capabilities is critical for developing a better understanding of the adaptive immune response to cancer; leveraging this understanding will be key in the development of successful cellular and transgenic immunotherapies.

P130

A measurable immune response in the tumors and lymph nodes of patients with lymph node positive and lymph node negative breast cancer.

Archana Thakur, PhD[1], Dana Schalk[1], Tayson Lin[2], Johnson Ung[1], Griffin Calme, BS[2], Johnson Ung[1], Lawrence G. Lum, MD, DSc[1], Lydia Choi[3]

[1]*University of Virginia Cancer Center, Charlottesville, VA, USA*
[2]*Wayne State University, Detroit, MI, USA*
[3]*Karmanos Cancer Institute, Detroit, MI, USA*

Background

The functional significance of various immune cell subsets may provide important information for maximizing the prognostic value of immunoscoring. In early stage breast cancer patients with no detectable lymph node invasion relapse rate is about 20-30% while one-third of lymph node positive breast cancer patients remain free of distant metastasis. The prognostic gap in this group of patients remains and the vast majority of the patients in both groups had no prognostic marker to assist in driving clinical management based on risk factors. We hypothesize that immune cell population and its T cell activation status (Th1 type) in the resected breast tumors and sentinel lymph nodes may serve as immunological biomarkers of tumor aggressiveness and offer useful prognostic information to facilitate specific therapy related clinical decision as well as response to therapeutic options. Since the nodal immune environment is influenced in part by tumor-derived factors, we tested a small cohort for cytoplasmic expression of IFN-gamma and IL-10 to explore the association between Th1 and Th2 status of the TILs along with the triple staining for the CD3+ T cells, CD20+ B cells and CD68+ macrophages in tumors and lymph nodes biopsies with clinical outcomes of breast cancer patients.

Methods
Biopsies from four groups of patients were examined for T cell activation status, 1) no recurrence until present and node negative; 2) no recurrence until present and node positive; 3) recurrence in last 5 years and node negative; 4) recurrence in last 5 years and node positive. Tissue slides from sentinel node biopsies and tumor resections from thirty women who underwent sentinel node biopsy with invasive breast cancer resection were dual stained for CD3/IL-10, CD3/IFN-gamma or triple stained for CD3/CD20/CD68. Slides were imaged using a Digital Scanner, the density and intensity of each cell type and cytokine was recorded as the number of positive cells per unit tissue surface area.

Results
Our data show that patients who had no evidence of disease after 5 years had weak to moderate expression of IFN-gamma by T cells while patients who progressed rapidly had no expression of IFN-gamma by T cells in the tumors or in the lymph nodes.

Conclusions
Understanding of the immune cell environment within the tumors and lymph nodes may have implications for improving clinical outcome of cancer patients.

Ethics Approval
The study was approved by Wayne State University's IRB, approval number 634183

P131

High-plex predictive marker discovery for melanoma immunotherapy treated patients using NanoString® Digital Spatial Profiling

Maria Toki, MD, MSc[1], Pok Fai Wong, MD, MPhil[1], James Smithy, MD, MHS[2], Harriet Kluger, MD[1], Chris Merritt, PhD[3], Giang Ong, MS[3], Sarah Warren, PhD[3], Joseph Beechem, PhD[3], David Rimm, MD, PhD[1]

[1]*Yale University School of Medicine, New Haven, CT, USA*
[2]*Brigham and Women's Hospital Department, Boston, MA, USA*
[3]*NanoString Technologies, Seattle, WA, USA*

Background
NanoString Digital Spatial Profiling (DSP)*, a technology previously validated to quantitative immunofluorescence, offers the capacity of highly multiplexed immune marker quantitative measurements with spatial resolution within specific regions of interest (ROI) on formalin-fixed, paraffin-embedded (FFPE) tissue. Here, we used NanoString DSP to explore the predictive value of a 44plex panel of immune markers measured in multiple compartments in a melanoma immunotherapy (ITx) treated cohort.

Methods
NanoString DSP technology uses a cocktail of primary antibodies conjugated to indexing DNA oligos. ROI on the tissue are selected with fluorescently labeled antibodies, and oligos from that region are UV cleaved, sipped up, and quantified on the nCounter® platform. Here, we used a tissue microarray (TMA) cohort which includes 60 Itx treated melanoma patients to identify potential predictive markers of survival and response using a 44plex panel of immune markers collected sequentially and quantified in three different compartments: in macrophage, leukocyte and the melanocyte ROI, defined by CD68+, CD45+ and S100+HMB45+ respectively. Each patient was represented by two cores and the counts for each marker were averaged.

Results
Biomarker counts were highly concordant across unique TMA cores from the same patient tumor. High concordance between DSP and quantitative

fluorescence was also seen as a validation for the DSP method. Out of the 44plex panel measured in three different ROIs, 13 and 16 immune markers were found to be associated with prolonged progression free survival (PFS) and overall survival (OS). Perhaps the most striking finding was that, using a CD68 specific compartment marker measurement, we found that PD-L1 expression in macrophages and not in tumor was a predictive marker for PFS, OS and response. Other notable compartment-specific biomarkers found to be associated with outcome included beta 2-microglobulin, HLADR, CD8 and IDO1.

Conclusions

NanoString DSP capacity for highly multiplexed immune marker measurements on selected compartments allowed the discovery of multiple predictive markers in a single TMA section of a melanoma ITx cohort. This tool represents the highest multiplexed spatially informed method for discovery without the liabilities of cycling methods. These findings can be used for the construction of predictive signatures involving multiple compartments reflecting the complexity of the tumor microenvironment. Future studies on the DSP platform are underway with multiplexing capacity to nearly 1000 biomarkers on the same tissue section.*FOR RESEARCH USE ONLY. Not for use in diagnostic procedures.

Ethics Approval

The study was approved by the Yale Human Investigation Committee protocol #9505008219 and conducted in accordance with the Declaration of Helsinki.

P132

RNA sequencing of rare antigen-specific T cells and tissue micro-regions using the RareCyte platform

Lance U'Ren, DVM, PhD[1], Rebecca Podyminogin[1], Nolan Ericson[1], Eric Kaldjian, MD[1], Tad George, PhD[1]

[1]*RareCyte Inc., Seattle, WA, USA*

Background

The immune system provides antigen-specific protection against pathogens as well as malignancies, both of which evolve strategies to evade immune surveillance and containment. Effective immune response often depends on activation of rare immune cell sub-types, whose function are influenced by the tissue micro-environment, the pathogen or cancer, and other factors. The RareCyte platform provides integrated multi-parameter imaging and retrieval capabilities that allow phenotypic identification and isolation of rare cells and microscopic regions of interest for sequence and transcript level analyses in order to study the complexity of host defense.

Methods

We utilized RareCyte's CyteFinder platform to identify rare antigen-specific T cells by using tetramers against influenza-specific T cell receptors (TCR) in both unstimulated and influenza peptide stimulated samples. Additionally, we isolated 40 µm regions of interest (ROIs) from B and T cell regions of human tonsil tissue. Single cells and tissue ROIs were isolated with the integrated CytePicker module. SMART-seq2 whole transcriptome amplification was carried out on single retrieved cells and ROIs, followed by Illumina Nextera XT library preparation and sequencing on an Illumina MiSeq. Expression analysis was carried out with DESeq2 and TCR sequences were retrieved from the antigen-specific T cell RNAseq datasets utilizing the TraCeR software package. For 6-color imaging, tonsil and melanoma tissue sections were immunofluorescent stained with panels containing BV421, Alexa488, Alexa647, sytox orange, qDot-625, and qDot-800 fluorophores and scanned with the CyteFinder system.

Results
We validated T cell activation by gene expression analysis revealing upregulation of transcripts in pathways such as TCR signaling and inflammatory response/cytokine signaling and were able to match paired alpha/beta TCR sequences with previously published influenza antigen-specific T cell databases. Expression analysis referencing retrieved tonsil T cell zone ROIs against B cell zone ROIs resulted in an expected differential analysis, such as upregulation of CD8a, CCL19, and CCL21 and downregulation of CD38, CR2, and CXCL13.

Conclusions
We were able to confirm that anti-influenza T cells isolated with the RareCyte were specific for expected TCRs and that peptide stimulated cells had an activated phenotype through RNA sequencing. Additionally, we validate use of the instrument for the picking of tissue micro-regions with confirmation of the cell type and tissue micro-environment via RNA sequencing. We also demonstrate that the system can be used for 6-color tissue imaging of melanoma cells and tumor-associated immune cells.

Ethics Approval
Human samples in this study were procured from commercial vendors who collected them according to their established ethics policies

P133

Spatially resolved and multiplexed immunoprofiling of NSCLC using imaging mass cytometry reveals distinct functional profile of CD4 and CD8 TILs associated with response to immune checkpoint blockers

Franz Villarroel-Espindola, PhD[1], Miguel Sanmamed, MD, PhD[2], Jonathan Patsenker[1], Ya-Wei Lin[3], Brian Henick, MD[4], Jovian Yu[1], Mark Verburg[5], Tayf Badri[1], Jon Zugazagoitia, MD[1], Daniel Carvajal-Hausdorf, MD[6], Ruth Montgomery, PhD[1], Roy Herbst, MD, PhD[1], Lieping Chen, MD, PhD[1], David Rimm, MD, PhD[1], Tal Shnitzer, PhD[3], Ronen Talmon, PhD[3], Yuval Kluger, PhD[1]

[1]Yale School of Medicine, NEW HAVEN, CT, USA
[2]Clínica Universidad de Navarra, New Haven, CT, USA
[3]Israel Institute of Technology, Haifa, Israel
[4]Columbia University, New York, NY, USA
[5]Stony Brook University, New York, NY, USA
[6]Clinica Alemana Universidad Desarrollo, New Haven, CT, USA

Background
Reinvigoration of anti-tumor immunity by blocking co-inhibitory checkpoints has revolutionized the treatment of numerous human malignancies including non-small cell lung cancer (NSCLC). Understanding the mechanisms mediating anti-tumor effect and determinants of sensitivity/resistance to treatment remain major challenges. Efforts to comprehensively analyze intact tumor specimens have been limited by the number of targets that can be measured with preserved tissue architecture and in native cell conditions. We used a 29-marker IMC panel to study the immune composition of NSCLC and association with benefit to immune checkpoint blockers.

Methods
The IMC panel was established by validation of individual metal-conjugated primary antibodies in formalin-fixed/paraffin-embedded (FFPE) samples using cell-line controls, human tissue specimens and comparison with multiplexed immunofluorescence. Markers included structural tissue components: GAPDH/Histone-3/LipoR/DNAintercalators; cell-phenotype markers: Vimentin/Cytokeratin/CD3/CD4/CD8/CD20/CD68/FOXP3/CD45RO; functional indicators: TBET/PD-1/LAG-3/TIM-3/CD25/B2M/KI-67/GZB; and candidate immunomodulatory targets: PD-L1/PD-L2/B7-H3/B7-H4/PD-1H/VISTA/IDO-1/CD47. We studied 12 NSCLC/normal-lung tissue pairs and 30 baseline

tumor specimens from patients receiving PD-1 axis blockers represented in tissue microarrays. Treated cases included 12 with durable clinical benefit (DCB) and 18 without benefit (NDB). We analyzed the overall levels of the markers and profiles of individual T-cell subpopulations using MCDviewer software. We performed integrated and spatially-resolved analysis in marker-selected patches using mathematical integration of signal and training of a support vector machine classifier to distinguish patients with response/resistance to treatment.

Results

The IMC panel showed specificity for individual markers, reproducibility across experimental runs and concordance with immunofluorescence. NSCLCs showed increased CD4+/CD8+/CD20+ TILs with higher expression of functional markers than case-matched non-tumor lung tissue. In cases treated with immune checkpoint blockade we identified prominent differences in the T-cell profile between patients with benefit/DCB compared with those without response to treatment/NDB characterized by higher levels of effector memory CD8+/CD45RO+ TILs and lower levels of T-cell immune inhibitory receptors. Cases with primary resistance to treatment were associated with CD4+ or CD8+ TILs containing increased levels of both activation (CD25/TBET/GZB/Ki-67) and immune suppression/dysfunction markers (PD-1/LAG-3/FOXP3). The spatially resolved machine learning classifier stratified DCB/NDB cases with 90% of concordance.

Conclusions

We have standardized a 29-marker immuno-oncology multiplexed IMC panel for simultaneous, quantitative and spatially resolved analysis of multiple protein targets in FFPE specimens. Our results show higher adaptive immune response in NSCLC relative to patient-matched non-tumor lung and identify a distinct activated/dysfunctional profile of T-cells in patients with primary resistance to immune checkpoint blockers. Our work supports further exploration of machine learning-based classifiers to objectively integrate markers and use as biomarkers.

Acknowledgements

Thanks to Yale CyToF core facility and Fluidigm(R).Funding: Department of Defense Lung Cancer Research Program Career Development Award #LC150383; Yale SPORE in Lung Cancer P50CA196530; Stand Up To Cancer - American Cancer Society Lung Cancer Dream Team Translational Research Grant SU2C-AACR-DT17-15; Lung Cancer Research Foundation grant.

Ethics Approval

The study was approved by Yale Human Investigation Committee protocol #1608018220

P134

Prognostic and predictive value of baseline biomarkers in advanced non-small cell lung cancer (NSCLC)

Huifen Wang, PhD[1], Robert McEwen[1], Ketan Patel, PhD[1], Binbing Yu[1], J Carl Barrett[1], Kris Sachsenmeier, PhD[1]

[1]*AstraZeneca, Gaithersburg, MD, USA*

Background

Expression levels of biomarkers measured prior to treatment may indicate high tumor burden and be useful to inform or optimize treatment options or be predictive of response.

Methods

We studied baseline status (post hoc) for several biomarkers that are commonly used in the “real world” clinical oncology setting, lactate dehydrogenase (LDH), neutrophil to lymphocyte ratio (NLR), carcinoembryonic antigen (CEA), and

prostate-specific antigen (PSA). We used the FlatIron Health database to correlate baseline biomarker data with respect to overall survival (OS) to predict immune oncology (IO)/chemo/targeted therapy response in NSCLC. The study included patients diagnosed with stage IIIB/IV NSCLC, aged ≥18 years at diagnosis, who had a non-missing value of blood-based baseline biomarkers of interest, received ≥1 IO/chemo/targeted therapy, and who were not participating in clinical trials. Pre-specified values along with median values of each biomarker served as cutoffs to define patients with high and low level of each biomarker. Time from NSCLC diagnosis to first line (1 L) treatment start, and from 1 L treatment start to end of follow-up/death were used to define baseline and OS, respectively. Covariates of practice type, age at diagnosis, gender, histology, stage at diagnosis, smoking status, performance status, number of treatment lines, and 2 L treatment type (IO vs chemo/targeted therapy) were studied and included in the multivariate model to assess biomarkers' prognostic value, and used for propensity score matching between the IO and chemo/targeted therapies.

Results

Of 10,678 patients included, most received 1 L (57.6%) and 2 L (26.8%) therapies. Of 716 patients on 1 L IO therapy, 18% remained on IO therapy; while 16.5% of patients on 1 L chemo/targeted therapy switched to IO therapy in 2 L. Baseline LDH, CEA, and NLR showed significant prognostic benefit for all treatments. A potential predictive value of LDH and CEA in response to IO therapy was observed: Patients on IO therapy with a low baseline biomarker level had improved OS vs patients on IO therapy with a high baseline biomarker level and chemo/targeted therapy-treated patients.

Conclusions

These data support the hypothesis that in NSCLC, patients with high tumor burden and/or specific leukocyte profiles are generally non-responsive to IO therapies.

P135

Integrative genomic and proteomic analysis identifies cancer subtypes and signaling networks associated with aberrant tumor expression of VISTA

Duncan Whitney, PhD[1], Anna Ma, MS[1], Ramachandra Katabathula, PhD[2], Timothy Wyant[1], Jefferson Parker[1], Salendra Singh, MS[2], David Tuck[1], Vinay Varadan, PhD[2]

[1]*Curis Inc, MA*
[2]*Case Western Reserve University, Cleveland, OH, USA*

Background

VISTA is a negative regulator of T-cell and myeloid cell function and is gaining importance as a target for cancer immunotherapy [1-3]. VISTA is highly expressed in tumor-infiltrating leucocytes, particularly within the myeloid lineage. Recent evidence suggests that tumor cells themselves also express VISTA, exacerbating the immunosuppressive milieu within the tumor microenvironment [4]. Determining tumor subtypes that overexpress VISTA can inform the indication selection for VISTA-targeting agents and design of clinical trials in specific patient populations.

Methods

Genome-scale data was obtained from the TCGA Pan-Cancer Atlas dataset spanning 33 cancer types and >11,000 tumor samples [5]. DNA Methylation profiles were utilized to model leukocyte infiltration in individual tumor samples. The immune-cell component of VISTA expression was modeled using a nonlinear non-parametric regression model (LOESS). Non-immune compartment tumors with high VISTA expression, independent of leukocyte infiltration scores, were selected as likely over-expressing VISTA. VISTA-High tumor types and subtypes were

determined and signaling network activities on a per-sample basis were derived using the InFlo systems framework. Pathways associated with aberrant VISTA expression were identified using a multivariate Gaussian model of gene expression and immune infiltration. Quantitative immunofluorescence (QIF) of VISTA protein expression was run on tissue microarrays (TMA): breast (n=602), lung (n=271), colorectal (n=2017), and ovarian (n=250) tumors. VISTA expression in stromal and tumor compartments was differentiated using labeled anti-cytokeratin and anti-VISTA antibodies.

Results

We identified 703 cancer samples (6.4%) exhibiting likely aberrant tumor cell expression of VISTA on tumor cells. VISTA-high tumors were enriched ($P << 0.01$) for Low Grade Glioma (LGG), Glioblastoma Multiforme (GBM), Kidney Renal Clear Cell Carcinoma (KIRC), Head and Neck Squamous Cell Carcinoma (HNSC), Sarcoma (SARC) and Mesothelioma (MESO). The CpG Island Methylator Phenotype (CIMP)-high of LGG and GBM, as well as the Atypical and Classical subtypes of HNSC were markedly enriched within the VISTA-High tumor population. We also identified subpopulations of lung (5.2%), breast (4.5%), colorectal (3.9%), and ovarian (4.1%) cancers to exhibit VISTA over-expression in the tumor compartment. Signaling networks identified as significantly associated with VISTA over-expression ($P < 0.05$) were identified. VISTA protein was expressed primarily in the stroma in nearly all (90-100%) of the TMA histospots, whereas between 5-10% showed VISTA expression in the tumor compartment, consistent with findings from the TCGA analysis.

Conclusions

Overexpression of VISTA on tumor cells was consistent between RNA analysis of TCGA and QIF-analyses of proteins in TMAs. This study represents the most comprehensive analysis of VISTA expression to date.

References

1. Lines JL, Sempere LF, Broughton T., Wang L, Noelle R. VISTA is a novel broad-spectrum negative checkpoint regulator for cancer immunotherapy. Cancer Immunol Res. 2014; (2): 510-7.
2. Nowak EC, Lines JL, Varn FS, Deng J, Sarde A, Mabaera R, Kuta A, Le Mercier I, Cheng C, Noelle RJ. Immunoregulatory functions of VISTA. Immunol Rev. 2017. 276: 66-79.
3. Gao J, Ward JF, Pettaway CA, Shi LZ, Subudhi SK, Vence LM, Zhao H, Chen J, Chen H, Efstathiou E, Troncoso P. VISTA is an inhibitory immune checkpoint that is increased after ipilimumab therapy in patients with prostate cancer. Nature medicine. 2017; 23(5): 551.
4. Boger C, Behrens HM, Kruger S, Rocken C. The novel negative checkpoint regulator VISTA is expressed in gastric carcinoma and associated with PD-L1/PD-1: A future perspective for a combined gastric cancer therapy? Oncoimmunology. 2017.
5. Thorsson V, Gibbs DL, Brown SD, Wolf D, Bortone DS, Ou Yang TH, Porta-Pardo E, Gao GF, Plaisier CL, Eddy JA, Ziv E, Culhane AC, Paull EO, Sivakumar IKA, Gentles AJ, Malhotra R, Farshidfar F, Colaprico A, Parker JS, Mose LE, Vo NS, Liu J, Liu Y, Rader J, Dhankani V, Reynolds SM, Bowlby R, Califano A, Cherniack AD, Anastassiou D, Bedognetti D, Rao A, Chen K, Krasnitz A, Hu H, Malta TM, Noushmehr H, Pedamallu CS, Bullman S, Ojesina AI, Lamb A, Zhou W, Shen H, Choueiri TK, Weinstein JN, Guinney J, Saltz J, R. A. Holt RA, Rabkin CE, Cancer Genome Atlas Research Network, Lazar AJ, Serody JS, Demicco EG, Disis ML, Vincent BG, Shmulevich L. The immune landscape of cancer. Immunity. 2018; 48: 812-30

P136

Genetic immunosignatures associate with progression-free survival in advanced soft tissue sarcoma patients treated on a Phase 2 trial of the VEGF receptor inhibitor axitinib plus pembrolizumab

Breelyn Wilky, MD[1], SuFey Ong[2], Sarah Warren, PhD[2], Alessandra Cesano, MD, PhD[2], Despina Kolonias[1], Eric Wieder, PhD[1], Deukwoo Kwon, PhD[1], Andrew Rosenberg, MD[1], Jonathan Trent, MD, PhD[1], Krishna Komanduri, MD[1]

[1]*University of Miami - SCCC, Miami, FL, USA*
[2]*NanoString Technologies, Seattle, WA, USA*

Background
Vascular endothelial growth factor (VEGF) maintains the immunosuppressive tumor microenvironment by limiting T cell infiltration and promoting suppressive immune cell phenotypes. Accordingly, simultaneous blockade of VEGF with checkpoint inhibitors has led to improved immune cell infiltration and tumor responses in melanoma and renal cell carcinoma. In soft tissue sarcomas (STS), response rates to PD-1 monotherapy or dual CTLA4/PD-1 blockade are modest at 16-19% [1,2]. We hypothesized that addition of VEGF receptor inhibitor axitinib plus anti-PD1 checkpoint inhibitor pembrolizumab would improve responses in STS. In a Phase II study of axitinib/pembrolizumab in 30 patients with advanced STS (NCT02636725), we observed 4 month progression-free survival (PFS) of 47.7%. We obtained tumor biopsies from study patients and evaluated expression of immune-related gene signatures in respect to clinical outcomes.

Methods
Formalin-fixed, paraffin embedded core needle tumor biopsies were obtained from study patients at baseline and after 12 weeks on study treatment. RNA was extracted from unstained slides and hybridized with NanoString® IO360 beta gene expression panel (for research use only) prior to analysis on the nCounter® platform. After normalization with housekeeping genes and technical controls, expression of immune subset signatures was analyzed using research algorithms developed by NanoString.

Results
28 baseline and 14 on-treatment biopsies contained sufficient tumor for analysis after pathologist review. STS histologies included alveolar soft part sarcoma (ASPS, n=9), leiomyosarcomas (LMS, n=6), undifferentiated pleomorphic sarcoma (UPS, n=5), and other (n=9). Higher baseline expression of antigen presentation machinery, type 1 interferons, immunoproteosome, and interferon downstream signaling signatures was significantly associated with PFS > 4 months, whereas B cell, NK cell, and NK CD56dim signatures were negatively associated with PFS. Higher glycolysis gene expression in on-treatment samples relative to baseline was associated with PFS > 4 months. UPS significantly differed from other subtypes with higher baseline expression of proliferation, stroma, myeloid inflammation, PD-L2, B7-H3, and TGF-beta signatures. UPS immunoprofiles were significantly altered with treatment relative to other subtypes, with higher expression of myeloid inflammation, inflammatory chemokine, B cell, dendritic cell, and TGF-beta signatures. ASPS demonstrated higher baseline expression of endothelial cell, antigen presentation machinery, and apoptosis signatures, with lower proliferation relative to other subtypes.

Conclusions
This is the first analysis in STS patients treated with immunotherapy to correlate genetic expression signatures with clinical outcomes. Pathways identified by the NanoString IO360 beta panel will require prospective validation, but may ultimately serve as predictive biomarkers, and suggest alternative targets to further enhance efficacy of

immunotherapy in STS.

Trial Registration
Clinicaltrials.gov: NCT02636725

References
1. Tawbi HA, Burgess M, Bolejack V, Van Tine BA, Schuetze SM, Hu J, D'Angelo S, Attia S, Riedel RF, Priebat DA, Movva S, Davis LE, Okuno SH, Reed DR, Crowley J, Butterfield LH, Salazar R, Rodriguez-Canales J, Lazar AJ, Wistuba II, Baker LH, Maki RG, Reinke D, Patel S. Pembrolizumab in advanced soft-tissue sarcoma and bone sarcoma (SARC028): a multicentre, two-cohort, single-arm, open-label, phase 2 trial. Lancet Oncol. 2017; 18(11):1493-1501.
2. D'Angelo SP, Mahoney MR, Van Tine BA, Atkins J, Milhem MM, Jahagirdar BN, Antonescu CR, Horvath E, Tap WD, Schwartz GK, Streicher H. Nivolumab with or without ipilimumab treatment for metastatic sarcoma (Alliance A091401): two open-label, non-comparative, randomised, phase 2 trials. Lancet Oncol. 2018; 19(3):416-426.

Ethics Approval
The study was approved by the University of Miami Institutional Review Board, approval number 20150932.

P137

A systematic literature review (SLR) of tumor mutational burden (TMB) and efficacy with immunotherapy (IO) in lung cancer

Connor Willis, PharmD[1], Michelle Fiander[1], Dao Tran, PharmD[2], Beata Korytowsky[3], John-michael Thomas, PharmD[3], Signe Fransen[3], Florencio Calderon[3], Teresa Zyczynski[3], Lisa Siegartel[3], Diana Brixner[1], David Stenehjem[2]

[1]*University of Utah, Salt Lake City, UT, USA*
[2]*University of Minnesota, Duluth, MN, USA*
[3]*Bristol-Myers Squibb, Plainsboro, NJ, USA*

Background
TMB is an emerging biomarker that may predict response to IO. This SLR evaluates published evidence on TMB as a biomarker for efficacy of IO in lung cancers.

Methods
Cochrane SLR methodology was followed [1]. Searches were conducted through April 2018 using: Medline; EMBASE; EMCARE; and SCOPUS. Two clinical trial registries (clinicaltrials.gov; ICTRP) and published conference abstracts were also searched. Studies of any design assessing clinical efficacy (objective response rate [ORR], progression-free survival [PFS], overall survival [OS]) in lung cancer (NSCLC/SCLC) by TMB or the association of TMB with other biomarkers or enrichment factors were included.

Results
Database searches identified 3662 unique references, full text screening of 809 articles was conducted, and 81 studies met all inclusion criteria. TMB was reported primarily as total mutation count (n=32) or by mutations/megabase (mut/Mb) (n=40). TMB was categorized as low, intermediate, or high in 32 of 81 studies. Methods used to categorize TMB were predetermined thresholds (n=21), the 50th percentile (n=9), or other percentiles (n=2). All studies showed improved PFS (n=8) [2-9] and ORR (n=8) [2-4, 8-12] of IO in TMB high vs. low/intermediate. Significant efficacy results ($p<0.05$) for IO in TMB high were observed in 6 of 8 studies for PFS and 4 of 8 studies for ORR. Improved OS was observed in 7 of 9 studies with 2 of 9 studies showing significant results [2-4, 10, 12-16]. Results on OS are presented (Table 1) and highlight the small sample size of included studies. TP53 and EGFR mutations were positively and negatively associated with high TMB, respectively [17-19] [19-21]. The literature showed a mixed association of PD-L1 and TMB [2, 7, 22-29]. High TMB was associated with

smoking history [7, 19, 30-40], squamous cell carcinoma [18, 33, 41, 42], and male gender [19, 39, 40].

Conclusions

This is the first SLR to assess the association of TMB and efficacy in lung cancer. Robust, adequately powered observational and prospective clinical studies should continue to assess TMB and other biomarkers to IO with clinical outcomes. This will validate ongoing data sets and further support precision treatment planning.

References

1. Cochrane handbook for systematic reviews of interventions, J.P.T. Higgins and S. Green, Editors. 2011.
2. Carbone DP, et al. First-line nivolumab in stage iv or recurrent non-small-cell lung cancer. N Engl J Med, 2017; 376(25): 2415-2426.
3. Goodman AM, et al. Tumor mutational burden as an independent predictor of response to immunotherapy in diverse cancers. Mol Cancer Ther, 2017; 16(11): 2598-2608.
4. Griesinger F, et al. Tumor mutation burden (TMB) is associated with improved efficacy of atezolizumab in 1l and 2l+ NSCLC patients. Oncology Research and Treatment, 2017; 40((Hellmann M.D.) Memorial Sloan Kettering Cancer Center, New York, USA): 220-221.
5. Hellmann MD, et al. Molecular determinants of response and resistance to anti-pd-(l)1 blockade in patients with NSCLC profiled with targeted next-generation sequencing (ngs). Journal of Clinical Oncology, 2017. 35(15).
6. Hellmann MD, et al., Nivolumab plus ipilimumab in lung cancer with a high tumor mutational burden. N Engl J Med, 2018. 378(22): 2093-2104.7. Mahadevan, N., et al., Non-synonymous mutation burden in lung carcinoma is associated with durable clinical response to immune checkpoint blockade. Journal of Thoracic Oncology, 2017. 12(1): p. S428-S429.
8. Rizvi NA, et al., Cancer immunology. Mutational landscape determines sensitivity to PD-1 blockade in non-small cell lung cancer. Science, 2015. 348(6230): p. 124-8.
9. Roszik J, et al. Novel algorithmic approach predicts tumor mutation load and correlates with immunotherapy clinical outcomes using a defined gene mutation set. BMC Medicine, 2016; 14(1): 168.
10. Gettinger S, et al. Predictive value of measuring somatic mutations and tumor infiltrating lymphocytes for PD-1 axis therapy in non-small cell lung cancer (NSCLC). Journal of Thoracic Oncology, 2017; 12(1): S430-S431.
11. Haratani K, et al. Tumor immune microenvironment and nivolumab efficacy in EGFR mutation-positive non-small-cell lung cancer based on t790m status after disease progression during EGFR-tki treatment. Annals of Oncology. 2017; 28(7): 1532-1539.
12. Singal G, et al. Analyzing biomarkers of cancer immunotherapy (cit) response using a real-world clinico-genomic database. Annals of Oncology. 2017; 28((Abernethy A.) Medical Group, Flatiron Health, Inc., New York, USA): p. v404-v405.
13. Owada Y, et al. Correlation between mutation burden of tumor and immunological/clinical parameters in considering biomarkers of immune checkpoint inhibitors for non-small cell lung cancer (NSCLC). Journal of Clinical Oncology. 2017; 35(15).
14. Rothberg B G, et al. The prognostic impact of EGFR, KRAS and TP53 somatic mutations in curatively resected early-stage lung adenocarcinomas. Journal of Thoracic Oncology. 2017; 12(1): S623.
15. Schrock A B, et al. Pulmonary sarcomatoid carcinomas commonly harbor either potentially targetable genomic alterations or high tumor mutational burden as observed by comprehensive genomic profiling. J Thorac Oncol. 2017; 12(6): 932-942.
16. Chen M. et al. The potential clinical application of comprehensive genomic profiling in targeted therapy and immunotherapy of lung cancer. Journal of Thoracic Oncology. 2017;12(11):S2010.

17. Dong, Z.Y., et al., EGFR mutation correlates with uninflamed phenotype and weak immunogenicity, causing impaired response to PD-1 blockade in non-small cell lung cancer. Oncoimmunology, 2017. 6(11): p. e1356145.
18. Choi, M., et al., Mutation profiles in early-stage lung squamous cell carcinoma with clinical follow-up and correlation with markers of immune function. Annals of Oncology, 2017. 28(1): p. 83-89.
19. Goldberg, M.E., et al., The interaction of PD-L1, TMB, and genomic alterations in NSCLC. Cancer Research, 2017. 77(13).
20. Liu, S.Y., et al., Dual positive PD-L1 and cd8+ til represents a predominant subtype in NSCLC and correlates with augmented immunogenicity. Journal of Thoracic Oncology, 2017. 12(1): p. S237.
21. Liu, X., et al., Molecular biomarker study of programmed death receptor ligand 1 (PD-L1) in korean patients with lung adenocarcinoma [#4213], in AACR 2018 Proceedings: Abstracts 3028-5930. 2018, CTI Meeting Technology: Chicago.
22. Nakagomi, T., et al., New therapeutic targets for pulmonary sarcomatoid carcinomas based on their genomic and phylogenetic profiles. Oncotarget, 2018. 9(12): p. 10635-10649.
23. Schabath, M., et al., Molecular epidemiology of programmed cell death 1-ligand 1 (PD-L1) protein expression in non-small cell lung cancer. Journal of Thoracic Oncology, 2017. 12(1): p. S475-S476.
24. Senarathne, W., et al., Composition of the immune microenvironment differs between carcinomas metastatic to the lungs and primary lung carcinomas. Annals of Diagnostic Pathology, 2018. 33: p. 62-68.
25. Ross, J., et al., Immune checkpoint inhibitor (ICPI) efficacy and resistance detected by comprehensive genomic profiling (CGP) in non-small cell lung cancer (NSCLC) [#1138] Annals of Oncology, 2017. 28(Suppl 5).
26. He, L., et al., Evaluating genomic signatures predicting veliparib sensitivity in non-small cell lung cancer (NSCLC). Journal of Thoracic Oncology, 2017. 12(1): p. S267-S268.
27. Kadara, H., et al., Whole-exome sequencing and immune profiling of early-stage lung adenocarcinoma with fully annotated clinical follow-up. Annals of Oncology, 2017. 28(1): p. 75-82.
28. Kim, H.S. and J.Y. Han, Association of PD-L1 expression with tumor infiltrating immune cells and mutation burden in the high grade neuroendocrine carcinoma of the lung. Journal of Clinical Oncology, 2017. 35(15): p. Suppl 1.
29. Ono, A., et al., Clinical factors associated with mutation burden in non-small cell lung cancer. Annals of Oncology, 2017. 28((Yamaguchi K.) Hospital and Research Institute, Shizuoka Cancer Center, Shizuoka, Japan): p. v578-v579.
30. Quek, K., et al., Mutational landscape of non-small cell lung adjacent normal [#5363], in AACR 2018 Proceedings: Abstracts 3028-5930. 2018, CTI Meeting Technology: Chicago.
31. Reck, M., et al., Smoking history predicts sensitivity to parp inhibitor veliparib in patients with advanced non-small cell lung cancer. J Thorac Oncol, 2017. 12(7): p. 1098-1108.
32. Schrock, A.B., et al., Characterization of 298 patients with lung cancer harboring MET exon 14 skipping alterations. J Thorac Oncol, 2016. 11(9): p. 1493-502.
33. Shim, H.S., et al., Unique genetic and survival characteristics of invasive mucinous adenocarcinoma of the lung. J Thorac Oncol, 2015. 10(8): p. 1156-62.
34. Wang, C., et al., The correlation between mutation burden and disease free survival in patients with lung adenocarcinomas. Journal of Clinical Oncology, 2017. 35(15).
35. Xiao, D., et al., Analysis of ultra-deep targeted sequencing reveals mutation burden is associated with gender and clinical outcome in lung adenocarcinoma. Oncotarget, 2016. 7(16): p. 22857-64.
36. Xiao, D., et al., Integrative analysis of genomic sequencing data reveals higher prevalence of lrp1b mutations in lung adenocarcinoma patients with copd. Sci Rep, 2017. 7(1): p. 2121.
37. Isaka, M., et al., Integrated genomic analysis to

assess the molecular signature of Japanese patients with non-small cell lung cancer. Journal of Thoracic Oncology, 2017. 12(11): p. S2292.
38. Kojima, H., et al., Genomic analysis to assess a molecular signature in Japanese patients with pulmonary high grade neuroendocrine carcinoma. Journal of Thoracic Oncology, 2017. 12(11): p. S2186.
39. Davis, A.A., et al., Association of tumor mutational burden (TMB) with DNA repair mutations and response to anti-PD-1/PD-L1 therapy in non-small cell lung cancer (NSCLC). Cancer Research, 2017. 77(13).
40. Park, W., et al., Correlating isend and tumor mutation burden (TMB) with clinical outcomes of advanced non-small cell lung cancer (ansclc) patients on nivolumab. Journal of Thoracic Oncology, 2017. 12(11): p. S2005-S2006.
41. Patel, K., et al., In silico analysis of non-synonymous snps (nsSNPs) and outcomes in non-small cell lung cancer (NSCLC) patients (pts) treated with immunotherapy (it). Journal of Clinical Oncology, 2017; 35(15).

Table 1. Overall survival with IO by TMB

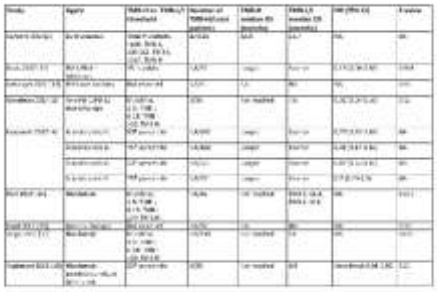

P138

Quantitative assessment of cancer-associated fibroblasts and immunotherapy outcome in metastatic melanoma

Pok Fai Wong, MD, MPhil[1], Wei Wei, MD, PhD[2], Swati Gupta, PhD[1], James Smithy, MD, MHS[3], Harriet Kluger, MD[1], David L. Rimm, MD, PhD[1]

[1]*Yale School of Medicine, New Haven, CT, USA*
[2]*Yale School of Public Health, New Haven, CT, USA*
[3]*Brigham and Women's Hospital, Boston, MA, USA*

Background

Clinical benefit from programmed cell death 1 (PD-1) immune checkpoint blockade is limited to a subset of metastatic melanoma patients, so there is a need for predictive biomarkers. Because the cancer-associated fibroblast (CAF) population is the predominant stromal cell type within the tumor immune microenvironment, we hypothesized that pretreatment CAF profiles could be associated with immunotherapy outcome.

Methods

Pretreatment whole tissue sections from 117 melanoma patients treated with anti-PD-1 therapy (pembrolizumab, nivolumab, or ipilimumab plus nivolumab) from 2011–17 were collected from Yale Pathology archives. Multiplex immunofluorescence for CAF profiling was achieved by simultaneous detection of nuclei (DAPI), melanoma cells (S100, HMB45), and the CAF markers, Thy1 (7E1B11, Abcam), smooth muscle actin (SMA; 1A4, Dako), and fibroblast activation protein (FAP; EPR20021, Abcam). Cell phenotyping and counting were performed using inForm software (PerkinElmer) and protein expression was measured by the AQUA method of quantitative immunofluorescence (QIF). CAF parameters by both methodologies were correlated with best overall response as defined by Response Evaluation Criteria in Solid Tumors (RECIST) 1.1, progression-free survival (PFS), overall survival (OS), and immune markers previously measured in this cohort.

Results

Pretreatment CAF parameters, by cell counts or QIF, were not associated with RECIST tumor burden classifications for best overall response, objective

response rate or disease control rate. In contrast, PFS (all $P < 0.05$) and OS (all $P < 0.003$) had significant positive associations with Thy1 and FAP cell counts, and negative associations with SMA cell count, which were specific to anti-PD-1 treated patients. Similar associations were not observed in a historical untreated melanoma cohort. In the absence of therapy, FAP was instead a negative prognostic biomarker ($P = 0.01$). The specific association of FAP with anti-PD-1 survival advantage suggests mechanistic involvement and warrants further study. Multivariable analyses also revealed statistically significant PFS and OS associations with the CAF parameters, particularly for FAP, independent of age, sex, mutation, stage, treatment, and prior immune checkpoint blockade. The QIF data showed similar trends. There was no correlation between the CAF parameters and CD8 or PD-L1 by either method of assessment.

Conclusions

Pretreatment CAF parameters, by cell counts or QIF, are associated with immunotherapy outcome in metastatic melanoma patients. Multiplex analysis of the tumor microenvironment has potential to be used as a companion diagnostic for precision immunotherapy and may be complementary to existing markers (CD8 and PD-L1).

Ethics Approval

The study was approved by the Yale Human Investigation Committee protocol #9505008219.

P139

Pharmacodynamic effects of CA170, a first-in-class small molecule oral immune checkpoint inhibitor (ICI) dually targeting V-domain Ig suppressor of T-cell activation (VISTA) and PD-L1

Timothy Wyant, PhD[1], Funda Meric-Bernstam, MD[2], David Tuck[3], Yung-Jue Bang, MD PhD[4], Anna Ma, MS[3], Jeffrey Sosman, MD[5], Adil Daud, MBBS MD[6], John Powderly, MD, CPI[7], Javier Garcia-Corbacho[8], Manish Patel, MD[9], James Lee, MD, PhD[10], Kyu-Pyo Kim[11], Joshua Brody, MD[12], Sun Young Rha[13], Erika Hamilton, MD[14], Marta Gil Martin[15], Santiago Ponce Aix, MD[16], Radhakrishnan Ramchandren, MD[17], Myung-Ju Ahn[18], James Spicer, MD, PhD[19], Simon Pacey[20*], Gerald Falchook, MD[21], Funda Meric-Bernstam, MD[2]

[1]Curis Inc, Lexington, MA, USA
[2]MDACC, Houston, TX, USA
[3]Curis, Lexington, MA, USA
[4]Seoul National University Hospital, Seoul, Korea
[5]Northwstern, Chicago, IL, USA
[6]UCSF, San Francisco, CA, USA
[7]Carolina BioOncology Institute, Huntersville, NC, USA
[8]Hospital Clinic Barcelona, Barcelona, Spain
[9]FLorida Cancer Specialists SCRI, Sarasota, FL, USA
[10]UPMC, Pittsburgh, PA, USA
[11]AMC, Seoul, Korea, Republic of
[12]Mt.Sinai, New York, NY, USA
[13]Yonsei University Health, Seoul, Korea, Republic of
[14]Tenn Oncology SCRI, Nashville, TN, USA
[15]Catalan Institute of Oncology, Catalon, Spain
[16]Hosptial Univesitario, Madrid, Spain
[17]Karmanos, Detroit, MI, USA
[18]Samsung Medical center, Seoul, Korea, Republic of
[19]King's College Guy's Hospital, London, UK
[20]University of Cambridge, Cambridge, UK
[21]SCRI Healthone, Denver, CO, USA

Background

VISTA was shown to independently suppress T cell responses and is expressed on both immune and tumor cells. VISTA expression is upregulated in tumors as a potential resistance mechanism after ICI therapy. As such, it has been considered a target for cancer immunotherapy. Pre-clinical studies have demonstrated dual blockade of PD-1 and VISTA can be synergistic. CA-170, novel oral dual inhibitor of VISTA and PD-L1/L2 is in phase 1 study with exploratory pharmacodynamic endpoints.

Methods
Longitudinal blood samples were collected for PBMC phenotyping. Archival tumor tissue was acquired on all patients and paired tumor biopsies (baseline and C2) were collected when feasible. IHC using select markers of interest and Nanostring immune transcriptome analyses were conducted on paired tumor samples.

Results
At the time of this analysis 41 patients had been treated across 6 dose levels (50 – 800 mg QD) with 39 having blood samples available for PBMC phenotyping, 19 patients had sufficient paired tumor biopsies for IHC, and 9 for Nanostring-based analysis. In the 39 patients with available blood samples, within 24 hours after the initial CA-170 dose, 28% showed an increase in the percentage of peripheral blood CD8 T cells that expressed CD69 (median +3.2 fold) and 21% showed an increase in CD8 T cells that expressed CD134+ (median + 2.8 fold). IHC staining analysis of paired tumor biopsies showed increases of CD8+ T cell population in 39% (1.5 fold to 13.8 fold) and CD11b+ myeloid population in 36% of samples (1.5 fold to 5 fold) at cycle 2. Additionally there tended to be increased expression of VISTA in 38% of evaluated samples (1.5 fold to 14.5 fold) post-treatment. Nanostring immune panel transcriptome analysis showed a trend for increased expression of signatures of T-helper (3/9 pairs), myeloid (9/9 pairs), and T-reg cells (3/9 pairs). Activation of IFN-γ gene signature and certain induced genes (CXCL9, CXCL10, CXCL11) showed an increase of at least one transcript ranging from 1.97 to 7.6 fold (7/9 pairs).

Conclusions
These data suggest that CA-170 treatment results in modulation of peripheral and intra-tumoral immune profile in treated patients. CA-170 treatment was associated with altered myeloid cell as well as T helper cell populations more frequently than CD8+ T cells. Increased expression of VISTA in tumor biopsies were noted post CA-170 treatment. Correlation between the PD effects and tumor response to CA-170 treatment is being explored.

Trial Registration
NCT02812875

Ethics Approval
The following institutions ethics boards have approved this study:MD Anderson Cancer Center, Seoul National University Hospital, Northwestern, UCSF, Carolina BioOncology Institute, Hospital Clinic de Barcelona, Florida Cancer Specialists/Sarah Cannon Research Institute, UPMC, Asian Medical Center, Mt. Sinai, Yonsei University Health System - Severance Hospital, Tennessee Oncology/Sarah Cannon Research Institute, Catalan Institute of Oncology, Hospital Universitario 12 de Octubre, Karmanos, Samsung Medical Center, King's College London, Guy's Hospital, University of Cambridge,Sarah Cannon Research Institute at HealthONE

Consent
Written informed consent was obtained from the patient for publication of this abstract and any accompanying images. A copy of the written consent is available for review by the Editor of this journal

P140

Deep profiling of Asian NSCLC to identify the tumor antigen-specific T cells and the predictive potential of the patients treated with PD-1/PD-L1 blockade

Joe Yeong, MBBS, PhD[1], Lisda Suteja[2], Yannick Simoni[3], Kah Weng Lau[4], Sherlly Lim[4], Jie Hua, Josh Loh[4], Angela Takano[4], Eng Huat Tan, MD[2], Kiat Hon, Tony Lim[4], S. W. Daniel Tan[2], Evan W. Newell, PhD[3]

[1]Singapore Immunology Network/ Singapore General Hospital, Singapore, Singapore

[2]National Cancer Center Singapore, Singapore, Singapore
[3]Singapore Immunology Network, Singapore, Singapore
[4]Singapore General Hospital, Singapore, Singapore

Background

Although PD-L1 tumor proportion score (TPS)(1), microsatellite instability status (MSI)(2) and interferon gamma (IFN-$_\gamma$)(3) gene signature have been widely recognized as biomarkers to predict the responsiveness of PD-1/PD-L1 blockade treatment, more clinically robust and practical markers are needed to more precisely identify potential responders and also to warn of potential toxicity especially when combination immunotherapies are used. Asian Non-Small Cell Lung Cancer (NSCLC) are differ from their western counterparts in terms of etiology with low prevalence of smoking and high incidence of EGFR mutant positive adenocarcinoma(4). Following up on our recent study (Nature 2018)(5) that profiled and implicated CD39+CD8+ T cells as tumor antigen-specific T cell populations in both Asian NSCLC and colorectal cancer tumors, here we investigate the tissue localization and predictive potential of CD39+CD8+ T cells in the context of NSCLC. Because CD39 expression by CD8+ T cells in these tumors appears to be associated with tumor-reactivity, we hypothesize that patients with higher frequencies or densities of these cells should respond better to checkpoint blockade immunotherapy.

Methods

Quantifying these cells in-situ using formalin-fixed paraffin-embedded (FFPE) archival tissue is difficult due to the often-abundant expression of CD39 by tumor cells or other infiltrating immune cells, which confounds accurate quantification of densities/frequencies of CD39+CD8+ T cells by standard immunohistochemistry. To overcome this challenge, we developed a fully automated multiplex Immunohistochemistry (m-IHC) protocol with clinical autostainer to visualize and quantitate tumor infiltrating lymphocytes (TILs) on FFPE samples (Pathology 2018)(6). In addition to manual scoring by two pathologists, CD39+CD8+ T cells frequencies/densities, TILs and tumor cells expression were assessed using pathological image analysis software.

Results

Based on this approach, we found that the quantification of CD39+CD8+ T cells by CyTOF and m-IHC yield decent correlation which lays the foundation to translate this to clinical practice in near future. We also identified that the abundances of such subsets are associated with clinicopathological parameters such as EGFR mutation status. We then applied such quantification method on the pre-treatment FFPE biopsies samples of a pilot retrospective cohort of NSCLC treated with PD-1/PD-L1 blockade (N=20) and found that the abundance of these CD39+CD8+ T cells population are of predictive value. The prediction is independent to the abundance of CD8+ T cells as well as other TILs and CD39 expression on tumor cells.

Conclusions

Further study is ongoing to expand the cohort and explore the predictive potential of this biomarker compared to the TPS, MSI and FN-$_\gamma$ gene signature.

References

1. Reck M, Rodríguez-Abreu D, Robinson AG, Hui R, Csőszi T, Fülöp A, et al. Pembrolizumab versus Chemotherapy for PD-L1–Positive Non–Small-Cell Lung Cancer. New Engl J Med. 2016;375(19):1823-33.
2. Le DT, Uram JN, Wang H, Bartlett BR, Kemberling H, Eyring AD, et al. PD-1 Blockade in Tumors with Mismatch-Repair Deficiency. New Engl J Med. 2015;372(26):2509-20.
3. Ayers M, Lunceford J, Nebozhyn M, Murphy E, Loboda A, Kaufman DR, et al. IFN-γ–related mRNA profile predicts clinical response to PD-1 blockade.

The Journal of Clinical Investigation. 2017;127(8):2930-40.
4. Cheng T-YD, Cramb SM, Baade PD, Youlden DR, Nwogu C, Reid ME. The International Epidemiology of Lung Cancer: Latest Trends, Disparities, and Tumor Characteristics. Journal of Thoracic Oncology. 2016;11(10):1653-71.
5. Simoni Y, Becht E, Fehlings M, Loh CY, Koo S-L, Teng KWW, et al. Bystander CD8+ T cells are abundant and phenotypically distinct in human tumour infiltrates. Nature. 2018;557(7706):575-9.
6. Lim JCT, Yeong JPS, Lim CJ, Ong CCH, Wong SC, Chew VSP, et al. An automated staining protocol for seven-colour immunofluorescence of human tissue sections for diagnostic and prognostic use. Pathology. 2018;50(3):333-41.

Ethics Approval
The Centralized Institutional Review Board of SingHealth provided ethical approval for the use of patient materials in this study (CIRB ref: 2011/411/B)

Consent
Written informed consent was obtained from the patient for publication of this abstract and any accompanying images. A copy of the written consent is available for review by the Editor of this journal.

P141

Circulating tumor DNA (ctDNA) a novel biomarker for immunotherapy response in advanced lung cancer

Meera Yogarajah, MD[1], Ebenezer Appah, MD[1], Katherine Neblett[2], Clive Morris[2], Greg Jones[2], Vincent Plagnol[2], Paul Walker, MD[1]

[1]East Carolina University, Greenville, NC, USA
[2]Inivata, Research Triangle Park, NC, USA

Background
Circulating tumor DNA (ctDNA) can be predicative of outcomes in lung cancer. Moreover the ctDNA levels can correlate with changes in tumor burden in response to therapy. We assessed the utility of (ctDNA) levels as an early indicator of response to immune-therapy.

Methods
Twenty-nine patients with advanced non-small cell lung cancer initiated on immune therapy with anti-PD1/PDL-1 therapy either alone or in combination with platinum-based chemotherapy were enrolled in this prospective trial. Patients had baseline plasma samples collected prior to therapy and serially with the initial 4 cycles of immuno- or chemo-immunotherapy. ctDNA was assessed in plasma by InVisionFirst™ (Inivata) ctDNA NGS assay for detection and quantification of genomic alterations in 36 genes commonly mutated in NSCLC. The early trends of the ctDNA allele fractions were correlated with imaging responses post 4 cycles of therapy and subsequently with interval imaging.

Results
Patients included 31% male, 62 years median age, 21% squamous, 72% adeno, 7% others, median cycles 4. Of the 29 patients, 7 were not evaluable at the time of analysis as they only had baseline values or did not have response assessment imaging. Twenty two patients had evaluable imaging assessments which was done on completion of C4 and later at intervals determined by the treating oncologist. Clinical benefit was demonstrated in 16 (55%) patients (complete response (CR, n =4), partial response (PR, n = 5) or stable disease (SD, n = 7)); 6 patients had progressive disease (PD). In patients achieving CR/PR there was no detectable ctDNA at baseline (n=4) or there was complete clearance of ctDNA after completion of 3-4 cycles of immune therapy (n=4), except for 1 patient who demonstrated persistent ctDNA. Follow up imaging demonstrated continued beneficial responses, with most patients who had CR continuing to be in CR and patients who had PR persisting as PR or improving to

CR. Patients with stable disease had varying levels of ctDNA with mildly increasing levels in some and stable low levels in others. All 6 patients with PD had detectable ctDNA at progression and some showed increasing levels.

Conclusions

Early decrease or clearance of ctDNA during immune therapy was correlated with positive clinical responses. Absence of detectable ctDNA was indicative of overall a good response and prognosis. Increasing or newly detectable ctDNA was indicative of progressive disease or poor overall outcome. These results suggest a value for validation in an expanded patient cohort.

P142

The immunogenomic impact of indoximod on the tumor microenvironment of melanoma patients

Jiayi Yu, PhD[1], Gabriela R. Rossi, PhD[1], Ravindra Kohle, MD, PhD[2], David Munn, MD[2], Yousef Zakharia, MD[3], Nicholas Vahanian, MD[1], Eugene Kennedy, MD, FACS[1], Charles Link, MD[1]

[1]NewLink Genetics, Ames, IA, USA
[2]Medical College of Georgia, Augusta Univ, Augusta, GA, USA
[3]University of Iowa, Iowa City, IA, USA

Background

The indoleamine 2,3-dioxygenase (IDO) pathway mediates immunosuppressive effects through the metabolism of tryptophan (Trp) to kynurenine (Kyn). This metabolic pathway triggers downstream signaling through the Trp sensors (GCN2 and mTOR) and the Kyn sensor (aryl hydrocarbon receptor, AhR) [1-4]. Indoximod is an orally administered, small-molecule IDO pathway inhibitor that reverses the immunosuppressive effects of low Trp and high Kyn that result from IDO activity. Preclinical studies demonstrate that indoximod has immunostimulatory effects involving three main cell types: CD8+ T cells, Tregs, and DCs. Indoximod increases proliferation of effector T cells, reprograms Tregs into helper T cells, and downregulates IDO expression in DCs. These effects are observed in both the presence and absence of IDO activity [5].

Methods

Patients with newly diagnosed unresectable locally advanced or metastatic melanoma in Phase 2 trial (NCT02073123) underwent pre-treatment tumor biopsy followed by a repeat biopsy after cycle 3 of pembrolizumab and indoximod. Fourteen pairs of tumor specimens (6 patients with objective response, and 8 non-responders) underwent RNA sequencing analysis and multiplex immunofluorescence staining to assess the phenotype and functional status of multiple immune populations in the tumor microenvironment (TME), define changes in the tumor genomic profile and gene expression. Baseline samples from the trial were used for predictive biomarker assessment (n= 38).

Results

Expression profiling identified up-regulation of multiple immune regulation pathways previously reported following pembrolizumab treatment. Importantly, comparison against published studies suggested immunologic and metabolic changes contributed exclusively by indoximod, including genes suggestive of increasing cytotoxicity and innate immune cell infiltration and activation (CD14, CD33, CD86, GZMM, CD11c, IRF8 among others). Melanoma-related genes were markedly decreased in responding patients compared to non-responding patients. Pro-inflammatory immunologic changes were observed only in the clinical-responder patients, while the non-responder patients showed minimal immunologic response. Consistent with the hypothesized mechanism of action for indoximod [5], IDO1 expression within the TME was downregulated upon treatment, especially in Ki67neg population.

Considered as a predictive biomarker, patients with high IDO expression showed higher probability of response to treatment and longer progression-free survival (PFS). This result was independent of the expression levels of PD-L1.

Conclusions

The combination of indoximod and pembrolizumab induced multiple immunologic and metabolic changes in the TME. Comparison analysis indicates that some of these changes appear to be contributed exclusively by indoximod. High IDO1 expression at baseline shows correlation with clinical response to treatment.

Trial Registration

ClinicalTrials.gov Identifier NCT02073123

References

1. McGaha TL, et al. Immunol Rev. 2012;249(1):135-157.
2. Munn DH, et al. Immunity. 2005;22(5):633-642.
3. Metz R, et al. OncoImmunology. 2012;1(9):1460-1468.
4. Opitz CA, et al. Nature. 2011;478(7368):197-203.
5. Brincks EL, et al. Presented at: Annual Meeting of the American Association for Cancer Research (AACR); April 14-18, 2018; Chicago, IL. Abstract 3753.

P143

Rational combination of GITR agonism with PD-1 blockade in cancer patients

Roberta Zappasodi, PhD[2], Cynthia Sirard, MD[3], Yanyun Li, PhD MD[2], Sadna Budhu, PhD[2], Moshen Abu-Akeel[2], Cailian Liu, MD[2], Xia Yang[2], Hong Zhong, BS[2], Walter Newman, PhD[3], Jingjing Qi[2], Phillip Wong, PhD[2], David Schaer[2], Henry Koon, MD[4], Vamsidhar Velcheti, MD FACP[5], Michael Postow, MD[2], Margaret K. Callahan, MD, PhD[2], Jedd Wolchok, MD, PhD[2], Taha Merghoub, PhD[2]

[1]Memorial Sloan Kettering Institute, New York, NY, USA
[2]MSKCC, New York, NY, USA
[3]Leap Therapeutics, Walpole, MA, USA
[4]Case Western Reserve University, Cleveland, OH, USA
[5]Cleveland Clinic, Pepper Pike, OH, USA

Background

Despite the clinical successes of checkpoint blockade, many patients are refractory to these therapies, highlighting the need of more effective combination programs targeting alternative immune pathways. Engaging the T-cell co-stimulatory receptor glucocorticoid-induced TNFR-related protein (GITR) with agonist antibodies has shown promising activity in preclinical mouse models. Based on this rationale, we initiated the first in-human phase-I trial of GITR stimulation with the agonist antibody TRX518 in advanced solid cancer patients (NCT01239134). Treated patients showed frequent reductions in circulating regulatory T cells (Tregs) that correlated with intra-tumor Treg reductions. However, this was not sufficient to achieve a clinical benefit. Here, we investigate the mechanisms underlying resistance of advanced tumors to GITR agonism and provide the rationale to combine anti-GITR with checkpoint blockade in clinical trials.

Methods

Mice were implanted with B16F10 murine melanoma and treated with the anti-GITR DTA-1 alone or in combination with the anti-PD-1 RMP1-14. Composition, phenotype and function of tumor-infiltrating T cells were analyzed by flow cytometry, in vitro killing assays and molecular profiling.

Results

We modeled tumor sensitivity and refractoriness to anti-GITR therapy by treating B16F10-bearing mice on day 4 (responsive tumors) or day 7 (refractory tumors) after tumor implantation respectively. We found that intra-tumor Tregs were significantly

reduced and effector-T-cell:Treg ratios increased in both responding and refractory tumors. However, time course analyses revealed complete lack of Treg accumulation in day-4-treated responding tumors, suggesting that Tregs may limit T-cell functionality during tumor development. Accordingly, in refractory compared to responding tumors, CD8+ T cells down-regulated activation/memory T-cell markers and up-regulated exhaustion markers. To overcome resistance to anti-GITR, we co-administered anti-PD-1 with the day-7 anti-GITR suboptimal treatment. This combination controlled tumor growth similar to the day-4 curative anti-GITR monotherapy and achieved 50% long-lasting complete responses. These effects were associated with intra-tumor infiltration of highly activated and cytolytic CD8+ T cells. Based on these results and considering the biologic activity and safety profile of TRX518, we have initiated the clinical investigation of TRX518 in combination with anti-PD-1 in patients with advanced solid tumors (NCT02628574). Noteworthy, 3 of the first patients enrolled in this study have manifested clinical responses.

Conclusions

These findings indicate that Treg elimination from advanced tumors is not sufficient to activate cytotoxic CD8+ T-cell responses unless the T-cell exhaustion process is concurrently blocked, underscoring the need to combine Treg-inhibiting/depleting immunotherapies with strategies that counteract exhaustion to regress advanced tumors. This study highlights the importance of developing rational, evidence-based combination immunotherapies.

Ethics Approval

All mouse procedures were performed in accordance with institutional protocol guidelines at MSKCC. All procedures involving human subjects, human material, or human data, or involving animals were in compliance with the ethical regulations.

P144

A fully-automated multiplex fluorescence IHC assay with whole slide multispectral imaging on mouse tissue: phenoptics™ quantitative pathology solutions translational workflow

Yi Zheng, PhD[1], Carla Coltharp, PhD[1], Ryan Dilworth, PhD[1], Rachel Schaefer[1], Linying Liu[1], Victoria Duckworth[1], William Kennedy[1], Darryn Unfricht, PhD[1], Peter Miller, MS[1], Milind Rajopadhye, PhD[1]

[1]PerkinElmer Inc., Hopkinton, MA, USA

Background

Developing biomarker research strategies for clinically relevant therapies in immuno-oncology is predicated on the ability to execute fully translational research studies. Phenoptics™ quantitative pathology solutions (QPS) is a comprehensive, end-to-end solution consisting of multiplex fluorescence immunohistochemistry staining along with multispectral imaging and tissue analysis. It provides an effective and quantitative method to reveal multiple biomarkers or cell types and their interaction within tissue on a per-cell and per-tissue-context basis. It enables a deeper understanding of the biology of the tumor microenvironment. Recently, the applications for Phenoptics have been expanded from regional areas of interest in human tissue Immuno-oncology research into whole slide IO tissue research, including animal studies, creating a truly translational platform. Here we describe a robust, fully-automated 7-color Opal staining procedure on Formalin-fixed paraffin-embedded (FFPE) section of mouse breast cancer followed by a multispectral whole slide scan and image analysis.

Methods

FFPE samples from mouse breast cancer were immunostained using Opal Polaris™ 7-color Automation IHC Kit on the Leica BOND RX™

automated stainer. Multispectral fluorescence imagery was acquired on a Vectra Polaris® automated imaging system and analyzed with inForm® and MATLAB® software.

Results

We've applied the fully-automated Opal staining procedure to a mouse breast cancer sample by using the new Opal Polaris 7-Color Whole Slide reagents plus the newly developed Opal Polymer anti-Rabbit HRP Secondary Antibody. Opal multiplexed fluorescence IHC in conjunction with tissue and cell segmentation and phenotyping using inForm image analysis software allowed us to reliably interrogate subsets of T cells, macrophages, tumor cells and proliferating cells. With the ability to spectrally unmix the whole slide image, we are able to analyze and examine spatial relationships between specific phenotypes in a much larger scale, across tissue types for fully translational studies.

Conclusions

The fully-automated Opal multiplex fluorescence staining assay and whole slide multispectral imaging that we developed for FFPE tissue research is illustrated here with a mouse breast cancer model, expanding the Phenoptics workflow into animal studies. It allows for unique tumor microenvironment assessment in the whole tissue section that is translational across models. With a comprehensive immune profiling of tumors and better understanding of cellular relationships across the whole slide, this approach provides us with a deeper understanding of the complex interactions of systems biology inherent in multiple models and tissue types in situ in solid tumors.

P145

Computational assessment of IDO1 feedback modulation

Jain Zhu, PhD[1], Rebecca Zhu[2]

[1]*OmicsHealth LLC, Bethesda, MD, USA*
[2]*Winston Churchill High School, Potomac, MD, USA*

Background

IDO1 is a cancer-related immunosuppressive gene. With recent unfavorable results in clinical studies of IDO1 inhibitors, it is imperative to address questions such as its interactions with validated oncology targets, its involvement in drug resistance and feasible combination strategies for its inhibitors. With a wide range of experimental data, efficient computational tools are indispensable for managing and exploring the current knowledge space of IDO1.

Methods

As of July 2018, there were ~1,500 publications on IDO1 and cancer in PubMed. Abstracts of these articles were downloaded and systemically analyzed. Information on molecular/cellular interactions together with results from preclinical and clinical studies was extracted, standardized and integrated into a graph-based database. A network-oriented querying and visualization system was established to model the interactions between cellular components, pathways and drugs.

Results

As many oncology targets, IDO1 is regulated by feedback loops (FBL). Positive (+)FBLs sustain IDO1 expression and activity when it is induced. Negative (-)FBLs restrict IDO1 activity upon its own induction, but rescue it upon inhibition. The computationally generated IDO1 feedback network (Figure 1) comprises 100 nodes (protein, miRNA, pathway, immune cell etc.), 227 interactions (induction, suppression, activation, inhibition etc.) with 1981 possible FBLs (969 positive vs 1012 negative). Genes involved in (+)FBLs include AKT, NF-kappaB, PD-L1, IL-10, HIF1A, IL-6, AhR, TIM-3 and STAT3. Modulation of these genes by IDO1 further enhances IDO1 activity. Kynurenine, produced by IDO1 and a ligand for AhR, is implicated in the (+)FBLs. Immune cells

including MDSCs, TILs, Tregs and macrophages are also identified with (+)FBLs. On the other hand, IFN-gamma, TP53, p21, STAT1, along with effectorT, CD8+T and NK cells are predominantly involved in (-)FBLs. Mechanistically, IDO1 suppresses activities of effectorT, NK and CD8+T cells with reduction in IFN-gamma leading to a decrease in IDO1 expression. Some gene products are bi-functional, associated with both types of feedbacks. For example, IL6, being up-regulated by IDO1, induces IDO1 transcription through activation of STAT3 (IDO1->IL-6->STAT3->IDO1). Paradoxically, IL-6 up-regulates SOCS3 which promotes degradation of phosphorylated IDO1 (IDO1->IL-6->SOCS3-|IDO1). The feedback network is further refined with key factors identified (Figure 2).

Conclusions

The cellular components involved in the FBLs are potential targets of drug combination with IDO1 inhibitors and biomarkers for treatment outcome. However, the roles of bi-functional genes need to be carefully evaluated. To provide a more complete picture of IDO1 in immune regulation, the feedback models need be constantly refined with newer data and expanded by incorporating data of other drug targets.

Figure 1. IDO1 feedback regulation network

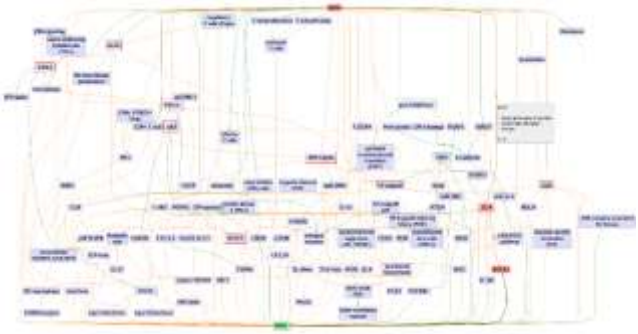

Figure 2. Key factors in IDO1 feedback regulation

P146

Cell proliferation improves prediction for immune checkpoint inhibitors (ICIs) response in PD-L1 positive TMB high non-small cell lung cancer (NSCLC)

Jason Zhu, MD[1], Matthew Labriola, MD[1], Daniele Marin, MD[1], Shannon McCall, MD[1], Edwin Yau, MD, PhD[2], Grace Dy[2], Sarabjot Pabla, MSc, PhD, BS[3], Sean Glenn, PhD[3], Carl Morrison, MD, DVM[3], Daniel George, MD[1], Tian Zhang, MD[1], Jeffrey Clarke, MD[1]

[1]*Duke University, Durham, NC, USA*
[2]*University at Buffalo, Buffalo, NY, USA*
[3]*OmniSeq Inc., Buffalo, NY, USA*

Background

Treatment for metastatic NSCLC is now highly dependent upon ICIs. Although some patients have durable treatment responses, the majority of patients will have either primary resistance or acquired resistance to treatment. While PD-L1 and tumor mutational burden (TMB) status has demonstrated predictive value for multiple ICIs, both are imperfect biomarkers. More accurate biomarkers are necessary to predict treatment response and resistance in metastatic NSCLC. Here, we describe the use of cell proliferation to evaluate response in PD-L1+ TMB high NSCLC.

Methods
113 formalin-fixed, paraffin-embedded (FFPE) tumor samples of metastatic NSCLC were evaluated by RNA-seq to measure transcript levels of genes related to cell proliferation, DNA-seq of 409 genes for tumor mutational burden (TMB), and PD-L1 status (Dako 22C3 antibody assay). Tumors were defined as PD-L1+ with a tumor proportion score >50% and as TMB high with 10 or greater mutations per megabase of DNA. Cell proliferation, defined as the mRNA expression of either 10 genes (BUB1, CCNB2, CDK1, CDKN3, FOXM1, KIAA0101, MAD2L1, MELK, MKI67, TOP2A) was evaluated for association with PD-L1 IHC expression, TMB, and response to ICIs by RECIST 1.1 criteria.

Results
Among the cohort of 113 cases, 14 (12%) were PD-L1 positive and TMB high, with 7 responders and 7 non-responders (50% objective response rate [ORR]). Of these 14 cases, 7 were proliferative and 7 were non-proliferative. The ORR for proliferative tumors was 29% (2/7) and ORR for non-proliferative tumors was 71% (5/7). Tumor proliferation status therefore improves upon clinical prediction for response to ICIs, even within the PD-L1 positive/TMB high population.

Conclusions
The 50% ORR in PD-L1+ TMB high NSCLC (14 cases) was within the expected range. Using proliferation status, non-proliferative tumors had ORR of 71%. This evidence would support that cell proliferation can be used for additional stratification of PD-L1+ TMB high NSCLC.

Ethics Approval
OmniSeq's analysis utilized deidentified data that qualified as non-human subject research under IRB-approved protocols, approved by both Roswell Park Comprehensive Cancer Center (Buffalo, NY, BDR #080316) and Duke Cancer Institute (Durham, NC, PRO00088762).

P147

Quantitative assessment of co-expression of PD-L1 and CMTM6 in the tumor microenvironment in non-small cell lung cancer (NSCLC) patients treated with PD-1 pathway blockade

Jon Zugazagoitia, MD, PhD[2], Fahad Shabbir, MD[2], Yuting Liu, PhD candidate[2], Brian Henick, MD[2], Scott Gettinger, MD[2], Roy Herbst, MD, PhD[2], Kurt Schalper, MD, PhD[2], David l. Rimm, MD, PhD[1]

[1]*Yale School o Medicine, New Haven, USA*
[2]*Yale School of Medicine, New Haven, USA*

Background
The importance of tumor versus immune cell PD-L1 expression in predicting benefit to PD-1 pathway blockade in NSCLC, and the role of PD-L1 regulators as potential contributors to these outcomes are poorly understood. Mechanistic studies have suggested that CMTM6 is a main regulator of PD-L1 expression by preventing its lysosomal degradation. Here we assess CMTM6 co-localized with PD-L1 in tumor and immune cells as a predictive biomarker.

Methods
We used multiplexed immunofluorescence (IF) to quantify the expression of PD-L1 and CMTM6 in 73 pre-treatment NSCLC cases represented in tissue microarrays, 56 of whom received only monotherapy. We performed target measurement with a Tyramide-based IF panel (PD-L1/CMTM6/CD68/Cytokeratin[CK]) and analyzed the data using the PM2000 microscope and AQUA software. Targets were measured in CK+ tumor cells, CD68+ macrophages and the non-CK stromal compartment, then split by the median.

Results
PD-L1 and CMTM6 showed a modest association with each other, particularly in the stroma (R2 = 0.46) and CD68 (R2 = 0.40) compartments. In the

monotherapy group, median OS was numerically longer, but not statistically significant, for patients with high PD-L1 in tumor cell, stroma or CD68 as compared to low PD-L1 tumors. However, OS was significantly longer for patients with concurrent high PD-L1 and high CMTM6 expression as compared to the remaining cases in stroma (23m vs. 6m, p = 0.02) and CD68 (22m vs. 6m, p = 0.03), but NOT in the tumor cell compartment (22m vs. 12m, p = 0.15). In contrast, OS was significantly shorter for patients with high PD-L1 but low CMTM6 expression in stroma (3m vs. 14m, p = 0.02) or CD68 (6m vs. 15m, p = 0.02), but not in the tumor cell compartment (21m vs. 12m, p = 0.80). Patients with low PD-L1 tumors derived no significant benefits in survival, regardless of CMTM6 status.

Conclusions

This works supports the hypothesized role for CMTM6 in stabilization of PD-L1 in patient tumors where co-expression in macrophages appears to be associated with benefit from PD-1 pathway blockade. Larger validation datasets are required to confirm this observation.

Ethics Approval

The study was approved by the Yale Human Investigation Committee protocol #9505008219.

Cancer Vaccines, Personal Vaccines and Tech

P148

Viral based vaccine for personalized neoantigen-directed cancer therapies

Christian Ottensmeier, MD PhD FRCP[1], Natalia Savelyeva[1], Katy McKann[1], Chuan Wang[1], Jason Greenbaum[2], Finn Nielsen[3], Chantal Hoffmann[4], Huguette Schultz[4], Nathalie Silvestre[4], Jean-Baptiste Marchand, pHD[4], Maud Brandely-Talbot, MD, PhD[4], Eric Quemeneur, PharmD, PhD[4], Kaidre Bendjama[4]

[1]*University of Southampton, Southampton, UK*
[2]*La Jolla Institute for allergy and immun, La Jolla, CA, USA*
[3]*Rigshospitalet, Copenhagen, UK*
[4]*Transgene, Illkirch Graffenstaden, France*

Background

Anarchic cellular proliferation and deficient DNA repair mechanisms result in accumulation of mutations in cancer cells potentially leading to expression of tumor specific neoantigens (TSNA). Given their ad hoc onset in the tumor, TSNA are not subject central tolerance and may constitute ideal targets for therapeutic cancer vaccines. However, clinical implementation of TSNA directed vaccination requires a potent immunizing vaccine formulation allowing the reproducible generation of a bespoke vaccine for every patient within acceptable time and cost. Herein, we propose a workflow to meet both requirements using a modified vaccinia Ankara (MVA) based vaccine. Technical feasibility was shown, and immunogenicity of the vaccine demonstrated in HLA-A02 expressing mice.

Methods

Blood and Tumor tissue from a patient with adenocarcinoma of the lung was sequenced and compared to reference genome to identify 2218 variants. Variants were filtered for their expression at transcriptomic level in tumor tissue but not in normal tissue (blood) to select 18 variants (17 missenses and 1 frameshift variant) in 18 different genes. Consequently, 18 mutated sequences covering the mutations and flanking sequences were cloned in an MVA virus. This viral vaccine was generated using a process of less than 8 weeks and compatible with GMP requirements. The said viral vaccine was used to immunize HHD mice and CD4 and CD8 cellular responses against the target neoantigens were assessed by ELISPOT.

Results
Responses were observed in all vaccinated animals for 4 mutations while 3 other mutations led to sporadic responses. Stimulation with wild type (non-mutated) human peptides did not evidence any cross reactivity with the wild type proteins. The responses appeared to be of both CD4 and CD8 T-cell nature. Interestingly, 2 out of the 4 strongest responses observed in mice were detected in PBMC from the donor patient without immunization suggesting that these mutations are relevant neoantigens and that vaccination would boost these responses.

Conclusions
We propose here a new approach for patient specific neoantigenic vaccination based on a platform with a remarkable safety track record in clinical setting. We have previously shown that successful antitumor immunization using an MVA viral vaccine against a shared antigen was related to an improved clinical outcome. Targeting neoantigens lacking self-tolerance is therefore a very promising approach, we are intending to translate to the clinic as early as 2019. Plans for clinical translation and study designs will be presented.

P149

A phase I study of the safety and immunogenicity of a multi-peptide personalized genomic vaccine in the adjuvant treatment of solid tumors and hematological malignancies

Ana Blazquez, PhD[1], Alexander Rubinsteyn, PhD[1], Julia Kodysh, MSc[1], John Finnigan[1], Thomas Marron, MD PhD[1], Rachel Sabado, PhD[1], Marcia Meseck, MS, JD[1], Timothy O'Donnell[1], Jeffrey Hammerbacher, BA[1], Michael Donovan[1], John Holt[1], Millind Mahajan[1], John Mandeli, PhD[1], Krysztof Misiukiewicz[1], Eric Genden[1], Brett Miles, DDS MD[1], Hooman Khorasani[1], Peter Dottino[1], Hanna Irie[1], Amy Tiersten, MD[1], Elisa Port[1], Andrea Wolf, MD[1], Hearn Cho, MD, PhD[1], Ashutosh Tewari, MD[1], Samir Parekh, MD[1], Sujit Nair[1], Matthew Galsky, MD[1], William Oh, MD[1], Sacha Gnjatic, PhD[1], Eric Schadt[1], Philip Friedlander, MD PhD[1], Nina Bhardwaj, MD, PhD[1]

[1]*Mount Sinai, New York, NY, USA*

Background
Mutation-derived tumor antigens (MTAs) arise as a direct result of somatic variations that occur during carcinogenesis and can be characterized via genetic sequencing. We developed a platform for a fully-personalized MTA-based vaccine in the adjuvant treatment of solid and hematological malignancies.

Methods
This is a single-arm, open label, proof-of-concept phase I study designed to test the safety and immunogenicity of Personalized Genomic Vaccine 001 (PGV001) that targets up to 10 predicted personal tumor neoantigens based on patient's HLA profile (ClinicalTrials.gov: NCT02721043).

Results
Five subjects have been enrolled. PGV001_002 (head and neck squamous cell cancer), who has completed vaccination, received 10 doses of vaccine comprising 10 long peptides (LP) combined with poly-ICLC (toll-like receptor-3 agonist) intracutaneously. Vaccine-induced T-cell responses were determined, at weeks 0 and 27 (before and after treatment, respectively), ex vivo by interferon (IFN)-g enzyme-linked immunospot assay and after expansion by intracellular cytokine staining. Overlapping 15-mer peptides (OLPs) spanning the entirety of each LP and 9-10-mer peptides corresponding to each predicted class I epitope (Min) were pooled. Ex vivo responses to these peptide pools were undetectable at week 0 but were evident at week 27 against 2 OLPs out of 10 (20%) and in 5 Min out of 10 (50%). After in vitro expansion, neoantigen-specific CD4+ and CD8+ T-cell responses were found in 5 out of 10 pooled peptides (50%). 7 out of 10 (70%) epitopes elicited polyfunctional T-cell responses (secretion of INF-γ,

TNF-α, and/or IL-2) from either CD4+ or CD8+ T cells.Deconvolution studies showed ex vivo IFN-γ production detection in 1 (15-mer) peptide out of 15 (6.7%) and in 4 (9-mer) peptides out of 22 (18.2%). After expansion, of 22 peptides tested, CD8+ T-cells were reactive against 13 peptides (59%), while CD4+ responses were found in 11 of 15 peptides tested. Both CD4+ and CD8+ T-cell responses were polyfunctional.

Conclusions

The PGV001 vaccine in our first patient showed both safety and immunogenicity, eliciting CD4+ and CD8+ responses to the vaccine peptides. As we enroll additional patients in this clinical trial, and perform deeper phenotyping of their tumor-reactive T cells, we will learn the determinants necessary for successful induction of immunity, while informing future immunotherapeutic approaches and rational combinations

Trial Registration

NCT02721043

Ethics Approval

The study was approved by the Icahn School of Medicine at Mount Sinai's Institutional Review Board, Approval Number HSM 15-00841

P150

A Phase II open labeled, randomized study of poly-ICLC matured dendritic cells for NY-ESO-1 and Mean-A peptide vaccination compared to Montanide, in melanoma patients in complete clinical remission

Anna Pavlick, MD, MBA[1], Ana Blazquez, PhD[2], Marcia Meseck, MS, JD[2], Michael Donovan[2], Mireia Castillo-Martin[2], Tin Htwe Thin, PhD[2], Rachel Sabado, PhD[2], John Mandeli, PhD[2], Sacha Gnjatic, PhD[2], Philip Friedlander, MD PhD[2], Nina Bhardwaj, MD, PhD[2]

[1]*NYU University, New York, NY, USA*
[2]*Mount Sinai, New York, NY, USA*

Background

Dendritic cells (DC) play a critical role in tumor immune-surveillance. Combination therapies by utilizing check point inhibitors may revert tumor-induced-T cell exhaustion; however, DCs are necessary to prime/activate T cells to target tumor cells. Montanide is a mineral oil-based adjuvant that enhances the immune response to vaccination. In this study, we compared the immunogenicity of Montanide and poly-ICLC-matured DCs.

Methods

This is a Phase II open label, randomized two arm study to compare Poly-ICLC matured DC with systemic administration of Poly-ICLC on days 1 and 2 (ARM A) to Montanide ISA-51 and Poly-ICLC as adjuvants for NY-ESO-1 and Melan-A/MART-1 peptide vaccination with systemic administration of Poly-ICLC on day 2 (ARM B) in study subjects with melanoma in complete clinical remission but at high risk of disease recurrence (NCT02334735). Evaluation of primary tumor expression of NY-ESO-1 and Melan-A tumor was determined by immunohistochemistry (IHC). Humoral responses were assessed by Seromics (ELISA) and T-cell responses were performed ex-vivo by interferon (IFN)-g enzyme-linked immunospot assay (ELISPOT) and after expansion by intracellular cytokine staining (ICS).

Results

Twenty-nine patients have been enrolled in this study. IHC studies demonstrated tumor expression of NY-ESO-1 and Melan-A in 78% and 81% of the patients, respectively. 100% of patients within arm B became seropositive for NY-ESO-1 peptide by cycle 2 day 8 (C2D8). 80% of patients within arm A also seroconverted to this antigen but titers were significantly lower. Melan-A-specific antibody responses were also found in arm B patients, but to a

lesser degree. However, arm A patients failed to develop seroreactivity to Melan-A. Cellular responses are under analysis. Preliminary data show that subjects in both arms develop T cell responses to both antigens.

Conclusions
This vaccine trial reached the primary endpoint of safety and tolerability. Patients vaccinated with either DC or Montanide had demonstrable antibody titers to immunizing antigens, although the latter reproducibly induced higher titers. Evaluation of cellular responses is ongoing.

Trial Registration
NCT02334735

Ethics Approval
The study was approved by the Icahn School of Medicine at Mount Sinai's Institutional Review Board, Approval Number HSM 14-00821

P151

Improving neoantigen identification for therapeutic and diagnostic use in immuno-oncology using mass spectrometry and machine learning

Sean Boyle, PhD[1], Eric Levy, PhD[1], Gabor Bartha[1], Jason Harris[1], Rena McClory[1], John S. West, MBA[1], Richard Chen[1]

[1]*Personalis, Menlo Park, CA, USA*

Background
Neoantigens are increasingly critical in immuno-oncology as therapeutic targets for neoantigen-based personalized cancer vaccines (PCVs) and as potential biomarkers for immunotherapy response. However, the methods for identifying which neoepitopes are more likely to provoke an immune response remains an important challenge for improving both the effectiveness of PCVs and enabling the potential use of neoantigens as a biomarker in immunotherapy. Current MHC binding prediction algorithms are trained using in vitro MHC binding data. One shortcoming of this approach is data generated using this methodology does not consider important upstream processing and shuttling components which occur for natural neoantigen presentation. Recent advances in immuno-affinity purification and mass spec technology makes it possible to identify processed cell surface MHC bound peptides in an in vivo setting, providing the opportunity for development of improved neoantigen prediction pipelines.

Methods
We sought to enhance the prediction of neoepitope binding \by improving both the training data and predictive algorithms. Mono-allelic HLA class I cell lines were generated by transfecting individual class I HLA alleles into the HLA class I null cell line K562, prioritizing HLA class I alleles that were of high abundance in different populations. Cell surface bound MHC class I peptides were then identified through immuno-affinity purification followed by mass spectrometry. We then developed and trained neural networks to predict MHC class I presentation for each assayed HLA class I allele. The predictive algorithms were incorporated into our overall neoantigen pipeline (NeoantigenID), which integrates DNA and RNA based somatic variant calling, somatic HLA mutation calling, peptide phasing, identification of indel and fusion derived neoepitopes, and comprehensive immuno-genomics biomarker reporting.

Results
We applied paired transfection and mass spec in an allele specific manner to identify thousands of MHC bound peptides bound to dozens of HLA class I alleles. Our neoantigen prediction algorithm, trained on our own in vivo peptide data, consistently achieves a higher overall sensitivity and specificity than other tools based primarily on in vitro MHC

binding data, when tested on the same HLA class I alleles. Our MHC class I-epitope binding prediction algorithm demonstrated an aggregative precision value of 0.88 across HLA alleles, as opposed to 0.50 for other widely used tools.

Conclusions
Effective neoantigen identification requires an accurate variant detection and characterization pipeline built upon a comprehensive exome and transcriptome platform. We have developed an accurate solution for detection of neoantigens with emphasis on improved MHC presentation prediction from a broad genomic footprint.

P152

Nanofluidic drug-eluting seed for sustained intratumoral immunotherapy for cancer treatment

Ying Xuan Chua, PhD[1*], Antonia Susnjar[1], Jeremy Ho[1], Jessica Rhudy[1], Priya Jain, BS[1], Marco Folci[1], Andrea Ballerini[1], Shailbala Singh[2], Carly Filgueira, PhD[1], Cassian Yee, MD[2], Brian Butler[1], Alessandro Grattoni[1]

[1]Houston Methodist Research Institute, Houston, TX, USA
[2]UT MD Anderson Cancer Center, Houston, TX, USA

Background
While the clinical breakthrough of immune checkpoint inhibitors such as anti-programmed death-1 (PD-1) or cytotoxic T-lymphocyte-associated protein 4 (CTLA-4) in certain cancers has fueled optimism in immunotherapy, the efficacy is limited to a small subset of patients. In addition to insufficient anti-tumor immune response, systemic immunotherapy administration causes adverse side effects, whereby up to 91% of treated patients experienced clinically significant immune-related adverse events (irAEs). Intratumoral immunotherapy delivery has demonstrated anti-tumor efficacy in preclinical and clinical studies with minimal systemic toxicity. However despite encouraging results, the feasibility of intratumoral injections is restricted to accessible solid tumors whereas inaccessible tumors require technically challenging image-guided injections.

Methods
To fulfill the unmet need for sustained local drug delivery and to avoid repeated intratumoral injections, we developed the nanofluidic drug-eluting seed (NDES), a device the size of a grain of rice for intratumoral drug delivery. The NDES is inserted intratumorally using a minimally invasive trocar method similar to brachytherapy seed insertion and offers a clinical advantage of drug elution. Drug release from the NDES is driven by a difference in concentration, allowing for sustained immunotherapy delivery without the need for injections, actuation or clinician intervention. In this study, the NDES was used to deliver immunotherapeutics intratumorally in the 4T1 orthotopic murine mammary carcinoma model, which recapitulates triple negative breast cancer (Figure 1A).

Results
We demonstrated that NDES-mediated intratumoral release of agonist monoclonal antibodies, OX40 and CD40, resulted in potentiation of local and systemic anti-tumor immune response and inhibition of tumor growth compared to control. Further, mice treated with NDES-CD40 showed minimal systemic drug exposure and liver damage compared to systemically treated mice. As CD40 monotherapy was insufficient to eliminate tumor burden, we speculated that therapeutic synergy could be maximally achieved by combination treatment with radiation to induce immunogenic cell death. In line with this, NDES-CD40 in combination with localized radiation was more effective at reducing tumor burden than monotherapy (Figure 1B).

Conclusions

Overall we present the NDES as an effective platform for sustained intratumoral immunotherapy delivery with tremendous potential for clinical translation given that the NDES is applicable to a broad spectrum of drugs and solid tumors.

Acknowledgements
We thank Carlos Favela and Dr. Kemi Cui from the advanced cellular and tissue microscopy core, Dr. Jianhua (James) Gu from the electron microscopy core, Dr. Andreana L. Rivera, Dr. Yulan Ren, and Sandra Steptoe from the research pathology core of Houston Methodist Research Institute. This work was supported by Golfers Against Cancer, Nancy Owens Breast Cancer Foundation and start-up funds from Houston Methodist Research Institute (AG). Nanofluidic membranes were provided by NanoMedical Systems, Inc.

Ethics Approval
All animal experiments conducted were approved by the Institutional Animal Care and Use Committee (IACUC) of Houston Methodist Research Institute and performed in accordance with the National Institute of Health Guide for the Care and Use of Laboratory Animals and the Animal Welfare Act.

P153

Vaccination with HSP70i$_{Q435}$ DNA elicits a broad, functional antibody response that may contribute to tumor control of melanoma

Cormac Cosgrove, PhD[1], Caroline Le Poole[1], Emilia Dellacecca[1], Steven Henning[1]

[1]*Northwestern University, Chicago, USA*

Background
On target, off tumor side effects during cancer immunotherapy remain a major concern. Vitiligo is an autoimmune disease resulting in severe skin depigmentation and often occurs in melanoma patients receiving immunotherapy. Importantly, cytotoxic T cells recognize the same antigens in both conditions, drive depigmentation in vitiligo and are the target of immunotherapies in melanoma treatment. Inducible HSP70 activates dendritic cells (DCs), mediates autoimmune reactivity in vitiligo and is overexpressed in melanomas. However, vaccination with a mutated form of HSP70i (HSP70i$_{Q435A}$), developed in our lab, tolerizes DCs, prevents depigmentation and elicits tumor control in mouse models, pointing to a separation of tumor immunity and autoimmune responses, testable in Sinclair swine with melanoma and vitiligo. Experiments in CD8 knockout mice and B cell adoptive transfer experiments suggest that that beyond T cells, there is a key role for B cell or antibody-mediated tumor control in HSP70i$_{Q435A}$ DNA vaccinated mice.

Methods
C57BL/6 mice were vaccinated abdominally 5Q6days with either HSP70i$_{Q435A}$ or empty vector DNA using the Helios Gene Gun platform (Biorad). Serum was collected by cardiac bleed at euthanasia. ELISA was used to determine antibody isotype/subclass titers in serum and anti-HSP70-mediated ADCC was measured in an ELISA-based NK cell degranulation assay. Sinclair swine received 4 weekly doses of HSP70i$_{Q435A}$ plasmid DNA by jet injection directly to the perilesional border. Changes in lesion and melanoma size were tracked over 6 months.

Results
Significant anti-HSP70i IgG and IgM titers were present in HSP70i$_{Q435A}$ versus empty vector DNA-vaccinated mice. Antibodies titers were observed for IgG1, 2a, 2b, 2c, 3, and 4 subclasses and there was significant degranulation of NK cells in response to anti-HSP70 serum antibodies. In Sinclair swine, repigmentation of lesions was observed in HSP70i$_{Q435A}$ DNA-treated but not PBS-treated animals. Further, while the presence of vitiligo was associated with tumor shrinkage, melanomas in

HSP70i$_{Q435A}$ DNA-treated sites showed a trend towards accelerated shrinkage compared to vitiligo alone.

Conclusions

Vaccination with HSP70i$_{Q435A}$ DNA elicits a broad antibody isotype and IgG subclass response, capable of activating NK cells to degranulate. Coupled with the overexpression of HSP70i by melanomas, antibodies therefore may contribute to tumor control through ADCC. Furthermore, experiments in Sinclair swine suggest that local vaccination can also reverse vitiligo without impacting tumor control. Thus, anti-HSP70i antibodies may support tumor control during repigmentation in response to HSP70i$_{Q435A}$ DNA vaccination. These data suggest a potentially important role for active anti-HSP70i vaccination to support tumor control.

Ethics Approval

The Ethics Boards at Loyola University, Chicago, and Northwestern University at Chicago approved the study.

P154

Empiric profiling of neoantigen-specific T cell responses in NSCLC patients with ATLAS™ reveals unexpected neoantigen and inhibitory antigen profiles

Kyle Ferber, PhD, BS[1], Michael O'Keeffe[1], Crystal Cabral, BS, MSc[1], Christopher Warren[1], Erick Donis[1], Mariya Croll, MS[1], James Loizeaux[1], Melissa W. Hayes, PhD[1], James Perry[1], Wendy Broom, PhD[1], Pamela Carroll[1], Jessica Flechtner, PhD[2], Jason Dobson, PhD, BS[1]

[1]*Genocea Biosciences, Cambridge, MA, USA*
[2]*Genocea Biosciences, Inc., Cambridge, MA, USA*

Background

Immunotherapy of non-small cell lung cancer has resulted in unprecedented, but sometimes short-lived efficacy in first- and second-line settings. The importance of T cells recognizing patient-specific mutations, or neoantigens, in successful immune checkpoint blockade (ICB) treatment is well established. Given the role of neoantigens in successful ICB treatment, coupled with the aspiration to improve response rates to ICB in the absence of added toxicity, efforts are underway to develop neoantigen vaccines to enhance specific T cell responses. The challenge is identifying which mutation, out of the tens to thousands present in a patient's tumor, to include in their vaccine. Here we comprehensively identify neoantigen-specific T cell responses in the peripheral blood of NSCLC patients to identify their characteristics.

Methods

The ex vivo ATLAS™ technology enables comprehensive screening of a subject's tumor mutanome by using subject-specific T cells and monocyte-derived dendritic cells (MDDCs). PBMC were isolated from nine consented NSCLC patients and viably frozen. Whole exome sequencing of paired tumor and saliva samples from the same subjects was performed. CD8 and CD4 libraries of putative antigens were constructed by cloning and expressing regions spanning each somatic mutation in E. coli ± a co- cytoplasmic variant of listeriolysin O. Unique libraries were pulsed in an ordered array onto MDDCs from each patient, and then their CD8+ and/or CD4+ T cells added and incubated overnight. Recall responses were measured by detection of cytokines in the supernatants.

Results

Subject tumors had medians of 700 somatic mutations with 100 unique sequences. More than 1,000 mutations were screened and both stimulatory and inhibitory CD4+ and CD8+ T cell responses to neoantigens, which were rarely shared between subsets, were identified. Inhibitory neoantigens made up a greater proportion overall. Up to 66% of

neoantigens were not expressed (by RNAseq). Most of the identified neoantigens were not algorithm-predicted epitopes, nor could they be classified based on expression level or mutation type. T cell responses to driver mutations were infrequent. No obvious associations between neoantigen frequency and tumor mutational burden were identified. The impact of ICB on neoantigen response profiles will be discussed.

Conclusions
The ex vivo ATLAS platform can be used to identify and characterize neoantigens in the peripheral blood of oncology patients. Identified neoantigens are unexpected relative to epitope prediction algorithms and common neoantigen prioritization criteria. A Phase 1/2a clinical trial of a targeted personalized cancer vaccine, GEN-009, using ATLAS-identified antigens is ongoing.

Acknowledgements
US Oncology

Ethics Approval
This study was approved by US Oncology, Inc., Institutional Review Board; Committee #1- Dallas

P155

A DNA-based CSPG4 cancer vaccine designed by SynCon® technology is highly immunogenic and extends survival in a mouse model of melanoma

Bradley Garman, MS[1], Jewell N. Walters, BS PhD[1], Elizabeth K. Duperret, BS, PhD[2], Aspen Trautz[2], Jaemi Chu[2], Jian Yan, BS PhD[1], Laurent Humeau, BS, MS, PhD[1], David B. Weiner BS, MS, PhD[2]

[1]*Inovio Pharmaceuticals, Inc., Plymouth Meeting, PA, USA*
[2]*The Wistar Institute, Philadelphia, PA, USA*

Background
Chondroitin sulfate proteoglycan 4 (CSPG4), a transmembrane glycoprotein with functional roles in tumor migration, invasion, angiogenesis, and metastasis, has emerged as a promising tumor antigen target due to its overexpression in several solid cancer types and limited expression in normal tissue. In this study, we used Inovio's proprietary SynCon® technology to design a synthetic consensus DNA vaccine targeting CSPG4 (SynCon® CSPG4) and assessed its immunogenicity and preclinical efficacy in a tumor-bearing mouse model of melanoma.

Methods
C57BL/6 mice (n=5 per group) were immunized with 25 µg of SynCon® CSPG4 or vector control. Four immunizations were administered, two weeks apart, with electroporation following each immunization. Cellular immune responses were measured by mouse IFN-γ ELISpot and flow cytometry. The breadth and magnitude of antigen-specific T-cell epitopes was further assessed by epitope mapping using consensus matched peptides. Vaccine-induced anti-tumor immunity was assessed in C57BL/6 mice transplanted with 5x10^4 YUMM1.7 murine melanoma cells (n=10). One week following implantation, these mice were immunized with 25 µg of SynCon® CSPG4. At the same time, naïve mice (n=10) were challenged with 5x10^4 YUMM1.7 tumor cells as a control.

Results
SynCon® CSPG4 generated strong cellular immune responses in mice, as assessed by IFN-γ ELISpot and flow cytometry. An average of over 800 SFU/10^6 splenocytes were elicited in mice vaccinated with SynCon® CSPG4. The percentage of CD8+IFN-γ+ cells in mice immunized with SynCon® CSPG4 (0.552%) was significantly higher than that of the control mice (0.09%) ($p<0.0442$). Additionally, the SynCon® CSPG4-vaccinated mice showed a significant increase in the percentage of CD8+CD107a+ T cells, an indicator of cytotoxic potential, compared to control

mice (1.07% vs. 0.034%, respectively ($p<0.01$)). Epitope mapping revealed that SynCon® CSPG4 could elicit broad T-cell immune responses. Notably, SynCon® CSPG4 generated cellular responses against three peptide sequences identical to native mouse CSPG4 sequences, suggesting SynCon® CSPG4 is capable of breaking tolerance. Importantly, SynCon® CSPG4 significantly slowed tumor growth and increased survival in the YUMM1.7 mouse model of melanoma.

Conclusions

Herein, we demonstrate that a DNA-based, synthetic consensus CSPG4 immmunogen induced robust anti-tumor immunity. DNA immunogens designed by SynCon® technology have the potential to break tolerance and induce anti-tumor immunity in cancer patients. Clinical investigation of SynCon® immunogens is warranted, both alone and in combination with checkpoint inhibitors.

Ethics Approval

The study was approved by the University of Pennsylvania Institutional Animal Care and Use Committee.

P156

Developing a cross-reactive heteroclitic peptide cancer vaccine targetting poorly immunogenic mutant calreticulin in myeloproliferative neoplasms

Mathieu Gigoux, PhD[1], Shannon Elf, PhD[2], Michele Ciboddo[2], Roberta Zappasodi, PhD[1], Stephane Pourpe, MSc[1], Nouran Abdelfattah, MSc[2], Timothy Chan, MD, PhD[1], Omar Abdel-Wahab, MD[1], Ann Mullally, MD[2], Taha Merghoub, PhD[1], Jedd Wolchok, MD, PhD[1]

[1]*Memorial Sloan Kettering Cancer Center, New York, NY, USA*
[2]*Harvard, Boston, MA, USA*

Background

Disease-initiating mutations in calreticulin (CALR), an endoplasmic reticulum (ER) chaperone protein, are present in approximately 40% of myeloproliferative neoplasms (MPN). In recent work we demonstrated that expression of mutant CALR alone is sufficient to engender MPN in mice. We further showed that the thrombopoietin receptor, MPL is required for mutant CALR-driven transformation and that the oncogenicity of mutant CALR is dependent on the C-terminus of mutant CALR, which is necessary for physical interaction between mutant CALR and MPL. Although more than thirty CALR mutations have been identified, all result in the generation of a common, 36-amino acid novel C-terminal CALR peptide, representing a tumor-specific neo-antigen. We predicted that the tumor-specific neo-epitopes generated by the mutant CALR C-terminus induce immune responses in MPN patients.

Methods

Unfortunately, HLA-A*02:01, the MHC-I allele most frequently found in the Caucasian population, is unable to bind to any neo-antigens generated by the CALR mutations, based on the predictive algorithm and confirmed by in vitro assay. As expected, none of these peptides could generate T cell reactivity, as measured by the presence of IFNγ and TNFα-expressing T-cells after 10 days. We therefore hypothesized that T cell reactivity against the CALR mutants could be activated using heteroclitic peptides, which are peptides with a single amino-acid mutation that increases MHC-I binding 10 to 1000-fold, and have the potential to generate cross-reactivity against the native CALR mutant peptides. To predict high-quality heteroclitic peptides, we used the NetMHC-Epitoptimizatron (NEOn) algorithm developed by our group, which generates candidate heteroclitic peptides for any MHC-I allele in mice and humans. To test this strategy, we took advantage of the fact H2-Kb and H2-Db, MHC-I alleles expressed in C57BL/6J mice, also do not bind efficiently to CALR mutant peptides.

Results
We are currently in the process of evaluating the response in mice immunized with H2-Kb and H2-Db heteroclitic CALR mutant peptides. In addition, we are also testing the relevance of this findings in PBMCs from HLA-A*02:01 healthy donors with HLA-A*02:01 heteroclitic peptides in vitro. Once hetercolclitic peptides are validated they will be tested in MPN derived PBMCs.

Conclusions
The design of a heteroclitic vaccine based apporach in MPN patients provides an attractive stragey to elicit antitumor immunity in MPN patients.

Ethics Approval
The study was approved by the MSKCC ethics board. IRB# 06-107 A(15) and IACUC# 96-04-017

P157

ISA101 and nivolumab for HPV-16+ Cancer: Updated clinical efficacy and immune correlates of response

Bonnie Glisson, MD[1], Erminia Massarelli, MD, PhD, MS[3], William William, MD[4], Faye M. Johnson, MD, PhD[4], Renata Ferrarotto, MD[4], Ming Guo[4], Lei Feng[5], J Jack Lee[6], Hai Tran[6], Jaime Rodriguez-Canales, MD[7], Tomas Zecchini Barrese[6], Ignacio Wistuba, MD[6], Jing Wang[5], Sjoerd van der Burg, PhD[8], Kimal Rajapakshe, PhD[9], Cornelis Melief, MD, PhD[10], Michael Curran, PhD[6]

[1]MD Anderson Cancer Center, Houston, TX, USA
[2]U T M D Anderson Cancer Center, Houston, TX, USA
[3]City of Hope, Duarte, CA, USA
[4]M. D. Anderson Cancer Center, Houston, TX, USA
[5]M D. Anderson Cancer Center, Houston, USA
[6]M D Anderson Cancer Center, Houston, USA
[7]Medimmune, Gaithersburg, MD, USA
[8]Leiden University, Leiden, Netherlands
[9]Baylor College of Medicine, Houston, USA
[10]ISA Pharmaceuticals, Leiden, Netherlands

Background
Therapy with ISA101, an HPV16 peptide vaccine, and nivolumab demonstrated a promising overall response rate (ORR) of 33% (8/24) in pts with incurable HPV16+ cancer (1). We now present updated clinical efficacy and immune correlative analyses.

Methods
Patients with HPV16 tumors and ECOG PS 0-1, and <2 prior regimens for recurrence were eligible. ISA101 100 mcgs/peptide D1, 22, 50 and Nivolumab 3 mg/kg iv q 2 wks starting D8, were given for up to 1yr. Baseline tumor samples (FFPE) were stained with multiplex immunofluorescence (mIF) for PD-L1, PD-1, CD3, CD8, CD68, and pancytokeratin in a single panel, scanned with the Vectra 3.0™ multispectral microscope, and analyzed using inForm™ 2.3.1 software. Whole transcriptome analysis of baseline tumors was performed on Affymetrix Clariom™ D arrays. Differential gene expression analysis was performed on responders (PR + CR) vs. non-responders (SD +PD). P-values were corrected for multiple hypothesis testing

Results
All responding patients had oropharynx primaries. Of the 8 responders, 4 remain in response > 1 yr (13.6-18.7 months) with a median duration of 10.3 months (3.8-18.7+) . Median OS is 17.5 months (95% CI: 13.8 – inestimable) with median f/u of 17 months in censored patients. The scores for activated T cells [(CD3+PD-1+) + (CD3+CD8+PD-1+)], activated cytotoxic T cells (CD3+CD8+PD-1+), and total macrophages [(CD68+PD-L1-)+ (CD68+PD-L1+)] in tumor tissue were directly correlated with clinical response (p values all < 0.05, Wilcoxon), and depth of response with the two CR pts having the highest degree of CD8+ T cell infiltration. Gene expression analysis revealed differential regulation of 225 genes

(1.25 fold or >) in responders vs non-responders (p = 0.05). High expression of interferon response genes and low expression of genes reflecting oxidative phosphorylation were correlated with clinical response. Enrichment in gene sets associated with interferon response and immune infiltration strongly predicted response to therapy, whereas elevated expression of genes associated with oxidative phosphorylation predicted progression."

Conclusions

Efficacy of ISA101 and nivolumab remains promising in long-term f/u. A randomized trial is ongoing to test this strategy. Similar to data with anti-PD-1 alone, increased infiltration by PD-1+ T cells (CD3+ and CD3+CD8+) was predictive of response. The correlation between macrophages and clinical response fits with data from preclinical models and possibly involves IFNγ. Enrichment in gene sets associated with interferon response and immune infiltration strongly predicted response to therapy, whereas elevated expression of genes associated with oxidative phosphorylation predicted progression."

Trial Registration

clinicaltrials.gov NCT0246892

References

1. Massarelli E, William WN, Johnson F et al Combining Immune Checkpoint Blockade and Tumor-specific Vaccine: Phase II Trial of Nivolumab and ISA101 in Patients with Incurable Human Papillomavirus 16-Related Cancers JAMA Oncology In Press

Ethics Approval

The study was approved by U. T. M. D. Anderson Cancer Center's IRB March 24, 2015.

P158

IFN-α and 5'-Aza-2'-deoxycytidine enhance the anti-tumor efficacy of a dendritic-cell targeting MIP3α-Gp100-Trp2 DNA vaccine by affecting T-cell recruitment and tumor microenvironment gene expression

James Gordy, PhD[1], Richard Markham, BS, MD[2]

[1]*Johns Hopkins Bloomberg School of Public, Baltimore, MD, USA*
[2]*Johns Hopkins BSPH, Baltimore, MD, USA*

Background

The chemokine MIP-3α (CCL20) binds to CCR6 found on immature dendritic cells. DNA vaccines fusing MIP-3α to melanoma-associated antigens Gp100 and Trp2 have been shown to be effective in therapeutically reducing melanoma tumor burden in mouse models. To further enhance the therapy, our laboratory has added agents designed to overcome immunoregulatory mechanisms of the tumor microenvironment. Here, we report that the combination of type-I interferon therapy (IFN) with 5'-Aza-2'-deoxycitidine (Aza) profoundly enhanced the therapeutic anti-melanoma efficacy of a MIP-3α-Gp100-Trp2 DNA vaccine.

Methods

The current studies utilize the B16F10 mouse melanoma model. Vaccinations are administered intramuscularly followed by electroporation. Vaccinations are given thrice at one-week intervals, beginning day 5 post challenge. Two days post vaccination, CpG adjuvant is administered into the vaccinated muscle. Aza is given i.p.at 1mg/kg on the first two vaccination days. IFN is given in a series of one high dose followed by three low doses, beginning on the first two vaccination days. Tumor sizes, growth, and survival were assessed by Anova, linear regression, and log-rank survival respectively. Tumor microenvironment gene expression levels

were explored by RT-PCR, with dCt values tested by Anova. Tumor-infiltrating lymphocytes (TILs) were assessed by measuring vaccine-stimulated TILs by intracellular cytokine staining flow cytometry, tested by Anova. All experiments have been repeated with sample sizes of 3-8 mice per group.

Results

We demonstrate that the addition of IFN and Aza significantly enhances the anti-tumor efficacy of a MIP-3α-Gp100-Trp2 vaccine. At day 19 post challenge, the triple treatment has tumors 69% smaller than vaccine alone. Mouse survival was also significantly increased, with the median survival increasing compared to vaccine by 39% and to negative control by 86%. Importantly, this increase in efficacy was dependent on the presence of all three components: vaccine, IFN, and Aza. All permutations of one or two treatments provided inferior efficacy. Aza and IFN additions to the vaccine increase T-cell tumor infiltration and alter the proportion of CD8+T-cells. Finally, we show that Aza and IFN induce durable changes in IFN-stimulated gene transcription that remain long after administration.

Conclusions

Efficient targeting of antigen to immature dendritic cells with a chemokine-fusion vaccine offers a potential alternative approach to ex vivo dendritic cell antigen-loading protocols currently undergoing clinical investigation. Combining this approach with IFN and Aza therapy significantly improved vaccine efficacy. This enhancement is correlated with changes in TILs and IFN-stimulated gene expression. This line of investigation has great potential to become a novel melanoma therapy.

Ethics Approval

This study was approved by the IACUC of Johns Hopkins University, protocol MO16H147

P159

Correlation between response and HLA type in a randomized phase IIb trial of NeuVax + trastuzumab in HER2 low-expressing breast cancer patients to prevent recurrence

Annelies Hickerson, MD[1], Guy T. Clifton, MD, FACS[1], Tommy Brown, MD[1], John Myers, III, MD[1], Jessica Campf, MD[1], Kaitlin Peace, MD[1], Jennifer K. Litton[2], Rashmi Murthy[2], Timothy J. Vreeland, BS MD[2], Diane Hale, MD[1], Garth Herbert, MD[1], Jason Lukas, MD/PhD[3], Nicholas J. Sarlis[4], Jarrod P. Holmes[5], Elizabeth A. Mittendorf[2], George E. Peoples, MD, FACS[6],

[1]Brooke Army Medical Center, Houston, TX, USA
[2]The University of Texas, Houston, TX, USA
[3]Providence Regional Cancer Partnership, Everett, WA, USA
[4]Sellas Life Sciences Group, Inc., New York, NY, USA
[5]Redwood Regional Medical Group, Santa Rosa, CA, USA
[6]Cancer Vaccine Development Program, San Antonio, TX, USA

Background

MHC class I (MHCI) peptide vaccines are HLA-restricted but may bind to multiple HLA-types. HLA types have been associated with response to multiple immunotherapies to include checkpoint inhibitors. The relationships between HLA-type, predicted peptide binding potential, and clinical response have implications for the design and development of active immunotherapy. In a planned interim analysis of a randomized phase IIb trial of the MHCI peptide, E75 (HER2 369-377), + GM-CSF (NeuVax) + trastuzumab versus GM-CSF + trastuzumab to prevent recurrences in node positive (NP) and/or triple negative (TNBC), HER2 low-expressing breast cancer patients we demonstrated a significant disease free survival (DFS) benefit specifically in triple negative (TNBC) patients to NeuVax + trastuzumab. This analysis examines the effect of HLA-type on trial outcomes.

Methods

Clinically disease-free HER2 low-expressing (IHC1+/2+, FISH nonamplified) NP (AJCC N1, N2, or N3) and/or TNBC patients after standard therapy were tested for the presence of the A2, A3, A24, and A26 alleles by flow cytometry. HLA-A2, A3, A24, and/or A26+ patients were randomized to receive trastuzumab + NeuVax (vaccine group; VG) or trastuzumab + GM-CSF (control group; CG). All patients received 1 year of trastuzumab per label. NeuVax or GM-CSF was given every three weeks x 6 starting with the third trastuzumab dose, and then boosted every six months x 4. The pre-specified interim analysis was triggered six months after last patient enrollment. The primary endpoint was DFS evaluated by log rank. The MHCI binding predictions were made using the IEDB Analysis Resource Consensus tool.

Results

275 patients were randomized in the study (VG n=136, CG n=139). 146 were HLA-A2+ (VG=71, CG=75), 133 HLA-A24+ (VG=71, CG=61), 88 HLA-A3+ (VG=44, CG=44), and 19 HLA-A26+ (VG=10, CG=9). Median follow up was 18.8 months. There were no significant clinicopathologic difference between the VG and CG as a whole or within HLA-allele subgroups, except that fewer HLA-A24+ VG patients received radiation therapy (p=0.02). In TNBC patients, active treatment benefited all HLA-types (Figure 1) especially HLA-A24+ patients (Figure 2, p=0.02). HLA-A24+ VG patients also showed a trend toward improved DFS study-wide (Figure 3, p=0.07). HLA-A24+ has the lowest predicted binding affinity of the four HLA alleles.

Conclusions

HLA-A24+ TNBC patients had a significant improvement in DFS despite the lowest predicted binding potential between E75 and this HLA-type. This suggests that lower-affinity peptides may generate a favorable immunologic response possibly due to decreased exposure and tolerance to epitopes.

Trial Registration

Combination Immunotherapy With Herceptin and the HER2 Vaccine E75 in Low and Intermediate HER2-expressing Breast Cancer Patients to Prevent Recurrence, NCT01570036

Ethics Approval

The study was approved by Western Institutional Review Board, approval number 20130058.

Figure 1.

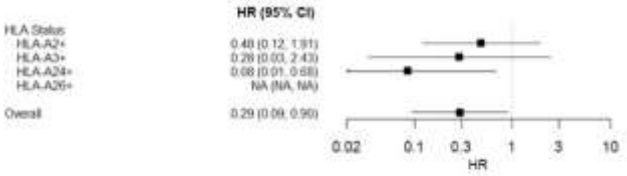

Figure 2.

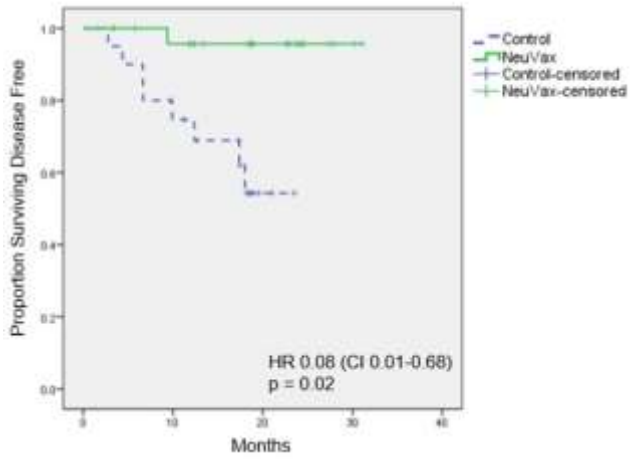

Figure 3.

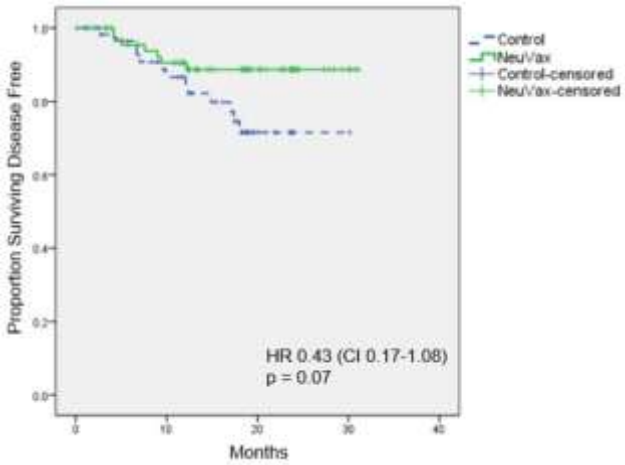

P160

Engineering a T cell stimulating extra-cellular matrix for immunotherapy

John Hickey, BS[1], Yi Dong[1], Hai-Quan Mao, PhD[1], Jonathon P. Schneck, MD, PhD[1], John Hickey, BS[1]

[1]*Johns Hopkins University, Baltimore, MD, USA*

Background

T cells are the target of many immunotherapies; many, such as adoptive T cell therapy, require expansion of T cells to several thousand-fold. Expansion often comes at the cost of losing cytotoxic functionality and ability to persist as a memory cell which limits the success of these therapies. In tissue engineering, much effort has been taken to control environmental cues for differentiation, phenotype skewing, and proliferation of stem cells. We hypothesized that by controlling factors surrounding the microenvironment we could further activate T cells which would retain functionality to give improved immunotherapy.

Methods

We engineer an extracellular matrix out of hyaluronic acid and polyethylene glycol diacrylate. We can control stiffness and easily attach additional cell-attachment and stimulatory cues such as anti-CD3 or peptide-loaded MHC (major histocompatibility complex) and anti-CD28.

Results

First, we demonstrate that the extracellular matrix environment provides a “signal 3” to T cells being stimulated. This is mediated by CD44 receptors on the surface of T cells and involves a crosstalk between the mTOR and Ras-Erk pathways with an ultimate upregulation of IL7 and IL15 receptors. Second, we engineered the extracellular matrix to present T cell stimulatory molecules to eliminate additional sources of stimulation. Here we found important biophysical properties of stiffness and extracellular matrix proteins influenced both the proliferation and phenotype of resultant T cells. Third, we stimulated rare antigen-specific T cells and adoptively transferred into a murine melanoma model and showed significant reduction of tumor burden compared to conventionally expanded T cells in plastic culture dishes.

Conclusions

Our studies demonstrate the importance of the environment, specifically the extracellular matrix in T cell stimulations. Additional engineering of the extracellular matrix enabled enhanced in vitro and in vivo functionality within an adoptive T cell therapy model. Further study and engineering of these extracellular environments could lead to substantial improvements in cellular therapies.

Acknowledgements

JWH is supported by NSF and ARCS Graduate Research Fellowships.

P161

The effects of IGF-1R antisense on cells of the glioma tumor microenvironment promotes immunostimulatory antigen release

D. Craig Hooper[1], Samantha Garcia, PhD[1], Rhonda Kean, MS[1], Aurore LeBrun, PhD[1], Emily Bongiorno[1], David Andrews, MD[1]

[1]*Thomas Jefferson University, Philadelphia, PA, USA*

Background
Glioblastoma (GBM) is the most lethal form of primary brain cancer. A highly anti-inflammatory tumor microenvironment (TME), in part due to the presence of tumor associated macrophages (TAMs) with M2-like properties, presents a significant obstacle to immunotherapy. While excised GBM tissues can be used as the basis of a personalized vaccine, this requires a strategy to generate antigens in an immunogenic format. Targeting the IGF-1R expressed in GBM tissues, which sensitizes the cells to radiation [1] and modulates the function of other IGF-1R-expressing cells in the TME may have utility in this regard. We show here that immune-stimulating antigens are released by tumor tissue treated ex-vivo in biodiffusion chambers with immunomodulatory IGF-1R antisense oligodeoxynucleotide and radiation.

Methods
GL261 cells were implanted stereotactically in the CNS of C57BL/6 mice and tumor tissue harvested at the appearance of clinical signs. Tumor tissues were dispersed, and aliquots subjected to different treatments prior to encapsulation in biodiffusion chambers. Fully-formulated chambers contained tumor tissues that had been cultured overnight with the IGF1-R antisense and then encapsulated with additional antisense and irradiated. Chambers were incubated in PBS or implanted in the flanks of naïve C57BL/6 mice overnight, then contents were retrieved and used to pulse naïve bone marrow dendritic cells (BMDCs). CD4+ T cells recovered from GL261-immune C57BL/6 mice were used to detect tumor antigenic determinants presented by the BMDCs with the readout being the number of cells producing IFNγ.

Results
The strongest IFNγ response was elicited by antigens recovered from fully-formulated chambers cultured in PBS overnight. If the overnight incubation with antisense was omitted a similarly immunogenic antigen preparation was generated only if the amount of antisense added to the chamber was increased. The contents of fully-formulated chambers implanted in mice overnight failed to stimulate immune CD4+ T cells in vitro suggesting that the antigen had been lost in the animals. However, these animals had been immunized and were protected against the growth of GL261 cells subsequently implanted in their CNS. Comparable results have been obtained in similar studies in other mouse tumor models.

Conclusions
Biodiffusion chambers containing irradiated glioma cells, prepared from excised tumor tissues, and an immunostimulatory IGF-1R antisense selectively produce glioma antigens in an immunogenic format appropriate for vaccination. The approach is currently under investigation in a clinical trial for patients with GBM (ClinicalTrials.gov, NCT01550523) and there is support from other mouse tumor models for its utility in diverse cancers.

References
1. Turner BC, et. al. Insulin-like growth factor-I receptor overexpression mediates cellular radioresistance and local breast cancer recurrence after lumpectomy and radiation. Cancer Res. 1997; 57:3079-83.

Ethics Approval
The study was approved by Thomas Jefferson

University's Animal Care and Use Committee AWA A3085-10, AUP00902.

P162

Single cell sequencing to identify TCRs that recognize autologous tumor cells after vaccination with allogeinic DRibble vaccine

Hong-Ming Hu, PhD[1], Christopher C. Paustian, PhD[2], Zhifa Wen[3], Tarsem L. Moudgil, MS[3], Traci L. Hilton, PhD[2], Sam Bookhardt, BA[2], Guangjie Yu[3], Eric Tran, PhD[3], Venkatesh Rajamanickam[3], Walter Urba, MD, PhD[3], Rachel E. Sanborn, MD[3], Bernard A. Fox, PhD[1]

[1]Providence Portland Medical Center, UbiVac, Portland, OR, USA
[2]UbiVac, Portland, OR, USA
[3]Providence Portland Medical Center, Portland, Oregon, OR, USA

Background

Adoptive immunotherapy with tumor-specific TCR gene-modified T cells has the potential to eradicate bulky disease. Traditional methods of TCR identification require lengthy in vitro culture to generate clonal T-cell populations, which adds time and complexity to this promising therapy. Here we described a simplified and reliable method to identify TCRs by single cell TCR sequencing of cells sorted with antibodies against T-cell surface markers that are up-regulated only when they are stimulated with specific tumor cell antigens.

Methods

A tumor-infiltrating lymphocyte (TIL) culture with T cells reactive against autologous tumor was generated from a brain metastasis of a patients with NSCLC. A panel of antibodies against T-cell surface antigens was screened to identify markers that are specifically up-regulated after stimulation with autologous tumors but not with related allogeneic tumor cells. Tumor-specific T cells were sorted from TIL with three suitable antibodies and expanded by a rapid expansion protocol. Expanded T cells were examined for their tumor-specificity and subjected to single cell TCR sequencing using the 10X genomic system. The top 10 TCRs were identified by bio-informatics approach and the corresponding alpha and beta chains were synthesized and cloned into a retroviral vector based on MSG backbone. PBMC from healthy donors were transduced with the retrovirus supernatant after activation. Tumor-reactivity of transduced T cells was determined after expansion in media supplemented with IL-2, IL-7, and IL-15. To identify tumor-specific TCRs in PBMC from the same patient after vaccination with allogeneic DRibbles, we also developed a protocol to expand tumor-specific T cells from PBMC with in vitro stimulation with DRibble-loaded PBMC.

Results

We identity CD94, CD137(4-1BB), CD355 (CRTAM) as specific markers for antigen-specific activation of T-cells by autologous tumor cells, whereas other "check point" markers such as CTLA-4, PD-1, Tim3, CD39, CD103 were up-regulated by stimulation with unrelated tumor cells. These antibodies were successfully used to sort and enrich tumor-specific T cells. The top 10 TCRs from each sorting were different but with overlapping clones. Five TCR clones were tumor-specific and capable to recognize the autologous tumor cells when they were expressed on T-cells from health donors. Additionally, ex-vivo culture of vaccine stimulated PBMC from a post-vaccine timepoint generated T cells enriched for activity against autologous tumor.

Conclusions

We developed a simplified work flow to identify tumor-specific TCRs. This flow will be further improved with antibody with DNA bar codes and used to identify tumor-reactive TCRs in a streamlined fashion.

Acknowledgements

The study was supported by Providence Portland

Medical Foundation and NCI SBIR grant R44 CA121612.

Ethics Approval

The study was approved by EACRI Institutution's Ethics Board, approval number IRB: PDX06-108

P163

Humoral immune responses elicited by Globo H vaccine and the impact of Globo H expression levels on clinical response to Globo H vaccine in metastatic breast cancer

Jung-Tung Hung[1], I-Ju Chen[2], Wei-Chien Tang[2], Shir-Hwa Ueng[3], Tsai-Hsien Hung[1], Fei-Yun Lo[1], Hope Rugo, MD[4], Chiun-Sheng Huang[5], Alice Yu, MD, PhD[1]

[1]Institute of Stem Cell & Translational Cancer Research
[2]OBI Pharma, Inc., Taipei, Taiwan, Province of China
[3]Chang Gung Memorial Hospital, Taoyuan, Taiwan, Province of China
[4]University of California San Francisco Comprehensive Cancer Center, San Francisco, USA
[5]National Taiwan University Hospital, Taipei, Taiwan, Province of China

Background

An international randomized phase II trial of Globo H (GH) vaccine Adagloxad simolenin (OBI-822/821) in 349 patients with metastatic breast cancer (MBC) showed longer PFS in vaccinated patients who developed anti-Globo H (anti-GH) antibodies versus those who did not. The impact of immune responses to OBI-822/821 and GH expression on clinical outcome was further evaluated.

Methods

Anti-GH and anti-KLH antibodies were determined by ELISA. The binding ability and antibody-dependent cellular cytotoxicity (ADCC)/complement dependent cytotoxicity (CDC) of antisera were examined by flow cytometry and cytotoxicity assay, respectively. GH expression on tumors was detected by immunohistochemistry (IHC).

Results

OBI-822/821 elicited anti-GH IgM responses reached a maximum of ≥1:80 between week 4 and 12 (after 3 to 5 injections) and then declined. The mean anti-GH IgG titer peaked at week 40 (after 9 injections) and decreased once vaccination was complete. In the OBI-822/821 group, both GH responders (anti-GH IgG titer ≥1:160 at any time, N=64) and GH non-responders (anti-GH IgG titer <1:160, N=31) developed similar levels of anti-KLH IgG titers at week 40 (p=0.94, median titer=128,000, t-test on log transformed data). The sera of 40 patients with high anti-GH titers were assessed for their biological activities. By flow cytometry, 77.5% (31/40) and 17.5% (7/40) of their post-immune IgM and IgG, respectively, showed > 10% increase in binding to MCF7 cells. A 1.5-fold increase in CDC activity of post-immune sera over pre-immune sera was noted in 62.5% (25/40) of patients. ADCC responses were observed in 50% of the 40 patient samples tested.Among patients with higher GH expression by IHC (H score ≥ 80), there was a trend toward better PFS for the vaccinated (N=42) vs placebo group (N=23) (Hazard Ratio=0.59; 95% CI: 0.32, 1.10, P-value=0.10). For those with H score < 80, there was no difference in PFS between vaccinated and placebo groups (N=83 and 44 respectively. HR=1.22; 95% CI: 0.79-1.89, P-value=0.36).

Conclusions

Adagloxad simolenin induced antibodies against GH and KLH antigens in MBC. The anti-GH elicited by the vaccine was biologically active in binding to GH-positive cancer cells and mediating CDC/ADCC. Notably, in the vaccinated group, immune non-responders produced equivalent levels of anti-KLH antibody as immune responders, suggesting a similar capacity to respond to foreign antigens. A trend for better PFS in subjects with higher GH expression

treated with OBI-822/821 versus placebo suggests the need for pre-screening GH expression in future trials of OBI-822/821.

Trial Registration
NCT03562637

Ethics Approval
The study was approved by Chang Gung Medical Foundation Institututional Review Board, approval number 102-3670A3.

P164

Personalized cancer vaccines based on peptide-TLR-7/8a conjugates induce CD8 T cell responses to neoantigens in primates that are dependent on TLR-7/8a potency

Andrew Ishizuka, DPhil[1], Andrei Ramirez-Valdez[2], Hide Yamane, PhD[2], Yaling Zhu, PhD[1], Vincent Coble[1], Faezzah Baharom[2], Kennedy Tobin[2], Brennan Decker[1], Geoffrey Lynn[1], Robert A. Seder, MD[2]

[1]Avidea Technologies, Baltimore, MD, USA
[2]VRC, NIAID, NIH, Bethesda, MD, USA

Background
Personalized cancer vaccines (PCVs) aim to enhance neoantigen-specific T cell responses. We developed a PCV platform based on peptide-TLR-7/8 agonist conjugates that self-assemble into nanoparticles (termed SNP-7/8a). SNP-7/8a ensures co-delivery of neoantigens with TLR-7/8a, and significantly expands the breadth of neoantigen-specific CD8 T cell responses in mice. Here, we determined how the potency of the co-delivered TLR-7/8a affected the magnitude and quality of neoantigen-specific CD8 T cells in mice and primates.

Methods
Mice were vaccinated with SNP-7/8a co-delivering an MC38 neoantigen (Adpgk) and either a high potency (EC50 = ~20 nM) imidazoquinoline TLR-7/8a (termed '2BXy') or moderate potency (EC50 = ~ 600 nM) TLR-7/8a (termed '2B'). CD8 T cell responses were evaluated by tetramer staining. Studies were subsequently conducted in rhesus macaques (RM) as TLR expression in RM and humans is highly similar. RM with the MHC-I allele Mamu-A*01 were vaccinated subcutaneously with SNP-7/8a co-delivering mock neoantigens predicted to bind Mamu-A*01 and either 2BXy or 2B. CD8 T cell responses were measured directly ex vivo by peptide stimulation and intracellular cytokine staining for IFN-g.

Results
After the first immunization, the CD8 T cell response was higher in mice vaccinated with 2BXy-based SNP-7/8a. However, there was no difference in the magnitude of the Adpgk-specific T cell responses after subsequent vaccinations. Interestingly, 2BXy-vaccinated mice had a significantly higher proportion of Adpgk-specific cells that had differentiated into KLRG1+CD127– short-lived effector cells (SLECs), whereas 2B-vaccinated mice had a higher proportion of KLRG1–CD127+ memory-precursor effector cells (MPECs). In primates, neoantigen-specific CD8 and CD4 T cells were identified directly ex vivo after a single vaccination with SNP-7/8a. While 2BXy-vaccinated RM trended towards a higher magnitude neoantigen-specific CD8 and CD4 T cell response after the first vaccination, the responses underwent a greater expansion in 2B-vaccinated animals compared to 2BXy-vaccinated animals. Moreover, 2BXy-vaccinated RM showed a trend towards having a higher proportion of IFN-g+ neoantigen-specific CD8 T cells that had terminally differentiated into CCR7–CD45RA+ (TEMRA) cells compared to 2B-vaccinated RM, where the response favored less differentiated CCR7+CD45RA– (Tcm).

Conclusions
SNP-7/8a induced neoantigen-specific CD8 and CD4 T cell responses in primates. Interestingly, the

moderate potency TLR-7/8a led to T cell responses that were balanced between effectors and memory cells, which may be optimal for tumor vaccines. Efforts to define the innate mechanisms controlling CD8 T cell differentiation following SNP-7/8a vaccination are underway.

Ethics Approval

These studies were approved by the Animal Care and Use Committee of the VRC, NIAID, NIH.

P166

Ex vivo ATLAS-identified inhibitory neoantigens promote mouse melanoma tumor progression

Hanna Starobinets, PhD[1], Kyle Ferber, PhD, BS[1], Jason R. Dobson, PhD, BS[1], Michael O'Keeffe[1], Crystal Cabral, BS, MSc[1], Matthew Lanchantin, BS[1], Erick Donis[1], Peri Matatia[1], Erik Carter[1], Adrienne Li, PhD[1], James Loizeaux[1], Jamie Foti, PhD[1], Wendy Broom, PhD[1], Pamela Carroll[1], Paul Kirschmeier[2], Jessica B. Flechtner, PhD[1], Hubert Lam, PhD[1]

[1]*Genocea Biosciences, Cambridge, MA, USA*
[2]*Dana-Farber Cancer Institute, Boston, USA*

Background

Neoantigens are attractive targets for personalized cancer immunotherapy due to their recognition as foreign antigens not subject to central tolerance. Personalized cancer vaccines leverage neoantigens to direct the immune system to specifically recognize tumor cells for their coordinated attack and destruction. Although not well understood, published data also suggest that some immunotherapies result in hyperprogression. One hypothesis for this phenomenon is antigen-specific immune modulation by T cells. ATLAS™ is a T cell profiling platform whereby putative antigens can be screened ex vivo using autologous antigen presenting cells (APCs) and T cells. Antigens are differentially characterized as stimulatory or inhibitory by significant up- or downregulation of T cell cytokine secretion relative to control responses; thus, the ATLAS assay allows for identification and characterization of desired as well as potentially unwanted antigen-specific T cell responses

Methods

A melanoma model was employed to identify murine neoantigens and inhibitory antigens using ATLAS. Mice were implanted subcutaneously with B16F10 tumors, which were subsequently resected for whole exome sequencing and assessed for non-synonymous mutations. ATLAS libraries individually expressing each mutation were constructed and used to screen splenic T cells from tumor bearing mice to identify stimulatory or inhibitory neoantigens. Candidate neoantigens were manufactured as synthetic long peptides and delivered subcutaneously to C57BL/6 mice with or without adjuvant to elucidate the ability of stimulatory or inhibitory vaccines to impact tumor growth.

Results

Non-synonymous mutations (>1600) were identified and incorporated into the ATLAS library. After T cell screening, multiple neoantigens were identified that differentially modulated the secretion of inflammatory cytokines. ATLAS-identified neoantigens were not enriched for NetMHCpan-predicted epitopes, known oncogenes, or tumor suppressor genes. In addition, there was no preferential enrichment of frame-shift mutations, insertions or deletions. After vaccination with ATLAS-identified antigens, significant T cell responses to stimulatory vaccine neoantigens were observed as well as modest anti-tumor efficacy against B16F10 tumor challenge. Strikingly, therapeutic immunization with inhibitory neoantigen peptides led to a marked and significant increase in tumor growth kinetics. Studies to further investigate the immunological mechanisms will be reported.

Conclusions
These studies demonstrate proof of concept in mice for therapeutic efficacy using the ex vivo ATLAS platform to prioritize neoantigens included in personalized vaccines. In addition, they demonstrate the existence and biological importance of vaccine antigens that lead to hyperprogression. A Phase 1/2a clinical trial of a targeted personalized cancer vaccine, GEN-009, filtered for inclusion of ATLAS-identified stimulatory antigens and exclusion of inhibitory antigens, is ongoing.

Acknowledgements
We would like to thank Catarina Nogueira for early exploratory work.

P167

Characterization of antigen specific immune responses from a first-in-human study evaluating the anti-ASPH cancer vaccine SNS-301 in biochemically relapsed prostate cancer patients

Michael Lebowitz, PhD[1], Kanam Malhotra[1], M.S. Walker[1], Hong Dai, MD, PhD[1], Michael S. Lebowitz, PhD[1], Steven Fuller, PhD[1], Amir Shahlaee, MD[1], James J. Elist, MD[2], Neal Shore, MD[3], Luke Nordquist, MD, FACP[4], Hossein Ghanbari, PhD[1]

[1]*Sensei Biotherapeutics, Gaithersburg, MD, USA*
[2]*James J. Elist, MD, Beverly Hills, CA, USA*
[3]*Carolina Urologic Research Center, Myrtle Beach, SC, USA*
[4]*GU Res. Network/Urology Cancer Center, Omaha, NE, USA*

Background
SNS-301 (formerly PAN-301) is a first-in-class immunotherapeutic cancer vaccine candidate targeting human aspartyl (asparaginyl) β-hydroxylase (ASPH). ASPH is an oncofetal antigen expressed prevalently in multiple human cancers but not in healthy adult tissue and that has not been targeted in any prior clinical studies. As a biologic modifier of the NOTCH pathway, ASPH is associated with tumor cell growth, motility and invasiveness. SNS-301 is a vaccine which delivers over 400 copies of an extracellular domain of the ASPH protein displayed on the coat of a bacteriophage vector. Previously presented pre-clinical data demonstrated the vaccine's ability to overcome tumor self-tolerance and to provide immune-mediated anti-tumor effects [1,2]. The safety and tolerability of SNS-301 have also been presented previously [3].

Methods
SNS-301 was administered intradermally every 21 days in a 3+3 dose-escalation trial evaluating 3 dose levels to patients with biochemically (rising PSA) relapsed prostate cancer with evidence of ASPH over-expression as detected in serum. Secondary immunologic endpoints included the calculation of geometric mean titers of anti-ASPH antibodies; stimulation of innate immune responses; production and persistence of antigen-specific B cell and T cell responses; and the correlation of anti-ASPH titers and serum ASPH levels.

Results
Twelve patients with measurable serum levels of ASPH received 6-18 doses of SNS-301 (median = 10 doses). All patients experienced dose-dependent ASPH-specific immune responses including B-cell, T-cell and antibody responses. Specifically, increases in activated, IFN-γ releasing T-cells were demonstrated, including activated patient-derived CD4+ helper T cells as demonstrated by cytokine release subsequent to in vitro stimulation with either SNS-301 or recombinant ASPH. Anti-ASPH antibody titers also increased in a dose-dependent fashion over the first 4-6 cycles (80-120 days) of vaccination. This increase correlated with concomitant increases in the percentages of ASPH-specific B-cells as measured by flow cytometry. Immune responses occurred faster and were more robust at the two higher doses vs. the lower dose. Immunologic efficacy generally

correlated with biochemical responses in these patients.

Conclusions
In this phase I setting, the SNS-301 vaccine induced vibrant and durable antigen-specific immune responses, which generally correlated with biochemical responses. Based on these cumulative results, a multi-site phase 2 efficacy clinical trial will commence enrollment in the 2nd half of 2018.

Trial Registration
ClinicalTrials.gov Identifier: NCT03120832

References
1. Tomimaru Y, Mishra S, Safran H, Charpentier KP, Martin W, De Groot AS, Gregory SH, Wands JR. Aspartate-β-hydroxylase induces epitope-specific T cell responses in hepatocellular carcinoma. Vaccine. 2015; 33:1256-66.
2. Iwagami Y, Casulli S, Nagaoka K, Kim M, Carlson RI, Ogawa K, Lebowitz MS, Fuller S, Biswas B, Stewart S, Dong X, Ghanbari H, Wands JR. Lambda phage-based vaccine induces antitumor immunity in hepatocellular carcinoma. Heliyon. 2017; 3:e00407.
3. Nordquist LT, Shore ND, Elist JJ, Oliver JC, Gannon W, Shahlaee AH, Fuller SA, Ghanbari HA. Phase 1 open-label trial to evaluate the safety and immunogenicity of PAN-301-1, a novel nanoparticle therapeutic vaccine, in patients with biochemically relapsed prostate cancer. J Clin Oncol. 2018;36:suppl; abstr e15166.

Ethics Approval
The study was approved by Schulman IRB, approval number 201606469.

P168

Induction of chemokine receptor and suppression of inhibitory receptors of CD8 T cell controlled effectively cervicovaginal tumor in mouse

Daewoo Lee, MD[1], Daeun Nam[1], Sungjong Lee, PhD, MD[2]

[1]*The Catholic University of Korea, Bucheon, Korea, Republic of*
[2]*St. Vincent's Hospital, Suwon, Korea, Republic of*

Background
Activation of exhausted CD8 T cell and migration of immune cells into tumor site is an important for overcoming resistance to cancer therapy. We evaluated the role of suppression of inhibitory receptors and chemokine axis in cervicovaginal tumor bearing mouse.

Methods
C57BL/6 mice were categorized into four groups according to treatment modality. Mice were challenged with 1×105 TC-1 cells on cervix and vagina. HPV DNA therapeutic vaccine was injected intramuscularly and intratumoral injection of GMCSF was performed. The mice were harvested on day 21 and immune cells were investigated by flow cytometry. We checked the expression of inhibitory receptors of CD8 T cells, including PD1, TIM3 and LAG3. Chemokine axis such as CXCL9, CXCL10, and CXCR3 were evaluated to know migration mechanism.

Results
Combination of HPV DNA vaccine and GMCSF resulted in significantly lower expression of TIM3 inhibitory receptors of CD8+ T cells in tumor ($p<0.05$) (Fig 1). However, expression level of PD1 and LAG3 was not changed after combination therapy. They significantly induced accumulation of tumor specific CD8 T cell in tumor site and increased expression of CXCR3 on tumor infiltration CD8 T cell ($p<0.05$). CXCL9, chemokine, was overexpressed in cervicovaginal tumor after combination therapy ($p<0.05$) (Fig 2). However, expression level of CXCL10 was not changed after combination therapy. Finally, mice treated with combination therapy survived

significantly longer than other groups with single therapy ($p<0.05$).

Conclusions

In conclusion, we overcame T cell exhaustion and identified chemokine axis during migration of CD8 T cell into cervicovaginal tumor using HPV DNA vaccine and GMCSF. This mechanism can be ideal target for future immunotherapy.

Figure 1 and 2. Inhibitory marker and chemokine

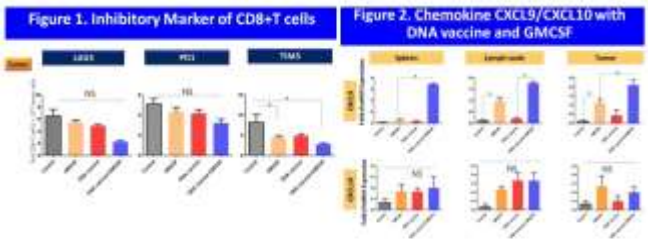

P169

In-Depth Characterization of Immune Responses Induced Against Patient-Specific Neoantigens using NEO-STIM™

Divya Lenkala[1], Brian McCarthy[1], Michael Nelson[1], Rachel Debarge[1], Janani Sridar[1], Yusuf Nasrullah, Master's in Biological Research, UK[1], Jessica Kohler, PhD[1], Matthew Goldstein, MD, PhD[1], Richard Gaynor, MD[1], Marit M. Van Buuren, PhD[1]

[1]*Neon Therapeutics, Cambridge, MA, USA*

Background

Neoantigens are tumor-specific antigens important in eliciting and directing effective anti-tumor immune responses. These antigens are not subject to central immune tolerance and are therefore potentially more immunogenic than tumor-associated antigens (1,2). A better understanding of the rules governing neoantigen immunogenicity will improve our ability to select high-quality targets for T cell responses with the potential to treat patients.

Methods

Patient-specific neoantigens were predicted using our bioinformatics pipeline, RECON®, and were used as immunogens in our proprietary ex-vivo stimulation protocol NEO-STIM to assess immunogenicity. Peptides were loaded into antigen presenting cells (APCs) and utilized to induce memory and de novo T cell reactivity from autologous peripheral blood mononuclear cells (PBMCs). In-depth analysis of the induced responses was performed through combinatorial coding analysis using peptide MHC (pMHC) multimers (3); functional analyses with multiplexed, multiparameter flow cytometry and cytotoxicity assays. Data from these analyses were used to characterize the specificity, functionality, sensitivity, phenotype and killing capacity of the induced T cells.

Results

Here we show exemplary data from one patient (ClinicalTrials.gov: NCT02897765) in which we induced multiple CD8+ and CD4+ T cell responses, both memory and de novo, towards predicted patient-specific neoantigens. These induced responses were reactive to the mutated neoantigens and not to the corresponding wild type antigen. These mutant-specific responses exhibited polyfunctionality in response to peptide stimulation along with capability to kill antigen expressing tumor cell lines. In conclusion, patient-specific neoantigens predicted by RECON were confirmed to be immunogenic by NEO-STIM induction of neoantigen-specific T cell responses.

Conclusions

NA

References

1. Yarchoan M, Johnson III BA, Lutz ER, et al. Targeting neoantigens to augment antitumor immunity. Nature Reviews Cancer. 2017; 17:209–

222.
2. Martin SD, Coukos G, Holt RA, et al. Targeting the undruggable: immunotherapy meets personalized oncology in the genomic era. Annals of Oncology. 2015; 26:2367–2374.
3. Andersen RS, Kvistborg P, Frøsig TM, et al. Parallel detection of antigen-specific T cell responses by combinatorial encoding of MHC multimers. Nature Protocols. 2012; 7:891–902.

P170

Identification of breast cancer neoantigens exposed by radiation therapy

Claire Lhuillier, PhD[1], Nils-Petter Rudqvist, PhD[1], Takahiro Yamazaki, PhD[1], Tuo Zhang, PhD[1], Lorenzo Galluzzi, PhD[1], Sandra Demaria, MD[1]

[1]*Weill Cornell Medical College, New-York, NY, USA*

Background

Recent studies have highlighted the key role of mutation-generated neoantigens in tumor response to immunotherapy [1]. We have previously shown in the BALB/c-derived 4T1 mouse model of immune-checkpoint blockade (ICB)-resistant metastatic breast cancer that tumor-targeted radiation therapy (RT) combined with CTLA-4 blockade induces the CD8+ T cell-mediated regression of irradiated tumors and inhibits lung metastases [2]. Analysis of the T-cell receptor repertoire indicated that unique clonotypes expand in treated tumors, suggesting that tumor rejection involves T cells reactive to a set of tumor antigens that are made available to the immune system by RT [3]. Therefore, we hypothesize that RT increases the expression of genes containing immunogenic mutations and hence promote priming of neoantigen-specific T cells.

Methods

We performed whole-exome sequencing and RNA sequencing of untreated and irradiated (8GyX3) 4T1 cells *in vitro* to identify tumor-specific neoantigens and determine which ones are upregulated by RT. In addition, these mutations were documented *in vivo*, in 4T1 tumors harvested before and after treatment (8GyX3 + anti-CTLA-4). Several algorithms were used to predict MHC-I and MHC-II-binding epitopes from these mutated genes. Peptides with a predicted affinity <500 nM were synthesized and tested *in vitro* for binding to H2-Ld or H2-Kd in a MHC stabilization assay using RMA-S cells. Peptides showing stable binding in this assay were used to vaccinate BALB/c mice, followed by challenge with 4T1 cells to test for the induction of protective anti-tumor immunity.

Results

Out of 309 total mutations initially identified in 4T1 cancer cells, 22 predicted MHC-I-binding epitopes were tested *in vitro* and 6 of them were confirmed to bind to H2Ld or H2Kd. For MHC-II, we identified two I-Ad-predicted binders, which were tested in vaccination experiments. Results showed that 2 MHC-I and 1 MHC-II neoepitopes were immunogenic, as assessed by IFNγ/TNFα response after T cells re-stimulation. Two of the three neoepitopes were encoded by genes upregulated by RT. Although a vaccine based on these three neoepitopes is not sufficient to inhibit tumor growth, a significant tumor growth delay was seen when vaccination was combined with tumor-targeted RT and an OX40 agonist.

Conclusions

Further analyses are ongoing to understand the regulation of RT-exposed neoantigens *in vivo* and their contribution to T cell-mediated tumor rejection. In conclusion, these data provide initial proof-of-principle evidence that RT can expose existing neoantigens to the immune system.

References

1. Schumacher TN, Schreiber RD. Neoantigens in cancer immunotherapy. Science. 2015; 348:69-74.
2. Demaria S, Kawashima N, Yang AM, Devitt ML,

Babb JS, Allison JP, Formenti SC. Immune-mediated inhibition of metastases after treatment with local radiation and CTLA-4 blockade in a mouse model of breast cancer. Clin Cancer Res. 2005; 11:728-734.
3. Rudqvist NP, Pilones KA, Lhuillier C, Wennerberg E, Sidhom JW, Emerson RO, Robins HS, Schneck J, Formenti SC, Demaria S. Radiotherapy and CTLA-4 Blockade Shape the TCR Repertoire of Tumor-Infiltrating T Cells. Cancer Immunol Res. 2018; 6:139-150.

P171

Safety and immunogenicity of a DNA vaccine encoding PSA and PSMA in patients with biochemically recurrent prostate cancer

Li Liu, PhD[1], Neal Shore, MD[2], Elisabeth Heath[3], Matthew Morrow, PhD[4], Kimberly Kraynyak, BS PhD[4], Kamal Bhatt, LCEH MS[4], Trevor McMullan[4], Jessica Lee, MS, MPH[4], Brian Sacchetta[4], Samantha Rosencranz[4], Ildiko Csiki, BS MD, PhD[4], Mark Bagarazzi, MD[1]

[1]*Inovio Pharmaceuticals Inc, Plymouth Meeting, PA, USA*
[2]*Carolina Urologic Research Center, Myrtle Beach, SC, USA*
[3]*Wayne State University, Detroit, MI, USA*
[4]*Inovio Pharmacetuicals, Plymouth Meeting, PA, USA*

Background
After definitive therapy, approximately one third of prostate cancer (PCa) patients (pts) will experience rising prostate specific antigen (PSA) levels, a condition known as biochemical recurrence. Active immunotherapies, or antitumor vaccines, are appealing as potential treatments to eradicate micrometastatic disease. The choice of vaccine antigens in prostate cancer has largely been guided by the presence of proteins whose expression is known to be essentially restricted to the prostate, including PSA and prostate-specific membrane antigen (PSMA). Various prostate cancer vaccine platforms targeting these antigens have been reported. In the current study, we evaluated the immunogenicity and safety of INO-5150, a DNA vaccine encoding PSA and PSMA, with or without INO-9012 (encoding IL-12 immune adjuvant), in men with biochemically relapsed prostate cancer.

Methods
62 post-prostatectomy/radiation therapy pts with rising PSA were divided into 4 cohorts in a phase I, open-label, multi-center study and received INO-5150 ± INO-9012 (A, 2mg INO-5150; B, 8.5 mg INO-5150; C, 2mg INO-5150+1mg INO-9012; D, 8.5mg INO-5150+1mg INO-9012). INO-5150±INO-9012 was administered via intramuscular (IM) injection followed by electroporation with the CELLECTRA® device on day 0, weeks 3, 12 and 24 then followed through study week 72. Safety, immunogenicity and efficacy were assessed for all evaluable pts.

Results
50/62 (81%) pts have completed all visits. 90% pts had Grade (Gr) 1-3 AEs, primarily injection site reactions, which were Gr1. 48/61(79%) evaluable subjects demonstrated immune responses to PSA/PSMA antigens. The response rate in ELISpot and ELISA assays were 70% (40/57) and 23% (14/61) respectively. In addition, analysis of antigen specific CD8+ T cells with lytic potential was conducted using flow cytometry. CD8+ T cells co-expressing CD38 and perforin were induced in 23/50 (46%) pts, who also experienced attenuated PSA increase (p=0.05 for PSA attenuation). In pts with stable disease (SD, N=20), treatment with INO-5150±INO-9012 significantly increased PSMA-specific CD8+ T cells with cytolytic potential as evidenced by the co-expression of the activation markers CD38 and CD69, expression of PD1 and upregulation of granulysin, granzyme A, granzyme B, and perforin compared to pts with progressive disease (PD) (p=0.024, N=30). 75% (27/36) of the patients with baseline (D0) PSADT≤12 months became stabilized with a significantly

prolonged PSADT at WK72 (p<0.0001, N=27).

Conclusions
INO-5150 +/- INO-9012 was safe and immunogenic. A therapeutic effect was demonstrated in patients with D0 PSADT of≤ 12 months, as manifested by their dampening % rise in PSA and prolonged PSADT up to 72 weeks follow up.

P172

Personalized cancer vaccines based on self-assembling nanoparticles co-delivering peptide antigens and TLR-7/8 agonists (SNP-7/8a) enhance the breadth and magnitude of anticancer CD8 T cell immunity

Geoffrey Lynn[1], Faezzah Baharom[2], Yaling Zhu, PhD[1], Ramiro A. Ramirez-Valdez, BA Cantab[2], Tobin Kennedy[2], Vincent Coble[1], Brennan Decker[1], Hide Yamane, PhD[2], Andrew S. Ishizuka, DPhil[1], Robert A. Seder, MD[2]

[1]Avidea Technologies, Inc., Baltimore, MD, USA
[2]National Institutes of Health

Background
Advances in genomic sequencing and in silico prediction algorithms have enabled the development of personalized cancer vaccines (PCVs) targeting tumor-specific neoantigens. With current peptide- and RNA-based PCVs, only ~10% of predicted neoantigens induce de novo CD8 T cell responses. Here, we show that the efficiency for inducing CD8 T cells to peptide antigens can be significantly improved and is highly dependent on the physical form of the peptide. Accordingly, particulate peptide antigens, unlike soluble peptide antigens, are taken up efficiently by dendritic cells in lymphoid tissue and promote CD8 T cell expansion through prolonged antigen presentation. Thus, a major challenge for peptide-based PCVs is ensuring consistent particle formulations despite the broad range of neoantigen physicochemical properties.

Methods
We developed a novel PCV platform based on charge-modified peptide-TLR-7/8 agonist conjugates that are chemically programmed to self-assemble into nanoparticles ("SNP-7/8a") of a defined size (20–50 nm) irrespective of the underlying neoantigen composition. Several hundred unique SNP-7/8a compositions were synthesized to systematically screen how different parameters of SNP-7/8a (size, charge, peptide antigen length, etc.) impact formulation characteristics and in vivo immunogenicity.

Results
Bioinformatics analysis of the characteristics of 72 million human genome-derived neoantigens was used to demonstrate that SNP-7/8a ensures consistent nanoparticle formation with neoantigens at extremes of charge (-6 to +6) and hydropathy (GRAVY, -2 to +2). Vaccination of mice with SNP-7/8a using predicted neoantigens (n = 179) from three tumor models induced CD8 T cells against ~50% of those with high predicted MHC-I binding affinity (IEDB consensus score < 0.5). Importantly, SNP-7/8a induced CD8 T cells that inhibited tumor growth against several neoantigens that were reported non-immunogenic using conventional peptide- or RNA-based vaccines.

Conclusions
SNP-7/8a based on charge modified conjugate vaccines represents a universal approach for co-delivering peptide antigens and adjuvants in nanoparticles to increase the magnitude and breadth of anticancer T cell immunity.

P173

Early results of a phase I clinical trial of a HER2 dendritic cell cancer vaccine

Hoyoung Maeng, MD[2], Lauren V. Wood, MD[2], Lee England, PA-C[2], Brenda Roberson, BSN, RN, OCN[3], Santhana Webb[2], Brittni Moore[2], David F. Stroncek, MD[3], John C. Morris, MD[4], Jay A. Berzofsky, MD, PhD[2]

[1]NCI, Bethesda, MD, USA
[2]National Cancer Institute, Bethesda, MD, USA
[3]National Institute of Health, Bethesda, MD, USA
[4]University of Cincinnati, Cincinnati, OH, USA

Background
We have developed a therapeutic cancer vaccine targeting HER2 based on autologous dendritic cells (DCs) transduced with an adenovirus (AdHER2) expressing the non-signaling extracellular and transmembrane domains of HER2, a driver oncogene in many cancers that is often associated with worse outcome. In mice, the homologous vaccine cured virtually all mice with established tumors up to 2 cm or with established macroscopic lung metastases. The protection was dependent on antibodies against HER2 that inhibited HER2 phosphorylation, but was FcR (ADCC) independent, unlike the mechanism of trastuzumab, an FDA approved anti-HER2 antibody. We translated this discovery to a clinical trial in the NIH Clinical Center.

Methods
This is an open-label, non-randomized phase I clinical trial (NCT01730118) in patients with advanced metastatic cancers who have progressed after a minimum of one standard therapy, whose tumor is HER2 immunohistochemistry (IHC) score 1+, 2+ or 3+ or HER2/CEP17 ratio ≥ 1.8 by FISH. Part 1 of the study enrolled cancer patients naïve to any HER2-directed therapies to assess the safety and immunologic response.

Results
In Part 1, excluding the lowest dose level (5 million viable DCs) where no responses were seen (n=6), at the second and third dose level (10 and 20 million viable DCs, n=6 each), 45% (5/11 evaluable patients) had clinical benefit, including one CR lasting 89 weeks (BRCA WT high grade serous ovarian cancer), one PR lasting 24 weeks (gastric adenocarcinoma), and 3 cases of stable disease (1 ovarian carcinosarcoma and 2 colon cancers). The patient with a CR (HER2 IHC score 3+ and FISH HER2/CEP17 ratio 1.3) recurred with HER2 IHC score 0 and FISH HER2/CEP17 ratio 1.2 metastasis, and the patient with ovarian carcinosarcoma (HER2 IHC score 1+ and FISH HER2/CEP17 ratio 1.0) who had initial tumor shrinkage (-24.8%) progressed with new lesions showing HER2 IHC score 0 and FISH HER2/CEP17 ratio 1.2, suggesting immune escape. Adverse reactions were mainly Grade 1 injection-site reactions. Serial echocardiograms showed preserved cardiac function. Currently, dose-expansion cohorts (40 million viable DCs) in patients who are anti-HER2 therapy naïve (Part 1) or who progressed after standard-of-care anti-HER2 therapy (Part 2) are ongoing.

Conclusions
We have translated a cancer vaccine from mice to human clinical trials with promising early results, and intend to combine this vaccine with checkpoint inhibitors, as vaccines can induce T cell responses, turning “cold” tumors into “hot” ones. This combination strategy can potentially improve the response rate and effectiveness.

Ethics Approval
The study was approved by IRB, National Cancer Institute, National Institute of Health, project number P12990, protocol 13C0016

P174

A phase 1/2a study to evaluate the safety, tolerability, immunogenicity, and anti-tumor activity of GEN-009 adjuvanted neoantigen vaccine in adult patients with selected solid tumors

Roger Cohen[1], Michael S.Gordon, MD[2], Wendy Hill[3], Lisa K McNeil, PhD[3], Tingting Ge, PhD[3], Arthur P. DeCillis, MD[3], Melissa L. Johnson, MD[4], Mark Awad, MD PhD[5],

[1]*University of Pennsylvania, Philadelphia, PA, USA*
[2]*Honor Health, Scottsdale, AZ, USA*
[3]*Genocea, Cambridge, MA, USA*
[4]*The Sarah Cannon Research Institute, Nashville, TN, USA*
[5]*Dana-Farber Cancer Institute, Boston, MA, USA*

Background
GEN-009 is a personalized adjuvanted neoantigen vaccine for the treatment of patients with solid tumors. Genocea's proprietary Antigen Lead Acquisition System (ATLAS™) is used to prioritize tumor neoantigens that will be synthesized into peptides for inclusion in GEN-009. ATLAS uses a patient's peripheral blood T cells and antigen presenting cells to screen for every patient-specific tumor mutation. The ATLAS neoantigen selection is based on a cytokine read-out. Neoantigens prioritized by ATLAS contain an epitope that is recognized by the patient's T cells and should elicit patient-specific stimulatory CD4 or CD8 T cell responses. Unlike *in silico* models, ATLAS is also able to identify inhibitory neoantigens. Inhibitory neoantigens will be excluded from each patient's vaccine.

Methods
GEN-009-001 is a first-in-human study conducted in three parts. For each patient, neoantigens will be selected by ATLAS, manufactured as synthetic long peptides, and co-administered with poly-ICLC adjuvant on 5 treatment days. The primary objectives in all parts are safety and immunogenicity. T cell responses before and after vaccination will be assessed in peripheral blood mononuclear cells by interferon-gamma/granzyme B FluoroSpot assay. Part A (n~9) is enrolling patients with melanoma, NSCLC, SCCHN or urothelial carcinoma who have completed treatment with curative intent and are without disease. Part B will enroll patients in 5 disease-specific cohorts (15 patients in each cohort including the tumor types noted above and renal cell carcinoma). Patients will initiate treatment with nivolumab monotherapy according to the FDA-approved label. Following ATLAS screening and vaccine production, GEN-009 will be added to the patient's nivolumab treatment. Antitumor activity will be defined by response improvement with the addition of GEN-009 to nivolumab compared with nivolumab monotherapy as described in (Table 1).Part C will treat patients who have the above-noted tumor types and have previously received standard therapy that included a PD-1 or PD-L1 inhibitor with GEN-009 as a monotherapy. An interim analysis based on response using RECIST 1.1 will be conducted after 15 patients have been analyzed. An additional 25 patients may be enrolled.

Conclusions
GEN-009-101 Part A is currently enrolling patients.

Ethics Approval
The study was approved by Western Institutional Review Board (WIRB), approval number 1-P210

Table 1.

Best Response to Nivolumab	Improved Response to Nivolumab + GEN-009
Partial response (PR)	Complete response (CR)
Stable disease (SD)	PR or CR
Progression of Disease	SD, PR, or CR

P175

Targeting arginase in tumor microenvironment

Evelina Martinenaite, MSc[1], Shamaila Munir Ahmad[1],

Simone Kloch Bendtsen, MSc[1], Mia Aaboe Jørgensen[1], Stine Emilie Weis-Banke[1], Inge Marie Svane, MD[1], Mads H. Andersen, PhD[1]

[1]*Center for Cancer Immunotherapy, Herlev, Denmark*

Background
Cancer progression is associated with an increased immune suppression at the tumor site. Arginase-1 is an enzyme expressed by immune inhibitory cells, such as myeloid derived suppressor cells (MDSCs), that reduces arginine availability to the tumor infiltrating immune cells and thus reduces T cell functionality in the tumor milieu. To target arginase-mediated immune inhibition we aimed to identify and characterize T cell responses against arginase-1 derived peptides.

Methods
We characterized spontaneous immune responses against optimized 38-mere arginase-1-derived peptide epitope in cancer patients and healthy donors using ex vivo and in vitro IFNγ ELISPOT and intracellular staining for IFNγ and TNFα. T cell responses were further characterized by combining the magnetic bead sorting of CD4+ and CD8+ memory T cells and IFNγ ELISPOT. The natural mechanism of arginase-1 specific T cell activation through upregulation of arginase-1 expression was investigated by IL-4 stimulation.

Results
We have previously identified arginase-1 hotspot region that contains multiple peptide epitopes commonly recognized by T cells from cancer patients and healthy donors. We have shown that arginase-specific T cells can be isolated, expanded and are able to recognize arginase-1 expressing immune cells. In this study, we were able to demonstrate that T cells recognizing an optimized 38-mere arginase-1 peptide epitope are a natural part of the T cell repertoire. Strong ex vivo responses against arginase peptide were detected in IFNγ ELISPOT and arginase-1 specific CD4+ and CD8+ memory T cells were found in both healthy donors and cancer patients. We have also shown that arginase-1 specific T cells could be activated by the IL-4-induced upregulation of arginase-1 expression, which suggests the potential role of arginase-specific T cells in the immune regulation.

Conclusions
Our study shows that arginase-1 specific CD4+ and CD8+ T cells are a natural part of the immune system, which makes vaccination using arginase-1 derived peptides a promising approach to effectively target arginase producing tumors and inhibitory immune cells such as M2 macrophages and MDSCs in the cancer microenvironment.

P176

Identification and analysis of critical immune molecules and signaling pathways to improve the immunogenicity of dendritic cell vaccines

Deena Maurer, MS[1], Deena Maurer, MS[1], Deena Maurer, MS[1], Patricia Santos, PhD[2], John Kirkwood, MD[2], Ahmad Tarhini, MD, PhD[3], Hussein Tawbi, MD, PhD[4], David Stroncek, MD[5], Ping Jin, PhD[5] , Lisa H. Butterfield, PhD[2]

[1]*University of Pittsburgh, Pittsburgh, PA, USA*
[2]*UPMC Hillman Cancer Center, Pittsburgh, PA, USA*
[3]*Case Western Reserve University, Cleveland, OH, USA*
[4]*MD Anderson Cancer Center, Houston, TX, USA*
[5]*National Institutes of Health, Bethesda, MD, USA*

Background
Melanoma is the leading cause of skin cancer-related death in the USA. Clinical trials have revealed important successes with checkpoint blockade treatments. However, many patients do not respond, and those who do often have previously mounted an immune response.

Methods

To elicit a strong antitumor immune response, we created a dendritic cell (DC) vaccine loaded with three full-length tumor-associated antigens: Tyrosinase, MART-1, and MAGE-A6 (TMM2). DC were generated from patient monocytes, matured with IFNγ + LPS, and transduced with a recombinant adenovirus encoding these antigens. Patients received three intradermal injections of the vaccine. Human genome RNA microarrays were used to analyze the gene expression profiles of the DC vaccines at immature (day 5 iDC), mature (day 6 mDC), and antigen loaded (day 7 previously matured AdVTMM2 DC) stages.

Results

To understand the mechanisms of the DC based vaccine induced immune and clinical responses, microarray gene expression profiles from patients are being investigated. We are examining costimulatory and immune checkpoint molecules and their downstream signaling pathways that are induced upon maturation and/or transduction.Preliminary protein data on 32 patients reveal a decrease in the surface expression of the costimulatory molecule, ICOSL, post maturation and viral transduction, compared to healthy donors (HD). ICOSL protein expression positively correlates with antitumor T cell responses specific to TMM2. ICOSL is reported to be regulated by NFκB [1]. Analysis of the microarray data revealed that NFκB signaling is predicted to be inactivated in patient mDC. mRNA expression of the reported NFKB inhibitor, NLRP2, negatively correlates with clinical outcome.Microarray data on a similar HD dataset showed that several metabolic pathways (oxidative phosphorylation and fatty acid beta-oxidation) are inactivated in HD mDC [2]. Inactivation of these pathways at the mDC stage are associated with an immune stimulatory phenotype. Patient data does not show these pathways are being inactivated in mDC. The mRNA expression of genes involved in these pathways are decreased post maturation, but not significantly, and correlate with clinical response.

Conclusions

The decrease in ICOSL protein expression observed after maturation and/or transduction may influence the antitumor immune response. In addition, our microarray data suggests that melanoma patient DC may not be metabolically “fit” to generate an optimal antitumor immune response. By understanding the mechanisms in DC, we will be able to generate superior DC-based vaccines and combination therapies, that may lead to improved outcomes for advanced melanoma patients.

Trial Registration

This study is related to the Clinical Trial, Multiple Antigen-Engineered DC Vaccine for Melanoma, identifier number NCT01622933.

References

1.Hu H, Wu X, Jin W, Chang M, Cheng X, Sun SC. Noncanonical NF-kappaB regulates inducible costimulator (ICOS) ligand expression and T follicular helper cell development. Proc Natl Acad Sci U S A. 2011; 108:12827–12832.

2. Jin P, et al. Molecular signatures of maturing dendritic cells: implications for testing the quality of dendritic cell therapies. J. Transl. Med. 2010;8:4. doi: 10.1186/1479-5876-8-4.

Ethics Approval

This study was approved by the University of Pittsburgh Institution's Ethics Board, approval numbers 0403105 (UPCI #09-021) and 12010416 (UPCI #04-001).

P177

Boosting T cell immunity against IDO1: Proof of concept for a novel cancer vaccine approach

Souvik Dey, PhD[1], Souvik Dey, PhD[1], Souvik Dey,

PhD[1], Erika Sutanto-Ward, BS[1], Katharina Kopp, BS[2], Mai-Britt Zocca, PhD[2], Ayako Pedersen, PhD[2], Mads Andersen, PhD[3], Alexander J. Muller, PhD[1]

[1]*Lankenau Institute for Medical Research, Wynnewood, PA, USA*
[2]*IO Biotech ApS, Copenhagen, Denmark*
[3]*University of Copenhagen, Herlev, Denmark*

Background
IDO1 (indoleamine 2,3-dioxygenase 1) is a tryptophan-catabolizing enzyme that fosters a tumor-promoting inflammatory microenvironment. IDO1 acts to subvert T cell immunity at multiple levels, including suppressing effector T cells and inducing/activating regulatory T cells. In this context, a particularly intriguing finding has been the observation that humans exhibit T cell reactivity against IDO1-expressing cells. IDO1-reactive T cells are found not only in cancer patients, where pathophysiological elevation of IDO1 has been frequently noted, but even in healthy individuals. This finding implies the existence of a T cell-mediated, counter-regulatory mechanism directed against IDO1. Initial clinical studies employing a peptide-based vaccine approach to harness this anti-IDO1 response for the benefit of cancer patients have thus far been encouraging. However, there is a pressing need to establish preclinical models for investigating the underlying basis of the anti-IDO1 response.

Methods
See Figure Legends.

Results
The CT26 colon carcinoma model was chosen for these studies based on high levels of IDO1 expression and responsiveness to IDO1 inhibition reported for these tumors. Predicted H2d MHC class I and II-restricted IDO1 peptide sequences, identified by computer algorithms, were selected so as to be compatible with the Balb/c strain-based CT26 model. Prophylactic vaccination identified a subset of these peptides that caused tumor growth suppression, including a class II-directed as well as class I-directed peptides. Therapeutic treatment of established CT26 tumors with a combination of anti-PD-1 antibody and class I, but not class II, peptide vaccine produced a combinatorial anti-tumor response beyond what was achieved with either agent alone. Interestingly, the combination of class I and class II peptides likewise elicited an enhanced combinatorial response, suggesting distinct mechanisms of action. Consistent with this interpretation, adoptive transfer of isolated CD8 and CD4 T cells from vaccinated responder mice reciprocally delayed growth of established tumors, such that CD8 (but not CD4) T cells were effective from a class I-vaccinated mouse while CD4 (but not CD8) T cells were effective from a class II-vaccinated mouse. Studies into the underlying nature of the IDO1-directed, anti-tumor response are currently ongoing.

Conclusions
As noted in humans, our results demonstrate that IDO1 is immunogenic in mice confirming that T cell responses against this endogenous protein are not fully tolerized. Initial findings that IDO1 peptide-derived vaccines can elicit effective anti-tumor responses demonstrate the utility of mouse models for further exploration and refinement of this novel approach to IDO1-directed cancer therapy.

Ethics Approval
This study was approved by the Lankenau Institute for Medical Research IACUC; protocol number A04-2097.

P178

Identification of shared phosphopeptide tumor targets in colorectal carcinoma for novel off-the-shelf vaccine development

Paisley T. Myers, PhD[1], Erin D. Jeffery, PhD[1], Benjamin Morin, PhD[1], Christine Brittsan, MA[2], Bishnu Joshi[1], Antoine Tanne, PhD[1], Karen Smith, BS[1], Albert Hurwitz[1], Kara L. Cummings, PhD[3], Amanda M. Lulu[3], Daniel L. Levey, PhD[1], Linh Mach[1], Mark A. Findeis, PhD[1], Gayle C. Hunt, PhD[3], Jeffrey Shabanowitz, PhD[4], Donald F. Hunt, PhD[4], Arthur A. Hurwitz[5], Robert N. Stein, MD PhD[1], Alex Duncan, PhD[1], Dennis Underwood, PhD[1]

[1]*Agenus Inc., Charlottesville, VA, USA*
[2]*Agenus Inc, Lexington, MA, USA*
[3]*University of Virginia School of Medicine, Charlottesville, VA, USA*
[4]*University of Virginia, Charlottesville, VA, USA*
[5]*AgenTus Therapeutics, Inc., Lexington, MA, USA*

Background

The high mortality rate of colorectal cancer (CRC) reflects limitations of current treatment modalities aimed at targeting the disease. Immunotherapy is a promising alternative to traditional chemotherapy, yet its benefit has been limited to patients with high mutational burden. Here, we describe a novel class of post-translationally modified neoantigens – phosphopeptide tumor targets (PTTs) – for use in a CRC vaccine. PTTs arise from dysregulated cellular signaling, are presented by HLA class I molecules, and are recognized as antigenic by circulating cytotoxic T cells. PTTs are highly prevalent among CRC patients, illustrating their role as excellent targets for the development of novel immunotherapeutics.

Methods

HLA:peptide complexes were immunopurified from CRC tissues using pan-HLA class I antibodies. Associated peptides were acid-eluted, concentrated, and enriched via immobilized metal affinity chromatography. Enriched phosphopeptides were analyzed on an Orbitrap Fusion Lumos mass spectrometer using complementary fragmentation methods and sequenced via Byonic™ software. Immunogenicity of PTTs was assessed by in vitro simulation of T cells derived from healthy donors.

Results

We applied our workflow to 26 CRC patient tissues. The patient population represents primary and metastatic tumors, microsatellite instable and stable classifications, and numerous HLA alleles, allowing for a broad assessment of PTT neoantigens associated with CRC. We identified over 500 unique PTTs, ranging from less than 1 to 100 copies per cell, with assignments to over 20 HLA alleles, highlighting the robust and sensitive nature of our ligandomic approach. Stringent selection criteria were employed to select strong candidates for inclusion in a CRC PTT vaccine aimed at targeting large patient populations. Thirty PTTs were selected based on 1) assignment to frequent HLA alleles, 2) derivation from proteins involved in dysregulated signaling pathways associated with malignancy, and 3) observation of memory T cell responses in healthy individuals. Based on frequencies of expression of prioritized HLA alleles, 70% of US/EU CRC patients would be eligible for vaccination and the majority of eligible patients' tumors will contain multiple PTTs included in the vaccine.

Conclusions

The development of a novel PTT-based vaccine for CRC may improve survival outcomes compared to standard-of-care treatments. The inclusion of highly-prevalent, multiple allele-associated epitopes from diverse source proteins expands the eligible patient population and increases the likelihood of stimulating an effective, anti-tumor immune response. Furthermore, the shared frequency observed in the PTT repertoire allows for advancement towards the development of an off-the-shelf cancer vaccine with broad therapeutic potential within CRC regardless of tumor mutational burden.

P179

Use of Jurkat T cells for high throughput screening of chimeric antigen receptor constructs

Tina Nguyen, PhD[1], Scott McComb, PhD[1], Risini Weeratna, PhD[1], Tina Nguyen, PhD[1]

[1]*National Research Council of Canada, Ottawa, Canada*

Background
Developing successful CAR T therapy requires identification of tumor targeting moieties that can recognize tumors with high degree of specificity with none to minimal auto activation of T cells. Easy, accurate, and rapid high throughput in vitro screening assays are necessary to help select lead candidates for further development of chimeric antigen receptor (CAR) T therapy.

Methods
Our model simplifies the workflow of testing by utilizing transient transfection of widely available Jurkat cells. Using electroporation, rather than relying on lentiviral transduction of CAR expression plasmids, we have developed a high throughput flow cytometry based assay wherein Jurkat CAR cells are exposed to human tumour cell lines with and without cognate target antigens. CAR activation can be readily observed for of via CD69 expression within 6 hours and remains stable for up to 24 hours post activation. We provide data from a number of validation assays, including testing with varying target cells lines, CAR constructs carrying varying signaling domains, and CAR constructs consisting of ScFv and single domain antibodies targeting different tumor specific and tumor-associated antigens.

Results
Using our screening method, we were able to identify lead candidate CARs targeting EGFRvIII, HER2, and EGFRWT with strong potential for pre-clinical development. Testing with CAR constructs carrying various signalling domains (41BB, CD28, 41BB/CD28) indicates that while providing information as to the autoactivation and specificity of the extracellular domain of CARs this model does not necessarily provide insight as to the strength or quality of activation signalling.

Conclusions
Thus, we developed a tool made for enabling the discovery of lead candidate tumour target binding moieties suitable for CAR-T application.

P180

From infectious disease to personalized cancer vaccines: Integrated CD4, CD8, and regulatory T cell neo-epitope screening platform for the design of safe and customized vaccines

Guilhem Richard, PhD[1], Randy F. Sweis, MD[3], Leonard Moise, PhD[2], Matthew Ardito, BA[2], William Martin, BA MD[2], Gad Berdugo, MSc, MBA[4], Gary D. Steinberg, MD[3], Anne S. de Groot, MD[1]

[1]*EpiVax Inc., Providence, RI, USA*
[2]*EpiVax, Inc., Providence, RI, USA*
[3]*University of Chicago, Chicago, IL, USA*
[4]*EpiVax Oncology, Inc., Providence, RI, USA*

Background
Precision cancer immunotherapy has proven to effectively control the tumor of patients in multiple clinical trials. However, the selection of immunogenic T cell neo-epitopes using traditional methodologies remains a challenging exercise. Poor vaccine performance may partially be due to inclusion of mutated epitopes cross-conserved with self-epitopes recognized by regulatory (Treg), anergic, or deleted T cells. In addition, most cancer vaccine studies focus on the selection of CD8 T cell neo-epitopes while overlooking CD4 T cell neo-epitopes.

Methods

We have developed Ancer, an integrated and streamlined neo-epitope selection pipeline, that accelerates the selection of both CD4 and CD8 T cell neo-epitopes. Ancer leverages EpiMatrix and JanusMatrix, predictive algorithms that have been extensively validated in prospective vaccine studies for infectious diseases [1]. Distinctive features of Ancer are its ability to accurately predict Class II HLA ligands and to identify tolerated or Treg epitopes.

Results

Ancer was evaluated on data from the BLCA bladder cancer cohort hosted at The Cancer Genome Atlas (TCGA) database. An initial analysis was carried out on a representative set of eleven patients to derive the best vaccine candidate sequences from high-quality missense mutations. A median number of 24 [interquartile range: 15-64] candidate sequences were generated for each patient under study. This initial analysis demonstrates the capacity of Ancer to define a sufficient number of candidate sequences for vaccinating bladder cancer patients in a precision immunotherapy setting.We also assessed Ancer's ability to predict patient outcomes on a larger subset of 58 individuals. While the disease-free status of the BLCA patients could not be explained by their tumor mutational burden (AUC=0.55, p-value=0.13), nor by their load of missense mutations (AUC=0.54, p-value=0.17), the number of neo-epitopes highly different from self significantly segregated disease-free patients from patients who recurred or progressed (AUC=0.68, p-value=0.02). These results suggest that defining the number of true neo-epitopes using Ancer may represent a novel biomarker for more robust anti-tumor immune response and higher likelihood of disease-free survival.

Conclusions

Our preliminary analysis of the BLCA cohort from the TCGA database showcases the value of Ancer in clinical settings. Our next step will be to investigate whether Ancer-defined neo-epitope load will serve as a biomarker for prognosis and response to therapy in the full BLCA cohort.

References

1. Moise L, Gutierrez A, Kibria F, et al. iVAX: An integrated toolkit for the selection and optimization of antigens and the design of epitope-driven vaccines. Hum. Vaccines Immunother. 2015;11:2312–2321.

P181

Pseudocowpox virus (PCPV), a potent tumor antigen-independent viral vector for cancer immunotherapy

Karola Rittner, PhD[1], Caroline Tosch, engineer[1], Thioudellet Christine[1], Christelle Remy-Ziller, Engineer[1], Marie-Christine Claudepierre, Ms[1], Benoit Sansas[1], Johann Foloppe[1], Philippe Erbs[1], Kaïdre Bendjama[1], Eric Quemeneur,PharmD, PhD[1]

[1]*Transgene, Illkirch-Graffenstaden, France*

Background

Viral vectors expressing tumor antigens and/or cytokines have proven to be clinically promising approaches to stimulate anti-tumor immunity and to modulate the tumor microenvironment. However, novel viral strains with improved immunogenic properties are sought. By screening a variety of wild-type poxviridae for their immunostimulant effects, we identified PCPV as a strong inducer of IFN-alpha expression in human PBMCs, with secretion rates up to 1000-fold higher than observed for Modified Vaccinia virus Ankara (MVA) or oncolytic Vaccinia virus (VV). PCPV was also superior to MVA in terms of activation of APCs, and increased CD86 expression in human M2-macrophages, suggesting a shift toward a less suppressive, antigen-presenting phenotype [1]. A recombinant PCPV encoding for the

HPV E7 antigen was generated to assess the anti-tumor activity, and immunogenicity in syngeneic murine tumor models TC1, and MC38.

Methods

TC1 or MC38 tumors were implanted subcutaneously (sc) in C57BL/6 mice. PCPV-E7 (107 pfu) was injected either intratumorally or intravenously. Immune cells were analyzed both from spleen, or lung, as previously reported [2]. Cytokines and chemokines were analyzed by Luminex after dissociation of either skin or tumor. Tumor infiltration was analyzed after enzymatic dissociation, and TILs enrichment using CD45+ magnetic beads. Subpopulations were identified by flow cytometry.

Results

Like MVA-E7, PCPV-E7 induced a strong cellular response, as demonstrated by ELISPOT on splenocytes, and frequency analysis of antigen-specific short-lived effector cells. Noteworthy, PCPV displayed a distinct cytokine/chemokine profile at the site of injection, with increased levels of pro-immune cytokines (IP-10, IFN-gamma, GM-CSF, IL-18, MIP-1alpha, MIP-1beta, IL-12, and IL-6). PCPV-E7 and MVA-E7 displayed similar effect on large TC1 tumors. Interestingly, intratumoral injection of PCPV-E7 into fast-growing E7-negative MC38 tumors led to tumor growth control, and increased survival rates that were never observed with MVA or VV vectors. Unlike VV, PCPV displayed no oncolytic activity on MC38 cells in vitro, thus the effect did not result from direct tumor cell lysis after infection. Analysis of tumor infiltrates showed that PCPV treatment decreased the frequency of Ly6C-positive cell populations, and increased that of Ly6G-positive neutrophils. This observation was associated with an increase of G-CSF concentration in the treated tumors. Depletion experiments are underway to monitor the contribution of either neutrophils, CD4+, or CD8+ T cells, and MC38-specific T cell responses in survivors.

Conclusions

Our recent data demonstrate that PCPV represents a promising agent for anti-tumor vaccination, in particular for its intrinsic ability to control tumor growth in a tumor antigen-independent manner.

References

1. Rittner et al. AACR 2018, poster LB-287; manuscript in preparation. 2. Remy-Ziller et al. Human Vaccines & Immunotherapeutics 2018, 14(1):140-145.

P182

Identification of prevalent immunogenic tumor antigens in microsatellite unstable patients with uterine corpus endometrial carcinoma.

Vladimir Roudko, PhD[1], Cansu Cimen Bozkus, PhD[2], Orfanelli Theofano, MD[2], Stephanie Blank, MD[2], Benjamin Greenbaum, PhD[2], Nina Bhardwaj, MD, PhD[2]

[1]Icahn School of Medicine at Mount Sinai Hospital, New York, NY, USA
[2]Icahn School of Medicine at Mount Sinai, New York, NY, USA

Background

Personalized vaccines using “neoantigens” that arise from tumor-specific genomic alterations are gaining momentum as a new approach of immunotherapy and are currently in evaluation in multiple clinical trials. However, these tumor antigens are highly personalized and require patient specific sequencing approaches for their identification. Here we report on a new computational pipeline, called UniVac (Universal Vaccine), that identifies highly frequent shared tumor epitopes. We applied our approach to microsatellite unstable (MSI-H) patient cohorts from The Cancer Genome Atlas (TCGA) as a proof-of-concept to determine if such shared antigens could be identified and be immunogenic.

Methods
A computational analysis of MSI-H patients from TCGA cohort, comprising 332 subjects was undertaken. The set of custom scripts were written in R and python, suitable for execution under UNIX environment. Immunogenicity of selected neopeptides were validated by standard immunological experiments, in which T cells were stimulated in vitro by overlapping long peptides spanning each neopeptide. T cell responses were determined by enzyme-linked immunospot assay (ELISPOT) and intracellular staining.

Results
We identified highly frequent, prevalent peptides, encoding MHC-I epitopes that originated from frameshift mutations in the MSI-H cohort of endometrial, colorectal and stomach tumors: 9, 34 and 33 peptides, respectively. In particular, we determined that the epitopes derived from 9 shared endometrial peptides are predicted to bind to the most frequent HLA alleles, thus targeting ~80% of all endometrial patient HLAome. The average frequency of the original 9 frameshifts in each tumor is estimated at ~40% rate, indicating a wide presence of those mutations in patients' tumors. Moreover, the frameshift load does not affect gene expression, as revealed by transcriptome analysis. We validated common 9 frameshift peptides from endometrial patients in an array of immunological experiments. First, we tested them in T cell stimulation assays using peripheral blood mononuclear cells (PBMCs) isolated from healthy donors. Majority of peptides induced CD8+ T cell responses, as determined by TNF-alpha and IFN-gamma production. Next, we tested whether we could elicit neopeptide-specific T responses in MSI-H endometrial cancer patients. T cell responses were also observed in some patients. Selected endometrial shared frameshift peptides appear to be clonal and prevalently found in MSI-H patients, thus laying a foundation for a shared antigen cancer vaccine design.

Conclusions
We developed a computational pipeline to predict the most frequent and shared peptides across patients with MSI-H tumors.

P183

Immunogenicity and specificity of neoantigens derived from tumor-specific mutations in gastric cancer

Tetsuro Sasada, MD, PhD[1], Junya Ohtake[1], Susumu Iizumi[1], Taku Kouro, MD, PhD[1], Yuka Igarashi[1], Mamoru Kawahara[1], Erika Yada[1]

[1]Kanagawa Cancer Center, Yokohama, Japan

Background
Neoantigens derived from tumor-specific genetic mutations can be recognized as foreign by the host immune system, and might be suitable target for cancer immunotherapy possibly due to their higher immunogenicity. In this study, to know the immunogenicity and specificity of tumor-specific neoantigens, we comprehensively examined T cell responses against neoantigens derived from genetic mutations in gastric cancer.

Methods
Missense mutations were identified in tumor cells from two gastric cancer patients by using next-generation sequencing. Amino acid sequences, which were derived from the identified mutations and predicted to bind to HLA-class I (A*0201, A*0206, or A*2402), were selected by an epitope prediction server, IEBD. Long peptides (27-mer), in which the mutated sequences were located in the center, were synthesized. Peripheral blood mononuclear cells (PBMC) from healthy donors were cultured in the presence of the synthetic peptides and antigen-specific T cell responses were evaluated by cytokine production assay.

Results

Using next-generation sequencing, 156 missense mutations were identified in two gastric cancer patients. From them, 30 potentially immunogenic peptide sequences derived from the identified mutations were selected. In the analysis with PBMC from 18 healthy donors, 27/30 (90%) synthetic peptides showed an ability to induce antigen-specific T cell responses in at least one donor, assessed by cytokine production assay. Among them, 15 peptides were immunogenic in more than one donor. The antigen-specific responses in CD4+ T cells (70%) were observed more frequently than those in CD8+ T cells (43%). Most of the mutated peptides were shown to induce much higher antigen-specific T cell responses than the corresponding wild type peptides. The specificity of T cell responses to mutated sequences, but not to the corresponding wild type sequences, were confirmed in 5 of 8 (62%) peptides examined.

Conclusions

Our findings demonstrated high immunogenicity and specificity of neoantigens derived from tumor-specific genetic mutations. In addition, PBMC from healthy donors were suggested to be useful for assessing the immunogenicity of neoantigens derived from cancer patients. Further studies would be recommended to develop a novel immunotherapeutic approach, “personalized cancer vaccination”, targeting mutation-derived neoantigens in gastric cancer.

Ethics Approval

This study was approved by the Institutional Review Board of Kanagawa Cancer Center. Informed consents for the study were obtained from all participants.

P184

High tumour burden mandates a cancer vaccine targeting many neoantigens combined with check point inhibition

Elisa Scarselli, MD[1], Anna Morena D'Alise[1], Guido Leoni[1], Gabriella Cotugno[1], Fulvia Troise, Dr[1], Francesca Langone[1], Imma Fichera, Maria De Lucia[1], Rosa Vitale[1], Adriano Leuzzi[1], Veronica Bignone, , Elena Di Matteo[1], Fabio Tucci[1], Lidia Avalle[2], Valeria Poli, Professor[2], Armin Lahm[1], Maria Teresa Catanese[1], Antonella Folgori[1], Stefano Colloca, Mr[1], Alfredo Nicosia[1]

[1]Nouscom srl, Rome, Italy
[2]University of Turin, Turin, Italy

Background

Neoantigens (nAgs) are a promising class of tumor antigens for cancer vaccination. with the potential of inducing robust and selective anti-tumor T cell responses. Adenoviruses derived from non-human Great Apes (GAds) represent novel genetic vaccines inducing potent cell-mediated immunity. Here, we developed a novel neoantigens vaccine approach based on the use of viral vectors, Great Apes Adenovirus (GAd), encoding multiple cancer neo-epitopes in tandem.

Methods

Balb/c mice were implanted either subcutaneously or intravenously with CT26 colon carcinoma cells. In early therapeutic vaccination, mice were vaccinated with a single intramuscular injection of GAd encoding CT26 neoantigens 3 days after cell inoculum. In advanced therapeutic setting, combined treatment of GAd and anti-PD1 started on established subcutaneous tumors (70-100 mm3). Tumor growth was monitored after vaccination and neo-antigen specific T cells were measured both in the periphery and in the tumors. DNA and RNA was extracted from tumors under treatment for NGS analysis of exome

and transcriptome.

Results

Prophylactic or early therapeutic vaccination with GAds encoding nAgs in mice induced CD8+ and CD4+ T cells and efficiently controlled tumor growth, irrespective of the number of encoded nAgs. In presence of high tumor burden, GAd has no anti-tumor effect unless combined with anti-PD1 treatment. Moreover, in the presence of high tumor burden effectiveness of vaccination required a vaccine encoding many neoantigens. An increased breadth of T cell immune response was measured by IFN-γ ELISpot analysis in mice cured by the combined treatment. Finally, transcriptome analysis of unique TCR beta CDR3 sequences, revealed presence of an increased number of clonotypes in tumor biopsies of combo treated animals compared to anti-PD-1.

Conclusions

Vaccination with Great Apes Adenovirus (GAd) encoding neoantigens is very effective to strengthen and broaden T cells against tumor neoantigens. Growth of vaccine-induced T cells in established tumours can be successfully achieved with a vaccine encoding many neoantigens combined with the administration of anti-PD-1. The data presented here warrant further testing of cancer vaccines based on GAd into the clinic supporting their use as stand-alone treatment in tumor prevention or in minimal residual disease/adjuvant clinical setting. Conversely, in the presence of established tumors, combination with check-point inhibition is required.

P185

CUE-101, a novel Fc fusion protein comprised of HLA-A*0201-bound HPV16 E7 peptide and IL-2, for selective targeting and expansion of anti-tumor T cells for treatment of HPV-driven malignancies

Mary C. Simcox, PhD[1], Steven Quayle[1], Dharma R. Thapa, PhD[1], Sandrine Hulot, PhD[1], Alyssa Nelson, BS[1], Lauren Kraemer, BS[1], Zohra Merazga, MS[1], Robert Ruidera, MSc[1], Dominic Beal, PhD[1], Gurpanna Saggu, PhD[1], Maria Hackett, MSc[1], Mark Haydock, BS[1], Jonathan Soriano, MSc[1], Joey Lee[1], Luke Witt, BS[1], Kelly Malone[1], Jessica Ryabin, BS[1], Simon Low, MSc[1], Natasha Girgis, PhD[1], Emily Spaulding, PhD[1], John Ross, PhD[1], Anish Suri, PhD[1], Rodolfo Chaparro, PhD[1], Ronald Seidel, PhD[1], Kenneth Pienta, MD[2]

[1]Cue Biopharma, Cambridge, MA, USA
[2]Johns Hopkins School of Medicine, Baltimore, MD, USA

Background

Human papilloma virus (HPV) is responsible for 72% of oropharyngeal,70% of cervical, 90% of anal and 71% of vulvar, vaginal, or penile cancers, causing significant morbidity and mortality worldwide [1,2].CUE-101, a novel fusion protein designed to activate tumor antigen-specific T cells to treat HPV16-driven cancers, is comprised of a human leukocyte antigen (HLA) complex, HLA-A*0201, a peptide epitope derived from the human HPV16 E7 protein (amino acid residues 11-20), a reduced affinity human interleukin-2 (IL-2) variant, and an effector attenuated human immunoglobulin G (IgG1) Fc domain.

Methods

CUE-101 cellular binding, specificity, TCR- and IL-2 receptor (IL-2R)-induced signaling, and induction of activation and cytotoxic T lymphocyte markers were measured using flow cytometry with human E7-specific T cells (Astarte Biologics, Bothell, WA). Enzyme-Linked ImmunoSpot (ELISPOT) assays were performed to measure peptide-specific secretion of interferon gamma (IFNg). Anti-tumor efficacy with a murine surrogate molecule was assessed in the TC-1 model [3], and tumor antigen-specific T cell expansion in vivo was assessed via tetramer staining.

Results

CUE-101 binds to HPV16-E7–specific CD8 T cells

(EC50 = 10-20 nM) and activates signal transduction downstream of TCR and IL-2R, whereas no activation of TCR signaling was observed upon CUE-101 treatment of bulk CD8 T cells or with a CUE-101 analog presenting a CMV peptide. Upon binding and receptor engagement, CUE-101 induces potent and dose-dependent secretion of IFNg (EC50 = 0.69 nM). Effector cytokine secretion is dependent on the peptide specificity of the HLA complex, and an analog lacking the IL-2 moieties exhibited >100-fold reduction in potency. Pharmacokinetic (PK) data in rats and monkeys suggest that exposures sufficient to promote antigen-specific T cell activation and expansion will be achievable in humans. In vivo, a murine surrogate of CUE-101 demonstrates anti-tumor activity both as a monotherapy and in combination with an anti-PD-1 antibody in the TC-1 E6/E7+ tumor model. Efficacy in this model was associated with expansion of HPV16 E7 reactive T cells, and establishment of immunologic memory was demonstrated via tumor rejection upon rechallenge with TC-1 cells in absence of any additional administration of the murine surrogate.

Conclusions

CUE-101 demonstrates selective binding, activation, and expansion of HPV16 E7-specific CD8+ T cells in vitro and a favorable PK profile in animals. A murine surrogate of CUE-101 exhibits anti-tumor efficacy both as a monotherapy and in combination with anti-PD-1. These data support the potential for CUE-101 to enhance anti-tumor immunity in patients with HPV16-driven malignancies.

References

1. de Sanjosé S, Diaz M, Castellsagué X, et al. Worldwide prevalence and genotype distribution of cervical human papillomavirus DNA in women with normal cytology: a meta-analysis. Lancet Infect Dis. 2007;7:453-459. 2. Frazer IH. Prevention of cervical cancer through papillomavirus vaccination. Nat Rev Immunol. 2004;4(1):46-54 3. Lin K, Guarnieri F, Staveley-O'Carroll K, Levitsky H, August J, Pardoll D, Wu T. Treatment of established tumors with a novel vaccine that enhances major histocompatibility class II presentation of tumor antigen. Cancer Res. 1996;56:21-26.

Ethics Approval

All animal activities and procedures were performed in accordance with the protocols approved by the Institutional Animal Care and Use Committee (IACUC) for ethical review of animal care and use.

P186

A multi-center study of hTERT immunotherapy in adults with solid tumors at high risk of relapse post-standard therapy: updated results from complete patient set

Anthony Shields, MD PhD[1], Autumn J. McRee, MD[2], Jennifer Johnson, MD[3], Weijing Sun, MD, FACP[4], Ashish Chintakuntlawar, MBBS, PhD[5], Naseem Prostak, BS MS[6], Kimberly Kraynyak, BS, PhD[6], Matthew P. Morrow, PhD[6], Jeffrey M. Skolnik, MD[6], Robert H. Vonderheide, MD, DPhil[8]

[1]*Karmanos Cancer Center, Detroit, MI, USA*
[2]*UNC Chapel Hill, Chapel Hill, NC, USA*
[3]*Thomas Jefferson University, Philadelphia, PA, USA*
[4]*University of Pittsburgh, Pittsburgh, PA, USA*
[5]*Mayo Clinic, Rochester, MN, USA*
[6]*Inovio, Plymouth Meeting, PA, USA*
[7]*Inovio Pharmaceuticals Inc, Plymouth Meeting, PA, USA*
[8]*University of Pennsylvania, Phildelphia, PA, USA*

Background

Human telomerase (hTERT) is a reverse transcriptase that recognizes and elongates telomeric DNA ends. hTERT is expressed in up to 90% of cancers, and can be recognized by cytotoxic T cells. As a result, hTERT is an excellent target for T cell-enabling therapy. The administration of optimized full-length DNA sequences followed by electroporation (EP) in vivo

has generated potent CD4+ and CD8+ T cell responses against hTERT in preclinical studies. In this phase 1 dose-escalation study, synthetic optimized DNA plasmids that target hTERT (INO-1400, or mutant hTERT; and INO-1401, or SynCon® TERT) were delivered intramuscularly followed by EP with the CELLECTRA® device, to assess safety, tolerability and immune effects of immunotherapy with INO-1400 or INO-1401, alone or co-administered with a plasma encoding for human IL-12 (INO-9012) in adult patients with cancer.

Methods

Following standard of care neoadjuvant or adjuvant chemoradiotherapy and/or surgery, patients with one of 9 solid tumors at high risk of relapse, but without evidence of residual disease, were enrolled to one of 10 arms and received four doses, four weeks apart, of either INO-1400 or INO-1401 alone or in combination with INO-9012 by IM injection, followed by EP. Patients were followed for tolerability, immunogenicity and clinical response.

Results

As of 18 July, 2018, the study has completed enrollment and dosing of 93 patients. Doses of 2 or 8 mg of INO-1400/01, and of 0.5 or 2 mg INO-9012 were well-tolerated, with a majority of reported adverse events (AE) being low-grade and related to IM+EP administration. Two related SAEs have been previously reported (breast cellulitis; abdominal pain/elevated lipase), and one dose-limiting toxicity (DLT) has been previously reported (rash). No other reported SAEs or DLTs have been reported for this study. Immunogenicity by ELISpot for antigen-specific interferon-gamma (IFN-g) secreting T cells suggests that patients can generate hTERT-specific T cells across multiple doses, with or without IL-12, and with both INO-1400 and INO-1401. The majority of patients continue on study, with several patients having completed two years of study follow- up.

Conclusions

INO-1400/01 with or without INO-9012 given IM with EP is well-tolerated in adults with solid tumors, and can generate active hTERT-specific T cells, suggesting an ability to break immune tolerance. Dosing is complete, and follow-up is ongoing.

Ethics Approval

The study was approved by each participating Institutution's Ethics or Institutional Review Board(s).

P187

Preclinical evidence for the potency and tumor selective activation of a novel EpCAM-CD3 Protease-Triggered Immune Activator (ProTIA) T-cell bispecific therapeutic

Tillman Pearce, MD[1], Bee-Cheng Sim[1], Desiree Thayer[1], Fan Yang[1], Tillman Pearce, MD[1], Zach Lange[1], Ulrich Ernst, PhD[1], Volker Schellenberger[1]

[1]*Amunix, Mountain View, CA, USA*

Background

The regulatory approval of blinatumomab (Blincyto) provided proof-of-concept that a bi-specific T cell engager could redirect human T cells (via a CD3 binding site) to act against a hematologic malignancy (via a CD19 binding site). Extending this general strategy to solid tumors is intriguing, especially in immunologically cold tumors; however, the potential for on-target, off-tumor toxicity may limit the feasibility of this approach.Amunix is developing a novel class of molecules called Protease-Triggered Immune Activators, or ProTIA, as a strategy for selective activation of T cells within the tumor microenvironment (Figure 1). ProTIA molecules include single chain Fv fragments targeting both a cell surface antigen overexpressed on tumor cells and the CD3 epsilon molecule on T cells. This core bi-specific molecule is then modified by addition of

proprietary recombinant polymers of defined length and sequence but of undefined structure called XTEN polymers. XTEN polymers are linked to the scFvs by a protease-cleavable site. ProTIA provides tumor selectivity by the antigen specificity of the ScFv, reduced penetration into normal tissue via the enhanced permeability and retention effect, and selective activation by tumor associated proteases.

Methods

An EpCAM-CD3 bispecific ProTIA was constructed with or without a tumor protease cleavable sequence (ProTIA-X vs. ProTIA-B), along with a pre-activated form without XTEN (active ProTIA, or ProTIA-A). In vitro cytotoxicity assays were performed using several cancer target cells and human PBMC effector cells. In vivo efficacy experiments in NOG mouse models were performed by implanting colorectal HCT-116 cells, then injecting human PBMC and test article when tumor was established. A mouse surrogate EpCAM-CD3 ProTIA was also constructed and assessed in vivo for on-target, off-tumor toxicity.

Results

In vivo, both ProTIA-A and ProTIA-X treatment, but not ProTIA-B treatment, resulted in tumor regression (Figure 2) with no adverse effect on body weight (effect on weight not shown). The mouse surrogate EpCAM-CD3 ProTIA-X had a 10-fold improved tolerability in C57BL/6 mice compared with the non-protected bispecific (ProTIA-A) (Figure 3).

Conclusions

T-cell redirecting therapies have great therapeutic potential for immunologically cold solid tumors or checkpoint inhibitor resistant tumors which have lost the capacity for cell surface neoantigen presentation, but pose a significant risk for on-target, off-tumor toxicity. These experiments confirmed that a novel ProTIA EpCAM-CD3 has similar potency as an unprotected bispecific (ProTIA-A) but with significantly reduced normal tissue toxicity.

Figure 1.

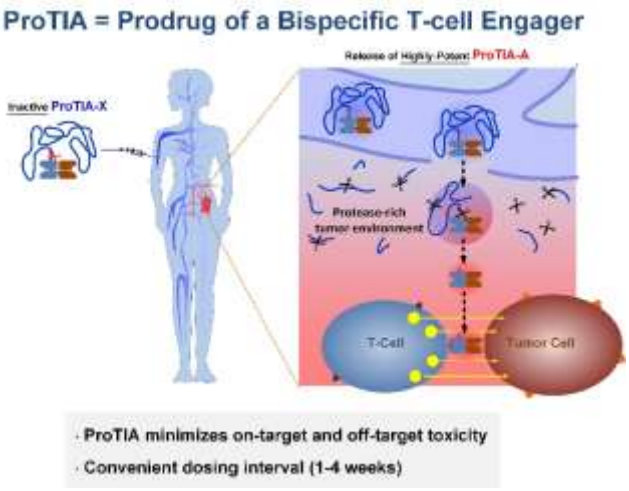

Figure 2.

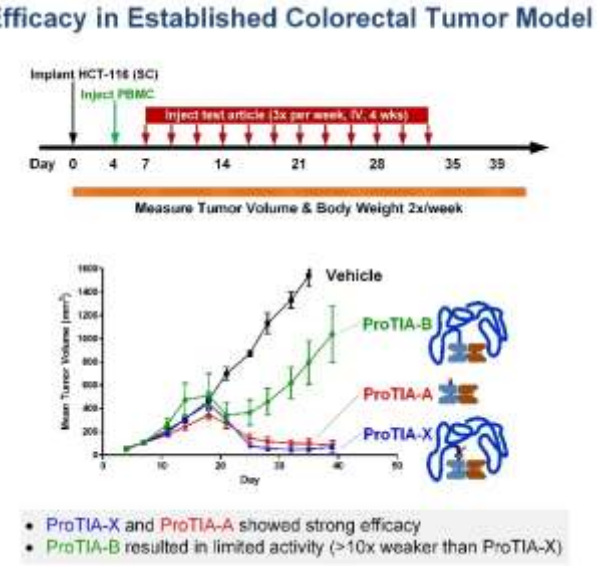

Figure 3.

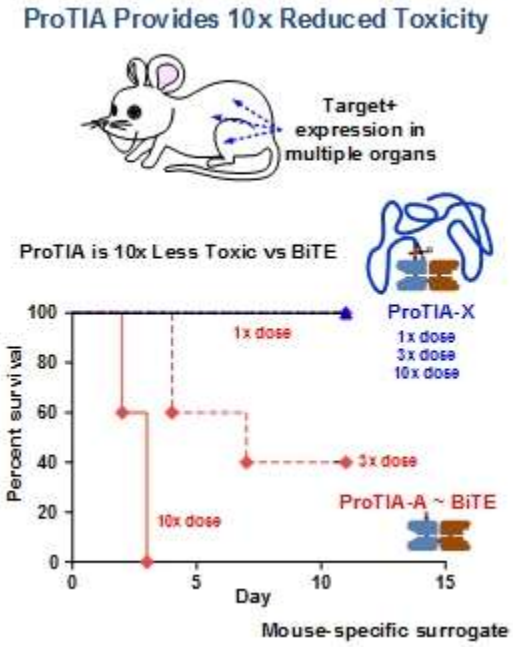

P188

Patient's autologous T cells recognize tumor specific neoantigens in PDX models of ovarian cancer

Muzamil Want, PhD[2], Muzamil Want, PhD[1], Muzamil Want, PhD[2], Anna Konstorum, PhD[3], Ruea-Yea Huang, PhD[1], Richard Koya, MD, PhD[1], Sebastian Battaglia, PhD[1*]

[1]Roswell Park Comprehensive Cancer Center, Buffalo, NY, USA
[2]Roswell ParkComprehensive Cancer Center, Buffalo, NY, USA
[3]UConn Health, Farmington, CT, USA

Background

Ovarian cancer (OC) is the fifth leading cause of cancer death in the USA and has the highest mortality rate of all gynecologic cancers. Since OC patients are often diagnosed at late stage with local and distal metastases, this offers a clinical challenge, with 70% of the patients developing chemoresistant disease. Private cancer neoantigens are derived from somatic mutations and represent an attractive target for ovarian malignancies, allowing for a fully personalized therapeutic approach.

Methods

We established patient-derived xenografts (PDX) model from one primary tumor of a Roswell Park ovarian cancer patient by injecting subcutaneously NSG mice with 2x106 cells. Tumor mutational landscape was interrogated in the primary tumor and two passages (P0, P1) via whole exome sequencing (WES) using the patient's PBMCs as germline control. NetMHC was used to predict affinity to the patient's HLAs and neoantigens were ranked based on differential binding of the wild type (WT) versus mutated (MUT) peptide. Potential neoantigens T cell activation by neoantigens was tested in vitro via ELISA and flow cytometry and in vivo by using neoantigen activated T cells for adoptive T cell therapy (ACT) infusing 5 x 106 cells intravenously in PDX mice (P1) 12 days post tumor implantation. TCRSeq was performed with 10XGenomics and analyzed with custom R scripts.

Results

We identified 184 non-synonymous mutations leading to 30 potential neoantigens with high affinity for the patient's HLAs. Interferon-gamma production and upregulation of CD137 identified a core set of 6 neoantigens specifically recognized by patient's autologous CD8+ T cells (Figure 1A-B), 4/6 neoantigens were common between PDX and primary tumor. Patient's T cells were activated in vitro by PDX tumor lysate (Figure 1C). In vivo ACT studies showed that mice injected with neoantigen-stimulated PBMCs (ACT_MUT) have reduced tumor growth when compared to mice injected with unstimulated patient's PBMCs (ACT_NP) (Figure 1D). Furthermore, ACT_MUT mice have higher levels of circulating T cells 15 days post-ACT and higher intratumoral T cells at end point than ACT_NP

(Figure 1E-F). We then sought to identify the TCR moieties that determine T cell response. TCRSeq analyses on the two strongest neoantigens identified multiple TCR activated by a single cancer neoantigen (Figure 1G), suggesting oligoclonal T cell activation.

Conclusions

PDX models reflect the tumor mutational landscape of OC patient and presence of neoantigen reactive T cells in the blood of OC patient can be used to develop a personalized immunotherapeutic approach.

Acknowledgements

This work is supported by RPCI-UPCI ovarian cancer SPORE CEP grant. NGS services were provided by Genomics shared resources supported by NCI P30CA16056 and for Cytometry services were provided by the Flow and Image Cytometry Core facility at the Roswell Park Comprehensive Cancer Center which is supported in part by the NCI Cancer Center Support Grant 5P30 CA016056.

Figure 1.

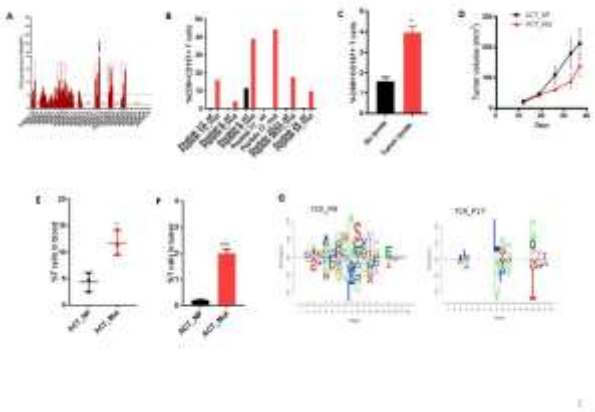

P189

A phase 1 study of safety and tolerability of AutoSynVax™ vaccine in patients with advanced cancer.

Robert Wesolowski, MD[1], Breelyn M. Wilky, MD[2], Allison O'Neill[3], Ana M. Gonzalez, MD PhD[3], Elise E. Drouin, PhD[3], Edward Dow[3], Mohamed Uduman[3], Antoine J. Tanne[3], Maria Agarwal, PhD[3], Bishnu Joshi[3], Benjamin Morin, PhD[3], Mark A. Findeis, PhD[3], Sandra Craig[3], Igor Proscurshim, MD[3], Ricardo Soto[3], Jennifer S. Buell, PhD[3], Robert Stein, MD PhD[3], John C. Castle[3], Daniel L. Levey, PhD[3]

[1]The Ohio State University, Columbus, OH, USA
[2]Miami University, Miami, FL, USA
[3]Agenus, Lexington, MA, USA

Background

Agenus AutoSynVax™ (ASV™), AGEN2003, is an individualized, fully synthetic neoantigen vaccine comprised of computationally defined peptide immunogens complexed to recombinant heat shock protein (HSP) and administered with QS-21 Stimulon® adjuvant. In animal models and clinical trials, vaccines employing HSP-peptide complexes mixed with QS-21 elicit antigen-specific CD8+ and CD4+ T-cell responses.

Methods

After signing an informed consent form, patients (pts) with advanced cancer, considered incurable/without approved therapies were treated with AGEN2003. The vaccine was administered subcutaneously at 240µg with 50µg QS-21 bi-weekly. Study primary objective was safety and tolerability. Other objectives included objective response rate (ORR), overall survival (OS) and tumor specific immune response. Given the small cohort, data was summarized using descriptive statistics. An Institutional Review Board at each participating site has approved the study.

Results

Nine pts were enrolled on the Phase I study, 3 received treatment with vaccine derived from their tumor. Of six enrolled but not treated; 5 progressed prior to treatment. An additional 2 pts (<18 yr)

received AGEN2003 through compassionate access (IND 16962). Among the treated pts, no Serious Adverse or grade (G) ≥3 toxicities attributed to vaccine were reported. The most common AE's (G 1-2) were nausea and myalgia at injection site. One compassionate use pt with metastatic hepatocellular carcinoma, refractory to PD-1 inhibition, has been treated intermittently with AGEN2003 alone or in combination with pembrolizumab for 13 months. Of 3 study pts: 2 (1 with uterine leiomyosarcoma, 1 with inflammatory breast cancer) received 8 doses each; a third pt with pleiomorphic leiomyosarcoma received 3 doses. Neoantigen-immunogenicity was positively associated with survival and as of July 2018, 2 patients (both with a quantifiable immune response) remain alive.

Conclusions
AGEN2003 was well tolerated with no serious AE's attributable to vaccine. We plan to combine future versions of ASV with immunomodulatory antibodies.

Trial Registration
NCT02992977

Ethics Approval
The study was approved by institutional review board at each participating institution (IRB study # 1174684)

Consent
Not applicable as no identifiable information is disclosed.

P190

Identification of antigenic epitopes of EGFR for lung cancer vaccine development

Juhua Zhou, PhD[1], Ge Guo[1], Jianzhong Zhang[2], Shaoyan Huang[2], Yanmin Li[1]

[1]*Ludong University, Yantai, China*

[2]*Yantaishan Hospital, Yantai, China*

Background
It has been documented that approximately 85% of the patients with lung cancer are non-small cell lung cancer (NSCLC). The mutation rate of human epidermal growth factor receptor (EGFR) gene is about >60% in NSCLC patients. The mutation loci of EGFR are mostly concentrated in the regions of exons 18-21. In addition, it has been reported that EGFR exon 19 T790M mutation is responsible for drug resistance of more than 90% of NSCLC patients to tyrosine kinase inhibitors. Thus, EGFR is a good candidate for developing non-small cell lung cancer vaccines.

Methods
In the current study, 40 peptides with 10 amino acids from EGFR protein were designed and synthesized using Immune Epitope Database (IEDB) online software for the prediction of T cell antigenic epitopes. Reverse immunology method was employed to screen T cell antigenic epitopes from 40 EGFR peptides, which was used to stimulate the expansion and interferon gamma release of peripheral blood mononuclear cells from 30 patients with NSCLC.

Results
Three unique peptides of EGFR were identified to be T cell antigenic epitopes due to their ability in the stimulation of cell expansion and cytokine release. Further studies in vivo showed that three unique peptides of EGFR could stimulate anti-lung cancer immune responses in both wild-type mice and NUDE mouse tumor model. The clinical trials of three unique peptides of EGFR as NSCLC cancer vaccines are under way.

Conclusions
Three unique peptides of EGFR may be used as cancer vaccines in the treatment of patients with NSCLC.

Trial Registration
This work was supported by "Taishan Scholar" special fund (No. tshw20120718) from Shandong Government, China

Ethics Approval
The study was approved by Ludong University's Institutional Review Board (IRB), approval number LDU-IRB2015002.

Case Studies

P191

Combination of Sorafenib and anti-PD-1 for advanced hepatocellular carcinoma- real world experience

San-chi Chen, MD[1], Muh-Hwa Yang[1], Yee Chao[1]

[1]*Taipei Veterans General Hospital, Taipei, Taiwan, Province of China*

Background
Advanced hepatocellular carcinoma (HCC) portends dismal prognosis. Recently, two anti-PD-1 monoclonal antibodies have demonstrated favorable responses in HCC. Nivolumab was proved for second line treatment based on CheckMate-040, in which nivolumab demonstrated the objective response rate (ORR) of 15% in sorafenib-experienced HCC. Similarly, pembrolizumab also achieved ORR of 16% in Keynote-224. However, there is still an unmet need to achieve a better response. Sorafenib that has been proved for the treatment of HCC for a decade is found to have immune modulation effect. Researches showed that sorafenib inhibited regulated T cells and promoted effector T cells, especially in low dose. These data support the rationale for sorafenib to combine with immunotherapy.

Methods
We retrospectively analyzed 43 HCC patients who received the combination therapy of sorafenib and anti-PD-1.

Results
Among 43 patients in this cohort, mean age was 63 (+/-12) year-old, 79% were male, 49% were HBV(+) and 21% were HCV(+). The Child-Pugh Score of A, B and C were 51%, 26% and 23%, respectively. Best responses were CR in 3 patients (7%), PR in 9 (21%), SD in 7 (16%) and PD in 15 (35%); the response rate was 28% and disease control rate (DCR) 44%. Patients had no significant difference of response in etiologies, Child-Pugh Score and initiate AFP levels. Eighteen patients (42%) developed grade 1/2 toxicities and 9 (21%) grade 3/4 toxicities including 4 immune hepatitis and three skin rash. Patients who developed grade 1/2 toxicities has ORR of 50% and grade 3/4 toxicities has ORR of 11%. Median PFS in responders and non-responders were 10.5 and 2.0 months, and median OS were 12.7 and 2.0 months, respectively. In univariate analysis, grade 1/2 toxicity (HR 0.35) and grade 3/4 toxicity (HR 5.11) were risk factors for disease progression; Child-Push Score C and BCLC stage D were risk factors for survival.

Conclusions
Combination therapy of sorafenib and anti-PD-1 has a favorable response in patients with HCC, event in those who have been previously treated with sorafenib. The adequate dose, synergistic effect and safety of this combination need a large-scale of clinical trial to confirm.

Ethics Approval
The study was approved by Taipei Veterans General Hospital's Ethics Board, approval number 2017-10-005BC.

P192

A case of nivolumab-induced gastrointestinal toxicity treated with vedolizumab in the context of metastatic non-small cell lung cancer

Cynthia N. Tran, MD[1], Yinghong Wang, MD, PhD[2], Wenyi Luo, MD[2]

[1]*Baylor College of Medicine, Houston, TX, USA*
[2]*MD Anderson Cancer Center, Houston, TX, USA*

Background
Immune checkpoint inhibitors have emerged as a novel therapeutic class for a wide variety of malignancies through their action on the immune system. This action promotes significant anti-tumor effect but, simultaneously, can also result in immune-related adverse events (irAEs) that may limit their use [1]. Multiple case reports and case series of lower gastrointestinal irAEs have been reported; however, the data on upper gastrointestinal tract is very sparse [2]. We herein describe a case with severe and steroid-dependent upper gastrointestinal toxicity with nivolumab treatment who eventually achieved clinical and histological remissions with vedolizumab treatment.

Methods
N/A

Results
A 65 year old male patient with lung cancer initially diagnosed in 2013, previously treated with pemetrexed and carboplatin regimen, was started on Nivolumab since January 2017 for progressive disease involving the left upper lung, retroperitoneal lymphadenopathy, possible liver metastases, and several small brain lesions. Following sixteen cycles of nivolumab, he developed multiple episodes of severe nausea, vomiting, and abdominal cramps requiring five hospitalizations total for dehydration and poor oral intake with associated weightloss. His initial EGD showed active inflammation in both the stomach and duodenum (Figure 1A, B). Due to this severe GI irAE, nivolumab was stopped even though his underlying cancer had demonstrated good response to nivolumab maintenance treatment. He was treated with multiple courses of steroid (intravenous methylprednisolone to oral prednisone) at each hospitalization but always developed symptomatic recurrence on prednisone taper dose at 20 mg/day. Additionally, the patient developed oral thrush and Clostridium difficile infection while on steroids that required antibiotic treatment. Two trials of budesonide were attempted but unsuccessful. After the fifth hospitalization, he was initiated on vedolizumab infusion and achieved clinical remission within two weeks without further requirement of hospitalization or steroids for the following six months. His most recent EGD and biopsy after five doses of vedolizumab demonstrated complete resolution of active inflammation on histologic evaluation (Figure 2A, B). His lung cancer has since relapsed and the treatment plan is to resume nivolumab with concurrent use of vedolizumab.

Conclusions
Immune checkpoint inhibitors, such as nivolumab, have emerged as treatment for a variety of malignancies [1]. Their use can be associated with various immune-related adverse events (irAEs) involving the upper gastrointestinal tract which is not commonly seen [2]. This case scenario showed that vedolizumab can provide steroid-sparing therapeutic effect to achieve clinical and histological remission even in cases that failed multiple steroid courses with good safety profile.

References
1. Postow M, Callahan M, Wolchock J. Immune checkpoint blockade in cancer therapy. J Clin Oncol. 2015; 33:1974-1982.
2. Abdel-Rahman O, El Halawani H, Fouad M. Risk of gastrointestinal complications in cancer patients

treated with immune checkpoint inhibitors: A meta-analysis. Immunotherapy, 2015; 7:1213-1217.

Ethics Approval
Institutional Review Board protocol is exempted at the University of Texas MD Anderson Cancer Center for single case report.

Consent
This study was granted waiver for consent.

Figure 1. Pathology of stomach and duodenum pre vedolizumab

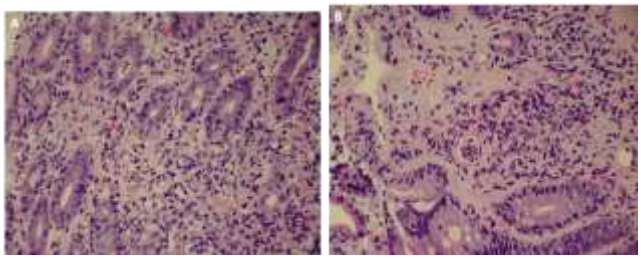

Figure 2. Pathology of stomach and duodenum post vedolizumab

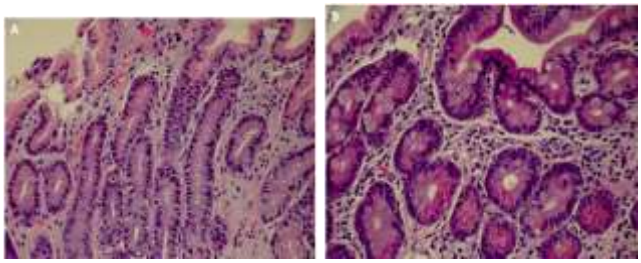

P193

Exceptional response of MSH6-null castration-resistant prostate cancer patient with myelophthisic pancytopenia to pembrolizumab

Panagiotis Vlachostergios, MD, PhD[1], Julia T. Geyer, MD[1], Ana M. Molina, MD[1], David M. Nanus, MD[1], Himisha Beltran, MD[1], Scott T. Tagawa, MD[1], Panagiotis J. Vlachostergios, MD, PhD[1]

[1]*Weill Cornell Medicine, New York, NY, USA*

Background
Metastatic castration-resistant prostate cancer (mCRPC) remains lethal despite recent advances in AR-directed therapies. Myelophthisis is not rare in advanced PC and often limits chemotherapeutic options. The tissue-agnostic activity of the anti-programmed cell death-1 (PD-1) inhibitor pembrolizumab in tumors harboring mismatch-repair (MMR) defects may offer an important therapeutic option in such patients.

Methods
We describe a MMR-deficient mCRPC patient with widespread metastases involving the bone marrow causing myelophthisis, who responded to immune checkpoint inhibition with pembrolizumab.

Results
A 74 year old man initially presented in 1999 with early prostate cancer, Gleason 4+3 = 7 underwent prostatectomy and salvage radiation but had PSA recurrence 9 years later. He was started on combined androgen blockade with leuprolide and bicalutamide to which he responded (PSA nadir <0.1 ng/ml) for 7 months, but then experienced PSA and radiologic progression with osseous metastases. He received consecutively sipuleucel-T, abiraterone, enzalutamide, 177Lu-J591, Radium-223 and docetaxel for his mCRPC. However he had further disease progression with diffuse osseous, lymph node and visceral (bilateral lung, solitary liver, bilateral adrenal) metastases and a rising PSA level at 2,048 ng/ml. Due to persistent pancytopenia (WBC: 3.2 x103/uL, Hb: 7.5 g/dl, PLT: 30 x103/uL) a bone marrow biopsy was performed. Hematoxylin and eosin staining revealed extensive metastatic PC (PSMA+, synaptophysin+, ERG–). Additionally, whole exome tumor sequencing was performed and disclosed somatic loss of MSH2 and MSH6. Germline mutation testing (father with multiple myeloma) showed a pathogenic germline MSH6 mutation [c.2731C>T (p.Arg911*)]. The patient started

pembrolizumab which he tolerated well. After 14 months on treatment, he has demonstrated complete PSA response (0.1 ng/ml) and complete resolution of soft-tissue (visceral and lymph node) metastases and CBC recovery (3.5 x103/uL, Hb: 11.8 g/dl, PLT: 132 x103/uL).

Conclusions

This is the first report of very good and durable response to immune checkpoint inhibition in a mCRPC patient with biallelic MSH6 inactivation who had extensive disease and myelophthisis. Personalized therapy of advanced PC with pembrolizumab in the context of MMR deficiency can be effective in the bone marrow.

Ethics Approval

The patient consented to participate in the Precision Medicine protocol at Weill-Cornell Medicine (WCM). The study was approved by our Institutional Review Board and Ethics Committee (WCM / New York-Presbyterian IRB protocol #: 1305013903).

Consent

Consent was received.

P194

Fecal microbiota transplantation for refractory immune checkpoint inhibitor-associated colitis

Yinghong Wang, MD, PhD[1], Hamzah Abu-Sbeih, MD[1], Diana Wiesnoski[1], Beth Helmink, MD PhD[1], Vancheswaran Gopalakrishnan, MPH, PhD[1], Kati Choi, MD[2], Hebert DuPont, MD[3], Zhi-Dong Jiang[3], Michael T. Tetzlaff, MD PhD[1], Jennifer A. Wargo, MD, MMSc[1], Robert Jenq, MD[1]

[1]Univ of Texas MD Anderson Cancer center, Houston, TX, USA
[2]Baylor College of Medicine, Houston, TX, USA
[3]Univ of Texas School of Public Health, Houston, TX, USA

Background

Background: Immune checkpoint inhibitors (ICIs) can lead to a severe immune-mediated colitis (IMC), which is treated with immunosuppressive therapy that is associated with significant morbidity. Pre-clinical models demonstrated that patients who develop IMC have differential bacterial signatures in their gut microbiome and that targeting specific bacterial-taxa may abrogate such toxicities.[1-4] Herein, we report the first reported case series of two-patients with refractory IMC successfully treated with FMT.

Methods

Methods: Included two-patients had a refractory IMC that was treated with FMT (50 grams). Clinical courses and immunohistochemical analysis of the colonic mucosa are detailed in Figures 1-7. Stool microbiome prior to and post-FMT was assessed via 16S sequencing (Figures 8-9).

Results

Results: Patient-1: a 50-year-old female with metastatic urothelial carcinoma received combined CTLA-4 and PD-1 blockade. Two-weeks after treatment initiation, she developed CTCAE grade ≥2 IMC. Infectious workup was negative. Colonoscopy demonstrated severe ulceration. She received corticosteroids, infliximab and vedolizumab for 3 months, but her symptoms and ulcers persisted. She then received a single-FMT via colonoscopy with complete resolution of symptoms and healed ulcers within 2 weeks. Prior to FMT, analysis in the colonic mucosa demonstrated high-density of CD8+ and low-density of CD4+ FoxP3+ T-cells. Post-FMT, CD8+ T-cell decreased and CD4+ FoxP3+ increased. Patient-2: a 78-year-old male with prostate cancer received ipilimumab. Three-months after treatment initiation, he developed grade ≥2 IMC. Infectious etiologies were excluded. Colonoscopy confirmed IMC. His symptoms and mucosal ulcerations persisted despite corticosteroids, infliximab and vedolizumab for 5

months. Then he received the first-FMT with partial response, however, after the second-FMT he had complete resolution of symptoms and ulcers. The density of all T-cell subtypes decreased post-FMT with persistence of CD4+ FoxP3+ cells. Principal coordinates analyses demonstrated the similarity to the donor microbiome most noticeably immediately post-FMT, but later deviated away, still, distinct from pre-FMT. At time of IMC diagnosis, patient-1 had a predominance of Clostridia and absence of Bacteroidia and Verrucomicrobiae and patient-2 had a predominance of Gammaproteobacteria (predominantly Escherichia). Immediately post-FMT, donor FMT-derived bacteria colonized the intestines of patient-1 (~75%) with abundance of Akkermansia that later decreased with expansion of Bifidobacterium. In patient-2, there was a notable increase in Blautia, Bacteroides and Bifidobacterium species post-FMT and a decrease in Escherichia.

Conclusions

Conclusion: These cases provide provocative and novel evidence that refractory IMC could be treated successfully with FMT, which reconstitutes the gut microbiome with relative increase in the proportion of regulatory T cells within the colonic mucosa.

References

Dubin, K., et al., Intestinal microbiome analyses identify melanoma patients at risk for checkpoint-blockade-induced colitis. Nat Commun, 2016. 7: p. P341

*Corresponding author email: Ulrike.Gnad-Vogt@curevac.com.2. Vetizou, M., et al., Anticancer immunotherapy by CTLA-4 blockade relies on the gut microbiota. Science, 2015. 350(6264): p. 1079-84.3. Chaput, N., et al., Baseline gut microbiota predicts clinical response and colitis in metastatic melanoma patients treated with ipilimumab. Ann Oncol, 2017. 28(6): p. 1368-1379.4. Wang, F., et al., Bifidobacterium can mitigate intestinal immunopathology in the context of CTLA-4 blockade. Proc Natl Acad Sci U S A, 2018. 115(1): p. 157-161.5. Borody, T.J. and A. Khoruts, Fecal microbiota transplantation and emerging applications. Nat Rev Gastroenterol Hepatol, 2011. 9(2): p. 88-96.

Ethics Approval

This study was approved by the Institutional Review Board at The University of Texas MD Anderson Cancer Center (PA18-0372)

Consent

Enrolled patients signed consent for the treatment protocol (CIND17-0036, CIND17-0058).

Figure 1.

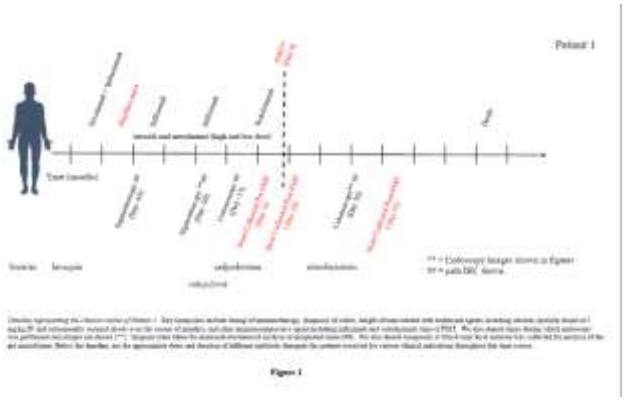

Figure 2.

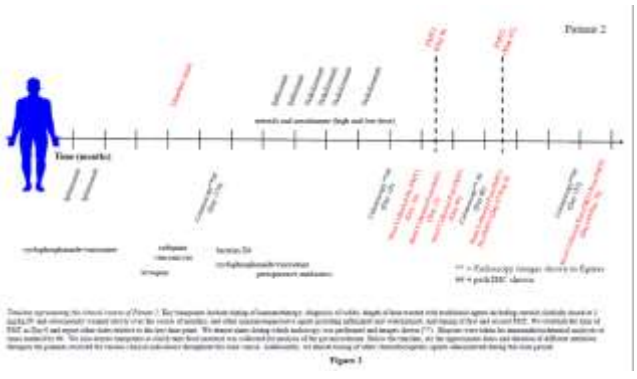

Figure 3.

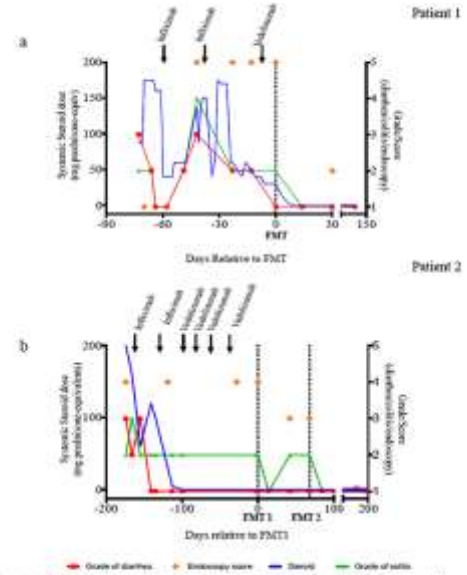

Severity of colitis. Various measures of disease severity are plotted throughout clinical course for (a) Patient 1 and (b) Patient 2, including daily dosage of systemic steroids (blue line), grade of diarrhea (red squares) and colitis (green triangles) as assessed by CTCAE Version 4 and endoscopic severity score (orange diamonds) which incorporates presence of erythema/ erosions, presence of ulcers, and number (≥ 2), size (≥1cm) and depth (≥3mm) of mucosal ulcerations (each feature counts one point). Vertical dotted line indicates date of FMT. The endoscopic scoring criteria was created based on institutional expertise. Timing of doses of immunosuppressive agents is also noted.

Figure 3

Figure 4.

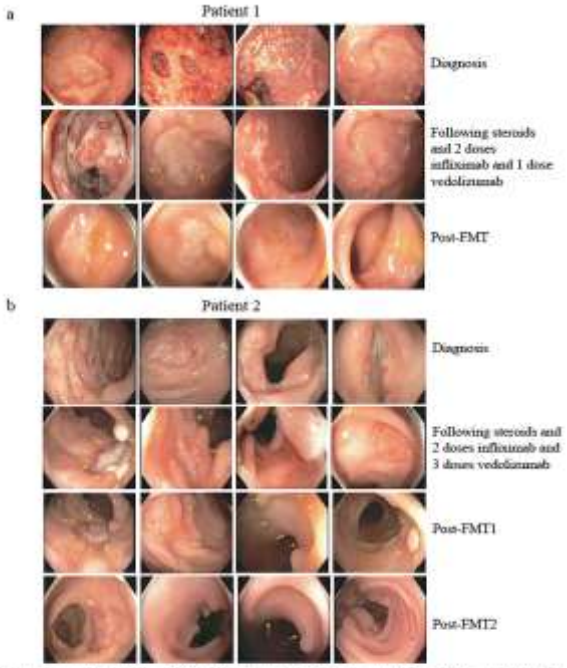

Additional endoscopic images from colonoscopy. (a) For Patient 1, images of colon and rectum near the time of diagnosis (row 1), after unsuccessful treatment with steroids and biologic immunosuppressive agents (steroid + 2 doses infliximab + 1 dose vedolizumab) (row 2) and approximately one month after FMT (row 3). (b) For Patient 2, images of colon and rectum near the time of diagnosis (row 1), after unsuccessful treatment with steroids and biologic immunosuppressive agents (steroid + 2 doses infliximab + 4 dose vedolizumab) (row 2), approximately 5 weeks following the first FMT (row 3), and approximately three months after the second FMT (row 4). Yellow arrows point to ulcerative lesions. Each photo represents a unique portion of the left colon and rectum. It is important to note that the photos directly beneath one another in subsequent rows do not necessarily correlate to the exact same location within the colon or rectum.

Figure 4

Figure 5.

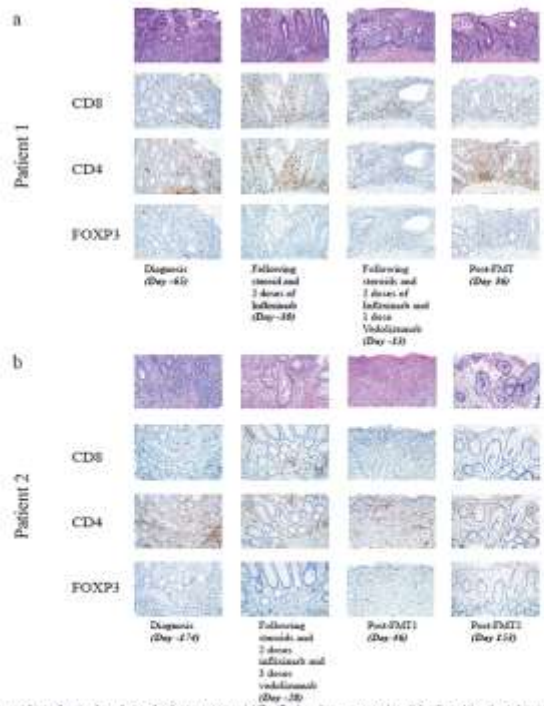

Immunohistochemical analysis of colonic mucosa. (a) For Patient 1, representative slides from biopsies taken at each of clinically relevant time points including at time of diagnosis, following unsuccessful treatment with steroids and 2 doses of infliximab, following additional one dose of vedolizumab, and following FMT (b) For Patient 2, representative slides from biopsies taken at time of diagnosis, following unsuccessful treatment with steroids and biologic immunosuppression, and following first FMT and following second FMT. Shown is H&E staining for each as well as staining for individual markers common to T lymphocytes: CD8, CD4 and FoxP3. Date of FMT1 is considered as Day 0.

Figure 5

Figure 6.

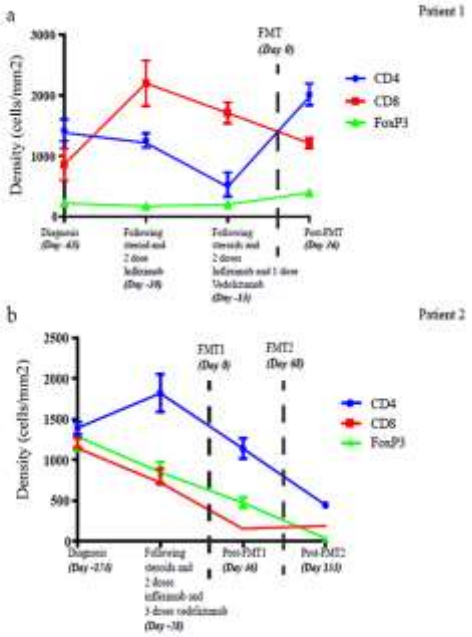

Quantification of immunohistochemical analysis of colonic mucosa (a) For Patient 1, absolute densities of different immune cells (cells/mm2) at time of diagnosis, during initial treatment with steroids and 2 doses of infliximab, following additional one dose of vedolizumab treatment, and following FMT. Vertical dotted line represents timing of the FMT (Day 0). (b) For Patient 2, absolute densities of different immune cells (cells/mm2) at time of diagnosis, following unsuccessful treatment with steroids and biologic immunosuppression, following FMT 1 and following the second FMT. For both, these data represent the average (+/- standard error of mean) cell density from 4 regions of interest per sample with each ROI measuring 500 µm x 500 µm. Vertical dotted line represents timing of FMT for each patient. Date of FMT1 is considered as Day 0.

Figure 6

Figure 7.

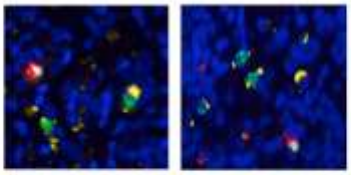

Figure 7

Figure 8.

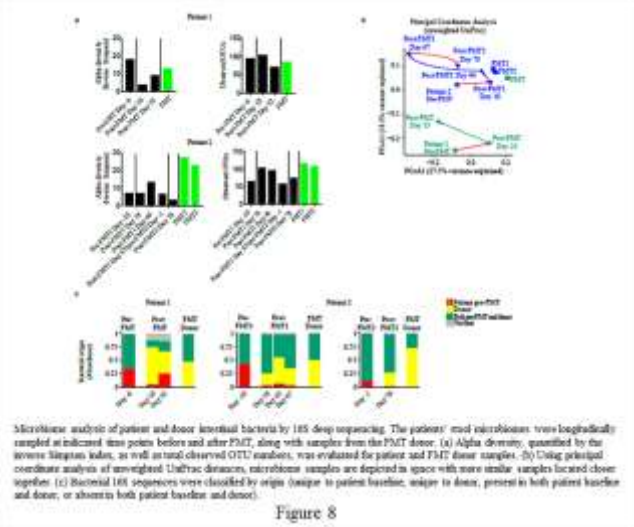

Figure 8

Figure 9.

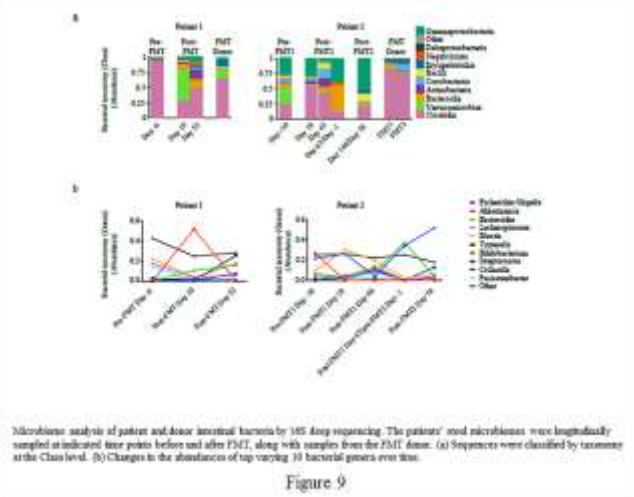

Figure 9

Cellular Metabolism and Antitumor Immunity

P195

Transcriptomic profiling of specific populations of T-cells in Acute Myeloid Leukemia

Milad Abolhalaj, MSc[1], Milad Abolhalaj, MSc[1], Milad Abolhalaj, MSc[1], Henrik Lilljebjörn[1], Carl Sandén[1], Karin Hägerbrand[2], Peter Ellmark, PhD[2], Carl Borrebaeck[1], Thoas Fioretos[1]

[1]*Lund University, Lund, Sweden*
[2]*Alligator Bioscience AB, Lund, Sweden*

Background

Acute myeloid leukemia (AML) has a 5-year survival of <5% among patients over 65 years. Checkpoint inhibitors have shown extraordinary effects in certain cancer patient groups and have been approved for different cancers. However, the results have been modest in AML and alternative strategies are thus warranted. Our study focuses on the transcriptome of specific T cell populations in AML patients to pinpoint novel targets for T cell-based interventions.

Methods

CD8+ T-cells (CTL), CD4+ T cells (Th), and regulatory T-cell (Tregs) populations were sorted from peripheral blood of AML patients (n=5), harbouring TP53-mutations, and controls (n=3) using flow cytometry. RNA was extracted and sequenced and data was analysed using Qlucore Omics Explorer software. Differentially expressed genes in each T-cell population from AML patients, as compared to its counterpart in controls, were identified (fold change>2, one-tailed t-test, FDR<0.1). Additionally, using ANOVA (FDR<0.1), transcriptomes of the three T-cell populations were compared in AML and then similarly in controls. Furthermore, genes expressed at a higher level in CTLs from AML as compared to Tregs in AML were identified (fold change>2, one-tailed t-tests, FDR<0.1) and those associated with plasma membrane were extracted. Additionally, plasma membrane-associated genes expressed higher in Th as compared to Tregs, and higher in Tregs as compared to both Th cells and CTL, were identified.

Results

ANOVA of the T-cell populations in AML identified 161 differentially expressed genes and the same analysis on control subjects resulted in 338 (38

overlapping). Furthermore, 577/498 genes were found to be expressed at higher/lower level by CTLs from AML compared to CTLs in control subjects. The corresponding numbers for Th cells and Tregs were 181/141 and 390/387, respectively. Interestingly, 10 plasma membrane-associated genes were expressed at higher levels by CTLs in AML patients compared to Tregs in AML. Furthermore, 5 membrane-associated genes were expressed higher in AML Th cells than AML Tregs. Finally, 1 membrane-associated gene was expressed higher by AML Tregs compared to both AML Th and CTLs, clearly supporting our strategy to identify novel targets.

Conclusions

The gene expression profiles of T-cells from AML differ from T-cells of control subjects and the differentially expressed genes give mechanistic insights into the impact of AML. Additionally, the plasma membrane-associated genes identified as selectively expressed by different T-cell populations in AML are potential targeting candidates for specific therapeutic interventions.

Ethics Approval

Study was performed in accordance with guidelines/regulations, approved by the Regional Ethics Committee.

Consent

Informed consent obtained from all donors.

P196

Comparison of culture media for in citro T cell assays and expansion

Ponni Anandakumar[1], Anne Lodge, PhD[1], Anne Lodge, PhD[1], Benjamin Tjoa, Ph D[1],

[1]*Astarte Biologics, Inc, Bothell, WA, USA*

Background

Identification of a reliable culture media to support in vitro T cell studies has become an important link in the chain of various Immuno-Oncology strategies. While many labs have chosen one favorite media for their T cell culture needs, it may be prudent to identify alternatives that can perform suitably, whether one works in the development of cell-based assays to screen potential drug candidates or generates and expands antigen-specific T cells. To address this issue, we have conducted a series of studies comparing the performance of several culture media.

Methods

A list of culture media (including several classic media + supplements as well as several new media) was compared to several commercially available T cell media in the generation of primary MLR (mixed-lymphocyte reaction), antigen-recall assay (e.g., CMV, tetanus), antigen-specific T cell proliferation assay, as well as in anti-CD3/CD28 driven T cell expansion culture.

Results

Classical media supplemented with several defined components can support primary in vitro responses as measured by cytokine production. Sustained T cell proliferation demanded additional supplementation and revealed greater differences between media. One representative data from these studies is included in this abstract. This experiment demonstrates the effect of human AB serum (HS) or fetal bovine serum (FBS) added to the culture medium X-VIVO 15 (Lonza, Walkersville, MD). At low peptide concentrations (3 and 10 ng/mL), the presence of HS and FBS inhibits T cell proliferation compared to X-VIVO 15 alone.

Conclusions

Media selection affects both T cell proliferation and function and therefore is critical to the success of adoptive T cell therapies. The strengths and

shortcomings of several media are revealed in these data.

Figure 1. Effect of supplements on antigen specific T cells

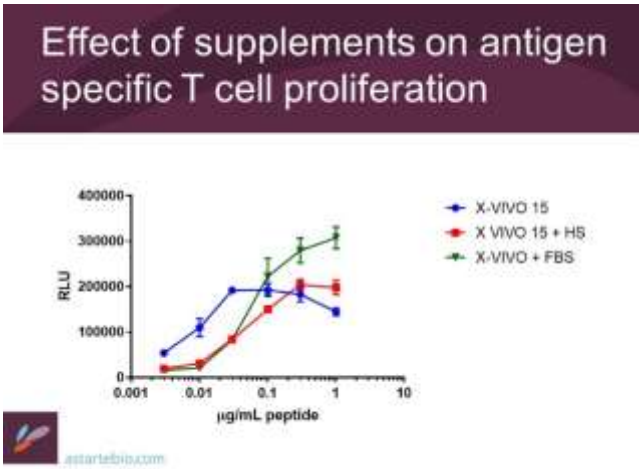

P197

Modulating hexokinase 2 as a novel approach for simultaneous targeting of the tumor and its immunosuppressive microenvironment

Vered Behar, PhD[1], Reut Yosef, PhD[1], Eyal Dor-On, PhD[1], Nofar Amsalem, MSc[1], Yuval Ariel, MSc[1], Oren Becker, PhD[1]

[1]*Vidac Pharma, Jerusalem, Israel*

Background

During malignant cell transformation and thereafter, many cancer types undergo metabolic reprograming to aerobic glycolysis to support their growth and proliferation, a phenomenon known as the Warburg effect. Elevated aerobic glycolysis results in excess lactate secretion to the tumor microenvironment, contributing to its immunosuppressive qualities. Hexokinase 2 (HK2), which catalyzes the first step of glucose metabolism and is key to aerobic glycolysis, is also a key gateway for apoptosis. HK2 becomes overexpressed in many cancer types, either in conjunction or instead of the normal HK1 isozyme, where it binds to the outer mitochondrial membrane via the VDAC1 channel. This VDAC1/HK2 association entails multiple advantages to cancer cells: a) blocks pro-apoptotic signals; b) fuels glycolysis with a continuous flux of mitochondrial ATP; and c) reduces sensitivity to feedback inhibition by HK2 product, glucose-6-phosphate. Temporal high HK2 expression, and binding to VDAC, is also found in a variety of activated immune cells to support their changing metabolic needs. Detachment of HK2 from VDAC1 in activated immune cells leads to various responses ranging from glycolysis inhibition, NLRP3-mediated inflammasome activation, and metabolic reprogramming to activate immunity.

Methods

VDA-1102 is a novel small molecule that detaches HK2 from the mitochondria (it is not an inhibitor). We present here in vitro and in vivo studies demonstrating its mechanism of action, both in cancer cells and in immune cells, resulting in immune-mediated anti-tumor response.

Results

In vitro studies demonstrated that VDA-1102 selectively detaches HK2, but not HK1, from VDAC1 leading to cancer cell apoptosis as well as glycolysis inhibition and reduction in lactate secretion, culminating in proliferation inhibition. Effects on macrophages (activating the M1 phenotype) and T cells were also demonstrated. In vivo efficacy studies in various syngeneic mouse models demonstrated significant tumor growth delay, prolongation of survival, and metastasis prevention. Analysis of tumor-associated immune cells in vivo indicated a favorable treatment-induced change in these cells, especially in macrophages and T cells.

Conclusions

This data supports the notion that VDA-1102's multiple effects target both cancer and the immune system. In cancer cells it induces apoptosis and

prevents secretion of lactate to the tumor microenvironment, whereas in macrophages it stimulates an anti-tumor immune response. Our findings support further development of VDA-1102 to evaluate its potential as an anti-cancer therapy, either as a monotherapy or in combination with immunotherapies in high HK2-expressing solid tumors.

Ethics Approval
All mouse studies were performed in compliance with "The Israel Animal Welfare Act" and following "The Israel Board for Animal Experiments" approval No IL-17-7-244.

P198

IDH1-R132H, a rate determining mutation in the timeline of anaplastic astrocytoma

Jonathan Fraser, MD[1], Mikhail Prosniac, PhD[1], Larry Harshyne[1], David Andrews, MD[1], D. Craig Hooper, PhD[1]

[1]*Thomas Jefferson University, Philadelphia, PA, USA*

Background
Until recently, the WHO classified the differences between grade III anaplastic astrocytomas (AA) and grade IV astrocytomas, or glioblastomas (GBM) by histological findings including neovascularization and necrosis. However, it is now recognized that isocitrate dehydrogenase (IDH1/2) mutation status differentiates 2 subsets of AA. Standard of care survival for AA patients with tumors expressing IDH1 with the R132H mutation (IDH1R132H) is commonly 5-7 years. In comparison, AA tumors with wild-type IDH1 (IDH1wt), like the majority of GBM, shares the poor prognosis of GBM, with median survival of 15-17 months. These tumors differ in their content of CD163+ tumor associated macrophage (TAM) that resemble M2 monocytes. The objective of the current is to determine if there is an association between the expression of IDH1 isoforms and TAM infiltration, and whether or not this is reflected in features of peripheral immunity.

Methods
Patients were diagnosed at surgery with AA by WHO histologic criteria. Pre-operative MRIs were assessed for extent of enhancement. Peripheral blood obtained prior to surgery was examined for immune cell distribution by flow cytometry, cytokine expression by RT-PCR, and local cytokine levels by Luminex. Tumor tissue obtained at surgery was assessed for IDH1-R132H expression and CD163+ TAM infiltration by immunohistochemistry.

Results
The majority of IDH1wt tumors enhanced in MRI while most IDH1R132H did not. However several tumors from both IDH1 subsets exhibited the opposite MRI characteristics. CD163+ TAM were abundant in tumors that enhanced but rare in those that did not. Circulating CD163+ monocytes were also elevated in patients with enhancing tumors. Differences in the expression by PBMC of a variety of genes encoding M2 phenotype markers as well as immune factors and their receptors were also detected; these also discriminate between subjects with enhancing versus non-enhancing tumors. MRI enhancement was more closely associated than IDH1wt with evidence of type 2 immune properties in PBMC and sera.

Conclusions
The data indicates that there is a closer association between the loss of tumor vascular integrity than IDH1 mutational status in the appearance of CD163+ TAM. Differences in the tumor microenvironment evidenced by TAM content are correlated with changes in measures of peripheral immune function suggestive of a type 2 immune bias. IDH1wt and IDH1R132H AA evidently progress through similar stages, albeit at different rates.

Acknowledgements
Funded by the Albert Stevens Foundation

Ethics Approval
the study was performed with de-identified specimens obtained through Thomas Jefferson University under IRB approval number:16D.424

P199

Myo-inositol up-regulates PD-L1 in non-small cell lung cancer

Eileen Fung, PhD[1], Jane Yanagawa[1], Jessica Kim[1]

[1]UCLA, Los Angeles, CA, USA

Background
Myo-inositol, an isomer of glucose, has shown to have preclinical promise for chemoprevention in multiple cancer models including lung cancer. However, results are conflicting in small randomized trials whether there is clinical benefit. While the molecular mechanisms driving chemoprevention are unclear, myo-inositol has been reported to affect the Akt1 signaling transduction pathway. Activation of Akt1 signaling pathway is associated with progression of non-small cell lung cancer (NSCLC) and enhanced expression of programmed death ligand-1 (PD-L1), an immunoregulatory protein. Binding of PD-L1 with its receptor, programmed death 1 (PD-1), results in T-cell exhaustion and, ultimately, immune evasion. We hypothesize that myo-inositol may impact signaling pathways that regulate PD-L1 expression.

Methods
A549, H441, H460, H1299, H1437, and H2291 lung cancer cell lines were treated with increasing doses of myo-inositol (0, 0.1, 1, 10, 100, and 200mM) for 72 hours in culture. PD-L1 cell surface expression was quantified using flow cytometry. Akt1 activation was determined by western blot analysis.

Results
Heterogeneous levels of basal PD-L1 expression were exhibited in A549, H441, H460, H1299, H1437, and H2291. Exposure of 200mM myo-inositol for 72 hours, cell surface PD-L1 expression were increased (1.1~2.25 fold, flow cytometry) in all 6 NSCLC cell lines. Western blot analysis showed increased phosphorylation of Akt1 (1.1~2.2 fold, western blot) in all NSCLC cell lines following myo-inositol treatment.

Conclusions
Upregulation of PD-L1 expression is exhibited following treatment with myo-inositol in NSCLC cell lines. This is the first report linking myo-inositol to regulation of PD-L1 expression through the AKT pathway.

P200

Cell competition and flower code regulates competitive interactions between tumor and its microenvironment

Rajan Gogna, PhD, MS, MBA[1], Esha Madan, PhD, MS, MBA[1], Masaki Nagane[2], Christopher Pelham[3], Taylor Parker[4], Antonio Beltran[5], Carlos Carvalho, MD[5]

[1]Champalimaud Center For Unknown, Lisbon, Portugal
[2]Azabu University, Tokyo, Japan
[3]St. Louis College of Pharmacy, Lisbon, Portugal
[4]Simon Cancer Center, IU, Libon, Portugal
[5]Champalimaud Centre for the Unknown, Lisbon, Portugal

Background
In living tissues, cells continuously interact, compete and compare their relative fitness levels[1, 2]. Cell competition explains oncogenic growth as an overarching phenomenon, it is the process where unfit cells, when confronted with fit cells, are

recognized and progressively eliminated[3-5]. Cancerous cells cheat this mechanisms and project themselves as super-fit to neighboring cells[1, 6-10]. These cells instead of being eliminated, induce apoptosis in surrounding normal cells. This promotes oncogenic growth by creating space and availability of nutrients (Fig-1a). Recently a novel molecular mechanism termed “Flower-code” which helps in recognition of unfit cells via cell surface marks called “Fitness fingerprints” was elucidated[8, 12]. In humans these fingerprints are encoded by 4 different isoforms of the transmembrane protein Flower (C9ORF7). The isoforms that indicate reduced fitness are called Lose and are expressed in viable cells marked to be eliminated, by fitter cells which express Win isoforms.

Methods

We have used techniques including CRISPR-assisted genetic engineering, a molecular cell competition assay in human cells (Fig-2a), live-cell imaging, gene expression analysis via FISH, qPCR in human cancer cells and FFPE patient cancer samples of multiple origins and development of humanized anti-Flower antibodies, via phage display.

Results

Novel results demonstrate the functional properties of Flower. Isoforms 2 and 4, with N-terminus internalized, are termed “Win” isoforms as they provide competitive advantage over cells expressing Flower “Lose” isoforms 1 and 3, with N-terminus externalized (Fig-1b). Importantly, Lose-expressing cells do not undergo apoptosis if neighboring cells have similar levels of Lose, therefore acting as canonical fitness comparison markers. Flower-/- MCF-7 cells ectopically expressing Lose isoforms, are eliminated by Flower-/- cells expressing Win isoforms (Fig-2b). FISH and qPCR show very poor expression of flower in normal tissue, but significantly high expression of Win isoforms within breast, colon, lung, SCC, liver and prostate cancers (n=95). Interestingly high expression of Lose isoforms in observed in the stromal cells 400-600µm from the edge of the tumor (Fig-2c).

Conclusions

First-time evidence is presented that Win and Lose isoforms of Flower, a fitness fingerprint protein, are expressed in cancer and stromal tissue, respectively. Win isoforms provides competitive advantages to cancer cells and expression of Lose isoforms on stromal cells marks them for progressive elimination, thereby supporting oncogenic growth. Flower is poorly expressed in normal tissues, thus is a high potential target for immune-therapy. We are presenting data highlighting the potential of monoclonal anti-Flower antibody in treatment of triple negative breast cancer PDX in abstract-P237

Acknowledgements

We acknowledge Champalimaud Research Foundation for supporting and funding this research.

References

1. Levayer R, Moreno E. Mechanisms of cell competition: themes and variations. J Cell Biol. 2013;200(6):689-98. Epub 2013/03/20. doi: 10.1083/jcb.201301051. PubMed PMID: 23509066; PubMed Central PMCID: PMCPMC3601360.
2. Amoyel M, Bach EA. Cell competition: how to eliminate your neighbours. Development. 2014;141(5):988-1000. Epub 2014/02/20. doi: 10.1242/dev.079129. PubMed PMID: 24550108; PubMed Central PMCID: PMCPMC3929405.
3. Merino MM, Rhiner C, Lopez-Gay JM, Buechel D, Hauert B, Moreno E. Elimination of unfit cells maintains tissue health and prolongs lifespan. Cell. 2015;160(3):461-76. Epub 2015/01/21. doi: 10.1016/j.cell.2014.12.017. PubMed PMID: 25601460; PubMed Central PMCID: PMCPMC4313366.
4. Morata G, Ripoll P. Minutes: mutants of drosophila autonomously affecting cell division rate. Dev Biol. 1975;42(2):211-21. Epub 1975/02/01. PubMed PMID: 1116643.

5. Moreno E, Basler K, Morata G. Cells compete for decapentaplegic survival factor to prevent apoptosis in Drosophila wing development. Nature. 2002;416(6882):755-9. Epub 2002/04/19. doi: 10.1038/416755a. PubMed PMID: 11961558.
6. Di Gregorio A, Bowling S, Rodriguez TA. Cell Competition and Its Role in the Regulation of Cell Fitness from Development to Cancer. Dev Cell. 2016;38(6):621-34. Epub 2016/09/28. doi: 10.1016/j.devcel.2016.08.012. PubMed PMID: 27676435.
7. Moreno E. Is cell competition relevant to cancer? Nat Rev Cancer. 2008;8(2):141-7. Epub 2008/01/11. doi: 10.1038/nrc2252. PubMed PMID: 18185517.
8. Rhiner C, Lopez-Gay JM, Soldini D, Casas-Tinto S, Martin FA, Lombardia L, et al. Flower forms an extracellular code that reveals the fitness of a cell to its neighbors in Drosophila. Dev Cell. 2010;18(6):985-98. Epub 2010/07/16. doi: 10.1016/j.devcel.2010.05.010. PubMed PMID: 20627080.
9. Levayer R, Hauert B, Moreno E. Cell mixing induced by myc is required for competitive tissue invasion and destruction. Nature. 2015;524(7566):476-80. Epub 2015/08/20. doi: 10.1038/nature14684. PubMed PMID: 26287461.
10. Moreno E, Rhiner C. Darwin's multicellularity: from neurotrophic theories and cell competition to fitness fingerprints. Curr Opin Cell Biol. 2014;31:16-22. Epub 2014/07/16. doi: 10.1016/j.ceb.2014.06.011. PubMed PMID: 25022356; PubMed Central PMCID: PMCPMC4238900.
11. Merino MM, Rhiner C, Portela M, Moreno E. "Fitness fingerprints" mediate physiological culling of unwanted neurons in Drosophila. Curr Biol. 2013;23(14):1300-9. Epub 2013/07/03. doi: 10.1016/j.cub.2013.05.053. PubMed PMID: 23810538.
12. Gogna R, Shee K, Moreno E. Cell Competition During Growth and Regeneration. Annu Rev Genet. 2015;49:697-718. Epub 2015/12/04. doi: 10.1146/annurev-genet-112414-055214. PubMed PMID: 26631518.

Ethics Approval

All animal studies performed in this research are approved by Champalimaud Institutional Review Board and the Portuguese Gov Ethical board (DGAV), the approval number is 0421/000/000.

Figure 1.

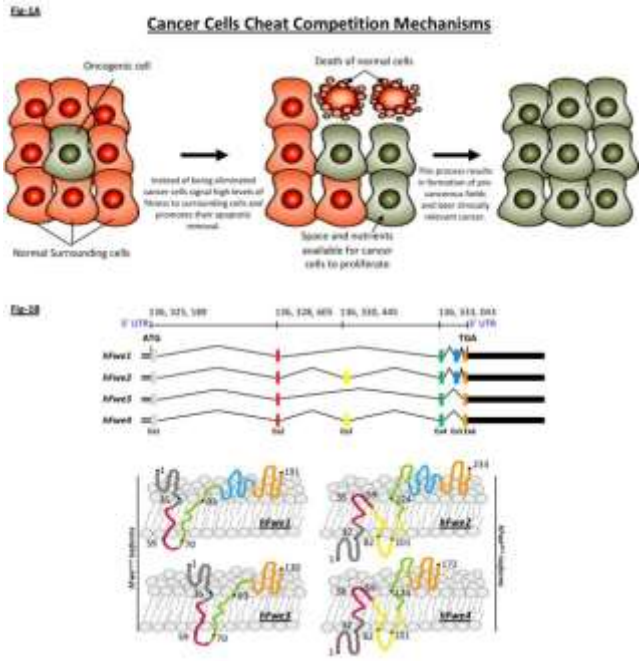

Figure 2.

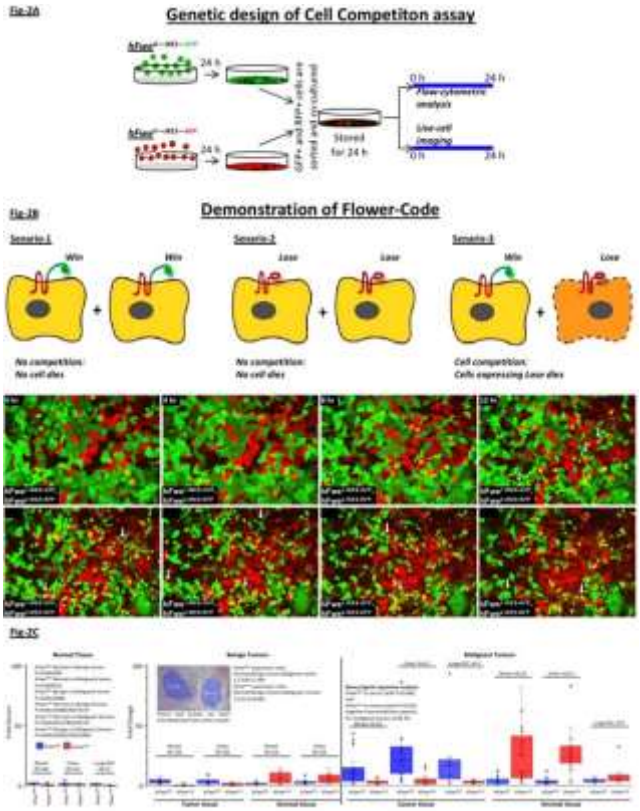

P201

Cell competition genes drive donor cell leukemia in AML patients

Rajan Gogna, PhD, MS, MBA[1], Esha Madan, PhD, MS, MBA[1], Christopher Pelham[2], Taylor Parker[3]

[1]*Champalimaud Center For Unknown, Lisbon, Portugal*
[2]*St. Louis College of Pharmacy, Lisbon, Portugal*
[3]*IUPUI, Simon Cancer Center, Libon, Portugal*

Background

Allogeneic hematopoietic stem cell transplantation (alloHSCT) improves overall survival in AML patients[1-4]. However, secondary leukemia is a major clinical problem, and surprisingly this can arise from healthy allogenic donor cells, termed donor cell leukemia (DCL)[5-8]. DCL is a rare complication (5%) associated with alloHSCT, where normal donor cells become transformed into aggressive leukemia or myelodysplastic syndrome in the host environment[9]. The mechanisms behind DCL remain unknown, however, some dormant donor cell mutations have been proposed to play some role. DNA sequencing has revealed that de-novo AML patients carry DNMT3A mutations (22%), which are associated with intermediate-risk cytogenetic profile and poor outcome[10]. Interestingly, the role of DNMT3A mutations was also highlighted in DCL. For example, an AML patient that received peripheral blood stem cells (PBSCs) from his HLA-matched brother developed DCL 27 months post-transplant. Whole-exome sequencing from specimens of the initial AML, first complete remission after chemotherapy, the first relapse, donor PBSCs, DCL at 27 and DCL at 36 months revealed that IDH2(R140Q) and DNMT3A(V150Gfs) mutations were present in the healthy donor cells at a low frequency and were potentially responsible for DCL[11]. Based on literature sets available and our preliminary data, we hypothesize that cell competition between host and donor cells contributes to DCL development, as its mechanisms allow the donor cells to acquire a Win phenotype and colonize the weak cellular microenvironment of the allogenic host. Cell competition results in the elimination of the less fit cells by the fitter cells through direct or indirect mechanisms[12-16]. Please refer to abstracts: P200

Methods

Flower-knockout MCF-7 cells were created using CRISPR and Win/Lose cell types were generated with help of lentiviral particles. These Win and Lose cells were allowed to compete (Fig-1a) and both populations were captured using Fluidigm single-cell capture technique (Fig-1b). Following which, both cell types were processed for single-cell RNA seq.

Results

RNA-seq results show that during competition the Winner cells have significantly reduced DNMT3A expression and activity. RNA-seq has revealed a novel set of uncharacterized genes that participate in this process.

Conclusions

Our results demonstrate a parallel behavior in DNMT3A status between alloHSCT donor cells which result in DCL and Winner cells from cell competition assay. We have identified a list of novel uncharacterized genes that may serve as biomarkers to select the appropriate alloHSCT donor cells that can help minimize the risk of DCL development.

Acknowledgements

We acknowledge Champalimaud Research Foundation for supporting and funding this research.

References

1. Li D, Wang L, Zhu H, Dou L, Liu D, Fu L, Ma C, Ma X, Yao Y, Zhou L, Wang Q, Wang L, Zhao Y, Jing Y, Wang L, Li Y, Yu L. Efficacy of Allogeneic Hematopoietic Stem Cell Transplantation in Intermediate-Risk AcuteMyeloid Leukemia Adult Patients in First Complete Remission: A Meta-Analysis of Prospective Studies. PLoS One. 2015 Jul 21;10(7):e0132620. doi: 10.1371/journal.pone.0132620. eCollection 2015. PubMed PMID: 26197471

2. Schiller GJ, Tuttle P, Desai P. Allogeneic Hematopoietic Stem Cell Transplantation in FLT3-ITD-Positive Acute MyelogenousLeukemia: The Role for FLT3 Tyrosine Kinase Inhibitors Post-Transplantation. Biol Blood Marrow Transplant. 2016 Jun;22(6):982-990. doi: 10.1016/j.bbmt.2016.01.013. Epub 2016 Jan 16. PubMed PMID: 26785334

3. Xu Y, Sun Y, Shen H, Ding L, Yang Z, Qiu H, Sun A, Chen S, Wu D. Allogeneic hematopoietic stem cell transplantation could improve survival of cytogenetically normal adult acute myeloid leukemia patients with DNMT3A mutations. Am J Hematol. 2015 Nov;90(11):992-7. doi: 10.1002/ajh.24135. PubMed PMID: 26223865.

4. Wang Y, Chen G, Cao R, Li J, He L, Guo X, Liang J, Shi P, Zhou Y, Xu B. Allogeneic hematopoietic stem cell transplantation improves the prognosis of p16-deleted adultpatients with acute lymphoblastic leukemia. Pharmacogenomics. 2017 Jan;18(1):77-84. doi: 10.2217/pgs-2016-0075. Epub 2016 Dec 14. PubMed PMID: 27967319.

5. Flynn CM, Kaufman DS. Donor cell leukemia: insight into cancer stem cells and the stem cell niche. Blood. 2007 Apr 1;109(7):2688-92. PubMed PMID: 17132724.

6. Gondek LP, Zheng G, Ghiaur G, DeZern AE, Matsui W, Yegnasubramanian S, Lin MT, Levis M, Eshleman JR, Varadhan R, Tucker N, Jones R, Gocke CD. Donor cell leukemia arising from clonal hematopoiesis after bone marrow transplantation. Leukemia. 2016 Sep;30(9):1916-1920. doi: 10.1038/leu.2016.63. Epub 2016 Mar 15. PubMed PMID: 26975880.

7. Ma H, Liu T. Development of donor cell leukemia following peripheral blood stem cell transplantation for severe aplastic anemia: A case report. Oncol Lett. 2016 Jun;11(6):3858-3862. Epub 2016 Apr 18. PubMed PMID: 27313707.

8. Wiseman DH. Donor cell leukemia: a review. Biol Blood Marrow Transplant. 2011 Jun;17(6):771-89. doi: 10.1016/j.bbmt.2010.10.010. Epub 2010 Oct 15. PubMed PMID: 20951819.

9. Shah NN, Bacher U, Fry T, Calvo KR, Stetler-Stevenson M, Arthur DC, Kurlander R, Baird K, Wise B, Giralt S, Bishop M, Hardy NM, Wayne AS. Myelodysplastic syndrome after allogeneic hematopoietic stem cell transplantation: diagnosticand therapeutic challenges. Am J Hematol. 2012 Sep;87(9):916-22. doi: 10.1002/ajh.23174. Epub 2012 Apr 4. PubMed PMID: 22473867.

10. Ley TJ, Ding L, Walter MJ, McLellan MD, Lamprecht T, Larson DE, Kandoth C, Payton JE, Baty J, Welch J, Harris CC, Lichti CF, Townsend RR, Fulton RS, Dooling DJ, Koboldt DC, Schmidt H, Zhang Q, Osborne JR, Lin L, O'Laughlin M, McMichael JF, Delehaunty KD, McGrath SD, Fulton LA, Magrini VJ, Vickery TL, Hundal J, Cook LL, Conyers JJ, Swift GW,

Reed JP, Alldredge PA, Wylie T, Walker J, Kalicki J, Watson MA, Heath S, Shannon WD, Varghese N, Nagarajan R, Westervelt P, Tomasson MH, Link DC, Graubert TA, DiPersio JF, Mardis ER, Wilson RK. DNMT3A mutations in acute myeloid leukemia. N Engl J Med. 2010 Dec 16;363(25):2424-33. doi: 10.1056/NEJMoa1005143. Epub 2010 Nov 10. PubMed PMID: 21067377.

11. Yasuda T, Ueno T, Fukumura K, Yamato A, Ando M, Yamaguchi H, Soda M, Kawazu M, Sai E, Yamashita Y, Murata M, Kiyoi H, Naoe T, Mano H. Leukemic evolution of donor-derived cells harboring IDH2 and DNMT3A mutations after allogeneicstem cell transplantation. Leukemia. 2014 Feb;28(2):426-8. doi: 10.1038/leu.2013.278. Epub 2013 Sep 26. PubMed PMID: 24067491.

12. Gogna R, Shee K, Moreno E. Cell Competition During Growth and Regeneration. Annu Rev Genet. 2015;49:697-718. Epub 2015/12/04. doi: 10.1146/annurev-genet-112414-055214. PubMed PMID: 26631518.

13. Amoyel M, Bach EA. Cell competition: how to eliminate your neighbours. Development. 2014;141(5):988-1000. Epub 2014/02/20. doi: 10.1242/dev.079129. PubMed PMID: 24550108; PubMed Central PMCID: PMCPMC3929405.

14. Petrova E, Lopez-Gay JM, Rhiner C, Moreno E. Flower-deficient mice have reduced susceptibility to skin papilloma formation. Dis Model Mech. 2012;5(4):553-61. Epub 2012/03/01. doi: 10.1242/dmm.008623. PubMed PMID: 22362363; PubMed Central PMCID: PMCPMC3380718.

15. Petrova E, Soldini D, Moreno E. The expression of SPARC in human tumors is consistent with its role during cell competition. Commun Integr Biol. 2011;4(2):171-4. Epub 2011/06/10. doi: 10.4161/cib.4.2.14232. PubMed PMID: 21655431; PubMed Central PMCID: PMCPMC3104570.

16. Merino MM, Rhiner C, Portela M, Moreno E. "Fitness fingerprints" mediate physiological culling of unwanted neurons in Drosophila. Curr Biol. 2013;23(14):1300-9. Epub 2013/07/03. doi: 10.1016/j.cub.2013.05.053. PubMed PMID: 23810538.

Ethics Approval

All animal studies performed in this research are approved by Champalimaud Institutional Review Board and the Portuguese Gov Ethical board (DGAV), the approval number is 0421/000/000.

Figure 1.

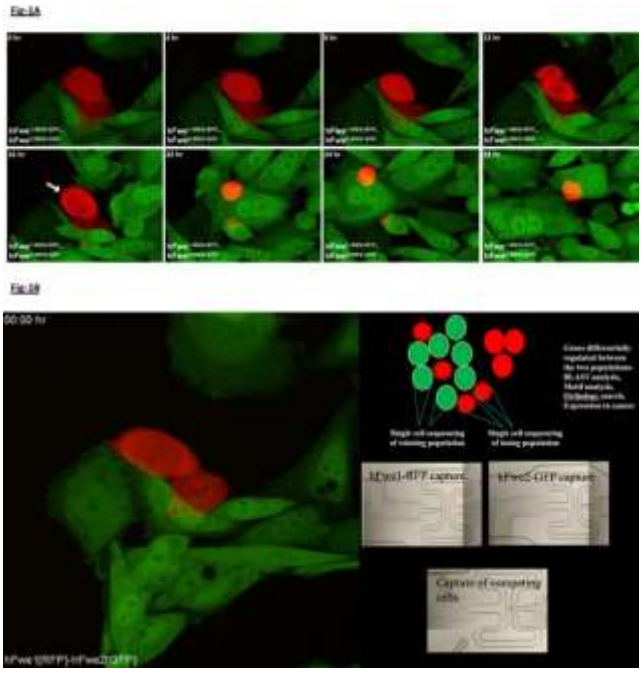

P202

Targeting the stress response kinase GCN2 to restore immunity in the tumor microenvironment

Lisa Marshall[1], Buvana Ravishankar[1], Lavanya Adusumilli[1], Mikhail Zibinsky, PhD[1], Deepa Pookot[1], Emily Huang[1], Oezcan Talay, PhD[1], Silpa Suthram[1], Jeffrey Jackson[1], Grant Shibuya[1], Akinori Okano[1], Paul Leger[1], Scott Jacobson, BS[1], Steve Wong[1], Sherra Johnson[1], Parcharee Tivitmahaisoon[1], Angela Wadsworth, BA[1], Jerick Sanchez[1], Martin Brovarney[1], David Chian, BA[1], Abood Okal, PhD[1], Delia Bradford[1], Christophe Colas[1], Andrea Kim[1], Gene Cutler, PhD[1], Jacob Schwartz[1], David Wustrow, PhD[1], Paul Kassner,

PhD[1], Dirk Brockstedt[1]

[1]*FLX Bio, Inc, South San Francisco, CA, USA*

Background

The tumor microenvironment (TME) is characterized by deficiencies in oxygen and key nutrients, such as glucose and amino acids. Stromal cells and Myeloid-derived suppressor cells (MDSC) within the tumor create a nutrient-poor environment that inhibits immune function and supports tumor growth [1]. GCN2 (general control nonderepressible 2), a stress response kinase, plays a key role in sensing and modulating the response to amino acid deprivation. GCN2 activation leads to an induction of the integrated stress response pathway in T cells leading to T cell anergy and apoptosis [2,3]. Here, we demonstrate that the pharmacologic inhibition of GCN2 restores the T cell proliferation and effector function in amino-acid deficient media and in MDSC-induced T cell suppression.

Methods

Mouse and human T cell viability, proliferation and function were assessed in vitro under amino-acid deprived conditions and in a co-culture with MDSCs. Pharmacodynamic markers including phospho-GCN2, phospho-EIF2α, and ATF4 were measured via western blot. Cell proliferation (CFSE dye dilution) and effector markers (IFNγ and Granzyme B) were measured by flow cytometry. Our FLX selective, sub-micro molar GCN2 inhibitor (GCN2i) was used to examine the role of GCN2 in T cell and MDSC function.

Results

Culturing mouse or human CD8+ T cells under low L-Tryptophan (TRP) conditions activated the GCN2/eIF2α/ATF4 pathway as shown by increased phospho-GCN2 and phospho-eIF2α levels, and enhanced ATF4 protein expression. GCN2/eIF2α pathway suppressed eIF2α phosphorylation and inhibited the increase in ATF4. Under these low TRP conditions or in MDSC co-culture, a GCN2i resulted in rescue of CD8+ T cell proliferation and improvement of cell viability. Additionally, increased levels of IFNγ and Granzyme B were observed in the presence of GCN2i.

Conclusions

The GCN2/eIF2α pathway is activated in immune cells during amino acid deprivation, and this induces a functional suppression of the immune response. Our results demonstrate that inhibition of GCN2 is an attractive approach for relieving immune suppression and promotion of T effector activation in the TME

Acknowledgements

Cesar Meleza, Minna Bui and Nathan Kozon

References

1. Turley S, Cremasco V, Astarita J. Immunological hallmarks of stromal cells in the tumor microenvironment. Nature Reviews Immunology. 2015: 15: 669–682.
2. Munn DH, Sharma MD, Baban B, Harding HP, Zhang Y, Ron D, Mellor AL. GCN2 kinase in T cells mediates proliferative arrest and anergy induction in response to indoleamine 2,3-dioxygenase. Immunity. 2005; 22(5): 633-42.
3. Rodriguez P, et al. L-arginine deprivation regulates cyclin D3 mRNA stability in human T cells by controlling HuR expression. Journal of immunology. 2010; 185.9: 5198–5204.

Ethics Approval

The study was approved by FLX Bio's IACUC committee, approval number FL0002

P203

Immunomodulatory effects through inhibition of monocarboxylate transporters in melanoma

Satish Noonepalle, PhD[1], Jennifer Kim, PhD[2], Namratta Manhas, PhD[1], Sophiya Ephrame, BS[1], Erica Palmer, BS[1], Melissa Hadley, MS[1], Vincent Sandanayaka, PhD[3], Alejandro Villagra, PhD[1]

[1]*George Washington University, Washington DC, DC, USA*
[2]*Brigham and Women's Hospital, Boston, MA, USA*
[3]*Nirogyone Therapeutics LLC, Worcester, MA, USA*

Background

Solid tumors under hypoxic conditions rely on glycolysis rather than oxidative phosphorylation for energy needs thereby generating lactate as a metabolic byproduct. Lactate is transported across the tumor cell membrane using monocarboxylate transporters, MCT1 & MCT4. Lactate is known to suppress immune cell function especially the cytotoxic CD8+ T-cells and NK cells resulting in local immune suppression of the tumor microenvironment (TME). Additionally, acidosis of local TME through lactate/H+ results in inflammation and angiogenesis by activation of VEGFR signaling. The net result of an increased lactate in TME is that it creates a conducive milieu for tumor growth and metastasis. Studies thus far have shown that MCT inhibitors mitigate the effects of lactate and promote immune function; however, the effect of lactate on immune cells in the context of tumor infiltration, immune cell composition, lineage differentiation and cytokine profiles are yet to be explored.

Methods

In this study, we used a novel MCT1/4 dual inhibitor NGY-A to demonstrate the effect of suppressing lactate in the local TME and restoring the anti-tumor immunity. In vivo experiments were performed with syngeneic mouse model of SM1 melanoma cells in C57BL/6 mice treated with NGY-A at a dosage of 10mg/kg administered intraperitoneally 5 days/week for 2 weeks. Total protein and RNA was extracted to perform immunoblot and real time PCR analyses. Expression of MCT1/4 was analyzed using skin cancer melanoma datasets on Cbioportal and R2 genomics platforms.

Results

Our preliminary data indicates that (1) MCT1/4 expression is upregulated in a subset of melanoma patients and it is associated with poor survival (2) In vivo analysis of SM1 melanoma mouse model in C57BL/6 mice, treatment with NGY-A significantly delayed tumor growth compared to the control group. (3) Analysis of tumors revealed that expression of immune suppressive B7 family genes Cd274 (PD-L1), Cd276 (B7-H3) and Lgals9 (Galactin-9) were significantly down regulated at both RNA and protein levels in NGY-A treated group compared to the control group. (4) Cytokine expression profiling of NGY-A treated tumors by RT-PCR indicated an increase in anti-tumor cytokines IFNγ, TNFα, IL-1β and decrease in pro-tumor cytokines TGFβ, IL-10 compared to control group tumors suggesting that NGY-A treatment can increase anti-tumor CD8+ T-cells, M1 macrophages and suppress tumor promoting M2-phenotype.

Conclusions

Our preliminary data strongly suggests that intervention of lactate transporters MCT1/4 with NGY-A exhibits significant anti-tumor effect by positively modulating the local TME to promote immune cell function.

P204

Characterization of novel dual A2A_A2B adenosine receptor antagonists for cancer immunotherapy

Mateusz Nowak[1], Michal Galezowski[1], Paulina Wegrzyn[1], Aneta Bobowska[1], Katarzyna Dziedzic[1], Joanna Szeremeta-Spisak[1], Marcin Nowogrodzki[1], Grzegorz Satala[1], Alicja Obara[1], Iwona Lozinska[1], Marcelina Dudek[1], Anita Janiga[1], Jacek Reus[1], Marek Wronowski[1], Magdalena Zastawna[1], Grzegorz Statkiewicz[1], Maciej Rogacki[1], Mateusz Swirski[1], Jakub Woyciechowski[1], Magdalena Ziembik[1], Karolina Grycuk[1], Foteini Soukou[1], Agnieszka Adamus[1], Karolina Wiatrowska[1], Natalia Lewandowska[1], Aniela Golas[1], Olga Pierzchala[1], Roderick Porter[1] Krzysztof Brzozka[1]

[2]Selvita S.A, Krakow, Poland

Background

Adenosine functions as a messenger molecule in many tissues including central nervous and cardiovascular systems. Recently the attention of researchers was attracted to immunological aspects of adenosine signaling and its involvement in the suppression of immune response in tumor microenvironment. Adenosine inhibits the biological functions of T lymphocytes infiltrating the cancer tissue by binding to the A2A receptor. The affinity to A2B receptor is believed to attenuate the response of innate system ie: dendritic cells. Thus blocking of both A2A and A2B signaling seems to be a viable approach for either standalone therapy or combination with other immunomodulating agents.

Methods

The activation of A2a R and A2b R increases intracellular levels of cAMP, subsequent phosphorylation of the CREB protein, which translates to lower excretions of certain types of cytokines by specific populations of primary cells. To assess the potency of antagonists under tumor like conditions either 100uM adenosine or 10uM synthetic adenosine agonist (NECA) was used. cAMP level was measured by TR-FRET based method. Cytokines levels were measured by alphaLISA method. Flow cytometry was used to measure adenosine related inhibition of CREB phosphorylation on T cells and B cells in blood harvested form animals dosed with our antagonist and ex vivo treated with NECA.

Results

We have developed a novel series of potent and dual A2A/A2B antagonists that retain its nanomolar potency in tumor-like adenosine rich environment. Our antagonists restore the cytokine release by activated CD4+ and CD8+ human T-lymphocytes after treatment with high concentrations of adenosine. We observe also the reversal of functional adenosine-induced suppression of NK cells. Most importantly presented compounds show improved pharmacological profile in comparison to A2A inhibitors tested in clinical trials. Currently our most advanced lead A2A/A2B inhibitors undergo an extensive in vivo efficacy and safety characterization.

Conclusions

Due to the abnormally elevated adenosine levels in tumor microenvironment, the efficacious adenosine receptor antagonist should be able to displace adenosine even in very high concentrations. We have demonstrated several in vitro models that dual A2A/A2B antagonists discovered in Selvita are able to reverse the immune suppression induced by adenosine concentration corresponding to those present in tumors.

P205

Preclinical and initial phase I clinical characterization of CPI-006: an anti-CD73 monoclonal antibody with unique immunostimulatory activity

Emily Piccione, PhD[1], Andrew Hotson, PhD[1], Glen Mikesell, BS[1], Barbara Daine-Matsuoka, BS[1], Chunyan Gu[1], Trang Dao-Pick[1], Craig Hill, PhD[1], Antonett Madriaga[1], Jennifer Rudnick[1], Liang Liu[1], W Jones[1], Linda Hammerich, PhD[2], Joshua Brody, MD[2], Ginna Laport[1], Richard Miller, MD[1], Joseph Buggy[1]

[1]Corvus Pharmaceuticals, Burlingame, CA, USA
[2]Icahn School of Medicine at Mount Sinai, New York, NY, USA

Background

The ecto-5'-nucleotidase CD73 generates immunosuppressive adenosine and functions as a co-stimulatory protein on lymphocytes [1]. CPI-006 is a humanized, FcγR binding-deficient anti-CD73 that fully inhibits enzymatic activity and does not induce antigen internalization. We report in vitro mechanistic studies, in vivo studies in cynomolgus monkeys, and preliminary data from an ongoing Phase 1/1b clinical trial.

Methods

CPI-006 was evaluated in vitro in human peripheral blood mononuclear cells (PBMCs) or purified B cells. Safety and toxicokinetic studies were performed in 16 cynomolgus monkeys; CPI-006 was dosed IV once weekly for five weeks up to 120 mg/kg. CPI-006 was given by IV infusion every 3 weeks in a Phase 1/1b trial (NCT03454451) to evaluate safety and biologic effects in advanced cancer patients.

Results

CPI-006 completely inhibited conversion of AMP to adenosine (IC50, 17nM). Blocking adenosine production with CPI-006 enhanced immune-cell mediated tumor killing (220pM) and reversed suppression of T cell proliferation (EC50, 70nM) and IFNγ secretion (EC50, 66nM). In vitro treatment of normal PBMCs or purified B cells with CPI-006 induced B lymphocyte activation leading to ERK phosphorylation and increased CD69, CD25, and CD83 expression. B cell activation was independent of adenosine and completely blocked by the BTK inhibitor ibrutinib (0.1µM). No B cell death or apoptosis was observed. Cynomolgus monkeys showed complete occupancy of CD73 on CD8+ T cells in peripheral blood up to 7 days post-treatment at doses ≥ 10 mg/kg. The NOAEL was 120 mg/kg, the highest dose tested. CPI-006 was administered to five cancer patients at 1 or 3 mg/kg (data cutoff July 30, 2018). Serum levels of CPI-006 were detected up to 24 hours post-dose with complete elimination by day 8. Full target occupancy was achieved 0.5 hours after dosing with no occupancy by day 15, concordant with serum levels of antibody. At 0.5 hours, a decrease in peripheral B cells (median reduction 60%, range 33-82%), but not T cells, was observed in all five patients. B cell depletion was transient and was restored to baseline levels by day 15, consistent with the pharmacokinetics. No grade 3/4 adverse

Conclusions

CPI-006 both inhibits the enzymatic activity of CD73 and stimulates an intracellular signal to activate B cells. Expression of CD69 and reversible reduction of circulating B cells is consistent with B cell activation and redistribution to lymphoid tissues through inhibition of S1P1 receptors [2]. These effects may have immunotherapeutic potential for patients with cancer.

Trial Registration

NCT03454451

References
1. Resta R, Yamashita Y, and Thompson LF. Ecto-enzyme and signaling functions of lymphocyte CD73. Immunological Revs. 1998; Vol 161: 95-109.
2. Shiow LR, Rosen DB, Brdickova N, Xu Y, An J, Lanier LL, Cyster JG, and Matloubian M. CD69 acts downstream of interferon-a/b to inhibit S1P1 and lymphocyte egress from lymphoid organs. Nature. 2006; Vol 440: 540-544.

P206

Using clear cell like-RenCa and papillary like-RenCa models of Kidney Cancer to study metabolic influences on the microenvironment and metastasis

Bradley Reinfeld, BA[1], Katy Beckermann[2], W. Rathmell, MD, PhD[2], Peter Siska[3], Jeffrey Rathmell, PhD[1], Melissa Wolf[1], Kirsten Young[1], Gabriella Andrejeva, PhD[1], Jamie Weyandt[4]

[1]*Vanderbilt University School of Medicine, Nashville, TN, USA*
[2]*Vanderbilt University Medical Center, Nashville, TN, USA*
[3]*University Hospital Regensburg, Nashville, TN, USA*
[4]*Aegis, Nashville, TN, USA*

Background
The genetics of renal cell carcinoma (RCC) surround loss of function mutations in genes that regulate metabolism. The most common genetic event in clear cell RCC (ccRCC) is loss of Von Hippel Lindau (VHL). In type II papillary RCC, 20% of patients lose key Krebs cycle enzyme, fumarate hydratase (FH). Through separate mechanisms, both mutations result in elevated hypoxia related signaling and demonstrate glycolytic phenotypes. This project focuses on how these mutational events create an immunoinhibitory metabolic milieu that ultimately promotes tumor establishment, progression, and metastasis.

Methods
Previously our lab has demonstrated differences in tumor interstitial fluid composition when comparing adjacent normal kidney parenchyma and RCC malignant tissue via 13C NMR. This work surrounds modeling the abnormal metabolic microenvironment of kidney cancer in relation to genetic features of the major classification sof RCC in vitro. By combing the OT-1 model antigen system with novel ribonucleic CRISPR/Cas9 approaches, we have a more genetically relevant tumor model whose elimination is antigen dependent. This approach has resulted in the establishment of clear cell-like RenCas (containing VHL knock out) and papillary-like RenCas (containing FH KO).

Results
From a metabolic standpoint, these cell lines both demonstrate the phenotypes of HIF elevated tumors with significantly increased glucose uptake, lactate production and glutaminolysis, but with varying metabolic demands. Additionally both KO cell lines accumulate lipid droplets via Oil Red O and electron microscopy. The FH-KO RenCas form larger tumors when grown in immunocompetent mice then their vector control. Intriguingly, this significant difference disappear is Rag deficient mice. By using these novel cell lines, we can evaluate how clinically relevant genetic events result in metabolic changes in the tumor microenvironment impacting immune cells and potential responsiveness to immunotherapy.

Conclusions
Our lab has developed novel immunocompetent models of RCC, which will allow us to investigate how tumor metabolic demands promote dysfunctional immune phenotypes. In doing so, we hope to find new synergistic therapeutic combinations that will increase the efficacy of immune checkpoint blockade via altering the metabolic components of the tumor microenvironment.

P207 **Abstract Travel Award Recipient**

Chronic T cell activation and metabolic stress promote the exhausted T cell state by inducing epigenetic inflexibility

Nicole Scharping, BS[1], Natalie Rittenhouse[1], Ashley Menk, BS[1], Ronal Peralta[1], Paolo Vignali, BA[1], Roderick O'Sullivan[1], Amanda Poholek[1], Greg Delgoffe, PhD[1]

[1]*University of Pittsburgh, Pittsburgh, PA, USA*

Background

CD8+ tumor-infiltrating T lymphocytes (TIL) progressively succumb to a dysfunctional state known as 'exhaustion', characterized by poor effector function and sustained co-inhibitory marker expression, but the factors causing this hyporesponsive phenotype remain unclear. We recently demonstrated that exhausted TIL also exhibit progressive loss of functional mitochondria, due in part to repression of the transcriptional co-activator PGC1α, resulting in suppressed mitochondrial fusion and biogenesis. Enforcing PGC1α expression in tumor-specific T cells not only led to increased mitochondria, but improved functionality, decreased tumor burden, and increased survival in mouse B16 melanoma. These results lead us to hypothesize that T cell exhaustion may be driven by metabolic insufficiency.

Methods

To characterize both the drivers and consequences of T cell exhaustion, we developed models to identify how tumor-derived signals – hypoxia and chronic T cell receptor activation – induce metabolic insufficiency and T cell exhaustion *in vitro*. These *in vitro* findings were analyzed in correlation with *ex vivo* exhausted TIL from mouse B16 melanoma for comparison.

Results

Exploring the drivers of T cell exhaustion, we found T cells experiencing chronic activation or hypoxia alone < i >in vitro< /i > could carry out similar or superior effector functions, but experiencing both chronic activation and hypoxia simultaneously generated profound, persistent T cell dysfunction. This dysfunction was characterized by high PD-1, Tim-3, and Lag3 expression, loss of IFNγ cytokine production, decreased oxygen consumption due to loss of functional mitochondria, and required the transcriptional repressor Blimp1. Our studies suggest metabolic insufficiency does not contribute to exhaustion energetically, but rather causes alterations in epigenetic remodeling both in our < i >in vitro< /i > exhaustion assay and in TIL, leading to increased repressive histone methylation and decreased expression of essential T cell effector genes. We next identified a mechanism for this hypermethylation signature and found TIL have excessive mitochondrial reactive oxygen species (ROS), which caused DNA damage. Consequently, we metabolically reprogrammed tumor-specific T cells and found metabolic reprogramming was sufficient to reduce ROS, reduce repressive chromatin methylation, and prevent DNA damage.

Conclusions

Our findings support a model in which chronic activation drives transcriptional repression, fundamentally altering how T cells respond to hypoxic conditions and exposing a mechanism of T cell exhaustion. These data reveal potential metabolic avenues to rescue exhausted T cells and improve immunotherapy.

P208

Metabolic reprogramming augments CAR T cell function

Yiyang Wang, N/A[1], Jason Lohmueller, PhD[2], McLane Watson, BS[2], Dayana Rivadeneira, PhD[2], Greg Delgoffe, PhD[1]

[1]*UPMC Hillman Cancer Center, Pittsburgh, PA, USA*
[2]*University of Pittsburgh, Pittsburgh, PA, USA*

Background
CAR T immunotherapy has emerged as an exciting approach for cancer treatment. Remarkable success has been demonstrated in the treatment of hematologic malignancies, yet to be replicated in solid tumors. This is thought to be due to many hurdles including tumor-associated immune suppression and alterations in the tumor metabolic environment. Current preclinical CAR T research has taken advantage of tumor graft models in immunodeficient mice, which may lead to neglect of the effect posed by the immune system. Our aim is to establish a fully murine model with mouse CAR T cells against antigens expressed in murine solid tumors. Furthermore, to combat the metabolic restrictive tumor microenvironment (TME), we attempt to develop gene-therapy strategies to make metabolically superior CAR T cells.

Methods
Murine CAR constructs containing the single-chain variable fragment that can recognize human CD19 were synthesized and transduced into mouse CD8+ T cells to generate murine CAR T cells. MC38 cells, (derived from murine adenocarcinoma) were modified to overexpress human CD19 and intradermally inoculated onto immunocompetent mice to establish the model. CAR T cells were first tested by in vitro cytotoxicity assay, then adoptively transferred into tumor bearing mice for tumor-infiltrating lymphocyte analysis. Retroviral transduction of genes involved in the mitochondrial biogenesis pathway served to reprogram these CAR T cells, which were further tested by bioenergetic assays including Seahorse extracellular flux analysis.

Results
In our murine model, tumor-infiltrating CAR T cells manifest an insufficient metabolic phenotype with repressed glucose uptake and loss of mitochondria mass. Their ability to produce antitumor cytokines is also suppressed. Retroviral overexpression of Ppargc1a (encoding PGC1α) and Tfam (Transcription Factor A, Mitochondrial) in CAR T cells increases their basal oxygen consumption rate (both genes) and spare respiratory capacity (Ppargc1a), while leading to an elevated expression of markers for central memory phenotype, suggesting their potential to perform better antitumor function in the TME. Preliminary data in the treatment of established MC38 tumor suggests that mice treated with metabolically reprogrammed CAR T cells have slower tumor growth compared to those treated with normal CAR T cells.

Conclusions
CAR T cells that infiltrate solid tumors function at a metabolic disadvantage. Metabolic reprogramming of CAR T cells to favor mitochondrial biogenesis increases their respiratory capacity, thus enhancing the effector function and longevity of these cells in the tumor microenvironment. The utilization of gene therapy targeting metabolism of T cells may improve the efficacy of adoptive T cell therapies for solid malignancy.

Ethics Approval
Animal work was done in accordance with the Institutional Animal Care and Use Committee of the University of Pittsburgh.

P209

Antagonism of peroxisome proliferator activated receptor alpha by TPST-1120 suppresses tumor growth and stimulates anti-tumor immunity

Chan Whiting, PhD[1], Nick Stock, PhD[2], Davorka Messmer, PhD[2], Austin Chen, PhD[2], Lisa Rahbaek, PhD[2], Allison Gartung, PhD[3], Karin Stebbins, PhD[2], Traci Olafson[2], Alex Broadhead[2], Ryan Clark, PhD[2], Catherine Lee, MS[2], Chris Baccei[2], Dan Lorrain, PhD[2], Alicia Levey, PhD[1], Derek Metzger, BA[1], Amanda Enstrom, PhD[1], Jennifer McDevitt, PharmD, PhD[1], David Spaner, MD, PhD[4], Peppi Prasit, PhD[2], Dipak Panigrahy, MD[3]

[1]*Tempest Therapeutics, San Francisco, CA, USA*
[2]*Inception, San Diego, CA, USA*
[3]*BIDMC, Boston, MA, USA*
[4]*Sunnybrook, Toronto, Canada*

Background
TPST-1120 is a first-in-class selective antagonist of human PPARα, a transcription factor that induces expression of fatty acid oxidation (FAO) genes. Metabolic adaptions promote tumor survival and suppress tumor-specific immunity by upregulation of FAO. Results from multiple syngeneic and xenograft mouse models suggest PPARα blockade has intrinsic and extrinsic anti-tumor activity and induces tumor-specific immunity.

Methods
The effects of TPST-1120 as monotherapy or in combination with chemotherapy or anti-PD1 were evaluated in multiple syngeneic mouse models including B16 melanoma, MMTV mammary carcinoma, MC38 colon, Lewis lung carcinoma, ID8 ovarian, Panc07 pancreatic cancer, and xenograft CLL, melanoma, pancreatic and AML models. To characterize its mechanism of anti-tumor immunity, TPST-1120 was evaluated in knock-out models of CCL2, MBL, TSP-1, STING and BatF3. Immune modulation was characterized by M2/M1 macrophage flow cytometry phenotyping and ELISA measurement of plasma and tumor matrix protein thrombospondin-1 (TSP-1), which is involved in granulocyte migration and angiogenesis.

Results
TPST-1120 mediated PPARα antagonism resulted in potent anti-tumor immune responses and significant tumor regression, either as a monotherapy or in combination with chemotherapy or anti-PD1. TPST-1120 showed anti-tumor efficacy against syngeneic models of breast, lung, colon, pancreatic and melanoma in addition to xenograft models of CLL, AML, pancreatic and melanoma as monotherapy or with chemotherapy. TPST-1120 demonstrated cytotoxic effect on tumor cells in vitro. In pancreatic and breast cancer models, TPST-1120 together with chemotherapies gemcitabine and eribulin, respectively, had additive effects on controlling tumor growth. TPST-1120 with anti-PD1 in ovarian orthotopic (ID8) and colon (MC38) models showed suppression of tumor growth and complete remission in some mice compared with either TPST-1120 or the checkpoint inhibitor alone. The combination also conferred protection against autologous tumor re-challenge in the ID8 model, strongly suggesting induction of immunological memory against the primary tumor. Preliminary studies in genetic knock-out mice, suggest macrophages and antigen cross-presenting dendritic cells are required for TPST-1120 activity, potentially through STING activation and TSP-1. Consistent with prior reports of the involvement of PPARα activation in promoting M2 macrophages, TPST-1120 skews toward an M1 effector macrophage phenotype and in vivo pretreated peritoneal macrophages enhance the uptake of whole tumor cells by FACS.

Conclusions
Through its unique mechanism of restricting FAO, TPST-1120 targets a metabolic pathway critical for survival of both tumor cells and suppressive immune

cell populations infiltrating the tumor microenvironment and represents a promising new approach for patients with advanced malignancies.

Cellular Therapy Approaches

P210

PD-1-positive tumor-infiltrating lymphocytes (TIL) for the next generation of adoptive T cell therapy

Michelle Abelson, PhD[1], Kenneth D'Argio[1], Angel Cedano-Hilton[1], Ian Frank[1], Krit Ritthipichai, DVM, PhD[1], Cecile Chartier[1]

[1]*Iovance Biotherapeutics, Tampa Bay, FL, USA*

Background

Adoptive T cell therapy with autologous TIL has demonstrated high response rates in patients with metastatic melanoma [1]. TIL products used for treatment are comprised of heterogenous T cells, which recognize tumor-specific antigens, mutation-derived patient-specific neoantigens, and non-cancer related antigens [2, 3]. Among them, neoantigen-specific T cells are main contributors to the anti-tumor activity of TIL [4]. Strategies enriching TIL for such T cells are thus expected to yield more potent therapeutic products, especially in epithelial cancers known to contain a high proportion of bystander T cells [5]. Several studies have demonstrated that expression of PD-1 on TIL identify tumor-specific T cells [6-8]. Presented here is the development of a new process to produce tumor antigen-specific-enriched TIL products for clinical application.

Methods

PD1-positive (PD1+) cells were sorted via flow cytometry directly from fresh tumor digests and expanded in vitro. Samples from 4 melanomas, 3 sarcomas, 3 breast cancers, and 2 lung cancers were evaluated. Sorted PD-1+ TIL-derived product, sorted PD-1- TIL-derived product, and whole tumor digest (unsorted)-derived product were compared for cell count, phenotype, function, TCR Vβ repertoire, and tumor reactivity.

Results

PD-1+ cells, ranging between 1-90% of the CD3+ cells, were isolated from tumor digests. Upon expansion, the PD-1+ cells proliferated 3-fold less than the PD-1 cells, and high TIL numbers were obtained in 9 of the 12 products. Phenotypic analyses revealed no significant differences in terms of T cell lineages and memory subsets, or expression of various activation, differentiation, and exhaustion markers between the 3 types of products. The PD1+ TIL-derived products responded to PMA and to anti-CD3 stimulations by inducing CD107a mobilization and IFN gamma secretion to extents similar to the control products. Profiling of the TCRvβ repertoire demonstrated that PD-1+ TIL-derived CD8+ cells displayed greater oligoclonality than their PD1- counterparts, likely reflecting antigen-driven clonal expansion at the tumor site. Whether this oligoclonal expansion will translate into superior tumor-specific recognition and killing is the subject of further investigation.

Conclusions

A process has been developed for the expansion of PD1+ TIL from a variety of histologies. Resulting products were shown to be phenotypically and functionally comparable with bulk TIL products. Consistent with prior reports [6, 8], our results suggest that in vitro expansion of PD1+ TIL can restore their effector functions and support the development of PD1+ TIL-derived product for the treatment of cancer.

References

1. Rosenberg SA, et al. Durable complete responses in heavily pretreated patients with metastatic melanoma using T-cell transfer immunotherapy. Clin Cancer Res. 2011; 7(13):4550-7.
2. Kvistborg P, et al. TIL therapy broadens the tumor-

reactive CD8(+) T cell compartment in melanoma patients. Oncoimmunology. 2012;1(4):409-418.
3. Simoni Y, et al. Bystander CD8(+) T cells are abundant and phenotypically distinct in human tumour infiltrates. Nature. 2018; 557(7706):575-579.
4. Schumacher TN, Schreiber RD. Neoantigens in cancer immunotherapy. Science. 2015; 348(6230): 69-74.
5. Turcotte S, et al. Phenotype and function of T cells infiltrating visceral metastases from gastrointestinal cancers and melanoma: implications for adoptive cell transfer therapy. J Immunol. 2013; 191(5): 2217-25.
6. Inozume T, et al. Selection of CD8+PD-1+ lymphocytes in fresh human melanomas enriches for tumor-reactive T cells. J Immunother. 2010; 33(9): 956-64.
7. Gros A, et al. PD-1 identifies the patient-specific CD8(+) tumor-reactive repertoire infiltrating human tumors. J Clin Invest, 2014; 124(5): p. 2246-59.
8. Thommen DS, et al. A transcriptionally and functionally distinct PD-1(+) CD8(+) T cell pool with predictive potential in non-small-cell lung cancer treated with PD-1 blockade. Nat Med. 2018.

P211

Oxygen and pressure promote primary T cell expansion and can regulate population dynamics and cytokine release

Yunmin Li, PhD[1], Zachary Pappalardo[1], Mauricio Montano[1], Ann Lu[1], Bruce Adams[1]

[1]Xcell Biosciences Inc., San Francisco, CA, USA

Background

T cell immunotherapy workflows typically require expansion of autologous T cells or genetic modification of T cells in vitro, followed by infusing of those cells back into the patients. Typically, T cells or genetically modified T cells are expanded using CD3 and CD28-based activation under standard cell culture conditions (18-20% O2). However, this approach is not always ideal or preferred because, for example, some donors fail to expand. Furthermore, expansion of T cells using activating agents can change cell phenotypes and states, and the state of cells could contribute to risk elements such as cytokine release syndrome. Because T cells in the body experience a broad range of O2 levels (ranging from 13%O2 in arterial blood to 5%O2 in venous blood), as well as a range of blood pressures (60 mmHg/1.2 PSI, 120 mmHg/2.3 PSI), we studied how environmental control might be used to optimize T cell growth and phenotype in workflows including: 1) activation-based expansion, 2) standard expansion, and 3) post-transfection viability.

Methods

To address expansion, human CD3+ T cells were seeded in expansion medium supplemented with IL2 (for activation, we used CD3 and CD28-based stimulation). A range of O2 concentrations and forces were tested for the ability to influence T cell growth and phenotype for up to 14 days using the AVATAR™ cell control system. Next, to address the issue of post-transfection viability, activated T cells were transfected by electroporation, and were recovered under a variety of different conditions and assessed for viability and expansion.

Results

CD3+ T cells grew faster, both without or with activation, resulting in as much as 51% more T cells compared to standard incubation at 2 weeks. T cells cultured under different O2 and pressure levels showed different proliferation rates but in general, T cell grew faster and had different cytokine secretion profiles when additional pressure was applied n the culture. In the case of transfection, we were able to improve post-transfection viability by as much as 35% with more than twice the number of cells after three days compared to those cultured under standard recovery conditions.

Conclusions
Environmental influences such as oxygen and pressure can be used to optimize expansion and/or state of T cells, including in difficult to grow samples, or cells that have been stressed by upstream manipulations such as transfection. This control can also be used to study phenotypic changes in cytokines release, metabolic markers and checkpoint receptor expression.

P212

Preinfusion product doubling time is associated with CAR T cell expansion and outcomes in ZUMA-1, the pivotal study of axicabtagene ciloleucel (axi-cel) in refractory large B cell lymphoma

Tiffany Adolf[1], Frederick Locke, MD[2], John Rossi, MS[3], Caron Jacobson, MD[4], David Miklos, MD[5], Armin Ghobadi, MD[6], Olalekan Oluwole, MBBS, MPH[7], Lazaros Lekakis, MD[8], Patrick Reagan, MD[9], Yizhou Jiang, PhD[3], Lianqing Zheng, PhD[3], William Go, MD, PhD[3], Adrian Bot, MD, PhD[3]

[1]Nexus GG Science LLC
[2]Moffitt Cancer Center, Tampa, FL, USA
[3]Kite, a Gilead Company, Santa Monica, CA, USA
[4]Dana-Farber Cancer Institute, Boston, MA, USA
[5]Stanford University School of Medicine, Stanford, CA, USA
[6]Washington University School of Medicine, St. Louis, MO, USA
[7]Vanderbilt-Ingram Cancer Center, Nashville, TN, USA
[8]University of Miami Health System, Miami, FL, USA
[9]University of Rochester Medical Center, Rochester, NY, USA

Background
Axi-cel, an FDA-approved autologous anti-CD19 chimeric antigen receptor (CAR) T cell therapy, demonstrated an 82% objective response rate (ORR), including a 58% complete response (CR) rate in patients with refractory large B cell lymphoma (median 15.4 months follow-up) [1]. Grade ≥3 cytokine release syndrome (CRS) and neurologic events occurred in 12% and 31% of patients, respectively. This analysis examined associations of preinfusion product characteristics with CAR T cell expansion and clinical outcomes.

Methods
ORR and blood CAR T cell levels (peak and area under the curve from days 0–28 [AUC_{0-28}] in ZUMA-1 were examined for associations with axi-cel product cell population doubling time (DT), a measure of preinfusion product T cell expansion kinetics. DT, measured between day 3 and final day of manufacturing, depends on the rates of cell proliferation and death during incubation with recombinant interleukin (IL)-2–supplemented medium. Major product T cell phenotypes were evaluated by flow cytometry. Associations were evaluated using logistic regression (nominal P values <.05 considered meaningful associations; not adjusted for multiplicity) and pairwise Spearman analysis (rs values) and visualized using quartile analysis bar charts and logistic regression predicted probability curves.

Results
Patients treated with products with shorter DT had higher ORR (P=.025; Figure A-B). Patients in the lowest product DT quartile (DT≤1.33 days) had 100% ORR. Patients in the highest product DT quartile (DT≥1.79 days) had 73% ORR. DT was also negatively associated with greater CAR T cell expansion post-infusion (peak CAR T cell levels, rs = -0.27; AUC_{0-28}, rs = -0.29; quartile analysis, Figure C). Of 17 nonresponders, 12 had product DT>1.5 days. A precise CD4/CD8 T cell ratio of 1:1 was not required for achieving lowest DT and maximal CAR T cell expansion or ORR. Additional analyses, including associations between product DT, T cell phenotypes, and other clinical outcomes including toxicities and durable response, will be presented.

Conclusions

Preinfusion product T cell expansion kinetics, as measured by DT during manufacturing in presence of IL-2–supplemented medium, may be associated with ORR and in vivo CAR T cell expansion in patients treated with axi-cel. Poor product DT may limit in vivo CAR T cell expansion. Indices related to product DT, a component of product T cell fitness, may be useful in optimizing CAR T cell therapy.

Trial Registration

NCT02348216

References

1. Neelapu SS, Locke FL, Bartlett NL, et al. Axicabtagene ciloleucel CAR T-cell therapy in refractory large B-cell lymphoma. N Engl J Med. 2017;377:2531-2544.

Figure 1.

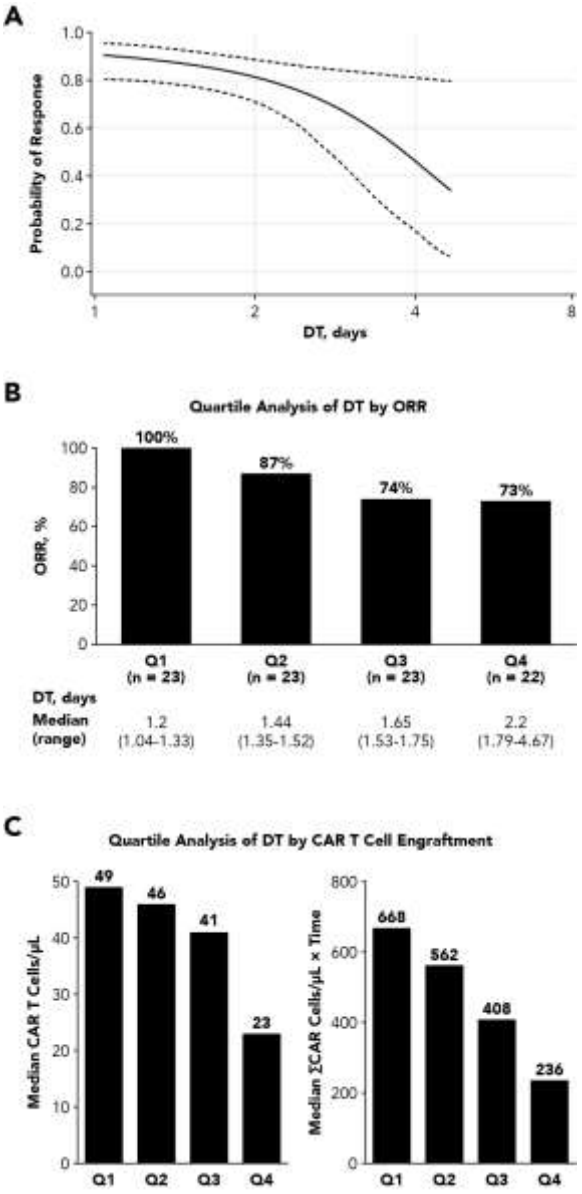

P213

CYAD-101: an allogeneic NKG2D CAR T cell therapy using a TCR inhibitory molecule

Sophie AGAUGUE, PhD[1], Alexandre Michaux, PhD[1], Eytan Breman, MSc[1], Sebastien Mauen, PhD[1], David Gilham, PhD[1]

[1]*Celyad SA, Mont Saint Guibert, Belgium*

Background
Chimeric antigen receptor (CAR) T cells have demonstrated impressive clinical results in B cell malignancies. Most CAR T cell therapies rely on autologous peripheral blood cells that present some challenges including manufacturing time and product variability. Allogeneic T cells derived from a healthy donor may circumvent these issues. However, allogeneic T cells can induce graft versus host disease (GvHD), a response triggered by the recognition of non-self Human Leukocyte Antigen molecules expressed on recipient cells by the T Cell Receptor (TCR) of donor cells. To avoid GvHD, we targeted the TCR signalling by using a TCR inhibitory molecule (TIM) peptide consisting of a truncated form of CD3zeta. Our mechanistic studies suggest that TIM is acting as a dominant negative form of CD3zeta reducing downstream TCR signaling pathway activity. To assess TIM in the context of a CAR therapy, an allogeneic CAR T cell was developed by co-expressing TIM and a NKG2D-based CAR (referred as CYAD-101).

Methods
CYAD-101 CAR T cells were produced from five different healthy donors. In vitro and in vivo experiments have been performed to evaluate the culture parameters, phenotype, alloreactivity and potency against NKG2D ligand-expressing tumor targets.

Results
In vitro experiments confirmed the suppression of TCR alloreactivity of the TIM-combined CAR as compared to control cells. However, the CYAD-101 T cells showed variability between donors in terms of CD4/CD8 ratio and percentage of central and effector memory populations potentially relating to the variability of the starting material to produce CAR T cells. In addition, harvested CYAD-101 cells were mainly composed of a non-activated and non-exhausted population (i.e. CD25-/CD69- and PD1-/LAG3-). A concomitant reduction in the level of phospho-ZAP-70 was observed in cells expressing the TIM. Importantly, in vitro cytotoxicity and cytokine production of CYAD-101 cells upon co-culture with NKG2D ligand-expressing tumor cell lines was not affected by the insertion of TIM. Finally, compared to control T cells, CYAD-101 cells efficiently delayed in vivo tumor progression and increased survival of NSG mice bearing orthotopic colorectal tumors while avoiding the induction of GvHD.

Conclusions
Following these promising preclinical results showing the combination of effective anti-cancer activity and inhibition of alloreactivity of CYAD-101 CAR T cells, a phase I clinical trial will be shortly initiated to assess the safety, cell kinetics and clinical activity of CYAD-101 CAR T cells in patients with unresectable metastatic colorectal cancer.

Ethics Approval
Animal studies were approved by VetAgro-Sup / Lyon National Veterinary School ethical committe (project n° APAFIS#8565-2017010413316369 v4) and french authorities.Use of whole blood of healthy donors was approved by local ethical committees.

P214

Development of allogeneic gene-edited CAR T-cells: from preclinic to clinical proof of concept

Beatriz Aranda Orgilles, PhD[1], Agnes Gouble[1], Roman Galetto, PhD[1], Julianne Smith[1], Philippe Duchateau[1], David Sourdive[1], Laurent Poirot, PhD[1], Stephanie depil[1]

[1]*Cellectis, New York, USA*

Background
Adoptive immunotherapy using engineered T-cells has emerged as a powerful approach to treat cancer. The potential of this approach relies on the ability to redirect T-cell specificity through ex vivo genetic engineering and transfer of chimeric antigen

receptors (CARs) or engineered TCRs. Transduction of patients' blood cells with an anti-CD19 CAR for the treatment of Acute Lymphoblastic Leukemia (ALL) has led to complete response in the large majority of treated patients and the early approval of two CAR T-cell products. Autologous treatments require a complex manufacturing process and depend on the existence of a healthy T-cell population despite previous heavy chemotherapy treatments. The use of allogeneic cells (derived from healthy donors rather than the patients themselves) allows preparation of cells well ahead of a patient's need for treatment. Moreover, allogeneic CAR T-cells offer the possibility to characterize in depth the starting material, generate multiple treatment doses from one process and, ultimately, more affordable access to treatment.

Methods

Using our proprietary nuclease-based gene editing technologies, we showed our capability to efficiently edit any gene in primary T-cells with very high precision.

Results

Here, we describe how TALEN® gene-editing technology allows to create CAR T-cells that can be used in allogeneic setting and, additionally, empowers them with improved safety and efficacy attributes. Among others, new features include expression control properties, resistance to standard oncology treatments, and prevention of fratricide of engineered CAR T-cells.

Conclusions

We have successfully developed GMP-compliant manufacturing of TALEN®-edited CAR T-cells for clinical use, which has led to two allogeneic CAR T-cell product candidates in the clinic. Preliminary data show expansion of allogeneic cells associated with antitumor activity, providing first clinical proof of concept for allogeneic CAR T-cell approaches. This technology offers unparalleled possibilities to design next generation cell immunotherapies not only in hematological malignancies but also in solid tumors.

P215

Preclinical evaluation of Deep™ IL-15 Primed PMEL cells demonstrates highly improved safety compared to systemic administration of IL-15

Philip Bardwell, PhD[1], Elena Geretti[1], Xiaoyan Liang[1], Santina Caruso[1], De-Kuan Chang, PhD[1], Jesse Lyons[1], Carlos Tassa[1], Sanela Bilic[1], Janice Lanista[1], Becker Hewes, MD[1], Jonathan Fitzgerald, PhD[1], Thomas Andresen, PhD[1]

[1]*Torque Therapeutics, Cambridge, MA, USA*

Background

Interleukin-15 (IL-15) is a promising candidate for tumor immunotherapy, since it is a strong activator of both CD8+ T and NK cells and in contrast to IL-2 does not activate regulatory T cells. Systemic administration of IL15-Fc to patients resulted in dose-limiting toxicities, likely due to activation of NK cells. Here we describe the safety of T cells loaded with Deep™ IL-15, a multimer of reversibly crosslinked IL-15/IL-15 Rα/Fc subunits (IL15-Fc). Deep IL-15 acts as an autocrine source of IL15-Fc providing T cell activation, expansion, and promotion of memory phenotypes. Additionally, Deep IL-15 limits systemic exposure to IL15-Fc thus avoiding hyperproliferation of endogenous cells, including NK cells, the primary mediators of IL-15 immunotoxicity.

Methods

Deep IL-15 was evaluated in an adoptive T cell therapy model by treatment of B16-F10 tumor-bearing mice with PMEL CD8+ T (PMEL) cells (10-27 x 106), carrying up to 158 µg of Deep IL-15 (>15-fold the maximum tolerated dose, MTD, of IL15-Fc). The toxicity of Deep-15 PMEL was compared with PMEL (10 x 106) co-injected with IL15-Fc (MTD of 10 µg/mouse) (PMEL + IL15-Fc). Readouts included IL15-

Fc exposure, cytokine release, changes in endogenous T cells and histopathology. Additionally, Deep™ IL-15 was administered to naïve C57BL/6 mice (10-100 µg/mouse) to evaluate direct effects of systemic Deep IL-15.

Results

Deep-15 Primed PMEL cells deliver significantly improved anti-tumor activity compared to PMEL cells alone in the B16-F10 model. Compared to systemic co-administration of IL15-Fc with PMEL, treatment with Deep-15 PMEL obtained a 300-fold lower systemic exposure to IL15-Fc, 41-fold lower IFN-γ release, and no expansion of endogenous cells (CBC; flow cytometry: CD4+, CD8+ and NK cells). Histopathology of lungs, liver and spleen revealed minimal findings with Deep-15 PMEL, less pronounced when compared to PMEL + IL15-Fc. Additionally, injection of Deep™ IL-15 alone resulted in no weight loss, no IFN-γ release and no changes in endogenous CD4+, CD8+ and NK cells.

Conclusions

Torque's novel Deep Primed technology offers the advantage of loading Deep™ IL-15 prior to cell infusion in ACT, at doses unachievable with systemic injection of IL15-Fc, resulting in controlled, cell-specific activation. Systemic injection of Deep IL-15 up to 15-fold of the IL15-Fc MTD resulted in no toxicity findings. Deep-15 PMEL cells were well tolerated, did not expand endogenous cells and resulted in minimal histopathological changes. Deep IL-15 Primed multi-targeted human T cells, TRQ15-01, are expected to start clinical evaluation in hematologic and solid tumors in late 2018.

Ethics Approval

All personnel received training from the Torque's Animal Care and Use Committee (IACUC). All animal procedures were in strict accordance with the National Institutes of Health Guide for the Care and Use of Laboratory Animals and were approved by the Torque Animal Care and Use Committee.

P216

Select metabolic and costimulatory bolt-on transgenes enhance chimeric receptor-bearing T cell activity against solid tumors

Luke Barron, PhD[1], Kathleen Whiteman[1], Madaline Gilbert[1], Tapasya Pai[1], Megan Snyder, BS[1], Michael Fray[1], Allison Nelson[1], Tyler Johnson[1], Kelsey Lakeman[1], John Shin[1], Ryan Boomer[1], Seth Ettenberg[1], Kathleen McGinness[1], Greg Motz[1]

[1]Unum Therapeutics, Cambridge, MA, USA

Background

The immunosuppressive features within solid tumors may limit the success of engineered T cell therapies. We sought to overcome key challenges in solid tumors by co-expressing novel transgenes in T cells bearing either Antibody-Coupled T cell Receptors (ACTRs) or Chimeric Antigen Receptors (CARs). We evaluated >100 metabolic and costimulatory genes for their ability to improve chimeric receptor T cell function in vitro and in vivo.

Methods

We compared the activity of T cells expressing parental ACTR or CAR constructs to T cells expressing these same parental constructs in combination with novel "bolt-on" transgenes. Constructs were virally transduced into primary human T cells. In vitro screening assays were developed to mimic a solid tumor microenvironment using common immunosuppressive factors like PGE2, TGF-beta, adenosine, kynurenine, low glucose, and immune-suppressive cells. T cell function was determined in these assays by monitoring T cell proliferation, IL-2 production, or resistance to chronic stimulation. In vivo anti-tumor activity was assessed against solid tumor xenograft mouse models.

Results

In vitro screening identified multiple classes of bolt-on costimulatory and metabolic genes that enhanced function in solid tumor-relevant assays in vitro. These genes represented diverse classes of costimulatory gene families and metabolic pathways, including glycolysis, the Krebs cycle, amino acid synthesis, and lactate pathways. Hits from in vitro screening were evaluated in tumor xenograft mouse models. Metabolism and costimulation bolt-on variants significantly improved activity over their respective chimeric receptor parents in both sensitive tumor models, where the parental construct is active and reduces tumor growth, and resistant tumor models where the parental construct is inactive. For example, the glucose transporter GLUT1 enabled bolt-on, but not parental, chimeric receptor-expressing T cells to proliferate in vitro despite limited glucose and cause regression of multiple solid tumor xenografts (Figure 1).

Conclusions

We have generated a panel of bolt-on transgenes to address challenges for T cells in the solid tumor microenvironment and evaluated a select set of these bolt-ons for their ability to enhance chimeric receptor T cell function, independent of parental chimeric receptor design. Variants were screened in assays established to mimic immunosuppressive aspects of solid tumors and in xenograft mouse models. We have shown that specific metabolism and costimulation bolt-on transgenes impart improved function to both ACTR- and CAR-expressing T cells relative to the parent chimeric receptor. Our results demonstrate a screening strategy to identify bolt-on transgenes that can overcome immunosuppressive challenges faced by T cell therapies in solid tumors.

Consent

This study was approved by Unum Therapeutics' Institutional Animal Care and Use Committee (IACUC), approval number 2016-04-004.

Figure 1.

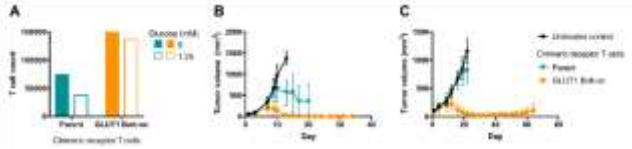

P217

Small molecule control of inducible MyD88/CD40 regulates Natural Killer cell expansion and anti-tumor activity

Joseph Bayle[1], Xiaomei Wang, PhD[1], Wei-Chun Chang, PhD[1], Daniel Jasinski, PhD[1], Jan Medina[1], Aaron Foster, PhD[1], David Spencer, PhD[1]

[1]*Bellicum Pharmaceuticals, Houston, TX, USA*

Background

The intrinsic anti-tumor activity of Natural Killer (NK) lymphocytes has the potential to be used as an allogeneic cell therapy with reduced GvHD risk relative to αβ T cells, however its potential has been limited NK by poor expansion in vivo. Previously, we developed a Chimeric Antigen Receptor-T cell (CAR-T) strategy that uses rimiducid-based dimerization of inducible MyD88/CD40 (iMC) to control T cell expansion and survival [1]. Here we demonstrate that iMC can also be applied to NK cell growth and anti-tumor efficacy in vitro and in vivo. Furthermore, an orthogonally regulated switch, rapamycin-inducible Caspase-9 (iRC9), was used to provide safety.

Methods

Human donor-derived PBMCs were selected for CD56 positivity, activated with IL-15 and K562 feeder cells, and transduced with γ-retrovirus encoding control iRC9-2A-ΔCD19, iRC9-2A-ΔCD19-2A-iMC (dual-switch NK) or iRC9-2A-IL-15-2A-ΔCD19-2A-iMC (dual-switch/IL-15 NK).

Results

In cell growth assays iMC-expressing dual-switch NK cells selectively outgrew iRC9-only NK cells, and this effect was further stimulated by 1 nM rimiducid (Figure 1). Inflammatory cytokine and chemokine production was also dramatically (10 to 1000-fold) elevated by the expression and activation of iMC in NK cells. In cocultures with THP1 acute myeloid leukemia cells at increasing Target:Effector (T:E) ratios, presence ($P < 0.001$, two way ANOVA) and activation ($P < 0.001$) of iMC dramatically increased tumor killing activity. Dual-switch NK anti-tumor activity was determined in xenografts of immunodeficient NSG mice bearing THP1 tumors (Fig 1). Unstimulated iMC with IL-15 or activation of iMC without IL-15 expression supported modest NK cell expansion, but rimiducid stimulation of iMC plus autocrine IL-15 showed enhanced NK expansion in vivo. Moreover, in tumor-free animals only dual-switch/IL-15 NK cells with weekly rimiducid stimulation expanded and persisted in vivo (up to 7 weeks). Cotransduction of a first generation CD123-targeted CAR to produce dual-switch/IL-15 CD123CAR-NK cells led to rimiducid-dependent control of THP1 tumor outgrowth in vivo beyond 40 days. Conversely, temsirolimus-mediated activation of the iRC9 safety switch rapidly (< 24 hours) ablated dual-switch NK cells in vivo.

Conclusions

Inducible MyD88/CD40 is an activation switch that supports NK cell expansion, persistence and anti-tumor activity in vitro and in vivo when paired with autocrine IL-15 expression. Tumoricidal activity can be further activated by target-specific CAR expression with safety controlled by the orthogonal iRC9 switch. This novel, regulated NK cell platform solves several of the challenges of NK cell-based therapy and should be readily translatable as an off-the-shelf cellular therapy for malignancies.

References

1. Foster, et al., Regulated expansion and survival of Chimeric Antigen Receptor-modified T cells using small molecule-dependent inducible MyD88/CD40. Molecular Therapy. 2017; 25: 2176-2188.

Figure 1.

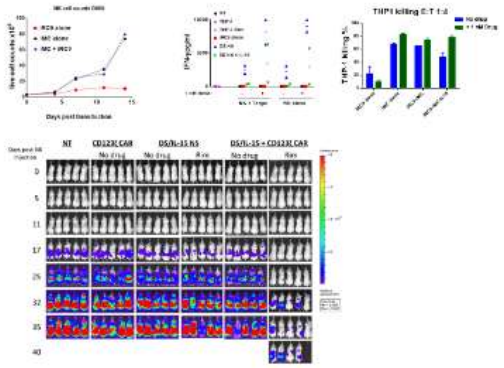

P218

Endogenous DAP10 provides optimal co-stimulation to NKG2D-based CAR T cells

Jennifer Bolsée[1], Eytan Breman, MSc[1], Thuy Nguyen[1], Sophie AGAUGUE, PhD[1], David Gilham, PhD[1]

[1]*Celyad, Mont-Saint-Guibert, Belgium*

Background

Chimeric antigen receptor (CAR) proteins are artificial proteins created by the fusion of an extracellular domain targeting one or several cell surface antigens, a hinge, a transmembrane domain and an intracellular part responsible for signal initiation and transmission to activate T cells. This part is usually composed of the intracellular domain of CD3ζ and one or two co-stimulatory domains (e.g. the cytoplasmic domain of CD28 and/or 4-1BB) leading to second and third generation CARs respectively. We developed a NKG2D-based CAR composed of the full length human NKG2D and the intracellular part of CD3ζ. NKG2D is a receptor expressed on NK cells and some T cell subsets,

existing as a dimer that interacts with a co-adaptor protein called DAP10. Upon interaction of NKG2D with one of its ligands, the DAP10 cytoplasmic tail induces downstream signaling and provides co-stimulation. Thus, the NKG2D-based CAR T cell (termed CYAD-01) despite appearing as a first-generation CAR, functions as a second generation. Here, we investigated whether CYAD-01 efficacy could be enhanced by the addition of costimulatory domains or overexpression of DAP10.

Methods

In this study, different NKG2D-based constructs were created and compared side by side to our current construct. Two different modifications of CYAD-01 CAR T cells were performed: DAP10 overexpression and addition of CD28 or 4-1BB co-stimulatory domains to generate "classical" CAR designs.

Results

Co-expression of DAP10 increased CAR expression at the surface of T cells without increasing IFN-γ secretion or cytolytic activity upon co-culture with target cells. Interestingly, addition of a co-stimulatory domain significantly decreased CAR expression, though that was not accompanied by any reduction in IFN-γ secretion or cytolytic activity when T cells were cultured with cancer cells. Further characterization of the cytokine secretion profile of the distinct CAR T cells by Luminex showed that no difference was observed in the cytokine secretion pattern in response to tumor cell lines or recombinant NKG2D ligands.

Conclusions

Our results uncover that the co-signaling delivered by the endogenous DAP10 is optimal for the in vitro NKG2D CAR T function, and that this signaling was as potent as traditional CD28 or 4-1BB based co-stimulation. Overexpression of DAP10 did not further affect CAR T cell function. These results pinpoint that CAR design is likely to be optimal for the generation of effective NKG2D-based CAR T cells. In vivo studies are ongoing to assess whether anti-tumor efficacy and persistence could be affected by overexpression of DAP10 or addition of co-stimulatory domains.

P219

SQZ'ing cells to engineer next generation antigen presenting cell (APC) therapies

Matthew Booty, PhD[1], Scott Loughhead[1], Kelan Hlavaty[1], Ildefonso Vicente-Suarez[1], Katarina Blagovic, PhD[1], Melissa Myint[1], Brittany Stokes, MS[1], Defne Yarar[1], Howard Bernstein, MD, PhD[1], Armon Sharei[1]

[1]*SQZ Biotechnologies, Watertown, MA, USA*

Background

The presentation of sufficient antigen on major histocompatibility complex class I (MHC-I) is a potential barrier to generating potent cancer immunization strategies. In this work, we use microfluidics-based Cell Squeeze® technology to deliver antigen directly to the cytosol of target APCs – resulting in the enhanced presentation of antigen on MHC-I. In addition to facilitating potent CD8+ T cell priming by professional APCs, this approach can make T cells effective, unorthodox APCs capable of priming CD8+ T cell responses in murine and human systems.

Methods

Protein and peptide antigens were delivered to the cytosol of purified murine or human T cells with Cell Squeeze®. The response to in vivo immunization was assessed by flow cytometry in a series of experiments using wild type C57BL/6 mice, MHC-I knockout mice, and/or adoptively transferred transgenic OT-I CD8+ T cells. Tumor experiments were conducted with the TC-1 cell line, which expresses the viral antigens E6 and E7 from human papilloma virus type 16 (HPV16).Human T cells were loaded with synthetic long peptides containing

antigens from cytomegalovirus (CMV) or HPV16. These T cells were co-cultured with epitope-reactive human responder CD8+ T cells, and interferon gamma production was quantified to assess antigen-specific responses in vitro.

Results

In murine systems, we demonstrate that Cell Squeeze® delivers protein antigen to T cells effectively and that the immunogenic epitope is processed and presented on MHC-I. When adoptively transferred in vivo, T cells squeezed with ovalbumin drive the expansion of CD8+ T cells in both transgenic (OT-1) and endogenous response assays. In a tumor model for HPV associated cancers, TC-1, E7 loaded T cells have strong anti-tumor effects both prophylactically and therapeutically. Following therapeutic immunization, the anti-tumor responses correlate with an increase in antigen-specific CD8+ tumor infiltrating lymphocytes compared to untreated mice. In human cells, we demonstrate that primary donor-derived unstimulated T cells can be effectively loaded with CMV and HPV16 antigens using Cell Squeeze®. These T cells are capable of stimulating antigen-specific CD8+ T cell responses in vitro using both T cell clones and patient-derived memory populations. The SQZ process has been scaled to engineer >1 billion T cells per minute in preparation for clinical translation.

Conclusions

Through the direct cytosolic delivery of antigen, we have engineered T cells to function as potent APCs. This strategy has demonstrated significant potential to generate CD8+ T cell responses in both murine and human systems and has been scaled up for clinical implementation.

Ethics Approval

Human samples were supplied by an approved vendor and animal studies were conducted in accordance with SQZ Biotech's Animal Care Program and IACUC which operate according to principles set forth in the PHS Policy, the Guide for the Care and Use of Laboratory Animals - 8th edition.

P220

Generating allogeneic CAR T cells without gene editing

Simon Bornschein, PhD[1], Alexandre Michaux, PhD[1], Susanna Raitano, PhD[1], Eytan Breman, MSc[1], Céline Jacques-Hespel[1], Fanny Huberty[1], Laura Saerens[1], Dorothée Daro[1], Steven Lenger, PhD[2], Hidevaldo Machado, PhD[2], Jonathan Moore, PhD[2], David Gilham, PhD[1]

[1]Celyad S.A., MONT-SAINT-GUIBERT, Belgium
[2]Horizon Discovery, Lafayette, CO, USA

Background

Current licensed CAR T products are an autologous therapy requiring collection, manufacture and formulation of the patients own T cells. Whilst clearly effective, there remain timely challenges to generate the cells (vein to vein) as well as a variability in patient's cells, resulting in manufacturing failure and product inconsistency.Allogeneic, off-the-shelf CAR T cell therapy is attractive since the cells are generated from a single healthy donor, thus maintaining consistency, reducing vein to vein time and allowing for treatment of multiple patients from the same manufactured batch. However, the main limitation of allogeneic therapy is the recognition of patient Human Leukocyte Antigen by the donor T cell receptor (TCR) driving Graft-versus-Host Disease (GvHD). Gene editing to eliminate the TCR is currently the most used approach in the allogenic CAR T cell field. Whilst efficient, there are potential limitations to gene-editing. Consequently, we have explored non-gene edited based technologies for their applicability in the allogeneic CAR T cell field.

Methods
To disrupt functionality of the TCR complex, we engineered a TCR inhibitory peptide, TIM, consisting of a truncated, signaling incompetent, form of CD3z. In parallel, several shRNAs were tested for their ability to reduce TCR expression by means of targeting the CD3 complex in primary T cells. The best shRNA candidates were also combined with TIM and all these types of engineered T cells were then tested in vitro for response against mitogenic antibody stimulation (OKT3) and in vivo for control of xenoGvHD in the NSG mouse strain.

Results
shRNA specific for CD3e and CD3z reduced expression of their relevant targets but also significantly reduced cell surface expression of the TCR by contrast to TIM. Interestingly, combining TIM with shRNA led to a recovery in TCR expression. Preliminary results indicate that T cells, engineered with non-genome editing technologies showed reduced in vitro mitogenic response when challenged with anti-CD3 antibodies. In vivo experiments also indicated an inhibition of GvHD with all those technologies when the T cells were adoptively transferred to the NSG mouse. The potency of the combination of TIM and shRNA and the comparison with gene edited knock-out of the TCR will be presented during the conference.

Conclusions
These experiments demonstrate that non-gene editing approaches to the generation of allogeneic CAR T cells using single vector approaches are feasible and may offer an attractive alternative to gene editing.

Ethics Approval
The study was approved by local authorities and the Ethics Board.

P221

The co-expression of a single shRNA targeting MICA and MICB with a NKG2D-CAR (CYAD-01) generates CAR-T cells resistant to target driven fratricide and improves CYAD-01 cell persistence in vivo

Simon Bornschein, PhD[1], Susanna Raitano, PhD[1], Jérôme Marijsse, master[1], Dorothée Daro[1], Steven Lenger, PhD[2], Hidevaldo Machado, PhD[2], Jonathan Moore, PhD[2], Sophie AGAUGUE, PhD[1], David Gilham, PhD[1]

[1]Celyad S.A., MONT-SAINT-GUIBERT, Belgium
[2]Horizon Discovery, Lafayette, CO, USA

Background
NKG2D is an activating receptor most commonly expressed on NK cells and subsets of T cells. NKG2D is known to engage 8 different stress induced ligands (NKG2DL) broadly present on tumors but largely absent on healthy tissue. T cells bearing a CAR consisting of the full human NKG2D receptor fused to the intracellular domain of CD3z (CYAD-01 T cells) specifically recognize and kill cancer cell lines derived from hematological and solid tumors in vitro and in vivo. These data have supported translation into phase 1 clinical trials. However, while working through the dose levels of these trials, it has become clear that the ability to manufacture large numbers of CYAD-01 T cells is problematic. The underlying reason appears to be self-killing (fratricide) mediated by the transient expression of NKG2DL on activated T cells. Given the potential breadth of ligand binding, our efforts have focused upon identifying the main NKG2DL that are expressed on activated T cells and to develop a translationally relevant strategy to modulate this expression. We then questioned whether this strategy enabled CYAD-01 T cells to avoid fratricide and thereby achieve an improved in vivo persistence.

Methods
Molecular and cellular analyses identified the key NKG2DL on activated T cells. We then explored specific targeting of the ligands through the co-expression of shRNA within the CAR vector to determine the subsequent impact upon in vitro and in vivo function of T cells bearing the NKG2D CAR.

Results
Of the eight NKG2DL, MICA and MICB were transiently expressed on activated T cells while ULBP1 was restricted to CD8+ T cells. There was little evidence of expression of the other ligands on T cells. Parallel studies having identified MICA and MICB as major stimulators of the NKG2D CAR, we screened shRNA to target these ligands. Two shRNA were identified that reduced cell surface expression of MICA/MICB. Engineering of a single vector encoding the NKG2D CAR and shRNA generated T cells that had much reduced in vitro fratricide, maintained NKG2D specific effector function and improved engraftment in NSG mice. The anti-tumor efficacy of these cells is currently under investigation and will be reported during the conference.

Conclusions
A single vector encoding the NKG2D CAR with a single shRNA generates CYAD-01 T cells that are resistant to CAR-T driven fratricide. We continue to explore the characteristics of these CAR T cells with the intention of translating to a clinical trial during 2019.

Ethics Approval
The study was approved by local authorities and the Ethics Board.

P222

Genetic engineering of tumour infiltrating lymphocytes (TIL) with a novel recombinant growth factor receptor for treatment of solid tumours

John Bridgeman, BSc, MSc, PhD[1], Michelle Le Brocq[1], Joanne McCaffrey[1], Tania Katopodi, PhD[1], Gemma Owens, MB BCh, BSc, MRes[2], Aysha Patel[1], Ryan Guest[1], Robert Hawkins[1]

[1]*Immetacyte Ltd, Manchester, UK*
[2]*University of Manchester*

Background
Lymphocytes isolated from tumour biopsies can be expanded ex vivo to huge numbers before readministration to patients whereupon theyimpart therapeutic benefit. So called Tumour infiltrating lymphocyte (TIL) therapy has proved hugely successful in numerous clinical trials for treatment of metastatic melanoma, and have also shown benefit in other indications. Persistence of therapeutic T-cells post infusion remains an issue which can be improved. In most situations preconditioning chemotherapy allows successful engraftment, and post-infusion IL-2 further potentiates the engraftment and persistence of T-cell infusions. However both treatments are associated with potentially severe toxicity and significantly increases the cost of treatment.

Methods
We have investigated the use of recombinant growth factor receptors to increase growth and survival of TIL. Recombinant growth factor receptors (rGFR) based on the thrombopoietin receptor (TpoR) were delivered to primary T-cells or TIL using lentiviral gene transfer. These engineered cells were then cultured with IL-2 or the agonist mimetic drug Eltrombopag. In some situations the engineered cells were coculcured with continuous patient matched

Melanoma or Ovarian tumour lines which were generated from dissociated tumour.

Results
Administration of the TpoR agonist mimetic drug Eltrombopag resulted in enrichment of engineered cells when cultured alone, furthermore, we observed enhanced growth and survival of engineered cells in an in vitro model of tumour targeting of melanoma and ovarian cancer against matched autologous tumour lines. We have further developed the basic receptor format to derive an optimised receptor with enhanced activity. We have also developed a method to deliver these rGFRs to TIL at high efficiency and in a GMP complient manner which will expedite their translation into a manufacturing process for clinical trial.

Conclusions
We have developed a technology based on the use of recombinant growth factor receptors which allows us to preferentially select engineered cells using a clinically available drug. We have demonstrated this technology in vitro in the setting of melanoma and ovarian cancer thus paving the way for use of this engineering approach in gene engineered TIL trials.

Ethics Approval
This study was approved by the UK Research Ethics Committee: Approval Number 169632

P223

In vitro analysis of Tumour Infiltrating Lymphocytes engineered with costimulatory antigen receptors delivering targeted costimulation

John Bridgeman, BSc, MSc, PhD[1], Michelle Le Brocq[1], Aysha Patel[1], Martina Sykorova[1], Tania Katopodi, PhD[1], Joanne McCaffrey[1], Ryan Guest[1], Robert Hawkins[1]

[1]*Immetacyte Ltd, Manchester, UK*

Background
Tumour infiltrating lymphocyte (TIL) therapy involves the ex vivo culture and expansion of lymphocytes - in particular T-cells – obtained from tumour biopsies, before readministration into the same patient. TIL therapy has proved effective in the amelioration of metastatic melanoma which has failed other standard treatment options, furthermore, trials in other cancer indications have shown encouraging results. As in other adoptive cell therapy settings, the anti-tumour response may, in certain circumstances, be inefficient, leading to tumour escape. This anti-tumour response may be subverted by the lack of adequate support signals delivered to the anti-tumour T-cells, for example, tumour cells rarely express any ligands for costimulatory receptors which are essential for full and sustained T-cell activation and cytokine secretion, the latter important for successful T-cell engraftment post infusion.

Methods
We have therefore sought to investigate the use of targeted costimulation, to this end T-cells were engineered using lentiviral vectors to express a chimeric costimulatory antigen receptor (CoStAR) which provides costimulation in response to defined tumour associated antigens. We have evaluated a number of target antigens across a spectrum of malignancies and have optimised assays using CoStARs targeting CEA and CA-125.

Results
Here we demonstrate that CoStARs targeting CEA (Colorectal, Gastric, Oesophageal) and CA-125 (Ovarian) enhance cytokine production upon engagement with their cognate antigen when signal 1 is delivered through the TCR. We have investigated a number of different CoStAR iterations with distinct signalling capacities and have optimised an engineering strategy which enables efficient delivery

of CoStAR to TIL in a GMP compliant manner.

Conclusions
Targeted costimulation offers a means to enhance the activity, survival and proliferation of TIL. Our strategy and efficient gene transfer technologies paves the way for clinical trial of CoStAR in a spectrum of cancer indications.

Ethics Approval
The study was approved by the UK Research Ethics Committee - approval number 169632

P224

Adoptive cell therapy using tumor infiltrating lymphocytes for the treatment of bladder cancer

Brittany Bunch, PhD[1], Matthew Beatty, PhD[1], Jennifer Morse, MS[1], Michael Kidd[1], MacLean Hall[1], Autumn Joerger[1], Charles Peyton[1], Mayer Fishman, MD, PhD[1], Amod Sarnaik, MD[1], Michael Poch[1], Shari Pilon-Thomas, PhD[1]

[1]H. Lee Moffitt Cancer Center, TAMPA, FL, USA

Background
Patients with advanced bladder cancer have limited therapeutic options and a median overall survival between 12 and 15 months. Apart from the recent FDA approval of checkpoint inhibitors for patients with metastatic disease, therapy options have not changed in decades. Adoptive cell therapy (ACT) using tumor infiltrating lymphocytes (TIL) has improved the median overall survival in patients with metastatic melanoma to 52 months. Our goal is to study ACT of TIL in bladder cancer using both human tumor specimens and in vivo studies.

Methods
TIL was expanded from resected lymph node metastasis or primary bladder tumors after radical cystectomy. Tumors were minced into fragments and plated in high dose IL-2 alone or in combination with agonistic 4-1BB. Reactivity was tested by co-culture with autologous tumor and IFN-gamma ELISAs. In vivo, mice were inoculated with syngeneic MB49 bladder tumor cells expressing OVA. Murine TIL was isolated from subcutaneous tumors and tested for reactivity by co-culture and IFN-gamma ELISAs. In mice bearing orthotopic MB49-OVA tumors, OVA-specific T cells were delivered intravesically. Tumor volume was monitored via ultrasound.

Results
We were able to expand TIL from 32 out of 39 primary and metastatic patient samples. Reactive TIL was detected in 19 out of 30 samples (63%, 2 samples did not have autologous tumor for testing). The addition of 4-1BB improved TIL expansion from primary tumors. In vivo, murine TIL isolated from subcutaneous tumors were reactive against tumor digest and MB49-OVA cell lines, but not against irrelevant tumor. Finally, we have determined that T cells can infiltrate into bladder tumors within 3 hours after intravesical delivery. Intravesical T cell delivery resulted in a decrease tumor burden compared with PBS treated mice.

Conclusions
From these studies we have demonstrated the feasibility of expanding reactive TIL from bladder cancer specimens. In addition, we have developed an in vivo murine model to study TIL therapy for the treatment of bladder cancer. Further studies will compare the response between systemic and intravesical delivery of TIL in vivo and characterize immune cell infiltrates within the tumor microenvironment.

Ethics Approval
These studies were approved by Moffitt Cancer Center's Ethics Board and USFs Institutional Animal Care and Use Committee .

P225

Adoptive cell transfer with NY-ESO-1 specific TCR T cells (TBI-1301) results in persistence, cytokine release syndrome and anti-tumor activity

Marcus Butler, MD[1], Valentin Sotov[1], Megan Nelles[1], Sarah Boross-Harmer[1], Luisa Bonilla[1], Sawako Elston[1], Michael Fyrsta[1], Diana Gray, MSc[1], Abha Gupta[1], Sevan Hakgor[1], Ausmeema Hossain[1], Michael Le[1], Darya Lemiashkova[1], Diane Liu[1], Charlotte Lo[1], Mark Comacho[1], Aaron Hansen[1], David Hogg, MD, FRCPC[1], Habeeb Majeed[1], Kiichi Murakami[1], Jessica Nie[1], Marc Ouellette[1], Albiruni Razak[1], Kendra Ross[1], Adrian Sacher, MD[1], Sam Saibil[1], Elizabeth Scheid[1], Anna Spreafico, MD PhD[1], Brendan Van As[1], Jennifer Yam[1], Pamela Ohashi, PhD[1], Shuichi Takahashi[2], Shinya Tanaka[2], Linh Nguyen, PhD[1]

[1]Princess Margaret Cancer Centre, Toronto, ON, Canada
[2]Takara Bio, Inc, Kasatsu, Japan

Background
TBI-1301 is a novel cell therapy product produced by engineering autologous lymphocytes to express an affinity-enhanced NY-ESO-1-specific TCR using a proprietary retrovirus vector that encodes siRNA to silence endogenous TCR expression. Previously, Kageyama et al. reported that the adoptive transfer of TBI-1301 could result in anti-cancer responses and cytokine release syndrome (CRS) in patients (ASH Annual Meeting, 2017). In parallel to this Japanese study, we are conducting a single site phase Ib study at the Princess Margaret Cancer Centre where patients with NY-ESO-1-expressing solid tumors are infused with NYESO-1 specific T cells (TBI-1301).

Methods
Eligibility for study participation includes informed consent, HLA-A*02:01 or A*02:06 haplotype, NY-ESO-1 expression confirmed by immunohistochemistry, disease progression, and lack of curative standard therapy. Eligible patients undergo phlebotomy to harvest PBMC which are then processed locally using the same standard operating procedures and reagents as used for the Kageyama study to generate engineered TBI-1301 cells. The study design is to manufacture and infuse 5x10^9 cells (day 0) to 9 patients following modest lymphodepletion with cyclophosphamide (750 mg/m2 on day -3 and -2). Endpoints include safety assessment, evaluation of efficacy, and biological correlates for persistence of NY-ESO-1 T cells post infusion.

Results
Thus far, 6 patients (1 endometrial cancer, 3 synovial sarcoma, 2 melanoma) have been enrolled and undergone study treatment. An additional 3 patients are undergoing manufacture (2 synovial sarcoma and 1 ovarian cancer). 5/6 treated patients received 5x10^9 cells while 1 patient with synovial sarcoma received 2.1x10^9 cells due to lower dose of manufactured cells. To date, no DLTs have been observed. Despite the lack of fludarabine in the lymphodepletion regimen, all 3 patients with synovial sarcoma experienced clinical and laboratory evidence of grade 1 CRS with increased CRP, ferritin, and IL-6 levels. CRS resolved spontaneously in 2 patients while the third received tocilizumab with rapid resolution of fevers. In this patient, grade 3 pain at his tumor site prolonged his admission. Thus far, 2 confirmed partial responses by RECIST have been observed. Moreover, biomarker analysis demonstrated transient reduction over 3 weeks in Tregs (CD4+CD25+CD127lowFoxp3+) and persistence of NY-ESO-1 specific T cells for greater than 100 days post infusion. Interestingly, persisting NY-ESO-1 T cells expressed CD27, as well as PD-1 and TIGIT.

Conclusions
TBI-1301 appears to be safe and to possess anti-tumor activity. Ongoing biomarker analysis will allow for further development of this technology and potential development of combination clinical trials.

Trial Registration
NCT02869217

Ethics Approval
The study was approved by the University Health Network Ethics Board, approval number 15-9534.

P226

Deep™ IL-15 primed multi-targeted T cells demonstrate potent antigen-specific cytotoxic activity against human cancer cells

Shawn Carey, PhD[1], Beth Pearce[1], Darren Smith[1], Pengpeng Cao, PhD[1], Christine McInnis, PhD[1], Amy Shaw[1], Jonas Bruun, PhD[1], FABIO FACHIN, PhD[1], Becker Hewes, MD[1], Jonathan Fitzgerald, PhD[1], Thomas Andresen, PhD[1], Andy Rakestraw, PhD[1]

[1]*Torque Therapeutics, Cambridge, MA, USA*

Background
Adoptive transfer of tumor-directed T cells has demonstrated encouraging clinical efficacy in some hematological and solid tumors. However, widespread success of such therapies has been limited by (1) single-epitope targeting by genetically modified TCR and CAR T cell therapies and (2) insufficient support of transferred T cell survival and function. To direct immune activation in the tumor microenvironment, Torque has developed the *Deep-Primed™* T cell therapy platform in which cytotoxic T lymphocytes (CTLs) simultaneously targeting multiple tumor associated antigens (TAA) are primed with immune-stimulatory drugs tethered to their surface to provide localized and sustained support to tumor-directed CTLs. This study evaluates cancer cell-directed cytotoxicity by multi-target CTLs with and without *Deep™ IL-15*, which is a cell-associated crosslinked multimer of human IL15-Fc.

Methods
CTLs directed against cancer cells expressing TAA including MART-1 or PRAME were generated from healthy donors using Torque's modular TAA-priming approach. CTL-mediated cytotoxicity was assessed using a panel of partially HLA-matched human cancer cells with diverse TAA expression. Cytotoxic activity was compared with and without Deep IL-15, and kinetic analysis of CTL function including expansion, activation, and cytotoxicity was used to provide mechanistic understanding of Deep IL-15 impact on anti-cancer cell activity by CTLs.

Results
Using time course mixed culture models, we show that Deep IL-15 enhances the performance of tumor-directed CTLs. MART-1-targeted and PRAME-targeted CTLs elicit specific cytotoxicity against human cancer cells expressing their respective antigen target, and Deep IL-15 augments this activity. Multiplexed analysis of CTL function revealed that this Deep IL-15-driven improvement in cytotoxicity is accompanied by IL-15-mediated CTL support both pre- and post-exposure to cognate antigen. First, Deep IL-15 provides autocrine signaling that drives survival and expansion of antigen-specific CTLs prior to antigen exposure, enabling a more robust CTL response against TAA-positive cancer cells upon encounter. Additionally, once Deep IL-15 primed CTLs are exposed to antigen, they show prolonged antigen-specific activation, survival, and expansion, as well as persistent antigen-specific cytotoxicity, indicating the Deep IL-15 improves the durability of anti-tumor activity.

Conclusions
Tumor-directed CTLs generated using Torque's modular TAA-priming approach elicit potent cytotoxicity against cancer cells expressing multiple TAA including MART-1 and PRAME. By acting as a cell-tethered cytokine source of bioactive IL-15, Deep IL-15 enhances CTL survival, proliferation, function, and cytotoxicity. Clinical trials evaluating TRQ15-01,

Torque's Deep IL-15 Primed multi-targeted T cells, will initiate later this year.

P227

Tethering IL-12 to the surface of T cells induces a broad immune activation and potent anti-tumor activity in mice without inducing systemic toxicities

De-Kuan Chang, PhD[1], Gulzar Ahmad[1], Jonathan Nardozzi, PhD[1], Douglas Jones, PhD[1], Thomas Andresen, PhD[1]

[1]*Torque Therapeutics, Cambridge, MA, USA*

Background

T cell-based immunotherapy has shown dramatic efficacy in some hematologic malignancies but translating these successes to solid tumors has been limited. A key challenge has been overcoming the immunosuppressive tumor microenvironment, which inhibits T cell activity and survival. Interleukin-12 (IL-12) holds strong potential for reshaping the anti-inflammatory environment in solid tumors. Its clinical utility, however, has been limited by severe toxicities both from systemic administration and from genetic engineering of tumor-specific T cells. To overcome these obstacles, we developed the Deep Primed< sup >TM< /sup > platform to anchor potent immune modulators on T cells to support immune activation in the tumor microenvironment. Our approach is versatile and enables tunable loading and persistence of IL-12 on the T cell surface.

Methods

Safety and efficacy profile of an engineered Deep IL-12 cytokine was evaluated in an immune-competent adoptive cell therapy model. Briefly, we utilized CD8 T cells from PMEL mice, which contain a T cell receptor specific to the gp100 antigen expressed in B16-F10 melanoma cells. Deep IL-12 was loaded ex vivo onto PMEL T cells and adoptively transferred into C57BL/6J mice bearing B16-F10 tumors. Here we present tumor growth inhibition, cytokine secretion, toxicity biomarkers, blood and tissue chemistry, and immune cell activity from adoptive transfer of tumor-specific T cells primed with Deep IL-12.

Results

Deep IL-12 significantly improved anti-tumor efficacy of adoptively transferred PMEL T cells against established B16-F10 tumors as compared with cell therapy alone or systemic co-administration of IL-12. Deep IL-12 increased peak expansion and long-term engraftment of PMEL T cells, without inducing expansion of circulating NK cells, which are believed to be a key mediator of IL-12 toxicity. There were no observed overt toxicities despite a modest, transient increase in circulating IFNg. Doses of Deep IL-12 more than 100-fold above the efficacious dose level similarly induced modest, transient circulating cytokine levels and did not induce overt toxicities in the form of body weight loss, suggesting a strong therapeutic window for Deep IL-12. Multiple doses of PMEL T cells loaded with Deep IL-12 further improved anti-tumor activity, in contrast to multiple doses of PMEL T cells in the absence of the Deep IL-12, which provided minimal anti-tumor activity.

Conclusions

Our data demonstrates that tethering IL-12 to the immune cell surface using Deep IL-12 dramatically improves the efficacy of tumor-targeted cell therapy, while mitigating toxicities associated with systemic IL-12.

P228

Novel electroporation method for T cells enables quick CAR-T cell manufacture

Jian Chen, PhD[1], Xiaofeng Xia, PhD[1]

[1]*Celetrix LLC, Manassas, VA, USA*

Background
CAR-T cells are currently manufactured for clinical use by infection of human T cells with viral vectors containing the CAR gene. T lymphocytes have to be stimulated and expanded ex vivo because the viral vectors infect fresh natural lymphocytes very poorly. The viral vector approach is extremely expensive due to the high cost of virus production and the high cost of long-term cell expansion that could take 10-14 days in a GMP facility. The viral vector approach also has a huge biological downside: ex vivo expanded T cells become bulky and lose efficacy against tumor cells. The use of electroporation technology in CAR-T cell manufacturing has attracted increasing interests for its low cost and the wide range of application including transposon based stable CAR expression, transient expression and genome editing. However, actual clinical use of electroporation technology in CAR-T has been difficult and several clinical trials have met significant problems due to the poor transfection efficiency and decreased T cell survival with traditional electroporation methods.

Methods
Through theoretical analysis of the other existing electroporation technologies, we found that they all have problems in electrophysical design. The problems include physical design of devices, electrical pulse selection, and buffer composition. The common electroporation cuvettes were changed to sealed cylindrical electroporation tubes. The buffer was also redesigned to support high efficiency and non-toxic electroporation. Specific protocols for PBMC were generated for the new electroporation system.

Results
With the new electroporation system, we can now achieve very high transfection efficiency for T cells while maintaining cell survival. For Sleeping Beauty transposon-based CAR expression, we found that over a period of two to three weeks the efficiency can get to 60% to 90% with fast cell proliferation. The protein expression time after electroporation is very short. For simple GFP plasmids we can observe GFP expression after only 30 minutes. Compared to other electroporation systems such as Amaxa Nucleofector, the new system produces at least two-fold increase in a combined efficiency/viability score.

Conclusions
Unlike viral vectors, electroporation works well on fresh natural T cells, thereby eliminating the need for expensive cell expansion and virus production altogether and cutting the huge economic burden of CAR-T therapy. By re-infusion of more natural T cells, the anti-tumor efficacy of CAR-T cells could be improved while the side effects of cytokine release syndrome could be minimized.

P229

Adapter mediated transduction with lentiviral vectors: A novel tool for cell-type specific gene transfer

Nicole Cordes, Master of Science[1], Carolin Kolbe[1], Thomas Schaser[1], Andrew Kaiser[1]

[1]*Miltenyi Biotec, Bergisch -Gladbach, Germany*

Background
Efficient and safe gene transfer is essential for immunotherapeutic applications like CAR T cell therapy. Restricting lentiviral vector entry to the cell type of interest increases safety and efficacy. This has been shown for lentiviral vectors pseudotyped

with measles virus envelope proteins (MV-LV). They are generated by ablating binding to the natural receptors and fusion of single-chain antibodies (scFV) specific for the target protein of choice to the viral envelope protein. Furthermore, MV-LVs enable gene transfer into quiescent T and B cells making it interesting for sophisticated applications. [1, 2]However, for each specificity a novel lentiviral vector has to be engineered and optimized. This process is laborious but also limited to the scFVs or targeting ligands that are available.

Methods

We describe here the development of a second generation MV-LV system in order to increase the flexibility and control of targetable lentiviral vectors. To this end, universally targetable MV-LV vectors were generated that are specific for a tag that is only present on adapter molecules that are specific for the antigen on the target cell.

Results

These vectors were shown to be functional in the presence of tagged adapter molecules. So far, tagged antibodies and antibody fragments (Fabs) were shown to be suitable adapter formats. No transduction was observed in the absence of adapter or in presence of untagged adapter molecules. Exclusive and selective transduction of the target population was demonstrated using marker gene transferring lentiviral vectors on co-cultures of cell lines. Flow cytometry analysis of transduced cells revealed a 100-1000 fold on-target to off-target ratio depending on the presence or absence of transduction enhancers. The flexibility and efficiency of the novel lentiviral vector system was demonstrated by changing the specificity and concentration of the adapter molecule. Selective transduction of CD4 and CD8 positive T cells within Pan T cells or even PBMC was initially shown with EGFP and confirmed with therapeutically active CARs. Furthermore, transduction of other relevant cell types like CD19 and CD20 expressing B cells as well as CD34 positive hematopoietic stem cells was demonstrated.

Conclusions

A highly selective, second generation lentiviral vector system was engineered that is superior in terms of flexibility and control. The gene transfer to the target cell population is now easily adjusted by using an antibody of choice, which renders laborious protein engineering obsolete. This adapter mediated transduction system may thereby be used for a variety of applications in the field of immunotherapy.

References

1. Funke S, et al. Targeted cell entry of lentiviral vectors. Mol Ther, 2008; 16(8): 1427-36.
2. Zhou, Q, et al. T-cell receptor gene transfer exclusively to human CD8(+) cells enhances tumor cell killing. Blood, 2012; 120(22): 4334-42.

P230

Identification of CD4+ and CD8+ T lymphocyte-epitopes from the cancer testis antigen Lactate dehydrogenase C

Julie Decock, PhD[1], Hibah Shaath[1], Remy Thomas[1], Salman Toor[1], Eyad Elkord, PhD[1]

[1]Qatar Biomedical Research Institute, Doha, Qatar

Background

Cancer testis antigens (CTA) form a large family of tumor-associated antigens that have gained interest as candidate targets for immunotherapy. Several CTAs have been shown to be re-expressed in tumor cells and to elicit spontaneous strong immune responses. Lactate dehydrogenase C (LDHC) is an archetypical CTA with a restricted expression in normal non-germline tissues. Upregulation of LDHC has been observed in a variety of cancer types and has been associated with a shorter progression free survival in renal cell carcinoma [1,2]. Preliminary

work in our group shows that LDHC is strongly expressed in breast cancer, thereby supporting its potential as a biomarker and/or immunotherapeutic target for breast cancer, including the aggressive triple negative breast cancer subtype.

Methods

A 15mer LDHC peptide library consisting of 81 peptides with an 11-residue overlap and different MHC preferences was subdivided into peptide subpools (PP) each containing 10-11 individual peptides. In vitro peptide stimulation of peripheral blood mononuclear cells from 7 healthy individuals was used to investigate cytotoxic immune responses against each subpool. Specific T cell responses were assessed using the interferon-γ ELISPOT assay and were defined positive if SFU/105 PBMCs ≥ 10. Multi-marker flow cytometry was used to phenotype the peptide-induced T lymphocytes as CD4+/CD8+ central memory cells (TCM), CD4+/CD8+ effector memory cells (TEM), naïve CD8+ cells and/or effector CD8+ cells.

Results

None of the donors tested HLA-A2 positive, warranting moderate resolution HLA typing of all donors in our study, which comprises the less well-studied Arab and Asian ethnic populations. We obtained a range of LDHC peptide-specific responses among the healthy donors. In 3 donors, no increase in IFN-γ release was observed. Donor 4 showed a response against PP2. Donor 2 showed responses against PP2, PP4 and PP5. Donor 3 and donor 7 showed responses to all peptide pools, with the highest responses against PP1, PP3 and PP6. Phenotyping of donor 3's immune response against PP1 demonstrated a marked increase in IFN-γ secreting CD4+/CD8+ TEM cells (CD45RA- CD45RO+ CCR7- CD62L-) and CD8+ TCM cells (CD45RA- CD45RO+ CCR7+ CD62L+). Further analyses using additional donors are ongoing, including peptide-pulsed dendritic cell assays and individual peptide response analyses.

Conclusions

We observed several cytotoxic immune responses against LDHC-specific epitopes, including an increase in central and effector memory CD8+ T lymphocytes in a female Arab donor. Although preliminary, these results suggest that LHDC could be a potential target for cancer immunotherapy in addition to being a potential biomarker.

References

1. Koslowski M, Türeci Ö, Bell C, Krause P, Lehr H-A, Brunner J, Seitz G, Nestle FO, Huber C, Sahin U. Multiple Splice Variants of Lactate Dehydrogenase C Selectively Expressed in Human Cancer. Cancer Res. 2002;62:6750–5.

2. Hua Y, Liang C, Zhu J, Miao C, Yu Y, Xu A, Zhang J, Li P, Li S, Bao M, Yang J, Qin C, Wang Z. Expression of lactate dehydrogenase C correlates with poor prognosis in renal cell carcinoma. Tumor Biol 2017;39:1010428317695968.

Ethics Approval

The study was approved by the QBRI-HBKU (approval number 2016-002) and Hamad Medical Corporation's Ethics Boards (approval number 17132/17).

P231

Uncovering the phenotype, the functional and homing properties of NKG2D CAR T cells

Benjamin Demoulin[1], Eytan Breman, MSc[2], Sophie AGAUGUE, PhD[2], David Gilham, PhD[2], Panagiota Sotiropoulou, PhD[2]

[1]*Celyad SA*
[2]*Celyad, Mont-St-Guibert, Belgium*

Background

T cells bearing a chimeric antigen receptor (CAR) consisting of the fusion of human NKG2D with the

intracellular domain of CD3zeta (CYAD-01) can bind eight stress ligands expressed in many cancers. Initial observations of clinical responses in patients with relapsed/ refractory AML after treatment with CYAD-01 (THINK clinical trial; NCT03018405) supports the potential of this therapeutic approach. To better understand CYAD-01, we performed a thorough characterization of CYAD-01 cells from both healthy donors and AML patients.

Methods

CYAD-01 cells were produced from healthy donors and AML patients. Cell culture parameters, as well as the T cell phenotype, the activation / exhaustion status and chemokine receptor expression were assessed at regular intervals during and at the end of the process. CYAD-01 cells were evaluated for their cytotoxic activity and cytokine production upon co-culture with cancer cell lines.

Results

CYAD-01 cells from healthy donors consisted predominantly of CD8+ T cells, while the CD4/CD8 ratio of AML-derived CYAD-01 cells was more heterogeneous. In both, CYAD-01 cells consisted mainly of effector memory T cells. The chemokine receptor profile of healthy donor-derived CYAD-01 cells showed relatively high levels of CXCR3, CXCR4 and CCR4 and lower levels of CCR3 for CD8+ cells, and additionally high levels of CCR10 for CD4+ cells. The expression of CXCR4 in particular, suggests that CYAD-01 cells may respond positively to chemokine signalling driving the T cells towards the bone marrow, potentially important for AML treatment. Upon co-culture with cancer cell lines or autologous blasts in an AML sample, CYAD-01 cells secreted high levels of IFN-γ. Upon target challenge, healthy donor-derived CYAD-01 cells secreted a broad array of cytokines including IL-2, IL-4, IL-6 and IL-17A.

Conclusions

CYAD-01 cells present as an activated, non-exhausted, predominantly effector memory T cell population. Interestingly, the expression of CXCR4 may support the ability of CYAD-01 cells to home to the bone marrow, an important property to facilitate targeting of AML leukemic stem cells. The breadth of cytokines produced by CYAD-01 cells confirms the ability of the NKG2D CAR to provide strong activation and co-stimulatory signalling. These results support the encouraging preliminary results from the THINK clinical trial.. Importantly, we are performing large scale investigation of patient material to investigate whether CYAD-01 cells can respond effectively to bone marrow chemokines and to understand if this feature is critical for the clinical responses seen to date in our THINK clinical trial. This will be presented during the conference.

P232

Differential effects of target ligands upon NKG2D CAR T cell activation.

Eytan Breman, MSc[2], Benjamin Demoulin[1], Eytan Breman, MSc[2], Martina Fontaine, PhD[2], Nancy Ramelot, Master[2], Sophie AGAUGUE, PhD[2], David Gilham, PhD[2], Panagiota Sotiropoulou, PhD[2]

[1]*Celyad SA*
[2]*Celyad, Mont-St-Guibert, Belgium*

Background

The Natural Killer group 2D (NKG2D) receptor binds to eight stress-induced ligands (NKG2DL): the major histocompatibility complex class I chain-related A and B (MICA, MICB) and the UL16 binding protein family (ULBP1-6). These ligands are absent from most normal tissues but frequently expressed in many tumors rendering NKG2D a promising means for cancer immunotherapy. We created a chimeric antigen receptor (CAR) T cell containing the full length human NKG2D fused to the CD3zeta signalling

domain (termed CYAD-01). As different ligand profiles may elicit differing responses to CYAD-01 cells, we investigated the effect on the distinct ligands on CYAD-01 function in vitro.

Methods

To elucidate whether a specific NKG2DL expression pattern is required for NKG2D-based CAR function, CYAD-01 cells were cocultured with cancer cell lines or in the presence of plate-bound NKG2DLs. Supernatants were harvested and analysed for cytokine secretion, and cytolytic activity was analysed by flow-cytometry.

Results

While most cell lines triggered cytotoxicity and cytokine production by CYAD-01 cells, there was a correlation of magnitude of response with relative MICA/B expression and no correlation with ULBP4 expression. To further understand the interaction of NKG2D with each specific ligand, CYAD-01 cells were cultured with individual plate-bound NKG2DL.Both MICA and MICB induced cytokine secretion by CYAD-01 cells from concentrations as low as 0.25 µg/mL, while 5µg/mL or higher concentrations of ULBP1, 2 or 3 were required. No cytokine production could be measured with ULBP4, 5 or 6. However, all the recombinant NKG2DL bound CYAD-01 cells as determined by flow cytometry. These data thus confirmed the trend observed with tumor cell lines.

Conclusions

Our data indicate that in a CAR-T context, MICA and MICB are potent activators of T cells engrafted with a NKG2D CAR, while ULBP1, 2 and 3 can induce NKG2D CAR T cell function. Recombinant ULBP4, 5 and 6 bind NKG2D but do not induce a strong effector response in vitro. Importantly, MICA and MICB are the predominant NKG2DL present in human tumors along with ULBP1 and 3. For instance, near 100% of AML blasts express one or more of these specific ligands. While the role of ULBP4,5 and 6 remains unclear, these observations demonstrate that there is a bias of ligand engagement by NKG2D CAR T cells towards target ligands that are broadly expressed across a wide variety of tumors making the approach highly attractive as a therapy.

P233

CD8+ tumor-infiltrating lymphocytes expanded from a NSCLC immunosuppressive environment display neoantigen-specific recognition

Lorenzo Federico, PhD[1], Andrea Ravelli[1], Cara Haymaker, PhD[1], Marie-Andrée Forget, PhD[1], Tatiana Karpinets, MS[1], Jason Roszik, PhD[1], Donastas Sakellariou-Thompson, BS[1], Young Uk Kim, PhD[1], Ankit Bhatta, MSc[1], May Celestino, BS, MA[1], Alexandre Reuben[1], Annikka Weissferdt[1], Ara Vaporciyan, MD[1], Mara Antonoff, MD[1], Garret Walsh[1], Phillip Andrew Futreal, PhD[1], Ignacio Wistuba, MD[1], Jack Roth[1], Zhang Jianjun[1], Emily Roarty, PhD[2], Lara Alvarez de Lacerda-Landry[1], Stephen Swisher, MD[1], Tina Cascone, MD, PhD[1], Gregory Lizee, PhD[2], John Heymach[1], Boris Sepesi, MD[1], Don Gibbons, MD[1], Chantale Bernatchez[1]

[1]MD Anderson Cancer Center, Houston, TX, USA
[2]MD Anderson, Houston, TX, USA

Background

The data presented here is part of the ImmunogenomiC prOfiling of Non-small cell lung cancer (ICON) project, a multigroup, cross-disciplinary prospective study designed to identify key immunophenotypic characteristics of early-stage non-small cell lung cancer (NSCLC).

Methods

Here, we report the results of ongoing analyses of multiparameter flow cytometry datasets and ex-vivo growth data of lymphocytes present in freshly resected fragments of tumors and matched uninvolved lung tissues from 133 patients. In addition, we present ELISPOT data providing

preliminary evidence of selective mutant peptide recognition by sorted CD8+ tumor-infiltrating lymphocyte (TIL) rapidly expanded from 4 patients.

Results

Comparison of immunophenotype data in a subgroup of tumor and uninvolved-matched lung tissues (N=53) revealed that cytotoxic CD8+ T cells were on average significantly less abundant in the CD3+ T-cell fraction of the tumor in comparison to uninvolved lung tissues (44% vs. 52%, $p< 0.01$). CD8+ TIL showed higher mean expression of ICOS (37.6% vs. 11.2%, $p< 0.000001$) and of the proliferation marker Ki67 (17.3% vs. 6.4%, $p< 0.00001$). In addition, the CD8+ TIL fraction was found to be composed of a larger percentage of PD1 (57.9% vs 32.5%, $p< 0.0001$), TIM3 (7.1% vs 3.0%, $p< 0.0001$), LAG3 (3.7% vs 0.4%, $p< 0.00001$), and CD103 (56.6% vs 26.2%, $p< 0.0001$) positive cells as compared to uninvolved lung tissues, and contained significantly less cells expressing granzyme B (6.3% vs. 27.3%, $p< 0.000001$) and perforin (2.3% vs. 19.1%, $p< 0.0000001$), indicating that TIL were activated but functionally inhibited.Unsupervised clustering analysis revealed that T-cell infiltrates from tumors grouped in two distinct phenotypic clusters mainly characterized by differential enrichment in LAG3, TIM3, Ki67, and ICOS expressing cells in both CD4+ and CD8+ non-resident (CD103-) T cell fractions. Moreover, tumors segregated according to the percentage of CD8+ TIL and their expression of PD-1.Successful TIL expansion (>12 million cells in 5 weeks) was achieved in 90 of 133 patients tested (67.7% success rate). IFNg ELISPOT analysis of TIL activation in response to predicted neoantigen peptide challenge identified TIL reactivity against 8 private mutations of potential interest in 3 of 4 patients tested suggesting that expanded TIL products contain reactive clones capable of selective neoantigen peptide recognition.

Conclusions

Our work indicates that in spite of a highly immunosuppressive microenvironment, TIL can be expanded from the majority of early-stage NSCLC patients, display possible specific reactivity toward mutated peptides, and could thus represent a possible therapeutic option for NSCLC patients.

Acknowledgements

We thank all the dedication of our research nurses Mary Ann Gianan and Craig DeGraaf, blood team Patrice Lawson, Heather Napoleon, Mayra Vasquez and Eric Prado, all thoracic OR nurses and anesthesiologists at MD Anderson Cancer Center, and Heidi Wagner, Elena Bogatenkova and the Institutional Tissue Bank team. We could not have completed this work without them. This work was supported by generous philanthropic contributions to The University of Texas MD Anderson Cancer Center Lung Cancer Moon Shots Program and by the NIH/NCI under award number P30CA016672 and used the Tissue Biospecimen and Pathology Resource, Research Histopathology Facility, Bioinformatics Shared Resource, and Biostatistics Resource Group). Special thanks to our patients and their families.

Ethics Approval

The study was approved by MD Anderson's IRB (LAB90-020, PA13-0589 and PA15-1112).

Consent

Written informed consent was obtained from the patient for publication of this abstract and any accompanying images. A copy of the written consent is available for review by the Editor of this journal

P234

NF-κB p50 deficient immature myeloid cell (p50-IMC) adoptive cell transfer activates the tumor microenvironment to slow tumor growth

Alan Friedman, MD[1], Rahul Suresh, PhD[1], Theresa Barberi, PhD[1], David Barakat, PhD[1], Kenneth Pienta, MD[1]

[1]*Johns Hopkins University, Baltimore, MD, USA*

Background

NF-κB p50 binds DNA, but unlike NF-κB p65, it lacks a trans-activation domain and recruits co-repressors. Absence of p50 results in activation of both macrophages and dendritic cells. Multiple solid tumors, including melanoma, fibrosarcoma, colon, prostate, pancreatic, and glioblastoma, exhibit impaired growth in syngeneic C57BL/6 p50-/- hosts, with M2-to-M1 tumor myeloid cell reprogramming and increased activated tumor T cells. We envision a cell-based therapy wherein patient-derived myeloid progenitors are expanded while targeting their p50 alleles, and then infused back into patients. Immature myeloid cells may localize to the tumor more effectively than mature macrophages. Administering chemotherapy prior to cell infusion may eliminate tumor myeloid cells, release neoantigens to encourage anti-tumor T cell activation, and reduce competing marrow-derived myeloid cell production.

Methods

Mice were inoculated with Hi-Myc prostate cancer (PCa), GL261-Luc GBM, or K-Ras(G12D)-Luc pancreatic ductal carcinoma (PDC) cells, the latter two orthotopically. 1-2 weeks later, mice received one intraperitoneal dose of 5-fluorouracil (5FU). 5 days later, lineage-negative marrow cells from p50-/- or WT mice that were expanded in media containing SCF/TPO/FL and transferred to M-CSF for one day were administered intravenously every 3-4 days (1E7 cells x 3). Tumor growth was monitored with calipers or IVIS imaging; myeloid and T cells were analyzed by flow cytometry.

Results

Mice bearing PCa showed significantly slowed tumor growth after receiving 5FU on d13 followed by p50-IMC on days 18, 21, and 25, versus mice receiving WT-IMC or 5FU alone (p=0.001), with ~5-fold reduced tumor volume on day 35. For mice implanted with GBM, 3 of 5 manifested very small tumors on day 21, in contrast to the control groups, and 4 of 10 PDC tumors shrank >10-fold in response to 5FU/p50-IMC. WT-IMC from CMV-Luc mice localized preferentially to tumor sites, with infused cells also in lung, spleen, and marrow. Progeny of CD45.2+ IMC were tracked in CD45.1+ tumor hosts. p50-IMC-derived CD11b+ myeloid cells were evident in prostate tumor, draining lymph nodes, spleen, and marrow, with tumor and nodal F4/80+ macrophages displaying an activated MHCII+CD11c+ phenotype. Total PCa CD8 T cells from 5FU/p50-IMC mice were ~5-fold higher than those from 5FU/WT-IMC mice, with increased IFNγ expression in response to PMA/ionomycin and increased surface PD-1, indicative of T cell activation and then exhaustion.

Conclusions

Adoptive cell transfer of murine p50-IMC, following a dose of 5FU, activates tumor myeloid and T cells to slow tumor growth and predicts the therapeutic utility of human p50-IMC against multiple solid tumors.

P235

STACT-TREX1: A novel tumor-targeting systemically-delivered STING pathway agonist demonstrates robust anti-tumor efficacy in multiple murine cancer models

Laura Glickman, PhD[1], Justin Skoble, PhD[1], Chris Rae, PhD[1], Anastasia Makarova, PhD[1], Marc D'Antonio[1],

Andrew McGeehan[1], Christopher Thanos, PhD[1]

[1]*Actym Therapeutics, Inc, Berkeley, CA, USA*

Background

Delivery of immunotherapy to directly activate tumor-resident immune cells is required to elicit durable anti-tumor immunity. To this end, we have generated a microbial-based immunotherapy platform (STACT- Salmonella Typhimurium and Checkpoint Therapy) that utilizes a highly attenuated strain engineered to: (a) enhance tumor-specific colonization due to auxotrophic consumption of immunosuppressive adenosine, (b) reduce TLR activation to enhance tolerability and limit immunosuppressive inflammation, (c) enable delivery of engineered RNAi towards any tumor/immune target of interest (alone or in combination), and (d) enhance plasmid maintenance and nuclear delivery. For our initial RNAi target selection, a STACT-TREX1 strain was designed. TREX1 is a 3' exonuclease immune checkpoint that degrades cytosolic DNA, thereby preventing it from binding cGAS and activating the STING pathway[1]. Mutations in TREX1 cause autoimmune disease and chilblain lupus, characterized by cGAS/STING-dependent overactivation of the type I interferon pathway[2,3]. Systemic delivery of small-molecule inhibitors targeting TREX1 are intractable due to its ubiquitous expression in healthy tissue. We have engineered our systemically-administered therapy to specifically deliver RNAi against TREX1 within the tumor microenvironment. This enables localized cGAS/STING signaling, production of type I interferon, and adaptive immunity against tumor neoantigens, rather than to the delivery vehicle itself.

Methods

A potent RNAi against murine TREX1 was selected by screening designed RNAi's for knockdown of TREX1 gene expression in HEK293 cells, as assessed by qPCR and western blot. A TREX1 RNAi-encoding plasmid was electroporated into an engineered, highly attenuated Salmonella strain with multiple chromosomal modifications that attenuate pathogenicity and enhance tumor-specific plasmid delivery. STACT-TREX1 was evaluated for therapeutic efficacy in subcutaneous CT26 and MC38 colon carcinoma models, and B16.F10 melanoma.

Results

Tumor-specific colonization of STACT-TREX1 therapy was observed after tail vein administration. For the dual flank model, distal tumor colonization was observed following intratumoral injection. The therapy was well tolerated, and found to be 1000-fold enriched in tumors relative to spleen and liver. In multiple single and dual flank tumor models, potent tumor growth inhibition and complete tumor regressions were observed. Immune correlates were consistent with STING activation, and the anti-tumor effect was shown to be CD8+ T-cell dependent.

Conclusions

A microbial immunotherapy engineered to stimulate the STING pathway in the TME demonstrated significant potency in several murine models of cancer. This therapeutic platform can address multiple solid tumor types without the need for antigen-specific targeting. Beyond TREX1, this platform can be engineered to accommodate combinations of immunostimulatory genes and immune checkpoints in a single therapeutic modality.

P236

Flower-code: A novel immunotherapy target

Rajan Gogna, PhD, MS, MBA[1], Christopher Pelham[2], Esha Madan, PhD, MS, MBA[1], Taylor Parker[3], Carlos Carvalho, MD[1], Antonio Beltran[1]

[1]Champalimaud Centre For Unknown, Lisbon, Portugal
[2]St. Louis College of Pharmacy, Lisbon, Portugal
[3]IUPUI, Simon Cancer Center, Libon, Portugal

Background

Cell competition is emerging as a strong concept that explains oncogenic growth as an outcome of competition between neoplastic and stromal cells[1-9]. The enhanced growth potential of cancer cells allows them to behave as super-competitors that eliminate the surrounding normal stromal cell populations. Elimination of normal cells increases space and availability of nutrients, thereby promoting oncogenic growth[1,4-5]. We hypothesize that human cancers are constantly competing with the surrounding stromal tissue, and they use mechanisms governed by cell competition genes such as Flower (C9ORF7). Expression of Flower protein is low in normal body; but is upregulated in cancers; Flower Win and Lose isoforms are expressed in tumor and surrounding stromal tissue, respectively (Fig-1a). This information suggests Flower may serve as a valuable target for cancer immune-therapy.

Methods

The functional epitopes of the Win and Lose isoforms of Flower proteins were identified and monoclonal and polyclonal antibodies were raised against those epitopes. Breast, colon, and squamous cell carcinoma FFPE cancer samples were IHC stained. The anticancer potential of anti-Flower monoclonal antibodies was observed in nude mice bearing patient-derived (PDX) triple negative breast (TN) cancer xenografts. The mice were treated with standard care of therapy for TN cancers. The treatment cycles included TAC (5mg/kg docetaxel, 1 mg/kg doxorubicin, 35 mg/kg cyclophosphamide, 1x week) administered in cycles (3 weeks on, 1 week off) to tumor-bearing mice. Tumor growth and mouse survival (120 days) were observed in presence and absence of anti-Flower Ab (80 mg/kg). The effect of this combination therapy was observed on tumor growth, mice survival, and frequency and sites of metastatic lesions.

Results

IHC results show that tumor tissue is enriched with Flower Win, whereas Flower Lose isoforms are present in the stromal tissue surrounding the tumors (Fig-1b). Results show a significant reduction in volume of TN PDX observed over a period of 45 days ($p<0.0001$). Further the KM curves reveal that the mice survival (over 120 days) was significantly longer in the Anti-Flower Ab + TAC compared with TAC alone ($P<0.0001$) and with controls ($P<0.0001$). Lastly, combination therapy resulted in a significant reduction in metastatic frequency to kidney, liver, lung, brain, axillary and inguinal lymph nodes ($P<0.0001$).

Conclusions

This preclinical study demonstrated a significant improvement of survival, metastatic events and tumor regression of triple negative patient-derived tumors in mice treated with monoclonal anti-Flower ABs, compared with TAC alone. Preliminary data reveals comparable results with colon and pancreatic PDX tumor models.

Acknowledgements

We acknowledge Champalimaud Research Foundation for supporting and funding this research.

References

1. Gogna R, Shee K, Moreno E. Cell Competition During Growth and Regeneration. Annu Rev Genet. 2015;49:697-718. Epub 2015/12/04. doi: 10.1146/annurev-genet-112414-055214. PubMed PMID: 26631518.
2. Penzo-Mendez AI, Chen YJ, Li J, Witze ES, Stanger BZ. Spontaneous Cell Competition in Immortalized Mammalian Cell Lines. PLoS One. 2015;10(7):e0132437. Epub 2015/07/23. doi: 10.1371/journal.pone.0132437. PubMed PMID: 26200654; PubMed Central PMCID: PMCPMC4511643.
3. Tamori Y, Deng WM. Tissue repair through cell competition and compensatory cellular hypertrophy in postmitotic epithelia. Dev Cell. 2013;25(4):350-63. Epub 2013/05/21. doi: 10.1016/j.devcel.2013.04.013. PubMed PMID: 23685249; PubMed Central PMCID: PMCPMC3891806.
4. Moreno E, Rhiner C. Darwin's multicellularity: from neurotrophic theories and cell competition to fitness fingerprints. Curr Opin Cell Biol. 2014;31:16-22. Epub 2014/07/16. doi: 10.1016/j.ceb.2014.06.011. PubMed PMID: 25022356; PubMed Central PMCID: PMCPMC4238900.
5. Levayer R, Moreno E. Mechanisms of cell competition: themes and variations. J Cell Biol. 2013;200(6):689-98. Epub 2013/03/20. doi: 10.1083/jcb.201301051. PubMed PMID: 23509066; PubMed Central PMCID: PMCPMC3601360.
6. Amoyel M, Bach EA. Cell competition: how to eliminate your neighbours. Development. 2014;141(5):988-1000. Epub 2014/02/20. doi: 10.1242/dev.079129. PubMed PMID: 24550108; PubMed Central PMCID: PMCPMC3929405.
7. Petrova E, Lopez-Gay JM, Rhiner C, Moreno E. Flower-deficient mice have reduced susceptibility to skin papilloma formation. Dis Model Mech. 2012;5(4):553-61. Epub 2012/03/01. doi: 10.1242/dmm.008623. PubMed PMID: 22362363; PubMed Central PMCID: PMCPMC3380718.
8. Petrova E, Soldini D, Moreno E. The expression of SPARC in human tumors is consistent with its role during cell competition. Commun Integr Biol. 2011;4(2):171-4. Epub 2011/06/10. doi: 10.4161/cib.4.2.14232. PubMed PMID: 21655431; PubMed Central PMCID: PMCPMC3104570.
9. Merino MM, Rhiner C, Portela M, Moreno E. "Fitness fingerprints" mediate physiological culling of unwanted neurons in Drosophila. Curr Biol. 2013;23(14):1300-9. Epub 2013/07/03. doi: 10.1016/j.cub.2013.05.053. PubMed PMID: 23810538.

Ethics Approval

All animal studies performed in this research are approved by Champalimaud Institutional Review Board and the Portuguese Gov Ethical board (DGAV), the approval number is 0421/000/000.

Figure 1.

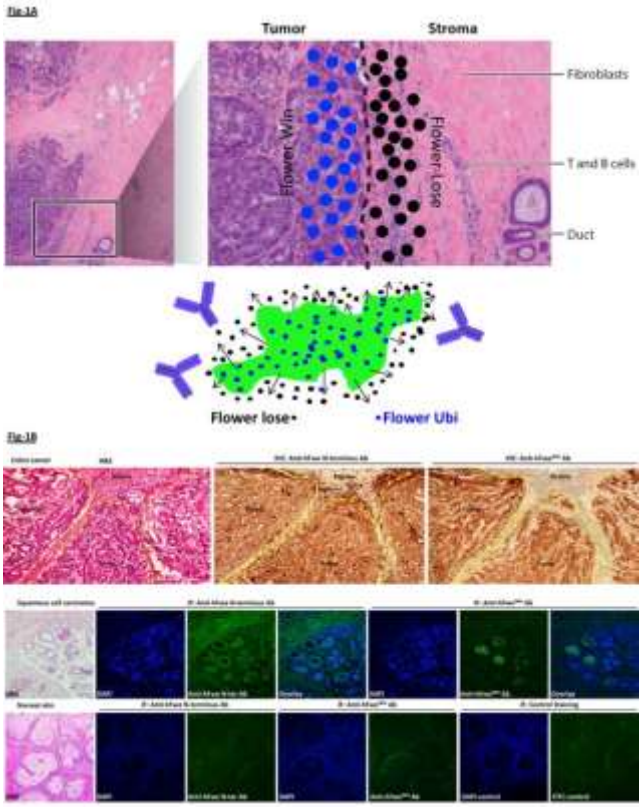

P237

CAR-modified killer MSC targeting GD2-positive Ewing sarcoma

Giulia Golinelli, PhD[1], Massimo Dominici[1], Giulia Grisendi[2], Carlotta Spano[2], Filippo Rossignoli[1], Malvina Prapa[1], Angela d'Esposito[1]

[1]*University of Modena and Reggio Emilia, Modena, Italy*
[2]*Rigenerand S.R.L., Modena, Italy*

Background
Ewing sarcoma (ES) is an aggressive mesenchymal-derived tumor representing the second most common malignancy in children and young adults. Despite a marked improvement in the prognosis of patients, the mortality caused by metastases and recurrent disease remains high calling for novel strategies to sustain remission and improve outcome. New avenues of research have been opened by using the pro-apoptotic agent TNF-related apoptosis inducing ligand (TRAIL) and cells carrying TRAIL close to tumor have shown to increase its bioavailability. Mesenchymal stromal cells (MSC) have been under investigation as vehicles for the delivery of anti-tumor agents. We previously demonstrated that MSC expressing TRAIL can induce apoptosis in a variety of sarcomas exerting also a relevant antitumor activity against in vivo models of ES. However, while the interaction between TRAIL and receptors is clear, more obscure is the manner in which MSC can selectively target tumors. As metastases are a great challenge in ES patients, dedicated strategies to drive MSC targeting and persistence to metastatic sites, particularly involving lungs in ES, shall be required. Here, in an effort to maximize the therapeutic profile of MSC TRAIL, minimize off-target effects and accounting for metastatic disease, we originally developed a strategy where TRAIL is delivered by MSC that are also modified by an anti-GD2 chimeric antigen receptor (CAR) to target GD2-positive ES cells.

Methods
The anti-GD2 CAR was expressed in MSC by viral transduction together with TRAIL. The anti-tumor activity of these functionalized MSC was in vitro assessed targeting GD2-positive or negative ES lines. The enhanced binding ability of functionalized MSC to GD2-positive ES cells and the specificity of interaction was investigated, as well, both in vitro and in vivo.

Results
The functionalized MSC expressed high levels of both TRAIL and CAR preserving a robust anti-tumor activity against ES lines. Most importantly, the functionalized MSC killing was further reinforced by an enhanced targeting thanks to improved cell-to-cell interactions. Based on in vitro findings, we started to assess the anti-GD2 CAR potential in an in vivo lung metastases ES model to better elucidate the advantage conferred by the CAR on MSC-based delivery.

Conclusions
Our results suggest that the CAR here described might be a powerful tool to redirect MSC carrying TRAIL against GD2-expressing tumors. This targeting strategy holds the promise to combine site-specific and prolonged retention of MSC in ES metastases, thereby providing a more effective delivery of TRAIL against this still incurable cancer even after metastatic dissemination.

Acknowledgements
The work is supported in parts by the "Associazione Italiana per la Ricerca sul Cancro" (AIRC, IG 2015), the Associazione Sostegno Ematologia Oncologia Pediatrica (ASEOP) and by "Progetto Dipartimenti Eccellenti MIUR 2017"

Ethics Approval
The study was approved by the Ministry of Health (Italy), approval number 1278/2015-PR.

P238

Regulation of in vivo anti-tumor activity of adoptively transferred CAR-T cells using FDA approved small molecule drugs

Jennifer Gori, PhD[1], Brian Dolinski, BS[1], Scott Heller, MS[1], Mara Inniss[1], Abhishek Kulkarni[1], Dan Jun Li, MD[1], Christopher Reardon[1], Dexue Sun[1], Karen Tran, MS[1], Michelle Ols, PhD[1], Jennifer Gori, PhD[1], Vipin Suri[1], Celeste Richardson[1], Steven Shamah, PhD[1]

[1]Obsidian Therapeutics, Cambridge, MA, USA

Background
Adoptive cell therapy with chimeric antigen receptor (CAR)-modified T cells has demonstrated clinical efficacy in the treatment of B cell malignancies and multiple myeloma. More widespread application of CAR-T cell therapy has been restricted by concerns about safety and observations of limited efficacy. Uncontrolled expansion of CD19-targeting CAR-T cells has caused severe CRS-related toxicity in many patients. Tumor antigen expression on healthy tissues can lead to on-target/off-tumor toxicity. Furthermore, prolonged antigen-dependent or independent CAR signaling may contribute to functional exhaustion, limiting efficacy. Adoptive transfer of T cells expressing a reversible, titratable, regulated CAR would support exogenous control of the level, activity, and timing of CAR expression for sustained anti-tumor efficacy and a more favorable safety profile. To exert control over CAR-T cells, we used destabilizing domain (DD) technology, fusing CAR to small protein domains which are unstable and degraded intracellularly but are reversibly stabilized by small molecule ligand binding, enabling exogenous control.

Methods
Using structure-guided engineering and mutagenesis screens, we identified mutations that destabilize human phosphodiesterase 5 (PDE5) protein and restabilize in the presence of FDA approved PDE5 inhibitors. To provide exogenous control over CAR-T cells, we fused destabilizing mutant-containing PDE5 domains (PDE5-DDs) to CD19-CAR (CD19-CAR-PDE5-DD), transduced human T cells with DD-modified CAR, and evaluated ligand dose-responsive CAR expression and activity. To evaluate anti-tumor activity in vivo, we implanted NSG mice with CD19+luciferase+Nalm6 cells and transplanted unmodified T cells or CD19-CAR-PDE5-DD T cells. We orally dosed mice with ligand or vehicle and monitored tumor growth by bioluminescent imaging to track tumor progression. We applied Kaplan-Meier analysis and the log-rank test to compare survival curves and median survival time.

Results
Human T cells transduced with CD19-CAR-PDE5-DD and treated with PDE5 ligands showed ligand-dependent CAR expression and activity in vitro. CD19 tumor-bearing mice treated with CD19-CAR-PDE5-DD T cells and stabilizing ligand showed a dose-dependent delay in tumor progression relative to ligand treated unmodified T cell recipients. Tumor growth inhibition was significant across ligand doses for CD19-CAR-PDE5-DD T cell recipients relative to unmodified T cell recipients. A significant survival advantage was observed in mice treated with CD19-CAR-PDE5-DD T cells relative to mice treated with unmodified T cells ($P<0.005$).

Conclusions
PPDE5-regulated CD19-CAR-T cell activity supported robust anti-tumor efficacy and increased survival in vivo. These preclinical studies demonstrate the potential to reversibly stabilize a DD-regulated CAR in vivo using FDA approved small molecules, toward enhancing safety and efficacy of CAR-T therapies for

the treatment of cancer

P239

Novel solid tumor gene therapy approach mediated by engineered Bifidobacterium longum generates efficient tumor-derived IL-12 expression and results in local and systemic anti-tumor immunity

Sheetal Raithatha[1], Umesh Ramachandran[1], Melissa Dennis[1], Elena Topchy[1], Steven Zhao[1], Alexander Graves[1]

[1]*Symvivo Corporation, Burnaby, Canada*

Background

Intravenous infusion of the probiotic obligate anaerobe, Bifidobacterium longum, selectively colonizes solid tumor tissues in preclinical models. Seeking to therapeutically exploit this observation, bifidobacteria was engineered to selectively shuttle plasmid DNA (pDNA) into solid tumor tissues resulting in membranous expression of therapeutically relevant transgenes such as interleukin-12 (IL-12).

Methods

An engineered, multi-domain fusion protein expressed locally by tumor-colonizing bacteria coordinates the binding and secretion of therapeutic pDNA molecules into the tumor microenvironment, mediating efficient genetic transfection of cancer cells, ultimately achieving tumor-derived expression of therapeutic genes. Membrane-bound IL-12 tumor expression was achieved in syngeneic mouse tumor models of colorectal cancer (CT-26) and melanoma (B16F10).

Results

In both models, B.longum engineered to deliver the IL-12 gene administered intravenously was well-tolerated and selectively colonized tumors. Robust and increasing expression of IL-12 was demonstrated within tumor tissues. Bacteria and/or transgene expression was undetectable in a comprehensive assessment of normal tissues. As predicted, IL-12 expression by the tumor resulted in the activation of both adaptive and innate immune responses. Increased pro-inflammatory cytokine levels and elevated tumor CD8+/Treg ratios were associated with the recognition of cancer specific antigens. B.longum mediated IL-12 gene delivery significantly inhibited tumor growth and combination therapy with anti-PD1 and anti-CTLA4 synergistically improved these outcomes.

Conclusions

Taken together, selective bacterial colonization of solid tumors employing intravenously-infused, genetically-engineered B.longum achieves robust and enduring tumoral expression of therapeutically relevant genes such as IL-12. A first-in-human clinical trial is planned for 2019.

Table 1.

Table 1. Biodistribution of engineered *B.longum* upon intravenous infusion

	SALINE (CFU/g)			Engineered *B. longum*:IL-12 (CFU/g)		
TISSUE	10 Days Post	16 Days Post	30 Days Post	10 Days Post	16 Days Post	30 Days Post
Tumor	0	0	0	$1.1x10^{8}$	$2.0x10^{7}$	$6.0x10^{7}$
Liver	0	0	0	0	0	0
Kidney	0	0	0	0	0	0
Lung	0	0	0	0	0	0
Spleen	0	0	0	0	0	0
Heart	0	0	0	0	0	0
Brain	0	0	0	0	0	0
Blood Cell Pellet	0	0	0	0	0	0
Blood Plasma	0	0	0	0	0	0

Figure 1.

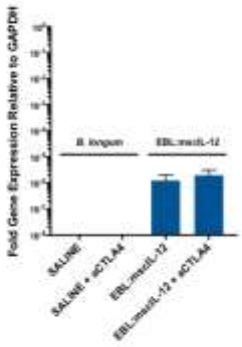

Figure 1. qRT-PCR analysis of IL-12 transgene expression in tumor tissues. aCTLA4 corresponds to anti-CTLA-4 therapy, and EBL:mscIL-12 corresponds to the engineered *B.longum* delivering the single chain Il-12 fusion gene.

Table 2.

Table 2: qRT-PCR analysis of transgene expression in tumor and non-tumor tissues

Tissues	SALINE	bacTRL:X3
TUMOR	0/3	3/3
BRAIN	0/3	0/3
HEART	0/3	0/3
KIDNEYS	0/3	0/3
LUNGS	0/3	0/3
LIVER	0/3	0/3

Figure 2.

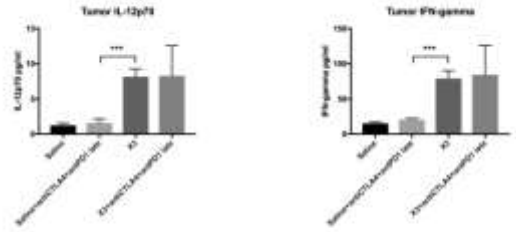

Figure 2. Intratumoral cytokine levels quantified using ELISIA analysis. X3 corresponds to engineered *B.longum* delivering the single chain Il-12 fusion gene

Figure 3.

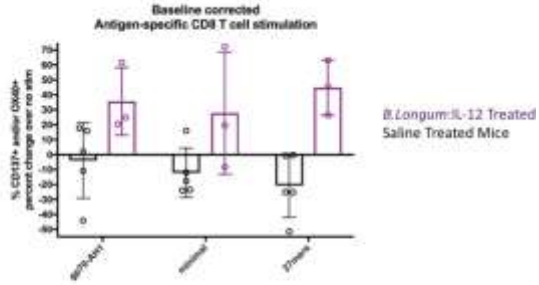

Figure 3. T-cells isolated from spleen and stimulated with synthetic neo-antigens (gp70, minimal and 27mers), proliferation above baseline reported. Flow cytometric analysis of activation markers on CD8+ T-cells.

Figure 4.

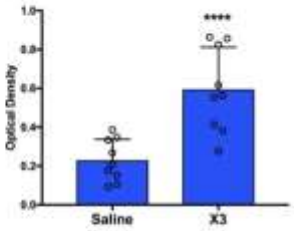

Figure 4. Circulating anti-tumor antibodies in mice treated with B.longum:IL-12. Plasma from each treatment arm was analyzed for anti-CT-26 antibodies by ELISIA. X3 corresponds to engineered *B.longum* delivering the single chain Il-12 fusion gene

Figure 5.

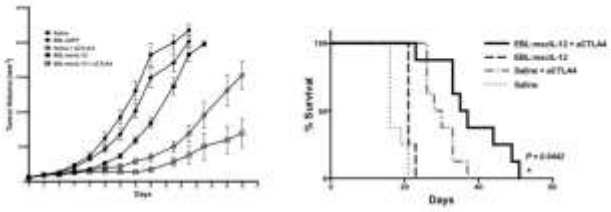

Figure 5. Anti-tumor effects of *B.longum*:IL-12 alone and in combination with anti-CTLA-4 in CT-26 tumors.

Figure 6.

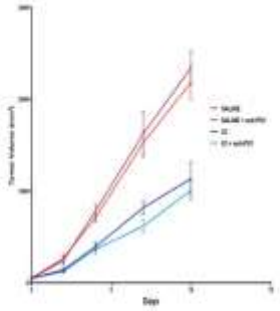

Figure 7. Anti-tumor effects of *B.longum*:IL-12 alone and in combination with anti-PD1 in B16F10 tumors.

P240

Autologous Epstein-Barr virus (EBV)-specific T cells (baltaleucel T): preliminary results from a multicenter, multinational phase 2 study for treatment of EBV-associated NK/T cell lymphoma

Kurt Gunter, MD[1], Yasuhiro Oki, MD[2], Won Seog Kim[3], Kirit Ardeshna, MB BChir MA MD FRCP FRCPath[4], Yi Lin, MD PhD[5], Jia Ruan, MD, PhD[6], Pierluigi Porcu, MD[7], Jonathan Brammer, MD[8], Eric Jacobsen, MD[9], Dok Hyun Yoon, MD[10], Cheolwon Suh, MD PhD[10], Felipe Suarez, MD PhD[11], John Radford, MD[12], Lihua Budde, MD PhD[13], JIN SEOK Kim, MD PhD[14], Gilles Salles, MD[15], Hun Ju Lee, MD[2], Catherine Bollard, MD[16], Arnaud Jaccard, MD PhD[17], Hye Jin Kang, MD PhD[18], Shannon Inman, BS[1], Maryann Murray[1], Katherin Combs, RN[1], Daniel Lee, MD PhD[19], Ranjana Advani, MD[20], Center director Rooney, PhD[21], Helen Heslop, MD[21]

[1]Cell Medica Inc, Houston, TX, USA
[2]MD Anderson Cancer Center, Houston, TX, USA
[3]Samsung Medical Center, Seoul, Korea, Republic of
[4]University College London Hospitals, London, UK
[5]Mayo Clinic, Rochester, MN, USA
[6]Weill Cornell Medical School, New York, NY, USA

[7]Thomas Jefferson University, Philadelphia, PA, USA
[8]The Ohio State University, Columbus, OH, USA
[9]Dana Farber Cancer Institute, Boston, MA, USA
[10]Asan Medical Center, Seoul, Korea, Republic of
[11]Hôpital Universitaire Necker, Paris, France
[12]University of Manchester, Manchester, UK
[13]City of Hope National Medical Center, Duarte, CA, USA
[14]Yonsei University College of Medicine, SEOUL, Korea, Republic of
[15]Centre Hospitalier - Université de Lyon, Pierre Benite, Auvergne, France
[16]Children's National Medical Center, Houston, TX, USA
[17]CHU de Limoges, Limoges, France
[18]Korea Cancer Center Hospital, Seoul, Korea, Republic of
[19]Houston Methodist Research Institute, Houston, TX, USA
[20]Stanford Cancer Institute, Stanford, CA, USA
[21]Baylor College of Medicine, Houston, TX, USA

Background

Advanced NK/T-cell lymphoma (NKTL) is a rare lymphoma associated with EBV expression and an aggressive course. Standard treatment for advanced disease involves asparaginase based regimens, however relapses are common. Herein we report early results from a phase 2 study (CITADEL, NCT01948180) of autologous EBV-specific T cells (baltaleucel T) for the treatment of NKTL.

Methods

The study was conducted in France, South Korea, the UK and the US. Patients with relapsed NKTL who had received prior asparaginase based therapy were eligible. 200 mL of whole blood was collected from the patient and the product was manufactured using EBV peptide stimulation and cytokines. Patients received 2 to 5 doses of 2x10e7 CD3+ cells/m2. The primary endpoint was overall response rate (ORR) by Lugano criteria, as assessed by independent review.

Results

As of 10 April 2018, 15 patients with relapsed NKTL were administered baltaleucel T, either as adjuvant therapy for patients without measurable disease due to bridging chemotherapy during manufacturing (n=5) or as treatment for patients with measurable active disease (n=10). Manufacturing success rate was approximately 71% under current release specifications. Two serious adverse events (AEs) (lymphoma pain and hyperbilirubinemia) were observed and attributed as possibly related to baltaleucel T. There were 10 unique non-serious product-related AEs of mild/moderate severity observed in 3 patients. No cytokine release syndrome or neurotoxicity was observed. Of the 5 patients with non-measurable disease, 2 remain on study without disease progression while 3 progressed. Of the 10 patients with measurable disease, 8 patients were evaluable for response and 2 patients withdrew early due to progression. In the predefined evaluable population (patients with measurable disease and imaging at 8 weeks), the ORR is 62.5% (5/8), and in all patients with measurable disease 50% (5/10). In the responding patients, the best response was 3 complete remissions (CRs) and 2 partial remissions (PRs). Median duration of response (DoR) was 3.5 months by Kaplan-Meier analysis. (DoR censored for hematopoietic stem cell transplantation or ongoing response.) For all 15 patients, the median overall survival (OS) is 13.4 months and the OS at 1 year is 60% with a median follow up 10.0 months (Figure 1). All responding patients remain alive.

Conclusions

Our study demonstrates feasibility, clinical activity and safety of administration of single agent autologous EBV-specific T cells in patients with advanced, relapsed NKTL in a multicenter, multinational trial. These results require validation in a larger cohort.

Acknowledgements
We thank the participating patients and their families.

Trial Registration
NCT01948180

Ethics Approval
The study was approved by all applicable institutional review boards and ethics committees.

Figure 1: CITADEL OS estimated by Kaplan-Meier method (n=15)

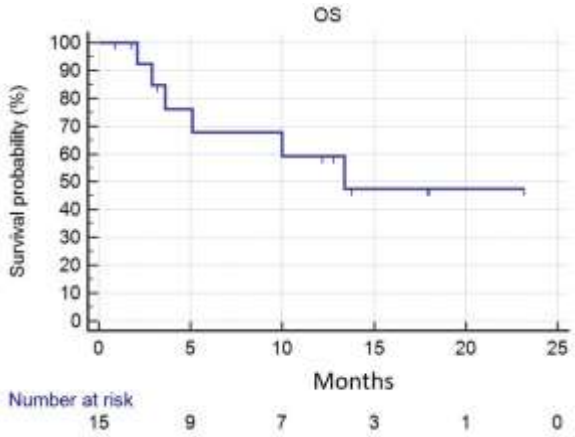

P241

Melanoma-derived human CD4+ tumor-infiltrating lymphocytes (TIL) demonstrate a functional response to autologous tumor

MacLean Hall[1], Autumn Joerger[1], Ellen Scott[1], Ben Schachner[1], Allison Richards[1], Valerie Stark[1], Jeani Rich[1], Amy Weber[1], Doris Wiener[1], Krithika Kodumudi, PhD[1], Matthew Beatty, PhD[1], Amod Sarnaik, MD[1], Shari Pilon-Thomas, PhD[1]

[1]*Moffitt Cancer Center, Tampa, FL, USA*

Background
Current strategies of Adoptive Cell Therapy (ACT) with Tumor-Infiltrating Lymphocytes (TIL) involve the expansion and selection of tumor-reactive CD8+ T cells for infusion into metastatic melanoma patients. Recent studies point to an expanded role of CD4+ T cells in anti-tumor immunity, warranting further investigation into the function and potential efficacy of this underexplored TIL population. [1,2]

Methods
TIL were isolated from surgically resected tissues from patients with metastatic melanoma at Moffitt Cancer Center. TIL were expanded in media containing IL-2 and subjected to the Rapid Expansion Protocol (REP). CD4+ and CD8+ TIL were isolated using magnetic bead negative selection. TCRbeta sequencing was performed using Adaptive Biotechnologies AdaptImmune platform. CD4+ TIL were stimulated with autologous tumor or dendritic cells (DC), or anti-CD3/CD28 and assayed for cytokine production by ELISA and flow cytometry.

Results
A complete response (CR) was achieved following infusion of predominantly (88%) CD4+ TIL in one metastatic melanoma patient. TCRbeta analysis showed a 64.4% overlap between CD4+ infused TIL clones and peripheral blood two weeks after adoptive transfer, which declined to 2.3% at six weeks. CD4+ TIL from 11 additional patients stimulated with anti-CD3/CD28 showed a pleiotropic cytokine repertoire (IFN-gamma, TNF-alpha, IL-5, IL-6, and IL-13), which was confirmed by flow cytometry. Responders (n=4) displayed an elevated Th1/Th2 cytokine profile compared to non-responders (n=7; p=0.0725). CD4+ TIL from four additional patients displayed robust IFN-gamma production in response to DC loaded with autologous tumor. Upregulation of MHC class II on autologous tumor cells stimulated CD4+ TIL to produce both IFN-gamma (4.0%) and TNF-alpha (5.9%). Recognition of autologous tumor was diminished in the presence of antibody blockade of MHC class II.

Conclusions
CD4+ TIL persisted in vivo and demonstrated a MHC class II-restricted response to autologous tumor, marked by a Th1 polarized cytokine profile. These data support further examination of the mechanisms by which CD4+ TIL may improve therapeutic efficacy in ACT.

References
1. Bailey SR, et al. Human CD26high T cells elicit tumor immunity against multiple malignancies via enhanced migration and persistence. Nat Commun. 2017; 8(1): 1961.
2. Tran E, et al. Cancer immunotherapy based on mutation-specific CD4+ T cells in a patient with epithelial cancer. Science. 2014; 344(6184): 641-5.

Ethics Approval
MCC15781 was approved by USF IRB approval number Ame5_P112

*Corresponding author email: m.rucevic@olink.com5.MCC16992 was approved by Advarra IRB approval number 14.03.0083.MCC17057 was approved by USF IRB approval number Ame13_Pro00009061.MCC18377 was approved by Advarra IRB approval number MOD00206092.

P243

Tumour infiltrating lymphocyte therapy: clinical outcomes in pre-treated metastatic melanoma patients and biomarker correlations

Robert Hawkins, MD, PhD[1], Manon Pillai, MB BS MD[1], Ryan Guest[2], Natallia Kirillova[2], Paul Lorigan[1], Michelle Le Brocq[2], John Bridgeman, BSc, MSc, PhD[2]

[1]*Chrisitie Hospital, Manchester, UK*
[2]*Immetacyte Ltd, Manchester, UK*

Background
Adoptive cell therapy (ACT) with tumour infiltrating lymphocytes (TIL) has consistently demonstrated impressive clinical results in several studies in the management of metastatic melanoma. For patients who progress on current therapies (checkpoint inhibitors and B-RAF inhibitor based therapy) the outlook is poor and there is a clear unmet medical need. We describe our experience as the only UK cancer centre providing TIL therapy.

Methods
TIL are cultured from resected tumour samples as previously described. The process is GMP compliant with cells manufactured under an MHRA specials licence and the process is applicable to large scale use. Infusion is preceded by non-myeloablative lymphodepleting chemotherapy (high dose cyclophosphamide and fludarabine) and followed by intravenous high dose interleukin 2 (HD-IL2). A range of biomarkers were assessed for potential correlation with outcome.

Results
Nineteen patients with progressive metastatic cutaneous melanoma who have failed other therapies have been treated to date. All patients had metastatic disease and were heavily pre-treated with a combination of targeted agents and immunotherapies (anti-CTLA4 and anti-PD1 antibodies). 11/19 (57%) achieved an objective clinical response according to the response evaluation criteria in solid tumours. 4/19 (21%) achieved a complete response and all of those are on-going (18+ to 72+ months). Treatment is well tolerated. All patients experienced anticipated toxicities associated with pre-conditioning chemotherapy and HD-IL2, which were short lived and manageable on the medical ward. The only autoimmune toxicity seen is vitiligo and there was no clinically significant cytokine release syndrome seen. The median overall survival is 15 months but several patients also had prolonged stable disease or partial responses and there is a plateau in the Kaplan-Meir survival curve with estimate 5 year survival of 40%. A

range of biomarkers correlate with response and survival.

Conclusions

We show that at our centre lympho-depleting chemotherapy followed by transfer of TIL and HD-IL2 is feasible and clinically effective, demonstrating tumour regression in over 50% of patients with metastatic cutaneous melanoma. Importantly long-term durable responses were seen including 21% complete durable remissions. Overall, there is clear durable clinical benefit in a group of patients with no other good current options for therapy. Biomarker analysis suggest the potential to select patients for treatment and way to improve the outcome even more. Base on pre-clinical data (1,2) we are also starting to explore TIL based therapy and engineered TIL in other cancers.

References

1. Owens GL, Price MJ, Cheadle EJ, Hawkins RE, Gilham DE, Edmondson RJ. Ex vivo expanded tumour-infiltrating lymphocytes from ovarian cancer patients release anti-tumour cytokines in response to autologous primary ovarian cancer cells. Cancer Immunol Immunother. 2018 Jul 23; doi: 10.1007/s00262-018-2211-3. 2. Baldan V, Griffiths R, Hawkins RE, Gilham DE. Efficient and reproducible generation of tumour-infiltrating lymphocytes for renal cell carcinoma. Br J Cancer. 2015 Apr 28; 112(9):1510-8.

P244

Reactive myelopoiesis triggered by lymphodepletion limits the efficacy of adoptive T cell therapy

Patrick Innamarato, BS[1], Shari Pilon-Thomas, PhD[1], Krithika Kodumudi, PhD[1], Amy Weber[1], Amod Sarnaik, MD[1], Doris Weiner[1], Jennifer Morse, MS[1], Michael Kidd[1], Patrick Verdugo[1]

[1]Moffitt Cancer Center, Tampa, FL, USA
[2]University of South Florida, Tampa, FL, USA

Background

Lymphodepleting chemotherapy administered before adoptive T cell therapy (ACT) enhances anti-tumor immune responses by increasing availability of cytokines necessary for the persistence and function of infused T cells. However, the induction of lymphopenia by nonmyeloablative chemotherapy also initiates the rapid expansion of highly immunosuppressive myeloid derived suppressor cells (MDSCs) that inhibit anti-tumor responses elicited by adoptively transferred T cells. Here, we investigated the role of lymphodepletion-induced MDSCs (LD-MDSCs) on ACT using mouse models and patients that received autologous tumor infiltrating lymphocytes (TIL).

Methods

In B16 tumor-bearing mouse models, single doses of cyclophosphamide and fludarabine were used to induce lymphodepletion. T cell proliferation was assessed by co-culturing MDSCs from C57BL/6 (WT) and IL-6KO mice and ACT models were carried out using donor pmel T cells. MDSC frequency and function were evaluated in a cohort of melanoma patients that received ACT with TIL pre- and post-infusion using flow cytometry and co-culture assays.

Results

Using mouse models, we show that the ability of IL-6KO MDSCs to suppress T cell proliferation is no different compared to WT mice. However, upon lymphodepletion the suppressive capacity of IL-6KO MDSCs is significantly attenuated, indicating that MDSCs arising after lymphodepletion are dependent on IL-6 signaling. We then confirmed these findings in a myeloid-specific IL-6R knockout model (IL-6RM-KO). In ACT models, we demonstrate that IL-6KO and IL-6RM-KO recipient mice exhibit significant delays in tumor growth and increased survival compared to WT mice receiving ACT. Melanoma patients that

received ACT with TIL exhibited a dramatic increase (3-250 fold) of MDSCs one week after treatment with lymphodepleting chemotherapy and TIL infusion compared to the pre-treatment frequency. Serum levels of IL-6 in these patients are also elevated compared to healthy donors. At one week post-infusion of TIL, we assessed 24 patient PBMCs and show that patients with <10% PMN-MDSCs have improved overall survival, progression-free survival, and objective response rates. Furthermore, we show that at week one and week two post-infusion, one patient exhibited >60% PMN-MDSCs (CD15+LOX-1+CD11b+) that inhibited T cell proliferation, expressed IL-6R, PD-L1, and high levels of ROS.

Conclusions

Together, these data suggest that targeting IL-6 signaling inhibits the immunosuppressive functions of MDSCs in a lymphodepleted setting and may enhance the efficacy of ACT with TIL. To our knowledge, this is the first study to demonstrate that MDSCs have a significant impact on the survival of patients receiving adoptive T cell therapy.

Ethics Approval

All animal protocols were reviewed and approved by the Institutional Animal Care and Use Committee at the University of South Florida. MCC15781 was approved by USF IRB approval number Ame5_P112

*Corresponding author email:
m.rucevic@olink.com5.MCC16992 was approved by Advarra IRB approval number 14.03.0083.MCC17057 was approved by USF IRB approval number Ame13_Pro00009061.MCC18377 was approved by Advarra IRB approval number MOD00206092.

P245

Enrichment of rare antigen-specific CD8+ T cells directly from splenocytes improves output and throughput

Ariel Isser[1], John Hickey, BS[1], Kayla Gee[1], Sebastian Salathe[1], Yi Dong[1], Jonathan Schneck, MD, PhD[1]

[1]*Johns Hopkins University, Baltimore, MD, USA*

Background

Adoptive immunotherapy, which involves expanding a patient's tumor antigen-specific cytotoxic (CD8+) T cells, presents a unique challenge as only 1 in 10,000-1,000,000 CD8+ T cells are specific to a particular antigen, leading to production processes that are generally low throughput, expensive, and difficult to standardize. Our laboratory has previously reported that paramagnetic iron dextran artificial antigen presenting cells (aAPCs) conjugated with peptide loaded major histocompatibility complex (pMHC) and anti-CD28, a costimulatory molecule, can be used to enrich and expand antigen-specific CD8+ cells to clinically relevant levels using a magnetic column [1]. To make this technique more translational, we aimed to decrease cost and complexity while improving throughput by performing enrichments directly from splenocytes without a prior CD8+ purification step and by using larger particles compatible with a 96 well plate magnet to batch multiple antigens.

Methods

To compare splenocyte to CD8+ enrichments, purified splenocytes from C57BL/6 mice were split into two equal fractions, only of which underwent a CD8+ isolation. Both fractions were enriched with 100 nm KbSIY/anti-CD28 or KbTRP2/anti-CD28 aAPCs over a magnetic column and then cultured for a week, after which cell counts and MHC-Ig dimer stains were used to assess fold expansion and antigen-specificity. Plate based enrichments were performed in a similar manner, except that larger 300 nm aAPCs compatible with a plate magnet were used for the enrichments.

Results

Enrichment directly from splenocytes is not only

feasible but results in 80% antigen-specificity and triple the number of antigen-specific cells as from CD8+ enrichments after a week of expansion. The expanded cells are polyfunctional as seen through intracellular cytokine stains. Helper T cells and dendritic cells are vital to the improved expansions seen in the splenocyte enrichments. Plate-based enrichments work effectively at a particle to cell dose above 680:1, result in robust expansions, and can be successfully used to expand three different populations of antigen-specific cells simultaneously.

Conclusions

Splenocyte as opposed to CD8+ enrichments provide a faster, cheaper, and more effective method to expand large populations of mostly antigen-specific cells, improving the scalability of cellular therapies that target patient-specific rare cancer neoantigens, lowering the risks of nonspecific off-target effects, and suggesting similar improvements may be seen with human PBMC as opposed to CD8+ enrichments. Moreover, 96 well plate based platforms can allow for wider screens of rare antigen-specific populations and simultaneous targeting of multiple cancer neoantigens.

References

1. Perica K, Bieler JG, Schütz C, Varela JC, Douglass J, Skora A, et al. Enrichment and expansion with nanoscale artificial antigen presenting cells for adoptive immunotherapy. ACS Nano. 2015; 9(7):6861–71.

P246

Targeting novel tumor-associated antigens with TCR-engineered T Cells

Mamta Kalra, PhD[1], Ali Mohamed, PhD[1], Zoe Coughlin[1], Thorsten Demberg, PhD[1], Amir Alpert, BS[1], Leoni Alten[1], Sebastian Bunk, PhD[1], Claudia Wagner[1], Jens Fritsche, PhD[1], Oliver Schoor, PhD[1], Agathe Bourgogne[1], Yannick Bulliard, PhD[1], Geoffrey Stephens[1], Dominik Maurer, PhD[1], Harpreet Singh, PhD[1], Carsten Reinhardt, MD, PhD[1], Tony Weinschenk[1], Steffen Walter, PhD[1]

[1]*Immatics US Inc., Houston, TX, USA*

Background

A major constraint to the broad applicability of Adoptive Cellular Therapy is the limited number of known tumor-specific targets that are safe and effective, especially against solid tumors. Unlike CAR-T cells that recognize only surface expressed tumor antigens, T-Cell Receptor (TCR) engineered T cells can access a wider repertoire of tumor targets including intracellular antigens presented in context of HLA molecules.

Methods

Here, we present the development of TCR-engineered T-cell products against 3 novel peptide-MHC antigens identified and validated by Immatics' proprietary XPRESIDENT® platform. This platform combined with an extensive safety assessment program supports our proprietary TCR Discovery platform to screen TCR candidates for potential off-target toxicities. Selected TCRs against specific peptide targets are prioritized into Immatics' ACT pipeline for translational development into safe and effective T-cell therapeutics under ACTengine® (Adoptive Cellular Therapy with autologous engineered T cells) program. Under the first three ACTengine® programs (IMA201,202,203), we developed 3 unique T-cell products each expressing a transgenic TCR targeted against its own respective proprietary novel HLA-A*02:01 restricted tumor antigen.

Results

The manufacturing of ACTengine® products is based on a short and robust process with a "turnaround" time of 23-30 days from leukapheresis collection to released product, which includes a 14-day compendial sterility testing. Overall manufacturing

scheme involves activation of T cells, followed by transduction with the viral vector expressing the respective TCRs, and expansion in the presence of cytokines. The ACTengine® products IMA201 and IMA202 generated for process qualification GMP runs consistently consisted of 20-80% (Avg-50%) transduced CD8+ T cells that rapidly expanded within a week's time to meet clinical doses. Both ACTengine® IMA201 and IMA202 products comprised a substantial proportion of naïve and central memory T cells, known to be associated with long-time persistence in vivo. Further, these T-cell products demonstrated potent anti-tumor response in vitro as evaluated by cytokine release and cytotoxicity assays. Continued process improvement past the first 2 programs has led to further shortening of the expansion phase for IMA203 manufacturing to 3-4 days post-transduction compared to 5-8 days for IMA201 & IMA202. Consequently, IMA203 T cell products exhibit further improved phenotype and functionality. Taken together, all three ACTengine® products are best-in-class product candidates for cancer ACT awaiting clinical proof of concept. Phase I clinical studies of ACTengine® IMA201 and IMA202 are currently underway, in collaboration with MD Anderson Cancer Center; the ACTengine® IMA203 trial is expected to start enrolling patients in Q1, 2019.

P247

Potent ex vivo expanded, human CD34+ cord blood-derived natural killer cells for glioblastoma immunotherapy

Lin Kang, PhD[1], Shuyang He[1], William van der Touw[1], Bhavani Stout[1], Valentina Rousseva[1], Rathna Ravishankar[1], Robert Hariri[1], Xiaokui Zhang[1]

[1]*Celularity, Warren, NJ, USA*

Background

Glioblastoma Multiforme (GBM) is the most aggressive brain malignancy in adults, where the 5-year survival rate is less than 10%. Novel therapies are urgently needed. Celularity, Inc. is developing PNK-007, a culture-expanded NK cell population derived from human umbilical cord blood (UCB) hematopoietic stem/progenitor cells, for treatment of hematological malignancy and solid tumors including GBM.

Methods

UCB CD34+ cells were cultivated in the presence of cytokines including thrombopoietin, SCF, Flt3 ligand, IL-7, IL-15 and IL-2 for 35 days to generate PNK-007. Flow cytometry was used to evaluate the phenotypic characteristics of PNK-007. Cytotoxicity of PNK-007 against GBM cell lines was assessed by a 4h PKH26/TO-PRO-3 FACS based assay. The supernatants were collected from co-culturing PNK-007 with GBM cell lines for 24h and subjected to analysis of secreted cytokines. To identify killing mechanisms, blocking antibodies or perforin inhibitors were employed in cytotoxicity assay. The U-87MG orthotopic NSG mouse model was used for PNK-007 in vivo efficacy study.

Results

Multiple GBM cell lines were assessed for susceptibility to PNK-007-mediated cytotoxicity in vitro. In 4h cytotoxicity assay at an E:T ratio of 10:1, PNK-007 (n=6 donors) exhibited 59.4%±1.5%, 47.6%±10.5%, 37.7%±12.3%, and 8.5%±3.9% cytotoxicity against U-251, LN-18, U-87MG, and U-118MG cells, respectively. Increased production of IFN-γ, GM-CSF, and TNF-α was observed in the supernatants of PNK-007 co-cultured with GBM cell lines compared with those of PNK-007 alone or tumor cells alone. By using blocking antibodies and/or perforin inhibitor (Concanamycin A), we have identified that Perforin or TRAIL, or a combination of them; NKG2D or DNAM-1, or a combination of them; played an important role in PNK-007-mediated cytotoxicity. PNK-007 in vivo anti-GBM activity was assessed in a U-87MG orthotopic NSG model. 1E4

luciferase-expressing U-87MG cells were stereotactically injected into the cranium of NSG mice at Day0. Single dosing of 5E5 PNK-007 at Day14 or repeated dosing of 5E5 PNK-007 at Day14 and Day21 by intracranial injection (IC) significantly reduced Bioluminescence Imaging (BLI) compared with the PBS control ($P<0.01$ by T-test). Furthermore, PNK-007 with two repeated IC doses significantly reduced BLI compared with single IC dose ($P<0.05$ by T-test).

Conclusions

The results demonstrated that PNK-007 exhibited in vitro cytotoxicity against GBM cell lines and cytokine secretion activity following exposure to tumor cells. In vivo efficacy studies further demonstrated anti-tumor activity of PNK-007 in a U-87MG orthotopic NSG model. Taken together, our data support the application of PNK-007 for the development of an allogeneic adoptive immunotherapeutic for GBM patients.

P248

IL-2, IL-15 and IL-21 expanded tumor-infiltrating lymphocytes (TIL) for the treatment of patients with solid cancer

Dragan Kiselicki[1], Julia Karbach[1], Martin Rao, PhD[2], Ernest Dodoo[2], Evgueni Sinelnikov[3], Akin Atmaca[1], Markus Maeurer[2], Elke Jaeger[1]

[1]Krankenhaus Nordwest, Frankfurt, Germany
[2]Champalimaud Foundation, Lisboa, Portugal
[3]Zellwerk GmbH, Oberkrämer, Germany

Background

Checkpoint inhibitors and cellular therapies for patients with solid cancers provide new immunological treatment options

Methods

TIL were expanded from primary (P) or metastatic lesions (ML) in medium containing IL-2, IL-15 and IL-21 from 2 patients with pancreatic cancer (PDAC), 1 patient with glioblastoma (GB), 1 patient with fibrosarcoma (FS) and 1 patient with uveal melanoma (UVM). The GB patient received 2 subsequently clinical infusions from the same pre-expansion culture. 1 of the PDAC patients received 3 clinical TIL infusions also from the identical pre-expansion culture. The other patients received a single TIL dose with 2x10e9 TIL. All patients received preconditioning treatment with a single cyclophosphamide dose (60mg/kg) followed by up to 5x IL-2 infusions (600,000 IU/kg and 60,000 IU/kg in the GB patient). Immunophenotyping of TIL was performed by flow cytometry. Functional assays included IFN-γ production and CD107 induction. T-cell reactivity against autologous tumor cells was tested by standard Cr51 assay and IFN-γ production. Tumor lesions underwent whole exome sequencing. Patients were clinically evaluated according to RECIST criteria. Immune responses were analyzed by flow cytometry, including Th1/Th2/Th17 subsets, T-cell maturation and differentiation defined by CD45RA/CCR7, LAG-3, PD1, TCR analysis, TCR sequencing and recognition of synthetic peptide mutation-specific T-cell responses.

Results

TIL were reliably expanded using IL-2, IL-15 and IL-21 for 5/5 patients resulting in 8 individual TIL doses for i.v. infusion. TIL recognized the (i) autologous tumor cells defined by IFN-γ production and cytotoxicity, resided in the memory T-cell subset, (ii) exhibited a restricted TCR repertoire, (iii) strongly expressed CXCR3, reflecting tissue homing capacity and (iv) recognized individual tumor mutations presented as synthetic peptides. TIL infusion to a single patient with GB resulted in necrosis and complete tumor remission. More detailed analysis of resected stable or regressing lung metastatic lesions from a patient with pancreatic cancer who received 3 TIL infusions revealed a diverse yet restricted T-cell repertoire with preferential expansion of individual TCR VB

families with a Th1/Th1* phenotype pattern suggesting a focused, local immune repertoire directed against metastatic tumor lesions (Figure 1).

Conclusions

IL-2, IL-15 and IL-15 expanded TIL from primary solid cancer and metastatic lesions promotes the cultivation of a focused T-cell product directed against the patient's autologous tumor cells and offers a viable treatment modality for patients with solid cancer. .

Ethics Approval

Written informed consent has been obtained.

Consent

Written informed consent was obtained from the patients for publication of this abstract and any accompanying images. A copy of the written consent is available for review by the Editor of this Journal.

Figure 1.

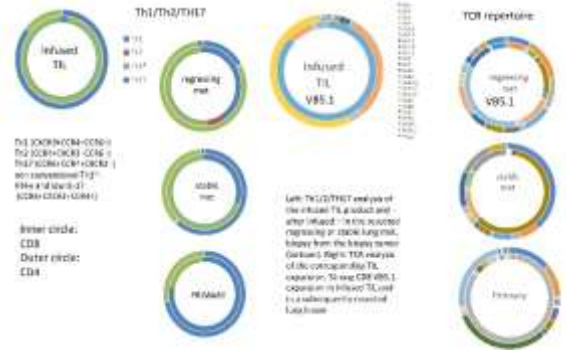

P249

Glypican-1 (GPC-1) specific CAR-T cells eradicate established solid tumor without adverse effects and synergize with anti-PD1 antibody therapies

Daiki Kato, DVM[1], Tomonori Yaguchi, MD, PhD[2], Kenji Morii, MS[2], Satoshi Serada[3], Tetsuji Naka[3], Takayuki Nakagawa[1], Ryohei Nishimura[1], Yutaka Kawakami, MD, PhD[2]

[1]The University of Tokyo, Tokyo, Japan
[2]Keio University School of Medicine, Tokyo, Japan
[3]National Institute of Biomedical Innovat, Osaka, Japan

Background

Chimeric antigen receptor transduced T cells (CAR-T) targeting CD19 are effective for B cell malignancies. Although clinical trials of CAR-T therapies for patients with solid tumor have been challenged, these trials have not been successful due to problems including insufficient activities in tumor tissues, on-target/off-tumor lethal toxicities and antigen-loss. We have previously shown that glypican-1 (GPC-1) was preferentially overexpressed on squamous cell carcinoma, and generated anti-GPC-1 human CAR-T cells (hGPC1-CART) using our anti-GPC-1 Ab which recognizes both human and murine GPC-1. Although strong anti-tumor effects of the hGPC1-CART were shown in a xenograft model implanted with GPC-1+ human cancer cells, this model was not sufficient to evaluate adverse effects of CART due to severe xenoGVHD and to evaluate induction of CTL against endogenous tumor antigens, which may be important for augmenting anti-tumor effects and overcoming antigen-loss problem in solid tumors. Therefore, in this study, we generated anti-GPC-1 "murine" CAR-T cells (mGPC1-CART) using the same anti-GPC-1 Ab used for hGPC1-CART, and evaluated their characteristics in syngeneic mouse models.

Methods

C57BL/6 mice bearing murine GPC-1 transduced MC38 (MC38-mGPC1) or MCA205 (MCA205-mGPC1) were treated with mGPC1-CART, and antitumor effects, adverse effects, induction of endogenous tumor antigen specific T cells, and combination with anti-PD-1 Ab were evaluated.

Results

Intravenous administration of mGPC1-CART showed

strong anti-tumor effects against GPC-1 transduced murine tumors in vivo without any overt adverse effects. Complete eradication of tumors was observed in the MCA205-mGPC1 model. No obvious damage or CAR-T cell infiltration was observed in evaluated normal tissues of the treated mice by immunohistochemical analyses. Furthermore, CTL responses against endogenous tumor antigens were enhanced by mGPC1-CART, indicating antigen spreading occurred. Since both tumor infiltrating mGPC1-CART and endogenous CD8+ T cells expressed PD-1, we also performed a combination therapy of mGPC1-CART and anti-PD-1 Ab in the MC38-mGPC1 model, and synergistic anti-tumor activities were shown without adverse effects.

Conclusions
These results indicate that GPC-1 specific CAR-T adoptive cell therapy in combination with anti-PD-1 Ab may be an attractive immunotherapy for solid cancers.

P250

Shorter ex vivo expansion of Th17 cells mediates potent anti-tumor regression in melanoma

Hannah Knochelmann[1], Michelle Nelson, PhD[1], Jacob Bowers[1], Megan Wyatt, MS[1], Aubrey Smith[1], Connor Dwyer, PhD[1], Chrystal Paulos, PhD[1]

[1]*Medical University of South Carolina, Charleston, SC, USA*

Background
Adoptive T cell transfer therapy mediates potent immunity in patients with bulky metastatic malignancies but proves difficult to translate clinically due to production costs, time, and labor required to generate personalized T cell products. Though several CAR-T cell preparations were recently FDA approved, patients indicated for these therapies are at risk of insurance coverage denial due to the large costs of T cell manufacturing. As a result, methods of reducing production costs by generating T cells with potent antitumor properties more quickly are in high demand.

Methods
We proposed a method of shortened ex vivo expansion using Th17 cells to treat melanoma using the TRP-1 transgenic mouse model in which CD4+ T cells express a TCR that recognizes tyrosinase-related protein 1 on melanoma. Naïve CD4+ T cells were polarized to secrete IL-17, and infused into mice with B16F10 melanoma after a nonmyeloablative total body irradiation (5 Gy) preparative regimen. Antitumor efficacy of Th17 cells was studied kinetically over ex vivo expansion spanning 12 hours to 14-days. Functionality and biology of T cells was determined using flow cytometry, and serum cytokines were measured with multiplex array.

Results
We found that Th17 cells expanded only four days ex vivo can eradicate tumors even when only few cells (~200K) are infused into the animal. These day-4 cells mediate more potent antitumor responses than greater numbers (>25X more) of Th17 cells expanded up to two weeks. In contrast to long-term expanded cells, day-4 Th17 cells 1) express peak levels of IL-2Ralphaα and costimulatory molecules (CD28, OX40, ICOS), 2) persist at greater fold once infused in the animal, 3) induce significantly increased production of IL-6, IL-17, and GM-CSF within the tumor-bearing host, and 4) provide long-lived protection against tumor recurrence.

Conclusions
Our findings indicate that day-4 Th17 cells regress large melanoma tumors even in very low number. Four days after activation, Th17 cells are highly activated and induce a robust inflammatory response with the host compared to Th17 cells expanded long-term. These results highlight that transferring T cells only 4-days after activation,

despite a lower yield than long-term expansion, can potentially improve efficacy, reduce expense, and improve accessibility of adoptive cell therapy to patients clinically.

Ethics Approval
Animal studies were approved by the IACUC of the MUSC Animal Resource Center (number 3039).

P251

Tumor-infiltrating lymphocytes (TIL) for the adoptive treatment of patients with pancreatic cancer

Joana Lerias, PhD[1], Georgia Paraschoudi, MSc[1], Martin Rao, PhD[1], Nuno Couto[1], Davide Valentini[1], Mireia Castillo-Martin[1], Antonio Beltran[1], Evgueni Sinelnikov[2], Hans Hofmeister[2], Ana Vieira[1], Javier Martin-Fernandez[1], Andreia Maia[1], Dário Ligeiro[3], Carlos Carvalho[1], Dragan Kiselicki[4], Akin Atmaca[4], Julia Karbach[4], Elke Jäger[4], Markus Maeurer[1], Joana Lerias, PhD[1]

[1]Champalimaud Foundation, Lisbon, Portugal
[2]Zellwerk, Berlin, Germany
[3]Centro de Sangue e Transplantação de Lisboa, IPST, Lisbon, Portugal
[4]Krankenhaus Nordwest, Frankfurt, Germany

Background
New treatment options are needed to offer the best suitable therapy for patients with pancreatic cancer. We studied in detail the quality and quantity of cellular immune response of a 65-year old female patient diagnosed with pancreatic ductal adenocarcinoma (PDAC) and stage IV peritoneal metastasis, who received a single dose of 60mg/kg cyclophosphamide, followed by 2x10e9 TIL at day 2, with sequent 5 doses of IL-2 (600,000 IL-2/kg). TIL were obtained from metastatic lesion and could be compared to TIL from the primary lesion as well as to T-cells obtained from a colon biopsy several weeks after TIL infusion.

Methods
Fresh tumor from primary (P) and peritoneal metastasis (PM) cancer lesions and colon tissue (C) were cultured in medium containing IL-2, IL-15 and IL-21. Immunophenotyping of TILs and peripheral blood mononuclear cells (PBMCs) was performed by high-content flow cytometry. Tumor exome sequencing was performed in primary and metastatic lesions, CD4+ and CD8+ TIL, as well as PBMCs were analyzed for TCR composition by CDR3 length analysis and tested for recognition of individual tumor mutations (represented by synthetic peptides) by IFN-γ production.

Results
P-TILs and PM-TILs were mainly effector memory (TEM), PBMCs were mostly comprised of central memory CD4+ T-cells (TCM) prior to T-cell therapy – as well as after immune-constitution. Comparison of TCR Vβ repertoire between P- and PM-TILs (86% Vβ13.1 in CD8+ P-TILs) showed a greater diversity in PM-TILs. 53/146 mutations were recognized in TIL from the primary lesion, 6/146 mutations in TIL from the metastatic lesion and 25/146 private antigens from T-cells expanded from colon biopsy after TIL infusion defined by IFN-gamma production. 60% of CD8+ PM-TILs tested CCR9 positive. Antigen-specific IFN-γ production in TIL from primary and metastatic cancer lesion showed strong responses to the melanoma-associated antigen Melan-A/MART-1 (AAGIGILTV) with high homology to common gram-negative bacterial species suggesting molecular mimicry (Figure 1).

Conclusions
The detailed molecular and functional examination of TIL from primary and metastatic pancreatic cancer lesions shows that TIL harvested from primary tumor lesion recognize a broad repertoire of private mutant target antigens, some which were shared among TIL from the metastatic lesion. TIL harvested from

primary lesions may be used for later tumor recurrences – dependent on the mutational diversity. TIL recognition pattern may be driven by molecular mimicry for common bacterial species present in the intestine.

Ethics Approval

This study was approved by the Champalimaud Foundation Ethics Committee and some individuals patient signed as well the informed consent at the KHNW, Frankfurt, Germany.

Consent

Written informed consent was obtained from the patient for publication of this abstract and any accompanying images.

Figure 1.Characterization TILs derived from pancreatic tumor

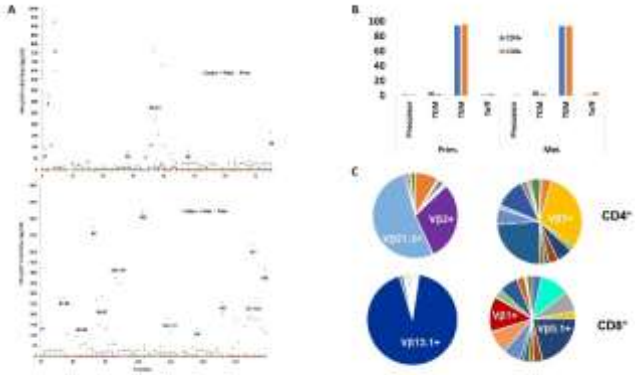

P252

Fast quality gauging of tumor-infiltrating lymphocytes (TIL) for the treatment of patients with solid cancer

Georgia Paraschoudi, MSc in Cell and Molecular Biology, Sweden[1], Joana Lérias[1], Martin Rao, PhD[1], Mireia Castillo-Martin[1], Antonio Beltran[1], Evgueni Sinelnikov[2], Hans Hofmeister[2], Javier Martin-Fernandez[1], Andreia Maia[1], Dário Ligeiro[3], Carlos Carvalho[1], Dodoo Ernest[4], Dragan Kiselicki[4], Julia Karbach[4], Elke Jäger[4], Ana Vieira[1], Georgia Paraschoudi, MSc in Cell and Molecular Biology, Sweden[1]

[1]*Champalimaud Foundation, Lisbon, Portugal*
[2]*Zellwerk, Oberkrämer, Germany*
[3]*Centro de Sangue e Transplantação de Lisboa, IPST, Lisbon, Portugal*
[4]*Krankenhaus Nordwest, Frankfurt, Germany*

Background

Individually tailored therapy using Tumor- infiltrating T-cells (TILs) represents a viable treatment option for patients with advanced solid cancer.

Methods

Freshly harvested tumor tissue from 12 patients was tested for TIL expansion: one patient with glioblastoma (2 TIL expansions), one patient with fibrosarcoma, one with uveal melanoma, one patient with esophagus cancer, one patient with a benign lipoma, and 6 patients with pancreatic cancer (with 5 TIL expansions for an individual case harvested from different tumor sites) targeting between 1 to 2x 10e9 TILs for a single infusion. TIL were further characterized by phenotypic analysis by flow cytometry including CD3, CD4, CD8, CD45RA, CCR7, CXCR3, CCR4, CCR6, CCR9, CD103, LAG-3, CD57, HLA-DR and PD-1 and Tregs (CD4+CD25highCD127neg). The molecular diversity of TIL was gauged by TCR CDR3 analysis in sorted CD3+ and CD4+ TIL. Immunohistochemistry included detection of immune cells and NY-ESO-1 (Figure 1). Prior to testing of individual target mutant epitopes, identified by tumor exome sequencing, T-cell recognition was gauged using a broad panel of antigens associated with common viral pathogens (e.g. CMV, EBV, Flu), tumor–associated antigens (e.g. NY-ESO-1, Melan-A/MART-1, survivin, mesothelin). Wildtype, as well as the most common KRAS mutations, wildtype MUC4 and MUC16 and a broad

array of MUC4 and MUC16 mutations were tested for recognition by IFN-γ production (Figure 2).

Results

TIL could be reliably expanded using IL-2, IL-15 and IL-21: TIL expansion could be achieved in 12/12 patients with different cancer histologies resulting in 17 individual TIL preparations with an oligoclonal TCR repertoire and a strong CXCR3 expression in both CD4+ and CD8+ TIL enabling access to tissue. A fast orientation of TIL recognizing common targets, including common pathogens, non-mutant tumor associated antigens, as well as mutant tumor driver mutations (e.g. KRAS) aids to define very fast the quality and nature of individual TIL preparations. Strong IFN-production could be identified in individual TIL preparations against single KRAS mutants or against individual TAAs, e.g. NY-ESO-1 epitopes that was also associated with antigen protein expression in the matching tumor lesion.

Conclusions

IL-2, IL-15 and IL-21 expanded TILs from primary solid cancer or metastatic lesions lead to expansion of a focused T-cell product even from small biopsy lesions. 'Fast' functional screening of TIL for common TAAs and frequent tumor mutations may aid to select very fast individual TIL preparations for adoptive therapy or present a starting point to further expand T-cells with antigen-specific TCRs directed against defined target antigens.

Ethics Approval

This study was approved by the Champalimaud Foundation Ethics Committee and some individuals patient signed as well the informed consent at the KHNW, Frankfurt, Germany.

Consent

Written informed consent was obtained from the patient for publication of this abstract and any accompanying images.

Figure 1. Immunohistochemical analysis of NYESO-1

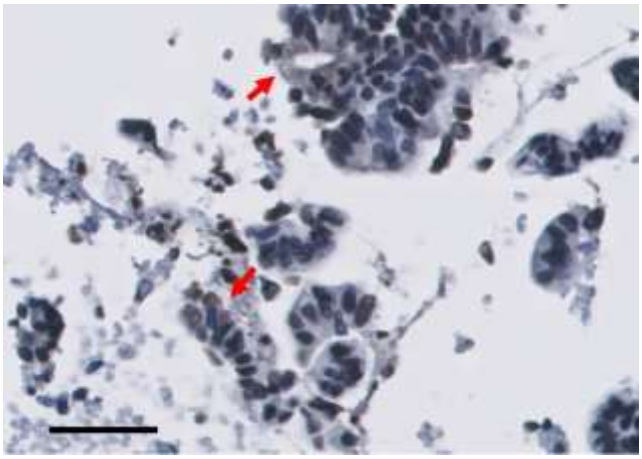

Figure 2. Characterization of TILs derived pancreatic tumor

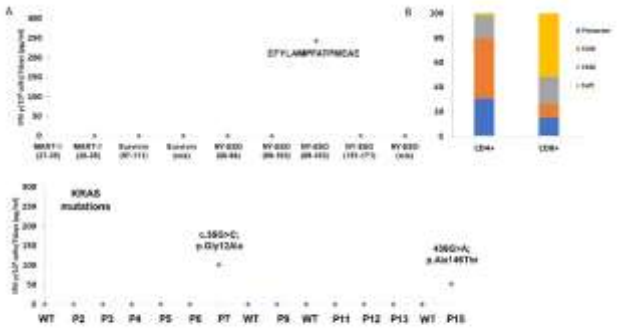

P253

B cell structural diversity in early cultured tumor-infiltrating lymphocytes

Dario Ligeiro, PhD[1], Hélder Trindade[1], Joana Lérias[2], Georgia Paraschoudi, MSc in Cell and Molecular Biology, Sweden[2], Andreia Maia[2], Catarina de Oliveira[2], Javier Martin-Fernandez[2], Martin Rao, PhD[2], Carlos Carvalho, MD[2], Mireia Castillo-Martin[2], Markus Maeurer[2]

[1]Centro de Sangue e Transplantação de Lisboa, IPST, Lisbon, Portugal
[2]Champalimaud Foundation, Lisbon, Portugal

Background

The tumor-infiltrating B cells (TIB) role in anti-cancer immune responses is under debate with reports showing an association of B cell densities in tumor with either higher recurrence rates or a more favorable outcome. B-cells may serve as antigen presenting cells and producers of cytokines, suggesting both pro- and antitumor effects. The regulatory mechanisms and cell type of TIB in the tumor immune landscape, as well as their antigen-specificity remains largely unknown. Here we classify the B-cell repertoire diversity in early cultures of tumor infiltrating lymphocytes (TILs) and report their antigen-specificity for individual patients.

Methods

Freshly harvested tumor tissues (colorectal and pancreatic cancer) were procured for TIL expansion using IL-2, IL-15 and IL-21. Immunohistology with CD3 and CD20 mAbs was used to identify TLS (tertiary lymphoid structures). Flow cytometric analysis was performed with anti-CD19, CD20, CD27, IgM, CD5, CD3, CD4, and CD8. Diversity of immunoglobulin heavy chain (IGH) transcripts was evaluated with a CDR3 spectratyping assay for heavy chain variable segments (IGHV) IGHV1-6 families and common primers specific for IGHM and IGHG gene segments. TIB diversity was profiled based on number and distribution of in-frame peaks acquired by fluorescent capillary electrophoresis. B-cell specificity was tested using EBV-immortalization and testing wild type, as well as mutant target epitopes on streptavidin-biotin scaffold, followed by IgG detection with standard ELISA.

Results

TLS, containing CD20+ B-cells, can be identified in the tumor periphery of colorectal or pancreatic cancer specimens. B-cells can be identified up to 3% in early TIL cultures that are accessible for BCR receptor analysis, which showed IgM and IgG transcripts from most families of IGHV gene segments (Figure 1). The clonotype repertoire of TIB was found skewed with a predominance of oligo and monoclonal profiles; however, some TIL cultures did show significant structural diversity even for IgG BCR transcripts. B-cells could be immortalized and showed reactivity to mutant, but not to wildtype target antigens in individual cancer specimens.

Conclusions

B-cells constitute a set of viable immune cells with a diverse Ig repertoire in early cultured TIL. Detection of IgG shows that Ig switching took place and the recognition of mutant epitopes suggests antigen-driven Ig affinity maturation. Such mutant – reactive B-cells may augment tumor-specific T-cell responses, yet may also be tumor promoting, depending on the cytokine production pattern. Identification of individual IgG transcripts targeting mutant cancer targets may provide blueprints for the tailored therapy of cancer targeting individual cancer mutations.

Ethics Approval

This study was approved by Champalimaud Foundation Ethics Committee.

Consent

Written informed consent was obtained from the patient for publication of this abstract and any accompanying images. A copy of the written consent is available for review by the Editor of this Journal.

Figure 1. TIB repertoire in early-cultured TILs

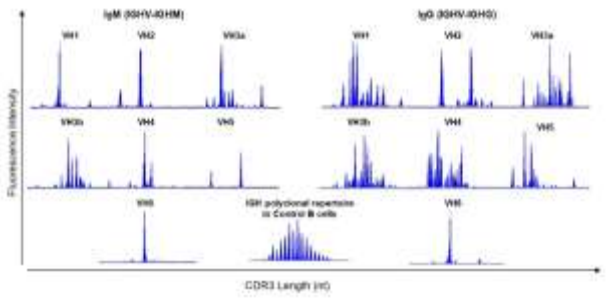

P254

Natural Killer cells propagated under pressurized culture conditions show enhanced tumor killing activity

James Lim[1], Ann Lu[1], Nick Wilson[1], Albert Wong[1]

[1]*Xcellbio, San Francisco, CA, USA*

Background

Novel cell-based immunotherapies are in advanced clinical trials, transforming the way we treat cancers. These therapies, however, are currently limited to blood-based cancers. Critical challenges remain in treating solid tumors, where hypoxic and high pressure microenvironments can limit the efficacy of current cell-based therapies. Recent research have shown that T-cells propagated under normoxic conditions (21% O2) have decreased cytolytic activity and reduced tumor-killing rates than cells grown under hypoxic conditions [1]. This observation would indicate that improvements in cell culturing and manufacturing processes could generate therapeutically-superior cell products through the simple modulation of oxygen and pressure control. To test this hypothesis we examined the effects of hypoxia and high pressure conditions on another therapeutic lymphocyte, donor-derived Natural Killer (NK) cells.

Methods

NK cells were enriched using magnetic-bead based separation from the peripheral blood of 12 healthy donors. NK cells were expanded for 1 week under varying oxygen concentrations (1%, 5%, 15%, 21%) and pressurized conditions mimicking the arterial vasculature pressure (~2PSI). We performed FACS analysis against NK markers (CD16 and CD56), and against mediators of cell cytolysis, perforin and granzymeB. mRNAseq was performed on NK datasets at time of collection and after 7 days of expansion. Differential gene expression and pathway analysis was performed to compare conventional culture conditions (21% O2, 0 PSI) against conditions mimicking the arterial vasculature (15% O2 and 2PSI) and bone marrow environments (5% O2 and 2PSI). NK-Tumor cell killing assays were performed using an electrical impedance-based system against a prostate cancer cell line (DU145).

Results

We report that NK cells propagated under low oxygen and pressurized conditions show comparable expansion rates compared to conventional culture conditions. However, NK cells grown under conditions mimicking the bone marrow and arterial vasculature systems exhibited strong expression of both CD16 and CD56 markers. In addition, these NK cells showed elevated levels of both granzyme B and perforin. NK-tumor cell killing assays revealed superior cell-killing abilities of these NK cells compared to conventionally grown NK cells. mRNAseq analysis revealed both exhaustive and activated gene expression signatures for all samples, but NK cells grown under pressurized conditions (2PSI) were defined by a significant shift in their metabolic gene expression profile.

Conclusions

In summary, the insights generated from this study can enable advancements in cell-manufacturing processes to create effective therapies.

References

1. Gropper et. al., Culturing CTLs under hypoxic

conditions enhances their cytolysis and improves their anti-tumor function. Cell Reports. 2017; 20, 2547-2555

P255

Results and perspectives from Phase 1 studies assessing the safety and clinical activity of multiple doses of a NKG2D-based CAR-T therapy, CYAD-01, in metastatic solid tumors

Alain Hendlisz, MD[1], Sylvie Rottey, MD[2], Mateusz Opyrchal, MD PhD[3], Kunle Odunsi, MD, PhD[3], Jean-Pascal Machiels, MD, PhD[4], Solmaz Sahebjam, MD[5], Leila Shaza, MD[1], Sandrine Aspeslagh[1], Marc Van den Eynde, MD[4], Jean-Luc Canon, MD[6], Javier Carrasco[6], Ahmad Awada[1], Eytan Breman, MSc[7], Panagiota Sotiropoulou, PhD[7], Sarah Snykers, PhD[7], Nathalie Braun[7], Caroline Lonez, PhD[7], Anne Flament[7], Bikash Verma, MD[7], Frédéric Lehmann, MD[7]

[1]*Institut Jules Bordet, BRUSSELS, Belgium*
[2]*Ghent University Hospital, Ghent, Belgium*
[3]*Rosswell Park Comprehensive Cancer cente, Buffalo, NY, USA*
[4]*Cliniques Universitaires Saint Luc, Brussels, Belgium*
[5]*Moffitt Cancer Center, Tampa, FL, USA*
[6]*Grand Hôpital de Charleroi (GHdC), Charleroi, Belgium*
[7]*Celyad, Mont-St-Guibert, Belgium*

Background
Chimeric antigen receptor T-cell (CAR-Ts) therapies have yet to demonstrate positive results in the context of solid tumors likely because of the inability of classical CAR-Ts to infiltrate into the tumor and overcome a hostile immunosuppressive tumor microenvironment (TME). CYAD-01, a NKG2D receptor-based CAR-T, targets eight stress ligands expressed across the hematological/solid tumor divide and thus provides a unique opportunity to explore the challenges facing CAR-T cell therapy. Promising reports of objective responses in refractory AML patients by CYAD-01 as a standalone therapy provide confidence in the relevance of the target. Here, we provide an overview of our clinical observations relating to CYAD-01 in the solid tumor setting.

Methods
The THINK study evaluates multiple i.v. administrations of CYAD-01 with or without prior preconditioning therapy. The SHRINK trial is evaluating the CYAD-01 treatment i.v. administered concurrently to a standard-of-care (SoC) FOLFOX chemotherapy for metastatic colorectal cancer (mCRC) with the aim to favor infiltration into the immunosuppressive TME but also engraftment of the CYAD-01 cells.

Results
As of August 1, 2018, 14 patients with solid tumor indications (11 mCRC, 1 pancreatic and 2 ovarian) have been enrolled at three different dose-levels (DL, 3x10E8, 1x10E9 and 3x10E9 CYAD-01) without prior preconditioning in the THINK study. Over 28 injections 3 were associated with treatment-related grade 3/4 adverse events, with 1 cytokine release syndrome (CRS) grade 3 in DL-2 and 1 grade 4 CRS in DL-3. The CRS observed in the DL-3 patient was considered a dose limiting toxicity (DLT) and 5 patients recruited at the same dose showed no further evidence of severe toxicity. Two patients showed disease stabilization. A peak of MCP-1 in patient's sera correlated with CYAD-01 injections, while other pro-inflammatory cytokines were induced after the 2nd and 3rd CYAD-01 injections. The first of the 3 DL-1 patients (1x10E8) in the SHRINK study completed his full schedule of concomitant administration without any DLT occurrence.

Conclusions
As a standalone therapy, CYAD-01 has shown a reassuring safety profile and promising clinical activity in refractory AML but activity is not clear yet

in solid tumors. Our initial attempts to boost the potency of CYAD-01 involve combining with SoC or preconditioning chemotherapy. Safety, clinical and translational research data comparing potential impact of these approaches on CYAD-01 potency will be presented, including any potential difference in terms of CYAD-01 kinetics. These studies will provide critical information to support the development of CAR-T therapy for solid tumors.

Trial Registration
NCT03018405, NCT03310008

Ethics Approval
The studies were approved by all relevant Belgian and US Institution's Ethics Boards and authorities.

P256

Evaluation of therapeutic T cell manufacture using long amplicon TCRβ immune repertoire sequencing

Geoffrey Lowman, PhD[1], Lauren Miller, BS[1], Timothy Looney, PhD[1], Tor Espen Stav-Noraas[1], Reidun Hartberg, PhD[2], Hilde Almåsbak[1], Mark Andersen, PhD[1], Sjoerd van der Burg, PhD[2], Elizabeth (Els) Verdegaal, PhD[2], Noel de Miranda, PhD[2]

[1]*ThermoFisher Scientific, Carlsbad, CA, USA*
[2]*Leiden University Medical Center, Leiden, Netherlands*

Background
Following the demonstration of the tremendous potential of T cell therapies in blood cancers, the field is evolving rapidly with focus on commercial, cost-effective manufacture to offer therapies for larger treatment groups. There exists a need for streamlined and quality-controlled manufacturing processes, with closed-system operations and simplified workflows. We demonstrate the utility of long amplicon T cell receptor beta (TCRβ) sequencing to sample repertoire features of therapeutic T cells at various timepoints during the manufacturing process.

Methods
T cell populations from multiple donors are tracked in each step of the therapeutic T cell manufacture process, beginning with baseline repertoire measurement after isolation from the donor and expansion using CTS™Dynabeads™CD3/CD28 in CTS™ OpTmizer™ T Cell Expansion Serum Free Media with 5% CTS™ Immune Cell Serum Replacement. The repertoire is then examined after the viral transduction process, and final T cell product. We survey the TCRβ repertoire of therapeutic T cell populations using the OncomineTM TCR Beta – LR Assay, sequencing on the Ion Torrent S5 system, and repertoire analysis using Ion Reporter immune repertoire analysis software.

Results
Donor PBMC-derived T cells were isolated with high recovery (>90%) and purity (>95%) and uniformly stimulated (>95% CD25+day 3 post-activation). Activated T cells were expanded and preserved a young phenotype (CD28+CD62L+) at day 7-10. TCRβ sequencing was used to measure the initial pre-isolation T cell population revealing a diverse polyclonal repertoire (evenness = 0.76-0.88). Importantly, this clonal diversity persists and often increases post-isolation, through activation, expansion, bead removal, transduction, and in the final product (evenness = 0.90-0.96). The consistent increase in evenness with cell culture time suggests that the manufacturing process used here promotes a polyclonal (unbiased) T cell expansion.

Conclusions
Measurement of a therapeutic T cell repertoire provides a sequence level understanding of the diversity within a cell product. We demonstrate that repertoire sequencing can ensure a diverse repertoire of T cells are maintained during manufacture. A 48h turnaround time, from sample

to analysis result allows this testing to occur at multiple timepoints in the manufacturing process using both the richness and evenness of the repertoire to track therapeutic T cell populations longitudinally. In addition, TCRβ repertoire sequencing of a therapeutic T cell product provides a rich baseline for further monitoring of the T cell repertoire after administration.

P257

Natural Killer and TCR gamma-delta T-cells are present in the tumor microenvironment and can be expanded for adoptive immunotherapy for epithelial cancer

Andreia Maia[1], Joana Lérias[1], Catarina de Oliveira[1], Javier Martin-Fernandez[1], Georgia Paraschoudi, MSc in Cell and Molecular Biology, Sweden[1], Martin Rao, PhD[1], Dário Ligeiro[2], Tin Htwe Thin, PhD[3], Ana Isabel Vieira[1], Carlos Cordon-Cardo, MD, PhD[3], Carlos Carvalho, MD[1], Markus Maeurer[1]

[1]*Champalimaud Centre for the Unknown, Lisbon, Portugal*
[2]*IPST - Instituto Portugues do Sangue e T, Lisbon, Portugal*
[3]*Icahn School of Medicine at Mount Sinai, New York, NY, USA*

Background

The immune system may control tumors, mainly through CD8+ T cells by recognition of major histocompatibility complex class I (MHC-I) molecules. Frequently, MHC-I loss occurs – which represents one of tumor immune evasion mechanisms. Natural Killer (NK) and TCR gamma-delta T-cells may still be able to recognize MHC-I negative tumor cells. NK and TCR gamma-delta T-cells, harvested from cancer lesions, can serve as immune effector cells in addition to conventional TCR alpha-beta T-cells, particularly in case of MHC-I negative tumors. The goal of this study is to evaluate MHC-I expression in different primary and metastatic tumors and to expand NK and TCR gamma-delta T-cells in sufficient numbers for adoptive therapy.

Methods

Paraffin-embedded tissue sections from one primary lung, four primary colon, two primary pancreas adenocarcinomas and four pancreatic adenocarcinoma metastases were analyzed by immunohistochemistry (IHC) with antibodies against CD56 (Novocastra), TCR γδ (Invitrogen) and HLA class I (Abcam). Number of NK and TCR gamma-delta T-cells/mm2 and percentage of MHC-I expression in tumor cells were recorded. From the same cases, fresh tumor tissue was cultured in medium containing IL-2, IL-15 and IL-21 to cultivate TILs, and percentage of TCR gamma-delta T-cells (CD3+ TCR γδ+) and NK cells (CD3- CD56+ CD16+) was analyzed by flow cytometry (FC). CD3+ TCR gamma-delta cells were further analyzed by TCR CDR3 analysis and NK cell receptors were genotyped.

Results

IHC analyses revealed presence of NK cells in all tumor samples, mostly in the peri-tumoral stroma, but also intraepithelially in a few cases (Figure 1A). The mean NK cells/mm2 was of 50.2 (range 14.1–155.7 cells/mm2). FC analyses from these samples showed that NK cells represented between 0%-27% in cytokine-expanded TILs (Figure 1E). TCR gamma-delta T-cells were observed in all tissue specimens except for the lung adenocarcinoma, showing a mean of 15.4 cells/mm2 (range 0-61.1 cells/mm2, Figure 1B). Interestingly, the tumor from which we expanded the highest percentage of TCR gamma-delta T-cells (52.3% in TILs) corresponded to a colon adenocarcinoma that showed the highest number of tissue TCR gamma-delta T-cells. TCR gamma-delta T-cells from colon adenocarcinoma specimens showed the presence of oligoclonal TCR Vdelta1+ TILs (Figure 1F). MHC-I evaluation showed consistent staining in all tumors, with absence of membranous expression in scattered tumor cells that accounted for 1%-10%

of the entire tumor area (Figure 1C-D).

Conclusions

This study shows that NK and TCR gamma-delta T-cells are present and can reliably be expanded for functional analysis and adoptive TIL therapy.

Ethics Approval

This study was approved by the Champalimaud Foundation Ethics Committee

Consent

Written informed consent was obtained from the patient for publication of this abstract and any accompanying images. A copy of the written consent is available for review by the Editor of this journal

Figure 1.

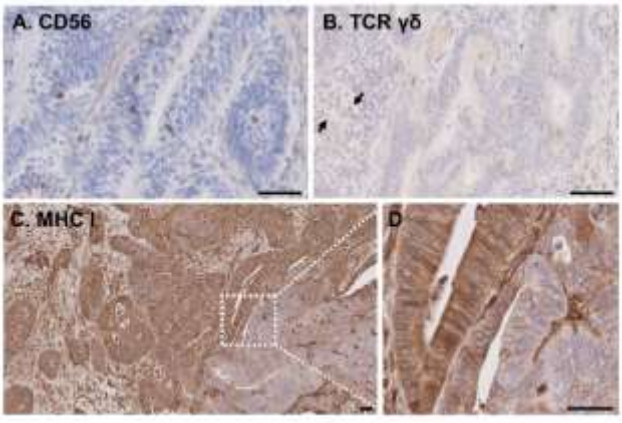

F

Centromeric Region									
Content	KIR3DL3	KIR2DS2	KIR2DL2	KIR2DL3	KIR2DL5	KIR2DS3	KIR2DS5	KIR2DP1	KIR3DP1
Con-A/Con-A	3DL3	_	_	2DL3	_	_	_	2DP1	3DP1

Telomeric Region									
Content	KIR2DL1	KIR2DL4	KIR3DL1	KIR3DS1	KIR2DS1	KIR2DS4	KIR3DL2	KIR2DL1	KIR2DL4
Tel-A/Tel-A	2DL1	2DL4	3DL1	_	_	2DS4	3DL2	2DL1	2DL4

P258

sd-rxRNA to enhance NK cell activity for adoptive cell transfer

Melissa Maxwell, MS[1], James Cardia[1], Dingxue Yan, Ph D[1], Gerrit Dispersyn, PhD[1]

[1]*RXi Pharmaceuticals, Marlborough, MA, USA*

Background

NK cells are the body's first line of defense against cancer cells. They are able to rapidly recognize and kill tumor cells without prior sensitization. Adoptive cell therapy (ACT) using NK cells shows promise against hematological cancers but the cytotoxic activity of these cells is limited by inhibitory receptors and pathways. Overexpression of such receptors has been shown to reduce NK cell-mediated cytotoxicity. Overcoming this inhibition would allow for a more potent antitumor response following ACT. We have developed a new class of stable, self-delivering RNAi compounds (sd-rxRNAs) that incorporate features of RNAi and antisense technology. sd-rxRNAs demonstrate potent activity, stability, and are rapidly and efficiently taken up by cells. We believe that sd-rxRNA targeting inhibitory receptors such as TIGIT and cbl-b may enhance the cytotoxic activity of NK cells used in ACT.

Methods

Freshly isolated human NK cells were isolated using negative selection and cultured in standard culture media containing IL-2. Twenty-four hours after isolation, cells were collected for transfection and the cell concentration was adjusted to ~1 x 106 cells/mL in RMPI media containing IL-2. Cells were seeded directly into 24-well plates containing chemically-optimized sd-rxRNAs ranging in final concentration from 0.125 µM to 2 µM. Taqman gene expression assays were used to determine expression levels of inhibitory receptors following the RNA to Ct 1-step protocol. In addition, cells were

stained using fluorescently labeled antibodies for flow cytometry. Cytotoxic capabilities of these transfected NK cells against cancer cell lines were tested in a Real Time Cell Analysis (RTCA) assay

Results

Transfection with sd-rxRNA targeting inhibitory receptors resulted in consistent silencing without negative impact on NK cell viability. For example, 2 µM TIGIT sd-rxRNA results in a 90% reduction in TIGIT mRNA. The reduction is seen at least 7 days post-transfection and results in a 38% reduction in surface expression of TIGIT by flow cytometry. Similar results were obtained with cbl-b silencing. The effects of this downregulation resulted in increased cytotoxic capabilities of NK cells against cancer cell lines in an RTCA assay.

Conclusions

This is the first data to demonstrate the potential of sd-rxRNA to improve NK cell potency in ACT. By treating NK cells with sd-rxRNA targeting inhibitory receptors such as TIGIT ex vivo, prior to ACT, the anti-tumor response of these cells may be enhanced resulting in a more effective therapy for hematological malignancies.

P259

Regional delivery of chimeric antigen receptor (CAR)-engineered T cells with 4-1BB co-stimulation effectively targets TAG72-positive peritoneal ovarian tumors

John Murad, BS, MS[1], Anna Kozlowska, MSc, PhD[1], Maya Ramamurthy[1], Wen-Chung Chang, MS[1], Paul Yazaki, PhD[1], David Colcher, PhD[1], John Shively, PhD[1], Mihaela Cristea, MD[1], Stephen Forman, MD[1]

[1]*City of Hope, Duarte, CA, USA*

Background

Obstacles in developing effective Chimeric Antigen Receptor (CAR)-engineered T cell therapies for solid cancers include avoiding off-tumor on-target toxicity due to the lack of truly restricted tumor antigens, and achieving durable responses usually limited by T cell persistence, and tumor trafficking. Aberrant glycosylation of cell surface proteins on tumors represent unique targets for cell based immunotherapy. One of these targets, TAG72 is over-expressed in multiple solid tumors including epithelial ovarian cancers. Recent optimization of CAR T cell design to include intracellular co-stimulatory signaling has improved anti-tumor activity, cytokine production, and T cell persistence. Furthermore, route of T cell delivery in solid tumors seems to be important to the anti-tumor activity in some settings. Herein we evaluate TAG72 CARs with 4-1BB co-stimulation for the treatment of advanced ovarian cancers.

Methods

TAG72 targeting CARs with CD3-ζ stimulation and 4-1BB co-stimulation (TAG72-BBζ) were evaluated for activation and anti-tumor activity using in-vitro co-culture assays with TAG72-positive and negative ovarian cancer target cell lines and primary cancer patient samples, using flow cytometry and ELISA. Anti-tumor activity of TAG72-BBζ CARs was evaluated in-vivo by intravenous or intraperitoneal routes of administration in clinically relevant peritoneal ovarian cancer models in NSG mice.

Results

TAG72-CAR T cells containing a 4-1BB co-stimulatory domain demonstrated selective activation and targeting of TAG72-positive ovarian cancer cells. Furthermore, our CARs targeted TAG72-positive cancer cells obtained from ovarian cancer patient ascites in-vitro. Analysis of in-vivo therapeutic activity of TAG72-BBζ CARs in two clinically relevant ovarian peritoneal cancer models show that regional intraperitoneal, but not intravenous, delivery of TAG72-BBζ CARs exhibited more potent anti-tumor activity and extended survival in mice. Importantly, repeat administration of TAG72-BBζ CARs more

effectively controlled tumor burden and extended overall survival. Tumor recurrences following CAR T cell therapy, in part due to tumor antigen heterogeneity and/or limited T cell persistence, were also observed.

Conclusions

TAG72-BBζ CAR T cells showed potent antigen-dependent cytotoxicity and cytokine production against multiple TAG72-positive ovarian cancer cell lines and patient-derived ovarian cancer ascites. Using in-vivo xenograft models of peritoneal ovarian tumors, regional intraperitoneal delivery of TAG72-BBζ CAR T cells significantly reduced tumor growth and extended overall survival of mice, and was further improved with repeat infusions of CAR T cells. However, antigen loss was observed in early recurring tumors, which coincided with a lack of T cell persistence. Taken together, we demonstrate efficacy with TAG72-CAR T cells for ovarian cancer, warranting further investigations as a therapeutic strategy for this disease.

Ethics Approval

The study was approved by the COH Institutional Review Board (IRB) and Office of Human Subjects Protection.

P260

Automated perfusion-based systems for research- and clinical-scale dendritic cell generation

Shashi Murthy, BS, PhD[1], Andrew Kozbial, BS, PhD[1], Lekhana Bhandary, BS, PhD[1]

[1]*Northeastern University, Boston, MA, USA*

Background

Dendritic cells (DCs) are effective vehicles for personalized therapies and there is substantial interest in leveraging their capabilities for improving patient outcomes [1,2]. However, the process of generating these DCs, typically from monocytes (MOs), in an efficient and reproducible process has proved challenging. We have developed automated closed systems, EDEN (large scale) and MicroDEN (small scale), for generating clinically relevant numbers of DCs from precursor MOs which can be sterile-transferred for downstream applications. These systems overcome many of the constraints of manual processing and are designed for the research environment as well as clinical manufacturing.

Methods

Enriched MOs were seeded into EDEN at a density of 206,000 MOs/cm2 using RPMI 1640 medium supplemented with 10% HI-FBS and 500 U/mL IL-4 and GM-CSF (R&D). Medium was continuously perfused and immature DCs were harvested on Day 6.Enriched MOs were seeded into MicroDEN at densities of 200k, 400k, and 600k MOs/cm2 using CellGenix DC Medium supplemented with 350 U/mL IL-4 and GM-CSF (CellGenix). Medium was continuously perfused and DCs were harvested on Day 6.

Results

Flow cytometry indicated that immature DCs (iDCs) from EDEN exhibited standard DC-SIGN (CD209), CD14, and CD80/83/86 (Figure 2). Antibody expression is comparable to prior results collected in MicroDEN and well plate controls. Approximately 25 million viable iDCs were harvested from EDEN for an iDC yield of 32% with the relatively low seeding density. These results indicate that EDEN can be used to generate clinically relevant numbers of iDCs in a single closed system. Flow cytometry indicated that MicroDEN generated phenotypically similar iDCs at each seeding density with an iDC yield of ~30% (Figure 3), similar to well plate controls. Allogeneic functional assays indicated that MicroDEN iDCs exhibited improved proliferative activity than well plate iDCs and generally exhibited better activity at lower seeding densities (Figure 4).

Conclusions

DCs generated in both EDEN and MicroDEN are phenotypically comparable and exhibit increased proliferative activity to standard manual culture. Upto 26 million DCs can be generated by MicroDEN at the highest seeding density whereas the output of EDEN is 26 million DCs at the lowest seeding density.

Acknowledgements

Funding from the NIH via U24 AI118665 is gratefully acknowledged.

References

1. Wang Z, Wu Z, Liu Y, Han W. New development in CAR-T cell therapy. J Hematol Oncol. 2017;10:53.2. Carreno BM, Magrini V, Becker-Hapak M, Kaabinejadian S, Hundal J, Petti AA, et al. A dendritic cell vaccine increases the breadth and diversity of melanoma neoantigen-specific T cells. Science. 2015;348:803-808.

Figure 1.

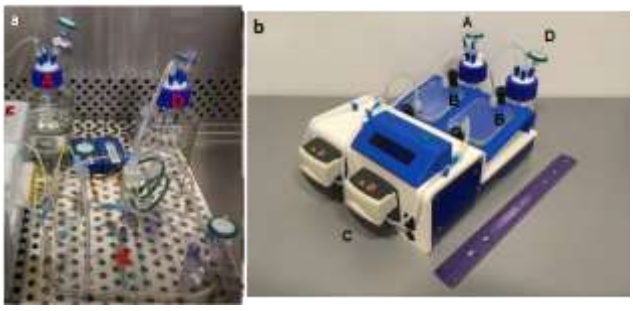

Figure 2.

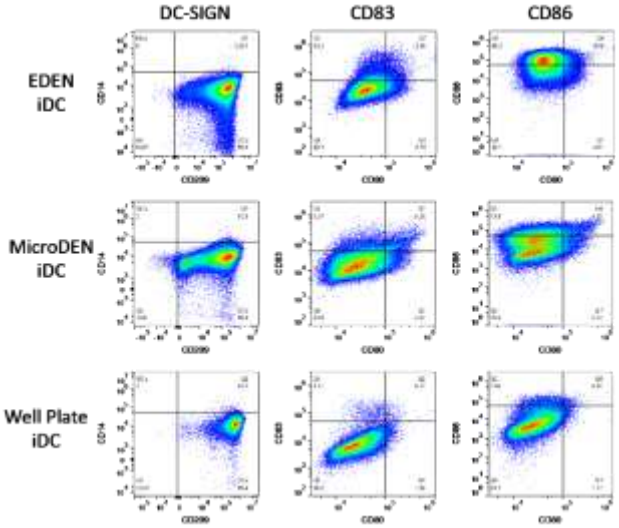

Figure 3.

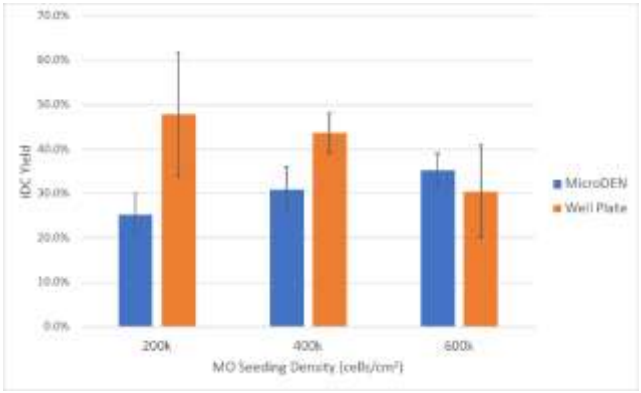

Figure 4.

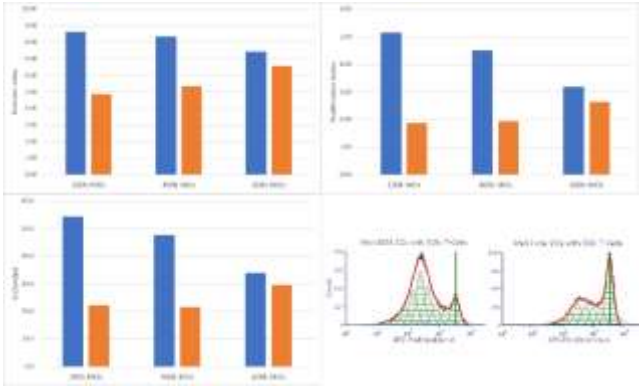

P261

Identification and pre-clinical development of tumour-reactive T-cell receptors from tumour-infiltrating lymphocytes

Natasha Myhill, MRes[1], John Bridgeman, Dr[2]

[1]*University of Manchester, Manchester, UK*
[2]*Immetacyte Ltd., Manchester, UK*

Background

Background: In the treatment of metastatic melanoma, tumour-infiltrating lymphocyte (TIL) therapy is one of the most promising immunotherapeutic options, with response rates of over 50% regularly reported. However, the tumour-reactive populations within the TIL products often remain poorly characterised, for example, whether the targets are comprised mainly of 'neoantigens' which are patient-specific or more common antigens shared between patients. By investigating whether T-cell receptors (TCRs) from TIL products reactive to common melanoma antigens can be utilised for treatment of multiple patients, we can better understand and shape TIL and TCR therapy to better target patient tumours.

Methods

Five HLA-A*02-restricted TCRs from one patient TIL sample that all recognise the shared melanoma antigen gp100 have been identified using an innovative paired TCR single cell sequencing technique. Initially, the gp100-TCRs have been cloned first into a TCR-negative Jurkat cell line for characterising their reactivity profiles using a series of flow cytometry based co-culture assays, before transduction into primary cells for assessment of tumour-killing potential. Matched and mismatched tumour lines, derived from patient tumour digest, were also characterised according to their tumour antigen expression using flow cytometry.

Results

Using the Jurkat cell model, results show that there are differences in the activation profile of the five TCRs, regarding their sensitivity to the gp100 index peptide when presented by T2 cells. The results also show that there is limited cross-reactivity between the TCRs, and that their activation profiles in response to HLA-A*02-expressing tumours derived from patient tumour samples reflect those seen for the gp100-index peptide. When the gp100-TCRs were cloned into primary CD8+ T-cells, intracellular cytokine staining by flow cytometry shows that all the TCRs respond to the gp100 index peptide and are capable of killing HLA-A*02 restricted tumour cells. The relative gp100 expression between the different tumours explains some of the differences in T-cell responses.

Conclusions

Out of the five candidate TCRs, gp100-5 exhibits the strongest activation profile when shown to the patient matched tumour line, indicating it might be the best at responding to lower levels of the antigen. These data allow us to better interrogate the overall reactivity profiles of TIL and investigate the specific shared antigen responses contained within these therapeutic cell populations.

Acknowledgements

I would like to acknowledge GigaGen for their involvement in the identification of the gp100-TCRs using their paired TCR single cell sequencing method.

P262

AIM ACT, a novel nanoparticle-based technology that generates therapeutic numbers of functional tumor-specific CD8+ T cells with central and effector phenotype in 14 days

Mathias Oelke, PhD[1], Sojung Kim[1], Juan Varela[1], Tatsuya Yoshida[2], Jeffrey Weber, MD, PhD[2], Lauren Suarez[1], Emily Lu[1], Celine Walmacq[1], Daniel Dembrow[1], Daniel Bednarik[1], Kenneth Carter, PhD[1], Scott Carmer, MBA[1]

[1]NexImmune, Gaithersburg, MD, USA
[2]New York University Medical Center, New York, NY, USA

Background
Efficient ex-vivo generation of functional tumor-specific T cells with memory phenotype remains a significant hurdle for the broad application of adoptive cell transfer (ACT) protocols for the treatment of cancer. Genetically engineered T cells represent one option, but genetic manipulation of T cells presents significant challenges in terms of complexity and generation time. Here, we describe a novel nanoparticle-based approach for generating tumor-specific T cells at clinical grade and scale from the endogenous T cell repertoire using artificial antigen presenting cells (aAPC).

Methods
Our aAPC consist of a paramagnetic nanoparticle to which humanized HLA-A2-Ig dimer-molecules and anti-CD28 antibodies are covalently linked. aAPC are loaded with multiple HLA-A2 restricted peptides and used to magnetically enrich and expand tumor-specific CD8+ T cells. Using peptide loaded aAPC, a fully enclosed, semi-automated, GMP T cell expansion platform has been developed that consistently generates clinically relevant numbers of tumor-specific, central and effector memory CD8+ T cells in 14 days, providing an alternative to genetic manipulation of T cells.

Results
Starting from a healthy donor leukopak, CD8+ T cells were generated using an aAPC cocktail loaded with 5 HLA-A2 epitopes from AML tumor antigens WT1, PRAME and cyclin A1. On average (n>20), 1-2 x109 T cells were generated that were 90% memory T cells with about 50% central memory and 40% effector memory CD8+ T cells. AML-specific T cells were expanded 500 to >5000-fold from low frequency precursor populations. These T cells were fully functional, as demonstrated by intra-cellular cytokine analysis and tumor cell killing. The system was also used to generate Mart-1 specific T cells of the same quality from cryopreserved PBL from melanoma patients. Additional data analyzing the TCR repertoire of the expanded AML and melanoma-specific T cells will be presented.

Conclusions
AIM ACT is a novel nanoparticle-based T cell expansion platform for the rapid, streamlined generation of clinically-relevant numbers of tumor-specific, central and effector memory CD8+ T cells from donor and patient PBMC in 14 days. The results reported here describe a platform that will be used in a multi-institution phase I clinical trial of adoptive T cell transfer for the treatment of AML patients pre- and post-allogeneic hematopoietic stem cell transplant. The flexibility of the AIM ACT system, as demonstrated using both AML and melanoma antigens, shows the potential for clinical application in other heme and solid tumors. Additionally, the system can be used for targeting both known and neo-epitopes.

P263

IL13RA2 as a new target for T-cell based therapies of melanoma brain metastases

Maria Ramello, PhD[1], Ismahene Benzaid, PhD[1], Maritza Lienlaf[1], Vincent Law[1], Nikhil Khushalani, MD[1], Amod Sarnaik, MD[1], Inna Smalley, PhD[1], Keiran Smalley, PhD[1], Peter Forsyth, MD[1]

[1]Moffitt Cancer Center, Tampa, FL, USA

Background
Melanoma brain metastases (MBM) represent a common complication of advanced cutaneous melanoma, and a major unmet need. Adoptive T cell therapies using genetically modified T cells to express chimeric antigen receptors (CAR) have shown evidences of disease control in primary brain

tumors. Based on the observation of immunologically relevant expression of IL13RA2 mRNA in metastatic lesions of melanoma patients, we tested the potential of this cancer/testes antigen as a target for cellular immunotherapies.

Methods

IL13RA2 expression was analyzed in patient-samples by flow cytometry. Activity of CAR-T cells was analyzed in vitro in co-cultures with target cells and in vivo, in a murine model of leptomeningeal disease (LMDz).

Results

Flow cytometry analyses confirmed the surface expression of IL13RA2 in MBM, as well as in soft tissues, in 12 out of 14 surgically resected lesions. We generated 2 novel 2nd generation CARs targeting IL13RA2 based on humanized monoclonal antibodies, which recognized the IL13RA2-expressing melanoma cell lines A375 and A375BR. Moreover, CAR-T cells exhibited a potent cytotoxic effect against Lu1205, M299 and WM1366 melanoma cell lines as measured by ACEA's xCELLigence real-time cytotoxic assay. In order to test whether T cell function may be affected by soluble factors present in the cerebrospinal fluid (CSF), we stimulated PBMCs with anti-CD3/CD28 beads in presence or absence of CSF. We observed higher proliferation in presence of melanoma patient-derived CSF compared to IL-2-containing media, suggesting that CAR-T cells are not intrinsically inhibited by (and might benefit from) exposure to CSF. In order to study CAR-T function in vivo, we developed a murine model of LMDz, an aggressive form of progression of MBM. To induce LMDz, A375BR cells were injected into cisterna magna of NSG mice. At day 10, all mice exhibited a significant reduction in total body weight, suggesting disease progression. On day 11, 25*10^6 CAR-T cells or untransduced controls (UT) were intravenously administered. Following treatment, mice treated with IL13RA2-CAR-Ts exhibited stabilization in the body weight while those receiving UTs continued to lose weight. At day 10 post-adoptive cell transfer we found higher counts of T cells in CSF of CAR-T-treated mice compared to UT.

Conclusions

In summary, our results suggest that IL13RA2 is a plausible target for CAR-T-based therapy of MBM. In addition, we demonstrate that human CSF does not exert an intrinsically inhibitory effect on T cell proliferation. Our current efforts are focused on further characterizing the in vivo therapeutic efficacy of anti-IL13RA2 CAR-T cells against MBM.

Acknowledgements

We acknowledge Margaret Baldwin, Assistant Director, Direction of Comparative Medicine, USF, for cisterna magna injections.

Ethics Approval

This study was approved by USF and Chesapeake IRB approval numbers 50102 and pro00014483, respectively, and by USF IACUC R2385.

P264

Identification of tyrosine phosphorylation sites in CD28 domain and their role in CAR-T cell function

Maria Ramello, PhD[1], Bin Fang, PhD[1], John Koomen, PhD[1], Eric Haura, MD[1]

[1]*Moffitt Cancer Center, Tampa, FL, USA*

Background

Chimeric antigen receptors (CARs) contain an antigen-sensing ectodomain and a signaling endodomain responsible for the initiation of a phosphorylation cascade that drives T-cell activation. Numerous pathway-focused attempts to characterize CAR signaling properties have been described. However, a global system-level assessment of CAR-triggered signaling network has not been described.

Methods
In order to conduct an unbiased analysis of CAR-initiated signaling events, we designed a phosphoproteomic assay in which PSCA-specific CAR-T cells are stimulated with metabolically heavy-labeled pancreatic cancer cells naturally expressing PSCA. Phosphorylation events (pY and pS/T) were detected by LC-MS/MS in the co-culture extracts. Post-hoc analyses allowed us to discriminate signals corresponding to T cells, based on exclusion of heavy-labeled tumor proteins. Ingenuity Pathway Analysis™ was used to identify pathways that were significantly overrepresented among the differentially phosphorylated proteins. CARs bearing phosphomimetic or non-phosphorylatable substitutions in key Y residues were generated, to validate their functional relevance in co-culture experiments and in in vivo models of adoptive immunotherapy.

Results
We found 40 peptides (of 791) differentially phosphorylated between CAR-Ts and mock-transduced T cells, spanning multiple pathways. Following tumor cells recognition, 2nd generation CAR-Ts exhibited more pronounced changes in phosphorylation than 3rd generation counterparts. Interestingly, we detected phosphorylation in all four tyrosine (Y) residues contained in the CD28 cytoplasmic tail. Two of these residues (Y191/YNMN and Y209/PYAP) are well characterized in terms of their functional relevance. However, the role of Y206 and Y218 residues is poorly understood. To evaluate their biological relevance, we generated 8 different versions of PSCA-CARs, each one including a non-phosphorylatable alanine-substitution or a phosphomimetic glutamic-acid-substitution in one of the identified Y residues. Upon transduction of human T cells, we observed that alanine-substitution of Y218 and glutamic-acid-substitution of Y191 severely compromised CAR expression as well as cytokine production after co-culture with target cells. Moreover, IFNγ and IL-2 production in response to tumor recognition were reduced when Y206 and Y209 were mutated with either of both alanine or glutamic-acid residues. Most importantly, we found that Y206A and Y218A substitutions reduced the anti-tumor efficacy of PSCA-CAR-Ts in vivo.

Conclusions
In summary, we developed a mass spectrometry platform to assess signaling events in CAR-Ts in a co-culture system. We identified four Y residues within the CD28 domains that are phosphorylated upon CAR activation, and established their relevance for CAR expression and/or function. A deeper understanding of molecular events controlled by these phosphosites will allow us to design new CARs with enhanced functional properties.

Acknowledgements
We acknowledge Christopher Anermann for technical assistance.

Ethics Approval
This study was approved by USF's IACUC, approval number R2385

P265

Inhibiting immune evasion in CNS tumors by reversing epigenetic gene silencing of chemoattractant cytokines

Nivedita Ratnam, PhD[1], Heather Sonnemann[1], Amber Giles, PhD[1]

[1]*National Cancer Institute, Bethesda, MD, USA*

Background
While immunotherapy may be a potential therapeutic strategy for CNS malignancies, concerns remain regarding the successful trafficking of cytotoxic immune cells into the tumor. CNS tumors have multiple strategies of immune evasion including

the epigenetic silencing of chemoattractant cytokines. However, interferon gamma (IFNg) from activated T cells can induce tumor cells to express chemoattractants CXCL9 and CXCL10. In ovarian cancer models, the histone methyltransferase inhibitor, GSK126, enhanced expression of these chemokines, thereby increasing T cell trafficking to the tumor. Here, we tested if GSK126 could likewise increase T cell migration to glioma tumors.

Methods

Gene expression of CXCL9 and 10 by qRT-PCR was determined in human and murine gliomas cell lines after treatment with a combination of IFNg and GSK126. ELISA assays were conducted to quantify secreted chemokines under similar treatment conditions. Cell migration assays were performed using tumor condition media (TCM) from human and mouse glioma cells treated with IFNg and GSK126 using healthy donor T cells (from PBMC) or mouse splenic T cells. Expression of CXCR3, the receptor for CXCL9 and 10 on T cells was measured in response to treatment with GSK126.

Results

CXCL9 and CXCL10 were enhanced both at the RNA and protein level in glioma cells treated with IFNg and GSK126 compared to vehicle treatment. This corresponded to increased T cell migration to GSK126-treated TCM. Treatment with GSK126 caused an increase in CXCR3 expression as well as an upward trend in gene expression of IFNg on T cells.

Conclusions

Our data support that epigenetically silencing the expression of chemoattractant cytokines is a mechanism of inhibiting immune cell trafficking into primary brain tumors. Histone methyltransferase inhibitors such as GSK126 reverse this gene silencing, resulting in increased T cell migration towards tumor cells. Thus, combinatorial treatment strategies involving GSK126, could potentially increase therapeutic efficacy by inhibiting immune evasion and increasing immune cell trafficking to the tumor; providing a potential rational combination with other immunotherapy regimens under investigation for primary brain tumors including checkpoint blockade using anti-PD-1 and/or anti-CTLA-4.

P266

Improving T cell functionality for adoptive cell transfer therapy in metastatic colon cancer

Sruthi Ravindranathan, PhD[1], Mohammad Raheel Jajja[1], Christopher Petersen[1], Ramireddy Bommireddy[1], Periasamy Selvaraj[1], Lily Yang[1], Bassel El-rayes, MD[1], Brianna Flynn, MS[2]

[1]*Emory University, Atlanta, GA, USA*
[2]*Isoplexis, Branford, CT, USA*

Background

Checkpoint inhibitors have shown promise in the management of several solid cancers, however this has not been replicated in colon cancer. This poor response has been attributed to high molecular heterogeneity and low frequencies of tumor infiltrating lymphocytes. We have previously demonstrated that T cells isolated from heavily treated lymphoma patients when treated with inhibitors of PI3K delta (idelalisib) and vasoactive intestinal peptide (VIP) signaling results in decreased levels of senescent T cells and increased frequency of stem memory and central memory T cells [1]. Additionally, we have demonstrated that tumor membrane vesicles (TMVs) prepared from human tumor cells decorated with IL-12 and B7-1 (IL-12. B7-1 TMVs), stimulate expansion of tumor antigen specific T cells [2]. Thus, current study aims to combine both strategies to obtain tumor antigen specific T cells with enhanced anti-tumor activity and in-vivo persistence.

Methods

PBMCs were obtained from four consented colon

cancer patients by Ficoll lymphocyte separation medium. Cells were then cultured for 14 days in RPMI complete media with 10% FBS, 50uM 2-mercaptoethanol, 30U/ml IL-2, anti-CD3/CD28 beads and in the presence or absence of idelalisib and/or antagonist for VIP (VIPhyb). The polyfunctionality strength index (PSI) of the expanded cells was determined via single cell analysis measured using in-depth cytokine analysis on the IsoCode Chip from Isoplexis. Fresh colon cancer tissue obtained from consented patients with metastatic colorectal cancer was implanted into immunocompromised mice NOD-SCID-gamma (NSG) and monitored for tumor growth. After sequentially transplanting in NSG mice for 3-5 passages, the tumors were isolated, lysed to generate cell membranes and incorporated with human IL-12 and B7-1 using glycosylphosphatidylinositol (GPI) anchor. The expression of IL-12 and B7-1 on the TMVs was confirmed using flow cytometric analysis.

Results

PBMCs from colon cancer patients expanded with VIPhyb and idelalisib resulted in enhanced PSI in CD4+ T cells (Figure 1). The elevated PSI was predominated by effector proteins associated with anti-tumor profile. Flow cytometric analysis of hIL-12. hB7-1 TMVs confirmed expression of human IL-12 and B7-1 (Figure 2).

Conclusions

Treating PBMCs isolated from colon cancer patients with VIPhyb and idelalisib increases the polyfunctionality strength index of CD4+ T cells. Further, if TMVs decorated with IL-12 and B7-1 are included in the culture, we expect to successfully expand tumor antigen specific T cells that can be adoptively transferred to colon cancer patients. Experiments are underway to test this hypothesis in vitro and in PDX mice with human colon cancer.

References

1. Petersen CT, Hassan M, Morris AB, Jeffery J, Lee K, Jagirdar N, Staton AD, Raikar SS, Spencer HT, Sulchek T, Flowers CR, Waller EK. Improving T-cell expansion and function for adoptive T-cell therapy using ex vivo treatment with PI3Kdelta inhibitors and VIP antagonists. Blood Adv. 2018;2(3):210-23.2.
Nagarajan S, Selvaraj P. Human tumor membrane vesicles modified to express glycolipid-anchored IL-12 by protein transfer induce T cell proliferation in vitro: a potential approach for local delivery of cytokines during vaccination. Vaccine. 2006;24(13):2264-74.

Ethics Approval

The study was approved by Emory's Institutional review board, approval number 00054023 The study was approved by Emory's Institutional Animal Care and Use Committee, protocol number 2005055

Figure 1. Polyfunctional strength index (PSI) of CD4+ cells

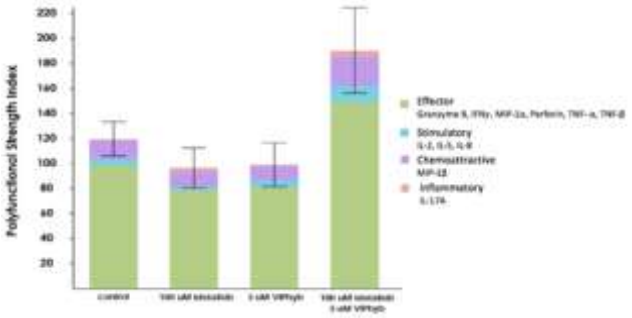

Figure 2. TMVs generated from PDX tumor decorated IL-12 B7-1

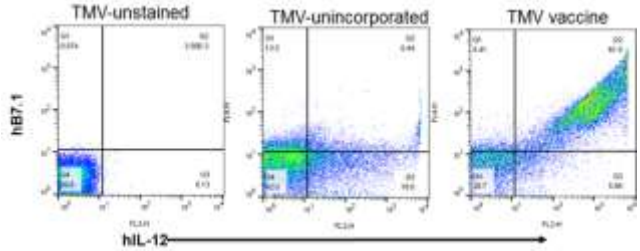

P267

Hijacked CAR19 T cells have potent activity against solid tumors

Paul Rennert, PhD[1], Fay Dufort, PhD[1], Lihe Su, PhD[1], Lan Wu, PhD[1], Alyssa Birt[1], Roy Lobb, PhD[1], Christine Ambrose, PhD[1]

[1]*Aleta Biotherapeutics, Natick, MA, USA*

Background

CAR T cells targeting CD19 (CAR19s) can eradicate B cell leukemias and lymphomas. The effectiveness of CAR19s is driven by their robust expansion and persistence properties, supported by normal CD19+ B cells. Thus CD19+ B cells serve as a non-tumor dependent, self-renewing source of antigen. We re-engineer CAR19s to secrete retargeting fusion proteins (FPs) by encoding expression cassettes downstream of the CAR sequence. By hijacking CAR19s, we utilize their inherent persistence properties. By designing multi-specific FP, we directly counter the clinically critical issues of tumor heterogeneity and antigen loss.

Methods

A MCSV promoter-based lentiviral vector was used to express the CAR19 construct and FPs. FP expression cassettes were designed to encode the CD19 proteins extracellular domain and one or two scFv sequences, separated from the CAR sequence by a P2A cleavage site. This modular design is termed IMPACTtm (Integrated Modular Proteins for Adoptive Cell Therapy). Primary T cells were transduced with an IMPACT- lentiviral vector encoding a CD19-anti-Her2 FP. FP secretion was measured across multiple donors. Next, an anti-EGFR scFv was added, creating a CD19-anti-Her2-anti-EGFR FP. FP activity was analyzed using binding and cytotoxicity assays. Primary T cells transduced with the CAR19/CD19-anti-Her2+ FP were assayed for in vivo efficacy using Her2+ tumor cells implanted into NSG mice.

Results

The CD19/anti-Her2 and anti-Her2/EGFR FPs were highly potent in cytotoxicity assays targeting Her2+, EGFR+ and dual positive solid tumor cell lines. The concentration of CD19/anti-Her2 fusion protein required redirect the CAR19 to kill 50% of the tumor cells was 10 pM (0.7 ng/ml). Transduced primary donor T cells secreted ~ 20 ng/ml of the CD19/anti-Her2 FP in cell culture and expressed CAR19 on the cell surface. All CAR19-based primary T cells killed CD19+ Nalm6 tumor cells. Redirected cytotoxic activity against Her2+ SKOV3 tumor cells was demonstrated in vitro and in vivo. A bispecific FP containing CD19 linked to anti-Her2 and anti-EGFR scFv was very potent against tumor cells expressing both antigens (IC50=0.75 pM). For each antigen, cytotoxicity was specifically mediated by the secreted fusion protein. Additional program examples of multi-specific targeting for diverse hematologic and solid tumor types will be shown.

Conclusions

The IMPACT platform addresses critical issues in cell therapy including CAR persistence, antigen escape and antigen heterogeneity, and provides important solutions for treating both hematologic and solid tumors. The potency of redirected cytotoxicity supports clinical development of CAR19/IMPACT programs, four of which are now ready for IND enabling studies.

P268

Heterogeneity of pancreatic cancer tumor-infiltrating T cells at the single cell level

Donastas Sakellariou-Thompson, BS[1], Aislyn Schalck[1], Mark Hurd, PhD[1], Gauri Varadhachary[1], Milind Javle, MD[1], Anirban Maitra, MBBS[1], Nicholas Navin, PhD[1]

[1]*MD Anderson Cancer Center, Houston, TX, USA*

Background
Pancreatic ductal adenocarcinoma (PDAC) has a 5-year survival rate of only 8%, and attempts to improve its outcome with checkpoint blockade have been ineffective. Although the T-cell infiltrate is poor, the presence of CD3+ tumor-infiltrating lymphocytes (TIL) in PDAC is correlated with better survival and our previous work demonstrated that tumor-reactive CD8+ TIL can be expanded from PDAC. While exploring the TIL repertoire, high frequency T-cell clones overlapping between the tumor and uninvolved-tissue were observed, suggesting the presence of tissue-resident memory T cells (Trm). These cells are often marked by expression of CD103, and recent work in other cancer types showed that tumor-reactive cells can be found in the Trm subset of CD8+ TIL.

Methods
High-order flow cytometry was performed on TIL from 5 primary human PDAC tumor samples examining expression of CD103 and several costimulatory and inhibitory markers. Additionally, single-cell RNA sequencing (scRNA-seq) was performed on the same samples to generate gene expression profiles paired with T-cell receptor sequences. Unbiased clustering was used to visualize the TIL clusters. TIL clones were defined as significantly expanded if they had a < 0.05 FDR-adjusted probability of being observed at, or above, the measured frequency when sampled from a multinomial distribution of all observed clones at even frequencies.

Results
Flow cytometry revealed that most PDAC samples did not contain substantial CD103+ population except for one. Therefore sequencing data was explored to find a Trm gene signature in PDAC that may not be principally defined by CD103. To date, 2,237 TIL have been sequenced. Initial clustering of CD8+ TIL showed a Trm-like group (e.g. CXCL13, LAG3, CTLA4 and CD39) and an associated mitotic subset (e.g. STMN1, H2AFZ, TUBB, and Ki67) whose phenotype aligned with assessed markers by flow cytometry. However, these groups were almost exclusively mapped to the sole CD103+ sample. After removing this sample to better define the CD103- populations, the resulting CD8+ clusters revealed a cytotoxic TIL population with no clear Trm-like signature within the effector memory subset. CD4+ TIL split into two distinct groups containing an activated Treg cluster and a conventional CD4+ T-cell cluster. The expression profile of expanded TCR clonotypes was also explored and will be discussed.

Conclusions
This study shows the potential of combining multi-parameter flow cytometry and scRNA-seq in defining functional heterogeneity of TIL in PDAC.

Ethics Approval
The study was approved by the Institutional Review Board of the University of Texas MD Anderson Cancer Center (LAB00-396, PA15-0014).

Consent
Written informed consent was obtained from the patients for publication of this abstract. A copy of the written consent is available for review by the Editor of this journal.

P269 Abstract Travel Award Recipient

Global phosphoproteomic analysis of chimeric antigen receptor and T cell receptor signaling enables design of modified receptors with distinct properties

Alexander Salter, BS[1], Richard Ivey[1], Anusha Rajan[1], Jacob Kennedy[1], Valentin Voillet, PhD[1], Jeffrey Whiteaker[1], Raphael Gottardo, PhD[1], Stanley Riddell, MD[1], Alexander Salter, BS[1]

[1]*Fred Hutchinson Cancer Research Center, Seattle, WA, USA*

Background
Chimeric antigen receptors (CARs) are synthetic proteins that redirect T cell specificity to tumor-associated antigens by mimicking certain aspects of T cell receptor (TCR) signaling. Most CARs contain the T cell-activating CD3z endodomain and a costimulatory domain from CD28 or 4-1BB. T cells expressing CD28/CD3z or 4-1BB/CD3z CARs are effective at treating refractory B cell malignancies but exhibit differences in effector function and cell fate that impact clinical efficacy and toxicity. These differences are assumed to result from activation of divergent signaling cascades, but the signaling pathways initiated by CARs and how these pathways compare to TCRs are poorly understood.

Methods
We developed a shotgun mass spectrometry platform to study CAR and TCR stimulation-induced protein phosphorylation events in primary human T cells. By coupling this technology to RNAseq, immunoprecipitations, in vitro measures of T cell function, and xenograft mouse models, we comprehensively traced how CAR and TCR-induced changes in protein phosphorylation alter T cell fate and function.

Results
Stimulation of CD28/CD3z or 4-1BB/CD3z CAR T cells activated nearly identical phosphoprotein signaling cascades. Instead, the major difference between the two CARs related to signaling kinetics and intensity whereby CD28/CD3z CAR stimulation produced faster and greater magnitude changes in protein phosphorylation. Increased CD28/CD3z CAR signal strength was related to CAR-Lck association and promoted an effector cell-like transcriptional profile and greater susceptibility to T cell exhaustion in a xenograft model of disseminated lymphoma. Mass spectrometry-guided mutagenesis of the CAR CD28 signaling domain enabled creation of fully-functional mutant CD28/CD3z CARs with reduced intensity. Further comparison of CAR to TCR signaling identified signaling adapters not engaged by CAR stimulation and provided a framework for altering CAR structure to engage these molecules.

Conclusions
CD28/CD3z and 4-1BB/CD3z CAR signaling is qualitatively similar and differs primarily in kinetics and magnitude. Increased TCR signaling strength is known to promote short-lived effector responses at the expense of memory formation and we propose that signal strength is also a major determinant of CAR T cell function and fate. Modification of CAR structure to fine-tune signal quantity and/or engage accessory signaling adapters may lead to more effective therapeutic receptors.

Acknowledgements
This work was supported by R01CA114536, FHCRC Bezos Immunotherapy Pilot Award, and FHCRC Interdisciplinary Cancer Research Training Grant.

Ethics Approval
Primary T cells were obtained from peripheral blood of healthy adults under a Fred Hutchinson Cancer Research Center Institutional Review Board-approved protocol (# 344). Informed consent was obtained from all enrollees.

P270

A novel, human sdAb-based, CAR against CD33, effectively targets AML in vitro and in vivo, and spares hematopoietic stem cells

Dina Schneider, PhD[1], Ying Xiong, PhD[1], Peirong Hu[1], Darong Wu, MS[1], Weizao Chen[2], Tianlei Ying[2], Zhongyu Zhu[1], Dimiter Dimitrov, PhD[3], Boro Dropulic, PhD, MBA[1], Rimas Orentas, PhD[4]

[1]*Lentigen, a Miltenyi Biotec Company, Gaithersburg,*

MD, USA
[2]National Cancer Institute, NIH, Frederick, MD, USA
[3]University of Pittsburgh, Frederick, MD, USA
[4]Seattle Children's Research Institute, Seattle, WA, USA

Background
Acute myeloid leukemia (AML) remains a challenging disease, and better treatment options are needed. Therapies targeting the AML cell surface antigen CD33 include the approved antibody drug conjugate gemtuzumab ozogamycin (My96) and investigational CART approaches incorporating CD33-binding domains derived from humanized scFvs. Single-domain antibodies (sdAbs), due to their small size, lack of mispairing risk, and human origin, are an attractive alternative option to scFv targeting domains for CARs, but have not been extensively evaluated.

Methods
We designed a novel chimeric antigen receptors utilizing sdAb-based targeting sequence (CAR33VH) derived by screening a human sdAb phage-display library, or the My96 scFv (My96CAR), serving as a comparator. Lentiviral expression vectors encoding each CAR construct incorporating the targeting domain in frame with a CD8 hinge and transmembrane domain, a 4-1BB costimulatory domain and a CD3 zeta activation domain, were transduced into activated primary human T cells. CAR T cells were characterized in vitro and in vivo for efficacy, specificity and toxicity against AML and for reactivity to hematopoietic stem cells (HSC) in vitro.

Results
The novel sdAb-based CAR33VH demonstrated robust and CD33-specific cytotoxicity in short-term and long-term killing assays against leukemic cell lines, and target-specific induction of IFN-gamma, TNF-alpha and IL-2 in response to CD33+ lines HL-60, MOLM-14 and KG-1a. Studies in A431 cells stably transduced with either full length or the clinically relevant truncated isoform of CD33, revealed that CAR33VH targets the V Ig-like domain of the full length CD33M isoform, as does the My96 CAR. Colony forming unit assays using human CD34+ HSCs pre-incubated with CAR T cells at E:T ratio of 20:1 overnight, and then transferred together to MethoCult medium supplemented with SCF, IL-3, IL-6, EPO, G-CSF, and GM-CSF for fourteen days, revealed no apparent toxicity to hematopoiesis of erythroid or myeloid lineages. In an in vivo AML model, NSG mice engrafted with the MOLM-14 leukemia cell line stably expressing firefly luciferase, both CAR33VH and CARMy96 efficiently eliminated tumors as documented by IVIS imaging.

Conclusions
We demonstrate for the first time the feasibility and efficacy of employing a human sdAb-derived binding domain in an anti-AML CAR design. CAR33VH was efficient in tumor killing in vitro and in vivo, and showed comparable functionality to the scFv-based My96CAR. Notably, CAR33VH had no detrimental effect on the development of myeloid or erythroid lineages in vitro, suggesting a potential for hematopoietic recovery following appropriate regulation of CAR expression in the therapeutic T cell population.

P271

Titratable and reversible regulation of IL12 or IL15 with FDA-approved drugs enhances CAR-T therapy

Steven Shamah, PhD[1], Brian Dolinski, BS[1], Kutlu Elpek[1], Tucker Ezell[1], Michelle Fleury[1], Jennifer Gori, PhD[1], Jia Gwee[1], Scott Heller, MS[1], Mara Inniss[1], Abhishek Kulkarni[1], Meghan Langley, BS[1], Dan Jun Li, MD[1], Grace Olinger, MS[1], Michelle Ols, PhD[1], Benjamin Primack[1], Christopher Reardon[1], Michael Schebesta[1], Dexue Sun[1], Zoe Tarasiewicz, BA[1], Karen Tran, MS[1], Michael Briskin[1], Celeste Richardson[1], Vipin Suri[1], Steven Shamah, PhD[1], Steven Shamah, PhD[1]

[1]*Obsidian Therapeutics, Cambridge, MA, USA*

Background
Adoptive cell therapy with chimeric antigen receptor (CAR) modified T cells has demonstrated clinical efficacy in the treatment of B cell malignancies and multiple myeloma. Efficacy of CAR-Ts in other indications has been hindered by limited CAR-T cell expansion, immunosuppression by the tumor microenvironment, and on-target/off-tumor toxicity. Armoring CAR-Ts to produce interleukin-15 (IL15) or interleukin-12 (IL12) has been shown to drive CAR-T expansion and resistance to immunosuppression, respectively, enhancing anti-tumor activity. However, published data suggest that the uncontrolled expression of either would likely compromise safety. Technologies that provide precise control over cytokine activity could therefore broaden clinical application of CAR-T therapies.

Methods
We developed a platform that equips immune cells with functionalities regulated via the administration of FDA-approved small molecule ligands. We utilize small, fully human protein sequences called destabilizing domains (DDs) that confer reversible destabilization to a fused target protein. In the absence of ligand, the fusion protein is degraded, whereas the presence of ligand restores expression and functionality. Stabilization is titratable by small molecule ligand dosing and reversible, providing fine-tuned control over the timing and concentration of target protein levels.

Results
We developed DDs based on the human phosphodiesterase 5 (PDE5), dihydrofolate reductase (DHFR), and estrogen receptor (ER) proteins, each of which can be regulated by FDA-approved ligands with distinct pharmacokinetic properties. Using these clinically translatable DDs, we created regulated IL12 and IL15 constructs that provide exogenous regulation of cytokines for enhanced CAR-T function. Transduction of T cells with lentivirus expressing cytokine-DD fusions led to titratable cytokine production upon exposure to ligands that stabilize PDE5, DHFR or ER-regulated DDs. ER-based DDs fused to IL12, led to low levels of basal IL12 expression in the absence of ligand and rapid induction of IL12 in an ER ligand concentration-dependent manner. Treatment of T cells expressing PDE5-based DDs fused to a membrane-bound IL15-IL15 receptor alpha chimera (mbIL15) supported rapid dose-dependent increases in cell surface mbIL15 expression upon exposure to PDE5 stabilizing ligands. These findings demonstrate how cytokine levels can be precisely regulated by manipulation of drug concentration and kinetics. The functional regulation of DD-fused cytokines and enhancement of anti-tumor activity using FDA-approved drugs in a mouse CAR-T tumor model is currently in testing.

Conclusions
Destabilizing domains fused to proteins, coupled with FDA-approved drug administration, support exogenous control of cytokines toward the development of CAR-T cell products with enhanced efficacy and more favorable safety profiles.

P272

A fully-closed, high efficiency manufacturing technology platform for the production of T cell therapies targeting multiple tumor antigens

Christine McInnis, PhD[1], Amy Shaw[1], Shawn Carey, PhD[1], Jonas Bruun, PhD[1], Rachel Klaski[1], Pengpeng Cao, PhD[1], Elisabeth Brown[1], Andy Rakestraw, PhD[1], Becker Hewes, MD[1], Jonathan Fitzgerald, PhD[1], Thomas Andresen, PhD[1], FABIO FACHIN, PhD[1]

[1]*Torque Therapeutics, Cambridge, MA, USA*

Background
Adoptive cell therapy (ACT) is a promising approach

for treating tumors refractory to other treatment modalities. ACTs, however, are still largely limited to genetically-modified approaches that recognize a single antigen, require harsh pre-treatments or adjuvant drugs to enable ACT survival and function *in-vivo*, and are often associated with severe toxicities. Torque's *Deep-Primed™* cell therapy platform uses novel cell process engineering to generate cytotoxic T lymphocytes (CTLs) that target multiple tumor antigens and that are tethered to Deep-IL15, a crosslinked multimer of human IL15-Fc,to deliver directed immune activation in the tumor microenvironment. Torque's *Slipstream™* cell process is semi-automated and fully closed, and its modular automation design enables both large-scale and decentralized manufacturing.

Methods

Following apheresis, patients' T cells and monocytes are enriched, and monocytes
are rapidly differentiated into peptide-loaded mature dendritic cells (mDC) for presentation to autologous T cells. Antigen-presenting mDC are co-cultured with T cells, promoting expansion of low-frequency, antigen-specific T cells directed towards multiple tumor associated antigens (TAA). Following expansion, the multi-target T cells are loaded with Deep IL-15, cryopreserved and formulated for multiple infusions. Here, we present product composition, specificity, cytotoxicity, and the advantage of Deep IL-15 across development and GMP lots of CTLs generated from healthy donors.

Results

Torque's modular antigen-priming process reliably generates billions of T cells to obtain multiple drug doses via a single manufacturing run. Across donors and across both process development and GMP sites, Torque's process reliably expands endogenous antigen-specific CTLs and results in a balanced ratio of CD8+ and CD4+ T cells. The CTL products display a mixture of memory and effector phenotypes, with low expression of exhaustion markers. The products are further characterized by a unique signature against multiple TAA epitopes, with a mean 11% TAA-specificity [5-20%]. TCR sequencing reveals that the majority of clones in the final product originate from rare clones, undetectable in the incoming apheresis. Post thaw, the Deep IL-15 tethered to the CTLs ensures prolonged survival, increased expansion, and cytotoxicity against antigen-expressing cell lines.

Conclusions

Torque's Slipstream™ manufacturing process uses proprietary biology processes and automation to produce Deep-Primed™ T-Cells with high efficiency using a cGMP process. Torque's lead clinical program, TRQ15-01, is expected to start in 2018 addressing indications in both hematologic and solid tumors.

P273

T cells cultured in the presence of TLR9 agonist gain a CD25(high)CD39(low), pro-inflammatory phenotype and regress melanoma in vivo

Aubrey Smith[2], Hannah Knochelmann[2], Connor Dwyer, PhD[2], Aubrey Smith[2], Aubrey Smith[2], Megan Wyatt, MS[2], Michelle Nelson, PhD[3]

[1]*Medical University of South Carolina, Charleston, SC, USA*
[2]*MUSC, Charleston, SC, USA*
[3]*Aptevo Therapeutics, Seattle, WA, USA*

Background

ACT therapy effectiveness is enhanced by preconditioning patients with a non-myeloablative lymphodepleting regimen [1-3]. In a mouse model of ACT one mechanism by which lymphodepletion enhances transferred T cells efficacy is by activating the innate immune system[4]. Microbes, which translocated from the radiation-injured gut, were responsible for activating innate immune cells

through Toll-like receptors (TLRs), which in turn, enhanced the function of CD8+ T cells[4]. Recently, administration of TLR agonists directly to the animal has proven an efficacious therapy[5, 6]. Additional immunostimulatory molecules such as IL-2, vaccine, or anti-OX40 agonist are necessary for antitumor efficacy with TLR agonist injection[5, 6]. Thus, we questioned whether generating a potent T cell product could be achieved by simply culturing anti-tumor T cells ex vivo with TLR9 agonist, CpG.

Methods

We employed the Pmel mouse model of ACT in which murine T cells express a transgenic TCR that specifically recognizes the peptide gp100 expressed by melanoma. Splenocytes acquired from this mouse were cultured in the presence of CpG-ODN 1668. Following culture cells were interrogated at the phenotypic and functional level in culture and/or infused into melanoma-bearing mice to determine their anti-tumor efficacy.

Results

We found that cells treated with CpG in vitro have a unique, proinflammatory, phenotype with high expression of IL-2Rα(CD25), but diminished expression of the ectonucleotidease CD39 (known to promote an immunosuppression). Further cells treated with CpG in vitro have enhanced anti-tumor efficacy in vivo compared to vehicle-expanded cells. CpG does not act directly on murine T cells in culture, as neither CD8+ isolated T cells nor day 3 cultured cells (>90% T cells) do not gain the CD25highCD39low when treated with CpG. Cells treated with CpG on day 3 of culture also do not have anti-tumor efficacy above that of vehicle treated cells. Finally, removing B cells from the culture on day 0 prevents the acquisition of the phenotype associated with CpG.

Conclusions

A potent T cell product can be generated by the addition of the TLR9 agonist, CpG, to the cell culture. These cells have a distinct, pro-inflammatory phenotype; they are CD25highCD39low and secrete overt INFgamma, Granzyme A and Granzyme B. Further, this phenotype and the potency of T cells generated is dependent on the presence of B cells in the culture as the removal of B cells prior to treatment with CpG in culture yielded a cell product with a similar phenotype and anti-tumor efficacy to that of vehicle treated cells.

References

1. Goff SL, et al. Randomized, prospective evaluation comparing intensity of lymphodepletion before adoptive transfer of tumor-infiltrating lymphocytes for patients with metastatic melanoma. J Clin Oncol. 2016; 34(20):2389-97. 2. June CH. Adoptive T cell therapy for cancer in the clinic. J Clin Invest. 2007; 117(6):1466-76. 3. June CH. Principles of adoptive T cell cancer therapy. J Clin Invest. 2007; 117(5):1204-12. 4. Paulos, CM, et al. Microbial translocation augments the function of adoptively transferred self/tumor-specific CD8+ T cells via TLR4 signaling. J Clin Invest. 2007; 117(8): 2197-204. 5. Nelson MH, et al. Toll-like receptor agonist therapy can profoundly augment the antitumor activity of adoptively transferred CD8(+) T cells without host preconditioning. J Immunother Cancer. 2016; 4: 6.6. Sagiv-Barfi I, et al. Eradication of spontaneous malignancy by local immunotherapy. Sci Transl Med. 2018; 10(426).

P274

Functional screening of different anti-B7H6 CAR designs

Sophie Agaugué, PhD[1], Lorraine Springuel[1], Benjamin Demoulin[1], Martina Fontaine, PhD[1], Adam Hargreaves, Dr[2], Dorothée Daro[1], Jennifer Bolsée, PhD[1], Céline Jacques-Hespel[1], Valérie Steenwinckel, PhD[1], David Gilham, PhD[1], Sophie Agaugué, PhD[1]

[1]Celyad, SA, Villejuif, France

[2]PathCelerate, Alderley Park, UK

Background

B7H6, a stress-induced ligand for the NK-activating receptor Nkp30, is widely expressed on the surface of transformed cells yet absent from healthy tissues under steady state conditions. In cancers, B7H6 expression is associated with tumor progression, poor prognosis and lymph node metastasis, while B7H6 expression on tumor cells can be upregulated by conventional cancer therapies. Therefore, B7H6 represents a highly attractive target for the immunotherapy of a broad range of high risk cancers. In this work, we investigated the optimal CAR design to develop an effective B7H6-targeted CAR T cell therapy.

Methods

B7H6 expression was assessed on a large panel of cancer cell lines by qRT-PCR and Flow Cytometry, as well as in patient samples from neuroblastoma, colorectal and ovarian tumors by IHC. The optimal CAR design to redirect T cells against B7H6 was investigated by engineering various constructs differing in the origin of their targeting moiety (murine versus humanized scFv) and the nature of the costimulatory signaling module (CD28, 4-1BB or a combination thereof). Primary human T cells transduced with the distinct CARs were assessed for proliferation, viability, CAR expression, cellular phenotype and in vitro functionality, cytotoxicity and cytokine production, upon co-culture with B7H6-bearing cancer cells.

Results

We verified that B7H6 RNA and protein were expressed by human cancer cell lines of various types and confirmed by immunohistochemistry B7H6 expression in primary tumors, validating B7H6 as an attractive target for immunotherapy. Importantly, B7H6 was highly expressed in ovarian cancer, a tumor type with high unmet medical need. Based on preliminary results, CAR T cells bearing the different generations of anti-B7H6 CAR were successfully produced, although the 4-1BB-containing 2nd generation murine CAR showed very low levels of membrane expression. Expansion and viability of CAR T cells bearing the humanized scFv were reduced compared to their murine counterparts. Moreover, humanized CAR T cells released interferon γ in their supernatant and expressed markers of activation and exhaustion, reminiscent of self-reactivity. Importantly, the 2nd generation CAR comprised of the murine scFv fused to CD28-CD3ζ tail endowed T cells with the best functionality to all other constructs when co-cultured with B7H6-expressing cancer cell lines.

Conclusions

Functional screening of different designs indicate the B7H6-targeting CAR comprised of murine scFv fused to CD28-CD3ζ signaling tail as our prime candidate warranting further preclinical investigation for the development of a clinical product. In vivo experiments using xenograft models for assessing anti-tumor efficacy will soon be initiated.

Ethics Approval

All tissue samples (primary tumors and normal tissues) were acquired under appropriate IRB/ethical approvals in place in the country from which the tissue was sourced. All animal and human samples study protocols were approved by local ethical committees and authorities.

P275

Pooling signaling and costimulatory domains in a flexible CARpool design

Jennifer Bolsée, PhD[2], Lorraine Springuel[1], Amélie Velghe[2], Sophie AGAUGUE, PhD[2], David Gilham, PhD[2]

[1]Celyad, SA, Villejuif, France
[2]Celyad, Mont-saint-Guibert, Belgium

Background
CARs are modular receptors that consist of a target binding moiety fused to structural domains including an extracellular spacer, a transmembrane region and intracellular signaling domains. These signaling regions typically comprise a tandem alignment of co-stimulatory (e.g. CD28, CD137) and activatory (CD3ζ) domains that upon target binding initiate activation of T cell effector functions. This linear configuration displays a rigid spatial orientation and ratio of co-stimulation to activation domains. To address this, we have developed a novel mix-and -match approach (CARpool) where the costimulatory signal is provided in trans on accessory proteins that associate with the antigen binding chain via transmembrane-mediated interactions, potentially driving the ability to tailor T cells responses upon CAR activation.

Methods
Exploiting the ability of NK activating receptors to assemble as multi-subunit complexes via membrane-embedded opposite charge interactions, several CD3ζ-containing CAR chains were designed using the transmembrane and cytoplasmic domains of NKG2D or NKp44, able to associate with DAP10 and DAP12 respectively. Each CAR included a B7H6 specific scFv. The CAR- and accessory protein-encoding sequences were co-expressed using 2A self-cleaving sites within the pSFG vector backbone. These constructs were compared to a classical second-generation CAR construct containing an intracellular CD28 costimulatory domain. Primary human T-cell populations expressing the diverse constructs were screened for CAR expression, T cell phenotype and in vitro function (cytokine secretion and cytolytic activity) upon co-culture with B7H6-expressing cell lines.

Results
NKG2D-based CAR complexes were moderately expressed at the cell surface but bound B7H6 and released cytokines upon co-culture with B7H6-expressing cancer cells. Modification of the position of the charged residue within the transmembrane domain of the CAR is being used to modulate the surface expression of the receptor. NKp44-based CAR complexes were more frequently expressed on primary T cells and binding to B7H6 was confirmed, validating the feasibility of the approach although functionality of these NKp44 based receptors appears currently to be more limited. We are optimizing these receptors including hinge domains in order to enhance functionality.

Conclusions
These studies provide proof-of-concept for a novel modulatory CAR design where it is possible to incorporate or interchange optimal costimulatory domain(s) depending on the target of interest and in a stoichiometrically controlled way. Notably, this does not necessitate subcloning the CAR chain itself. Importantly, recapitulating physiological TCR activation by providing co-stimulation in trans within the CARpool may result in optimal downstream signaling, thereby enhancing anti-tumoral activity of CAR T cells.

Ethics Approval
Human samples study protocols were approved by local ethical committees and authorities.

P276

Characterization of systemic and local immunity following adoptive transfer of NY-ESO-1 SPEAR T-cells in synovial sarcoma (NCT01343043)

Samik Basu, MD[1], Justina Stadanlick[1], Indu Ramachandran, PhD[1], Daniel Lowther[1], Rebecca Dryer-Minnerly, PhD[1], Ruoxi Wang[1], Svetlana Fayngerts[1], Daniel Nunez[1], Natalie Bath, MSc[1], Gareth Betts, PhD[1], Karen Chagin, MD[1], Thomas Faitg, PhD[1], Wayne Higgins[1], Malini Iyengar, PhD[1], Luca Melchiori[1], Siva Samavedam[1], Jonathan Silk, PhD[1], Alex Tipping, PhD[1], Trupti Trivedi, MS[1], Erin

Van Winkle[1], Lilli Wang[1], Rafael Amado, MD[1], Gwendolyn Binder[1], Samik Basu, MD[1]

[1]*Adaptimmune, Philadelphia, PA, USA*

Background
Gene-modified autologous T-cells expressing NY-ESO-1c259, an affinity-enhanced T-cell receptor (TCR) reactive against the NY-ESO-1-specific HLA-A*02-restricted peptide SLLMWITQC (SPEAR T-cells; GSK 794), have demonstrated clinical activity in patients with advanced synovial sarcoma (SS). The factors contributing to gene-modified T-cell expansion and the changes within the tumor microenvironment following T-cell infusion remain unclear. Here, we report on phenotypic and functional studies on T-cells, sera, and tumor biopsies from SS patients treated with NY-ESO-1 SPEAR T-cells.

Methods
Engineered T-cell persistence was determined by qPCR for the vector backbone in post-infusion PBMC samples. Serum cytokines were measured via a multiplexed electrochemiluminescent MSD immunoassay. Multiplexed gene expression analysis and immunohistochemistry for immune markers (e.g. CD8) were performed on formalin-fixed paraffin-embedded (FFPE) tumor biopsies from patients prior to and following adoptive T-cell transfer. Additionally, RNA in situ hybridization (RNAish) was performed on FFPE tumor biopsies to detect the presence or absence of gene-modified T-cells within the tumor microenvironment following adoptive transfer. Clinical responses were assessed by RECIST v1.1.

Results
The magnitude of gene-modified T-cell expansion within two weeks after infusion was associated with response in patients with high expression of intra-tumoral NY-ESO-1 antigen expression (2+ or 3+ in ≥ 50% cells by IHC). Patients receiving a fludarabine-containing conditioning regimen experienced an increase in serum levels of the homeostatic lymphocyte cytokines IL-7 and IL-15. Prior to infusion, the SS microenvironment exhibited minimal leukocyte infiltration. CD163+ tumor-associated macrophages (TAMs) were the dominant population. An increase in leukocytes and lymphocytes within the tumor microenvironment was observed at the post-infusion tumor biopsy, at approximately 8 weeks. At time points greater than 8 weeks post infusion, the tumor microenvironment was minimally infiltrated with a TAM-dominant leukocyte infiltrate. Notably, genes encoding tumor-associated antigens and antigen presentation did not significantly change within the tumor post-T-cell infusion. Gene-modified NY-ESO-1c259TCR T-cells were capable of infiltrating the SS tumor microenvironment in a subset of tumor samples tested.

Conclusions
Our studies elucidate some of the factors that underpin response and resistance to adoptive gene-modified T-cell transfer in solid malignancies. Furthermore, these data demonstrate that non-T-cell inflamed tumors of a type that are often resistant to immune checkpoint blockade can be successfully treated with adoptive T-cell based immunotherapy.

Trial Registration
NCT01343043

Ethics Approval
The protocol was approved by each center's Institutional Review Board, and all patients signed informed consent forms.

P277

Genetic modification of IL13Rα2-CAR T cells to express secretory or membrane-bound IL-15 enhances their anti-glioma activity without discernible differences

David Steffin, MD[1], Haley Houke[2], Tim Sauer, MD[1], Irina Balyasnikova, PhD[3], Stephen Gottschalk[2], Center director Rooney, PhD[1], Giedre Krenciute, PhD[2]

[1]Texas Children's Hospital, Houston, TX, USA
[2]St. Jude Children's Research Hospital, Memphis, TN, USA
[3]Northwestern University, Chicago, IL, USA

Background

Immunotherapy with genetically modified T cells expressing chimeric antigen receptors (CARs) has the potential to improve outcomes for patients with glioblastoma (GBM), a type of brain cancer with dismal outcomes [1]. We have shown that IL13Rα2-CAR T cells have potent antitumor activity in preclinical GBM models, and that expression of secretory (s) IL15 further enhances their anti-glioma activity [2]. Several studies have suggested that membrane bound (mb) IL15 has greater biological activity than sIL15 [3]. However, the effector function of CAR T cells expressing mbIL15 or sIL15 have never been directly compared. Thus, the aim of this study was to generate IL13Rα2-CAR.sIL15 and IL13Rα2-CAR.mbIL15 T cells, and compare their anti-glioma activity.

Methods

We generated two retroviral vectors encoding an IL13Rα2-CAR with a CD28.ζ endodomain and sIL15 or mbIL15 separated by 2A sequence; mbIL15 consisted of IL15 linked to the CD8α stalk and transmembrane domain. In addition, both vectors encoded CD20 to facilitate detection of transduced T cells and to serve as a potential suicide switch. Genetically-modified T cells were generated by retroviral transduction. Transgene expression was confirmed by FACS analysis (IL13Rα2-CAR, CD20, mbIL15) or ELISA (sIL15).

Results

In cytotoxicity assays, IL13Rα2-CAR, IL13Rα2-CAR.sIL15 and IL13Rα2-CAR.mbIL15 T cells readily killed IL13Rα2+ U373 glioma cells with no significant differences between effector T-cell populations. Expression of sIL15 or mbIL15 significantly enhanced the expansion of IL13Rα2-CAR T cells upon stimulation with U373 glioma cells and CAR T cells expressing sIL15 secreted significantly higher amounts of INFg when compared to IL13Rα2-CAR.mbIL15. However, there was no significant difference in the fold-expansion of IL13Rα2-CAR.sIL15 and IL13Rα2-CAR.mbIL15 T cells.

Conclusions

We demonstrate here that expression of sIL15 or mbIL15 in IL13Rα2-CAR T cells enhance their anti-glioma activity. Our in vitro studies indicate so far that there is no significant difference in the effector function of IL13Rα2-CAR.sIL15 and IL13Rα2-CAR.mbIL15 T cells. In vivo studies are in progress to confirm our findings. Thus, genetic modification of IL13Rα2-CAR T cells with sIL15 or mbIL15 presents a promising strategy to enhance their anti-glioma activity.

References

1. Fangusaro, J. Pediatric high grade glioma: a review and update on tumor clinical characteristics and biology. Frontiers in oncology. 2012;2:105.
2. Krenciute, G.; Krebs, S.; Torres, D.; Dotti, G.; Lesniak, M.S.; Balyasnikova, I.V.; Gottschalk, S. Charachterization and functional analysis of scFv-based CARs to redirect T cells to IL13Rα2-positive glioma. Journal for immunotherapy of cancer. 2015;3(S2):P116.
3. Imamura, M.; Shook, D.; Kamiya, T.; Shimasaki, N.; Chai, S.M.; Coustan-Smith, E.; Imai, C.; Campana, D. Autonomous growth and increased cytotoxicity of natural killer cells expressing membrane-bound interleukin-15. Blood. 2014:blood-2014-2002-556837.

P278

Identification of senescent T-cell subsets that impact gene-engineered T cell manufacturing success and product consistency

Jeffrey Teoh, PhD[1], Daniel Cossette[1], Sara Cooper[1]

[1]*Juno Therapeutics, a Celgene Company, Seattle, WA, USA*

Background

Autologous chimeric antigen receptor (CAR) T-cell therapy has demonstrated significant clinical benefit in hematological malignancies. The autologous nature of CAR T-cell therapeutic modalities introduces heterogeneity into the manufacturing process. Both pre- and post-manufacturing memory T-cell phenotypes have been demonstrated to correlate with clinical outcome [1,2], and enrichment for early memory T-cell subsets is associated with improved manufacturing success [3]. However, little is known regarding the mechanisms by which T-cell phenotypic heterogeneity impacts the manufacturing process and pre-infusion CAR T-cell profiles. Here we demonstrate the presence of a T-cell subset that does not appear to expand in CAR T cell manufacturing, but continues to consume growth factors as well as drive process and product heterogeneity.

Methods

CD19-directed CAR T cells were activated through engagement of CD3/CD28, transduced, and expanded in vitro. Throughout this process, T cells were assessed for expansion, viability, activation, memory differentiation state, and cell cycle state. Functionality of the final drug product was also assessed, including cytokine production and cell survival following CAR-specific stimulation.

Results

The majority of T cells upregulated activation markers, including CD25 and CD69, in the presence of the CD3/CD28 stimulus, whereas only a subset of activated T cells entered cell cycle based on Ki67 expression. The Ki-67+ fraction primarily comprised cells expressing CD27 and CD28, whereas Ki67- populations were enriched for CD57+ cells and corresponded with CD27-CD28- phenotypes. CD57+ cells exhibited activated phenotypes and persisted throughout early process stages. The proportion of CD57+ T cells decreased after 48hrs, which coincided with T-cell expansion and increased viability. To directly assess the impact of CD57+/- T cells in CAR T-cell manufacturing, CD57+ cells were positively selected from starting material and combined with CD57- cells at various ratios prior to activation. The proportion of CD57+ cells in starting material correlated with process duration, and CAR T cells did not expand in the condition containing 95% CD57+ T cells.

Conclusions

Whereas CD27+ T cells appear to contribute to the majority of expanded cells in process manufacturing, CD57+ cells do not expand and appear to contribute minimally to the final drug product. CD57+ cells consume IL-2, occupy activation reagents, and contribute to cell counts used for establishing and maintaining cell culture. Thus, CD57+ T cells can directly impact upstream process operations and introduce variability in downstream expansion processes and product attributes. Selective depletion of CD57+ T cells at process initiation could augment cellular manufacturing success and further improve drug product consistency.

References

1. Fraietta JA, Lacey SF, Orlando EJ, Pruteanu-Malinici I, Gohil M, Lundh S, Boesteanu AC, Wang Y, O'Connor RS, Hwang WT, Pequignot E, Ambrose DE, Zhang C, Wilcox N, Bedoya F, Dorfmeier C, Chen F, Tian L, Parakandi H, Gupta M, Young RM, Johnson FB, Kulikovskaya I, Liu L, Xu J, Kassim SH, Davis MM, Levine BL, Frey NV, Siegel DL, Huang AC, Wherry EJ,

Bitter H, Brogdon JL, Porter DL, June CH, Melenhorst JJ. Determinants of response and resistance to CD19 chimeric antigen receptor (CAR) T cell therapy of chronic lymphocytic leukemia. Nat Med. 2018; 24(5):563-571.
2. Larson RP, Lower R, DeVries T, Jiang Y, Hause RJ, Getto R, Christin B, Yee NK, Bowen MA, Weber C, Li D, Albertson T, Sutherland C, Ramsborg CG. Defined cell composition and precise control over JCAR017 dose enables identification of relationships between chimeric antigen receptor T cell product attributes, pharmacokinetics, and clinical endpoints in NHL. Cancer Res. 2018; 78(13 Suppl):Abstract nr 960.
3. Singh N, Perazzelli J, Grupp SA, Barrett DM. Early memory phenotypes drive T cell proliferation in patients with pediatric malignancies. Sci Trans Med. 2016; 8(320):320ra3

P279

CRISPR/Cas9 enables the efficient production of allogeneic CAR-T cells engineered to contain multiple genome edits to enhance therapeutic T-cell function

Demetrios Kalaitzidis, PhD[1], Ashley Porras, BA[1], Dan Henderson[1], Sushant Karnik[1], Katie Levitsky, BS[1], Jason Sagert, PhD[1], Zinkal Padalia, MS[1], Mary Lee Dequeant, PhD[1], melanie allen, BS[1], Hanspeter Waldner[1], Henia Dar, PhD[1], Chandirasegaran Massilamany, PhD[1], Paul Tetteh[1], Dakai Mu, BA[1], Elaine Huang, PhD[1], Thao Nguyen[1], Sarah Spencer, PhD[1], Kelly Maeng[1]

[1]*Crispr Therapeutics, Cambridge, MA, USA*

Background
The CRISPR/cas9 system allows for rapid assessment of the consequences of perturbing many genes while at the same time deriving potentially lead molecules for cell and gene therapies

Methods
This technology was applied to primary human T cells to produce allogeneic CAR-T cells by multiplexed genome editing. A robust system has been developed for site-specific integration of CAR and multiplexed KO generation by utilizing homology-directed repair (HDR) with Cas9 ribonucleoprotein (RNP) and an AAV6-delivered donor template.

Results
The CRISPR/cas9 multi editing system was used to discover the following in the allogeneic CAR T cell setting: 1) multiple edits (>5) can be applied efficiently producing stable non transformed CAR T cells, 2) the effects of single and multiple edits on CAR T function can be examined efficiently to determine gene edits that improve CAR T cell function, 3) the consequence of these effects for on target and off target activity can be used to rapidly generate lead gRNAs, 4) next generation cell therapies can be defined towards targeting solid tumors with allogeneic CAR T cells. Here we show the effects in vitro and in vivo of knocking out multiple genes singly and in combination, including the response to multiple antigen challenges and the ability to overcome PDL1 induced resistance.

Conclusions
Producing CAR T cells with multiple edits could be an important step towards enhancing the ability of this therapeutic class to tackle solid tumors with improved efficacy over the current therapeutics.

P280

IL-12 cytokine priming of low avidity tumor specific T cells enhances tumor clearance and prevents exhaustion

Christopher Tucker, BS[1], Jason Mitchell[1]

[1]*University of Minnesota, Minneapolis, MN, USA*

Background
Checkpoint blockade therapy has largely failed in patients that lack immune infiltration of their tumor. To generate a de novo immune response in these patients, adoptive cellular therapy (ACT) has been attempted with the transfer of high avidity tumor reactive T cells. This has resulted in significant autoimmunity and long term therapeutic failure. We and others have hypothesized this autoimmunity is due to this use of high avidity T-cells reacting to healthy tissue. We therefore hypothesized that low avidity T-cells could provide comparable tumor control but limit these autoimmune side effects with the optimal cytokine priming regimen.

Methods
Using high and low avidity transgenic tumor reactive CD8+ T-cells specific for tyrosinase-related protein-2 (TRP2) we investigated how IL-2 alone or IL-12/IL-2 priming affected these two different T-cell populations. We crossed these TRP2 specific transgenic mice to GFP and Brainbow Red mice to track antigen specific T-cell populations during adoptive transfer and investigated cytokine production and cell surface markers with flow cytometry and two-photon microscopy.

Results
Low avidity TRP2 T-cells primed with IL-2 alone failed to control melanoma growth, and became tolerized within the tumor environment. Additionally these T-cells were poorly cytolytic to tumor targets and underwent increased apoptosis when co-cultured with tumor cells. To overcome this deficiency, our lab had previously published that IL-12 cytokine priming during activation of adoptively transferred T-cells provided superior tumor control. With these experiments we show that IL-12 restores low avidity T-cell functionality and tumor cytolysis potential while preventing T-cell exhaustion by down regulation of PD-1. We additionally show that PD-1 checkpoint blockade provides no additional therapeutic benefit when transferring IL-12 primed CD8+ T-cells. Finally we show that with tumor antigen overexpression and IL-12 priming low avidity T-cells can provide long term tumor control.

Conclusions
Taken together these data indicate that IL-12 priming of low avidity T-cells could be an effective approach in clinical ACT protocols. This protocol could provide superior safety margins in cancer patients by avoiding autoimmunity while maintaining therapeutic efficacy.

P281 Abstract Travel Award Recipient

Endogenous MHC class II restricted CD4+ T cell responses to recurrent driver mutations in melanoma and non-small cell lung cancer (NSCLC)

Joshua Veatch, MD, PhD[1], Brenda Jesernig, MS[1], Sylvia Lee[2], Stanley Riddell, MD[1]

[1]*Fred Hutchinson Cancer Research Center, Seattle, WA, USA*
[2]*University of Washington, Seattle, WA, USA*

Background
T cell responses to mutated neoantigens are thought to mediate clinical responses to immune checkpoint inhibition and adoptive cell transfer in cancers with high mutation burdens. Most T cell responses to neoantigens recognize patient specific mutations, posing an obstacle for design of vaccination or adoptive transfer strategies. Here, we identify endogenous T cell responses in patients with cancer to 3 different recurrent oncogenic driver mutations: BRAF V600E, KRAS G12V and the ERBB2 (Her2) internal tandem duplication (Her2-ITD).

Methods
Neoantigen-reactive T cells were expanded and cloned after stimulating lymphocytes from

melanoma and NSCLC patients with peptide panels spanning mutations identified by exome sequencing.

Results

MHC class II restricted CD4+ T cells specific to the BRAF V600E mutation found in 40% of melanoma were isolated from a melanoma patient following a durable complete response to tumor infiltrating lymphocyte therapy. BRAF V600E specific cells showed a Th1 memory phenotype, were preferentially localized to the tumor site, and expanded and persisted in blood greater than 2 years after TIL therapy. The tumor from this patient had fewer than 30 somatic mutations and the BRAF V600E specific CD4+ T cell response was correlated with robust and persistent CD8+ T cell responses to multiple self–antigens. We also identified CD4+ T cell responses to the recurrent KRAS G12V and Her-ITD mutations in 2 different patients with lung adenocarcinoma. In all cases, the T cells recognized MHC class II expressing cells expressing the mutant but not wildtype sequences, and the Her2-ITD specific T cells localize preferentially to the tumor relative to the normal lung. T cell receptors (TCR) were isolated and conferred specificity to BRAF V600E, KRAS G12V and Her2-ITD following gene transfer. Each TCR was restricted by common class II HLA allele found in 10-25% of the population.

Conclusions

This study greatly expands the number of driver mutations that can be targeted by immunotherapy. Clinical evaluation of adoptive transfer or vaccination strategies should help interrogate the role of MHC class II restricted CD4+ T cells in human anti-tumor immunity, and could have clinical activity across multiple patients.

Ethics Approval

These studies were approved by the Institutional review board at the Fred Hutchinson Cancer Research Center, approval numbers 2643, 1765 and 1246.

P282

Pathogen-reduced human platelet lysate as a serum replacement maintains CAR T cells in a less-differentiated phenotype associated with superior anti-tumor function

Norihiro Watanabe, PhD[1], Alejandro Torres Chavez[1], Emanuele Canestrari, PhD[2], Christina Dann, PhD[2], Ann Leen[1], Juan Vera[1]

[1]*Baylor College of Medicine, Houston, TX, USA*
[2]*Cook Regentec, Indianapolis, IN, USA*

Background

Many groups have shown that the maintenance of a naive-like (TN) and central memory (TCM) CAR T cell phenotype during in vitro production is associated with prolonged in vivo T cell persistence resulting in potent anti-tumor effects. In this study we explored the impact of different media supplements on CAR T cell phenotype and function.

Methods

As a model system we used T cells modified with a second generation CAR targeting prostate stem cell antigen (PSCA) containing a CD28/CD3z endodomain, as previously published by our group. Three days post-retrovirus transduction in the presence of IL2 with 10% fetal bovine serum (FBS), CAR T cells were divided into 3 groups that were cultured in medium supplemented with either 10% FBS, 10% human AB serum (ABS) or 10% pathogen reduced human platelet lysate (PR HPL). Following a minimum of 7 days in culture under these conditions we evaluated CAR T cell growth, phenotype, and short- and long-term *in vitro* cytolytic activity and *in vivo* anti-tumor effects.

Results

We monitored T cell expansion over a 14-day period and found that CAR T cell growth was similar among the conditions. Interestingly, populations of CCR7+

cells (TN and TCM) were dramatically increased when CAR T cells were maintained in 10% PR HPL (CD4+: 66.7±2.1%; CD8+: 69.6±4.7%) compared to 10% FBS (CD4+: 36.2±3.3%; CD8+: 20.8±3.1%) or 10% ABS (CD4+: 15.8±1.6%; CD8+: 7.3±1.5%). Although CAR T cells maintained in PR HPL exhibited slightly lower cytolytic ability in a 5 hr 51Cr release assay because of highly enriched/less differentiated T cell populations, they showed potent anti-tumor effects with enhanced T cell expansion in a 9 day coculture assay. Importantly, these CAR T cells (1x10e6 cells/mouse) were able to eliminate established subcutaneous tumors in xenograft mice engrafted with PSCA-expressing tumors while cells maintained in either FBS or ABS only delayed but did not eliminate tumors. Furthermore, when we performed a tumor re-challenge experiment in mice who cleared their primary tumor by injecting with 2x10e6 cells/mouse, only animals that initially received PR HPL cultured CAR T cells exhibited CAR T cell accumulation and expansion at the re-challenge tumor site, resulting in anti-tumor effects, suggesting their capacity for long-term *in vivo* persistence.

Conclusions

Our work indicates that exposure of CAR T cells to PR HPL during *ex vivo* culture leads to improved maintenance of less differentiated T cells with enhanced persistence and *in vivo* anti-tumor killing ability.

P283

Allogeneic CAR T-cells resistant to both T- and NK-cell cytotoxicity

Alan Williams[1], Laurent Poirot, PhD[2], Philippe Duchateau[2], brian Busser[2], Alexandre juillerat[3], Stephane depil[2], Sonal Temburni-Blake, MS[3]

[1]*Cellectis. Inc, NYC, NY, USA*
[2]*Cellectis, Paris, France*
[3]*Cellectis.Inc, NYC, USA*

Background

The last years have seen the adoptive transfer of engineered autologous T-cells making great strides in the development of new treatments against cancer. The use of third party donor-derived T-cells represents an attractive alternative to generate CAR T-cells readily accessible to patients. These off-the-shelf cells derived from a possibly non-HLA-matched donor nevertheless carry the risk of graft-versus-host-disease (GvHD) through the expression of their endogenous T-cell receptors (TCRs).The recent advances in precise genome editing using designer nucleases allowed to mitigate this issue as demonstrated by the molecular remissions observed in patients after infusion of universal TALEN® multiplex gene-edited CAR T-cells. In particular, these universal CAR T-cells were engineered to reduce the risk of graft versus host disease (GvHD) by TALEN® inactivation of TCRαβ. The clinical outcome of CAR T-cell therapies is intimately linked to the ability of effector cells to engraft and proliferate in order to eradicate tumor cells within patients. Although the transient activity of off-the-shelf CAR T-cells represents an important safety feature, the possibility to extend their therapeutic window may be desirable in particular disease indications and after lymphodepleting regimens where the patient's immune system has been restored. Thus, we are developing novel approaches to render these cells less visible to both host T- and NK-cells.

Methods

The single genetic disruption of the beta-2 microglobulin (B2M) gene, a required component of all MHC class I molecules, promotes resistance to host CD8+ T-cell attack but may trigger NK-cell activation, leading to the rejection of the edited T-cells lacking MHC-I. We therefore further engineered these B2M negative cells via a TALEN®-mediated and B2M gene-specific targeted integration matrix to express inhibitors of NK cytotoxicity.

Results
We have identified an NK-cell inhibitor that successfully blocks the so-called NK-cell "missing self-response" in vitro and in vivo. Altogether, the precise TALEN®-mediated inactivation of B2M coupled with insertion of an NK-cell inhibitor enabled the generation of allogeneic CAR T-cells, resistant to host T- and NK-cells, with improved persistence and long-term anti-tumor activity.

Conclusions
We believe that this strategy provides a frame work to generate a universal CAR T-cells that will enable large scale utilization of adoptive T-cell therapies and thus benefit a broader range of patients.

P284

Importance of the enzymatic activity of CD26 expressed on tumor-specific Th17 cells for adoptive cell therapy

Megan Wyatt, MS[2], Stefanie Bailey[2], Hannah Knochelmann[2], Aubrey Smith[2], Connor Dwyer, PhD[2], Michelle Nelson, PhD[2]

[1]MUSC, Charleston, SC, USA
[2]Medical University of South Carolina, Charleston, SC, USA

Background
Adoptive T-cell immunotherapy (ACT), an exciting breakthrough in cancer treatment, utilizes patients' own tumor-specific T-cells to fight their cancer. However, not all T cells are equal in their tumor-fighting ability. We have recently discovered that CD4+ T cells that express dipeptidylpeptidase 4, or CD26, possess enhanced antitumor properties in three different aggressive models [1]. CD26 has several important functions that may play a role in antitumor responses, including enzymatic cleavage of chemokines involved in T cell migration. We sought to determine whether the CD26 protein is necessary for the observed enhanced anti-tumor efficacy, or if it is just a marker of an excellent memory cell population.

Methods
B16F10 melanoma tumors were subcutaneously injected on either wild-type (WT) mice or CD26-/- mice, both on a C57BL/6 background. Prior to ACT, the mice were given drinking water +/- 75 mg/kg daily dose of sitagliptin, an inhibitor of CD26 enzymatic activity. CD26+ Th17 cells isolated and expanded from TYRP transgenic mice expressing the TRP-1 T cell receptor that recognizes tyrosinase were adoptively transferred into the tumor-bearing mice, and tumor burden was measured for 128 days, during which sitagliptin treatment was constant.

Results
As has been previously demonstrated [2], sitagliptin treatment enhanced anti-tumor response of the Th17 cells in WT hosts initially. However, as the experiment progressed many of the initial responders regressed, so that survival +/- sitagliptin in WT mice was not significantly different. In the absence of host CD26, the Th17 cells drastically decreased tumor burden and increased survival (8/10 responders; survival of WT vs CD26-/- p=0.016, WT+sitagliptin vs. CD26-/- p=0.008, Mantel-Cox Logrank test). In sitagliptin-treated CD26-/- mice, the anti-tumor effect of the Th17 cells was diminished and 9/10 mice lost control of their tumor by day 78 post-treatment (survival of CD26-/- vs. CD26-/- +sitagliptin p=0.005, Mantel-Cox Logrank test).

Conclusions
The results of this study indicate that CD26 enzymatic activity is important for the ability of Th17 cells to produce an anti-tumor response, as the antitumor response of Th17 cells was lost in CD26-/- mice treated with sitagliptin. Further studies utilizing CD26-/- TYRP donor cells to ensure the specificity of the sitagliptin-mediated effects are planned, as are experiments with human T cells with CD26 removed

via CRISPR/Cas9 methods. This work will help define the antitumor role of CD26 in cells utilized for adoptive cell therapy.

References

1. Da Silva RB, Laird ME, Yatim N, Fiette L, Ingersoll MA, Albert ML. Dipeptidylpeptidase 4 inhibition enhances lymphocyte trafficking, improving both naturally occurring tumor immunity and immunotherapy. Nat Immunol. 2015;16(8):850-858.2. Bailey SR, Nelson MH, Majchrzak K, Bowers JS, Wyatt MM, Smith AS, Neal LR, Shirai K, Carpenito C, June CH, Zilliox MJ. Human CD26 high T cells elicit tumor immunity against multiple malignancies via enhanced migration and persistence. Nat Commun. 2017;8(1):1961.

Ethics Approval

The study was approved by the Institutional Animal Care and Use Committee at the Medical University of South Carolina, approval number 3039.

P285

A clinical study on CD33-directed chimeric antigen receptor modified NK cells

Qiao Li, PhD[4], Leiming Xia[1], Jing Zhang[2], Liu Liu[1], Bin Li[1], Tan Li[1], Yi Wang[1], Lin Yang[3], Yangyi Bao[1], Alfred Chang[4], Max Wicha, MD[4]

[1]*The First People's Hospital of Hefei, Hefei, China*
[2]*University of Michigan Rogel Cancer Center*
[3]*Persongen Biomedicine (Suzhou) Co., Ltd, Suzhou, China*
[4]*University of Michigan Rogel Cancer Cent, Ann Arbor, USA*

Background

About 20-40% of the patients with acute myeloid leukemia (AML) show no response to current therapy, and 50-70% of the patients relapse after complete response. These patients are categorized as refractory and relapsed (R/R) AML. The 1-year survival rate of these patients is limited to <30% and further dropped to approximately 10% for 5-year survival. More effective treatment for this disease is urgently needed. As a novel immune cell-based therapy, chimeric antigen receptor (CAR) modified NK (CAR-NK) cell treatment may represent a promising strategy in treating hematological malignancies.

Methods

Higher CD33 is expressed on both AML cells and leukemia stem cells (LSCs), compared with normal hematopoietic stem cells. Therefore, CD33-directed CAR-NK (CD33-CAR-NK) treatment may lead to the development of a novel strategy for R/R AML. In this clinical study, three patients with R/R AML expressing high levels of CD33 (40-70%) were enrolled. Two were M1 subtypes, and the other was M2a subtype. All three patients had received a series of standard chemotherapy regimen with no significant therapeutic effect before 3×109 allogeneic CD33-CAR-NK cells were infused. 1×109 CD33-CAR-NK cells were infused every other day for a total of three infusions.

Results

After CD33-CAR-NK cell infusion, the main side effects include repeated low-grade fever and significant rises of serum cytokines, e.g. IFN-γ, TNF-α, IL-2, IL-6 and IL-10. However, these cytokines reduced to normal level before discharge. In addition, we detected serum K+, Ca2+, creatinine and glutamic-pyruvic transaminase after CD33-CAR-NK infusion, and found none of these three indexes was significantly changed, compared with those before the CD33-CAR-NK infusion. After CD33-CAR-NK cell infusions, the proportion of leukemic cells in the patients' bone marrow significantly decreased from 40% to 26%; the proportion of CD33+ cells in bone marrow reduced from 48.82% to 32.56%, and the proportion of CD33+CD34+ cells in bone marrow reduced from 40.59% to 27.26% respectively in a 53

years old male patient with AML-M1.

Conclusions
This initial clinical work indicates that CD33-CAR-NK therapy may offer a new therapeutic option for R/R AML, which aims to reduce the tumor burden, eliminate LSCs, and provide opportunity to combine it with other therapies for more effective treatment of the R/R AML patients.

Acknowledgements
Medicine and technique Foundation of Hefei city, China; Longenbaugh Foundation, USA.

Trial Registration
NCT02944162.

Ethics Approval
This study was approved by the Ethics Board of the First People's Hospital of Hefei, China, approval number 2016-001-01.

P286

Combination of PD-1 blockade and RetroNectin-activated cytokine-induced killer cells in pre-heavily treated NSCLC: a retrospective study

Lingdi Zhao[1], Lu Han[2], Yong Zhang[2], Tiepeng Li[2], Yonghao Yang[2], Wei Li[2], Yiman Shang[2], Hongwei Lin[2]

[1]Affiliated Cancer Hospital of Zhengzhou University & Henan Cancer Hospital, Zhengzhou, Peoples Republic of China
[2]Affiliated Cancer Hospital of Zhengzhou, Zhengzhou, China

Background
Lung cancer is one of the most common malignancies worldwide, with high morbidity and mortality. Great advances have been made recently in the treatment of advanced non-small cell lung cancer (NSCLC); however, almost all patients eventually fail after first- or second-line therapy. There is no standard regimen for patients with advanced NSCLC after failure of second-line therapy. Therefore, it is of great importance to explore treatment regimens for these patients.

Methods
We retrospectively analyzed patients with advanced NSCLC who received anti-programmed cell death protein (PD)-1 antibody combined with RetroNectin activated cytokine-induced killer (R-CIK) cells after failure of at least two regimens from October 2015 to April 2018 in our department. A total of seven patients were included in this study. Descriptive statistics were used to summarize the patients' characteristics, treatment-related adverse events (AEs), overall responses, and R-CIK cell phenotypes. Survival was calculated using the Kaplan-Meier method.

Results
Of the seven patients, five were men and two were women. The median age was 54 years (range 42-64 years). The median number of previous treatment regimens was 3 (range 2-7). Partial remission was achieved in two patients, stable disease in four patients, and one patient experienced progressive disease. The median time-to-progression was 4.8 months. At present, there are four patients still alive, and the median overall survival has not been reached. During treatment, grade 2 fever occurred in two patients and grade 2 interstitial pneumonia in one patient; no AEs over grade 2 occurred.

Conclusions
PD-1 blockade combined with R-CIK cells is safe and effective in patients with advanced NSCLC who have failed at least two treatment regimens.

Clinical Trials (Completed)

P287

HyPeR: A phase 1, dose escalation study of Guadecitabine (SGI-110) a second generation hypomethylating agent in combination with Pembrolizumab (MK3475) in patients with refractory solid tumours

Malaka Ameratunga, MBBS[1], Maxime Chénard-Poirier[2], Sanjena Mithra[3], Ricardo Morilla[4], Ruth Riisnaes[4], Penny Flohr[4], Rita Pereira, BSc[4], Ana Ferreira, MSc[4], Ines Figueiredo[4], Suzanne Carreira[4], Claudia Bertan[4], Wei Yuan[4], David Dolling[4], Mateus Crespo[4], Bora Gurel[4], Bob Brown[5], Naina Patel[5], Joanna Dawes[4], Toby Prout[4], Mona Parmar[4], Alison Turner[4], Holly Tovey[1], Emma Hall[1], Anna Minchom[1], Udai Banerji[1], Nina Tunariu[1], Juanita Lopez[1], Dionysis Papadatos-Pastos[6]

[1]Royal Marsden Hospital, Sutton, UK
[2]CHU de Québec - Université Laval, Sutton, UK
[3]University College London Hospitals, London, UK
[4]Institute of Cancer Research, London, UK
[5]Imperial College London, London, UK
[6]University College Hospitals London, London, UK

Background
Guadecitabine is a second-generation DNA hypomethylating agent which induces epigenetic expression of immune related genes and increases the infiltration of interferon-producing T-cells into tumours; it can potentially enhance the anti-cancer activity of pembrolizumab [1,2]. The aim of this investigator-initiated study is to evaluate the safety and efficacy of guadecitabine in combination with pembrolizumab and identify the recommended phase 2 dose (RP2D).

Methods
Patients with advanced solid tumours, refractory to standard therapy received guadecitabine via subcutaneous injection on days 1-4 and pembrolizumab intravenously on day 1 of each 21-day cycle following a 4-week sensitising run-in period with guadecitabine. The study used a 3+3 design, with a dose-finding cohort (Part A) followed by an ongoing expansion cohort (Part B) at the RP2D and includes correlative pharmacokinetic and pharmacodynamic studies. Paired pre- and post-treatment tumour biopsies are to be evaluated for PD-L1 expression, tumour infiltrating lymphocytes, gene expression by RNAseq and methylome studies. Longitudinal analysis of peripheral blood CD3, CD4 and CD8 lymphocytes by flow cytometry using a multi-level mixed effect model was performed. The trial was reviewed by a central research ethics committee (REC#16/LO/1605).

Results
Following completion of Part A, 12 evaluable patients (2 mesothelioma, 2 PD-L1 negative NSCLC, 2 cholangiocarcinoma, 2 cervical, 2 breast, an ovarian and colorectal cancer) have been treated (6 each at 45mg/m2 and 30mg/m2 guadecitabine). Two DLTs (neutropenia, febrile neutropenia) were reported at 45mg/m2, whereas none were at 30mg/m2. The most common toxicities were reversible neutropenia, fatigue and abdominal pain. The recommended Phase II doses (RP2D) were 30mg/m2 for guadecitabine days 1-4 with 200mg IV pembrolizumab q21 days. Overall, 3 patients (colorectal cancer, NSCLC, cervical cancer) had prolonged stable disease > 6 months' duration. A patient with cervical adenocarcinoma had a 69% drop in Ca125. A patient with PD-L1 negative NSCLC with a STK11 aberration (associated with resistance to PD-1 inhibition [3]) had a PFS of 8 months. (Figure 1) A further patient with PD-L1 negative NSCLC was taken off study for PD, but on follow-up CT demonstrated a partial response, in the absence of intervening therapy. Longitudinal analysis of peripheral blood lymphocytes by flow cytometry over time showed evidence of increasing CD3 counts by 0.16%/day (p=0.03) and for CD4 by 0.17%/day

(p=0.007), but not CD8 counts. Enrollment in the expansion phase is ongoing.

Conclusions

The RP2D of this combination is 30mg/m2 guadecitabine D1-4 and pembrolizumab 200mg q21 with evidence of biological and anti-tumour activity.

Trial Registration

Eudra-CT 2016-000760-41

References

1. Coral S, Parisi G, Nicolay HJ, et al. Immunomodulatory activity of guadecitabine, a 5-aza-2'-deoxycytidine-containing demethylating dinucleotide. Cancer Immunol Immunother.2013;62:605-14
2. Wang LX, Mei ZY, Zhou JH, Yao YS, Li YH, Xu YH, et al. Low dose decitabine treatment induces CD80 expression in cancer cells and stimulates tumour specific cytotoxic T lymphocyte responses. PLoS One. 2013;8(5):e62924
3. Skoulidis, Ferdinandos, et al. "STK11/LKB1 Mutations and PD-1 Inhibitor Resistance in KRAS-Mutant Lung Adenocarcinoma." Cancer discovery (2018): CD-18.

Ethics Approval

The trial was reviewed by a central research ethics committee (REC#16/LO/1605).

Figure 1: Swimmer's plot

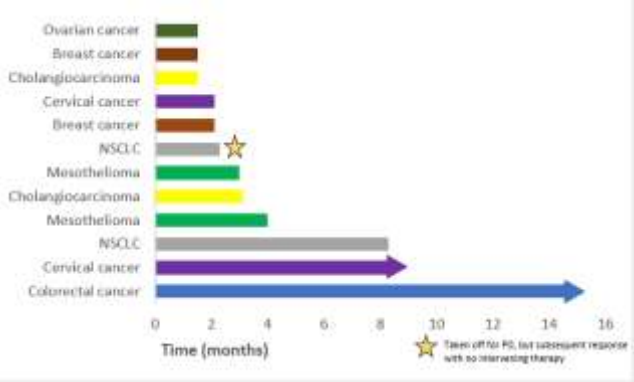

P288

IMAGE 1 (Immune Modulation And Gemcitabine Evaluation 1), a randomized, open-label phase II trial comparing gemcitabine with and without IMM-101 in advanced pancreatic cancer.

Angus Dalgleish, MD, PhD[1]

[1]*St. George's University of London, London, UK*

Background

The effectiveness of immunotherapy for pancreatic cancer is limited by the impenetrable nature of the primary tumor and the complex mix of cellular and biochemical negative regulators in the tumor microenvironment. To complement previously published encouraging results from the IMAGE 1 trial [1], we present here updated results to include the long- term follow-up of this study.

Methods

Patients (n=110) with advanced pancreatic cancer and WHO performance status 0-2 were allocated randomly to receive IMM 101 (a myeloid dendritic cell activator containing heat-killed Mycobacterium obuense [NCTC 13365]) + gemcitabine (Gem) (n=75) or Gem alone (n=35) for a 12-cycle maximum. Twelve of the thirteen patients who completed this protocol, (11 IMM-101 + Gem, 1 Gem alone) entered a follow-up sub-study to monitor long-term survival and tolerability, all receiving IMM 101 with or without adjunctive chemotherapy.

Results

Median overall survival (OS) was longer for patients from the IMM-101 + Gem group (6.7 v. 5.6 months, hazard ratio [HR] 0.67, 95% confidence interval [CI] 0.44 to 1.04; log rank p-value 0.0706) with the OS increase more pronounced for the pre-defined subset of patients (n=92) with metastatic disease (7.0 v. 4.4 months, HR 0.53, 95% CI 0.33 to 0.86; log rank p-value 0.0093). Longer follow-up of this

metastatic group, including data from the sub-study, revealed survival probabilities for the IMM-101 treated group of 18.3% at 18 months, 11.4% at 24 and 30 months and 5.7% at 36 months. The Gem-alone group had a survival probability of 2.3% at 18 months with no patients with survival data beyond this time point. Extended exposure to IMM-101 did not appear to compromise tolerability with maximum exposure of 46.5 months observed.

Conclusions

First line IMM-101 in combination with Gem produced extended survival benefits for metastatic pancreatic cancer patients compared to Gem alone. The survival probabilities beyond 24 months are comparable to those seen with the nab-paclitaxel-Gem combination [2], but without any notable incremental toxicity burden.

Acknowledgements

Funded by Immodulon Therapeutics, London, UK

Trial Registration

IMAGE 1: EUDRACT Number: 2010-022757-42; multiple ethics committee approvals obtained in accordance with requirements of participating countries and trial centers.

References

1. Dalgleish AG, et. al. Randomised, open-label phase II study of gemcitabine with and without IMM-101 for advanced pancreatic cancer. Br J Cancer 2016; 115, 789-796.
2. Goldstein D, et. al. nab-Paclitaxel plus gemcitabine for metastatic pancreatic cancer: Long-term survival from a phase III trial. J. Natl. Cancer Inst. 2015; 107 (2), dju413.

Ethics Approval

multiple ethics committee approvals obtained in accordance with requirements of participating countries and trial centers.

P289

Initial results from a phase 1a/b study of etigilimab (OMP-313M32), an anti-T cell immunoreceptor with Ig and ITIM domains (TIGIT) antibody, in advanced solid tumors

Sunil Sharma, MD[1], Kathleen Moore[2], Niharika Mettu[3], Ignacio Garrido-Laguna[4], Susanna Ulahannan, MD, MMed[2], Vivek Khemka, MD[1], Ann Kapoun[5], Leonardo Faoro[6]

[1]Honor Health Research Intitute, Scottsdale, AZ, USA
[2]University of Oklahoma, Oklahoma City, OK, USA
[3]Duke University, Durham, NC, USA
[4]University of Utah, Salt Lake City, UT, USA
[5]OncoMed Pharmaceuticals, Redwood City, CA, USA
[6]Oncomed Pharmaceuticals Inc, Redwood City, CA, USA
[7]Sarah Cannon Research Institute, Nashville, TN, USA

Background

TIGIT is an immune-checkpoint expressed on T and NK cells. Etigilimab is a novel IgG1 anti-TIGIT antibody that has inhibitory as well as ADCC characteristics. Anti-TIGIT demonstrates preclinical in-vivo anti-tumor effects as a single agent and with anti-PD-1. Initial results from the phase 1a dose escalation portion of the study are presented.

Methods

This study enrolled subjects with advanced solid tumors into either a Ph 1a single-agent portion (dose escalation in all comers + expansion in selected tumor types) or a Ph 1b combination [PD-(L)1 refractory] portion with nivolumab (dose escalation). Objectives included safety, maximum tolerated dose (MTD), determining the recommended Ph 2 dose (RP2D), pharmacokinetics, immunogenicity, efficacy and biomarkers. Dose escalation followed a modified 3+3 framework.

Results
18 subjects were treated in the dose escalation portion of the Phase 1a with doses ranging from 0.3 to 20 mg/kg Q2W. Tumor types included colorectal cancer (6), endometrial cancer (3), pancreatic cancer (3), and 6 other tumor types (1 each). No dose-limiting toxicities were observed; thus, the RP2D was 20 mg/kg Q2W. The most frequent treatment-related AEs were rash (33.3%), fatigue (16.7%), nausea (16.7%), pruritus (16.7%), and cough (11.1%). Immune-related adverse events included rash (33.3%), pruritus (16.7%), autoimmune hepatitis (5.5%) and stomatitis (5.5%). Grade 3 or higher treatment-related AEs included rash (16.7%), and fatigue, hypophosphatemia, and autoimmune hepatitis (5.5% each). Four (22%) subjects had stable disease as best response (longest durations were 210 and 226 days), 12 had progressive disease, and 2 were not evaluable. The expansion cohort in phase 1a and dose-escalation in phase 1b are ongoing. Updated data, including PK and biomarker data will be presented.

Conclusions
TIGIT is a potential therapeutic target against cancer. Etigilimab has been well tolerated at doses up to 20 mg/kg Q2W. Evidence of immune activation was shown in multiple subjects with immune-related AEs. Early signs of potential efficacy have been observed in subjects with prolonged stable disease.

Trial Registration
clinicaltrials.gov NCT03119428

Ethics Approval
The study was approved by the Institutional Review Boards of all participating institutions.

P290

Immunologic biomarkers in a multi-center, single arm, open label Phase II clinical trial of mFOLFOX6 and pembrolizumab in patients with advanced colorectal cancer

Matthew Farren, PhD[1], Yan Tong[2], Ziuye Liu[2], Bert O'Neil[2], Tanios Bekaii-Saab, MD[3], Anne Noonan[4], Christopher McQuinn, MD[5], Thomas Mace, PhD[5], Walid Shaib, MD[1], Christina Wu, MD[1], Bassel El-rayes, MD[1], Safi Shahda, MD[2], Matthew Farren, PhD[1]

[1]*Emory University, Atlanta, GA, USA*
[2]*Indiana University, Indianapolis, IN, USA*
[3]*Mayo Clinic, Phoenix, AZ, USA*
[4]*Ohio State University, Columbus, OH, USA*
[5]*The Ohio State University, Hilliard, OH, USA*

Background
Colorectal cancer (CRC) accounts for an estimated 135,000 new cases and 50,000 deaths annually in the USA. Although PD-1/PD-L1-targeted immune checkpoint blockade has survival benefit in CRC patients with microsatellite instable (MSIhigh) tumors, most patients remain refractory to this therapy. We hypothesized that chemotherapy might potentiate the clinical response to pembrolizumab and improve outcomes in CRC.

Methods
Advanced/recurrent CRC patients received pembrolizumab (200mg IV every 3 weeks) and mFOLFOX6 (oxaliplatin, leucovorin, and 5`fluorouracil) on days 1 and 15 of a 28-day cycle. To assess the immunological impact of treatment, peripheral blood was collected at baseline and prior to treatment on cycle 1 day 15 (C1D15), on C3D1, and at the end of treatment. Plasma and leukocytes were isolated and cryopreserved. 40 soluble factors (via bioplex) and >200 immune cell phenotypes and populations (via FACS) were characterized. All studies were IRB-approved and registered on

clinicaltrials.gov (NCT02375672).

Results

Patients on this trial experienced a median progression free survival (PFS) of 7.4 months, and a median overall survival (OS) of 17.7 months. Patients were dichotomized based on outcome (i.e. greater-than or less-than median PFS or OS) and analyzed to determine how baseline levels of, or changes in, individual (univariate) soluble biomarkers or immune cell phenotypes were associated with patient outcome. Our analysis found that patients who experienced greater OS had significantly greater baseline levels of circulating cytokines that could broadly be described as pro-inflammatory, such as IL-2 (p=0.0366) or CD40L (p=0.0045), among others. Moreover, these patients had a greater relative frequency of circulating CD8+ T cells (compared to CD4+) at baseline (p=0.0181) and, perhaps more interestingly, had a lower proportion of naïve CD4+ and CD8+ T cells at baseline (p=0.0131 and 0.0437, respectively). This suggests greater responsiveness to FOLFOX + pembrolizumab among patients with a greater preexisting anti-tumor immune response. Conversely, patients with higher baseline frequencies of circulating regulatory T cells experienced shorter OS (p=0.0343), as did those patients whose circulating levels of VEGF increased over the course of treatment (p=0.0276), arguing that preexisting or emergent immunosuppression antagonized treatment efficacy. Ongoing analyses are exploring additional hypotheses related to longitudinal immunologic changes and impact upon biomarkers of immunogenic cell death relative to clinical outcomes.

Conclusions

Overall, our data identifies several potential immune mediators through which chemotherapy acts to potentiate the response to immunotherapy in CRC and several immunological predictors for benefit from combined pembrolizumab + FOLFOX therapy.

Trial Registration

ClinicalTrials.gov registry number NCT02375672

Ethics Approval

This study was approved by the Indiana University IRB. Protocol number 1502701251A010

P291

A targeted modified IL-2 (NHS-IL2) combined with stereotactic body radiation therapy (SBRT) in patients with advanced melanoma refractory to checkpoint inhibitors: Results from a Phase IIa trial

Omid Hamid, MD[1], David Lawson, MD[2], Karl Lewis, MD[3], Jose Lutzky, MD, FACP[4], C. Lance Cowey[5], Beatrice Brunkhorst[6], Meng Li[6], Wanping Geng[6], Christine Hicking[7], Vijay Kasturi, MD[6], Howard Kaufman[8], Lisa Jolly[9]

[1]*The Angeles Clinic and Research Institute, Los Angeles, CA, USA*
[2]*Emory University, Atlanta, GA, USA*
[3]*University of Colorado, Aurora, CO, USA*
[4]*Mount Sinai Comprehensive Cancer Center, Miami Beach, FL, USA*
[5]*Baylor Taylor Charles A. Sammons Cancer, Dallas, TX, USA*
[6]*EMD Serono, Inc, Billerica, MA, USA*
[7]*Merck KgaA, Darmstadt, Germany*
[8]*Massachusetts General Hospital, Boston, MA, USA*
[9]*Bioscript Group, Macclesfield, Cheshire, UK*

Background

Benefits of IL-2 in cancer patients are limited by toxicity. NHS-IL2 is a fusion protein comprising IL-2, modified to bind high-affinity IL-2 receptors, and a human IgG2 monoclonal antibody (NHS76) targeting DNA from necrotic tumor cells. Phase I studies demonstrated a tolerable safety profile, and preclinical studies demonstrated activity as monotherapy and in combination [1–3]. We report data from a Phase IIa open-label, parallel-group

dose-escalation trial designed to determine the maximum tolerated dose (MTD) and tolerability of NHS-IL2 combined with SBRT in patients with advanced melanoma refractory to checkpoint inhibition (NCT01973608).

Methods

Adults with unresectable/metastatic melanoma who failed ipilimumab +/- anti-PD1, and ECOG PS 0–1 were randomized to one of three dose groups: low (0.3mg/kg), intermediate (1.0mg/kg), and high (dose escalation: 3+3 design 1.8–3.6mg/kg, dose-expansion at MTD or 3.6mg/kg). Patients received NHS-IL2 (1-hour intravenous infusion) 4 days after SBRT to a single lesion in 21-day cycles until disease progression, unacceptable toxicity, or consent withdrawal. Primary objective: MTD of NHS-IL2 + SBRT. Exploratory objectives included efficacy (best overall response [BOR] by RECIST and immune-related [ir]RECIST), safety, immunohistochemistry, pharmacokinetics, pharmacodynamics, biomarker assessments. Paired biopsies were obtained and CD8+/FOXP3-positive cells were counted manually. Peripheral T-cell subsets were assessed by flow cytometry.

Results

Twelve patients were treated before early study termination (June 2015, reassessment of pipeline priorities; 0.3mg/kg n=2; 1.0mg/kg n=2; 1.8mg/kg n=6; 2.4mg/kg n=2). MTD was not reached; one patient (1.8mg/kg) had a dose-limiting toxicity (angioedema). Serious drug-treatment-emergent adverse events (AEs) occurred in 4/12 patients (1.8mg/kg n=3; 2.4mg/kg n=1); none were considered study drug-related, none were fatal. No severe cardiovascular AEs were observed, no new risks were identified. BOR was unevaluable in 4/12 patients. BOR was SD in 5/12 patients (four patients with disease control ≥4.3 months; 3/5 patients with previous ipilimumab + anti-PD1 treatment) and PD in 3/12 by irRECIST. BOR was SD in 2/12 patients and PD in 6/12 by RECIST. Serum NHS-IL2 exposure increased dose-proportionally up to 2.4mg/kg; t1/2 was 8–16 hours, with no significant accumulation following multiple doses. Changes in soluble serum factors, PBMC subsets, gene signatures, and immune cell infiltration upon NHS-IL2 treatment will be presented.

Conclusions

NHS-IL2 combined with SBRT had acceptable safety and tolerability, and demonstrated disease control in heavily pretreated patients with advanced melanoma who failed ipilimumab +/- anti-PD1 without the toxicities often associated with IL-2 treatment. Further evaluation of NHS-IL2, including combination with immune checkpoint inhibitors, may be warranted.

Acknowledgements

Medical writing assistance, provided by Lisa Jolly (Bioscript Science, Macclesfield, UK) was funded by Merck KGaA, Darmstadt, Germany.

Trial Registration

NCT01973608

References

1. Gillies SD, Lan Y, Hettmann T, Brunkhorst B, Sun Y, Mueller SO, Lo KM. A low-toxicity IL-2-based immunocytokine retains antitumor activity despite its high degree of IL-2 receptor selectivity. Clin Cancer Res. 2011;17:3673-3685.
2. Gillessen S, Gnad-Vogt US, Gallerani E, Beck J, Sessa C, Omlin A, Mattiacci MR, Liedert B, Kramer D, Laurent J, Speiser DE, Stupp R. A phase I dose-escalation study of the immunocytokine EMD 521873 (Selectikine) in patients with advanced solid tumours. Eur J Cancer. 2013;49:35–44.
3. van den Heuvel MM, Verheij M, Boshuizen R, Belderbos J, Dingemans AM, De Ruysscher D6, Laurent J, Tighe R, Haanen J, Quaratino S. NHS-IL2 combined with radiotherapy: preclinical rationale and phase Ib trial results in metastatic non-small cell lung cancer following first-line chemotherapy. J

Trans Med. 2015;13:32.

Ethics Approval
This study was approved by Copernicus IRB (CGIRB) approved under IRB Tracking #: QUI1-13-405 .

P292

Changes in intra- and perinodular heterogeneity patterns on serial computed tomography are associated with overall survival in Nivolumab-treated non-small cell lung cancer

Mohammadhadi Khorrami, PhD[1], Prateek Prasanna, PhD[1], Anant Madabhushi, PhD[1], Mohammadhadi Khorrami, PhD[1]

[1]*Case Western Reserve University, Cleveland, OH, USA*
[2]*Cleveland Clinic, Pepper Pike, OH, USA*

Background
Programmed cell death (PD)-1 immune checkpoint inhibitors have been approved to treat stage III unresectable, or stage IV metastatic Non-Small Cell Lung Cancer (NSCLC) patients. There are no validated clinical biomarkers to identify the patients who are likely to derive benefit from checkpoint inhibitor therapy such as Nivolumab. Apart from changes in RECIST measurements, changes in other image characteristics post immunotherapy are poorly understood. Previous studies have shown that more heterogeneous tumors with irregular patterns of intensities have a better overall survival in patients treated with Nivolumab. In addition to heterogeneity in PD-L1 status, other micro-environmental factors like heterogeneous and inefficient vasculature which contributes to regions of hypoxia and acidosis may cause treatment failure. These characteristics may manifest as distinct patterns within and around nodules on computed tomography (CT) images. Our work shows that changes between baseline, and post-treatment radiomic textural features within nodules and surrounding habitat on CT are associated with overall patient survival (OS).

Methods
Non-contrast CT scans from 73 NSCLC patients, with pre- and 2-week post-Nivolumab treatment, were acquired retrospectively from Cleveland Clinic Foundation. 454 intra-nodular texture features as well as 7426 features from annular rings around the nodule (0-30mm from nodule boundary) were extracted from the baseline and post-treatment temporal CT scans. The normalized differences in feature statistics across the two time-points were then computed to yield a set of 'delta-radiomic' descriptors. Cox proportional hazard model was employed to evaluate the ability of the features in predicting OS in a univariate and multivariate setting. In addition, Kaplan–Meier survival analysis and log-rank statistical tests were performed to assess the discriminative ability of the features.

Results
A multivariate Cox regression analysis indicated that intranodular Laws Energy (Hazard ratio (HR): 1.924; 95% CI: 1.220, 3.038; log-rank p = 0.0049), intranodular Haralick sum average (HR: 4.06; 95% CI: 1.890, 8.738; p = 0.00033), intranodular Haralick difference average (HR: 1.098; 95% CI: 1.0256, 1.177; p = 0.0074) and perinodular Laws Energy (HR: 1.86; 95% CI: 1.049, 3.318; p = 0.017) were predictors of OS, while no significant differences were observed in age or gender. The concordance index (CI) of the multi-variate radiomic model was 0.70. Figure 1 shows KM curve using Linear Discriminate Analysis (LDA) classifier and 3-fold cross validation for top 4 features. (Figure 1)

Conclusions
Our results suggest that changes in certain radiomic texture features between baseline and post-treatment CT scans following Nivolumab could potentially identify overall survival in NSCLC patients.

Figure 1.

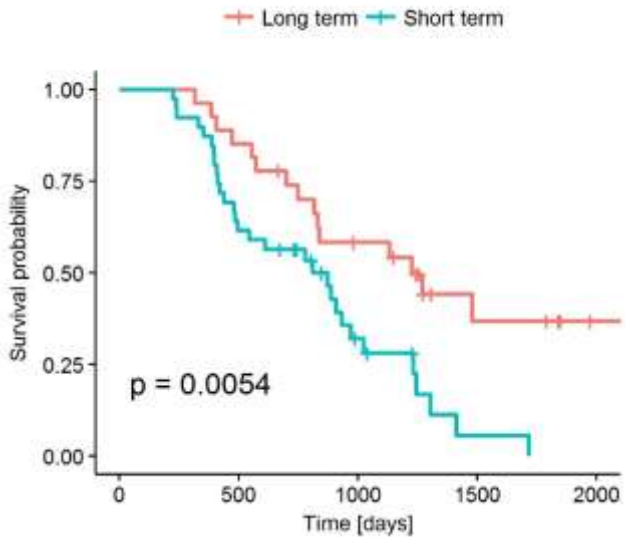

P293

Autologous tumor cell vaccination combined with systemic CpG-B and IFNα promotes activation of dendritic cells and T cells and induces clinical responses in metastatic Renal Cell Carcinoma

Bas Koster, MD[1], Saskia Santegoets[2], Jorien Harting, MD[1], Arnold Baars, MD, PhD[1], Marieke van Ham, PhD[3], Rik Scheper, PhD[1], Erik Hooijberg, PhD[4], Tanja de Gruijl, PhD[1]

[1]Amsterdam UMC, Cancer Center Amsterdam, Amsterdam, Netherlands
[2]Leiden University Medical Center, Leiden, Netherlands
[3]Sanquin Research, Amsterdam UMC, Amsterdam, Netherlands
[4]Netherlands Cancer Institute, Amsterdam, Netherlands

Background

Currently, immune checkpoint blockade is overtaking targeted therapy as first-line treatment of metastatic Renal Cell Carcinoma (mRCC). However, a majority of patients still fails to respond. It has become clear that response to immune checkpoint inhibitors relies on T cells reactive to highly individualized neo-antigens. In this light, there is a resurgence in interest for autologous tumor vaccination approaches. In this study the toxicity and efficacy of vaccination with irradiated autologous tumor cells in combination with a class B CpG oligodeoxynucleotide (CpG-B, CPG7909) and Granulocyte-macrophage colony-stimulating factor (GM-CSF) followed by systemic CpG-B and interferon-α (IFNα) administration was examined in patients with mRCC.

Methods

A single-arm Phase II trial was conducted, in which patients with mRCC were intradermally vaccinated with a minimum of three whole-cell vaccines containing 0.7 – 1.3 x 10^7 irradiated autologous tumor cells (ATC), admixed with 1 mg CpG-B and 100 µg GM-CSF, followed by bi-weekly subcutaneous (SC) injections with 8 mg CpG-B and SC injections with 6 MU IFNα three times per week.

Results

Fifteen patients were treated according to the protocol. Treatment was well tolerated. Objective clinical responses occurred in three patients, including one long-term complete response and two partial responses. Disease stabilization occurred in another three patients. Positive delayed type hypersensitivity (DTH) responses to ATC were absent before the treatment but present in 13 out of the 15 patients during treatment, suggestive for a treatment induced specific antitumor response. Further immune monitoring on circulating mononuclear cells revealed that treatment resulted in activation of plasmacytoid dendritic cells, non-classical monocytes and upregulation of both PD-1 and CTLA4 on effector T cells. Moreover, a pre-existing ex vivo IFNγ response to ATC was associated with clinical response on treatment.

Conclusions

Autologous tumor cell vaccination combined with systemic CpG-B and IFNα is tolerable, safe, immunogenic and able to elicit anti-tumor responses in patients with advanced RCC. Immune activation and treatment-induced up-regulation of PD-1 and CTLA4 on circulating T cells further suggest an added benefit of combining this approach with immune checkpoint blockade.

Ethics Approval

The study was approved by the Institutional Review Board of the VU University Medical Center, approval number 2003-37.

P294

Confirmatory study validates a MALDI prognostic signature for IL-2 response and the adverse prognostic role of the serum apoptotic marker Hepatocyte Growth Factor (HGF) in Renal Cell Carcinoma (RCC)

Michael Lotze, MD[1], Shuyan Zhai, PhD[1], Daniel Normolle, PhD[1], Ryan Sullivan, MD[2], Heinrich Roder, DPhil[3], Joanna Roder, PhD[4], David McDermott, MD[5], Theodore Logan, MD[6], Marc Ernstoff, MD[7], Thomas Olencki, DO[8], David Friedland, MD[1], Rahul Parikh, MD, PhD[1], Jodi Maranchie, MD[1], Mary Jo Buffo, BS[9], Lisa Butterfield, PhD[1]

[1]*University of Pittsburgh, Pittsburgh, PA, USA*
[2]*Massachusetts General Hospital, Needham, MA, USA*
[3]*Biodesix, Inc., Boulder, CO, USA*
[4]*Biodesix, Inc, Steamboat Springs, CO, USA*
[5]*Beth Israel Deaconess, Boston, MA, USA*
[6]*University of Indiana, Indianapolis, IN, USA*
[7]*Dartmouth University, Buffalo, NY, USA*
[8]*Ohio State University, Columbus, OH, USA*
[9]*University of Pittsburgh Medical Center, Pittsburgh, PA, USA*
[10]*UPMC Hillman Cancer Center, Pittsburgh, PA, USA*

Background

Aldesleukin (recombinant interleukin-2, IL-2) was FDA-approved for mRCC in 1992 with a 5-10% rate of durable CRs and 25% ORR. Hydroxychloroquine (HCQ) inhibits autophagy, promoting tumor apoptosis. In murine models, IL-2 and HCQ is associated with diminished toxicity and increased efficacy [1]. We hypothesized that a MALDI mass spectrometric signature associated with response to IL-2 in melanoma could stratify outcomes in RCC and that the adverse role of HGF [2], an apoptotic marker [3] promoting autophagy [4] could be confirmed.

Methods

We studied high-dose IL-2 in combination with oral HCQ for patients with mRCC. Patients (pts) received IL-2, 600,000 IU/kg, every 8 hours up to 14 doses/cycle. HCQ was administered orally, starting 2 weeks prior to IL-2 and continued up to one year. The HCQ dose was 600 mg (17pts) or 1200 mg (13pts) daily. MALDI mass spectra were generated for pretreatment (and on D1 after 14d HCQ) serum samples, blindly classified as Early/Late (poor/good outcomes, respectively), based on the melanoma algorithm. Pretreatment serum was also tested for HGF. Overall survival (OS) was compared between Early/Late groups and between high and low HGF (dichotomized at the median) using log-rank test and proportional hazards ratios (PHR).

Results

Of 30 patients in the study, 29 were evaluable for response. MALDI test classification and HGF (high vs low) were both univariate significant predictors of OS at Day 1 after IL-2. HGF also predicted OS at Day -14. Although MALDI test classification was associated with HGF level (Mann-Whitney p = 0.042 (Day-14) and p=0.021 (Day 1), an exploratory investigation of simultaneous stratification by both markers revealed that Early and low HGF and Late patients regardless of HGF level had very good OS, significantly better than Early patients and high HGF (p=0.002).Table 1. Classifiers MALDI and HGF PHR (95% CI) Log-rank

pDay -14 HGF (high vs low) 10.516 (1.233-89.702) 0.009 MALDI test (Early vs Late) 4.998 (0.582-42.929) 0.104Day 1 HGF (high vs low) 12.581 (1.425-111.084) 0.005 MALDI test (Early vs Late) >100 (no deaths in late) 0.030

Conclusions

IL-2 plus HCQ was well tolerated and clinically active with encouraging PFS of >17 months at the 600 mg HCQ dose (>4x greater than historical controls). A MALDI test developed in melanoma predicting OS in mRCC was validated. The prognostic power of the apoptotic marker and cMET ligand, HGF was confirmed. A combination of both markers showed potential for improved stratification, requiring future validation.

Trial Registration

NCT01550367; approved as IRB 11-074.

References

1. Liang X, De Vera ME, Buchser WJ, Romo de Vivar Chavez A, Loughran P, Beer Stolz D, Basse P, Wang T, Van Houten B, Zeh HJ 3rd, Lotze MT. Inhibiting systemicautophagy during interleukin 2 immunotherapy promotes long-term tumor regression. Cancer Res. 2012 Jun 1;72(11):2791-801.
2. Tanimoto S, Fukumori T, El-Moula G, Shiirevnyamba A, Kinouchi S, Koizumi T, Nakanishi R, Yamamoto Y, Taue R, Yamaguchi K, Nakatsuji H, Kishimoto T, Izaki H, Oka N, Takahashi M, Kanayama HO. Prognostic significance of serum hepatocyte growth factor in clear cell renal cell carcinoma: comparison with serum vascular endothelial growth factor. J Med Invest. 2008 Feb;55(1-2):106-11.
3. Vogel S, Trapp T, Börger V, Peters C, Lakbir D, Dilloo D, Sorg RV. Hepatocyte growth factor-mediated attraction of mesenchymal stem cells for apoptoticneuronal and cardiomyocytic cells. Cell Mol Life Sci. 2010 Jan;67(2):295-303.
4. Wang Y, Liu J, Tao Z, Wu P, Cheng W, Du Y, Zhou N, Ge Y, Yang Z. Exogenous HGF prevents cardiomyocytes from apoptosis after hypoxia via up-regulating cell autophagy. Cell Physiol Biochem. 2016;38(6):2401-13.

Ethics Approval

The study was approved by the University of Pittsburgh Institution's Ethic Board as IRB 11-074.

P295

A Phase 1, open-label, multicenter, dose escalation study of mRNA-2416, a lipid nanoparticle encapsulated mRNA encoding human OX40L, for intratumoral injection to patients with advanced malignancies

Shilpa Gupta, MD[1], Todd Bauer, MD[2], Ryan Sullivan, MD[3], Robert Andtbacka, MD, CM, FACS, FRCSC[4], Ding Wang, MD[5], Geoffrey Shapiro, MD, PhD[6], Khanh Do, MD[6], Kurt Schalper, MD, PhD[7], Patricia Gaule, PhD[7], Tal Zaks, MD, PhD[8], Joshua Frederick, PhD[8], Lisa Johansen[8], Kristen Hopson, PhD[8], William Randolph[8], Sima Zacharek, PhD[8], Robert Meehan, MD[8], Antonio Jimeno, MD, PhD[9]

[1]University of Minnesota, Minneapolis, MN, USA
[2]Sarah Cannon at Tennessee Oncology, Nashville, TN, USA
[3]Massachusetts General Hospital, Needham, MA, USA
[4]University of Utah Huntsman Cancer, Salt Lake City, UT, USA
[5]Henry Ford Health System, Detroit, MI, USA
[6]Dana Farber Cancer Institute, Boston, MA, USA
[7]Yale Cancer Center, New Haven, CT, USA
[8]Moderna Therapeutics, Cambridge, MA, USA
[9]University of Colorado Denver, Denver, CO, USA

Background

Blocking co-inhibitory checkpoints has become a standard treatment in diverse solid and hematologic malignancies, however, checkpoint inhibitors alone are not sufficient to induce robust and durable tumor regressions in the majority of patients.

Generating optimal anti-tumor T-cell responses requires T-cell receptor activation and co-stimulation, which may occur via ligation of tumor necrosis factor (TNF) receptor family members, such as OX40. The OX40 receptor (TNFRSF4, cluster of differentiation [CD]134) is expressed on activated immune effector cells such as T-cells and natural killer (NK) cells [1]. It's ligand, OX40L, is a homo-trimeric transmembrane protein normally expressed on antigen-presenting cells upon immune stimulation [2]. Binding of OX40 by OX40L in the presence of a recognized antigen promotes the expansion CD4+ and CD8+ T-cells and enhances memory responses while inhibiting regulatory T cells. Induction of OX40L expression by tumor cells, or other cells presenting tumor antigens may trigger a specific cell-mediated immune response with systemic anti-tumor effects. mRNA-2416 is a novel mRNA-based therapy that encodes human OX40L. Durable tumor regressions have been observed in preclinical models treated with mRNA-2416 at both injected and un-injected distal tumor sites.

Methods

Patients with locally advanced, recurrent or metastatic solid malignancy or lymphoma were treated with mRNA-2416 in a standard 3+3 phase 1 dose escalation study to assess safety and efficacy of intratumoral injection every 2 weeks in 28-day cycles. Tumor biopsies were collected at screening and on-treatment from one of three timepoints/locations (C1D2 or C2D2 from injected tumor, or C1D22-28 from un-injected tumor). All paired biopsies are evaluated by multiplexed Quantitative Immunofluorescence (QIF) and by RNA sequencing to characterize OX40L expression, and biomarkers of adaptive anti-tumor immune response following treatment.

Results

As of the July 2018 data cut off, 23 patients have been treated (melanoma 8, sarcoma 5, HNSCC 3, ovarian 2, neuroblastoma 1, salivary 1, appendiceal 1, NSCLC 1, colorectal 1) during dose escalation at dose levels from 1-8 mg. No dose limiting toxicities have been reported. Related adverse events (AEs) of at least grade 3 consisted of 2 serious AEs; a skin ulceration due to tissue defect after regression of injected tumor, and an injection related reaction. No related grade 4/5 AEs were reported. Increased expression of OX40L protein in both tumor and immune cells post-treatment was detected by preliminary QIF analyses.

Conclusions

mRNA-2416 is tolerable at all dose levels studied, and yielded productive expression of OX40L protein. Translational data continues to be collected and analyzed.

Trial Registration

NCT03323398

References

1. Compaan DM, Hymowitz SG. The crystal structure of the costimulatory OX40-OX40L complex. Structure. 2006;14(8):1321–1330.
2. Mallett S, Fossum S, Barclay AN. Characterization of the MRC OX40 antigen of activated CD4 positive T lymphocytes--a molecule related to nerve growth factor receptor. EMBO J. 1990;9(4):1063-1068.

Ethics Approval

This study was approved by each Institution's IRB. e.g. University of Minnesota approval number STUDY00000068.

P297

Systemic activation and polyclonal expansion of CD8 T cells in cancer patients on Pegilodecakin alone or in combination with anti-PD-1

Martin Oft, MD[4], Aung Naing, MD, FACP[1], Jeffrey Infante, MD[2], Kyri Papadopoulos[3], Ivan Chan, PhD[4], Cong Shen[5], Navneet Ratti, BS, MBA[6], Bianca Rojo,

MSc[4], Karen Autio, MS, MD[5], Deborah Wong, MD PhD[7], Manish Patel, MD[8], Patrick Ott, MD, PhD[9], Gerald Falchook, MD[10], Shubham Pant, MBBS[1], Annie Hung, BA[4], John Mumm, PhD[11], Matthew Adamow[5], Scott McCauley, BA[12], Phillip Wong, PhD[5], Peter Van Vlasselaer, PhD[13], Joseph Leveque[4], Edward Garon, MD[7], Nizar Tannir, MD, FACP[1]

[1]MDACC, Houston, TX, USA
[2]SCRI, Nashville, TN, USA
[3]START, San Antonio, TX, USA
[4]ARMO BioSciences, Redwood City, CA
[5]MSKCC, New York, NY, USA
[6]ARMO, Redwood City, CA, USA
[7]UCLA, Santa Monica, CA, USA
[8]Florida Cancer Specialists, Sarasota, FL, USA
[9]DFCI, Boston, MA, USA
[10]SCRI at Health One, Denver, CO, USA
[11]AROM BioSciences, Gaithersburg, MD, USA
[12]ARMO BioScinces, Redwood City, CA, USA
[13]Armo BioScience, Redwood City, CA, USA

Background

Immunooncology therapies aim to induce activation and expansion of tumor reactive CD8+ T cells. Tumors with low mutational burden have a reduced response rate to checkpoint inhibition, presumably due to a reduced number of tumor reactive T cells. Pegilodecakin induces the expansion of tumor reactive T cells in preclinical tumor models. Pegilodecakin (PEGylated IL-10 or AM0010) monotherapy has been reported to achieve 25% objective tumor responses (ORR) in intermediate to poor risk renal cell cancer (RCC) in median 4th line of treatment (LOT) (range 1-8) (Naing A et al, JCO, 2016).

Methods

Patients received pegilodecakin (daily self-administration) alone or combination with pembrolizumab or nivolumab (following standard schedule and dose). Samples were collected post written consent from patients enrolled in a multi-basket trial and analyzed in accordance with the IRB. Systemic and cellular immune responses were assessed by serum cytokine analysis, PBMC flow cytometry and T cell clonal analysis by TCR deep sequencing. Immune fluorescence (IF) or immunohistochemistry was performed on formaldehyde fixed archival, pretreatment biopsies and on-treatment biopsies (CD8, granzyme B, phospho-STAT-3 or LAG-3, T-bet/CD3, HLA-A).

Results

Pegilodecakin treatment induced a systemic immune response biased towards Th1 cytokines and cytotoxic effector molecules (GranzymeB, FasL, lymphotoxinB) in the serum. PBMC analysis by Flow cytometry in pre and post treatment samples show invigoration of exhausted, T cells, with increased proliferation of LAG3+PD1+ CD8+ T cells throughout pegilodecakin treatment. The magnitude of PD-1+Lag-3+Ki-67+CD8+ T cells correlated with the objective response to pegilodecakin. T-cell clonal analysis (TCR sequencing of PBMCs) on pegilodecakin showed >10fold expansion of several hundred, previously undetected T-cell clones per patient, correlating with objective tumor response. On-treatment biopsies showed that Pegilodecakin increased GzmB+, Phospho-Stat3+ and Lag-3+ CD8+ T cells and HLA-A expression in the tumor. Patient on pegilodecakin + anti-PD-1 had an increased overall response rate compared to historical control (Table 1, 2), including responses in NSCLC patients with low tumor mutational burden.

Conclusions

Pegilodecakin treatment induced the hallmarks of CD8+ T-cell immunity in cancer patients, including the systemic elevation of IFNg and GranzymeB levels, expansion and activation of CD8+ TILs, invigoration and expansion of PD-1+/Lag-3+ CD8+ T-cell sub-set and the de-novo expansion of T-cell clones. The elements of the pegilodecakin induced immune activation correlated with the achievement of objective response. Combination of pegilodecakin

with anti-PD-1 may provide a treatment alternative for patients and indications with low tumor antigen and tumor mutational burden.

Trial Registration
NCT0200944

Ethics Approval
The study was approved by the IRBs of all contributing Institutions.

Table 1. Pegilodecakin + anti-PD-1 in NSCLC

Table 2. Pegilodecakin + anti-PD-1 in RCC

P298

T cell response induced by the addition of IL-7 treatment following sipuleucel-T immunotherapy in metastatic castration resistant-prostate cancer

Russell Pachynski, MD[2], Lauren Harshman, MD[4], Leonard Appleman, MD, PhD[5], Paul Monk, MD[6], Rhonda Bitting[7], Omer Kucuk, MD[8], Frederick Millard, MD[9], John Seigna[10], Steven Fling, PhD[11], Nirasha Ramchurren, PhD[11], Bruce Hess, BS[11], Leonard D'Amico, PhD[11], Andreanne Lacroix, BS[11], Judith Kaiser, MBA, BSN, RN[11], Michel Morre, DVM, MSc[12], Anne GREGOIRE, phD[12], Martin Cheever, MD[11], Evan Yu, MD[13]

[1]Washington University School of Medicine, St Louis, MO, USA
[2]Washington University, St Louis, MO, USA
[3]University of Chicago, Chicago, IL, USA
[4]Dana Farber Cancer Institute, Boston, MA, USA
[5]University of Pittsburg, Pittsburgh, PA, USA
[6]Ohio State University, Columbus, OH, USA
[7]Wake Forest Baptist Health, Winston-salem, NC, USA
[8]Emory University, Atlanta, GA, USA
[9]UCSD, San Diego, CA, USA
[10]Dartmouth-Hitchcock, Lebanon, NH, USA
[11]Fred Hutchinson Cancer Research Center, Seattle, WA, USA
[12]Revimmune, Boulogne, MD, France
[13]University of Washington, Seattle, WA, USA
[14]UCSF, San Francisco, CA, USA

Background
Sipuleucel-T is a FDA-approved autologous cellular immunotherapy for asymptomatic or minimally symptomatic metastatic castration resistant prostate cancer (mCRPC). Treatment with sipuleucel-T results in humoral B cell responses, and can induce robust, antigen-specific T cell responses that correlate with overall survival. IL-7 is a homeostatic cytokine that can enhance the generation of naïve T cells and promote the generation of memory T cells. We hypothesized that treatment with IL-7 after sipuleucel-T would augment and prolong cellular immune responses compared to observation.

Methods
We performed a randomized phase 2 clinical trial where chemotherapy-naïve mCRPC patients receiving sipuleucel-T were either followed (observation arm) or treated (within 7 days) with recombinant human IL-7 10mcg/kg SC weekly x 4. Peripheral immune responses were evaluated at weeks 1 (pre-IL-7), 6, and 11 after completion of sipuleucel-T. T cell responses to PAP and PA2024 were assessed by ELISPOT, while ELISAs were used to assess antibody responses to these antigens. Flow cytometry was used to assess any treatment-induced

modulation of peripheral T cells and other leukocyte subsets.

Results

A total of 54 patients were enrolled from 2015 to 2017 and randomized 1:1 into observation (n=26) or IL-7 (n=28) arms. Treatment with IL-7 was generally well tolerated, with injection site reactions being the most common toxicity. Clinical data will be further evaluated and presented later. For the IL-7, but not the observation arm, an expansion of all lymphocyte subsets was seen, with 2-3-fold increases over baseline in CD3, CD4, CD8 T cells, and CD56bright NK cells. Within the IL-7 arm, statistically significant increases over baseline were seen in T cells at weeks 6 and 11. However, compared to the observation arm, increases in absolute lymphocyte and T cell numbers for the IL-7 arm were statistically significant only at week 6. Patients in the IL-7 arm, but not observation arm, showed a significant reduction in neutrophil to lymphocyte ratio (NLR) over the course of treatment. However, there were no significant differences seen in frequencies of antigen-reactive (PAP or PA2024) T cells or antibody responses between observation and IL-7 arms.

Conclusions

Here, we present results from the first randomized trial comparing IL-7 vs observation following sipuleucel-T treatment in mCRPC patients. While IL-7 treatment did not increase the frequency of antigen specific T cells, it significantly expanded lymphocyte populations, suggesting IL-7 may result in an increase in absolute number of antigen-specific T cells in patients. Further analysis of T-cell clonal expansion is pending.

Trial Registration

NCT01881867

Ethics Approval

The study was IRB approved at each participating institution.

P299

Combination of subcutaneously administered TLR9 agonist lefitolimod with CTLA-4 checkpoint inhibitor ipilimumab - A phase I trial in patients with advanced solid tumors

Matthew Reilley, MD[1], Casey Ager, BS[2], Martin Meng[2], Apostolia Tsimberidou, MD, PhD[2], Sarina Piha-Paul, MD[2], Timothy Yap, MD[2], Siqing Fu, MD, PhD[2], Aung Naing, MD, FACP[2], Jordi Rodon[2], Ly Nguyen[2], Priya Bhosale, MD[2], Manuel Schmidt, MSc[3], Matthias Baumann[3], Funda Meric-Bernstam, MD[2], Michael Curran, PhD[2], David Hong, MD[2]

[1]*University of Virginia, Charlottesville, VA, USA*
[2]*MD Anderson Cancer Center, Houston, TX, USA*
[3]*Mologen AG, Berlin, Germany*

Background

Toll-like receptors (TLR) have generated significant interest as an effective means of stimulating the immune system that results in the killing of tumor cells. TLR9 agonists can function as immunomodulators and are therefore useful targets for immunotherapy. Counter-regulatory signals exist that suppress the development of an anti-tumor response, such as IL-10, Treg cells, and PD-L1. Therefore, the efficacy of TLR9 against advanced malignancies may be enhanced by addition of an immune check-point blockade inhibitor to improve immune activation. Lefitolimod (MGN1703) is a covalently-closed dumbbell-shaped DNA molecule that functions as a TLR9 agonist. We developed a clinical trial combining lefitolimod with ipilimumab (anti-CTLA4) in patients with advanced malignancies.

Methods

This is a single-center investigator-initiated trial conducted at the University of Texas MD Anderson Cancer Center. Eligible patients with advanced solid tumors without prior exposure to TLR agonists were enrolled in a dose escalation 3+3 phase 1 trial.

Lefitolimod was administered subcutaneously weekly at 4 increasing dose levels and ipilimumab infused intravenously every 3 weeks at 3mg/kg. Peripheral blood and tumor biopsies were collected for analysis of changes in tumor immunity.

Results

To date 18 patients have enrolled and received at least one treatment. No dose-limiting toxicities (DLTs) have been encountered at any dose level. Thus, the maximum tolerated dose (MTD) of the combination was determined to be the highest dose level with lefitolimod at 120mg weekly and ipilimumab 3mg/kg every 3 weeks. The most common adverse events (AEs) include fatigue (72%), hepatic enzyme elevation (50%), anemia (44%), dyspnea (44%), myalgias (44%), abdominal pain (39%), anorexia (39%), cough (39%), rash (33%), fever (28%), hyperglycemia (28%), and nausea (28%). Grade 3 AEs occurring in more than one patient include dyspnea, hyperglycemia, fatigue, abdominal pain, and hypokalemia; only one episode of fatigue was felt to be possibly related to therapy. Two patients experienced a best response of stable disease for 45 weeks (primary peritoneal carcinoma) and 24 weeks (high-grade pancreatic neuroendocrine tumor) respectively at 30mg and 60mg dose levels of lefitolimod. Flow analysis of tumor cell immune infiltrates shows increased proportion and activation of cytotoxic T lymphocytes. PD-1 expression increased after treatment suggesting potential benefit from additional PD-1 blockade.

Conclusions

The combination is safe and well tolerated in patients with advanced cancers. Expansion cohorts with intratumoral administration are ongoing.

Trial Registration

ClinicalTrials.gov Identifier: NCT02668770.

Ethics Approval

This study was approved by MD Anderson Cancer Center institution's review board approval number 2015-0135.

Consent

Written informed consent was obtained from the patient for participation in the study. A copy of the written consent is available for review by the Editor of this journal.

P300

First-in-human phase 1 study of IT1208, a defucosylated humanized anti-CD4 depleting antibody, in patients with advanced solid tumors

Kohei Shitara, MD[1], Satoshi ueha[2], Shigeyuki Shichino[2], Hiroyasu Aoki[3], Haru Ogiwara, MD, PhD[2], Tetsuya Nakatsura[4], Toshihiro Suzuki[4], Manami Shimomura[4], Toshiaki Yoshikawa[4], Kayoko Shoda[4], Shigehisa Kitano[5], Makiko Yamashita[5], Takayuki Nakayama[5], Akihiro Sato[6], Sakiko Kuroda[6], Masashi Wakabayashi[6], Shogo Nomura[6], Satoru Ito[7], Kouji Matsushima[2], Toshihiko Doi, MD, PhD[6]

[1]*National Cancer Hospital East, Kashiwa, Japan*
[2]*Tokyo University of Science, Tokyo, Japan*
[3]*The University of Tokyo, Tokyo, Japan*
[4]*National Cancer Center, Kashiwa, Japan*
[5]*National Cancer Center Hospital, New York, NY*
[6]*National Cancer Center Hospital East, kashiwa, Japan*
[7]*IDAC Therapeutics Inc, Tokyo, Japan*

Background

Transient CD4+ T cell depletion led to the proliferation of tumor-specific CD8+ T cells in the draining lymph node and increased infiltration of PD-1+CD8+ T cells into the tumor, which resulted in strong anti-tumor effects in tumor-bearing mice. [1] Here we report a first-in human study of IT1208, a defucosylated humanized anti-CD4 monoclonal antibody engineered to exert potent antibody-

dependent cellular cytotoxicity.

Methods
Patients with advanced solid tumors for whom no standard therapy was available, were treated with intravenous infusion of IT1208 at dose of 0.1 or 1.0 mg/kg. First patient in each cohort was treated as single administration and other patients received two administrations of IT1208 on day 1 and 8 followed by safety and efficacy assessment. To assess cellular and molecular effects of IT1208 on the tumors, histological and transcriptomic analyses of pre- and post-treatment tumor samples were performed. The study was approved by ethics board in each institution.

Results
Eleven patients were enrolled in 0.1 mg/kg (n=4) and 1.0 mg/kg cohort (n=7), having gastric or gastro-esophageal (n=6), colorectal (n=3), esophageal (n=1) and pancreatic cancer (n=1, also having colon cancer). Grade 1 or 2 infusion-related reaction was observed in all patients but manageable. No other treatment related immune mediated adverse events or infections were observed. Decreased CD4+ cells in peripheral bloods by IT1208 were observed in all patients, especially in patients with two administrations of 1.0 mg/kg, reducing CD4+ cells count from median 395/μL at baseline to 3.5/μL at nadir. CD8+ cells increased on day 29 compared with baseline in most patients, which resulted in remarkably decreased CD4/8 ratios. One microsatellite stable colon cancer patient with lung and liver metastases achieved durable partial response, showing increased infiltration of Ki67+CD8+ cells into tumors after IT1208. Moreover, transcriptomic profiling of the liver metastatic site of the patient revealed upregulation of the expression of interferon-stimulated genes, T cell activation-related genes and antigen presentation-related genes after IT1208. Additional 3 patients with gastric or esophageal cancer achieved stable disease lasting at least 3 months.

Conclusions
Single agent IT1208 successfully depleted CD4+cells with manageable safety profile and encouraging preliminary efficacy signals, which warrants further investigations especially in combinations with immune check point inhibitors.

Trial Registration
UMIN000026564

References
1. Ueha S, Yokochi S, Ishiwata Y, et al. Robust Antitumor Effects of Combined Anti-CD4-Depleting Antibody and Anti-PD-1/PD-L1 Immune Checkpoint Antibody Treatment in Mice. Cancer Immunol Res. 2015;3:631-40.

P301

MLH1/ MSH2 expression and the prognosis of colorectal cancer in 978 Chinese patients

Yu Wang, MD*, Shuiming Wang[1], Youping Deng[1]

[1]*Oncology, nanjing, China*

Background
The purpose of this study was to evaluate the prognostic significance of MLH1/ MSH2 status in a large cohort of stage I to IV colorectal cancer (CRC) patients using the immunohistochemical analysis. The relationship among MLH1/ MSH2, clinical outcome and OS (Overall Survival) was also investigated.

Methods
The study included 978 patients with colorectal cancer (173 stage I, 395 stage II, 286 stage III and 124 stage IV) who underwent curative surgical resection. We used immunohistochemical to analyze MMR status through MLH1 and MSH2 expression. And we also used gene scanning to verify the microsatellite state of the patients.

Results
801 (81.99%) colorectal cancers showed positive MLH1/ MSH2 status while 177 (18.01%) colorectal cancers demonstrated negative MLH1/ MSH2 status using immunohistochemical analysis. Patients with positive MLH1/ MSH2 more frequently suffered from right-side colon, with 1-3 lymph nodes metastasis, with mucus, positive surgical margin ($P < 0.05$), but with no evidence related with age, gender, tumor size, differentiation and TNM stage.Patients with negative MLH1/MSH2 showed significantly better OS than positive one($P < 0.05$).Univariate and multivariate analysis demonstrated that the independent predictive factors of colorectal cancer were TNM stage, lymph nodes metastasis, mucus, surgical margin and MLHl/MSH2 status($P < 0.05$). Gene scan denmostrated that 173(90.02%) were MSS, 12 (6.38 %) were MSI-H and 3(1.60%) were MSI-L. That is consistent with the immunohistochemical results.

Conclusions
This study confirmed the positive prognostic role of MLHl/MSH2.

P302

Phase II trial of reirradiation (ReRT) plus Pembrolizumab for locoregional inoperable recurrence or second primary squamous cell carcinoma of the head and neck (SCCHN): Analysis of early toxicity

Dan Zandberg, MD[1], Tejan Diwanji, MD[2], Robert Morales, MD[2], Tiffani Tyer[2], James Snider, MD[2], Alexander Engelman, MD[2], Soren Bentzen, PhD[2], Thomas DeMora, MD[3], Robert Malyapa, MD[2], Navid Saeidi[2], Ana Ponce Kiess, MD[4], Josh Lubek, MD[2], Robert Ord, MD[2], Donita Dyalram, MD[2], Kyle Hatten, MD[2], Jeffrey Wolf, MD[2], Rodney Taylor, MD[2], John Papadimitriou, MD, PhD[2], Ranee Mehra, MD[4], Harry Quon, MD[4], Hyunseok Kang, MD, MPH[4], John Ridge, MD, PhD[3], Jessica Bauman, MD[3], William Regine, MD[2], Mohan Suntharalingam, MD[2], Scott Strome, MD[2], Kevin Cullen, MD[2]

[1]*UPMC Hillman Cancer Center, Pittsburgh, PA, USA*
[2]*University of Maryland, Baltimore, MD, USA*
[3]*Fox Chase Cancer Center, Philadelphia, PA, USA*
[4]*Johns Hopkins University, Baltimore, MD, USA*

Background
Based on pre-clinical synergy between radiation and anti-PD-1 mAb, we initiated a phase II trial of ReRT plus pembrolizumab. The trial includes a stopping boundary for toxicity for the first 20 patients that completed 7 weeks of therapy. This abstract reports the early toxicity (up to 3 months post RT) for these patients. To our knowledge this is the first report of ReRT plus immunotherapy in SCCHN.

Methods
Main inclusion criteria are: unresectable (or declined resection) locoregional recurrence or second primary SCCHN (excluding salivary or cutaneous), prior RT completed >6 months ago and >50% of tumor volume previously radiated at doses > 45 Gy. ReRT is 1.2Gy BID for 5 weeks to total 60Gy (IMRT or Proton RT). Pembrolizumab is dosed 200mg IV q 3 weeks starting the first day of radiation. PET/CT is done 3 months after ReRT (after 6th cycle of pembrolizumab) to evaluate response with continued pembrolizumab until progression or 2 years. Primary endpoint is PFS (n=48) and the trial design used continuous monitoring of the incidence of G4/5 non-hematologic toxicity within the first 7 weeks of treatment using a Pocock-type stopping boundary in the first 20 patients.

Results
Twenty patients completed 7 weeks of therapy as of 7/18/18. Median age was 61 (50-79), primary sites were oral cavity (40%), oropharynx (40%), larynx (5%), and nasopharynx (15%), median time from prior RT was 72 months (10-300), 1 patient received proton RT, all others IMRT. All patients completed

prescribed ReRT and the 2 cycles of pembrolizumab concurrent, and 79% completed all 6 cycles (1 patient is still on pembrolizumab within 3 months of RT). There were 423 AEs and 88 were treatment related (TRAEs: probable/definite from treatment either ReRT and/or pembrolizumab). Common TRAEs (any grade) experienced by patients' included: mucositis (60%), radiation dermatitis (40%), fatigue (30%), dysphagia (25%), weight loss (15%), dysgeusia (15%). Hyperthyroidism (1 patient) and Hypothyroidism (2 patients) were the only immune related AEs. There were 4 G3 TRAEs which occurred in 2 patients (1 patient with dysphagia, radiation dermatitis, salivary duct inflammation) consistent with an incidence of 10% with an exact binomial upper 1-sided 95% CI of 28.3%. There were no treatment related G4/5 adverse events.

Conclusions

Evaluation of early toxicity shows that ReRT plus pembrolizumab was overall well tolerated. The pre-specified toxicity boundary was not crossed and accrual will continue towards the primary endpoint of PFS.

Ethics Approval

The study was approved by the IRB and University of Maryland, Baltimore. Approval Number HP-00061458

Clinical Trials (In Progress)

P303

Correlation between prior surgery and immune related gastrointestinal toxicity among women receiving olaparib and tremelimumab for the treatment of recurrent ovarian cancer

Jaryse Harris, BA[1], Carolyn Muller, MD[1], Teresa Rutledge[1], Olivier Rixe, MD, PhD[1], Aisha Sethi[1], Phyllis Gimotty, PhD[2], Katherine Morris, MD, FACS[3], Sarah Adams, MD[1,2]

[1]University of New Mexico, Albuquerque, NM, USA
[2]University of Pennsylvania, Philadelphia, PA, USA
[3]University of Oklahoma, Oklahoma City, OK, USA
[4]University of New Mexico Comprehensive C, Albuquerque, NM, USA

Background

Ovarian tumors have been relatively resistant to immune checkpoint blockade, despite a strong rationale for immune therapy in this disease [1]. We recently demonstrated that targeted therapy with a poly(adenosine diphosphate-ribose) polymerase (PARP) inhibitor synergized with CTLA4 immune checkpoint blockade to achieve long-term survival in ovarian tumor models [2]. Based on these results, we launched INST 1419: A phase I/II study of the combination of olaparib and tremelimumab in BRCA1 and BRCA2 mutation carriers with recurrent ovarian cancer (NCT02571725). This ongoing trial has demonstrated clinical responses among patients treated to date. In keeping with prior studies of CTLA4 antibody therapy we have observed immune related adverse events [3]. Here we report an association between prior enteric surgery and the emergence of Grade 3 gastrointestinal toxicity.

Methods

Women with a confirmed germline mutation in BRCA1 or BRCA2 who have recurrent ovarian, tubal or peritoneal cancer with measurable disease are eligible for this study. Olaparib is administered orally at 300 mg twice daily, and tremelimumab intravenously at 10mg/kg every 28 days for four to six cycles followed by maintenance dosing every 12 weeks. The primary endpoint is overall response rate measured by modified WHO immune related response criteria [4]. Adverse events are scored using Common Terminology Criteria for Adverse Events. The target enrollment is 50 subjects. Response data is currently available for 13 patients.

Results
Of 13 patients who completed at least 3 cycles of treatment and were assessable for response, five (38%) experienced Grade 3 gastrointestinal toxicity. Four had colitis and one had gastritis requiring hospitalization for supportive care and steroids. Notably, four of these patients had a history of gastrointestinal surgery: three women with Grade 3 colitis had a history of colon resection and one patient with Grade 3 gastritis had a prior gastric sleeve surgery. None of the eight patients without Grade 3 gastrointestinal toxicity had a history of gastrointestinal surgery. The association between prior enteric surgery and Grade 3 gastrointestinal toxicity is significant (Fisher's exact test, p=0.007).

Conclusions
Emerging data from our ongoing phase II trial demonstrates an association between prior enteric surgery and immune related gastrointestinal toxicity in response to combination therapy with a CTLA4 antibody and a PARP inhibitor. While these results will need to be validated in a larger patient cohort, they suggest that surgical history can be used to anticipate immune related toxicity in patients receiving immune checkpoint antibodies.

Trial Registration
This study is registered at clinicaltrials.gov NCT02571725.

References
1. Lavoue V, et al. Immunity of human epithelial ovarian carcinoma: the paradigm of immune suppression in cancer. J Transl Med, 2013;11:147.
2. Higuchi T, et al. CTLA-4 blockade synergizes therapeutically with PARP inhibition in BRCA1-Deficient ovarian cancer. Cancer Immunol Res, 2015; 3(11): 1257-68.
3. Hodi FS, Mihm MC, Soiffer RJ, Haluska FG, Butler M, Seiden MV, et al. Biologic activity of cytotoxic T lymphocyte-associated antigen 4 antibody blockade in previously vaccinated metastatic melanoma and ovarian carcinoma patients. Proceedings of the National Academy of Sciences of the USA of America 2003;100(8):4712-17.
4. Wolchok JD, Hoos A, O'Day S, et al. Guidelines for the evaluation of immune therapy activity in solid tumors: immune-related response criteria. Clin Cancer Res. 2009 Dec 1;15(23):7412-20.

Ethics Approval
This study was approved by the Western IRB in March 2016, study number 1159154, approval number 20152180.

P304

A phase 1 study of MGD007, a humanized gpA33 x CD3 DART® protein, in combination with MGA012, an anti-PD-1 antibody, in patients with relapsed/refractory metastatic colorectal cancer

Richard Kim, MD[1], David Ryan, MD[2], Stacey Stein, MD[3], James Cleary, MD, PhD[4], Liqin Liu, PhD[5], Ralph Alderson, PhD[5], Francine Chen, MD[5], Peter Lung, BS, HT (ASCP)[5], Allan Reduta, BA[5], Syd Johnson, PhD[5], Jan Baughman, MPH[5], Ezio Bonvini[5], Paul Moore, PhD[5], Joanna Lohr, PhD[5], Jon Wigginton, MD[5], Jan Davidson-Moncada, MD, PhD[5], John Powderly, MD, CPI[6]

[1]*Moffitt Cancer Center, Tampa, FL, USA*
[2]*Massachusetts General Hospital, Boston, MA, USA*
[3]*Yale Cancer Center, New Haven, CT, USA*
[4]*Dana Farber Cancer Institute, Boston, MA, USA*
[5]*MacroGenics, Inc., Rockville, MD, USA*
[6]*Carolina BioOncology, Huntersville, NC, USA*

Background
The benefit of checkpoint blockade for colorectal cancer (CRC) is restricted to mismatch repair deficient patients, indicating the need for other means to further leverage T-cell mediated antitumor responses in this population. MGD007 is a gpA33 x CD3 bispecific DART protein designed to

recruit/expand host T cells, via their CD3 component, and to mediate tumor cell killing through engagement of glycoprotein A33 (gpA33), a cell surface target on >95% of CRC tumors. MGA012, also known as INCMGA00012, is an anti-PD-1 antibody undergoing Phase 1 investigation. MGD007 demonstrated drug targeting to both CD3 T cells and gpA33 in a Phase 1 monotherapy trial. Concomitant with its ability to mediate T-cell killing of CRC tumor cells, preclinical data show that MGD007 induces expression of PD-1/PD-L1 on T cells and CRC tumor cell lines, respectively. Furthermore, MGA012 enhances MGD007-mediated CTL activity and interferon gamma release upon exposure to gpA33-positive CRC and T cells, while MGD007 anti-tumor activity in preclinical mouse models is enhanced upon combination with anti-PD-1. Based on the two molecules' intended complementary mechanisms of action, the current study will investigate whether the novel, mechanism-based combination of MGD007 (T-cell agonist) and MGA012 (checkpoint inhibitor) could mediate enhanced antitumor activity compared to either modality alone.

Methods

This Phase 1b/2 study is designed to characterize safety, tolerability, dose-limiting toxicities (DLTs), and maximum tolerated dose (MTD)/maximum administered dose (MAD) of MGD007+MGA012 in patients with relapsed/refractory metastatic CRC. Patients are eligible irrespective of KRAS/MMR status, after treatment with 2-5 prior standard therapy regimens in the metastatic setting, or if they did not tolerate fluoropyrimidines, oxaliplatin or irinotecan chemotherapy or are not good candidates for standard of care. Secondary objectives include characterization of pharmacokinetics, pharmacodynamics, and immunogenicity of the combination, and investigation of the preliminary antitumor activity as measured by objective response rate, disease control rate, and progression-free survival rate at 16 weeks using both Response Evaluation Criteria in Solid Tumors (RECIST 1.1), and immune-related RECIST. Translational studies will investigate the immune modulatory activity of MGD007+MGA012. The study will include a 3+3+3 design Dose Escalation Phase to determine the MTD or MAD of the combination, followed by a Cohort Expansion Phase treating patients at the MTD or MAD to further define the safety and initial antitumor activity of the combination. Patients may be treated for up to 12 cycles in the absence of disease progression, DLT, or other criteria for permanent discontinuation. Enrollment is ongoing.

Trial Registration

NCT03531632

Ethics Approval

The study was approved by each institution's Insitutional Review Board.

P305

A phase 1, open label, dose escalation study of MGD009, a B7-H3 x CD3 DART® protein, in combination with MGA012, an anti-PD-1 antibody, in patients with relapsed or refractory B7-H3-expressing tumors

Alexander Spira, MD, PhD, FACP[1], Stacie Goldberg, MD[2], James Strauss, MD[3], Johanna Bendell, MD[4], Gregory Cote[5], E Rahma, MD[6], Marwan Fakih, MD[7], Ralph Alderson, PhD[2], Liqin Liu, PhD[2], Ross La Motte-Mohs, PhD, BS[2], Amy Worth[2], Ashley Lowe[2], Jan Baughman, MPH[2], Tony Wu, PhD[2], Syd Johnson, PhD[2], Ezio Bonvini[2], Paul Moore, PhD[2], Jon Wigginton, MD[2]

[1]*Virginia Cancer Specialists, Fairfax, VA, USA*
[2]*MacroGenics, Inc., Rockville, MD, USA*
[3]*Mary Crowley Cancer Research, Dallas, TX, USA*
[4]*Sarah Cannon Research Institute, Nashville, TN, USA*
[5]*Massachusetts General Hospital, Boston, MA, USA*
[6]*Dana Farber Cancer Institute, Boston, MA, USA*
[7]*City of Hope, Duarte, CA, USA*

Background

T cells naturally undergo activation-induced upregulation of co-inhibitory pathways, which may limit the antitumor immune response. Blocking these inhibitory pathways may enhance the antitumor activity of CD3 bispecifics. MGD009 is a clinical stage B7-H3 x CD3 DART protein designed to redirect T cells to kill B7-H3-expressing tumor cells. B7-H3, a member of the B7 family of immune regulators, is overexpressed in a variety of solid tumors and has limited expression in normal tissues. In preclinical studies, MGD009 causes T-cell infiltration, activation and expansion in the tumors. MGD009 upregulates PD-1 on T cells and PD-L1 on tumor cells and immune cells in vitro. Preliminary observations in patients enrolled in the ongoing Phase 1 dose escalation trial with MGD009 alone indicate evidence of PD-1 up-regulation on both peripheral CD4 and CD8 T cells. MGA012, also known as INCMGA00012, is an anti-PD-1 antibody that has shown clinical activity in an ongoing Phase 1 trial. In vitro and in vivo studies have shown enhanced antitumor activity with the combination of MGD009 and MGA012 beyond that achieved with MGD009 alone. It is hypothesized that T-cell checkpoint inhibition with MGA012, combined with activation and enhancement of redirected T-cell killing with MGD009, could mediate greater anti-tumor activity than either agent alone in patients with B7-H3 expressing solid tumors.

Methods

This is a Phase 1, open-label, dose escalation, and cohort expansion study (NCT03406949) designed to characterize the safety, tolerability, pharmacokinetics, pharmacodynamics, immunogenicity, and preliminary antitumor activity of MGD009 in combination with MGA012. Dose escalation uses a 3+3+3 design, with patients treated every 2 weeks with escalating doses of IV MGD009 (starting dose 3 µg/kg), and MGA012 at a dose of 3 mg/kg in all cohorts. Antitumor activity is assessed by both conventional Response Evaluation Criteria in Solid Tumors (RECIST) 1.1 and immune-related RECIST. The study consists of a Dose Escalation Phase to determine the maximum tolerated dose (MTD) or maximum administered dose (MAD -- if no MTD is defined) of the combination, followed by a Cohort Expansion Phase to further define the safety and initial antitumor activity of the combination with the doses established in the Dose Escalation Phase. Patients with B7-H3-expressing, unresectable, locally advanced or metastatic solid tumors of any histology will be enrolled in the Dose Escalation Phase. Expansion cohorts will be limited to 6 tumor types (N=20/cohort) treated at the MTD/MAD of the combination. The study is ongoing at approximately 6 U.S. centers.

Trial Registration

NCT03406949

Ethics Approval

This study was approved by each participating institution's Institutional Review Board.

P306

A phase 1/2, first-in-human, dose escalation study of MGC018 (anti-B7-H3 antibody-drug conjugate) alone and in combination with MGA012 (anti-PD-1 antibody) in patients with advanced solid tumors

John Powderly, MD, CPI[1*], Deryk Loo[2], Anthony Joshua, MD[3], Johanna Bendell, MD[4], Alexander Spira, MD, PhD, FACP[5], Joanna Lohr, PhD[2], Pepi Pencheva, MD[2], Jichao Sun, PhD[2], Jan Baughman, MPH[2], Ezio Bonvini[2], Jennifer Brown[5], Nehal Lakhani, MD, PhD[6], Jon Wigginton, MD[2]

[1]Carolina BioOncology, Huntersville, NC, USA
[2]MacroGenics, Inc., San Francisco, CA, USA
[3]St. Vincent's Hospital, Syndey, Australia
[4]Sarah Cannon Research Institute, Nashville, TN, USA
[5]Virginia Cancer Specialists, Fairfax, VA, USA
[6]START Midwest, Grand Rapids, MI, USA

Background
Antibody-drug conjugates (ADCs) are a powerful class of agents for targeted cancer treatment, combining the specificity of a monoclonal antibody with highly-potent cytotoxic "payloads" for selective delivery of cytotoxic agents to cancer cells, offering potential for increased efficacy while minimizing exposure to normal tissues. Immune-checkpoint blockade is a promising approach, and inhibitors of programmed death-1 (PD-1), PD-1 ligand, and cytotoxic T-lymphocyte–associated protein 4 (CTLA-4) are approved for patients with various solid tumors; however, a significant proportion do not derive clinical benefit. B7-H3, a member of the B7 family of immune regulators, is overexpressed in a wide range of solid tumors, with limited normal tissue expression. MGC018 is an ADC targeted against B7-H3 with a linker-duocarmycin payload, conjugated to an anti-B7-H3 monoclonal antibody. MGC018 demonstrated favorable binding properties; potent cytotoxic activity toward multiple B7-H3-expressing human tumor cells in vitro; antitumor activity in B7-H3 human tumor xenografts (breast cancer, ovarian cancer, lung cancer and melanoma); a favorable tissue cross-reactivity profile across 34 normal human tissues; and acceptable safety following repeat-dose administration in cynomolgus monkeys. It is hypothesized that MGC018 monotherapy will mediate antitumor activity against B7-H3-positive tumors. Further, that administration of this B7-H3-directed cytotoxic agent could enhance tumor cell death and drive "auto-vaccination" of the host immune system, with added engagement of a T-cell response by sequenced administration of MGC018 in combination with anti-PD-1 antibody (MGA012; also known as INCMGA00012).

Methods
This Phase 1/2, bifurcated-design study will characterize safety, dose-limiting toxicities (DLTs), and maximum tolerated/administered dose (MTD/MAD) for MGC018 as monotherapy (Module A) or in combination with MGA012 (Module B) in patients with advanced solid tumors. Pharmacokinetics, immunogenicity, and impact of treatment on various measures of immune function and tumor cell death will be assessed. Tumor assessments will occur every 42-84 days, and response status will be defined using RECIST v1.1 and irRECIST. Module B will commence after the MTD/MAD of MGC018 monotherapy (Module A) is defined. Each module consists of a Dose Escalation (3+3+3 design) followed by a Cohort Expansion Phase. Patients with solid tumors of any histology will be enrolled in the Dose Escalation Phases; Cohort Expansion will include patients with SCCHN, prostate carcinoma, triple negative breast cancer, and uveal melanoma. Patients who do not experience DLT/unacceptable toxicity or meet criteria for permanent discontinuation may undergo additional cycles. Patients will be followed for survival every 3 months for 2 years following last dose.

Trial Registration
Pending

Ethics Approval
Each institution will obtain Institutional Review Board approval prior to enrollment of subjects.

P307

An open-label, phase 1B study of NEO-PV-01 + CD40 agonist antibody (APX-005M) or Ipilimumab with Nivolumab in patients with advanced or metastatic melanoma

Omid Hamid, MD[1], David Spigel, MD[2], Patrick Ott, MD, PhD[3], Siwen Hu-Lieskovan, MD, PhD[4], Karl Lewis, MD[5], Michael Gordon, MD[6], Lisa Cleary[7], Melissa Moles[7], Richard Gaynor, MD[7], Matthew Goldstein, MD, PhD[7], Les Brail[7], Keith Flaherty, MD[8]

[1]*Angeles Clinic, Los Angeles, CA, USA*
[2]*Sarah Cannon, Nashville, TN, USA*

[3]Dana-Farber Cancer Institute, Boston, MA, USA
[4]UCLA, Los Angeles, CA, USA
[5]University of Colorado Denver, Aurora, CO, USA
[6]Honor Health, Scottsdale, AZ, USA
[7]Neon Therapeutics, Cambridge, MA, USA
[8]Massachusetts General Hospital, Boston, MA, USA

Background

Cancer cells contain unique DNA mutations that result in altered amino acid sequences known as neoantigens. Growing evidence supports a central role for neoantigens as targets for tumor directed immune responses. Tumor mutational burden and neoantigen load have been associated with anti-tumor activity of checkpoint inhibitors. NEO- PV-01 is a personal neo-antigen vaccine designed specifically for the molecular profile of each individual's tumor. In the ongoing NT-001 study, NEO-PV-01 administered in combination with nivolumab has been shown to be well tolerated and to generate neoantigen specific immune responses in patients with melanoma. Here we describe a clinical trial, NT-003, combining NEO-PV-01 in combination with either nivolumab, nivolumab and ipilimumab, or the CD40 agonist antibody APX-005M and nivolumab. Immune modulatory antibodies that enhance T cell priming offer a rational combination partner with vaccines to further enhance induction of de novo T cell reactivity and to expand existing T cell responses against neoantigens.

Methods

NT-003 is a multi-arm, phase 1B study designed to evaluate the safety of administering NEO-PV-01 using an alternative vaccination schedule, or combination regimens with APX005M or ipilimumab with nivolumab in patients with advanced or metastatic melanoma. Please see Figure 1 for design. Patients undergo a baseline tumor biopsy and HLA typing. DNA and RNA sequencing is performed on tumor as well as peripheral blood. NEO-PV-01 is custom designed for each individual patient and contains up to 20 peptides approximately 14-35 amino acids in length. The peptides are pooled into four groups and mixed with poly-ICLC at the time of administration. On Day 1, patients will begin treatment with nivolumab (Q2W). Beginning at Week 12, patients begin immunizations with NEO-PV-01. Also at beginning at week 12, patients will begin to receive the co-administered therapy/(s) depending upon their cohort and arm assignment (Figure 1). The primary endpoint is safety. Secondary endpoints are ORR, CBR, PFS, and assessment of response conversion beginning on Week 12. Exploratory objectives include extensive immune monitoring with antigen-specific analyses over multiple timepoints of both peripheral blood and tumor (NCT03597282).

Trial Registration

NCT03597282

Figure 1.

P308

A Phase 1 study of MEDI5752, a bispecific antibody that preferentially targets PD-1 and CTLA-4 expressing T cells, in patients with advanced solid tumors.

Jeffery Brubaker[1], Ben Tran[2], Mark Voskoboynik[3], James Kuo[4], Yung-Lue Bang, MD[5], Hyun-Cheo Chung, MD, PhD[6], Myung-Ju Ahn[7], Sang-We Kim[8], Ayesh Perera[1], Daniel Freeman[1], Ikbel Achour, PhD[1],

Raffaella Faggioni, PhD[1], Feng Xiao[1], Charles Ferte, MD, PhD[1], Charlotte Lemech, MBBS BSc(med) MD(res)[4]

[1]*MedImmune, Gaithersburg, MD, USA*
[2]*Peter MacCallum Cancer Center, Melbourne, Australia*
[3]*Nucleus Network, Melbourne, Australia*
[4]*Scientia Clinical Research, Sydney, Australia*
[5]*Seoul National University Hospital, Seoul, Korea, Republic of*
[6]*Yonsei Cancer Center, Yonsei University, Seoul, Korea, Republic of*
[7]*Samsung Medical Center, Seoul, Korea, Republic of*
[8]*Asan Medical Center, Songpa-Gu, Korea, Republic of*

*Corresponding author email: fertec@MedImmune.com

Background

Based on demonstrated clinical activity and manageable safety profiles, checkpoint inhibiting antibodies blocking PD 1, PD-L1, or CTLA-4 have received regulatory approvals for the treatment of various malignancies [1-5]. The combination therapy with anti-PD-1 and anti-CTLA-4 agents is approved by FDA for metastatic melanoma, renal cell carcinoma and microsatellite instability-high (MSI-H) or mismatch repair deficient (dMMR) metastatic colorectal cancer, based on improved overall survival versus either agent alone [6-10]. Numerous clinical studies of combination immunotherapy are currently investigating the same combination across a range of solid tumors [11-15]. Although the efficacy of these drug combinations is dose dependent, the toxicity associated with anti-CTLA-4 agents, in particular, is dose limiting, thereby potentially affecting treatment outcomes with combination therapy.MEDI5752 is a bispecific humanized IgG1 monoclonal antibody that binds PD-1 and CTLA-4. In contrast to the combination therapy, MEDI5752 exhibits a novel T cell targeting mechanism that could provide a favorable toxicity profile. In addition, we have shown that MEDI5752 can impact cell surface expression of PD-1. Based on these novel mechanisms of action, MEDI5752 may show improved efficacy and safety in comparison to co-administration of conventional anti-PD-1/anti-PD-L1 and anti-CTLA-4 antibodies.

Methods

This is a Phase 1, first-time-in-human, multicenter, open-label study in patients with advanced solid tumors. The dose-escalation phase will evaluate approximately six MEDI5752 dose levels to identify a maximum tolerated dose. Dose escalation will be followed by two dose-expansion cohorts in defined setting with patients with advanced or metastatic solid tumor and tested against a control arm. Subjects will remain on treatment until confirmed progressive disease, initiation of alternative cancer therapy, unacceptable toxicity, or other reason for discontinuation. The primary endpoints are safety and efficacy (objective response in the dose-expansion phase). Secondary endpoints include additional efficacy assessment across both phases, pharmacokinetics, and immunogenicity.

Trial Registration

NCT03530397

References

1. Opdivo Prescribing Information. Princeton, NJ: Bristol-Myers Squibb Company, 2018. [revised 2018 Apr].
2. Keytruda Prescribing Information. Whitehouse Station, NJ: Merck Sharp & Dohme Corp, 2018 [revised 2018 Jun].
3. Tecentriq Prescribing Information. San Francisco (CA): Genentech, Inc, 2018. [revised 2019 Jul].
4. Imfinzi Prescribing Information. Wilmington (DE): AstraZeneca Pharmaceuticals LP, 2018.[revised 2018 Feb].
5. Yervoy Prescribing Information. Princeton (NJ): Bristol-Myers Squibb Company, 2018. [revised 2018 Apr].

6. Larkin J, Chiarion-Sileni V, Gonzalez R, Grob JJ, Cowey CL, Lao CD, et al. Combined nivolumab and ipilimumab or monotherapy in untreated melanoma. N Engl J Med. 2015;373:23-34.
7. Postow MA, Chesney J, Pavlick AC, Robert C, Grossmann K, McDermott D, et al. Nivolumab and ipilimumab versus ipilimumab in untreated melanoma. N Engl J Med. 2015;372:2006-2017.
8. Motzer RJ, Tannir NM, McDermott DF, Frontera OA, Melichar B, Choueiri TK, et al. Nivolumab plus ipilimumab versus sunitinib in advanced renal-cell carcinoma. N Engl J Med. 2018;378:1277-1290.
9. Overman MJ, Lonardi S, Wong KYM, Lenz H-J, Gelsomino F, Aglietta M, et al. Durable clinical benefit with nivolumab plus ipilimumab in DNA mismatch repair–deficient/microsatellite instability–high metastatic colorectal cancer. J Clin Oncol. 2018;36:773-779.
10. Broderick JM. Nivolumab, ipilimumab combo approved by FDA for MSI-H/dMMR colorectal cancer. Pharmacy Times, 11 July, 2018. Available at: https://www.pharmacytimes.com/news/nivolumab-ipilimumab-combo-approved-by-fda-for-msihdmmr-colorectal-cancer. Accessed 18 July, 2018.
11. Antonia S, Goldberg SB, Balmanoukian A, Chaft JE, Sanborn RE, Gupta A, et al. Safety and antitumour activity of durvalumab plus tremelimumab in non-small cell lung cancer: a multicentre, phase 1b study. Lancet Oncol. 2016a;17(3):299-308.
12. Haddad R, Gillison M, Ferris RL, Harrington K, Monga M, Baudelet C, et al. Double-blind, two-arm, phase 2 study of nivolumab (nivo) in combination with ipilimumab (ipi) versus nivo and ipi-placebo (PBO) as first-line (1L) therapy in patients (patients) with recurrent or metastatic squamous cell carcinoma of the head and neck (R/M SCCHN)—CheckMate 714. Ann Oncol. 2016;27(suppl_6):1017TiP-TiP.
13. Kelley RK, Abou-Alfa GK, Bendell JC, Kim T-Y, Borad MJ, Yong W-P, et al. Phase I/II study of durvalumab and tremelimumab in patients with unresectable hepatocellular carcinoma (HCC): Phase I safety and efficacy analyses. J Clin Oncol. 2017;35(15_suppl):4073.
14. Janjigian YY, Ott PA, Calvo E, Kim JW, Ascierto PA, Sharma P, et al. Nivolumab ± ipilimumab in patients with advanced (adv)/metastatic chemotherapy-refractory (CTx-R) gastric (G), esophageal (E), or gastroesophageal junction (GEJ) cancer: CheckMate 032 study. J Clin Oncol. 2017;35(15_suppl):4014.
15. Escudier B, Tannir NM, McDermott DF, Frontera OA, Melichar B, Plimack ER, et al. LBA5CheckMate 214: Efficacy and safety of nivolumab + ipilimumab (N+I) v sunitinib (S) for treatment-naïve advanced or metastatic renal cell carcinoma (mRCC), including IMDC risk and PD-L1 expression subgroups. Ann Oncol. 2017;28(suppl_5):mdx440.029- mdx440.029.

P309

Phase I dose-finding study of MIW815 (ADU-S100), an intratumoral STING agonist, in patients with advanced solid tumors or lymphomas

Janis Callister[1], Funda Meric-Bernstam, MD[2], Theresa Werner[3], Stephen Hodi[4], Wells Messersmith, MD[5], Nancy Lewis[6], Craig Talluto[7], Mirek Dostalek[6], Aiyang Tao[6], Sarah McWhirter[8], Damian Trujillo[8], Jason Luke, MD, FACP9

[1]Articulate Science, Manchester, UK
[2]MD Anderson Cancer Center, Houston, TX, USA
[3]University of Utah, Salt Lake City, UT, USA
[4]Dana-Faber Cancer Institute, Boston, MA, USA
[5]University of Colorado Cancer Center, Aurora, CO, USA
[6]Novartis Pharmaceuticals Corporation, East Hanover, NJ, USA
[7]Novartis Institutes for BioMedical Resea, Cambridge, MA, USA
[8]Aduro Biotech Inc, Berkeley, CA, USA
[9]The University of Chicago Medicine, Chicago, IL, USA

Background

MIW815 (ADU-S100) is a novel synthetic cyclic dinucleotide that can activate human STING

(STimulator of INterferon Genes) in antigen-presenting cells. In preclinical models, STING pathway activation can induce tumor antigen-specific T-cell priming within the tumor microenvironment, leading to antitumor immunity and tumor destruction.

Methods

Eligible patients (≥2 accessible tumors; Eastern Cooperative Oncology Group Performance Status ≤1) include those with advanced/metastatic solid tumors or lymphomas with progressive disease despite standard of care or for whom there is no standard treatment. MIW815 (ADU-S100) is administered by weekly intratumoral injections (3 weeks on/1 week off) at escalating doses (starting dose: 50 µg) in 28-day cycles. Primary objectives are to characterize safety and tolerability and to identify a recommended dose for future studies. Secondary objectives include preliminary efficacy, pharmacokinetics (PK), and pharmacodynamics (PD). The study is currently in dose escalation.

Results

As of June 15, 2018, 41 heavily pretreated patients (median age 62 years; range 26–80 years) with various solid tumors or lymphomas were enrolled. Thirty-five patients have discontinued from the study for the following reasons: disease progression (n=26), physician/patient decision (n=8), and death (n=1); 6 patients continue to receive treatment. No dose-limiting toxicities (DLTs) were reported during the first cycle at any dose level. The most common (≥10% of patients) treatment-related AEs (TRAEs) were pyrexia (n=7; 17.1%), injection site pain (n=6; 14.6%), and headache (n=6; 14.6%). Grade 3/4 TRAEs included increased lipase (n=2; 4.9%) and elevated amylase, tumor pain, dyspnea, respiratory failure, and injection site reaction (n=1 each; 2.4%). Systemic MIW815 (ADU-S100) exposure increased with dose. On-treatment tumor biopsies showed increases in CD8 T cells infiltrating the injected tumors in a subset of patients. Preliminary antitumor activity, PK analysis, and PD data from injected lesions, non-injection lesions, and peripheral blood, will be presented.

Conclusions

Intratumoral injection of MIW815 (ADU-S100) was well tolerated in doses tested thus far in patients with advanced solid tumors and lymphoma, with no DLTs reported to date. Trials evaluating combinations of MIW815 (ADU-S100) with anti-PD1 or anti-CTLA4 antibodies are ongoing.

Ethics Approval

This study was approved by an independent ethics committee or institutional review board at each site.

P310

NANT Cancer Vaccine an orchestration of immunogenic cell death by overcoming immune suppression and activating NK and T cell therapy in patients with third line or greater TNBC and head & neck SCC

Eric Carlson[1], Mira Kistler, MD[2], Patrick Soon-Shiong, MD, FRCS, FACS[1], John Lee, MD[1], Chaitali Nangia, MD[2], Leonard Sender[2], Frank Jones, PhD[3]

[1]*Nantkwest, Los Angeles, CA, USA*
[2]*Chan Soon-Shiong Institute for Medicine, El Segundo, CA, USA*
[3]*NantCell, CULVER CITY, CA, USA*

Background

Triple negative breast cancer (TNBC) and head & neck squamous cell cancer (HNSCC) have multiple mechanisms to prevent immune recognition and immune eradication that lead to the creation of an immune suppressive tumor microenvironment. We hypothesize that effective and sustained response against tumors requires a coordinated approach that: 1. reverses the immune-suppressive tumor microenvironment, 2. induces immunogenic tumor

cell death and 3. reengages NK and T-cell tumor response against a 4. cascade of tumor antigens. To test this hypothesis, we have developed the NANT Cancer Vaccine: a temporospatial approach that combines: metronomic low dose chemotherapy, SBRT, off-the-shelf cryopreserved allogeneic NK cells, yeast and adenoviral tumor associated antigen vaccines, IL-15RαFc superagonist N-803 immunostimulatory cytokine, with checkpoint inhibitor.

Methods

A phase 1b, single-arm, open-label trial of the NANT Cancer Vaccine in patients with recurrent metastatic third line or greater TNBC and HNSCC was initiated. Treatment occurred in 3-week cycles of low-dose chemotherapy (aldoxorubicin, cyclophosphamide, cisplatin, nab-paclitaxel, 5-FU/L), antiangiogenic therapy (bevacizumab), SBRT, engineered allogeneic high affinity CD-16 NK-92 cells (haNK), IL-15RαFc (N-803), adenoviral vector-based CEA, MUC1, Brachyury, HER2 vaccine (Ad), yeast vector-based RAS, Brachyury and CEA vaccine (Ye), and an IgG1 PD-L1 inhibitor, avelumab plus cetuximab. The primary endpoint is incidence of treatment-related adverse events. Secondary endpoints include ORR, DCR, PFS, and OS.

Results

To date, 3 patients with 3rd-line or greater TNBC and 2 patients with 4th-line or greater HNSCC have been treated with the NANT Cancer Vaccine. All treatment was completed in the outpatient setting, with no immune-related adverse events. Two of the three patients with TNBC experienced partial response (78% and 62% decrease by irRC). Both patients with HNSCC experienced objective tumor response (100% and 47% decrease by irRC). Four hematologic DLT's were observed and managed with a planned dose reduction of cisplatin. All responding patients are still undergoing therapy.

Conclusions

This preliminary data suggests that the NANT Cancer Vaccine of low-dose chemoradiation combined with innate and adaptive immunotherapy can be administered safely in an outpatient setting without any observed increased irAE's. Preliminary efficacy result of four out of five patients (80%) with confirmed overall responses, with one of these four patients demonstrating a complete response with 5th-line metastatic disease is encouraging.

Trial Registration

NCT03387111 NCT03387085

Ethics Approval

These studies were approved by IRB Company, approval numbers 2018-0001-CSSIFM and 18-0002-CSSIFM.

P311

Positive identification of neoepitope specific T cell by tumor-normal DNA & RNA sequencing from breast cancer patient leading to yeast-based vaccine phase 1 trial delivering tumor specific neoepitopes

Peter Sieling, PhD[1], Steve Benz[2], Zach Sanborn, PhD[1], Kayvan Niazi[1], Tom King[3], Shahrooz Rabizadeh, PhD[1], Andrew Nguyen[2]

[1]NantBio, Culver City, CA, USA
[2]Nantomics, Rockville, MD, USA
[3]NantCell, Culver City, CA, USA

Background

Patient specific neoepitope discovery and subsequent vaccine development promise an opportunity for immunological memory, tumor clearance, and durable remission. Screening for neoepitope specific T cells in breast cancer patients utilizing our proprietary tumor-normal DNA & RNA sequencing technology led to successful identification of peptide-specific T cell clones

isolated from biopsied tissue. All T cell clones specifically recognized the same tumor-specific mutations and not their wild-type counterpart, and demonstrated CDR3 T cell receptor diversity. The polyclonal nature of isolated T cells and the specificity with which they engaged mutant protein demonstrated the validity of this bioinformatic approach to neoepitope identification and formed the basis for this clinical trial. Based on this platform, we have initiated a clinical trial of neoepitope vaccine delivery using a yeast vehicle.

Methods

This study requires tumor-normal DNA and RNA sequencing to identify tumor specific DNA mutations expressed by tumor RNA and presented by patient MHC I and II (also identified by DNA sequencing). Tumor specific neoepitopes are expressed as a polytope in S. cerevisiae and delivered subcutaneously to patients enrolled in this trial. This phase 1 study aims to determine primarily, safety, dosing, including recommended phase 2 dose (RP2D), and secondarily, efficacy (disease recurrence rate, disease-free survival and overall survival) of a personalized neoepitope yeast-based vaccine in subjects who have completed potentially curative therapy for their solid cancer (eg, colorectal cancer, breast cancer, head and neck squamous cell carcinoma, melanoma) (NCT03552718).

Results

Our data demonstrate that our proprietary algorithms accurately predict tumor specific neoepitopes, which appropriately engender CD4+ and CD8+ T cell responses. These responses enable tumor clearance in combination with immunostimulants such as IL-15RαFc (N-803) and IL-12. Our previous ex vivo studies of patient-derived TILs further provide evidence of neoepitope engagement, establishing clonal T cell populations reactive against predicted neoepitopes in a patient specific manner [1]. The yeast delivery vehicle in this trial has previously induced immunogenicity against tumor associated antigens in previous clinical studies [2]. Trial sites are being actively recruited and activated.

Conclusions

Neoepitopes have been successfully identified using tumor-normal next generation sequencing. Personalized neoepitope technology promises significant advances against cancer. Data from this trial will establish safety and an immunological strategy to direct patients with cancer towards durable responses.

Trial Registration

NCT03552718

References

1. Würfel F, Erber R, Huebner H, Hein A, Lux MP, Jud S, Kremer A, Kranich H, Mackensen A, Haberle L, Hack C, Rauh C, Wunderle M, Gaß P, Rabizadeh S, Brandl A, Langemann H, Volz B, Nabieva N, Schulz-Wendtland R, Dudziak D, Beckmann MW, Hartmann A, Fasching P, Rübner M. TILGen: A Program to Investigate Immune Targets in Breast Cancer Patients – First Results on the Influence of Tumor-Infiltrating Lymphocytes. Breast Care. 2018; 13:8-14.
2. King T, Guo Z, Hermreck M, Bellgrau D, Rodell T. Construction and Immunogenicity Testing of Whole Recombinant Yeast-Based T-Cell Vaccines. Methods Mol. Biol. 2016; 1404:529-545.

Ethics Approval

This study was approved by IRB company, approval number 2018-0033-CSSIFM.

P313

INCMGA 0012-201: A phase 2 study of INCMGA00012 in patients with metastatic Merkel cell carcinoma (mMCC)

Geoffrey Gibney, MD[1], Inderjit Mehmi, MD[2], Sadhna Shankar[3], Jeffrey Marine[3], Chuan Tian[3], Igor Puzanov,

MD, MSCI, FACP[4]

[1]*MedStar Georgetown Cancer Institute, Washington, DC, USA*
[2]*WVU Cancer Institute, Morgantown, WV, USA*
[3]*Incyte Corporation, Wilmington, DE, USA*
[4]*Roswell Park Comprehensive Cancer Center, Buffalo, NY, USA*

Background
INCMGA00012 is a humanized IgG4 monoclonal antibody against human PD-1 that lacks antibody-dependent cell-mediated cytotoxicity directed against effector lymphocytes. It has demonstrated acceptable tolerability with no dose-limiting toxicity at doses up to 10 mg/kg administered every 2 weeks in an ongoing phase 1 study. Clinical activity has been seen in multiple tumor types. Full and sustained receptor occupancy of INCMGA00012 on both CD4+ and CD8+ T cells along with complete loss of competing fluorescently labeled anti–PD-1 staining (eJBio105 clone) were seen at all dose levels evaluated in the phase 1 study.In patients with mMCC, response rates decline with increasing number of previous chemotherapy regimens [1]. Blockade of the PD-1/PD-L1 pathway has resulted in objective responses in up to 60% of chemotherapy-naive patients. Approximately 30% of chemotherapy-refractory patients showed an objective response to treatment with the anti–PD-L1 antibody avelumab. Additionally, there is no clear correlation of response rates with PD-L1 or Merkel cell polyomavirus status of the tumor.INCMGA00012 offers the convenience of once every 4 weeks (Q4W) flat dosing.

Methods
This is a phase 2, open-label study designed to characterize the efficacy and safety of INCMGA00012 in patients with mMCC. The primary endpoint is the overall response rate (ORR) in chemotherapy-naive patients with mMCC. The secondary endpoints include ORR in the full study population (chemotherapy-naive plus chemotherapy-refractory patients). Other secondary endpoints consist of duration of response, disease control rate, progression-free survival, and overall survival in the chemotherapy-naive patients alone, and the full study population. Patients with mMCC and measurable disease per RECIST v1.1, who have not been previously treated with any anti–PD-1 or anti–PD-L1 therapy and are either chemotherapy-naive or have received no more than 3 prior chemotherapy regimens, are eligible for participation. Approximately 90 patients will be enrolled globally. INCMGA00012 will be administered at a flat dose of 500 mg as an intravenous infusion over 60 minutes Q4W. Disease assessments will be conducted every 8 weeks. Study treatment may continue up to 2 years if there is no unacceptable drug-related toxicity or disease progression.

Trial Registration
NCT03599713

References
1. Colunga A, Pulliam T, Nghiem P. Merkel cell carcinoma in the age of immunotherapy: Facts and hopes. Clin Cancer Res. 2018; 24:2035-2043.

Ethics Approval
The study was approved by institutional review boards or independent ethics committees of participating institutions.

P314

An open-label, phase 1B study of NEO-PV-01 with Pembrolizumab plus chemotherapy in patients with advanced or metastatic nonsquamous Non-small Cell Lung Cancer

Mark Awad, MD PhD[1], David Spigel, MD[2], Lisa Cleary[3], Melissa Moles[3], Richard Gaynor, MD[3], Matthew Goldstein, MD, PhD[3], Ramaswamy Govindan, MD[4]

[1]Dana Farber Cancer Institute, Boston, MA
[2]Sarah Cannon Cancer Institute, Nashville, TN, USA
[3]Neon Therapeutics, Cambridge, MA, USA
[4]Washington University in St. Louis, Saint Louis, MO, USA

Background
Neoantigens arise from unique DNA mutations in cancer cells and are attractive targets for tumor directed immune responses. The anti-tumor activity of checkpoint inhibitors has been associated with tumor mutational burden as well as neoantigen load. The combination of carboplatin/pemetrexed plus anti-PD1 therapy for the treatment of front-line non-squamous NSCLC has demonstrated improved efficacy over chemotherapy alone [1]. This combination reduces the risk of early progression and may also modulate the tumor microenvironment. Vaccines targeting neoantigens offer a rational combination with chemotherapy and anti-PD1 as a highly specific way to induce de novo T cell reactivity and to expand existing T cell responses against neoantigens. Here, we describe a clinical trial combining NEO-PV-01, a personal neoantigen vaccine designed specifically for the molecular profile of each individual's tumor, with carboplatin/pemetrexed plus anti-PD1.

Methods
NT-002 is a single-arm, phase 1B study designed to evaluate the safety of administering NEO-PV-01 + adjuvant (Poly-ICLC) with pembrolizumab plus carboplatin and pemetrexed in patients with advanced non-squamous non-small cell lung carcinoma who have received no prior systemic treatment. Patients undergo a baseline tumor biopsy and HLA typing. DNA and RNA sequencing are performed on tumor as well as peripheral blood to serve as normal DNA controls. NEO-PV-01 is custom designed for each individual patient and contains up to 20 peptides 14-35 amino acids in length. The peptides are pooled into four groups and mixed with the adjuvant Poly-ICLC at the time of subcutaneous administration. On Day 1, patients will begin with 4 treatment cycles of pembrolizumab plus chemotherapy. Beginning on Cycle 5 (Week 12), patients will receive pembrolizumab monotherapy Q3W up to Week 103. Also beginning at Week 12, patients receive five priming immunizations with NEO-PV-01 over a three-week period followed by booster vaccinations at Weeks 19 and 23. The primary endpoint is safety. Secondary endpoints are ORR, CBR, PFS, and assessment of response conversion between Week 12 and Week 24. Exploratory endpoints include extensive immune monitoring with antigen-specific analyses over multiple timepoints of both peripheral blood and tumor.

Trial Registration
NCT03380871

References
1. Gandhi L, et. al. Pembrolizumab plus chemotherapy in metastatic Non–Small-Cell Lung Cancer. New England Journal of Medicine. 2018; 378:2078-2092

Ethics Approval
This study was approved by institutional ethic's boards at the Dana Farber Cancer Institute, Washington University in St. Louis, and Sarah Cannon Cancer Center.

P315

Phase I/II study of the anti–LAG-3 antibody MK-4280 in combination with pembrolizumab for the treatment of hematologic malignancies

Gareth Gregory[1], Pier Zinzani[2], John Palcza, MS[3], Jane Healy[3], Robert Orlowski, MD[3], Arun Balakumaran, PhD, MD[3], Philippe Armand[4]

[1]School of Clinical Sciences at Monash Health, Monash University, Melbourne, Austrailia

[2]Institute of Hematology "Seràgnoli" University of Bologna, Bologna, Italy
[3]Merck & Co., Inc., Kenilworth, NJ, USA
[4]Dana-Farber Cancer Institute, Boston, MA, USA

Background
Most lymphomas, including classic Hodgkin lymphoma (cHL), diffuse large B-cell lymphoma (DLBCL), and indolent B-cell lymphomas are not readily curable in the relapsed/refractory (R/R) setting, and new options for treating those malignancies are urgently needed. Pembrolizumab, a humanized, high-affinity antibody against programmed death 1 (PD-1), has demonstrated effective antitumor activity and acceptable safety in patients with R/R cHL and R/R primary mediastinal large B-cell lymphoma. Lymphocyte activation gene-3 (LAG-3) is a cell surface immunomodulatory receptor commonly co-expressed with PD-1 on exhausted T cells and may serve as an escape pathway for lymphoma subjected to PD-1 blockade. Dual blockade of PD-1 and LAG-3 demonstrated synergistic activity in mouse models of colon adenocarcinoma and fibrosarcoma. MK-4280 is a humanized anti–LAG-3 monoclonal antibody that blocks the interaction between LAG-3 and its ligand MHC class II. This study will evaluate the safety and efficacy of MK-4280 plus pembrolizumab in patients with selected hematologic malignancies.

Methods
This phase 1/2 multisite study (ClinicalTrials.gov: NCT03598608) will enroll patients with PD-1/PD-L1 inhibitor–naive cHL (cohort 1), PD-1/PD-L1 inhibitor–refractory R/R cHL (cohort 2), R/R DLBCL (cohort 3), and R/R indolent B-cell lymphoma (cohort 4). The study will have a safety lead-in phase to establish the preliminary recommended phase 2 dose (RPTD) followed by an efficacy expansion phase. In the safety lead-in phase, a modified toxicity probability interval design will be used to establish RPTD of MK-4280 plus pembrolizumab. Dose-limiting toxicities will be assessed during the first cycle. Eligibility criteria are age ≥18 y, ECOG PS 0/1, adequate organ function, and meeting the standard eligibility criteria for pembrolizumab studies, such as no prior receipt of anti–PD-1 antibody and no active infection necessitating systemic therapy. Patients will receive pembrolizumab 200 mg Q3W and MK-4280 for 35 cycles or until disease progression, unacceptable toxicity, or withdrawal from study. Tumor response will be assessed by CT/PET Q12W to confirm complete response or as clinically indicated, using revised response criteria for malignant lymphoma. Patients will be monitored for adverse events (AEs) until 30 days after study treatment end (90 days for serious AEs). The primary objective of this study is to determine the safety, tolerability, and to establish a preliminary RPTD. Secondary end points include objective response rate per investigator review and pharmacokinetics of MK-4280 and pembrolizumab. The safety lead-in phase will enroll ≥14 patients and the efficacy expansion phase will enroll approximately 120 patients (30 per cohort).

Trial Registration
ClinicalTrials.gov: NCT03598608

Ethics Approval
The protocol and its amendments were approved by the appropriate institutional review board or independent ethics committee.

Consent
All patients will provide written informed consent.

P316

Phase 1b dose-escalation and dose-expansion study to evaluate safety, tolerability, pharmacokinetics, and antitumor activity of ADCT-301 (Camidanlumab Tesirine) in patients with advanced solid tumors

Igor Puzanov[1], Shivaani Kummar, MD[2], Patricia LoRusso, DO[3], Kyri Papadopoulos[4], Francesca Zammarchi, PhD[5], Hans Cruz[5], Jens Wuerthner, MD

PhD[5], Johanna Bendell, MD[6]

[1]Roswell Park Comprehensive Cancer Center, Buffalo, NY, USA, Buffalo, NY, USA
[2]Stanford University, CA, USA, Stanford, CA
[3]Yale Cancer Center, New Haven, CT, USA, New Haven, CT, USA
[4]South Texas Accelerated Research Therapeutics (START), San Antonio, TX, USA
[5]ADC Therapeutics, London, UK
[6]Sarah Cannon Research Institute, Tennessee Oncology, Nashville, TN, USA, Nashville, TN, USA

Background

CD25+ regulatory T-cells (Tregs) suppress tumor-specific T-cell–mediated immune responses and contribute to cancer progression [1]. Modifying the intra-tumoral balance of effector T-cells and Tregs by blocking or depleting CD25+ Tregs is a strategy for tumor eradication, either as a standalone approach or in combination with other immuno-oncology therapies [1,2]. ADCT-301 (camidanlumab tesirine [Cami-T]), an anti-CD25 human monoclonal antibody conjugated to a potent pyrrolobenzodiazepine dimer toxin (Figure 1), is a candidate for selective depletion of tumor-infiltrating CD25+ Tregs. A surrogate of Cami-T, sur301, has shown strong and durable antitumor activity in mouse colon adenocarcinoma-derived models. This study aims to characterize the safety and tolerability of Cami-T in patients with selected advanced solid tumors. A separate study of Cami-T in patients with relapsed/refractory Hodgkin lymphoma and non-Hodgkin lymphoma (NCT02432235) is ongoing.

Methods

This is a Phase 1b, multicenter, open-label, dose-escalation and dose-expansion study planned for adult patients with locally-advanced or metastatic solid tumors. Patients should be refractory to or intolerant of existing therapies. The primary objective of the study is to characterize the safety and tolerability of Cami-T and to identify the recommended dose(s) and schedule(s) for future studies. Secondary objectives are to evaluate the preliminary antitumor activity, pharmacokinetics and immunogenicity of Cami-T. A fresh tumor biopsy for biomarker investigations is required to participate. Based on the literature on CD25+ Treg tumor content, patients with the following tumor types will be eligible: head and neck, non-small cell lung, gastric and esophageal, pancreas, bladder, renal, melanoma, triple negative breast, and ovarian cancers. Patients who had a prior organ or allogeneic bone marrow transplant, history of symptomatic autoimmune disease, significant medical comorbidities, or received major surgery or antitumor therapies within the last 14 days will be excluded. The first cohort will receive a dose of 20 µg/kg every 3 weeks, selected as the minimum dose with potential antitumor activity based on mouse models and data from the Phase I study of Cami-T in hematological malignancies. Subsequent dose escalation up to 300 µg/kg is planned to identify the recommended dose(s) for expansion. The study plans to enroll up to 50 patients with an expected start in Q3 2018.

Conclusions

A new Phase 1 study is planned to assess the safety and preliminary efficacy of Cami-T for the management of advanced solid tumors.

Acknowledgements

Study sponsored by ADC Therapeutics

References

1. Sasidharan Nair V, Elkord E. Immune checkpoint inhibitors in cancer therapy: a focus on T-regulatory cells. Immunol Cell Biol. 2018;96:21–33.
2. Arce Vargas F, Furness AJS, Solomon I, et al. Fc-optimized anti-CD25 depletes tumor-infiltrating Regulatory T cells and synergizes with PD-1 blockade to eradicate established tumors. Immunity. 2017;46:577–586.

Figure 1.

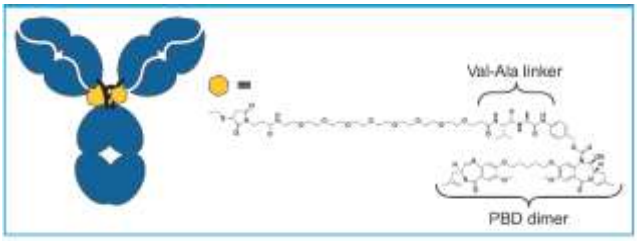

PBD, pyrrolobenzodiazepine

P318

HITM-SURE: Phase Ib CAR-T hepatic artery infusion trial for stage IV adenocarcinoma using Pressure-Enabled Drug Delivery technology

Steven Katz, MD[1], Prajna Guha, PhD[2], John Hardaway, MD, PhD[2], Ethan Prince, MD[3], Ashley Moody, BSN, RN[2], Jill Slansky, PhD[4], Kimberly Jordan, PhD[4], Richard Schulick, MD, FACS[4], Robert Knight, MD[5], Jerry Zeldis, MD, PhD[5], Vincent Armenio, MD[1], N. Joseph Espat, MD, FACS[1], Richard Junghans, PhD, MD[6]

[1]*Roger Williams Medical Center, Boston University, Providence, RI, USA*
[2]*Roger Williams Medical Center, Providence, RI, USA*
[3]*Roger Williams Medical Center, Warren Alpert Medical School of Brown University, Providence, RI, USA*
[4]*University of Colorado, Aurora, CO, USA*
[5]*Sorrento Therapeutics, Inc., San Diego, CA, USA*
[6]*Immunotherapy Consultations, Boston, MA, USA*

Background

Prior Hepatic Immunotherapy for Metastases (HITM) phase I/Ib studies demonstrated the safety and biologic activity of anti-CEA CAR-T cell hepatic artery infusions (HAI) for CEA+ liver metastases (LM). Here we report preliminary HITM-SURE data using Pressure-Enabled Drug Delivery (PEDD) technology for HAI to overcome high intra-tumoral pressures.

Methods

Candidates had unresectable CEA+ LM and failed ≥ 1 line of systemic chemotherapy. Enrolled patients received 3 HAI of 10^10 second generation (IgCD28TCR) anti-CEA CAR-T cells (Sorrento Therapeutics) via a PEDD (Surefire Medical) device and low dose IL-2 (50,000 IU/kg/day). Objectives were to evaluate the safety profile of CAR-T HAI with PEDD and to secondarily assess clinical response.

Results

At study conclusion, 4 male and 1 female pts completed treatment—mean age 56.3 yrs (38-64) with 1-2 lines of prior chemotherapy. There was an average of 7.4 LM with an average maximal diameter of 2.8 cm. Mean CAR expression was 68.1% and production time of 14.6 d. In vitro targeted cytotoxicity was 53.5%. Reduction in serum CEA was observed in all pts (avg decrease 15 ng/mL, range 3-39 ng/mL). Compared to previous HITM CAR-T HAI trials with a standard catheter, PEDD significantly increased the frequency of CAR-T 5.2-fold within LM, as detected by quantitative PCR (p=0.03). No Grade (G) 4 or 5 AEs related to CAR-T HAIs via PEDD were detected. G1/2/3 events were largely attributed to IL-2 infusion and were comparable to prior HITM studies. One pt experienced grade 3 colitis, which resolved with IL-2 dose reduction and had colon biopsies that were negative for CAR-T by PCR and immunofluorescence. Twelve-month follow-up imaging in one pt with stage IV pancreatic carcinoma revealed no evidence of LM on PET and his primary pancreatic tumor was stable. Serum and LM biopsies from this pt reveal increased expression of IFN-g and IL-6 in LM, with decreased expression of IL-17, PD-L1, IDO and GM-CSF. A second pt with stage IV pancreatic cancer had no evidence of LM on PET at 6 weeks following CAR-T infusions. Average overall survival post-treatment is 8.3 mo (2.3-16.3) with 4 pts alive at the time of data evaluation.

Conclusions
Early results from the HITM-SURE study indicate that HAI of CAR-T using PEDD is well tolerated and results in encouraging activity against CEA+ LM. The median OS compares favorably with prior HITM studies and presently approved second/third line regimens. Final results will inform design and device choice for larger studies.

Trial Registration
NCT02850536

Ethics Approval
The study was approved by the Roger Williams Medical Center institutional review board, approval number 16-350-74.

P319

PD-1 Blockade with pembrolizumab during concurrent chemoradiation for locally advanced non-small cell lung cancer

Salma Jabbour, MD[1], Abigail Berman[2], Roy Decker, MD PhD[3], Andrew Zloza[1], Steven Feigenberg[2], Scott Gettinger, MD[3], Charu Aggarwal, MD MPH[2], Corey Langer, MD[2], Charles Simone, MD[4], Jeffrey Bradley[5], Yong Lin[1], Jyoti Malhotra, MD[1]

[1]Rutgers Cancer Institute of New Jersey, New Brunswick, NJ, USA
[2]University of Pennsylvania, Philadelphia, PA, USA
[3]Yale University, New Haven, CT, USA
[4]University of Maryland, Baltimroe, MD, USA
[5]Washington University, St. Louis, MO, USA
[6]Rutgers Cancer Institute, New Brunswick, NJ, USA

Background
Despite the curative potential of chemoradiation therapy (CRT) for inoperable, locally advanced non-small cell lung cancer (LA-NSCLC), the historical 2-year overall survival rate is only 55-60%. A recent trial showed that Programmed Death Ligand 1 (PD-L1) blockade in Stage III NSCLC improves progression-free survival when used as consolidation after CRT. Limited data exist about incorporation of PD-L1 inhibition during CRT. We sought to assess the safety and toxicity of PD-1 inhibition using pembrolizumab during CRT for LA-NSCLC.

Methods
In this multi-center Phase I clinical trial using a 3+3 trial design, for Stage III NSCLC, we evaluated the timing and dosing of pembrolizumab with concurrent chemotherapy (carboplatin + paclitaxel weekly) and RT (60 Gy in 2 Gy/day). In Regimen 1, we started pembrolizumab at full dose (200 mg IV Q3weeks) 56-84 days after the first day of CRT (2-6 weeks after CRT end). In Regimen 2: we gave pembrolizumab at reduced dose (100 mg IV Q3weeks) throughout the full course of treatment starting on Day 28 of CRT. In Regimen 3: we gave pembrolizumab at full dose starting on Day 28 of CRT. In Regimen 4: we gave pembrolizumab at reduced dose starting on Day 0. In Regimen 5: we gave pembrolizumab at full dose starting on Day 0. In all regimens, we continued pembrolizumab for up to 18 doses and delivered pembrolizumab as monotherapy after CRT. Dose Limiting Toxicity (DLT) was defined as Grade ≥4 Pneumonitis.

Results
We enrolled 19 subjects from 8/2016-7/2018, and 15 received pembrolizumab on Regimens 1-5. In Regimen 1, the DLT assessment period could last up to 15 weeks from the Day 0 of CRT. Median age was 71 years (range 53-84 years). We observed no DLT upon completion of Regimen 5 or in any of the cohorts. Therefore, we recommended the dose for further study as CRT + pembrolizumab 200 mg IV on the first day of CRT. Treatment-related adverse events (AE) included: Grade 2 nephritis (n=1, Regimen 1); Grade 3 pneumonitis (n=1, Regimen 2; 7 months after CRT); Grade 3 hyperglycemia (n=1, Regimen 5). We continue for an enrollment of an

additional 6 patients on Regimen 5.

Conclusions
In evaluating pembrolizumab during CRT for LA-NSCLC, we did not observe any DLT of Grade ≥4 Pneumonitis. We plan to perform additional correlative testing including, baseline PD-L1 status and CD8+ T cell vs CD4+FoxP3+ T cell infiltration during therapy.

Trial Registration
NCT02621398

Ethics Approval
The study was approved by the Rutgers Institutional Review Board, approval number Pro20150002247.

Consent
Written informed consent was obtained from the patient for publication of this abstract and any accompanying images. A copy of the written consent is available for review by the Editor of this journal

P320

A phase 1/1b study to evaluate the safety and tolerability of AB928, a novel dual adenosine receptor antagonist, in combination with chemotherapy in patients with breast or gynecologic malignancies

Paul de Souza, MBBS, MPH, PHD, FRACP[1], Chee Khoon Lee[2], Katrin Sjoquist[2], Shu Pan[3], Amanda Idan[3], Aimee Rieger, BS[4], Wade Berry, BA[4], Lixia Jin[4], Lisa Seitz, MSc[4], Devika Ashok, PhD[4], Matthew Walters, PhD[4], Dana Piovesan, MSc[4], Joanne Tan, PhD[4], Susan Lee, PhD[4], Adam Park, BS[4], Daniel DiRenzo, PhD[4], Joyson Karakunnel, MD, MSc[4]

[1]University of Western Sydney, Sydney, Australia
[2]St George Public Hospital, Kogarah, Australia
[3]St George Private Hospital, Kogarah, Australia
[4]Arcus Biosciences, Inc., Hayward, CA, USA

Background
In many tumors, extracellular adenosine contributes to an immunosuppressed tumor microenvironment via activation of the A2a receptor (A2aR) and A2b receptor (A2bR) expressed on intratumoral immune cells. AB928 is a novel, selective, small molecule antagonist of both A2aR and A2bR with the ability to potently block the immunosuppressive effects of high concentrations of adenosine in the tumor microenvironment. AB928 differs from other known A2aR antagonists based on its dual mode of action, its minimal loss of potency due to nonspecific binding to plasma proteins, and its lack of penetrance through a healthy blood-brain barrier. Preclinically, combining adenosine receptor inhibition with either chemotherapy or anti-programmed cell death-1 resulted in greater tumor control in mouse models, suggesting that AB928 may have synergistic activity when paired with either chemotherapy or checkpoint inhibitors in oncology patients. A phase 1 study with AB928 in healthy volunteers has been completed.

Methods
A phase 1/1b, open-label, dose-escalation (3+3 design) study is evaluating the safety/tolerability (including dose-limiting toxicities), pharmacokinetics, pharmacodynamics, and clinical activity of AB928 in combination with pegylated liposomal doxorubicin (PLD) in patients with breast or gynecologic malignancies. Patients are eligible if they have pathologically confirmed triple-negative breast cancer or ovarian cancer that is metastatic, advanced or recurrent with progression for which no alternative or curative therapy exists. Patients may have received up to 5 lines of prior therapies for advanced/recurrent and progressive disease (unlimited number of hormonal therapies permitted). AB928 is administered orally once daily at a starting dose of 75 mg (Cohort 1) escalating to 150 mg (Cohort 2) and 200 mg (Cohort 3), and PLD is administered at the standard regimen of 40 mg/m2 intravenously every 4 weeks. Intermediate AB928

doses may be evaluated based on data from cohorts that have been explored. Doses that have exceeded the maximum tolerated dose will not be evaluated. Following identification of the recommended phase 2 dose of AB928 and PLD during dose escalation, each tumor cohort (triple-negative breast and ovarian cancer) may be expanded to further evaluate the combination. The primary endpoint is safety/tolerability, and secondary endpoints are pharmacokinetics, pharmacodynamics (receptor occupancy in peripheral blood and immunomodulatory activity in select immune subsets), and clinical activity (objective response rate, duration of response, disease control rate [complete response, partial response, or stable disease for >6 months], and progression-free survival per Response Evaluation Criteria in Solid Tumors v1.1, and overall survival). The study is recruiting.

Ethics Approval

This study was approved by Bellberry Human Research Ethics committee (HREC), 129 Glen Osmond Road Eastwood South Australia 5063; Institutional Review Board; approval number 2018-04-306.

P321

A phase 1/1b study to evaluate the safety and tolerability of AB928, a novel dual adenosine receptor antagonist, in combination with chemotherapy in patients with gastrointestinal malignancies

Paul de Souza, MBBS, MPH, PHD, FRACP[1], Chee Khoon Lee[2], Katrin Sjoquist[2], Shu Pan[3], Amanda Idan[3], Aimee Rieger, BS[4], Wade Berry, BA[4], Lixia Jin[4], Lisa Seitz, MSc[4], Devika Ashok, PhD[4], Matthew Walters, PhD[4], Dana Piovesan, MSc[4], Joanne Tan, PhD[4], Susan Lee, PhD[4], Adam Park, BS[4], Daniel DiRenzo, PhD[4], Joyson Karakunnel, MD, MSc[4]

[1]University of Western Sydney, Sydney, Australia
[2]St George Public Hospital, Kogarah, Australia
[3]St George Private Hospital, Kogarah, Australia
[4]Arcus Biosciences, Inc., Hayward, CA, USA

Background

In many tumors, extracellular adenosine contributes to an immunosuppressed tumor microenvironment via activation of the A2a receptor (A2aR) and A2b receptor (A2bR) expressed on intratumoral immune cells. AB928 is a small molecule A2aR and A2bR antagonist with the ability to potently block the immunosuppressive effects of high adenosine concentrations in the tumor microenvironment. Preclinically, combining adenosine receptor inhibition with either chemotherapy or anti-programmed cell death-1 resulted in greater tumor control in mouse models, suggesting AB928 may have synergistic activity when paired with either chemotherapy or checkpoint inhibitors in oncology patients. A phase 1 study with AB928 in healthy volunteers has been completed.

Methods

A phase 1/1b, open-label, dose-escalation (3+3 design) study is evaluating the safety/tolerability, pharmacokinetics, pharmacodynamics, and clinical activity of AB928 in combination with mFOLFOX in patients with gastrointestinal malignancies. Patients are eligible if they have histologically confirmed gastroesophageal or colorectal cancer that is metastatic or locally advanced and unresectable for which no alternative or curative therapy exists, or standard therapy is not considered appropriate by the participant and treating physician. Patients must have received ≤5 lines of prior therapies and must not have received prior oxaliplatin treatment, except those who have received prior oxaliplatin-based therapy as the most recent regimen in the adjuvant setting if completed ≥6 months prior to enrollment. AB928 is administered orally once daily at a starting dose of 75 mg (Cohort 1) escalating to 150 mg (Cohort 2) and 200 mg (Cohort 3), and mFOLFOX is administered at the standard regimen (oxaliplatin 85 mg/m2 intravenously [IV] every 2 weeks, leucovorin

400 mg/m2 IV every 2 weeks, and 5-fluorouracil 400 mg/m2 IV bolus + 2400 mg/m2 [continuous 46-hour infusions on Days 1 and 2]). Intermediate AB928 doses may be evaluated based on data from cohorts that have been explored. Doses that have exceeded the maximum tolerated dose will not be evaluated. Following identification of the recommended phase 2 dose of AB928 and mFOLFOX during dose escalation, each tumor cohort (gastroesophageal and colorectal cancer) may be expanded to further evaluate the combination. The primary endpoint is safety/tolerability and secondary endpoints are pharmacokinetics, pharmacodynamics (receptor occupancy in peripheral blood and immunomodulatory activity in select immune subsets), and clinical activity (objective response rate, duration of response, disease control rate [complete response, partial response, or stable disease for >6 months], progression-free survival per Response Evaluation Criteria in Solid Tumors v1.1, and overall survival). The study is recruiting.

Ethics Approval

This study was approved by Bellberry Human Research Ethics committee (HREC), 129 Glen Osmond Road Eastwood South Australia 5063; Institutional Review Board; approval number 2018-04-307.

P322

A phase 1/1b study to evaluate the safety and tolerability of AB928, a novel dual adenosine receptor antagonist, in combination with carboplatin/pemetrexed and pembrolizumab in lung cancer patients

Paul de Souza, MBBS, MPH, PHD, FRACP[1], Chee Khoon Lee[2], Katrin Sjoquist[2], Shu Pan[3], Amanda Idan[3], Aimee Rieger, BS[4], Wade Berry, BA[4], Lixia Jin[4], Lisa Seitz, MSc[4], Devika Ashok, PhD[4], Matthew Walters, PhD[4], Dana Piovesan, MSc[4], Joanne Tan, PhD[4], Susan Lee, PhD[4], Adam Park, BS[4], Daniel DiRenzo, PhD[4], Joyson Karakunnel, MD, MSc[4]

[1]*University of Western Sydney, Sydney, Australia*
[2]*St George Public Hospital, Kogarah, Australia*
[3]*St George Private Hospital, Kogarah, Australia*
[4]*Arcus Biosciences, Inc., Hayward, CA, USA*

Background

In many tumors, extracellular adenosine contributes to an immunosuppressed tumor microenvironment via activation of the A2a receptor (A2aR) and A2b receptor (A2bR) expressed on intratumoral immune cells. AB928 is a novel, selective, small molecule antagonist of both A2aR and A2bR with the ability to potently block the immunosuppressive effects of high concentrations of adenosine in the tumor microenvironment. Preclinically, combining adenosine receptor inhibition with either chemotherapy or anti-programmed cell death-1 has resulted in greater tumor control in mouse models, suggesting that AB928 may have synergistic activity when paired with either chemotherapy or checkpoint inhibitors in oncology patients. A phase 1 study with AB928 in healthy volunteers has been completed.

Methods

A phase 1/1b, open-label, dose-escalation (3+3 design) and dose-expansion study was designed to evaluate the safety/tolerability (including dose-limiting toxicities), pharmacokinetics, pharmacodynamics, and clinical activity of AB928 in combination with standard-of-care carboplatin/pemetrexed plus pembrolizumab [1] in patients with nonsquamous non small-cell lung cancer (NSCLC). Patients are eligible if they have pathologically confirmed nonsquamous NSCLC that is metastatic or recurrent with progression. Patients may have received up to 5 lines of prior therapies in dose escalation and up to 3 lines of prior therapies in dose expansion. AB928 is administered orally once daily at a starting dose of 75 mg (Cohort 1) escalating to 150 mg (Cohort 2) and 200 mg (Cohort 3), and

carboplatin/pemetrexed plus pembrolizumab is administered at the standard regimen (carboplatin: AUC 5 mg/mL/min intravenously [IV] every 3 weeks [Q3W]; pemetrexed: 500 mg/m2 IV Q3W; pembrolizumab 200 mg IV Q3W). Intermediate AB928 doses may be evaluated based on data from cohorts that have been explored. Doses that have exceeded the maximum tolerated dose will not be evaluated. Following identification of the recommended phase 2 dose of AB928 in combination with carboplatin/pemetrexed plus pembrolizumab during dose escalation, the lung cancer cohort will be expanded to further evaluate this combination. The combination of AB928 and carboplatin/pemetrexed without pembrolizumab may also be evaluated in dose expansion. The primary endpoint is safety/tolerability and secondary endpoints are pharmacokinetics, pharmacodynamics (receptor occupancy in peripheral blood and immunomodulatory activity in select immune subsets), and clinical activity (objective response rate, duration of response, disease control rate [complete response, partial response, or stable disease for >6 months], and progression-free survival per Response Evaluation Criteria in Solid Tumors v1.1, and overall survival). FDA submission completed with start-up for recruitment ongoing.

References

1. Gandhi L, Rodriguez-Abreu D, Gadgeel S, et al. Pembrolizumab plus chemotherapy in metastatic non-small-cell lung cancer. N Engl J Med. 2018;378:2078-2092.

P323

A phase 1 study to evaluate the safety and tolerability of AB928, a novel dual adenosine receptor antagonist, with AB122, a programmed cell death-1 inhibitor, in patients with advanced malignancies

Lisa Seitz, MSc[1], Aimee Rieger, BS[1], Wade Berry, BA[1], Lixia Jin[1], Devika Ashok, PhD[1], Matthew Walters, PhD[1], Dana Piovesan, MSc[1], Joanne Tan, PhD[1], Susan Lee, PhD[1], Adam Park, BS[1], Daniel DiRenzo, PhD[1], Joyson Karakunnel, MD, MSc[1]

[1]*Arcus Biosciences, Inc., Hayward, CA, USA*

Background

In many tumors, extracellular adenosine contributes to an immunosuppressed tumor microenvironment via activation of the A2a receptor (A2aR) and A2b receptor (A2bR) expressed on intratumoral immune cells. AB928 is a novel, selective, small molecule antagonist of both A2aR and A2bR with the ability to potently block the immunosuppressive effects of high concentrations of adenosine in the tumor microenvironment. Preclinically, combining adenosine receptor inhibition with either chemotherapy or anti-programmed cell death-1 resulted in greater tumor control in mouse models, suggesting that AB928 may have synergistic activity when paired with either chemotherapy or checkpoint inhibitors in oncology patients. A phase 1 study with AB928 in healthy volunteers has been completed. AB122 is a fully human monoclonal antibody targeting PD-1.

Methods

A phase 1, open-label, dose-escalation (3+3 design) study is evaluating the safety/tolerability (including dose-limiting toxicities), pharmacokinetics, pharmacodynamics, and clinical activity of AB928 in combination with AB122 in patients with advanced malignancies. Patients are eligible if they have pathologically confirmed non-small cell lung cancer, squamous cell carcinoma of the head and neck, renal cell carcinoma, breast cancer, colorectal cancer, melanoma, bladder cancer, ovarian cancer, endometrial cancer, Merkel cell carcinoma, or gastroesophageal cancer that is metastatic, advanced or recurrent with progression for which no alternative or curative therapy exists. Patients must have received standard of care, and may have

received up to 5 lines of prior therapies. AB928 is administered orally once daily at a starting dose of 75 mg (Cohort 1) escalating to 150 mg (Cohort 2) and 200 mg (Cohort 3), and AB122 is administered intravenously every 2 weeks at 240 mg. Intermediate AB928 doses may be evaluated based on data from cohorts that have been explored; however, doses must not exceed the maximum tolerated dose. Following identification of the recommended phase 2 dose of AB928 and AB122 during dose escalation, select tumor cohorts may be expanded to further evaluate this combination. The primary endpoint is safety/tolerability and secondary endpoints are pharmacokinetics, pharmacodynamics (receptor occupancy in peripheral blood and immunomodulatory activity in select immune subsets), immunogenicity, and clinical activity (objective response rate, duration of response, disease control rate [complete response, partial response, or stable disease for >6 months], and progression-free survival per Response Evaluation Criteria in Solid Tumors v1.1, and overall survival). This study is recruiting.

Ethics Approval

This study was approved by Bellberry Human Research Ethics committee (HREC), 129 Glen Osmond Road Eastwood South Australia 5063; Institutional Review Board approval number 2018-05-360.

P324

A phase II clinical trial of Ipilimumab/Nivolumab combination immunotherapy in patients with rare upper gastrointestinal, neuroendocrine and gynaecological malignancies

Oliver Klein[1,4], Kee Damien[2], Ben Markman[3], Rachael Chang Lee, FRACP[4], Siddharth Menon[3], Jodie Palmer, BA/BSc, PhD, Grad Dip Law (IP)[5], Andreas Behren, PhD[5], Jonathan Cebon, MD, PhD[4]

[1]Medical Oncology, Austin Health, Heidelberg, Australia
[2]Peter MacCallum Cancer Centre, Melbourne, Australia
[3]Monash Medical Centre, Melbourne, VIC, Australia
[4]Olivia Newton John Cancer Centre, Melbourne, Australia
[5]Olivia Newton John Cancer Research Insti, Heidelberg, Australia

Background

Ipilimumab/Nivolumab combination treatment is so far the most efficacious immunotherapy regimen. It has demonstrated significant clinical activity in patients with metastatic melanoma, renal cell carcinoma, microsatellite instable colorectal cancer and non-small cell lung cancer and response rates are higher compared to single agent anti-PD-1 therapy. Patients with rare cancers represent an unmet medical need and have an inferior overall survival compared to patients with more common malignancies. No therapies including immunotherapies have systematically been investigated in this patient population. This trial investigates the efficacy of Ipilimumab/Nivolumab immunotherapy in patients with rare cancers and aims to identify tumour type agnostic biomarkers that can predict for response.

Methods

60 patients with advanced rare upper gastrointestinal, neuroendocrine and gynaecological malignancies and an ECOG performance status of 0 or 1 were included in the trial. All patients received nivolumab 3mg/kg and ipilimumab 1mg/kg every 3 weeks for four doses, followed by nivolumab 3mg/kg every 2 weeks. Treatment continued for 96 weeks, until disease progression or the development of unacceptable toxicity. The primary endpoint is clinical benefit rate (overall response rate and stable disease at week 12) with overall survival for each tumour type being a descriptive endpoint. Acquisition of tumour tissue prior to study

enrolment was mandatory and a panel of genomic assays and immuno- histochemistry- and - fluorescence are used to identify tumour type agnostic biomarkers

Background
Ipilimumab/Nivolumab combination treatment is so far the most efficacious immunotherapy regimen. It has demonstrated significant clinical activity in patients with metastatic melanoma, renal cell carcinoma, microsatellite instable colorectal cancer and non-small cell lung cancer and response rates are higher compared to single agent anti-PD-1 therapy. Patients with rare cancers represent an unmet medical need and have an inferior overall survival compared to patients with more common malignancies. No therapies including immunotherapies have systematically been investigated in this patient population.

Methods
60 patients with advanced rare upper gastrointestinal, neuroendocrine and gynaecological malignancies and an ECOG performance status of 0 or 1 were included. All patients received nivolumab 3mg/kg and ipilimumab 1mg/kg every 3 weeks for four doses, followed by nivolumab 3mg/kg every 2 weeks. Treatment continued for 96 weeks, until disease progression or the development of unacceptable toxicity. The primary endpoint is clinical benefit rate (overall response rate and stable disease at week 12) with overall survival for each tumour type being a descriptive endpoint. Acquisition of tumour tissue prior to study enrolment was mandatory and a panel of genomic assays and immuno-histochemistry and - fluorescence are used to identify tumour type agnostic biomarkers.

Results
As per 31 July 2018 43 patients have been enrolled and an updated efficacy and safety analysis will be presented at the meeting. So far 23 patients have undergone their first restaging at week 12. The objective response rate for the evaluable patient population is 43 % with responses being seen in a wide range of malignancies including biliary tract cancers, adrenocortical carcinoma, atypical bronchial carcinoid and rare gynaecological cancers as uterine clear cell carcinoma. Grade 3/4 immune related adverse events were detected in 19% of patients.

Conclusions
Our preliminary data demonstrate that Ipilimumab/Nivolumab combination treatment has considerable efficacy in a wide range of advanced rare malignancies for which treatments are very limited or no standard treatments are available. The rate of high grade immune related toxicity is in keeping with the experience in previously reported clinical trials using the same dosing regimen. Biomarker studies are ongoing to identify tumour agnostic markers of response.

P325

A phase 1 dose escalation study of TSR-033, an anti-LAG3 monoclonal antibody, in patients with advanced solid tumors

Kelly Stratton, MD[1], Aurélien Marabelle, MD PhD[2], Geoffrey Shapiro, MD, PhD[3], Jong Chul Park, MD[4], Solmaz Sahebjam, MD[5], Srimoyee Ghosh, PhD[6], Jian Chen[6], Taylor Eves[6], Ying Wang[6], Amita Patnaik, MD FRCP(C)[7]

[1]College of Medicine, The University of Oklahoma, Oklahoma City, OK, USA
[2]Gustave Roussy, Villejuif Cedex, France
[3]Dana-Farber Cancer Institute, Boston, MA, USA
[4]Massachusetts General Hospital, Boston, MA, USA
[5]Moffitt Cancer Center & Research Institute, University of South Florida, Tampa, FL, USA
[6]TESARO, Inc., Waltham, MA, USA
[7]South Texas Accelerated Research Therapeutics, San Antonio, TX, USA

Background
Lymphocyte activation gene 3 (LAG3) is an immune checkpoint receptor found on effector and regulatory T cells that controls T cell response, activation, and growth. Progressive expression of immune checkpoint receptors, including LAG3, contributes to T cell exhaustion and compromises antitumor immune response. LAG3 is frequently co-expressed with PD-1 on tumor-infiltrating T cells across a variety of tumor types and has been shown to interact with major histocompatibility complex (MHC) class II, on antigen-presenting cells, to attenuate T cell activation.TSR-033 is an investigational, humanized, anti-LAG3 monoclonal antibody that blocks the interaction of the LAG3 receptor with MHC class II. LAG3 blockade with TSR-033 in combination with anti-PD-1 therapy (TSR-042) boosts immune function and elicits antitumor immunity in preclinical models. Clinical data demonstrate that combined anti-PD-1 and anti-LAG3 checkpoint blockade leads to increased antitumor activity compared with anti-PD-1 alone in patients who have progressed on anti-PD-1 therapy.

Methods
TSR-033 is being investigated in a multicenter, open-label, first-in-human phase 1 trial enrolling patients with advanced or metastatic solid tumors who have progressed after, or are intolerant to, available or approved therapies. The primary objective of the current part of this study is to evaluate the safety and tolerability of TSR-033 as a monotherapy. Patients received IV infusion of TSR-033 monotherapy every 14 days in 4 escalating dose levels.

Results
As of July 13, 2018, 26 patients have been treated with monotherapy: 3 patients at 20 mg, 10 patients at 80 mg, 8 patients at 240 mg, and 5 patients at 720 mg. Adverse events that occurred in >15% of patients were arthralgia (5 patients, 19%), back pain (5 patients, 19%), decreased appetite (5 patients, 19%), and nausea (5 patients, 19%). No adverse events of grade 3 or higher were considered related to study drug. Adverse events occurring in >5% of patients and considered to be immune related were arthralgia (2 patients, 8%). One dose-limiting toxicity (grade 1; myasthenia gravis) occurred with TSR-033 monotherapy at 80 mg. Exposure increased in a dose proportional manner and importantly, receptor occupancy on peripheral T cells increased as the exposure increased, confirming target engagement in the periphery.

Conclusions
TSR-033 monotherapy was well tolerated across multiple dose levels. Adverse events were manageable and consistent with the safety profiles of other immune checkpoint inhibitors. Dose escalation of TSR-033 in combination with TSR-042 (anti-PD-1) is ongoing.

Trial Registration
clinicaltrials.gov NCT03250832

P326

GARNET: Preliminary safety, efficacy, pharmacokinetic, and biomarker characterization from a phase 1 clinical trial of TSR-042 (anti-PD-1 monoclonal antibody) in patients with recurrent/advanced NSCLC

Desamparados Roda Perez, PhD, MD[1], Janakiraman Subramanian[2], Joanna Pikiel[3], Maria-Pilar Barretina-Ginesta[4], José Trigo, MD[5], Wei Guo[6], Sharon Lu[6], David Jenkins, PhD[6], Kai Yu Jen[6], Hadi Danaee[6], Steven Dunlap[6], Ellie Im[6], Victor Moreno, PhD, MD[7]

[1]University Hospital, Valencia, Spain
[2]Saint Luke's Cancer Institute, Kansas City, USA
[3]Regional Center of Oncology, Gdansk, Poland
[4]Institut Català d'Oncologia, Hospital Universitari Dr. J. Trueta, Girona, Spain
[5]Hospital Universitario Virgen de la Victoria, Málaga,

Spain
[6]TESARO, Inc., Waltham, USA
[7]START Madrid-FJD, Hospital Fundación Jiménez Díaz, Madrid, Spain

Background
TSR-042 is a humanized monoclonal antibody targeting programmed death (PD)-1 receptor, effectively blocking interaction with its ligands PD-L1 and PD-L2. TSR-042 is being evaluated in patients with advanced solid tumors in the ongoing phase 1 GARNET trial (NCT02715284). Weight-based dose escalation (part 1) and fixed-dose safety studies (part 2A) have been completed. We present safety/efficacy data from the non-small cell lung cancer (NSCLC) cohort at the recommended phase 2 dose (RP2D).

Methods
NSCLC patients with previously treated recurrent/advanced disease were enrolled. Patients received the RP2D of TSR-042: 500 mg Q3W for cycles 1-4 and 1000 mg Q6W thereafter. Serum was collected for pharmacokinetic (PK) analysis. Antitumor activity was assessed with immune-related Response Evaluation Criteria in Solid Tumors (irRECIST). Tumor PD-L1 expression was measured and PD-L1 tumor proportion scores (TPS) were categorized as <1%, 1-49%, and ≥50%.

Results
A total of 35 patients were enrolled. The median number of prior lines of therapy for metastatic disease was 1. Among these patients, 34 (97%) experienced ≥1 treatment-emergent adverse event (AE), 11 (31%) had grade ≥3 AEs, and 1 (3%) experienced a grade ≥3 drug-related AE (fatigue). The most common AEs were fatigue/asthenia (31%), nausea (29%), and diarrhea (20%). Two patients (6%) had drug-related immune-related AEs of hypothyroidism and hyperthyroidism, respectively. No cases of drug-related pneumonitis were observed. PD-L1 TPS results were available for 26 patients; of these only 1 patient (4%) had TPS ≥50%, 25 (96%) had TPS<50%, and 13 (50%) had TPS <1%. In the overall population of 35 patients there were 9 (26%) partial responses (confirmed and unconfirmed), and 11 patients (31%) had stable disease. Of the 9 patients who responded, treatment is ongoing for 7 patients. PK at RP2D was consistent with previous studies.

Conclusions
TSR-042 demonstrated robust clinical activity in previously treated recurrent/advanced NSCLC patients whose tumor PD-L1 status was predominantly TPS <50%, including in patients with TPS <1%. Both overall response rate and toxicity appear competitive with approved anti-PD-1 agents studied in the same setting.

Trial Registration
clinicaltrials.gov NCT02715284

P327

Higher dose single-agent intratumoral G100 (a TLR4 agonist) results in increased biomarker activity and improved clinical outcomes in patients with follicular lymphoma

Christopher Flowers, MD, MS[1], Carlos Panizo[2], Weiyun Ai, MD, PhD[3], Iris Isufi, MD[4], Alex Herrera, MD[5], Nancy Bartlett, MD[6], Craig Okada, MD, PhD[7], Bela Kis, MD, PhD[8], Luis de la Cruz Merino Sr.[9], Javier Briones[10], Jorge Chaves, MD[11], Elizabeth Cull[12], Locke Bryan, MD[13], Roch Houot, MD, PhD[14], Kim Linton, PhD[15], Ian Chau[16], Gottfried von Keudell[4], Hailing Lu, MD, PhD[17], Frank Hsu, MD[17], Ahmad Halwani, MD[18]

[1]Emory University, Atlanta, GA, USA
[2]Clinica Universidad de Navarra, Pamplona, Spain
[3]University of California San Francisco, San Francisco, CA, USA
[4]Yale University, New Haven, CT, USA

[5]*City of Hope, Duarte, CA, USA*
[6]*Washington University, St. Louis, MO, USA*
[7]*Oregon Health and Science University, OR, USA*
[8]*Moffitt Cancer Center, Tampa, FL, USA*
[9]*Hospital Universitario Virgen Macarena, Seville, Spain*
[10]*Hospital De La Santa Creu I San Pau, Barcelona, Spain*
[11]*Northwest Medical Specialties, Tacoma, WA, USA*
[12]*Greenville Health System Cancer Institute, Tocoma, WA, USA*
[13]*Georgia Cancer Center,Augusta University, Augusta, GA, USA*
[14]*Centre Hospitalier Universitaire Pontchaillou, Rennes, France*
[15]*The Christie NHS Foundation Trust & The University of Manchester, UK*
[16]*Royal Marsden Hospital, London, USA*
[17]*Immune Design, Seattle, WA, USA*
[18]*Huntsman Cancer Institute, Salt Lake City, UT, USA*

Background

G100 (G) is a toll-like receptor 4 (TLR4) agonist that activates the innate and adaptive immune system. This ongoing phase 1/2 study demonstrated that intratumoral (IT) G100 alone or with pembrolizumab (P) was safe, induced systemic clinical responses in follicular lymphoma (FL) patients (pts) including relapsed/refractory (R/R) disease. Compared to G alone, the addition of P resulted in a higher response rate, abscopal (untreated sites) tumor shrinkage and increased CD8 tumor infiltrating lymphocytes (TILs), which were associated with clinical responses. An association between baseline tumor TLR4 expression by immunohistochemistry (IHC) and clinical response was observed. We now present clinical and biomarker data for G100 alone at a higher 20µg dose (Part 3) and compare it to 10µg (Part 2).

Methods

14 (9 R/R) FL (Part 3) and 13 (7 R/R) FL (Part 2) pts were enrolled. Pts received 6-9 doses of IT G100 weekly to a site treated with low dose radiation (RT, 2Gy x2 doses). A 2nd course of G100 could be given without RT. Responses were evaluated by IrRC criteria. Blood samples and tumor biopsies from treated and/or abscopal sites were obtained pre- and post-G100 for TLR4 expression by IHC, lymphocyte markers and RNA expression.

Results

Median observation was 15mo vs 8mo for Part 2 vs Part 3. Best overall response rate (ORR) and 9mo ORR were 23% vs 29% and 15% vs 29% for 10 vs 20µg dose. Abscopal tumor shrinkage (≥10%) was 54% vs 79% (all pts) and 29% vs 78% (R/R pts) at 10µg vs 20µg dose. Among pts with baseline TLR4high (≥50%) tumor expression, ORR was 17% for 10µg (n=6) vs 57% vs for 20µg (n=7) dose. No Grade ≥3 adverse events were observed. At the 20µg dose, a trend toward higher CD8 TILs and greater reduction of CD20+ tumor cells was observed (p=0.03). Clinical response was associated with baseline TLR4high expression (p=0.002) as well as post-G100 increase in CD8 TILs (p=0.02), and a decrease in CD20+ tumor cells (p=0.03) (all pts). G100 significantly increased T- and NK-cell, and macrophage (CD163, CD68, FcgR2A, FcgR3A, IRF1, MRC1, MSR1, granzyme) gene expression ($p<0.05$) as analyzed by NanoString.

Conclusions

G100 20µg dose is safe and demonstrates an early trend toward better clinical responses. This dose induces greater changes in tumor biomarkers that are associated with clinical response (increase of TILs, decrease of CD20+ tumor cells) and supports further development of the 20µg dose of IT G100.

Trial Registration

NCT02501473

Ethics Approval

The study was approved by participating institutions' Ethics Board.

P328

Preoperative window of opportunity trial of nivolumab with or without tadalafil in patients with squamous cell carcinoma of the head and neck

Adam Luginbuhl, MD[1], Jennifer Johnson, MD[1], Larry Harshyne[1], Joseph Curry, MD[1], Rita Axelrod, MD[1], Ralph Zinner, MD[1], Benjamin Leiby, PhD[1], Madalina Tuluc, MD[1], Christopher Snyder[1], David Cognetti, MD[1], Ulrich Rodeck, MD PhD[1], Athanassios Argiris, MD PhD[1]

[1]*Thomas Jefferson Univesity, Philadelphia, PA, USA*

Background

Checkpoint modulation to augment or inhibit components of the immune system is of great interest to the clinical management of squamous cell carcinoma of the head and neck (SCCHN). PD-1 blockade using nivolumab has proven to be efficacious in the metastatic and recurrent disease setting, whereas efficacy in treatment naïve patients amenable to curative surgery is yet to be determined. Combining PD-1 blockade with other therapeutic modalities has emerged as a promising strategy in several malignancies. This window of opportunity trial is designed to test molecular and therapeutic effects of the combination of nivolumab with tadalafil. Tadalafil is a phosphodiesterase-5 inhibitor and has been found to augment tumor specific immunity in SCCHN patients. Both in mouse and human studies, tadalafil decreases myeloid-derived suppressor cells (MDSCs) associated with reduced arginase and iNOS expression and intratumoral Treg abundance. Conversely, tadalafil reportedly increases cytotoxic effector T cells (CD8+) within the tumor. The window of opportunity format allow us to relate treatment-associated changes in the tumor environment to therapeutic outcomes.

Methods

This is an investigator-initiated, multi-institutional window of opportunity randomized trial in patients with SCCHN, who are candidates for complete surgical resection. Patients are randomized 1:1 to receive nivolumab 240 mg intravenously every 2 weeks for 2 doses with or without oral tadalafil 10 mg once daily for 4 weeks. Surgery is performed at approximately 4 weeks from first nivolumab infusion. The primary endpoint is correlative analysis of immune cell polarization in peripheral blood and tumor specimens pre and post treatment. Secondary endpoints include additional immune profiles, exosomes, and tissue surgical wound healing and tumor response assessed by repeat imaging before surgery. The sample size is 25 patients per arm (50 total). Enrollment began in September 2017 and 25 patients have been enrolled over 10 months.

Acknowledgements

Sidney Kimmel Cancer Center at Thomas Jefferson UniversityBristol-Myers Squibb

Trial Registration

NCT03238365

Ethics Approval

The study was approved by Thomas Jefferson University Institutution's Ethics Board, approval number #17P.210

P329

Phase 3 KEYNOTE-716 study: Adjuvant therapy with pembrolizumab versus placebo in resected high-risk stage II melanoma

Jason Luke, MD, FACP[1], Paolo Ascierto, MD[2], Matteo Carlino, MBBS, PhD, BMedSC, F[3], Alexander Eggermont[4], Jean-Jacques Grob, MD[5], Axel Hauschild[6], John Kirkwood, MD[7], Georgina Long, MBBS, PhD, BSc, FRAC[8], Peter Mohr[9], Caroline Robert[4], Jeffrey Gershenwald, MD[10], Andrew Poklepovic, MD[11], Merrick Ross, MD[10], Richard Scolyer[12], James Anderson[13], Sama Ahsan[13], Nageatte

Ibrahim, MD PhD[13], Vernon Sondak[14]

[1]*University of Chicago, Chicago, MA, USA*
[2]*Istituto Nazionale Tumori IRCCS "Fondazi, Napoli, Italy*
[3]*Westmead Hospital, Blacktown, Australia*
[4]*Gustave Roussy Cancer Centre, Villejuif, France*
[5]*Aix-Marseille Université, Marseille, France*
[6]*University Hospital Schleswig-Holstein, Kiel, Germany*
[7]*UPMC Hillman Cancer Center, Pittsburgh, PA, USA*
[8]*The University of Sydney, Sydney, Australia*
[9]*Elbe Kliniken Buxtehude, Germany*
[10]*MD Anderson Cancer Center, Houston, TX, USA*
[11]*VCU Massey Cancer Center, Richmond, VA, USA*
[12]*Royal Prince Alfred Hospital, Sydeney, Australia*
[13]*Merck & Co., Inc., Kenilworth, NJ, USA*
[14]*Moffit Cancer Center, Tampa, FL, USA*

Background

Adjuvant pembrolizumab showed significantly longer recurrence-free survival compared with placebo in resected stage III melanoma in the KEYNOTE-054 study [1]. KEYNOTE-716 (NCT03553836) is a randomized, placebo-controlled, multicenter phase 3 study of adjuvant pembrolizumab in patients with surgically resected high-risk stage II melanoma.

Methods

Patients must be ≥12 years of age and have newly diagnosed, completely resected stage IIB/IIC cutaneous melanoma, defined by the AJCC Cancer Staging Manual, 8th edition [2] (including negative sentinel lymph node biopsy and no evidence of distant metastasis). Patients cannot have mucosal or uveal melanoma or have received prior treatment for melanoma, including radiation, beyond resection of primary disease within 12 weeks of the start of study therapy. The study has a 2-part design. In the double-blind phase (part 1), patients will be randomly assigned 1:1 to receive pembrolizumab 200 mg for patients ≥18 years or 2 mg/kg for patients 12-17 years (maximum dose, 200 mg) or placebo every 3 weeks for 17 cycles. Stratification: 1 stratum for pediatric patients (12-17 years); 3 strata for adult patients per T stage (T3b/T4a/T4b). Study treatment will begin within 12 weeks of complete resection. Tumor imaging will be performed every 24 weeks while treatment is ongoing, at the end of treatment, every 6 months for the first 3 years off treatment, and then yearly for up to 2 years or until recurrence (up to 5 years of total imaging). Adverse events will be graded per NCI Common Terminology Criteria for Adverse Events, version 4.0. In the unblinded phase (part 2), patients with confirmed recurrence may be rechallenged (patients received pembrolizumab in part 1) or crossed over to pembrolizumab (patients received placebo in part 1). Resected local or distant recurrence or unresectable disease will be treated for an additional 17 or 35 cycles, respectively. Tumor imaging in part 2 will occur every 12 weeks while treatment is ongoing. The primary end point is recurrence-free survival; secondary end points are distant metastasis-free survival, overall survival, and safety. Approximately 954 patients will be enrolled.

Trial Registration

ClinicalTrials.gov identifier, NCT03553836

References

1. Eggermont AMM, et al. N Engl J Med. Adjuvant pembrolizumab versus placebo in resected stage III melanoma. 2018;378:1789-801.2. Amin MB et al., eds. AJCC Cancer Staging Manual, 8th edition. New York: Springer International Publishing; 2017.

Ethics Approval

The study was approved by the relevant Institutional Review Boards for each institution.

P330

Harnessing the power of lymphodepletion and checkpoint blockade: A Nivolumab/Ipilimumab-primed immunotransplant for relapsed/refractory diffuse large B cell lymphoma patients

Thomas Marron, MD PhD[1,2], Netonia Marshall, PhD[2], Dana Ostrowski, BA[2], Amir Steinberg, MD[2], Linda Hammerich, PhD[2], Sacha Gnjatic, PhD[2], Nina Bhardwaj, MD, PhD[2], Joshua Brody, MD[2], Thomas Marron, MD PhD[2]

[1]*Tisch Cancer Institute, The Mount Sinai Hospital, New York, NY, USA*
[2]*Icahn School of Medicine at Mount Sinai, New York, NY, USA*

Background

Patients with relapsed/refractory diffuse large B-cell lymphoma (DLBCL) have a poor prognosis, with only a quarter of patients achieving a CR following autologous stem cell transplant (ASCT)(1). Novel immunotherapies offer promise, however, checkpoint blockade achieves a very low complete response rate(2), and chimeric antigen receptor T cells (CAR-T) achieve durable complete remissions in fewer than a third of patients, often due to exhaustion or antigen loss(3,4). Cellular therapies like CAR-T utilize lymphodepleting chemotherapy to achieve rapid proliferation and anti-tumor activity of cytotoxic T cells infused after chemotherapy(5-7), and we have documented similar homeostatic proliferation of T cells following ASCT, however, these cells develop an exhausted phenotype. We therefore hypothesized that combined checkpoint blockade and lymphodepletion may result in synergistic clinical efficacy and provide the added benefit of a poly-clonal/multiantigen-specific T cell response. In the A20 lymphoma murine model we treated mice growing tumors with dual checkpoint blockade (DCBA, anti-PD-1 and anti-CTLA-4)—priming polyclonal anti-tumor T cells in vivo—and then transferred their cells into tumor bearing recipients following lymphodepletion(8). As in humans, following adoptive transfer into a lymphodepleted recipient CD8 T cells expand but also upregulate functional checkpoint receptors limiting their activity. The addition of DBCA before and after adoptive transfer into a lymphodepleted host—termed immunotransplant—increases anti-tumor response by increasing activation, cytokine production, and proliferation in a common gamma chain cytokine-dependent manner. Immunotransplant improved survival over either component given alone.

Methods

We have translated these murine findings into an immunotransplant trial in DLBCL patients with chemo-insensitive disease or disease relapsed following ASCT or CAR-T therapy. Patients will receive 2 cycles of DCBA (ipilimumab and nivolumab) given at three-week intervals, and subsequently undergo apheresis and cryopreservation of their PBMCs. Patients then receive lymphodepleting conditioning with fludarabine and cyclophosphamide, according to the dosing schedule used in the ZUMA-1 trial of KTE-C19 CAR-T cells[9]. Patients then are infused with their pre-chemotherapy cells, and upon count recovery patients will receive an additional two cycles of DCBA followed by maintenance nivolumab.The primary endpoint is clinical efficacy, defined as the proportion of patients who achieve complete response. Secondary endpoints include correlation of imaging with molecular remission (determined by blood IgVH), one and two-year overall survival and progression-free survival, overall response rate, as well as assessment for dynamic changes in the stool microbiome and correlates with outcome.

Results

This trial opened to accrual in May of 2018 (NCT0330544), enrollment is ongoing.

Trial Registration
NCT0330544

References
1. Vose JM, Zhang MJ, Rowlings PA, et al. Autologous transplantation for diffuse aggressive non-Hodgkin's lymphoma in patients never achieving remission: a report from the Autologous Blood and Marrow Transplant Registry. Journal of clinical oncology : official journal of the American Society of Clinical Oncology. 2001;19(2):406-413.
2. Lesokhin AM, Ansell SM, Armand P, et al. Nivolumab in Patients With Relapsed or Refractory Hematologic Malignancy: Preliminary Results of a Phase Ib Study. Journal of clinical oncology : official journal of the American Society of Clinical Oncology. 2016;34(23):2698-2704.
3. Schuster SJ, Bishop MR, Tam CS, et al. Primary analysis of Juliet: a global, pivotal, phase 2 trial of CTL019 in adult patients with relapsed or refractory diffuse large B-cell lymphoma. Am Soc Hematology; 2017.
4. Turtle CJ, Hay KA, Hanafi L-A, et al. Durable Molecular Remissions in Chronic Lymphocytic Leukemia Treated With CD19-Specific Chimeric Antigen Receptor–Modified T Cells After Failure of Ibrutinib. Journal of Clinical Oncology. 2017;35(26):3010-3020.
5. Dudley ME, Wunderlich JR, Robbins PF, et al. Cancer regression and autoimmunity in patients after clonal repopulation with antitumor lymphocytes. Science. 2002;298(5594):850-854.
6. Gattinoni L, Finkelstein SE, Klebanoff CA, et al. Removal of homeostatic cytokine sinks by lymphodepletion enhances the efficacy of adoptively transferred tumor-specific CD8+ T cells. J Exp Med. 2005;202(7):907-912.
7. Kochenderfer JN, Dudley ME, Kassim SH, et al. Chemotherapy-refractory diffuse large B-cell lymphoma and indolent B-cell malignancies can be effectively treated with autologous T cells expressing an anti-CD19 chimeric antigen receptor. Journal of clinical oncology : official journal of the American Society of Clinical Oncology. 2015;33(6):540-549.
8. Marshall N, Hammerich L, Upadhyay R, Marron TU, Brody J. Converting a tumor from checkpoint blockade-resistant to checkpoint blockade-sensitive: Immunotransplant for aggressive lymphoma. Journal of Clinical Oncology. 2016;34(15_suppl):e14538-e14538.
9. Locke FL, Neelapu SS, Bartlett NL, et al. CT019 - Primary results from ZUMA-1: a pivotal trial of axicabtagene ciloleucel (axicel; KTE-C19) in patients with refractory aggressive non-Hodgkin lymphoma (NHL) AACR; April 2, 2017, 2017; Washington D.C.

Ethics Approval
The protocol for this clinical trial has been approved by the Icahn School of Medicine Institutional Review Board (IRB, GCO#17-2164) and FDA. This trial is being performed under the supervision of the Mount Sinai IRB and in accordance with principles of the Declaration of Helsinki.

Figure 1. Trial Schematic

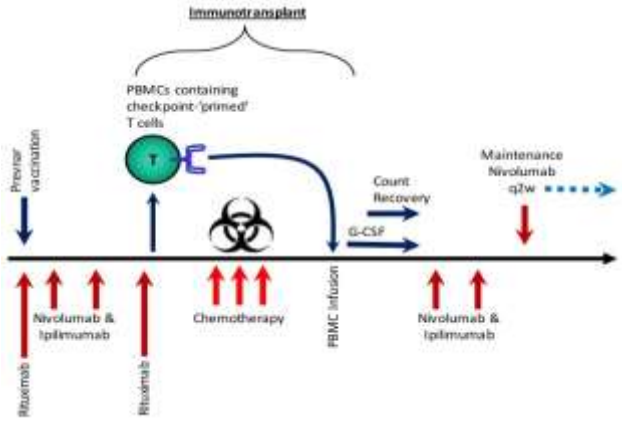

P331

A phase 1a clinical trial of NLG802, a prodrug of indoximod with enhanced pharmacokinetic properties

Olivier Rixe, MD, PhD[1], Thomas George, MD[2], Heloisa Soares[1], Agnieszka Marcinowicz[3], Nicholas Vahanian, MD[3], Charles Link, MD[3], Edouard Dupis[1], Eugene Kennedy, MD, FACS[3], Mario Mautino, PhD[3]

[1]*University of New Mexico, Albuquerque, NM, USA*
[2]*Univ of Florida Health Cancer Center, Gainesville, FL, USA*
[3]*NewLink Genetics, Ames, IA, USA*

Background
Indoximod contributes to enhanced antitumor immunity by relieving IDO-mediated immunosuppression by mechanisms that involve modulation of AhR signaling and mTOR activation, which leads to multiple immunomodulatory effects including a shift from suppressive Foxp3+ Treg toward Th17 helper T cells as well as the downregulation of IDO expression in DCs. Indoximod has demonstrated an excellent safety profile in human clinical trials at doses of up to 1200 mg bid. Increasing doses above this level generally does not result in increased plasma concentration or drug exposure due to limiting dose-dependent oral bioavailability. In order to improve bioavailability of indoximod we developed NLG802, a prodrug of indoximod that increases oral bioavailability of indoximod ~ 5-fold in non-human primates.

Methods
NLG802 is being evaluated in a standard 3+3 dose escalation Phase 1a study in patients with recurrent advanced solid malignancies. Doses being evaluated include 180, 360, 720, 1080 and 1440 mg bid. NLG802 is administered orally in repeating 28 day cycles until toxicity or disease progression. Endpoints include safety, toxicity, pharmacokinetics, and determination of an MTD or MBED.

Results
Single oral dosing of NLG802 at 180 mg (n=3) and 363 mg (n=4) resulted in indoximod Cmax of 7.2±2.7 µM and 11.8±1.6 µM and AUC(0-inf) 49±8 and 92±25 µMh, respectively. Multiple oral dosing of NLG802 at 180 mg bid (n=3) and 363 mg bid (n=4) resulted in indoximod Cmax of 6.5±2.8 µM and 18.5±3.1 µM and AUC(0-inf) 52±22 and 125±24 µMh, respectively. Among NLG802 treated patients the most common adverse events, regardless of attribution, are fatigue (50%), nausea (40%), and peripheral edema (40%). Serious adverse events include constipation, weakness, and esophagitis all attributed to underlying disease. The most common NLG802 related adverse events are fatigue (20%) and nausea (20%). No subjects have experienced a Grade 4/5 adverse event. No subjects discontinued therapy due to an adverse event.

Conclusions
Oral doses of NLG802, as compared to a molar equivalent oral dose of indoximod, produce an average increase of 4-fold in Cmax and AUC after a single dose and 5-6 fold increase in AUC and Cmax after continuous bid dosing. Additional data on other dose cohorts will be available at the time of the presentation.

Ethics Approval
The study was approved by Western Institutional Review Board (WIRB) on 28May2017, WIRB PRO NUM 2017011

P332

CheckMate 9TM: Phase 3 study of nivolumab + cisplatin + radiotherapy in cisplatin-eligible patients with intermediate- or high-risk locally advanced squamous cell carcinoma of the head & neck

Maura Gillison, MD, PhD[1], Vincent Gregoire, MD,

PhD[2], Makoto Tahara[3], Quynh Thu Le, MD[4], Wilfried Budach[5], Mark Lynch, PhD[6], Justin Kopit[6], Vijayvel Jayaprakash, MBBS, PhD[6], Peng Sun[6], Robert Ferris, MD, PhD[7]

[1]MD Anderson Cancer Center, Houston, TX, USA
[2]Centre Léon Bérard, Brussels, Belgium
[3]National Cancer Center, Kashiwa, Japan
[4]Stanford University, Stanford, CA, USA
[5]University of Düsseldorf, Düsseldorf, Germany
[6]Bristol-Myers Squibb, Wallingford, CT, USA
[7]University of Pittsburgh Cancer Institute, Pittsburgh, PA, USA

Background

Squamous cell carcinoma of the head and neck (SCCHN) is the most common pathological type of head and neck cancer [1]. Approximately 60% of patients present with locally advanced disease [2], for which cisplatin-based chemoradiotherapy is the standard of care [3]. However, for patients with intermediate- and high-risk SCCHN, outcomes remain poor [4]. In preclinical models, radiotherapy in combination with or preceded by administration of an immune checkpoint inhibitor enhances antitumor immune responses in addition to having a direct cytotoxic effect [5]. Nivolumab is an anti–PD-1 antibody that has shown improved survival in patients with recurrent/metastatic SCCHN post-platinum therapy [6]. CheckMate 9TM (NCT03349710) is an ongoing, randomized, double-blind, placebo-controlled, phase 3 trial investigating nivolumab-based treatment in intermediate- or high-risk locally advanced SCCHN. The study is enrolling patients in 2 cohorts: cisplatin-eligible and cisplatin-ineligible; here, we discuss the cisplatin-eligible cohort of the study.

Methods

The cisplatin-eligible cohort of CheckMate 9TM includes patients who are considered eligible for cisplatin-based chemoradiation due to having creatinine clearance ≥60 mL/min. Eligibility for enrollment in CheckMate 9TM includes: histologically confirmed SCCHN of the oral cavity, oropharynx, hypopharynx, or larynx with locally advanced disease that is unresectable or resectable but suitable for an organ-sparing approach, no prior radiotherapy or systemic treatment, and Eastern Cooperative Oncology Group status of 0-1. Patients eligible for inclusion in this trial could have tumors with either intermediate or high risk of recurrence based on baseline factors including human papillomavirus p16 status, tumor staging and smoking history. Approximately 580 patients will be enrolled and randomized 1:1 to treatment with either nivolumab plus cisplatin in combination with radiotherapy or corresponding placebo plus cisplatin in combination with radiotherapy (Figure 1). Treatment will continue until progression or completion of maintenance treatment. Primary endpoint: event-free survival. Secondary endpoints: duration of loco-regional control, overall survival, and proportion of patients without meaningful symptom deterioration at 24 weeks after treatment completion. Enrollment is ongoing in 11 countries with an estimated study completion date of November 2022.

Acknowledgements

The patients and families for making this trial possible; the contributions of the study teams from the various sites involved in the trial; the protocol manager for this study, Anne Delvaux; Bristol-Myers Squibb (Princeton, NJ) and ONO Pharmaceutical Company Ltd. (Osaka, Japan); the study was supported by Bristol-Myers Squibb; all authors contributed to and approved the submission; writing and editorial assistance was provided by Brooke Middlebrook, Evidence Scientific Solutions Inc., funded by Bristol-Myers Squibb.

Trial Registration

Clinicaltrials.govNCT03349710

References
1. Ferlay J, Soerjomataram I, Dikshit R, et al. Cancer incidence and mortality worldwide: sources, methods and major patterns in GLOBOCAN 2012. Int J Cancer. 2015;136:E359-386.
2. SEER Cancer Statistics Review (CSR) 1975-2014.
3. Georges P, Rajagopalan K, Leon C, et al. Chemotherapy advances in locally advanced head and neck cancer. World J Clin Oncol. 2014;5:966-972.
4. Szturz P, Vermorken JB. Treatment of elderly patients with squamous cell carcinoma of the head and neck. Front Oncol. 2016;6:199.
5. Teng F, Kong L, Meng X, Yang J, Yu J. Radiotherapy combined with immune checkpoint blockade immunotherapy: Achievements and challenges. Cancer Lett. 2015;365:23-29.
6. Ferris RL, Blumenschein G, Jr., Fayette J, et al. Nivolumab for recurrent squamous-cell carcinoma of the head and neck. N Engl J Med. 2016;375:1856-1867.

Ethics Approval
This study was approved by each institution's Review Board/Independent Ethics Committee.

Figure 1.

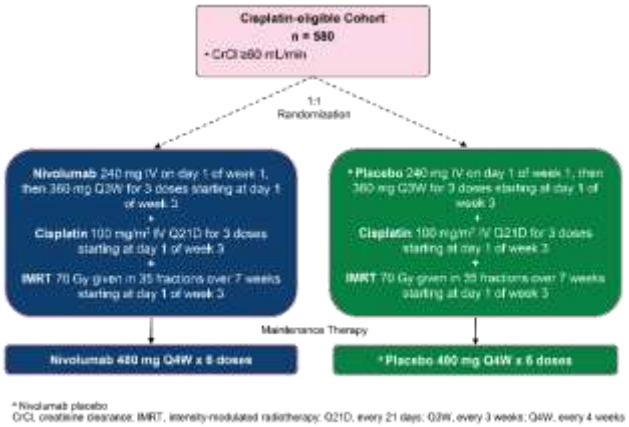

P333

CheckMate 9TM: Phase 3 study of nivolumab + radiotherapy (RT) vs cetuximab + RT in cisplatin-ineligible patients with intermediate-/high-risk locally advanced squamous cell carcinoma of the head/neck

Robert haddad, MD[1], Kevin Harrington, MD[2], Lisa Licitra, MD[3], Peter Brossart[4], Dennis Soulières[5], Loren Mell, MD[6], Laurence Toms[7], Justin Kopit[7], Mark Lynch, PhD[7], Vijayvel Jayaprakash, MBBS, PhD[7], Ezra Cohen, MD[8]

[1]*Dana-Farber Cancer Institute, BOSTON, MA, USA*
[2]*Royal Marsden NHS Foundation Trust/The Institute of Cancer Research, UK*
[3]*Fondazione IRCCS Istituto Nazionale dei Tumori and University of Milan, Milan, Italy*
[4]*University Hospital of Bonn, Bonn, Germany*
[5]*Centre Hospitalier de l'Université de Montréal, Montreal, Canada*
[6]*University of California San Diego School of Medicine, San Diego, CA, USA*
[7]*Bristol-Myers Squibb, Princeton, NJ, USA*
[8]*University of California San Diego, Moores Cancer Center, La Jolla, CA, USA*

Background
The standard of care for patients with locally advanced squamous cell carcinoma of the head and neck (SCCHN) is cisplatin-based radiotherapy [1]. Treatment options for patients ineligible to receive cisplatin due to advanced age or comorbidities [2] are limited to radiotherapy alone or in combination with cetuximab, and associated with modest efficacy or increased toxicity [3]. As the majority of patients with locally advanced SCCHN eventually develop recurrent/metastatic disease, there is an unmet need for better treatment options [4]. Nivolumab is an anti–PD-1 antibody that has shown improved survival and acceptable tolerability in patients with recurrent/metastatic SCCHN post-platinum therapy

[5]. CheckMate 9TM (NCT03349710) is an ongoing, randomized, double-blind, placebo-controlled, phase 3 trial investigating nivolumab-based treatment in intermediate- or high-risk locally advanced SCCHN. The study is enrolling patients in 2 cohorts: cisplatin-eligible and cisplatin-ineligible; here, we discuss the cisplatin-ineligible cohort of the study.

Methods

The cisplatin-ineligible cohort of CheckMate 9TM includes patients who are considered ineligible for cisplatin-based chemoradiation due to the presence of ≥1 of the following: age ≥70 years, creatinine clearance <60 and >30 mL/min, or severe hearing loss (minimal hearing threshold ≥80 dB in either ear). Eligibility for enrollment in CheckMate 9TM includes: histologically confirmed SCCHN of the oral cavity, oropharynx, hypopharynx, or larynx with locally advanced disease that is unresectable or resectable but suitable for an organ-sparing approach, no prior radiotherapy or systemic treatment, and Eastern Cooperative Oncology Group status of 0-1. Patients eligible for inclusion in this trial could have tumors with either intermediate or high risk of recurrence based on baseline factors including human papillomavirus p16 status, tumor staging and smoking history. Approximately 466 patients will be enrolled and randomized 1:1 to either nivolumab plus radiotherapy or cetuximab plus radiotherapy (Figure 1). Patients in each treatment arm will also be administered the corresponding placebo. Treatment will continue until progression or completion of maintenance treatment. Primary endpoint: event-free survival. Secondary endpoints: duration of loco-regional control, overall survival, and proportion of patients without meaningful symptom deterioration at 24 weeks after treatment completion. Enrollment is ongoing in 11 countries with an estimated study completion date of November 2022.

Acknowledgements

The patients and families for making this trial possible; the contributions of the study teams from the various sites involved in the trial; the protocol manager for this study, Anne Delvaux; Bristol-Myers Squibb (Princeton, NJ) and ONO Pharmaceutical Company Ltd. (Osaka, Japan); the study was supported by Bristol-Myers Squibb; all authors contributed to and approved the submission; writing and editorial assistance was provided by Brooke Middlebrook, Evidence Scientific Solutions Inc., funded by Bristol-Myers Squibb.

Trial Registration

Clinicaltrials.govNCT03349710

References

1. Georges P, Rajagopalan K, Leon C, et al. Chemotherapy advances in locally advanced head and neck cancer. World J Clin Oncol. 2014;5:966-972.
2. Ahn MJ, D'Cruz A, Vermorken JB, et al. Clinical recommendations for defining platinum unsuitable head and neck cancer patient populations on chemoradiotherapy: A literature review. Oral oncology. 2016;53:10-16.
3. Baxi SS, O'Neill C, Sherman EJ, et al. Trends in chemoradiation use in elderly patients with head and neck cancer: Changing treatment patterns with cetuximab. Head Neck. 2016;38 Suppl 1:E165-171.
4. Szturz P, Vermorken JB. Treatment of elderly patients with squamous cell carcinoma of the head and neck. Front Oncol. 2016;6:199.
5. Ferris RL, Blumenschein G, Jr., Fayette J, et al. Nivolumab for recurrent squamous-cell carcinoma of the head and neck. N Engl J Med. 2016;375:1856-1867.

Ethics Approval

This study was approved by each institution's Review Board/Independent Ethics Committee.

Figure 1.

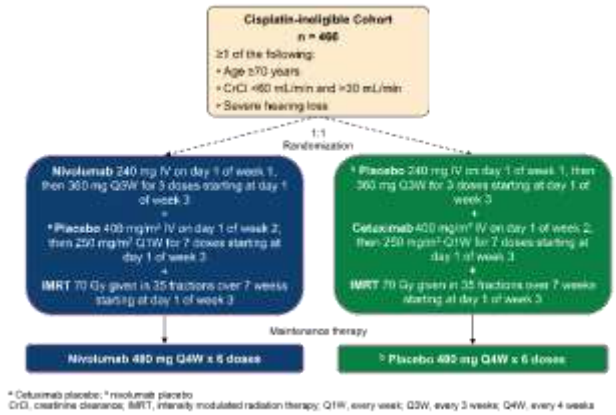

P334

AI-designed dual peptide vaccine plus novel combination adjuvant showed markedly induction of antigen-specific CTLs with disease stabilization in last line patients with GI cancers

Masao Nakajima, MD[1], Shoichi Hazama[2], Koji Tamada, MD PhD[3], Keiko Udaka[4], Yasunari Kouki[5], Toshinari Uematsu[5], Hideki Arima[5], Shun Doi, PhD[6], Hiroto Matsui[1], Sinsuke Kanekiyo[1], Yoshitaro Shindo[1], Yukio Tokumitsu[1], Shinobu Tomochika[1], Shin Yoshida[1], Michihisa Iida[1], Nobuaki Suzuki[1], Shigeru Takeda[1], Shigeru Yamamoto[1], Shigefumi Yoshino[5], Tomio Ueno[7], Hiroaki Nagano[1]

[1]*Yamaguchi Univ. Graduate school of medicine, Ube, Japan*
[2]*Yamaguchi Univ. School of Medicine, Ube, Japan*
[3]*Yamaguchi University, Ube, Japan*
[4]*Kochi Medical School, Kochi, Japan*
[5]*Yamaguchi University hospital, Ube, Japan*
[6]*CYTLIMIC Inc, Tokyo, Japan*
[7]*Kawasaki University School of Medicine, Kurashiki, Japan*

Background

Based on the exploratory analysis of our previous studies of peptide vaccine, we concluded that the combination of adjuvants hLAG-3Ig + Poly-ICLC was essential to overcome the therapeutic limitation of the traditional peptide studies by controlling negative immune checkpoints and enhancing CTLs induction. Another issue with peptide vaccines is human leukocyte antigen (HLA) restriction. Hence, we developed novel multi-HLA-binding peptides derived from the tumor antigens, HSP70 and GPC3, and confirmed the high expression in many types of cancer. After the presentation at ASCO 2017, we expanded pts in recommended dose to confirm safety and explored biomarkers for efficacy.

Methods

We identified HSP70- and GPC3-peptide that have high binding affinity to each of HLA-A2402, 0201, and 0206 by a binding prediction system (NEC Corporation). In this phase I study of a novel peptide cancer vaccine therapy for patients with metastatic solid cancer, the primary objective was to evaluate its safety and toxicity. Secondary objective was to examine the immune and clinical response, and also to confirm the recommendable dose. This study used a three-tiered dose-escalation strategy with 3 pts' cohorts. In addition to the 3 scheduled cases, 8 more cases were added and 11 cases were enrolled at the recommended dose. Moreover, to explore biomarkers for efficacy, we analyzed the exhaustion markers on T cells and immune-suppressive cells in PBMC of the treated patients.

Results

Seventeen HLA-A*24:02-, 02:01-, and 02:06-matched pts (esophagus (EC), 5; colon (CRC), 6; liver (HCC), 4; pancreas, 1; stomach, 1) were treated in this study. No severe adverse effects related to the treatment were encountered. Peptide-specific CTL induction to HSP70 and GPC3 was observed in 15 and 16 pts, respectively. We observed decreased tumor marker expression in 10 cases, and disease control was observed in 5 pts (18, 4, 3, 3, 2 M). OS rates in CRC, HCC, and EC were 80%, 100%, and 60% at 6M, and 60%, 75% and 0% at 12M, respectively. Low expression of PD1 on CD4+ T cells (p = 0.02) and low

proportion of Treg Fraction II (p = 0.03) in the PBMC were the significant favorable biomarker for OS.

Conclusions
The combination cancer vaccine therapy using multi-HLA-restricted peptides and hLAG-3Ig + Poly-ICLC was safe and effective for treating the last line patients with metastatic solid tumors. The proportion of the PD-1+/CD4+ T cells and Treg Fraction II were the significant biomarker for OS.

Ethics Approval
The study was approved by Yamaguchi University's Ethics Board, approval number 12345. (UMIN ID: 000020440)

Consent
Written informed consent was obtained from the patient for publication of this abstract and any accompanying images. A copy of the written consent is available for review by the Editor of this journal.

P335

A phase 1 study of ALX148: CD47 blockade in combination with anticancer antibodies to bridge innate and adaptive immune responses for advanced malignancy

Nehal Lakhani, MD, PhD[1], Patricia LoRusso, DO[2], Laura Chow, MD[3], Yung-Jue Bang, MD PhD[4], Philip Fanning[5], Yonggang Zhao, PhD, MBA[5], Jaume Pons[5], Hong Wan[5], Sophia Randolph, MD, PhD[5], Wells Messersmith, MD[6]

[1]START Midwest, Grand Rapids, MI, USA
[2]Yale Cancer Center, New Haven, CT, USA
[3]Seattle Cancer Care Alliance, Seattle, WA, USA
[4]Seoul National University Hospital, Seoul, Korea
[5]ALX Oncology Inc., Burlingame, CA, USA
[6]University of Colorado Cancer Center, Aurora, CO, USA

Background
Tumors upregulate CD47, a marker of self, to evade the anticancer immune response. Blocking CD47 disrupts a key myeloid immune checkpoint and enhances innate and adaptive immunity against cancer[1]. ALX148 is a fusion protein comprising a high affinity CD47 blocker with an inactive human Fc domain to extend serum half-life and minimize toxicity. ALX148 safely enhances activity of anti-cancer targeted antibodies and checkpoint inhibitors (CPI) in nonclinical models[1]. Single agent ALX148 is well tolerated by patients with no maximum-tolerated dose (MTD) reached, a maximum-administered dose (MAD) of 30 mg/kg every other week, and no dose-dependent hematologic toxicity (SITC 2017, #241; ASCO 2018, #3068), negating the need for priming/loading administration strategies. Part 2 of this study evaluates the safety of ALX148 in combination with pembrolizumab, trastuzumab or rituximab in patients with advanced malignancy.

Methods
The primary objective of Part 2 is to characterize the safety profile of ALX148 administered with established anticancer antibodies. Patient cohorts with solid tumor malignancy receive escalating doses of intravenous ALX148 in combination with pembrolizumab or trastuzumab (HER2-positive tumors). Patients are also evaluated for response, PK, and CD47 target occupancy (TO). Preliminary combination data from the fully enrolled solid tumor dose escalation and ongoing expansion cohorts are reported as of July 20, 2018 and will be updated at the time of presentation.

Results
Twenty-five patients with advanced solid tumors received ALX148 in combination with pembrolizumab or trastuzumab as of data cutoff. Patients were heavily pretreated with a median of 5 (2-12) prior regimens. Median age was 56 (32-74) yrs. Thirteen patients (52%) experienced predominantly single and low grade treatment-

related adverse events (TRAEs). No ALX148 MTD was reached with a MAD of 10 mg/kg, once weekly. Of the initial 8 evaluable patients in the pembrolizumab cohort, there was 1PR with 48% tumor reduction at first evaluation (NSCLC, PD-L1 <10%, CPI-refractory), 2SD (NSCLC, PD-L1 0%, > 24 weeks; appendiceal cancer, MSS). Of the initial 8 evaluable patients in the trastuzumab cohort, there were 3SD (1-gastroesophageal junction with 27% tumor reduction at first evaluation, trastuzumab-resistant; 2-breast). Initial PK and CD47 TO of ALX148 in combination were similar to that of single agent administration.

Conclusions

ALX148 is well tolerated with preliminary antitumor activity in combination with pembrolizumab or trastuzumab in patients with advanced solid tumors. No MTD was reached in either combination. Combination expansion cohorts are ongoing, with ALX148 administered 10 mg/kg, once weekly.

Trial Registration

ClinicalTrials.gov identifier NCT03013218.

References

1. Kauder S, et al., ALX148 blocks CD47 and enhances innate and adaptive antitumor immunity with a favorable safety profile. PLOS ONE. In Press.

P336

An international, single-arm, phase 2 study of INCMGA00012 in patients with advanced squamous carcinoma of the anal canal (SCAC) who have progressed following platinum-based chemotherapy (NCT03597295)

Sheela Rao[1], May Cho[2], Anne Demols[3], Talal Kayyal[4], Hiral Parekh[5], Gerard Kennealey, MD[6], Chuan Tian[6], Melissa Catlett[6], Marwan Fakih, MD[7]

[1]The Royal Marsden, London, UK
[2]UC Davis Comprehensive Cancer Center, Sacramento, CA, USA
[3]CUB Hôpital ERASME, Brussels, Belgium
[4]Renovatio Clinical, Houston, TX, USA
[5]University of Florida, Gainesville, FL, USA
[6]Incyte Corporation, Wilmington, DE, USA
[7]City of Hope Comprehensive Cancer Cente, Duarte, CA, USA

Background

A standard treatment for refractory advanced SCAC has not yet been established; however, preliminary phase 2 results with PD-1 inhibitors showed promising activity [1,2]. INCMGA00012 is a humanized IgG4 monoclonal antibody that recognizes human PD-1 and has demonstrated acceptable tolerability with evidence of clinical activity in a phase 1 study of solid tumors (NCT03059823) [3]. This trial will evaluate the safety and efficacy of INCMGA00012 in patients with locally advanced or metastatic SCAC, including those with well-controlled human immunodeficiency virus (HIV) infection.

Methods

INCMGA 0012-202 is a phase 2, open-label, single-arm study, with planned enrollment of 81 patients who have locally advanced or metastatic SCAC following ≤2 prior systemic treatments, at least 1 of which included platinum. HIV+ patients should be well controlled on highly active antiretroviral therapy (HAART). Other key eligibility criteria include age ≥18 years, measurable disease by RECIST v1.1, and Eastern Cooperative Oncology Group performance status of 0 to 1. Daily prednisone dose of ≤10 mg or equivalent is allowed. Patients will receive INCMGA00012 500 mg by intravenous infusion once every 28 days up to 2 years in the absence of clinical disease progression or intolerable toxicity, or discontinuation for any other reason. Disease assessments will be performed every 8 weeks. The primary endpoint is overall response rate. Secondary endpoints include duration of response, disease control rate, progression-free survival, overall

survival, safety, and pharmacokinetics. Health-related quality of life and relevant biomarkers are exploratory endpoints.

Acknowledgements
Clinical trial management was provided by Tristan Richard (Incyte Corporation, Wilmington, DE).

Trial Registration
NCT03597295

References
1. Morris VK, Salem ME, Nimeiri H, et al. Nivolumab for previously treated unresectable metastatic anal cancer (NCI9673): a multicentre, single-arm, phase 2 study. Lancet Oncol. 2017; 18:446-453.
2. Ott PA, Piha-Paul SA, Munster P, et al. Safety and antitumor activity of the anti-PD-1 antibody pembrolizumab in patients with recurrent carcinoma of the anal canal. Ann Oncol. 2017; 28:1036-1041.
3. Lakhani N, Mehnert J, Rasco D, et al. A phase 1 study of the safety, tolerability, and pharmacokinetics (PK) of MGA012 (anti-PD-1 antibody) in patients with advanced solid tumors. J Immunother Cancer. 2017; 5(Suppl 2):Abstract P249.

Ethics Approval
The study was approved by institutional review boards or independent ethics committees of participating institutions.

P337

Phase I dose-escalation and expansion study of intratumoral CV8102, a RNA-based TLR- and RIG-1 agonist with or without anti-PD1antibodies in patients with advanced solid tumors

Lucie Heinzerling[1], Juergen Krauss[2], Carsten Weishaupt[3], Patrick Terheyden[4], Benjamin Weide, MD[5], Ralf Gutzmer[6], Peter Mohr[7], Juergen Becker, MD, PhD[8], Felix Kiecker[9], Angelika Daehling[10], Fatma Doener, PhD[10], Regina Heidenreich[10], Sarah-Katharina Kays[10], Ute Klinkhardt, MD[10], Birgit Scheel[10], Oliver Schönborn-Kellenberger[11], Tobias Seibel[10], Tanja Strack[10], Ulrike Gnad-Vogt, MD[10], Madelaine Schroth[10]

[1]University Hospital of Erlangen, Germany
[2]Nationales Centrum für Tumorerkrankungen, Heidelberg, Germany
[3]Universitaetsklinikum Muenster, Muenster, Germany
[4]Universitätsklinikum Schleswig-Holstein, Lübeck, Germany
[5]Universitäts-Hautklinik Tuebingen, Tuebingen, Germany
[6]Haut-Tumor-Zentrum Hannover, Germany
[7]Elbe Kliniken Stade-Buxtehude GmbH, Germany
[8]Translational Skin Cancer Research, Essen, Germany
[9]Charité Universitätsmdizin Berlin, Berlin, Germany
[10]CureVac AG, Tuebingen, Germany
[11]Cogitars GmbH, Heidelberg, Germany

Background
Intratumoral (IT) activation of innate immune signaling pathways is a promising approach to overcome the immunosuppressive tumor microenvironment andinduce/restore anti-tumor immunity. CV8102, a single-stranded non-coding RNA complexed with a cationic peptide that signals via TLR-7/-8 and RIG-I [2], has shown to stimulate transient upregulation of inflammatory cytokines, chemokines and IFN-γ related genes at the injection site, followed by activation of T, NK, NKT and migratory dendritic cells in the draining lymph nodes [1]. IT CV8102 demonstrated dose-dependent anti-tumor activity and synergized with systemic PD1 inhibition in preclinical models. This Phase I study investigates CV8102 as single agent and in combination with systemic anti-PD1 antibodies.

Methods
Patients (pts) with advanced inoperable melanoma (MEL), cutaneous/head and neck squamous cell or adenoid cystic carcinoma (cSCC, SCCHN, ACC) are

eligible for single agent CV8102, MEL and SCCHN pts without response after 12 weeks of anti-PD1 treatment are eligible for the combination part.Pts are treated with up to 8 IT injections of CV8102 into a single tumor lesion over a 12 week period. Dose-escalation for single agent and anti-PD1 combination follows a Bayesian logistic regression model. Responses are assessed Q8W/Q12W per RECIST 1.1/irRECIST and. pre- and on-treatment samples collected for biomarker analyses.. After determination of the recommended dose expansion cohorts are planned.

Results

As of July 06, 2018, 9 pts (4 MEL, 2 SCCHN, 2 ACC, 1 cSCC) have been treated with single agent CV8102 (doses from 25 µg up to 150µg). 2 pts have been treated with CV8102 (25 and 50 µg) in combination with anti-PD1 antibodies. No dose limiting toxicities occurred, most common AEs were mild to moderate injection site reactions and flu-like symptoms.So far 6 pts are evaluable for tumor response after single agent CV8102 at their initial assessment. Notably, one MEL pt treated at the 150 µg dose experienced a complete regression of the injected as well as non-injected lesions. This patient also experienced a marked increase of IL-6 and CRP at 6 and 24 hours after the first injection, respectively. 4 pts achieved stable disease, including one SCCHN pt treated at 100 µg who experienced shrinkage of a non-injected lymph node metastasis. Dose escalation is continuing and updated safety and efficacy results will be presented.

Conclusions

CV8102 was so far well tolerated and early signs of clinical activity including regression of non-injected lesions were observed after single agent treatment.

References

1. Heidenreich R, Jasny E, Kowalczyk A, Lutz J, Probst J, Baumhof P, Scheel B, Voss S, Kallen KJ, Fotin-Mleczek M. A novel RNA-based adjuvant combines strong immunostimulatory capacities with a favorable safety profile. Int J Cancer. 2015 ;137:372-84. 2. Ziegler A, Soldner C, Lienenklaus S, Spanier J, Trittel S, Riese P, Kramps T, Weiss S, Heidenreich R, Jasny E, Guzmán CA, Kallen KJ, Fotin-Mleczek M, Kalinke U. A New RNA-Based Adjuvant Enhances Virus-Specific Vaccine Responses by Locally Triggering TLR- and RLH-Dependent Effects. J Immunol. 2017 ;198:1595-1605.

Ethics Approval

The study was approved by Universitätsklinikum Tübingen Medizinische Fakultät Ethik-Kommission, approval number 785/2016AMG1

P338 Abstract Travel Award Recipient

Phase II neoadjuvant and immunologic study using the anti B7-H3 antibody, Enoblituzumab, in patients with localized prostate cancer

Eugene Shenderov, MD, PhD[1], Karim Boudadi, MD[1], Angelo Demarzo, MD, PhD[1], Mohamad Allaf, MD[1], Onur Ertunc, MD[1], Igor Vidal, MD[1], Carolyn Chapman, AAS[1], Hao Wang[1], Jim Vasselli, MD[2], Jon Wigginton, MD[2], Jan Davidson-Moncada, MD, PhD[2], Rehab Abdallah, MB BCh[1], Tanya O'Neal, BS, MS[1], Christian Pavlovich, MD[1], Trinity Bivalacqua, MD PhD[1], Ashley Ross, MD[1], Charles Drake, MD, PhD[3], Drew Pardoll, MD, PhD[1], Emmanuel Antonarakis, MD[1]

[1]*Johns Hopkins Hospital, Baltimore, MD, USA*
[2]*Macrogenics, Rockville, MD, USA*
[3]*Columbia University, New York, NY, USA*

Background

Prostate cancer (PCa) is the second-most-common cause of cancer-related deaths in men [1, 2]. Immune-checkpoint blockade has resulted in unprecedented treatment advances in multiple tumor types, despite yielding modest results in PCa.

While CTLA-4 and PD-L1 are infrequently expressed in PCa, B7-H3 (another B7 superfamily member) is highly expressed in many PCas, may modulate anti-tumor immune responses, and is associated with worse prognosis [3-5]. Binding (blocking) B7-H3 is now clinically possible with the recent development of enoblituzumab (MacroGenics), a humanized Fc-optimized (for antibody-dependent cell-mediated cytotoxicity [ADCC]) monoclonal antibody that binds B7-H3 with high affinity and specificity [6, 7]. Here we describe a study to test the hypothesis that neoadjuvant enoblituzumab treatment in patients with high-risk localized PCa will lead to partial pathological responses and reduced biochemical recurrence following prostatectomy, initially by modulating T cell immunity in the tumor microenvironment (TME) and also through direct tumor killing via ADCC.

Methods

Thirty two (32) men with intermediate- and high-risk localized prostate cancer (Gleason sum 7-10) were consented on an IRB-approved single-center, single arm, phase 2 study evaluating the safety, anti-tumor effect, and immunogenicity of neoadjuvant enoblituzumab given prior to radical prostatectomy at Johns Hopkins. Participants receive enoblituzumab at a dose of 15 mg/kg IV given weekly for 6 doses prior to radical prostatectomy. Two weeks after the last dose of enoblituzumab, prostates are harvested at radical prostatectomy, and examined for secondary and correlative endpoints.

Results

To-date, the trial has enrolled 20/32 patients, with minimal clinical toxicity having been noted. We have optimized B7-H3 immunohistochemical (IHC) staining, showing specific B7-H3 staining (Figure 1) and the ability to stain for the CD8+ T cell infiltrate in enoblituzumab-treated prostatectomy samples (Figure 2). Furthermore, B7-H3 detection in post-treatment biopsies is consistent with preferential B7-H3 expression in tumor versus normal cells. Moreover, CD8+ T cell quantitation in the initial enoblituzumab-treated prostatectomy samples shows a statistically significant increase in infiltrate compared to age- and stage-matched untreated prostatectomy controls (Figure 3, median 98 vs 46 cells/mm2, P=0.003).

Conclusions

This study aims to explore the impact of B7-H3 blockade on PSA recurrence following prostatectomy, the effects on the prostate gland TME, and whether B7-H3 IHC staining can be used to predict response or resistance to B7-H3–targeted therapies. The described finding of enhanced CD8 infiltration suggests that enoblituzumab alters the TME in a fashion that results in enhanced CD8 T cell infiltration – a hallmark of responsiveness to immunotherapy.

Acknowledgements

Study sponsors: Emmanuel Antonarakis, M.D. (PI); MacroGenics, Inc., Rockville, MD; 2018 Conquer Cancer Foundation Young Investigator Award

Trial Registration

ClinicalTrials.Gov NCT02923180

References

1. Murphy SL, Xu J, Kochanek KD, Curtin SC, Arias E. Deaths: Final Data for 2015. National vital statistics reports : from the Centers for Disease Control and Prevention, National Center for Health Statistics, National Vital Statistics System. 2017;66(6):1-75.
2. Siegel RL, Miller KD, Jemal A. Cancer statistics, 2018. CA: A Cancer Journal for Clinicians. 2018;68(1):7-30.
3. Benzon B, Zhao SG, Haffner MC, Takhar M, Erho N, Yousefi K, Hurley P, Bishop JL, Tosoian J, Ghabili K, Alshalalfa M, Glavaris S, Simons BW, Tran P, Davicioni E, Karnes RJ, Boudadi K, Antonarakis ES, Schaeffer EM, Drake CG, Feng F, Ross AE. Correlation of B7-H3 with androgen receptor, immune pathways and poor outcome in prostate cancer: an expression-

based analysis. Prostate Cancer Prostatic Dis. 2017;20(1):28-35.
4. Parker AS, Heckman MG, Sheinin Y, Wu KJ, Hilton TW, Diehl NN, Pisansky TM, Schild SE, Kwon ED, Buskirk SJ. Evaluation of B7-H3 Expression as a Biomarker of Biochemical Recurrence After Salvage Radiation Therapy for Recurrent Prostate Cancer. International Journal of Radiation Oncology Biology Physics. 2011;79(5):1343-9.
5. Roth TJ, Sheinin Y, Lohse CM, Kuntz SM, Frigola X, Inman BA, Krambeck AE, Mckenney ME, Karnes RJ, Blute ML, Cheville JC, Sebo TJ, Kwon ED. B7-H3 Ligand Expression by Prostate Cancer: A Novel Marker of Prognosis and Potential Target for Therapy. Cancer Research. 2007;67(16):7893-900.
6. Powderly J. 2015 Society for Immunotherapy of Cancer (SITC) Annual Meeting in National Harbor, MD. Dr. John Powderly II of the Carolina BioOncology Institute, Huntersville, NC, presented "Interim Results of an Ongoing Phase 1, Dose Escalation Study of MGA271 (Fc-optimized Humanized Anti-B7-H3 Monoclonal Antibody) in Patients with Refractory B7-H3-Expressing Neoplasms or Neoplasms Whose Vasculature Expresses B7-H3".
7. Loo D, Alderson RF, Chen FZ, Huang L, Zhang W, Gorlatov S, Burke S, Ciccarone V, Li H, Yang Y, Son T, Chen Y, Easton AN, Li JC, Rillema JR, Licea M, Fieger C, Liang TW, Mather JP, Koenig S, Stewart SJ, Johnson S, Bonvini E, Moore PA. Development of an Fc-Enhanced Anti–B7-H3 Monoclonal Antibody with Potent Antitumor Activity. Clinical Cancer Research. 2012;18(14):3834-45.

Ethics Approval

The study was approved by Johns Hopkins Institutions's Ethics Board, approval number IRB00070748.

Figure 1. Enoblituzumab binds B7-H3 with high affinity and specificity

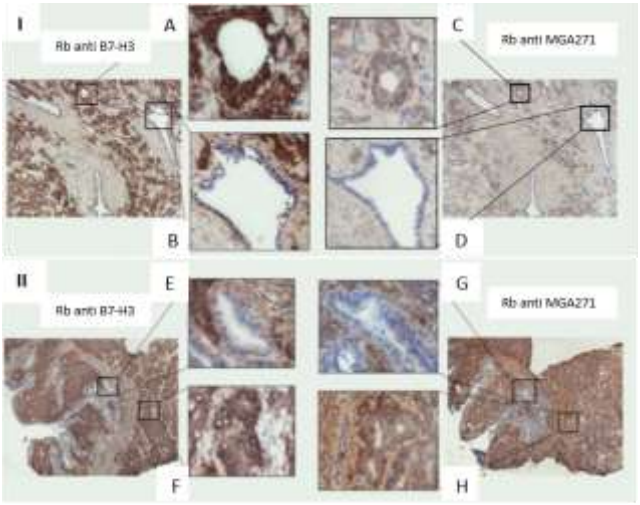

Figure 2. Enoblituzumab Treated Prostatectomy CD8+ T Cell Infiltrates

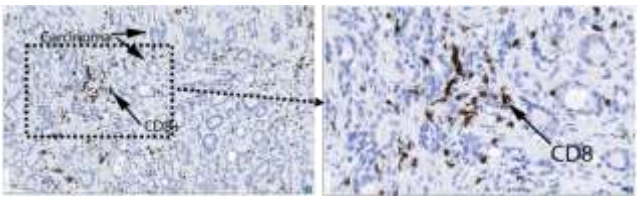

Figure 3. CD8+ T Cell Quantitation in Enoblituzumab-treated Prostates

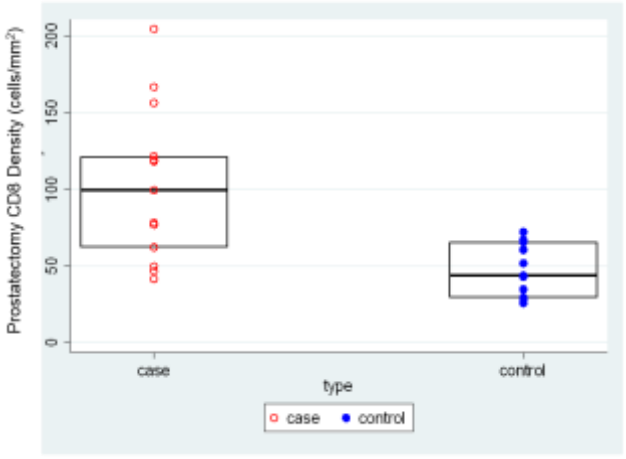

P339

HCRN GI16-288: A phase II trial of perioperative CV301 vaccination in combination with nivolumab and systemic chemotherapy for resectable hepatic-limited metastatic colorectal cancer

Kristen Spencer, DO, MPH[1], Daniella Portal, BS[1], Christopher Heery, MD[2], Lynne Bauman, MS[2], Howard Hochster, MD[1], Elizabeth Poplin, MD[1], Usha Malhotra, MD[1], Richard Alexander, MD[1], David August, MD[1], Timothy Kennedy, MD[1], Miral Grandhi, MD[1], Russell Langan, MD[1], Edmund Lattime, PhD[1], Dirk Moore, PhD[1], Michael Kane, RPh, BCOP[1], Liesel Dudek, RN, OCN, CCRP[1], Sarah Nabeel[1], Darren Carpizo, MD, PhD[1]

[1]*Rutgers Cancer Institute of New Jersey, New Brunswick, NJ, USA*
[2]*Bavarian Nordic, Morrisville, NC, USA*

Background

Approximately 50% of patients with colorectal cancer (CRC) develop metastatic disease, most frequently in the liver. Surgical resection is the only potential cure, however recurrence occurs in a majority of cases. To date, perioperative chemotherapy has not translated into an overall survival (OS) benefit [1, 2]. Immune checkpoint inhibitors are active in mCRC patients with high microsatellite instability [3], however studies in an array of CRCs have demonstrated a relationship between the tumor immune microenvironment and outcomes, implying immune strategies may be used in a broader population [4, 5].CV301, formerly PANVAC, is a vector-based vaccine that expresses the tumor antigens carcinoembryonic antigen (CEA) and mucin 1 (MUC1), and in a phase II study in patients with mCRC who had undergone complete resection of liver metastases did not improve RFS, but significantly improved OS as compared to an unvaccinated contemporary control cohort (median OS NR vs 44.1 mos) [6]. This study highlighted that: 1) the optimal use of this vaccine may be in patients free of detectable (and immunosuppressive) disease and 2) the gradual immune response generated through epitope spreading may mean long-term outcomes such as OS is a more appropriate primary endpoint. Additionally, CV301 up-regulates PD-L1 in the tumor microenvironment, suggesting a role for rational immunotherapy combinations [7].

Methods

This is a multi-center Phase II randomized study to determine whether the addition of CV301 vaccination to perioperative Nivolumab and mFOLFOX improves 3-year OS in 78 patients undergoing surgical resection for mCRC. Eligible patients are those with resectable hepatic-limited mCRC and ECOG performance status

Acknowledgements

This trial is managed by Hoosier Oncology Group and sponsored by Bavarian Nordic and Bristol-Myers Squibb.

Trial Registration

Clinicaltrials.gov: NCT02840994

References

1. Nordlinger B, Sorbye H, Glimelius B, Poston GJ, Schlag PM, Rougier P, Bechstein WO, Primrose JN, Walpole ET, Finch-Jones M, Jaeck D, Mirza D, Parks RW, Collette L, Praet M, Bethe U, Van Cutsem E, Scheithauer W, Gruenberger T. Perioperative chemotherapy with FOLFOX4 and surgery versus surgery alone for resectable liver metastases from colorectal cancer (EORTC Intergroup trial 40983): a randomised controlled trial. Lancet. 2008;371(9617):1007-16.
2. Nordlinger B, Sorbye H, Glimelius B, Poston GJ, Schlag PM, Rougier P, Bechstein WO, Primrose JN, Walpole ET, Finch-Jones M, Jaeck D, Mirza D, Parks RW, Mauer M, Tanis E, Van Cutsem E, Scheithauer W, Gruenberger T. Perioperative FOLFOX4 chemotherapy and surgery versus surgery alone for

resectable liver metastases from colorectal cancer (EORTC 40983): long-term results of a randomised, controlled, phase 3 trial. Lancet Oncol. 2013;14(12):1208-15
3. Overman MJ, McDermott R, Leach JL, Lonardi S, Lenz HJ, Morse MA, Desai J, Hill A, Axelson M, Moss RA, Goldberg MV, Cao ZA, Ledeine JM, Maglinte GA, Kopetz S, Andre T. Nivolumab in patients with metastatic DNA mismatch repair-deficient or microsatellite instability-high colorectal cancer (CheckMate 142): an open-label, multicentre, phase 2 study. Lancet Oncol. 2017;18(9):1182-1191.
4. Galon J, Costes A, Sanchez-Cabo F, Kirilovsky A, Mlecnik B, Lagorce-Pagès C, Tosolini M, Camus M, Berger A, Wind P, Zinzindohoué F, Bruneval P, Cugnenc PH, Trajanoski Z, Fridman WH, Pagès F. Type, density, and location of immune cells within human colorectal tumors predict clinical outcome. Science. 2006; 313(5795):1960-4.
5. Pagès F1, Berger A, Camus M, Sanchez-Cabo F, Costes A, Molidor R, Mlecnik B, Kirilovsky A, Nilsson M, Damotte D, Meatchi T, Bruneval P, Cugnenc PH, Trajanoski Z, Fridman WH, Galon J. Effector memory T cells, early metastasis, and survival in colorectal cancer. N Engl J Med. 2005;353(25):2654-66.
6. Morse MA, Niedzwiecki D, Marshall JL, Garrett C, Chang DZ, Aklilu M, Crocenzi TS, Cole DJ, Dessureault S, Hobeika AC, Osada T, Onaitis M, Clary BM, Hsu D, Devi GR, Bulusu A, Annechiarico RP, Chadaram V, Clay TM, Lyerly HK. A randomized phase II study of immunization with dendritic cells modified with poxvectors encoding CEA and MUC1 compared with the same poxvectors plus GM-CSF for resected metastatic colorectal cancer. Ann Surg. 2013;258(6):879-86
7. Foy SP, Sennino B, dela Cruz T, Cote JJ, Gordon EJ, Kemp F, Xavier V, Franzusoff A, Rountree RB, Mandl SJ. Poxvirus-based active immunotherapy with PD-1 and LAG-3 dual immune checkpoint inhibition overcomes compensatory immune regulation, yielding complete tumor regression in mice. PLoS One. 2016 Feb 24;11(2):e0150084.

Ethics Approval
This study was approved by the Rutgers Cancer Institute of New Jersey Institutional Review Board (Pro20170000595).

Figure 1.

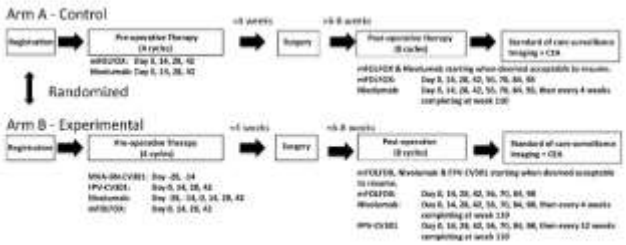

P340

Pharmacokinetic and pharmacodynamic characterization of ALX148, a CD47 blocker, in patients with advanced malignancy and non-Hodgkin lymphoma

Hong Wan[1], Feng Jin, PhD[1], Nehal Lakhani, MD, PhD[2], Patricia LoRusso, DO[3], Laura Chow, MD[4], Wells Messersmith, MD[5], Sangetha Bollini[1], Laura Doyle[1], Steven Kauder, PhD[1], Philip Fanning[1], Jaume Pons[1], Sophia Randolph, MD, PhD[1]

[1]ALX Oncology, Burlingame, CA, USA
[2]START Midwest, Grand Rapids, MI, USA
[3]Yale Cancer Center, New Haven, CT, USA
[4]Seattle Cancer Care Alliance, Seattle, WA, USA
[5]University of Colorado Cancer Center, Aurora, CO, USA

Background
ALX148 is a fusion protein comprising a high affinity CD47 blocker with an inactive human Fc domain to extend serum half-life and minimize toxicity[1]. ALX148 safely enhances the activity of anticancer antibodies in nonclinical models[1] and is currently being investigated in a Phase 1 study (SITC 2017,

#241; ASCO 2018, #3068). The objective of this analysis was to characterize the pharmacokinetics (PK) and pharmacodynamics (PD) of ALX148 in patients with advanced solid tumors and lymphomas as a single agent and in combinations with pembrolizuab or trastuzumab. Translational PK and PD modeling was conducted to estimate target occupancy (TO) in human tumors.

Methods

Data from the first-in-human Phase 1 study in 48 patients with advanced malignancy were used for this analysis. Multiple intravenous (IV) doses in the range 0.3 – 30 mg/kg were administered once weekly (QW) or once every two weeks (QoW). ALX148 was quantitated using an immunoassay in serum samples collected after first and subsequent doses. CD47 TO was measured in peripheral blood by flow cytometry. Noncompartmental PK analysis and PK/PD modeling were conducted with Phoenix and NONMEM programs. Preclinical PK/PD analysis was performed with ALX148 in tumor bearing mice, and serum PK and TO in peripheral blood, spleen and tumor compartments were measured.

Results

Maximum serum concentration (Cmax) and area under the concentration curve (AUC) of ALX148 exhibited greater than dose-proportional increase at 0.3 - 3 mg/kg QW, indicating nonlinearity in PK. At 10 mg/kg QW and 30 mg/kg QoW, increases in Cmax and AUC were dose proportional. The PK parameters and observed TO data were consistent with the presence of a CD47 antigen sink saturated at doses ≥ 3 mg/kg QW. ALX148 PK profile (10 mg/kg QW) was not changed when dosed in combination with pembrolizumab or trastuzumab, with a steady-state half-life of ~ 16 days. In tumor bearing mice, administration of ALX148 demonstrated dose dependent TO in peripheral blood, spleen and tumor. Using PK/PD models established from preclinical data and extrapolated based on human PK and peripheral PD data, a tissue/tumor TO >85% was projected to be maintained at ≥ 5 mg/kg QW in patients over the dosing interval.

Conclusions

ALX148 exhibited clinical PK properties typical of antibody-type protein therapeutics directed towards cell-surface targets. ALX148 PK approached linear range and maintained complete peripheral TO over the dosing interval at ≥ 3 mg/kg QW. Initial data suggests ALX148 PK/PD profiles are not impacted by combination drugs.

Trial Registration

ClinicalTrials.gov identifier NCT03013218

References

1. Kauder S et al., ALX148 blocks CD47 and enhances innate and adaptive antitumor immunity with a favorable safety profile. PLOS ONE. In Press.

P341

Phase 1 study of CA-170, a first-in-class, orally available, small molecule immune checkpoint inhibitor (ICI) dually targeting VISTA and PD-L1, in patients with advanced solid tumors or lymphomas

Timothy Wyant, PhD[1], Yung-Lue Bang, MD[2], Jeffrey Sosman, MD[3], Adil Daud, MBBS MD[4], Funda Meric-Bernstam, MD[5], Javier Garcia-Corbacho[6], Manish Patel, MD[7], James Lee, MD, PhD[8], Kyu-Pyo Kim[9], Joshua Brody, MD[10], Sun Young Rha[11], Marta Gil Martin[12], Santiago Ponce Aix, MD[13], Erika Hamilton, MD[14], Radhakrishnan Ramchandren, MD[15], Myung-Ju Ahn[16], James Spicer, MD, PhD[17], Simon Pacey[18], Gerald Falchook, MD[19], Hongwei Wang, MD, PhD[1], Guangxin Xu[20], Lisa Adams, BS[20], Anna Ma, MS[20], Robert Ghararvi[20], David Tuck[20], John Powderly, MD, CPI[21]

[1]Curis Inc, Lexington, MA, USA
[2]Seoul National University, Seoul, Korea, Republic of
[3]Northwestern, Chicago, IL, USA

[4]UCSF, San Francisco, CA, USA
[5]MDACC, Houston, TX, USA
[6]Hospital Clinic i Provincial, Barcelona, Spain
[7]Florida Cancer Specialist SCRI, Sarasota, FL, USA
[8]UPMC, Pittsburgh, PA, USA
[9]Asan Medical Center, Seoul, Korea, Republic of
[10]Mt. Sinai, New York, NY, USA
[11]Yonsei University Health System - Severa, Seoul, Korea, Republic of
[12]Catalan Institute of Oncology, Catalon, Spain
[13]Hospital Universitario 12 de Octubre, Madrid, Spain
[14]Sarah Cannon Research Insitute/Tennessee, Nashville, TN, USA
[15]Karmanos, Detroit, MI, USA
[16]Samsung Medical Center, Seoul, Korea, Republic of
[17]King's College Guy's, London, UK
[18]Cambridge University Hospitals NHS Found, Cambridge, UK
[19]SCRI, Denver, CO, USA
[20]Curis, Lexington, MA, USA
[21]Carolina BioOncology Institute, Huntersville, NC, USA

Background

VISTA and PD-1 are independent immune checkpoints that negatively regulate T-cell function. VISTA is expressed on immune and tumor cells and is found to be upregulated in tumors as a potential resistance mechanism after ICI therapy. Pre-clinical studies demonstrated that dual blockade of both checkpoints can be synergistic. CA-170 directly targets VISTA and PDL1/L2 and demonstrated significant anti-tumor activity in multiple preclinical models.

Methods

Enrollment initially followed accelerated titration and subsequently switched to 3+3 design. Two dosing schedules [once daily (QD) and twice daily (BID)] were evaluated in dose escalation. Cohorts of selected dose levels were expanded with additional patients. The expansion phase allows for enrollment of patients with selected indications. Primary objectives: safety, maximum tolerated dose (MTD) and recommended Phase 2 dose. Secondary objectives: pharmacokinetics (PK) and anti-tumor activity.

Results

A total of 59 patients have been treated across 9 dose levels (50 – 800 mg QD and 600 – 1200 mg BID) with 52 evaluable for dose limiting toxicities (DLTs). Enrolled tumor types included lung (20%), colorectal (17%), head and neck (14%), and ovarian cancer (8%). No DLT has been observed thus far. The most common treatment-emergent AEs (all grades) were fatigue (30%), nausea (27%), vomiting (21%), decreased appetite (20%), anemia (18%), constipation (18%), cough (16%), headache (13%), pyrexia (13%), and insomnia (12%). These were predominantly low grade and self-limiting events. Two reversible SAEs possibly related to drug were reported: one grade 3 lipase elevation and one grade 3 vomiting at 800 mg QD. Three newly enrolled patients are pending restaging. Fifty-one patients were evaluable for anti-tumor activity with 25 showing stable disease, 9 on study for ≥ 6 cycles (2 ongoing in cycle 26 and 8; most prolonged SD = 18 months), and 7 showing tumor shrinkage. CA-170 exhibited approximately dose proportional plasma exposure for both QD and BID schedules with T1/2 no longer than 12 hours. Compared with QD steady state plasma levels, BID dosing at the same dose resulted in approximately 50% increase in Cmax, 4.3-fold increase in Cmin, and an approximately two-fold increase in AUC/day.

Conclusions

These data suggest CA-170 has an acceptable safety profile with preliminary signs of anti-tumor activity and approximately dose proportional PK profile. MTD has not been reached. These data warrant the continued clinical development of CA-170. The study is ongoing with evaluation of potentially pharmacologically active BID dose in selected VISTA-expressing cancer types, such as mesothelioma.

Trial Registration
NCT02812875

Ethics Approval
This study was approved by the ethics committees of the following institutions: Seoul National University Hospital, Northwestern, UCSF, MDACC, Hospital Clinic de Barcelona, Florida Cancer Specialists/Sarah Cannon Research Institute, UPMC, Asan Medical Center, Mt. Sinai, Yonsei University Health System - Severance Hospital, Catalan Institute of Oncology, Hospital Universitario 12 de Octubre, Tennessee Oncology/Sarah Cannon Research Institute, Karmanos, Samsung Medical Center, King's College London, Guy's Hospital, University of Cambridge, Sarah Cannon Research Institute at HealthONE, Carolina BioOncology Institute

Consent
Written informed consent was obtained from the patient for publication of this abstract and any accompanying images. A copy of the written consent is available for review by the Editor of this journal

P342

Nivolumab plus cisplatin/pemetrexed or cisplatin/gemcitabine as induction in resectable NSCLC

Ralph Zinner, MD[2], Scott Cowan, MD[2], Charalambos Solomides, MD[2], Craig Hooper, PhD[2], Larry Harshyne, PhD[2], Grace Lu-Yao, PhD[2], Hushan Yang, PhD[2], Linda Phan, BS[2], Dawn Poller, BS[2], Sung Whang, DNP, CRNP[2], Benjamin Leiby, PhD[2], Marie Werner-Wasik, MD[2], Bo Lu, MD[2], Jennifer Johnson, MD[2], Rita Axelrod, MD[2], Argiris Athanassios, MD PhD[2], Natathiel Evans, MD[2]

[1]*Thomas Jefferson University Hospital, Philadelphia, PA, USA*
[2]*Thomas Jefferson University, Philadelphia, PA, USA*

Background
For patients (pts) with stage IB (>4cm)-IIIA Non-small-cell lung cancer (NSCLC), multi-modality therapy yields a modest improvement in 5 year post-surgical overall survival (OS), with comparable benefit for induction and postoperative adjuvant chemotherapy (chemo). Induction can speed the discovery of promising regimens by using pathologic response as a surrogate for OS. About 20% of pts treated with induction chemo have major pathologic response (MPR) (< 10% viable tumor) at primary and lymph nodes while pathologic complete responses (pCR) average 4%. MPR was strongly associated with improved OS [1]. PD-1 checkpoint inhibitors (CI), nivolumab (nivo), pembrolizumab (pembro), and the PD-L1 CI, atezolizumab, are established in advanced NSCLC as 2nd line therapy, and pembro is approved as a single agent as 1st line treatment of pts with PD-L1 high expressing tumors. In a phase III 1st line NSCLC study, pts with high mutational burden tumors had superior OS with nivo plus ipilimumab compared to doublet chemo. Pembro plus carboplatin with pemetrexed (P) was approved as 1st line therapy based on a randomized phase II study in advanced NSQ NSCLC showing improved clinical response and PFS compared to chemo alone with no increase in grade III toxicity. We therefore hypothesize that the addition of nivo to induction cisplatin (C) P or C gemcitabine (G) will increase the MPR rate over induction chemo alone compared to historical controls.

Methods
This is an investigator initiated trial for pts with newly diagnosed clinical stage I-IIIA (stage I > 4cm) SQ and NSQ NSCLC. Induction is C 75mg/m2 IV q 3w x 3 plus either P 500 mg/m2 IV q 3wks x 3 or G 1250mg/m2 IV d1, d8 q 3 wks x 3 plus nivo 360mg IV q 3w x 3. Surgery is planned 3 wks after the last dose. The primary outcome is MPR. Secondary outcomes include safety, pCR, overall clinical response rate, clinical CR, 1 year PFS, OS and

exploratory outcomes assessing markers of immune bias. Enrollment will be 34 pts. NCT03366766

References

1. Hellmann MD, Chaft JE, William WN Jr., Rusch V, Pisters KM, Kalhor N, Pataer A, Travis WD, Swisher SG, Kris MG. Pathological response after neoadjuvant chemotherapy in resectable non-small-cell lung cancers: proposal for the use of major pathological response as a surrogate endpoint. Lancet Oncol. 2014;15;e42-50.

Ethics Approval

The study was approved by Thomas Jefferson University Hospital Internal Review Board approval number 17P545

Consent

There is no identifiable information on any of the patients.

P343

Nivolumab plus weekly carboplatin and paclitaxel as induction therapy in resectable locally advanced head and neck cancer

Ralph Zinner, MD[1], David Cognetti, MD[2], Joseph Curry, MD[2], Adam Luginbuhl, MD[2], Richard Goldman, MD[2], Charalambos Solomides, MD[2], Madalina Tuluc, MD[2], Stacey Mardekian, MD[2], Craig Hooper, PhD[2], Larry Harshyne, PhD[2], Grace Lu-Yao, PhD[2], Hushan Yang, PhD[2], Linda Phan, BS[2], Dawn Poller, BS[2], Benjamin Leiby, PhD[2], Voichita Bar-Ad, MD[2], Jennifer Johnson, MD[2], Rita Axelrod, MD[2], Argiris Athanassios, MD PhD[2]

[1]*Thomas Jefferson University Hospital, Philadelphia, PA, USA*
[2]*Thomas Jefferson University, Philadelphia, PA, USA*

Background

Despite multimodality standard therapy, patients (pts) with resectable locally advanced squamous cell carcinoma of the head and neck (SCCHN) are at high risk for locoregional and distant recurrence. Although induction chemotherapy followed by surgery and postoperative radiotherapy did not show improved overall survival (OS) in 2 phase III trials of pts with resectable oral cancer, pts with pathologic complete response (pCR) and/or major pathologic response (MCR) had improved progression free survival (PFS) and OS [1,2]. In addition, major tumor responses may decrease surgical morbidity and reduce postoperative radiation fields [2]. Therefore, induction regimens which improve pCR/ MCR rates may improve survival and morbidity. PD-1 checkpoint inhibitors, nivolumab and pembrolizumab, are established in recurrent or metastatic SCCHN as 2nd line therapy. In a randomized phase III in 1st-line advanced non-squamous non-small cell lung cancer, carboplatin plus pemetrexed plus pembrolizumab improved clinical response, PFS, and OS compared to chemotherapy alone. We hypothesize that pts with newly diagnosed, previously untreated SCCHN, induction nivolumab in combination with weekly carboplatin and paclitaxel will increase the pCR rate at the primary cancer compared to the historical control chemotherapy alone.

Methods

This is an investigator-initiated trial for pts with newly diagnosed (AJCC 8th) stage III or IV HPV negative and stage III HPV positive SCCHN (oral cavity, oropharynx, hypopharynx, and larynx) who are surgical candidates. Pts receive induction with carboplatin AUC IV Q1 wk x 6 plus paclitaxel 100 mg/m2 IV Q1 wk x 6 with nivolumab 240mg IV Q2 wks x 3, all beginning on day 1 with surgery wk 8. The primary objective is pCR at the primary site. Secondary objectives include safety, pCR at all sites, MCR at primary site, overall clinical response, clinical complete response, 1 year PFS, OS and exploratory objectives assessing markers of immune bias. Two of planned 37 pts have been enrolled. NCT03342911

References
1. Zhong LP, Zhang CP, Ren GX, Guo W, William WN Jr, Hong CS, Sun J, Shu HG, Tu WY, Li J, Cai YL, Yin QM, Wang LZ, Wang ZH, Hu YJ, Ji T, Yang WJ, Ye WM, Li J, He Y, Wang YA, Xu LQ, Zhuang Z, Lee JJ, Myers JN, Zhang ZY. Long-term results of a randomized phase III trial of TPF induction chemotherapy followed by surgery and radiation in locally advanced oral squamous cell carcinoma.Oncotarget,2015;6:18708-14.
2.Bossi P, Lo Vulio S, Buzzo M, Mariani L, Granata R, Orlandi E, Locati L, Scaramellini G, Fallai C, Licitra L. Preoperative chemotherapy in advanced resectable OCSCC: long-term results of a randomized phase III trial. Ann Oncol. 2014;25:462-6

Ethics Approval
This study was approved by Thomas Jefferson University Internal Review Board approval number 17P502

Consent
There is no identifiable information on any patient.

Combination Therapy

P344

Spherical Nucleic Acid (SNA) TLR9 agonists induce long-term tumor-specific immune responses in synergy with PD-1 checkpoint inhibition

Bart Anderson, PhD[1], SubbaRao Nallagatla, PhD[1], Richard Kang, PhD[1], Ekambar Kandimalla, PhD[1]

[1]*Exicure, Skokie, IL, USA*

Background
Novel spherical nucleic acid (SNA) configuration of toll-like receptor (TLR) 9 agonist oligonucleotides are designed to trigger innate and adaptive immune responses against tumor cells in cancer patients. SNAs are densely-packed, radially-oriented 3-dimensional arrangements of oligonucleotides surrounding a liposomal nanoparticle. This 3D-architecture increases cellular uptake compared to conventional “linear” oligonucleotides that are not in SNA configuration. SNAs enter cells and localize to endosomes, which is where TLR9 proteins are localized, making SNAs ideal TLR9 agonists.Immune checkpoints are inhibitory pathways crucial for maintaining self-tolerance and modulating the duration and amplitude of physiological immune responses. However, tumors use immune-checkpoint pathways, particularly the PD-1 / PD-L1 pathway, as a major mechanism of immune resistance. TLR9 agonists combined with anti-PD-1 antibodies show synergistic anti-cancer effects. Here, we assess SNA immunostimulation and anti-tumor effects combined with an anti-PD-1 antibody.

Methods
Uptake of fluorescently-labeled oligonucleotides was measured by microscopy and flow cytometry. Mouse serum cytokines were measured by multiplex ELISA.Subcutaneously implanted EMT-6 cells were used as a tumor model. PD-1 and PD-L1 expression were measured using RT-qPCR. Tumor growth was assessed following SNA and anti-PD-1 treatment. Surviving mice were re-challenged with EMT-6 cells or with distinct syngenic tumor cells.The immunological response to subcutaneously administered SNAs in monkeys was assessed by Luminex-based measurement of serum cytokines and flow cytometric measurement of immune cell activation.

Results
Oligonucleotide uptake in SNA format was significantly increased ($P<0.0001$) compared to linear oligonucleotide (Fig.1). TH1-type cytokines were induced in wild-type but not TLR9-deficient mice, confirming TLR9-dependent immunostimulation (Fig.2).SNA treatment upregulated PD-1 and PD-L1

expression in EMT-6 tumors (Fig.3). Combined SNA plus anti-PD-1 treatment, but not anti-PD-1 monotherapy, produced complete anti-tumor responses. Re-challenge with EMT-6 tumor cells in mice previously experiencing a complete response resulted in tumor rejection, but tumors were not rejected when mice were re-challenged with distinct tumor cell lines, verifying adaptive immune responses against EMT-6 cells (Fig.4).SNA administration to NHP elicited both TH1-type cytokines in serum and activated immune cells including B-cells and pDCs (Fig.5).

Conclusions

TLR9-agonist SNAs induced potent, TLR9-dependent TH1-type immune responses in mice and monkeys and increased checkpoint inhibitor expression in the tumor. SNA plus anti-PD-1 combination therapy induced tumor-specific immunity and memory. These data support the clinical investigation of SNAs in immuno-oncology. One such SNA, AST-008, is undergoing a Phase 1a clinical trial and is planned for testing in cancer patients combined with an anti-PD-1 antibody.

Figure 1.

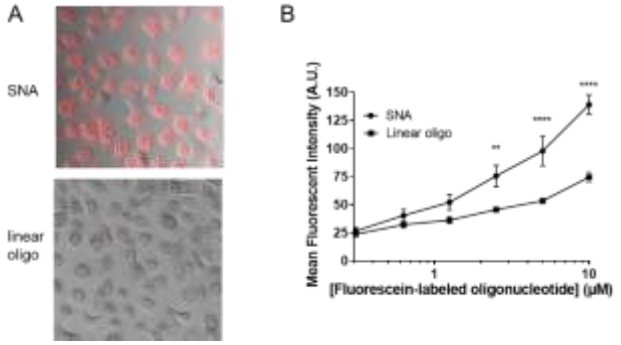

Figure 2.

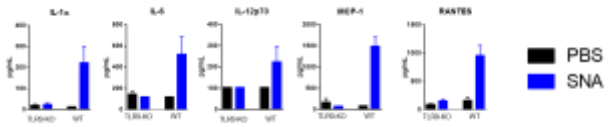

Figure 3.

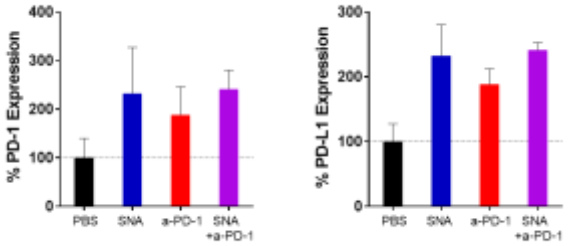

Figure 4.

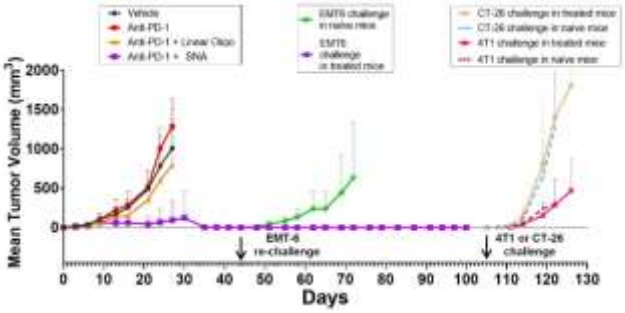

Figure 5.

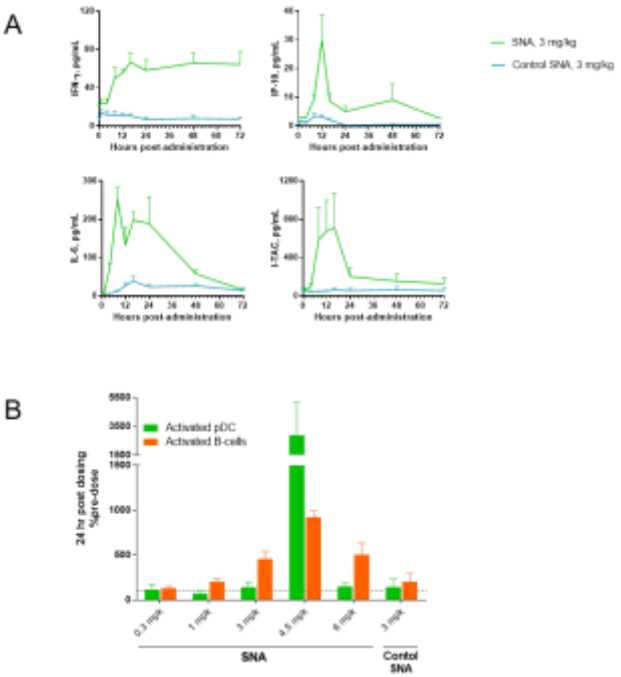

P345

Depletion of plasma arginine with pegzilarginase enhances the anti-tumor activity of immune checkpoint inhibitors

Mark Badeaux, PhD[1], Giulia Agnello, PhD[1], Danlee Enzler, BS[1], Leslie Priddy, BS[1], Jason Wiggins, BS[1], Christopher Daige[1], Scott Rowlinson, PhD[1]

[1]*Aeglea Biotherapeutics, Austin, TX, USA*

Background

Tumors unable to endogenously synthesize L-Arginine (arginine) due to defects in the arginine biosynthetic pathway are highly sensitive to arginine depletion. Pegzilarginase is a bioengineered human PEGylated arginase 1 with enhanced pharmacological properties that displays single-agent anti-tumor activity in a number of preclinical solid tumor models and clinical activity in dose escalation studies. Extracellular depletion of arginine directly impairs tumor cell growth, inducing both autophagy and apoptosis [1]. Given the relationship between autophagy and antigen presentation [2], we hypothesized that pegzilarginase activity could enhance immune cell recruitment and function in the tumor microenvironment, and therefore may exhibit enhanced anti-tumor activity in combination with immuno-oncology (IO) agents.

Methods

Pegzilarginase, either as a monotherapy or in combination with IO agents (anti-CTLA-4 Ab, anti-PD-L1 Ab), was administered to Balb/c mice bearing subcutaneous CT26 tumors. Tumor volumes were measured at regular intervals until survival endpoints were reached. At pre-determined time points, blood was collected for cytokine analyses, and flow cytometry was employed to assess intratumoral cell viability and immunophenotyping.

Results

Treatment with pegzilarginase or IO agents alone demonstrated greater anti-tumor activity relative to control treatment. The combination regimen of either anti-CTLA-4 Ab or anti-PD-L1 Ab with pegzilarginase induced greater anti-tumor activity than either IO monotherapy, including an increase in complete responses (CRs) in anti-PD-L1 Ab studies (37.5% CRs in combination arm vs. 0% in anti-PD-L1 Ab arm). Tumors treated with pegzilarginase underwent autophagy and early apoptosis during the initial period of systemic arginine depletion. Pegzilarginase treatment increased the fraction of CD8+ T cells expressing early activation markers CD69 and CD25. The combination treatment regimen induced a significant increase in serum interferon-gamma levels, as well as an increase in total and activated intratumoral CD8+ T cells relative to either monotherapy.

Conclusions

Pegzilarginase monotherapy enhances tumor immune infiltration and early CD8+ T cell activation. The combination of pegzilarginase with IO agents results in greater anti-tumor activity than either IO agent alone and is marked by an increase in tumor-infiltrating immune cells, including a large number of activated cytotoxic T cells. These findings support pursuit of clinical studies combining pegzilarginase with immuno-oncology agents.

References

1. Patil M et al. Arginine dependence of tumor cells: Targeting a chink in cancer's armor. Oncogene. 2016; 35: 4957-722. You L et al. The crosstalk between autophagic and endo-exosomal pathways in antigen processing for MHC presentation in anticancer T cell immune responses. J Hematol Oncol. 2017; 10: 165.

P346

A phase 1b/2 study of the safety and efficacy of HBI-8000-nivolumab combination in melanoma (MEL), renal cell carcinoma (RCC) and non-small cell lung cancer (NSCLC)

Reid Bissonnette[1], Nikhil Khushalani, MD[2], Zeynep Eroglu, MD[2], Andrew Brohl, MD[2], Thai Ho, MD, PhD[3], Heather Yeckes-Rodin, MD[4], Michael Kurman, MD[1], Mireille Gillings, PhD[1], Gloria Lee, MD, PhD[1]

[1]HUYA Bioscience International, San Diego, CA, USA
[2]H. Lee Moffitt Cancer Center, Tampa, FL, USA
[3]Mayo Clinic Arizona, Phoenix, AZ, USA
[4]Hematology-Oncology Associates of the Treasure Coast, Port St Lucie, FL, USA

Background
HBI-8000 is a Class I selective oral benzamide histone deacetylase inhibitor (HDACi). It is in registration trials in Japan and Korea for lymphoma and marketed in China. Its demonstrated immune modulatory effects include (i) enhanced immune cell-mediated cytotoxicity; (ii) enhanced tumor infiltration, and (iii) decreased tumor infiltration and expansion of T-regulatory and myeloid derived suppressor cells that suppress antitumor immunity.

Methods
The safety of HBI-8000 in combination with standard dose nivolumab (NIVO) was evaluated in a Phase 1b trial utilizing a 3+3 design escalating from 20, 30 to 40 mg twice weekly (BIW). The recommended Phase 2 dose (RP2D) was determined by dose limiting toxicity (DLT). In Phase 2, the disease cohorts were expanded to explore the efficacy of HBI-8000 at RP2D in combination with NIVO. Pharmacokinetics (PK), thorough QTc and pharmacodynamics (PD) were also studied.

Results
Phase 1b evaluated 15 pts (6 RCC, 5 MEL, 4 NSCLC,) for DLT; DLTs (1 fatigue G3 and 1 headache G3) were observed at 40 mg BIW. 30 mg BIW was selected as the RP2D. Tumor responses were 6 PRs (40%; 3 MEL, 2 RCC, 1 NSCLC); 5 SD; and 4 PD. At RP2D, 47 pts with Mel, NSCLC and RCC with or without prior checkpoint inhibitor (CPI) therapy were enrolled. As of Jul 20 2018, 20 MEL CPI-naïve pts (including Ph1) were evaluable for response with an objective response rate of 65% (1 CR, 10 PR). The median follow-up was 110 days, median time to response 56 days (range: 53-112) and the median progression-free survival had not been reached (range: 12 – 515+). Thirteen patients continue on treatment. The most common side effects attributed to HBI-8000 were Grade 3 hypophosphatemia (N=11), neutropenia (N=6), lymphopenia (N=5), fatigue (N=3), thrombocytopenia (N=2), nausea/anorexia (N=2), headache, diarrhea, anemia, transaminase elevation (N=1 each), and G4 lymphopenia (N=1). No increase of irAEs were detected. A QTc study with time-matched PK found no evidence of QTc prolongation. Patient accrual is ongoing.

Conclusions
The combination of HBI-8000 and nivolumab was well tolerated without new toxicity concerns. Preliminary efficacy is encouraging, especially in CPI-naïve MEL. Investigations in additional indications, including NSCLC and RCC are ongoing.

Trial Registration
NCT02718066

Ethics Approval
The study was approved by participating study site's Institutional Review Board, and sponsor is in full compliance with all GCP and FDA regulations

P347

Targeting phosphatidylserine enhances the anti-tumor response to radiation therapy and immune checkpoint blockade in a preclinical melanoma model

Sadna Budhu, PhD[1], Rachel Giese, MD[1], Aditi Gupta, BA[1], Sara Schad, BS[1], Olivier De Henau, MD[1], Roberta Zappasodi, PhD[1], Luis Campesato, PhD[1], Christopher Barker, MD[1], Jedd D. Wolchok, MD, PhD[1], Taha Merghoub, PhD

[1]*Memorial Sloan-Kettering Cancer Center, New York, NY, USA*

Background

Phosphatidylserine (PS) is a phospholipid that is exposed on surface of apoptotic cells, viable tumor cells, and activated immune cells. It has been shown to promote immunosuppressive signals in the tumor microenvironment. In a mouse B16 melanoma model, targeting PS in combination with immune checkpoint blockade promoted greater anti-tumor activity than either agent alone. This combination was shown to enhance T cell infiltration and activation in the tumors of treated animals. Radiation therapy (RT) is an effective focal treatment of primary solid tumors but is less effective in treating metastatic solid tumors as a monotherapy. RT induces immunogenic tumor cell death and enhances tumor-specific T cell infiltration in treated tumors.

Methods

8-10 mice/group were injected intradermally on the right hind limb with 100,000 B16F10 melanoma cells. 7-10 days after implantation, tumors were treated locally with a single dose of 15Gy RT or 3-doses of 8Gy or 15Gy given every 2 days. 1 day after RT, mice were given antibodies to PS (mch1N11) and PD-1 (RMP 1-14) intraperitoneally every 3 days. Tumor surface area and overall survival of mice were used to determine efficacy of the combinations. For FACS analysis, tissues were collected between 1-10 days after RT in all treated groups.

Results

Local RT of B16 melanoma causes an increase in PS expression on the surface of viable tumor and immune infiltrates. Treatment of animals with an antibody that targets PS (mch1N11) synergizes with RT to improve anti-tumor activity and overall survival. The triple combination of mch1N11, RT and anti-PD-1 treatment displayed greater anti-tumor and survival benefit. We found an increase in proinflammatory M1-macrophages after treatment with RT and mch1N11. There was also an increase in CD8 T cell activation in the triple combination. We found that treatment of mice whose tumors are refractory to anti-PD-1 benefited from the combination RT and mch1N11 in both reduction of tumor burden and overall survival. Finally, we found an increase of PS expression on immune cells in the blood of melanoma patients 4-7 days post RT supporting the rationale for translating of this therapy into the clinic.

Conclusions

This finding highlights the potential of combining these agents to improve outcome in patients that are refractory to anti-PD-1 and may inform the design of future clinical trials with the human PS targeting antibody (Bavituximab) in multiple cancers.

P348

Survival and immune modulation in homologous recombination deficient murine ovarian tumors using the PARP inhibitor, rucaparib and immune agonist, NKTR-214

Deborah Charych, PhD[1], Liliane Robillard, PhD[2], Andrew Simmons, PhD[2], Thomas Harding, PhD[2], Minh Nguyen[2], Rachel Dusek, PhD[2]

[1]Nektar Therapeutics, San Francisco, CA, USA
[2]Clovis Oncology, San Francisco, CA, USA

Background

Ovarian cancer is the most lethal cancer of the female reproductive system and its treatment remains an unmet medical need.[1] One major advance is the use of poly(ADP-ribose)polymerase (PARP) inhibitors, now approved for both treatment and maintenance-treatment of recurrent ovarian cancer. Although ovarian cancer has low response to checkpoint inhibitors, IL2 has shown clinical promise in platinum-resistant and refractory disease.[2] The IL2-pathway agonist NKTR-214 activates and mobilizes CD8T and NK cells to tumor in human and mouse via the IL2R$\beta\gamma$ complex. The unique mechanistic combination of synthetic lethality (rucaparib) plus lymphocytic immune activation (NKTR-214) may enhance durable responses.

Methods

Two ovarian lines with genetic alterations frequent to human high grade serous ovarian cancer were used: ID8-BRCA2-/- (ID8) orthotopic primary tumors form direct contact with murine ovarian stroma, secondary carcinomatosis and extensive ascites with disease progression similar to human and BR5FVB1 (BR5) with p53-/-, BRCA1-/-, myc and Akt. Tumor cells were implanted orthotopically into immune competent mice (n=10/group) by intraperitoneal injection (ID8) or subcutaneously (BR5) and monitored respectively for frank ascites/survival or growth inhibition of established (125 mm3) tumors. Mice were treated with rucaparib (150mg/kg BID×28 days), NKTR-214 (0.8mg/kg Q9D×3), or combination. A triplet was included in ID8 (rucaparib+NKTR-214+anti-pD1). Immune modulation was evaluated by IHC and gene expression.

Results

In the orthotopic ovarian survival model, treatment with rucaparib or NKTR-214 increased median survival compared to vehicle (70 and 81 days respectively versus 53 days, p<0.0005). In contrast, median survival was 101 days for rucaparib+NKTR-214 doublet. Triplet therapy rucaparib+NKTR-214+anti-PD1 did not significantly add survival, median 104 days. In BR5, treatment with NKTR-214+rucaparib suppressed tumor growth by 88.5% by day 59 with 50% tumor-free mice by day 113 compared to 0% for either single agent. An increase in infiltrating cytotoxic CD8 T and NK cells to the tumor with complementary induction of dendritic cells, neutrophils and interferon-gamma-induced chemokines was observed in tumors after rucaparib+NKTR-214.

Conclusions

The combination of synthetic lethality (rucaparib) with lymphocytic stimulation (NKTR-214) provided significantly increased survival and durable complete response in orthotopic and subcutaneous ovarian cancer models. These unique murine tumors demonstrated disease progression and genetic aberrations parallel to human tumorigenesis, atypical of syngeneic preclinical studies. Profiling of tumors suggested the activity of this combination is through antigen priming of infiltrating memory T cells, increased NK cell recruitment and enhanced cytotoxicity of tumor infiltrates.

References

1. Torre LA, Trabert B, DeSantis CE, Miller KD, Samimi G, Runowicz CD, Gaudet MM, Jemal A, Siegel RL: Ovarian cancer statistics, 2018. CA Cancer J Clin (2018).2. Vlad AM, Budiu RA, Lenzner DE, Wang Y, Thaller JA, Colonello K, Crowley-Nowick PA, Kelley JL, Price FV, Edwards RP: A phase ii trial of intraperitoneal interleukin-2 in patients with platinum-resistant or platinum-refractory ovarian cancer. Cancer immunology, immunotherapy (2010) 59(2):293-301.

Ethics Approval

The study was conducted in accordance with humane, responsible, ethical and scientifically sound

use of animals at Crown Biosciences International, Santa Clara, CA (HQ) in compliance with US and Chinese governments, international regulations, and AAALAC accreditation requirements. These include coordination with IACUC for implementation of the company's animal care and use policies, programs and Standard Operating Procedures.

P349

Spatial distribution analysis reveals increased PD1 expression on cytotoxic T cells leading to tumor regression upon combined MEK and HDAC inhibition in spontaneous PDAC mouse model

Phyllis Cheung, PhD[1], Jens T. Siveke[1], Anna Bazarna[1], Christian Neander[1], Konstantinos Savvatakis[1], Sven-Thorsten Liffers[1], Marija Trajkovic-Arsic[1], Aayush Gupta[2], Alexander Herner[2], Phyllis Cheung, PhD[1]

[1]*University Hospital Essen, DKFZ, Essen, Germany*
[2]*Technischen Universität München, Munich, Germany*

Background
Immunotherapy has demonstrated limited efficacy in pancreatic ductal adenocarcinoma (PDAC), which is likely due to the extensive desmoplasia comprising heterogeneous cell populations with complicated interactions. Integrated, multi-omic and multiplexed technologies are essential for understanding the cellular changes in the complex microenvironment upon therapeutic treatments. Emerging preclinical studies have demonstrated the ability of MEK and HDAC inhibitors (MEKi and HDACi) to sensitize tumor cells to immune checkpoint inhibition. Here, we evaluated the impact of MEKi alone, or in combination with HDACi, on the immune landscape of PDAC using gene expression array, multiplexed immunofluorescence imaging and spatial distribution analysis.

Methods
Spontaneous PDAC mouse models were treated with MEKi and/or HDACi and the tumors were profiled using Nanostring PanCancer Immune Panel and gene expression array, followed by validation using immunohistochemical (IHC) and immunofluorescent (IF) staining at protein level. Spatial distribution of immune cells and tumor cells was investigated by multiplexed IF staining and analyzed computationally for quantification, co-expression and spatial distribution.

Results
Nanostring analysis and GSEA demonstrated that MEKi treatment alone resulted in M2 macrophage reduction, and increase in infiltrating cytotoxic T cells and PD1 expression. Upon combination with HDACi, PD1 level was further augmented, while iNOS and cleaved caspase 3 were increased when compared to MEKi alone. Multiplexed IF staining and computational analysis showed that the augmented PD1 expression induced by combined treatment was largely found on CD8+ T cells. Notably, spatial distribution analysis showed that the tumor cells in close proximity of PD1+CD8+ cells expressed high levels of iNOS and cleaved caspase 3, and low level of proliferation marker Ki67. The findings suggest that the PD1+CD8+ cells are spatially associated with increased apoptosis and reduced proliferation in tumor cells. Indeed, better survival was observed in mice with combined treatment, although statistical significance cannot be reached due to small sample size.

Conclusions
Our findings provide evidence for the beneficial role of PD1 expression on CD8+ cytotoxic cells in anti-tumor responses induced by combined MEK and HDAC inhibition. Besides, the application of multiplexed imaging and spatial distribution analysis improve our understanding of cellular interactions upon treatment and therefore provide new insights into the optimization of potential therapies.

Ethics Approval
Animal experiments for establishment and analysis of immune-based therapeutic strategies as described above in the genetically-induced, spontaneous, immunocompetent PDAC model have been approved by the Landesamt für Natur, Umwelt und Verbraucherschutz (LANUV) Nordrhen-Westfalen.

P350

First-line nivolumab plus ipilimumab is associated with lower costs per responder versus sunitinib among patients with advanced renal cell carcinoma

Toni Choueiri[1], Keith Betts, PhD[2], Shuo Yang, PhD[3], Ella Du, MESc[2], Sumati Rao, PhD[3], Saby George, MD, FACP4

[1]Dana-Farber Cancer Institute, Boston, MA, USA
[2]Analysis Group, Inc., Los Angeles, CA, USA
[3]Bristol-Myers Squibb, Lawrence Township, NJ, USA
[4]Roswell Park Comprehensive Cancer Center, Buffalo, NY, USA

Background
In the CheckMate 214 (CM214) clinical trial, nivolumab plus ipilimumab (N+I) demonstrated superior objective response rates (ORRs), more durable responses, and longer overall survival compared with sunitinib (S) as first-line treatment for patients with intermediate/poor-risk advanced renal cell carcinoma (aRCC). This study compared the cost per responder (CPR) and cost per month of response (CPMR) of N+I versus S as first-line treatment from a third-party US payer perspective, to better assess the value of this immuno-oncology combination and optimize treatment decisions.

Methods
CPR and CPMR over 1 year and over the available trial follow-up period were calculated by dividing the total cost per patient by the ORR and mean duration of response (mDOR), respectively, over each assessment period. ORR and mDOR, as well as other clinical inputs (drug dosage, adverse event frequency, subsequent treatments, and death rates) were obtained from CM214 for each treatment arm. Costs of drug acquisition and administration, all-cause adverse events, subsequent treatment, and terminal care were included in calculating total cost per patient accrued in each assessment period from a US payer perspective. The statistical differences in CPR and CPMR between the two treatments were assessed using the delta method.

Results
With a median follow-up of 25.2 months in CM214, N+I had a higher ORR and mDOR in each assessment period than S, and the incremental benefit of N+I in mDOR versus S increased over time. For both assessment periods, N+I had a lower CPR and CPMR (Table 1). Over 1 year, the CPR for N+I was $55,036 lower than S (P=0.260). The difference in CPR between N+I and S increased over time, and over the available follow-up period the CPR for N+I was $126,249 lower than S (P=0.113). Considering duration of response, the CPMR for N+I was $9,099 lower (P=0.094) over 1 year and $15,973 lower (P=0.004) over the available follow-up period compared with S. The cost savings of N+I increased over time as well.

Conclusions
First-line N+I for aRCC was associated with lower CPR and CPMR, due in part to superior ORR and mDOR compared with S. With longer follow-up time, the clinical benefits of N+I were more pronounced compared with S, indicating that the combination immunotherapy is a more cost-effective first-line choice for intermediate/poor-risk aRCC.

Acknowledgements
The authors thank Matt Driver and Yichen Lu (Analysis Group, Inc.) for analytical support, and PPSI (a PAREXEL company) for editorial support, funded

by Bristol-Myers Squibb.

Trial Registration
NCT02231749

Table 1.

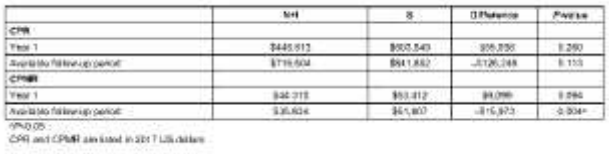

P351

ADU-S100 (MIW815) synergizes with checkpoint inhibition to elicit an anti-tumor CD8+ T cell response to control distal tumors

Kelsey Sivick Gauthier, PhD[1], Anthony Desbien, PhD[1], Gabrielle Reiner[1], Leticia Corrales[1], Weiwen Deng[1], Laura Glickman, PhD[2], Natalie Surh[1], Brian Francica[1], David Kanne[1], Justin Leong, PhD[1], Ken Metchette[1], Lianxing Zheng[3], Charles Cho[4], Yan Feng[3], Jeffrey McKenna[3], Steve Bender, PhD[4], Chudi Ndubaku[1], Meredith Leong[1], Thomas Dubensky, Jr.[5], Andrea van Elsas[6], Sarah McWhirter[1]

[1]Aduro Biotech, Berkeley, CA, USA
[2]Aduro Biotech, currently Actym Therapeutics, Berkeley, CA, USA
[3]Novartis Institutes for BioMedical Research, Cambeidge, MA, USA
[4]Genomics Institute of the Novartis Research Foundation, San Diego, CA, USA
[5]Aduro Biotech, currently Tempest Therapeutics, Berkeley, CA, USA
[6]Aduro Biotech Europe, Oss, Netherlands

Background
STimulator of Interferon Genes (STING) is a critical component of an innate immune pathway that activates robust anti-viral and anti-tumor responses in mouse models [1,2,3,4]. Small molecule agonists of STING are being developed as cancer immunotherapeutics due to potent anti-tumor efficacy and induction of immunity to rechallenge in pre-clinical models [5]. Activation of the STING pathway by intratumoral (IT) injection of synthetic cyclic dinucleotides (CDNs) induces type I interferons in tumor resident-myeloid subsets, activation of antigen presenting cells, expansion of tumor-specific CD8+ T cells and control of tumors [5,6,7].

Methods
In this study, we explored the benefit of combining CDN IT therapy with immune checkpoint blockade. ADU-S100 (MIW815), a CDN under clinical evaluation, was administered by IT injection in syngeneic mouse tumor models to assess the efficacy in combination with checkpoint inhibition.

Results
In mice bearing dual flank 4T1 mammary carcinoma tumors resistant to anti-PD-1 treatment, adding a single dose of ADU-S100 with anti-PD-1 induced eradication of both injected and non-injected tumors, leading to complete responses, demonstrating that ADU-S100 potentiates the activity of checkpoint blockade. Tumor control was CD8+ T cell-dependent and correlated with an enhanced CD8+ T cell effector profile in both the periphery and in non-injected tumors. Combining a single injection of ADU-S100 with anti-PD-1 also elicited enhanced tumor control in the MC-38 colon carcinoma model compared to ADU-S100 or anti-PD-1 treatment alone. Moreover, in the poorly immunogenic B16.F10 model, adding ADU-S100 to the ineffective combination therapy of anti-PD-1 and anti-CTLA-4 induced tumor-specific CD8+ T cell responses and tumor control, leading to multiple complete responses and durable immunity in surviving animals.

Conclusions

Together, these results highlight the immune correlates of STING-mediated anti-tumor efficacy and illustrate the potential of combining ADU-S100 (MIW815) with checkpoint inhibitors for the treatment of human cancer. Clinical trials of ADU-S100 in combination with anti-PD-1 or with anti-CTLA-4 are ongoing and could further elucidate the immunological mechanism of action and therapeutic effect in humans.

References

1. Diamond MS, Kinder M, Matsushita H, Mashayekhi M, Dunn GP, Archambault JM, et al. Type I interferon is selectively required by dendritic cells for immune rejection of tumors. The Journal of Experimental Medicine. 2011;208(10):1989–2003. 2. Fuertes MB, Kacha AK, Kline J, Woo S-R, Kranz DM, Murphy KM, et al. Host type I IFN signals are required for antitumor CD8 T cell responses through CD8α dendritic cells. The Journal of Experimental Medicine. 2011;208(10):2005–16. 3. Ishikawa H, Barber GN. STING is an endoplasmic reticulum adaptor that facilitates innate immune signalling. Nature. 2008;455(7213):674–8. 4. Woo S-R, Fuertes MB, Corrales L, Spranger S, Furdyna MJ, Leung MY, et al. STING-Dependent Cytosolic DNA Sensing Mediates Innate Immune Recognition of Immunogenic Tumors. Immunity. 2014;41(5):830–42 5. Corrales L, Glickman LH, McWhirter SM, Kanne DB, Sivick KE, Katibah GE, et al. Direct activation of STING in the tumor microenvironment leads to potent and systemic tumor regression and immunity. Cell Reports. 2015;11(7):1018-30. 6. Francica BJ, Ghasemzadeh A, Desbien AL, Theodros D, Sivick KE, Reiner GL, et al. TNFα and radioresistant stromal cells are essential for therapeutic efficacy of cyclic dinucleotide STING agonists in nonimmunogenic tumors. Cancer Immunology Research. 2018;6(4):422–33. 7. Corrales L, McWhirter SM, Dubensky TW, Gajewski TF. The host STING pathway at the interface of cancer and immunity. Journal of Clinical Investigation. 2016Jan;126(7):2404–11.

Ethics Approval

All animals were used according to protocols approved by Institutional Animal Use Committee of Aduro Biotech and maintained in specific pathogen-free conditions in a barrier facility.

P352

Blocking colony stimulating factor 1 receptor (CSF-1R) and tropomyosin receptor kinase A (TrkA) improves the anti-tumor efficacy of immune checkpoint blockade

Colm Duffy, BA[1], Stephen Mok[1], James Allison, PhD[1]

[1]*The University of Texas MD Anderson Cancer Center, Houston, TX, USA*

Background

Established tumors can escape immune responses by secreting the cytokine colony stimulating factor 1 (CSF-1), stimulating the proliferation and recruitment of immunosuppressive myeloid cells to the tumor microenvironment by binding to colony stimulating factor-1 receptor (CSF-1R). Additionally, the neurotrophin nerve growth factor (NGF) is a ligand for tropomyosin receptor kinase A (TrkA), which is over-expressed on multiple tumor types. Signaling through TrkA via the Akt and MAPK pathways regulates the survival, proliferation and invasion of tumor cells. PLX7486 is a novel orally bioavailable small molecule Trk and CSF-1R dual-inhibitor that is now being studied in Phase I clinical trials. We hypothesized that PLX7486 would synergize with immune checkpoint blockade to result in a greater antitumor effect, by targeting Trk signaling directly on cancer cells and by inhibiting the recruitment of immunosuppressive myeloid cells through CSF-1R, thus enabling an improved antitumor T cell response.

Methods
Various cancer cell lines were assessed by Western blot to determine whether TrkA and CSF-1 are expressed. Murine cancer cells, myeloid cells and T cells were treated with various concentrations of PLX7486 to determine effects on cell viability. Mice were subcutaneously implanted with MC38, B16F10 or MT4 cancer cells and treated with combined PLX4786 and anti-CTLA-4 or anti-PD-1 to determine the effects on tumor growth and on subpopulations of immune cells within the tumor microenvironment.

Results
We confirmed the expression of TrkA receptor on multiple murine cancer cell lines in vitro and exposed them to PLX7486, showing a direct cytotoxic effect with an IC50 of 5-8µM on most of the cell lines and an inhibition of AKT pathway signaling in MC38 cells. PLX7486 also had a direct cytotoxic effect on bone marrow-derived macrophages and the murine macrophage cell line RAW264.7 with an IC50 <1µM, while it had no effect on activated T cells in vitro. Combining PLX7486 and anti-CTLA-4 or anti-PD-1 in vivo in MC38, B16F10 or MT4 tumor models resulted in increased antitumor effects and a reduction in immune suppression within the tumor microenvironment.

Conclusions
The combined treatment groups of PLX7486 and anti-CTLA-4 or anti-PD-1 showed significant superiority in vivo in multiple tumor models. Our work provides rationale for testing this combined therapy in cancer patients.

Acknowledgements
We thank F. Hasan for illustration and members of the Allison lab for helpful discussions. This work was supported by a grant from Cancer Prevention and Research in Texas to J.P.A. (R1203). C.R.D. was supported by the CPRIT Research Training Grant (RP170067). S.M. is a CRI Irvington Postdoctoral Fellow. J.P.A. is a Co-Director of the Parker Institute for Cancer Immunotherapy.

Ethics Approval
The study was approved by MD Anderson Cancer Center`s Institutional Animal Care and Use Committee, Study # 00001221-RN01

P353

Strategic combination of multiple immune-oncology agents to engage, expand, and enable immune responses against tumors

Kellsye Fabian, PhD[1], Michelle Padget[1], Anthony Malamas[1], Rika Fujii[1], John Lee, MD[2], Jeffrey Schlom, PhD[1], James W. Hodge, PhD, MBA[1]

[1]CCR, NCI, NIH, Bethesda, MD, USA
[2]NantKwest, Culver City, CA, USA

Background
We hypothesize that in order for immunotherapy mount an effective and sustainable response against tumors, multiple levels of immune cell-tumor interaction must be interrupted. Therefore, optimal therapy of established tumors would require multiple agents that would 1) engage the immune response and generate tumor specific effector cells; 2) expand the number and breadth of the immune effector cells; and 3) enable the anti-tumor activity of these immune cells in the tumor microenvironment.

Methods
4T1-bearing Balb/c mice and MC32a-bearing C57BL/6 mice were treated with vaccine (adenovirus-Twist or adenovirus-CEA), cytokine (IL-15 superagonist), antibody agonist for co-stimulatory receptors (anti-OX40 and anti-4-1BB), immune checkpoint inhibitor (anti-PD-L1), and chemotherapy (docetaxel). Primary and metastatic tumor growth inhibition and generation of anti-tumor immune effector cells were used as primary efficacy

endpoints.

Results
Administration of 1-2 agents had no antitumor activity while the combination of 3-5 agents had modest antitumor effects. On the other hand, the concurrent treatment with all six agents (hexatherapy) was able to significantly induce anti-tumor responses and reduce tumor burden. Hexatherapy modified the tumor immune landscape by favoring effector T cells and limiting the immunosuppressive cell populations, thus improving the CD4+ T cell:Treg and CD8+:Treg ratios. Furthermore, tumor infiltrating T cells in the mouse cohort that received hexatherapy have higher proliferative capacity (Ki67+) and have significantly less exhausted phenotype showing less PD-1 and CTLA-4- expression.

Conclusions
These data demonstrate that strategic combination of multiple immune-oncology agents that can engage, expand, and enable the immune response is imperative for optimal anti-tumor therapy.

Ethics Approval
The study was approved by the NCI ACUC, protocol number LTIB-30.

P354

Co-clinical trials of MEK inhibitor, anti PD-L1 and anti CTLA-4 combination treatment in Non-Small Cell Lung Cancer

Pierre-Olivier Gaudreau[1], David Peng, PhD[1], Bertha Leticia Rodriguez[1], Jared Fradette[1], Laura Gibson[1], Samrat Kundu, PhD[1], Limo Chen, PhD[1], Jennifer Wargo, MD, MMSc[1], Don Gibbons, MD, PhD[1]

[1]MD Anderson Cancer Center, Houston, USA

Background
Immunotherapies involving the PD-1 / PD-L1 axis have revolutionized the treatment of non-small cell lung cancer (NSCLC), but novel combination therapies are needed to improve the overall response rate. Current work by our group using mutant KRAS and TP53 (KP) mouse models of NSCLC have shown that rationally designed therapies combining PD-L1 immune checkpoint blockade with MEK inhibitors significantly decrease tumor growth and metastasis compared to either monotherapies in syngeneic KP mice tumors. Despite these encouraging results, therapeutic resistance still occurs. Reverse Phase Protein Array (RPPA) and FACS analyses from these tumors showed an increase in Tregs and CTLA-4 immune checkpoint expression. As anti CTLA-4 checkpoint blockade is particularly effective in increasing the CD8 / Treg lymphocyte ratio [1], we hypothesized that the addition of this agent as a novel triple combination therapeutic strategy may improve the outcome by depleting Tregs and neutralizing CTLA-4 expression.

Methods
Using in vivo KP subcutaneous tumors (sv129 genetic background), we compared the triple combination of the MEK inhibitor selumetinib, anti PD-L1 and anti CTLA-4 or IgG2b isotype control antibodies. Tumor sizes were assessed weekly with digital calipers, and tumor weights and lung metastasis were quantified visually at the end of treatment following mice euthanasia. Fresh cells were characterized by FACS to establish the tumor-infiltrating immune cell profile. Tumor specimens were processed for RPPA and custom codeset Nanostring analyses for further mechanistic insights. In an upcoming single center, Phase I / II clinical trial, two combination schedules of selumetinib, tremelimumab and durvalumab will be compared with historical controls in patients (n = 40) with previously treated, metastatic NSCLC. The primary objective is to assess progression-free survival, and secondary objectives include further clinical outcomes and markers of response and resistance in pre- and on- treatment biopsies.

Results
The addition of anti CTLA-4 to anti PD-L1 and MEK inhibitor treatment improved survival in the epithelial KP mouse model (log-rank test, p=0.0078) (Figure 1). Animal trials using the mesenchymal KP model, along with correlative analyses (i.e., FACS, RPPA, Nanostring) for both models, are currently underway. The Phase I / II clinical protocol is undergoing regulatory review.

Conclusions
The combination of a MEK inhibitor, anti PD-L1 and anti CTLA-4 improves survival in epithelial KP tumor models of NSCLC. Correlative analyses to gain mechanistic insights of efficacy are ongoing. Accrual for the Phase I / II clinical trial is expected to start in early 2019.

Acknowledgements
This work is supported by an operating grant to D.L. Gibbons from the NIH/NCI ("The Role of Epithelial-Mesenchymal Transition in Re-Wiring KRAS Mutant Lung Cancer"; grant number: 1R37CA214609-01A1). P.O. Gaudreau is supported by the Fonds de Recherche Québec–Santé's (FRQS) Resident Physician Health Research Career Training Program program (grant number: 32667).

Trial Registration
ClinicalTrials.gov identifier: NCT03581487MD Anderson Cancer Center trial number: 2017-0888

References
1. Wei SC, Levine JH, Cogdill AP et al. Distinct Cellular Mechanisms Underlie Anti-CTLA-4 and Anti-PD-1 Checkpoint Blockade. Cell 2017; 170: 1120-1133.

Ethics Approval
The clinical trial discussed in the abstract was approved by the MD Anderson Cancer Center IRB (protocol 2017-0888).

Figure 1.

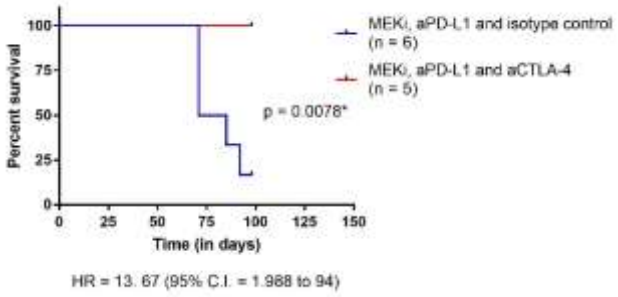

P355

Nivolumab plus ipilimumab is associated with lower number needed to treat compared with sunitinib for preventing death in advanced renal cell carcinoma

Saby George, MD, FACP[1], Keith Betts, PhD[2], Shuo Yang, PhD[3], Ella Du, MESc[2], Jennifer Johansen, PharmD, BCPS[3], Sumati Rao, PhD[3], Toni Choueiri[4]

[1]*Roswell Park Comprehensive Cancer Center, Buffalo, NY, USA*
[2]*Analysis Group, Los Angeles, CA, USA*
[3]*Bristol-Myers Squibb, Lawrence Township, NJ, USA*
[4]*Dana-Farber Cancer Institute, Boston, MA, USA*

Background
Nivolumab plus ipilimumab (N+I) demonstrated superior efficacy and safety outcomes compared with sunitinib (S) as first-line treatment of intermediate/poor-risk advanced or metastatic renal cell carcinoma (aRCC) in the CheckMate 214 trial. To further quantify the clinical benefits and risks associated with these two treatments, this study estimated the number needed to treat (NNT) and number needed to harm (NNH) for N+I versus S in

previously untreated intermediate/poor-risk aRCC.

Methods

For patients with intermediate/poor-risk aRCC in CheckMate 214, the rates of objective response (ORR), overall survival (OS), and grade 3/4 adverse events (AEs) over 12 and 24 months were calculated using patient-level data. The NNTs were calculated for ORR and OS as the inverse of the absolute risk reduction between N+I and S over 12 and 24 months among all randomized patients (N+I, 425; S, 422). Similarly, the NNHs were calculated as the reciprocals of the absolute risk differences between the two treatments for treatment-related and all-cause grade 3/4 AEs among all treated patients (N+I, 423; S, 416).

Results

The NNT and NNH analyses showed consistent benefits of N+I over S in clinical efficacy and safety. At month 12, one death would be prevented if 12.50 (95% confidence interval [CI], 7.30-43.39) patients were treated with N+I instead of S (Table). At month 24, the NNT to prevent one death with N+I versus S was reduced to 8.18 (95% CI, 5.20-19.23). When ORR was assessed, the NNT to achieve one additional responder with N+I versus S was 6.32 (95% CI, 4.53-10.48) at month 12 and 6.62 (95% CI, 4.67-11.36) at month 24. When safety was evaluated, for every 4.32 (95% CI, 3.24-6.47) patients treated with S instead of N+I, one additional patient would have experienced a treatment-related grade 3/4 AE over 12 months (Table). The NNH for an all-cause grade 3/4 AE over 12 months was 6.02 (95% CI, 4.37-9.64) and remained similar over 24 months.

Conclusions

The NNT/NNH analysis showed that among previously untreated patients with intermediate/poor-risk aRCC, N+I provides greater clinical benefits and is associated with significantly lower risks of grade 3/4 AEs compared with S. The survival benefit of N+I over S was even more pronounced when a longer follow-up period was evaluated, indicated by the reduction in NNT from month 12 to month 24. Future analyses based on longer-term data are warranted to quantify the benefits and risks associated with N+I beyond 2 years.

Acknowledgements

The authors thank Matt Driver and Lei Yin from Analysis Group for analytical support. Editorial support was provided by PPSI (a PAREXEL company), funded by Bristol-Myers Squibb.

Trial Registration

NCT02231749

Table 1.

Outcome	Time horizon, months	Outcome rate of N+I	Outcome rate of S	Absolute rate difference	NNT (95% CI) of N+I vs S	NNH (95% CI) of S vs N+I
OS	12	80.08%	72.08%	8.00%	12.50 (7.30-43.39)	–
	24	64.76%	52.54%	12.22%	8.18 (5.20-19.23)	–
Treatment-related grade 3/4 AE	12	49.14%	72.30%	23.16%	–	4.32 (3.24-6.47)
	24	56.49%	77.70%	21.22%	–	4.71 (3.38-7.76)

P356

CXCR4 antagonism converts the cold tumor into hot tumor by enhancing the infiltration of antigen-specific CD8 T-cells in the TME leading to increased anti-tumor effects of anti-OX40

Pankaj Gaur, PhD[1], Vivek Verma[1], Rahul Nandre, PhD[1], Ella Sorani, PhD[2], Abi Vainstein-Haras, MD[2], Galia Oberkovitz[2], Amnon Peled, PhD[3], Seema Gupta, PhD[1], Samir Khleif, MD[1], Stephen Shaw, PhD[4], Osnat Bohana-Kashtan[4]

[1]Georgetown University Medical Center, Washington, DC, USA
[2]BiolineRx Ltd., Modi'in, Israel
[3]Hadassah Hebrew University Hospital, Jerusalem,

Israel
[4]Bioline Rx, Sandwich, UK

Background
CXCR4 helps to retain the hematopoietic stem cells (HSC) in the bone marrow (BM). CXCR4 binds to its ligand CXCL12/SDF1 which is constitutively expressed in the BM thereby inhibiting the mobilization of CXCR4 expressing immune progenitor cells. Moreover, increased numbers of effector cells in the tumor microenvironment (TME) are directly correlated to enhanced immunotherapeutic efficacy. Therefore, CXCR4 antagonism will result in movement of immune cells to the periphery, increasing the infiltration of effector cells into the TME. Furthermore, signaling through OX40 is known to enhance the effector functions of CD8 T-cells and also generate immune memory. However, as a single agent anti-OX40 has not yet shown promising results in the clinic. Therefore, we hypothesized that combining anti-OX40 with CXCR4-antagonist will enhance the functionality of tumor-infiltrated effector cells as well as produce durable anti-tumor responses by augmenting immune memory.

Methods
To assess the anti-tumor response of CXCR4 in combination with anti-OX40, tumor-bearing mice were treated with anti-OX40 antibody (1 mg/kg twice weekly) and/or CXCR4 antagonist (BL-8040; 4 doses; 24 h apart; 20 mg/kg) in the presence of tumor-specific antigen priming (E7-peptide; 3 doses/ one week apart). Tumor growth and mice survival were recorded. Anti-tumor immune responses were determined in the tumors obtained 3-4 days after the second vaccination using flow cytometry.

Results
We found that BL-8040 given with specific antigenic stimulation results in increased anti-tumor immune response leading to significant decrease in tumor growth ($p \leq 0.001$ at day 21) and prolonged mice survival. BL-8040 significantly increases the numbers of total and antigen-specific CD8+ T-cells in the TME. Furthermore, in accordance with our hypothesis combination of CXCR4-antagonist and anti-OX40 treatment resulted in an increase in the functionality of tumor-infiltrated effector cells as determined by the numbers of total and antigen-specific granzyme B+ and IFN-gamma+ CD8+ T-cells, leading to significant delay in tumor growth and prolonged mice survival. In addition, this combination increased the central memory (CD62+ CD44+) in the TME, enhancing the durability of anti-tumor immune response.

Conclusions
Based on these findings, we conclude that CXCR4 antagonism converts cold tumors into hot tumors by facilitating the infiltration of tumor-specific effector cells into the TME. Further, anti-OX40 enhances the anti-tumor immune response by augmenting the effector functions of the tumor-infiltrated CD8+ T-cells and maintaining the durability of response by generation of immune memory. Hence, we demonstrate that the combination of agonist anti-OX40 with CXCR4-antagonist is a promising immunomodulatory strategy for cancer immunotherapy.

P357

Entinostat increases the frequency of tumor-specific effector T-cells and their functionality is enhanced by anti-OX40 leading to durable anti-tumor effects

Rahul Nandre, PhD[1], Vivek Verma[1], Pankaj Gaur, PhD[1], Hua Wang[2], Peter Ordentlich, PhD[3], Lei Wang, PhD[3], Seema Gupta, PhD[1], Samir Khleif, MD[1]

[1]Georgetown University Medical Center, Washington, DC, USA
[2]Augusta University, Augusta, GA, USA
[3]Syndax Pharmaceuticals, Waltham, MA, USA

Background

The epigenetic deregulation of T-cells and enhanced numbers of immunosuppressive cells in the TME are associated with decreased anti-tumor effects. Hence, targeting the epigenetic modifications using modulators such as histone-deacetylase inhibitors (HDACi) provides the basis for a potential role for these agents in cancer immunotherapy. Entinostat, an HDACi has been shown to reprogram the TME by impacting the numbers of CD8T-cells and immunosuppressive cells, resulting in enhanced anti-tumor activity when combined with immune-checkpoint blockade [1]. However, the combination effect of Entinostat with anti-OX40 remains poorly explored. Signaling through OX40 is known to enhance the effector functions of CD8T-cells. However, as a single agent anti-OX40 has not yet shown promising results in the clinic. Therefore, we hypothesized that the combination of Entinostat with anti-OX40 will enhance the effector-functions of CD8T-cells while simultaneously reducing the immunosuppressive cells in the TME, leading to improved anti-tumor effects.

Methods

In TC-1 mouse tumor model, Entinostat (3mg/kg) in combination with anti-OX40 (1mg/kg) and tumor-specific vaccine (E7-peptide; 3 doses one-week apart) was given. Tumor growth and mice survival were recorded. Three days after the second immunization, immune-responses were determined in the tumors.

Results

We show that Entinostat significantly increases the numbers of tumor-infiltrated CD8 and CD4 cells and reduces the frequency of immunosuppressive Tregs and MDSCs leading to a significant delay in tumor growth. However, none of the mice show complete tumor rejection and ultimately succumb to tumor burden. Importantly, Entinostat synergizes with anti-OX40, resulting in complete tumor regression in 100% of the mice that remain tumor free for rest of their lives. This effect is found to be associated with enhanced total and antigen-specific granzymeB+ and IFN-gamma+ CD8T-cells in the TME. In addition, anti-OX40 further reduces the Tregs and MDSCs in the TME. To test the durability of the anti-tumor response induced by Entinostat+anti-OX40, the mice with complete tumor rejection were re-challenged with the tumor. Although, the tumors grew avidly in untreated animals, none of the treated mice showed tumor development, clearly establishing a durable anti-tumor response after combination treatment.

Conclusions

These results highlight the ability of Entinostat in increasing the numbers of effector T-cells in the TME. Anti-OX40 significantly enhanced the functionality of these tumor-infiltrated effector cells leading to induction of robust and durable anti-tumor responses. Importantly, anti-OX40 further decreased the numbers of immunosuppressive populations in the TME. These data highlight that Entinostat enhances the anti-tumor efficacy of anti-OX40, which can be a promising strategy for cancer-immunotherapy.

References

1. Terranova-Barberio M, et al. HDAC inhibition potentiates immunotherapy in triple negative breast cancer. Oncotarget. 2017; 8:114156-114172.

P358

ROR-gamma agonist induces long-lived Th17 cells in the TME leading to increased anti-tumor effects of agonist anti-OX40

Pankaj Gaur, PhD[1], Vivek Verma[1], Rahul Nandre, PhD[1], Laura Carter, PhD[2], Xiao Hu, PhD[2], Xikui Liu, PhD[2], Seema Gupta, PhD[1], Samir Khleif, MD[1]

[1]Georgetown University Medical Center, Washington, DC, USA
[2]Lycera Corp, Ann Arbor, MI, USA

Background
T-cell costimulation through OX40 has been shown to promote expansion and proliferation of effector T-cells leading to enhanced effector functions, memory generation and immune inflammatory anti-tumor responses. However, treatment with anti-OX40 as a single agent has not led to major positive clinical outcomes. In preclinical models, we have recently shown that combining anti-PD-1 concurrently with anti-OX40 negates the effects of agonist anti-OX40 making identification of combination partners crucial for anti-tumor therapy. ROR-gamma-t, a master transcription factor is known to drive Type 17 T-cell differentiation. Synthetic, small molecule ROR-gamma agonists have been shown to enhance Type 17 T-cell effector functions and survival, decrease immune suppressive mechanisms and modulate expression of a number of costimulatory and coinhibitory molecules. We hypothesized that ROR-gamma agonist could enhance the anti-tumor effects of anti-OX40.

Methods
We tested using TC-1, a mouse tumor model where vaccine is used to prime the immune system and assessed the effects of agonist anti-OX40 antibody (1 mg/kg twice weekly) combined with a ROR-gamma agonist (LYC-54143; 100 mg/kg BID given continuously till the end of study) on growth of established tumors and survival.

Results
We found that the ROR-gamma agonist significantly delayed tumor growth and prolonged mice survival, which was by induction of Th17 cells in the TME. Analysis of the tumor microenvironment revealed that the functionality of ROR-gamma induced Th17 cells was significantly enhanced upon anti-OX40 treatment. Moreover, this treatment increased the numbers of total CD4+ T-cells including ROR-gamma-t+ and highly activated INF-gamma+ cells and decreased the Treg numbers. Furthermore, we found that ROR-gamma agonist+anti-OX40 resulted in an increase in the numbers of total and antigen-specific, granzyme B+, and IFN-gamma+ CD8+ T-cells as well as increased the central memory (CD62+ CD44+) in the TME.

Conclusions
ROR-gamma agonist enhances the anti-tumor effects of anti-OX40 leading to reduced tumor growth and prolonged mouse survival. These anti-tumor effects are mediated by generation of activated antigen-specific CD8+ and IFN-gamma+ Th17 cells with simultaneous decrease in the numbers of Tregs in the TME.

P359

Immune cell responses and dose scheduling optimization of radiation and anti-PD-L1 treatment combination using a joint experimental and systems modeling approach

Gabriel Helmlinger, PhD[1], Yuri Kosinsky, PhD[2], Simon Dovedi, PhD[3], Kirill Peskov, PhD[2], Veronika Voronova, MSc[2], Lulu Chu, PhD[1], Donald Stanski, MD[1]

[1]*AstraZeneca, Waltham, MA, USA*
[2]*M&S-Decisions LLC, Moscow, Russian Federation*
[3]*MedImmune, Manchester, UK*

Background
We explored the mechanistic interactions between radiation therapy (RT) and the host immune system using a quantitative systems modeling approach to investigate how distinct variables may impact the immunogenicity of RT + immuno-oncology (IO) combination therapies. In addition to its cytoreductive effect RT also modulates the tumor microenvironment (TME) to facilitate an anti-tumor immune response. Combination therapies of RT + anti-PD-L1 mAb blockade have indeed shown synergy in a number of preclinical studies [1,2]. In the PACIFIC clinical trial, Imfinzi, an anti-PD-L1 mAb, was effective as a consolidation therapy following

platinum-based chemoradiotherapy, with statistically and clinical significant improvements in OS over placebo [3,4].

Methods

Based on data from [1], we developed an externally validated mechanistic population model of the origination and development of an anti-tumor T cell immune response linked to CT26 tumor size dynamics, following treatment with anti-PD-L1 mAb therapy alone and in combination with RT in a mouse model (Fig 1A). Variability in individual tumor size dynamics was taken into account using a mixed-effects model at the level of tumor infiltrating T cell influx.

Results

Upon external validation, the model was used prospectively to predict anti-tumor efficacy in a broad range of therapeutically-realistic RT and anti-PD-L1 mono- and combination dosing schedules. In full agreement with [1], scheduling of an anti–PD-L1 mAb with concomitant administration of RT – and not preceding RT - was required to maximize efficacy benefits (Fig 1B). The model also highlighted a pivotal role for the immune response in RT-induced tumor shrinkage: RT may indeed accelerate the development of an immune response by improving tumor antigen presentation, thereby inhibiting tumor growth and delaying the accumulation of immuno-suppressive regulatory T cells (Treg) as a result. The model accounted for the adaptive expression of PD-L1 in response to inflammatory changes in the local TME as a negative feedback which could be overcome by blockade of this axis. Combinations of RT and anti-PD-L1 treatments may offset the immuno-suppressive impact of Treg and PD-L1 expression over time, thereby inducing a sufficiently robust accumulation of cytotoxic T cells with subsequent tumor shrinkage or rejection.

Conclusions

This modeling study provides quantitative mechanistic insights into the links between RT and anti-tumor immune responses. The model may be used to determine appropriate combinations and schedules of immuno-modulation and RT to maximise the therapeutic potential of RT/IO combination therapy.

References

1. Dovedi S, et al. Acquired resistance to fractionated radiotherapy can be overcome by concurrent PD-L1 blockade. Cancer Res. 2014;74:5458-5468. 2. Deng L, et al. Irradiation and anti–PD-L1 treatment synergistically promote antitumor immunity in mice. J Clin Invest. 2014;124:687–695. 3. Antonia S, et al. Durvalumab after chemoradiotherapy in stage III non-small-cell lung cancer. N Engl J Med. 2017;377:1919-1929. 4. https://www.astrazeneca.com/media-centre/press-releases/2018/imfinzi-significantly-improves-overall-survival-in-the-phase-iii-pacific-trial-for-unresectable-stage-iii-non-small-cell-lung-cancer-25052018.html

Figure 1.

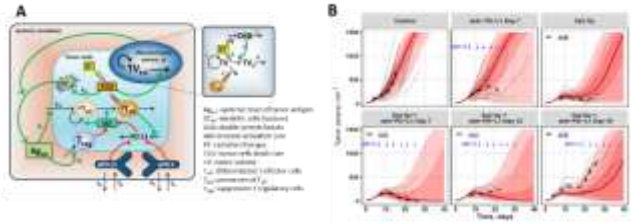

P360

Enhanced anti-tumor efficacy of mesothelin-targeted immunotoxin LMB-100 combined with anti-PD-1 antibody

Qun Jiang, PhD[1], Daniel Rathkey[1], Jingli Zhang[1], Ira Pastan, MD[1], Raffit Hassan, MD[1]

[1]*National Institutes of Health, Bethesda, MD, USA*

Background
LMB-100 is a recombinant immunotoxin, currently in phase I clinical trials that targets mesothelin (MSLN) a cell surface protein highly expressed in mesothelioma and lung adenocarcinoma. Given the high expression of PD-L1 in mesothelioma and lung cancer and promising clinical activity of PD-1/PD-L1 checkpoint inhibitors in these cancers, we aimed to evaluate if LMB-100 in combination with αPD-1 antibody will result in greater anti-tumor efficacy.

Methods
We established a human MSLN expressing syngeneic mouse model using PD-L1 positive mouse lung adenocarcinoma cell line 531LN2 stably transfected with a vector encoding hMSLN. Mice bearing 531LN2-hMSLN subcutaneous tumors were given no treatment, or intravenous LMB-100 alone, or intraperitoneal αPD-1 antibody alone, or LMB-100 plus αPD-1 antibody. Tumor growth and overall survival was analyzed. Using NanoString gene expression assay, we analyzed cancer associated immune gene expression induced by the drug administration. We then depleted CD8+ T cells using αCD8 antibody to identify its role in the drug induced anti-tumor effects. Finally, we evaluated LMB-100/αPD-1 combination in a mesothelin and PD-L1 positive patient derived mesothelioma RH63 humanized mouse model transplanted with healthy donor PBMCs.

Results
In mice bearing 531LN2-hMSLN tumors, tumor growth was significantly inhibited by LMB-100/αPD-1 treatment compared to mice treated with either drug alone. The median tumor volumes were 865mm3, 420mm3, 277mm3, and 65mm3 in untreated, LMB-100 treated, αPD-1 treated, and combination treated groups respectively on day 34 post tumor inoculation ($p<0.001$). The median overall survival was 38 days without treatment, 52 days with either LMB-100 or PD-1 antibody alone, and 74 days with the combination ($p<0.05$). We observed a significant increase of CD8+ T cells and Th1 cytokine signaling gene expression in tumors treated with LMB-100 /αPD-1 compared to either agent alone. After depletion of CD8+T cells, the anti-tumor benefits were significantly negated in LMB-100/αPD-1treated mice, suggesting their important roles. Furthermore, we observed similar LMB-100/αPD-1 combination-enhanced anti-tumor efficacy in healthy donor PBMCs transplanted mesothelioma RH63 humanized mouse model. The median tumor volumes were 350mm3, 306mm3, 248mm3, 216mm3and 135mm3 in untreated, PBMCs transplanted, LMB-100 treated, PBMCs plus αPD-1 treated, and PBMCs plus LMB-100/αPD-1 combination treated groups respectively on day 41 post tumor inoculation ($p<0.001$).

Conclusions
Our study demonstrates that LMB-100/αPD-1 antibody combination enhances CD8 T cells mediated anti-tumor efficacy in hMSLN expressing syngeneic lung cancer mouse model and humanized mesothelioma mouse model. Combination treatment with immune checkpoints and LMB-100 could be useful to treat patients with mesothelin positive cancers.

Acknowledgements
We thank Dr. Jonathan M. Kurie from MD Anderson Cancer Center for providing us 531LN2 cell line as a gift.

P361

Phase 1/2 study of mogamulizumab (anti-CCR4), to deplete regulatory T-cells, in combination with PD-1 checkpoint inhibitor nivolumab in subjects with locally advanced or metastatic solid tumors

David Hong, MD[2], Olivier Rixe, MD, PhD[3], Vi Chiu, MD, PhD[3], Patrick Forde, MD[4], Tomislav Dragovich, MD[5], Yanyan Lou, MD[6], Asha Nayak, MD[7], Rom Leidner, MD[8], James Atkins, MD[9], Agron Collaku,

PhD[1], Floyd Fox, PhD[1], Margaret Marshall, MD[1], Anthony Olszanski, MD, RPh[10]

[1]*Kyowa Kirin Pharmaceutical Development, Inc., Princeton, NJ, USA*
[2]*MD Anderson Cancer Center, Houston, TX, USA*
[3]*University of New Mexico Comprehensive Cancer Center, Albuquerque, NM, USA*
[4]*Sidney Kimmel Comprehensive Cancer Center, Johns Hopkins University School of Medicine, Baltimore, MD, USA*
[5]*Banner MD Anderson Cancer Center, Gilbert, AZ, USA*
[6]*Mayo Clinic Cancer Center, Jacksonville, FL, USA*
[7]*Georgia Cancer Center, MARTINEZ, GA, USA*
[8]*Providence Cancer Center, Portland, OR, USA*
[9]*Southeastern Medical Oncology Center, Goldsboro, NC, USA*
[10]*Fox Chase Cancer Center, Phildelphia, PA, USA*

Background
Tumors induce an immunosuppressive environment by recruiting regulatory T-cells (Tregs) that inhibit immune antitumor activity and T-cell activation via cell cycle checkpoints. Mogamulizumab (Moga), an antibody targeting anti-CC-chemokine receptor 4 (CCR4), eliminates CCR4+ cells in T cell malignancies, depletes a subset of high expressing CCR4+ Tregs, and is approved to treat CCR4+ T cell lymphomas in Japan. Nivolumab (Nivo), an antibody targeting the programmed cell death-1 (PD-1) checkpoint, is approved to treat several solid and hematologic tumors. We hypothesized that simultaneously blocking two suppressive pathways by combining Moga and Nivo may enhance antitumor activity.

Methods
We conducted a Phase 1 dose finding study in the U.S. to identify the maximum tolerated dose (MTD) for Moga+Nivo combination, and a Phase 2 expansion using the MTD regimen in tumor-specific cohorts. Subjects were excluded if previously treated with any drug targeting T cell stimulation or checkpoint pathways. The primary objective was to assess safety and tolerability. The secondary objectives were to evaluate antitumor activity based on overall response rate (ORR), time to response (TTR), duration of response, progression-free survival (PFS), and overall survival (OS). Exploratory objectives included examination of biomarkers by flow cytometry and immunohistochemistry

Results
A total of 114 subjects were enrolled and treated: n=4 in a single Phase 1 cohort and n=110 in 7 tumor-specific Phase 2 cohorts (see Table 1). There were no dose-limiting toxicities in Phase 1, and all Phase 2 subjects received the planned dose of 1 mg/kg Moga + 240 mg Nivo. Treatment emergent adverse event rates for all cancer types are shown in Table 2 (Table 2). There were 2 complete responses (both in subjects with ovarian cancer) and 10 partial responses, for an ORR (Table 1) of 10.5% (95% CI, 5.6, 17.7) and a median TTR of 2.34 months. For all subjects, median PFS was 2.6 months (95% CI, 2.3, 3.7) and median OS was 9.5 months (95% CI, 6.0, 13.8). The Moga+Nivo combination depleted effector Treg immunosuppressive populations in peripheral blood and within tumor stroma; however, this expected depletion was not correlated with treatment response.

Conclusions
Moga+Nivo combination therapy in multiple solid tumors demonstrated an expected safety profile and some antitumor activity. There was no additive antitumor effect seen with the combination of the two agents in this study. Further study may elucidate the effects of Moga on effector T cells.

Trial Registration
NCT02705105

Ethics Approval
This study was approved by an Institutional Review

Board at each investigative site.

Table 1.

Primary Tumor Type	Subjects Enrolled (n)	Overall Response Rate[a] n (%) (95% CI)
All cancer types	114	12 (10.5) (5.6, 17.7)
All in Phase 1 cohort	4	1 (25.0) (0.6, 80.6)
NSCLC, squamous cell	5	1 (20.0) (0.5, 71.6)
NSCLC, non-squamous, PD-L1 non-expressing	4	1 (25.0) (0.6, 80.6)
Squamous cell carcinoma of head and neck	10	3 (30.0) (6.7, 65.2)
Colorectal carcinoma, non-MSI high	29	1 (3.4) (0.1, 17.8)
Ovarian/Fallopian tube/primary peritoneal	21	3 (14.3) (3.0, 36.3)
Hepatocellular carcinoma	24	2 (8.3) 1.0, 27.0)
Pancreatic adenocarcinoma	17	0 (0.0, 19.5)

a: Number of Subjects with CR or PR; by RECIST v1.1 (from first dose of IMP to initiation of subsequent anti-cancer therapy)
CI=confidence interval, IMP=investigational medicinal product, MSI=microsatellite instability, NSCLC=non-small cell lung cancer, PD-L1=programmed death-ligand 1, RECIST=Response Evaluation Criteria in Solid Tumors

Table 2.

Adverse Event Category	All Cancer Types (Mega 1 mg/kg + Nivo 240 mg) N=114
Any treatment-emergent adverse event (TEAE)[a] (n, %)	114 (100.0)
Any IMP-related	104 (91.2)
Mega-related	101 (88.6)
Nivo-related	101 (88.6)
Any ≥Grade 3 TEAE (n, %)	90 (78.9)
Any IMP-related	45 (39.5)
Mega-related	41 (36.0)
Nivo-related	44 (38.6)
Any serious adverse event (SAE) (n, %)	68 (59.6)
Any IMP-related	24 (21.1)
Mega-related	20 (17.5)
Nivo-related	23 (20.2)

a: TEAEs during any cycle
IMP=investigational medicinal product; Mega=megagonadimumab, Nivo=nivolumab

P362

TTI-621 (SIRPαFc), an immune checkpoint inhibitor blocking the CD47 "do not eat" signal, enhances the anti-tumor effect of radiation and targeted therapy in ovarian cancer models

Lei Cui, PhD, BS[2], Hui Chen, BS[2], April Lewtak, MSc[2], Sean Oh[2], Carole Galligan, PhD[2], Simone Helke[2], Julia Berchadsky, PhD[2], Bob Uger, BS, PhD[2], Lisa Johnson, PhD[2]

[1]*Trillium Therapeutics, Mississauga, Canada*
[2]*Trillium Therapeutics Inc., Mississauga, Canada*

Background

Ovarian cancer (OVCa) is the most lethal gynecologic malignancy. With standard treatment demonstrating a high relapse rate, novel treatment strategies are needed. PARP inhibitors are approved as monotherapy agents for BRCA mutated OVCa, and function as radiosensitizers. Both radiotherapy (RT) and PARP inhibitors induce immunogenic cell death, release tumor antigens, and enhance the infiltration of immune cells, including macrophages, to tumor sites. Thus, innate checkpoint inhibition may enhance the anti-tumor effect of DNA damaging agents.CD47 is an immune checkpoint that binds signal regulatory protein alpha (SIRPα) and delivers a "do not eat" signal to suppress macrophage phagocytosis. It is frequently overexpressed by tumors to evade macrophage mediated destruction. TTI-621 (SIRPαFc), an immune checkpoint inhibitor consisting of the CD47 binding domain of human SIRPα linked to the Fc region of IgG1, blocks the CD47 "do not eat" signal and engages macrophages Fcγ receptors, thereby enhancing phagocytosis and antitumor activity. Here we report the efficacy of the combination of TTI-621 and DNA damaging therapeutics, RT and PARP inhibition, in BRCA competent and knock-down OVCa xenografts.

Methods

TTI-621, RT and niraparib (a PARP inhibitor) was evaluated alone or in combination in intraperitoneal tumor xenografts of BRCA competent and knock-down luciferase-expressing OVCa cells in NOD/SCID mice. TTI-621 (10 mg/kg) was administered intraperitoneally 1 hour prior to RT, 3 times per week for 3 weeks. Niraparib (50 mg/kg) was administered 1 hour prior to RT, 5 times per week for 1 week. Mice were treated with whole abdomen RT at a dose of 2

Gy for 2 fractions. Treatment efficacy was assessed by bioluminescent imaging (BLI) and survival. Systemic toxicity was evaluated by clinical parameter scoring.

Results

While TTI-621 monotherapy inhibited tumor growth in the BRCA competent xenograft model, the combination of TTI-621 and RT significantly improved survival compared to RT alone. Mice bearing BRCA knock-down tumors had improved survival with the TTI-621+niraparib combination compared to vehicle control. TTI-621 significantly enhanced survival when combined with RT, with extended survival observed in the RT+TTI-621+niraparib group. No chronic toxicity was observed for all the treatments.

Conclusions

The current study provides supportive evidence for combining innate modulation (TTI-621) with radiation therapy to improve overall survival in patients with OVCa. Additionally, patients with BRCA mutated tumors may benefit from triple therapy with TTI-621, niraparib and RT. Further studies are needed to assess the effect in models with intact adaptive immune systems.

Ethics Approval

The study was approved by the University Health Network's Animal Use Committee, protocol number 5603.

P363

Pegzilarginase in combination with agonist anti-OX40 therapy enhances T cell priming and effector function leading to improved tumor regression and survival

Melissa Kasiewicz, BS[1], Annah Rolig, Ph D[1], Elizabeth Sturgill, PhD[1], Mark Badeaux, PhD[2], Scott Rowlinson, PhD[2], William L. Redmond, PhD[1]

[1]*Earle A. Chiles Research Institute, Portland, OR, USA*
[2]*Aeglea BioTherapeutics, Austin, TX, USA*

Background

Tumor cells defective in enzymes required for arginine biosynthesis are dependent upon arginine uptake from the environment. Extracellular depletion of arginine directly affects tumor cells, inducing autophagy and apoptosis. Pegzilarginase (AEB1102) is a bioengineered, pegylated, human arginase 1 (Aeglea Biotherapeutics) currently in phase I clinical trials. This arginine-depleting agent has been shown to both inhibit arginine auxotrophic tumor growth and to enhance the efficacy of PD-L1 blockade in preclinical models. In the current study, we investigated the therapeutic efficacy and mechanism of action of combined pegzilarginase/anti-OX40 (aOX40) immunotherapy. We hypothesized that pegzilarginase/aOX40 treatment would synergize to enhance T cell priming and effector function leading to improved tumor regression and survival.

Methods

Efficacy studies were conducted in CT26 (colon) or MCA-205 (sarcoma) tumor-bearing mice. Eight days after subcutaneous tumor implantation, mice were treated with pegzilarginase (3 mg/kg; q7dx4; ip) and/or aOX40 mAb (10 mg/kg; d8, d12; ip). Seven days post-treatment (d15), the phenotype and effector status of T cells and myeloid populations within the lymph nodes (LN) and tumor were evaluated by flow cytometry. In additional cohorts, gene expression profiling (single cell RNAseq; scRNAseq) was performed 3 days post-treatment (d11). Survival studies were conducted in both models with tumor measurements taken twice weekly until tumor burden was greater than 150mm2. Data represents the results of 2-3 independent experiments (n=10/group) and for phenotyping assays, significance was determined by using a one-way ANOVA with a p-value cut-off of

0.05.

Results
We observed a significant reduction in tumor growth and increased overall survival following pegzilarginase/aOX40 therapy versus monotherapy in CT26 ($p<0.01$) and MCA-205 ($p<0.01$) tumor-bearing mice. Flow analysis revealed increased CD8+ T cell activation and effector function, as evidenced by higher levels of granzyme A, IFN-g and TNF-a. Evaluation of tumor infiltrating lymphocytes (TIL) showed increased granzyme A+ CD8+ T cells, but no differences among effector CD4 T cells, supporting the hypothesis that pegzilarginase /aOX40 therapy augments CD8 T cell-mediated anti-tumor immunity. Preliminary analysis of MDSC populations suggests a trend toward higher PD-L1 expression following combination therapy.

Conclusions
Collectively, these data demonstrate that pegzilarginase in combination with OX40 agonists can significantly impair tumor growth while promoting both T cell proliferation and effector function. These insights support further exploration of this novel combination approach in future clinical trials.

P364

Systemic anti-tumor immunity and immune memory formation by a novel TLR7/8 targeting agent NKTR-262 combined with CD122-biased immunostimulatory cytokine NKTR-214

Saul Kivimae, PhD[1], Marlene Hennessy, BS[1], Rhoneil Pena[1], Yolanda Kirksey, MSc[1], Wildaliz Nieves, PhD[1], Phi Quach, BS PhD[1], Janet Cetz, BS[1], Zhongxu Ren, PhD[1], Haiying Cai, BS[1], BoLiang Deng, PhD[1], Wen Zhang, PhD[1], Fiore Cattaruzza[1], Christie Fanton, PhD[1], Neel Anand, PhD[1], Werner Rubas, PhD[1], Stephen Doberstein, PhD[1], Loui Madakamutil[1], Jonathan Zalevsky, PhD[1]

[1]Nektar Therapeutics, San Francisco, CA, USA

Background
NKTR-262 is a novel intratumorally administered TLR7/8 agonist currently being investigated in the clinic in combination with NKTR-214, a systemically administered CD122-biased cytokine. NKTR-262 promotes an immune stimulatory environment and local injection site tumor antigen production limiting agonist release to systemic circulation. When NKTR-262 is administered in combination with NKTR-214 the combined effect of innate immune stimulation and enhanced antigen presentation with sustained T cell activation leads to systemic tumor immunity.

Methods
Syngeneic mouse tumor models with diverse histologies (CT26, EMT6, 4T1) were assessed for NKTR-262 and NKTR-214 combination treatment efficacy and immune system activation. Tumors were inoculated bilaterally to assess abscopal efficacy and systemic dissemination of anti-tumor CD8+ T cells. Once established, tumors were treated with a single unilateral peritumoral dose of NKTR-262, while NKTR-214 was administered i.v. on q9dx3 schedule. Efficacy correlating immune cell phenotyping was conducted from tumors and blood by flow cytometry to assess combination treatment synergy. Regression of NKTR-262-injected and contralateral tumors was assessed by tumor size measurements. NKTR-262 and NKTR-214 combination effect on T cell clonality and TIL infiltration were assessed by Adaptive ImmunoSEQ platform in the CT26 tumor model. Durable anti-tumor immune memory formation was assessed by tumor volume and immune phenotyping measurements in tumor rechallenge studies in CT26 and EMT6 models.

Results
NKTR-262 and NKTR-214 in combination showed efficacy in all tested tumor models, from significant tumor growth inhibition to complete tumor clearance in multiple models. Synergistic efficacy

correlated with sustained systemic expansion of tumor antigen specific CD8+ T cells that specifically required coordinated activation of the innate and adaptive arms of the immune system. NKTR-262 treatment significantly increased clonality and infiltration of NKTR-214 expanded T cells, accelerating expansion of tumor infiltrating clones. NKTR-262 and NKTR-214 combination treatment led to durable immune memory and resistance to secondary tumor challenge in multiple models correlating with spontaneous cytotoxic T cell response in secondary tumor lesions.

Conclusions

We present a designed combination therapy that mimics a natural immune response by activating a broad immune cell network in multiple nonclinical tumor models. Combining NKTR-262 with NKTR-214 engages the entire immune activation cascade required for systemic tumor clearance. Combination treatment coordinates tumor antigen presentation and costimulatory signaling with tumor antigen recognizing CD8+ T cell expansion to produce a sustained systemic anti-tumor immune response. A comprehensive anti-tumor immune activation by coordinated engagement of innate and adaptive immune cells may increase the success of immune therapy for patients.

Ethics Approval

All animal care and procedures were ethically approved and performed according to the AAALAC accredited Nektar Therapeutics IACUC guidelines, approval number 2017-001.

P365

Triple checkpoint blockade targeting PD-1, TIM-3, and LAG3 improves T cell reinvigoration and antitumor efficacy over single and double combinations

Johanna Kaufmann, PhD[1], Geeta Sharma[1], Srimoyee Ghosh, PhD[1], Sujatha Kumar, PhD[1], Kevin Coleman, PhD[1], Sridhar Ramaswamy, MD[1], David Jenkins, PhD[1]

[1]*TESARO, Inc., Waltham, MA, USA*

Background

Single T cell checkpoint blockade (CPB) with anti-PD-1/PD-L1 antibodies induces durable antitumor responses in subsets of patients. However, multiple immune checkpoint receptors (ICRs) are sequentially upregulated upon T cell activation and are also markers of an exhausted phenotype after chronic activation in the context of infections and cancer. We and others have described expression of the ICRs PD-1, TIM-3, and LAG3 on various tumor-infiltrating immune cell types across tumor types, suggesting their targeting may have applicability for the treatment of multiple cancer types. Here, we explore the functional effects of triple blockade of PD-1, TIM-3, and LAG3 on T cell activation, tumor immune contexture, and antitumor activity in preclinical models.

Methods

To examine the ability of combination CPB to reverse T cell exhaustion, splenocytes from mice with a transgenic $CD4^+$ T cell receptor were stimulated with 2 different peptide sequences of myelin basic protein to produce responsive effector or exhausted T cells. $CD4^+$ T cells were restimulated in the presence of antibodies and activity was quantified by IFN-γ release. To examine antitumor activity and pharmacodynamic effects in vivo, Balb/c mice were inoculated with the syngeneic breast cancer cell line EMT6 and treated with antibodies alone or in combination. Tumor growth was measured, and tumor-infiltrating lymphocytes were characterized by flow cytometry.

Results

Triple combination treatment with anti-PD-1, anti-TIM-3, anti-LAG3 antibodies was able to fully reverse the exhausted phenotype of $CD4^+$ T cells in vitro, as

determined by restored IFN-γ release. In contrast, single antibody treatments only partially reinvigorated T cells, while double combinations displayed an intermediate effect. This improved reinvigoration translated into increased antitumor efficacy in vivo. Control of tumor growth increased incrementally from single (6-24% tumor growth inhibition [TGI]) to double (40-50% TGI) and triple combinations (61% TGI). This reduction of tumor growth was associated with significant increases in overall immune cell infiltrate, $CD8^+$ T cell infiltration, and M1/M2 macrophage ratios and a decrease in intratumoral $CD11b^+$ cell numbers after triple combination treatment, suggesting a broad modulation of the tumor microenvironment.

Conclusions

Triple blockade of PD-1, TIM-3, and LAG3 resulted in highly effective reversal of T cell exhaustion and achieved improved tumor control over single or double combinations. By targeting immune checkpoints expressed on multiple cell types, additional mechanisms of tumor immune control were engaged. Taken together, these data support the concept of double and triple combinations of blocking antibodies to PD-1, TIM-3, and LAG3.

P366

Blockade of the PD-1/PD-L1 pathway with the Anti-PD-1 mAb, MGA012, enhances the biological activity of the B7-H3 x CD3 bispecific DART® molecule, MGD009

Liqin Liu, PhD[1], Yinhua Yang[1], Ralph Alderson, PhD[1], Jonathan Li, PhD[1], Qihong Xu[1], Daorong Liu[1], Robert Burns[1], Vatana Long[1], Syd Johnson, PhD[1], Ezio Bonvini[1], Paul Moore, PhD[1*]

[1]*MacroGenics, Rockville, MD, USA*

Background

While checkpoint inhibitors have dramatically improved disease outcomes for patients with certain types of tumors, a significant proportion of patients do not benefit from these agents. Moreover, checkpoint inhibitors are most effective in immunogenic tumors with high mutational burden and pre-existing T-cell infiltration, an indication of an ongoing but thwarted immune response. Combinations with agents that have complementary mechanisms of actions, such as T-cell recruiting agents, may provide expanded benefit to patients with resistance or limited response to checkpoint inhibitor treatment. MGD009, is a clinical stage B7-H3 x CD3 bispecific DART molecule designed to redirect T cells to lyse B7-H3-positive tumor cells. Preclinical studies demonstrated that MGD009 mediates potent anti-tumor activity associated with T-cell activation, expansion and infiltration into tumor sites. Notably, MGD009 activity is also associated with upregulation of PD-1 on T cells and PD-L1 on both tumor and T cells. To address whether the antitumor activity of MGD009 could be further enhanced by coordinating blockade of the PD-1/PD-L1 pathway, we have performed combination studies of MGD009 with MGA012, a clinical-stage anti-PD-1 mAb. also known as INCMGA012.

Methods

T-cell receptor (TCR)-mediated signaling was evaluated using a PD-1/PD-L1 dependent co-culture reporter system in the presence of MGD009 ± MGA012. In vitro redirected T-cell killing assays were performed using JIMT-1/Luc as target cells and T cells as effectors. In vivo studies were conducted in human PBMC-reconstituted xenografts in MHC class I-null NSG™ mice. Flow cytometry and cytokine multiplex assays were used to evaluate surface/intracellular markers and cytokine levels.

Results

Blockade of the PD-1/PD-L1 checkpoint axis with MGA012 enhanced B7-H3 expression-dependent, MGD009-induced NFAT signaling beyond that observed with MGD009 alone in a co-culture

reporter assay. MGA012 augmented MGD009-mediated tumor cell lysis of B7-H3+ve tumor cells in redirected T-cell killing assays. In vivo anti-tumor activity of MGD009 was further enhanced by the addition of MGA012 in a human PBMC-reconstituted mouse xenograft model. Mechanism of action studies revealed that MGD009 and MGA012 co-operate to augment granzyme A/B, perforin expression, T-cell activation and expansion beyond that achieved with MGD009 alone and in a B7-H3-dependent manner. Significantly, MGA012 further increased the fraction of central and effector memory T-cells induced by MGD009.

Conclusions
The combination of MGD009 with MGA012 exerts enhanced cellular signaling and T-cell responses in vitro and increased anti-tumor activity in vivo beyond that achieved with MGD009 alone. These proof-of-principle studies provides rationale for clinically testing this combination approach.

Ethics Approval
All in vivo studies were reviewed and approved by MacroGenics Institutional Animal Care and Use Committee (IACUC)

P367

Synergistic anti-tumor effects of TLR4 agonist G100 and anti-OX40 antibody

Hailing Lu, MD, PhD[1], Alec Betancur[1], Howard Lee[1], Jan Ter Meulen, MD, PhD[1]

[1]*Immune Design, Seattle, WA, USA*

Background
Intratumoral injection of G100 (Glucopyranosyl Lipid A in stable emulsion) has shown potent anti-tumor effects. Clinical trials evaluating G100 in patients with follicular lymphoma (FL) (NCT02501473) have shown significant objective responses in treated and non-treated (abscopal) lesions (Flowers, ASH 2017). Mechanistic studies have shown that the systemic anti-tumor effects of G100 are mediated by CD8 T cells. Tumor biopsies from FL patients demonstrated increased CD8 T cell infiltration post-G100 treatment, which correlate with clinical response. We hypothesize that the ability of G100 to increase T cell infiltration into tumors will synergize with therapies that separately activate T cells via OX40.

Methods
The combination therapy (G100+α-OX40 Ab) was studied in a bilateral A20 lymphoma and B16 melanoma models. In the A20 model, BALB/c mice received inoculation with 5E6 A20 cells on both flanks on Day 0. In the B16 model, C57BL/6 mice received an inoculation with 1E5 B16-ova or B16-F10 cells on Day 0 on the right flank and in some studies a 2nd tumor inoculation on Day 3 on the left flank. Treatment started after tumors were established (Days 5-8). Mice received treatment with G100 alone (10 µg, IT, 3x/week, injected into tumor on one side only), α-OX40 Ab (clone OX86, 200 µg, IP, 1x/week), or the combination of G100 plus α-OX40 Ab. Tumor growth was monitored via caliper measurement.

Results
G100+α-OX40 was more potent than either single agent in controlling the growth of both G100-treated and abscopal tumors. In the A20 model, the overall survival rate after complete regression of both treated and abscopal tumors was 20% in the G100 monotherapy group, 10% in the α-OX40 monotherapy group, and 60% in the G100+α-OX40 group ($p=0.01$ for G100+α-OX40 vs. G100 alone; $p=0.0037$ for G100+α-OX40 vs. α-OX40). At three months post primary tumor inoculation, all survival mice rejected a tumor re-challenge with A20 cells. In the B16 melanoma model, G100+α-OX40 resulted in better tumor control and significantly longer survival compared to either monotherapy ($p=0.0016$ for G100+α-OX40 vs. G100 or α-OX40 alone). Complete regression of treated and abscopal lesions only occurred in mice receiving combination therapy. The

survival mice rejected re-challenge with B16-ova and with wildtype B16-F10 tumors, indicating long-term memory responses.

Conclusions
Combination therapy using intratumoral injection of G100 with systemic delivery of anti-OX40 has synergistic anti-tumor effects in preclinical tumor models, which supports clinical evaluation.

P368

Combination of a dipeptidyl peptidase inhibitor BXCL701 and biased CD122 agonist NKTR-214 with anti-PD1 provides functional immunological memory through inflammatory cell death.

John MacDougall, PhD[1], Snigdha Gupta, PhD[2], Veena Agarwal[1], Luca Rastelli[1], Annie An[3], wenqing yang, PhD[3], Henry Li[3], Deborah Charych, PhD[4], Jonathan Zalevsky, PhD[4], Vincent O'Neill[1]

[1]BioXcel Therapeutics, New Haven, CT, USA
[2]BioXcel Corporation, Gurugram, India
[3]Crown Bioscience, San Diego, CA, USA
[4]Nektar Therapeutics, San Francisco, CA, USA

Background
BXCL701 (Talabostat; Val-boroPro) is a potent inhibitor of dipeptidyl peptidases, including DPP8, DPP9, and fibroblast activation protein (FAP). Utilizing Artificial Intelligence approaches BXCL701 was uncovered as an agent that would potentially synergize with existing immunotherapies as novel combinations for cancer treatment. Our hypothesis was confirmed with the observation that BXCL701, in combination with an anti-PD-1 antibody and NKTR-214 (a CD122-biased agonist) results in complete and durable response with functional demonstration of immunologic memory in a syngeneic mouse model of pancreatic cancer (Pan02) [1]. In this case, it was only the triple combination that generated complete and durable responses implying that immune activation by these three agents were non-redundant and complementary.

Methods
Here we extend those observations to other syngeneic mouse models (MC-38, Wehi-164) in which this combination of agents was similarly able to generate complete and durable responses with functional immunologic memory. However, complete and durable responses were not observed in all models tested (RM-1, B16F10). We used the differential responses observed in these models to assess what tumor associated immune cells might correlate with response to this triple combination.

Results
Using IHC and flow cytometry based immunophenotyping data we found that tumor models which were responsive to the triple combination had high densities of tumor associated macrophages, whereas those models that were less responsive had low macrophage densities. Recent literature demonstrating that inhibition of DPP8 and DPP9 in macrophages by BXCL701 activates the Nlrp1b inflammasome, resulting in an inflammatory cell death termed pyroptosis, supports a mechanistic based hypothesis for tumor responses [2,3].

Conclusions
Thus, it is proposed that BXCL701 stimulated macrophages rapidly prime the tumor microenvironment for other immune effector cells, those of which are similarly primed by a combination of checkpoint inhibition and NKTR-214 stimulation. These data validate that a complete anti-tumor response in these models requires engagement of multiple cell types of the immune system, both innate and adaptive. These data provide the basis for a mechanistically based predictive biomarker that can potentially be used in the clinical application of this triple combination therapy.

References
1. Rastelli L, Gupta S, Dahiya A, Jagga Z, Nandabalan K, Upmanyu S. Efficacy and immune modulation by BXCL701 a dipeptidyl peptidase inhibitor, NKTR-214 a CD122-biased immune agonist with PD1 blockade in murine pancreatic tumors. 2018 ACSO Annual Meeting, Abstract #3085
2. Okondo MC, Johnson DC, Sridharan R, Go EB, Chui AJ, Wang MS, Poplawski SE, Wu W, Liu Y, Lai JH, Sanford DG, Arciprete MO, Golub TR, Bachovchin WW, Bachovchin DA. DPP8 and DPP9 inhibition induces pro-caspase-1-dependent monocyte and macrophage pyroptosis. Nat Chem Biol. 2017 Jan;13(1):46-53.
3. Okondo MC, Rao SD, Taabazuing CY, Chui AJ, Poplawski SE, Johnson DC, Bachovchin DA. Inhibition of Dpp8/9 Activates the Nlrp1b Inflammasome. Cell Chem Biol. 2018 Mar 15;25(3):262-267

P369

Pegilodecakin, a pegylated human IL-10 (AM0010), enhances the cytotoxicity of CAR-T cells *In Vitro*

Scott McCauley, BA[1], Rakesh Verma, PhD[1], Martin Oft, MD[1]

[1]*ARMO Biosciences, Redwood City, CA, USA*

Background
Immune therapies rely on expansion of anti-tumor T cells for tumor regression and successful therapeutic outcomes. Recent studies of Pegilodecakin, a pegylated interleukin-10 (IL-10), have demonstrated that doses greatly exceeding typical endogenous levels can drive a productive tumor specific T cell expansion and response. In a large Phase I/Ib study, Pegilodecakin achieved objective responses across multiple tumor types, alone and in combination with chemotherapies and Programmed Cell Death-1 (PD-1) inhibitors. Agents that improve the functional expansion of chimeric antigen receptor (CAR) T cells, post adoptive transfer, hold promise to improve the therapeutic efficacy of CAR-T therapy in patients. Here we report on early *in vitro* studies to demonstrate that Pegilodecakin significantly enhances the anti-tumor cytotoxic T lymphocyte (CTL) activity of CAR-T cells.

Methods
The engineered Primary CD19 CAR-T cells were generated by isolating human T cells from whole blood and transducing these T cells with a CD19-targeted CAR. The CD19 CAR-T cells were then activated, expanded, and tested in a Real-time Cytotoxicity Assay (RTCA) against HeLa cells stably expressing human CD19 (CD19-HeLa). Multiple effector-to-target (E:T) ratios were tested and the CTL activity was measured through cell-sensor impedance in an electronic microtiter plate. Cytotoxicity was measured for CD19 CAR-T alone or in combination with varied concentrations of Pegilodecakin, and was directly compared with controls, including Pegilodecakin alone or Pegilodecakin with non-transduced T cells. To functionally validate the CTL activity, we measured the levels of Granzyme-B and Interferon-gamma (IFNg) in the culture supernatants by ELISA at the end of the RTCA.

Results
The RTCA revealed that Pegilodecakin in combination with the CD19 CAR-T showed a significant increase in CTL activity ($P<0.001$) against CD19-HeLa cells as compared to the CD19 CAR-T alone. Functionally, when combined with Pegilodecakin, CD19 CAR-T cells produced significantly higher levels of Granzyme-B ($p<0.0005$) and IFNg ($p<0.02$) as measured at the end of the RTCA. Controls, including Pegilodecakin alone (without CAR-T or non-transduced T cells) and non-transduced T cells in combination with Pegilodecakin, had significantly lower CTL activity by RTCA or ELISA (Granzyme-B or IFNg).

Conclusions
We demonstrate that when combined with Pegilodecakin, the CTL activity of the CD19 CAR-T is significantly improved. Additionally, this combination demonstrates significantly improved functional activity of these CD19 CAR T cells, including significantly increased Granzyme-B and IFNg levels relative to controls. These encouraging results warrant further examination of Pegilodecakin/CAR-T therapy combinations *in vivo*, with an aim towards improving the clinical use and activity of CAR-T therapies.

Acknowledgements
CAR-T platform was made available by ProMab Biotechnologies, who generated the *in vitro* data in this study

P370

Forced expression of OX40L and inhibition of IDO within the murine glioblastoma microenvironment creates a potent anti-tumor immune response.

Teresa Nguyen, BS[2], Yisel Rivera-Molina, PhD[2], Francisco Puerta-Martinez, PhD[2], Debora Kim[2], Xuejun Fan, BS[2], Frederick Lang, MD[2], Hong Jiang, PhD[2], Candelaria Gomez-Manzano, MD[2], Juan Fueyo[2]

[1]*The University of Texas, Houston, TX, USA*
[2]*MD Anderson Cancer Center, Houston, TX, USA*

Background
An immunosuppressive tumor-microenvironment characterizes glioblastoma (GB). Regulatory T-cells can activate indolamine-2,3-dioxygenase (IDO) causing immunosuppression. IDO is upregulated in GB patients, and correlates with a poor prognosis. The use of the oncolytic adenovirus, Delta-24-RGD, has been shown to induce complete responses in a subset of GB patients by immune mechanisms that activate anti-tumor cytotoxic properties of T-cells. This cytotoxic effect can be enhanced by the addition of immune agonists, such as OX40L, a T-cell co-stimulator. We hypothesized that combining IDO inhibition (Indoximod) and Delta-24-RGD armed with OX40L (D24-RGDOX) will have an enhanced therapeutic effect in GB.

Methods
A GB mouse model was used to determine therapeutic efficacy of D24-RGDOX and Indoximod as single agents or in combination. C57BL/6 mice were intracranially implanted with syngeneic GB cells, followed by intratumoral viral injections and/or Indoximod treatments. We sacrificed the mice on day 24 post-tumor implantation for immunological studies, including co-culture of splenocytes from differentially treated mice with cancer cells for determining secretion levels of IFN-gamma. We also quantified T-cells of different immunophenotypes of brain infiltrating lymphocytes (BILs) by flow cytometry. Lastly, we performed a survival study.

Results
The co-culture experiment showed that splenocytes from the combination-treated mice produced the highest amount of IFN-gamma compared to either single agent treatment (ANOVA, $p<0.0001$). Additionally, immunophenotyping of murine BILs by flow cytometry revealed that combination-treated mice led to the highest percentage of CD45+ cells (ANOVA, <0.0001). Moreover, mice treated with the combination therapy yielded the highest infiltration of PD-1+TIM-3+ exhausted CD8 T-cells compared to the Delta-24-RGDOX or Indoximod treated groups (ANOVA, $p<0.0001$), and correlated with complete tumor elimination as shown by H&E staining. Interestingly, the survival data shows that the combination treatment induced a greater survival benefit compared to Indoximod or D24-RGDOX alone, resulting in the most long-term survivors (mean survival, days, Indoximod=37, D24-RGDOX=47, combination=109 days, Logrank test for trend, $p<0.0001$) and re-challenged survivors.

Conclusions
The co-culture results indicate increased activation of T-cells by the combination treatment. The increase of CD45 cells in combination-treated mice compared to Delta-24-RGDOX indicate enhanced infiltration of immune cells by Indoximod. Moreover, the increase of exhausted T-cells in combination-treated mice and the accompanied complete tumor regression suggest there is a process of active tumor-targeting T-cells converting into exhaustive T-cells during therapy. The re-challenge survival data indicate the establishment of immune memory by D24-RGDOX and Indoximod, and support the use of IDO inhibitors with armed oncolytic adenoviruses as a potential treatment for GB.

P371

Reprogramming the immune phenotype of Rb-deficient tumor cells using BET inhibition

Brian Olson, PhD[1], Christina Hong[1], Riyue Bao, PhD[2], Gregory Lesinski, PhD, MPH[1], Akash Patnaik, MD, PhD[2]

[1]*Emory University, Atlanta, GA, USA*
[2]*University of Chicago, Chicago, IL, USA*

Background
Immune checkpoint blockade has revolutionized the treatment of several malignancies. However, subsets of patients fail to respond, highlighting the urgency of identifying predictive biomarkers to guide rational combinatorial treatment strategies. We have previously shown tumors lacking a T cell-inflamed gene signature (a predictor of immunotherapeutic efficacy) are enriched for loss of the tumor suppressor RB1. Based on this observation, we examined the immunological consequences of RB1 loss in prostate tumor cells and whether targeted therapeutics aimed at reversing the molecular consequences of RB1 loss (namely inhibitors of the bromodomain and extraterminal (BET) domain family of proteins) can reprogram the immune phenotype of Rb-deficient tumors.

Methods
Isogenic murine prostate tumor cells with or without Rb expression were generated and interrogated for changes in markers related to an immunosuppressive phenotype, including chemokine and checkpoint ligand expression and effects on T cell migration in vitro and in vivo. These cell lines were then evaluated for the effects of RB1 loss towards susceptibility to BET inhibition, in terms of effects on tumor cell viability as well as effects on immune phenotype.

Results
Loss of RB1 in prostate tumor cells resulted in decreased expression of chemokines associated with immune infiltration and function, increased expression of multiple checkpoint ligands, as well as soluble factors resulting in decreased T cell migration. When examined in tumor-bearing animals in vivo, RB1 loss translated into decreased immune infiltration into the tumor microenvironment. Tumor cells lacking RB1 had increased susceptibility to BETi-mediated tumor cell death, with cells surviving BET inhibition displaying pharmacodynamic inhibition of BET family member function. Rb-deficient tumor cells also displayed increased susceptibility to BETi-mediated reprogramming of their immune phenotype, including decreased expression of checkpoint ligands such as PD-L1, Gal9, and VISTA, decreased expression of chemokines associated with tumor growth and immune suppression such as CXCL1 and CXCL5, as well as a complete restoration of T cell migration.

Conclusions
We show that loss of RB1 results in an immunosuppressive tumor microenvironment, and that Rb-deficient tumor cells have increased susceptibility to BET inhibition in terms of tumor cell-intrinsic and extrinsic efficacy. Targeting the

immunological consequences following BET inhibition in Rb-deficient tumors may provide a rational approach for combined pharmacological and immune-based treatment strategies for individuals with Rb-deficient malignancies.

Acknowledgements
American Cancer Society (BMO), Prostate Cancer Foundation (AP/BMO), NCI National Cancer Institute Prostate SPORE-University of Chicago/Northwestern University (AP).

Ethics Approval
This study was approved by the Emory University Institutional Animal Care and Use Committee; protocol number 3000268.

P372

BETAMUNE, a replication competent type 5 adenovirus carrying a TGF-Beta trap, reverses resistance to a PD-L1 inhibitor in an immunocompetent mouse model

Christopher Larson, MD PhD[1], Corey Carter, MD[1], Bryan Oronsky, MD, PhD[1], Tony Reid, MD PhD[1]

[1]*EpicentRx Inc, La Jolla, CA, USA*

Background
Checkpoint inhibitors have permanently changed the therapeutic landscape for multiple tumor types previously associated with a dismal prognosis. However, for the subset of patients that initially benefit from these inhibitors, lethal secondary resistance often develops. We evaluated combination therapy with a preclinical oncolytic adenovirus called BETAMUNE, armed with a TGF-β "trap" that neutralizes the immunosuppressive cytokine, TGF-β, and a checkpoint inhibitor, anti-PD-L1, in PD-L1 resistant tumors. The study, which was performed in an immunocompetent mouse model, demonstrated that the combination of BETAMUNE with PD-L1 blockade reversed PD-L1 resistance, potentially representing a future paradigm shift for patients that are primarily or secondarily resistant to checkpoint inhibitors.

Methods
Murine KRAS mutant lung adenocarcinoma cell line, ADS-12, was established in house. BETAMUNE, produced in HEK-293 cells, carries a disruption in E1A and a TGFβR-IgG fusion using the mouse isoforms of those genes for immunologic compatibility with an immunocompetent mouse. 129S4/SvJae mice, implanted with subcutaneous ADS-12 tumors, were randomized into treatment groups 10 mice per group. Treatment involved intratumoral injections of either viral storage buffer or BETAMUNE at 10(to the power of 9) PFU/dose on days 0, 4, and 8, plus intraperitoneal injections of either phosphate buffered saline (PBS) or 200 µg anti-PD-L1 antibody (clone 10F.9G2, BioXcell) diluted in PBS on days 1, 5, 9, and 13.

Results
All mice tolerated the treatments without obvious signs of toxicity. No activity was evident with anti-PD-L1 antibody alone. Treatment with BETAMUNE alone in these larger tumors led to complete responses in four of ten mice, and combination therapy led to complete responses in seven of ten mice. Tumor volume was smaller in the combination therapy group compared to 19k-mTGFβR-IgG alone ten days after starting treatment ($p<0.01$).

Conclusions
This study demonstrates that localized oncolytic infection with BETAMUNE is safe and abrogates resistance to systemic PD-L1 immunotherapy, which strongly supports further evaluation of this combination in upcoming Phase 1 and Phase 2 clinical studies in 2019.

Ethics Approval
All applicable international, national, and/or

institutional guidelines for the care and use of animals were followed.

P373

Synergistic efficacy of duvelisib with checkpoint or co-stimulatory antibodies in a B cell lymphoma model: Advantages of dual inhibition of PI3K-delta and PI3K-gamma

Jonathan Pachter, PhD[1], David Weaver, PhD[1]

[1]*Verastem, Needham, MA, USA*

Background

Duvelisib is an oral dual inhibitor of phosphoinositide 3-kinase (PI3K)-delta and PI3K-gamma which has shown clinical activity as monotherapy in chronic lymphocytic leukemia (CLL), small lymphocytic lymphoma (SLL), follicular lymphoma (FL), and T cell lymphoma [1,2]. Recent publications have demonstrated that PI3K-delta inhibition reduces immunosuppressive Tregs and enriches memory T cells [3,4], whereas PI3K-gamma inhibition reduces immunosuppressive myeloid cells [5,6]. Hence, we postulated that duvelisib may augment the efficacy of immune checkpoint or co-stimulatory antibodies.

Methods

Mice bearing syngeneic A20 B cell lymphoma tumors (60-90 mm3) were treated with vehicle, duvelisib, anti-PD-1, anti-PD-1 + duvelisib, anti-OX40, or anti-OX40 + duvelisib. Tumor volumes were measured by caliper. Tregs, macrophages and MDSCs were quantified by flow cytometry from mice bearing A20 tumors after 8 days of treatment.

Results

In the A20 model, duvelisib, anti-PD-1 and anti-OX40 treatments each induced tumor growth delay. When duvelisib and anti-PD-1 were combined in mice with pre-existing A20 tumors, strong anti-tumor synergy was observed. When anti-OX40 and duvelisib were combined, tumor regression was observed which correlated with strong reduction of tumor Tregs, M2 macrophages and MDSCs. To assess immune memory, tumor-free mice following anti-OX40 alone or anti-OX40 + duvelisib were injected with A20 cells in the contralateral flank with no further treatment. Whereas mice that had received anti-OX40 alone grew new tumors upon A20 re-challenge, all tumor-free mice that had received anti-OX40 + duvelisib did not grow tumors upon re-challenge and showed elevated memory T cells in blood and spleen. These findings indicate that the anti-OX40 + duvelisib treatment established immune memory, potentially contributing to the observed tumor regression. Mechanistically, duvelisib was found to reduce Tregs, M2 macrophages and MDSCs in the context of combinations with PD-1 or OX40 antibodies, and duvelisib (dual PI3K-delta/gamma inhibition) was found to inhibit all 3 immunosuppressive cell populations more effectively than idelalisib (PI3K-delta only) or IPI-549 (PI3K-gamma only).

Conclusions

These data demonstrate that duvelisib treatment stimulates anti-tumor immunity. Furthermore, the unique dual inhibition of PI3K-delta and PI3K-gamma appears to make duvelisib especially effective in enhancing the anti-tumor efficacy of immune checkpoint and co-stimulatory antibodies. These data support further exploration of duvelisib in combination with anti-PD-1/PD-L1 or co-stimulatory antibodies in patients with various cancers.

References

1. Flinn IW, O'Brien S, Kahl B, Patel M, Oki Y, Foss FF, Porcu P, Jones J, Burger JA, Jain N, Kelly VM, Allen K, Douglas M, Sweeney J, Kelly P, Horwitz S. Duvelisib, a novel oral dual inhibitor of PI3K-delta gamma is clinically active in advanced hematologic malignancies. Blood 2018; 131:877-887.
2. Horwitz SM, Koch R, Porcu P, Oki Y, Moskowitz A, Perez M, Myskowski P, Officer A, Jaffe JD, Morrow SN, Allen K, Douglas M, Stern H, Sweeney J, Kelly P,

Kelly V, Aster JC, Weaver D, Foss FM, Weinstock DM. Activity of the PI3K-delta,gamma inhibitor duvelisib in a phase 1 trial and preclinical models of T-cell lymphoma. Blood 2018; 131: 888-898.
3. Ali K, Soond DR, Pineiro R, Hagemann T, Pearce W, Lim EL, Bouabe H, Scudamore CL, Hancox T, Maecker H, Friedman L, Turner M, Okkenhaug K, Vanhaesebroeck B. Inactivation of PI(3)K p110delta breaks regulatory T-cell-mediated immune tolerance to cancer. Nature 2014; 510:407-411.
4. Abu Eid R, Ahmad S, Lin Y, Webb M, Berrong Z, Shrimali R, Kumai T, Ananth S, Rodriguez PC, Celis E, Janik J, Mkrtichyan M, Khleif SN. Enhanced therapeutic efficacy and memory of tumor-specific CD8 T cells by ex vivo PI3K-delta inhibition. Cancer Res 2017; 77:4135-4145.
5. Kaneda MM, Messer KS, Ralainirina N, Li H, Leem CJ, Gorjestani S, Woo G, Nguyen AV, Figueiredo CC, Foubert P, Schmid MC, Pink M, Winkler DG, Rausch M, Palombella VJ, Kutok J, McGovern K, Frazer KA, Wu X, Karin M, Sasik R, Cohen EE, Varner JA. PI3Kgamma is a molecular switch that controls immune suppression. Nature 2016; 539:437-442.
6. De Henau O, Rausch M, Winkler D, Campesato LF, Liu C, Cymerman DH, Budhu S, Ghosh A, Pink M, Tchaicha J, Douglas M, Tibbitts T, Sharma S, Proctor J, Kosmider N, White K, Stern H, Soglia J, Adams J, Palombella VJ, McGovern K, Kutok JL, Wolchok JD, Merghoub T. Overcoming resistance to checkpoint blockade therapy by targeting PI3K-gamma in myeloid cells. Nature 2016; 539: 443-447.

P374

Sex-based heterogeneity of response to immunotherapy in non small cell lung cancer

Fabio Conforti, MD[1], Laura Pala[1], Vincenzo Bagnardi[2], Giuseppe Viale[1], Tommaso De Pas, MD[1], Elisabetta Pennacchioli[1], Emilia Cocorocchio[1], Pier Francesco F. Ferrucci, MD[1], Richard Gelber[3], Aron Goldhirsch[1]

[1]*European Institute of Oncology, Milan, Italy*
[2]*University of Milan-Bicocca, Milan, Italy*
[3]*Dana-Farber Cancer Institute, Harvard, Boston, MA, USA*

Background

Recently, four large randomized clinical trials (RCTs) demonstrated that pembrolizumab administered alone or in combination with chemotherapy as first line systemic treatment, improved overall survival (OS) of patients with advanced non-small cell lung cancer (NSCLC), as compared with standard chemotherapy alone. [1,4]We previously demonstrated a significant sex-based heterogeneity of the efficacy of anti-CTL4A and anti-PD-1 drugs in several solid tumors, with male patients obtaining higher benefit than females. [5] Given the complex sex-dimorphism of immune system function and response, we hypothesized that the direction of such heterogeneity could be different using different immunotherapeutic strategies. Here, we provide evidence suggesting that adding pembrolizumab to chemotherapy compared with chemotherapy alone in advanced NSCLC leads to an impressive greater OS benefit in women as compared with the benefit observed for men.

Methods

We performed a meta-analysis of four RCTs (i.e Keynote 24, 42, 189 and 407; Table1), to assess the interaction between patients' sex and the efficacy of the two experimental immunotherapeutic strategies (i.e. pembrolizumab alone or pembrolizumab plus standard chemotherapy).[1-4] We tested the null hypothesis that both evaluated immunotherapeutic strategies have homogeneous effect in the same sex.

Results

Analysis included 2754 patients, 847 (31%) of whom were females. Results showed that male patients treated with pembrolizumab monotherapy had a significantly reduced risk of death as compared with males treated with standard chemotherapy: pooled-OS HR 0.76 (95% CI, 0.65-0.88;fig.1). In females,

pembrolizumab alone was not better than standard chemotherapy: pooled-OS HR 0.90 (95% CI, 0.71-1.15). By contrast, pembrolizumab administered with chemotherapy was associated with a very large OS advantage compared with chemotherapy alone in female patients but a significantly smaller benefit was seen in males (female pooled-OS HR, 0.32; 95% CI, 0.23 -0,46; males pooled-OS HR, 0.69; 95% CI, 0.55 -0.87). The heterogeneity of the efficacy of the two immunotherapeutic strategies in male and female patients was highly significant: the pooled interaction (i.e. the pooled estimate of the ratios of the HRs in males and in females reported in each trial) was 0.82 (95% CI, 0.62-1.1) for pembrolizumab alone, indicating a greater effect of pembrolizumab alone in men with respect to women, and 2.1 (95% CI, 1.36-3.25) for pembrolizumab plus chemotherapy, indicating a greater effect of pembrolizumab plus chemotherapy versus chemotherapy alone in women as compared with men (p-heterogeneity=0.004; Figure1).

Conclusions

These data highlight the need for different immunotherapeutic strategies to be tested taking into account sex-related heterogeneity of responsiveness

Acknowledgements

We thank Shari Gelber for editorial assistance.

References

1. Reck M, Rodríguez-Abreu D, Robinson AG, et al. Pembrolizumab versus chemotherapy for PD-L1–positive non–small-cell lung cancer. N Engl J Med. 2016;375:1823-1833. 2. Gandhi L, Rodríguez-Abreu D, Gadgeel S, et al. Pembrolizumab plus chemotherapy in metastatic non-small-cell lung cancer. N Engl J Med. 2018;378:2078-2092. 3. Paz-Ares G, Luft A, Ali Tafresh A, et al. Phase 3 study of carboplatin-paclitaxel/nab-paclitaxel (Chemo) with or without pembrolizumab (Pembro) for patients (Pts) with metastatic squamous (Sq) non-small cell lung cancer (NSCLC). J Clin Oncol 2018; 36. (suppl; abstr 105) 4. Lopes G, Wu Y, Kudaba I, et al. Pembrolizumab (pembro) versus platinum-based chemotherapy (chemo) as first-line therapy for advanced/metastatic NSCLC with a PD-L1 tumor proportion score (TPS) ≥ 1%: Open-label, phase 3 KEYNOTE-042 study. J Clin Oncol 2018; 36 (suppl; abstr LBA4) 5. Conforti F, Pala L, Bagnardi V, et al. Cancer immunotherapy efficacy and patients' sex: a systematic review and meta-analysis. Lancet Oncol. 2018; (18)30261-4. pii: S1470-2045

Table 1.

Figure 1.

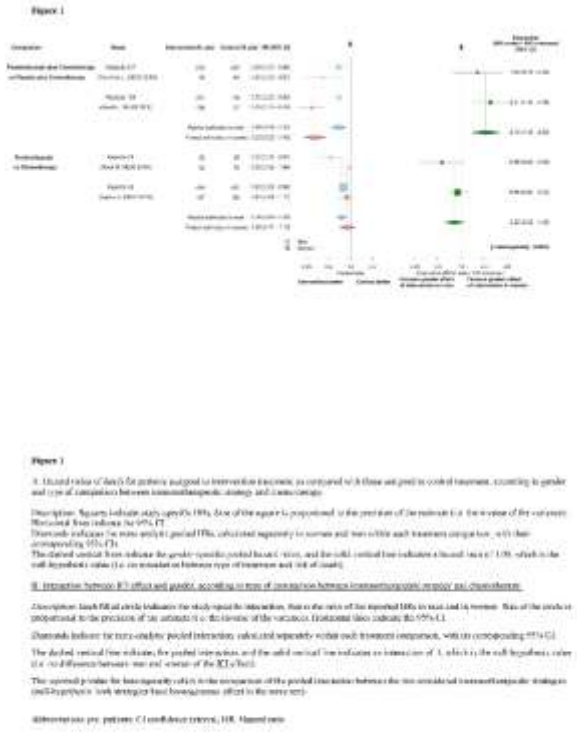

P375

Simultaneous costimulatory T-cell engagement and checkpoint inhibition by PRS-344/ONC0055, a 4-1BB / PD-L1 bispecific compound for tumor localized activation of the immune system

Marina Pavlidou, PhD[1], Janet Peper[1], Lucia Pattarini[2], Christian Barthels[1], Eva-Maria Hansbauer[1], Rachida Bel Aiba[1], Milan Blanusa[1], Alix Scholer-Dahirel[2], Maximilien Grandclaudon[2], Celine Grand[2], Jamila Elhmouzi-Younes[2], Matthieu Rivière[2], Véronique Blanc, PhD[2], Christine Rothe[1], Shane Olwill[1]
[1]*Pieris Pharmaceuticals, Freising, Germany*
[2]*Institut de Recherches Servier Oncology, Croissy Sur Seine, France*

Background

Multiple lines of evidence show that 4-1BB (CD137), a key costimulatory immunoreceptor, is a highly promising therapeutic target in cancer. Current antibody-based approaches showed immune cell activation not only in tumor tissues but also in the periphery, associated with dose-limiting on-target toxicity and a limited therapeutic window due to peripheral immune cell activation. To overcome this limitation, we generated PRS-344/ONC055, a 4-1BB/PD-L1 bispecific that is designed to promote 4-1BB clustering by bridging 4-1BB-positive T cells with PD-L1. PD-L1 is the primary ligand of the T cell receptor PD-1 and is expressed in a wide variety of tumors resulting in an inhibitory interaction with PD-1 in the tumor microenvironment. Preclinical evidence suggests that combining 4-1BB-induced T cell activation and expansion with “anti-PD-L1 mediated” immune checkpoint blockade may overcome the limitation of single agent therapy and offer benefit to ICP-resistant or non-responsive patients. PRS-344/ONC0055 has been designed to provide the potential of a combinatorial therapy in one molecule but also favors the localized activation of antigen-specific T cells in the tumor microenvironment, potentially reducing peripheral toxicity.

Methods

Anticalin® proteins are 18 kDa protein therapeutics derived from human lipocalins. We utilized phage display technologies to generate an Anticalin protein binding to 4-1BB with high affinity and specificity. PRS-344/ONC0055 was obtained by fusion of the 4-1BB-specific Anticalin protein to a PD-L1-targeting monoclonal antibody with an engineered IgG4 backbone.

Results

The bispecific fusion protein PRS-344/ONC0055 targets 4-1BB and PD-L1 with similar affinities as compared to parental building blocks and is capable of binding both targets simultaneously. We show

that the bispecific molecule retains its ability to block (PD-1 / PD-L1) receptor-ligand interaction with similar potency to the parental PD-L1 antibody. In ex vivo cell based assays, PRS-344/ONC0055 induces a dose-dependent T cell activation only in the presence of PD-L1 positive cells. We show that PRS-344/ONC0055 synergistic activity is stronger than that mediated by the combination of clinically relevant 4-1BB and PD-L1 benchmark antibodies.

Conclusions

We report potent costimulatory T cell engagement of the immunoreceptor 4-1BB in a PD-L1-dependent manner, utilizing the 4-1BB/PD-L1 bispecific compound PRS-344/ONC0055. This approach has the potential to provide a localized activation of the immune system with high efficacy and reduced peripheral toxicity. Furthermore, the direct, PD-L1-targeting activity of PRS-344/ONC0055 provides an additional therapeutic benefit by checkpoint blockade. Taken together our data outlines proof of concept functionality of PRS-344/ONC0055 and supports IND-enabling studies of this promising compound.

P376

Targeting vasoactive intestinal peptide signaling to enhance immunotherapy against solid tumors

Sruthi Ravindranathan, PhD[1], Rebecca Pankove, MS[1], Yiwen Li, MS[1], Shuhua Wang, MD[1], Edmund K. Waller, MD, PhD, FACP[1], Mohammad Zaidi, MD, MS[1], Gregory Lesinski, PhD, MPH[1]

[1]Emory University, Atlanta, GA, USA

Background

Vasoactive intestinal peptide (VIP) is a neuropeptide synthesized by nerve terminals, the pancreas, GI tract, and immune cells. VIP signaling represents an immune checkpoint pathway as it is produced upon inflammation and induces an immunosuppressive microenvironment. We have previously shown that daily administration of VIPhyb, a competitive peptide antagonist of VIP signaling, improves overall tumor free survival in mouse models of leukemia [1]. In solid tumors, human gene expression data shows VIP expression to greatly vary between different tumors, with highest levels in pancreatic exocrine cancers and lowest in melanoma. We hypothesize that VIP expression by cancers represents a targetable pathway for immune escape, and that antagonists of VIP signaling would induce an anti-tumor response when used alone or in combination with other immune checkpoint inhibitors.

Methods

Murine melanoma (B16F10, D4M.3A), breast cancer (4T1, 4T07) and pancreatic cancer (MT5, panc02) cells were cultured for 24 hours and their supernatants were tested for VIP concentration using an enzyme immunoassay. Growth of subcutaneously implanted melanoma (B16F10) and pancreatic cancer (MT5) in C57BL/6 mice was monitored every day following daily administration of 10ug VIPhyb (subcutaneously) starting from day -1 and/or 200ug of IgG2a or anti-PD-1 antibody (intraperitoneally) on day -1 and every 3 days thereafter. The treatment was continued until mice were euthanized when the tumor volume reached 500mm^3. The tumor tissues were stained for VIP, CD8 and DAPI, while the splenocytes were analyzed via flow cytometry for levels of CD3, CD4+, CD8+, CD4+PD1+ and CD8+PD1+ T cells.

Results

Supernatants from pancreatic cancer cells had significantly higher levels of VIP when compared to melanoma and breast cancer cells (Table 1).Treatment of immune competent mice bearing melanoma or pancreatic cancer cells with the combination of VIPhyb and anti-PD-1 (combination group) produced complete and durable regression of tumors in 20% of the mice in the melanoma model (Figure 1) and increased median survival in the

pancreatic cancer model (Figure 2). Also, there was a significant difference in the frequency of PD1 expressing CD4+ T cells in the spleen of mice in the combination group (Figure 3). Further, immunohistochemistry of the tumor tissue sections showed increased CD8+ T cell infiltration in the tumor of mice in the combination group (Figure 4).

Conclusions

Blocking VIP-signaling is a novel immunotherapeutic approach in preclinical solid tumor models. Improving half-life of VIPhyb are underway, to enhance the effectiveness of this peptide even in tumors with potentially high levels of VIP.

References

1. Petersen, C T, Li, J M, & Waller, E K, Administration of a vasoactive intestinal peptide antagonist enhances the autologous anti-leukemia T cell response in murine models of acute leukemia. OncoImmunology, 2017; 6(5), e1304336.

Ethics Approval

The study was approved by Emory's Institutional Animal Care and Use Committee (IACUC), protocol number 3000202

Table 1. Murine pancreatic cancer cells produce more VIP

Cancer	Cell line	Average concentration of VIP (ng/ml)
Pancreatic	MT5	297.5 ± 23.3
	Panc02	486.9 ± 62.4
Breast cancer	4T1	<2.66
	4T07	<2.66
Melanoma	B16F10	3.33 ± 2.4
	D4M.3A	<2.66

Figure 1. VIPhyb+anti-PD-1 in melanoma models

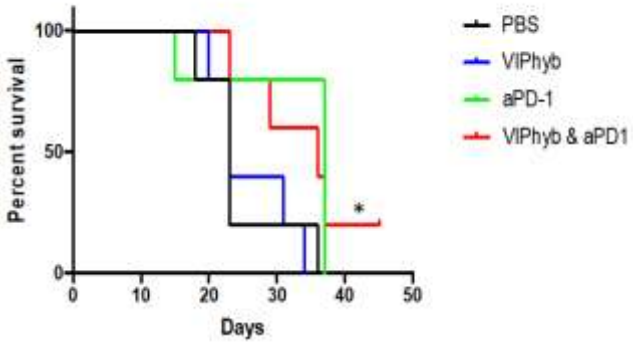

Figure 2. VIPhyb+anti-PD-1 in pancreatic cancer models

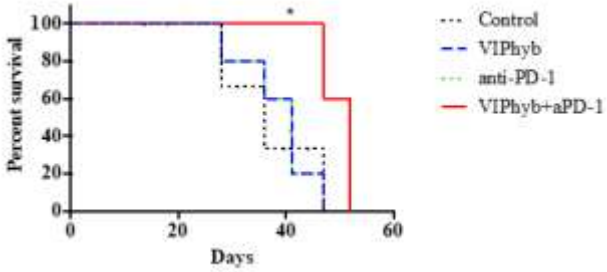

Figure 3. VIPhyb+anti-PD1 increases CD4+ PD1+ T cells

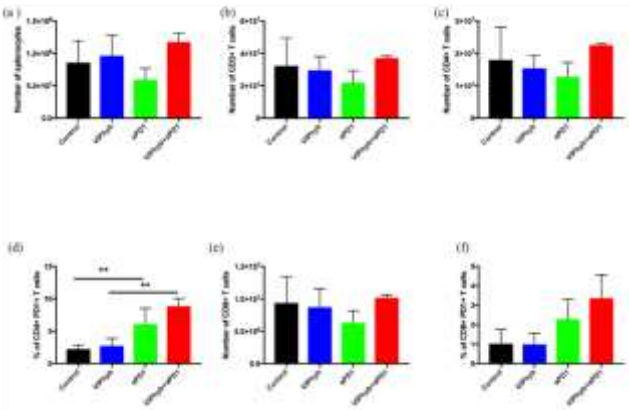

Figure 4. VIPhyb+ anti-PD-1 increases CD8+ T cells in tumor

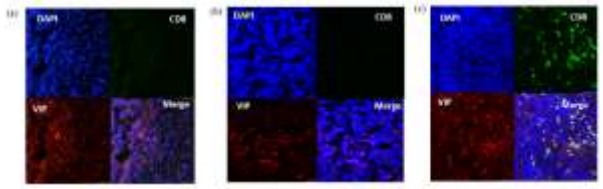

P377

Combination immunotherapy anti-PD-1 anti-body (Ab) with CBT-101 (c-MET inhibitor) demonstrates enhanced activity in tumors not dependent on c-MET

Mamatha Reddy[1], Gavin Choy, PharmD[1], Sarath Kanekal, PhD[1], Sanjeev Redkar, PhD[1]

[1]*CBT pharmaceuticals, Inc., Pleasanton, CA, USA*

Background
HGF/c-MET signaling mobilizes neutrophils in response to cancer immunotherapies. Neutrophils recruited to T-cell-inflamed microenvironments acquire immunosuppressive properties. c-MET+ neutrophils suppress therapy-induced T-cell expansion and effector functions. Glodde N et al [1] have shown that c-MET inhibition promoted adoptive T-cell transfer in murine cancer models by increasing effector T-cell infiltration in tumors. This therapeutic effect was independent of tumor cell-intrinsic c-MET dependence. In cancer patients, high serum levels of HGF correlated with high neutrophil counts and poor responses to checkpoint blockade therapies. Therefore, c-MET inhibitor (CBT-101) co-treatment may improve responses to cancer immunotherapy in settings beyond c-MET-dependent tumors.

Methods
Safety and efficacy of CBT-101, anti-PD-1Ab and combination were evaluated in three syngeneic mouse models, MC-38 (colorectal), H-22 (liver) and RENCA (renal). Tumor cells were inoculated in C57BL/6 mice and treatment was initiated when tumors reached a mean volume of approximately 100 mm3. Mice were randomized into four groups of ten animals per group and treated with either vehicle, CBT-101 (10 mg/kg oral daily in MC-38 and H-22 models and 20 mg/kg oral daily in RENCA), anti-PD-1 Ab (10 mg/kg intraperitoneally twice weekly), or a combination of CBT-101 plus anti-PD-1. Animals were checked daily for morbidity and mortality. Body weights (BW) and tumor volumes (TV) were measured twice weekly. In the MC-38 model, tumor tissue was collected at the end of the study and formalin fixed. Double IHC analysis of c-MET and neutrophils was used to quantify the expression of Met+ neutrophils.

Results
In MC-38 study, mean percent tumor growth inhibition (TGI) of combination demonstrated 65% tumor growth inhibition, versus 39% and 33% for anti-PD-1 and CBT-101 respectively. In H-22 study, there was no activity with CBT-101, 35% with anti-PD-1 and 60% TGI with combination. In RENCA study individual agents showed 60 to 65% activity while combination group demonstrated 80% TGI. The combination regimen was well tolerated by all animals with no loss in BW. Met+ neutrophils were significantly increased in the anti-PD-1 Ab group and dropped to the levels of vehicle group with combination treatment.

Conclusions
CBT-101 and Anti-PD-1 Ab combination treatment enhances host anti-tumor response in murine tumor models. Encouraged by these results, a Phase 1/2 clinical trial has been initiated to establish a safe dose combination of CBT-501 + CBT-101 primarily and nivolumab + CBT-101, secondarily in select solid tumors.

Trial Registration
Pending

References
1. Glodde N et al: Reactive Neutrophil Responses Dependent on the Receptor Tyrosine Kinase c-MET Limit Cancer Immunotherapy, Immunity, 47: p789–802, 2017

P378

NKTR-214 (CD122-biased agonist) and NKTR-262 (TLR7/8 agonist) combination treatment pairs local innate immune activation with systemic CD8+ T cell expansion to enhance anti-tumor immunity

Annah Rolig, Ph D[2], Daniel Rose, BS in biology[2], Saul Kivimäe[3], Deborah Charych, PhD[3], Werner Rubas, PhD[3], Jonathan Zalevsky, PhD[3], William L. Redmond, PhD[2]

[1]Earle A. Chiles Research Institute, Robert W. Franz Cancer Center, Portland, OR, USA
[2]Earle A. Chiles Research Institute, Portland, OR, USA
[3]Nektar Therapeutics, San Francisco, CA, USA

Background
Radiation therapy (RT) remains the standard of care for many human cancers. Combining NKTR-214, a CD122-biased cytokine agonist conjugated with releasable polyethylene-glycol (PEG) chains, with local RT significantly enhanced therapeutic efficacy in preclinical models. Mechanistically, NKTR-214 provides sustained signaling through the IL-2 receptor pathway (IL-2Rβγ) to preferentially activate and expand effector CD8+ T and NK cells and RT modulates the tumor microenvironment (TME) to induce antigen-release. Together, NKTR-214/RT treatment resulted in improved therapeutic responses compared to either treatment alone. However, abscopal responses in murine tumors were modest, leading us to explore alternative approaches with the potential to elicit more robust tumor-antigen specific responses. In the current study, we evaluated the extent to which NKTR-262, a polymer-modified TLR7/8 agonist prodrug, modulates the TME and synergizes with NKTR-214 treatment. We hypothesized that NKTR-214/NKTR-262 immunotherapy would promote synergistic activation of immunostimulatory innate immune responses along with systemic adaptive anti-tumor responses to significantly improve abscopal responses, tumor regression, and overall survival.

Methods
Tumor-bearing mice (CT26; 4T1) received NKTR-214 (0.8 mg/kg; iv), RT (16 Gy x 1), and/or intratumoral NKTR-262 (0.5 mg/kg). The activation status of CD4+, CD8+, and NK cells in the blood, lymph node, and/or tumor (7 days post-treatment) was evaluated by flow cytometry. Effects on innate immune subsets (macrophages, monocytes) including M1/M2 polarization were evaluated by flow cytometry and immunohistochemistry (1 day post-treatment). Data represents the result of 1-2 independent experiments (n=5-14/group). For immune markers, statistical significance was determined using a 1-way ANOVA with a p-value cut-off of 0.05.

Results
NKTR-214/RT resulted in increased absolute lymphocyte counts and expression of T cell activation markers (Ki-67, PD-1, granzyme A) in the blood and tumor. Compared to NKTR-214/RT, NKTR-214/NKTR-262 resulted in significantly improved survival ($p<0.05$) and expansion of activated CD8+ T cells (GzmA+; Ki-67+; ICOS+; PD-1+) in the blood ($p<0.05$). In the tumor, both combination treatments resulted in a similar CD8+ T cell density. NKTR-262/NKTR-214 induced higher frequencies of GzmA+ CD8+ T cells exhibiting reduced expression of suppressive checkpoint receptors PD-1+ and TIM-3+ ($p<0.05$). The increased CD8+ T cell differentiation was associated with a significant increase in M1 monocytes ($p<0.05$) and reduced presence of M2 monocytes.

Conclusions
Combined NKTR-214/NKTR-262 therapy induced robust anti-tumor immunity characterized by systemic CD8+ T cell expansion, enhanced intratumoral CD8+ T cell effector function, and favorable myeloid polarization resulting in improved tumor regression and tumor-free survival.

P379

Nanobodies® as a platform for multispecific targeting of immunomodulatory receptors.

Anandi Sawant, PhD[1], Douglas Linn, PhD[2]

[1]*Merck & Co., Palo Alto, CA, USA*
[2]*Merck & Co, Boston, MA, USA*

Background
While the clinical successes of immunotherapeutic antibodies targeting PD-1 and CTLA-4 have revolutionized the treatment of cancer, a majority of patients still fail to achieve objective responses. Tumors use several mechanisms to escape immune surveillance, and emerging clinical data suggest that targeting multiple immunomodulatory pathways can provide significant benefit over monotherapy. Nanobodies® (Nbs) are antibody-like therapeutic proteins based on immunoglobulin single variable domains.

Methods
Several Nbs can be linked together for multispecific targeting. In collaboration, Merck & Co., Inc. and Ablynx have developed bispecific PD-1/LAG-3 Nbs consisting of either one or two anti-PD-1 and LAG-3 modules (LAG-3mono/PD-1mono, LAG-3bi/PD-1bi) linked to an albumin-binding module for half-life extension.

Results
Nb panels were triaged through a number of in vitro binding, blocking, and functional assays to find highly potent PD-1 or LAG-3 leads that were then benchmarked against respective antibodies (Abs). In vivo, bispecific PD-1/LAG-3 Nbs demonstrated notable anti tumor effects in multiple tumor models. In certain models, both bispecific PD-1/LAG-3 Nbs performed favorably relative to the combination of anti-PD-1 and anti-LAG-3 antibodies. Interestingly, a bispecific Nb with single modules for each target (LAG-3mono/PD-1mono) was as efficacious as a bispecific Nb that allowed for avid bivalent interactions with each target (LAG-3bi/PD-1bi). Both bispecific Nbs induced infiltration and activation of T cells within tumors and the expression of anti-tumor immunity-associated genes.

Conclusions
Targeting two inhibitory immunomodulatory receptors with a single drug holds promise of achieving clinical benefit in patients that have failed monotherapy options.

P380

Treatment-free survival (TFS), with and without immunomodulatory medications (IMMs), as a novel outcome applied to immuno-oncology (IO) agents in advanced melanoma

Meredith Regan, PhD[1], Lillian Werner[1], Ahmad Tarhini, MD, PhD[2], Sumati Rao, PhD[3], Komal Gupte-Singh, PhD[3], Corey Ritchings, PharmD[3], Michael Atkins, MD[4], David McDermott, MD[5]

[1]*Dana-Farber Cancer Institute, Boston, MA, USA*
[2]*Cleveland Clinic Taussig Cancer Institut, Cleveland, OH, USA*
[3]*Bristol-Myers Squibb, Princeton, NJ, USA*
[4]*Georgetown Lombardi Comprehensive Cance, Washington, DC, USA*
[5]*Beth Israel Deaconess Medical Center, Boston, MA, USA*

Background

Patients discontinuing IO agents may experience periods of disease control without the need for subsequent systemic anticancer therapy, but may still require IMMs. This study simultaneously characterizes the disease control and IMM use during the treatment-free period.

Methods

Pooled data from the CheckMate 067 (phase 3) and 069 (phase 2) trials of nivolumab plus ipilimumab (NIVO+IPI; N=407), nivolumab (NIVO; N=313), and ipilimumab (IPI; N=357) for advanced melanoma were analyzed. IPI was given for 4 doses and NIVO was given until progression or unacceptable toxicity. Persistent use of IMMs and duration of IMM use initiated after IO protocol therapy cessation associated with any-grade treatment-related adverse events were included in the assessment. TFS was defined as the area between two Kaplan-Meier curves for conventional time-to-event endpoints from randomization: (A) time to IO protocol therapy cessation and (B) time to subsequent therapy or death [1]. TFS was subdivided as TFS with and without IMM use by a third endpoint: (C) time to cessation of both IO protocol therapy and IMM use. Area under each Kaplan-Meier curve was estimated by the 36-month restricted mean time-to-event. Area under the overall survival (OS) curve was partitioned as survival after subsequent therapy initiation (mean OS-B), TFS (mean B-A), time on IO protocol therapy (mean A), and as TFS with (mean C-A) and without (mean B-C) IMMs. Each area was summarized by its percentage of the 36-month period.

Results

At 36 months, 58% of NIVO+IPI, 52% of NIVO, and 36% of IPI patients were alive. Few patients remained on protocol therapy (11% NIVO+IPI, 17% NIVO, and 0% IPI) and many were surviving free of subsequent therapy initiation (47% NIVO+IPI, 37% NIVO, and 15% IPI). The 36-month restricted mean OS was longer for NIVO+IPI and NIVO than IPI (Table 1). Patients on NIVO spent a longer time on protocol therapy compared with NIVO+IPI or IPI. Mean TFS was longest for NIVO+IPI at 31% of the period; 13% with and 18% without IMMs. TFS without IMMs was longer for NIVO+IPI than NIVO (+3.2 months; 95% CI 1.7, 4.7) and shorter than IPI (-0.7 months; 95% CI -2.5, 1.2).

Conclusions

TFS, defined by the area between Kaplan-Meier curves for time to IO protocol therapy cessation and time to subsequent therapy or death, was longer for NIVO+IPI compared with NIVO or IPI in patients with advanced melanoma. When IMM use was considered, TFS without IMMs was longer for NIVO+IPI than NIVO.

References

1. Regan MM, Werner L, Tarhini A, et al. Treatment-free survival, a novel outcome applied to immune-oncology agents in advanced melanoma. Presented at ASCO June 1-5, 2018; abstract 9531.

Table 1.

Table 1. Estimated restricted mean months of different health states (of 36 months): TFS with and without IMM use

Restricted mean time, months (% of 36-month period)	NIVO+IPI (N=407)	NIVO (N=313)	IPI (N=357)
OS	25.7 (72)	24.9 (69)	21.4 (59)
Time on IO protocol therapy (A)	10.3 (29)	13.9 (39)	2.6 (7)
TFS (B-A)	11.1 (31)	4.6 (13)	8.7 (24)
TFS with IMMs (C-A)	4.5 (13)	1.2 (3)	1.4 (4)
TFS without IMMs (B-C)	6.6 (18)	3.4 (9)	7.2 (20)
Survival after subsequent therapy initiation (OS-B)	4.3 (12)	6.4 (18)	10.1 (28)

P381

Schweinfurthin natural products promote immune-dependent regression of murine melanoma and improve anti-PD-1-based immunotherapy to achieve durable complete responses and protective immunity

Kathleen Kokolus, MS, PhD[1], Jeremy Haley, MS[1], Emily Koubek[1], Raghavendra Gowda, PhD[1], Saketh Dinavahi, PhD[1], Arati Sharma, PhD[1], David Claxton, MD[2], Klaus Helm, MD[1], Joseph Drabick, MD[2], Gavin Robertson, PhD[1], Jeffrey Neighbors, PhD[1], Raymond Hohl, MD[2], Todd Schell, PhD[1]

[1]Penn State College of Medicine, Hershey, PA, USA
[2]Penn State Cancer Institute, Hershey, PA, USA

Background

Metastatic melanoma is a significant clinical problem with a 5-year survival rate of 15-20%. Recent approval of new immunotherapies and targeted inhibitors have improved the prognosis for these patients. In particular, antibody-based therapies that block the PD-1/PD-L1 checkpoint inhibitory pathway have achieved an increased overall response rate of 30-40% in metastatic melanoma. However, durable complete response rates are reported only around 15%, highlighting the need to identify approaches that can increase the therapeutic efficacy. Schweinfurthins are a family of plant-derived products that demonstrate anticancer activity against a variety of tumor types. Specific mechanisms of activity remain only partially defined but these compounds are known to modulate cholesterol metabolism. Given recent studies demonstrating that immune-based approaches may synergize with cholesterol inhibiting drugs, we investigated how schweinfurthins may impact anti-PD-1-mediated immunotherapy using an aggressive murine melanoma model.

Methods

Two different schweinfurthin analogs were tested for concentration-dependent in vitro growth inhibition of three human melanoma cell lines as well as the murine B16.F10 melanoma cells. B16.F10 cells treated with increasing concentrations of schweinfurthins were evaluated for surface expression of calreticulin using flow cytometry. Groups of B16.F10 melanoma-bearing C57BL/6 mice were administered schweinfurthin analogs for five consecutive days with or without administration of anti-PD-1 antibody twice a week for three weeks. Tumor growth and mouse survival was monitored. H&E stains were used to evaluate tumor regression. The impact of schweinfurthin administration on immune cell composition was determined by flow cytometry.

Results

Two schweinfurthin compounds differentially reduced the growth of human and murine melanoma cells in vitro and induced plasma membrane surface localization of the ER-resident protein calreticulin in B16.F10 melanoma cells, an indicator of immunogenic cell death. Both compounds improved anti-PD-1-mediated immunotherapy of established tumors in immunocompetent C57BL/6 mice either by delaying tumor progression or resulting in complete tumor regression. A 5-day course of schweinfurthin alone was associated with transient tumor regression in the absence of anti-PD-1 and this initial regression required an intact immune system as tumors were unaffected in NOD scid gamma (NSG) mice.

Conclusions

Schweinfurthins promote an immune-dependent initial tumor regression and improve the efficacy of anti-PD-1 therapy, leading to enhanced and durable anti-tumor immunity. This combination approach can potentially be translated to improve outcomes for metastatic melanoma patients treated with anti-PD1 therapy.

Acknowledgements
Supported, in part, by the Rose Dunlap Endowment and the Pennsylvania DOH using Tobacco CURE Funds (SAP #4100072562). KMK was supported by National Cancer Institute/National Institutes of Health training grant T32 CA060395. Schweinfurthin compounds were provided by Terpenoid Therapeutics Inc.

Ethics Approval
Animal studies were performed in accordance with institutional guidelines under protocol #46864 approved by the Penn State College of Medicine Institutional Animal Care and Use Committee

P382

CD28-negative memory tumor infiltrating lymphocytes (TILs) maintain an activated cytotoxic phenotype

Lillian Seu, PhD[1], Bijal Kakrecha, BS[1], Paul Fischer, MSc[1], Malinda Aitken[2], Alice Tang[3], Steven Nadler, PhD[2], Laurence Menard, PhD[2]

[1]*Bristol-Myers Squibb, ewing, NJ, USA*
[2]*Bristol Myers Squibb, Princeton, NJ, USA*
[3]*University of Pennsylvania, Philadelphia, USA*

Background
CD28 is constitutively expressed on human T cells, and promotes survival, proliferation signals, and induces the T cell growth factor interleukin-2. Enrichment of the senescent CD28-negative T cell population is a feature of an aging immune system, and is accelerated in various inflammatory conditions caused by chronic infections and/or autoimmune conditions. Recently, it has been shown that PD1 counteracts CD28 function via active de-phosphorylation of the cytoplasmic tail of CD28. Due to the repression by the critical immune checkpoint (IC) target PD-1, an understanding of CD28 regulation of tumor T cells would greatly aid in reinvigoration strategies with PD1/PDL1-based immunotherapies.

Methods
Flow cytometry of immune cells from freshly isolated tumors and matching peripheral blood was conducted across several tumor indications (renal cell carcinoma, non-small cell lung carcinoma, melanoma, colorectal cancer, head and neck squamous cell carcinoma, and others.) Boolean gating as well as high dimensionality tSNE analyses were performed to assess CD28 expression levels on CD4+ and CD8+ T cells, along with memory (CD45RO, CCR7), cytotoxic (CD107a), and activation (CD38) markers. (Figure 1, 2)

Results
In this report, we show that CD28 expression levels are diminished in TILs as compared to matching peripheral T cells. Concordant with observations in peripheral T cells, tumor associated CD4+ T cells retain higher levels of CD28 expression than CD8+ T cells. We additionally show that effector memory CD4+ TILs have highly correlated expression levels of CD28 and PD1 (CD4 Effector memory: Spearman r=0.62, P=0.001), while not true of the CD8 effector memory compartment in tumors (Spearman r=0.13, P=ns). Moreover, follow-up tSNE analysis revealed in a subset of tumors (e.g., renal cell carcinoma) a population of CD8+ CD45RO+ CD28-negative memory T cells with a CD107a (cytotoxic) and CD38 (activated) phenotype. Longitudinal immunophenotyping of PD1/PDL1-treated donors reveal extensive variability in CD28+ T cell frequencies across all peripheral T cell memory subsets.

Conclusions
We report an assessment of CD28 profiling in various tumor indications that show that CD28 expression is most significantly lost on central memory and effector memory CD8+ T cells in the tumor. Despite

the loss of this critical co-stimulatory receptor, a cytotoxic profile (CD107a) is retained on CD28-negative CD8+ T cells across many tumor indications. Studies are currently aimed at understanding which agonist signals are sufficient to maintain and activated phenotype of these CD28 negative memory T cell populations.

Ethics Approval

The study was approved by BMS Institutution's Ethics Board

Figure 1. tSNE T cell analysis: matching Blood and TILs

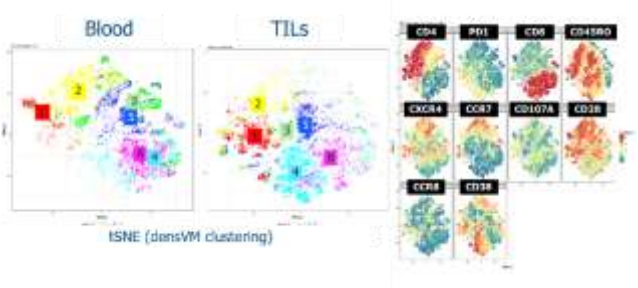

Figure 2. tSNE overlay using machine-learning approaches

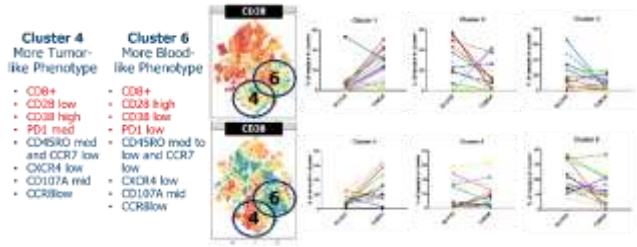

P383

Combination therapy with M7824 (MSB0011359C) and NHS-muIL12 enhances antitumor efficacy in preclinical cancer models

Colleen Stanton[1], Chunxiao Xu, PhD[2], Bo Marelli[2], Jin Qi[2], Guozhong Qin[2], Huakui Yu[2], Molly Jenkins[2], Kin-Ming Lo[2], Joern-Peter Halle[2], Yan Lan, MD[2]

[1]Nucleus Global
[2]EMD Serono Research and Development, Belmont, MA, USA

Background

PD-1/PD-L1 pathway inhibition is a clinically validated approach in cancer therapy. However, most patients do not respond to the monotherapy due to multiple immunosuppressive mechanisms. Combining anti-PD-1/PD-L1 with other immunotherapeutic agents targeting additional immunomodulatory pathways in the tumor microenvironment (TME) is one strategy to overcome resistance and improve response rates. M7824 is an innovative first-in-class bifunctional fusion protein composed of two extracellular domains of TGF-β receptor II (a TGF-β "trap") fused to a human anti-PD-L1 IgG1 monoclonal antibody. Through simultaneous blockade of the PD-L1 and TGF-β pathways, M7824 demonstrated enhanced anti-tumor activity in preclinical models [1]. NHS-IL12, and the surrogate NHS-muIL12, are immunocytokines designed to target tumor necrotic regions to deliver IL-12 into the TME, where they can activate NK cells and CD8+ T cells to increase their cytotoxic functions. The surrogate NHS-muIL12 has demonstrated antitumor efficacy in preclinical models [2]. This study is designed to investigate whether M7824 treatment may further benefit from combination therapy with NHS-muIL12.

Methods

Mice bearing MC38, EMT-6, or 4T1 tumors were treated with M7824, NHS-muIL12, or combination therapy. Tumor growth and survival were assessed in each model, and tumor recurrence following remission and rechallenge was evaluated in the EMT-6 model. Immune cell populations in the spleens and tumors were evaluated by flow cytometry and the frequency of tumor antigen-reactive IFNγ-producing CD8+ T cells was evaluated by an ELISpot assay in the MC38 model.

Results
Combination of M7824 and NHS-muIL12 enhanced antitumor activity and extended the survival relative to either monotherapy in preclinical tumor models. Combination therapy also enhanced the proliferation, infiltration, and cytotoxicity of CD8+ T cells relative to monotherapies. In addition, the combination therapy increased the frequency of tumor antigen-reactive T cells and induced the generation of tumor-specific immune memory, as demonstrated by protection against tumor rechallenge.

Conclusions
These data demonstrate that combination therapy with M7824 and NHS-muIL12 improved anti-tumor efficacy in multiple preclinical tumor models and suggest that combining these therapies may be a promising therapeutic strategy for patients with solid tumors.

References
1. Lan Y, et al. Enhanced preclinical antitumor activity of M7824, a bifunctional fusion protein simultaneously targeting PD-L1 and TGF-β. Sci Trans Med. 2018;10(424).
2. Fallon J, et al. The immunocytokine NHS-IL12 as a potential cancer therapeutic. Oncotarget 2014;5(7):1869-84.

P384

M7824 (MSB0011359C) is an effective combination partner with standard-of-care therapies in tumor models

Yan Lan, MD[2], Rinat Zaynagetdinov, MD, PhD[2], Kenneth Hance[4], Chia Lin Chu, PhD[5], Chunxiao Xu, PhD[2], Bo Marelli[2], Jin Qi[2], Guozhong Qin[2], Huakui Yu[2], Giorgio Kradjian[2], Yanping Zhang[2], Molly Jenkins[2], Joern-Peter Halle[2], Kin-Ming Lo[2]

[1]Nucleus Global
[2]EMD Serono Research and Development, Billerica, MA, USA
[3]EMD Serono Research & Development, Billerica, MA, USA
[4]GlaxoSmithKline, Collegeville, PA, USA
[5]EMD Serono Research and Development Inst, Billerica, MA, USA

Background
We have recently reported enhanced preclinical anti-tumor activity of M7824, which is an innovative first-in-class bifunctional fusion protein composed of two extracellular domains of TGF β receptor II (a TGF-β "trap") fused to a human anti–PD-L1 IgG1 monoclonal antibody [1]. In Phase 1 and Phase 1b expansion studies in patients with advanced solid tumors, M7824 has shown early evidence of clinical activity [2]. This study is designed to investigate the efficacy of M7824 in combination with standard-of-care therapies in different murine models.

Methods
Combination of M7824 with Ox/5-FU was tested in the MC38 colorectal cancer model, with cisplatin, doxorubicin, radiation therapy (RT), or anti-VEGF A (B20) in the 4T1 breast cancer model, with gemcitabine in the MB49 bladder cancer model, with pazopanib in the RENCA renal carcinoma model, and with anti-CTLA4 in the B16 melanoma model.

Results
Combination of M7824 and Ox/5-FU significantly decreased tumor volume and weight in the MC38 model and increased the frequency of p15E-reactive, IFNγ-producing CD8+ T cells. In the 4T1 model, combination of M7824 and doxorubicin or RT, enhanced tumor growth inhibition and extended survival, and combination of M7824 and cisplatin or anti-VEGF A likewise decreased tumor volume relative to monotherapies. Combination of M7824 and pazopanib significantly decreased tumor weight in the orthotopic RENCA model. Finally, combination of M7824 with anti-CTLA4 significantly decreased

tumor volume in the B16 model.

Conclusions

Taken together, these results support the combination of M7824 with conventional standard-of-care therapies. The enhanced efficacy seen in multiple murine models also supports the broad application of M7824 combination therapies in different cancer indications.

References

1. Lan Y, et al. Enhanced preclinical antitumor activity of M7824, a bifunctional fusion protein simultaneously targeting PD-L1 and TGF-β. Sci Trans Med. 2018;10(424).2. Strauss J, et al. phase I trial of M7824 (MSB0011359C), a bifunctional fusion protein targeting PD-L1 and TGFβ, in advanced solid tumors. Clin Cancer Res. 2018;24(6):1287-1295.

P385

Preliminary biomarker analysis of sitravatinib in combination with nivolumab in NSCLC patients progressing on prior checkpoint inhibitor

Vanessa Tassell[1], James Christensen[1], Peter Olson[1], Igor Rybkin, MD, PhD[2], Ticiana Leal, MD[3], Alexander Spira, MD, PhD, FACP[4], Collin Blakely, MD[5], Manish Patel, DO[6], Leora Horn, MD[7], Kai He, MD, PhD[8], David Berz, MD[9], Ryan Ramaekers, MD[10], Alison Savage[11], Timothy Larson[12], Donald Richards[13], Tammy Roque[14], Anthony Pham[15], Massarelli Erminia[16], James Uyeki[17], Abhinav Chandra, MD, FACP[18], Robert Jotte[19], Wangjian Zhong, MD[20], David Hong, MD[21], Joshua Lang, MD MS[3], Jennifer Schehr[3], Julio Fernandez Banet[22], Kai He, MD, PhD[23], Adam Pavlicek[22]

[1]Mirati Therapeutics, San Diego, CA, USA
[2]Henry Ford Health System, Detroit, MI, USA
[3]University of Wisconsin, Madison, WI, USA
[4]Virginia Cancer Specialists, Fairfax, VA, USA
[5]University of San Francisco, San Francisco, CA, USA
[6]University of Minnesota Masonic Cancer C, Minneapolis, MN, USA
[7]Vanderbilt University, Nashville, TN, USA
[8]The Ohio State University Comprehensive, Columbus, OH, USA
[9]Beverly Hills Cancer Center, Beverly Hills, CA, USA
[10]Saint Francis Cancer Treatment Center, Grand Island, NE, USA
[11]Hematology Oncology Associates - Barnett, Medford, OR, USA
[12]Minnesota Oncology Hematology, Minneapolis, MN, USA
[13]Texas Oncology - Longview Cancer Center, Houston, TX, USA
[14]Texas Oncology, Sherman, TX, USA
[15]Northwest Cancer Specialists, P.C., Tualatin, OR, USA
[16]City of Hope - Duarte, Duarte, CA, USA
[17]Texas Oncology - South Austin, Austin, TX, USA
[18]Yuma Regional Cancer Center, Yuma, AZ, USA
[19]Rocky Mountain Cancer Centers - Denver, Denver, CO, USA
[20]Baptist Health, Louisville, KY, USA
[21]MD Anderson, Houston, TX, USA
[22]Monoceros Biosystem Inc., San Diego, CA, USA
[23]x, Columbus, OH, USA

Background

Sitravatinib is a spectrum-selective tyrosine kinase inhibitor which targets TAM receptors (Axl, MER), VEGFR2, KIT and MET. Inhibition of these receptors may enhance anti-tumor activity of nivolumab by modifying the tumor microenvironment and enhancing a T cell-mediated anti-tumor immune response. Sitravatinib in combination with nivolumab has demonstrated signs of clinical activity in advanced non-squamous NSCLC patients (pts) who have become refractory to prior checkpoint inhibitor therapy (CIT). Understanding the mechanism of action and molecular characteristics of responding patients is critical and we report on the preliminary biomarker analysis.

Methods
Study objectives include evaluation of safety, efficacy, and correlative science endpoints in pts who have progression of disease (PD) on or after CIT. Sitravatinib is administered orally in continuous 28-day cycles; nivolumab is administered intravenously 240 mg every 2 weeks. Key objectives include overall response rate, safety, evaluation of tumor PD-L1 expression, tumor mutation profile, and circulating and tumor infiltrating immune cell populations.

Results
As of June 26, 2018, the CIT-experienced cohorts enrolled 64 pts and 46/64 have had at least one on-study tumor assessment. Clinical benefit (CB) defined as confirmed partial response (PR) and stable disease (SD) of >/= 14 weeks has been seen in 19/46 pts. Evaluation of tumor PD-L1 expression indicated a trend toward a positive PD-L1 result in pts with CB compared with pts with no CB (PD or SD < 14 weeks). Profiling of tumor mutation status in plasma (GuardantOMNITM) indicated no significant correlation of tumor mutation burden (TMB) with CB. Interestingly, pts exhibiting STK11 (LKB1) mutations (3) all demonstrated PD as best response. Baseline and post-treatment (C1D15) analysis of selected circulating immune cell populations in peripheral blood were evaluated utilizing flow cytometry. A significant increase in T-effector cells (CD8+/CD4-/CD3+/CD45RA/CD62L-) at C1D15 was observed in subsets of pts with CB compared with pts with no CB. In an exploratory analysis, MHC I expression in circulating tumor cells (CTCs) was evaluated. In one patient, baseline CTCs showed negative MHC I expression at PD and subsequently had increased expression of MHC I on CTCs after treatment with sitravatinib and nivolumab, which correlated with 13.3% reduction in target lesions. Additional baseline and post-treatment analyses will be included.

Conclusions
The combination of sitravatinib with nivolumab is clinically active in pts progressing on prior CIT regimens. Preliminary analysis of correlative endpoints suggests that PD-L1 positivity and induction of a T-effector cell response may correlate with clinical outcome.

Ethics Approval
This study was approved by Copernicus (WIRB), approval number PRA0-16-311.

P386

CTX-471, a novel agonistic antibody targeting CD137, enhances the anti-tumor activity of tumor antigen-targeted antibodies and immune checkpoint inhibitors when used in combination

Ugur Eskiocak, PhD[1], Wilson Guzman, BS[1], Robert Tighe, BS[1]

[1]Compass Therapeutics, Cambridge, MA, USA
[2]Compass Therapeutics LLC, Cambridge, MA, USA

Background
CD137 (4-1BB) is a member of the TNFR superfamily that provides costimulatory signals to activated cytotoxic lymphocytes. CTX-471 is a novel agonistic antibody that recognizes a unique epitope of CD137 that is shared by human, cynomolgus monkey, and mouse. CTX-471 displays a wide therapeutic window in preclinical studies, making it a promising agent for clinical IO combinations. Prior reports have identified CD137 agonists as effective combination partners for tumor antigen-targeted antibodies and immune checkpoint inhibitors (ICIs) [1,2].

Methods
Combination study of CTX-471 plus trastuzumab (IgG1 anti-Her2) or cetuximab (IgG1 anti-EGFR) in immunocompetent mice was conducted with CT26 murine CRC cells engineered to express the human targets. To circumvent spontaneous tumor rejection, the cell lines were inoculated into Balb/c-SCID mice

followed by adoptive transfer of Balb/c splenocytes and initiation of treatment five days later. In the CTX-471 plus cetuximab study, FACS-based immunophenotyping was performed. CTX-471 was tested in combination with PD-L1 blockade (CTX-PD-L1) in the EMT-6 orthotopic breast carcinoma model and the C1498 disseminated AML model. Combination with anti-PD-1 was assessed in the PANC-02 orthotopic tumor model.

Results

CTX-471 combination with trastuzumab was synergistically effective against CT26-huHer2 tumors curing 8/8 mice, while CTX-471 monotherapy achieved 3/8 cures and trastuzumab monotherapy was ineffective. CTX-471 combination with cetuximab had synergistic activity against CT26-huEGFR tumors, curing 4/8 mice. CTX-471 and cetuximab lacked monotherapy efficacy in this model. CTX-471 combined with cetuximab caused an increase in CD8+ TILs and a decrease in Treg, positively shifting the CD8/Treg ratio. Significant increases in MHC class II+ M1 macrophages was also observed. We compared sequential vs. concomitant dosing schedules of CTX-471 plus ICI. In the EMT6 tumor model, CTX-471 plus CTX-PD-L1 showed enhanced efficacy when given sequentially, whereas concomitant dosing negatively impacted efficacy. In the PANC02 model, CTX-471 plus anti-PD-1 showed improved efficacy that was unimpacted by dosing schedule. In the disseminated C1498 AML model both dose schedules of CTX-471 plus CTX-PD-L1 synergistically improved overall survival, with concomitant dosing curing 30% of the animals. All cured mice rejected tumors upon rechallenge.

Conclusions

Our promising preclinical results support the clinical testing of CTX-471 in combination with approved antigen-targeted antibodies and ICIs. Interestingly, the sequential dosing of costimulatory agonists and ICIs appears to be important in some, but not all, preclinical models. Understanding the clinical implications of this observation will require further research. IND-enabling toxicology studies for CTX-471 are ongoing and a Phase 1 clinical trial is planned for 2019.

References

1. Kohrt HE, Houot R, Weiskopf K, et al. Stimulation of natural killer cells with a CD137-specific antibody enhances trastuzumab efficacy in xenotransplant models of breast cancer. J Clin Invest. 2012;122(3):1066-75.2. Shindo Y, Yoshimura K, Kuramasu A, et al. Combination immunotherapy with 4-1BB activation and PD-1 blockade enhances antitumor efficacy in a mouse model of subcutaneous tumor. Anticancer Res. 2015;35(1):129-36.

Ethics Approval

The described animal studies were approved by Compass Therapeutics Institutional Animal Care and Use Committee under protocol CTX-016-01.

P387

A multicenter, phase II study in patients with first line NSCLC, or recurrent PD-X refractory NSCLC or with recurrent HNSCC receiving Eftilagimod Alpha in combination with Pembrolizumab (TACTI-002)

Frederic Triebel, MD, PhD[1], Christian Mueller, MSc[1], Chrystelle Brignone, PhD[1], Tatsiana Skrahina[1], Martin Forster[2]

[1]*Immutep, Orsay, France*
[2]*UCL Cancer Institute, London, UK*

Background

Eftilagimod alpha is a recombinant soluble LAG-3Ig fusion protein binding to MHC class II molecules and mediating antigen presenting cell (APC) activation followed by CD8 T-cell activation. Combining an APC activator with an immune checkpoint inhibitor (ICI)

aims to increase efficacy without additional toxicity. A Phase I study (abstract number: P398

*Corresponding author email: ftriebel@immutep.com) has assessed the safety of the eftilagimod alpha plus pembrolizumab combination.

Methods

The study is designed according to Simon's optimal two-stage design, with objective response rate as primary endpoint. Secondary endpoints include progression free survival and overall survival. During the first stage of the study patients (pts) will be recruited into this multicenter, open label, Phase II study for each of three indications: A: 1st line, PD-X naïve NSCLC; B: 2nd line, PD-X refractory NSCLC; C: 2nd line PD-X naive HNSCC. In case there are more responses than a certain threshold observed in patients recruited in the initial stage (N1), additional patients (N2) will be recruited. In total 110 patients are planned to be enrolled. Eftilagimod alpha will be administered as 30 mg subcutaneous injection every 2 weeks for the first 8 pembrolizumab cycles (200 mg every 3 weeks) and every 3 weeks for the 9 following cycles (clinicaltrial.gov link to be added).

Results

Trial in progress

Conclusions

Trial in progress

Trial Registration

EudraCT: 2018-001994-25

Figure 1. TACTI-002 trial design

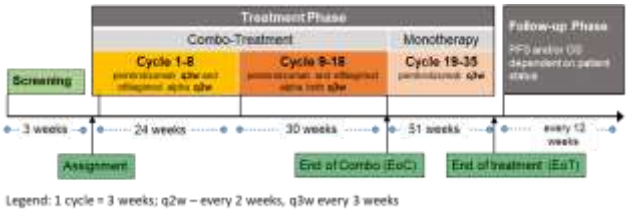

Legend: 1 cycle = 3 weeks; q2w – every 2 weeks, q3w every 3 weeks

P388

Combination of the Wee1 inhibitor adavosertib (AZD1775) with anti-PD-L1 shows activity in pre-clinical studies

Viia Valge-Archer, PhD[1], Matthew King, PhD[1], Chrysiis Michaloglou, PhD[1], Anisha Solanki[1], Jennifer Hare[1], PhD[1], Susan Critchlow, PhD[1]

[1]*AstraZeneca, Little Chesterford, UK*

Background

Inhibition of DNA damage repair (DDR) pathways may enhance anti-tumour immunity via immune recognition and response to increased DNA damage. Immune priming may be consolidated by combination with immune checkpoint blockade to further increase anti-tumour responses.Inhibition of Wee1 by adavosertib (AZD1775) can induce replication stress and aberrant entry into mitosis in cells, which can result in cell death via replication or mitotic catastrophe [1].

Methods

Human and murine T cell proliferation was measured as CTV dilution in response to anti-CD3 / anti-CD28 stimulation or mixed lymphocyte reaction in the presence or absence of compounds. Tumour cells were treated in vitro for 24 to 72 hours prior to assessment. Alterations in tumour or T cell phenotype were measured by flow cytometry or immunofluorescent microscopy.In vivo syngeneic tumour models were implanted subcutaneously into Balb/c (CT26) or C57/Bl6 (MC38) mice and treated with adavosertib or anti-murine PD-L1 at the indicated doses and schedules.

Results

Proliferation and viability of activated human T cells show dose-dependent inhibition by adavosertib treatment, along with increased S-phase gamma-H2AX expression and 53BP1 foci, which are markers

of DNA damage. Similar effects were observed in both human and murine T cells, with proliferation IC50's of 350 nM and 149 nM, respectively. Results of in vivo PD studies demonstrate that a 2-5-fold decrease in number or frequency of tumour infiltrating T cells under continuous adavosertib dosing can be mitigated by scheduling. Combination of adavosertib with anti-PD-L1 resulted in approx. 2-fold increased numbers of tumour infiltrating CD8+ T cells and significantly increased Ki67 expression of tumour infiltrating T cells over vehicle or anti-PD-L1 alone. Treatment with adavosertib also resulted in increases in tumour cytokine and chemokine gene expression consistent with increased immune priming and activation.Despite the impact of adavosertib on T cell proliferation, anti-tumour efficacy studies in a murine syngeneic tumour model do not show antagonism of anti-PDL1 activity by adavosertib. Rather, positive schedule-dependent combination anti-tumour activity of adavosertib + anti-PD-L1 is observed, including 3/10 complete responses (CR) with the combination using a schedule that showed no CR with either monotherapy.

Conclusions

Pre-clinical data provides support for further investigation of combinations of adavosertib plus immune checkpoint blockade. Studies are ongoing to explore further dose and scheduling, as well as molecular mechanisms underpinning combination activity, including interferon/STING and immunogenic pathways.

References

1. Matheson CJ, Backos DS, Reigan P. Targeting WEE1 Kinase in Cancer. Trends Pharmacol Sci. 2016; 37:872-881.

Consent

All studies were conducted in accordance with UK Home Office legislation, the Animal Scientific Procedures Act 1986 (ASPA) and with AstraZeneca Global Bioethics policy. All experimental work is outlined in project licence a which has gone through the AstraZeneca Ethical Review Process.

P389

Digital spatial profiling on uveal melanoma tissue treated with combined radiofrequency ablation and ipilimumab

Trieu My Van, PhD[1], Lisette Rozeman, MD[2], Sarah Warren, PhD[3], Joseph Beechem, PhD[3], John Haanen, MD PhD[2], Christian Blank, MD, PhD[2]

[1]NKI/Nanostring, Amsterdam, Netherlands
[2]NKI, Amsterdam, Netherlands
[3]Nanostring, Seattle, WA, USA

Background

Uveal melanoma (UM) is a rare disease which shows limited response to anti-CTLA4 and anti-PD1 antibodies [1,3-6]. Preclinical experiments in murine melanoma model indicated a durable response with additional radiofrequent ablation (RFA) and CTLA-4 blockade by enhancing antigen presentation within the tumor area [7,8]. However, RFA and immunotherapy are not suitable for all melanoma patients and the incidences of adverse events (AE) also vary. Thus, personalized therapy would lower the risk for AE and predict the response rate after cancer therapy. Here, we used the novel digital spatial profiling (DSP) technology to characterize the protein profiles in UM patients before and upon combination therapy.

Methods

The SECIRA-UM trial is a phase 1b/2 study assessing the safety and efficacy of the combination of RFA and IPI in UM patients with at least 2 unresectable liver lesions. In phase 1b, patients underwent RFA of one liver lesion and received 4 courses of ipilimumab (IPI) to define the recommended dose for phase 2. Primary endpoints of phase 2 were confirmed

objective response rate (ORR) and disease control rate (DCR) according to RECIST 1.1, secondary endpoints were progression free survival (PFS) and overall survival (OS).DSP technology uses a cocktail of primary antibodies conjugated to unique DNA oligos with a UV photocleavable linker. Oligos in the Region of interest (ROI) on formalin-fixed paraffin-embedded (FFPE) tissues are released via UV mediated linker cleavage and counted on the nCounter™ platform.

Results

The combination of RFA-IPI 10mg/kg slightly improved the median PFS and OS compared to RFA-IPI 3mg/kg. However, the most common RFA related toxicities, which were transient elevation of liver enzymes and flank pain, did not differ between the different dosing cohorts. To understand the response of UM after combination therapy we used the DSP technology to characterize the protein expression profiles in UM biopsies. Our DSP analysis provided a detailed profile of 39 proteins/biopsy. Here, we show the comparison of expression profiles in responding vs non-responding patients, before vs after combination treatment and between the different dosing cohorts.

Conclusions

Our trial results showed a safe but limited clinical activity of RFA-IPI 3mg/kg while RFA-IPI 10mg/kg had a higher toxicity rate but showed a trend towards longer overall survival. Moreover, usage of the DSP technologies strongly advances our knowledge of protein expression levels within the tumor area and will have a high impact on future trial designs.

Trial Registration

CA184-180/N11RFA

References

1. Krantz BA, Dave N, Komasubara KM, Marr BP, Carvajal RD. Uveal melanoma: epidemiology, etiology, and treatment of primary disease. Clin Ophthalmol. 2017; 11: 279-289.
2. Maio M, Danielli R, Chiarion-Sileni V, Pigozzo J, Parmiani G, Ridolfi R, De Rosa F, Del Vecchio M, Di Guardo L, Queirolo P, Picasso V, Marchetti P, De Galitiis F, Mandala M, Guida M, Simeone E, Ascierto PA. Efficacy and safety of ipilimumab in patients with pre-treated, uveal melanoma. Annals of Oncology. 2013; 2911-2915
3. Luke JJ, Callahan MK, Postow MA, Romano E, Ramaiya N, Bluth M, Giobbie-Hurder A, Lawrence DP, Ibrahim N, Ott PA, Flaherty KT, Sullivan RJ, Harding JJ, D'Angelo S, Dickson M, Schwartz GK, Chapman PB, Wolchok JD, Hodi FS, Carvajal RD. Clinical activity of ipilimumab for metastatic uveal melanoma: a retrospective review of the Dana-Farber Cancer Institute, Massachusetts General Hospital, Memorial Sloan-Kettering Cancer Center, and University Hospital of Lausanne experience. Cancer. 2013. 119(20):3687-95
4. Kelderman S, van der Kooij MK, van den Eertwegh AJ, Soetekouw PM, Jansen RL, van den Brom RR, Hospers GA, Haanen JB, Kapiteijn E, Blank CU. Ipilimumab in pretreated metastastic uveal melanoma patients. Results of the Dutch Working group on Immunotherapy of Oncology (WIN-O). Acta Oncol. 2013
5. Algazi AP, Tsai KK, Shoushtari AN, Munhoz RR, Eroglu Z, Piulats JM, Ott PA, Johnson DB, Hwang J, Daud AI, Sosman JA, Carvajal RD, Chmielowski B, Postow MA, Weber JS, Sullivan RJ. Clinical outcomes in metastatic uveal melanoma treated with PD-1 and PD-L1 antibodies. Cancer. 2016. 3344-3353
6. van der Kooij MK, Joosse A, Speetjens FM, Hospers GA, Bisschop C, de Groot JW, Koornstra R, Blank CU, Kapiteijn E. Anti-PD1 treatment in metastatic uveal melanoma in the Netherlands. Acta Oncol. 2017. 101-103.
7. den Brok MH, Sutmuller RP, van der Voort R, Bennink EJ, Figdor CG, Ruers TJ, Adema GJ. In situ tumor ablation creates an antigen source for the generation of antitumor immunity. Cancer Res. 2004. 4024-9
8. den Brok MH, Sutmuller RP, Nierkens S, Bennink

EJ, Frielink C, Toonen LWJ, Boerman OC, Figdor CG, Ruers TJM, Adema GJ. Efficient loading of dendritic cells following cryo and radiofrequency ablation in combination with immune modulation induces anti-tumour immunity. Br J Cancer. 2006. 896–905

P390

Vasoactive Intestinal Peptide Antagonist Synergizing with PD1 Antibody Inhibits the Tumor Growth of Breast Cancer.

Shuhua Wang, MD[1], Sruthi Ravindranathan, PhD[1], Yiwen Li, MS[1], Rebecca Pankove, MS[1], Parvin Forghani[1], Edmund K. Waller, MD, PhD[1]

[1]*Emory University, Atlanta, GA, USA*

Background

Breast cancer is known to be the most common cancer in women with annual incidence of 170 million globally [1]. Novel immunotherapeutic approaches that target the immunosuppressive tumor microenvironment (TME) are required to boost the endogenous immune response [2]. Several studies have shown that the inhibition of myeloid-derived suppressor cells (MDSCs) in the TME effectively promotes T cell immunity against breast cancer. We have previously shown that Silibnin, a natural flavonoid from milk thistle can effectively reduce MDSC accumulation in blood and tumor in 4T1 tumor bearing mice [3]. Additionally, in murine leukemia models, we have observed that inhibiting vasoactive intestinal peptide (VIP) signaling reduces tumor burden and increases survival. The current study thus explores the effect of inhibiting VIP signaling with/without checkpoint inhibitors in murine breast cancer model.

Methods

Balb/c mice were injected 2.5 x 105 4T1cells subcutaneously on the right flank on day 0 and treated with VIPhyb (subcutaneously), anti-PD-1 (aPD1) (intraperitoneally) or a combination of VIPhyb and anti-PD-1 (aPD1+VIPhyb) starting from day 1. Mice treated with PBS and IgG2a were considered as control. Tumor volume was measured every day and mice were euthanized either upon ulceration or when their tumors reached the IACUC endpoint (500mm3). Spleens were then harvested and analyzed for frequency of Ki67 or PD1 expressing T cells, NK cells, B cells and MDSCs.

Results

On day 13 and 14 post 4T1 inoculation, the combination treatment group had the smallest tumor burden ($P<0.05$, combination vs control group) (Fig 1). Higher frequencies of CD4+ PD1+ T cells were found in the combination group compared to control, anti-PD-1 or VIPhyb alone treated groups ($p<0.05$), consistent with result using the combination of VIPhyb and anti-PD1 in other solid tumor models studied in our lab. Higher levels of CD4+Ki-67+ cells were seen in the combination therapy treated group compared to control, aPD1 or VIPhyb treated group (p=NS). We observed a similar level of MDSC across all experimental groups (p=NS) (Fig 2).

Conclusions

Combination therapy with anti-PD-1 and VIPhyb treatment suppressed breast cancer growth and enhanced proliferation of antigen experienced CD4+ T cells. Inhibition of tumor growth was associated with increased numbers of antigen-experienced Ki67+ PD1+ T cells. Since silibinin has been previously shown to decrease the MDSC population, current experiments are testing the addition of silibinin to the combination therapy treatment.

References

1. Ferlay J, Soerjomataram I, Dikshit R, Eser S, Mathers C, Rebelo M, Parkin DM, Forman D, Bray F. Cancer incidence and mortality worldwide: sources, methods and major patterns in GLOBOCAN 2012. Int J Cancer. 2015 Mar 1; 136(5):E359-86.

doi:10.1002/ijc.29210. Epub 2014 Oct 9.
2. Umansky V, Blattner C, Gebhardt C, Utikal J. The Role of myeloid-derived suppressor cells (MDSC) in cancer progression.Vaccines (Basel). 2016 Nov 3; 4(4).pii: E36. Review.
3. Forghani P, Khorramizadeh MR,Waller EK.. Silibinin inhibits accumulation of myeloid-derived suppressor cells and tumor growth of murine breast cancer. Cancer Medicine. 2014; 3(2):215-224.

Ethics Approval
The study was approved by Emory Institute Animal Care and Use Committee, protocol number 3000202

Figure 1.

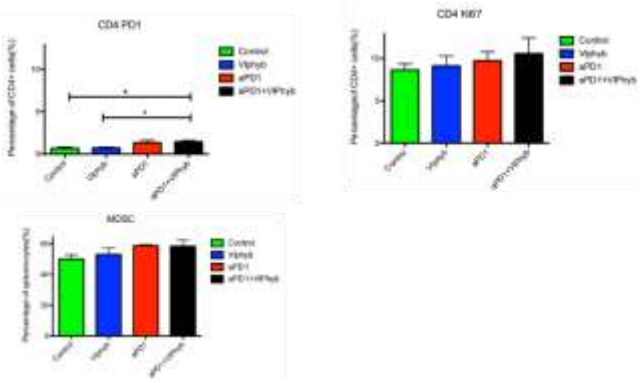

Figure 2.

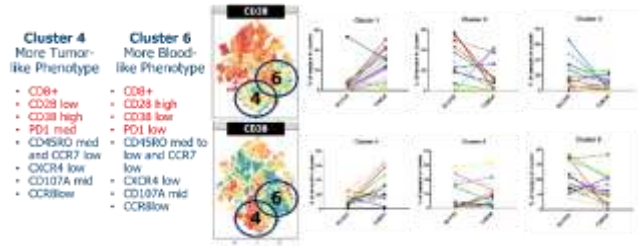

P391

A phase 1b/2 trial of lenvatinib in combination with pembrolizumab in patients with advanced melanoma

Matthew Taylor, MD[2], Nicholas Vogelzang, MD[3], Allen Cohn[3], Daniel Stepan[4], Robert Shumaker, PhD,[4], Corina Dutcus[4], Matthew Guo[4], Emmett Schmidt, MD PhD[5], Drew Rasco[6]

[1]*Oxford PharmaGenesis, Oxford, UK*
[2]*Oregon Health and Science University, Portland, OR, USA*
[3]*McKesson Specialty Health, Las Vegas, NV, USA*
[4]*Eisai Inc., Woodcliff Lake, NJ, USA*
[5]*Merck & Co., Inc., Kenilworth, NJ, USA*
[6]*South Texas Accelerated Research Therape, San Antonio, TX, USA*

Background
Lenvatinib is a multikinase inhibitor of VEGFR 1–3, FGFR 1–4, PDGFRα, RET, and KIT. Pembrolizumab, an anti-PD-1 antibody, is approved for the first-line treatment of patients with advanced melanoma, with objective response rates (ORR) of 21–34% [1,2]. Preclinical studies indicate that lenvatinib decreases the population of tumor-associated macrophages, increases $CD8^+$ T cell infiltration, and augments the activity of PD-1 inhibitors; therefore, lenvatinib is a rational combination partner for pembrolizumab [3,4]. We report interim results of an ongoing phase 1b/2 trial evaluating lenvatinib in combination with pembrolizumab in patients with solid tumors, focusing on the advanced melanoma cohort.

Methods
In this multicenter, open-label study (NCT02501096), patients with measurable, confirmed, metastatic melanoma and ECOG performance status ≤1 received lenvatinib (20 mg/day orally) + pembrolizumab (200 mg Q3W, IV). Patients were not preselected based on PD-L1 status. Tumor assessments were performed by study investigators using immune-related RECIST (irRECIST). The phase 2 primary end point was ORR at 24 weeks (ORR_{WK24}). Secondary end points included ORR, progression-free survival (PFS), and duration of response (DOR).

Results

At the data cutoff of March 1, 2018, 21 patients were enrolled: 14 (67%) patients were PD-L1(+), 4 (19%) were PD-L1(-), 3 (14%) were not tested; and 38% of patients had ≥1 prior anticancer therapy. The primary end point of ORR_{WK24} was 47.6% (95% CI, 25.7–70.2). Additional efficacy outcomes are summarized in the table (Table 1). All patients experienced ≥1 treatment-related adverse event (TRAE). Grade 3 and 4 TRAEs occurred in 13 (62%) and 1 (5%; adrenal insufficiency) patients respectively. There were no fatal TRAEs. The most common any-grade TRAEs were fatigue (52%), decreased appetite (48%), diarrhea (48%), hypertension (48%), dysphonia (43%), and nausea (43%). Dose reduction and interruption due to TRAEs occurred in 13 (62%) and 10 (48%) patients, respectively.

Conclusions

The lenvatinib and pembrolizumab combination regimen was well-tolerated and demonstrated encouraging clinical activity. The combination may potentially improve upon the antitumor activity of anti-PD-1 monotherapies, supporting further evaluation of this regimen in patients with advanced melanoma.

Trial Registration

NCT02501096

References

1. Ribas A, et al. Pembrolizumab versus investigator-choice chemotherapy for ipilimumab-refractory melanoma (KEYNOTE-002): a randomised, controlled, phase 2 trial. Lancet Oncology. 2015;16(8):908-18.
2. Robert C, et al. Pembrolizumab versus ipilimumab in advanced melanoma. N Engl J Med. 2015;372(26):2521-2532.
3. Kato Y et al. Effects of lenvatinib on tumor-associated macrophages enhance antitumor activity of PD-1 signal inhibitors. Mol Cancer Ther. 2015;14 (12Suppl2):A92.
4. Kato Y. Upregulation of memory T cell population and enhancement of Th1 response by lenvatinib potentiate antitumor activity of PD-1 signaling blockade. Cancer Res. 2017;77 (13 Suppl):4614.

Ethics Approval

This study was approved by all relevant institutional review boards.

Table 1.

Table 1. Summary of Tumor Response

Outcome	irRECIST (N = 21)
Best Overall Response, n (%)	
Complete response	1 (4.8)
Partial response	9 (42.9)
Stable disease	7 (33.3)
Progressive disease	3 (14.3)
Unknown or not evaluable	1 (4.8)
ORR, n (%) 95% CI	10 (47.6) 25.7–70.2
Median DOR, months (95% CI)	12.5 (2.7–NE)
Median PFS, months (95% CI)	7.6 (2.6–15.8)
PFS rate at 12 months, % (95% CI)	38.3 (16.5–60.0)
Median follow-up time for PFS, months (95% CI)	16.0 (5.3–22.0)

NE, not estimable.

P392

A phase 1b/2 trial of lenvatinib in combination with pembrolizumab in patients with non-small cell lung cancer

Marcia Brose[2], Nicholas Vogelzang, MD[3], Christopher Di Simone[3], Sharad Jain, MD[3], Donald Richards[3], Carlos Encarnacion[3], Drew Rasco[4], Robert Shumaker, PhD,[5], Corina Dutcus[5], Daniel Stepan[5], Matthew Guo[5], Emmett Schmidt, MD PhD[6], Matthew Taylor, MD[7]

[1]Oxford PharmaGenesis, Oxford, UK
[2]Abramson Cancer Center of the University, Philadelphia, PA, USA
[3]McKesson Specialty Health, Las Vegas, NV,USA
[4]South Texas Accelerated Research Therape, San Antonio, TX, USA
[5]Eisai Inc., Woodcliff Lake, NJ, USA
[6]Merck & Co., Inc., Kenilworth, NJ, USA
[7]Oregon Health and Science University, Portland, OR, USA

Background

Lenvatinib is a multikinase inhibitor of VEGFR 1−3, FGFR 1−4, PDGFRα, RET, and KIT. Pembrolizumab, an anti-PD-1 antibody, is approved as a monotherapy for previously treated patients with metastatic PD-L1–positive (tumor proportion score [TPS] ≥1%) non-small cell lung cancer (NSCLC), with an objective response rate (ORR) of 18% [1]. We report interim results of an ongoing phase 1b/2 trial evaluating lenvatinib in combination with pembrolizumab in patient with solid tumors, focusing on the metastatic NSCLC cohort.

Methods

In this multicenter, open-label study (NCT02501096), patients with measurable, confirmed metastatic NSCLC and ECOG performance status ≤1 received lenvatinib (20 mg/day orally) and pembrolizumab (200 mg Q3W, IV). In the phase 2 portion, patients must have had ≤2 prior lines of systemic therapy; there was no limit for phase 1b. Patients were not preselected based on PD-L1 status. Tumor assessments were performed by study investigators using immune-related RECIST (irRECIST). The phase 2 primary end point was ORR at 24 weeks (ORR_{WK24}). Secondary end points included ORR, progression-free survival (PFS), and duration of response (DOR).

Results

At the data cutoff of March 1, 2018, 21 patients were enrolled. 9 (43%) Patients were PD-L1(+) (TPS ≥1%); 5 (24%) were PD-L1(-); 7 (33%) were not tested. 3 (14%) Patients were treatment-naïve; 7 (33%), 10 (48%), and 1 (5%) patients had 1, 2, and ≥3 prior lines of systemic therapy, respectively. The primary end point of ORR_{WK24} was 33.3% (95% CI, 14.6–57.0). Additional efficacy outcomes are summarized in the table (Table 1). Grade 3 and 4 treatment-related adverse events (TRAEs) occurred in 10 (48%) and 1 (5%; increased aspartate aminotransferase) patients, respectively. There was 1 fatal TRAE (exsanguination; deemed “possibly related” to study treatment). The most common grade 3 TRAEs were hypertension (24%), fatigue (14%), diarrhea (14%), proteinuria (10%), and arthralgia (10%).

Conclusions

The combination of lenvatinib and pembrolizumab showed promising clinical activity with a manageable safety profile in previously treated patients with metastatic NSCLC who were not preselected for PD-L1 status. Further study is warranted.

Trial Registration

NCT02501096

References

1. Herbst RS et al. Pembrolizumab versus docetaxel for previously treated, PD-L1-positive, advanced non-small-cell lung cancer (KEYNOTE-010): a randomised controlled trial. Lancet. 2016;387(10027):1540-50.

Ethics Approval

This study was approved by all relevant institutional review boards.

Table 1.

Table 1. Summary of Tumor Response

Outcome	irRECIST (N = 21)
Best Overall Response, n (%)	
Complete response	1 (4.8)
Partial response	6 (28.6)
Stable disease	10 (47.6)
Progressive disease	2 (9.5)
Unknown or not evaluable	2 (9.5)
ORR, n (%)	7 (33.3)
95% CI	14.6–57.0
Clinical benefit rate[a], n (%)	13 (61.9)
95% CI	38.4–81.9
Median DOR, months (95% CI)	NE (2.4–NE)
Median PFS, months (95% CI)	7.4 (5.3–NE)
PFS rate at 12 months, % (95% CI)	35.5 (12.6–59.5)
Median follow-up time for PFS, months (95% CI)	11.7 (4.1–18.0)

NE, not estimable.
[a]Clinical benefit rate is defined as complete response plus partial response plus stable disease ≥ 23 weeks.

P393

A phase 1b/2 trial of lenvatinib in combination with pembrolizumab in patients with urothelial cancer

Nicholas Vogelzang, MD[2], Carlos Encarnacion[2], Allen Cohn[2], Christopher Di Simone[2], Drew Rasco[3], Donald Richards[2], Matthew Taylor, MD[4], Corina Dutcus[5], Daniel Stepan[5], Robert Shumaker, PhD,[5], Matthew Guo[5], Emmett Schmidt, MD PhD[6], James Mier, MD[7]

[1]*Oxford PharmaGenesis, Oxford, UK*
[2]*McKesson Specialty Health, Las Vegas, NV, USA*
[3]*South Texas Accelerated Research Therape, San Antonio, TX, USA*
[4]*Oregon Health and Science University, Portland, OR, USA*
[5]*Eisai Inc., Woodcliff Lake, NJ, USA*
[6]*Merck & Co., Inc., Kenilworth, NJ, USA*
[7]*Beth Israel Deaconess Medical Center, Boston, MA, USA*

Background
Pembrolizumab, an anti-PD-1 antibody, is approved in the second-line setting for patients (objective response rate [ORR] 21%) with advanced/metastatic urothelial cancer and in the first-line setting for patients who are ineligible for cisplatin with combined positive score ≥10 or ineligible for platinum-based chemotherapy, with ORR (overall ORR 29%) [1–3]. However, there is still an unmet need for effective therapeutic options for advanced urothelial cancer. Lenvatinib is a multikinase inhibitor of VEGFR 1-3, FGFR 1-3, PDGFRα, RET and KIT. Tyrosine kinase inhibitors, such as lenvatinib, have demonstrated activity in urothelial cancer and may reverse the immunosuppressive environment that leads to immuno-oncology (IO) therapy failure. Here we present a phase 1b/2 trial to determine the safety and efficacy of lenvatinib in combination with pembrolizumab in patients with advanced urothelial cancer.

Methods
In this multicenter, open-label study (NCT02501096), patients with confirmed metastatic urothelial cancer and an ECOG PS of 0 or 1 received lenvatinib 20 mg orally once daily and 200 mg pembrolizumab intravenously every 3 weeks. Patients were not preselected based on PD-L1 status. The phase 2 primary end point was ORR at week 24 (ORR_{wk24}), as assessed by study investigators using immune-related RECIST (irRECIST). Secondary end points included ORR, duration of response (DOR), and progression-free survival (PFS).

Results
At the time of data cutoff (March 1, 2018), 20 patients were enrolled. 9 (45%) Patients were PD-L1(+); 5 (25%) were PD-L1(-); 6 (30%) were not tested. 4 Patients (20%) were treatment-naïve, whereas 11 (55%) and 5 (25%) patients had had 1 and 2 lines of prior anticancer therapies, respectively. No patient had received prior IO therapy. The primary end point of ORR_{wk24} was 25% (95% CI: 8.7–49.1). Additional efficacy outcomes are summarized in the table (Table 1). 18 (90%) Patients experienced treatment-related adverse events (TRAEs). Grade 3 and 4 TRAEs occurred in 5 (25%) and 5 (25%) patients, respectively. There was 1 fatal TRAE (gastrointestinal hemorrhage). The most common any-grade TRAEs were proteinuria (45%), diarrhea (40%), fatigue (30%), hypertension (30%), and hypothyroidism (30%).

Conclusions
The tyrosine kinase inhibitor (lenvatinib) and immunotherapy (pembrolizumab) regimen demonstrated activity in this study, which included patients receiving later-line treatment. The combination of lenvatinib and pembrolizumab deserves further investigation in patients with metastatic urothelial cancer.

Trial Registration
NCT02501096

References
1. Bellmunt J, et al. Pembrolizumab as second-line therapy for advanced urothelial carcinoma. N Engl J Med. 2017;376(11):1015-26.
2. Vuky J et al. Updated efficacy and safety of KEYNOTE-052: A single arm phase 2 study investigating first-line pembrolizumab (pembro) in cisplatin-ineligible advanced urothelial cancer (UC). J Clin Oncol. 2018;36(15 Suppl):4524.
3. Keytruda® (pembrolizumab) [package insert]. Whitehouse Station, NJ: Merck & Co., Inc.; 2017.

Ethics Approval
This study was approved by all relevant institutional review boards.

Table 1.

Table 1. Summary of Tumor Response

Outcome	irRECIST (N=20)
Best Overall Response, n (%)	
Complete response	1 (5.0)
Partial response	4 (20.0)
Stable disease	9 (45.0)
Progressive disease	2 (10.0)
Unknown or not evaluable	4 (20.0)
ORR, n (%) 95% CI	5 (25.0) (8.7–49.1)
Median DOR, months (95% CI)	NE (6.5–NE)
Median PFS, months (95% CI)	5.5 (1.3–NE)
Median follow-up time for PFS, months (95% CI)	11.7 (2.6–16.5)

NE, not estimable.

P394

CX3CR1+CD8+ T cells is responsible to the clinical benefit of chemoimmunotherapy in metastatic melanoma patients after disease progression on PD-1 blockade

Yiyi Yan, MD PhD[1], Roxana Dronca, MD[1], Svetomir Markovic, MD, PhD[1], Haidong Dong, MD, PhD[1]

[1]*Mayo Clinic, Rochester, MN, USA*

Background
Clinical management of metastatic melanoma (MM) after PD-1 blockade failure remains a challenge and lacks a standard of care. Immunotherapy or chemotherapy alone provides limited benefit in this setting. Chemo-immunotherapy (CIT) combinations have demonstrated favorable efficacy and safety profiles in lung cancer patients. Our pre-clinical study in MM has shown that the addition of chemotherapy to PD-1 blockade can reshape a subset of therapy-responsive CD8+ T cells with resultant enhanced anti-tumor activities, suggesting the potential clinical benefits of CIT in MM patients whose disease have progressed after anti-PD-1 therapy. Further understanding of the clinical benefits and immunoregulatory mechanisms of CIT in this setting is crucial for the development of optimal combinatorial chemo-immunotherapeutic strategies to improve clinical outcomes in patients with advanced cancer.

Methods
MM patients (n=22) who have failed PD-1 blockade therapy were subsequently treated with CIT (paclitaxel and carboplatin in combination with pembrolizumab). The overall survival (OS), objective response rate (ORR), time-to-next therapy (TTNT), and toxicities were assessed. Using peripheral blood (PB) from MM patients, the phenotypic and functional changes induced by chemotherapy in therapy-responsive T cells, in the setting of anti-PD1 therapy, were examined. The immunoregulatory effects of CIT were also examined in melanoma mouse model.

Results
MM patients who have received subsequent CIT had a median OS of 5 years (95% CI: 2-NR) (median follow up of 3.9 years), with ORR of 61% (CR of 23%). The median TTNT was 8 months (95% CI: 6-15). No additional toxicities were identified. CX3CR1+CD8+ therapy-responsive T cells are low in MM patients who have failed to respond to anti-PD-1 monotherapy. However, in MM patients who responded to subsequent CIT, this subset of therapy-responsive T cells survived the chemotherapy with increased frequency and enhanced function. The clinical benefit of CIT is only observed in CX3CR1 wild type mice, not in KO mice, and ongoing PD-1

blockade is necessary to improve its anti-tumor activities.

Conclusions
In MM patients who have failed anti-PD-1 therapy, the chemo-immunotherapy combination showed favorable clinical outcomes and an acceptable toxicity profile. CX3CR1+ CD8+ effector T cells are responsible for the clinical benefit of CIT. This novel therapy-responsive population underlies the key cellular and molecular immunoregulatory mechanisms of chemotherapy. It serves as a meaningful marker to measure these collaborative effects and to develop the optimal chemo-immunotherapy strategy to improve clinical responses to current immune checkpoint blocking agents.

P395

PD-1 blockade synergies with RetroNectin-activated cytokine-induced killer cells in pretreated metastatic renal cell cancer

Lingdi Zhao[1], Yonghao Yang[2], Tiepeng Li[2], Yong Zhang[2], Wei Li[2], Lu Han[2], Hongwei Lin[2], Quanli Gao[2]

[1]Affiliated Cancer Hospital of Zhengzhou University & Henan Cancer Hospital, Zhengzhou, Peoples Republic of China
[2]Affiliated Cancer Hospital of Zhengzhou, Zhengzhou, China

Background
Metastatic renal cell carcinoma (MRCC) has a poor prognosis after failure of multitargeted kinase inhibitors. New immunomodulators, such as anti-programmed death (PD)-1 antibody, have made progress in the treatment of MRCC, while the objective response rate is low. Therefore, it is urgent to improve the efficacy of anti-PD-1 therapy. We hypothesised that RetroNectin-activated cytokine-induced killer (R-CIK) cells could be combined safely with anti-PD-1 antibody and yield anti-tumor activity in patients with targeted therapy failed renal cell carcinoma.

Methods
Patients with MRCC were eligible if they were failed to at least one tyrosine kinase inhibitors, Eastern Cooperative Oncology Group performance status (ECOG PS) less than 3. Eligible patients received nivolumab (3mg/kg, q2w) or pembrolizumab (2mg/kg, q3w), and a dose of R-CIK cells about 5 to 10×109given intravenously twice a month. The primary objective was to determine the safety, secondary objectives included objective response rate (ORR), progression-free (PFS) survival and overall survival (OS).

Results
From May 2015 to May 2018, 15 patients were enrolled (median age 59 [45-79]), among which 12 patients were male. There were three patients received pembrolizumab and 12 patients received nivolumab therapy. No unexpected toxicities were observed associated with the therapy. Grade 1 fever occurred in one patient, grade 1 hypothyroidism occurred in 3 patients, grade 1/2 elevated transaminase occurred in 4 patients. For 12 patients evaluable for response, overall response rate was 75%, with complete remission rate 41.7 percent (5/12). The incidence of pseudo-progression was 25% (3/12). The PFS and OS were not reached.

Conclusions
PD-1 antibody combined R-CIK cells was found to be well tolerated and to have a manageable safety profile, and have synergistic effects in pretreated patients with metastatic renal cell cancer. Although only a pilot study, the ORR was encouraging in tyrosine kinase inhibitors therapy failed MRCC patients.

P396

Phase I trial of interferon-gamma (IFN-g) combined with nivolumab (nivo) in patients with advanced solid tumors

Matthew Zibelman, MD[1], Alexander Macfarlane[1], Kimberly Costello[1], Thomas McGowan[1], John O'Neill, BA[1], Rutika Kokate[1], Igor Astsaturov[1], Hossein Borghaei, MS, DO[1], Christina Chu, MD[1], Crystal Denlinger[1], Efrat Dotan, MD[1], Daniel Geynisman[1], Angela Jain, MD[1], Lainie Martin, MD[1], Elias Obeid, MD, MPH[1], Joseph Treat, MD[1], Namrata Vijayvergia, MD[1], Rohit Walia[1], Jennifer Winn, MD, MS[1], Jeffery Nieves, PharmD[2], Amy Grahn, MS[2], Jeffrey Sherman, MD, FACP[2], Karthik Devarajan[1], Karen Ruth[1], R Alpaugh, PhD[1], Essel Al-Saleem[1], Edna Cukierman, PhD[1], Kerry Campbell, PhD[1], Elizabeth Plimack, MD MS[1]

[1]Fox Chase Cancer Center, Philadelphia, PA, USA
[2]Horizon Pharma, Lake Forest, IL, USA

Background
The presence of IFN-g is essential in the tumor microenvironment for a response to immune checkpoint blockade. We report a phase I trial evaluating the safety and preliminary efficacy of IFN-g/Nivo in patients with select solid tumors

Methods
Patients with advanced solid tumors (kidney, gastroesophageal, breast, ovarian, endometrial, small and non-small cell lung, anal, mesothelioma) who had progressed after > 1 prior therapy were recruited. Prior immunotherapy (ITx) was allowed. Eligible patients received IFN-g as part of four 6 patient cohorts, with dose levels ranging from 25-100 mcg/m2 (subq every other day), combined with nivo (3 mg/kg IV every 2 weeks). All patients had a baseline tumor biopsy, followed by one week of IFN-g induction alone, followed by an on-treatment biopsy and the addition of nivo. The primary endpoint was safety and to establish a recommended phase 2 dose (RP2D), with secondary efficacy endpoints.

Results
Twenty-six patients were accrued to four dose cohorts, with all evaluable for toxicity and 23 evaluable for efficacy. Median age was 60 years (33-76), 61.5% were female, and 26.9% had received prior ITx. Three dose limiting toxicities occurred, two at the highest dose level, thus 75 mcg/m2 was the max tolerated dose; however 50 mcg/m2 was selected as the RP2D based on study committee assessment of combined safety, efficacy, and correlative endpoints. The most common adverse events (AEs) irrespective of grade were predominantly known IFN-related side effects fatigue, fever, chills, and myalgias, and were predominantly < grade 3. Grade 3 AEs in three or more patients consisted of fatigue, hyponatremia, and leukopenia. No immune-related AE (irAE) was reported and no patient required steroids for an irAE. Nine patients had a new pleural effusion or ascites develop on study, two of whom came off study for a treatment-related AE. One patient with triple-negative breast cancer (TNBC) achieved a CR. Six patients had SD as best response, including 3/4 pts (75%) with renal cell carcinoma (RCC) evaluable for response, and 2/4 (50%) evaluable gastroesophageal cancer (GEC) patients. Two of seven patients (28.5%) who had received prior ITx achieved SD, including one patient each with RCC or GE cancer.

Conclusions
The combination of IFN-g and nivo was well tolerated and resulted in no irAEs. Further study in patients with RCC, GEC, and TNBC may be warranted, including in the post-immunotherapy setting.

Acknowledgements
Thank you to Horizon Pharma for providing funding

support for this study

Trial Registration
Registered at ClinicalTrials.gov: NCT02614456

Ethics Approval
The study was approved by the Fox Chase Cancer Center Institutional Review Board, IRB number 15-1048

Co-Stimulatory Ligand-Receptor Interactions

P397

Ectopic Tim-3 expression on T regulatory cells leads to lymphoproliferation and T cell activation.

Hridesh Banerjee[1], Héctor Nieves-Rosado[1], Lawrence P. Kane, Ph.D.[1]

[1]*University of Pittsburgh, Pittsburgh, PA, USA*

Background
T cell (or transmembrane) immunoglobulin and mucin domain 3 (Tim-3) is a transmembrane protein that has been associated with both inhibitory and co-stimulatory function in T cells. In tumor-infiltrating (TI) T cells and during chronic infection, Tim-3 has been seen to be expressed in terminally exhausted T cells and a significant proportion of regulatory T cells (Treg). However, what role Tim-3 plays in Treg is still unclear. Another factor complicating the role of Tim-3 is that along with Tim-3, other checkpoint receptors such as PD-1 are also upregulated in TI-Treg and very little is known about crosstalk between various checkpoint receptors in effector T cells and Treg.

Methods
To investigate the role of Tim-3 in Treg, we used two mouse models, a constitutive Tim-3/Treg model (Foxp3-YFP-Cre x flox-stop-flox Tim-3) and a tamoxifen-inducible Treg/Tim-3 model (Foxp3-CreERT2 x flox-stop-flox Tim-3).Basic characterisation of the immune system specifically the lyymphoid compartment and T cells including Treg cells was carried out. Functional assays on T regulatory cells was also done to look at effect of TIM-3 expression on T reg cells.

Results
At ten weeks after Tim-3 induction, Tim-3 transgenic mice had larger spleens and lymph nodes. This phenotype was observed to be milder in younger mice. Lymphoid organs in constitutive Tim-3 transgenic mice showed systemic lymphoid hyperplasia. T cells in these mice displayed a more activated phenotype. Overall frequency, numbers and phenotype of Treg cells in the peripheral lymphoid organs were also altered in constitutive Tim-3 transgenic mice. In the inducible Tim-3 mice however, we do not find systemic lymphoid hyperplasia but changes in numbers and phenotype of Treg were consistent with constitutive Tim-3 transgenic mice. Ectopic Tim-3 expression on Treg was also associated with changes in Treg function both in vitro and in vivo.

Conclusions
TIM-3 is sufficient to change the basic regulatory function of T reg cells, thereby studying how checkpoint therapies effect T reg in tumormicroenvironment and chronic infection may lead us to better Understanding the role of Tim-3 in Treg, and could contribute to novel therapeutic approaches for diseases such as cancer and chronic infection.

P398

Activation of the T Cell costimulatory protein CD137 using multivalent bicyclic peptides

Kristen Hurov[1], Punit Upadhyaya[1], Jessica Kublin[1], Xueyuan Zhou[1], Julia Kristensson[1], Rachid Lani[1], Gemma Mudd[1], Katerine van Rietschoten[1], W. Frank

An[1], Johanna Lahdenranta[1], Liuhong Chen[1], Gavin Bennett[1], Kevin McDonnell[1], Nicholas Keen[1], Peter U. Park, PhD[1]

[1]*Bicycle Therapeutics, Lexington, MA, USA*

Background

CD137 (4-1BB/TNFRSF9) is a costimulatory receptor belonging to the TNF receptor superfamily. It was originally cloned as an inducible gene from stimulated helper and cytotoxic T cells and has since been shown to also be expressed on natural killer (NK) cells. Agonistic anti-CD137 antibodies have shown potent, often curative anti-tumour activity in preclinical models. These effects are mainly mediated by cytotoxic T cells and generate long lasting, memory responses. Two human anti-CD137 antibodies, binding to the extracellular domain of CD137, urelumab and utomilumab are currently undergoing clinical testing. Urelumab has shown several single-agent, partial responses, but its use has been hampered by hepatoxicity, whilst utomilumab has shown little or no single agent activity.

Methods

Bicycles® are a new class of drugs - fully synthetic, constrained bicyclic peptides that combine the attributes of three therapeutic modalities (antibodies, small molecules, and peptides) by delivering high affinity, good PK, and rapid clearance. Their small size (1.5-2 kDa) delivers advantages in tumour penetration, and rapid renal elimination may avoid the liver and GI toxicity often associated with other drug modalities, including certain antibodies. We hypothesised that a fully synthetic Bicycle CD137 agonist with rapid renal clearance, minimal liver interaction and no Fc receptor interaction may induce CD137 mediated anti-tumour activity while avoiding liver toxicity. We screened for CD137 binders with a library of 10e12 Bicycles using phage display and following phage and chemical optimization, a high affinity lead BCY3814 (KD ~30 nM) was selected.

Results

BCY3814 binds to the human CD137 ligand-binding site. In common with many TNF receptors, CD137 activation requires receptor crosslinking, thus multivalent binders would be expected to recapitulate the action of its natural trimeric ligand. We generated more than 50 different bi-, tri- and tetra-valent variants of BCY3814 with chemical linkers and hinges of various lengths and rigidity using different sites of attachments, while maintaining a compact size (<15 kDa). We developed molecules exhibiting a wide range of potency in a cell-based CD137-dependent reporter assay. In addition, these molecules activate human T cells in vitro as monitored by increased cytokine release. Selected CD137 multimers are being tested in a humanized CD137 mouse model to demonstrate T cell activation and anti-tumour activity, without the liver toxicity reported for urelumab.

Conclusions

We hypothesise that such molecules could be promising, novel cancer immunotherapy candidates and importantly, they pave the way for development of synthetic agonists of other TNF receptors.

P399

Induction of tumor-specific immune responses and modulation of the tumor micro-environment by TLR9 agonist lefitolimod in murine syngeneic tumor models

Kerstin Kapp, PhD[1], Barbara Volz[1], Detlef Oswald[1], Burghardt Wittig, MD, PhD[2], Manuel Schmidt, MSc[1]

[1]*Mologen AG, Berlin, Germany*
[2]*Advisor to Mologen AG, Berlin, Germany*

Background

Preclinical and ongoing clinical studies support the

application of TLR9 agonists for immunotherapy. The immune surveillance reactivator (ISR) lefitolimod is in advanced clinical development for single-agent maintenance treatment in metastatic colorectal cancer (phase III, IMPALA) and extensive disease small cell lung cancer (phase II, IMPULSE). Lefitolimod activates plasmacytoid dendritic cells to secrete interferon-alpha, followed by a broad activation of cells of the innate and adaptive immune system. Lefitolimod therefore provides the necessary and sufficient signals for the initiation of an immunotherapeutic anti-tumor response.

Methods

It was evaluated, if lefitolimod is able to induce local and systemic anti-tumor immune responses in the murine syngeneic colon carcinoma CT26 and the breast cancer EMT-6 models. The presence and activation state of CD8+ T cells within tumor infiltrating cells was determined via flow cytometry. Tumor antigen-specific T cells were analyzed via IFN-gamma ELISpot using spleen cells stimulated with either tumor cells or the peptide AH1, derived from an immunodominant antigen of CT26 cells.

Results

Intratumoral administration of lefitolimod resulted in a beneficial modulation of the tumor micro-environment (TME) characterized by increased infiltration of activated CD8+ T cells, which showed an up-regulation of Granzyme B. Notably, an increase of IFN-gamma secreting CD8+ T cells within the spleen was detected after re-stimulation with the tumor-specific AH1 peptide antigen or CT26 tumor cells. This beneficial TME modulation and antigen-specific effects were associated with a markedly reduced tumor growth in the CT26 model. The anti-tumor effect was even more pronounced in the EMT-6 model, where nine out of ten mice showed complete tumor regression. The 9 tumor-free mice subsequently rejected both, the initially used EMT-6 as well as CT26 tumor cells in re-challenge studies, in contrast to age-matched naïve mice. This indicates that treatment with lefitolimod induces a sustained, long-lasting immune memory against shared antigens of both tumor types.

Conclusions

Treatment of tumors with lefitolimod resulted in a beneficial modulation of the TME with an increase in anti-tumor effector cells. A strong systemic immune response as well as a sustained immune memory against different tumors was induced. These data indicate that lefitolimod provides the essential requirements for use as mono-immunotherapy or as an optimal combination partner of other immunotherapeutic drugs like checkpoint inhibitors in immuno-oncological trials.

P400

Tumor-localizing NKp30/ICOSL vIgD fusion proteins direct effective dual CD28/ICOS T cell costimulation to B7-H6+ tumor cells in vitro and tumors in vivo

Steven Levin, PhD[2], Lawrence Evans, BS[2], Erika Rickel[2], Katherine Lewis, PhD[2], Daniel Demonte[2], Martin Wolfson, BS[2], Stacey Dillon, PhD[2], Ryan Swanson, BS[2], Kristine Swiderek, PhD[2], Stanford Peng, MD, PhD[2]

[1]*Alpine Immune Sciences, Inc., Seattle, WA, USA*
[2]*Alpine Immune Sciences, Seattle, WA, USA*

Background

Background: Although checkpoint inhibitor therapies have significantly improved outcomes in multiple cancers, complete and durable responses remain infrequent, possibly attributable to a lack of adequate T cell costimulation and/or activating signals. Novel therapeutic proteins which confer T cell costimulation may be particularly effective anti-tumor therapies, particularly in combination with checkpoint inhibitors. But at the same time, localization of such costimulatory activity to tumors,

such as via a tumor-specific targeting antigen, may be simultaneously important to maintain tolerability of such agonist therapeutics. B7-H6, a cell surface immunoglobulin superfamily (IgSF) member which binds the NKp30 receptor, appears to be expressed specifically in multiple tumor types, and may serve as such a tumor-specific antigen. Novel therapeutic proteins which localize costimulatory agonist domains to B7 H6 may therefore be capable of significant antitumor efficacy yet may be safely administered systemically by preferentially localizing agonist activity to the B7-H6 tumor microenvironment.

Methods

Methods: Using our platform technology, which is based on the directed evolution of IgSF members, NKp30/ICOSL variant immunoglobulin domain (vIgD) fusion proteins were created from NKp30 vIgDs with high affinity against B7-H6 and ICOSL vIgDs, which dually agonize the T cell costimulatory receptors ICOS and CD28. These tumor-localizing vIgD proteins were evaluated in vitro in T cell costimulation assays with target cells with or without B7-H6, and in vivo in a B7-H6+ CT26 mouse tumor model.

Results

Results: NKp30/ICOSL vIgD-Fc fusion proteins conferred effective B7-H6-dependent costimulation to T cells in vitro, with enhanced T cell proliferation and cytokine production (IFN-gamma, TNF-alpha, IL-2) in response to B7-H6-expressing but not B7-H6-negative target cells. Isolated ICOSL and NKp30 vIgDs alone were not efficacious. Importantly, NKp30/ICOSL vIgD-Fc fusion proteins demonstrated anti-tumor efficacy in a B7 H6+ mouse tumor model, especially when administered in combination with a PD-1 inhibitor (Figure 1).

Conclusions

Conclusions: Tumor-localizing NKp30/ICOSL vIgDs confer potent T cell costimulation via CD28 and ICOS dependent upon the tumor antigen B7-H6 and elicit encouraging efficacy against B7-H6+ tumors in vivo, including in combination with PD-1 inhibitors. Such fusion proteins may provide particularly effective therapeutics for B7-H6+ tumors either as monotherapy or in combination with checkpoint blockade. These findings further suggest tumor-localized immunomodulation is possible and may improve cancer outcomes.

Ethics Approval

All animal procedures were approved by the appropriate Institutional Animal Care and Use Committee overseeing the vivarium where the studies were conducted (Alpine Immune Sciences and Charles River Laboratories), and followed the guidelines set forth in the 8th Edition of the Guide for the Care and Use of Laboratory Animals (National Research Council, 2011).

Figure 1.

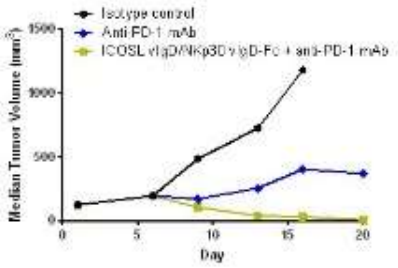

P401

Blockade of T cell immunoreceptor with Ig and ITIM domains (TIGIT) leads to increased proliferation of bone marrow T cells from patients with acute myeloid leukemia (AML)

Yoko Kosaka, PhD[1], Adam Lamble, MD[2], Fei Huang, PhD[3], Evan Lind, PhD[1]

[1]*Oregon Health & Science University, Portland, OR, USA*
[2]*Seattle Children's Hospital, Portland, OR, USA*
[3]*Janssen Pharmaceutical R&D, Spring House, PA, USA*

Background
Background: The success of immunotherapeutic checkpoint blockade in cancer has led to great interest in finding novel targets that play a pivotal role in immune responses. One such molecule is T cell immunoreceptor with Ig and ITIM domains (TIGIT), which has been shown to be inhibitory and expressed by nonresponsive and suppressive T cells in the tumor microenvironment.

Methods
Methods: In the present study, we investigate the role of TIGIT on immune suppression of T cell responses in bone marrow microenvironment of patients with AML. Bone marrow aspirates were subjected to T cell proliferation assays using stimulation though TCR with or without accompanying TIGIT blockade. Samples were also subjected to high parameter mass-spec based flow cytometry and both mutational and transcriptional profiling by deep sequencing and clinical parameters (age, sex, blast count, ELN risk stratification) were recorded.

Results
Results: Of 57 total samples tested, 24 (42.1%) showed a profound defect in T cell proliferation in response to anti-CD3 stimulation (<5% of T cells responding to stimulation). Of these 24 that showed the most functional impairment, 12 (50%) had at least a 2-fold and 6 (25%) at least a 5-fold increase in the frequency of dividing T cells with the addition of an anti-TIGIT blocking antibody.

Conclusions
Conclusions: These results indicate that in many samples, TIGIT blockade can partially overcome functional suppression of T cells in AML bone marrow, and suggest that TIGIT is involved in mediating immune defects in AML. A better understanding of the role of TIGIT in the AML microenvironment will provide insight in determining whether TIGIT blockade could represent an effective therapy in AML.

Acknowledgements
This work was also funded in part by generous support from the Leukemia and Lymphoma Society of America Beat AML project (PIs Brian Druker MD/Jeffrey Tyner PhD).

Ethics Approval
All human experiments are approved under IRB protocol #00004422 Marc Loriaux MD, PI.

P402

DuoBody-CD40x41BB conditionally enhances immune activation by crosslinking of CD40- and 4-1BB positive cells

Alexander Muik, PhD[1], Friederike Gieseke[1], Isil Altintas, PhD[2], Saskia Burm[2], Mustafa Diken[1], Christian Grunwitz[1], Sebastian Kreiter[1], David Satijn, PhD[2], Danita Schuurhuis[2], Ozlem Tureci[1], Ugur Sahin[1], Esther Breij, PhD[2]

[1]*BioNTech AG, Mainz, Germany*
[2]*Genmab B.V., Utrecht, Netherlands*

Background
Immune checkpoint inhibitor antibodies that can (re-)activate anti-tumor immunity show great promise for the treatment of cancer. Similarly, therapeutic agents that boost anti-tumor immunity by direct activation of immunostimulatory molecules may provide clinical benefit. In this context, targeting tumor necrosis factor (TNF) receptor superfamily members, which deliver essential co-stimulatory activity for immune responses, gained attention. We hypothesized that simultaneous engagement of the

T-cell co-stimulatory molecule 4-1BB and CD40 on antigen-presenting cells (APCs) using a bispecific antibody could be an elegant and potent mechanism to induce conditional activation of both CD40-positive immune cells and 4-1BB positive T cells.

Methods

DuoBody-CD40x4-1BB (GEN1042) is an IgG1 Fc-silenced bispecific antibody that was obtained by controlled Fab-arm exchange of humanized parental CD40- and 4-1BB-specific monoclonal antibodies. The binding characteristics and functional activity of DuoBody-CD40x4-1BB were analyzed in vitro using flow cytometry, cell-based reporter assay systems and primary human lymphocyte assays. To evaluate the capacity of DuoBody-CD40x4-1BB to induce proliferation of tumor-infiltrating lymphocytes (TILs) in the tumor microenvironment, ex vivo TIL expansion assays were conducted using freshly isolated human tumor specimen.

Results

DuoBody-CD40x4-1BB induced activation of both CD40 and 4-1BB intracellular signaling, which was dependent on simultaneous binding to CD40- and 4-1BB positive cells as measured by reporter assays. The monospecific control antibodies did not show agonist activity. This demonstrates that the bispecific antibody confers conditional activity upon receptor cross-linking. Using human primary T cells and monocyte-derived dendritic cells, both obtained from human healthy donor PBMCs, antigen-specific T-cell assays were conducted in vitro. DuoBody-CD40x4-1BB enhanced T-cell proliferation as well as concomitant pro-inflammatory cytokine secretion. Enhanced T-cell proliferation was again dependent on binding of DuoBody-CD40x4-1BB to both CD40 and 4-1BB. Importantly, DuoBody-CD40x4-1BB did not enhance proliferation of T cells that were not pre-activated by TCR stimulation. Furthermore, in ex vivo cultures of fresh human tumor tissue resections DuoBody-CD40x4-1BB increased the expansion of TILs up to 10-fold over control antibody treatment.

Conclusions

In summary, DuoBody-CD40x4-1BB is a bispecific antibody that crosslinks CD40 and 4-1BB positive cells, thereby inducing conditional stimulation and subsequently co-stimulatory activity. In the context of cancer, DuoBody-CD40x4-1BB can enhance anti-tumor immunity by (re-)activating tumor-specific T cells, either intratumorally or in the tumor-draining lymph nodes. The unique mechanism of action, its conditional agonist activity, distinguishes DuoBody-CD40x4-1BB from agonistic antibodies targeting CD40 or 4-1BB. Therefore, DuoBody-CD40x-4-1BB represents a novel therapeutic agent with potential for treatment of solid tumors.

Ethics Approval

The use of tumor tissue resections was approved by BioNTech AG's Ethics Board, approval number 837.309.12 (8410-F).

P403

Preliminary results from a first-in-human phase 1 study of the CD40 agonist monoclonal antibody (mAb) CDX-1140

Rachel Sanborn, MD[1], Michael S. Gordon, MD[2], Mark O'Hara, MD[3], Nina Bhardwaj, MD, PhD[4], Yi He, PhD[5], Tracey Rawls[5], Tibor Keler, PhD[5], Michael Yellin, MD[5]

[1]*Providence Portland Medical Center, Portland, OR, USA*
[2]*Scottsdale Healthcare Hospital, Scottsdale, AZ, USA*
[3]*Hospital of the University of PA, Philadelphia, PA, USA*
[4]*Icahn School of Medicine Mt. Sinai, New York, NY, USA*
[5]*Celldex Therapeutics, Inc., Hillsborough, NJ, USA*

Background

Agonist CD40 mAbs can mediate antitumor immunity through multiple mechanisms, including enhancing

tumor antigen presentation, activation of tumoricidal macrophages, and direct growth inhibition/killing of CD40-expressing tumor cells. To fully exploit these mechanisms may require the mAb to be dosed at levels that provide significant tumor and tissue penetration, without dose-limiting-toxicities (DLT) from systemic CD40 activation. Our agonist CD40 mAb, CDX-1140, was selected based on its unique and linear dose-dependent in vitro and in vivo activity and is postulated will achieve maximum agonist activity at dose levels associated with good systemic exposure. CDX-1140 is a fully human IgG2 agonist anti-CD40 mAb that activates dendritic cells (DCs) and B cells in an Fc receptor independent manner and has potent antitumor activity against CD40-expressing cancer cells. In addition, CDX-1140 does not block the natural CD40-CD40L interaction; combination of CDX-1140 with added soluble CD40L is synergistic in the activation of immune cells suggesting a potential to enhance in vivo CD40L dependent immune responses. In toxicology studies, CDX-1140 demonstrated potent CD40-mediated pharmacological effects without significant toxicities.

Methods

A phase 1 dose-escalation study of CDX-1140 (CDX1140-01; NCT03329950) is underway in patients with advanced tumors who have exhausted standard-of-care treatment options. The primary endpoint is determining the safety profile and maximum tolerated dose. Secondary endpoints include pharmacokinetics, immunogenicity, clinical and biological outcome assessments. Baseline and on-study biopsies will be used to explore the pharmacodynamic effects of CDX-1140 in the tumor microenvironment (TME). The dose escalation (DE) portion evaluates CDX-1140, given every 4 weeks, at doses from 0.01 to 3 mg/kg; the first 2 cohorts are single-patient cohorts and all subsequent DE cohorts are conducted utilizing a 3+3 design. Tumor-specific expansion cohorts will further explore the activity of CDX-1140. This study will also evaluate CDX-1140 in combination with CDX-301 (rhFLT3L), a DC growth factor that markedly increases DC numbers, including the CD141+ subset which are critical to an antitumor immune response and are often scarce within the TME.

Results

To date, CDX-1140 cohorts at 0.01 (n=2), 0.03 (n=1), and 0.09 (n=3) mg/kg have been completed without any drug-related serious adverse events, infusion reactions, or DLTs reported. The only drug related toxicity has been grade 1 fatigue (n=2) . Expected pharmacodynamic effects, including transient, dose-dependent decreases in lymphocyte counts and dose-dependent increases in serum IL-12p40 and TNF-Alpha, have been observed.

Conclusions

The early data suggest that CDX-1140 has the expected immune activating and safety profile.

Ethics Approval

The study was approved by University of Pennsylvania, approval number 828733; Mount Sinai School of Medicine, approval number IRB-18-00213; Providence Health and Services, approval number 201700532 and Western Institutional Review Board, approval number 115925

P404

The discovery and characterization of PTZ-522 (ASP1951), a fully-human, high affinity agonistic anti-GITR tetravalent monospecific monoclonal antibody

Cynthia Seidel-Dugan, PhD[3], Sonja Kleffel[1], Sandra Abbott[1], Heather Brodkin[1], Daniel Hicklin[1], Nels Nielson[2], Christopher Nirschl[1], Rebekah O'Donnell[1], Andreas Salmeron[1], Philipp Steiner, PhD[1], Christopher Thomas[1], William Winston[1]

[1]Potenza Therapeutics, Inc, Cambridge, MA, USA
[2]Adimab, LLC, Lebanon, NH, USA

[3]*Potenza Therapeutics, Cambridge, MA, USA*

Background

Multiple studies have demonstrated that tumors establish an immunosuppressive microenvironment (TME) to escape immune surveillance and promote tumor development. Tumor-infiltrating lymphocytes (TILs) become suppressed in the TME so their proliferative capacity and effector functions are impaired. Members of the TNF Receptor (TNFR) family and their ligands modulate the proliferation, differentiation, and activation of immune effector cells. Glucocorticoid-induced TNFR-related (GITR) is a receptor belonging to the TNFR family with costimulatory activity. In preclinical studies, GITR agonists increase effector T cell proliferation and function, and decrease the tumor infiltration, stability, and/or survival of Tregs, resulting in a more pro-inflammatory TME. In multiple syngeneic mouse tumor models, treatment with GITR agonists demonstrates compelling anti-tumor activity. Based on these promising preclinical data, a number of GITR agonist agents are being tested in the clinic.

Methods

Functional and structural studies have demonstrated that optimal activation of human GITR requires an adequate clustering of the receptor with trimeric GITR ligand (GITRL). Traditional bivalent agonistic antibodies are not as efficacious as trimeric GITRL and are expected to require FcR mediated cross-linking for full activity, which introduces potentially undesired FcR activation, cytokine release, and/or elimination of key effector cells expressing GITR. Potenza Therapeutics has identified PTZ-522 (also known as ASP1951), a novel, tetravalent monospecific (TM) anti-GITR agonist antibody designed to overcome these potential liabilities.

Results

PTZ-522 is a hinge-stabilized IgG4 antibody which binds with high affinity to human and cynomolgus monkey GITR. PTZ-522 has agonistic activity in engineered cell assays and primary T cells from peripheral blood of healthy donors. The TM-formatted antibody PTZ-522 is more active in cell assays than the same antibody in a bivalent format (522-IgG4) and has similar or greater activity than trimeric GITRL. Moreover, this activity was observed in the absence of any FcR cross linking. Analysis of GITR expression on T cells using human tumor samples as well as PBMCs demonstrates that GITR is more highly expressed on TILs, highlighting the different immune phenotype of cells found in the tumor microenvironment. The TM-formatted antibody PTZ-522 increases proliferation and inflammatory cytokine production by GITR expressing TILs. Increased activity in the TIL assay is also observed with the combination of PTZ-522 with a PD-1 inhibitor. Mechanistically, PTZ-522 binding to T cells results in rapid GITR activation and internalization not observed with bivalent antibodies.

Conclusions

These data support the continued development of PTZ-522 as a novel GITR agonist for the treatment of cancer.

P405

Agonistic IgM antibodies targeting immunostimulatory TNFRSF family members GITR and OX40 enhance immune responses beyond that of IgGs

Angus Sinclair, PhD[1], Dalya Rosner, PhD[1], Beatrice Wang[1], Tasnim Kothambawala[1], Ling Wang[1], Susan Calhoun[1], Avneesh Salini[1], Sachi Rahman[1], RAMESH BALIGA, PhD[1], Bruce Keyt[1]

[1]*IGM Biosciences, Mountain View, CA, USA*

Background

Tumor necrosis factor receptor (TNFR) superfamily T cell immunostimulatory receptors OX40 and GITR

require trimerization to induce agonistic signaling. Anti-OX40 and anti-GITR therapeutic IgG antibodies have demonstrated limited anti-tumor activity in the clinic, perhaps due to inefficient multimerization through FcγR engagement in the tumor microenvironment. We generated and evaluated the functional properties of agonistic anti-OX40 and anti-GITR IgM antibodies and have compared their activities to corresponding IgGs.

Methods

Agonistic anti-OX40 and anti-GITR IgG1 and IgM antibodies were generated using variable regions inserted into the same light chains and either the IgG or IgM heavy chain framework. Antibody binding was evaluated using antigen ELISAs or by flow cytometry with human T cells. Activated human T cells were used to evaluate antibody induced proliferation and cytokine release. Effects of these antibodies on regulatory T cell (Treg) suppression of T effector proliferation and cytokine release were measured.

Results

Agonistic anti-OX40 and anti-GITR IgM antibodies demonstrated superior binding potencies to recombinant antigens (>10 fold in molar comparisons) compared to IgG antibodies, which were amplified at low antigen density. Improved binding was due to the enhanced avidity of the multivalent IgMs compared to bivalent IgGs. As OX40 and GITR require trimerization with ligand or antibodies for function, the agonistic properties of the IgMs and IgGs were compared. In NF-kB-luciferase reporter assays driven by either GITR or OX40, a significant increase in potency was observed with the IgM in both EC50 and max activity compared to IgG in presence or absence of cross-linking agents. In primary human T cell activation assays, IgMs significantly enhanced T cell proliferation and cytokine secretion compared to IgGs. OX40 and GITR are also expressed on immunosuppressive Tregs. In co-culture of Tregs with T effector cells, IgM antibodies significantly reversed the suppressive activity of Tregs on T cell proliferation and inflammatory cytokine secretion, whereas IgGs had little to no effect.

Conclusions

We have discovered IgM antibodies significantly bind to and signal more efficiently through OX40 and GITR than corresponding IgGs, even in presence of cross linking agents. Efficient multimerization and agonism of OX40 and GITR with IgM antibodies may therefore enhance the anti-tumor immunostimulatory effects of immunotherapeutic antibodies targeting these T cell agonists.

Acknowledgements

We thank Sarah Wadsworth for her assistance with some of the studies.

P406

ALPN-202, a combined PD-L1/CTLA-4 antagonist and PD-L1-dependent CD28 T cell costimulator, elicits potent intratumoral T cell immunity superior to and differentiated from PD-L1 inhibitor monotherapy

Ryan Swanson, BS[1], Mark Maurer, BS[1], Chris Navas, BS[1], Chelsea Gudgeon, BS[1], Katherine Lewis, PhD[1], Martin Wolfson, BS[1], Sherri Mudri, BS[1], Kayla Susmilch, MS[1], Joe Kuijper[1], Stacey Dillon, PhD[1], Steven Levin, PhD[1], Kristine Swiderek, PhD[1], Stanford Peng, MD, PhD[1]

[1]*Alpine Immune Sciences, Seattle, WA, USA*

Background

ALPN-202 is a variant CD80 vIgD™-Fc fusion protein blocking the PD-L1 and CTLA-4 checkpoints while providing PD-L1-dependent T cell activation via CD28. This strategy delivers potent T cell costimulation, which is currently missing from checkpoint inhibitor only regimens, and may be critical for the generation of clinical anti-tumor

responses, seeking to broadly improve cancer outcomes. ALPN-202 has previously demonstrated preclinical anti-tumor activity superior to PD-L1 inhibition, but the specific mechanism(s) of superiority remain unreported.

Methods
In a hPD-L1-transduced MC38 tumor model treated with ALPN-202 or durvalumab, an approved PD-L1 inhibitor, anti-tumor responses were evaluated by serial tumor volume measurements, and intratumoral immune responses were assessed by RNA-Seq, flow cytometry, and immunoSEQ TCR repertoire analysis (Adaptive Biotechnologies).

Results
Multiple doses of ALPN-202 elicited anti-tumor responses superior to durvalumab as judged by tumor volume measurements. Efficacy was importantly also observed with single ALPN-202 doses administered intraperitoneally or intratumorally. RNA-Seq and flow cytometric analyses of tumors revealed higher T cell, NK cell, macrophage, and dendritic cell markers after ALPN-202 treatment vs. durvalumab, along with higher T cell effector transcripts, including IL-2, IFN-gamma, granzyme B, and T-bet. TCR repertoire analysis demonstrated increased clonality and richness in response to ALPN-202, two characteristics previously not reported in response to PD-(L)1 or CTLA-4 inhibition alone.

Conclusions
ALPN-202 elicits intratumoral immune responses superior to PD-L1 inhibition alone, including T cell infiltration and T cell effector molecules. This suggests it may translate into clinical anti-tumor responses in cancers currently resistant to checkpoint inhibition alone and/or may improve outcomes in cancers when administered in combination with existing therapies. Ongoing studies seek to further define such potential and specific clinical indications and modalities to guide upcoming clinical trials.

P407

CTX-471, a novel agonistic antibody targeting CD137, eradicates very large tumors in vivo by selectively reprogramming the tumor microenvironment without causing hepatic toxicity

Ugur Eskiocak, PhD[1], Wilson Guzman, BS[1], Nora Zizlsperger, PhD[1], Benjamin Wolf[1], Christine Cummings[1], Thomas Daly[1], Puru Nanjappa[1], Lauren Milling[1], Xianzhe Wang[1], Lucy Liu[1], Samantha Ottinger[1], Jason Lajoie[1], Michael Schmidt[1], Robert Tighe, BS[2]

[1]*Compass Therapeutics, Cambridge, MA, USA*
[2]*Compass Therapeutics LLC, Cambridge, MA, USA*

Background
CD137 (4-1BB) is a member of the TNFR superfamily that provides costimulatory signals to activated cytotoxic lymphocytes. Agonistic antibodies against CD137 have shown promising therapeutic activity in mouse tumor models. However, hepatic toxicity has been observed in animals and humans with a few anti-CD137 antibodies [1,2]. Recent advances in our understanding of TNFR agonist antibodies implicate epitope, affinity, and IgG subclass as important contributors to function [3,4]. Here we describe the preclinical characterization of CTX-471, a fully human IgG4 agonist of CD137 with a differentiated pharmacology and toxicology profile.

Methods
CTX-471 was identified based on epitope binning and antigen-binding assays. The in vitro bioactivity of CTX-471 was measured in a human IFN-γ release assay. The in vivo efficacy of CTX-471 was assessed in multiple syngeneic mouse tumor models that included various mechanistic endpoints: FACS analysis of TILs, effector cell depletion, tumor histology, and Fc receptor profiling. The efficacy of

CTX-471 was further evaluated in mice bearing very large (~500 mm3) CT26 tumors. Finally, the toxicity profile of CTX-471 was evaluated in mice and cynomolgus monkeys.

Results

CTX-471 binds to a unique epitope shared by human, cynomolgus monkey, and mouse CD137. In vitro, CTX-471 increased IFN-γ production by human T cells in an FcγR-dependent manner, displaying an intermediate level of activity between two clinical-stage anti-CD137 antibodies. In Vivo, CTX-471 exhibited curative monotherapy activity in CT26, A20, and EMT-6 models. When compared to known anti-CD137, OX-40, PD-1, PD-L1, and CTLA-4 antibodies, only an affinity-optimized version of CTX-471 showed the ability to eradicate very large tumors. All mice cured by CTX-471 rejected tumors upon rechallenge. CTX-471 profoundly reprogramed the TME, leading to an influx of inflammatory cells, decreased T cell exhaustion, Treg depletion, and TAM modulation, while having very little effect on the peripheral immune system. Tumor models with abundant expression of FcγR's responded more strongly to CTX-471 treatment, and Fc silencing mutations attenuated efficacy. In mice and monkeys, extremely high doses of CTX-471 (up to 100 mg/kg weekly for 4 weeks) were well-tolerated, with no signs of hepatic toxicity.

Conclusions

CTX-471 displays a favorable and well-differentiated efficacy-safety profile that is attributed to a unique epitope, optimized affinity, and FcγR-dependent activity. To our knowledge, CTX-471's level of monotherapy efficacy against very large tumors is unprecedented for an IO antibody. IND-enabling toxicology studies are underway, and a Phase 1 trial is planned for the first-half of 2019.

References

1. Bartkowiak T, Jaiswal AR, Ager CR, et al. Activation of 4-1BB on liver myeloid cells triggers hepatitis via an interleukin-27–dependent pathway. Clinical Cancer Research. 2018 Apr;24(5):1138–51.
2. Segal NH, Logan TF, Hodi FS, et al. Results from an integrated safety analysis of urelumab, an agonist Anti-CD137 monoclonal antibody. Clinical Cancer Research. 2016;23(8):1929–36.
3. Yu X, Chan HTC, Orr CM, et al. Complex interplay between epitope specificity and isotype dictates the biological activity of anti-human CD40 antibodies. Cancer Cell. 2018;33(4):664-675.e4. 4. Chodorge M, Züger S, Stirnimann C, et al. A series of fas receptor agonist antibodies that demonstrate an inverse correlation between affinity and potency. Cell Death Differ. 2012;19(7):1187-95.

Ethics Approval

All animal studies were approved by Compass Therapeutics Institutional Animal Care and Use Committee under protocol CTX-016-01.

P408

Preclinical identification of the pharmacologically active dose range of the tumor targeted 4-1BB agonist MP0310 based on tumor regression, receptor occupancy and CD8 T lymphocyte expansion

Elmar Vom Baur, PhD, MBA, MEng[1], Ivana Tosevski, PhD[1], Laurent Juglair, MSc[1], Alexander Link, PhD[1], Guy Lemaillet[1], Heïdi Poulet[1], Christian Reichen, PhD[1], Patricia Schildknecht, MSc[1], Joanna Taylor, MSc[1], Alexander Titz, MSc[1], Waleed Ali[1], Doris Schaible[1], Mirela Matzner[1], Christof Zitt, PhD[1], Jörg Herbst, PhD, DABT[1], Keith Dawson, PhD[1], Julia Hepp, PhD[1], Dan Snell, PhD[1], Michael T. Stumpp, PhD[1], Victor Levitsky, MD PhD[1], Hong Ji, MD, PhD[1], Ivana Tosevski, PhD[1]

[1]*Molecular Partners AG, Schlieren, Switzerland*

Background

In animal models, agonistic antibodies targeting the

T cell costimulatory receptor 4-1BB (CD137) have shown promise as anti-tumor agents, but clinical studies have shown only limited signs of efficacy as well as dose-limiting hepatotoxicity with one of the candidates. To avoid systemic toxicities and to direct immune activation to the tumor, we have generated the tumor-targeted 4-1BB agonist MP0310. MP0310 is a multi-domain DARPin® molecule comprising domains binding to 4-1BB, fibroblast activation protein (FAP), and human serum albumin, the latter for half-life extension. FAP binding targets MP0310 activity to tumors as FAP is highly expressed in many solid tumors and crucially, activation of 4-1BB by MP0310 is dependent on FAP-mediated clustering of 4-1BB. Previously we have shown, in vitro and in vivo, that MP0310 is at least as potent as the agonistic 4-1BB antibodies and, in contrast to the antibodies, does not induce hepatotoxicity or exacerbate graft versus host disease in humanized mouse models. Also, no systemic T cell activation has been observed in cynomolgus monkeys. The present study, in support of the clinical development of MP0310, is to establish the pharmacologically active dose range of MP0310 in a mouse model based on parameters such as receptor occupancy, CD8+ T cell expansion and anti-tumor activity.

Methods

NSG mice were implanted subcutaneously with HT-29 tumor cells and subsequently were injected with human PBMCs. Mice were then treated with a suboptimal dose of a tumor associated antigen binding T cell engager and with a variant of MP0310 containing a mouse FAP binding domain (mMP0310) at doses from 0.0128 to 40mg/kg. Tumor volume and potential biomarkers of T cell activation were measured.

Results

mMP0310 strongly increased intra-tumoral CD8 T cell expansion in a dose-dependent manner compared to monotherapy with the T cell engager. Maximal increases in intra-tumoral CD8 T cell numbers and the ratio of CD8 versus CD4 cells correlated with 100% receptor occupancy (RO) reached at a dose of 1.6mg/kg. Only marginal activity on T cells was seen at a dose of 0.0128mg/kg correlating with a 4-1BB RO level below 10%. In addition, mMP0310 enhanced tumor regression induced by the T cell engager in a manner suggesting dose-dependency starting at 0.32mg/kg

Conclusions

The novel FAP-targeted 4-1BB agonist mMP0310 has been shown to enhance T cell activation and antitumor activity without producing toxicity. Dose dependency of pharmacodynamic activities related to 4-1BB RO has been demonstrated and biomarkers for clinical development have been identified

P409

Pharmacodynamic activity of MEDI1873, a Glucocorticoid-Induced tumor necrosis factor family-related protein (GITR) agonist molecule, administered intravenously to patients with advanced solid tumors

Nicholas Durham, PhD[2], Nathan Standifer, PhD[2], Jennifer Cann, PhD[2], Christopher Morehouse, MD[2], Li Yan[2], Kristina Kovacina[2], Xu Liu[2], Jia Li[2], Yuling Wu[2], Katie Streicher, PhD[2], Paolo Vicini[2], Ayesh Perera[2], Rakesh Kumar, PhD[2], Raid Aljumaily, MD[3], Aung Naing, MD, FACP[4], Ashish Chintakuntlawar, MBBS, PhD[5], Naiyer Rizvi, MD[6], Helen Ross, MD[5], Michael Gordon, MD[7], Jeffrey Infante[8], Crystal Denlinger[9], Ani Balmanoukian, MD[10]

[1]*Ashfield Healthcare*
[2]*MedImmune, Gaithersburg, MD, USA*
[3]*Oklahoma University College of Medicine, Oklahoma City, OK, USA*
[4]*University of Texas, Houston, TX, USA*
[5]*Mayo Clinic, Rochester, MN, USA*
[6]*Columbia University Medical Center, New York, NY, USA*

[7]HonorHealth, Scottsdale, AZ, USA
[8]Sarah Cannon Research Institute, Spring House, PA, USA
[9]Fox Chase Cancer Center, Philadelphia, PA, USA
[10]The Angeles Clinic, Los Angeles, CA, USA

Background

MEDI1873 is a novel GITR-ligand/IgG1 agonist fusion protein that binds to the co-stimulatory molecule GITR, which is upregulated on activated T cells. This Phase 1 study (NCT02583165) evaluated safety, pharmacokinetics, pharmacodynamics, and preliminary antitumor activity in patients with advanced solid tumors.

Methods

MEDI1873 was administered IV Q2W in sequential dose escalation (DE) cohorts: 2 single patient cohorts (1.5 and 3 mg), followed by six 3+3 DE cohorts (7.5, 25, 75, 250, 500 and 750 mg). Antitumor response was assessed using RECIST v 1.1. Pharmacodynamic cohorts of patients with non-small cell lung cancer, head and neck squamous cell carcinoma (HNSCC) or colorectal cancer receiving 75 or 250 mg were evaluated for intratumoral CD8, FOXP3, GITR and tumoral PD-L1 expression by immunohistochemistry using matched biopsies from pretreatment and day 29. Peripheral blood from all patients was monitored for type-2 IFN cytokine levels, gene expression, and lymphocyte phenotype by flow cytometry up to day 43.

Results

As of 1 March 2018, 40 patients have been dosed in the DE (28) and pharmacodynamic (12) cohorts. MEDI1873 elimination half-life was ~2.0 days. MEDI1873 pharmacokinetics was dose-proportional over a range of 1.5 to 500 mg. Antidrug antibodies were rare and had minimal impact on pharmacokinetics. MEDI1873 engaged GITR as evidenced by >50% reductions in peripheral GITR-expressing memory CD4+ T cells using a competitive target engagement assay. The duration of GITR+ T-cell suppression correlated with MEDI1873 dose. At doses ≥75 mg, peripheral IFNγ, IP-10, I-TAC and MIG were elevated on days 2 and 3. This was followed by increased Ki67+CD4+ T cells on day 15. Additionally, patients with high baseline GITR levels (≥ median) had a sustained elevation of Ki67+CD4+ T cells to Day 43. Of 8 patients with evaluable paired tumor biopsies, one patient with HPV+ HNSCC and the highest baseline GITR on CD4+ T cells showed a 2x increase in intratumoral CD8+ and tumoral PD-L1+ cells. Intratumorally, MEDI1873 induced a ≥25% reduction in GITR+/FOXP3+ T cells in 5 of 5 evaluable patients. Patients with prolonged stable disease (≥40 weeks) had an average 2x elevation in Ki67+CD4+ peripheral T cells compared to all other patients.

Conclusions

MEDI1873 engages GITR on circulating blood cells resulting in increased peripheral IFNγ production and CD4+ memory T-cell proliferation coupled with a decrease in intratumoral GITR+/FOXP3+ cells. These pharmacodynamic effects are consistent with the compound's mechanism of action and may be enhanced in patients with high baseline GITR expression.

Trial Registration

ClinicalTrials.gov [NCT02583165]

Ethics Approval

Multicenter study conducted at 11 sites:(1) Pinnacle Oncology Hematology, 9055 E Del Camino Dr., Scottsdale, AZ 85358, USA [PI: Michael Gordon; IRB Registration No. IRB00002349](2) Mayo Clinic, AZ, 5777 E. Mayo Boulevard, Phoenix, AZ 85054, USA [PI: Helen Ross; IRB Registration No. IRB00000020](3) The Angeles Clinic and Research Institute, 11818 Wilshire Boulevard, Los Angeles, CA 90025, USA [PI: Ani Balmanoukian; IRB Registration No. IRB00002349](4) Mayo Clinic, MN, 200 First Street SW, Rochester, MN 55905, USA [PI: Asish Chintakuntlawar; IRB Registration No. IRB00000020](5) H Lee Moffitt Cancer Center and

Research Institute, 12902 Magnolia Drive, Tampa, FL 33612, USA [PI: Scott Antonia; IRB Registration No. IRB00000790](6) Sarah Cannon Research Institute, 250 25th Avenue North, Nashville, TN 37203, USA [PI: Howard Burris; IRB Registration No. IRB00001035](7) Columbia University Medical Center, 161 Fort Washington Avenue, Herbert Irving Pavilion Mezzanine, New York, NY 10032, USA [PI: Richard Carvajal; IRB Registration No. IRB00006882](8) Greenville Health System, 120 Dillon Drive, Spartanburg, SC 29307, USA [PI: Ki Chung; IRB Registration No. IRB00002227](9) Fox Chase Cancer Center, 333 Cottman Avenue, Philadelphia, PA 19111, USA [PI: Crystal Denlinger; IRB Registration No. IRB00002349](10) Oklahoma University, 1000 Stanton L Young Blvd, Oklahoma City, OK 73117, USA [PI: Raid Aljumaily; IRB Registration No. IRB00001035](11) MD Anderson, 1515 Holcombe Blvd, Houston, TX 77030, USA [PI: Aung Naing; IRB Registration No. IRB00002203]

Cytokines in Anti-Tumor Immunity

P410

MV-626, a potent and selective inhibitor of ENPP1 enhances STING activation and augments T-cell mediated anti-tumor activity in vivo

Jason Baird, PhD[1], Gregory Dietsch, PhD, DABT[2], Vincent Florio, PhD[2], Michael Gallatin, PhD[2], Clayton Knox, MD[2], Joshua Odingo, PhD[2], Marka Crittenden, MD, PhD[1], Michael J. Gough, PhD[1]

[1]EACRI Providence Portland Medical Center, Portland, OR, USA
[2]Mavupharma, Kirkland, WA, USA

Background
STING is an endogenous sensor of cGAMP, which is synthesized by cGAS following detection of cytoplasmic DNA. STING activation leads to interferon production and activation of inflammatory pathways that facilitate cytolytic T cell priming. STING agonists administered intratumorally show potent anti-tumor efficacy in a range of preclinical models; several agonists are in clinical development. Radiation therapy also increases cytoplasmic DNA levels in cancer cells, resulting in STING activation and secretion of inflammatory cytokines. Ectonucleotide pyrophosphatase/phosphodiesterase 1 (ENPP1) is the phosphodiesterase that negatively regulates STING by hydrolyzing cGAMP. MV-626, a highly potent and selective ENPP1 inhibitor with 100% oral bioavailability in rats and mice, blocks cGAMP hydrolysis and increases STING activation in cells where cGAS is active. We hypothesize that by conditionally enhancing STING activation, ENPP1 inhibitors will facilitate development of anti-tumor cellular immune responses, particularly following radiation therapy.

Methods
The effects of ENPP1 inhibition on STING activation using cGAMP or DNA treatment of cells were assessed. Panc02-SIY tumors were implanted in C57BL/6 mice and randomized to receive 20Gy CT-guided radiation therapy, 5 daily ip doses of MV-626, or both MV-626 and radiation. Mice were followed for outcome, tumor antigen specific T cell responses and changes in the tumor immune environment. Additional studies were conducted in mice bearing MC38 tumors.

Results
In vitro, MV-626 blocks ENPP1-mediated hydrolysis of cGAMP and enhances STING activation by DNA-mediated cGAS activation or exogenous cGAMP. Therapeutic doses of MV-626 were well tolerated in mice, with no evidence of toxicity or clinically-significant increases in systemic cytokine levels. Systemic administration of MV-626 monotherapy caused tumor growth delay. MV-626 combined with radiation therapy significantly increased overall survival, and most animals achieved durable tumor cures. Additional studies in the MC38 model

confirmed MV-626 activity. Studies characterizing effects of MV-626 in the tumor microenvironment are underway.

Conclusions

These data demonstrate that a potent, selective ENPP1 inhibitor augments STING activation and enhances immune responses to tumors. We demonstrate for the first time that, in combination with radiation therapy, ENPP1 inhibition improves outcomes and cures tumors in preclinical models through changes in the tumor immune environment. These translational studies represent a novel approach to enhancing tumor directed immune response following radiation, and provide a foundation for clinical development of an ENPP1 inhibitor as a cancer immunotherapy.

P411

An IL15/IL15Rα heterodimeric Fc-fusion engineered for reduced potency demonstrates an optimal balance of in vivo activity and exposure

Matthew Bernett, PhD[1], Rajat Varma, PhD[1], Christine Bonzon, PhD[1], Liz Bogaert, PhD[1], Rumana Rashid, PhD[1], Ke Liu, PhD[1], Irene Leung, PhD[1], Suzanne Schubbert, PhD[1], Sung-Hyung Lee, PhD[1], Daniel Kirouac, PhD[2], Fei Hua, PhD[2], Nicole Rodriguez, PhD[1], Yoon Kim, PhD[1], Kendra Avery, PhD[1], Connie Ardila[1], Nargess Hassanzadeh-Kiabi, PhD[1], Umesh Muchhal, PhD[1], Seung Chu, PhD[1], Gregory Moore, PhD[1], John R. Desjarlais[1]

[1]Xencor Inc., Monrovia, CA, USA
[2]Applied BioMath, LLC, Oakland, CA, USA

Background

IL15 and IL2 are similar cytokines that bind to the IL2Rβ/γc receptor complex and induce the proliferation of lymphocytes. Their therapeutic potential has been well established in animal models and human trials. As potential drugs, both IL2 and IL15 are extremely potent and suffer from low tolerability and very fast clearance that limits therapeutic window. To engineer a more druggable version of IL15, we created various IL15/IL15Rα heterodimeric Fc-fusions (IL15/IL15Rα-Het-Fc) with reduced potency to improve tolerability, slow receptor-mediated clearance, and prolong half-life.

Methods

We engineered IL15/IL15Rα-Het-Fc by fusing IL15 to one side of a heterodimeric Fc, and the sushi domain of IL15Rα to the other. Fc-fusions were tuned for optimal activity by engineering amino acid substitutions in IL15 - at the IL2Rβ or γc interface - that reduced in vitro potency. In vitro proliferation of lymphocytes in normal human PBMCs was monitored by counting Ki67+ cells after incubation with Fc-fusions for 4 days and by measuring signaling in a STAT5 phosphorylation assay. In vivo activity was evaluated using a huPBMC-NSG mouse model by measuring the extent of human leukocyte engraftment by flow cytometry and IFNγ. Tolerability, immune stimulation, and pharmacokinetics were evaluated in non-human primates (NHP). A computational PK/PD model was developed and trained on available data to quantify relationships between affinity, dose, and biological activity.

Results

IL15/IL15Rα-Het-Fc were produced with good yield and purity. The Fc-fusions enhanced proliferation of CD8+ T and NK cells in vitro. Variants with substitutions at the IL2Rβ and/or γc interface reduced potency up to ~700-fold compared to wild-type IL15/IL15Rα-Het-Fc. Treatment of huPBMC-NSG mice with IL15/IL15Rα-Het-Fc promoted enhanced T cell engraftment and elevated IFNγ. NHP studies indicated half-lives of several days for potency-reduced IL15/IL15Rα-Het-Fc, which are significantly longer than the <1 hr half-life of IL15. In both in vivo settings, a marked inverse correlation of pharmacodynamics and clearance was observed,

with reduced potency variants allowing higher, more tolerated doses and enhanced lymphocyte proliferation due to more sustained exposure. Our mechanism-based PK/PD model was used to predict optimal drug affinities, balancing potency vs. target-mediated clearance, and will be used to facilitate prediction of human PK/PD and regimen design. A lead candidate XmAb24306 was selected based on combined experimental observations and modeling predictions, and has been selected for clinical development.

Conclusions
Multiple IL15/IL15Rα heterodimeric Fc-fusions were engineered for reduced potency and evaluated in vitro and in vivo. We identified a variant, named XmAb24306, that optimally balanced potency and exposure.

P412

Tumor cell-intrinsic defects in STING pathway signaling

Blake Flood, BS[1], Leticia Corrales[2], Thomas Gajewski, MD, PhD[1]

[1]*University of Chicago, Chicago, IL, USA*
[2]*Aduro, Berkeley, CA, USA*

Background
Our laboratory has previously shown that immunogenic tumors spontaneously activate the innate immune system through the STING pathway. The STING pathway senses cytosolic DNA, which activates a signal transduction pathway culminating in phosphorylated IRF3 that translocates to the nucleus where it acts as a transcription factor to induce several genes including IFN-β. STING signaling and IFN-β receptor signaling in tumor-infiltrating immune cells, in turn, are required for optimal priming of CD8+ T cells against tumor antigens. Based on this notion, STING agonists have been pursued as a pharmacologic approach to activate the pathway. However, whether tumor cells themselves also can experience STING pathway activation through to IFN-β production has been unclear.

Methods
We stimulated various cell populations present in the tumor microenvironment as well as multiple tumor cell lines with STING agonists to test their ability produce IFN-β, and analyzed each step in STING pathway signaling. Further biochemical techniques including Western blotting and intracellular immunofluorescence were used to carefully analyze each step of the STING pathway in tumor cells or controls.

Results
We observed that tumor cells themselves usually fail to produce IFN-β in response to STING agonists or cytoplasmic DNA, arguing that loss of activation of this pathway might occur regularly as a component of oncogenesis. Surprisingly, we found that most tumor cells retain expression of each gene in the STING pathway, and that STING signal transduction was intact up to and including nuclear translocation of IRF3 in most instances. However, ChIP assays demonstrated that IRF3 was unable to bind the IFN-β promoter but could still bind the promoters of other genes. B16 melanoma cells, in particular, demonstrated a concurrent deficiency in NF-κB signaling downstream of STING pathway activation.

Conclusions
These results suggest that defective IRF3 DNA binding to the IFN-β locus may be a frequent alteration in cancer. Uncovering the detailed molecular mechanism of this effect could lead to new therapeutic interventions to restore the STING pathway in cancer cells.

P413

The FAP-IL2v immunocytokine is a versatile combination partner for cancer immunotherapy

Valeria Nicolini[1], Inja Waldhauer[1], Anne Freimoser-Grundschober[1], Federica Cavallo[2], Sara Colombetti[1], Marina Bacac[1], Gonzalo Acuna[1], Jehad Charo, PhD[1], Stefan Evers, PhD[1], Volker Teichgraeber, MD[1], Pablo Umana, PhD[1], Christian Klein, Dr rer nat[1]

[1]Roche Innovation Center Zurich, Schlieren, Switzerland
[2]University of Turin, Turin, Italy
[3]ROCHE Innovation Center Zurichoche, Schlieren, Switzerland

Background
FAP-IL2v (RG7461) is a novel FAP-targeted immunocytokine based on a novel IL-2 variant (IL2v) with abolished binding to CD25 (IL2Ra) to overcome preferential expansion of Tregs, activation induced cell death and to reduce IL-2 toxicities due to CD25 binding. Binding of FAP-IL2v to the intermediate affinity IL-2Rbg heterodimer is retained resulting in induction of activation and expansion of immune cells, particularly NK cells and cytotoxic CD8 T-cells. These properties make FAP-IL2v a promising partner for combination with checkpoint inhibitors, ADCC-competent/enhanced therapeutic and T-cell bispecific antibodies (TCBs).

Methods
muFAP-IL2v, a murinized surrogate of FAP-IL2v, was tested in combination with muPD-L1 and muCD40 specific surrogate antibodies and the T-cell bispecific muCEA-TCB surrogate in syngeneic orthotopic pancreatic Panc02 or Panc02-CEA models, in C57BL/6 or human CEA transgenic C57BL/6 mice, respectively. The combination of muFAP-IL2v with a anti-ratHER2 muIgG2a antibody was evaluated in the fully immunocompetent BALB-neuT genetically engineered mouse model for breast cancer, whereas the combination of FAP-IL2v with the glycoengineered Type II anti-CD20 antibody obinutuzumab was evaluated in the WSU-DLCL2 xenograft model in hCD16 transgenic Scid mice.

Results
In the pancreatic orthotopic Panc02 model in C57BL/6 mice, FAP-IL2v can boost the activation of pre-existing antigen specific T-cells in combination with anti-PD-L1 checkpoint inhibition. In the same model FAP-IL2v further enhances the efficacy of PD-L1 checkpoint inhibition when combined with an agonistic CD40 antibody resulting in long term survival in the majority of animals, and in the induction of immunological memory as evidenced by protection from tumor cell re-challenge. Furthermore, FAP-IL2v is able to enhance the activity of 1) an ADCC-competent HER2 antibody in the BALB-neuT genetically engineered mouse model and 2) the ADCC-enhanced CD20 antibody obinutuzumab in the aggressive non-Hodgkin's lymphoma model WSU-DLCL2 in human CD16 transgenic SCID mice. Finally, the activity of the T-cell bispecific antibody CEA-TCB was enhanced by combination with FAP-IL2v in the syngeneic pancreatic orthotopic Panc02 model stably expressing CEA in human CEA transgenic C57BL/6 mice.

Conclusions
The presented efficacy studies support the role of the FAP-targeted immunocytokine FAP-IL2v as a versatile combination partner for cancer immunotherapy and serve to inform the selection of combination partners for clinical studies. Particularly, they demonstrate FAP-IL2v's potential in combination with the PD-L1 checkpoint inhibitor atezolizumab, ADCC-competent antibodies e.g. trastuzumab, cetuximab or obinutuzumab, and T-cell bispecific antibodies such as CEA-TCB. Based on these data FAP-IL2v is currently being tested in Phase 1b clinical trials in combination with atezolizumab, trastuzumab and cetuximab.

P414

Efficacy of anti-PD-L1/IL-15 fusion protein in multiple tumor models

Stella Martomo, PhD[1], Dan Lu, MA[1], Zhanna Polonskaya[1], Xenia Luna[1], Kevin McCracken[1], Jeegar Patel[1]

[1]*Kadmon Corporation, New York, NY, USA*

Background

Therapeutic antibodies targeting immune checkpoint inhibitors such as PD-1/PD-L1 effectively expand and reactivate T cells in patients, leading to durable objective response rates in select cancers. However, a substantial number of patients fail to respond or become resistant to these therapies. Thus, combination therapies which include these agents as well as therapies targeting alternative effector cell types are needed. IL-15 promotes survival and cytotoxicity of both CD8 T and NK cells in the absence of the concomitant expansion of Treg population, making it a strong candidate for immunotherapy. Direct administration of IL-15 proved to be clinically challenging; durability of responses likely hindered by the short half-life and toxicity. To capitalize on the anti-tumor potential of IL-15, we generated a therapeutic fusion protein (KD033), combining a proprietary high affinity human-PD-L1 antibody (or mouse-PD-L1 surrogate antibody (KD033-surrogate)) with human IL-15. Initial assessment of this fusion antibody showed enhanced tolerability relative to a non-targeted IL-15 fusion antibody and potent anti-tumor activity.

Methods

Mouse syngeneic tumors were grown to 100 mm3 prior to a single IV administration of KD033-surrogate. Immune cell activation in cynomolgus monkeys was assessed following IV administration of KD033 (Day 1 and 15). Where applicable, tumor volumes were measured and immune cell infiltration and modulation was evaluated by immunohistochemistry, flow cytometry and Luminex.

Results

To assess broad anti-tumor potential of our molecule, single dose of KD033-surrogate was tested against a panel of 12 murine syngeneic tumors. Pronounced tumor growth inhibition was observed in multiple tumor types. In CT-26, colorectal tumor model, KD033-surrogate treatment achieved complete tumor regression in multiple animals, and consistent with generation of immune memory, tumors in these animals failed to regrow following CT-26 re-challenge. Interestingly, KD033-surrogate demonstrated synergistic response when co-administered with anti-PD-1 antibody, suggesting that KD033 could be effectively combined with other checkpoint modulators. Supporting the IL-15-dependent mechanism of action, KD033 (in monkeys) or KD033-surrogate (in mice) increased peripheral blood CD8, NK, NKT and/or gamma delta T (CD3+CD4-CD8-) cells. Additionally, an increase in tumor CD8 cells was observed in mice treated with KD033-surrogate compared to the non-targeted IL-15 fusion antibody.

Conclusions

KD033 treatment led to a robust activation of multiple effector cell types associated with a potent and durable anti-tumor activity. Based on the therapeutic activity and improved safety of the fusion protein, Kadmon is developing KD033 with the aim of clinical testing in 2019.

P415

Preclinical characterization of IL-2 Superkines engineered with biased CD8+ T cell stimulating properties

Fahar Merchant, PhD[1], Shafique Fidai[1], Aaron Ring[2]

[1]*Medicenna Therapeutics Inc., Toronto, Canada*
[2]*Yale University School of Medicine, New Haven, CT, USA*

Background
Interleukin-2 (IL-2) is a cytokine immunotherapy approved by the FDA in 1992 that shows rare, but dramatic activity in metastatic renal cell carcinoma and melanoma. However, IL-2 therapy is hampered by limited efficacy, severe toxicities, and a short circulating half-life that necessitates frequent administration. These limitations may be overcome by engineering IL-2 variants with extended half-life and decreased reliance on the IL-2 accessory receptor CD25 that is believed to mediate toxicity and unwanted stimulation of Tregs.

Methods
A series of novel IL-2 'Superkines' were engineered with biased potency towards the intermediate affinity IL-2 receptor (heterodimer of CD122 and CD132) and fused to a low-effector function Fc moiety for extended serum half-life. These Superkines were assayed for in vitro signaling potency on IL-2 receptor reporter cells lines and human peripheral blood mononuclear cells (PBMCs). Selected muteins were evaluated for their efficacy in syngeneic mouse models and for their in vivo PK and safety.

Results
A novel Fc-fused IL-2 mutein, MDNA109-Fc, was found to have a unique biased activation profile for cells expressing the intermediate affinity receptor, through a unique mechanism of action involving >1000 times increased affinity for CD122 vs. wild-type IL-2, while having similar affinity for CD25. This change improved IL-2 receptor dimerization in human cell lines and greatly enhanced phospho-STAT5 signaling and proliferation of CD8 lymphocytes vs. Tregs, leading to a 43-fold increase in potency at stimulating CD8+ T cells vs. wild-type IL-2. MDNA109-Fc also had improved potency on CD4+ Foxp3- T cells and NK cells. In vivo, this potency bias translates to an increased splenic CD8/Treg ratio. In addition, MDNA109-Fc demonstrated improved tumor growth inhibition over wild-type IL-2 in the aggressive B16F10 melanoma model. MDNA109-Fc was characterized at multiple doses and with several administration methods, demonstrating a greatly extended serum half-life that enabled a semiweekly to weekly subcutaneous dosing schedule in mice, paired with a good safety profile in vivo.

Conclusions
MDNA109-Fc is an improved interleukin-2 agent with a unique biased activation profile targeting effector versus immunosuppressive immune cells, and improved efficacy in a melanoma model. Unlike other next-generation IL-2 molecules in development, MDNA109-Fc specifically targets CD122, resulting in potent activation of effector T cells relative to Treg. MDNA109-Fc could improve the therapeutic potential of an effective, but limited use IL-2 immunotherapy by improving its efficacy, safety, and dosing convenience, a profile that may synergize well with immune checkpoint therapy.

P416

Short-course IL-15 given as a continuous infusion leads to massive expansion of NK cells: Implications for combination therapy with anti-tumor antibodies

Milos Miljkovic, MD, MSc[1], Sigrid Dubois, PhD[1], Thomas Fleisher, MD[2], Jennifer Albert, RN[1], Thomas Waldmann, MD[1], Kevin C. Conlon, MD[1]

[1]*National Cancer Institute, Bethesda, MD, USA*
[2]*NIH Clinical Center, Bethesda, MD, USA*

Background

Successful development of cytokines as immunotherapeutics for the treatment of cancer requires defining the optimal treatment regimen[1]. Post-infusional reactions limited dose escalation and immune activation in the first-in-human clinical trial of recombinant human IL-15 (rhIL-15) given as a 30-minute intravenous bolus (IVB)[2]. Ten-day treatment schedules of subcutaneous injection (SC) and continuous intravenous infusion (CIV-10) were better tolerated at 2 mcg/kg, with the CIV-10 schedule producing noteworthy increases in CD8 lymphocytes and NK cells[3, 4]. We report the results of the 5-day (CIV-5) rhIL-15 regimen, with a safety profile and stimulation of effector cells comparable to CIV-10, dosed up to 5 mcg/kg without dose-limiting toxicities.

Methods

Eleven patients were treated at 3 (n=4), 4 (n=3), and 5 mcg/kg/day (n=4, Table 1) with the CIV-5 regimen in a standard phase I dose-escalation study of rhIL-15 for patients with refractory metastatic cancers.

Results

There were no dose-limiting toxicities, but two patients did not complete cycle 1 for reasons unrelated to rhIL-15 (NSAID-induced SIADH and infectious gastroenteritis). The most common adverse events were fever, chills, fatigue, nausea, transient liver function test abnormalities, anemia, and thrombocytopenia (Tables 2-3). The best response was stable disease. Impressive expansion of NK cells was seen at all dose levels (21 to 44-fold, mean 33-fold) as well as an increase in CD8 cells (1.6-8.9-fold, mean 3.8-fold). The mean increase was greatest at 4 mcg/kg: NK cells 42-fold, and CD8 cells 4.8-fold. This effector lymphocyte expansion exceeded results seen with other rhIL-15 dosing regimens or other IL-15 formulations (Table 4). The emergence of pulmonary capillary leak symptoms and slower patient recovery from toxicities at 5 mcg/kg dose level, without a further rise in immune cell subsets, led to our choice of 4 mcg/kg as the highest CIV-5 dose to be tested in new combination treatment trials.

Conclusions

The shorter duration of the CIV-5 rhIL-15 regimen and its safety profile may make outpatient administration via an ambulatory infusion pump feasible. The massive expansion of NK cells and increases in CD8 cells it produced were greater than other IL-15 regimens. NK cells are key mediators of antibody-dependent cell cytotoxicity (ADCC); in mice, the increase of NK cell number following CIV IL-15 was associated with increased ADCC of anti-tumor antibodies and their efficacy[5]. Our upcoming trials of CIV-5 rhIL-15 with obinutuzumab or avelumab will leverage the observed massive NK cell expansion to augment the ADCC and therefore their efficacy as anti-tumor antibodies.

References

1. Conlon, K.C., M.D. Miljkovic, and T.A. Waldmann, Cytokines in the Treatment of Cancer. J Interferon Cytokine Res, 2018. [epub ahead of print]2. Conlon, K.C., et al., Redistribution, hyperproliferation, activation of natural killer cells and CD8 T cells, and cytokine production during first-in-human clinical trial of recombinant human interleukin-15 in patients with cancer. J Clin Oncol, 2015. 33(1): p. 74-82.3. Conlon, K.C., et al., Abstract 1596: Phase I trial of

recombinant human Interleukin 15 (rhIL-15) administered as continuous intravenous infusion (CIV) for 10 days (240 hours) in patients with refractory metastatic cancers. Cancer Research, 2017. 77(13 Supplement): p. 1596-1596.4. Miller, J.S., et al., A First-in-Human Phase I Study of Subcutaneous Outpatient Recombinant Human IL15 (rhIL15) in Adults with Advanced Solid Tumors. Clinical Cancer Research, 2018. 24(7): p. 1525-1535.5. Miljkovic, M.D., et al., IL-15-enhanced antibody-dependent cellular cytotoxicity mediated by NK cells and macrophages: Implications for immunotherapy of T-cell lymphoma [abstract], In: Proceedings of the 2018 AACR Meeting on Advances in Malignant Lymphoma. 2018, Philadelphia (PA): AACR: Boston, Massachusetts.

Ethics Approval

The study was approved by the National Cancer Institute's Institutional Review Board, approval number 385250.

Table 1.

Diagnosis	Age	Gender	Dose level (µg/kg/day)	No. of doses	NK cell increase (fold)	CD8+ T-cell increase (fold)
Melanoma	63	M	5	5	32.01	4.21
Small bowel	69	M	5	10	39.13	4.74
Colorectal	60	F	5	4	-	-
Small bowel	51	F	5	10	32.03	5.66
Colorectal	66	F	4	10	44.90	3.65
Renal cell	56	M	4	15	43.65	8.94
Esophageal	60	M	4	10	39.63	2.01
Colorectal	67	F	3	20	21.40	1.65
Colorectal	56	F	3	15	23.66	2.03
Endometrial	70	F	3	3	-	-
Colorectal	47	F	3	10	24.15	1.66

Table 2.

	3 µg/kg n=4				4 µg/kg n=3				5 µg/kg n=4			
CTC V4 Grade	1	2	3	4	1	2	3	4	1	2	3	4
Arthritis						1						
Bladder infection		1										
Chills	1	1				2				2		
Constipation	1								1			
Diarrhea	2				1				1	1		
Dizziness					2							
Dry mouth	1				2							
Dry skin						1						
Edema limbs	1	1										
Fatigue	1	1							2	1		
Fever	2	2			1	1			2	2		
Headache	1				1							
Hypotension		1				1			1			
Nausea	2				2				3			
Pulmonary edema		1										
Rash maculo-papular	2								2			
Vomiting	2				1				2			

Table 3.

	3 µg/kg n=4				4 µg/kg n=3				5 µg/kg n=4			
CTC V4 Grade	1	2	3	4	1	2	3	4	1	2	3	4
Anemia			2			2			1	1	1	
ALT increased	1	1			1	1			3			
AST increased		2			2				4			
Alkaline phosphatase		1			1		1		2	1		
Hyperbilirubinemia	1	1				1			1		1	
Hypoalbuminemia		2			1	1			2	2		
Creatinine increased					1				1	2		
Hyperglycemia										1		
Hypernatremia	2										1	
Hyponatremia	1		1		2				3			
Hypocalcemia	1				1				4			
Hypokalemia	2	1							1		2	
Hypomagnesemia					1				3			
Hypophosphatemia		1	2			2				1	2	
Lymphocytosis				2				2			1	2
Lymphopenia		1				1	1			2	1	1
Neutropenia	1				1		1			1		
Thrombocytopenia		2			2				1	1		
Leucopenia		2				1	1		1	1	1	

Table 4.

Regimen	RP2D (mcg/kg)	Mean fold increase at RP2D NK	CD56^{bright}	CD8 T
IVB	0.3	2.5		8
SC	2	10.8	37	3.3
CIV-10	2	31	400	3.3
CIV-5	4	42	pending	4.8

P417

SYTX80-013-A: an engineered IL-2 for the treatment of solid tumors with superior pre-clinical efficacy and safety evidence

Marcos Milla, PhD[1], Jerod Ptacin, PhD[1], Carolina Caffaro[1], Hans Aerni, PhD[1], Lina Ma[2], Kristine San Jose[1], Michael Pena[1], Robert Herman[1], Yelena

Pavlova[1], David Chen[1], Laura Shawver[2], Lilia Koriazova[1], Ingrid Joseph[1]

[1]*Synthorx, Inc., La Jolla, CA, USA*
[2]*Synthorx.com, La Jolla, CA, USA*

Background
Aldesleukin, a recombinant form of IL-2, is the first approved immuno-oncology drug leading to complete, durable remissions in metastatic melanoma and renal cell carcinoma patients. Yet, its use is very limited because of vascular leak syndrome (VLS), a severe dose-limiting adverse event stemming from the engagement of the high affinity IL-2 receptor alpha chain in group 2 innate lymphoid cells, eosinophils and vascular endothelial cells. IL-2's high potency for activation of CD4+ regulatory T cells (Tregs) that suppress T cell-mediated tumor killing responses further reduces its therapeutic window.

Methods
N/A

Results
We applied our Expanded Genetic Alphabet technology platform to the engineering of SYTX80-013-A: a site-directed, singly pegylated form of IL-2 completely lacking IL-2 receptor (IL-2R) alpha chain engagement yet retaining normal binding to the intermediate affinity beta-gamma IL-2R signaling complex present at the surface of natural killer (NK) and CD8+ tumor-killing cells. SYTX80-013-A potently induces pSTAT5, Ki67 and the proliferation of peripheral NK and CD8+ effector T cells in vivo in mice. Remarkably, dosing of SYTX80-013-A in those animals has minimal effect on molecular and clinical markers of VLS, even at high dose levels. In the mouse CT-26 and B16F10 syngeneic tumor models, SYTX80-013-A induces NK and CD8+ T cell tumor infiltration with marked elevation of CD8+/Treg TIL ratios. In non-human primates, SYTX80-013-A can be dosed for maximal elevation in lymphocytes (pharmacodynamic marker) with negligible elevation in eosinophils (toxicology marker).

Conclusions
This demonstrates that SYTX80-013-A is a re-programmed IL-2 that changes the pharmacological profile of that cytokine from low lymphocyte/high eosinophil to high lymphocyte/no eosinophil induction: an IL-2 with a therapeutic window. We are now advancing this molecule into GLP toxicology studies, in preparation for FIH studies in 2019.

P418

Pre-clinical investigation of NKTR-255, a polymer-conjugated human IL-15 with a potent NK cell dependent anti-tumor efficacy

Takahiro Miyazaki, MS[1], Murali Addepalli, PhD[1], Arunasree Lanka, PhD[1], Amol Murkar, MSc[1], Ravikumar Nutakki[1], Palakshi Obalapur, PhD[1], Peiwen Kuo, PhD[1], Phi Quach, BS PhD[1], Mekhala Maiti, PhD[1], Laurie VanderVeen, PhD[1], Ping Zhang, MS PhD[1], Loui Madakamutil[1], Jonathan Zalevsky, PhD[1]

[1]*Nektar Therapeutics, San Francisco, CA, USA*

Background
IL-15 is a cytokine that activates and provides survival benefit to T and NK cells and has potential as an immunotherapeutic agent for the treatment of cancer. Exploiting the therapeutic value of native IL-15 has been challenging due to, for example, its unfavorable pharmacokinetic properties and tolerability. NKTR-255 is a polymer-conjugated human IL-15 that retains binding affinity to the alpha subunit of IL-15 receptor and exhibits reduced clearance to thereby provide a sustained pharmacodynamics response. Here we investigate the pharmacological properties of NKTR-255 on NK cells and the effect of NKTR-255 in NK cell-dependent tumor models.

Methods
For in vivo NK cell characterization, mice received single IV doses of 0.03, or 0.3 mg/kg of NKTR-255. Blood and spleen samples were collected to assess the NK population and function. Flow cytometry was used to measure pSTAT5 and Ki-67 in NK cells. Purified splenic NK cells were co-cultured with YAC-1, a mouse T lymphoma cell line, to measure cytotoxic function. In the CT26 model, 1x105 cells were administered intravenously on Day 0, treatment was initiated on Day 1 at 0.3, 1, or 3 mg/kg, and on Day 13 lungs were scored for metastases. In the orthotopic 4T1 model, 5x105 cells were implanted in the mammary fat pad on Day 0, treatment was initiated on Day 5 at 0.3 mg/kg, and on Day 14, metastases were determined from culture of single lung cell isolates.

Results
In vitro, NKTR-255 showed a dose-dependent phosphorylation of STAT5 and enhancement of cytotoxic function in mouse NK cells. NKTR-255 administration increased thebpSTAT5+ populations, the Ki67+ populations and the absolute number of NK cells. In addition, NKTR-255 provided sustained effects of NK cell activation, as determined by enhanced Granzyme B and CD16 expression and cytotoxic function. In the disseminated CT26 model, NKTR-255 treatment resulted in a significant increase of NK cells in lung and a dose-dependent reduction in the number of lung metastases in a NK cell-dependent manner. In the physiological 4T1 metastasis model, NKTR-255 also showed a significant anti-metastatic effect although it did not affect primary tumor growth.

Conclusions
NKTR-255 is a powerful immune stimulator of NK cells that provides a dose-dependent effect in the proliferation and activation of NK cells. This property of NKTR-255 translates into enhanced anti-metastatic activity in mouse lung metastasis models. These results indicate that NKTR-255 has the therapeutic capacity to be an anti-tumor agent that enhances NK cell expansion and survival.

Ethics Approval
All animal care and procedures were ethically approved and performed according to AAALAC accredited Nektar Therapeutics IACUC guidelines.

P419

NKTR-214 in combination with radiation produces a potent in situ vaccine in the syngeneic B78 melanoma model.

Alexander Pieper, BS[1], Alexander Rakhmilevich, MD, PhD[1], Jacob Slowinski, Mr[1], Amy Erbe, PhD[1], Jacquelyn Hank, PhD[1], Zachary Morris, MD, PhD[1], Deborah Charych, PhD[2], Paul Sondel, MD, PhD[1]

[1]University of Wisconsin Madison, Madison, WI, USA
[2]Nektar Therapeutics, San Francisco, CA, USA

Background
NKTR-214 is an engineered agonist of the IL2 pathway, biased to the CD122 receptor resulting in sustained signaling and increased CD8/Treg ratios in human and murine tumors. NKTR-214 has shown promising clinical results by enhancing systemic anti-tumor responses. Radiation therapy (RT) alone rarely generates an effective in situ vaccination due, in part, to poor persistence of activated tumor-specific lymphocytes. However, RT can increase tumor immunogenicity by local release of immune stimulatory cytokines, immunogenic tumor cell death, and phenotypic changes that enhance immune susceptibility of tumor cells surviving RT. NKTR-214 may sustain, expand, and drive the systemic anti-tumor response initiated by RT leading to tumor clearance and tumor specific immunologic memory.

Methods
C57BL/6 mice were inoculated with B78 melanoma cells on the right flank. Once average tumor volumes reached 125mm3 (~4 weeks), mice were randomized and treated with 12 Gy external beam local RT to this tumor site (defined as treatment day 0). Cohorts of mice were then treated with one of the following: 1) intravenous (IV) IL-2 (0.47 mg/kg), qdx5 starting on day 5; or 2) intra-tumoral (IT) IL2 (0.47 mg/kg), qdx5 starting on day 5; or 3) IV NKTR-214 (0.8 mg/kg) q9dx3 starting on day 5; or 4) buffer alone, q9dx3 starting on day 5. Tumor growth was monitored biweekly. All mice with complete response (CR) were rechallenged at day 90 with a second inoculation of B78 melanoma to test for immunologic memory.

Results
Both RT and NKTR-214 alone slowed tumor growth compared to the buffer alone group; however, neither RT nor NTKR-214 alone caused tumor regression. In contrast, the combination of RT + NTKR-214 resulted in significant tumor regression ($p<0.01$). The rate of complete response (CR) was significantly greater with RT + NKTR-214 compared to RT + IV IL-2 (80% CR vs. 16% CR, $p<0.05$). RT + NKTR-214 also performed better than RT + IT IL-2 causing significantly more tumor regression ($p<0.01$) and a higher CR rate (80% CR vs. 60% CR). The combination of RT + NKTR-214 resulted in stronger immunologic memory than RT + IT IL-2 as more mice receiving RT + NKTR-214 rejected a second B78 inoculation (100% rejection vs. 55% rejection, $p<0.01$).

Conclusions
Previously, IT IL-2 was required to activate and sustain tumor-specific lymphocytes generated from RT of B78. Here we showed that this effect of in-situ vaccination can be realized through IV administration of systemic NKTR-214 coupled with standard RT.

P420

Outpatient staccato pulse intravenous Interleukin-2 in metastatic melanoma

Walter Quan, MD[1], Leah Gutierrez, RN BSN[2], Erin Johnson[1], Francine Quan, RN MSN OCN[3]

[1]*Loma Linda University, Loma Linda, CA, USA*
[2]*Western Regional Medical Center, Goodyear, AZ, USA*
[3]*Loma Linda University Beaumont, Tempe, AZ, USA*

Background
Daily single intravenous Interleukin-2 (IL-2) infusions (pulses) have been developed to decrease toxicity while maintaining anticancer activity of this molecule against melanoma. Such IL-2 schedules have previously been shown to elicit Lymphokine Activated Killer cell (LAK) activity [1]. Hank has demonstrated in vitro that LAK generated by IL-2 then subsequently exposed to additional IL-2 displayed enhanced cytotoxicity [2]. In patients receiving IL-2 therapy, a rebound lymphocytosis occurs approximately 2-3 days later. The staccato schedule was developed to administer an additional IL-2 pulse during the time of rebound lymphocytosis.

Methods
In this retrospective study, twenty-two patients with metastatic melanoma were treated with IL-2 18 Million IU/M2 intravenously over 15-30 minutes on days 1-3 and 21.6 Million IU/M2 intravenously over 15-30 minutes on day 5 on an outpatient basis. Cycles were repeated every 3 weeks.

Results
Patient characteristics: 9 males/13 females, median age-55 (range: 21-74), median ECOG performance status-1 (0-1); common metastatic sites: lymph nodes (17), lungs (15), subcutaneous (12), bone (6), liver (4). Prior systemic therapy: Ipilimumab (8); Interferon (7); Pembrolizumab or Nivolumab (7);

Interleukin-2 (5); oral targeted therapy (4); none (4). Most common toxicities were nausea/emesis, decreased appetite, sinus/catarrhal symptoms, myalgia/arthralgia, peripheral swelling, and rigors. No patients required hospitalization for toxicity of therapy. One patient (5%) has had a complete response (ongoing at 12.5+ months) while ten other patients (45%) had partial responses (total response rate =50%; 95% CI: 28-72%). Two of the patients with partial responses have been rendered free of disease following surgical resection of their residual cancer. Responses occurred in lung, bones, lymph nodes, pancreas, peritoneum, breast, small bowel, and subcutaneous sites. Median response duration is 10.1 months.

Conclusions

Outpatient staccato pulse intravenous Interleukin-2 has activity in melanoma.

References

1. Mitchell MS, Kempf RA, Harel W, Shau H, Boswell WD, Lind S, Dean G, Moore J, Bradley EC. Low-dose cyclophosphamide and low-dose interleukin-2 for malignant melanoma. Bull NY Acad Med 1989; 65:128-144.
2. Hank JA, Weil-Hillman G, Surfus JE, Sosman JA, Sondel PM. Addition of interleukin-2 in vitro augments detection of lymphokine-activated killer activity generated in vivo. Cancer Immunol Immunother 1990; 31:53-59.

Ethics Approval

The study was approved by Loma Linda University's Institutional Review Board, approval number 5180218.

P421

Combination of Pegilodecakin (AM0010) with Docetaxel improves immune cell-mediated anti-tumor response in mouse 4T1 tumor model

Navneet Ratti, BS, MBA[1], Rakesh Verma, PhD[1], Martin Oft, MD[1]

[1]ARMO BioSciences, a wholly owned subsidiary of Eli Lilly and Company, Redwood City, CA, USA

Background

Pegilodecakin is a PEGylated-recombinant hIL-10 that has single agent and combination efficacy with chemotherapy and checkpoint inhibitors across multiple cancers. Pegilodecakin stimulates the survival, proliferation and cytolytic ability of the $CD8^+$ T-cells. Clinical studies with Pegilodecakin have reported 41% ORR in combination with anti-PD1 in 2nd line NSCLC. Pegilodecakin induced expansion of $PD1^+Lag3^+CD8^+$ T-cells correlates with clinical response. Microtubule inhibiting molecules are used as chemotherapeutic agents but combination efficacy with immuno-oncology therapies is not well understood. Here we report the enhanced immune responses and efficacy of AM0010 when combined with Docetaxel.

Methods

Pegilodecakin is active, but immunogenic in mice. Therefore, B-cell deficient mice were employed for in-vivo studies. $5x10^3$ 4T1 cells were inoculated subcutaneously and allowed to reach a median tumor volume of 100 mm^3 prior to treatment. Mice received Pegilodecakin alone at 0.5mpk/qd and/or Docetaxel alone at 40mpk/qw. Tumor size and body weights were monitored twice weekly. Immune cells were phenotyped by flow cytometry. Sera were analyzed for cytokines.

Results

The control cohort reached the terminal tumor size by Day 39 PI. Compared to control, Tumor Growth Inhibition percentage (TGI) was 80.91% on Pegilodecakin, 21.39% on Docetaxel and 97.04% on the combination cohort.Docetaxel cohort showed body-weight loss in mice, which was alleviated on Pegilodecakin+Docetaxel. Systemic metastases were

only observed in control and Docetaxel cohorts.In the tumors, Pegilodecakin showed an increase of 82-fold in tumor infiltrating T-cells (TILs), 622-fold increase in $PD1^+Lag3^+CD8^+$ T-cells and a 545-fold increase in proliferative $Ki67^+PD\text{-}1^+Lag\text{-}3^+CD8^+$ T-cells compared to the control cohort.Docetaxel showed an 11-fold increase of TILs but no significant changes in further subsets ($CD8^+$/$PD1^+Lag3^+CD8^+$/$Ki67^+PD1^+Lag3^+CD8^+$ T-cells).Pegilodecakin+Docetaxel showed the largest increase in TILs (>400-fold), $PD1^+Lag3^+CD8^+$ (>1300-fold) and proliferating $Ki67^+PD1^+Lag3^+CD8^+$ TILs (1641-fold).Serum IFNG was increased on Pegilodecakin+Docetaxel (6.03pg/mL), compared to 3.39pg/mL on Pegilodecakin, 0.30pg/mL on Docetaxel and 0.72pg/mL in untreated mouse. IFNG was undetectable in control mice at 3 weeks and not available at the terminal endpoint.

Conclusions

Pegilodecakin stimulated T-cell mediated tumor regression of 4T1 breast cancers was increased on Pegilodecakin/Docetaxel. Tumor regression correlated with presence and proliferation of $PD1^+Lag3^+CD8^+$ T-cells in the tumor. Tumor regression and TIL activation was most enhanced on Pegilodecakin+Docetaxel. The immune stimulation of the combination therapy is further reflected in the systemic increase of IFNG in the combination arm compared to monotherapy. These results provide rationale to clinically test a combination Docetaxel with Pegilocakin in tumors with low T-cell infiltration and resistance to available immunotherapies.

P422

A polymer-associated human IL-15 (NKTR-255) has optimized biological activity and unique mechanisms of action on CD8 T Cells and NK Cells

Tanya Robinson, PhD[1], Shweta Hegde, Research Assistant[1], Sarai Rivas, BS[1], Takahiro Miyazaki, MS[2], Kimberly S. Schluns, PhD[1]

[1]*University of Texas MD Anderson Cancer Center, Houston, TX, USA*
[2]*Nektar Therapeutics, San Francisco, CA, USA*

Background

IL-15 has anti-tumor activity but with limited efficacy due to its unfavorable pharmacokinetic properties and tolerability. Nektar Therapeutics has developed a polymer-conjugated human IL-15 (NKTR-255) that exhibits a prolonged in vivo half-life and enhanced potency, which is currently being examined as a potential cancer immunotherapeutic agent. Since responses by IL-15 can be mediated by transpresentation via the IL-15Rα, as soluble IL-15/IL-15Rα complexes, or by cis-presentation, we investigated the role of IL-15Rα in driving NKTR-255 responses by naïve and memory CD8 T cells and NK cells in mice.

Methods

The effects of NKTR-255 were examined by the adoptive transfer of CFSE-labeled naïve ovalbumin-specific CD8 T cells (OT-I) or established memory OT-I T cells followed by systemic administration of NKTR-255. To assess responses by central and effector memory T cell subsets, sorted CD44hi memory phenotype CD8 T cells were transferred into wild-type (Wt) recipients followed by NKTR-255 treatment. Additionally, NK cell responses to NKTR-255 were analyzed in IL-15Rα bone marrow (BM) chimeras by BrdU incorporation.

Results

Naïve CD8 OT-I T cells transferred into Wt and IL-15Rα-/- mice proliferated at similar levels and acquired a central memory phenotype in response to NKTR-255. Interestingly, naive IL-15Rα-/- OT-I T cells had a deficient response to NKTR-255 but not to rhIL-15 or soluble IL-15 complexes. Additionally, proliferation by memory IL-15Rα-/- OT-I T cells in response to NKTR-255 was partially impaired compared to Wt OT-I cells. Sorted memory CD8 T

cells maintained their proportion of CD62L+ and - subsets after NKTR-255-stimulated proliferation. Since IL-15Rα expression is essential for NK cell development, BM chimeras were generated with either IL-15Rα-/- or Wt BM in Wt recipients. In this model system, similar levels of BrdU were incorporated in IL-15Rα-/- and Wt NK cells after treatment with NKTR-255.

Conclusions

These findings suggest naive CD8 T cells are critically dependent on cis-presentation of NKTR-255, while memory CD8 T cells are only partially dependent. For both naive or memory CD8 T cells, transpresentation of NKTR-255 was not required. In contrast to CD8 T cells, NK cell responses to NKTR-255 are not dependent on cis-presentation. Overall, these findings highlight the potential of polymerized IL-15 to modify IL-15Rα dependency leading to different mechanisms of action on CD8 T cells and NK cells and unique therapeutic effects.

Ethics Approval

All animal procedures were conducted in accordance with the animal care and use protocols (00000851-RN01) approved by the IACUC at the UT MD Anderson Cancer Center.

P423

Safety, pharmacokinetics and pharmacodynamic effects of ALKS 4230 in patients with advanced solid tumors from the ongoing dose escalation portion of a first in human (FIH) study

Ulka Vaishampayan, MD[1], Vamsidhar Velcheti, MD FACP[2], David McDermott, MD[3], Mayer Fishman, MD, PhD[4], Chris Hoimes, MD[5], Daniel Cho, MD[6], Lei Sun, Ph.D[7], Juan Alvarez, PhD[8], Heather Losey, PhD[7], Rose Marino, MD[7], Emily Putiri, PhD[7], Sean Rossi[7], Lisa Von Moltke, MD[7], William Slichenmyer, MD[9], Marc Ernstoff, MD[10]

[1]*Barbara Ann Karmanos Cancer Institute, Detroit, MI, USA*
[2]*Cleveland Clinic, Pepper Pike, OH, USA*
[3]*Beth Israel Deaconess Medical Center, Boston, MA, USA*
[4]*Moffitt Cancer Center, Tampa, FL, USA*
[5]*University Hospital, Cleveland, OH, USA*
[6]*New York University, New York, NY*
[7]*Alkermes, Inc., Waltham, MA, USA*
[8]*Merck, Boston, MA, USA*
[9]*Alacrita, Waltham, MA, USA*
[10]*Roswell Park Cancer Institute, Buffalo, NY, USA*

Background

ALKS 4230 is a fusion of circularly permuted IL-2 and IL-2 Receptor (IL-2R) α designed to selectively activate the intermediate-affinity IL-2R, comprised of IL-2Rβ and γ, for activation of cytotoxic CD8+ T cells and NK cells. ALKS 4230 has previously been shown to have enhanced antitumor activity relative to IL-2 in murine models.

Methods

In the ongoing FIH Phase 1 study in patients with advanced solid tumors, ALKS 4230 is administered as a 30 minute intravenous infusion once daily for 5 consecutive days repeating in treatment cycles of 14 days (first cycle) or 21 days (subsequent cycles). The primary objectives are to investigate ALKS 4230 safety and tolerability and to determine the maximum tolerated dose and recommended Phase 2 dose. Other assessments include pharmacokinetics, lymphocyte sub-population expansion, immunogenicity, and anti-tumor activity.

Results

Twenty-four patients have received ALKS 4230 at doses ranging from 0.1 to 3 µg/kg/day. Patients with multiple tumor types were enrolled, including 5 with prostate carcinoma, 4 with renal cell carcinoma, and 3 with melanoma. Patients had a median of 3 (range 1-8) prior lines of systemic therapy. The most common treatment emergent adverse events (AEs)

seen in ≥ 60% of patients were fever and chills. Grade 3 treatment-related AEs seen in 1-2 patients occurred at the 3 µg/kg/day dose level and included neutropenia, leukopenia, jaundice, febrile neutropenia, lymphopenia, diarrhea, cholangitis, hyperbilirubinemia and hypoalbuminemia. There were no Grade 4 or 5 AEs. Systemic exposure to ALKS 4230 increased with increasing dose and serum ALKS 4230 concentrations at 3 µg/kg/day have exceeded the EC50 values for NK and CD8+ T cell activation determined in in vitro pharmacology studies. Treatment with ALKS 4230 resulted in a dose-dependent increase in circulating NK and CD8+ T cells with an approximately 4-fold and 2-fold expansion at 3 µg/kg/day, respectively, and minimal, non-dose dependent change in Tregs. Transient, dose dependent elevations in serum IL-6 levels occurred 4-6 hours post-dose and were associated with transient fever and chills but not cytokine storm. No objective responses have been seen, and dose escalation is ongoing.

Conclusions

ALKS 4230 was well tolerated at the doses tested, with treatment-related AEs that were manageable and transient. The 3 µg/kg/day dose level induced expected immunologic effects, supporting the rationale for assessing combination therapies with ALKS 4230, as well as continued dose escalation in the monotherapy setting.

Acknowledgements

Study was sponsored by Alkermes, Inc. The authors gratefully acknowledge the patients and their families who participated in this study.

Trial Registration

Trial Registration at Clinicaltrials.gov: NCT02799095

Ethics Approval

The study was approved by Beth Israel Deaconesses Medical Center Investigation Review Board (IRB), approval number 16-229, Roswell Park Cancer Institute IRB, approval number MOD00002327 / PH 285316, Cleveland Clinic IRB, approval number 16-804, Western IRB, approval number 1166122, New York University IRB, approval number i15-01394, University Hospitals IRB, approval number 16-804, and Chesapeak IRB approval number 00000790.

P424 Abstract Travel Award Recipient

NKTR-214, an engineered IL-2, selectively depletes intratumoral Tregs and expands immunotherapy-induced effector T cell responses

Meenu Sharma, PhD[1], Hiep Khong, PhD[1], Faisal Fa'ak, MD[1], Brent Chesson[1], Barbara Pazdrak[1], Laura Maria S Kahn[1], Louise Janssen, MSc[1], Uddalak Bharadwaj[1], Binisha Karki[1], Zhilan Xiao, MD[1], Yared Hailemichael, PhD[1], Manisha Singh, PhD[1], Christina Vianden, MSc[1], David Tweardy[1], Salah Eddine Bentebibel[1], Cara Haymaker, PhD[1], Chantale Bernatchez[1], Adi Diab, MD[1], Ute Hoch, PhD[2], Jonathan Zalevsky, PhD[2], Willem W. Overwijk, PhD[1]

[1]UT MD Anderson Cancer Center, Houston, TX, USA
[2]NEKTAR Therapeutics, San Francisco, CA, USA

Background

High dose IL-2 has been used in treatment of metastatic melanoma and renal cell carcinoma. However, expansion of suppressive Tregs and physiologic toxicities associated with IL-2 has limited its use in anti-cancer therapies. NKTR-214 is an engineered IL-2 cytokine that provides sustained activation of the IL-2 pathway through controlled release of IL-2 with a bias to the IL-2 receptor CD122 (IL-2Rbeta gamma), so that it can selectively enhance CD8+ T cell over regulatory T cells (Tregs). We tested this idea by assessing the therapeutic synergy of NKTR-214 with CTLA-4 and PD-1-based checkpoint blockade therapy or with peptide-vaccination in CT26 colon carcinoma and B16 melanoma models. We investigated impact of treatment on proliferation

and apoptosis of effector CD8+ T cells and immunosuppressive CD4+Foxp3+ Tregs, as well as effector cytokines and chemokines in tumor and peripheral tissues. In vivo cytokine neutralization experiments and in vitro assays revealed that NKTR-214 plus vaccine treatment induced CD8+ effector T cell responses and enhanced associated cytokines IFN-gamma and TNF-alpha that mediate specific depletion of intratumoral, but not peripheral, Tregs.

Methods

CT26 colon carcinoma tumor bearing mice were treated with NKTR-214 or CTLA-4 and/or PD-1 checkpoint blockade. Tumor size, survival and tumor-specific effector T cell response was analyzed. To monitor antigen-specific immune response, we adoptively transferred naïve gp100-specific pmel-1 CD8+ T cells into mice bearing established B16 tumors, followed by a single vaccination (gp100 peptide + anti-CD40 mAb + TLR-7 agonist) alone or in combination with NKTR-214 or Aldesleukin (IL-2) given every 8 days. Detailed analysis of CD8+ T cells and Tregs was done by flow cytometry. Chemokines/cytokines levels in tumor and spleen were measured by luminex-based assay.

Results

NKTR-214 efficiently synergized with checkpoint blockade and with vaccination, improving overall survival and cure of mice in models of colon carcinoma and melanoma. NKTR-214 promoted the CD8+ T cell survival, expansion and release of associated cytokines, IFN-gamma and TNF-alpha, which synergized to induce apoptosis and inhibited proliferation of Tregs specifically in tumors (Figure 1) while preserving Tregs in peripheral tissues. In vitro cytokine treatment also confirmed that IFN-gamma and TNF-alpha together are both sufficient and required to block Treg proliferation. Preliminary results confirm similar therapeutic effects with cancer patients receiving clinical doses of NKTR-214.

Conclusions

NKTR-214 synergizes with checkpoint blockade as well as with vaccination to improve the survival, proliferation and tumor infiltration of effector CD8+ T cells while promoting selective intratumoral depletion of Tregs to establish effective anti-tumor immunity.

Figure 1. NKTR-214 mediated intratumoral Treg depletion

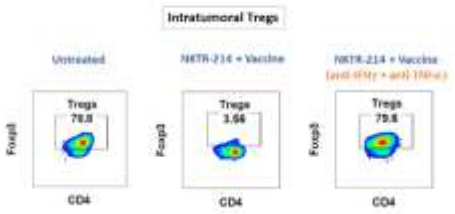

P425

Pharmacokinetics and pharmacodynamic effects of ALKS 4230, an investigational immunotherapeutic agent, in cynomolgus monkeys after intravenous and subcutaneous administration

Lei Sun, PhD[1], Jared Lopes, PhD[1], Heather Flick, MS[1], Erin Murphy, MS[1], Heather Losey, PhD[1]

[1]*Alkermes, Inc., Waltham, MA, USA*

Background

ALKS 4230 is an engineered cytokine designed to selectively activate the intermediate-affinity interleukin-2 receptor (IL-2R), expressed predominantly on natural killer (NK) cells and CD8+ T cells, which play an important role in driving immune responses in cancer. A first-in-human study of intravenous administration of ALKS 4230 in patients with advanced solid tumors (NCT02799095) is currently ongoing. To compare the pharmacodynamic responses in response to the

intravenous and subcutaneous administration of ALKS 4230, two studies were carried out in cynomolgus monkeys.

Methods
In the first study, a single dose of ALKS 4230 was administered intravenously or subcutaneously. In the second study, ALKS 4230 was administered intravenously once daily on Days 1-5 or subcutaneously on Days 1 and 4. Serial blood samples were collected from each animal for determination of serum concentrations of ALKS 4230 and multiple proinflammatory cytokines as well as for immunophenotyping by flow cytometry.

Results
Overall systemic exposure to ALKS 4230 as measured by area under the serum concentration vs. time (C-T) curve (AUC) after a single subcutaneous dose of 1 mg/kg was comparable to that after an intravenous dose of 0.3 mg/kg, suggesting a subcutaneous bioavailability of ~30%. With comparable AUC but lower Cmax, subcutaneous administration elicited greater expansion of CD8+ T cells and CD56+ NK cells as well as a superior ratio of CD8+ T cells to CD4+CD25+FoxP3+ Tregs compared to intravenous administration. In addition, expansion of CD8+ T cells and CD56+ NK cells was sustained up to 12 days after a single dose. Total systemic exposure to ALKS 4230 was comparable after 5 daily intravenous doses of 0.1 mg/kg and 2 subcutaneous doses of 0.5 mg/kg (on Days 1 and 4) and resulted in similar expansion of total CD8+ T cells, NK cells and Tregs between the two dosing regimens. The serum IL-6 C-T profile mirrored the ALKS 4230 C-T profile, with a higher peak IL-6 level and a higher Cmax of ALKS 4230 following the last intravenous dose of 0.1 mg/kg compared to the last subcutaneous dose of 0.5 mg/kg.

Conclusions
Subcutaneous administration of ALKS 4230 can achieve similar total systemic exposure to ALKS 4230 compared to intravenous administration with less frequent dosing and a lower Cmax, leading to similar expansion of total CD8+ T cell and NK cell populations. Therefore subcutaneous administration may be a practical alternative to intravenous dosing and merits clinical evaluation.

Emerging Models and Imaging

P426

Chaos-based fractal radiomic features of nodule vasculature predicts response to immunotherapy on non-contrast lung CT

Mehdi Alilou, PHD[1], Marjan Firouznia, PHD[1], Pradnya Patil[2], Kaustav Bera, MBBS[1], Robert Gilkeson[3], Prabhakar Rajiah[3], Vamsidhar Velcheti, MD FACP[2], Anant Madabhushi, PhD[1]

[1]Case Western Reserve University, Cleveland, OH, USA
[2]Cleveland Clinic, Cleveland, OH, USA
[3]University Hospital Case Medical Center, Cleveland, OH, USA

Background
Immune-checkpoint blockade treatments, particularly drugs inhibiting programmed death-ligand 1 (PD-L1) with its receptor, programmed cell death protein-1 (PD-1) has demonstrated promising clinical efficacy in patients with advanced non-small cell lung cancer (NSCLC). In spite of recent regulatory approval of several immunotherapy (IO) drugs, the objective response rate of these drugs is modest (~20%) at best. The complex nature of the host immune response makes tissue based biomarker development for IO response assessment challenging. Consequently, there is an urgent and critical unmet need to develop accurate, validated biomarkers to predict which NSCLC patients will

benefit from IO. Previous research has shown that the morphology of the tumor feeding vessels plays a role in cancer aggressiveness as well as therapeutic refractoriness. Post-treatment tumors show significant improvement in vessel tortuosity abnormalities when compared before therapy initiation. Hence, we sought to evaluate whether computer extracted measurements of fractal features of nodule associated vessel morphology on baseline CT scans in NSCLC patients treated with Nivolumab could distinguish between patients who did and did not respond to the PD-1 inhibitor.

Methods

Our study comprised non-contrast CT scans of 61 patients obtained retrospectively from the Cleveland Clinic, including 31 patients who responded to Nivolumab and 30 non-responders. Patients who did not receive Nivolumab after 2 cycles due to lack of response or progression as per RECIST were classified as 'non-responders', patients who had radiological response or stable disease as per RECIST were classified as 'responders'. From nodule annotations provided by a trained radiologist, a region-growing algorithm was used to segment the surrounding vasculature (Figure1A). A set of 12 vessel fractal radiomic (VFR) measurements pertaining to the fractal analysis, the state space reconstruction and Lyapunov exponent were extracted from each nodule associated vasculature. A Naive Bayes classifier was then used, in a 3-fold cross-validation setting through 200 iterations, to construct a classifier to identify which patients respond to nivolumab therapy.

Results

VFR features (Figure1B) were found to distinguish responders from non-responders to Nivolumab with an AUC=0.73±0.08 . Statistically significant difference was observed for two VFR features between responders and non-responders (p<0.009).

Conclusions

VFR were able to distinguish responders from non-responders for patients with NSCLC and treated with Nivolumab. The VFR could potentially serve as a predictive tool for response assessment for immune checkpoint inhibitors and enable selection of NSCLC patients who will benefit from IO; paving the way for design of more rational clinical trials with combination of IO agents.

Ethics Approval

The study protocol was approved under University Hospitals (UH) IRB 02-13-42C.

Figure 1.

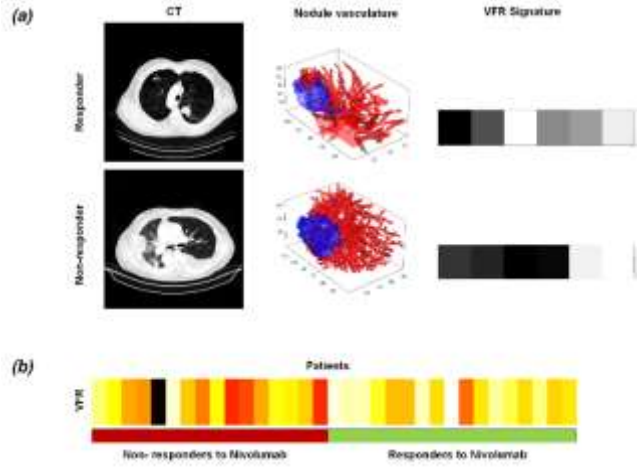

P427

Novel immune competent murine glioblastoma models derived from Nestin-CreER^{T2} Quaking$^{L/L}$; P53$^{L/L}$; PTEN$^{L/L}$ mice

Chao-Hsien Chen, MD[1], Renee Chin, MS[1], Genevieve Hartley, PhD[1], Takashi Shingu, PhD[2], David Hong, MD[1], Jian Hu, PhD[1], Michael A. Curran, PhD[1]

[1]The University of Texas MD Anderson Cancer Center, Houston, TX, USA
[2]University of Texas MD Anderson Cancer Center, Houston, TX, USA

Background

Despite the success of immunotherapy in several cancers, antibody blockade of the immune checkpoint receptor PD-1 failed to improve the survival of recurrent glioblastoma multiforme (GBM) patients [1]. In contrast to this clinical reality, the widely used immunocompetent mouse model of GBM, GL261, is highly immunogenic and readily cured by T-cell checkpoint blockade therapy [2]. The resulting inability to model the immunotherapeutic sensitivity of human GBM preclinically prevents effective translation of murine observations to clinical therapies. Quaking (QKI) is a GBM tumor suppressor gene which is deleted, mutated or downregulated in the majority of human GBM [3,4], the expression level of which strongly correlates with patient survival [5]. We describe novel murine immunocompetent glioblastoma stem cell (GSC) lines derived from Nestin-CreER^{T2} Quaking (QKI)$^{L/L}$; P53$^{L/L}$; PTEN$^{L/L}$ (QPP) mice [5] and determine their sensitivities to immunotherapies.

Methods

We selected four lines, namely QPP4, 5, 7 and 8, after validation of their engraftment in C57BL6/J mice. The immunotherapeutic sensitivities in response to systemic CTLA-4 and PD-1 blockade therapies were determined by tumor growth kinetics and survival. The tumor microenvironment (TME) was evaluated by flow cytometry analysis.

Results

All four QPP lines express GSC markers, such as CD171 and α2β5, but lack PD-L1 or PD-L2 expression *in vitro* and *in vivo*, excepting limited PD-L1 expression by QPP7 *in vivo*. This fits the observation that only a small proportion of human GBM expresses PD-L1 [6]. These QPPs have distinct sensitivities to systemic checkpoint blockade in different niches. Subcutaneously, QPP4, 5 and 8 are sensitive to CTLA-4 blockade, and QPP7 is sensitive to both PD-1 and CTLA-4 blockades. In the brain, QPP5 and 7 remain sensitive to CTLA-4 blockade (n= 8-15, p<0.05), while QPP4 and 8 resist both PD-1 and CTLA-4 blockades (n= 9-15, p>0.05) (Figure 1). Preliminary analysis of the orthotopic TME of the checkpoint-resistant QPP8 line reveals no significant change in CD8 T cells, regulatory CD4 T cells (Treg), myeloid-derived suppressor cells (MDSCs), tumor associated macrophages (TAMs) and microglia infiltration, or CD8/Treg and CD8/MDSCs ratios with either CTLA-4 or PD-1 blockade (n=3-5). PD-L1 expression on monocytic MDSCs, TAMs and microglia in the PD-1 or CTLA-4 blockade group are significantly increased (p<0.05) (Figure 2), however, which could reveal the origins of the prognostic value of the PD-1/PD-L1 axis in human GBM [7].

Conclusions

The distinct checkpoint blockade sensitivities of QPP lines could fill the critical need for preclinical GBM models suitable for evaluating immunotherapeutics.

References

1. Reardon DA, Omuro A, Brandes AA, Rieger J, Wick A, Sepulveda J, Phuphanich S, de Souza P, Ahluwalia MS, Lim M, Vlahovic G, Sampson J OS10.3 Randomized phase 3 study evaluating the efficacy and safety of nivolumab vs bevacizumab in patients with recurrent glioblastoma: CheckMate 143. Neuro-Oncology. 2017; 19: iii21-iii21.

2. Reardon DA, Gokhale PC, Klein SR, et al. Glioblastoma eradication following immune checkpoint blockade in an orthotopic, immunocompetent model. Cancer Immunol Res. 2016; 4(2):124-135.

3. Hu J, Ho AL, Yuan L, et al. From the cover: neutralization of terminal differentiation in gliomagenesis. Proc Natl Acad Sci U S A. 2013; 110(36):14520-14527.

4. Brennan CW, Verhaak RG, McKenna A, et al. The somatic genomic landscape of glioblastoma. Cell. 2013; 155(2):462-477.

5. Shingu T, Ho AL, Yuan L, et al. Qki deficiency maintains stemness of glioma stem cells in suboptimal environment by downregulating

endolysosomal degradation. Nat Genet. 2017; 49(1):75-86.
6. Hodges TR, Ott M, Xiu J, et al. Mutational burden, immune checkpoint expression, and mismatch repair in glioma: implications for immune checkpoint immunotherapy. Neuro Oncol. 2017; 19(8):1047-1057.
7. Nduom EK, Wei J, Yaghi NK, et al. PD-L1 expression and prognostic impact in glioblastoma. Neuro Oncol. 2016; 18(2):195-205.

Figure 1. Orthotopic survival and immune sensitivities.

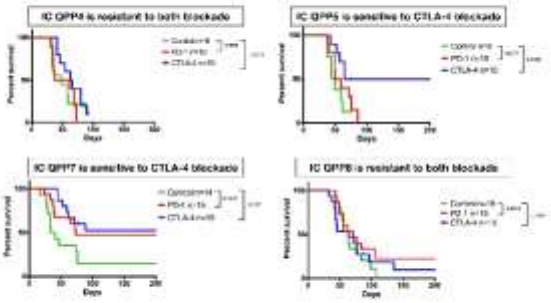

Figure 2. PD-L1 expression on myeloid cells in QPP8 TME.

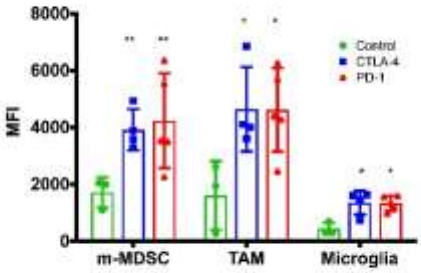

P428

Spatially-resolved, high-plex digital profiling enables characterization of complex immune biology of the colorectal cancer microenvironment

Sarah Church[1], Chris Merritt, PhD[1], Andrew White, BSc[1], Douglas Hinerfeld, PhD[1], Dan Zollinger[1], Giang Ong, MS[1], Kristi Barker, MS[1], Sarah Warren, PhD[1], Joseph Beechem, PhD[1]

[1]*NanoString Technologies, Seattle, WA, USA*

Background

Spatial characterization of the tumor microenvironment (TME) interface between cancer cells, stroma and immune cells is essential for understanding tumor progression and discovering prognostic and predictive biomarkers. However, it has proven difficult to perform such studies in a highly multiplexed manner using limited sample quantity. Digital Spatial Profiling (DSP) has been developed as a research use instrument, software and chemistry for hi-plex profiling of mRNA and protein using an optical-barcode read-out. In this study, microsatellite stable (MSS) or instable (MSI) characterized colorectal tumors were characterized using DSP with 40 proteins or 48 RNA probes to evaluate active and suppressive immune mechanisms in both immune dense regions and tumor versus stroma.

Methods

Sixteen FFPE colorectal tumors that were characterized for Microsatellite stability status were mounted on slides. Tissue sections were stained with a cocktail of pan-cytokeratin, CD45, CD3 and DNA fluorescent markers and 48 RNA probes or 40 antibodies, each conjugated to a UV-photocleavable DNA barcode. Regions of interest (ROI) were delineated using the immunofluorescence followed by UV excitation of the defined ROIs, which releases

the DNA barcodes for downstream quantitation on the NanoString nCounter® platform. Two strategies were used for selecting ROIs, 1) Geometric profiling of CD45-enriched hotspots in the tumor center and invasive margin and 2) Segment profiling of cytokeratin-positive tumor regions compared to cytokeratin-negative regions.

Results
We show that deep profiling of CD45-enriched regions from the invasive margin and tumor center of MSS and MSI tumors have different immunosuppressive and activated immune phenotypes. Comparing colorectal tumors characterized as MSS, DSP was able to differentiate immune hot and cold tumors despite MSS status. Further evaluation using segment profiling of tumors versus stroma also identified specific immune proteins and RNA pathways that were distinctly related to each compartment and were different between MSI and MSS tumors.

Conclusions
Our results suggests DSP has the potential to be used to predict patients' response to PD-1 immune checkpoint blockade with greater sensitivity than standard MSS/MSI profiling, and furthermore DSP may allow identification of unique localized immune characteristics that would guide combination therapeutic approaches.

P429

Integrative spatially-resolved, high-plex digital profiling enables characterization of complex immune biology in the tumor microenvironment of mesothelioma

Carmen Ballesteros Merino, PhD[1], Moritz Widmaier, PhD[2], Sarah Church[3], Thomas Herz, PhD[2], Alexei Budco, MSC[2], Dasa Medrikova, PhD[2], Ivan Kanchev, PhD[2], Andrew White, BSc[3], Douglas Hinerfeld, PhD[3], Shawn Jensen, PhD[1], John Handy, MD[1], Rachel Sanborn, MD[1], Carlo Bifulco, MD[1], Sarah Warren, PhD[3], Joseph Beechem, PhD[3], Bernard A. Fox, PhD[1]

[1]*Providence Portland Cancer Center, Portland, OR, USA*
[2]*Definiens, Munich, Germany*
[3]*NanoString Technologies, Seattle, WA, USA*

Background
Malignant mesothelioma is an aggressive cancer with poor prognosis and few effective therapies. Since mesothelioma is derived from the mesothelium of the lung, we hypothesize that immune cells in the tumor microenvironment (TME) may behave differently than other solid tumors. In our previous studies, utilizing multi-plexed immunofluorescence, we did not find immune phenotypes associated with improved patient survival. Here we describe a novel combination of two technologies to spatially characterize the interface between mesothelioma cells, stroma and immune cells in the TME in a high-plex capacity.

Methods
Ten FFPE mesothelioma tumors were characterized by Definiens' Immune-Oncology Profiling (IOP) and NanoString Digital Spatial Profiling (DSP). Three alternating sequential sections were stained with Definiens' IOP (CD8/PD-1/FOXP3, CD68/PD-L1/CD3, Granzyme B). Definiens analysis was combined to identify localization of each marker in the tumor center, invasive margin or stroma. Twelve regions-of-interest (ROIs) were then selected based on the Definiens analysis for high-plex analysis on DSP on the interleaving slide: 4 CD68-enriched, 6 CD8-enriched and 2 CD3-low. For DSP analysis, each slide was stained with a combination of fluorescent-labeled antibodies (pan-cytokeratin, CD3, CD68) and a panel of 38-antibodies each conjugated to a unique UV-photocleavable DNA barcode. ROIs from Definiens' defined analysis were overlayed on DSP fluorescent scans, followed by UV excitation of the defined ROIs, which releases the DNA barcodes for

downstream quantitation on the NanoString nCounter® platform.

Results

We found strong correlation between Definiens and NanoString analysis of T cell and macrophage markers in selected regions. Generally, patients with longer survival (>6 months) had increased density of immune infiltrates including higher density of T cells, T-cell activation markers (PD-1), higher cytokeratin levels and decreased Ki67 in the tumor center and increased tertiary lymphoid structure makers (B cells) in the invasive margin. Furthermore, STING and VISTA were highly expressed across all mesotheliomas. However, the patient with the longest survival (>31 months) expressed an immune-excluded phenotype. Co-localization analysis revealed that high CD68 density was tightly correlated to PD-L1 expression and in at least one case additional suppressive macrophage markers, including CD163 and B7-H3.

Conclusions

Already this small data set demonstrates that integration of two novel high-plex spatial analysis techniques separates distinct immune mechanisms in the TME. Our analysis suggests that macrophages are highly associated with expression of immune-inhibitory signals in mesothelioma. Therefore, we hypothesize that analysis of additional mesotheliomas may guide the development of combination immunotherapy trials that will be effective against this incurable disease.

P430

Radiomic texture features from MR perfusion images predicts pseudoprogression from true progression in glioblastoma patients: A multi-institutional study

Nabil Elshafeey[1], Aikaterini Kotrotsou[1], Srishti Abrol[1], Islam Hassan[1], Ahmed Hassan[1], Kamel El Salek, MD[1], Fanny Moron[2], Meng Law[3], Pascal Zinn[2], Rivka Colen, MD[4]

[1]MD Anderson Cancer Center, Houston, TX, USA
[2]Baylor College of Medicine, Houston, TX, USA
[3]University of Southern California, Los Angeles, CA, USA
[4]The University of Texas, Houston, TX, USA

Background

Pseudoprogression (PsP) is an inflammatory response associated with radiation and necrotic induced changes reflective of treatment, appearing as areas of increased enhancement on postcontrast T1-weighted images. Response assessment criteria, such as RANO, struggle to distinguish between true progression and PsP. Advanced imaging techniques (MR perfusion, MR diffusion) have been proposed as an alternative way of distinguishing between PsP and progressive disease (PD). However, the outcome of such studies underscores the need for novel tools distinguish between these. In this study, we sought to evaluate the utility of radiomic analysis of MR perfusion [Dynamic contrast enhancement (DCE) and Dynamic susceptibility contrast (DSC)] maps in differentiating PsP from PD.

Methods

Patients: A total of 98 patients were included in this multi-institutional IRB-approved study. All had pathological confirmation; 78 patients with PD and 20 patients with PsP. Radiomic Analysis: All patients underwent DSC and DCE perfusion MRI as part of their routine clinical care. Images were analyzed using Nordic ICE 2.3 (NordicNeuroLab); rCBV and Ktrans maps were obtained. Subsequently, an experienced radiologist delineated the entire tumor on DCE and DSC maps using 3D slicer (http://www.slicer.org) (Figure 1). The extracted 3D region-of-interest (ROI) parametric maps were imported in the radiomic pipeline. A total of 475 features (10 histogram-based and 375 higher-order

texture features) were calculated for each parametric map. Statistical Analysis: An advanced feature selection method based on Minimum Redundancy Maximum Relevance (MRMR) was used to analyze the featureset and extract core features. Selected features were used to build a Support Vector Machine (SVM) model for prediction of PD versus PsP. To evaluate the robustness of the estimates made with the SVM models, leave-one-out cross-validation (LOOCV) was conducted. Finally, box plots of the 10 most relevant features and probability maps were calculated.

Results

MRMR identified 50 radiomic features that were further used to build the SVM model. The prediction of progression by LOOCV was significant p-value=0.031. Area under the curve (AUC), sensitivity and specificity were 89.26%, 81.82% and 100% respectively and the most discriminating features were variance and sum entropy (Figure 2). Box plots of the 10 most relevant features are shown in Figure 3.

Conclusions

This study demonstrates that MR perfusion radiomic analysis can discriminate between PsP and PD. Further validation and a comparative study of radiomic analysis of MR perfusion maps and conventional MR images would be valuable to determine which approach is more effective, and the added value in combining the two approaches.

Figure 1.

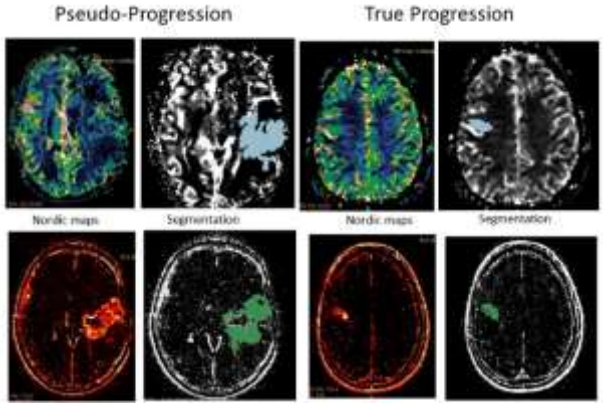

Figure 2.

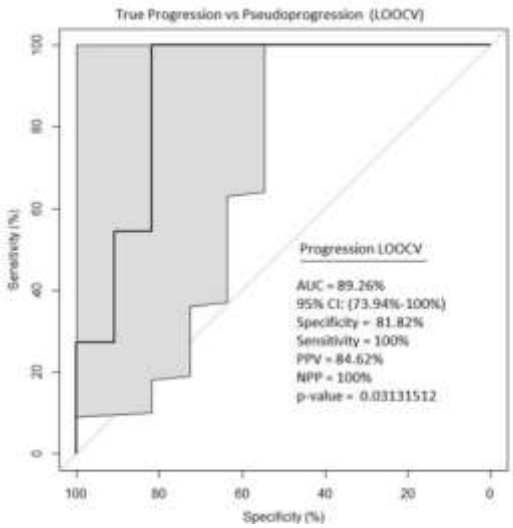

Figure 3.

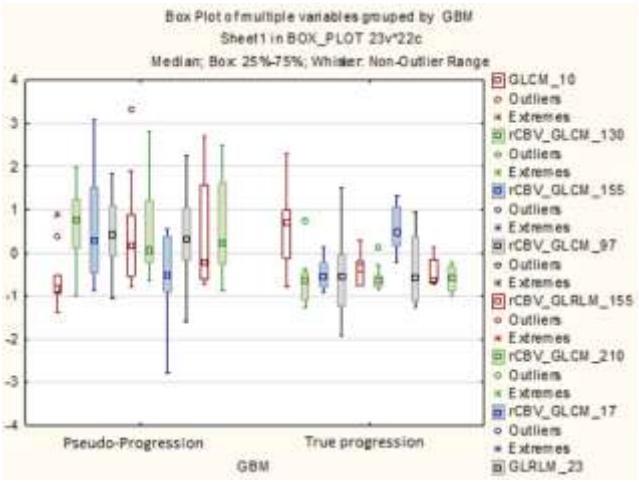

P431

Radiomic Analysis differentiates between True Progression and Pseudo-progression in Glioblastoma patients: A large scale multi-institutional study

Srishti Abrol[1], Aikaterini Kotrotsou[1], Nabil Elshafeey[1], Islam Hassan[1], Ahmed Hassan[1], Tagwa Idris, MD[1], Kamel El Salek, MD[1], Ahmed Elakkad, MD[1], Kristin Alfaro-Munoz[1], Shiao-Pei Weathers[1], Fanny Moron[2], John deGroot[1], Meng Law[3], Rivka Colen, MD[1]

[1]MD Anderson Cancer Center, Houston, TX, USA
[2]Baylor College of Medicine, Houston, TX, USA
[3]University of Southern California, Los Angeles, CA, USA
[4]The University of Texas, Houston, TX, USA

Background

Treatment-related changes can occur as a result of multiple factors; these changes are often difficult to distinguish from true progression (PD) of the tumor using conventional MRI. Treatment-related changes or pseudoprogression (PsP) subsequently subside or stabilize without any further treatment, whereas progressive tumor requires a more aggressive approach. PsP mimics PD radiographically and may potentially alter the physician's judgement. Hence, it can predispose a patient to overtreatment or be categorized as a non-responder and exclude him from clinical trials. Radiomic analysis results in the quantification of grey tone spatial variation thereby providing textural features that characterize the underlying structure of the object under investigation. This study aims at assessing the potential of radiomics to discriminate PsP from PD in glioblastoma (GBM) patients.

Methods

In this multi-institutional study, we evaluated 304 GBM patients retrospectively. All patients showed radiographic worsening in MRI, with/without clinical deterioration, and were evaluated for PD our PSP. 149 patients had histopathological evidence of PD and 27 of PsP. Remaining 128 patients were categorized into PD or PsP based on RANO criteria . Conventional MR images were acquired using typical clinical acquisition parameters. Three tumor phenotypes (ROIs), namely edema/invasion, necrosis, and enhancing tumor, were delineated by an experienced radiologist. A total of 1800 radiomic features were obtained for each patient. Statistical Analysis: An advanced feature selection method based on Minimum Redundancy Maximum Relevance (MRMR) was used to analyze the featureset and extract core features. Selected features were used to build a Support Vector Machine (SVM) model for prediction of PD versus PsP status. To evaluate the robustness of the estimates made with the SVM models, leave-one-out-cross-validation (LOOCV) and a 70-30% split was performed.

Results

Using the MRMR feature selection method, we could identify 100 significant features that were further used to build a SVM model. On LOOCV, the area under curve (AUC) was 90%, with a sensitivity and specificity of 97% and 72% respectively (Figure 3).

Using 70% of the patient data for training and 30% for validation an AUC of 94% was achieved, with sensitivity of 97% and specificity of 75%. Five texture features i.e. energy, cluster shade, sum average, maximum probability and cluster prominence were found to be most predictive of nature of disease progression.

Conclusions

The proposed tool has the potential to advance clinical management strategies. Apart from its non-invasive nature, our methodology doesn't require additional imaging and may act as a complementary tool for the clinicians.

Figure 1.

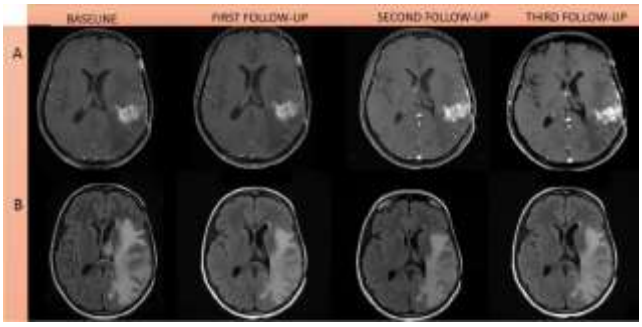

Figure 2.

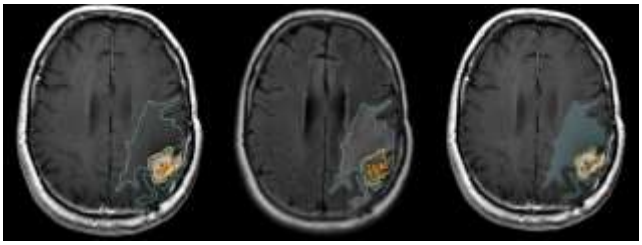

Figure 3.

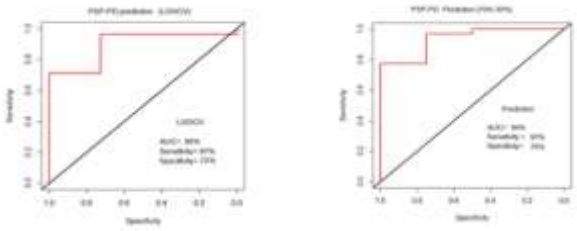

P432

High tumor mutation burden (Hypermutation) in gliomas exhibit a unique predictive radiomic signature

Islam Hassan[1], Aikaterini Kotrotsou[1], Carlos Kamiya Matsuoka[1], Kristin Alfaro-Munoz[1], Nabil Elshafeey[1], Nancy Elshafeey[1], Pascal Zinn[2], John deGroot[1], Rivka Colen, MD[3]

[1]MD Anderson Cancer Center, Houston, TX, USA
[2]Baylor College of Medicine, Houston, TX, USA
[3]The University of Texas, Houston, TX, USA

Background

Increase in tumor mutation burden (TMB) or hypermutation is the excessive accumulation of DNA mutations in cancer cells. Hypermutation was reported in recurrent as well as primary gliomas. Hypermutated gliomas are mostly resistant to alkylating therapies and exhibit a more immunologically reactive microenvironment which makes them a good candidate for immune checkpoint inhibitors. Herein, we sought to use MRI radiomics for prediction of high TMB (hypermutation) in primary and recurrent gliomas.

Methods

In this IRB-approved retrospective study, we analyzed 101 patients with primary gliomas from the University of Texas MD Anderson Cancer Center. Next generation sequencing (NGS) platforms (T200 and Foundation 1) were used to determine the Mutation burden status in post-biopsy (stereotactic/excisional). Patients were dichotomized based on their mutation burden; 77 Non-hypermutated (<30 mutations) and 24 hypermutated (>=30 mutations or <30 with MMR gene or POLE/POLD gene mutations). Radiomic analysis was performed on the conventional MR images (FLAIR and T1 post-contrast) obtained prior to tumor tissue surgical sampling; and rotation-invariant radiomic

features were extracted using: (i) the first-order histogram and (ii) grey level co-occurrence matrix. Then, we performed Logistic regression modelling using LASSO regularization method (Least Absolute Shrinkage and Selection Operator) to select best features from the overall features in the dataset. ROC analysis and a 50-50 split for training and testing, were used to assess the performance of logistic regression classifier and AUC, Sensitivity, Specificity, and p-value were obtained. (Figure 1)

Results

LASSO regularization (alpha = 1) was performed with all the 4880 features for feature selection and 40 most prominent features were selected for logistic regression modelling. Our entire dataset ROC analysis showed an accuracy of 100%, sensitivity of 100% and specificity of 100% with p-value of 1.256-12, while our 70-30 split ROC analysis showed an accuracy of 96.7%, sensitivity of 85% and specificity of 100% and a p-value of 0.003; Our 50-50 split ROC analysis showed an accuracy of 94%, sensitivity of 75%, and specificity of 100% and a p-value of 0.0008. (Figure 2, 3, 4)

Conclusions

An MRI-radiomic phenotype is predictive of the increase in TMB (Hypermutation) in both primary and recurrent gliomas.

Figure 1.

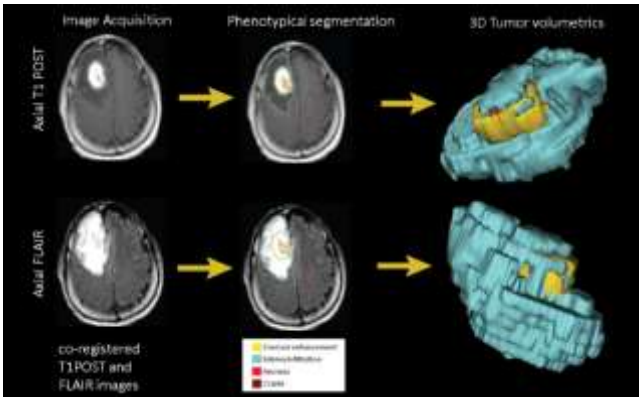

Figure 2.

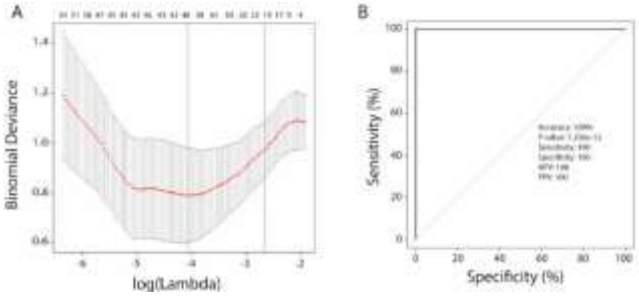

Figure 3.

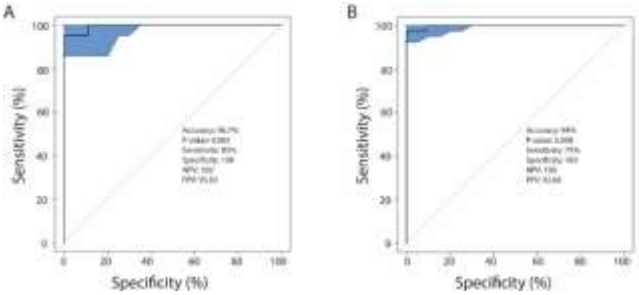

Figure 4.

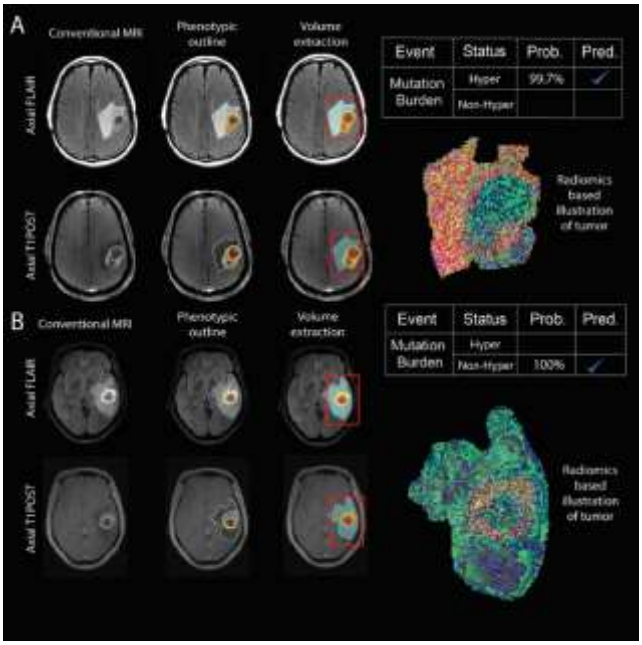

P433

Advances in multiplex fluorescence immunohistochemistry: 9 color imaging; whole slide multispectral

Carla Coltharp, PhD[1], Yi Zheng, PhD[1], Rachel Schaefer[1], Ryan Dilworth, PhD[1], Linying Liu[1], Chichung Wang[1], Kristin Roman, MS[1], Clifford Hoyt, MS[1], Peter Miller, MS[1]

[1]PerkinElmer, Inc., Hopkinton, MA, USA

Background

We describe two advances in multispectral fluorescence immunohistochemistry, a powerful tool for quantifying interactions within the tumor microenvironment. First, a fully-automated 8-plex assay plus DAPI counterstain on the same tissue section. Second, a novel scanning method that produces a multispectral whole slide scan of 6 markers plus DAPI counterstain in ~6 minutes (1x1.5 cm tissue section).

Methods

FFPE primary tumors were immunostained using Opal™ reagents manually or on a Leica BOND RX™. Imagery was acquired on a Vectra Polaris® automated imaging system and analyzed with inForm® and MATLAB® software.

Results

Two new Opal™ reagents (Opal 480 and Opal 780) were combined with currently available Opal 7-color kits to stain and distinguish 8 markers plus DAPI when imaged on the Vectra Polaris®.Figure 1 shows a 9-color panel on lung cancer: CD20 (Opal 480), PD-L1 (Opal 520), CD8 (Opal 540), FoxP3 (Opal 570), CD68 (Opal 620), PD-1 (Opal 650), Ki67 (Opal 690), and PanCK (Opal 780). Colors assigned to each marker, and associated component planes, are shown in Figure 1B.These 8 markers combine to generate more than 20 phenotypes relevant to immuno-oncology that can be studied in relation to local PD-L1 expression and proliferation state (Ki67+/-). For example, while the density of CD8+ cells was 8-fold lower in tumor than stroma (150 vs 1200 cells/mm^2), those CD8+ cells were >4x more likely to be proliferating in tumor vs stroma (28% vs. 6%).To interrogate interactions across a whole section, we additionally developed a multispectral whole-slide scanning method, demonstrated on lung cancer using a subset of 7 stains from the 9-color panel above. Phenotype and expression-level assessments of the unmixed whole slide scan describe distribution patterns of immune cells across the entire section.In measurements of crosstalk and dynamic range, whole-slide multispectral scanning performed comparably to established field-based multispectral imaging, and outperformed conventional fluorescence scanning by reducing crosstalk from up to 8% to under 2% (typically <0.5%) and extending the dynamic range of some channels by more than 50-fold.

Conclusions

We introduce a 9-color fIHC assay that distinguishes 8 markers plus DAPI counterstain on the same tissue section, increasing the depth of cellular interactions that can be studied within the tumor microenvironment.Additionally, we introduce a whole slide multispectral imaging method that provides rich quantitation of interactions among 6 markers at length scales spanning from cell biology to tumor physiology.

Figure 1.

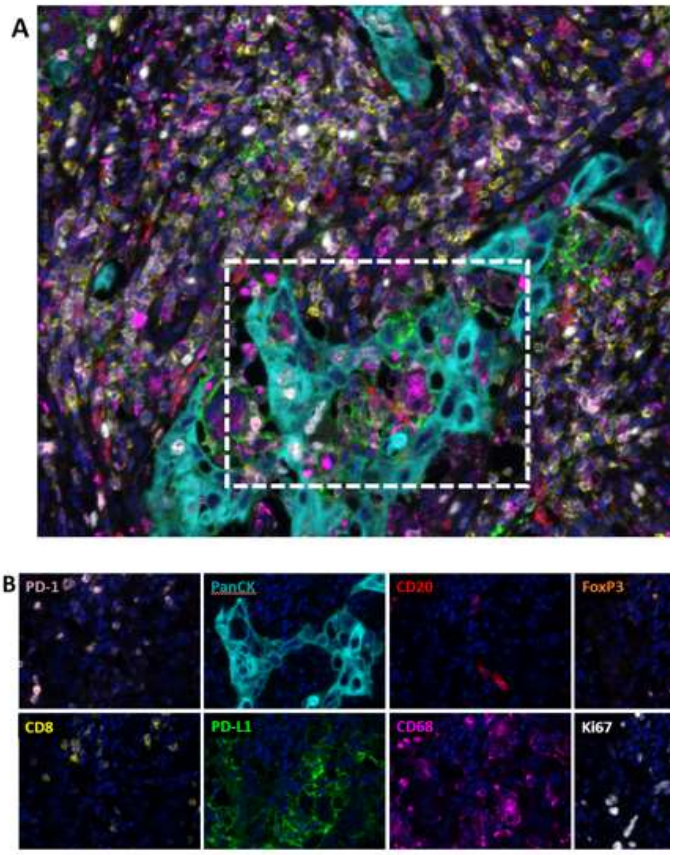

P434

Mathematical modeling of CAR T cell therapy outcomes to develop design specifications for CAR T cell engineering

Amritava Das, PhD[1], Rachel Grosser, undergraduate[2], Ambar Velazquez Albino, BS Student[3], Krishanu Saha[2], Christian M. Capitini, MD[2]

[1]*Morgridge Institutes for Research, Madison, WI, USA*
[2]*University of Wisconsin - Madison, Madison, WI, USA*
[3]*University of Puerto Rico - Mayaguez, Mayaguez, PR, USA*
[4]*Morgridge Institute for Research, Madison, WI, USA*

Background

Chimeric antigen receptor (CAR) T cell therapy has demonstrated success in clinical trials [1], and two such therapies have now been approved within the USA [2]. Due to the heterogeneity of apheresis products from heavily treated cancer patients, no algorithms exist to predict the efficacy of manufactured CAR T cell products. CAR T cells are living drugs, that are capable of division, anti-tumor cytotoxicity and cytokine secretion post infusion. Based on previous models of virus-T cell interaction [3], we developed new models to estimate post-infusion CAR T cell division and cytotoxicity. Simulation results reveal important characteristics when elite populations of CAR T cells are present in the pool of infused CAR T cells.

Methods

Models were implemented in COPASI [4], a biochemical network simulation platform. Patient CAR T cell performance data extracted from previously published studies using WebPlotDigitizer [5]. Fitting of model parameters to published patient data and model inference performed using ABC-SysBio [6], a python-based toolkit implementing Approximate Bayesian Computation. Post-processing of outputs from COPASI and ABC-SysBio was performed on MATLAB.

Results

Any of the models developed (selection shown in Figure 1) could be fit to patient data, and ABC-SysBio can be implemented to select between the models given patient data. Model presented in figure 1A was used to determine the effects of having a large population of CAR T cells which can only undergo one cell division and a smaller elite population (1/1000th of maximum at infusion) capable of unlimited expansion. Broadly, the rates of division of high performance clonal CAR T cells (at most 4 h doubling time), and the rates of memory formation of CAR T cells (at least 0.383/day) were found to most significantly impact tumor clearance, while the

cytotoxicity of the CAR T cells (ranging from 2 – 16 /day/cell) did not significantly impact tumor clearance in the mathematical models (Figure 2).

Conclusions

Surprisingly memory formation is more associated with complete remission than cytotoxicity and mirrors previous findings that correlate therapeutic success with memory formation [7]. Estimation of the parameter values for number of CAR T cell divisions, rates of division, memory formation, memory reactivation, CAR T cell depletion (exhaustion and non-exhaustion induced death) and anti-tumor cytotoxicity can be useful in determining the design specifications of successful CAR T cell therapy administrations across various clinical trials. Extrapolation of this model in a prospective setting will be needed for further validation.

References

1. Gill S, Maus MV,Porter DL. Chimeric antigen receptor T cell therapy: 25years in the making. Blood Rev. 2016; 30(3): 157-67.
2. June, CH, Sadelain M. Chimeric Antigen Receptor Therapy. N Engl J Med. 2018; 379(1): 64-73.
3. Wodarz D,Thomsen AR. Effect of the CTL proliferation program on virus dynamics. International Immunology. 2018; 17(9): 1269-1276.
4. Hoops S, et al. COPASI--a COmplex PAthway SImulator. Bioinformatics. 2006; 22(24): 3067-74.
5. Burda, BU, et al. Estimating data from figures with a Web-based program: Considerations for a systematic review. Res Synth Methods. 2017; 8(3): 258-262.
6. Liepe J, et al. ABC-SysBio--approximate Bayesian computation in Python with GPU support. Bioinformatics. 2010; 26(14): 1797-9.
7. Fraietta JA, et al. Determinants of response and resistance to CD19 chimeric antigen receptor (CAR) T cell therapy of chronic lymphocytic leukemia. Nat Med. 2018; 24(5): 563-571.

Figure 1. Mathematical modeling frameworks developed

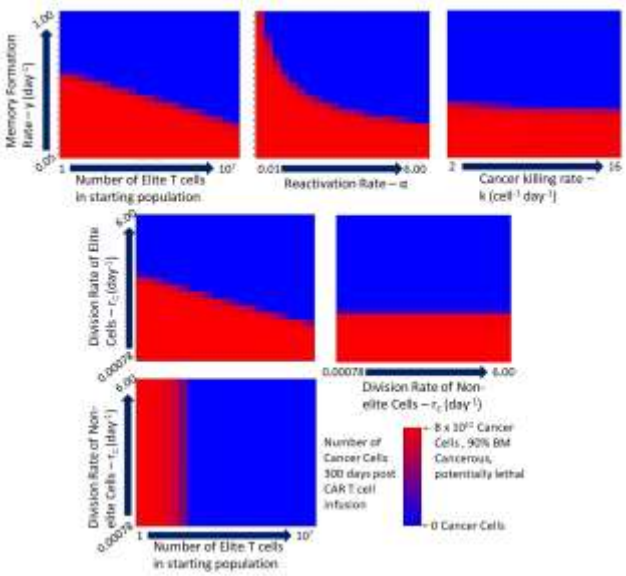

Figure 2: Heatmaps indicating the number of cancer cells

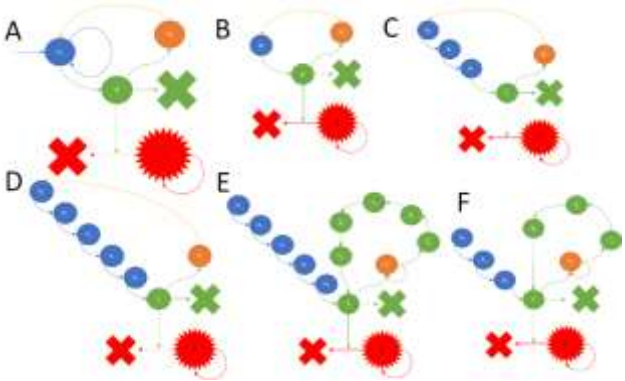

P435

Image-based analysis of the myeloid cell landscape in the 3D co-culture with tumor cells

Gera Goverse, PhD[1], Kuan Yan, PhD[1], Lars Geulen[2], Paul Vink, BS[2], Leo Price[1], Lidia Daszkiewicz, PhD[1]

[1]*OcellO B.V., Leiden, Netherlands*
[2]*Aduro Biotech, Oss, Netherlands*

Background
The myeloid cell compartment plays an important role in anti-tumor immune responses and represents a heterogeneous population with both cancer-promoting and cancer-restraining actions. Unleashing the full potential of cancer immunotherapies requires an understanding of the cellular mechanisms that govern these opposite actions. To date, high throughput relevant preclinical models for dissecting the interactions between different cellular players in the tumor microenvironment are lacking. Previously we have shown that our 3D image-based co-culture system allows assessing efficacy of immune modulators to enhance PBMC infiltration and tumoroid killing. Our main goal was to improve this model by incorporating a more complete human immune system. To do that we first generated diverse myeloid populations in a 3D environment and then used our image-based platform to describe the different subsets. The image analysis software was trained on a set of features that reproducibly allowed discrimination between undifferentiated monocytes, M1 and M2 macrophages and dendritic cells. The different myeloid subsets were next co-cultured with tumor cells to analyze the complex cellular interplay of the TME.

Methods
Different myeloid populations were generated in 3D from monocytes derived from healthy donors PBMCs. Polarized M1 and M2 macrophages, DCs and undifferentiated monocytes were then co-cultured in 3D with SKBR3 tumor cells or 3D tumoroids derived from this cell line. The cellular interactions were visualized using high-content microscopy and quantified with multiparametric morphometric analysis with OMinerTM software.

Results
3D image analysis enabled the discrimination of immune-tumor cell interactions and revealed the effect of myeloid cells on tumor growth in co-culture. Our approach also enables the analysis of how tumor-driven mechanisms regulate myeloid cell differentiation and contribute to the immunosuppressive microenvironment. These results provide a means to elucidate the bi-directional interplay between tumor and immune cells and allows for analysis of functional reprograming of the suppressive population towards a M1 phenotype induced by drug candidates.

Conclusions
The 3D assay presented here enables visualization and measurement of effects of immunotherapies on cells that engage in a more physiologically relevant spatial setting than when culturing them in traditional 2D cultures. Using morphological measurements different myeloid cell subsets can be distinguished, which offers a very attractive alternative for complex and labor-intensive phenotyping based on markers expression and cytokine release profiling. The ultimate goal is to develop a highly sophisticated platform for testing cancer immunotherapies that combines the complexity of the TME and the robustness of a high throughput screening platform.

P436

Image analysis simulations of needle biopsy tumor specimens to investigate CD8+ TIL heterogeneity

Thomas Herz, PhD[1], Victor Matvienko[1], Tobias Wiestler, PhD[1], Rene Korn, PhD[1], Keith Steele, DVM, PhD[2]

[1]Definiens AG, Munich, Germany
[2]MedImmune, Gaithersburg, MD, USA

Background
Core needle biopsies are used to histologically assess tumors when surgical excision is impractical. Such small samples may not be representative given the known heterogeneity of immune cell distribution,

including CD8+ tumor infiltrating lymphocytes (TILs)[1].

Methods

Initially, 20 immunolabeled slides from purchased non-squamous NSCLC tumor resections were scanned and tumor region was manually annotated[1]. CD8(+) TILs were detected using Definiens Developer XD™ software[1,2]. Needle biopsies were simulated using an elliptical shape, with multiple iterations applied by varying the size, angle and positioning of that ellipse across the full resection using Python programming language[3], totaling in 24,200 single needle simulations per case. CD8(+) TIL density was determined for the tumor region contained within each simulated portion. Using the statistical software R[4], individual cores were compared to other cores in each sample, to the full tumor region and across all 20 cases.

Results

The heterogeneity of the CD8(+) TIL distribution is very well reflected in the statistical analysis of the number of CD8(+) TILs actually found within the needle biopsy to the expected number, based on the size of the needle ellipse and full slide CD8(+) TIL density. Even in cases with generally high correlation, a single biopsy location with changing the needle size or the angular component of the needle direction only can already produce a set of non-representative CD8(+) TIL densities. In a about 15% of all simulated cores, no CD8(+) TIL was found in the tumor region, spanning all dimensions of variation used in the simulation equally as well as cases.

Conclusions

One needle biopsy insufficiently represents the CD8+ TIL density of resected non-squamous NSCLC. Determining a clinically-feasible number of cores to accurately assess CD8 requires further study. Systematic measurement of sampling error should be extended to other markers of the immune response to cancer whose expression is known to be heterogenous, such as PD-L1.

References

1. Steele K, Tan TH, Korn R. Measuring multiple parameters of CD8+ tumor-infiltrating lymphocytes in human cancers by image analysis. J Immunother Cancer 2018;6:202. Baatz M, Zimmermann J, Blackmore CG. Automated analysis and detailed quantification of biomedical images using Definiens Cognition Network Technology®. Combinatorial Chemistry & High Throughput Screening 2009;12:908–163. Python Software Foundation [https://www.python.org]4. R Core Team (2017). R: A language and environment for statistical computing. R Foundation for Statistical Computing, Vienna, Austria. [https://www.R-project.org]

P437

In vivo synergistic effect of checkpoint blockade and radiation therapy against chordomas in a humanized mouse model

Wataru Ishida, MD[1], Kyle McCormick, BA[2], Aayushi Mahajan, MS[2], Eric Feldstein, BS[2], Michael Lim, MD[1], Jeffrey Bruce[2], Peter Canoll, MD PhD[2], Sheng-fu L. Lo, M.D.[1]

[1]Johns Hopkins University, Baltimore, MD, USA
[2]Columbia University Medical Center, New York, NY, USA

Background

It has been a challenge to apply immunotherapy (IT) to patients with chordomas, due to lack of clinically-translatable *in vivo* models. Currently, there are no well-established murine chordoma cell lines that can be injected to syngeneic mice or no transgenic mouse models that develop chordomas spontaneously, which would allow us to study the interaction between murine chordomas and murine immune cells. Hence, we aimed to develop a

humanized mouse model, where human immune cells are engrafted into immunodeficient mice,[1,2] to overcome this limitation by studying the interaction between human immune system and human chordomas. We also sought to utilize it to study synergistic effect between IT and radiation therapy (RT) against chordoma.

Methods

Fifteen 10-12-week-old NSG mice were sub-lethally (1.5Gy) irradiated and then implanted with fetal thymic tissue and CD34+ stem cells that had been harvested from a fetus, whose HLA-types were partially-matched with those of the U-CH1 chordoma cell line. Reconstitution of immune cells in NSG mice was confirmed 8 weeks post-transplantation and then each animal (15 humanized NSG mice and 12 naïve NSG mice) was injected with U-CH1 cell suspension bilaterally and subcutaneously. Next, they were treated for 4 weeks as follows: A) control, isotype antibodies (Abs) injection (n=3), B) anti-human-PD-1 Abs (n=4), C) RT + isotype Abs (n=3, unilaterally to the left-sided tumor, 8Gy x 4), D) anti-human-PD-1 Abs and RT (n=5), E) naïve NSG mice (n=6, without the engraftment of human immune cells) + isotype, and F) naïve NSG mice (n=6) + anti-human-PD-1 Abs. During and after the treatment, anti-tumor activities were monitored via tumor size, flow cytometry, qRT-PCR, and immunohistochemistry.

Results

One week after the treatment, on the irradiated side, (D) demonstrated lowest tumor volume (Figure 1), highest number of human PBMCs, highest % of CD8+ human T cells, highest % of CD45RO+CD4+ human (memory) T cells, and lowest % of PD-1+CD8+ human T cells in the tumors via flow cytometry (Figure 2), and highest IFN-gamma in the tumors via qRT-PCR, compared to the other five groups with statistical significance. On the non-irradiated side, similarly D) had the smallest tumor compared to the others (P=0.09).

Conclusions

We demonstrated that this humanized mouse model could be a revolutionary platform to investigate IT against rare cancers such as chordomas, where murine equivalent cell lines are currently unavailable. The direct synergistic effect between IT and RT against chordoma as well as the potential abscopal effect was observed.

Acknowledgements

We would like to thank all members of Herbert Irving Comprehensive Cancer Center at Columbia University Medical Center for generous support and its shared resource as well as CCTI, especially Drs. Hui Wang and Yong-Guang Yang at the CCTI humanized mouse core as well as Dr. Siu-Hong Ho, the director of the CCTI flow cytometry core and Assistant Professor of Medical Sciences. We also would like to thank The Sidney Kimmel Comprehensive Cancer Center at Johns Hopkins University and its oncology shared resources, particularly Drs. Alan Meeker and Sujayita Roy. These studies used the resources of the Herbert Irving Comprehensive Cancer Center Flow Cytometry Shared Resources funded in part through Center Grant P30CA013696. Research reported in this publication was performed also in the CCTI Flow Cytometry Core, supported in part by the Office of the Director, National Institutes of Health under awards S10RR027050. The content is solely the responsibility of the authors and does not necessarily represent the official views of the National Institutes of Health.

References

1. Kalscheuer H, Danzl N, Onoe T, et al. A model for personalized in vivo analysis of human immune responsiveness. Sci Transl Med. 2012;4(125):125ra130.2. Zitvogel L, Pitt JM, Daillere R, Smyth MJ, Kroemer G. Mouse models in oncoimmunology. Nat Rev Cancer. 2016

Ethics Approval
This study was approved by Columbia IACUC, protocol number AAAQ8458.

Figure 1.

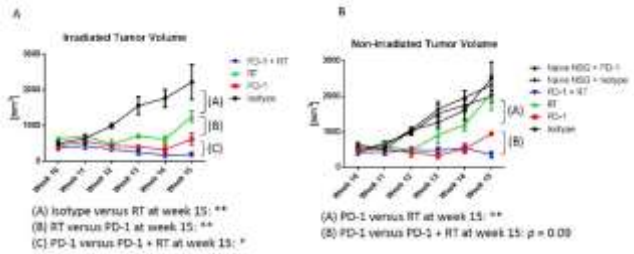

Figure 2.

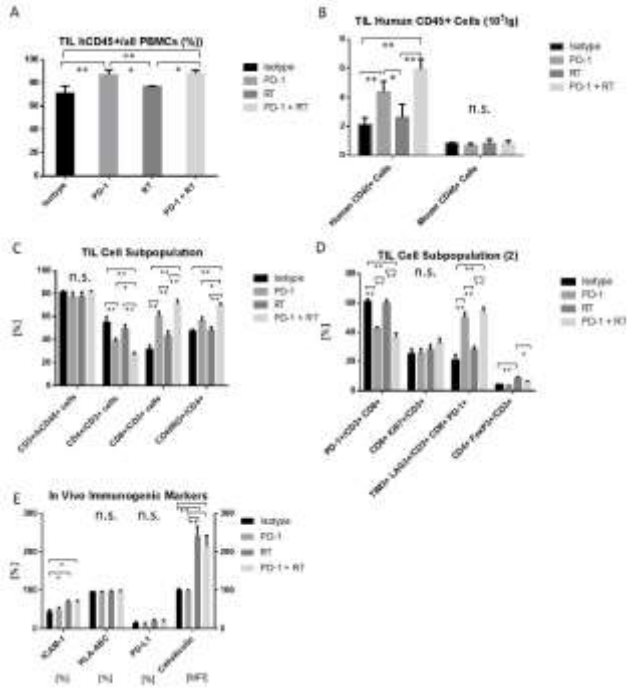

P438

Effect of CD3 affinity and normal tissue expression on the biodistribution and tumor targeting of MUC16xCD3 bispecific antibodies in MUC16 and CD3 humanized mice

Marcus Kelly, PhD[1], Alison Crawford, PhD[1], Jason Giurleo, PhD[1], Richard Tavaré, PhD[1], Sosina Makonnen[1], Carlos Hickey[1], Makenzie Danton[1], Cody Arnold[1], Lauric Haber[1], Eric Smith, PhD[1], Dangshe Ma[1], William Olson, PhD[1], Gavin Thurston, PhD[1], Jessica Kirshner, PhD[1]

[1]*Regeneron Pharmaceuticals Inc., Tarrytown, NY, USA*

Background
The tumor associated glycoprotein MUC16 is highly expressed in ovarian cancer with limited normal tissue expression, making it a suitable target for the development of CD3 binding T-cell engaging bispecific antibodies. Here we used non-invasive immuno-PET imaging as a powerful tool to determine the impact of each antigen binding arm on bio-distribution of MUC16-CD3 bispecific antibodies in mice. To dissect the role of CD3 affinity on antibody distribution, we assessed two bispecifics with varying CD3 affinity; MUC16-$CD3_{low}$ and MUC16-$CD3_{high}$, alongside the bivalent parental MUC16 antibody.

Methods
Antibodies were radiolabeled with positron emitting radionuclide Zirconium-89 (^{89}Zr) using the chelator deferoxamine (DFO) and demonstrated high radiochemical purity and immunoreactivity. Initial imaging and biodistribution studies were performed in SCID mice bearing MUC16+ OVCAR3 ovarian tumor xenografts to validate the MUC16 binding arm of the antibodies. Localization of ^{89}Zr-MUC16-$CD3_{low}$ and ^{89}Zr-MUC16-$CD3_{high}$ was next measured in tumor-free MUC16 and CD3 double humanized immunocompetent mice. A subsequent study assessed blocking CD3-dependent localization of ^{89}Zr-MUC16-$CD3_{high}$ by a control CD3 antibody. Parental ^{89}Zr-MUC16-MUC16 antibody was assessed in matched humanized and normal mice to determine localization to MUC16 expressing normal tissues. Lastly, the uptake of ^{89}Zr-MUC16-$CD3_{low}$ or ^{89}Zr-MUC16-$CD3_{high}$ to ID8/VEGF/hMUC16 tumors was assessed in the double humanized mice.

Results

Immuno-PET imaging of ^{89}Zr-MUC16-CD3$_{low}$, ^{89}Zr-MUC16-CD3$_{high}$ and ^{89}Zr-MUC16-MUC16 all demonstrated high and specific targeting to OVCAR3 xenografts (~70%ID/g). In the MUC16 and CD3 humanized mice, very high localization of ^{89}Zr-MUC16-CD3$_{high}$ to CD3+ lymphoid tissues (spleen and lymph nodes) was observed. Relative ^{89}Zr-MUC16-CD3$_{low}$ uptake in lymphoid tissues was greatly reduced. Conversely, blood levels of ^{89}Zr-MUC16-CD3$_{high}$ were lower than ^{89}Zr-MUC16-CD3$_{low}$, resulting in higher tissue:blood ratios by ^{89}Zr-MUC16-CD3$_{high}$. Blocking with control CD3 bispecific significantly reduced localization of ^{89}Zr- MUC16-CD3$_{high}$ to lymphoid tissues. Specific uptake of ^{89}Zr-MUC16-MUC16 in normal tissues was not observed. ^{89}Zr-MUC16-CD3$_{low}$ and ^{89}Zr-MUC16-CD3$_{high}$ both showed significant uptake (50-60%ID/g) in ID8/VEGF/hMUC16 tumors. Tumor uptake between the antibodies was generally not significantly different despite the high lymphoid uptake of ^{89}Zr-MUC16-CD3$_{high}$.

Conclusions

^{89}Zr-MUC16-CD3$_{low}$ and ^{89}Zr-MUC16-CD3$_{high}$ demonstrated specific localization to MUC16+ tumors and CD3+ lymphoid tissues, with lymphoid distribution correlating to relative CD3 affinity. Both MUC16-CD3 bispecifics demonstrated clear tumor localization in the presence of CD3+ tissues. This work demonstrates that immuno-PET is an ideal technology to monitor bispecific localization in vivo. Further studies may investigate any correlation between antibody biodistribution as monitored by immuno-PET and toxicity or efficacy observed during the optimization of these promising therapeutics.

P439

A novel high-throughput, high-content real-time imaging platform to assess immunogenic cell killing activity of immunotherapeutic agents using patient-derived tumor samples.

Jenny Kreahling, PhD[1], Melanie Mediavilla-Varela, PhD[1], Melba Marie Page, PhD[1], Soner Altiok, MD, PhD[1]

[1]*Nilogen Oncosystems, Tampa, FL, USA*

Background

Immuno-oncology has revolutionized cancer care for many cancer types, however, the development of novel immunotherapeutics still faces many challenges due to lack of drug screening platforms that represent the complexity of the tumor microenvironment. Conventional cytotoxicity assays, such as chromium 51 and LDH release are limited in providing clinically relevant data about immunogenic cell death. The goal of this study was to develop an integrated confocal-based high-throughput, high-content real-time imaging platform to assess immunogenic cell killing activity of novel immunotherapeutic agents and to develop rational drug combinations using patient-derived tumor samples.

Methods

All patient tumor samples were obtained with patient consent and relevant IRB approval. For the confocal imaging platform, unpropagated 3D tumoroids measuring 100-150 micron in size were prepared from fresh tumor samples of non-small cell lung cancer using a proprietary technology developed at Nilogen Oncosystems. Cell-match studies utilized autologous patient-derived cell lines that were isolated and propagated from each patient's tumor.

Results

In Cell-match studies, tumor cells and tumor infiltrating lymphocytes (TILs) were labeled with different cell tracker fluorescent dyes to monitor cell movements and locations. For 3D tumoroid assays samples were pre-labeled with proprietary fluorogenic markers to identify live and dead tumor cells. After treatment with different immune-

stimulatory agents, real-time confocal imaging analysis was performed to assess apoptotic tumor cell death which was evaluated via the detection of changes in the permeability of cell membranes and activation of caspase 3 pathway. Comprehensive flow cytometry analysis was performed to corroborate confocal imaging findings on immunogenic tumor cell death (LIVE/DEAD viability markers and cleaved caspase 3) and TIL activation (CD25, CD69, Ki-67 and granzyme expression in CD4 and CD8 positive lymphocytes). A custom image analysis algorithm was developed for the collection of data in a structurally relevant environment on quantification of marker-specific cell number, cell viability and apoptosis in addition to structural and functional analysis of cells in intact 3D tumoroids.

Conclusions

The confocal-based high-throughput and high-content real-time imaging platform described here is physiologically relevant and allows rapid screening of multiple drugs and drug combinations based on their immunogenic cell killing activity in a cost-effective manner to accelerate drug discovery.

P440

Open-source digital image analysis of whole-slide multiplex immunohistochemistry

Nikhil Lonberg, HSDG[1], Carmen Ballesteros Merino, PhD[1], Shawn Jensen, PhD[1], Bernard Fox, PhD

[1]*Robert W Franz Cancer Center, Earle A Chiles Research Institute, Portland, OR, USA*

Background

Successful digital image analysis (DIA) of cancer tissue is accurate and reproducible. These points of emphasis have brought procedures like the tissue microarray (TMA) and hotspot regions of interest (ROI) under scrutiny. The nature in which a pathologist selects TMAs and ROIs is conducive to bias. Whole Slide Imaging (WSI) offers a solution in its unbiased region selection and consideration of a larger tissue sample. However, options for softwares that can handle such large throughput are scarce. Additionally, while multiplex immunohistochemistry (mIHC) is becoming popular [1], documentation of its digital analysis tools remains minimal [2]. The combination of these procedures potentiates a deeper understanding of the tumor microenvironment. This study presents the whole-slide mIHC analysis capabilities of QuPath, an open-source application developed at Queen's University Belfast [3].

Methods

A multiplex fluorescent stain panel was performed on patient samples. The slides were imaged and cells were detected and segmented in QuPath. QuPath parallelizes its workload to manage whole-slide throughput efficiently. Custom scripts were written that exhibit machine-learning and thresholding techniques to aggregate cell phenotype totals. Additionally, cell detection numbers were generated for specific ROIs and compared to a commercial DIA software. All scripts and protocols in this study are made public for replication and improvement by the community.

Results

QuPath's automated cell segmentation and classification were demonstrated as a proof-of-concept for whole-slide multiplex immunohistochemistry analysis. Across an entire slide, cells positive for multiple markers were effectively segmented and properly phenotyped.

Conclusions

Open-source applications have become a driving force for innovation and collaboration in the field of digital image analysis. In litigating the strengths and weaknesses of QuPath for whole-slide mIHC analysis, we aim to advance the field's knowledge of available software tools and bring attention to necessary

points of growth in this rapidly changing industry.

References
1. Feng Z, Jensen SM, Messenheimer DJ, Farhad M, Neuberger M, Bifulco CB, Fox BA. Multispectral imaging of T and B cells in murine spleen and tumor. J Immunol. 2016;196:3943-3950. 2. Blom S, Paavolainen L, Bychkov D, Turkki R, Mäki-Teeri P, Hemmes A, Välimäki K, Lundin J, Kallioniemi O, Pellinen T. Systems pathology by multiplexed immunohistochemistry and whole-slide digital image analysis. Sci Rep. 2017; 7:1-13. 3. Bankhead P, Loughrey MB, Fernández JA, Dombrowski Y, McArt DG, Dunne PD, McQuaid S, Gray RT, Murray LJ, Coleman HG, James JA, Salto-Tellez M, Hamilton PW. Qupath: open source software for digital pathology image analysis. Sci Rep. 2017; 7:1-7.

P442

Automated quantification of whole-slide multispectral immunofluorescence images to identify spatial expression patterns in the lung cancer microenvironment

Lorenz Rognoni, PhD[1], Vinay Pawar, PhD[1], Tze Heng Tan, MSc, PhD, DiplIng[1], Felix Segerer, PhD[1], Philip Wortmann, PhD[1], Sara Batelli, PhD[1], Pierre Bonneau[1], Andrew Fisher, PhD[2], Gayathri Mohankumar, MS[2], David Chain, PhD[3], Michael Surace, PhD[3], Keith Steele, DVM, PhD[3], Jaime Rodriguez-Canales, MD[3]

[1]*Definiens AG, Munich, Germany*
[2]*Definiens Inc., Cambridge, MA, USA*
[3]*Medimmune, Gaithersburg, MD, USA*

Background
Advancement in cancer immunotherapy is associated with unraveling the complexities of immune suppressive mechanisms across different cancers. Quantification on multispectral multiplex-immunofluorescence (mIF) images allows detection of several biomarkers in a single section. In addition, new evidence using mIF techniques suggests that spatial analysis reveals novel insights in the tumor microenvironment. However, multispectral imaging is tile based due to long scanning periods, which leads to insufficient data acquisition for significant spatial analysis. In this study, our goal is to develop an automated workflow to study the spatial patterns of infiltrating cells in the tumor microenvironment based on multispectral mIF whole slide scans. This was used to study the relationship between tumor proliferation and immune-response in non-small cell lung cancer (NSCLC) resections.

Methods
45 formalin fixed, paraffin embedded NSCLC resection samples were stained with a custom-developed 7-plex mIF panel (CD68, CD8, Ki67, PD1, PD-L1, pancytokeratins-CK & DAPI) using the Opal method (PerkinElmer). Tiled scans were acquired with a Vectra Polaris (PerkinElmer) multispectral imaging system. Definiens Insights services with custom algorithms was used to analyze the unmixed multispectral data as whole slide images.

Results
The 7-plex Opal staining was optimized for an automated staining platform to ensure high throughput and consistent sample processing. We developed a workflow which composes the tiled unmixed multispectral data to a whole-slide image and optimizes the layers for screen display and automated image analysis. Furthermore, images were shared on Definiens collaboration platform along with a chromogenic-IHC pseudocolor of the IF CK/DAPI signals and co-registered H&E section for pathologist annotations. These annotations were used in defining tumor center and invasive margin. The image analysis includes single-cell detection on the complete slide along with classification of subpopulations based on multi-marker positivity of individual cells. Part of the analysis is a high-quality tumor stroma separation based on the CK signal. The

single-cell readouts were used to construct spatial biomarker-expression patterns (Figure 1), which shows distinct immunological areas in the tumor region and a possible correlation between tumor proliferation (Ki67) with the immune activity in the invasive margin.

Conclusions

We developed an automated workflow for quantitative mIF image analysis on whole-tissue slides. Additionally, our image analysis permitted identification of spatial patterns for immunoprofiling, where we could overcome the limitation of small regions of interests and provide significant amount of data on the whole tumor region.

Ethics Approval

Commercially available samples were obtained according to the declaration of Helsinki for this study.

Figure 1.

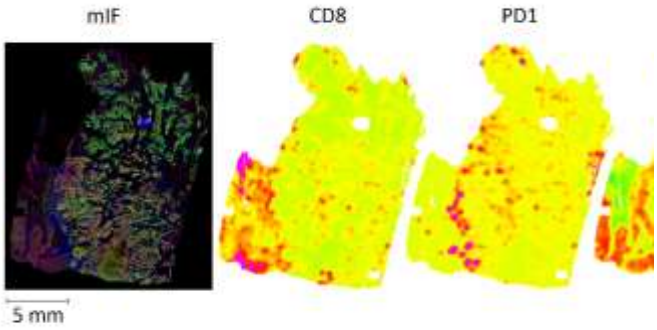

P443

Haplotype human immune system (HIS) modeling and co-engraftment of PDX: ImmunoGraft® platform for evaluation of pharmacodynamics of Immuno Oncology therapeutics

Bhavana Verma, PhD[1], Champions Oncology c/o Mancini, PhD[1], Angela Davies, MD[1], David Sidransky, MD[2], Amy Wesa, PhD[1], Neal Goodwin, PhD[1]

[1]*Champions Oncology, Rockville, MD, USA*
[2]*Johns Hopkins University, Baltimore, MD, USA*

Background

Recent success of several immunotherapeutic regimens, such as checkpoint modulators has boosted development of next generation IO agents underscoring the need for robust preclinical platform to evaluate IO-therapies. The Champions ImmunoGraft® model utilizing humanized NOG mice is an innovative pre-clinical model for assessing the efficacy of IO agents against solid tumors. Improved immunodeficient mouse strains, such as triple transgenic NOG-EXL mice expressing huIL-3 and huGM-CSF, allows for superior HIS development. In this study, we evaluated human immune lineage development, tumor infiltrating leukocytes, and tumor response to checkpoint inhibitor utilizing this humanized mouse platform.

Methods

Human immune system component development in peripheral blood was assessed by flow cytometry across 9 donors 8 weeks post intravenous transplantation of cord-blood (CB) C34+ hematopoietic cells (HSC) in NOG and NOG-EXL mice. Next, NOG-EXL mice were humanized with CB-HSC from 2 donors, monitored for engraftment then implanted with a patient-derived xenograft (PDX) tissue from a non-small cell lung carcinoma (NSCLC) patient. Immune cell populations (T cells, macrophages, myeloid-derived suppressor cells (MDSC) and dendritic cells (DC)) were evaluated by flow cytometry at 4 and 6 weeks post-tumor implantation in various tissues. For nivolumab (α-PD-1; 10mg/kg) treatment, dosing was initiated at a tumor volume of 80-150 mm3. Responses were determined as changes in tumor volume.

Results
NOG-EXL (100%) consistently engrafted more readily than NOG (80%), with greater than 25% huCD45+ cells in the periphery. Some donor to donor variability was observed in HIS engraftment in both mouse strains; both strains permitted T cell, B cell and some myeloid cell development. T cell lineage development was equivalent in both strains at 12-weeks post–HSC transplantation. Improved myeloid lineage (CD33+) development was found in NOG-EXL animals. Macrophage, MDSC, as well as T cells were found in tumor infiltrates. Evaluation of PD-1 blockade in NSCLC PDX ImmunoGraft® in NOG-EXL mice indicated HIS donor variability impacted treatment efficacy in vivo.

Conclusions
ConclusionsImproved mouse strains that allow for robust reconstitution of immune compartments enhances value of ImmunoGraft® platform for screening new IO therapies. We demonstrated that NOG-EXL mice allow better engraftment and HIS development compared to NOG. Evaluation of nivolumab efficacy in NSCLC PDX model in this enhanced ImmunoGraft® indicates that PD-1 blockade is feasible, and offers an opportunity to evaluate therapeutics targeting myeloid populations. The ImmunoGraft® has the potential to advance translational IO drug discovery and development.

P444

Autologous human immune system (HIS) ImmunoGraft®: Mobilized peripheral blood (MPB) derived CD34 engraftment and lineage development

Bhavana Verma, PhD[1], Georgia Chen, PhD[2], Edmund Waller, MD, PhD, FACP[2], Neal Goodwin, PhD[1], Angela Davies, MD[1] , Amy Wesa, PhD[1], Nabil Saba, MD[2]

[1]*Champions Oncology, Rockville, MD, USA*

[2]*Winship Cancer Institute of Emory University, Atlanta, GA, USA*

Background
Humanized mice generated by hematopoietic stem cells (HSC) transplant and co-engrafted with a patient-derived xenograft (PDX) represents a promising pre-clinical platform for studying immunological response to cancer and evaluation of immunotherapeutic interventions. These models are limited by the fact that the immune system developed in these mice is allogeneic to the tumor. To address this, we have innovated a platform to reconstitute autologous HIS in immunodeficient NOG-EXL mice with mobilized peripheral blood (MPB)-CD34 cells derived from a head and neck cancer patients along with PDX generated from the same patient tumor tissue.

Methods
Patients with head and neck squamous cell carcinoma (HNSCC) were consented for tumor and IRB approved apheresis for stem cell collection at Winship Cancer Institute of Emory University. The HSC collection protocol included mobilization with G-CSF and Plerixafor, prior to apheresis, isolation and cryopreservation of MPB-CD34 cells. PDX were established from biopsies or surgical specimens by passaging in immunodeficient mice. In parallel, Irradiated NOG-EXL mice were humanized by intravenous transplantation of HSC. Engraftment of human immune components (T cells, B cells and myeloid cells) in peripheral blood was assessed by flow cytometry up to 25 weeks, with terminal collections and assessment of immune components in spleen and bone marrow at 30 weeks.

Results
Twenty-eight PDX models were generated from 43 patients with HNSCC and evaluated by next-generation sequencing. In parallel, HIS engraftment assessed in circulation was observed at 8 weeks post-transplant in 100% of NOG-EXL mice; with 5-

20% hCD45+ cells present. B cell development was predominant at early timepoints and declined over time. T cell development was observed starting at 15 weeks, with both CD4 and CD8 T cell subsets observed. Strong myeloid lineage (CD33+) development was observed starting at 8 weeks and persisted throughout the study. At 30 weeks we plan to evaluate immune compartments in blood, spleen and bone marrow of the humanized mice.

Conclusions

HSC mobilized from an adult patient with HNSCC was used to engraft and generate HIS-mice with B cells, T cells, and myeloid cells. In parallel, a matched PDX model was established from the same patient. The co-engraftment of HIS mice with an autologous PDX is in progress. This data demonstrate that mobilization and apheresis of HNSCC patients is technically and clinically feasible, and may permit the establishment of autologous HIS-PDX mice. The advanced autologous CD34-ImmunoGraft® has the potential to advance translational ImmunoOncology drug discovery and development.

Ethics Approval

Apheresis was performed based on an IRB approved protocol implemented at Winship Cancer Institute of Emory University

P445

Human CD33+ myeloid cells support metastatic colonization in a humanized mouse model of melanoma

Chun Yu, PhD[1], Jan Martinek, PhD[1], Te-Chia Wu[1], Kyung Kim[1], Elaheh Ahmadzadeh, PhD[1], Rick Maser[2], Florentina Marches[1], Patrick Metang[2], Pierre Authie[2], Hannah Brookes[1], Joshy George, PhD[1], Jacques Banchereau[1], A. Karolina Palucka, MD, PhD[2]

[1]*The Jackson Laboratory for Genomic Medicine, Farmington, CT, USA*

[2]*The Jackson Laboratory for Mammalian Gen, Bar Harbor, ME, USA*

Background

Metastatic melanoma remains an incurable disease for some patients due to treatment resistance and metastatic dissemination. Here we show that metastatic melanoma tumor samples from patients are infiltrated with myeloid cells and display STAT3-driven transcriptional profiles.

Methods

To study the biology of myeloid cells and melanoma cells in vivo, we used NSG mice with transgenic expression of human hematopoietic cytokines SCF/GM-CSF/IL-3 (NSG-SGM3) engrafted with human CD34+ hematopoietic progenitor cells.

Results

Humanized NSG-SGM3 mice when implanted with Me275 human melanoma cell line subcutaneously, developed multi-organ distant melanoma tumors. This was linked with the presence of circulating tumor cells and elevated serum biomarker lactate dehydrogenase (LDH). Among six melanoma cell lines analyzed, potential to form distant tumors was correlated with G0/G1 cell cycle status and proliferative capacity. Treatment with VEGF inhibitor Avastin significantly decreased the number of melanoma tumors in the spleen but not in the liver. Adoptive transfer experiments confirmed the critical role of human CD33+ myeloid cells in metastatic colonization and these cells displayed STAT-3-driven transcriptional profiles.

Conclusions

Thus, our model enables mechanistic and pre-clinical studies for the development of novel treatment strategies targeting human-specific molecular pathways controlling melanoma dissemination.

P446

Using monocytes to instill brain tumors with TILs

Tomasz Zal, PhD[1], Meenakshi Shanmugasundaram[1], Anna Zal[1], Shouhao Zhou[1], Amy Heimberger, MD[1], Tomasz Zal, PhD[1], Felix Nwajei, PhD[1]

[1]*University of Texas MD Anderson Cancer Center, Houston, TX, USA*

Background

Tumors that localize in brain, including primary cancers and brain metastases, typically contain infrequent lymphocytic infiltrates. The paucity of tumor infiltrating lymphocytes (TILs) in brain tumors (BTs) presents a challenge for current immunotherapies reliant on TIL reactivation or lymphocyte (T cell) delivery. In emergent view, TILs are hailed by various types of tumor-associated myeloid cells, which can originate either from the organ's tissue-resident macrophages, or from bone marrow sources. In healthy brain, the myeloid compartment is dominated by the resident microglia, whereas extracranial-derived myeloid cell subsets are rare outside of brain inflammation. However, the basis of TIL recruitment to brain tumor (BT) sites, or lack thereof, remains unclear.

Methods

We investigated TIL dynamics in BTs using longitudinal skull window multiphoton microscopy in multi- reporter mouse strains. Cyan fluorescent brain metastases were induced by infusing, into the carotid artery, syngeneic MCA205 (sarcoma), LLC (lung adenocarcinoma) or B16F10 (melanoma) cells, and GL261 glioblastoma was deposited directly into the brain. Endogenous T cells (hCD2-DsRed) were co-imaged with the microglia and monocytes and/or dendritic cells (CX3CR1-GFP and CD11c-YFP). We further distinguished the microglia, monocytic and dendritic cell subsets using three-color myeloid reporter mice (CX3CR1-GFP/CD11c-YFP/CCR2-RFP).

Results

Present in various densities across BT models, TILs were accompanied by myeloid cells expressing the fractalkine receptor CX3CR1, which is expressed predominantly on the microglia and monocytes or monocyte-derived cells. Fractalkine (CX3CL1) was upregulated on BT-juxtaposed neurons and CX3CR1-expressing monocytes adhered to and scanned the local vasculature. TILs were decreased, and their motility aimless, in mice lacking CX3CR1, resulting in increased BT growth. However, the TIL's spatial and temporal densities correlated with dendritic-form cells expressing high levels of CD11c (DCs), rather than CD11c-negative monocytes or microglia. TIL migration was confined around CD11c-high DCs and the confinement radius was tighter, in coincidence with cancer cell killing, in tumors undergoing T-cell mediated immune rejection, compared with BTs that were progressing. Depletion of CD11c cells from mice with established BTs led to a rapid abandonment of BTs by the TILs, whereas infusion of (CD11c-negative) monocytes into the blood gave rise to intratumoral CD11c-high dendritic cells, which could attract TILs.

Conclusions

Our results identify the patrolling monocytes and their development into intratumoral DCs as critical cellular mediators of the adaptive immune surveillance of tumors in brain. Moreover, our results establish a proof of principle for the use of monocyte adoptive cell transfer as a potential therapeutic strategy for instilling BTs with TILs.

Acknowledgements

Funding was provided by the NCI (5R01CA137059, 5P50CA127001/DP150072), the University of Texas MD Anderson Cancer Center (IRG 30026195, MRP1152014) and the Schissler Family Fellowship (FN).

Ethics Approval

The study was approved by the MD Anderson

Institutional Animal Care and Use Committee, protocol number 00000878-RN02.

Immune Effects of Chemotherapy

P447

A case of checkpoint inhibitor-induced celiac disease

Dana Alsaadi[1], Neil Shah, MD[1], Aline Charabaty, MD[1], Michael Atkins, MD[1]

[1]*Georgetown University, Washington, DC, USA*

Background
Immune checkpoint inhibitors (ICIs) have now become standard of care treatment for many malignancies. ICIs are associated with unique immune mediated adverse events (irAEs) due to dysregulation of immune activation. As treatment with ICIs is becoming more common, rare irAEs are also being recognized. Here we report a case of ICI-induced celiac disease.

Methods
N/A

Results
A 74-year-old Caucasian female with metastatic renal carcinoma received second line nivolumab (anti-PD1 antibody) after initial disease progression on sunitinib. Ipilimumab was added after she failed to respond to six cycles of nivolumab monotherapy. One week after her first cycle of combo treatment, she presented with nausea, vomiting, grade 1 diarrhea, and weight loss. She underwent endoscopy, which showed bile stasis in the stomach, normal appearing stomach mucosa, and non-bleeding erythematous mucosa in the duodenal bulb. Stomach biopsy showed moderate active chronic gastritis. Duodenal biopsy showed moderate chronic active duodenitis with focal neutrophilic cryptitis, mucosal erosions, villous atrophy, mildly increased intraepithelial lymphocytes, and moderate chronic inflammation in the lamina propria pathognomonic of celiac disease. Symptoms improved with gluten-free diet, twice-daily omeprazole and anti-emetics and she was able to continue on treatment.

Conclusions
There has been only one published case reporting ICI-induced celiac disease.[1] Our case report highlights a rare irAE (celiac disease) associated with ICI treatment. It is unclear whether the patient had previously undiagnosed celiac disease or whether ICIs triggered her enteritis. Our patient was able to continue treatment with ICIs with dietary modifications, suggesting correct diagnosis is critical for optimal patient outcome.

References
1. Gentile NM, D'Souza A, Fujii LL, Wu TT, Murray JA. Association between ipilimumab and celiac disease. Mayo Clin Proc 2013; 88: 414-417.

Consent
Consent was received.

P448

Blockade of EphB4-ephrin-B2 interaction remodels the tumor immune microenvironment in head and neck cancers

Shilpa Bhatia[1], Sana Karam, MD, PhD[2]

[1]*University of Colorado, Anschutz Medical Campus, Aurora, CO, USA*
[2]*University of Colorado Denver, Aurora, CO, USA*

Background
Identifying targets in the tumor microenvironment (TME) that act as barriers to an effective anti-tumor immune response has become an area of intense

investigation. In the current study, we established EphB4-ephrin-B2 signaling as a key pathway that regulates both innate and adaptive arms of the immune system. Eph receptor tyrosine kinases and their membrane-bound ephrin ligands have been implicated in human malignancies and in immune cell development, migration, and activation in inflammatory models. However, direct evidence that supports the role of Eph-ephrin interaction in cancer-related immune response is lacking. We hypothesized that EphB4-ephrin-B2 interaction regulates TME by sustaining immunosuppressive cells-Tregs and TAMs thus negatively impacting the functional ability of CD8 T cells.

Methods

We used orthotopic models of head and neck squamous cell carcinoma to determine the role of EphB4-ephrin-B2 interaction in tumor immune microenvironment. Mice were treated with control agent or an EphB4-ephrin-B2 blocker in the absence or presence of radiation (RT). Tumor immune cell infiltrates were analyzed using mass cytometry and flow cytometry applications. ELISA or multiplex cytokine array were utilized to determine circulating cytokine/chemokine levels in plasma.

Results

We observed that inhibition of EphB4-ephrin-B2 signaling in vivo significantly reduced tumor growth and decreased the infiltration of Tregs, TAMs, and increased infiltration and activation of Teffector cells, without affecting CD4 T cell numbers. This was correlated with decreased Treg proliferation and activation when EphB4-ephrin-B2 signaling is inhibited. Since RT remains the mainstay in treatment of head and neck squamous cell cancer (HNSCC) patients, we combined EphB4-ephrin-B2 inhibitor with RT in our tumor model and observed further increase in CD8 and CD4 T cell infiltrates and activation status, and a significant decline in circulating IL-10 and TGF-β1 levels compared to the control group. A significant reduction of TAMs, favoring a polarization towards an anti-tumoral M1 phenotype, was also observed in EphB4-ephrin-B2 inhibitor+RT group. We also compared the efficacy of combining EphB4-ephrin-B2 inhibitor with RT to anti-PDL1+RT in an in vivo model known to develop resistance to anti-PDL1+RT therapy. Our data demonstrated that combining EphB4-ephrin-B2 inhibitor with RT was equally effective to that of anti-PDL1+RT in terms of anti-tumor growth response.

Conclusions

Our study provides the first insight into a novel role for EphB4-ephrin-B2 interaction in modulating tumor immune microenvironment in HNSCC. Our findings present a potential alternative in the form of EphB4-ephrin-B2 targeted therapeutics that can be tested in clinical trials in combination with RT for HNSCC patients.

P449

Improving PDAC outcomes through targeting immune populations and fibrosis by EphB4-ephrinB2 or Treg inhibition combined with radiation

Sana Karam, MD, PhD[1]

[1]*Univ. of Colorado Denver, Aurora, CO, USA*

Background

A driving factor in pancreatic ductal adenocarcinoma (PDAC) treatment resistance is the tumor microenvironment, which is highly immunosuppressive. One potent immunological adjuvant is radiation therapy (RT). Radiation, however, has also been shown to induce immunosuppressive infiltration, which can contribute to tumor progression. Another negative effect is the potential contribution to formation of fibrotic tumor stroma. To capitalize upon the immunogenic effects of radiation and obtain a durable tumor response, radiation must be rationally combined with targeted therapies to mitigate the

influx of immunosuppressive cells and fibrosis. One such target is ephrinB2, which is overexpressed in PDAC and correlates negatively with prognosis. Based upon previous studies of ephrinB2 ligand-EphB4 receptor signaling, we hypothesized that inhibition of ephrinB2-EphB4 combined with radiation would regulate the microenvironment response post radiation, leading to increased tumor control in PDAC.

Methods

Immunocompetent C57BL/6 and immune compromised athymic nude mice were injected subcutaneously with either a patient derived xenograft (PDX) tumor, PANC 272, or a mouse pancreata derived cell line (FC1242) and randomized into PBS, B11 (an inhibitor of ephrinB2-EphB4 interaction), RT and B11+RT groups. Depletion studies were conducted using anti-IgG or anti-CD35 antibodies. To determine tumor immune cell infiltration, tumors were subjected to flow cytometric analysis. Plasma samples were subjected to ELISA to determine circulating TGFβ1 levels in control and treatment groups. Fibrosis was quantified following Masson's Trichrome staining and PicroSirius Red staining.

Results

Our data show that combining ephrin-B2-EphB4 inhibitor with RT significantly reduces regulatory T-cell and neutrophil infiltration, TGFβ1 secretion, and stromal fibrosis, enhancing effector T-cell activation and decreasing tumor growth. Further, our data demonstrate that depletion of regulatory T-cells in combination with radiation reduces tumor growth and fibrosis as demonstrated by Masson's Trichrome staining and PicroSirius Red staining.

Conclusions

These are the first findings to suggest that in PDAC, ephrinB2-EphB4 interaction has a profibrotic, pro-tumorigenic role, presenting a novel and promising therapeutic target.

P450

The stapled peptide ALRN-6924, a dual inhibitor of MDMX and MDM2, displays immunomodulatory activity and enhances immune checkpoint blockade in syngeneic mouse models

Luis Carvajal, PhD[1], Narayana Narasimhan, PhD[1], Jian-Guo Ren, PhD[1], Solimar Santiago, MS[1], Manoj Samant, PhD[1], David Sutton, PhD[1], Vincent Guerlavais, PhD[1], D. Allen Annis, PhD[1], Manuel Aivado, MD, PhD[1]

[1]*Aileron Therapeutics, Inc., Cambridge, MA, USA*

Background

The tumor suppressor p53 is one of the most pursued targets in oncology, playing a central role inducing cell cycle arrest, apoptosis and senescence in response to cellular stress and oncogenic signals. In addition to its intrinsic anti-tumor activity in cells, p53 activation can induce anti-tumor immunity and plays an important role in the regulation of innate and adaptive immunity. Therefore, p53-reactivating agents in combination with immune checkpoint blockade (ICB) may represent a powerful approach to optimize the body's immunological response against cancer. ALRN-6924 is an α-helical stapled p53 peptide currently in clinical testing that has demonstrated anticancer activity as monotherapy [1]. In this study, we investigated whether p53 reactivation with ALRN-6924 can be leveraged as new combination partner for ICB.

Methods

Peripheral blood mononuclear cells (PBMCs) were stimulated with ALRN-6924 ex vivo for 24 hr. Gene expression and cytokine levels were measured using a validated TaqMan assay (ThermoFisher) and the Human XL Cytokine Array Kit (R&D Systems). Immune profiles from pre- and post-treatment

tumor biopsy samples were evaluated by NanoString PanCancer IO360 and Immune Profiling RNA gene expression panels. Immunophenotyping of PBMCs was done by flow cytometry. Efficacy and immune cell profile (determined by flow cytometry and IHC) were evaluated in CloudmanS91 and MC38 syngeneic murine tumor models following treatment with ALRN-6924 alone and in combination with anti-PD-1 or anti-PD-L1, including re-challenge studies to test for immunological memory.

Results

Ex vivo stimulation of PBMCs with ALRN-6924 promotes transcriptional activation of genes involved in innate and adaptive immunity, and the production of immune-stimulating cytokines including INF-γ, IL-6 and IL-12. mRNA analysis of pre- and post- treatment tumor biopsies from patients treated with ALRN-6924 revealed a differential gene expression pattern consistent with conversion to an inflamed tumor phenotype. In syngeneic mouse models, ALRN-6924 was sufficient to promote infiltration of CD8+ T cells, polarization of M1 macrophages in mouse tumors and immunological memory. Moreover, ALRN-6924 synergizes with anti-PD-1 and anti-PD-L1 to induce anti-tumor immunity resulting in an increased number of mice achieving complete regressions (CR), in both p53 wild-type and mutant tumors, compared to single agents.

Conclusions

Reactivation of p53 with ALRN-6924 enhanced the effects of ICB therapy in mice. Furthermore, the present study suggests that ALRN-6924 modulates anti-tumor immunity in p53 wild type, and p53 mutant tumors, possibly via tumor cell extrinsic effects in the tumor microenvironment.

References

1. Funda Meric-Bernstam, M. S. Saleh, J. R. Infante, S. Goel, G. S. Falchook, G. Shapiro,K. Y. Chung, R. M. Conry, D. S. Hong, J. S. Wang, U. Steidl, L. D. Walensky, V. Guerlavais, M. Payton, D. A. Annis, M. Aivado, M. R. Patel, Phase I trial of a novel stapled peptide ALRN-6924 disrupting MDMX- and MDM2-mediated inhibition of WT p53 in patients with solid tumors and lymphomas. J. Clin. Oncol. 35, 2505–2505 (2017).

Ethics Approval

All studies involving human material or animal (in vivo) studies were approved under Aileron's IND122392 protocol and by the Institutional Animal Care and Use Committee at Charles River Laboratories, Morrisville, N.C. ASP #: 990202, respectively.

P451

Gal9/Tim-3 expression level is higher in patient with failed chemotherapy in AML

Justin Kline, MD[1], Paola Dama, PhD[1], Hongtao Liu, MD, PhD[1]

[1]*University of Chicago, Chicago, IL, USA*

Background

Activation of immune checkpoint pathways in Acute Myeloid Leukemia (AML) may interfere with effective T-cell anti-tumor immunity, and is associated with immune evasion in pre-clinical leukemia models as it has been demonstrated. [1,2] It was previously reported that overexpression of CTLA4 and PD-1 is associated with more aggressive leukemia and progression from MDS to AML or AML relapse. While PD-1/PD-L1 blockade therapy can be effective as cancer immunotherapy, interruption of PD-1/PD-L1 interactions alone does not completely restore T cell function in some patients indicating the involvement of additional negative regulatory pathways, such as Tim-3/Gal-9, in T cell exhaustion. Immune checkpoint pathways active in Acute Myeloid Leukemia (AML) patients, especially during the course of remission induction chemotherapy, have not been well-studied. We characterized these

pathways in newly diagnosed AML patients enrolled in a phase I dose escalation trial that combined Selinexor a Selective Inhibitor of Nuclear Export (SINE) with high-dose cytarabine (HiDAC) and mitoxantrone (Mito) (NCT02573363) as induction therapy.

Methods

Multi-parameter flow-cytometry was performed on bone marrow specimens at diagnosis and following remission induction therapy in 26 patients with AML enrolled to the study to monitor the changes in expression of immune checkpoint receptors. Expression of CD47, PD-L1, PD-L2 and Gal-9 was assessed on CD34+ AML blasts and CD34- cell populations. In parallel, expression of inhibitory (PD1, CTLA4, LAG3, TIM3) and stimulatory co-receptors (CD28, ICOS, CD137, OX40, CD40L, HLA-DR) on CD4+ and CD8+ T cell subsets were evaluated. The positivity and frequency of parent in percentage of each markers was gauged by comparing with their FMO controls. Samples were analyzed using LSR Fortessa or LSRII Cytometers. The Mann Whitney Test, Spearman's rank correlation and Runs Test analysis were applied. For all analyses, P-values <0.05 were considered statistically significant.

Results

The percentage of CD34- Gal9+ cells was significantly higher and was positively correlated with higher numbers of TIM-3-expressing T cells at the time of diagnosis in patients who experienced treatment failure (TF) after chemotherapy, compared to those in complete remission (CR). When comparing TIM-3 expression on CD4+ and CD8+ T cells in pre-treatment (diagnosis) to post induction therapy samples, the magnitude of increase measured by median fluorescence intensity (MFI) inversely correlated to response to therapy with increase TIM-3 MFI of > 50% in patients with TF.

Conclusions

This study provides preliminary evidence to support a rationale for incorporating antibodies against the Gal9/TIM3 pathway during and/or following remission induction therapy for AML.

References

1. Zhang L, Gajewski TF, Kline J. PD-1 / PD-L1 interactions inhibit antitumor immune responses in a murine acute myeloid leukemia model. Blood. 2009; 114(8), 1545–1552.
2. Zhou Q, Munger ME, Blazar BR. Coexpression of Tim-3 and PD-1 identifies a CD8+T-cell exhaustion phenotype in mice with disseminated acute myelogenous leukemia. Blood, 2011;117(17), 4501–4510.

Ethics Approval

The study was approved by the Institutional Review Board at The University of Chicago, approval number 150412.

P452

Cisplatin treatment induces anti-tumor immune response in NSCLC by activation of the innate immune response pathway

Triparna Sen, PhD[2], Lixia Diao[2], Kavya Ramkumar[2], Carl Gay[2], Pan Tong[2], You-Hong Fan[2], Robert Cardnell[2], Don Gibbons, MD[2], John Heymach[2], Jing Wang[2], Lauren Byers, MD[2], CARMINIA DELLA CORTE, MD[2]

[1]The University of Texas MD Anderson Cancer Center, Houston, TX, Houston, TX, USA
[2]MD Anderson Cancer Center, Houston, TX, USA

Background

Platinum-based doublet chemotherapy plus anti-PD1 immunotherapy is a new standard of care for the treatment of advanced NSCLC patients. It is known that DNA damage can activate antitumor immune responses in cancer through release of cytosolic DNA leading to Stimulator of Interferon Genes (STING)

pathway activation, production of neo-antigens, and release of pro-inflammatory cytokines. Our group has previously demonstrated that mesenchymal tumors with high EMT scores have the highest expression of targetable immune markers (1). However, the underlying mechanism of how platinum-based chemotherapy modulate the immune microenvironment is far from being fully understood in NSCLC. The aim of this study is to elucidate the effect of platinum-based chemotherapy on anti-tumor immune response and identify novel biomarkers to aid patient selection for chemotherapy and immunotherapy combination clinical trials.

Methods

We analyzed transcriptomic and proteomic expression of immune markers in NSCLC samples from two clinical datasets (MDACC-PROSPECT, n= 209) and The Cancer Genome Atlas (TCGA, n=1016). We also treated NSCLC cell lines with cisplatin to investigate its effect on DNA damage and changes in immune markers expression by western blot and Reverse-Phase Protein Array (RPPA analysis).

Results

Treatment with cisplatin increased DNA damage (increased γH2AX), and significantly upregulated PD-L1 and STING pathway protein expression in a panel of NSCLC cell lines.In the TCGA cohort, immune checkpoints and inflammatory cytokines mRNA expression is highly coordinated and positively correlated with EMT genes. In the TCGA lung adenocarcinoma (LUAD, n=515) cohort, high expression of effector chemokines (CXCL10, CCL5) and mediators of STING pathway (TBK1, TMEM173) were associated with high levels of CD274 (PD-L1) and other targetable immune markers (LAG3, IDO1, PDCD1LG2, CTLA4). These findings were further validated both in lung squamous (LUSC) TCGA and the PROSPECT cohorts (LUAD and LUSC). Interestingly, in the LUAD TCGA cohort, smoking status (another source of DNA damage) was significantly correlated with higher expression of STING and other immuno-modulatory genes, and EMT signature.

Conclusions

Our results demonstrate that in treatment naïve-NSCLC tumors, expression of PDL1 and other targetable immune markers correlate with expression of STING, EMT, smoking status and DDR pathway genes, and that treatment with cisplatin further enhances the immunogenicity of tumors through activation of the STING pathway in NSCLC cells. Our findings identify a novel mechanism by which cisplatin activates an innate immune response pathway in NSCLC. Furthermore the results identify potential biomarkers (EMT, smoking status, DDR protein expression) for patient selection in clinical trials.

References

1. Mak MP, Tong P, Diao L, et al. A Patient-Derived, Pan-Cancer EMT Signature Identifies Global Molecular Alterations and Immune Target Enrichment Following Epithelial-to-Mesenchymal Transition. Clin Cancer Res. 2016;22:609-20.

P453

Enhancing the anti-tumor immunity elicited by alpha radiation-based brachytherapy using immunoadjuvants and blockade of suppressor cells

Vered Domankevich-Bachar, DR[1], Adi Cohen[2], Margalit Efrati[2], Michael Schmidt[2], Hans Georg Rammensee[3], Itzhak Kelson[2] , Yona Keisari[2]

[1]*Tel Aviv University, Tel Aviv, Israel*
[2]*Tel Aviv Uiniversity, Tel-Aviv, Israel*
[3]*University of Tübingen, Tübingen, Germany*

Background

Diffusing alpha emitters Radiation Therapy (DaRT) is a novel brachytherapy treatment for solid tumors.

DaRT seeds disperse short-lived alpha-emitting atoms in a therapeutically-significant range, which diffuse inside the tumor and destroy a sizeable part of it. Thus, for the first time, an efficient and safe method for treating the entire solid tumor by highly destructive alpha radiation is used. In situ tumor ablation is known to release tumor antigens and damage associated molecular pattern molecules (DAMPs) that lead to the induction of systemic anti-tumor immunity. Indeed, we previously reported that in the breast cancer carcinoma mice model DA3, DaRT-treated mice showed increased survival rates, and reduced rates of lung metastases and of primary- or challenged- tumor development. Here we aimed to boost the anti-tumor immune response induced by DaRT, locally and systematically, and to investigate the specificity of the response.

Methods

Mice breast (4T1) and colon (CT26) tumors, implanted subcutaneously, were treated with DaRT seeds with/without immunomodulatory agents. Immunomodulatory agents studied are the immunoadjuvants polyIC, CpG, and XS15, the MDSC inhibitor sildenafil, and the Treg inhibitor cyclophosphamide. Non-radioactive seeds (inert) served as control. Local- and systemic- responses were determined by tumor progression, host survival, response to challenge and lung metastasis. The specificity of the immune response was studied by Winn Assay and tumor challenge to cured tumor-bearing mice.

Results

It was found that in the CT26 colon cancer mice model: (1) combining DaRT with polyIC, CpG or XS15 significantly reduced tumor progression and prolonged survival. (2) Complete response was achieved when using DaRT combined with CpG and immune suppressor cells inhibitors. (3) Cured mice became resistant to CT26 cells but not to DA3 (breast cancer) cells. (4). Splenocytes from CT26 bearing mice cured by DaRT specifically reduced CT26 but not DA3 tumor take in naïve mice. In the triple negative breast cancer model, 4T1, treating the primary tumor with polyIC, prior to DaRT treatment, reduced tumor progression and eliminated lung metastases.

Conclusions

DaRT is currently tested under clinical trials in squamous cell carcinoma patients showing effective tumor control without adverse effects. The current results provide strong evidence for the induction of a specific- and systemic- immune response against tumor antigens following DaRT treatment. We propose DaRT as a safe and efficient novel strategy, not only for tumor ablation, but also for in situ vaccination of cancer patients.

P454

Elucidating the functional role of type-1 interferon signaling following a medium-dose intermittent cyclophosphamide schedule in preclinical breast cancer models

Kshama Doshi, PhD[1], Cameron Vergato[1], Kshama Doshi, PhD[1], Darren Roblyer, PhD[1], David Waxman, PhD[1]

[1]*Boston University, Allston, MA, USA*

Background

Many cytotoxic chemotherapy drugs, including the breast cancer standard of care drug cyclophosphamide (CPA), can induce immunogenic cell death when administered at medium-dose and intermittent (MEDIC) schedule [1]. Adaptive and innate immune responses generated in this manner can greatly potentiate chemotherapy drug efficacy and generate tumor-specific long-term immune memory. Cancer cells have also been shown to up-regulate type-1 interferon (IFNα/β) signaling in response to many chemotherapy drugs. Here we set

out to elucidate the effects and mechanisms of immune activation in a breast cancer preclinical model using a MEDIC schedule of CPA.

Methods

We used an in-vitro IFN-based biomarker strategy to identify breast cancer models that can induce immunogenic responses following treatment with 4-hydroperoxy cyclophosphamide (4HC), a chemically activated form of CPA. Sub-lethal concentrations of 4HC were established by MTS assay and used to study induction of interferon-stimulated genes by qPCR in five breast cancer cell lines: 4T1, E0771, Emt6, Py230 and MCF7. Anti-IFN receptor-1 antibody was used to verify the role of IFNα/β in 4HC-induced interferon-stimulated gene induction. CPA-induced immune activation was also evaluated in a syngeneic mouse tumor model. Mice with orthotopic tumors implanted in the 4th mammary fat pad were treated with a MEDIC schedule of CPA and tumor progression was monitored. Effects of drug treatment on IFN signaling and immune cell infiltration into the tumor compartment was evaluated by marker gene expression.

Results

Screening results revealed sub-lethal concentrations of 4HC significantly induced multiple interferon-stimulated genes, including Cxcl10 (~8 fold), Igtp (~15 fold) and Mx1 (~20 fold) in 4T1 breast cancer cells. In contrast partial to minimum induction was seen in E0771, Emt6, Py230 and Mcf7 cells. Further, anti-IFN receptor-1 antibody blocked > 90% of 4HC-induced interferon-stimulated gene induction in 4T1 cells. Conditioned media from 4HC-treated 4T1 cells also stimulated IFNα/β signaling in drug-naive recipient 4T1 cells. Finally, in syngeneic mouse tumor models, MEDIC CPA scheduling significantly reduced tumor progression resulting in tumor stasis. Diminished tumor growth kinetics was accompanied by significant increases in expression of interferon-stimulated genes and cytolytic enzymes in the tumor compartment.

Conclusions

Breast cancer cell autonomous activation of type-1 IFN signaling and downstream gene induction is activated in a syngeneic 4T1 breast cancer model treated with a MEDIC CPA regimen. Mechanistic features of this pathway, involving autocrine and paracrine type-1 IFN signaling loop, were characterized in-vitro. Studies assessing key immune players and their role in anti-tumor responses are in progress, and will be presented.

Acknowledgements

Grant support: DOD grant # U.S. Department of Defense (DOD) (W81XWH-15-1-0070)

References

1. Wu J, Waxman DJ. Immunogenic chemotherapy: Dose and schedule dependence and combination with immunotherapy. Cancer Lett. 2018;419:210-221.

P455

Inducible T cell Co-stimulator (ICOS) is upregulated on lymphocytes following radiation of tumors and ICOS agonism in combination with radiation results in enhanced tumor control

Michael Gough, PhD[1], Shelly Bambina[1], Monica Gostissa, PhD[2], Christopher Harvey, PhD[2], David Friedman, PhD[1] Marka Crittenden, MD, PhD[1]

[1]Earle A. Chiles Research Institute, Portland, OR, USA
[2]Jounce Therapeutics Inc., Cambridge, MA, USA

Background

Radiation and co-stimulatory ligands or checkpoint inhibitors have demonstrated improved anti-tumor immunity and overall survival in preclinical animal studies. However, the results of human trials suggest

we have not yet found the optimal combination. Here we demonstrate upregulation of ICOS expression on T cells following focal tumor radiation and test the hypothesis that ICOS agonism in combination with radiation will enhance the immunologic effect of radiation resulting in increased survival.

Methods

BALB/c mice bearing CT26 tumors or C57BL/6 mice bearing Panc02 tumors were treated at d14 with 20Gy CT guided radiation therapy and anti-ICOS antibody or isotype control antibody was administrated i.p. Mice were followed for overall survival to 100 days post implantation. Animals were euthanized when tumors reached 1.2cm in greatest diameter. Flow cytometry was performed using a T cell panel on fresh whole blood, PBMC, or tumor infiltrating immune cells.

Results

24 hours following 20Gy focal radiation to a CT26 tumor there was a significant increase in the percent of circulating CD4 Treg that express ICOS in the blood (27.42% vs 18.02%, p<0.0001, n=5/group). Similarly, 7 days following radiation there was an increase in non-Treg CD4 cells expressing ICOS in the blood (7.73% vs 3.68%, p<0.0001, n=5/group) and the tumor (62.16% vs 34.04%, p=0.004, n=5/group). ICOS expression was also increased on CD8 T cells in irradiated tumors (25.34% vs 14.02%, p=0.007). In mice bearing CT26 tumors, ICOS agonist antibody was administered prior to, concurrent with, or 7 days post radiation. Concurrent administration was associated with the most significant increase in survival (50%) when compared to isotype control (0%), ICOS agonist antibody alone (10%), or radiation plus isotype (0%). In the less immunogenic Panc02 tumor model, no survival benefit was seen with radiation and ICOS therapy. However in the same model, dual PD-1 antagonism and ICOS agonism plus radiation led to a significant increase in survival when compared to all other combinations, with an increase in median survival from 46 days to 68 days, p=0.01 compared to radiation alone and was associated with a 25% long term survival.

Conclusions

ICOS is upregulated on T cells following radiation and targeting ICOS in combination with radiation is associated with improved survival. Timing appears important as the benefit is optimal when ICOS agonism is delivered concurrent with radiation rather than preceding or 7 days post-radiation. In poorly immunogenic tumors, addition of PD-1 antagonism to the combination can lead to improved survival.

Ethics Approval

Animal protocols were approved by the Earle A. Chiles Research Institute IACUC (Animal Welfare Assurance No. A3913-01). All experiments were performed in accordance with relevant guidelines and regulations.

P456

Pressure-enabled delivery of CAR-T cells into the porcine pancreas results in highly-targeted pancreatic delivery with minimal systemic exposure and no pancreatitis or severe systemic cytokine release

John Hardaway, MD, PhD[1], James Chomas, PhD[2], David Jaroch, PhD[2], Prajna Guha, PhD[1], N. Joseph Espat, MD, FACS[3], Steven Katz, MD[3], Aravind Arepally, MD[4]

[1]*Roger Williams Medical Center, Providence, RI, USA*
[2]*Surefire Medical, Inc., WESTMINSTER, CO, USA*
[3]*Roger Williams Medical Center, Boston University, Providence, RI, USA*
[4]*Surefire Medical, Inc., Piedmont Medical Center, Westminster, CO, USA*

Background

The purpose of this preclinical study is to determine whether highly preferential delivery of T cells into the pancreas can be achieved while minimizing systemic exposure and avoiding systemic and pancreatic inflammation using the Surefire® Retrograde Venous-Pressure Enabled Drug Delivery (RV-PEDD) method and device, as compared to systemic venous infusion (SVI).

Methods

Healthy human donor CAR-T cells (Sorrento Therapeutics) or unmodified activated T cells were transferred into 10 normal adult swine by either (a) SVI (n=5) or (b) RV-PEDD via trans-hepatic access into pancreatic veins (n=5). Samples of peripheral blood (PB) were obtained at 15, 30, and 120 minutes after infusion. Serum was analyzed for porcine tumor necrosis factor-alpha (TNF-α) and interleukin-6 (IL-6) by enzyme-linked immunosorbent assay (ELISA) as indices of systemic inflammation, whereas circulating CAR-T were quantified using flow cytometry. Liver and pancreatic tissues were harvested for histology, immunofluorescence (IF) of human CD3, and determination of human CD3 mRNA expression via qPCR.

Results

After SVI, the donor CAR-T cell fraction among circulating mononuclear cells was 13.7% at 15 minutes, 31.7% at 30 minutes, and 20.5% at 120 minutes, versus RV-PEDD that yielded 1.8% detection at 15 minutes, and undetectable cells at 30 and 120 minutes. With SVI, IF found substantial accumulation of donor CAR-T cells in PB and minimal pancreatic staining, as opposed to RV-PEDD infusion where substantial pancreatic accumulation and minimal PB staining had occurred (Figure 1). qPCR analysis of pancreatic tissues from RV-PEDD specimens revealed a 147-fold increase in CAR-T penetration, as compared to SVI. Alternatively, analysis of PB following SVI revealed a 61-fold increase in systemic exposure with negligible detection in the pancreas.

Histologically defined pancreatic inflammation was not evident in any animal after RV-PEDD (Figure 2). Systemic inflammation, based on TNF-α and IL-6 levels, was not evident within 2 hours after RV-PEDD infusion, whereas pronounced increases of TNF-α and IL-6 levels were observed with systemic infusion.

Conclusions

RV-PEDD was associated with efficient and specific delivery of donor T cells into porcine pancreas compared to systemic infusion. RV-PEDD did not result in significant systemic exposure nor induce pancreatic or systemic inflammation. These data support clinical testing of Surefire® RV-PEDD technology to improve the therapeutic index with selective delivery of cellular therapeutics into the pancreas.

Ethics Approval

The study was approved by the T3 Labs IACUC on 6/15/16, with amendments on 11/17/16, 2/24/17.

Figure 1.

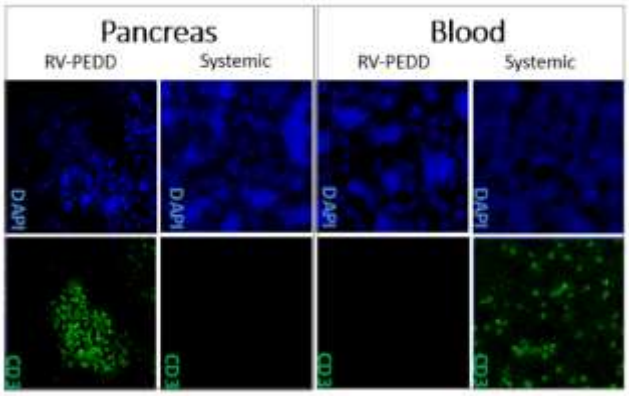

Figure 2.

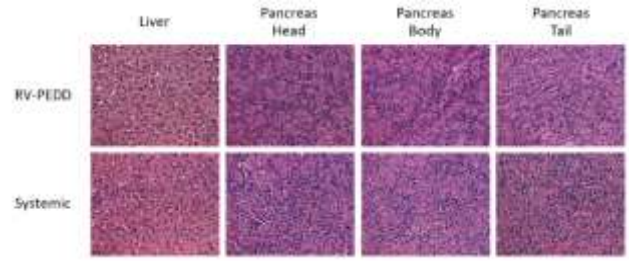

P457

TP53 gene therapy emanating from the investigational agent SGT-53 is capable of augmenting cancer immunotherapy in multiple murine syngeneic tumor models

Joe Harford, PhD[1], Sang-Soo Kim, PhD[1], Kathleen Pirollo, PhD[2], Antonina Rait, PhD[2], Manish Moghe[2], Esther Chang, PhD[2]

[1]SynerGene Therapeutics, Inc., Potomac, MD, USA
[2]Georgetown University Medical Center, Washington, DC, USA

Background

Manipulation of immune checkpoints has emerged as an important form of cancer immunotherapy [1,2]. However, a large number of patients do not respond or develop resistance to checkpoint blockade, and treatment-related toxicities can be limiting. The tumor suppressor p53 exerts anti-tumor activity by inducing apoptosis, but also participates in the regulation of cellular immune responses [3.4]. We have investigated the potential of TP53 gene therapy to augment cancer immunotherapy by combining an anti-PD1 antibody with SGT-53, an investigational nanomedicine that targets tumors and carries a plasmid encoding human wild-type p53 (Figure 1). SGT-53 is now in Phase II clinical trials [5,6].

Methods

We utilized mouse syngeneic tumor models that are relatively resistant to immunotherapy including an aggressive metastatic breast cancer (4T1), a non-small cell lung carcinoma (LL2), and a glioblastoma (GL261). Anti-tumor efficacies of an anti-PD1 antibody alone, SGT-53 alone or the combination of these agents were compared [7]. A number of markers with relevance to immune responses or tumor-induced immunosuppression were assessed by FACS or gene expression profiling.

Results

In all syngeneic models, SGT-53 increased tumor apoptosis and rendered the tumors immunologically "hot". SGT-53 plus anti-PD1 inhibited growth more than either single agent (Figure 2). The combination therapy dramatically reduced lung metastases by 4T1 breast tumors, while the anti-PD1 alone was ineffective. Based on relevant markers, SGT-53 treatment increased tumor immunogenicity, enhanced both innate and adaptive immune responses, and reduced tumor-induced immunosuppression. In mice bearing 4T1 tumors, injections of the anti-PD1 antibody killed the mice before tumors were themselves fatal. Addition of SGT-53 to the treatment regimen alleviated this fatal xenogeneic hypersensitivity to the anti-PD1 and extended the lives of 4T1-bearing mice (see Figure 3). We have identified genes that potentially underlie these observations.

Conclusions

Collectively, our data indicate that restoring p53 function via SGT-53 is able to boost anti-tumor immunity to enhance anti-PD1 immunotherapy by sensitizing tumors while reducing immune-related adverse events. Our data suggest that SGT-53, representing tumor-targeted TP53 gene therapy, has potential to augment immune checkpoint blockade agents while minimizing toxicity to improve outcomes in a variety of malignancies. Our data provide a strong mechanistic rationale for combining the investigational agent SGT-53 with checkpoint blockade agents in a clinical trial setting. It is possible that the SGT-53 would not only improve outcomes for cancer patients who already respond to immunotherapy, but also increase the percentage responding while minimizing adverse events related to the immunotherapy.

References

1. Mellman I, Coukos G, Dranoff, G, Cancer immunotherapy comes of age. Nature 2011; 480, 480-489.

2. Pardoll DM, The blockade of immune checkpoints in cancer immunotherapy. Nature Reviews Cancer 2012; 12, 252-264.
3. Lowe J, Shatz M, Resnick MA, Menendez D, Modulation of immune responses by the tumor suppressor p53. BioDiscovery 2013; 8, 2.
4. Munoz-Fontela C, Mandinova A, Aaronson SA, Lee SW, Emerging roles of p53 and other tumour-suppressor genes in immune regulation. Nature Reviews Immunology 2016; 16, 741-750.
5. Senzer D, Nemunaitis J, Nemunaitis D, Bedell C, Edelman G, Barve M, Nunan R, Pirollo KF, Rait A, Chang EH, Phase I study of a systemically delivered p53 nanoparticle in advanced solid tumors. Molecular Therapeutics 2013; 21, 1096-1103.
6. Pirollo K F, Nemunaitis J, Leung PK, Nunan R, Adams J, Chang EH, Safety and efficacy in advanced solid tumors of a targeted nanocomplex carrying the p53 gene used in combination with docetaxel: Phase 1b study. Molecular Therapeutics 2016; 24, 1697-1706.
7. Kim SS, Harford JB, Moghe M, Rait A, Chang EH, Combination with SGT-53 overcomes tumor resistance to a checkpoint inhibitor, OncoImmunology 2018; DOI: 10.1080/2162402X.2018.148498

Ethics Approval

All animal experiments were performed in accordance with and under approved Georgetown University GUACUC protocols.

Figure 1.

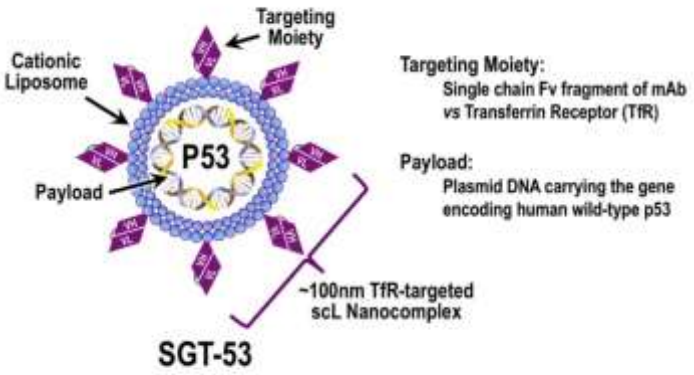

Figure 2

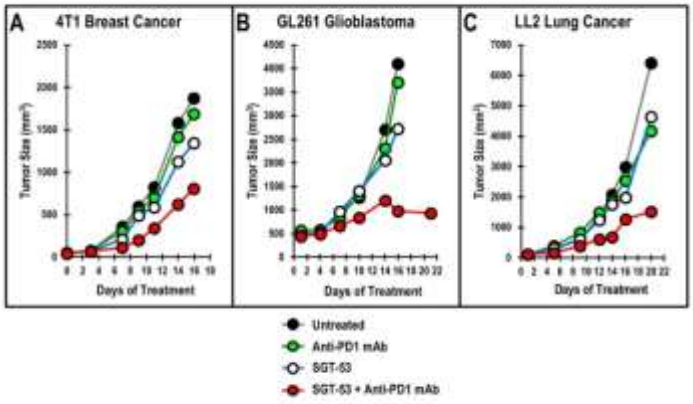

Figure 3.

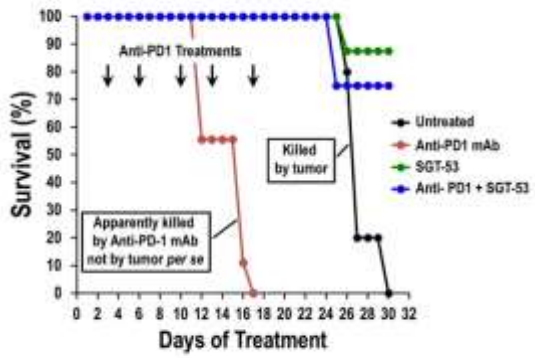

P458

Contribution of an immune system to RACPP mediated drug delivery

Dina Hingorani, PhD[1], Maria Camargo[1], Matthew Doan, BS[1], Joesph Aguilera[1], Stephen Adams[1], Sunil Advani[1],

[1]*University of California San Diego, La Jolla, CA, USA*

Background

The interaction of tumor and host derived stroma is a complex process involving enzymes including matrix metalloproteinases (MMPs), specifically MMP2 / 9 [1]. The lack of efficacy from small molecule inhibitors to MMPs [2,3] and new approaches of macrophage mediated drug delivery strategies [4], propelled us to test the contributions of intrinsic tumor cell vs host stroma in the recruitment of macrophages in-vivo. We tested the hypothesis that drug delivering peptides that target the tumor-immune interplay have improved therapeutic efficacy and specificity.

Methods

Cy5:Cy7 FRET based ratiometric activatable cell penetrating peptides (RACPPs) were used to image syngeneic WT and MMP2/9 KO Polyoma middle T (PyMT) orthotopic tumors in C57/Bl6 WT and KO mouse models. The excised tumors were stained F4/80 pan-macrophage antibody markers. ACPP carrying the tumor radiosensitiser monomethyl auristatin E (MMAE) along with Beta integrin targeting moiety cRGD was injected in syngeneic lung tumor cell line (LL2) implanted in immune compromised athymic Nu/Nu mice and immune competent C57/Bl6 mice. The amount of released MMAE drug was analyzed in tumor vs surrounding normal tissue by LC-MS.

Results

The normalized Cy5/Cy7 ratio for the WT tumors established in WT mice (1.87 ± 0.11) was significantly higher than the ratio for the DKO tumors in WT mice (1.34 ± 0.07; $p < 0.003$) or the DKO tumors in DKO mice (1.20 ± 0.08; $p < 0.0002$) (Figure 1A, 1B). As expected, the majority of the immune infiltration was at the periphery of the tumor with WT tumor having a significantly greater ability to recruit host macrophages into the tumor than DKO tumor cells (Figure 1C-1F). At 24 h, biodistribution measurements of released MMAE drug, revealed a higher tumor/muscle ratio of delivered drug (14 fold) in immune competent mice compared to immune-deficient mice(Figure 1G, 1H).

Conclusions

Interestingly, genotype tumor cells was more important than the host stromal component in promoting MMP-2/-9 activity in the tumors in this model system. Importantly, exploiting drugs that inhibit macrophage recruitment into tumors [4] and harnessing macrophage mediated drug delivery [5,6] in the tumor extracellular matrix may prove superior in eradicating tumors. In summary, our novel RACPP-drug conjugates can selectively localize to tumors and where they can be cleaved both by tumor cells and tumor-associated macrophages to provide improve the therapeutic index of systemically administered drugs [6,7].

References

1. Noël A, Jost M, Maquoi E. Matrix metalloproteinases at cancer tumor–host interface. InSeminars in cell & developmental biology 2008 Feb 1 (Vol. 19, No. 1, pp. 52-60). Academic Press.
2. Gura, Trisha. "Systems for identifying new drugs are often faulty." (1997): 1041-1042.
3. Richmond, Ann, and Yingjun Su. "Mouse xenograft models vs GEM models for human cancer therapeutics." (2008): 78-82.
4. Panni, Roheena Z., David C. Linehan, and David G. DeNardo. "Targeting tumor-infiltrating macrophages to combat cancer." Immunotherapy 5, no. 10 (2013): 1075-1087.
5. Li, Fu, Michelle Ulrich, Mechthild Jonas, Ivan J. Stone, Germein Linares, Xinqun Zhang, Lori Westendorf, Dennis R. Benjamin, and Che-Leung Law. "Tumor-Associated Macrophages Can Contribute to Antitumor Activity through FcγR-Mediated Processing of Antibody–Drug Conjugates." Molecular cancer therapeutics 16, no. 7 (2017): 1347-1354.
6. Buckel, Lisa, Elamprakash N. Savariar, Jessica L. Crisp, Karra A. Jones, Angel M. Hicks, Daniel J. Scanderbeg, Quyen T. Nguyen et al. "Tumor radiosensitization by monomethyl auristatin E: mechanism of action and targeted delivery." Cancer research 75, no. 7 (2015): 1376-1387.
7. Crisp, Jessica L., Elamprakash N. Savariar, Heather L. Glasgow, Lesley G. Ellies, Michael A. Whitney, and Roger Y. Tsien. "Dual targeting of integrin αvβ3 and matrix metalloproteinase-2 for optical imaging of tumors and chemotherapeutic delivery." Molecular cancer therapeutics 13, no. 6 (2014): 1514-1525.

Ethics Approval

All animal were performed under approved IACUC protocol number S15290 at the University of California San Diego.

Figure 1.

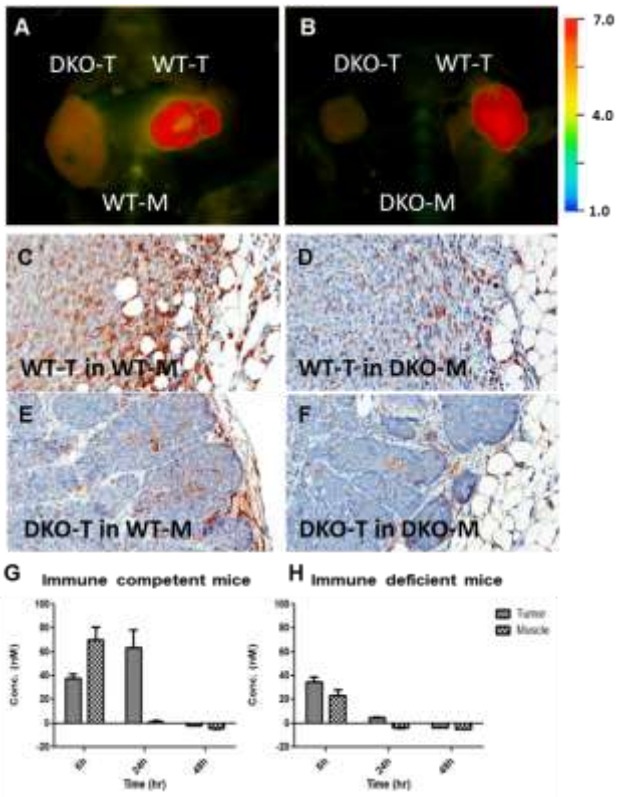

P459

Detection of tumor-specific antibodies and their binding regions in mice cured from B78 melanoma

Anna Hoefges, MS[1], Amy Erbe, PhD[1], Drew Melby[1], Alexander Rakhmilevich, MD, PhD[1], Jacquelyn Hank, PhD[1], Claire Baniel, BS, BA[1], Clinton Heinze, BS[1], Irene Ong, PhD[1], Sean Mcilwain, PhD[1], Hanying Li, PhD[2], Richard Pinapati, PhD[2], Bradley Garcia, PhD[2], Jigar Patel, PhD[2], Zachary Morris, MD, PhD[1], Paul Sondel, MD, PhD[1]

[1]University of Wisconsin Madison, Madison, WI, USA
[2]Roche Sequencing Solutions, Inc., Madison, WI, USA

Background
Antibodies can play an important role in both innate and adaptive immune responses against cancer. We present a study that identifies possible new targets for antibody-based immunotherapy. We have developed a peptide array to assess potential protein-targets for antibodies that are activated in melanoma-cured mice through a combined immunotherapy regimen. By using Roche-Nimblegen's unique technology, we were able to test antibody-reactivity to ~650 proteins, using 12 separate serum samples per array chip. This technology will enable us to accurately determine the linear peptide-binding sequences recognized by the anti-tumor antibodies produced in cured mice.

Methods
Mice bearing large GD2-expressing B78 melanoma tumors were treated with a triple-combination of immunotherapy capable of inducing an "in situ vaccine" effect, enabling mice to be cured of their tumors with long-term immune memory [1,2]. This triple combination therapy includes external beam radiation to the tumor, intratumoral injection of a tumor-specific immunocytokine (anti-GD2 mAb linked to IL2) and anti-CTLA-4. Serum was collected from mice when mice had macroscopic tumors, as well as after mice were cured of large tumors and rejected a re-challenge with the same tumor type. Using flow cytometry, mouse serum was tested for antibody-binding against B16 (parental cell line of B78). Afterwards, the serum was used on a Roche-Nimblegen peptide-array to determine specific antibody-protein binding sites and affinity towards the tumor.

Results
We analyzed sera from 4 mice that rejected established B78 tumors with this combination immunotherapy and compared their early-tumor and post-rejection serum antibody binding. We also included serum from mice bearing large tumors and analyzed the data generated by assessing differential expression in mice that rejected tumors vs mice that had large tumors or serum from naïve mice. Flow results showed increased signal after treatment. Multiple proteins of interest were selectively identified on the peptide array with sera from the 4 mice that rejected their tumors. We are continuing to investigate these proteins.

Conclusions
We were able to identify murine proteins that were selectively recognized by antibodies in mice that were cured of a tumor with immunotherapy but not by sera from to mice that were not cured of the same tumor or sera from naïve mice. The identified candidates may be new targets for antibody-based therapies, for adaptive recognition and could help in the development of new treatments.

References
1. Morris ZS, et al. Cancer Research, 76:3929-3941, 20162. Morris ZS, et al. Cancer Immunology Research, Published online, May 2018

P460

Chemotherapy induced immunogenic cell death and response to STING agonist in high-grade serous ovarian cancer

Sarah Nersesian, MSc[1], Nichole Peterson, MSc[1], Julie-Ann Francis[1], Madhuri Koti, DVM, MVSc, PhD[1]

[1]Queen's University, Kingston, ON, Canada

Background
High Grade Serous Carcinoma of the ovary (HGSC) is mostly diagnosed at late stages and primarily treated with surgery followed by platinum/taxane-based chemotherapy. Unfortunately, majority of the patients exhibit resistance to chemotherapy and ultimately succumb to the disease. We previously demonstrated that chemotherapy naïve HGSC patient tumours with early recurrence show an

immunosuppressed or immunologically cold pre-existing tumour immune microenvironment with decreased expression of genes involved in Type I Interferon (IFN1) and T helper type 1 response. We also reported the efficacy of a novel "Stimulator of Interferon Genes" agonist in combination with carboplatin chemotherapy and PD-1 immune checkpoint blockade using the ID8-Trp53-/- immunocompetent mouse model of HGSC. Based on previous reports on the distinct immunogenic cell death inducing potential of carboplatin and doxorubicin and that HGSC patients are treated with liposomal doxorubicin as a second line chemotherapy, the current study was performed to determine whether the effect of STING agonist can be further enhanced using a specific chemotherapy drug.

Methods

ID8-Trp53-/- and ID8-Trp53-/-;Brca1-/- cells were implanted in C57/BL6 immunocompetent mouse model of HGSC. At four-week time point established tumours were treated with carboplatin or doxorubicin chemotherapy followed by STING agonist treatment. Immune profiling was performed at early mid and late time points by measuring systemic responses in splenic immune cells, plasma cytokine profiles and tumour immune transcriptomic profiling. Overall survival was measured as per our previously established protocols.

Background

High Grade Serous Carcinoma of the ovary (HGSC) is mostly diagnosed at late stages and primarily treated with surgery followed by platinum/taxane-based chemotherapy. Majority of the patients exhibit resistance to chemotherapy and ultimately succumb to the disease. Contemporary immunotherapies targeting the PD-1/PD-L1 immune checkpoints have not proven be efficacious in HGSC patients. Based on our patient tumour based findings [1] that chemotherapy naïve HGSC patient tumours, with early recurrence and resistant to chemotherapy, show an immunologically cold pre-existing tumour immune microenvironment (TME), we conducted pre-clinical evaluation of a novel "Stimulator of Interferon Genes" (STING) agonist in combination with carboplatin chemotherapy and PD-1 immune checkpoint blockade using the ID8-Trp53-/- mouse model of HGSC [2]. This report demonstrated the potential of STING agonists in sensitization of ovarian tumours to PD-1 immune checkpoint blockade therapy, for ovarian cancer patients. Given the distinct immunogenic cell death (ICD) inducing potential of carboplatin and doxorubicin and that HGSC patients are treated with liposomal doxorubicin as a second line chemotherapy, the current study was performed to determine whether the effect of STING agonist can be further enhanced using a specific chemotherapy drug.

Methods

ID8-Trp53-/- cells were implanted in C57/BL6 immunocompetent mice. At four-week time point, established tumours were treated with carboplatin or doxorubicin chemotherapy followed by STING agonist treatment. A custom NanoString panel of 60 known ICD associated genes was used to measure the chemotherapy type related gene expression changes at early time point post single or combination treatments. Doxorubicin treated tumours showed significantly higher expression of Cxcl10, Cd274, Isg15, Psmb9 and Calr. Addition of STING agonist to each chemotherapy treatment showed significantly higher expression of Cxcl10 and IsG15 in the doxorubicin + STING agonist treated mice compared to carboplatin. Interestingly, Ccl5 gene expression was higher in the tumours from carboplatin treated mice compared to those treated with doxorubicin. Plasma cytokine profiles showed distinct profiles of interferon induced cytokines post treatment. Doxorubcin + STING agonist treated mice showed longer survival compared to carboplatin + STING agonist treated mice.

Results

Findings from our study demonstrate that efficacy of STING agonists can be further exemplified by selectively combining with potent ICD inducing chemotherapy.

Conclusions

Our study shows that clinical potential of STING agonists can be best achieved via combining with a potent ICD inducing chemotherapy and are key to the design of STING agonist based clinical trials.

Acknowledgements

This study was funded by the Canadian Institutes for Health Research and Early Research Award support to MK.

References

1. Au KK, Le Page C, Ren R, Meunier L, Clément I, Tryshkin K, Peterson N, Kendall-Dupont J, Childs T, Francis JA, Graham CH, Craig A, Squire JA, Mes-Masson AM, and Koti M. STAT1 induced intratumoural TH1 immunity predicts chemotherapy resistance in high-grade serous ovarian cancer. Journal of Pathology: Clinical Research. 2016. Sep 19;2(4):259-270.

2.Ghaffari A, Peterson, Khalaj N NK, Robinson A, Francis JA and Koti M. STING agonist therapy in combination with PD-1 immune checkpoint blockade enhances response to carboplatin chemotherapy in high-grade serous ovarian cancer. British Journal of Cancer. 2018. Jul 26. doi: 10.1038/s41416-018-0188-5.

P462

Fractionated radiation with PD-1 blockade promotes anti-tumor activity in mouse head and neck cancer

Go Inokuchi, MD, PhD[1], Elizabeth McMichael, PhD[2], Masahiro Kikuchi, MD, PhD[1], David Clump, MD PhD[1] Robert Ferris[1]

[1]University of Pittsburgh, Pittsburgh, PA
[2]University of Pittsburgh Hillman Cancer Center, Pittsburgh, PA, USA

Background

Resistance to RT could be explained by the increased myeloid cells and upregulation of PD-L1 on tumor and myeloid cells. As 2Gy fractionated radiation therapy (RT) is the standard of care in HNSCC, pre-clinical investigations suggest that the addition of PD-1 blockade to RT could be clinically beneficial. Here, we investigated the immune response in a murine model of HNSCC to fractionated irradiation with or without PD-1 blockade.

Methods

Mice were inoculated with 2x106 murine tonsil epithelium E6/E7/H-ras transformed head and neck cancer cells (MEER) s.c. into both the neck and flank. Ten days following implantation, the neck tumor was irradiated with 20 Gy in 10 fractions. Anti-PD-1 therapy began following the initial dose of RT and continued every 3-4 days thereafter. Tumor growth was monitored and tumor volume was determined. Splenic and tumors tissues were collected 4 days after the final radiation dose for flow cytometric analysis.

Results

The effects of conventional 2Gyx10 fractionated RT was found to be greatly enhanced by the addition of PD-1 blockade, reducing tumor volumes by 7.2-fold. No clear abscopal effect on the non-irradiated flank tumor was observed. 2Gyx10 RT was better able to recruit myeloid and CD8+ T cells to the tumor site, an increase of 1.5-fold, as compared to 2Gyx5 fractionation. RT was shown to upregulate PD-L1 both on CD45- tumor cells and CD45+CD11b+ myeloid cells ($p<0.05$). Fractionated RT was also shown to increase CD8+ T cells activation through the production of IFN-gamma and TNF-alpha ($p<0.001$).

Conclusions
Concurrent PD-1 blockade with fractionated 2Gyx10 RT could activate the anti-tumor response in mouse head and neck cancer and warrants further investigation.

P463

HfO2 nanoparticles exposed to radiotherapy generate abscopal effect through activation of CD8+ T cells.

Audrey Darmon, BS[1], Ping Zhang, MD, PhD[1], Sébastien Paris, PhD[1]

[1]*Nanobiotix, Paris, France*

Background
When exposed to radiotherapy (RT), nanoparticles of hafnium oxide (HfO2-NP) increase radiation dose deposition from within the cancer cells. HfO2-NP is intended for a single intratumor injection. Results of phase II/III in locally advanced Soft Tissue Sarcoma patients demonstrated a significant superiority and clinical benefits of HfO2-NP activated by radiotherapy compared to the standard of care, with a good local tolerance among this patient's population, validating their first-in-class mode of action. HfO2-NP+RT is currently evaluated in six other clinical trials including head and neck, prostate, liver and rectum cancers. Moreover, preclinical studies have demonstrated that HfO2-NP+RT can generate the abscopal effect, where RT alone cannot. Here, we further explored the role of T cells infiltrates in the establishment of abscopal effect following HfO2-NP intratumor injection and activation with RT.

Methods
In a first experiment, CT26 (murine colorectal cancer cells) were subcutaneously injected in both flanks of BALB/c mice. Once the right tumors reached a mean tumor volume of 115±30 mm3, they were intratumorally injected with HfO2-NP (or vehicle) and irradiated 24 hours later with 4Gy per fraction for 3 consecutive days. Tumors from both flanks were collected 3 days after the last RT fraction and immune cell infiltrates were measured using immunohistochemistry (IHC) and digital pathology analyses.In order to investigate the specific role played by CD8+ T cells in the antitumor immune response and the abscopal effect, the experiment was subsequently repeated with CD8+ T cells depletion prior treatment with HfO2-NP+RT or RT alone (use of anti-CD8 antibody).

Results
In the first experiment, the abscopal effect was observed in the group treated with HfO2-NP+RT only. Correspondingly, IHC analyses showed a stark increase of CD8+ T cells infiltrates and other immune cells in both flanks of mice with HfO2-NP+RT, while RT alone had no significant effect.In the CD8+ T cells depletion experiment, no abscopal effect was observed. Besides, the control of the tumor treated with HfO2-NP + RT was less efficient than the control of the tumor treated with HfO2-NP+RT in absence of CD8+ T cells depletion.

Conclusions
These in vivo data suggest that the immunogenic conversion of the tumor microenvironment induced by HfO2-NP+RT triggers the abscopal effect through the activation of CD8+ T cells. HfO2-NP+RT may potentiate a pro-inflammatory environment suitable for immune enabling drugs: it may act as effective in-situ cancer vaccine and be combined with immunotherapeutic agents across oncology.

Ethics Approval
All experiments were approved by the Institutional Animal Care and Use Committee of Institut Gustave Roussy, approval number 2016_ 031_4340.

P464 **Abstract Travel Award Recipient**

Molecular targeted radiotherapy (MTRT) enhances the efficacy of immunotherapy increasing complete response rates of both local and distant disease in a "cold" tumor models

Ravi Patel, MD, PhD[1], Reinier Hernandez, PhD[1], Peter Carlson[1], Ryan Brown[1], Abigail Jaquish[1], Luke Zangl[1], Raghava Sriramaneni, PhD[1], Joseph Grudzinski, PhD[1], Bryan Bednarz, PhD[1], Jamey Weichert, PhD[1], Paul Sondel, MD, PhD[1], Zachary Morris, MD, PhD[1]

[1]*University of Wisconsin, Madison, WI, USA*

Background

Studies have shown that in some immunologically "cold" tumor models, distant disease can suppress the effect of in situ vaccines (IS) even at the primary site[1]. This may be overcome by delivering low dose radiotherapy (RT) to all tumor sites; yet delivering large field RT to metastatic disease can cause systemic lymphopenia. We have developed a strategy using a molecular targeted RT (MTRT), Y90-NM600 (YN6), that has selective uptake in nearly any tumor type or location to deliver RT to all sites of disease in a functionally "cold" metastatic tumor model.

Methods

Large (~150-200 mm3) B78 melanoma primary tumors and occult secondary (non-palpable at treatment) as well as B16 melanoma lung metastases were established in syngeneic mice. Combinations of immune checkpoint inhibition (ICI; anti-CTLA-4 and anti PD-1), IS (12 Gy RT + IT anti-GD2-mAb + IL2), or MTRT (50 µCi) were given [Figure 1]. Tumor growth was tracked to day (D) 30, Survival to D60, and mice with complete response (CR) were re-challenged with injection of B78 cells (D90) and unrelated Panc02 cells(D120). Tumor growth and survival studies were replicated in syngeneic 4T1 breast and NXS2 neuroblastoma models. Mechanistic studies using T-cell depletion, whole body external beam RT (WBEBRT), histology, and gene expression profiling were conducted.

Results

Tumor response was significantly improved with the addition of MTRT to each group, with highest response rate in the triple combination treatment group which had a CR as well as tumor specific immune memory in 83% of mice ($p < 0.05$). Development of secondary tumors and distant metastatic disease was also reduced in the triple combination treatment group (ICI + IS + MTRT), while dual treatment groups had varying levels of efficacy in treating primary, occult secondary, or metastatic disease [Figure 2]. Similar response and survival was replicated in 4T1 and NXS2 models with addition of MTRT. T-cell depletion revealed a reversal of the enhanced response seen with MTRT. Unlike MTRT, delivering WBEBRT did not enhance efficacy of immunotherapy. QPCR of MTRT gene expression demonstrated upregulation of STING/IFN/apoptosis pathways (Mx1/Ifnb/PDL1/DR5/ICAM1) that were greater than that achieved with equivalent doses of EBRT. Histological analysis of tumor samples showed significantly increased CD8+ infiltrates in the combination treatment group ($p < 0.05$).

Conclusions

Our results demonstrate that MTRT can effectively stimulate and enhance the generation of an immune response to combination IS and ICI immunotherapy treatments, enabling tumor eradication at primary, occult secondary, and metastatic sites of disease.

Acknowledgements

RSNA Fellow Award, ASCO Young Investigator Award, UW 20/20 Award, UW Cancer Center Core Grant

References

1. Morris, ZS, et al. Cancer Immunol Res 2018

Jul;6(7):825-34

Ethics Approval

This study was approved by the UW Institutional Animal Care and Use Committee.

Figure 1.

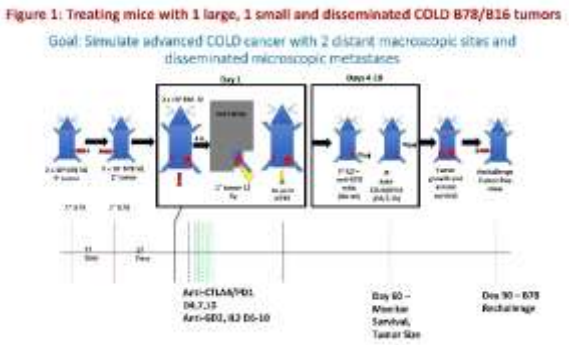

Figure 2.

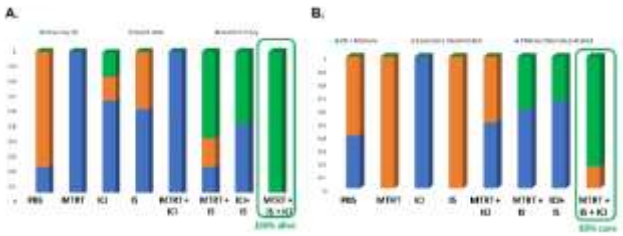

P465

Comparison of peripheral immune response during chemoradiotherapy (CRT) with and without PD-1 blockade in patients with head and neck squamous cell carcinoma (HNSCC)

Juan Callejas-Valera, PhD[1], Juan Callejas-Valera, PhD[1], Daniel Vermeer[1], Christopher Lucido[2], Caitlin Williamson[1], Marisela Killian[1], William Spanos, MD[1], Paola Vermeer, PhD[1], Steven F. Powell, MD[3]

[1]*Sanford Research, Sioux Falls, SD, USA*
[2]*University of South Dakota, Sioux Falls, SD, USA*
[3]*Sanford Cancer Center, Sioux Falls, SD, USA*

Background

While inhibitors of the programmed death-1 and its ligands (PD-1 and PD-L1/2) are active in recurrent/metastatic (R/M) HNSCC, their effects during curative intent therapy are unknown. Previous translational data demonstrated that standard, high-dose CRT decreases circulating CD4+ and CD8+ T-cell populations while increasing PD-1 expression and myeloid derived suppressor cells (MDSCs) [1]. To overcome this suppressive immunophenotype, we developed a clinical trial exploring the combination of the PD-1 inhibitor, pembrolizumab, with CRT using a low-dose chemotherapy regimen. Here we present data comparing the peripheral blood immune response during this novel therapy to standard CRT.

Methods

We evaluated peripheral blood mononuclear cells (PBMCs) from HNSCC patients from two clinical trials (NCT02586207, NCT01386632) and healthy volunteers (controls) to compare the peripheral blood immune response during CRT. Trial 1 used low-dose cisplatin (40 mg/m2 weekly x 6 doses) with pembrolizumab and Trial 2 used standard high-dose cisplatin (100 mg/m2 every 3 weeks x 3 doses) without PD-1 inhibition. We compared circulating immunocytes, including CD4+ and CD8+ T-cells, regulatory T-cells (T-regs), and MDSCs, utilizing multi-color flow cytometry at baseline, during (mid-treatment) and after (3 months post-radiation) CRT. Immune checkpoint expression (PD-1, TIM3, LAG3) on CD4/CD8+ cells was also compared between the groups. Changes in memory T-cell populations (effector memory; EM, central memory; CM, and effector memory RA; EMRA) were also evaluated.

Results

18 patient samples from trial 1 and 15 samples from trial 2 were viable for evaluation. Comparing the two treatments, there was no significant difference in key immunocyte populations during therapy (Figure 1).

However, there was a significant decline in PD-1 expressing CD4+ and CD8+ T-cell populations during treatment with PD-1 inhibition and low-dose chemotherapy compared to standard treatment (Figure 2). Expression of other markers of immune exhaustion (TIM3, LAG3) rise in both groups throughout treatment. Memory T-cell populations (Figure 3) show that the pembrolizumab-based treatment increased the percentage of both EM and EMRA helper T-cells in contrast with standard treatment.

Conclusions

Our data demonstrates that the addition of a PD-1 inhibitor to a low-dose cisplatin CRT regimen can reduce circulating PD-1+ T-cells during therapy. However, these populations, as well as other markers of T-cell exhaustion rise by the end of therapy and could play a role in immune escape. Further characterization of this immune response is needed to determine the best approach to add novel immunotherapy agents in this treatment setting.

Acknowledgements

Sanford Research Flow Cytometry CoreSupported by a Center of Cancer Biology Research Excellence (COBRE) grant (5P20GM103548-08) from the National Institutes of Health

References

1. Parikh F, Duluc D, Imai N, Clark A, Misiukiewicz K, Bonomi M, Gupta V, Patsias A, Parides M, Demicco EG, Zhang DY, Kim-Schulze S, Kao J, Gnjatic S, Oh S, Posner MR, Sikora AG. Chemoradiotherapy-induced upregulation of PD-1 antagonizes immunity to HPV-related oropharyngeal cancer. Cancer Res. 2014;74(24):7205-16.

Ethics Approval

Trial 1 (NCT02586207) was approved by the Western Institutional Review Board (WIRB), approval number 20152167. Trial 2 (NCT01386632)was approved by the Sanford Research Institutional Review Board (IRB), approval number MODCR00000588.

Figure 1. Peripheral Blood Immunocyte Response during CRT

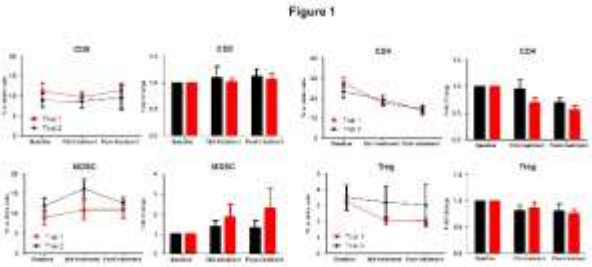

Figure 2. Changes in Immune Checkpoint Expression

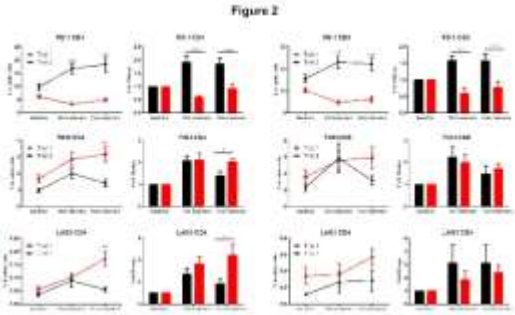

Figure 3. The Effect on Memory T-cell Response

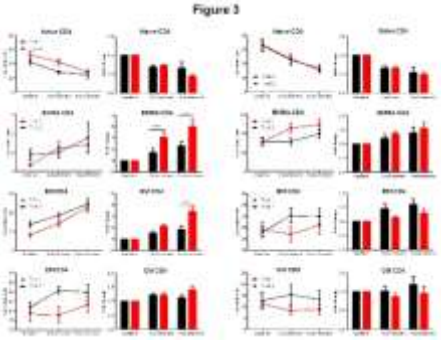

P466

TGF beta blockade enhances radiotherapy abscopal efficacy effects in combination with anti-PD1 and anti-CD137 immunostimulatory monoclonal antibodies.

Inmaculada Rodriguez[2], Lina Mayorga[1], Tania Labiano[3], benigno Barbes[1], inaki etxeberria[2], Mariano Ponz-Sarvise[1], arantza Azpilicueta[2], elisabeth Bolanos[2], Miguel F.Sanmamed[1], Pedro Berraondo[2], Felipe Manuel Alfonso Calvo[1], Mary Helen Barcelos-Hoff[4], Jose Luis Perez-Gracia[1], Ignacio Melero, MD, PhD[3*], Maria Rodriguez-Ruiz, MD, PhD[1]

[1]Clinica Universidad de Navarra, Pamplona, Spain
[2]Centro de Investigacion Medica Aplicada, Pamplona, Spain
[3]Complejo Hospitalario de Navarra, Pamplona, Spain
[4]University of California, San Francisco, San Francisco, CA, USA

Background

Radiotherapy can be synergistically combined with immunotherapy in mouse models, extending its efficacious effects outside of the irradiated field (abscopal effects) [1]. We previously reported that a regimen encompassing local radiotherapy in combination with anti-CD137 plus anti-PD-1 mAbs achieves potent abscopal effects against syngeneic transplanted murine tumors up to a certain tumor size. Knowing that TGFβ expression or activation increases in irradiated tissues, we tested whether TGFβ blockade may further enhance abscopal effects in conjunction with the anti-PD-1 plus anti-CD137 mAb combination [2].

Methods

Mice bearing bilateral MC38 or 4T1 tumors were randomly assigned to 6 groups receiving or not radiotherapy (8Gy/3fx), in combination or not with intraperitoneal antibodies (anti-PD1 plus anti-CD137 and/or anti-TGFβ). Tumor tissue was processed to obtain single-cell suspensions for flow cytometry analyses Levels of TGFβ-1 in mouse tumor tissue homogenates and IFNγ in mouse plasma samples were measured by commercial ELISAs.

Results

TGFβ blockade with 1D11, a TGFβ neutralizing monoclonal antibody, markedly enhanced abscopal effects and overall treatment efficacy against subcutaneous tumors of either 4T1 breast cancer cells or large MC38 colorectal tumors. Increases in CD8 T cells infiltrating the non-irradiated lesion were documented upon combined treatment, which intensely expressed Granzyme-B as an indicator of cytotoxic effector capability.

Conclusions

Radiotherapy-induced TGFβ hampers abscopal efficacy even upon combination with a potent immunotherapy combination. Therefore TGFβ blockade in combination with radioimmunotherapy regimens results in greater efficacy.

Acknowledgements

We are in debt to Dr. Alan Korman (BMS, San Francisco CA) for his kind gift of monoclonal antibodies. We acknowledge generous help from Drs. Martinez-Monge, Aristu, Castañon and Gil-Bazo from the department of oncology at CUN. Excellent dosimetry by Arantza Zubiria and dedicated animal care by Eneko Elizalde are also acknowledged.

Trial Registration

NA

References

1. Rodriguez-Ruiz ME, Rodriguez I, Barbes B. Abscopal effects of radiotherapy are enhanced by combined immunostimulatory mAbs and are dependent on CD8 T cells and crosspriming. Cancer Res. 2016 Oct 15;76(20):5994-6005.
2. Vanpouille-Box C, Diamond JM, Pilones KA. TGFβ is a master regulator of radiation therapy-induced antitumor immunity. Cancer Res. 2015 Jun 1;75(11):2232-42.

Ethics Approval

The study was approved by Navarra Institutution's Ethics Board, approval number 117/14

P467

Augmenting immunity with IAP antagonists in PDAC

Kevin Roehle, PhD[1], Michael Dougan, MD, PhD[1], Stephanie Dougan, PhD[2]

[1]Dana-Farber Cancer Institute, Bosotn, MA, USA
[2]Massachusetts General Hospital, Boston, MA, USA

Background
Pancreatic ductal adenocarcinoma (PDAC) is responsible for about 7% of all cancer-related deaths in the US. PDACs are fibrotic and dense tumors with little vasculature, and are rapidly metastatic. Thus far, cancer-immunotherapy with immune checkpoint blocking antibodies have largely failed in PDAC. The Inhibitor of Apoptosis (IAP) protein family comprises a diverse group of proteins, many of which have immunoregulatory roles. IAP antagonists are small molecule drugs that primarily inhibit cellular (c-)IAP1 and c-IAP2 protein leading to TNFa mediated apoptosis in tumor cells through alternative NF-kB signaling. In immune cells IAP antagonism leads to increased alternate NF-kB signaling, leading to increased survival of B cells, activation of dendritic cells and supporting activation of T cells in a costimulatory manner.

Methods
We evaluated the effects of the IAP antagonist LCL-161 in multiple syngeneic models of pancreatic cancer.

Results
Although LCL-161 did not induce TNFa mediated apoptosis in any of our tumor cell lines in vitro, we were able to induce robust immune-mediated regressions in an orthotopic and subcutaneous tumor models.

Conclusions
These responses were dependent on CD8 and CD4 T cells, and we show evidence for a direct effect of LCL-161 in augmenting T cell priming in pancreatic cancer.

P468

Transcriptomic profiles conducive to immune-mediated tumor rejection in human breast cancer skin metastases treated with Imiquimod

Mariya Rozenblit, MD[1], Wouter Hendrickx, PhD[2], Adriana Heguy[3], Luis Chiriboga[3], Cynthia Loomis[3], Karina Ray[3], Farbod Darvishian, MD[3], Mikala Egeblad, PhD[4], Davide Bedognetti, MD, PhD[5], Sylvia Adams, MD[3]

[1]Yale University, Connecticut, CT, USA
[2]Sidra Medicine, Doha, Qatar
[3]NYU, New York, USA
[4]Cold Spring Harbor Laboratory, Cold Spring Harbor, NY, USA
[5]SIDRA, Doha, Qatar

Background
Imiquimod is a topical toll-like-receptor-7 agonist currently used for treating basal cell carcinoma. Recently, imiquimod has demonstrated tumor regression in melanoma and breast cancer skin metastases. However, the molecular perturbations induced by imiquimod in breast cancer metastases have not yet been characterized. Here, we describe transcriptomic profiles associated with responsiveness to imiquimod in breast cancer skin metastases.

Methods
Baseline and post-treatment tumor samples from eight patients treated with imiquimod in a clinical trial were profiled using Nanostring nCounter ® Human v1.1 PanCancer Immune Profiling Panel. Two of the patients had stable disease during the initial study and were found to have a systemic complete clinical response after subsequent treatment with

fulvestrant after study completion which continued for several years. On follow up, these two patients also had disease remission for two years. An additional patient had a local partial anti-tumor response after eight weeks of imiquimod treatment and was labeled as a partial responder (PR). Five of the eight patients did not have an anti-tumor response and were defined as non-responders (NR). An integrative analytic pipeline was used to analyze gene expression data including pathway analysis and deconvolution.

Results

We showed that tumors from patients who achieved a durable clinical response displayed a permissive microenviroment, substantiated by the upregulation of transcripts encoding for molecules involved in leukocyte adhesion and migration, cytotoxic functions, and antigen presentation (Figure 1AB). Imiquimod triggered a strong T-helper-1 (Th-1)/cytotoxic immune response, characterized by the coordinated upregulation of Th-1 chemokines, migration of Th-1 and cytotoxic T cells into the tumor, and activation of immune-effector functions, ultimately mediating tumor destruction (Figure 1C).

Conclusions

Topical imiquimod can induce a robust immune response in breast cancer metastases, and this response is more likely to occur in tumors with a pre-activated microenvironment. In this setting, imiquimod could be utilized in combination with other targeted immunotherapies to increase therapeutic efficacy.

Acknowledgements

The work was supported by the AMA Foundation Seed Grant

Ethics Approval

The clinical trial was approved by the New York University Institutional Review Board

Figure 1.

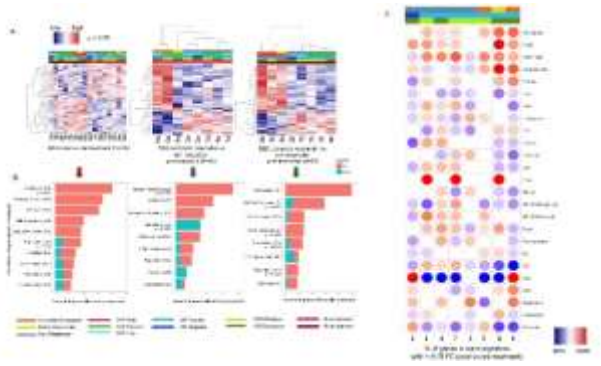

P469

TCR repertoire correlates of response in tumor-bearing mice treated with radiotherapy and CTLA-4 blockade

Nils-Petter Rudqvist, PhD[1], Claire Lhuillier, PhD[1], Erik Wennerberg, PhD[1], Jennifer Sims, PhD[2] , Sandra Demaria, MD[1]

[1]*Weill Cornell Medical College, New York, NY, USA*
[2]*Memorial Sloan Kettering Cancer Center, New York, NY, USA*

Background

Tumor-targeted radiation therapy (RT) in combination with immune checkpoint blockade can activate tumor-specific T-cells to reject tumors. Yet, predictive features of effectively primed T cell repertoires (TCR) remain poorly understood. Using the 4T1 mouse model of triple negative breast cancer, where RT+CTLA-4 blockade elicits an anti-tumor T cell response that controls both the irradiated tumor and non-irradiated lung metastases and extends survival, we previously reported increased intratumoral CD8/CD4 ratio and CD8+ T cell clonality following RT+anti-CTLA-4 treatment [1]. Here, we determined the longitudinal changes of the TCR repertoires in the 4T1 carcinoma and its

correlates with treatment response.

Methods

To analyze longitudinally the TIL repertoire before and after treatment with RT+anti-CTLA-4, mice were inoculated in both flanks with 4T1 cells (n=8/group). One tumor was resected 2 days before treatment (pre-TX) and the other was treated with RT (3X8 Gy) or anti-CTLA-4 antibody (3x200 μg i.p.) monotherapy or in combination and resected 1 day after treatment when immune-mediated tumor rejection is occurring in tumors treated with RT+anti-CTLA-4 (post-TX). No local tumor recurrence was observed, but mice succumbed of lung metastasis with the largest increase in survival (vs. untreated) in mice given RT+anti-CTLA-4 (p=0.0041). To assess the TIL TCR repertoire, dual-stage PCR amplification and high-throughput sequencing of the TCRa and b CDR3 regions was performed using mRNA isolated from total tumor.

Results

In tumors treated with RT and RT+anti-CTLA-4, both the TCRa and b repertoires increased in clonality compared to pre-TX, whereas a smaller increase in TCRb clonality was found after anti-CTLA-4 monotherapy. We have previously characterized the TCRb repertoire of expanded and activated CD8+ T cells recognizing the AH1 epitope from gp70 antigen (a tumor antigen expressed by 4T1 cells) in tumors of mice treated with RT+anti-CTLA-4 [1]. Using GLIPH [2], we identified a major AH1-specific CDR3b motif and found it present in pre-TX tumors of all animals, and its frequency increased in mice treated with RT or RT+anti-CTLA-4, consistent with our previous findings. In contrast, the V-J Jensen-Shannon divergence, assessed excluding AH1-specific T cells, was higher between pre- and post-TX tumors in all mice treated with RT, (independent of anti-CTLA-4 treatment) and correlated strongly with survival (cox regression; p=0.00054), suggesting priming and expansion of T cells targeting antigens other than AH1.

Conclusions

Together these data support the dominant role of RT in priming emergent or low-abundance T cell clonotypes, rather than the driving of already-prevalent clonotypes.

References

1. Rudqvist NP, Pilones KA, Lhuillier C, Wennerberg E, Sidhom JW, Emerson RO, Robins HS, Schneck J, Formenti SC, Demaria S. Radiotherapy and CTLA-4 blockade shape the TCR repertoire of tumor-infiltrating T cells. Cancer Immunol Res. 2018; 6(2): 139-150.
2. Glanville J, H. Huang A, Nau O, Hatton LE, Wagar F, Rubelt X, Ji A, Han SM, Krams C, Pettus N, Haas CSL, Arlehamn A, Sette SD, Boyd TJ, Martinez S, Davis MM. Identifying specificity groups in the T cell receptor repertoire. Nature. 2017; 547(7661): 94-98.

Ethics Approval

All experiments were approved by the Weill Cornell Medicine Institutional Animal Care and Use Committee, approval number 2015-0028.

P470

Targeting DNA damage response promotes anti-tumor immunity through STING-mediated T-cell activation in small cell lung cancer

Triparna Sen, PhD[1], Bertha Leticia Rodriguez[1], Limo Chen, PhD[1], Naoto Morikawa[1], Junya Fujimoto[1], Lixia Diao[1], Youhong Fan[1], Jing Wang[1], Bonnie Glisson[1], Ignacio Wistuba, MD[1], Julien Sage[2], John Heymach[1], Don Gibbons, MD[1], Lauren Byers, MD[1]

[1]UT MD Anderson Cancer Center, Houston, TX, USA
[2]Stanford University, Houston, TX, USA

Background

Despite recent advances in the use of immunotherapy, only a minority of small cell lung

cancer (SCLC) patients respond to immune checkpoint blockade (ICB) with programmed cell death protein 1 (PD-1) or programmed death ligand 1 (PD-L1) antibodies as monotherapy or combination. We have previously established that SCLC is vulnerable to agents targeting the DNA damage response (DDR) pathway, including inhibitors of PARP and CHK1, and these findings have led to several clinical trials of DDR inhibitors for SCLC. Our recent findings demonstrate that CHK1 inhibitor, prexasertib, potentiate the anti-tumor response of PD-L1 blockade in SCLC. In the present study we have established the efficacy of combined PARP (olaparib) and PD-L1 blockade and further elucidated the underlying mechanism of DDR-mediated anti-tumor immune response in SCLC models.

Methods

SCLC models were treated with small molecule inhibitors prexasertib or olaparib with or without anti-PD-L1. End point analyses were done by immunoblot, immunohistochemistry, qRT-PCR, flow cytometry and reverse phase protein array (RPPA).

Results

We treated the tumor bearing B6129F1 mice with either IgG, olaparib (100mg/kg,4/7), anti-PD-L1 or combination. By 10days, all mice treated with olaparib+anti-PD-L1 combination had a complete tumor regression with no tumor growth upto 80days. Co-targeting DDR+PD-L1 significantly increased the level of CD8+ cytotoxic-T cell infiltration and decreased PD-1+/TIM3+ exhausted T-cell population ($p<0.0001$). CD8 depletion was able to reverse the anti-tumor effect of the combination demonstrating the role of cytotoxic T-cell infiltration and function in DDR+PD-L1 response. Next, we established, by genetic knockdown studies, that DDR-mediated immune response was facilitated through activation of the STING/TBK1/IRF3 innate immune response pathway. STING pathway activation enhanced expression of Type-1 interferon gene IFNβ and downstream chemokines, CXCL10/CCL5 and resulted in T-cell recruitment.

Conclusions

Our results demonstrate,for the first time, the remarkable efficacy of the combination of PD-L1 blockade with PARP/CHK1 inhibition and provide a strong scientific rationale for combining these modalities in clinical trials for SCLC patients. Combining DDR inhibition with ICB leads to T-cell recruitment and enhanced effector cell function in SCLC tumors, mediated by the activation of the innate immune response pathway STING/TBK1/IRF3 and increased IFNβ. The immune profiling and correlative biomarker data from our study provide valuable mechanistic insight and indicate the subset of the patient population who are most likely to respond to these treatments. Because prexasertib, olaparib and other PARP inhibitors are already in clinical trials for SCLC, we expect that this hypothesis has the potential for rapid translation into the clinic.

P471

Mertk is a therapeutic target in combination with radiation to promote adaptive immune tumor responses

Garth Tormoen, MD, PhD[1], Jason Baird, PhD[2], Gwen Kramer, BS[2], Shelly Bambina[2], Marka Crittenden, MD, PhD[2], Michael Gough, PhD[2]

[1]Oregon Health & Science University, Portland, OR, USA
[2]Earl A. Chiles Research Institute, Portland, OR, USA

Background

Mertk is a member of the Tyro3-Axl-Mertk (TAM) family of receptors and regulates phagocytosis of dying cells by macrophages. Cancer cells killed by radiation therapy direct repolarization of macrophages into immune suppressive phenotypes. Mertk-/- mice grafted with immunogenic tumors have enhanced tumor control following ionizing

radiation compared to Mertkwt mice. Gas6 is the endogenous ligand for Mertk and its ability to signal through Mertk requires a post-translational vitamin k-dependent modification that is inhibited by warfarin.

Methods

Mertk-/- and WT mice were injected subcutaneously in the flank with 5E4 CT26 cells (BALB/c) or 5E6 Panc02-SIY cells (C57BL/6) and allowed to grow to 5 mm before treatment with 250 µg anti-CD8α antibodies, warfarin (0.5 mg/L drinking water) and subjected to a single dose of ionizing radiation (16 Gy) followed by 250 µg of OX40 or PBS I.P. 1-day post-RT. Peripheral blood was collected 6 days after RT and evaluated by Flow Cytometry for SIY-pentamer+CD8+ T cells.

Results

Radiation therapy results in tumor control in BALB/c mice, but tumor cure in Mertk-/- BALB/c mice. Tumor cure in Mertk-/- BALB/c mice was abrogated by depletion of CD8 T cells indicating that ligation of Mertk in tumor macrophages suppresses endogenous anti-tumor immunity following radiation therapy. Similarly, warfarin-treated mice had higher rates of tumor cure following radiation that was also abrogated by CD8 depletion. In C57BL/6 mice, Mertk-/- alone does not affect responses to radiation therapy in the Panc02 tumor model, but the combination of radiation therapy with anti-OX40 costimulation of T cell responses resulted in a significant increase in peripheral blood SIY+ CD8 T cells 5 days after treatment, and significantly improved survival compared to radiation alone.

Conclusions

Mertk-/- mice, and Mertkwt mice treated with warfarin to inhibit Gas6 experience increased tumor control following ionizing radiation in an adaptive-immune mediated manner in CT26 tumor models. In less immunogenic tumors, loss of Mertk-/- permitted tumor cure following radiation therapy when combined with the T cell costimulatory molecule OX40. These data demonstrate that Mertk suppresses adaptive immunity in irradiated tumors. Mertk is an attractive therapeutic target in combination with ionizing radiation and immune therapy to promote adaptive immune anti-tumor responses.

Ethics Approval

All animal studies were approved by the Earl A. Chiles Research Institute IACUC, Assurance No. A3913-01.

P472

Immunogenic tumor antigen is required in antitumor effect of cisplatin monotherapy and its combination with anti-PD-L1

Daiko Wakita, PhD[1], Toshiki Iwai, BS[1], Masamichi Sugimoto, PhD[1], Osamu Kondoh[1]

[1]*Chugai pharmaceutical CO., LTD., Kamakura, Japan*

Background

Although anti-PD-L1/PD-1 immunotherapy has shown marked clinical effect in a broad range of cancer, a subset of patients respond to monotherapy, and tumor mutation burden have been identified as potential predictive marker for responders. To extend the clinical benefits, combination of anti-PD-L1 and chemotherapy has been actively investigated. However the association of immunogenicity of neoantigen with antitumor effects of the combination of immunotherapy and chemotherapy is remained unknown. Here we investigated tumor antigen-specific T cell responses and antitumor effect of the anti-PD-L1 plus cisplatin combination therapy in mouse tumor models.

Methods

E.G7-OVA cell, expressing ovalbumin (OVA) gene as an immunogenic model tumor antigen, and its

parental less immunogenic EL4 cell were subcutaneously inoculated into C57BL/6 mouse. The tumor-bearing mice were intraperitoneally treated with anti-mouse PD-L1 mAb (anti-PD-L1; 10 mg/kg, three times a week) and cisplatin (CDDP; 1 mg/kg, once at Day1). For CD8+ cell depletion experiments, the tumor-bearing mice were treated with CDDP (4 mg/kg, once at Day1) and anti–mouse CD8 mAb (twice a week from one day before the treatment initiation). To evaluate cytolytic activity, CD8+ T cells isolated at Day7 were co-cultured with CFSE labeled-tumor cells and the frequency of dying-tumor cell was measured by flow cytometry.

Results

Anti-PD-L1 alone and CDDP alone exhibited significant antitumor effect in E.G7-OVA-bearing mice and the combination therapy resulted in further effect than the each monotherapy at Day15. In parallel with the therapeutic effect, CD8+ T cells from tumor-draining lymph node exhibited higher cytolytic activity against E.G7-OVA in monotherapy group than that in control group, and highest cytolytic activity was observed in combination group. In contrast, even after the combination therapy, cytolytic activity against parental EL4 cells was hardly detected. In addition, less immunogenic EL4 were insensitive to monotherapies with anti-PD-L1, CDDP and their combination. Moreover, in immunogenic E.G7-OVA-bearing model, the higher dose of CDDP (4 mg/kg) showed direct cytolytic activity as well as CD8+ T cell dependent antitumor effect, whereas only direct cytotoxic effect was observed in EL4-bearing model.

Conclusions

In our model, not only anti-PD-L1 alone but also CDDP alone enhanced T cell responses against immunogenic tumor antigen (OVA) but not neoantigens in EL4 cell, indicating the higher impact of immunogenic tumor antigen in antitumor effects during anti-PD-L1 therapy and chemotherapy. We are further exploring the contribution of subdominant epitopes of OVA or antigens other than OVA to antitumor effect.

P473

Enhancing abscopal responses to radiation therapy by manipulating autophagy

Takahiro Yamazaki, PhD[1], Marissa Rybstein[1], Aitziber Buqué, PhD[1], Ai Sato[1], Lorenzo Galluzzi, PhD[1]

[1]*Weill Cornell Medicine, New York, NY, USA*

Background

Macroautophagy (autophagy) is an evolutionary conserved cellular mechanism culminating with the lysosomal degradation of dispensable, damaged or potentially toxic cytoplasmic structures (e.g., permeabilized mitochondria). Autophagy helps cancer cells to adapt to harsh environmental conditions and to resist therapy. However, autophagy is also key for multiple steps of the anticancer immune response. Thus, whether autophagy should be inhibited or activated in the context of cancer therapy remains debated [1]. Since autophagy has been shown to play a key role in the removal of cytosolic DNA, which is one mechanism leading to type I interferon (IFN) secretion, and since type I IFN is required for systemic immune responses activated by radiation therapy (RT), we asked the question as to whether selectively inhibiting autophagy in cancer cells may boost the ability of RT to initiate anticancer immunity.

Methods

CRISPR/Cas9 technology was used to render mouse mammary carcinoma TSA and EO771 cells autophagy deficient, and chemical inhibitors of autophagy were employed. Autophagy-competent versus –deficient cells were characterized for autophagic proficiency (by immunoblotting), growth (in vitro and in vivo), resistance to cell death induced by starvation, chemotherapy and RT (by multicolor flow cytometry

and clonogenic assays) and production of type I IFN (by PCR and ELISA). Alongside, cancer cells were employed to generate synchronous tumors in immunocompetent syngeneic mice. Only one of these tumors (that was either autophagy-competent or-deficient) was irradiated in the context of CTLA4 inhibition, and the response of both the irradiated and non-irradiated (abscopal) tumor was monitored.

Results
Autophagy inhibition reduced the growth of mouse mammary carcinoma cells, in vitro and in vivo, limited their clonogenic potential (at baseline) and increased their sensitivity to multiple stressors. Moreover, pharmacological and genetic autophagy inhibition increased the capacity of mouse mammary carcinoma cells to secrete type I IFN in response to radiation. Finally, immunocompetent mice bearing syngeneic autophagy-deficient mouse mammary carcinoma cells mounted improved abscopal responses to RT (in the context of CTLA4 blockade) as compared to immunocompetent mice bearing syngeneic autophagy-competent cells, as determined by growth inhibition of a distant, non-irradiated, autophagy-competent lesion.

Conclusions
In conclusion, autophagy inhibits abscopal responses by limiting the release of type I IFN by irradiated cancer cells. We will test the innovative hypothesis that selective autophagy inhibition in cancer cells may synergize with autophagy activation at the whole-body level (by nutrient restriction or physical exercise), hence enabling superior therapeutic responses to radiation.

References
1. Rybstein MD, Bravo-San Pedro JM, Kroemer G, Galluzzi L. The autophagic network and cancer. Nat Cell Biol. 2018;20(3):243-251.

Ethics Approval
The study was approved by Weill Cornell Medicine's Ethics Board, approval number 2017-0007.

P474

Antibody targeting of WNT signaling modulator dickkopf1 (DKK1) enhances innate anti-tumor immunity and complements anti-PD-1 therapy

Mike Haas[1], Heidi Heather[1], Franziska Schürpf-Huber[1], Lane Newman[1], Walter Newman, PhD[1], Mike Kagey[1], Min Yang, PhD[1]

[1]*Leap Therapeutics, Cambridge, MA, USA*

Background
DKK1, a secreted modulator of the Wnt and PI3K/AKT signaling pathways, may contribute to an immunosuppressive tumor microenvironment by influencing Tregs, MDSCs and NK cell functions [1] while also affecting tumor cell NK target expression [2]. DKK1 is expressed in a variety of tumor types and elevated levels frequently correlate with poor survival. DKN-01 is a neutralizing IgG4 monoclonal against DKK1, and mDKN-01 is a murine version of DKN-01.

Methods
mDKN-01 has been evaluated in B16 and 4T1 syngeneic mouse tumor models as monotherapy and in combination with anti-PD-1

Results
As a monotherapy mDKN-01 demonstrated a highly reproducible inhibition of tumor growth in a B16 melanoma syngeneic model, with concomitant infiltrates of CD45+ CD11b immune cells. Intratumoral MDSC are reduced and show elevated expression of PD-L1. mDKN-01 anti-tumor activity is lost in immunocompromised NSG mice and following depletion of NK cells in immune competent mice. In addition, mDKN-01 anti-tumor activity is retained in a RAG1-/- mouse, highlighting the T cell independence and NK dependence of the anti-tumor

mechanism. Combination therapy with anti-PD-1 and mDKN-01 showed cooperative tumor growth inhibition in the B16 model, and reduction of lung metastasis in a 4T1 breast tumor model. These data indicate the potential for DKN-01 complementarity with checkpoint blockers.

Conclusions

In murine studies mDKN-01 is an innate-immune IO agent with effects on NK and MDSC cells. mDKN-01 plus anti-PD-1 are more active together than either agent alone in two murine syngeneic models. Preliminary clinical results demonstrate that DKN-01 in combination with pembrolizumab is well tolerated and is clinically active in esophagogastric cancer, including in patients previously treated with other checkpoint inhibitors or in immune resistant phenotypes not expected to respond to pembrolizumab alone. Clinical trial information: NCT02013154

Trial Registration

Clinical trial information: NCT02013154

References

1. Chae WJ, Ehrlich AK et al. The wnt antagonist dickkopf-1 promotes pathological type 2 cell-mediated inflammation immunity. 2016; 44:246-258.
2. Chae WJ, Park JH, et al. Membrane-bound dickkopf-1 in foxp3+ regulatory T cells suppresses T-cell-mediated autoimmune colitis. Immunology. 2017;265-275.
3. D'Amico L, Mahajan S. Dickkopf-related protein 1 (Dkk1) regulates the accumulation and function of myeloid derived suppressor cells in cancer. J Exp Med. 2016; 213:827-40.
4. Malladi S, Macalinao DG, et al. Metastatic latency and immune evasion through autocrine inhibition of WNT Cell. 2016;165:45-60.

P475

Avadomide in combination with nivolumab results in increased activated and memory T-cells and enhances CD8+ tumor infiltration in hepatocellular carcinoma patients

Patrick Hagner, PhD[1], Fadi Towfic, PhD[1], Alfredo Romano, MD[1], Julien Edeline, MD[2], Carlos Gomez-Martin, MD, PhD[3], Antoine Hollebecque, MD[4], Robin Kate Kelley, MD[5], Armando Santoro, MD, PhD[6], Michael Pourdehnad, MD[1], Anita Gandhi, PhD[1]

[1]*Celgene Corporation, Summit, NJ*
[2]*Centre Eugene Marquis, Rennes, France*
[3]*Hospital 12 de Octubre, Madrid, Spain*
[4]*Institut G. Roussy, Villejuif, France*
[5]*University of California San Francisco, San Francisco, CA, USA*
[6]*Humanitas University, Rozzano-Milan, Italy*

Background

Avadomide (CC-122) binds E3 ubiquitin ligase $CRL4^{CRBN}$, resulting in degradation of transcription factors Aiolos and Ikaros, and activation of T cells. Preclinical and clinical data indicate that avadomide exerts strong immunomodulatory activity through enhanced ADCC and a shift in T-cell subsets from naïve to effector and memory subsets. Avadomide is in clinical development in multiple hematologic diseases and has been explored in solid tumors, including hepatocellular carcinoma (HCC), as single agent (NCT01421524) and in combination with nivolumab (NCT02859324). In preclinical models, avadomide plus nivolumab demonstrates synergistic activation of T cells and significantly enhanced immune-mediated cytotoxicity against HCC cells. Here, we report the effects of combining avadomide with nivolumab on peripheral blood T-cell subsets and activation status and on trafficking of immune cells to the tumor in patients with HCC.

Methods
Peripheral blood T-cell subsets were analyzed by flow cytometry. Tumor biopsies were analyzed by immunohistochemistry or RNA sequencing with deconvolution analyses to identify immune cell populations.

Results
Avadomide, as single agent and in combination with nivolumab, results in decreased absolute peripheral CD4+ and CD8+ naïve (CD45RA+/CD45RO–) T cells and increased memory (CD45RA–/CD45RO+) and activated (HLA-DR+) T cells, without significantly affecting total CD3+, CD4+ or CD8+ populations. Interestingly, the combination demonstrated a trend towards greater increase in activated (+182%) and memory (+257.9%) CD4+ T cells compared with avadomide alone (+123.2% and +12.2%). Increased levels of peripheral Treg populations were detected within 15 days of treatment initiation, and the CD8/Treg ratio declined from 7.8 at screening to 2.7 on C1D15. To understand the effects on tumor microenvironment, we performed RNA sequencing on paired tumor biopsies from patients receiving combination treatment collected at enrollment and six weeks after treatment initiation (n=9). Deconvolution analyses identified increased infiltration of T-cell populations, dendritic cells and macrophages, and decreased B-cell populations in on-treatment biopsies relative to pre-treatment. Immunohistochemistry confirmed significantly increased CD8+ T-cells in on-treatment biopsies relative to pre-treatment in patients receiving the combination (*P*=0.04), while no significant changes in CD8+ T-cell infiltration were observed in patients receiving single agent avadomide (*P*=0.65).

Conclusions
Avadomide is a potent immunomodulating agent with multiple immune activating properties. Avadomide plus nivolumab leads to significantly greater CD8+ T-cell tumor infiltration compared with single agent avadomide. These findings provide proof-of-concept for the combination of avadomide with checkpoint blockade in solid tumors and demonstrate potential for further clinical and biomarker studies to ascertain relative contribution of avadomide over nivolumab monotherapy and assess efficacy.

Trial Registration
ClinicalTrials.gov identifier NCT01421524 and NCT02859324.

Ethics Approval
This study was approved by the research ethics boards of all participating institutions.

Consent
Written informed consent was obtained from the patient for publication of this abstract and any accompanying images. A copy of the written consent is available for review by the Editor of this journal.

Immunosuppressive Cells in the Tumor Microenvironment

P476

EWS-FLI1 expression level modulates T-cell mediated tumor apoptosis in Ewing sarcoma.

Claire Julian[1], Ariel Klinghoffer, -[1], Hether Bernard, MD[1], Linda McAllister-Lucas[1], Kelly Bailey, MD, PhD[1]

[1]*University of Pittsburgh, Pittsburgh, PA, USA*

Background
Metastatic Ewing sarcoma is a deadly bone cancer most commonly diagnosed in children and is driven by the fusion oncoprotein EWS-FLI1. The level of EWS-FLI1 expression can change Ewing cell behavior. Interestingly, lower levels of EWS-FLI1 are associated with increased expression of ICAM-1, a surface protein reported in some cancers to influence tumor cell: T-cell interaction and promote T-cell activation.

Very little is known about the immune response to Ewing sarcoma tumor cells and elucidating the mechanisms regulating the immune response to Ewing tumor cells may reveal much needed new treatment opportunities for patients with metastatic disease. In this study, we seek to determine the impact of tumor cell EWS-FLI1 expression level on T-cell mediated Ewing sarcoma tumor cell apoptosis.

Methods

We performed real-time monitoring of tumor cell caspase 3 activity in Ewing tumor cell/T-cell co-cultures. For this analysis, Ewing sarcoma tumor cell populations with 'high' or 'low' EWS-FLI1 expression were prepared by either: 1) using flow cytometry to isolate naturally occurring populations or 2) using EWS-FLI1 siRNA to generate EWS-FLI1 'low' cells. Human T-cells were isolated from random donor buffy coat, and T-cells were activated using a CD2/3/28 antibody cocktail. Surface expression of ICAM-1, PD-L1 and PD-L2 was determined by flow cytometry analysis. Blocking antibodies were also utilized.

Results

EWS-FLI1 'low' cells demonstrated a significant decrease in T-cell mediated tumor cell apoptosis upon introduction of ICAM-1 blocking antibody. Based on this, we questioned whether EWS-FLI1 'low' cells would be more susceptible to T-cell mediated apoptosis that EWS-FLI1 'high' cells (that lack surface ICAM-1). Notably, despite having higher ICAM-1, we found that EWS-FLI1 'low' cells are actually less susceptible to T-cell mediated apoptosis that EWS-FLI1 'high' cells, suggesting that EWS-FLI1 'low' cells possess an ability to evade T-cell-mediated tumor killing. Further, in comparison to EWS-FLI1 'high' cells, EWS-FLI1 'low' cells respond to interferon-gamma treatment with dramatically greater transcriptional upregulation of PD-L1 and PD-L2. We then assessed the impact of PD-1 blocking antibody on T-cell mediated tumor cell apoptosis and found that treatment of EWS-FLI1 'low' cell/T-cell co-cultures with blocking antibody significantly enhances T-cell-induced tumor cell apoptosis.

Conclusions

We have shown that Ewing cells with lower EWS-FLI1 are more resistant to T-cell mediated apoptosis than cells with higher EWS-FLI1. As such, EWS-FLI1 'low' cells may serve as negative regulators of the immune response in Ewing tumors. These data highlight that Ewing tumor cell heterogeneity can influence the anti-tumor immune response.

Acknowledgements

KMB is supported by Alex's Lemonade Stand Foundation Young Investigator Award, The Children's Cancer Research Fund Emerging Scientist Award and the NIH 2K12HD052892-11A1

P477

HMBD-002-V4: A novel anti-VISTA antibody that uniquely binds murine and human VISTA and potently inhibits tumor growth by remodeling the immunosuppressive tumor microenvironment

Jerome Boyd-Kirkup, PhD[1], Dipti Thakkar, PhD[1], Vicente Sancenon, PhD[1], Siyu Guan, PhD[1], Konrad Paszkiewicz, PhD[1], Piers Ingram, PhD[1]

[1]*Hummingbird Bioscience, South San Francisco, CA, USA*

Background

Immune checkpoint therapies have shown unprecedented clinical activity in several types of cancer, however, less than 30% of patients respond. VISTA is a co-inhibitory immune checkpoint receptor of the B7 family and functions to suppress human T-cell activity. VISTA is highly expressed on tumor infiltrating myeloid cells including myeloid derived suppressive cells (MDSC), which have been associated with resistance to immunotherapy. Increases in VISTA+ cells have also been observed in

response to PD1 and CTLA4 therapy. Targeting VISTA could represent a novel treatment axis in the non-responder population.Despite the promise of VISTA, limited structural information, lack of a definitive ligand, and incomplete data on expression in normal vs. disease contexts, have made development of drug candidates challenging. Further, previous anti-VISTA antibodies have only bound to rodent *or* human VISTA, making it impossible to translate pre-clinical efficacy and safety data to predict patient response.

Methods

HMBD-002-V4 is a humanized anti-VISTA antibody developed using Hummingbird Bioscience's proprietary Rational Antibody Discovery platform to target a specific epitope predicted by structural modeling to block ligand binding and be conserved between human, cyno and murine VISTA.

Results

In vitro, HMBD-002-V4 showed dose-dependent inhibition of the interaction between VISTA and the putative ligand VSIG3 for both human and mouse orthologs, and further demonstrated release of VISTA inhibition on T-cell activity and increased secretion of pro-inflammatory cytokines in human *ex vivo* assays.*In vivo*, HMBD-002-V4 showed single agent tumor growth inhibition (TGI) of up to 40% in syngeneic murine CDX models, however, efficacy was significantly improved if combined with anti-PD(L)1 antibody where TGI above 94% was possible. Profiling of representative tumors by FACS revealed MDSC infiltration in these models that was significantly increased after treatment with anti-PD(L)1 antibody and associated with an increase in immunosuppressive serum cytokines. Conversely, HMBD-002-V4 efficacy was associated with decreased MDSC infiltration for both monotherapy and combination arms and a remodeling of the tumor microenvironment towards a pro-inflammatory phenotype. In models without MDSC infiltration, HMBD-002-V4 showed poor efficacy. HMBD-002-V4 was evaluated for pharmacokinetics and toxicology and demonstrated excellent serum half-life of 11 days, with no observable toxicity in multiple animal models. Further, HMBD-002-V4 has been optimized for manufacturability, including high expression titers and stability.

Conclusions

HMBD-002-V4 represents a promising therapeutic candidate for the treatment of VISTA-mediated suppression of anti-tumor immunity. Predictive biomarkers of response to HMBD-002-V4 are currently being explored in multiple indications and the first-in-human trial of HMBD-002-V4 is planned for 2019.

Ethics Approval

The study was approved by the SingHealth Institutional Animal Care and Use Committee, approval number 2016/SHS/1230.

P478

Platelets as immune suppressors in anti-cancer immune responses

Ana Micaela Carnaz Simões[1], Morten Holström, PhD[1], Mads Andersen, PhD[1], Per Thor Straten, PhD[1]

[1]*Center for Cancer Immune Therapy, Herlev, Herlev, Denmark*

Background

Platelets (PLTs) are well-known players during cancer progression. For several cancers, an increased number of circulating PLTs correlates with poor prognosis. PLTs help cancer cells by modulating angiogenesis and/or directly binding cancer cells, which facilitates the metastatic process [1,2]. These cells and their soluble factors can also protect cancer cells from immune attack by mechanisms that are poorly understood. Studies focused on autoimmune conditions, have shown that exhausted PLTs form

aggregates with T cells, downregulating T cell activation, proliferation and interferon-ɣ production [3,4]. Nevertheless, no similar study has been conducted in the context of cancer.

Methods

Our study investigated the presence of circulating PLT-immune cell aggregates in myeloproliferative neoplasm (MPN) patients. To that purpose, cryopreserved peripheral blood mononuclear cells were analyzed by multicolor flow cytometry for PLT bound -T, -NK, -B and -CD3+/CD56+ cells, as well as CD4 and CD8 T cell subpopulations. Furthermore, to assess the effect PLT-binding has on T and NK cell anti-tumor reactivity, in vitro cytotoxic response was continuously monitored over 40 hours, using the xCELLigence technology.

Results

Our preliminary results show that, when compared to healthy donors, MPN patients have an increased number of PLT bound CD8+ T, NK and CD3+/CD56+ cells. Finally, our results indicate that platelets can modulate the T and NK cells tumor reactivity in distinct manners; the presence of PLTs impairs the killing capacity of T cell whereas it seems to enhance it on NK cells. However, further studies are needed to confirm our preliminary results.

Conclusions

N/A

References

1. Borsig L. The role of platelet activation in tumor metastasis. Expert Rev Anticancer Ther. 2008;8(8):1247-1255. doi:10.1586/14737140.8.8.1247.
2. Bambace NM, Holmes CE. The platelet contribution to cancer progression. J Thromb Haemost. 2011;9(2):237-249. doi:10.1111/j.1538-7836.2010.04131.x.
3. Zamora C, Canto E, Nieto JC, et al. Functional consequences of platelet binding to T lymphocytes in inflammation. J Leukoc Biol. 2013;94(3):521-529. doi:10.1189/jlb.0213074.
4. Zamora C, Cantó E, Nieto JC, et al. Binding of platelets to lymphocytes: A potential anti-inflammatory therapy in rheumatoid arthritis. J Immunol. 2017;198(8):3099-3108. doi:10.4049/jimmunol.1601708.

P479

NG-641: an oncolytic T-SIGn virus targeting cancer-associated fibroblasts in the stromal microenvironment of human carcinomas

Matthieu Besneux[1], Brian Champion, PhD[1], Nalini Marino[1], Marilena Patsalidou[1], Gianfranco di Genova[1], Sam Illingworth[1], Stefania Fedele[1], Lorna Slater[1], Darren Plumb[1], Katy West[1], Joshua Freedman, BS[2], Len Seymour[2], Kerry Fisher, MD PhD[1], Alice Brown, PhD[1]

[1]PsiOxus Therapeutics Ltd, Abingdon, UK
[2]Oxford University, Oxford, UK

Background

NG-641 is a modified variant of enadenotucirev (EnAd), an Ad11p/Ad3 chimeric group B adenovirus, which retains all the functional properties of enadenotucirev, while also mediating the expression of transgenes designed to target the breakdown of the stromal barrier and reverse immune suppression within the tumor microenvironment (TME). As an approach to immunogene therapy targeting stromal rich tumors, we have created a transgene-modified variant of EnAd expressing a bi-specific T-cell activator molecule (FAP-TAC) recognizing human fibroblast activating protein (FAP) on cancer associated fibroblasts (CAFs) and CD3 on T-cells. To enhance the activity of the bispecific molecule, particularly in tumors with poor immune cell infiltration (“excluded phenotype”), NG-641 also encodes an immune-enhancer module (IM), consisting of the chemokines CXCL9 and CXCL10 and

the type I interferon IFNa..

Methods
FAP-TAC constructs comprising linked ScFv antibodies specific for human FAP and CD3 were designed and used to generate EnAd viruses expressing the FAP-TAC transgene such that expression was under the virus major late promoter (MLP) to allow broad or tumor-selective expression, respectively. Tumor and fibroblast cell lines and freshly isolated malignant peritoneal ascites and surgically excised tumor samples from carcinoma patients were used to evaluate virus activities.

Results
Initial studies with different viruses expressing FAP-TAC alone or with different additional transgenes showed that FAP-TAC activity generated by NG-641 infection was essentially the same as that with viruses bearing only the FAP-TAC transgene. In tumor cell lines, NG-641 selectively secretes functional FAP-TAC molecules, as determined in cocultures of FAP+ fibroblasts and PBMC-derived T cells. Production of the IM transgenes CXCL9, CXCL10 and IFNa was confirmed by specific ELISA assays, with functionality evaluated by reporter cell, FACS and cell migration assays. T cell-activation mediated by FAP-TAC leads to cytokine secretion and cytotoxicity towards the fibroblasts. Studies with unseparated primary tumor samples (containing tumor cells, CAFs and infiltrated immune cells) also demonstrated potent activation of the endogenous T-cells, indicating that virus produced FAP-TAC is a potent T-cell activator despite suppressive influences of the TME.

Conclusions
In this study, we have shown that CAFs can be effectively targeted for T-cell mediated destruction by NG-641, a tumor stroma targeting transgene-bearing oncolytic virus. This is associated with strong activation of endogenous T-cells to kill CAFs even in the presence of an immunosuppressive microenvironment. Systemic dosing of such a virus to patients with stromal rich tumors may provide an effective approach for reversing immune suppression within the TME and driving effective anti-tumor immunity.

P480

Transcriptomic characterization of tumor vs. peripheral blood NK cells in head and neck cancer patients

Fernando Concha-Benavente, MD, PhD[2], Robert Ferris[1]

[1]*University of Pittsburgh, Pittsburgh, PA, USA*
[2]*UPMC Hillman Cancer Center, Pittsburgh, PA, USA*

Background
NK cells play a crucial role in tumor immunosurveillance with a unique capacity of killing cancer cells via antibody dependent cellular cytotoxicity (ADCC), particularly in the setting of head and neck cancer (HNC) where cetuximab, an EGFR-specific mAb, has been used since 2006. Cetuximab-activated NK cells induce dendritic cell (DC) activation, tumor antigen cross-presentation and expansion of EGFR-specific T cells, linking innate and adaptive antitumor immunity. However, the benefit of cetuximab is only seen in 10-15% of patients [1]. Moreover, NK cell dysfunction has been associated with increased risk of cancer [2-5] and poor clinical prognosis [6-8]. Therefore, characterizing whether NK cells infiltrate HNC tumors and their expression profile is important in order to reverse NK cell dysfunction and improve cancer immunotherapy

Methods
NK cells were sorted by flow cytometry from freshly isolated HNC peripheral blood lymphocytes (PBL) and paired tumor infiltrating lymphocytes (TIL). Sequential RT reactions produced amplified dsDNA which was fragmented, end labeled with biotin and

hybridized to the Human Clariom S array. First level data analysis was performed using Affymetrix Expression Console using RMA normalization algorithm

Results

Initial exploratory grouping analysis (EGA) showed that PBL (n=9) and TIL (n=6) NK cells had a divergent expression profile. Hierarchical clustering (HC) analysis of paired PBL and TIL NK cells (n=4) revealed that TIL NK cells had a total of 1345 differentially expressed genes, from which 713 were downregulated more than 2-fold when compared to PBL NK cells. We found that Th1 type transcription factors such as EOMES and BLIMP-1, activation/cytolytic markers such as CD38, NKG2F, CD247, granzyme A, granzyme H, perforin 1 and FCGR3A (CD16a) and FCGR3B (CD16b) which are key molecules for ADCC were significantly downregulated in TIL NK cells. Likewise, sphingosine-1-phosphate receptor 1 (S1PR1), a critical mediator of NK cell traffic and retention in inflamed tissues, Th1 type induced T/NK cell attracting chemokines CCL5 and CCL4 and innate immunity activator, toll-like receptor 3 (TLR3) were downregulated in TIL NK cells.

Conclusions

These findings suggest an exhausted phenotype of TIL NK cells characterized by downregulation of Th1 type activation markers compared to NK cells in the periphery. Reversing NK cell dysfunction is key in order to improve antitumor immunity of HNC patients.

References

1 Ferris R L, Jaffee E M, Ferrone S. Tumor antigen-targeted, monoclonal antibody-based immunotherapy: clinical response, cellular immunity, and immunoescape. J Clin Oncol 2010. 28: 4390-4399.

2 Hersey P, Edwards A, Honeyman M, McCarthy W H. Low natural-killer-cell activity in familial melanoma patients and their relatives. Br J Cancer 1979. 40: 113-122.

3. Fauriat C, Just-Landi S, Mallet F, Arnoulet C, Sainty D, Olive D, Costello R T. Deficient expression of NCR in NK cells from acute myeloid leukemia: Evolution during leukemia treatment and impact of leukemia cells in NCRdull phenotype induction. Blood 2007. 109: 323-330.

4. Saito H, Osaki T, Ikeguchi M. Decreased NKG2D expression on NK cells correlates with impaired NK cell function in patients with gastric cancer. Gastric Cancer 2012. 15: 27-33.

5 Schantz S P, Shillitoe E J, Brown B, Campbell B. Natural killer cell activity and head and neck cancer: a clinical assessment. J Natl Cancer Inst 1986. 77: 869-875.

6 Coca S, Perez-Piqueras J, Martinez D, Colmenarejo A, Saez M A, Vallejo C, Martos J A, Moreno M. The prognostic significance of intratumoral natural killer cells in patients with colorectal carcinoma. Cancer 1997. 79: 2320-2328.

7 Takeuchi H, Maehara Y, Tokunaga E, Koga T, Kakeji Y, Sugimachi K. Prognostic significance of natural killer cell activity in patients with gastric carcinoma: a multivariate analysis. Am J Gastroenterol 2001. 96: 574-578.

8. Ishigami S, Natsugoe S, Tokuda K, Nakajo A, Che X, Iwashige H, Aridome K, Hokita S, Aikou T. Prognostic value of intratumoral natural killer cells in gastric carcinoma. Cancer 2000. 88: 577-583.

P481

The epigenetic underpinnings of regulatory T cell fragility in the tumor microenvironment

Becky Dadey, BS[1], Abigail Overacre-Delgoffe, PhD[2], Ting Wang[1], Zhe Sun[1], Rong Zhang, MS[2], Wei Chen[2], Natalie Rittenhouse[2], Amanda Poholek[2], Tracy Tabib[1], Robert Lafyatis[1], Creg Workman, PhD[1], Dario Vignali, PhD[1]

[1]*University of Pittsburgh, Pittsburgh, PA, USA*

[2]*Children's Hopsital of Pittsburgh, Pittsburgh, PA, USA*

Background

Regulatory T cells (Tregs) are a suppressive cell population that limit the anti-tumor response. However, systemic ablation of Tregs cannot be utilized as a therapy due to massive autoimmune defects. Our lab has demonstrated that Treg-restricted deletion of cell surface protein Neuropilin (Nrp1, CD304) results in substantially reduced tumor growth with no autoimmune defects [1]. We have shown that Treg-restricted deletion of Nrp1 in the TME does not result in loss of Foxp3 expression and "ex-Treg" generation but rather causes them to exhibit an effector-like phenotype including loss of suppressive function and production of interferon gamma (IFNγ), which we refer to as Treg fragility [2].

Methods

We sought to understand the epigenetic underpinnings between Nrp1-sufficient and -deficient Tregs from the tumor microenvironment that could lead to this 'fragile' state. To do so we performed bisulfite treatment from ZymoEZ Direct Kit followed by Sanger Sequencing to identify differences in DNA methylation. We utilized ATAC sequencing to identify discrepancies in chromatin accessibility following the Greenleaf protocol [3]. We also utilized TCR sequencing from Adaptive Biotechnologies per the manufacturer's protocol. For single cell RNAseq, we loaded 3500 cells/sample using ChromiumTM Single Cell 3' Gel Bead Kit and Chromium Single Cell 3'v2 Library Kit. Samples were sequenced on a NextSeq500. Finally, CUT&RUN ChIP-seq was perform following the Henikoff protocol [4].

Results

We found that Tregs lacking Nrp1 in the TME have a differential methylation signature at the Conserved Non-coding Sequence 2 (CNS2) locus of the Foxp3 gene, albeit no difference in the chromatin accessibility at this locus, no change in single cell RNAseq, and maintenance of Foxp3 protein expression. We also found that Nrp1-deficient Tregs are not peripherally-induced Tregs but rather are thymically-derived.

Conclusions

We have identified an intriguing change in the DNA methylation status of the CNS2 locus of Foxp3 in the Nrp1-deficient Tregs from the tumor microenvironment but no loss in Foxp3 expression. This finding conflicts with current data suggesting that CNS2 hypermethylation shuts off Foxp3 expression. Additional experiments will be required to understand how this locus maintains Foxp3 protein despite DNA methylation. Future studies will also examine the epigenetic mediators that might cause this differential methylation or if extrinsic factors in the TME promote differential methylation.

References

1. Delgoffe GM, Woo SR, Tunis ME, Gravano DM, Guy C, Overacre AE, Bettini ML, Vogel P, Finkelstein D, Bonnevier J, Workman CJ, Vignali DA. Stability and function of regulatory T cells is maintained by a neuropilin-1-semaphorin-4a axis. Nature. 2013; 7466, 252-6

2. Overacre-Delgoffe AE, Chikina M, Dadey RE, Yano H, Brunazzi EA, Shayan G, Horne W, Moskovitz JM, Kolls JK, Sander C, Shuai Y, Normolle DP, Kirkwood JM, Ferris RL, Delgoffe GM, Bruno TC, Workman CJ, Vignali DAA. Interferon-γ derives treg fragility to promote anti-tumor immunity. Cell. 2017; 169, 1130-41

3. Buenrostro JD, Giresi PG, Zaba LC, Chang HY, Greenleaf WJ. Transposition of native chromatin for fast and sensitive epigenomic profiling of open chromatin, DNA-binding proteins and nucleosome position. Nat Methods. 2013; 10:1213-1218

4. Skene PJ, Henikoff S. An efficient targeted nuclease strategy for high-resolution mapping of DNA binding sites. Elife 2017; 6:e21856

P482

Humanization and characterization of novel, best in class isoform-specific anti-TGFβ monoclonal antibodies

Matteo Brioschi[1], Pamela Cheou[2], Jacques Van Snick, PhD[2], Catherine Uyttenhove, PhD[2], George Coukos, MD, PhD[3], Gerd Ritter[4], Steven Dunn, PhD[3], Steven Dunn, PhD[3]

[1]Ludwig Institute for Cancer Research, Epalinges, Switzerland., Epalinges, Switzerland
[2]Ludwig Institute for Cancer Research Ltd, Brussels, Belgium., Brussels, Belgium
[3]Ludwig Institute for Cancer Research, Epalinges, Switzerland. CHUV, Lausanne, Switzerland., Epalinges, Switzerland
[4]Ludwig Institute for Cancer Research, New York, NY., New York, NY, USA

Background

TGFβ is a conserved, highly pleiotropic and potent cytokine that has been implicated in tumor escape and progression via its modulation and suppression of multiple immune-cell related pathways within the tumor microenvironment [1]. Three homo-dimeric isoforms have been identified, which individually have been shown to drive context-dependent physiological and phenotypic responses, including aspects of proliferation, migration, differentiation, angiogenesis, and immune responsiveness [2]. Although a compelling target for tumor immunotherapy, the use of anti-TGFβ antibodies that do not adequately distinguish between the individual isoforms could give rise to on-target off-tumor toxicity, undesirable inflammatory adverse events or a zero-sum anti-tumor activity. To address this unmet need for more specific reagents, we have selected two antibodies for humanization from a panel of recently generated high-affinity murine mAb hybridomas which have extraordinary mono-isoform selectivity for TGFβ1 or TGFβ3 and which neutralize TGFβ-driven signalling in a cell reporter system with high potency [3]. Isoform specific TGFβ blockade with these antibodies is effective at delaying in-vivo tumor growth in melanoma and breast cancer models [4].

Methods

Antibody humanization was performed using a molecular engineering approach combining framework grafting, competitive screening of antibody fragments and selective back mutation of individual residues guided by assaying for TGFβ neutralization potency of the antibody constructs using a transformed mink lung epithelial cell (tMLEC) TGFβ reporter line. Binding kinetics were assayed by surface plasmon resonance. Physicochemical properties of the engineered antibodies and suitability for down-stream development were characterized using several techniques including transient expression in singular cell system, size-exclusion chromatography and thermal differential scanning fluorimetry.

Results

We report the successful conversion of two TGFβ isoform-specific mouse mAbs into humanized recombinant IgG4 molecules targeting human TGFβ1 or TGFβ3 respectively. Engineered variants of both parental TGFβ antibodies express efficiently in a transient human cell system, display good thermal stability and retain their potent binding and neutralization activity with regard to their cognate TGFβ isoforms. We were able to generate several humanized LCR1901 anti-TGFβ3 variants with significantly improved neutralization potency in cellular TGFβ signalling assays relative to the parental mAb, and with essentially undetectable levels of binding to TGFβ1 and TGFβ2.

Conclusions

We have generated a panel of humanized antibodies that specifically neutralize TGFβ3 or TGFβ1 signalling. Recent studies assigning a dominant gatekeeper role

for TGFβ3 in malignant glioblastoma progression [5], as well as specifically implicating TGFβ1 in breast and gastric cancers [6,7], support the continued pre-clinical and clinical investigation of these novel TGFβ antibodies.

References

1. Neuzillet C, Tijeras-Raballand A, Cohen R, Cros J, Faivre S, Raymond E, de Gramont A. Targeting the TGFβ pathway for cancer therapy. Pharmacol Ther. 2015 Mar;147:22-31
2. Poniatowski ŁA, Wojdasiewicz P, Gasik R, Szukiewicz D. Transforming growth factor beta family: Insight into the role of growth factors in regulation of fracture healing biology and potential clinical applications. Mediators Inflamm. 2015;2015:137823
3. Uyttenhove C, Marillier RG, Tacchini-Cottier F, Charmoy M, Caspi RR, Damsker JM, Goriely S, Su D, Van Damme J, Struyf S, Opdenakker G, Van Snick J. Amine-reactive OVA multimers for auto-vaccination against cytokines and other mediators: perspectives illustrated for GCP-2 in L. major infection. J Leukoc Biol. 2011 Jun;89(6):1001-7
4. Gupta A, Budhu S, Giese R, van Snick J, Uyttenhove C, Ritter G, Wolchok J, Merghoub T. Isoform specific TGF-β inhibition in combination with radiation therapy as a novel immune therapeutic approach to cancer therapy. Journal for ImmunoTherapy of Cancer 2017; 5 (suppl 2) :87 Abstract 326 AND Gupta A, Budhu S, Giese R, van Snick J, Uyttenhove C, Ritter G, Wolchok J, Merghoub T. Targeting specific TGF-β isoforms in combination with radiation therapy leads to differential antitumor effects in mouse models of cancer. Cancer Res. 2018; 78(13 suppl): Abstract 4716
5. Seystahl K, Papachristodoulou A, Burghardt I,Schneider H, Hasenbach K, Janicot M, Roth P, Weller M. Biological Role and Therapeutic Targeting of TGF-β3 in Glioblastoma. Mol Cancer Ther. 2017 Jun;16(6):1177-1186
6. Rodriguez G, Abrahamsson A, Jensen L, Dabrosin C. Estradiol Promotes Breast Cancer Cell Migration via Recruitment and Activation of Neutrophils. Cancer Immunol Res; 5(3); 234–47
7. Peng LS, Zhang JY, Teng YS, Zhao YL, Wang TT, Mao FY, Lv YP, Cheng P, Li WH, Chen N, Duan M, Chen W, Guo G, Zou QM, Zhuang Y. Tumor-Associated Monocytes/Macrophages Impair NK-Cell Function via TGFb1 in Human Gastric Cancer. Cancer Immunol Res. 2017 Mar;5(3):248-256

P483

Iron and HLA-G: Neglected immunosuppressive molecules in the human microenvironment

Xian Jiang[2], Robert Elliott[1]

[1]*Mastology, Baton Rouge, LA, USA*
[2]*the Breast Foundation, Baton Rouge, LA, USA*
[3]*EEB clinic, Baton Rouge, LA, USA*

Background

There are many immunosuppressive molecules in the tumor microenvironment that need to be inhibited, if we are to improve immunotherapy in the Stage IV patients. There are many reports on the possible role of HLA-G in cancer immunosuppression, but very little on the role of iron. The immunosuppressive effect of iron and HLA-G in the tumor microenvironment has been neglected and ignored as therapeutic targets. This study was implemented to determine if iron and HLA-G, as neglected molecules enhance tumor immunosuppression, and could be cancer immunotherapy targets.

Methods

We examined HLA-G expression in normal mammary and breast cancer cell lines and human normal and breast cancer tissue. This examination was done by reverse transcription polymerase chain reaction (RT-PCR) and immunohistochemistry (IHC). Intracellular iron levels were manipulated in the human MCF-7 and MDA-MB-231 breast cancer cell lines. Cytolysis

of these cell lines was measured after exposure to the natural killer cell line NK-92 MI (NK). The gene expression of ferritin heavy chain (FTH1) was determined as was the production of nitric oxide (NO) and tumor necrosis factor alpha (TNFa).

Results

RT-PCR confirmed HLA-G expression was absent in the normal epithelial MCF-12A cells showing no mRNA expression, however, the cell lines MCF-7, MDA-MB-231and T-47D had various levels of HLA-G mRNA expression. IHC was performed on 38 breast cancer specimens and on 12 normal breast specimens. Fifty-eight percent (22/38) of the cancer had medium to strong staining, but only 8.3% (1/12) of the normal specimens had medium staining. The difference was significant ($p<0.05$). When NK-92 MI cells were co-cultured with MCF-7 and MDA-MB-231 cells, NO and TNF-a were released into the media. The addition of iron inhibited the cytolysis of cancer cell lines. Deferoxamine (DFOM), an iron chelator, increased NK-92 MI cytolysis of MCF-7 and MDA-MB-231 cells. The cytotoxicity of the breast cancer cells was reversed by the addition of iron. This cytotoxicity is induced by NO released from S-nitro-N-acetyl – penicillamine (NO donor). RT-PCR showed the iron chelator reduced FTH1 expression, while iron upregulated the expression of FTH1.

Conclusions

HLA-G antigen is expressed in trophoblastic placental cells as an immunotolerant molecule to protect the fetus from maternal alloreactivity. Its expression in cancer cells contributes to cancer immunosuppression. Increased iron in the tumor microenvironment and cancer cells inhibited cancer cells cytolysis by NK cells by antagonizing NO and TNFa cytotoxicity and the upregulation of ferritin expression. We hope this study will stimulate researchers to investigate the role of HLA-G and iron as therapeutic targets of the cancer microenvironment. Cancer immunotherapy in Stage IV patients will be improved by the inhibition of these neglected molecules.

P484

Pharmacokinetics, pharmacodynamics, and safety of FLX475, an orally-available, potent, and selective small-molecule antagonist of CCR4, in healthy volunteers

Sjoerd van Marle, MD[2], Ewoud-Jan van Hoogdalem, PhD, RPh[2], Daniel Johnson[1], Abood Okal, PhD[1], Paul Kassner, PhD[1], David Wustrow, PhD[1], William Ho, MD, PhD[1], Steven Smith[1]

[1]FLX Bio, South San Francisco, CA, USA
[2]PRA Health Sciences, Groningen, Netherlands

Background

Regulatory T cells (Treg) are essential for immune tolerance to self antigens, but can also dampen anti-tumor immune responses in the tumor microenvironment (TME). The predominant chemokine receptor on human Treg is CCR4, the receptor for the chemokines CCL17 and CCL22 [1], which are produced by tumor cells, tumor-associated macrophages and dendritic cells, as well as by effector T cells (Teff) in the setting of an inflammatory anti-tumor response. Preclinical studies with orally-available CCR4 antagonists have demonstrated potent inhibition of Treg migration into tumors, an increase in the intratumoral Teff/Treg ratio, and anti-tumor efficacy as a single agent and in combination with checkpoint inhibitors. [2]

Methods

A first-in-human, randomized, double-blind, placebo-controlled trial was conducted to examine the safety, pharmacokinetics (PK), and pharmacodynamics (PD) in healthy volunteers (HVs) of single and repeat dosing of FLX475, an orally-available, potent, and selective small-molecule antagonist of CCR4. Seven cohorts of 8 subjects each (6 drug, 2 placebo) were

administered single doses ranging from 5 mg to 1000 mg. Six cohorts were administered daily doses of FLX475 for 14 days ranging from 25 mg to 150 mg, including two cohorts evaluating a loading dose administered on Day 1.

Results

FLX475 was well-tolerated, with no significant laboratory abnormalities or dose-limiting clinical adverse events. Dose-dependent increases in exposure were observed with low peak-to-trough ratios and a half-life of approximately 72 hours. Daily dosing without a loading dose demonstrated approximately 4-5x accumulation of FLX475 over 14 days. A receptor occupancy (RO) PD assay using study subject peripheral blood Treg [3] demonstrated a tight PK/PD relationship, suggesting that doses of approximately 75 mg PO QD and above are sufficient to maintain target drug exposure above the IC90 for human in vitro Treg migration.

Conclusions

In this first-in-human HV study, the oral CCR4 antagonist FLX475 was demonstrated to be well tolerated with outstanding PK properties. A robust PD assay measuring receptor occupancy on circulating Treg demonstrated the ability to safely achieve exposure levels predicted to maximally inhibit Treg recruitment into tumors via CCR4 signaling. These data have enabled the optimized design of an ongoing Phase 1/2 study of FLX475 both as monotherapy and in combination with checkpoint inhibitor in cancer patients.

Trial Registration

EudraCT 2017-003952-22

References

1. Talay O et al. Potent and selective C-C chemokine receptor (CCR4) antagonists potentiate anti-tumor immune responses by inhibiting regulatory T cells (Treg) [abstract]. In: Proceedings of the 110th Annual Meeting of the American Association for Cancer Research; 2017 Apr 1–5; Washington, DC. AACR; 2017. Abstract nr 4600.
2. Talay O et al. Potent and selective C-C chemokine receptor 4 (CCR4) antagonists inhibit regulatory T cell recruitment, increase effector T cell numbers, and potentiate anti-tumor responses in mice. J Immunother Cancer. 2017; 5(Suppl 2):467.
3. Okal A, Ho W, Wong B, Kassner P, Cutler G. Patient selection strategies and pharmacodynamic assays for CCR4 antagonists. J Immunother Cancer. 2017; 5(Suppl 2): 44.

Ethics Approval

Approved by the Independent Ethics Committee of the foundation “Stichting Beoordeling Ethiek Biomedisch Onderzoek” (Assen, The Netherlands), Study Code FLB307EC-173071, CCMO code NL63737.056.17.

P485

Testing of two bispecific SNIPER™ antibodies targeting mouse tumor-infiltrating Tregs

Anna Hoefges, MS[1], Bonnie Hammer[2], Amy Erbe, PhD[1], Alexander Rakhmilevich, MD, PhD[1], Jacquelyn Hank, PhD[1], Bryan Glaser, PhD[2], Lucas Bailey, PhD[2], Roland Green, PhD[2], Paul Sondel, MD, PhD[1]

[1]University of Wisconsin Madison, Madison, WI, USA
[2]Invenra, Madison, WI, USA

Background

T regulatory cells (Tregs) are essential to help prevent autoimmune diseases. In the setting of cancer, however, Tregs can help cancer evade anti-tumor immunity by suppressing immunity. Murine studies have shown that if Tregs are selectively depleted, anti-tumor immunity can be enhanced and synergistic immunotherapy achieved, promoting tumor regression. However, currently available Treg-depletion agents can be non-specific and deplete/suppress other T cells, can fail to sufficiently

deplete Tregs, or can potently deplete all Tregs, leading to toxic autoimmunity. We have developed and tested a way to selectively eliminate Tregs in the tumor microenvironment (TME) while leaving peripheral Tregs by using bispecific mAbs created using Invenra's SNIPER™ technology. SNIPER™ bispecific antibodies have relatively weak affinity for two separate targets, limiting their binding and activity when only one target is present. However, when both targets are present, binding is much stronger due to the avidity effect. This allows specific subpopulations of cells to be more specifically selected for elimination by antibody drug conjugates or antibody dependent cellular cytotoxicity.

Methods

Two separate SNIPER™ bispecific mAbs, Inv-1 and Inv-2, were created. C57Bl/6 mice were injected with B78 melanoma tumors. Established tumors and spleens were harvested from mice and analyzed by flow cytometry to identify T cell populations and binding specificity of Inv-1 and Inv-2.

Results

We analyzed binding of the Inv-1 and Inv-2 to lymphocytes harvested from spleens and tumors from the B78 tumor-bearing mice. We used a standard Treg verification panel (CD4, CD25, Foxp3) to identify known Treg populations. Separate panels included the bispecific antibodies (Inv-1 or Inv-2). We found that Inv-1 binds to 59% of Foxp3+ cells extracted from the TME, but only to 18% of the splenic Foxp3+ cells. This shows a preferential binding for tumor-infiltrating-Tregs. Separately, Inv-2 bound to 81% of Foxp3+ cells extracted from the TME, but only to about 51% of the splenic Foxp3+ cells.

Conclusions

Both Inv-1 and Inv-2 selectively target Tregs, with a preference for Tregs present in the TME. In vivo administration of these antibodies may allow for selective depletion of tumor-associated Tregs. Selective depletion of TME-Tregs may result in a reduction in toxic autoimmune side effects associated with immune-activation in the setting of global Treg depletion. In turn, the removal of Tregs specifically from the TME, coupled with a reduction of potential toxic side effects, may enhance the efficacy and applicability of combining Treg depletion with other immune-activating immunotherapies.

P486

Antisense oligonucleotides targeting CD39 and PD-L1 modulate the immunosuppressive tumor microenvironment and have potent anti-tumor activity

Frank Jaschinski, PhD[1], Tamara Thelemann[1], Richard Klar, PhD[1], Monika Schell[1], Lisa Hinterwimmer[1], Sven Michel[1], Melanie Buchi[2], Abhishek Kashyap[2], Alfred Zippelius, MD[2]

[1]*Secarna Pharmaceuticals GmbH & Co. KG, Planegg-Martinsried, Germany*
[2]*University of Basel, Basel, Switzerland*

Background

Antisense oligonucleotides (ASOs) are a new therapeutic modality and have the potential to suppress expression of any RNA target. On the one hand they allow selective targeting of factors previously considered as undruggable, on the other hand -due to their different pharmacokinetic and pharmacodynamic properties- they can offer a complementary approach to more established modalities such as small molecule drugs or antibodies. In the present study, locked-nucleic-acid (LNA)-modified antisense oligonucleotides targeting PD-L1 and the ectonucleotidase CD39 were designed and their activity was tested in cell culture and syngeneic mouse models

Methods

In vitro activity of ASOs on target mRNA and protein

expression was investigated in tumor cell lines and confirmed in isolated human T cells. Degradation of extracellular ATP and proliferation of immune cells were tested in isolated human T cells. In vivo, target activity and investigation of frequency of intratumoral Treg were investigated in the syngeneic MC38 mouse model. The MC38 model and the syngeneic EMT6 model were used to test effects on tumor growth or survival.

Results

In vitro, unformulated ASOs targeting PD-L1 and CD39 achieved potent target knockdown on mRNA and protein level in tumor cell lines and in isolated human T cells. CD39-specific ASOs potently reduced degradation of extracellular ATP in T cells. While treatment of T cells with ATP potently suppressed their proliferation, CD39-specific ASOs could reverse this effect. In syngeneic mouse tumor models, systemic treatment with CD39-specific ASO resulted in potent knockdown of CD39 expression e.g. in Treg, tumor-associated macrophages and myeloid-derived suppressor cells and in a reduction of the frequency of intratumoral Treg. Moreover, tumor growth was strongly reduced by CD39-specific ASO, as monotherapy. In combination with PD-1 antibodies, anti-tumor efficacy of antibodies was improved by ASO.Anti-tumor efficacy of-murine PD-L1 ASOs was demonstrated in syngeneic mouse models. In a breast cancer model, all tumor-bearing mice treated with the PD-L1 ASO rejected the tumor and remained tumor-free. Upon rechallenge, the vast majority of mice rejected the tumor cells demonstrating immunological memory formation. No signs of toxicity were observed.

Conclusions

We have shown, that ASOs targeting immunosuppressive factors are able to achieve potent target suppression in the relevant cell types in vivo and can induce potent anti-tumor effects as monotherapy and in combination therapy with antibody-based checkpoint inhibitors, thereby enhancing survival. Taken together, we developed innovative immunotherapeutic tools that will potentially improve treatment options for cancer patients in the future.

Ethics Approval

PBMC were obtained from leukapheresis products (Klinikum rechts der Isar, TU München, ethics commission reference: 329/16 S)

P487

The role of MultiOmyx in illustrating the pancreatic tumor microenvironment

Juncker-Jensen Juncker-Jensen, PhD[1], Jun Fang[1], Judy Kuo[1], Mate Nagy[1], Qingyan Au[1], Eric Leones[1], Flora Sahafi[1], RaghavKrishna Padmanabhan[1], Nicholas Hoe[1], Josette William, PhD, MD[1]

[1]*NeoGenomics, Aliso Viejo, CA, USA*

Background

Pancreatic ductal adenocarcinoma (PDAC) is characterized by an excessive amount of desmoplastic stroma seeded with inflammatory cells and it is one of the most aggressive forms of cancer with no current specific therapies. Tumor-associated macrophages (TAMs) are a major component of the tumor microenvironment (TME), and in most solid cancers increased TAM infiltration is associated with a poor prognosis. TAMs can be described as classically activated M1 types with pro-inflammatory antitumor functions, versus alternatively activated M2 types with immunosuppressive pro-tumor functions. The immunosuppressive functions of M2 TAMs can be exerted through release of cytokines and growth factors as well as via direct recruitment of T regulatory cells (Tregs), a subset of lymphocytes responsible for immune tolerance of the system to the tumor. While the differentiation from M1 to M2 in PDAC has been shown to be associated with a worse prognosis [1], not much is known about PDAC

TAM polarization and its potential correlation to Treg recruitment.

Methods
We have used MultiOmyx, a proprietary, multiplexing assay with similar staining characteristics as standard IHC stains but with the significant advantage that 60 protein biomarkers can be interrogated from a single FFPE section. MultiOmyx protein immunofluorescence (IF) assays utilize a pair of directly conjugated Cyanine dye-labeled (Cy3, Cy5) antibodies per round of staining. Each round of staining is imaged and followed by novel dye inactivation chemistry, enabling repeated rounds of staining and deactivation.

Results
Using the pan macrophage marker CD68 in combination with either M1 marker HLA-DR or M2 marker CD163 we confirmed the presence of M1 (CD68+HLA-DR+) and M2 (CD68+CD163+) populations in 9 stage IIB non-metastatic PDAC FFPE samples, the vast majority being of the M2 subtype. Moreover, we found a positive significant correlation (Pearson's correlation $p<0.05$) between the presence of M2 TAMs and Tregs (CD3+CD4+FoxP3+), but not between M1 TAMs and Tregs. Using our proprietary algorithms that takes into account the staining pattern for each specific biomarker, we will now examine the spatial relationship between the M1/M2 subtypes of TAMs and Tregs in the stromal and intratumoral areas and compare our findings to those found in samples from patients with stage IV metastatic PDAC.

Conclusions
We demonstrate a positive significant correlation between the presence of M2-TAMs and Tregs in the TME of PDAC, suggesting a possible pathway in which TAM-polarization plays an immunosuppressive function by recruiting Tregs.

References
1. Kurahara H et al. Significance of M2-polarized tumor-associated macrophages in pancreatic cancer. JSurgRes. 2011;167:e211-219

P488

Targeting hIDO1 with 3rd generation antisense oligonucleotides for modulation of the tumor microenvironment

Richard Klar, PhD[1], Sandra Kallert, PhD[2], Tamara Thelemann[1], Sven Michel[1], Monika Schell[3], Lisa Hinterwimmer[1], Alfred Zippelius, MD[2], Frank Jaschinski, PhD[3]

[1]*Secarna pharmaceuticals GmbH & Co. KG, Planegg/Martinsried, Germany*
[2]*University of Basel, Department of Biomedicine, Switzerland*
[3]*Secarna pharmaceuticlas GmbH & Co. KG, Planegg-Martinsried, Germany*

Background
Targeting the immunosuppressive microenvironment of tumors has emerged as a promising treatment option for oncologic indications in the last years. However, despite long lasting remissions in a small subset of patients the majority does not respond to the currently available immunotherapies, possibly caused by the existence of a plethora of immune suppressive factors. One of those factors is indoleamin-2,3-dioxygenase 1 (IDO1), an enzyme that degrades tryptophan to kynurenines which in turn can result in a suppression of immune effector cells.

Methods
As an alternative approach to small molecule IDO1-inhibitors, we designed antisense oligonucleotides (ASOs) with specificity for human IDO1 (hIDO1). ASOs were synthesized as GapmeRs with flanking locked nucleic acids to increase stability and affinity

to the target RNA. The knockdown efficacy of ASOs on the mRNA and protein level was investigated in cancer cells and human immune cells without addition of a transfection reagent. The effect of hIDO1 knockdown in cancer cells on the production of L-Kynurenine and the proliferation of cocultured T cells was investigated. We furthermore developed ASOs with specificity for murine IDO1 (mIDO1) to investigate the efficacy of ASO-mediated IDO1 knockdown in syngeneic tumor models.

Results

We identified a subset of ASOs that resulted in a hIDO1 mRNA knockdown of >90% in cancer cell lines. Two highly potent ASOs with IC50 values in the low nanomolar range were selected for further experiments. The treatment of cancer cells as well as human immune cells resulted in reduction of IDO protein levels by >85%. Importantly, we observed a complete block in the production of immunosuppressive L-Kynurenine in ASO treated cells and IC50 values in the low nanomolar range. In line with those results, we observed a strongly increased proliferation of T cells when hIDO1 was knocked down in cocultured tumor cells. Preliminary in vivo experiments suggest that treatment of tumor-bearing mice with mIDO1-specific ASOs results in the knockdown of IDO1 in tumor cells as well as tumor infiltrating myeloid cells.

Conclusions

We selected highly potent hIDO1 ASOs that efficiently knock down hIDO1 mRNA and protein in cancer cells as well as primary human cells and potently reduce the immunosuppressive capacity of cancer cells. Potent mouse specific IDO1 ASOs have been identified and will be used for in vivo efficacy studies in tumor-bearing mice. Taken together, we developed an innovative immunotherapeutic tool to block the expression of hIDO1 that will potentially improve treatment options for cancer patients in the future.

Ethics Approval

PBMC were obtained from leukapheresis products (Klinikum rechts der Isar, TU München ethics commission reference: 329/16 S)

P489

Prognostic significance of tumor-associated macrophage content in head and neck squamous cell carcinoma: A meta-analysis

Ayan Kumar, BS[1], Alexander Knops, BA[1], Brian Swendseid, MD[1], Ubaldo Martinez-Outschoom, MD[1], Larry Harshyne, PhD[1], Nancy Philp, PhD[1], Ulrich Rodeck, MD PhD[1], Christopher Snyder[1], Adam Luginbuhl, MD[1], David Cognetti, MD[1], Jennifer Johnson, MD[1], Joseph Curry, MD[1]

[1]*Thomas Jefferson University, Philadelphia, PA, USA*

Background

Head and neck squamous cell carcinoma (HNSCC) develops within a complex cellular microenvironment that promotes tumor growth, thus providing multiple potential therapeutic targets. Among those are macrophages, which are abundant in and around tumor tissue, and have been implicated in the growth, development, and persistence of HNSCC [1]. However, the relationship between the density and composition of tumor-associated macrophages (TAMs) and clinicopathologic markers of disease is poorly defined [2,3]. Inconsistent findings may be a result of differences in approach to TAM detection. Some authors have measured total macrophage content in tumor tissue, while others have stained tumor samples for individual subtypes of TAMs, which include M1 (pro-inflammatory) and M2 (immunosuppressive). Here we review the published evidence concerning the relationship of the phenotypes of tumor-associated macrophages with HNSCC prognosis.

Methods

We conducted a meta-analysis of the existing publications investigating the relationship between TAM density (total and M2 subtype) and T stage, nodal involvement, vascular invasion, lymphatic invasion, and tumor differentiation (Figure 1). A total of thirteen studies were included (Table 1) [2-14]. Forest plots and risk ratios were generated to illustrate overall effects.

Results

Higher density of both total and M2 subtype of TAMs in the tumor microenvironment is associated with advanced T stage, increased rates of nodal positivity, presence of vascular invasion, and presence of lymphatic invasion ($p < 0.0001$; Figures 2-5). There is no significant association between TAM density, either total or M2 subtype, and tumor differentiation (Figure 6).

Conclusions

Increased TAM density, particularly those of the M2 phenotype, correlates with poor clinicopathologic markers in HNSCC and is associated with poor clinical prognosis. Yet, it is unknown whether and how TAMs contribute to poor prognosis in this tumor type. Additional investigation into the mechanisms behind TAM recruitment and polarization will help define the feasibility of TAM-targeted therapies.

References

1. Marcus B, Arenberg D, Lee J, et al. Prognostic factors in oral cavity and oropharyngeal squamous cell carcinoma. Cancer. 2004; 101(12):2779-2787.
2. Fang J, Li X, Ma D, et al. Prognostic significance of tumor infiltrating immune cells in oral squamous cell carcinoma. BMC Cancer. 2017; 17.
3. Shigeoka M, Urakawa N, Nakamura T, et al. Tumor associated macrophage expressing CD204 is associated with tumor aggressiveness of esophageal squamous cell carcinoma. Cancer Science. 2013; 104(8):1112-1119.
4. Balermpas P, Rödel F, Liberz R, et al. Head and neck cancer relapse after chemoradiotherapy correlates with CD163+ macrophages in primary tumour and CD11b+ myeloid cells in recurrences. Br J Cancer. 2014; 111(8):1509-1518.
5. Fujii N, Shomori K, Shiomi T, et al. Cancer-associated fibroblasts and CD163-positive macrophages in oral squamous cell carcinoma: their clinicopathological and prognostic significance. Journal of Oral Pathology & Medicine. 2012; 41(6):444-451.
6. Hu Y, He M-Y, Zhu L-F, et al. Tumor-associated macrophages correlate with the clinicopathological features and poor outcomes via inducing epithelial to mesenchymal transition in oral squamous cell carcinoma. J Exp Clin Cancer Res. 2016; 35.
7. Huang H, Liu X, Zhao F, et al. M2-polarized tumour-associated macrophages in stroma correlate with poor prognosis and Epstein-Barr viral infection in nasopharyngeal carcinoma. Acta Otolaryngol. 2017; 137(8):888-894.
8. Liu S-Y, Chang L-C, Pan L-F, Hung Y-J, Lee C-H, Shieh Y-S. Clinicopathologic significance of tumor cell-lined vessel and microenvironment in oral squamous cell carcinoma. Oral Oncology. 2008; 44(3):277-285.
9. Lu C-F, Huang C-S, Tjiu J-W, Chiang C-P. Infiltrating macrophage count: a significant predictor for the progression and prognosis of oral squamous cell carcinomas in Taiwan. Head Neck. 2010; 32(1):18-25.
10. Matsuoka Y, Yoshida R, Nakayama H, et al. The tumour stromal features are associated with resistance to 5-FU-based chemoradiotherapy and a poor prognosis in patients with oral squamous cell carcinoma. APMIS. 2014; 123(3):205-214.
11. Sugimura K, Miyata H, Tanaka K, et al. High infiltration of tumor-associated macrophages is associated with a poor response to chemotherapy and poor prognosis of patients undergoing neoadjuvant chemotherapy for esophageal cancer. Journal of Surgical Oncology. 2015; 111(6):752-759.
12. Wang S, Sun M, Gu C, et al. Expression of CD163, interleukin-10, and interferon-gamma in oral squamous cell carcinoma: mutual relationships and

prognostic implications. Eur J Oral Sci. 2014; 122(3):202-209.
13. Yamagata Y, Tomioka H, Sakamoto K, et al. CD163-positive macrophages within the tumor stroma are associated with lymphangiogenesis and lymph node metastasis in oral squamous cell carcinoma. Journal of Oral and Maxillofacial Surgery. 2017; 75(10):2144-2153.
14. Zhu Y, Li M, Bo C, et al. Prognostic significance of the lymphocyte-to-monocyte ratio and the tumor-infiltrating lymphocyte to tumor-associated macrophage ratio in patients with stage T3N0M0 esophageal squamous cell carcinoma. Cancer Immunol Immunother. 2017; 66(3):343-354.

Figure 1.

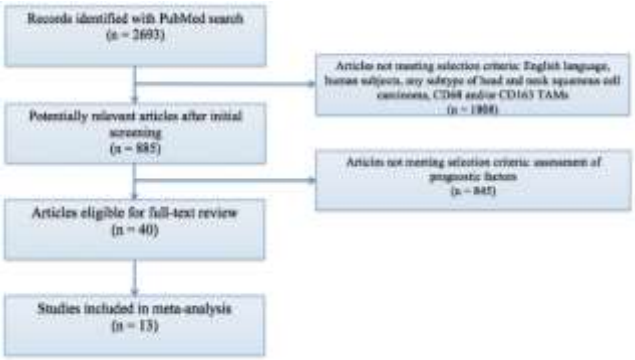

Table 1.

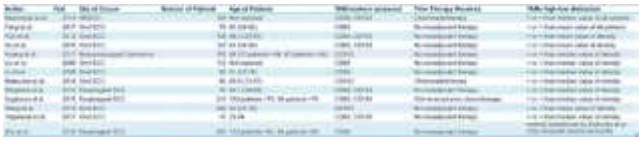

Figure 2.

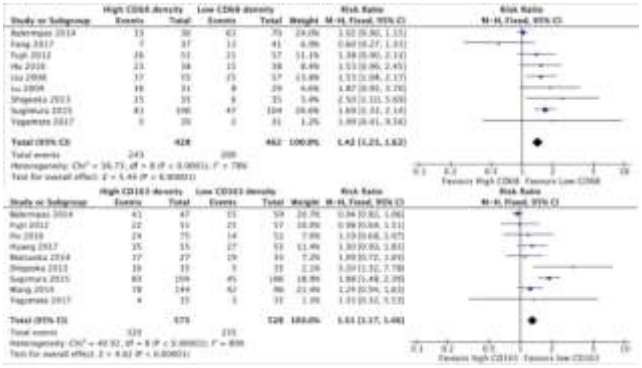

Figure 3.

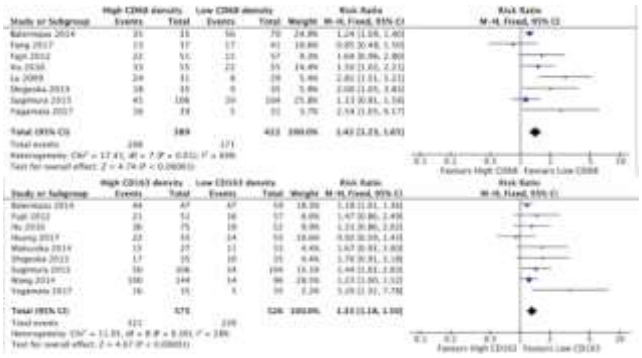

Figure 4.

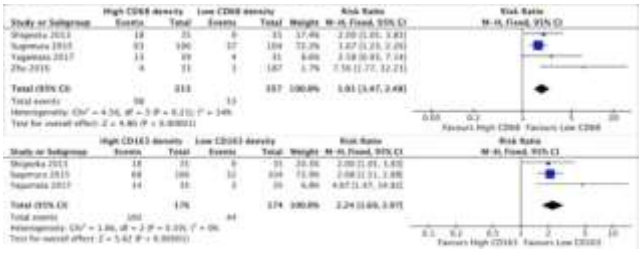

Figure 5.

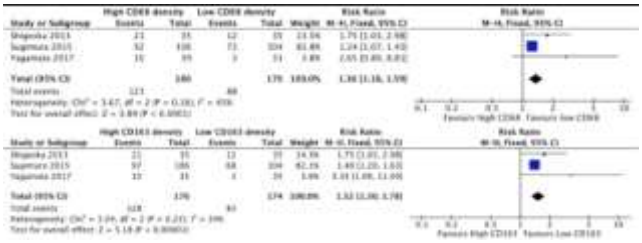

Figure 6.

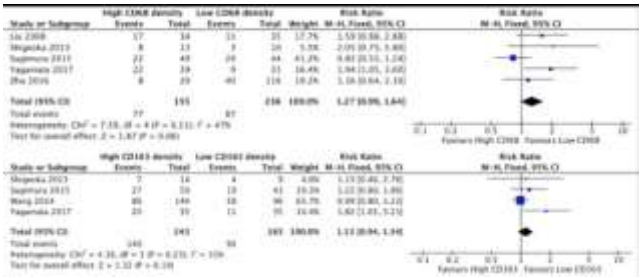

P490

Characterization of the tumor immune microenvironment in treatment-naïve EGFR-mutant NSCLC uncovers a suppressed immune phenotype

Xiuning Le[1], Alexandre Reuben[1], Marcelo Negrao, MD[1], Won-Chul Lee, PhD[1], Edwin Parra[1], Carmen Behrens, MD[1], Humam Kadara, PhD[2], Ignacio Wistuba, MD[1], Jianjun Zhang, MD, PhD[1], John Heymach[1]

[1]MD Anderson Cancer Center, Houston, TX, USA
[2]American University of Beirut, Beirut, Lebanon

Background

Although immune checkpoint blockade (ICI) has been successfully utilized in treating patients with non-small cell lung cancer (NSCLC), the benefit of ICI for patients with advanced EGFR-mutant NSCLC has been limited. Intriguingly, recent data from IMpower150 subgroup analysis demonstrated that combination of VEGF blockade with anti-PD-L1 and chemotherapy induces response in patients with EGFR/ALK driven NSCLC, suggesting modulating the tumor microenvironment may enhance response to anti-PD-1 blockade in EGFR/ALK lung cancers. In order to develop effective immune therapy combinations, it is critical to understand tumor immune microenvironment (TME) and identify negative regulators in EGFR-mutant lung cancer for rational design of clinical trials. [1]

Methods

We leveraged a published set of stage I-III lung adenocarcinomas with immune profiling and sequencing data (PROSPECT cohort, Kadara et al Ann Oncol 2018). We selected a set of 94 adenocarcinomas including 14 cases with EGFR-sensitizing mutations with immune profiling by immunohistochemistry for ten immune markers (PD-L1, PD-1, CD3, CD4, CD8, CD45RO, CD57, CD68, FoxP3 and Granzyme B). Gene microarray data were also available to evaluate the tumor microenvironment while CIBERSORT was used to infer immune cell subpopulations.

Results

PDL1 and GzmB were significantly lower in the EGFR-mutant cases, as expected. CD4 was higher in EGFR-mutant tumor center. Forty-four key immune regulators' levels we evaluated to further evaluate the tumor microenvironment. IFNG was lower while TGFbeta was higher in EGFR-mutant cases, suggesting a suppressive TME. Other negative regulators, including CTLA4, LAG3, TIM3, TIGIT, IL6 and VEGFA were not differentially expressed. Lastly, CIBERSORT analysis revealed CD4+ memory T cells were decreased in the EGFR-mutant cases.

Conclusions

Results from this analysis are consistent with prior knowledge of EGFR-mutant NSCLC, demonstrating a PD-L1 low, GzmB low, IFNG low and TGFbeta high immune phenotype, suggesting a suppressive tumor microenvironment. CD4+ T cells composition needs

to be further understood as subpopulation of CD4+ T cells (T regs) might be contributing to the suppressed TME. These results represent an initial step for rationale combination of immune therapy to modulate the suppressive TME, which might lead to enhanced treatment efficacy to benefit patients with EGFR-mutant lung cancers.

References
1. Kadara H, et al. Ann Oncol. 2018 29(4):1072

P491

The DNA methyltransferase inhibitor, guadecitabine, has beneficial immunomodulatory effects on myeloid derived suppressor cells, and augments adoptive immunotherapy for solid tumors

Andrea Luker, PhD candidate[1], Harry Bear, M.D., Ph.D. [1], Daniel Conrad, Ph.D. [1], Laura Graham[1]

[1]*Virginia Commonwealth University, Richmond, VA, USA*

Background
Myeloid Derived Suppressor Cells (MDSC) are a regulatory population that accumulates in tumor microenvironments. They are a significant hurdle in treating cancer because they dampen anti-tumor responses as well as hinder the effects of immunotherapy. Here we show that the DNA methyltransferase inhibitor (DNMTi), Guadecitabine, has beneficial immunomodulatory effects on MDSCs and 4T1 tumor cells, both *in vitro* and *in vivo*.

Methods
Purified MDSCs or 4T1 cells were cultured for 48-72 hours with 1μM Guadecitabine and then analyzed for surface molecules by flow cytometry or further incubated with fluorescently-labeled Ovalbumin for 30 minutes to allow for antigen uptake. 4T1 tumors (50k, flank) were established in syngeneic Balb/c mice for 10 days before administering four daily doses of Guadecitabine (50μg, i.p.); mice were sacrificed at day 16 to collect tissues for analysis. Guadecitabine and AIT (50 million expanded draining lymph node cells) were administered concurrently starting at day 3, and tumor size was monitored until a humane endpoint. All experiments include n=3+ with at least two experimental repeats.

Results
MDSCs cultured with Guadecitabine had increased expression of MHC II, CD80, and CD86 exclusively in Ly6C+ cells, with no effect on the Ly6G+ subpopulation. These Ly6C+ MDSCs also demonstrated significantly enhanced antigen uptake *in vitro*. Guadecitabine-treated 4T1 cells exhibited significantly increased MHC I and PD-L1 expression over vehicle-treated cells. Guadecitabine treatments in 4T1 tumor-bearing mice immediately reduced the tumor-induced MDSC accumulation in the spleen (Figure 1), bone marrow, and blood, thereby restoring normal cellularity. Similar to the *in vitro* findings, the remaining MDSCs in Guadecitabine-treated mice had increased levels of MHC II and co-stimulatory molecules. Subsequently, animals sacrificed at day 16 exhibited a significant reduction in tumor area (Figure 2). Finally, we tested the effectiveness of Guadecitabine in combination with T cell adoptive immunotherapy (AIT). Individually, Guadecitabine or AIT alone slowed the initial tumor progression over the first 2-3 weeks. When applied together, however, there was an additional synergistic effect that strongly suppressed tumor growth and prolonged overall survival for an additional 2+ weeks (Figure 3).

Conclusions
In vitro, the DNMTi Guadecitabine selectively alters the Ly6C+ MDSC subpopulation toward an immune-stimulatory phenotype, and induces expression of immunogenic surface molecules on 4T1 cells. *In vivo*, treatment with Guadecitabine reduces tumor burden by mainly affecting MDSC accumulation and

phenotype. In addition, Guadecitabine enhances the effectiveness of AIT to suppress tumor progression and prolong overall survival.

Acknowledgements
We would like to thank Astex Pharmaceuticals for providing the Guadecitabine, as well as the Massey Cancer Center for pilot grant funding.

Ethics Approval
These studies were conducted with the permission and oversight of the VCU Institutional Animal Care and Use Committee.

Figure 1.

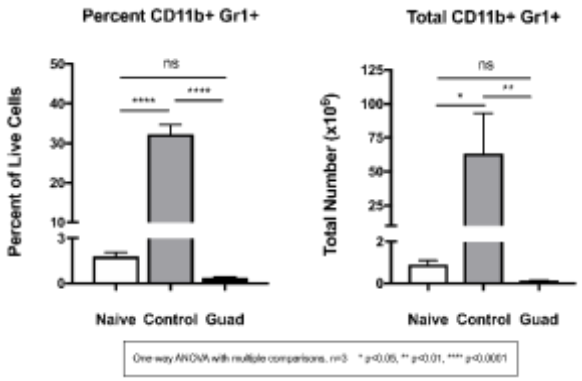

Figure 2.

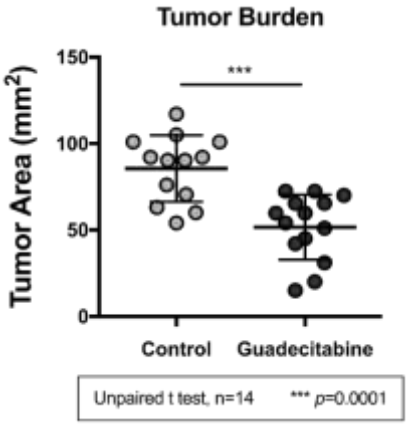

Figure 3.

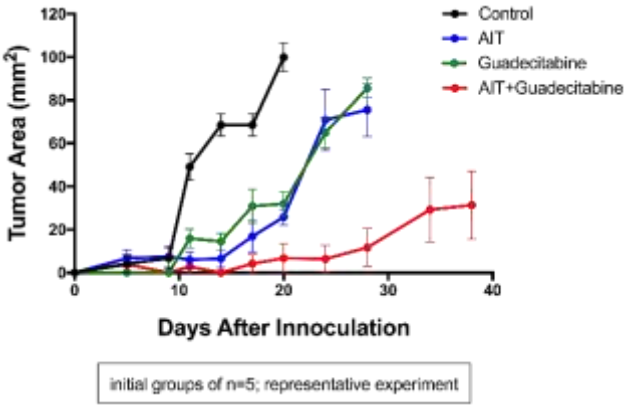

P492

Myeloid-derived suppressor cells (MDSC) assessment using a fully automated sequential chromogenic multiplex assay

Anna Martirosyan, Dr[1], Assil Benchaaben[1], Aurélie Collignon, MS[1], Emilie Bonzom, Trainee[1], Matthieu Duval, Apprentice[1], Emmanuel Prestat, PhD[1], Christophe Haond[1], Jacques Fieschi, PhD[1]

[1]*HalioDx, Marseille, France*

Background
Despite significant advances in the recent years, the response rate to immune checkpoint inhibitor therapies for non-small cell lung cancer (NSCLC) is only about 20%. There is a strong and urgent need to identify new diagnostic biomarkers to predict which patients can benefit from an immune checkpoint blocker treatment. Extensive animal data and several clinical trials indicate that immunosuppression is a limiting factor of effective anti-tumoral immunotherapy. In this context, the presence of immunosuppressive elements such as myeloid-derived suppressor cells (MDSC) in the tumoral microenvironment might be a major factor contributing to resistance to checkpoint inhibitors. In recent years, several studies have shown a

correlation between the level of MDSC and stage, overall survival, and response to therapy in NSCLC patients. For instance circulating MDSC were negatively associated with the immune response to cancer vaccine. Furthermore, the accumulation of MDSC has also been reported to correlate with the progression-free survival and the response to chemotherapy, as well as metastatic burden in NSCLC patients. Last, but not least the intra-tumoral accumulation of MDSC is associated with unfavorable prognosis.

Methods

Here we assessed the presence and abundance of this major immunoregulatory population within the NSCLC microenvironment by using an automated sequential chromogenic multiplex assay.

Results

A unique combination of biomarkers (CD11b, CD15, HLA-DR, CD14, LOX1, and S100A9) was developed to detect and quantify different populations of MDSC on a single FFPE tumor tissue section. Briefly, a tissue section was sequentially stained, digitized, unstained and re-stained with antibodies targeting the six markers. Images of the whole slide were then analyzed by digital pathology: first, a newly developed software was used to co-register the 6 virtual slides and perform colors deconvolution. Then detection of positive cells was performed for each marker independently, using Indica Lab's HALO software. The M-MDSC (monocytic MDSC) and PMN-MDSC (polymorphonuclear MDSC) populations were defined as being respectively CD11b+CD14+HLA-DRnegativeS100A9+cells and CD11b+CD15+HLA-DRnegativeLOX1+cells. In addition, tissue segmentation tools were used to assess MDSC densities in parenchyma, tumor stroma and invasive margin regions.

Conclusions

The detection and quantification of MDSC in NSCLC patients could be a key parameter to predict patient's responses to anti-tumoral immunotherapy. This new tool will allow to evaluate the immunosuppressive landscape of NSCLC tumors.

P493 Abstract Travel Award Recipient

B cells in glioblastoma are associated with diminished survival

Ileana Mauldin, PhD[1], Jasmin Jo, MD[1], Nolan Wages, PhD[1], Samuel Young, BS[1], Loren Erickson, PhD[1], Maria-Beatriz Lopes, MD, PhD[1], Craig Slingluff, MD[1], Camilo Fadul, MD, FAAN[1]

[1]*University of Virginia, Charlottesville, VA, USA*

Background

The demonstrated efficacy of immunotherapy, in the treatment of some cancers, has not been observed with glioblastoma (GBM). Characterization of the immune infiltrates in GBM may identify targets to drive the immune activation that improves the efficacy of immunotherapy. We have observed that GBM can harbor dense B cell infiltrates usually found cuffing blood vessels. B cells can act as antigen presenting cells driving local immune activation, or as regulatory B cells (Bregs) to suppress immune activation; they may also be localized in tertiary lymphoid structures (TLS) usually associated with better patient survival. The prevalence and role of B cell infiltrate in GBM is unknown.

Methods

Surgically-resected GBM from 48 patients were evaluated for immune infiltrate by multispectral Immunohistochemistry using the OPAL staining system, Vectra3 microscope, and Inform Software (PerkinElmer). Three multiplex panels were designed to enumerate CD20 infiltrates from three serial sections of tumors and to evaluate additional immune markers. RNA-seq gene expression data from the Cancer Genome Atlas (TCGA) was evaluated

from GBM patients.

Results

In univariate assessments, low CD20+ cell densities were associated with better overall survival (OS) (median OS 31.7 months for 12 CD20low patients vs. 18.7 months for 36 CD20high patients, p=0.019). Multivariate analyses were done to assess key prognostic factors (CD20 density (low vs high), Karnofsky performance status (KPS; high vs. low), age, and MGMT methylation (methylated vs unmethylated). Decreased OS was observed from patients with high CD20+ infiltrate (Hazard ratio (HR)=2.84, p=0.03) and longer OS was associated with MGMT methylation (HR=0.49, p=0.04). Differences in age (HR=1.13, p=0.05) and KPS (HR=0.49, p=0.08) were trending in significance. We found that B cell infiltrates in GBM do not constitute TLS when examined for high endothelial venules. TCGA data also suggests that in GBM overexpression of MS4A1 (encoding CD20) is associated with decreased OS (p=0.01).

Conclusions

Our studies suggest a correlation between B cells and diminished patient survival, thus CD20 infiltrates may constitute a novel prognostic factor for GBM. We hypothesize that B cells in GBM may function as Bregs which would suppress immune activation. However, this hypothesis needs to be further evaluated by examining Breg function in tumors and evaluating the impact of GBM-infiltrating B cells on tumor-infiltrating T cells.

Ethics Approval

The study was approved by the University of Virginia's Ethics Board, approval number 20210.

P494

Targeting the CCR2/MCP-1 chemokine axis for cancer therapy

Payal Mittal[1], Tatiana Akimova[2], Craig Leach[3], Jose Clemente[3], Matthew Sender[3], Liqing Wang[2], Joseph Marino[3], Yao Chen[3], Peiling Chen[3], Brandon Turunen[3], Wayne Hancock, MD, PhD[2]

[1]Children's hospital of Philadelphia/GSK, Philadelphia, PA, USA
[2]Children's hospital of Philadelphia, Philadelphia, PA, USA
[3]GlaxoSmithKline, Collegeville, PA, USA

Background

Host anti-tumor responses, including the actions of cytotoxic T cells, play a key role in curtailing tumors, but can be hindered by multiple mechanisms active within the tumor microenvironment. One such mechanism involves the recruitment and expansion of immunosuppressive cells such as myeloid derived suppressor cells (MDSCs) in the tumor microenvironment. We are targeting the signaling pathways implicated in recruitment of MDSCs in tumor microenvironment.

Methods

We have utilized transplantable lung tumor cell line (TC1) to address the role of the CCR2/MCP-1 axis in MDSC associated tumor progression. Additionally, I utilized CCR2 knockout mice to demonstrate the dependence of progression of TC1 tumor on CCR2 signaling.I also used a thioglycolate-induced peritonitis model of inflammation to validate the ability of a CCR2 antagonist to inhibit trafficking of MDSCs to the site of inflammation and then tested the compound at this inhibitory concentration for its ability to impair CCR2 chemokine signaling within established tumors.

Results
Phenotypic profiling of TC1 tumors revealed maximal expression of CCR2 by tumor resident MDSCs, and MCP-1 by transplanted tumor cells, tumor associated macrophages (TAMs) and tumor associated neutrophils (TANs) respectively. Additionally, utilization of CCR2 knockout mice showed the dependence of progression of TC1 tumor on CCR2 signaling (tumors were significantly smaller in CCR2KO mice compared to WT mice). We used a thioglycolate-induced peritonitis model of inflammation to validate the ability of a CCR2 antagonist to inhibit trafficking of MDSCs to the site of inflammation in a dose-dependent manner with a maximal effect at a dose of 10 mg/kg, and then tested the compound at this inhibitory concentration for its ability to impair CCR2 chemokine signaling within established tumors. CCR2 antagonist promoted antitumor immunity in TC1 tumors.

Conclusions
In summary, genetic and pharmacologic data indicate that CCR2 targeting may be an important new component of immuno-oncology based therapies.

P495

Pegfilgrastim, but not Plinabulin, generates a blood myeloid cell (BMC) repertoire with a predominant immunosuppressive phenotype

Douglas Blayney, MD[1], Stephan Ogenstad[2], Yuankai Shi[3], Lihua Du[4], Lan Huang[5], Ramon Mohanlal, MD, PhD, MBA[5*]

[1]*Stanford Cancer Institute, Stanford, CA, USA*
[2]*Statogen Consulting, LLC, Zebulon, NC, USA*
[3]*Chinese Academy of Medical Sciences, Beijing, China*
[4]*Wanchun Bulin Pharmaceuticals Limited, Dalian, China*
[5]*BeyondSpring Pharmaceuticals, Inc., New York, NY, USA*

Background
Tumors recruit BMC to the tumor microenvironment and modulate BMCs [immunosuppressive tumor-associated macrophages (TAM), neutrophils (TAN), and myeloid derived suppressor cells (MDSC)] in tumor microenvironment (Schupp, Cellular Immunology, 2017; Ginhoux, Nat Rev Immunology, 2014). Predominantly immature BMCs are associated with poor prognosis (Bergenfelz, PLoS One, 2015; Toor, Cancer Immunol Immunother, 2017). An elevated N-to-L Ratio (NLR) of NLR > 5, and reduced L-to-M ratio (LMR) of <3.2 are predictive of poor prognosis in cancer patients (pts) (Zhou; Nature, 2017; Sierzega; Ann Surg Onc, 2017). Chemotherapy (chemo) induced neutropenia (CIN) is mitigated with G-CSF such as pegfilgrastim (Peg). Plin is a novel non-G-CSF small molecule, with a different mechanism of action for CIN (LSK inhibition reversal; Lloyd AACR, 2017). Plin (by IV) and Peg (by SC) are given as a single dose-per-cycle. In contrast to Peg, Plin is given on the same day of chemo, 30 minutes after chemo, vs 24 hours after chemo with Peg. Plin does not cause bone pain, and has anti-cancer, immune-enhancing activity (Mohanlal, ASCO-SITC 2018). The Phase (Ph)2 portion of Study BPI-2358-105 (NCT03P171

*Corresponding author email: mbagarazzi@inovio.com6) in NSCLC pts, compared Plin (at different doses; n=55) with Peg for the prevention of Docetaxel (Doc) CIN. Plin (20 mg/m2) and Peg are equally effective for the prevention of Doc CIN, in respect to frequency and duration of severe neutropenia (Blayney, ASCO 2018). Since Plin and Peg both improve BMCs, we evaluated their respective immunosuppressive potential.

Methods
BMCs from cycle 1 of Ph2 study 105 was analyzed with either Plin (20 mg/m2; n=14) or Peg (6 mg; n=14). BMCs, including immature Ns ((pro)myelocytes and bands) were available through day (D) 15.

Results
In contrast to Peg, Plin did not show NLR>5 or LMR<3 (Table below). N bands were observed in 25% vs 0% of pts with Peg and Plin resp. (Pro)myelocytes were observed in 77% vs 14% of pts with Peg and Plin, resp (p<0.001).

Conclusions
Peg, but not Plin generates a BMC profile with a predominant immunosuppressive phenotype, while both are equally effective for the prevention of Doc CIN.

Table 1. Blood Immune Cell Repertoire after Peg or Plin

	Baseline	D6	D7	D8	D9	D10	D15
Plin NLR	2.63	3.01	1.83	1.26	1.13	1.15	1.96
Peg NLR	4.11	3.93	5.09	8.31	9.21	12.2	8.11
p-value NLR	NS	NS	0.03	<0.001	<0.001	<0.001	<0.001
Plin LMR	5.75	7.81	8.29	6.59	4.50	3.70	4.15
Peg LMR	3.84	4.43	2.74	3.15	2.95	2.99	3.24
p-value LMR	NS	0.005	<0.0001	0.026	NS	NS	NS

P496

Innate and adaptive immune responses to metastatic colorectal cancer differ by sex and correlate with survival

Anita Ray, PhD[1], Robert Nofchissey, BS[1], Sarah Adams, MD[2], William Berry[1], Katherine Morris, MD, FACS[3]

[1]OUHSC, Oklahoma City, OK, USA
[2]UNM, Albuquerque, NM, USA
[3]University of Oklahoma Stephenson Cancer Center, Oklahoma City, OK, USA

Background
Women with colorectal cancer (CRC) have a survival advantage over men. The mechanism behind this is unclear. CRC is strongly influenced by the tumor immune microenvironment (TME), with multiple immune cell types and signaling pathways implicated in its initiation, progression, and metastasis. Furthermore, murine models of sepsis have demonstrated increased numbers of peritoneal leukocytes and increased activation in females that correlate with improved survival [1,2]. Macrophages are vital participants in the CRC TME and can drive pro- and anti-inflammatory shifts. We hypothesized that the immune CRC TME is sex-dependent and contributes to improved survival in females.

Methods
Male and female C57/Bl6 mice were injected with 105 MC38 cells intraperitoneally. Age and sex-matched mice were sacrificed for normal controls (n=6 for all groups). Tumors and ascites developed in the peritoneal cavity in the tumor model. Mice were sacrificed when moribund or at Day 23 post-injection. Serum and tumor cytokine secretion were measured with Luminex™ 32-Plex Immunology assay and results compared by sex. Cells were stained with fluorescent antibodies and run on a flow cytometer alongside controls.

Results
Similar to human CRC patients, female mice survived longer than males (p=0.0354). While there were no significant differences in cytokine production in healthy mice, male and female mice bearing tumors had significant differences in both systemic and tumor-produced cytokines. In female TME, more G-CSF, IL-10, and GM-CSF were secreted. These cytokines influence macrophage polarization. Macrophage numbers at the tumor site were similar between the sexes, but tumors from female mice had increased IL-10 producing macrophages (p=0.0685), which is characteristic of M2-type macrophages. Mice with elevated IL-10+ macrophages survived longer (p=0.0005). M2 macrophages and G-CSF signaling cause differentiation of Th2 cells. Tumors from females showed increased total CD4+ T cells (p=0.0398), which also correlated with increased survival

(p=0.0222). Animals with elevated IL-4 producing CD4 T cells survived longer (p=0.0195), suggesting that sex-specific innate and adaptive responses to CRC may contribute to the survival benefit seen in women.

Conclusions

Shifts within the TME can alter the trajectory of tumor progression and patient outcome. We report here marked differences in the TME of females and males in immune cell populations and behavior. These changes within the tumor are strongly correlated with survival, suggesting that they play a role in the survival gap between men and women with CRC. The origins of these sex-linked responses, and the potential effects on immune therapies warrant further study.

Acknowledgements

We would like to acknowledge the American Cancer Society, the Stephenson Cancer Center, and the University of Oklahoma Health Sciences Center Department of Surgery for funding, and the Laboratory for Molecular Biology and Cytometry Research at OUHSC for the use of the Flow Cytometry and Imaging facility which provided equipment and services.

References

1. Scotland R, Stables M, Madalli S, et al. Sex differences in resident immune cell phenotype underlie more efficient acute inflammatory responses in female mice. Blood 2011; 118:5918-5927.
2. Angele M, Schwacha M, Ayala A, et al. Effect of gender and sex hormones on immune responses following shock. Shock 2000; 14(2):81-90.

Ethics Approval

The study was approved by the OUHSC IACUC, protocol number 17-008-C.

P497

Study of anti-HER2 CAR T cells in the immunosuppressive ependymoma tumor microenvironment

Marissa Kane[2], Andrea Griesinger[2], Andrew Donson[2], Vladimir Amani[2], Nicholas Foreman[2], Davis Witt[3], Jean Mulcahy Levy[2], Anandani Nellan, MD[2]

[1]Children's Hospital Colorado, Aurora, CO, USA
[2]University of Colorado Denver, Aurora, CO, USA
[3]Thomas Jefferson University, Philadelphia, PA, USA

Background

Ependymoma is the third most common childhood brain tumor and novel treatment methods are urgently needed. Complete surgical resection and radiation still results in a 10-year relapse rate of over 70%. Chemotherapy has failed to improve survival in patients with ependymoma. Chimeric antigen receptor (CAR) T cell therapy has been very effective in hematologic malignancies, but progress in solid tumors has lagged. The hostile tumor microenvironment of solid tumors has been implicated as a primary reason why CAR T cell therapy has only resulted in modest and temporary responses in patients. Previous research has shown that ependymoma tumor cells secrete cytokines that polarize surrounding monocytes into an immunosuppressive phenotype, which in turn renders tumor infiltrating T cells ineffective. Native T cells found in patients' ependymoma tumor samples are incapacitated and this phenomenon may also affect engineered CAR T cells.

Methods

811 and 928 are two high-risk patient derived ependymoma cell lines that have confirmed HER2

surface expression and are used for in-vitro experiments. Human peripheral blood mononuclear cells are activated to promote T cell proliferation and transduced with retrovirus to express anti-HER2 CAR on the surface. Monocytes are cultured in 811 and 928 tumor conditioned media to polarize cells into an immunosuppressive phenotype (polarized monocyte media). T cells and monocytes from the same donor are used in each experiment. Flow cytometry is used to characterize exhaustion markers, as well as surface CAR expression of transduced T cells. Cytokine secretion will be analyzed with a Millliplex Human Cytokine Panel. T cell function will be assessed with an Incucyte live cell imager to quantify immune cell killing of tumor cells over time.

Results

Anti-HER2 CAR T cells have excellent pre-clinical efficacy against 811 and 928 cells as demonstrated by cytokine release after co-incubation and robust tumor cell killing. Anti-HER2 CAR T cells co-cultured in 811 and 928 polarized monocyte media exhibit higher numbers of surface inhibitory markers (PD-1, TIM-3, and LAG-3) compared to anti-HER2 CAR T cells cultured in AIMV media. Anti-HER2 CAR T cells co-cultured in 811 or 928 polarized monocyte media also have decreased CAR surface expression and a trend towards decreased tumor cell killing.

Conclusions

Anti-HER2 CAR T cells cultured in 811 and 928 polarized monocyte media have increased inhibitory markers and decreased CAR expression. Understanding the mechanism of exhaustion and downregulation of CAR expression may have therapeutic implications to improve the efficacy of CAR T cells against solid tumors.

P498

Characterization of the tumor microenvironment in a spontaneous mouse model of cholangiocarinoma: a robust model for evaluating therapeutic interventions for treating the disease

Luis Ruffolo, MD[1], Katherine Jackson, MD[1], Joseph Murphy, MSc[1], Nathania Figueroa, MD[1], Brian Belt, JD[1], David Linehan, MD[1], Peter Prieto, MD, MPH[1]

[1]*University of Rochester Medical Center, Rochester, NY, USA*

Background

Cholangiocarcinoma is the second most common primary liver malignancy. Prognosis is dismal due to its resistance to conventional therapy and propensity to metastasize. Therefore, the development of effective strategies for treating cholangiocarcinoma represents a significant unmet clinical need, but models for evaluating more advanced approaches like targeted and immune based therapies are lacking. Cholangiocarcinoma is characterized by the presence of a dense fibro-inflammatory reaction and extensive tumor stroma that confers resistance to therapy. Although mice with targeted activation of Kras and loss of p53 (Kras-p53) in the liver spontaneously develop cholangiocarcinoma recapitulating the histological features of human disease, the composition of the tumor microenvironment (TME) remains largely unknown. Here, we examined the composition of the TME in Kras-p53 mice to identify additional targets for evaluating more advanced strategies for treating cholangiocarcinoma.

Methods

Histological staining and immunohistochemistry were performed on formalin-fixed, paraffin embedded and frozen tissue sections from human and mouse cholangiocarcinoma tumors for stromal and immune markers. Bone marrow (BM), peripheral

blood, spleen, and single cell tumor and normal liver suspensions from Kras-p53 mice and littermate controls were processed for flow cytometry analysis. RNA was extracted from tumor and normal liver tissue and RNA-seq and qRT-PCR analysis were performed. Myeloid cells from BM, spleen, and tumor were isolated and functional assays were performed in-vitro.

Results

Human cholangiocarcinoma featured prominent immunosuppressive signatures including a dense inflammatory leukocyte infiltrate mainly comprised of myeloid cells of both monocytic and granulocytic origin including tumor associated macrophages (TAM) and neutrophils (TAN) respectively. Tumors from Kras-p53 mice featured a prominent fibro-inflammatory reaction (Figure 1) with a dense network of fibroblasts, collagen deposition and, hyaluronic acid. Flow cytometry demonstrated Kras-p53 tumors were infiltrated with significantly elevated levels of inflammatory leukocytes (Figure 2) including TAM and TAN. RNA-seq and qRT-PCR demonstrated Kras-p53 tumors expressed elevated levels of cytokines associated with myelopoiesis and mobilization of myeloid cells. In addition, tumors expressed increased levels of soluble factors and checkpoint markers associated with immune suppression including Tgf-β, Il10, Arg-1, Pd-l1, Pd-1, and Ctla-4. Myeloid cells isolated from Kras-p53 tumors were functionally trophic and suppressed T cell proliferation. Thus, these data suggest the TME of cholangiocarcinoma features additional targets for testing more advanced strategies including immune based therapies.

Conclusions

Cholangiocarcinoma tumors derived from Kras-p53 mice are highly desmoplastic and feature a prominent inflammatory immune infiltrate including highly immunosuppressive myeloid cells. Thus, Kras-p53 mice are a robust model to evaluate targeted and immune therapeutic interventions.

Ethics Approval

The study was approved by the University of Rochester UCAR Committee, approval number 2014-037E

Figure 1.Tumors derived Kras-p53 mice highly desmoplastic

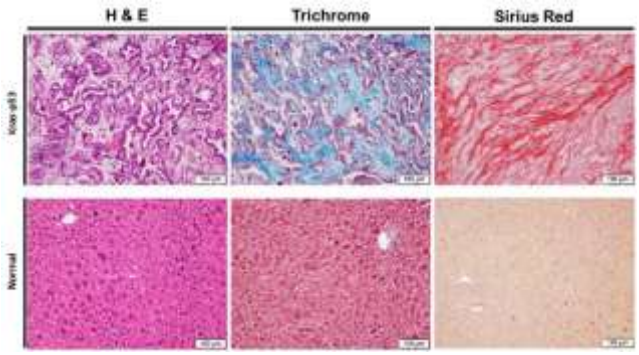

Figure 2. Kras-P53 tumors increased inflammatory leukocytes

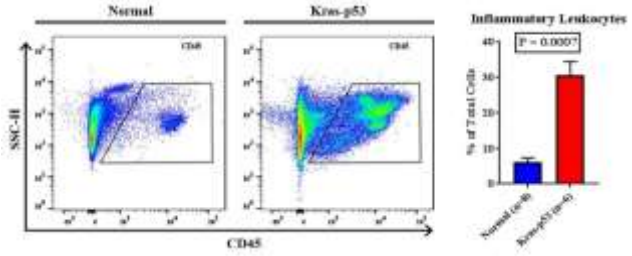

P499

Correlation of immune escape mediated defects in the HLA class I antigen-presenting machinery with the immune cell infiltration and prognosis in oral squamous cell carcinoma

Claudia Wickenhauser, MD, PhD[1], Barbara Seliger, MD, PhD[1]

[1]*Martin Luther University Halle-Wittenber, Halle, Germany*

Background
Progression of oral squamous cell carcinoma (OSCC) is often associated with an evasion of tumor cells from the host immune surveillance, which is accompanied by a worse outcome of patients and might influence the efficacy of immunotherapies.

Methods

Since little information exist about the molecular mechanisms leading to tumor immune evasion and its correlation with the immune cell contexture the expression of HLA class I antigens and components of the antigen processing machinery (APM) was analyzed in three untreated and interferon (IFN)-γ treated OSCC cell lines as well as a panel of 160 human papilloma virus (HPV)-negative OSCC lesions and correlated with the composition of immune cell infiltration and clinical parameters.

Results
Immunohistochemical analyses of the OSCC lesions revealed that HLA class I heavy chain and β2-microglobulin (β2-m) as well as selected HLA class I APM components were significantly downregulated in OSCC lesions vs. non-neoplastic cells. This was in accordance to the predominantly low basal mRNA and protein expression of HLA class I APM components in OSCC cell lines, which was accompanied by low HLA class I surface expression. The impaired HLA class I APM component expression was enhanced by IFN-γ treatment suggesting a deregulation rather than structural alterations as a major mechanism of impaired expression. This was in line with a positive association of HLA class I APM expression levels with the frequency and composition of the immune cell infiltration of OSCC lesions and mediated by the T cell produced IFN-γ: Intra- as well as peri-tumoral density of CD8+ T lymphocytes and intra-tumoral density of FoxP3+ regulatory T cells correlated with membranous HLA class I heavy chain (HC) and β2-m expression and the trimeric HLA classI/β2-m/peptide complex, while membranous β2-m and cytoplasmic HLA class I HC expression positively correlated with the intra-tumoral density of CD4+ T lymphocytes. High cytoplasmic expression levels of HLA class I HC and β2-m, low cytoplasmic expression of the peptide transporter associated with antigen processing (TAP) subunit 1 and a high nuclear expression of LMP2 were significantly correlated with a poor overall survival (OS) of OSCC patients.

Conclusions
In conclusion, this study revealed marked differences between HLA class I-positive and negative tumors related to tissue structure, the composition of intra- and peri-tumoral leukocyte infiltration of the TME and OSCC patients' prognosis. This knowledge might help to overcome immune escape and to improve the efficacy of immunotherapeutic strategies for OSCC patients in the future.

P500

Novel bispecific antibody preferentially and efficiently depletes tumor-associated immunosuppressive myeloid cells and enhances therapeutic responses to PD-L1 blockade in immune-excluded tumor model

Seng-Lai Tan, PhD[1], Sangeetha Palakurthi, PhD[1], Jacqueline Lee[1]

[1]*Elstar Therapeutics, Cambridge, MA, USA*

Background
Accumulation of tumor-associated macrophages (TAMs) and myeloid-derived suppressor cells (MDSCs) has been associated with tumor progression, poor prognosis, and inferior response to immune checkpoint therapy in many cancers. These cells render effector immune cells dysfunctional and promote angiogenesis and metastasis. Thus, TAMs and MDSCs are considered promising therapeutic targets in cancer immunotherapy.

Methods
We determined co-expression of CSF-1R and CCR2 on TAMs and MDSCs and generated a bispecific antibody (UniTI-01), which simultaneously binds CSF-1R and CCR2, to deplete these immunosuppressive cell populations, while sparing tissue-resident macrophages. In vitro and ex vivo assays using recombinant proteins, cell lines, and primary cells were conducted to determine UniTI-01 binding to both CSF-1R and CCR2 on the same cell and its effects on CSF-1 and CCL2-dependent functional assays. Plasma exposure, pharmacodynamic and therapeutic effects of UniTI-01 were assessed in murine syngeneic tumor models.

Results
We confirmed CSF-1R and CCR2 are co-expressed on TAMs and monocytic MDSCs (M-MDSCs) from ovarian and colorectal cancer patients as well as murine syngeneic tumors. Specific binding of the murine-reactive surrogate bispecific antibody UniTI-01 was demonstrated using murine CSF-1R and/or CCR2 in heterologous expression systems. Additionally, UniTI-01 effectively bound TAMs and M-MDSCs derived from several syngeneic tumor models. The monovalent anti-CSF-1R arm and anti-CCR2 arm of UniTI-01 exerted inhibitory activity in CSF-1- and CCL2-dependent functional assays in vitro, respectively. Importantly, UniTI-01 preferentially depleted TAMs and M-MDSCs over major organ tissue-resident macrophages, including Kupffer cells, in tumor-bearing mice. In contrast, an anti-CSF-1R monoclonal antibody induced significant depletion of tissue-resident macrophages in several organs. UniTI-01 treatment increased intratumoral T cells and CD8+ T cells:CD4+ Treg ratio across different syngeneic tumor models. In the immune-excluded model EMT6, a combination regimen of UniTI-01 and an anti-PD-L1 monoclonal antibody induced significant tumor regression compared to either agent alone. Finally, mice that cleared EMT6 tumor on the combination therapy developed specific and durable anti-tumor response demonstrated by their protection when re-implanted with EMT6 cells, but not with a different tumor cell line (CT-26).

Conclusions
Dual targeting of CSF-1R and CCR2 using a bispecific antibody efficiently depletes TAMs and M-MDSCs without significantly affecting tissue-resident myeloid cells and may serve as a novel approach to enhance therapeutic efficacy of checkpoint blockade immunotherapy with a wider therapeutic window. Our data support development of a synonymous human UniTI-01 for clinical evaluation.

P501

Multiplex immunofluorescence evaluation of immune cell relationships within PDAC resection tissues using tailored analysis of multi-spectral image component data

Hannah Thomson[1], Alison Bigley, CSci, FIBMS[2], Lorcan Sherry, PhD[2], Mark Anderson, BSc[2], Mariana Beltran[3], Dawn Lyster, MSc[3], Mike Millar[3]

[1]OracleBio Ltd., North Lanarkshire, Scotland, UK
[2]OracleBio, Glasgow, UK
[3]Aquila BioMedical, Edinburgh, UK

Background
Pancreatic ductal adenocarcinoma (PDAC) is an aggressive exocrine tumour with an extremely poor prognosis where the application of checkpoint inhibitors has proven to be disappointing. One of the characteristics of PDAC is a desmoplastic process that is thought to create a barrier to potential responses of immune cells and reduce accessibility of therapeutic agents. PDAC phenotype is also known to be immune cell deficient. However, M2 macrophage aggregations have been identified within the tumour milieu that often co-express programmed cell death markers. The evaluation of

PD-L1 expression and associated immune cell responses in Whipple's resection tissues may be utilised to aid predicting patient outcome [1]. Here we use a 7-plex evaluation to exemplify the potential of multiplex immunofluorescence (mIF) combined with multispectral imaging and quantitative image analysis to examine relationships in immune, inflammatory and checkpoint expressing cell populations within PDAC surgical resection samples.

Methods

Exemplar PDAC resection sections were mIF labelled by Aquila BioMedical for 5 cell markers, including PD-L1, CD3, CD8, FoxP3, CD163, a pan cytokeratin epithelial marker and DAPI nuclear marker. The stained slides were digitised using the Vectra Polaris multispectral scanner (Perkin Elmer) and defined region of interest (ROI) images exported in multi-layered component data format. The mIF images were analysed by OracleBio using tailored applications developed in Visiopharm Oncotopix Software. These enabled the identification of tumour and stroma ROI, facilitated cell detection, classification and analysis and the determination of cell relationships within the tumour microenvironment.

Results

Across the n=5 resection samples, selected ROI displayed a range of tumour, stroma, lymphoid aggregates and connective tissue content. Analysis of cell populations indicated varying levels of CD3, CD8 and FoxP3 immune cell infiltrations. PD-L1 also showed a varied expression within tumour cells across samples while higher numbers of CD163 positive macrophage aggregations were identified within tumour.

Conclusions

Although knowledge of the underlying mechanisms of PDAC have advanced over the recent years, much still remains unclear. Multiplex IF data potentially enables a greater understanding of the complex mechanisms involved in PDAC, thereby furthering the development of drugs that target immune cells and may be indicative of response to treatment or predicting patient outcome.

References

1. Yamaki S, Yanagimoto H, Tsuta K, Ryota H, Kon M. PD-L1 expression in pancreatic ductal adenocarcinoma is a poor prognostic factor in patients with high CD8+ tumor-infiltrating lymphocytes: highly sensitive detection using phosphor-integrated dot staining. International Journal of Clinical Oncology. 2017 March 18. 22(4): 726–733.

P502

Novel approach of modulating immune cell metabolism in the tumor microenvironment to enhance efficacy of immunotherapy

Frank Boriello, MD/PhD[2], HongBum Lee[3], Vincent O'Neil[3], Ted Kim, PhD[3], James Lederer, PhD[4], Sanghee Yoo, PhD[3]

[1]ImmunoMet Therapeutics Inc., Houston, TX, USA
[2]Alloplex Biotherapeutics, Boston, MA, USA
[3]ImmunoMet Therapeutics, HOUSTON, TX, USA
[4]Brigham and Women's Hospital/Harvard, Boston, MA, USA

Background

Cells adopt different metabolic strategies depending on their functional needs. Tumor cells deplete glucose by aerobic glycolysis, which can inhibit effector immune cells that may rely on aerobic glycolysis for effector activity [1]. It has been shown that immune cells that use mitochondrial oxidative phosphorylation (OXPHOS) for energy are able to co-exist with tumor cells in the TME. OXPHOS dependent immune cells include CD4+ regulatory T cells (Tregs), myeloid-derived suppressor cells (MDSC), and tumor associated macrophages (TAM).

These immune cell types are immune suppressive and metabolically compatible with tumor cells [2].

Methods

Human PBMC was used for immune suppressive cell differentiationCyTOF mass cytometry was used to characterize immune cellsSyngeneic in vivo animal studies using RENCA and CT26 were conducted for in vivo efficacy studies

Results

IM188 is an OXPHOS inhibitor drug with a biguanide core structure. Metformin is the canonical biguanide drug that has been safely used to control glucose levels in people with type II diabetes. The mechanisms for how biguanide drugs influence immune cells has not been well characterized. Since IM188 is an optimized biguanide targeting OXPHOS dependent immune cells, we studied the effects of IM188 on human blood immune cells (PBMCs) and on immune responses in mouse models of infection or cancer. PBMCs were differentiated under conditions to promote Treg or MDSC expansion in vitro in the absence or presence of IM188. Analysis of differentiated T cells by CyTOF mass cytometry showed reduced expression of multiple Treg markers such as Foxp3, CTLA4, and TGF-beta. In MDSC differentiation studies, we found that IM188 reduced MDSC expansion and their functional activity to suppress T cell proliferation. In mouse bacteria and virus infection studies, the most intriguing finding was the IM188 treatment caused increased CD8+ T cell expansion and increased IFN-gamma and TNF-alpha cytokine expression in CD8+ T cells. These observations suggest that IM188 can enhance T cell mediated immune responses. Finally, in syngeneic mouse tumor models, IM188 showed a good range of combination efficacy with anti-PD1 therapy. We measured increased T effector cells and decreased immune suppressive cell types at the tumor site in mice treated with IM188 or anti-PD-1 antibody.

Conclusions

In summary, IM188 shows metabolic reprogramming activity that may enhance immune functions by modulating immune cell differentiation and/or function by inhibiting OXPHOS-dependent cells and promoting aerobic glycolysis by effector immune cells.

References

1. Chang HA, Qiu J, O'Sullivan D, Buck MD, Noguchi T, Curtis JD, Chen Q, Gindin M, Gubin, MM, van der Wind GWJ, Tonc E, Schreiber,RD, Pearce EJ, and Pearce EL. Metabolic competition in the tumor microenvironment is a driver of cancer progression. 2015 ; 162:1229-1241.
2. Hossain F, Al-Khami AA, Wyczechowska D, Hermandez C, Zheng L, Reiss K, Valle LD, Trillo-Tinoco J, Maj T, Zou W, Rodriguez PC, Ochoa AC. Inhibition of fatty acid oxidation dodulates immunosuppressive functions of myeloid-derived suppressor cells and enhances cancer therapies. Cancer Immunol Res. 2015; 2:1236-127.

P503

Characterization of the immune desert in metastatic non-small cell lung cancer (NSCLC) and the use of cell proliferation to predict clinical response to immune checkpoint inhibitors (ICIs)

Jason Zhu, MD[1], Matthew Labriola, MD[1], Daniele Marin, MD[1], Shannon McCall, MD[1], Edwin Yau, MD, PhD[2], Grace Dy[2], Sarabjot Pabla, MSc, PhD, BS[3], Sean Glenn, PhD[3], Carl Morrison, MD, DVM[3], Daniel George, MD[1], Tian Zhang, MD[1], Jeffrey Clarke, MD[1]

[1]*Duke University, Durham, NC, USA*
[2]*University of Buffalo, Buffalo, NY, USA*
[3]*Omniseq Inc, Buffalo, NY, USA*

Background

Immune checkpoint inhibitors (ICIs) have profoundly reshaped the treatment landscape for advanced

NSCLC. While patients who have an ICI response may have a deep and durable response, in unselected populations, the majority of patients will not respond, but will be exposed to potential immune toxicities. Current biomarkers such as PD-L1 are not sensitive nor specific for predicting response, particularly for non-inflamed (NI) or "immune desert" tumor microenvironments. Here, we describe the use of cell proliferation to evaluate response in immune desert NSCLC.

Methods

113 formalin-fixed, paraffin-embedded (FFPE) tumor samples of metastatic NSCLC were evaluated by RNA-sequencing to measure transcript levels of genes related to tumor infiltrating lymphocytes and cell proliferation, DNA-sequencing of 409 genes for tumor mutational burden (TMB), and PD-L1 status (Dako 22C3 antibody assay). Tumors were defined as inflamed or NI based upon RNA-sequencing analysis of CD8 compared to a reference population of more than 500 cases of multiple tumors. NI/immune desert tumors were defined as the lower 15th percentile of rank for CD8+ T-cells. Cell proliferation, defined as the mRNA expression of 10 genes (BUB1, CCNB2, CDK1, CDKN3, FOXM1, KIAA0101, MAD2L1, MELK, MKI67, TOP2A) was evaluated for association with PD-L1 IHC expression, TMB, and response to ICIs by RECIST 1.1 criteria.

Results

In our cohort of 113 cases, 12% (15/113) were classified as having an NI, immune desert tumor microenvironment. Of these 15 NI cases, 8 (53%) were proliferative and 7 (47%) were non-proliferative; in addition, 10 of 15 cases (67%) had high TMB (TMB-H). The majority (11/15, 73%) of NI cases were non-responders, with 4 cases having an objective response. For the 4 responders, 3 were non-proliferative; conversely, for the 11 nonresponders,7 were proliferative. For NI/TMB-H there were 9 were nonresponders, with 7 proliferative and 1 responder who was non-proliferative. For NI/TMB-L the ORR was 60% (3/5) with 2 of 3 responders being non-proliferative. Only 2 of these NI cases were PD-L1 positive (TPS>50%), one of which as a non-proliferative responder (50%). PD-L1 was negative in the other 13 cases, 3 of whom were responders (23%).

Conclusions

Biomarkers such as PD-L1 and TMB on their own may not be sufficient in predicting overall response in immune desert tumor microenvironments. In these cases, cell proliferation may be important in distinguishing patients who may have a clinical benefit to ICI. These results support that NI non-proliferative tumors are more likely to respond to ICI than NI proliferative tumors.

Ethics Approval

OmniSeq's analysis utilized deidentified data that qualified as non-human subject research under IRB-approved protocols, approved by both Roswell Park Comprehensive Cancer Center (Buffalo, NY, BDR #080316) and Duke Cancer Institute (Durham, NC, PRO00088762).

Impact of Diet, Exercise, and/or Stress on Antitumor Immunity

P504

Nutritional measures to boost immunosurveillance of breast cancer by NK cells

Lorenzo Galluzzi, PhD[1], Aitziber Buqué, PhD[1], Maria Perez-Lanzon, MSc (Master of Science)[2], Takahiro Yamazaki, PhD[1], Guido Kroemer, MD, PhD[2]

[1]*Weill Cornell Medical College, New York, NY, USA*
[2]*Centre de Recherche des Cordeliers, Paris, France*

Background

Hormone receptor (HR+) breast cancer (BC) is currently responsible for the majority of BC-related

deaths in the US [1]. HR+ BC patients are usually managed by surgery, followed by adjuvant endocrine therapy ± chemotherapy. However, chemotherapy provides limited clinical benefits and is often associated with severe side effects[2], calling for the development of alternative treatment regimens. Over the past decade, immunotherapy with immune checkpoint blockers (ICBs) has achieved unprecedented clinical success in patients with a variety of tumors [3]. However, despite the fact that BC is also under immunosurveillance [4,5], BC patients are generally resistant to ICBs [6], especially in the case of HR+ disease [7]. Thus, there is an unmet need for improved therapeutic approaches to HR+ BC, at least in part reflecting the lack of adequate preclinical models to recapitulate the incidence, natural progression, metastatic dissemination and response to therapy of HR+ BC in immunologically competent hosts.

Methods

We extensively characterized endogenous BC driven in wild-type or genetically engineered C57BL/6 or BALB/c mice by slow-release medroxyprogesterone acetate (MPA) pellets and oral 7,12-dimethylbenz[a]anthracene (DMBA) for incidence, progression, histology, transcriptomic profile, and sensitivity to standard therapeutic agents as well as nutritional interventions.

Results

We demonstrate that MPA/DMBA-driven tumors resemble human HR+ BC in that (1) they display a similar morphology, (2) they express hormonal receptors, (3) they have a gene signature that largely overlaps with that of HR+/HER2- human BCs, (4) tumorigenesis depend on nuclear estrogen receptors, (5) tumor insurgence can initially be delayed by tamoxifen administration, but acquired resistance rapidly subsides, (6) they are under active immunosurveillance by the host immune system with a predominant role for NK cells, and once they form palpable nodules they exhibit limited immune infiltration, and (7) they develop according to rather heterogeneous kinetics. Moreover, MPA/DMBA-driven tumors resemble human HR+ BC because they respond to chemotherapy, PD-1 blockade and RT in a rather heterogeneous and poor fashion. We demonstrate that MPA/DMBA-driven carcinogenesis can be delayed by caloric restriction as well as administration of vitamin B6, vitamin D, and nicotinamide mononucleotide (NAM), in immunocompentent, but not immunodeficient, mice, an effect paralleled by increased amounts of NK cells in the spleen.

Conclusions

HR+ BC appears to evolve by evading NK cell-dependent immunosurveillance, suggesting that NK cell-activating strategies, including nutritional measures like NAM, as well as specific antibodies targeting NK cell receptors, may improve the efficacy of (immuno)therapeutic agents currently employed in the clinics for HR+ BC patients.

References

1. Munoz D, et al. Effects of screening and systemic adjuvant therapy on ER-specific US breast cancer mortality. J Natl Cancer Inst. 2014;106. 2. Jagsi R, et al. Impact of adjuvant chemotherapy on long-term employment of survivors of early-stage breast cancer. Cancer. 2014;120:1854-1862. 3. Sharma P, Allison JP. The future of immune checkpoint therapy. Science.2015;348:56-61. 4. Savas P, et al. Clinical relevance of host immunity in breast cancer: from TILs to the clinic. Nat Rev Clin Oncol. 2016;13:228-241. 5. Kroemer G, Senovilla L, Galluzzi L, Andre F, Zitvogel L. Natural and therapy-induced immunosurveillance in breast cancer. Nat Med. 2015;21:1128-1138. 6. Emens LA. Breast cancer immunotherapy: facts and hopes. Clin Cancer Res. 2018;24:511-520. 7. Rugo HS, et al. Safety and antitumor activity of pembrolizumab in patients with estrogen receptor-positive/human epidermal growth factor receptor 2-negative advanced breast cancer. Clin Cancer Res. 2018.

Ethics Approval
The study was approved by IACUC at the hosting institutions

P505

The gut microbiome of metastatic melanoma patients initiating systemic therapy is influenced by host factors including diet, probiotic and antibiotic use

Vancheswaran Gopalakrishnan, MPH, PhD[1], Christine Spencer, PhD[2], Jennifer McQuade, MD[1], Miles Andrews, MD, PhD[1], Beth Helmink, MD PhD[1], Alexandria Cogdill, MEng[1], Md Khan[1], Elizabeth Sirmans[1], Lauren Haydu, MS, BChe, MIPH[1], Eliza Posada[1], Elizabeth Burton[1], Isabella Glitza, MD, PhD[1], Rodabe Amaria, MD[1], Sapna Patel, MD[1], Adi Diab, MD[1], Michael Wong, MD PhD FRCPC[1], Hussein Tawbi, MD, PhD[1], Wen-Jen Hwu, MD, PhD[1], Michael Davies, MD, PhD[1], Patrick Hwu, MD[1], Robert Jenq, MD[1], Kelly Nelson, MD[1], Carrie Daniel-MacDougall, MPH, PhD[1], Lorenzo Cohen[1], Jennifer Wargo, MD, MMSc[1]

[1]UT MD Anderson Cancer Center, Houston, TX, USA
[2]Parker Institute for Cancer Immunotherapy, New York, NY, USA

Background
The diversity and composition of the gut microbiome has been implicated in differential responses to immune checkpoint blockade in melanoma and other cancers [1-3]. However, little is known about the impact of diet and other lifestyle factors in this population.

Methods
We assembled a large cohort of early and late-stage melanoma patients (n=312) initiating systemic treatment at UT MD Anderson Cancer Center. In addition to biological specimens, we collected a comprehensive lifestyle survey, including the NCI dietary screener questionnaire, in a subset of patients (n=113). The fecal microbiome was characterized via sequencing of the V4 region of the 16S rRNA gene to determine diversity and compositional structure. Dietary components were dichotomized into high and low categories based on the median of estimated consumption. Differences in compositional structure between groups was determined using analysis of similarity (ANOSIM) for unweighted UniFrac beta diversity distances, and pairwise Mann-Whitney tests for taxonomic comparisons.

Results
The median age of melanoma patients in our cohort was 62 yrs (59% male; 86% Stage III/IV), and the most common treatment type was anti-PD1 based therapy (53.1%). There were no significant associations observed between alpha diversity and age, sex or body mass index among the melanoma patients. “Biotic” use, defined as self-reported use of either biotic was quite common (29% antibiotics, 42% probiotics), and was associated with lower alpha-diversity (p=0.01), with significant associations observed for both antibiotics alone (p=0.05) and for probiotics alone (p=0.02). Additionally, consumption of red meat (p=0.006), sugar-sweetened beverages (SSB) (p=0.048), and fruits and vegetables (FV) (p=.049) were also associated with differences in compositional structure with selective enrichment of Desulfovibrionales (high vs. low red meat =0.03), Mollicutes (in low vs. high SSB consumers, p=0.008), and Porphyromonadaceae (in high vs low FV consumers, p=0.001).

Conclusions
Prospective longitudinal studies are underway to assess the relationships between “biotic” use, dietary factors and the gut microbiome, and treatment response among patients, as well as functional studies in preclinical models. These data provide preliminary evidence that the gut microbiome of melanoma patients may be modifiable by host factors such as diet, use of

antibiotics and probiotics, with potential therapeutic implications.

References

1. Gopalakrishnan V, et al. Gut microbiome modulates response to anti–PD-1 immunotherapy in melanoma patients. Science. 2018; 359(6371): 97-103.
2. Routy B, et al. Gut microbiome influences efficacy of PD-1–based immunotherapy against epithelial tumors. Science. 2018; 359(6371): 91-97.
3. Matson V, et al. The commensal microbiome is associated with anti–PD-1 efficacy in metastatic melanoma patients. Science. 2018; 359(6371): 104-108.

Ethics Approval

The study was approved by The University of Texas MD Anderson Center's Ethics Board, approval numbers LAB00-063, and PA15-0232

P506

Subcutaneous and intramuscular fat indices predict survival in advanced stage cancer patients treated with immunotherapy

Dylan Martini, BA[1], Julie Shabto, BA[1], Yuan Liu, PhD[2], Milton Williams[1], Amir Khan[1], Colleen Lewis[3], Hannah Collins[3], Mehmet Akce[3], Haydn Kissick[1], Bradley Carthon, MD, PhD[3], Walid Shaib, MD[3], Olatunji Alese, MD[3], Conor Steuer, MD[3], Christina Wu, MD[3], David Lawson, MD[3], Ragini Kudchadkar, MD[3], Bassel El-rayes, MD[3], Suresh Ramalingam, MD[3], Taofeek Owonikoko, MD, PhD[3], R. Donald Harvey, PharmD[1], Viraj Master, MD, PhD[1], Mehmet Bilen, MD[3]

[1]Emory University School of Medicine, Atlanta, GA, USA
[2]Emory University, Atlanta, GA, USA
[3]Winship Cancer Institute, Atlanta, GA, USA

Background

Obesity has been investigated as a prognostic indicator in patients with cancer [1]. In this study, we explored the association between different types of fat and clinical outcomes in advanced stage cancer patients treated with immunotherapy by developing a risk group classification.

Methods

We performed a retrospective analysis of 90 patients treated on immunotherapy-based phase 1 clinical trials at our center from 2009-2017. Baseline CT images at mid-L3 were obtained, and subcutaneous fat density, intramuscular fat density, and visceral fat density (cm2) were calculated using SliceOmatic (TomoVision, version 5.0) and converted to indices (SFI: subcutaneous fat index, IFI: intramuscular fat index, and VFI: visceral fat index) after dividing by height in meters-squared. Risk groups by PFS were created by a recursive partitioning and regression trees method for SFI and IFI, which were selected by a stepwise variable selection among all fat related variables (Figure 1). Cox proportional hazard model and Kaplan-Meier method were used for association with OS and PFS.

Results

Most patients (59%) were males and more than two-thirds (69%) had at least 2 prior lines of therapy. Melanoma (33%) and gastrointestinal (22%) tumors were the most common histologies. The medians for each of the indices were as follows: SFI = 62.78, IFI = 4.06, and VFI = 40.53. Low-risk patients (SFI 73) had significantly longer OS and PFS than intermediate-risk (SFI < 73 and IFI < 3.4) and poor-risk patients (SFI < 73 and IFI 3.4) (Table 1). Intermediate-risk patients also trended towards longer OS and PFS than poor-risk patients. Patients in the low-risk group had substantially longer median OS and PFS than intermediate and poor-risk patients per Kaplan-Meier estimation (Table 1, Figures 2-3).

Conclusions

Decreased subcutaneous fat and increased myosteatosis may decrease survival in advanced stage patients treated with immunotherapy. Future studies should investigate the interaction between different fat composition, the immune system, and the tumor microenvironment.

References

1. Demark-Wahnefried W, Platz EA, Ligibel JA, Blair, CK Courneya KS, Meyerhardt JA, et al. The Role of Obesity in Cancer Survival and Recurrence. Cancer Epidemiology, Biomarkers, and Prevention. 2012 Aug;21(8):1244-59.

Ethics Approval

The study was approved by the Emory University Institutional Review Board, approval number IRB00100973.

Figure 1.

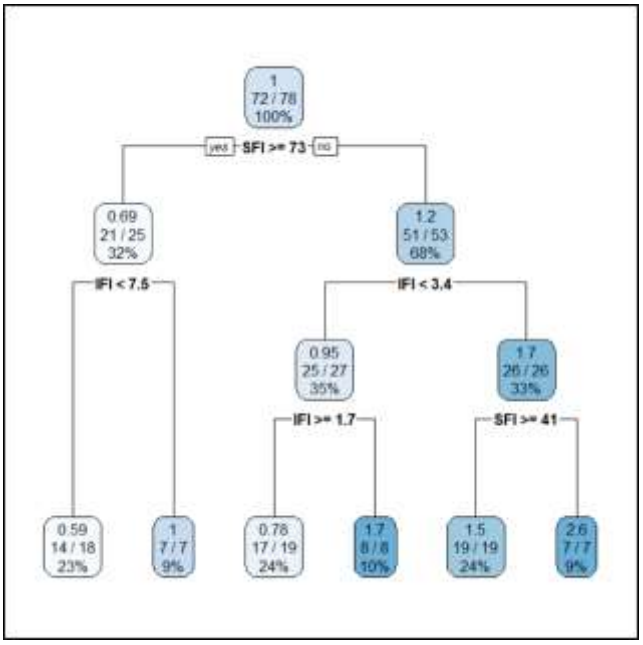

Table 1. MVA† of fat risk with survival

	OS		PFS	
	HR (CI)	**p-value**	**HR (CI)**	**p-value**
Low Risk: SFI ≥ 73	0.20 (0.09-0.46)	**<0.001***	0.38 (0.20-0.72)	**0.003***
	Median Survival: 24.4 months		**Median Survival:** 4.1 months	
Intermediate Risk: SFI < 73 and IFI < 3.4	0.58 (0.31-1.12)	0.105	0.79 (0.44-1.40)	0.414
	Median Survival: 8.7 months		**Median Survival:** 1.9 months	
High Risk: SFI < 73 and IFI ≥ 3.4	--	--	--	--
	Median Survival: 6.2 months		**Median Survival:** 1.9 months	

Figure 2.

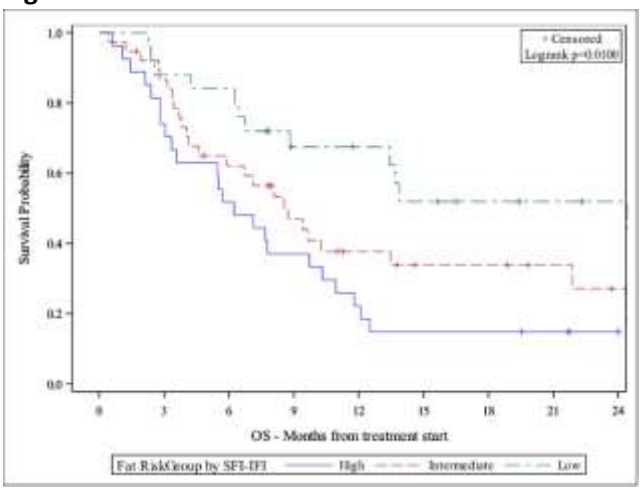

Figure 3.

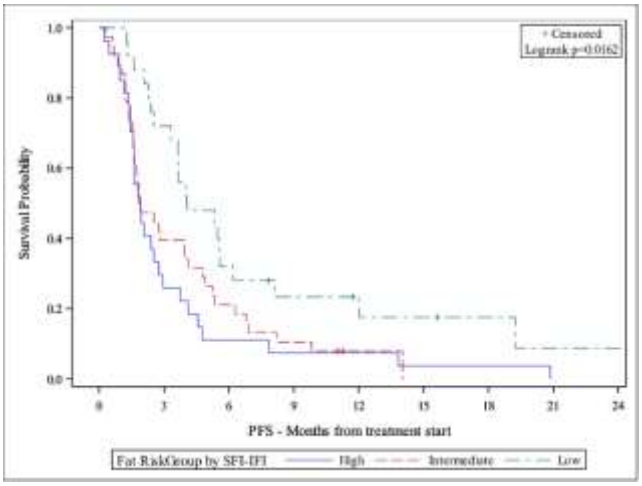

P507

Body mass index as a predictor of survival in advanced stage cancer patients treated with immunotherapy

Julie Shabto, BA[1], Dylan Martini, BA[1], Yuan Liu, PhD[2], Milton Williams[1], Amir Khan[1], Colleen Lewis[3], Hannah Collins[3], Mehmet Akce[2], Haydn Kissick[2], Bradley Carthon, MD, PhD[2], Walid Shaib, MD[2], Olatunji Alese, MD[2], Conor Steuer, MD[2], Christina Wu, MD[2], David Lawson, MD[2], Ragini Kudchadkar, MD[2], Bassel El-rayes, MD[2], Suresh Ramalingam, MD[2], Viraj Master, MD, PhD[2], Taofeek Owonikoko, MD, PhD[2], R. Donald Harvey, PharmD[2], Mehmet Bilen, MD[2]

[1]Emory University School of Medicine, Atlanta, GA, USA
[2]Emory University, Atlanta, GA, USA
[3]Winship Cancer Institute, Atlanta, GA, USA

Background
Body mass index (BMI) has been investigated as a prognostic factor for cancer patients [1], but the effect of BMI on clinical outcomes in patients on phase 1 clinical trials using immunotherapy-based treatment is not known. We investigated the association between BMI and survival in advanced staged cancer patients treated with immunotherapy.

Methods
We completed a retrospective analysis of 90 patients treated on phase 1 clinical trials using immunotherapy-based treatment regimens at Winship Cancer Institute of Emory University from 2009-2017. Baseline BMI was collected from the electronic medical records. Overall survival (OS) and progression-free survival (PFS) were measured from the first dose of immunotherapy to date of death or hospice referral and radiographic or clinical progression, respectively. Cox proportional hazard model was used for association with OS and PFS. BMI was analyzed as a continuous variable and as a categorical variable (normal or underweight: BMI < 25, overweight: 25 ≤ BMI < 30, obese: BMI ≥ 30).

Results
Most patients (59%) were males and the majority (81%) were Royal Marsden Hospital (RMH) good risk. Approximately two-thirds (69%) of patients received at least 2 lines of systemic therapy before being treated with immunotherapy on the clinical trial. Melanoma (33%), gastrointestinal (22%), and lung and head & neck (20%) were the most common tumor types. The median BMI was 27.4. When treated as a continuous variable in multi-variable analysis, a higher BMI was significantly associated with longer OS and PFS (Table 1). Patients with a normal or underweight BMI had significantly shorter OS (HR: 3.27, p-value: 0.005) and trended towards shorter PFS when compared to overweight and obese patients. The median OS and PFS of obese patients was 19.1 months and 4.7 months, respectively, while median OS and PFS of normal or underweight patients was 6.7 months and 1.9 months and median OS and PFS for overweight patients was 8.6 months and 2.3 months, respectively, per Kaplan-Meier estimation (Table 1, Figures 1-2).

Conclusions
Obesity may help prolong survival in advanced stage cancer patients treated with immunotherapy. Further studies are needed to elucidate the underlying biologic effect of adiposity on the tumor microenvironment and the immune system in patients treated with immunotherapy.

References
1. Azvolinsky A. Cancer Prognosis: Role of BMI and Fat Tissue. JNCI. 2014; Volume 106: page 6-7.

Ethics Approval
The study was approved by the Emory University Institutional Review Board, approval number

IRB00100973.

Table 1: MVA† of the association between BMI and survival

	OS		PFS	
	HR (CI)	p-value	HR (CI)	p-value
Continuous Variable Analysis				
BMI (n=82)	0.92 (0.87-0.97)	**0.001***	0.96 (0.92-1.00)	**0.03***
Categorical Variable Analysis				
Normal or underweight (BMI < 25, n=28)	3.27 (1.44-7.41)	**0.005***	1.84 (0.94-3.60)	0.073
	Median Survival: 6.7 months		**Median Survival**: 1.9 months	
Overweight (25 ≤ BMI < 30, n=30)	1.83 (0.84-3.95)	0.127	1.46 (0.80-2.68)	0.218
	Median Survival: 8.6 months		**Median Survival**: 2.3 months	
Obese (BMI ≥ 30, n=23)	-		-	
	Median Survival: 19.1 months		**Median Survival**: 4.7 months	

Figure 1.

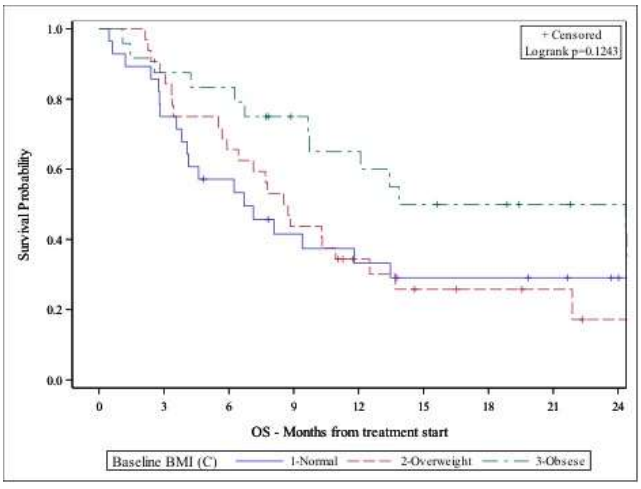

Figure 2.

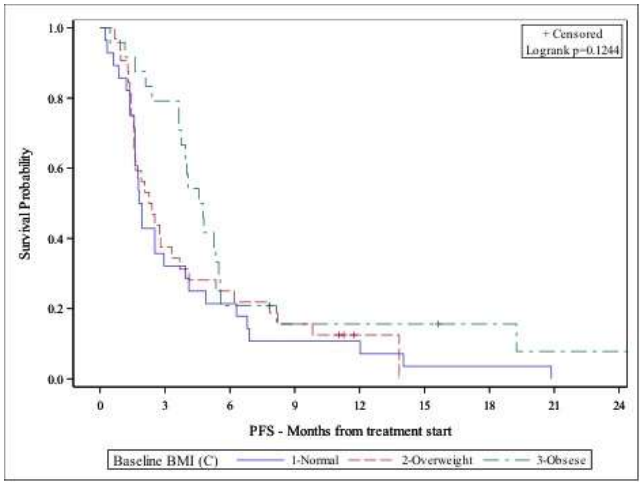

P508

Obesity promotes PD-1 mediated T cell dysfunction and tumor pro-gression but superior anti-tumor effects upon checkpoint blockade

Ziming Wang, MS[1], Jesus Luna, PhD[1], Cordelia Dunai, MS[1], Lam Khuat[1], Catherine Le, BS[1], Ethan Aguilar[1], Annie Mirsoian[1], Christine Minnar, PhD[1], Kevin Stoffel, MS[1], Ian Sturgill[1], Steven Grossenbacher[1], Robert Canter, MD, MAS, FACS[1], Arta Monjazeb, MD, PhD[1], William Murphy, PhD[1], Ziming Wang, MS[1]

[1]*University of California, Davis, Sacramento, CA, USA*

Background

PD-(L)1 signaling is central to T cell exhaustion which occurs with chronic antigen stimulation and results in T cell dysfunction. Blockade of the PD-(L)1 pathway augments T cell responses in a variety of viral and cancer models. Obesity, defined by high body mass index (BMI >30 kg/m2), is reaching pandemic proportions and is a major cancer risk factor. The impact of obesity on immune responses in general, and cancer immunotherapy in particular, is poorly understood.

Methods
Male B6 and female BALB/c mice were fed diets consisting of either 60% or 10% fat, respec-tively, starting from 6-week until 6-month old. DIO and control mice were injected with either B16-F0 (non-metastatic melanoma), B16-F10 (metastatic melanoma), 3LL (metastatic Lewis lung carcinoma), or 4T1 (metastatic breast carcinoma) cells. Tumor-bearing mice were treated intraperitoneally with aPD-1 mAb every other day at 250µg/mouse after an initial dose of 500µg/mouse for a total of 6 injections. Tumor progression was determined by caliber measure-ment, PET-CT, and quantification of metastases. Immune phenotypes and T cell function were measured by flow cytometry. Transcriptomes were analyzed by RNAseq.

Results
DIO mice were significantly heavier than control mice, with an average weight of 60g vs 42g in B6 mice, and 40g vs 20g in BALB/c mice. Tumors grew significantly faster in DIO mice com-pared to control counterparts as quantified by caliber measurement and PET-CT. T cells in the tumor microenvironment (TME) of DIO mice demonstrated features of exhaustion, including significantly increased expression of PD-1, Tim3 and Lag3, but decreased expression of Ki67. Transcriptomic analysis of sorted (>95% purity) CD8+ memory T cells from B16-bearing control and DIO mice also demonstrated the upregulation of exhaustion-related transcripts and down-regulation of effector-related transcripts in T cells from DIO mice. aPD-1 treatment led to signifi-cant reduction of tumor burden, inhibited development of metastases in DIO mice, and overall improved survival times. The enhanced checkpoint blockade responsiveness in DIO mice was associated with significantly increased CD8+ tumor-infiltrating lymphocytes (TILs), as well as increased TNFα and IFNγ-production by CD8+ T cells.

Conclusions
These data indicate a paradoxical impact of obesity on cancer in which immune dysfunction, and tumor progression are heightened, but checkpoint blockade efficacy is also enhanced. This study highlights obesity as a biomarker for cancer immunotherapy.

Innate Anti-Tumor Immunity

P509

Tumor spheroid model to dissect the interplay between myeloid cells and cancer cells

Elaheh Ahmadzadeh, PhD[1], Jan Martinek, PhD[1], Florentina Marches[1], Chun Yu, PhD[1], A. Karolina Palucka, MD[1]

[1]*The Jackson Laboratory, Farmington, CT, USA*

Background
The tumor microenvironment includes cancer cells as well as stromal cells, immune cells, epithelial cells, vasculature and extracellular matrix. Interactions between these components regulate tumor development, migration and metastasis. Current 2-dimensional (2D) in vitro culture methods fail to represent the multidimensional complexity of tumor microenvironment. The multicellular tumor spheroids support co-culture conditions and allow a 3D system that can be employed to investigate the integration of multiple cell types and gain insight into the interaction of cancer cells with other cells in their environment. We established such model to investigate the molecular mechanisms regulating the interactions between melanoma, myeloid cells and T cells.

Methods
Tumor Spheroids were developed using hanging drop technique with multiple melanoma cell lines,

dermal fibroblasts and immune cells. Preliminary experiments were carried out to determine the optimum conditions for spheroid formation. Spheroids were cultured at density of 104 per cell type per drop and incubated for 3, 4, or 5 days.

Results

Spheroid formation occurred within 72 hours and the integrity of spheroids were maintained throughout the experiments. Cell viability and cell proliferation was monitored within spheroids for up to 5 days using Live and dead staining and CellTrace™ CFSE Cell Proliferation Kit, respectively. Immunofluorescence analysis of spheroid cryosections showed a homogeneous distribution of fibroblasts in spheroids. However, spheroid compaction and fibronectin expression varied between spheroids formed by different cell lines. We assessed the integration and localization of monocytes within the spheroids by adding purified blood CD14+ cells to the mixture of tumor cells and dermal fibroblasts at equal density of 104 cells per drop. Immunofluorescence analysis of serial sections of spheroid showed CD45+ cells scattered throughout spheroid. Furthermore, addition of CD14+ cells to tumor spheroids on day 3 resulted in infiltration of monocytes into spheroids in less than 24 hours.

Conclusions

Thus, our 3D model can be used to assess the distribution of immune infiltrates and the interaction of cancer cells with myeloid cells.

P510

Monoclonal antibodies targeting the MerTK receptor de-repress the innate immune response

Diego Alvarado, PhD[1], Mike Murphy[1], Laura Vitale, BS[1], Thomas O'Neill, BA[1], Andrew Proffitt[1], Jay Lillquist[1], Gwenda Ligon[1], Craig Polson[1], Anna Wasiuk[1], Jeffrey Weidlick, BS[1], Jenifer Widger, BA[1], Laura Mills-Chen[1], Andrea Crocker, BS[1], Colleen Patterson[1], Russell Hammond[1], Li-Zhen He, MD[1], Joel Goldstein, PhD[1], Lawrence Thomas, PhD[1], Henry Marsh, BS PhD[1], Tibor Keler, PhD[1], Richard Gedrich[1]

[1]*Celldex Therapeutics, New Haven, CT, USA*

Background

MerTK, a member of the TAM (Tyro3/Axl/MerTK) family of receptor tyrosine kinases (RTKs), is an important negative regulator of innate immunity. Activation of MerTK in myeloid cells by its ligands Gas6 or Protein S (PROS) promotes phosphatidylserine-dependent efferocytosis of apoptotic cells, inducing a tolerogenic state and mediating resolution of inflammation. MerTK deficient mice exhibit phenotypes consistent with systemic inflammation and auto-immunity. Importantly, MerTK ablation confers tumor immunity, increased pro-inflammatory cytokines and tumor lymphocyte infiltration. We hypothesize that pharmacological targeting of MerTK with monoclonal antibodies (mAbs) may lead to a similar pro-inflammatory response and recapitulate the anti-tumor effects observed in MerTK-/- mice.

Methods

Cultured human PBMCs, or monocyte-derived dendritic cells and macrophages were treated with a panel of MerTK-targeting mAbs for 24 hours alone, or in the presence of pro-inflammatory stimuli (LPS, CD40L or IFN-gamma). A panel of cytokines (eg. IL-1RA, TNF-a) were measured in supernatants by ELISA, or using a multiplex approach. Phospho-immunoreceptor (R&D) profiling from PBMC lysates was performed after treatment with mAbs or saline for 1 hour in full serum. The generation and characterization of MerTK knock-out and human MerTK transgenic mice will be presented.

Results

From a panel of human anti-MerTK mAbs derived from phage-display libraries or human IgG mice we

identified several mAbs that enhanced cytokine and chemokine release from primary human immune cells, alone or in the presence of inflammatory stimuli. Surprisingly, mAb activity required Fc receptor binding as introduction of mutations in the Fc domain to abrogate FcR binding rendered the Abs ineffective, despite maintaining target binding. Surrogate mAbs targeting mouse MerTK elicited similar responses in vivo. Treatment of human PBMCs with a MerTK mAb resulted in reduced phosphorylation of ITIM-bearing immunoreceptors known to negatively regulate the immune response. In addition, human MerTK transgenic, and MerTK knockout mice have been generated and characterized with a view to establish in vivo proof-of-concept with human MerTK mAbs.

Conclusions

Pharmacological targeting of MerTK with monoclonal antibodies modulates cytokine production in human and murine model systems in a manner consistent with genetic ablation of the target. MerTK mAbs enhanced production of inflammatory cytokines and decreased the activity of inhibitory immunoreceptors. The anti-tumor activity of MerTK mAbs is planned using surrogate models and human MerTK transgenic mice.

P511

Co-expression of a chimeric NKG2D receptor with membrane bound IL-15 enhances natural killer cell function and long-term persistence in vitro and in vivo

Luxuan Buren[1], James Trager, PhD[1]

[1]*Nkarta Therapeutics, South San Francisco, CA, USA*

Background

Chimeric antigen receptors have been used successfully to retarget T cells in patients with hematologic malignancies. Natural killer (NK) cells offer an alternative to T cells for cellular immunotherapy, highly active and suitable for allogeneic use as they are not HLA-restricted and do not cause GVHD. A goal of NK cell engineering is to improve their in vivo persistence and recognition of cancer cells. Ligands of the natural killer group 2D (NKG2D) receptor are broadly expressed in solid tumor and hematological malignancies, making NKG2D an attractive target for NK cell engineering. This work was undertaken to demonstrate that NK activity and persistence can be elevated by simultaneous expression of chimeric constructs directing the expression of an activating NKG2D receptor (aNKr) and a membrane-bound form of IL-15 (mbIL-15).

Methods

NK cells were generated by co-culture of peripheral blood mononuclear cells (PBMC) with genetically modified irradiated K562 feeder cells. NK cells were transduced at an MOI of 1-2 with a bicistronic virus encoding an NKG2D aNKr and mbIL-15. NK expansion and NKG2D aNKr expression were evaluated by flow cytometry to detect the CD56+ CD3- cell population and the elevation of NKG2D expression over endogenous levels. In vitro cytotoxicity of transduced NK cells was measured using both flow cytometry and the IncuCyte S3 live cell analysis system. The in vivo activity of engineered NK cells was further assessed in a xenograft tumor model, using the osteosarcoma cell line U2OS engineered to express luciferase, with tumor growth measured using bioluminescence in NSG mice.

Results

NK cells were expanded for 7 days (40 fold to >100 fold) prior to transduction. Transduction increased of NKG2D expression in NK cells (>70%, N=8 donors) relative to control cells. NKG2D aNKr-mbIL15 NK cells could be maintained for up to 6 weeks in low IL-2 culture. aNKr-mbIL-15 expression significantly elevated cytotoxicity in NK cells against multiple tumor cell lines, inducing cell death of > 60% of

target cells within 4 hours at 1:1 E:T ratio. One infusion of transduced NK cells tumor-bearing NSG mice resulted in long-term anti-tumor responses. Moreover, co-expression of mbIL-15 significantly delayed tumor growth relative to that observed in cells expressing only the NKG2D aNKr.

Conclusions

Transduction of NK cells with an NKG2D aNKr and mbIL-15 increases their cytotoxic activity and persistence. Based on these data, further development of NKG2D aNKr-mbIL-15 NK cells for clinical use will be pursued.

P512

AO-176, a next generation CD47 antibody, induces immunogenic cell death

Ben Capoccia, PhD[1], Ronald Hiebsch[1], Michael Donio[1], Alun Carter[1], Robyn Puro[1], Benjamin Capoccia[1], W. Casey Wilson[1], Daniel Pereira[1], Pamela Manning[1], Robert Karr[1]

[1]*Arch Oncology, St. Louis, MO, USA*

Background

Recent success in cancer immunotherapy has targeted immune checkpoints such as PD-1, PDL-1, and CTLA-4 to enhance the cytotoxic activity of the adaptive T cell immune response. While the clinical response to these therapies has been dramatic for some, many others have shown partial or even no response highlighting the need for alternative or synergistic approaches that activate innate immunity. Disruption of the interaction between SIRPα and CD47, an innate checkpoint inhibitor, using anti-CD47 antibodies, for example, is known to enhance innate immunity by increasing the phagocytosis of tumor cells by macrophages and dendritic cells (DCs) leading to processing and presentation of tumor antigens. Recently, we described AO-176, a next generation anti-CD47 antibody that blocks the CD47/SIRPα interaction, induces phagocytosis and causes a direct tumor cell-autonomous death while negligibly binding RBCs.Herein, we characterize the ability of our CD47 antibodies such as AO-176, to induce Immunogenic cell death (ICD) and Damage Associated Molecular Patterns (DAMPs) in tumor cells and to potentiate chemotherapy-induced ICD/DAMPs. ICD is a process whereby an agent induces cell surface exposure and release of DAMPs from dying cells which stimulates DCs and adaptive immune responses.

Methods

Tumor cells were treated in vitro with our CD47 antibodies either alone or in combination with chemotherapeutics followed by assessment of ICD/DAMPs using flow cytometry and biochemical assays. RNAseq was also performed on cells undergoing CD47 antibody mediated ICD/DAMP induction to better understand how CD47 inhibition may regulate ICD.

Results

AO-176 and other CD47 antibodies, developed by Arch Oncology, caused mitochondrial stress and loss of outer-membrane integrity, typically observed prior to cells undergoing apoptosis. In addition, CD47 antibody treatment induced a significant ER stress response at the genetic level resulting in the surface exposure of ER chaperone proteins calreticulin, Hsp90, and PDIA3. Concomitantly, our CD47 antibodies increased autophagy and JAK/STAT signaling which resulted in both ATP and HMGB1 release, respectively. Finally, we demonstrated that in combination, our antibodies potentiated the effects of ICD/DAMP-inducing chemotherapy (eg. Doxorubicin).

Conclusions

Here, we describe the unique ability of a specific subset of next generation CD47 antibodies, such as AO-176 to induce ICD/DAMPs. RNAseq analysis of treated cells also revealed alteration of several

pathways, including those where DAMPs play a role. In summary, next generation CD47 antibodies such as AO-176 may provide a novel approach to enhancing the current landscape of checkpoint immunotherapy by enhancing both the innate and adaptive immune responses against tumors.

P513

Targeting adenosinergic immunometabolic suppression with engineered natural killer cells for immunotherapy of CD73+ solid tumors

Andrea Chambers, MS[1], Kyle B. Lupo[1], Jiao Wang, PhD[1]

[1]*Purdue University, Lafayette, IN, USA*

Background

Genetically engineered natural killer (NK) cells have shown promise as immunotherapies for hematologic malignancies; however, clinical treatment of solid tumors is lagging. This setback is caused by many mechanisms, including accumulation of immunosuppressive adenosine (ADO) [1,2,3] generated from ectoenzymes CD39 and CD73 by cancer cells [4]. We have shown that ADO suppresses NK cell anti-tumor immunity, resulting in downregulation of activating receptor expression and impaired metabolic activity. To overcome immunometabolic suppression due to adenosinergic signaling, we are engineering NK cells directed against CD73 by imparting in situ ADCC-like activation upon NK cells using a novel genetic construct.

Methods

Peripheral blood-derived NK cells were isolated from healthy human donors. For ADO studies, NK cells were primed 24 hours with IL-2 (200 IU/ml or 400 IU/ml), IL-15 (100 ng/ml), or IL-12 (20 ng/ml) and IL-15 (100 ng/ml) with or without exogenous ADO (1 mM). Treatments were performed with adenosine A2 receptor inhibitor SCH58261, and EHNA, an ADO deaminase inhibitor. Cytotoxicity against CD73+ cells was measured using 7-AAD/CFSE staining, while IFNγ and activating marker expression were measured by flow cytometry. Differential gene expression due to ADO was determined by RNAseq. Engineering NK cells using a novel genetic construct was made by fusing CD73 scFv with CD16a-derived signaling domains before transcribing into mRNA. CAR NK cells were generated by electroporation of the mRNA, and tested for NK transfection efficiency and effector function against CD73+ solid tumors.

Results

Results show that ADO reprograms NK cells' anti-tumor responses, and priming NK cells with IL-12 and IL-15 can partially mitigate ADO-induced immunosuppression. Using IL-12 and IL-15 was preferential to using IL-2, and IFNγ production in response to ADO was enhanced. Furthermore, ADO resulted in altered gene expression signatures that matched impaired IFNγ signaling and cellular metabolism in NK cells. To block adenosinergic signaling, a novel genetic construct that fuses CD73 scFv with in situ ADCC-like signaling was generated. Human NK cells were successfully electroporated with mRNA encoding the construct. These cells are currently being evaluated for effector function and ability to block CD73-induced immunosuppression on solid tumor targets.

Conclusions

The microenvironment of solid tumors is highly immunosuppressive via the activity of CD73 expressed on cancer cells. Our results demonstrate that ADO can act on specific NK cell pathways to cause NK cell inhibition. Harnessing these results, a novel CD73-targeting construct is currently being investigated to redirect NK cell function when targeting solid tumors.

References

1. Rezvani K, Rouce RH. The application of natural

killer cell immunotherapy for the treatment of cancer. Front Immunol. 2015; 6. 2. Rezvani K, Rouce R, Liu E, Shpall E. Engineering natural killer cells for cancer immunotherapy. Molec. Therapy. 2017;25: 1769-1781 3. Ohta A. A metabolic immune checkpoint: adenosine in tumor microenvironment. Front Immunol. 2016; 6. 4. Antonioli L, Blandizzi C, et al. Anti-CD73 immunotherapy: A viable way to reprogram the tumor microenvironment. Oncoimmunology. 2016;5.

P514

High efficiency electroporation of primary human NK cells

Jian Chen, PhD[1], Xiaofeng Xia, PhD[1]

[1]*Celetrix LLC, Manassas, VA, USA*

Background

(Looking to give a short talk as this technical breakthrough would help many labs in the field.) Natural killer (NK) cells have a great potential as a therapeutic agent against tumor cells. Genetic modifications of NK cells such as gene knock-out or exogenous protein expression are important for boosting NK cell expansion or NK cell killing specificity. Unfortunately, viral vectors that are commonly used for other types of cell immunotherapy have poor efficiency in NK cell transduction. As a physical method, electroporation theoretically should work well with NK cells but the special biology of NK cells have made it difficult to achieve high efficiency in NK cell electroporation and cell viability was also a major issue. For example, electroporation of plasmids used to have poor efficiency and high cell mortality in expanded NK cells.

Methods

Here we used a two-pronged approach to tackle the NK cell electroporation problem. First, a novel electroporation method was used involving a new device that has surpassed the performance of all other electroporation technologies on the market. Second, instead of using expanded NK cells, we used fresh un-expanded NK cells that were previously considered harder for electroporation.

Results

Using a relatively high cell concentration, we selected a high electric field strength and were able to quickly achieve a very high efficiency (40% to 50%) for fresh NK cells electroporated with plasmids. The viability of the NK cells after electroporation was between 85% and 95%. Electroporation of mRNA or Cas9/gRNA ribonucleoproteins (RNPs) is much easier than electroporation of plasmids and the new method would allow complex experimental designs such as co-transfection of RNP and plasmids for knock-in.

Conclusions

With the new high efficiency NK cell electroporation method, genetic modification for NK cells has become easily accessible, thereby allowing more possibilities of clinical anti-tumor applications of NK cells.

P515

Novel class of small molecule direct STING agonists as potential cancer immunotherapy

Monika Dobrzanska[1], Stefan Chmielewski, PhD[1], Magdalena Zawadzka[1], Adam Radzimierski[1], Karolina Gluza[1], Katarzyna Wojcik-Jaszczynska[1], Maciej Kujawa[1], Grzegorz Topolnicki[1], Grzegorz Cwiertnia[1], Aleksandra Poczkaj[1], Izabela Dolata[1], Jolanta Mazurek[1], Magdalena Mroczkowska[1], Agnieszka Gibas[1], Tushar Mahajan[1], Marcin Les[1], Wojciech Schonemann[1], Sylwia Sudol[1], Kinga Michalik[1],

Magdalena Sieprawska-Lupa[1], Katarzyna Banaszak[1], Charles-Henry Fabritius[1], Karolina Wiatrowska[1], Agnieszka Adamus[1]

[1]*Selvita S.A., Krakow, Poland*

Background

Type I interferons are major players in mounting immune response to cancer cells. IFNβ release by antigen-presenting cells promotes spontaneous anti-tumor CD8+ T cell priming being largely dependent on activation of Stimulator of Interferon Genes (STING). In preclinical murine models intratumoral injection of cyclic dinucleotide (CDN) STING agonists induced regression of established tumors and generated long-term immunologic memory. Relative instability and chemical nature of cyclic dinucleotides limit their use as systemically available immunotherapeutics. Therefore, herein we report the discovery of potent and selective first-in-class non-nucleotide, non-macrocyclic, small molecule direct STING agonists, structurally unrelated to known chemotypes with potential for systemic administration routes.

Methods

Cytokine release has been determined by ELISA or AlphaLisa in human peripheral blood mononuclear cells (PBMC) obtained from healthy human subjects. Activation of STING pathway was monitored in THP-1 Dual reporter monocytic cell line. Human monocyte-derived macrophages (HMDM) and human monocyte-derived dendritic cells (HMDC) were differentiated from CD14+ cells (obtained from PBMC) in the presence of GM-CSF and GM-CSF with IL-4 for HMDM and HMDC, respectively. Mouse bone marrow-derived macrophages (BMDM) were obtained from C57BL/6 mice. Surface expression of the antigen-presenting cell maturation markers i.e. CD80, CD86, CD83 and HLA-DR was assessed by flow cytometry with corresponding isotype controls. The binding affinity was confirmed by Fluorescence Thermal Shift, Fluorescence Polarisation and Microscale Thermophoresis.

Results

STING agonists have confirmed direct binding to both mouse and human STING protein in three independent biophysical binding assays (FTS, MST and FP) and by additional crystallography studies. The compounds have fine-tunable ADME properties with particularly good solubility, permeability and human plasma stability. They selectively activated STING-dependent signaling in both THP-1 reporter assays and in primary cells of human and mouse origin. In vitro functional assays demonstrated their ability to induce cytokine responses (IFNβ, TNFα) in a panel of human peripheral blood mononuclear cell (PBMC), human monocyte derived macrophage (HMDM) and human dendritic cells samples with various STING haplotypes. Additionally, the compounds efficiently induced cytokine release in mouse bone marrow-derived macrophages. Pro-inflammatory cytokine profile was accompanied by up-regulation of the maturation markers, CD80, CD86, CD83 and HLA-DRon the surface of human antigen presenting cells.

Conclusions

These data demonstrate potent, novel, next-generation small molecule STING agonists activating STING-dependent signaling in both mouse and human immune cells to promote potential antitumor immunity. The compounds show good selectivity and in vitro ADME properties enabling further development for systemic administration as a single agent or in combinatory cancer immunotherapies.

P516

SIRPα blockade increases the activity of multiple myeloid lineage cells, enhances dendritic cell cross-presentation, and aids in remodeling the tumor microenvironment

Brian Francica[1], Jay Hyok Chung[1], Brandy Chavez[1],

Erik Voets, PhD[1], Andrea van Elsas[1], Hans van Eenennaam, PhD[1], Meredith Leong[1]

[1]*Aduro Biotech Europe, Oss, Netherlands*

Background

Antagonizing the SIRPα-CD47 pathway is gaining traction as an effective and novel approach to immune manipulation as design of immunotherapies broadens to include blockade of innate immune checkpoints. Recently, the combination of tumor-targeting antibodies with SIRPα-CD47 blockade has provided promising clinical results, suggesting that increased phagocytosis of cancer cells is clinically relevant for treatment of hematologic cancers [1]. However, the ability for this combination to enhance phagocytosis in the context of solid tumors may be remarkably diminished for several reasons including reduced expression of "eat-me" signals like SLAMF7, increased immune suppression in the tumor microenvironment (TME), and the physical size of tumor cells when adhered in a complex heterogeneous environment. To achieve efficacy in solid tumor indications, it is important that therapies blocking the SIRPα-CD47 axis also potentiate adaptive immune mechanisms and not solely phagocytosis.

Methods

Subcutaneous mouse tumor models and a mouse bone marrow-derived dendritic cell (BMDC) cross-presentation assay were used to assess the efficacy of SIRPα blockade in solid tumors.

Results

Here we demonstrate that, in addition to increasing macrophage uptake of tumor cells in suspension, SIRPα blockade also functions to modify the myeloid compartment in the TME of solid tumors. In four independent subcutaneous mouse tumor models, we demonstrate that SIRPα blockade combines in a synergistic manner with PD-1 blockade to reduce tumor burden. In these models, anti-SIRPα therapy skews the DC population towards cross-presenting DC1 cells and increases the CD86 expression on myeloid cells in multiple immune tissues. In vivo and in vitro, SIRPα blockade correlates with lower levels of SIRPα present on the cell surface, and we hypothesize that a combination of downregulation and blockade may cause the skewing of myeloid lineages. Using a mouse BMDC cross-presentation assay, we also demonstrate that the blockade of SIRPα results in increased T cell expansion, supporting a role for SIRPα blockade in enhancing DC function.

Conclusions

Together, these data suggest that antagonizing SIRPα functions to skew myeloid cells. This results in enhanced T cell activation and that, when combined with PD-1 blockade, improves therapeutic efficacy in multiple mouse models. Based on these data in mouse models, an antibody with specificity for human SIRPα, ADU-1805, is being developed for use in clinical trials.

References

1. Liu X, Kwon H, Li Z, Fu Y-X. Is CD47 an innate immune checkpoint for tumor evasion? Journal of Hematology & Oncology. 2017Nov;10(1).

P517

Pan-allele anti-SIRPα antibodies that block the SIRPα–CD47 innate immune checkpoint

Erik Voets, PhD[1], Jay Hyok Chung[1], Paul Vink, BS[1], David Lutje Hulsik[1], Marc Paradé[1], Sanne Spijkers[1], Inge Reinieren-Beeren[1], Joost Rens[1], Wout Janssen, BS[1], Brian Francica[1], Meredith Leong[1], Andrea van Elsas[1], Hans van Eenennaam, PhD[1]

[1]*Aduro Biotech Europe, Oss, Netherlands*

Background

SIRPα immunoregulatory activity on myeloid cells is

activated by binding of its ligand CD47 [1,2], and blockade of the pathway may enhance anti-tumor immunity [3,4]. Hence the pathway is thought to represent a novel immune checkpoint. CD47, being ubiquitously expressed on normal cells and upregulated on many cancer cells, has been extensively studied in the context of "don't-eat-me" [5,6]. Alternative strategies are focusing on directly targeting SIRPα because of its more restricted expression to myeloid-derived lineages [7].However, the identification of functional human SIRPα antagonistic antibodies has been hampered by the allelic variation in the SIRPα locus and its homology with the activating receptor SIRPβ and the decoy receptor SIRPγ.

Methods

Using Aduro Biotech's B-select platform, we have identified and characterized ADU-1805: a highly selective pan-allele anti-SIRPα antibody (EC50 SIRPαV1/SIRPαV2 ≤ 3nM) that lacks appreciable SIRPβ binding (EC50 > 120nM) and cross-reacts with SIRPγ (EC50 ≤ 5nM).

Results

ADU-1805 potently blocks CD47 binding (IC50 ≤ 1.5nM) in all known human *SIRPA* genotypes (including homozygous and heterozygous genotypes) and antagonizes SIRPα–CD47 interaction on primary SIRPα+ myeloid cells (IC50 ≤ 4nM). In line with its antagonistic properties, ADU-1805 enhances tumor cell clearance by human granulocytes and macrophages. Furthermore, on the IgG2 subclass backbone selected during the humanization process, ADU-1805 exhibits improved activity relative to other IgG subclasses tested. Finally, unlike data with CD47-targeting antibodies, ADU-1805 does not trigger hemagglutination or platelet binding/aggregation *in vitro*, suggesting a reduced risk of red blood cell (RBC) and platelet depletion *in vivo*.

Conclusions

In summary, we have identified ADU-1805 as a potentially best-in-class antagonistic anti-SIRPα antibody with a unique binding profile as it binds all reported human SIRPα alleles but does not appreciably bind to the activating SIRPβ receptor. Blocking the SIRPα–CD47 innate immune checkpoint with ADU-1805 may modulate myeloid cells in the tumor microenvironment and promote antigen presentation and cross-priming of dendritic cells. We are currently advancing ADU-1805 through preclinical studies.

References

1. Oldenborg PA, Zheleznyak A, Fang YF, Lagenaur CF, Gresham HD, Lindberg FP. Role of CD47 as a marker of self on red blood cells. Science. 2000;288(5473):2051–4.
2. Oldenborg PA, Gresham HD, Lindberg FP. Cd47-signal regulatory protein α (Sirpα) regulates Fcγ and complement receptor–mediated phagocytosis. The Journal of Experimental Medicine. 2001Feb;193(7):855–62.
3. Tseng D, Volkmer J-P, Willingham SB, Contreras-Trujillo H, Fathman JW, Fernhoff NB, et al. Anti-CD47 antibody-mediated phagocytosis of cancer by macrophages primes an effective antitumor T-cell response. Proceedings of the National Academy of Sciences. 2013;110(27):11103–8.
4. Liu X, Pu Y, Cron K, Deng L, Kline J, Frazier WA, et al. CD47 blockade triggers T cell–mediated destruction of immunogenic tumors. Nature Medicine. 2015;21(10):1209–15.
5. Jaiswal S, Jamieson CH, Pang WW, Park CY, Chao MP, Majeti R, et al. CD47 is upregulated on circulating hematopoietic stem cells and leukemia cells to avoid phagocytosis. Cell. 2009;138(2):271–85.
6. Majeti R, Chao MP, Alizadeh AA, Pang WW, Jaiswal S, Gibbs KD, et al. CD47 is an adverse prognostic factor and therapeutic antibody target on human acute myeloid leukemia stem cells. Cell. 2009;138(2):286–99.

7. Yanagita T, Murata Y, Tanaka D, Motegi S-I, Arai E, Daniwijaya EW, et al. Anti-SIRPα antibodies as a potential new tool for cancer immunotherapy. JCI Insight. 2017Dec;2(1).

P518 Abstract Travel Award Recipient

Non-canonical cross-presenting dendritic cells mediate anti-tumor immunity

Ellen Duong, ScB[1], Stefani Spranger, PhD[1]

[1]*MIT, Cambridge, MA, USA*

Background

Recent studies revealed a critical role for cross-presenting CD103$^+$ dendritic cells (DC1) in both the induction and maintenance of CD8$^+$ T cell immunity in the tumor. Exclusion of DC1 from the tumor microenvironment (TME) is a mechanism of immune evasion by the tumor and contributes to impaired responses to checkpoint blockade therapy. Elucidating the contributions of different DC subsets to the TME will be instrumental towards improving current immunotherapies.

Methods

We compared the myeloid infiltrate of acutely cleared regressor tumors versus progressively growing tumors, an approach that was previously used to phenotype dysfunctional T cells in the TME [1]. Murine syngeneic tumor lines expressing SIY were categorized as 'progressor' or 'regressor,' and implanted in wild-type, Rag2$^{-/-}$, Batf3$^{-/-}$, Clec9a$^{GFP/GFP}$, and CD11c-DTR bone marrow (BM) chimera mice. Flow immunophenotyping was used to profile the intratumoral myeloid compartment, and ELISpot was performed to determine the number of IFNγ-producing CD8$^+$ T cells. To assess function, sorted myeloid cells were co-cultured with CD8$^+$ T cells to evaluate their ability to induce T cell proliferation. Single cell-RNA-sequencing was performed to profile the cellular components of the TME in an unbiased fashion.

Results

In contrast to progressor tumors, regressor tumors were more infiltrated with DC1 than other DC types (non-DC1). A high DC1/non-DC1 ratio was correlated with increased intratumoral CD8$^+$ T cell infiltration and was predictive of tumor control across different tumor types and mouse strains. Batf3$^{-/-}$ and Clec9a$^{GFP/GFP}$ mice, which lack functional DC1, were able to eliminate a subset of regressor tumors, suggesting that the regression of these tumors was independent of Clec9a-mediated cross-presentation by Batf3-driven DC1. By IFNγ-ELISpot, we found that while CD8$^+$ T cell priming was completely ablated in Batf3$^{-/-}$ and Clec9a$^{GFP/GFP}$ mice implanted with progressor tumors, mice with regressor tumors retained ~50% CD8$^+$ T cell priming. Ex vivo co-culture assays of 2C CD8$^+$ T cells with sorted myeloid cells from SIY-expressing tumors in Batf3$^{-/-}$ mice indicated the presence of CD11c$^+$ cells capable of non-canonical cross-presentation. Ablation of the CD11c$^+$ compartment using diphtheria toxin-treated CD11c-DTR BM chimeras resulted in loss of T cell priming and anti-tumor immunity in the regressor tumor. Single-cell sequencing of the regressor tumor indicated the presence of a novel DC subset capable of non-canonical cross-presentation in DC1-deficient mice.

Conclusions

Identifying the cell type(s) involved and the mechanism of non-canonical cross-presentation in regressor tumors can open new therapeutic avenues to stimulate the anti-tumor immune response when Batf3-driven DC1 are excluded from the tumor.

References

1. Williams et al. The EGR2 targets LAG-3 and 4-1BB describe and regulate dysfunctional antigen-specific CD8$^+$ T cells in the tumor microenvironment. J Exp Med. 2017; 214(2):381-400.

P519

Agonist redirected checkpoint platform (ARC), engineering bi-functional fusion proteins (SIRP -Fc-CD40L), for cancer immunotherapy

George Fromm, PhD[1], Suresh de Silva, PhD[2], Taylor Schreiber, MD, PhD[2]

[1]*Shattuck Labs, Inc, Apex, NC, USA*
[2]*Shattuck Labs, Inc., Durham, NC, USA*

Background

A majority of clinical responses to PD1/L1 blockade occur in patients with abundant intratumoral PD-L1 expression and lymphocyte infiltration, suggesting that additional efficacy may be found in combination therapies that increase either of these variables. Because PD1/L1 blockade augments the cytotoxic potential of T cells, synergistic pathways could include those that reduce immunosuppressive myeloid cells or enhance antigen presentation. Here we report the generation of a novel, two-sided human fusion protein (Agonist Redirected Checkpoint, ARC), incorporating the extra cellular domains of SIRPα and CD40L, adjoined by a central Fc domain; termed SIRPα-Fc-CD40L. The SIRPα-Fc-CD40L construct was designed to simultaneously enhance antigen uptake and cross-presentation (CD47 axis) and enhance antigen presenting cell maturation and function (CD40 axis), with a single compound.

Methods

Human and mouse SIRP -Fc-CD40L were produced and characterized using a range of biochemical assays to determine molecular weight, subunit composition & binding affinity; molecular assays to characterize in vitro/ex vivo binding, in vitro functional activity; and anti-tumor efficacy in multiple syngeneic tumor model systems. SIRP -Fc-CD40L has entered late stage manufacturing.

Results

The SIRPα end of the ARC bound immobilized CD47 at 3.59 nM affinity and also CD47 on the surface of human tumor cells both in vitro and in vivo, but importantly, did not bind human platelets, RBCs, nor induce hemolytic activity. The CD40L end of the ARC bound immobilized CD40 at 756 pM affinity and also CD40 on primary macrophages. The SIRP -Fc-CD40L ARC stimulated Fc receptor-independent NF B-luciferase signaling and also induced cytokine secretion from human PBMCs, both with and without TCR stimulation. Furthermore, when activated human dendritic cells or macrophages were co-cultured with CD47 positive human tumor cells, SIRPα -Fc-CD40L was shown to enhance phagocytosis of human tumor cells, and in vivo in mice, induced rapid activation of CD4+ and CD8+ dendritic cells. Finally, the therapeutic activity of SIRPα-Fc-CD40L in established murine MC38 and CT26 tumors was superior to CD47-blocking antibody, CD40-agonist antibody, and combination antibody therapy. Interestingly, anti-tumor response was heightened significantly when SIRPα-Fc-CD40L was combined with antibody blockade of CTLA4, PD1, or PDL1.

Conclusions

These data demonstrate feasibility of a novel chimeric fusion protein platform, providing checkpoint blockade and TNF superfamily costimulation in a single molecule. Signal replacement of CD47 by CD40L may uniquely poise DCs/macrophages in the tumor microenvironment for activation and cross-presentation of tumor antigens following enhanced tumor cell phagocytosis.

P520

Natural killer (NK) cells orchestrate the antitumor activities of Listeria monocytogenes (Lm)-based immunotherapy

Rachelle Kosoff, PhD[1], Lauren Pettit, MS[1], Nithya Thambi, MS[1], Kimberly Ramos[1], Jeff Jones[1], Skye Kuseryk[1], Robert Petit, PhD[1], Michael Princiotta, MS, PhD[1], Kim Jaffe, PhD[1], Sandy Hayes, PhD[2]

[1]ADVAXIS, INC, Princeton, NJ, USA
[2]Advaxis Immunotherapies, Inc, Princeton, NJ, USA

Background
Advaxis' Lm-based immunotherapies are antigen-based immunotherapies that are designed to elicit tumor antigen-specific T cell effectors that recognize and kill tumor cells. However, because the tumor antigens are delivered by a bacterial vaccine vector, innate cytotoxic effectors, such as NK cells, may also be recruited to play a role in controlling tumor growth. The purpose of this study is to determine whether and how NK cells contribute to the antitumor activities of Lm-based immunotherapy.

Methods
Tumor growth inhibition was evaluated in C57BL/6 mice that were implanted with human papillomavirus (HPV)16+ TC-1 tumor cells and then immunized on days 8, 15 and 22 after tumor implantation with PBS or with axalimogene filolisbac (AXAL), an Lm-based immunotherapy expressing the HPV16 E7 protein. To in vivo deplete NK cells, anti-asialo GM1 antibody (Ab) was administered 1 day before tumor implantation and at 3-day intervals during the PBS or AXAL treatment regimen. For mechanistic studies, flow cytometric analysis and immune-related gene profiling of tumor infiltrating leukocytes (TILs) were performed at various time points after tumor implantation.

Results
We first compared intratumoral NK cell frequency and maturation in PBS- and AXAL-treated mice. Although the percentages of intratumoral NK cells in PBS- and AXAL-treated mice were equivalent, NK cells in tumors of AXAL-treated mice were more functionally mature, based on their high expression of CD11b and granzyme A, than NK cells in tumors of PBS-treated mice. To determine whether AXAL-induced NK cell activity was required for AXAL-mediated tumor control, we used anti-asialo GM1 Ab to in vivo deplete NK cells. In AXAL-treated mice, NK cell depletion resulted in a complete loss of tumor growth inhibition. Phenotypic and functional analyses of TILs revealed impaired dendritic cell (DC) maturation and significantly reduced infiltration of functional HPV-specific CD8+ T cells in NK cell-depleted AXAL-treated mice compared to AXAL-treated mice. Gene profiling and pathway analysis showed that the genes significantly downregulated in tumors of NK cell-depleted AXAL-treated mice versus tumors of AXAL-treated mice were involved in NK cell signaling, DC maturation, and interferon signaling.

Conclusions
Treatment of tumor-bearing mice with AXAL leads to NK cell activation, DC maturation and, by extension, an effective antitumor T cell response. These data suggest that NK-DC cross-talk, which leads to activation and maturation of both cell types, is a mechanism by which NK cells contribute to AXAL's antitumor activities.

Ethics Approval
All mouse experiments were performed under approved IACUC protocols (0914A2016 and 0914B2016).

P521

T cell immunotherapies trigger innate immunity and aseptic inflammation leading to potent anti-tumor and off-targets effects

Daniel Hirschhorn-Cymerman, PhD[1], Jacob Ricca[2], Billel Gasmi, MD[2], Olivier De Henau, MD[2], Levi Mangarin, BS[2], Sadna Budhu, PhD[2], Yanyun Li, PhD MD[2], Czrina Cortez, BS[2], Cailian Liu, MD[2], Roberta

Zappasodi, PhD[2], Sean Houghton[3], Allison Betof[2], Katherine Panageas, PhD[2], Mario Lacuoture, MD[2], Tracvis Hollmann, MD PhD[2], Jean Albrengues, PhD[3], Mikala Egeblad, PhD[3], Taha Merghoub, PhD[2], Jedd Wolchok, MD, PhD[2]

[1]Memorial Sloan Kettering Cancer Center, New York, NY, USA
[2]MSKCC, New York, NY, USA
[3]Cold Spring Harbor Laboratory, Cold Spring Harbor, NY

Background
Mobilizing the immune system to treat advanced cancers is now a clinical reality. Successful immune-based therapies that treat tumors are often accompanied by immune-related adverse events (irAE) that can occasionally present with severe and lethal symptoms. Currently, there are no well-defined preventative approaches to uncouple anti-tumor immunity from irAEs. The primary immunotherapies currently in clinical use include agents that activate T cell responses such as checkpoint blockade of inhibitory pathways and infusion of ex-vivo tumor-derived, or T cell receptor (TCR)-transgenic or chimeric antigen receptor-modified T cells. While the beneficial and toxic effects of T cell-based immunotherapies in the clinic are being extensively explored, the precise mechanisms underlying their activity remain the subject of intense investigation.

Methods
In the present study, we treated established tumors with melanoma-specific adoptive CD4+ T cell transfer and costimulation via OX40 or CTLA-4 blockade.

Results
We found that, in spite of adequate T cell stimulation, acute local inflammation plays a fundamental role in tumor elimination and related irAEs. While stimulated T cells are necessary for initiating a therapeutic response, activation of endogenous neutrophils constitute an important and necessary effector mechanism of tumor destruction and irAEs. Extensive neutrophil extracellular traps (NETs) were associated with irAEs. Furthermore, melanoma patients treated with checkpoint blockade who developed skin rashes equivalent to irAEs found in mice, showed increased survival and NETs were found in biopsies from rashes and tumors.

Conclusions
Our results bring forward a novel paradigm where T cells enact an anti-tumor immune response that is followed by an inflammatory effector mechanism provided by the innate immune system with curative as well as morbid effects in mice and patients.

Ethics Approval
All tissues were collected at MSKCC following consent to an institutional biospecimen collection study protocol approved by the MSKCC Institutional Review Board. Informed consent was obtained for all patients. The study was in strict compliance with all institutional ethical regulations

P522

Immune-profiling reveals DNAM-1 downregulation in tumor-infiltrating lymphocytes of renal cell carcinoma patients

Veronika Kremer, MSc[1], Christina Seitz, MSc[1], Ann-Helen Scherman Plogell, MD[2], Eugenia Colon, MD, PhD[2], Evren Alici, MD, PhD[1], Andreas Lundqvist, PhD[1]

[1]Karolinska Institutet, Stockholm, Sweden
[2]Stockholm South General Hospital, Stockholm, Sweden

Background
Natural killer (NK) cells infiltrate renal cell carcinoma (RCC) tumors and may play a key role in modulating tumor progression, as high NK cell frequencies have been correlated with improved patient survival.

However, NK cells, as well as T cells, have been found be phenotypically and functionally suppressed in the tumor microenvironment.

Methods
We investigated immune cell phenotypes and secretion signatures in blood and primary tumors of RCC patients and applied the supervised multivariate analysis tool Orthogonal Projections to Latent Structures (OPLS) to correlate those with disease parameters.

Results
We found that DNAM-1 expression on intratumoral NK cells is associated with a lower Fuhrman grade, whereas PD-1 expression on peripheral blood lymphocytes correlates with a lower primary tumor stage. Furthermore, we identified differences in the immune profiles of blood and tumor of each patient using an OPLS approach. We showed that DNAM-1 is significantly downregulated on tumor-infiltrating T and NK cells compared with peripheral blood ($p=0.0006$). Indeed, our in vitro experiments suggested that this is likely triggered by contact with tumor cells.

Conclusions
Our results suggest that while T and NK cells can be activated by RCC tumors, they are also inhibited through DNAM-1 down-regulation, which seems to be a central mechanism of immune escape by RCC tumors.

Ethics Approval
The study was approved by the Regional Ethical Review Board in Stockholm, approval number #2013-570-31.

P523

Engineering responsive multi-functional natural killer cells derived from induced pluripotent stem cells capable of overcoming immunometabolic suppression for immunotherapy of solid tumors

Kyle B. Lupo[1], Andrea M. Chambers[1], Jiao Wang, PhD[1], Sandro Matosevic, PhD[1]

[1]*Purdue University, Lafayette, IN, USA*

Background
Targeted immunotherapy with engineered natural killer (NK) cells has proven to be a promising approach for the treatment of solid tumors. The pathogenesis of solid cancers, however, causes severe immunosuppression, due to mechanisms which include the generation of immunosuppressive adenosine by the cancer-associated enzyme CD73, as well as the expression of CD155, which causes immune cell dysfunction. Moreover, challenges in sourcing NK cells impair the development of immunotherapies for solid tumors, promoting interest in using induced pluripotent stem cells (iPSCs) as a source of allogeneic NK cells.

Methods
We have generated “off-the-shelf” NK cells differentiated from iPS cells using a novel feeder-free cell culture protocol. These cells can act as a source of allogeneic NK cells that can be genetically engineered for use in cancer immunotherapy. Additionally, we are genetically engineering NK cells with a responsive genetic construct which combines extracellular TIGIT, a ligand for CD155, with intracellular signaling elements that redirect inhibition induced by CD155/TIGIT interaction to trigger release of CD73 scFv. These multi-functional NK cells are capable of competitively binding to CD155+ cancer cells, displacing the inhibition induced by CD155/TIGIT interaction, and blocking CD73. Engineered NK cells are generated via

transfection using mRNA electroporation and assessed for cytotoxic function against CD73+ targets.

Results

Initially, iPS cells were differentiated into hematopoietic progenitor cells. These cells were characterized via flow cytometry using cell surface markers expressed on hematopoietic progenitors – CD34, CD43, and CD45. Differentiation yielded CD34+/CD45+ and CD34+/CD43+ cell populations of approximately 20% and 13%, respectively, consistent with results described in literature using feeder-based protocols [1]. Following four weeks of NK cell culture, cells were further analyzed and yielded high expression of several NK cell maturation markers under optimal conditions (greater than 70%, 45%, and 55%, for CD3-/CD56+, CD94+, and NKp46+ cell populations, respectively). In parallel, we have generated a responsive construct targeting CD155 with the concomitant release of CD73 scFv and are characterizing its effect on NK cells' anti-tumor immunity.

Conclusions

We have shown that NK cells can be generated from iPSCs using an efficient feeder-free protocol. We also synthesized a novel genetic construct which redirects TIGIT-induced inhibition and triggers release of therapeutic CD73 scFv. NK cells engineered with our construct are expected to inhibit immunometabolic suppression due to multi-functional CD73 and CD155 activity and enhance the killing ability of NK cells against solid tumor targets, allowing improved cancer targeting over traditional chimeric antigen receptor-NK therapies.

Acknowledgements

Jungil Moon, Ph. D., iPS Facility Coordinator, Purdue University, West Lafayette, I.N.

References

1. Bock A, Knorr D, and Kaufman D. Development, expansion, and in vivo monitoring of human NK Cells from human embryonic stem cells (hESCs) and induced pluripotent stem cells (iPSCs). Journal of Visualized Experiments : JoVE. 2013;74: 50337.

P524

Preclinical characterization of BMS-986299, a first-in-class NLRP3 innate agonist with potent antitumor activity, alone and in combination with checkpoint blockade

James Burke[2], Michael Wichroski, PhD[2], Huilin Qi[2], Jie Fang[2], Adam Bata[2], Ramola Sane[2], Anwar Murtaza, PhD[2], Ashvinikumar Gavai, PhD[2], Ragini Vuppugalla[2], Frederic Reu[2], Dana Banas[2], Julie Carman, PhD[2], Damien Bertheloot[3], Dennis Dean[3], Luigi Franchi[3], Shomir Ghosh[3], Gary Glick[3], Jonathan Graves[3], Ana Kitanovic, PhD[3], Eicke Latz[3], Xiaokang Lu, BS[3], Edward Olhava[3], William Roush[3], Brian Sanchez[3], Andrea Stutz[3], David Winkler, PhD[3], John Hunt, PhD[2], Miguel Sanjuan, PhD[2], James Burke[2]

[1]Chrysalis Medical, Hayward, CA, USA
[2]Bristol-Myers Squibb, Lawrence Township, NJ, USA
[3]IFM Therapeutics, Princeton, NJ, USA

Background

Immune checkpoint inhibitors (CPI) targeting adaptive immunity have significantly improved patient outcomes in many tumor types, but other approaches are needed to extend clinical benefit to more patients. Targeting innate immunity to provide broader activation of the immune system may be one approach to complement CPI activity. The NLRP3 inflammasome pathway, a key mediator of innate immunity and immune homeostasis, promotes pro-inflammatory response through the maturation of cytokines interleukin-1β (IL-1β) and IL-18, which drive augmented adaptive immune and T-cell memory responses. Targeting innate immune

activation through the NLRP3 inflammasome represents a novel and differentiated approach to activating the antitumor immune cycle. Here, we present the preclinical evaluation of a first-in-class NLRP3 agonist BMS-986299 ± CPI.

Methods

Cellular activation of the NLRP3 inflammasome was investigated using cell imaging, biochemical methods, and cytokine release assays. Selectivity of BMS-986299 was confirmed in NLRP3-deficient cells. To investigate whether local activation of NLRP3 could drive systemic antitumor immunity, resulting in abscopal antitumor effects, BMS-986299 (intratumorally 6 to 100 µg Q2D×3 or Q1W) ± anti-PD-1 or anti-CTLA-4 CPI (intraperitoneally) was evaluated in mouse syngeneic tumor models (eg, EG7 thymoma and MC38 colon adenocarcinoma); abscopal activity was measured in a noninjected distal tumor.

Results

BMS-986299 selectively activated the human and mouse NLRP3 inflammasome, resulting in inflammasome assembly (ASC speck formation), caspase-1 activation, and IL-1β and IL-18 cleavage/release. BMS-986299 induced IL-1β at EC_{50} ≈ 0.5 µM in human PBMCs. In allogeneic mixed lymphocyte reaction assays, single-agent BMS-986299 enhanced T-cell activation; the addition of CPI resulted in further improvements. Pharmacodynamic studies revealed that intratumoral administration of BMS-986299 led to localized release of IL-1β and IL-18 within injected tumors. In the EG7 model, BMS-986299 was sufficient to induce complete regression in both injected and abscopal tumors; efficacy was abrogated in NLRP3 deficient mice, confirming that antitumor activity was NLRP3-dependent for this molecule. In the MC38 model, BMS-986299 in combination with PD-1 blockade resulted in reduced tumor growth in both injected and abscopal tumors (≥ 50% complete tumor regressions). In both models, all mice achieving complete tumor regression with BMS-986299 ± CPI rejected fresh tumor cells when rechallenged without further treatment, demonstrating long-term, durable antitumor immunity.

Conclusions

BMS-986299 is a first-in-class, selective NLRP3 innate agonist, with robust preclinical antitumor activity ± CPI. These data support the ongoing clinical evaluation of BMS-986299 as a novel therapeutic for the treatment of solid tumors in combination with CPI [NCT03444753].

Ethics Approval

This preclinical study was conducted in accordance with ethical principles and local laws/regulations. The use of samples were reviewed and approved by an institutional review board or independent ethics committee.

P525

Preclinical characterization of BMS-986301, a differentiated STING agonist with robust antitumor activity as monotherapy or in combination with anti–PD-1

Gary Schieven, PhD[2], Jennifer Brown[2], Jesse Swanson, BS[2], Caitlyn Stromko[2], Ching-Ping Ho, BS[2], Rosemary Zhang[2], Bifang Li-Wang[2], Hongchen Qiu[2], Huadong Sun[2], Brian Fink, PhD[2], Anwar Murtaza, PhD[2], John Hunt, PhD[2]

[1]*Chrysalis Medical, Hayward, CA, USA*
[2]*Bristol-Myers Squibb, Princeton, NJ, USA*

Background

Immune checkpoint inhibitors (CPI) targeting adaptive immunity have improved patient outcomes in many tumors, but other approaches are needed to extend benefit to more patients. Targeting innate immunity to provide broader activation of the

immune system may be one approach to complement CPI activity. Stimulator of interferon genes (STING) enhances antitumor immunity by inducing innate immune responses leading to T-cell priming and activation, resulting in a more effective antitumor response. Here we present the preclinical evaluation of the novel STING agonist BMS-986301 ± anti–PD-1.

Methods

BMS-986301 activity was studied in reporter cell lines and mouse/human peripheral blood mononuclear cells (PBMCs). T-cell proliferation and survival were evaluated in resting and activated T cells. Antitumor activity of BMS-986301 (intratumorally) ± anti–PD-1 (intraperitoneally) was evaluated in bilaterally implanted staged (100 mm^3) CT26 or MC38 mouse tumor models; abscopal activity was measured in the noninjected distal tumor. Immune cell levels were measured by flow cytometry, with tetramer staining of tumor-reactive $CD8^+$ T cells. The STING agonist ADU-S100 was used as a reference.

Results

BMS-986301 induced cytokine and Type I interferon response gene expression, with comparable potency in human and mouse PBMCs. In human PBMCs, comparable activity was observed across major STING variants. No responses were observed in STING-deficient cells or mice, demonstrating specificity. Because STING agonists can inhibit T-cell proliferation and survival, BMS-986301 was tested and showed low cytotoxicity toward $CD8^+$ resting human T cells and decreased inhibition of proliferation of activated human T cells in vitro relative to ADU-S100. BMS-986301 monotherapy (250 ug every 4 days [Q4D]×3) achieved >90% complete regressions of injected and noninjected tumors in both tumor models, showing abscopal effects in a dose-dependent manner. Identical dosing with ADU-S100 (250 ug Q4D×3) provided 13% complete regressions in both tumor models. In the CT26 model, anti–PD-1 plus a single dose of BMS-986301 (100 ug) provided 80% complete regressions of injected/noninjected tumors; no complete regressions were observed with anti–PD-1 alone. BMS-986301 induced increased expression of genes associated with T-cell activation in tumors and draining lymph nodes, induced T-cell proliferation, and increased NK-cell infiltration into tumors. In the CT26 model, antitumor activity correlated with induction of circulating tumor-reactive T cells. All CT26 mice achieving complete regressions with BMS-986301 rejected fresh tumor cells without further treatment, demonstrating immunological memory.

Conclusions

BMS-986301 is a differentiated STING agonist, with promising preclinical antitumor activity alone and in combination with anti–PD-1, supporting its evaluation in future clinical studies.

Ethics Approval

This preclinical study was conducted in accordance with ethical principles and local laws/regulations. The use of samples were reviewed and approved by an institutional review board or independent ethics committee.

P526

The potential role of fibroblast activation protein as a natural killer cell immune checkpoint in pancreatic cancer

Louis Weiner, MD[1], Shangzi Wang, PhD[1], Allison O'Connell[1]

[1]*Georgetown University, Washington, DC, USA*

Background

Immunotherapy has been largely ineffective in pancreatic cancer, partially due to the dense stromal fibrosis surrounding the tumor that creates an

immunosuppressive microenvironment. The main cellular component of this fibrosis, activated pancreatic stellate cells (aPSCs), are marked by elevated expression of fibroblast activation protein (FAP). Here we investigate the relationship between FAP and the cytotoxic activity of natural killer (NK) cells.

Methods

To assess the relationship between aPSCs and NK cells we used a novel in vitro co-culturing system that utilizes primary donor-derived PSCs and a human NK cell line, NK92. We tested the ability of NK cells to kill aPSCs using CytotoxGlo and Annexin V assays. We monitored FAP expression and markers of activation in aPSC and NK cells using rt-qPCR, western blot and flow cytometry. To assess the effects of FAP inhibition we used a non-specific FAP inhibitor, talabostat, in vitro and in vivo. 1 µM of talabostat was added to coculturing conditions and NK lysis of aPSCs was determined. For in vivo studies forty female C57BL/6 mice were injected subcutaneously with 1X105 syngeneic MT3-2D cells (Kras+/G12D, p53+/-R172H derived from a PDAC KPC GEMM model [1]). Once tumors reached 40-50 mm3, ten mice per group were given either 30 ug of talabostat per mouse daily by oral gavage, 200 ug of anti-PD-1 per mouse twice a week by i.p., both, or neither. Control mice were treated with PBS. Treatment was terminated after 4 weeks and the mice were monitored, with tumor measurements occurring weekly.

Results

Here we demonstrate that the human NK cell line (NK92) is activated by and kills aPSCs, potentially via recognition of MICA/B on aPSCs by NK cell surface receptor NKG2D. Upon direct contact with PSCs, PSCs downregulate FAP expression and NK92 cells upregulate FAP. This is the first-time NK cells have been shown to produce FAP and that induction of FAP is mediated by cell-to-cell contact. Furthermore, FAP expression by NK92 cells is associated with an inactivate phenotype. FAP inhibition enhances NK92 killing of PSCs in vitro and enhances PDAC tumor clearance in vivo. The anti-tumor activity of FAP inhibition was enhanced upon addition of anti-PD-1 therapy. (Figures 1-5)

Conclusions

This suggests FAP functions as an NK cell immune checkpoint. FAP is expressed in NK cells after activation to attenuate cytotoxicity and can be inhibited to enhance anti-tumor immunity.

Acknowledgements

I'd like to acknowledge Dr. Stephen Byers and Dr. Ivana Peran for provided the PSCs and Dr. Kerry Campbell for providing the NK92 cells.

References

1. Boj SF, Hwang C-I, Baker LA, Chio IIC, Engle DD, Corbo V, Jager M, Ponz-Sarvise M, Tiriac H, Spector MS, et al. Organoid models of human and mouse ductal pancreatic cancer. Cell. 2015; 160:324–338.

Ethics Approval

This study was approved by Georgetown University's IACUC, protocol #2016-1254

Figure 1.

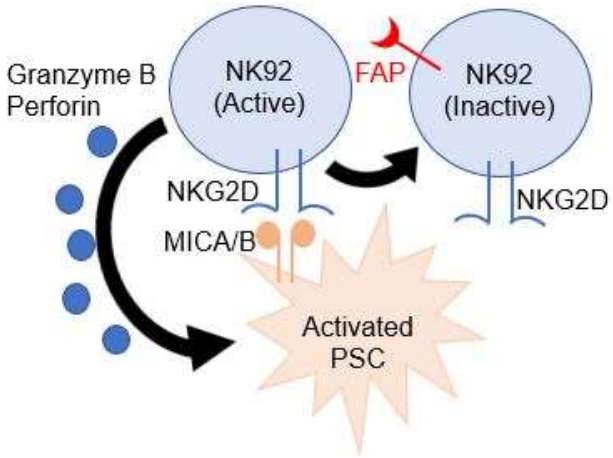

Figure 2.

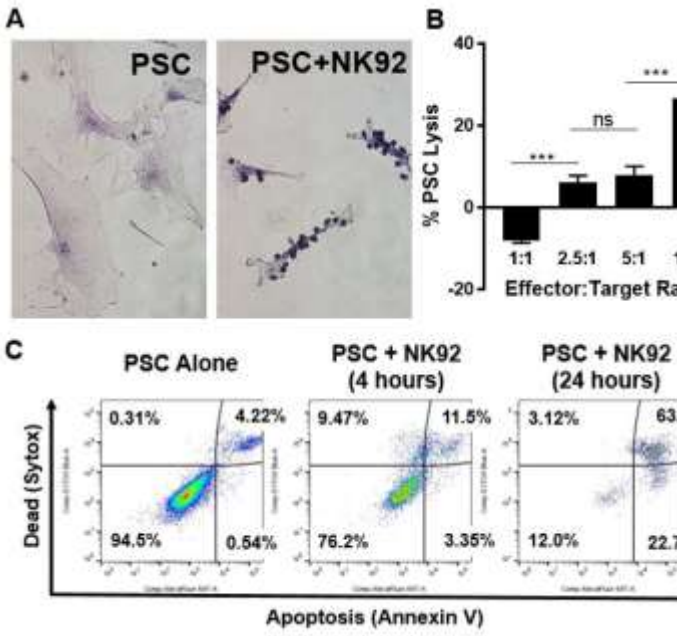

Figure 3.

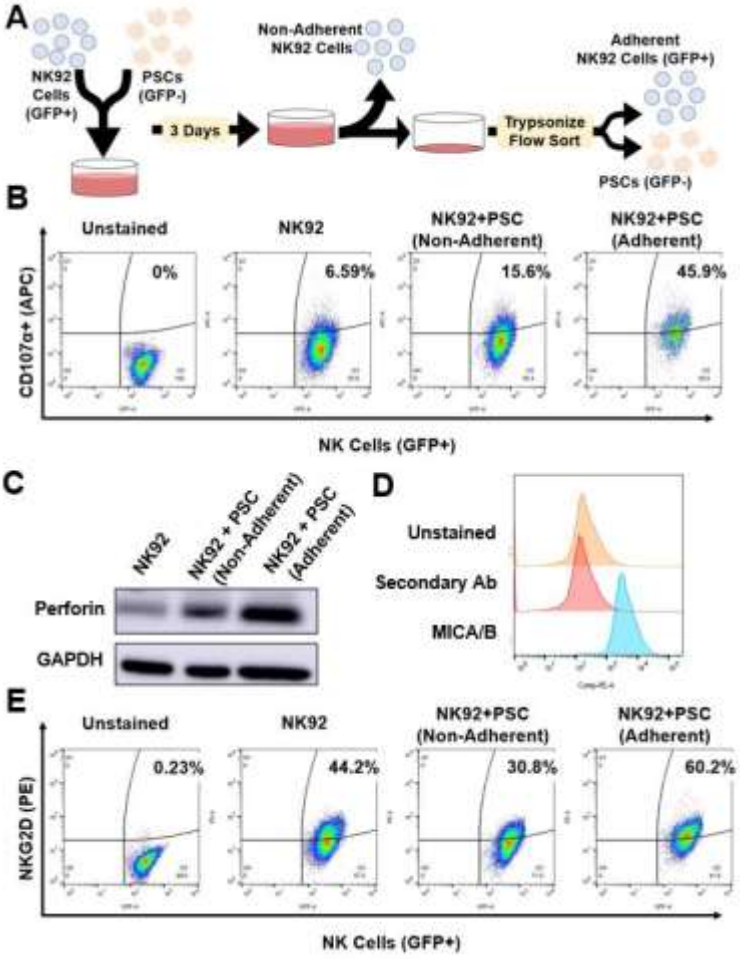

Figure 4.

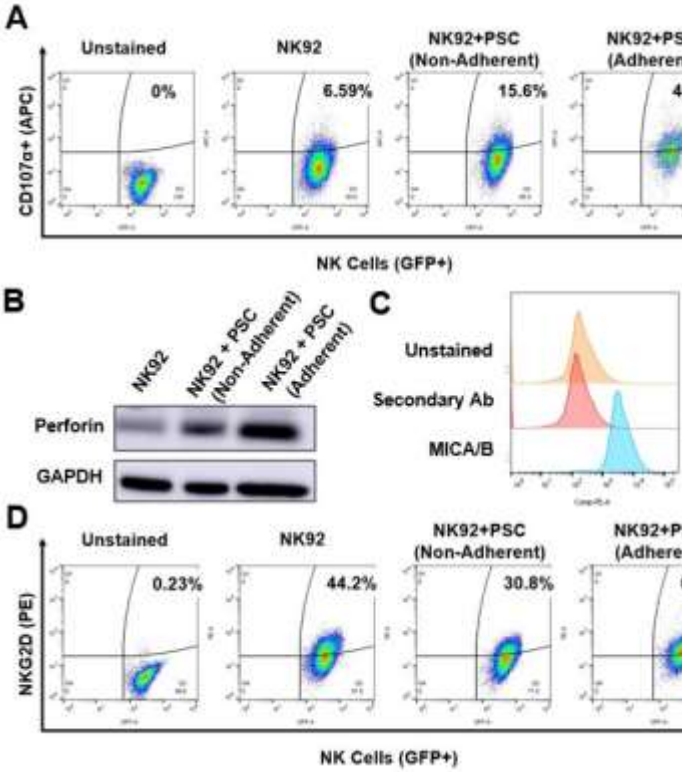

Figure 5.

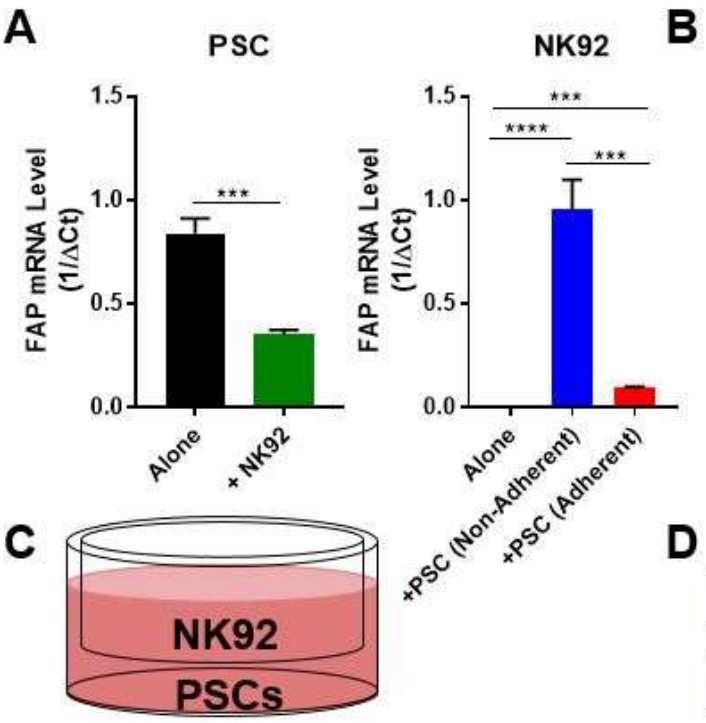

P527

Imprime PGG, a novel cancer immunotherapeutic, engages the complement system to prime innate immune effector functions

Xiaohong Qiu, BS[1], Ben Harrison, MS[1], Adria Jonas, MS[1], Anissa Chan, PhD[1], Nadine Ottoson, BS[1], Nandita Bose, PhD[1], Keith Gorden, BS[1]

[1]*Biothera Pharmaceuticals, Eagan, MN, USA*

Background

Imprime PGG (Imprime), an intravenously-administered soluble, yeast β-1,3/1,6-glucan, is currently in clinical development with tumor-targeting antibodies, anti-angiogenics, and checkpoint inhibitors. The fundamental mechanistic rationale for these therapeutic combinations is that Imprime, being a PAMP, primes innate immune

effector functions to ultimately inspire an adaptive immune response-based anti-cancer immunity cycle. Imprime forms a tripartite immune complex (IC) comprising of Imprime, naturally occurring anti-β-glucan antibodies (ABA) and iC3b complement opsonin in subjects with sufficient ABA levels. Ex vivo human and in vivo mouse studies have shown that the innate immune receptor, FcgRIIA, and the pattern recognition receptors, complement receptor 3 (CR3) and Dectin-1, are critical for Imprime's innate immune responses. However, the contributions of the complement system, a vital component of innate immunity, towards the functional activity of Imprime has not been thoroughly investigated. Imprime-ABA IC activates the classical complement pathway and releases C5a. As C5a is a well-known priming agent, and cross-talks with the other innate immune receptors, we hypothesized that Imprime-induced C5a will engage the C5a-C5a receptor (C5aR) signaling pathway to enhance Imprime binding and innate immune effector functionalities.

Methods

The role of C5a in Imprime-ABA binding to isolated neutrophils was evaluated by: a) adding exogenous C5a; b) using C5a-depleted serum, and c) using C5aR antagonist (C5aRA). Cytokine production in healthy subjects with sufficient ABA levels were measured 24hrs post-Imprime treatment in the presence or absence of C5aRA by multiplex luminex assays. The effect of C5a inhibitors was also evaluated in a chemiluminescence-based oxidative burst assay measuring reactive oxygen species (ROS) generated by Imprime-treated isolated neutrophils in response to Rituxan-bound B cell lymphoma cells. In order to test these endpoints in complement-depleted conditions, the whole blood was washed extensively to remove the plasma.

Results

Addition of exogenous C5a increased the percentage of neutrophils binding to Imprime in a dose-dependent manner. Furthermore, Imprime binding in the presence of C5aRA and C5a-depleted serum was significantly reduced. Functionally, C5aRA abrogated cytokine production (IL-8, MCP-1, MIP-1alpha, and IL-6) in Imprime-treated blood. Likewise, Imprime-ABA induced ROS in high-ABA blood was greatly inhibited in C5a-depleted serum and could be rescued by replenishing complements. C5aRA also inhibited Imprime-induced ROS production. In a non-physiological, complement-depleted condition, Imprime bound predominantly via FcgRIIA, resulting in diminished cytokine and ROS responses.

Conclusions

These results collectively demonstrate that Imprime-induced C5a play a critical role in enhancing Imprime binding and functional responses, potentially by lowering the signaling threshold of the other innate immune receptors.

P528

Tumor-derived alpha fetoprotein suppression of mitochondrial metabolism via PGC1-α and SREBP-1 expression and activity in human dendritic cells

Patricia Santos, PhD[1], Ashley Menk, BS[1], Jian Shi, MD[1], Allan Tsung, MD[1], Greg Delgoffe, PhD[1], Lisa Butterfield, PhD[1]

[1]*University of Pittsburgh, Pittsburgh, PA, USA*

Background

Alpha-fetoprotein (AFP) is an oncofetal antigen expressed during fetal development and by over 50% of hepatocellular carcinomas (HCC). AFP-L3 is the major isoform present in the serum of HCC patients and is associated with poor patient prognosis. While tumor-derived AFP (tAFP) contains >80% of AFP-L3, cord blood serum-derived AFP (nAFP) contains less than 5% of AFP-L3. We have previously shown that monocyte-derived dendritic cells (DC) cultured in the presence of AFP (in particular tAFP), retained a monocyte-like morphology, had decreased

expression of DC maturation markers, and are poor stimulators of antigen-specific T cell responses. In this study, the effect of AFP on DC metabolism was examined.

Methods

PBMC were isolated from healthy donor (HD) or HCC patients using Ficoll-Paque density gradient centrifugation. HD monocytes were isolated from PBMC and cultured for 5 days with IL-4 and GM-CSF to generate DC in the presence of 10 µg/mL ovalbumin (OVA), nAFP or tAFP. DC were collected and tested for 1) mitochondria levels and function by flow cytometry, 2) metabolic function by seahorse extracellular flux analyzer, 3) expression of oxidative phosphorylation proteins, SREBP-1 and downstream gene targets via Western Blot, and 4) expression of PGC1-α via flow cytometry. PBMC from HCC patients were stained with surface markers to identify different circulating DC subsets prior to intracellular staining with PGC1-α.

Results

DC cultured in the presence of nAFP and tAFP show reduced expression of mitochondrial regulator PGC1-α. Furthermore, nAFP- and tAFP-DC had reduced mitochondrial mass and mitochondrial activity compared to OVA-DC. This was confirmed by a reduction in the basal oxygen consumption rate (OCR) in nAFP-DC and a more severe reduction in basal OCR in tAFP-DC, with changes in DC metabolism occurring within 24 hours of AFP exposure. The decrease in oxygen consumption in DC exposed to nAFP and tAFP is attributed to downregulation of cytochrome c oxidase, responsible for the reduction of oxygen into water. Importantly, circulating myeloid DC from HCC patients have reduced PGC1-α expression compared to healthy donors. Lastly, there was a reduction in the expression of the transcription factor SREBP-1 and downstream targets FASN and ACLY in DC exposed to nAFP and tAFP, suggesting mechanistic inhibition of mTORC1 pathway in DC by AFP.

Conclusions

Collectively, these data show the profound negative effects of AFP on DC metabolism. These novel findings elucidate a key mechanism of immune suppression in HCC and may lead to new therapeutic approaches to reverse these effects.

Ethics Approval

The study was approved by the University of Pittsburgh's Institutional Review Board, approval number 0403105.

P529

Efficacy and safety profile of AU7R-104, a small molecule targeting CD47/SIRPα pathway

Murali Ramachandra, PhD[2], Pottayil Sasikumar, PhD[1], Chennakrishnareddy Gundala[2], Wesley Balasubramanian, PhD[2], Sudarshan Naremaddepalli, PhD[2], Archana Bhumireddy, MSc[2], Sandeep Patil, PhD[2], Amit Dhudashiya[2], Vijaysai Rayavarapu, MSc[2], Dodheri Samiulla, PhD[2], Sanjeev Giri, PhD[2], Rajesh Eswarappa, PhD, DABT, ERT[2], Kiran Aithal, PhD[2], Girish Daginakatte, PhD[2], Murali Ramachandra, PhD[2]

[1]Aurigene Discovery Technologies, Bangalore, India
[2]Aurigene Discovery Technologies Limited, Bangalore, India

Background

CD47 is over expressed on many different human cancers and it is also known as a “don’t eat me” signal. Many studies have demonstrated that there is great potential for targeting the CD47-SIRPα pathway as therapy for cancer. Efforts have been made to develop therapies inhibiting the CD47-SIRPα pathway, through antibodies directed against CD47 and recombinant SIRPα proteins. We have developed a novel small molecule CD47 antagonist, AU7R-104, as therapeutic agent for solid and hematological cancers. AU7R-104 enhances

phagocytosis of tumor cells and exhibits good drug-like properties with good anti-tumor activity. Here, we report the in vivo activity of AU7R-104 in different tumor models, biomarker characterization and safety profile of AU7R-104 in rodents and non-rodents.

Methods
We have identified preclinical candidate compound AU7R-104 with potent in vitro and in vivo activity. AU7R-104 was profiled extensively in different tumor models both as single agent and in combination with tumor specific antibodies and other anti-cancer agents. In the PK-PD and efficacy studies, efforts were made for biomarker characterization through multiplex and FACS analysis. Advanced profiling of AU7R-104 has been completed in DMPK and toxicological studies in rodents and non-rodents.

Results
AU7R-104 has potent anti-tumor activity both as a single agent and in combination with anti-cancer agents. In the PK-PD studies, AU7R-104 enhanced in vivo phagocytosis in both macrophages and dendritic cells. Multiplex analysis of serum samples indicated there was modulation of macrophage and T-cell mediated cytokines. In the advanced ADME assays, AU7R-104 demonstrated good drug-like properties without any significant alerts. AU7R-104 combination treatments were well tolerated. Preliminary safety evaluation of AU7R-104 in both rodents and non-rodents indicated the lack of safety concerns typically associated with anti-CD47 antibodies or SIRPα-Fc protein therapeutics.

Conclusions
The above findings support further development of these orally bioavailable agents for use in the clinic

P530

Novel bispecific antibody targeting NKp30 receptor enhances NK-mediated killing activity against multiple myeloma cells and overcomes CD16A deficiency

MONIA DRAGHI, PhD[1], Jennifer Watkins-Yoon[1], Jamie Schafer, PhD[1], Sara Haserlat[1], Sri Vadde[1], Xin Kai[1], Allison Nelson[1], Lucy Liu[1], Nora Zizlsperger, PhD[1], Amanda Oliphant[1], Michael Schmidt[1], Robert Tighe, BS[2],

[1]Compass Therapeutics, Cambridge, MA, USA
[2]Compass Therapeutics LLC, Cambridge, MA, USA

Background
Multiple myeloma (MM) is a malignant hematological disease characterized by a dysregulated growth of malignant plasma cells. Different therapeutic options are available for MM patients; however, the disease remains mostly incurable. B-cell maturation antigen (BCMA) is a promising target in MM because of its restricted expression in normal and malignant plasma cells [1]. NK cells have been implicated in the clinical efficacy of several therapies against MM and may contribute to the success of stem cell transplantation (SCT) by clearing residual cancer cells [2]. In patients with advanced MM, NK cell function is impaired by downregulation of activating receptors including NKG2D, 2B4, and CD16A (FcγRIIIA) [3,4]. Downregulation of CD16A is particularly problematic for conventional anti-BMCA antibodies seeking to elicit ADCC. In contrast, expression of NKp30 remains stable, providing a compelling rationale for the design of BCMA-targeted multispecific molecules that redirect NK cell killing by engaging NKp30 to overcome deficiencies in other activating NK receptors.

Methods
Our Stitchmabs™ and common light chain (LC) bispecific antibody platforms were employed to discover and engineer CTX-4419, a tetravalent, fully

human, bispecific molecule consisting of a novel IgG1 antibody recognizing BCMA fused at the c-terminus to two anti-NKp30 Fab fragments with a common LC sequence. The in vitro activity of CTX-4419 was compared against a conventional anti-BCMA IgG1 antibody format for its capacity to induce killing of MM cells and cytokine and chemokine production by primary NK cells and NK cell lines.

Results

When tested with primary NK cells expressing both CD16A and NKp30, CTX-4419 induced potent NK cell cytotoxicity and cytokine production against tumor cells which was superior to the monoclonal IgG1 anti-BCMA control. In contrast to the anti-BCMA IgG1 control that activated only CD16A+ NK cells, CTX-4419 induced potent killing of MM cells and IFN-γ production by KHGY-1, a CD16A- NKp30+ cell line, showing that CTX-4419 can redirect NK cell subsets with low expression of CD16A to kill MM cells. Additionally, an Fc-silent version of CTX-4419 retained activity, further supporting a CD16A-independent function. Importantly, CTX-4419 did not activate NK cells in the absence of BCMA-expressing tumor cells, indicating no off-target effects.

Conclusions

We have engineered and characterized a first-in-class, differentiated bispecific NK cell engager that potently redirects NKp30+ NK cells to kill BCMA+ tumor cells. Unlike traditional anti-BCMA mAbs, CTX-4419 remains highly active in the absence of CD16A engagement. CTX-4419 in undergoing monotherapy assessment in pre-clinical models including experiments with patient derived samples.

References

1. Tai YT, Anderson KC. Targeting B-cell maturation antigen in multiple myeloma. Immunotherapy. 2015;7(11):1187-99.
2. Cooley S, Parham P, Miller JS. Strategies to activate NK cells to prevent relapse and induce remission following hematopoietic stem cell transplantation. Blood. 2018;131(10):1053-1062.
3. Fauriat C, Mallet F, Olive D, Costello RT. Impaired activating receptor expression pattern in natural killer cells from patients with multiple myeloma. Leukemia. 2006;20(4):732-3.
4. Costello RT, Boehrer A, Sanchez C, et al. Differential expression of natural killer cell activating receptors in blood versus bone marrow in patients with monoclonal gammopathy. Immunology. 2013;139(3):338-41.

P531 Abstract Travel Award Recipient

Redirecting immunometabolic suppression by targeting purinergic signaling enhances immunotherapy of solid tumors with CAR-NK cells

Jiao Wang, PhD[1], Sandro Matosevic, PhD[1], Kyle B. Lupo[1], Andrea M. Chambers[1]

[1]*Purdue University, West Lafayette, IN, USA*

Background

Engineering natural killer (NK) cells with chimeric antigen receptors (CARs) can enhance their targeting of solid tumor malignancies [1]. However, the CD73-mediated generation of adenosine (ADO) within the hypoxic microenvironment of many solid tumors induces severe immunometabolic suppression which impairs their activation and anti-tumor immunity (Figure 1A) [2–4].

Methods

In an effort to overcome purinergic immunometabolic suppression and improve NK cell-mediated anti-tumor function, we have developed an immunotherapeutic treatment approach which combines non-virally engineered NKG2D-retargeted CAR-NK-92 (NKG2D.CAR-NK-92) cells alongside neutralization of CD73 ectonucleotidase activity (Figure 1B). We have quantified the cytotoxicity of these engineered cells in terms of IFN-γ expression

and degranulation activity, and characterized their anti-tumor effects and homing of on CD73+ solid tumors in vivo.

Results

CAR-NK-92 cells, expressing a chimeric immunoreceptor targeting NKG2D based on the piggyBac transposon system, showed significantly higher IFN-γ production, degranulation capacity, and lytic ability against solid tumor cells compared with wild-type NK cells. CD73 blockade was able to further enhance the killing ability of CAR-engineered NK cells against CD73+ solid tumor targets. In vivo, neutralization of CD73 activity promoted anti-tumor efficacy of the engineered NK cells against CD73+ human lung cancer xenografts, including a greater delay in tumor growth, no obvious toxicity, and increased tumor-infiltrating NK cells (Figure 1C-G). CD73 blockade could contribute to the delay in tumor growth in vivo independently of adaptive immune cells, innate immunity or NK cell-mediated ADCC, suggesting that CD73 might contribute to tumor metastasis via autocrine-like mechanisms outside of its ectonucleotidase activity.

Conclusions

Immunometabolism is emerging as a profound mediator of NK cell anti-tumor immunity. Immunotherapies targeting the adenosinergic signaling pathway, such as by neutralizing CD73 ectoenzymatic activity, had, however, not been evaluated on NK cells. Our studies demonstrate, for the first time, the potential of targeting CD73 to modulate purinergic signaling and enhance adoptive NK cell immunotherapy via mechanisms that could implicate autocrine tumor control as well as by mediating adenosinergic signaling. We also provided the basis for targeting the regulation of cancer metabolism as a promising strategy for enhancing the therapeutic efficacy of CAR-modified NK cells for immunotherapy of solid tumors. Based on these results, in order to achieve affective redirection of purinergic signaling while enhancing cancer targeting specificity, we are currently designing and characterizing a multi-functional CAR-NK cell which consists of a single chain antibody targeting CD73 alongside dual chimeric antigen receptor targeting, as a next-generation, single-agent immunometabolic therapy of solid tumors with NK cells.

References

1. Guillerey C, Huntington ND, Smyth MJ. Targeting natural killer cells in cancer immunotherapy. Nat Immunol. 2016;17(9):1025-36.
2. Zhang B. CD73: a novel target for cancer immunotherapy. Cancer Res. 2010;70(16):6407–11.
3. Antonioli L, Blandizzi C, Pacher P, Haskó G. Immunity, inflammation and cancer: a leading role for adenosine. Nat Rev Cancer. 2013;13(12):842-57.
4. Ohta A. A metabolic immune checkpoint: adenosine in tumor microenvironment. Front Immunol. 2016;7:109.

Figure 1.

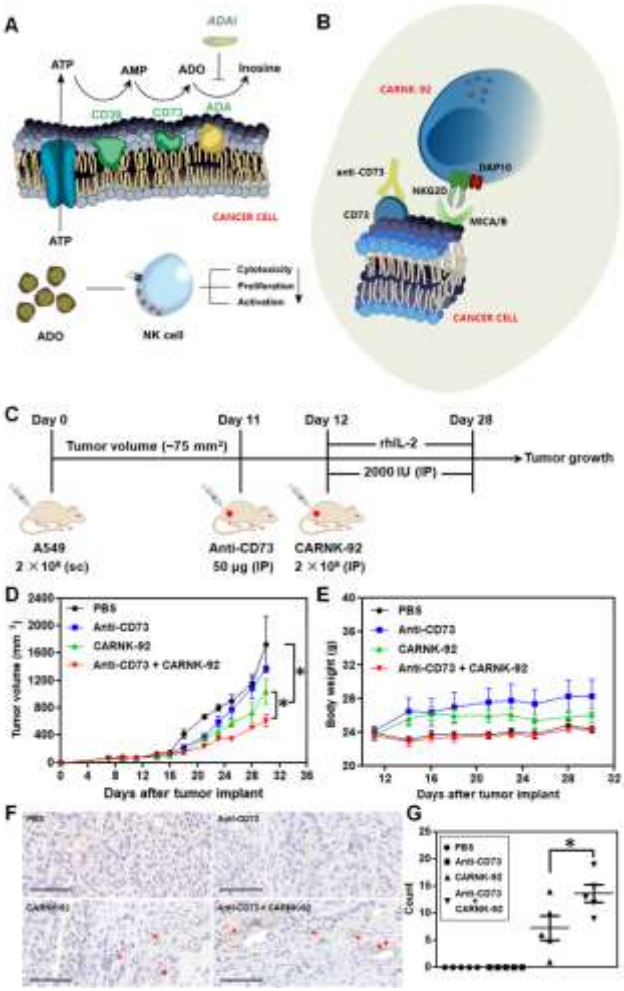

P532

Preclinical characterization of a first-in-class ILT4 antagonist, MK-4830

Luis Zuniga, PhD[1], Barbara Joyce-Shaikh, BS[1], Douglas Wilson[1], Holly Cherwinski[1], Yi Chen[1], Grein Jeff[1], Wendy Blumenschein, BA[1], Eric Muise, MS[1], Xiaoyan Du[1], Edward Hsieh[1], Sripriya Dhandapani[1], Gulesi Ayanoglu[1], Maribel Beaumont[1], Shuli Zhang[1], Michael Rosenzweig, DVM, PhD[1], Robert Kastelein, PhD[1], Robert Stein, MD PhD[2], Dennis Underwood, PhD[2], Milan Blanusa[3], Rachel Altura, MD[1], Daniel Cua[1]

[1]Merck Research Laboratories, Palo Alto, CA, USA
[2]Agenus Inc., Lexington, MA, USA
[3]Pieris Pharmaceuticals GmbH, Freising, Germany

Background

Myeloid-derived suppressor cells in the tumor microenvironment contribute to tumor immune evasion by suppressing local T cell activation, proliferation, and anti-tumor effector responses, identifying them as targets for therapeutic intervention. ILT4 is an inhibitory member of the immunoglobulin-like transcript (ILT) family of proteins. It is expressed primarily by myeloid cells, including those in the tumor microenvironment, and interacts with major histocompatibility (MHC) class I complexes and angiopoietin-like (ANGPTL) ligands. ILT4 signaling is associated with the induction of a tolerogenic phenotype in antigen presenting cells. We demonstrate the pre-clinical anti-tumor properties of a first-in-class anti-ILT4 monoclonal antibody which has now entered clinical trials in patients with advanced solid tumors.

Methods

The clinical candidate MK-4830 is a fully human monoclonal antibody that we selected for specificity, ligand blockade, and functional downstream signaling antagonism of ILT4. Primary human tumor tissue, blood, and serum were profiled for the expression of ILT4 and its ligands. Primary human PBMCs were used to discover MK-4830-dependent,

myeloid-associated cytokine responses in vitro. A humanized mouse model implanted with a patient-derived melanoma cell line (SK-MEL-5) was used to evaluate the mechanism of action of ILT4 antagonism and its anti-tumor efficacy.

Results
MK-4830 is specific to ILT4 and does not bind other ILT-family receptors. MK-4830 blocks ILT4 ligand binding and reverses ILT4-mediated suppression of signal transduction. Blocking ILT4 in vitro enhances proinflammatory cytokine expression of GM-CSF and TNFα in LPS-stimulated human PBMC cultures. ILT4 is expressed in primary human tumor samples and ILT4+ myeloid cells are observed both in the periphery and in the tumor infiltrate within the humanized mouse tumor model. Administration of MK-4830 in the humanized mouse tumor model resulted in approximately 50% reduction in tumor growth, alterations in both splenic and tumor myeloid subset distributions, as well as changes in myeloid-centric chemokine and cytokine profiles.

Conclusions
MK-4830, a novel first-in-class antagonist ILT4 antibody, induces robust anti-tumor activity in a humanized mouse tumor model. The preclinical data presented here support the ongoing clinical evaluation of MK-4830 as an anti-cancer therapy and suggests its potential to target tumor-associated myeloid cells in combination with other immune checkpoint blockers.

Trial Registration
Study of MK-4830 as Monotherapy and in Combination With Pembrolizumab (MK-3475) in Participants With Advanced Solid Tumors (MK-4830-001). (2018). Retrieved from https://clinicaltrials.gov/ct2/show/results/NCT03564691?term=NCT03564691&rank=1 (Identification No. NCT03564691)

Ethics Approval
In vivo experiments used in this study were approved by Merck Research Laboratories' Ethics Board, approval number P2021-400265-JAN.

P533

Gastrointestinal symptoms observed after chimeric antigen receptor T–cell therapy

Hamzah Abu-Sbeih, MD[1], Tenglong Tang, MD[1], Jason R. Westin, MD[1], David Richards, MD[1], Sattva S. Neelapu, MD[1], Yinghong Wang, MD, PhD[1]

[1]*MD Anderson Cancer Center, Houston, TX, USA*

Background
The new approach of chimeric antigen receptor T-cell therapy (CAR-T) has been proven to be a very effective treatment for hematological malignancies.[1, 2] The most notable drawbacks of CAR-T is cytokine release syndrome (CRS) and CAR-related encephalopathy syndrome (CRES).[3-6] Gastrointestinal adverse events (GI-AEs) associated with CAR-T have not been studied yet. Herein, we describe the incidence and features of GI-AEs observed after CAR-T.

Methods
This is a case series of patients with hematological malignancies who received CAR-T, as a clinical trial or standard of care where data publication was permitted by the primary investigators, and subsequently suffered from GI-AEs between 1/2012 and 5/2018. Other etiologies of diarrhea were excluded (Figure 1).

Results
Out of the 132 patients that received CAR-T, 21 (16%) experienced GI-AEs. The median age for the 21 patients was 59 years (range, 23-77; Table 1). Most patients had diffuse large B-cell lymphoma (67%). Ten patients experienced CRS, whereas, 7 experienced CRES. Interleukin-6 antagonist was

required in 10 patients. Diarrhea was present in all 21 patients (Table 2); 62% grade 1, 33% grade 2 and 5% grade 3. Other associated gastrointestinal symptoms among these 21 were abdominal pain (38%), nausea and vomiting (38%), fever (38%), abdominal distension (10%), and bloody stool (5%). The median duration from CAR-T infusion to diarrhea onset was 5 days (range, 1-40). Eleven patients required treatment for GI-AEs with a median duration of 6 days. Sixteen patients had abdominal imaging evaluation; 3 (19%) of them had findings suggestive of gastrointestinal tract inflammation. Three (14%) patients experienced GI-AEs recurrence after improvement initially. Colitis was confirmed endoscopically in 1 patient; a 76 year old male who received 2 infusions of CAR-T. Five months later, he developed grade 3 diarrhea with abdominal cramps and 15 pounds weight loss. A stool infectious workup including PCR-based multiplex was negative. Colonoscopy demonstrated diffuse inflammation of the entire colon with histology showing glandular drop out, increased apoptosis, and focal erosions. He had no improvement with steroids and mesalamine, and was subsequently treated with oral immunoglobulin with partial improvement. However, his colitis relapsed and an additional trial of cholestyramine was unsuccessful. Lastly, a complete resolution of his gastrointestinal symptoms was achieved by an antibiotics course (vancomycin and piperacillin/tazobactam) for his new onset of pneumonia.

Conclusions

GI-AEs occur in 16% of patients receiving CAR-T. They are typically mild and self-limiting requiring only symptomatic treatment. Nevertheless, of a rare occurrence, it could lead to a refractory colitis.

References

1. Sadelain M, Brentjens R, Riviere I. The basic principles of chimeric antigen receptor design. Cancer Discov. 2013;3(4): 388-98.
2. Sadelain M. CAR therapy: the CD19 paradigm. J Clin Invest. 2015;125(9):3392-400.
3. Magee M.S., Snook A.E. Challenges to chimeric antigen receptor (CAR)-T cell therapy for cancer. Discov Med. 2014;18(100):265-71.
4. Grigor E.J.M., et al., Efficacy and safety of chimeric antigen receptor T-cell (CAR-T) therapy in patients with haematological and solid malignancies: protocol for a systematic review and meta-analysis. BMJ Open, 2017. 7(12): p. e019321.
5. Leick M.B., Maus M.V. Toxicities associated with immunotherapies for hematologic malignancies. Best Pract Res Clin Haematol. 2018;31(2):158-165.
6. Neelapu S.S., et al. Chimeric antigen receptor T-cell therapy - assessment and management of toxicities. Nat Rev Clin Oncol. 2018;15(1):47-62.

Ethics Approval

This case series was approved by the Institutional Review Board at The University of Texas MD Anderson Cancer Center (IRB No.: PA18-0472).

Consent

This case series was granted waiver of consent.

Figure 1.

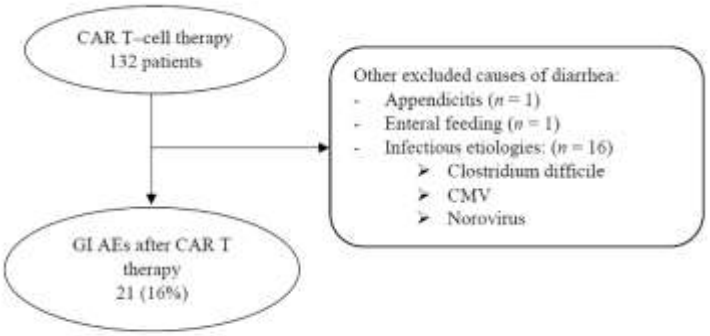

Figure 1. Included patients.

Table 1.

Table 1. Patient characteristics (Number of patients = 21).

Characteristic	No. of patien (%)
Median age, years (range)	59 (23-77)
Male sex	14 (67)
White race	14 (67)
Comorbidities present	5 (24)
Non-steroidal anti-inflammatory drugs	5 (24)
History of smoking	11 (52)
Prior hematopoietic stem cell transplant	11 (52)
Chemotherapy within 3-months of CAR T	17 (81)
Cancer type	
Diffuse large B-cell lymphoma	14 (67)
Follicular lymphoma	2 (10)
B-cell acute lymphocytic leukemia	2 (10)
B-cell chronic lymphocytic leukemia	2 (10)
Other	1 (5)
CAR T–cell therapy toxicities	
Cytokine release syndrome	10 (48)
CAR-related encephalopathy syndrome	7 (33)
Other	3 (14)
Treatment of CAR T toxicities	
Interleukin-6 antagonist	10 (48)
Corticosteroid treatment	9 (43)

Table 2. Characteristics of gastrointestinal adverse events observed in our cohort.

Characteristic	No. of patients (%)
Gastrointestinal (GI) symptoms	
Diarrhea	21 (100)
Abdominal pain	8 (38)
Nausea & vomiting	8 (38)
Fever	8 (38)
Abdominal distension	2 (10)
Blood per rectum	1 (5)
CTCAE grade of diarrhea	
1	13 (62)
2	7 (33)
3	1 (5)
Median duration of GI symptoms, days (range)	5 (1-40)
Mean absolute neutrophil count at diarrhea onset (SD)	0.59 K/μL (0.98)
Treatment for diarrhea	
Yes	11 (52)
Antimotility	10 (48)
Oral IVIG and cholestyramine	1 (5)
No	10 (48)
Median duration of treatment, days (range)	6 (2-60)
Suggestive findings of GI tract inflammation on imaging[a]	3 (19)
Recurrent diarrhea	3 (14)
Duration from improvement to recurrence, days (range)	21 (5-24)

Abbreviation: CTCAE, Common Terminology Criteria for Adverse Events v4.03; IVIG, intravenous immunoglobulin.
[a]Imaging evaluation was available for 16 patients.

Table 2.

P534

Timely endoscopic and histological evaluation is critical to provide appropriate management for immune checkpoint inhibitor induced colitis

Hamzah Abu-Sbeih, MD[1], Faisal S. Ali[1], Wenyi Luo, MD[1], Wei Qiao, PhD[1], Gottumukkala S. Raju, MD[1], Yinghong Wang, MD, PhD[1]

[1]*MD Anderson Cancer Center, Houston, TX, USA*

Background

Immune checkpoint inhibitors (ICI) are efficacious treatments for advanced malignancies but can result in immune mediated diarrhea and colitis (IDC). Currently, the guidelines for the treatment of IDC depend only on clinical symptoms. Endoscopic and histologic features of such adverse events are not well studied in a manner that can help to gauge treatment plans. We aimed to characterize endoscopic and histologic features of IDC and to assess their association with clinical outcomes.

Methods

Our study included patients who had undergone endoscopy for IDC (1/2010 to 4/2018). Patients with GI infection at time of onset were excluded. High-risk endoscopic features are ulcers deeper than 2mm, larger than 1cm, and extensive colonic involvement. Univariate and multivariate logistic regression were performed to assess the association of endoscopic and histological features with clinical outcomes.

Results

A total of 182 patients was included; most were white (92%), males (65%) with a mean age of 60 years. Median time from ICI initiation to IDC was 7 weeks. Fifty-three percent had grade 3–4 diarrhea, and 32% grade 3–4 colitis. One-hundred forty-one patients received immunosuppressant therapy, and 41 received symptomatic therapy only (Table 1). Forty-nine patients had mucosal ulcerations, 66 non-ulcerative inflammation and 67 normal endoscopy. Calprotectin was higher in patients with ulceration (P=0.04). The sensitivity of lactoferrin to detect histologic and endoscopic inflammation was 90% and 70% respectively. Patients who underwent endoscopy >30 days of symptom onset required longer duration of steroids (P=0.02), had more recurrent symptoms (P<0.01) and received later infliximab/vedolizumab add-on therapy than did those who underwent endoscopy ≤30 days (P=0.03; Table 2). High-risk features were associated with more frequent (P=0.03) and longer duration (P=0.02) hospitalization and infliximab/vedolizumab requirement (P<0.01; Table 3). Patients with active histological inflammation had more recurrence (P<0.01) and repeat endoscopy (P<0.01; Table 4). Repeat endoscopy was required in 47 patients. A multivariate logistic regression revealed that longer ICPI treatment was associated with more frequent hospitalizations (OR 1.00; 95%CI 1.00-1.01; P<0.01; Table 5) and high-risk endoscopic features were associated with the requirement of infliximab/vedolizumab (OR 3.89; 95%CI 1.68-9.01; P<0.01).

Conclusions

High risk endoscopic features and active histologic inflammation represent important markers of disease severity with clinical implications and should be used in a timely manner to devise IDC-focused treatment algorithms that incorporate a more intricate degree of specificity to improve upon the currently available guidelines.

Ethics Approval

This retrospective, single-center study was approved by the Institutional Review Board at The University of Texas MD Anderson Cancer Center (IRB No. PA18-0472).

Consent

This study was granted waiver for consent.

Table 1.

Table 1. Association between patient characteristics and treatment group

Characteristic	Immunosuppressant N = 141	No immunosuppressant N = 41	*P* value
Age in years, mean (SD)	60 (15)	58 (19)	0.371
Male sex, n (%)	94 (66.7)	25 (61.0)	0.576
White race, n (%)	135 (95.7)	32 (78.0)	0.001
Comorbidities present, n (%)	79 (56.0)	28 (68.3)	0.207
Smoking, n (%)	74 (52.5)	22 (53.7)	1.000
NSAID, n (%)	76 (53.9)	20 (48.8)	0.597
Malignancy type, n (%)			0.016
Melanoma	62 (44.0)	15 (36.6)	
Solid	74 (52.5)	19 (46.3)	
Hematological	5 (3.5)	7 (17.1)	
Cancer stage[a], n (%)			1.000
III	13 (9.6)	3 (8.8)	
IV	122 (90.4)	31 (91.2)	
Checkpoint inhibitor type, n (%)			0.051
CTLA-4	59 (41.8)	12 (29.3)	
PD-1/L-1	45 (31.9)	22 (53.7)	
Combination[b]	37 (26.2)	7 (17.1)	
Diarrhea grade			< 0.001
1	4 (2.8)	20 (48.8)	
2	43 (30.5)	17 (41.5)	
3-4	94 (66.7)	4 (9.8)	
Colitis grade			< 0.001
1	23 (16.3)	14 (34.1)	
2	59 (41.8)	27 (65.9)	
3-4	59 (41.8)	0 (0.0)	
Endoscopic evaluation			0.223
Flexible sigmoidoscopy	33 (23.4)	14 (34.1)	
Colonoscopy	108 (76.6)	27 (65.9)	
IBD like endoscopic pattern[c]			0.229
Crohn's colitis	32 (31.7)	7 (50.0)	
Ulcerative colitis	69 (68.3)	7 (50.0)	

Abbreviation: NSAID, non-steroidal antiinflammatory drugs; CTLA-4, cytotoxic T-lymphocyte antigen-4; PD-1/L-1, programmed cell death receptor-1 and ligand 1; SD, standard deviation.
[a] American Joint Committee on Cancer (AJCC) Cancer Staging System, 13 patients are missing
[b] Combination: ipilimumab + nivolumab
[c] Only 115 patients were included for the IBD like endoscopic pattern evaluation

Table 2.

Table 2. Clinical outcomes of patients according to the timing of endoscopy from IDC onset.

Characteristic	>30 days after diarrhea onset N = 40	≤30 days after diarrhea onset N = 142	P v
IV steroids, n (%)	23 (57.5)	60 (42.3)	0.
Duration of symptoms (days, SD)	54 (92)	26 (77)	0.
Duration of steroid (days, SD)	87 (120)	53 (41)	0.
Infliximab/vedolizumab, n (%)	8 (22.9)	34 (32.1)	0.
Duration from onset to first infliximab/vedolizumab dose (days, SD)	31 (23)	15 (14)	0.
Colonoscopy findings, n (%)			0.
Ulcer	9 (22.5)	40 (28.2)	
Non-ulcerative inflammation	11 (27.5)	55 (38.7)	
Normal	20 (50.0)	47 (33.1)	
High-risk endoscopic features, n (%)	14 (35.0)	57 (40.1)	0.
Active histological inflammation, n (%)	29 (72.5)	100 (70.4)	0.
Outcomes, n (%)			
Hospitalization	27 (67.5)	105 (73.9)	0.
Duration of hospitalization (days, SD)	9 (7)	7 (6)	0.
ICU admission	4 (10)	3 (2.1)	0.
Recurrence	20 (50.0)	31 (21.8)	0.

Abbreviation: ICU, intensive care unit; IV, intravenous; SD, standard deviation.

Table 3.

Table 3. Patients with endoscopic inflammation involvement

Characteristic	High-risk features N = 71	No high-risk features N = 111	P value
Duration of symptoms (days, SD)	41 (106)	27 (60)	0.301
IV steroids, n (%)	41 (66.1)	42 (58.3)	0.378
Infliximab/vedolizumab, n (%)	30 (46.2)	12 (15.8)	< 0.001
Mean duration from diagnosis to first recurrence (days, SD)	140 (147)	144 (121)	0.902
Outcomes, n (%)			
Hospitalization	58 (81.7)	74 (66.7)	0.028
Duration of hospitalization (days, SD)	9 (8)	6 (5)	0.016
ICU admission	3 (4.2)	4 (3.6)	0.656
Recurrence	20 (28.2)	31 (27.9)	1.000
Repeat endoscopy	18 (25.4)	18 (16.2)	0.181

[a]High-risk endoscopic features; deep ulcers >2 mm in depth, large ulcers > 1 cm, extensive i

Table 4.

Table 4. Association between histological active inflammation and clinical characteristics

Characteristic	Active inflammation N = 129	No-active inflammation N = 53	P value
Time from ICPI to onset (months, SD)	3 (4)	5 (9)	0.014
Duration of symptoms (days, SD)	39 (96)	17 (21)	0.102
Diarrhea grade, n (%)			0.001
1	9 (7.0)	15 (28.3)	
2	43 (33.3)	17 (32.1)	
3-4	77 (59.7)	21 (39.6)	
Colitis grade, n (%)			0.012
1	19 (14.7)	18 (34.0)	
2	63 (48.8)	23 (43.4)	
3-4	47 (36.4)	12 (22.6)	
IV steroids, n (%)	71 (54.0)	13 (24.5)	< 0.001
Duration of steroid (days, SD)	67 (77)	37 (34)	0.083
Infliximab/vedolizumab, n (%)	39 (33.6)	3 (12.0)	0.032
Colonoscopy findings, n (%)			< 0.001
Ulcer	49 (38.0)	0 (0.0)	
Non-ulcerative inflammation	51 (39.5)	15 (28.3)	
Normal	29 (22.5)	38 (71.7)	
High-risk endoscopic features, n (%)	63 (48.8)	8 (15.1)	< 0.001
Outcomes, n (%)			
Hospitalization	98 (76.0)	34 (64.2)	0.143
Duration of hospitalization (days, SD)	8 (6)	6 (8)	0.196
ICU admission	2 (1.6)	5 (9.4)	0.023
Recurrence	44 (34.1)	7 (13.2)	0.004
Repeat endoscopy	32 (24.8)	4 (7.5)	0.007

Abbreviation: ICPI, immune checkpoint inhibitor; ICU, intensive care unit; IV, intravenous; SD, standard deviation.

Table 5.

Table 5. Multivariate logistic regression analysis of infliximab/vedolizumab use and hospital admission

Characteristic	Infliximab/vedolizumab use		Hospital admission	
	OR (95% CI)	P value	OR (95% CI)	P value
Age	0.98 (0.95–1.01)	0.20	1.00 (0.98–1.02)	0.93
CTLA-4 based therapy	1.92 (0.68–5.37)	0.22	1.26 (0.58–2.74)	0.55
Duration of ICPI treatment	1.00 (0.99–1.01)	0.17	1.00 (1.00–1.01)	< 0.01
High-risk endoscopic features	3.93 (1.69–9.12)	< 0.01	1.74 (0.79–3.87)	0.17
Active histological inflammation	2.32 (0.60–8.99)	0.22	1.39 (0.64–3.02)	0.40

Abbreviation: ICPI, immune checkpoint inhibitor; CTLA-4, cytotoxic T-lymphocyte antigen-4; OR, odds ratio; CI, confidence interval.

P535

Upper gastrointestinal symptoms and associated endoscopic and histologic features in patients receiving immune checkpoint inhibitors

Hamzah Abu-Sbeih, MD[1], Tenglong Tang, MD[1], Wenyi Luo, MD[1], Wei Qiao, MD[1], David Richards, MD[1], Yinghong Wang, MD, PhD[1]

[1]*MD Anderson Cancer Center, Houston, TX, USA*

Background

Immune checkpoint inhibitors (ICPIs) have demonstrated high effectiveness in treating many

types of malignancies. Gastrointestinal (GI) immune-related adverse events (irAE) are commonly reported, however, limited literature describes upper gastrointestinal tract toxicity. Therefore, we aimed to describe clinical, endoscopic and histological characteristics of upper GI tract injury related to ICPI treatment.

Methods

We studied consecutive patients who received ICPIs between April 2011 and March 2018 and developed upper GI symptoms that required esophagogastroduodenoscopy (EGD). Patients with Helicobacter pylori gastritis were excluded from our study. We performed descriptive statistical analysis using means and standard deviations for continuous variables and frequencies and percentages for categorical variables.

Results

Sixty patients developed upper GI symptoms between ICPI initiation and 6 months after the last infusion (Table1); majority were of white race with a mean age of 59 years. In our cohort, 42 patients had other risk factors of gastritis such as chemotherapy, radiotherapy, and non-steroidal anti-inflammatory drugs (Table2). Patients without these risk factors had isolated gastric involvement on endoscopy. Overall, histologic inflammation of the stomach was evident in 83% of patients, and inflammation of the duodenum was evident only in 38% of patients. The rate of ulceration was the same in the cohorts with and without other risk factors for gastritis (11% vs. 12%). Among patients who had both upper and lower endoscopic evaluation (n=38), 17 (45%) had histological inflammation involving upper GI tract only; these patients developed GI toxicity later than patients with GI toxicity involving both upper and lower (P=0.060; Table3). Isolated upper GI tract involvement was more frequent in patients undergoing anti-PD-1/L1 treatment (P=0.071). Likewise, isolated upper GI toxicity was associated with more frequent mucosal ulceration (P=0.02; Table4). Patients with concurrent upper and lower GI tract involvement received immunosuppressive therapy more often than did patients with isolated upper GI tract involvement. Majority of the isolated upper GI symptoms were treated with proton pump inhibitors and H2 blockers, with less immunosuppressant use.

Conclusions

Overall ICPI-related upper GI-toxicities had gastric involvement more often than duodenal involvement on endoscopic and histological level, which is also observed more in patients treated with PD-1/L1. Mucosal ulcerations were more frequently found in isolated upper GI toxicity than concurrent upper and lower GI toxicities. Patients without other risk factors for gastritis had isolated gastric involvement on endoscopy, with duodenal inflammation in 39% of patients histologically. Concurrent GI tract involvement required immunosuppressive therapy more often than isolated upper GI tract involvement.

Ethics Approval

This retrospective, single-center study was approved by the Institutional Review Board at The University of Texas MD Anderson Cancer Center (IRB No. PA18-0472).

Consent

This study was granted waiver for consent.

Table 1.

Table 1. Patient baseline characteristics

Characteristic	No. (%) Gastritis patients N = 60
Mean age (years, SD)	59 (13)
Male sex	41 (68)
Race (white)	55 (92)
Underlying autoimmune disorder	5 (8)
Comorbidities	30 (50)
History of smoking	31 (52)
NSAID use	21 (35)
Prior PPI and H_2-blocker use	33 (55)
Concurrent chemotherapy	11 (18)
Concurrent core radiotherapy	7 (12)
Malignancy type	
Melanoma	25 (42)
Solid tumor	32 (53)
Hematologic	3 (5)
Cancer Stage[a]	
Stage III	1 (2)
Stage IV	57 (98)
ICPI therapy	
CTLA-4	20 (33)
PD-1/L1	29 (48)
Combination	11 (18)
Recurrence	9 (15)

Table 2.

Table 2. Comparison of EGD characteristics between patients who received ICPI and had other risk factors and those who received ICPI and had no other risk factors.

Characteristic	No. (%) ICPI without other risk factors N = 18	ICPI with other risk factors N = 42	p
EGD findings			0.022
Ulcer	2 (11)	5 (12)	
Non-ulcer inflammation	6 (33)	28 (67)	
Normal	10 (56)	9 (21)	
Distribution on EGD			0.023
Stomach	8 (44)	22 (52)	
Duodenum	0 (0)	3 (7)	
Both	0 (0)	8 (19)	
Gastric inflammation on histology			0.586
Active	4 (22)	13 (31)	
Chronic inactive	12 (67)	21 (50)	
Normal	2 (11)	8 (19)	
Duodenal inflammation on histology			0.617
Active	5 (28)	8 (19)	
Chronic inactive	2 (11)	8 (19)	
Normal	11 (61)	26 (62)	

Risk factors are NSAID, chemotherapy, radiotherapy

Table 3.

Table 3. Clinical characteristics according to the endoscopic involvement of GI tract (n = 38)

Characteristic	No. (%) Isolated upper GI tract N = 17	Concurrent (Upper and lower) N = 21	p
ICPI therapy			0.410
CTLA-4	7 (41)	9 (43)	
PD-1/L1	8 (47)	6 (29)	
Combination	2 (12)	6 (29)	
Mean duration of ICPI use, months (SD)	8 (9)	3 (6)	0.064
Mean time to onset, months (SD)	9 (9)	4 (5)	0.060
Number of ICPI doses at onset (SD)	6 (9)	7 (8)	0.484
Clinical presentation			
Nausea and vomiting	11 (65)	17 (81)	0.293
Abdominal pain	2 (12)	8 (38)	0.136
Dyspepsia	5 (29)	5 (24)	0.727
Diarrhea	12 (71)	20 (95)	0.071
GI bleeding and/or anemia	2 (12)	4 (19)	0.672
Treatment of GI injury			
Steroids	10 (59)	7 (33)	0.190
Mean duration of steroid (SD)	114 (92)	98 (85)	0.702
Infliximab/ vedolizumab	11 (65)	14 (67)	1.000
PPI	11 (65)	17 (81)	0.649
H_2-blocker	6 (35)	8 (38)	1.000
Hospitalization	7 (41)	10 (48)	0.752
Recurrence of upper GI symptoms	0 (0)	2 (10)	0.492

Table 4.

Table 4. Endoscopic characteristics of concurrent and isolated upper involvement

Characteristic	No. (%)	
	Isolated upper GI tract	Concurrent (Upper and lower)
	N = 17	N = 21
EGD findings		
Ulcer	1 (6)	0 (0)
Non-ulcer inflammation	6 (35)	16 (76)
Normal	10 (59)	5 (24)
Distribution on EGD		
Stomach	6 (35)	12 (57)
Duodenum	0 (0)	1 (45)
Both	1 (6)	3 (14)
Upper GI tract inflammation on histology		
Active	5 (29)	5 (24)
Chronic inactive	10 (59)	11 (52)
Normal	2 (12)	5 (24)

P536

The fate of immune–mediated diarrhea after the resumption of immune checkpoint inhibitor treatment

Hamzah Abu-Sbeih, MD[1], Faisal S. Ali[1], Jianjun Gao, MD, PhD[1], Yinghong Wang, MD, PhD[1]

[1]MD Anderson Cancer Center, Houston, TX, USA

Background

Immune–mediated diarrhea (IMD) is a leading cause for immune checkpoint inhibitor (ICPI) treatment discontinuation. Nonetheless, despite the occurrence of IMD initially, the remarkable efficacy of ICPIs encourages oncologists to resume ICPI treatment for cancer progression or as a maintenance. There is a paucity of evidence about the recurrence rate of IMD after ICPI resumption.[1] Hence, we assessed the risk and risk factors of IMD recurrence after ICPI resumption.

Methods

This is a cohort study of patients who had developed IMD and then resumed the same or different ICPI agent after improvement of IMD between 1/2010 and 4/2018. IMD was graded using CTCAE v4.03. A univariate followed by a multivariate logistic regression analyses were performed to assess the association of clinical covariates and IMD recurrence.

Results

Out of the 4864 patients who received ICPI treatment, 437 (8.9%) developed any grade IMD (Figure 1-2). Among them, 116 resumed ICPI treatment and were included in our analyses; 21 restarted anti-cytotoxic T-lymphocytes associated protein-4 (CTLA-4) and 95 anti-programmed death-1/ligand-1 (PD-1/L1). The median age was 60 years (Table 1). ICPI treatment discontinuation was due to IMD in 76 patients (66%). Seventy-nine patients (68%) required immunosuppressive therapy for the first event of IMD. The median duration from the last ICPI dose to the restart of ICPI treatment was 65 days (SD, 194). Overall, 37 (32%) patients experienced a recurrence of IMD (CTLA-4, 48%; PD-1/L1, 28%). Twenty-seven patients (73%) required immunosuppression for the recurrent IMD (Table 2); 15 of them discontinued ICPI treatment. The median duration from ICPI re-initiation to IMD recurrence was 63 days (range, 1–397). Severe IMD requiring immunosuppression initially was associated with higher grades (P<0.001) and more frequent immunosuppression requirement (P<0.001; Table 3) for the recurrent IMD. On multivariate logistic regression, patients who received anti-CTLA-4 based therapy initially had lower risk of IMD recurrence (odds ratio [OR], 0.20, 95% CI, 0.08-0.51; P=0.001; Table 4-5). The requirement for immunosuppression for IMD initially (OR, 3.04; 95% CI, 1.12-8.29; P=0.030) and the resumption of anti-CTLA-4 agents (OR, 3.89; 95% CI, 1.22-12.40; P=0.022) were associated with increased risk of IMD recurrence.

Conclusions

The resumption of anti-PD-1/L1 therapy has a lower IMD recurrence rate compared to anti-CTLA-4. Hence, ICPI therapy, especially anti-PD1-PD-L1, may be resumed in order to maximize the clinical benefit for patients who have limited alternative treatment

options. Severe IMD requiring immunosuppression initially was a risk factor for the recurrence of severe IMD after ICPI resumption.

References

1. Pollack, MH, et al., Safety of resuming anti-PD-1 in patients with immune-related adverse events (irAEs) during combined anti-CTLA-4 and anti-PD1 in metastatic melanoma. Ann Oncol, 2018. 29(1): 250-255.

Ethics Approval

This retrospective, single-center study was approved by the Institutional Review Board at The University of Texas MD Anderson Cancer Center (IRB No. PA18-0472).

Consent

This study was granted waiver for consent.

Table 1.

Table 1. General characteristics of the initial colitis event.

Characteristic	No. of patients (%)
Median age (years, SD)	60 (17)
Male sex	62 (53)
White race	107 (92)
Comorbidities present	65 (56)
Cancer type	
Melanoma	71 (61)
Solid	38 (33)
Hematological	7 (6)
Cancer stage	
III	13 (11)
IV	96 (83)
Median duration of ICPI (SD)	44 (88)
Median number of doses (SD)	3 (4)
Checkpoint inhibitor type	
CTLA-4	38 (33)
PD-1/L1	48 (41)
Combination	30 (26)
Reason to stop ICPI treatment	
Colitis	76 (66)
Disease progression	21 (18)
Non-GI irAEs	5 (4)
Complete remission	11 (10)
Still receiving at the end of study period	3 (3)
CTCAE grade of diarrhea	
1	32 (28)
2	35 (30)
3-4	49 (42)
CTCAE grade of colitis	
1	30 (26)
2	34 (29)
3-4	24 (21)
Median duration of symptoms (days, SD)	12 (51)
Treatment of colitis	
Symptomatic only	37 (32)
Steroids therapy only	58 (50)
Infliximab/vedolizumab	21 (18)
Other non-GI adverse events	45 (39)

Abbreviations: SD, standard deviation; ICPI, immune checkpoint inhibitor; CTLA-4, cytotoxic T-lymphocytes associated protein-4; PD-1/L-1, programmed death protein and ligand; CTCAE, Common Terminology Criteria for Adverse Events.

Table 2.

Table 2. Characteristics of the recurrent immune-mediated diarrhea based on the ICPI therapy resu

Characteristic	Resumed CTLA-4 N = 21	Resumed PD-1/L1 N = 95	*P* valu
Recurrence of symptoms	10 (48)	27 (28)	0.120
Time from ICPI resumption to recurrence (days, SD)	47 (58)	96 (95)	0.139
Treatment of recurrence			0.761
Symptomatic only	2 (20)	8 (30)	
Steroids therapy only	6 (60)	16 (59)	
Infliximab/vedolizumab add-on	2 (20)	3 (11)	
Diarrhea CTCAE grade of recurrence, n (%)			0.343
1	2 (20)	8 (30)	
2	7 (70)	19 (70)	
3-4	1 (10)	0 (0)	
Colitis CTCAE grade of recurrence, n (%)			1.000
1	7 (70)	17 (63)	
2	3 (30)	10 (37)	

Abbreviations: SD, standard deviation; ICPI, immune checkpoint inhibitor; CTLA-4, cytotoxic T-lymphocyte associated protein-4; PD-1/L-1, programmed death protein and ligand; CTCAE, Common Terminology Crite Adverse Events.

Table 3.

Table 3. Characteristics of the recurrent immune-mediated diarrhea for patients who needed immunosuppression for the initial immune-mediated diarrhea.

Characteristic	Immunosuppression N = 29	NO-immunosuppression N = 8	
Time from ICPI resumption to recurrence (days, SD)	85 (96)	77 (62)	
Treatment of recurrence			
Symptomatic only	2 (7)	8 (100)	
Steroids therapy only	22 (76)	0 (0)	
Infliximab/vedolizumab	5 (17)	0 (0)	
Diarrhea CTCAE grade of recurrence, n (%)			
1	2 (7)	8 (100)	
2	26 (90)	0 (0)	
3-4	1 (3)	0 (0)	

Abbreviations: SD, standard deviation; ICPI, immune checkpoint inhibitor; CTCAE, Common Terminology Cri for Adverse Events.

Table 4.

Table 4. Univariate logistic regression analysis of immune-mediated diarrhea recurrence.

Covariate	Odds ratio	95% confidence interval	*P*
Age	1.01	0.98-1.03	0.526
Cancer stage III	0.35	0.07-1.66	0.185
Duration of initial ICPI treatment	1.00	0.99-1.01	0.177
CTLA-4 based therapy initially	0.33	0.15-0.75	0.008
Resumption of CTLA-4 therapy	2.29	0.87-6.01	0.093
Time from ICPI stop to resumption	1.00	0.99-1.00	0.373
Required immunosuppression initially	2.10	0.85-5.21	0.108
CTCAE grade of diarrhea			
2	1.64	0.54-4.92	0.380
3-4	2.26	0.82-6.25	0.115
Required infliximab/vedolizumab	1.80	0.68-4.74	0.237
Duration of symptoms	1.00	0.99-1.01	0.389
Other irAEs	0.56	0.24-1.29	0.173

Abbreviations: ICPI, immune checkpoint inhibitor; CTLA-4, cytotoxic T-lymphocytes associated protein-4; CTCAE, Common Terminology Criteria for Adverse Events.

Table 5.

Table 5. Multivariate logistic regression analysis of immune-mediated diarrhea recurrence.

Covariate	Odds ratio	95% confidence interval	*P*
Initial ICPI type			
PD-1/L1		(reference)	
CTLA-4 based	0.20	0.08-0.51	0.001
ICPI type resumed			
PD-1/L1		(reference)	
CTLA-4	3.89	1.22-12.40	0.022
Required immunosuppression initially	3.04	1.12-8.29	0.030
Duration from last ICPI dose and resumption	1.00	0.99-1.00	0.240

Abbreviations: ICPI, immune checkpoint inhibitor; CTLA-4, cytotoxic T-lymphocytes associated protein-4; CTCAE, Common Terminology Criteria for Adverse Events.

Figure 1.

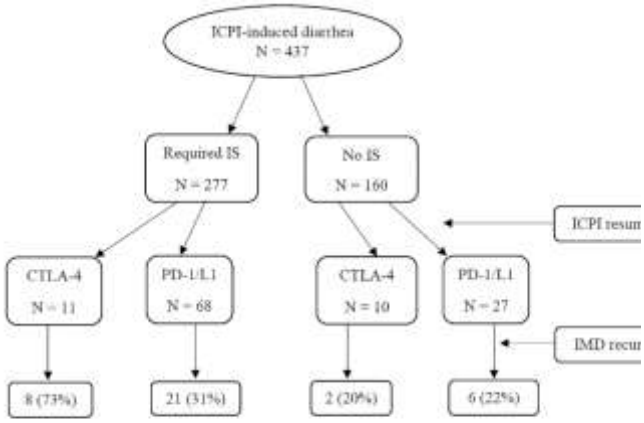

Figure 1. The recurrence rate of immune-mediated diarrhea (IMD) after ICPI resumption according to th immunosuppression (IS) requirement for the initial immune-mediated diarrhea.

Figure 2.

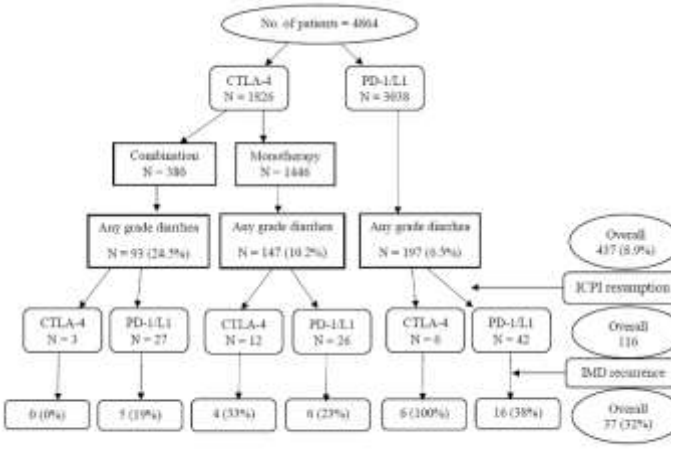

Figure 2. The recurrence of immune-mediated diarrhea after ICPI resumption by the type of ICPI.

P537

Immune checkpoint inhibitor–induced colitis as a predictor of survival in metastatic melanoma

Hamzah Abu-Sbeih, MD[1], Faisal S. Ali[1], Wei Qiao, PhD[1], Yang Lu, MD[1], Sapna Patel, MD[1], Adi Diab, MD[1], Yinghong Wang, MD, PhD[1]

[1]MD Anderson Cancer Center, Houston, TX, USA

Background

Gastrointestinal (GI) immune related adverse events (irAEs) commonly limit immune checkpoint inhibitors' (ICPIs) treatment, which is very effective for metastatic melanoma. The impact of GI-irAEs and their immunosuppressive therapy on patients' survival is not well studied. We aimed to assess the impact of GI-irAEs on overall survival (OS) and progression free survival (PFS) of patients with metastatic melanoma.

Methods

This is a retrospective study of patients with metastatic melanoma who received ICPI treatment and developed GI-irAEs from 1/2010 through 4/2018 with a mean follow-up duration of 1.7 years. A number of randomized patients who did not have GI-irAEs were included in our analysis. ICPI treatment response on CT and/or FDG PET/CT images was evaluated based on combined immune-modified Response Evaluation Criteria in Solid Tumors (RECIST) and immune-related RECIST 1.1. OS and PFS were defined as the time from ICPI initiation until death or last follow-up and until progression, death, or last staging, respectively. OS was redefined as the time from diarrhea onset to study the effect of immunosuppressive therapy. Kaplan-Meier curves were used to estimate unadjusted OS and PFS time distributions (Figure1-2). The Cox proportional hazards model was used to evaluate survival predictors. GI- and non–GI-irAE were included in the Cox model as time-dependent variables.

Results

A total of 243 patients were included in our analyses, majority were white (93%), males (64%) with a mean age of 58 years (Table 1). In our cohort, 173 patients (71%) had GI-irAEs; 124 (72%) received immunosuppression (Table 2). In multivariate Cox regression, ECOG 2-3 (HR 4.36, 95%CI 2.38-7.99; P<0.01), LDH ≥618 IU/L (HR 2.85, 95%CI 1.79-4.49; P<0.01), stage M1c (HR 4.66, 95%CI 1.69-12.78; P<0.01) were associated with worse OS rates (Table3). In contrast, longer duration of ICPI treatment (HR 0.86, 95%CI 0.81-0.92; P<0.01) and any grade GI-irAEs (HR 0.51, 95%CI 0.31-0.83; P<0.01) were associated with improved OS rates. Immunosuppressive treatment did not affect OS (HR 1.5, 95%CI 0.82-2.74; P=0.19). High-grade diarrhea was associated with improved OS (P=0.0492; Figure 3). Additionally, patients who developed GI-irAEs had longer PFS durations on multivariate Cox model (HR 0.44, 95%CI 0.29-0.64; P<0.01; Table 4).

Conclusions

GI-irAEs are associated with improved survival rates in patients with metastatic melanoma. Furthermore, higher grades of diarrhea are associated with improved patients' OS, which could explain the finding that immunosuppressive therapy did not adversely affect OS. Therefore, the onset of GI-irAEs should be conveyed to patients as a favorable sign rather than an alarming one.

Ethics Approval

This retrospective, single-center study was approved by the Institutional Review Board at The University of Texas MD Anderson Cancer Center (IRB No. PA18-0472).

Consent

This study was granted waiver for consent.

Table 1.

Table 1. Patient characteristics (n = 243).

Characteristic	No. of patients (%)
Mean age (standard deviation)	58.4 years (15.7 years)
Male sex	156 (64.2)
White race	226 (93.0)
Comorbidities present	107 (44.0)
Underlying autoimmune disorder	19 (7.8)
History of smoking	91 (37.4)
Eastern Cooperative Oncology Group performance status[a]	
0-1	218 (91.2)
2-3	21 (8.8)
Mean lactate dehydrogenase value (standard deviation)	629.6 IU/L (702 IU/L)
Lactate dehydrogenase[b]	
<618 IU/L	188 (79.0)
≥618 IU/L	50 (21.0)
Cancer stage	
III	36 (14.8)
IV	
M1a	18 (7.4)
M1b	49 (20.2)
M1c	140 (57.6)
Positive BRAF mutation	121 (49.8)
Positive lymph nodes	190 (78.2)
Mean duration of immune checkpoint inhibitor therapy (standard deviation)	3.5 months (5.1 months)
Checkpoint inhibitor type	
CTLA-4	137 (56.4)
PD/PD-L1	59 (24.3)
Combination	47 (19.3)

[a]Performance status was available in only 239 patients.
[b]Lactate dehydrogenase levels were available for only 238 patients.

Table 2.

Table 2. Adverse events observed in our cohort.

Adverse event	No. of patients (%
Total adverse events	190 (78.2)
Colitis/diarrhea[a]	173 (71.2)
Non-gastrointestinal	83 (34.2)
Mean time to diarrhea onset (standard deviation)	3.2 months (5.4 months)
Mean duration of diarrhea (standard deviation)	70 days (102 days)
Evidence of colitis among those with diarrhea (n = 173)	
Computed tomography imaging evaluation	48 (27.7)
Endoscopic/histologic evaluation	76 (43.9)
Diarrhea grade (n = 173)	
1	45 (26.0)
2	49 (28.3)
3-4	79 (45.7)
Colitis grade (n = 140)	
1	32 (22.9)
2	64 (45.7)
3-4	44 (31.4)
Treatment for colitis/diarrhea (n = 173)	
Immunosuppressive	124 (71.7)
Non-immunosuppressive	49 (28.3)
Mean duration of steroid treatment (standard deviation)	63.3 days (75.3 days)
Mean follow-up duration (standard deviation)	1.7 years (1.4 years)

[a]All of these patients had diarrhea and 140 also had colitis.

Table 3.

Table 3. Multivariable Cox regression analysis for overall survival.

Covariate	Hazard ratio	95% confidence interval	P
Age	1.01	0.99-1.02	0.49
Eastern Cooperative Oncology Group performance status 2-3	4.36	2.38-7.99	<0.01
Lactate dehydrogenase ≥ 618 IU/L	2.85	1.79-4.49	<0.01
M1c cancer stage	4.66	1.69-12.78	<0.01
Lymph node metastasis	1.53	0.79-2.96	0.21
Combination regimen	0.49	0.23-1.02	0.06
Any grade colitis/diarrhea	0.51	0.31-0.83	<0.01
Mean duration of immune checkpoint inhibitor therapy	0.86	0.81-0.92	<0.01

Table 4.

Table 4. Multivariable Cox regression analysis for progression free survival.

Covariate	Hazard ratio	95% confidence interval	P
Lactate dehydrogenase ≥ 618 IU/L	1.81	1.22-2.66	<0.01
Eastern Cooperative Oncology Group performance status 2-3	2.58	1.50-4.44	<0.01
M1c cancer stage	4.35	2.12-8.93	<0.01
Lymph node metastasis	1.67	1.03-2.69	0.03
Combination regimen	0.52	0.32-0.86	0.01
Mean duration of immune checkpoint inhibitor therapy	0.92	0.88-0.96	<0.01
Any grade colitis/diarrhea	0.44	0.29-0.64	<0.01

Figure 1.

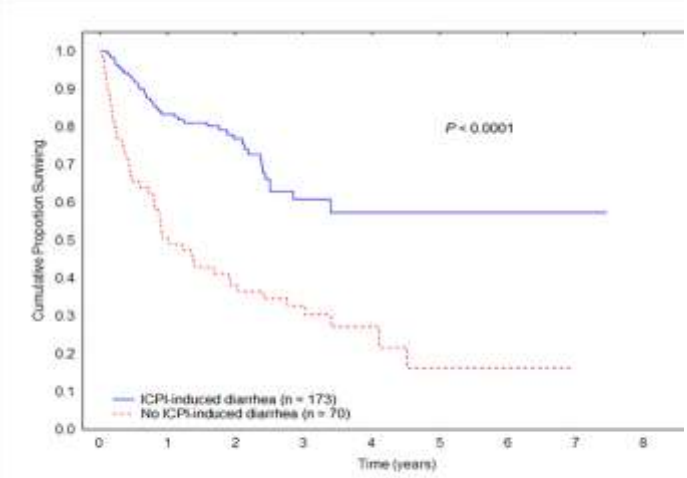

Figure 1. Kaplan-Meier overall survival curve stratified by immune checkp inhibitor (ICPI)-induced diarrhea/colitis status.

Figure 2.

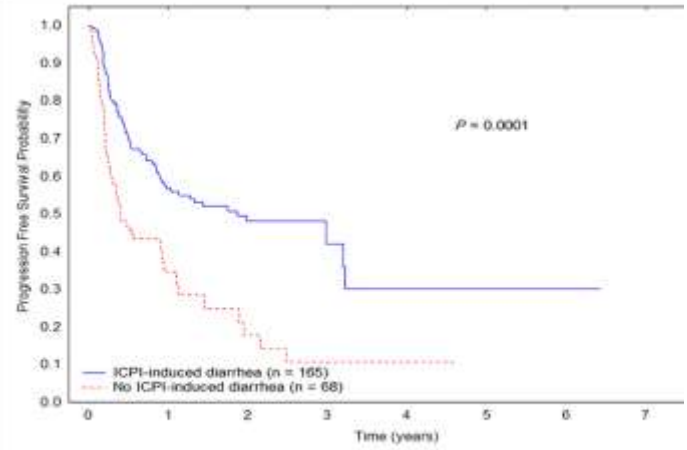

Figure 2. Kaplan-Meier progression-free survival curve stratified by immun checkpoint inhibitor (ICPI)-induced diarrhea/colitis status.

Figure 3.

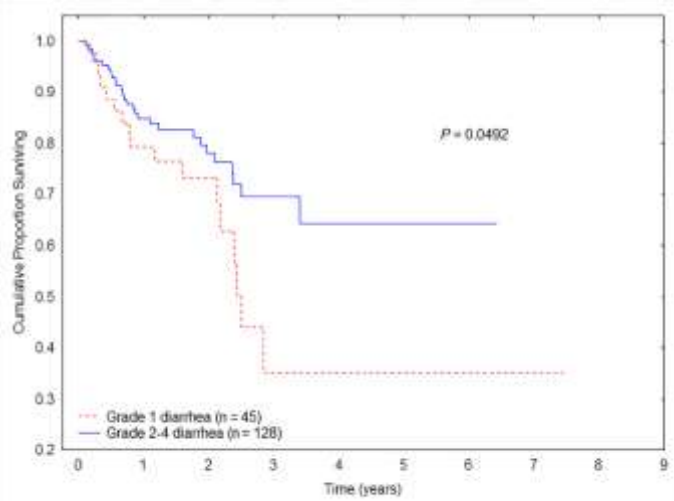

Figure 3. Kaplan-Meier overall survival curve stratified by diarrhea grade.

P538

Precision medicine in immune checkpoint inhibitor–induced diarrhea and colitis treatment: the advent of organ targeted vedolizumab therapy

Hamzah Abu-Sbeih, MD[1], Faisal S. Ali[1], Dana Alsaadi[2], Joseph Jennings, MD[2], Wenyi Luo, MD[1], Zimu Gong, MD[1], David Richards, MD[1], Aline Charabaty, MD[2], Yinghong Wang, MD, PhD[1]

[1]*MD Anderson Cancer Center, Houston, TX, USA*
[2]*Georgetown University, Washington, DC, USA*

Background

Immune checkpoint inhibitor (ICPI), which is an efficacious treatment for advanced malignancies, is commonly limited by immune mediated diarrhea and colitis (IMDC). Steroids and infliximab are often used to treat severe IMDC given its immune mediated mechanism. These agents induce systemic immunosuppression with its associated morbidity. Additionally, systemic immunosuppression might hamper the effect of ICPI. Hence, we aimed to assess clinical outcomes of vedolizumab (a gut-targeted

anti-integrin agent) as an alternative treatment for IMDC.

Methods

This is a retrospective multicenter case series of adult patients who had IMDC and received vedolizumab from 12/2016 through 4/2018 from MD Anderson Cancer Center and Medstar-Georgetown University. All patients had IMDC that is refractory to steroids and/or infliximab.

Results

Twenty-eight patients were included; 20 males (71%), 25 Caucasians (89%) with a mean age of 63 years (Table 1). The most common malignancy was melanoma in 7 patients (25%). Eight patients (29%) received anti-cytotoxic T-lymphocyte associated antigen-4 (CTLA-4), 12 (43%) programmed death protein-1 or its ligand (PD-1/L-1) and 8 (29%) combination therapy. Median time from ICPI to IMDC onset was 10 weeks (IQR 1-70). Fifteen patients (54%) had grade 2 and 13 (46%) had grade 3 or 4 IMDC. Diagnostic evaluations for IMDC are shown in (Table 2). The median reduction in fecal calprotectin values was 347 for vedolizumab initiation <14 days of IMDC onset and 197 for >14 days (Figure 1). Mucosal ulceration was present in 8 patients (29%), whereas non-ulcerative inflammation was present 13 (46%). All of our patients had features of active histological inflammation; 14 (50%) had concurrent features of chronicity, and 10 (36%) had features of microscopic colitis. The treatment and outcomes of IMDC are shown in (Table 3). Mean duration of steroid treatment was 96 days (SD 74). Seven patients received infliximab in addition to steroids and were refractory to it. Median number of vedolizumab infusions was 3 (IQR 1-4). Mean duration of follow-up was 15 months. Twenty four patients (86%) achieved and sustained clinical remission. Repeat endoscopic evaluation was performed in 17 patients. Endoscopic remission was attained in 7 (54%) of the 13 patients who had abnormal endoscopic findings initially with 5/17 (29%) patients reaching histological remission as well. (Table 4) lists the characteristics of patients who had clinical remission. In our cohort, 1 patient developed skin rash and 1 had joint pain.

Conclusions

Vedolizumab could be an appropriate treatment for steroid refractory IMDC, with favorable outcomes and good safety profile.

Ethics Approval

This retrospective, single-center study was approved by the Institutional Review Board at The University of Texas MD Anderson Cancer Center (IRB No. PA18-0472).

Consent

This study was granted waiver for consent.

Table 1.

Table 1. Patient clinical characteristics (n = 28).

Characteristic	No. of patients (%)
Mean age, years (SD)	63 (10)
Male sex	20 (71)
Cancer type	
Melanoma	7 (25)
Renal cell carcinoma	4 (14)
Prostate carcinoma	4 (14)
Urothelial	3 (11)
Other solid tumors	10 (36)
Cancer stage	
III	6 (21)
IV	22 (79)
ICPI type	
CTLA-4	8 (29)
PD-1/L1	12 (43)
Combination	8 (29)
Median no. of ICPI infusions (IQR)	3 (1-36)
Median time to diarrhea onset, weeks (IQR)	10 (1-70)
Peak grade of diarrhea	
2	15 (54)
3-4	13 (46)
Colitis symptoms	
Abdominal pain	14 (50)
Blood or mucous in stool	11 (39)

Abbreviations: SD, standard deviation; ICPI, immune checkpoint inhibitor; IQR, interquartile range.

Table 2.

Table 2. Patient diagnostic evaluation data (n = 28).

Characteristic	No. of patients (%
Endoscopy and histologic features	
Type of endoscopy	
Colonoscopy	22 (79)
Flexible sigmoidoscopy	6 (21)
Endoscopic findings on initial evaluation	
Ulceration	8 (29)
Nonulcerative inflammation	13 (46)
Normal	7 (25)
Endoscopic distribution	
Extensive	14 (50)
Left colon only	5 (18)
Isolated small bowel	2 (7)
Histological inflammation on initial evaluation	
Active features	28 (100)
Chronic features	14 (50)
Microscopic	10 (36)
Median no. of endoscopic procedures (IQR)	2 (1-7)
Diagnostic laboratory studies	
Mean duration of laboratory follow-up, months (SD)	3 (4)
Positive fecal lactoferrin at onset of diarrhea[a]	23 (100)
Positive fecal lactoferrin after vedolizumab therapy[b]	11 (79)
Mean fecal calprotectin value at onset of diarrhea µg/g (SD)[c]	329 (276)
Mean fecal calprotectin value at follow-up µg/g (SD)[d]	218 (262)

Abbreviations: IQR, interquartile range; SD, standard deviation.
[a]Lactoferrin was initially measured for 23 patients.
[b]Lactoferrin was measured at follow-up for 14 patients.
[c]Calprotectin was initially measured for 19 patients.
[d]Calprotectin was measured at follow-up for 13 patients.

Table 3.

Table 3. Treatment for colitis and outcomes (n = 28).

Characteristic	No. of patients (%)
Treatment	
Mean overall duration of steroid therapy, days (SD)	96 (74)
Diarrhea refractory to steroids	28 (100)
Infliximab therapy	9 (32)
Median no. of infliximab doses (IQR)	2 (1-3)
Recurrent symptoms while receiving infliximab	9 (100)
Median no. of vedolizumab doses (IQR)	3 (1-4)
Outcomes	
Mean duration of endoscopic follow-up, months (SD)	6 (4)
Clinical remission at last follow-up	24 (86)
Endoscopic remission at last follow-up[a]	7 (54)
Histologic remission at last follow-up[a]	5 (29)

Abbreviations: SD, standard deviation; IQR, interquartile range.
[a]Repeat endoscopic and histologic evaluations were performed in 17 patients. However, endoscopic remission was counted for only 13 patients who had abnormal endoscopic findings initially.

Table 4.

Table 4. Vedolizumab therapy outcomes and clinical characteristics (n = 28).

Characteristic	Clinical remission, no. (%)	Clinical failure, no. (%)
Total no. of patients	24	4
Checkpoint inhibitor type		
CTLA-4	6 (25)	2 (50)
PD-1/L1	11 (46)	1 (25)
Combination	7 (29)	1 (25)
Mean duration of steroid therapy, days(SD)	95 (79)	99 (52)
Mean time from symptom onset to vedolizumab/infliximab therapy, days (SD)	78 (86)	41 (40)
Median no. of vedolizumab doses (IQR)	3 (1-4)	3 (1-4)
Mean fecal calprotectin level at time of onset µg/g (SD)	299 (236)	586 (584)
Peak grade of diarrhea		
2	12 (50)	2 (50)
3-4	12 (50)	2 (50)
Initial endoscopic findings		
Ulceration	6 (25)	3 (75)
Nonulcerative inflammation	12 (50)	0 (0)
Normal	6 (25)	1 (25)
Initial histologic findings		
Active features	24 (100)	4 (100)
Chronic features	10 (42)	4 (100)
Microscopic	9 (38)	1 (25)
Mean overall duration of disease months (SD)	5 (3)	8 (5)
Mean fecal calprotectin level after vedolizumab therapy µg/g (SD)	187 (108)	270 (487)
Last repeat endoscopic findings[a]		
Ulceration	1 (8)	3 (75)
Nonulcerative inflammation	6 (46)	0 (0)
Normal	6 (46)	1 (25)
Active features on last repeat histologic analysis[a]	9 (69)	4 (100)

Abbreviations: SD, standard deviation; IQR, interquartile range.
[a]Repeat endoscopy and histologic analysis was performed in 13 patients with clinical remission.

Figure 1.

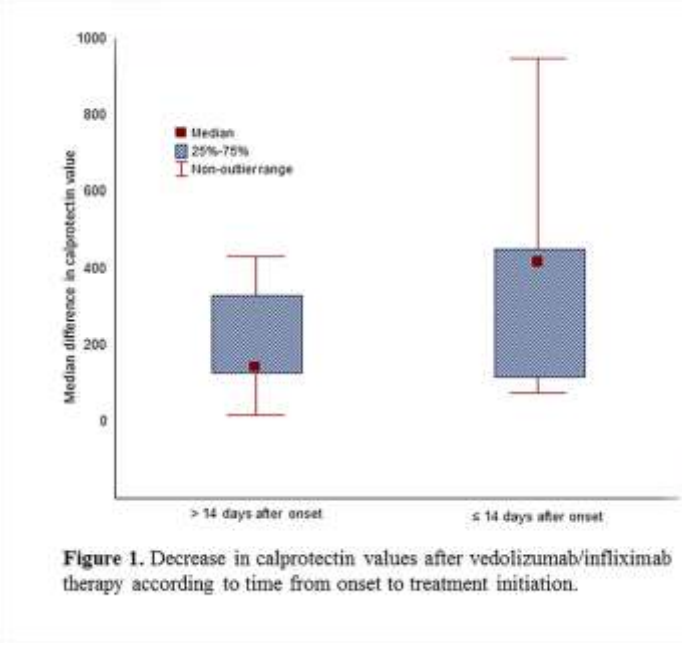

Figure 1. Decrease in calprotectin values after vedolizumab/infliximab therapy according to time from onset to treatment initiation.

P539

Development of cutaneous squamous cell carcinoma in patients receiving anti PD-1/PD-L1 therapy

Amanda Herrmann, MD, PhD[1], Priyadharsini Nagarajan, MD, PhD[1], Vivek Subbiah, MD[1], Kelly Nelson, MD[1], Alexander J. Lazar, MD, PhD[1], Courteny Hudgens, MS[1], Khalida Wani, PhD[1], Michael T. Tetzlaff, MD, PhD[1], Jennifer A. Wargo, MD, MMSc[1], Anisha B. Patel, MD[1]

[1]*UT MD Anderson Cancer Center, Houston, TX, USA*

Background

The utilization of immune checkpoint inhibitors (ICPI) has advanced in recent years. Antibodies targeting programmed cell death-1 (PD-1) and its ligand (PD-L1) are successfully used for treatment in a variety of cancers, including metastatic and inoperable cutaneous squamous cell carcinoma (cSCC). [1] Cutaneous adverse events are seen in approximately 40% of anti PD-1 treated melanoma patients [2], but few have described the development of new cSCC in the setting of anti PD-1 therapy [3].

Methods

We present a summary of 10 patients treated at MDACC with anti-PD-1/PD-L1 therapy for non-squamous cell cancers who developed cSCC. Seven patients presented to the dermatology clinic following development of skin lesions during the course of their anti-PD-1/PD-L1 therapy; three more were discovered with a limited retrospective chart review. Skin biopsies were interpreted from H&E stain as well as immunohistochemical antibody analysis for CD3, CD8, PD-1, and PD-L1.

Results

Two female and 8 male patients aged 51- 81 years, and developed biopsy-proven well-differentiated cSCC after a median of 4 months (range 3-16 months) following therapy initiation. Four patients developed multiple lesions over the course of several months, and in 70% of cases lesions developed during anti-PD-1/PD-L1 therapy. These lesions were treated conservatively with no complications or recurrence after 12 months follow up. Skin biopsies revealed well-differentiated cSCC, with full thickness keratinocyte atypia and at least superficial dermal invasion. Immunohistochemical analysis was performed using 8 biopsies from 4 patients. PD-L1 expression was present in 63% of samples [4]. The infiltrate was predominant and non-brisk at the periphery of the tumor with normal proportions of CD3:CD8 T lymphocytes. A median of 5% (range 1-13%) of the peripheral infiltrate had PD-1 expression.

Conclusions

There is a potential link between the development of cSCC lesions and anti-PD-1/PD-L1 therapy. While this link has yet to be solidified, we are actively investigating factors that may contribute to the development of these lesions in the setting of ICPI therapy, including whole exome sequencing,

RNAseq, and TCR sequencing. We plan to compare cSCC samples resulting from various etiologies, including BRAF inhibitor- induced cSCC and ultraviolet light-induced cSCC, to determine if there are unique characteristics in the cSCC from our ICPI-associated tumor cohort of patients. Preliminary data shows increased PD-L1 expression in the drug-induced tumors. [4] These results will be important to clinicians moving forward, as the use of this class of therapeutics rapidly increases, and may soon include the treatment of advanced cSCC.

References

1. Migden MR, Rischin D, Schmults CD, et al. PD-1 Blockade with Cemiplimab in advanced cutaneous squamous-cell carcinoma. N Engl J Med. 2018 Jul 26; 379(4):341-351.
2. Villadolid J, Amin A. Immune checkpoint inhibitors in clinical practice: update on management of immune-related toxicities. Transl Lung Cancer Res. 2015 Oct; 4(5):560-75.
3. Freites-martinez A, Kwong BY, Rieger KE, Coit DG, Colevas AD, Lacouture ME. Eruptive keratoacanthomas associated with pembrolizumab therapy. JAMA Dermatol. 2017; 153(7):694-697.
4. Gambichler T, Gnielka M, Rüddel I, Stockfleth E, Stücker M, Schmitz L. Expression of PD-L1 in keratoacanthoma and different stages of progression in cutaneous squamous cell carcinoma. Cancer Immunol Immunother. 2017; 66(9):1199-1204.

Ethics Approval

The study was approved by UT MD Anderson Cancer Center's Institutional Review Board, protocol number PA17-1060.

Consent

Not applicable. Waiver of consent obtained through the IRB for PA17-1060.

P540

Safety of cancer patients with preexisting autoimmune diseases presenting in the emergency center following immune checkpoint blockade

Mohsin Shah, MD[1], Mazen N. Jizzini, MD[1], Imad El. Majzoub, MD[1], Aiham Qdaisat, MD[1], Cielito C. Reyes, DrPH[1], Sai-Ching J. Yeung, MD, PhD[1]

[1]*The Univeristy of Texas MD Anderson Cancer Center, Houston, TX, USA*

Background

Immune checkpoint inhibitors (ICI) have dramatically increased the survival of cancer patients, but their use can be limited by the occurrence of immune related adverse events (irAE) that may be serious and infrequently life threatening. Cancer patients with preexisting autoimmune diseases (PAD) were excluded from clinical trials. The safety of ICI in these patients is currently unknown. [1] The aim of this study was to evaluate the safety of ICI in patients with PAD that presented to the Emergency Center (EC) at a comprehensive cancer center.

Methods

Cancer patients with PAD who received ICI and presented to the EC between March 1, 2011 and February 29, 2016 at MD Anderson Cancer Center. We extracted data on patient's characteristics (age, gender, preexisting autoimmune disease, treatment given for the underlying disease), type of checkpoint inhibitors used, reported irAE, how they were managed, whether immunotherapy was withheld or discontinued and their clinical outcome.

Results

Twenty two cancer patients with PAD were identified through institutional databases. Of these, 15 were males (68%). Mean age was 59.5 year (SD 11.6). Median Charlson Comorbidity Index was 9.5 (range 5-13). Most patients received anti PD-1 drugs (64%).

Melanoma was the most common cancer (45%). Most frequent PAD were autoimmune thyroiditis and eczema. Eleven patients were actively receiving treatment for PAD at initiation of ICI therapy, of which 3 received immunosuppressive therapy (steroids in 2, disease-modifying antirheumatic drug plus rituximab in 1). Eighty six percent of cases experienced de novo irAE or PAD exacerbation. Fourteen percent were severe (Grade ≥3). Of these, 6 were managed with corticosteroids. Resolution of de novo irAE or exacerbation of PAD was achieved in 10 cases without the need to withhold or discontinue immunotherapy. Median time to last follow up or death from first infusion was 16.8 months [range 2-80]. Death was reported in 17 cases due to cancer progression.

Conclusions

Despite frequent de novo irAE or exacerbation of PAD, most patients with PAD who visited the ED tolerated ICI therapy well. Prospective studies are needed to establish the risk-benefit profile of ICI therapy in patients with PAD including those who did not need to visit EDs.

References

1. June CH, Warshauer JT, Bluestone JA. Is autoimmunity the Achilles' heel of cancer immunotherapy? Nat Med. 2017; 23: 540-547.

Ethics Approval

The study was conducted under a clinical research protocol approved by the institutional review board of The University of Texas MD Anderson Cancer Center.

Mechanisms of Resistance to Immunotherapy

P541

The immunosuppressive tumor microenvironment (TME) in Epstein-Barr virus (EBV)-positive and EBV-negative gastric cancers: implications for immunotherapy

Sepideh Besharati, MD[1], Tracee McMiller, MS[1], Mark Yarchoan[1], Qingfeng Zhu, PhD[1], Elizabeth Engle, MSc[1], Janis Taube, MD, MSC[1], Alan Berger[1], Robert Anders, MD, PhD[1], Suzanne Topalian, MD[1]

[1]*Johns Hopkins University, Baltimore, MD, USA*

Background

Chemotherapy-refractory gastric carcinomas (GC) are aggressive malignancies, and only ~15% respond to drugs targeting the PD-1/PD-L1 pathway. EBV+ GCs (10% of GCs) often contain chromosomal amplifications for PD-L1 and PD-L2. They have been reported to contain robust CD8+ T cell infiltrates and an interferon-gamma (IFNg) gene signature, suggesting immune stimulation by strongly immunogenic EBV proteins. The current study aimed to characterize immune cell subsets and checkpoint expression in EBV+ GC compared to EBV(-) GC.

Methods

After screening >1000 cases, 25 invasive primary GC specimens AJCC stage 1A–4 (11 EBV+, 14 EBV-, confirmed with EBER ISH) were identified from treatment-naïve patients. Immunohistochemistry (IHC) was conducted for CD3, CD4, CD8, CD20, CD68, FoxP3, PD-1, PD-L1, LAG-3, GITR, IDO1, CSF1R and COX-2. Immune cell densities were quantified. RNA was isolated from macrodissected areas of dense CD3+ T cell infiltrates juxtaposed to PD-L1+ stromal cells, and gene expression profiling (GEP) was performed using multiplex qRT-PCR for a panel of 61 candidate immune-related genes.

Results

IHC revealed that 17/25 GCs contained PD-L1+

stromal cells (range 5-75% positive cells) with no significant difference between EBV+/- specimens; however, only 3/25 specimens contained PD-L1+ tumor cells (all EBV+). There was a higher proportion of CD8+ vs. CD4+ T cells in EBV+ tumors (p=0.051). IHC analysis of EBV+/- GCs did not show significant differences in the proportions of other immune cell subsets or expression of immune modulators. However, GEP revealed that EBV+ tumors had higher expression of IDO1 (11-fold, p=0.02). In contrast, EBV(-) tumors overexpressed CD163, CSF1R and IL10 associated with suppressive M2 macrophages (p<0.10). In addition, EBV(-) tumors overexpressed the cancer-promoting genes CXCR4 (p=0.09), IL32 (p=0.03), and IL1A (p=0.02). Notably, PTGS2 (COX-2) and IL1B, involved in prostaglandin production supporting cancer progression and metastasis, were the most highly overexpressed genes in EBV(-) tumors (270-fold, p<0.001; and 24-fold, p=0.06, respectively). IHC showed COX-2 overexpression by EBV(-) tumors (p=0.068), consistent with GEP. IHC also indicated expression of COX-2 by normal gastric epithelium.

Conclusions

Gastric cancers are characterized by an immunosuppressive TME regardless of EBV status, with abundant expression of PD-L1 and other immune checkpoints. GEP revealed that EBV(-) GCs, which are much more common than EBV+ GCs, overexpress molecules such as COX-2, IL-1A, IL-1B, IL-10 and CSF1R. Our findings provide novel insights into the immune microenvironment of EBV+ and EBV(-) GC, and offer potential targets to overcome resistance to anti-PD-1/PD-L1 therapies in this disease.

Acknowledgements

Funded by the Bristol-Myers Squibb International Immuno-Oncology Network and NCI R01 CA142779.

P542

Exposure to anti-PD-1 causes Functional Differences in Tumor-Infiltrating Lymphocytes in Solid Tumors

Caitlin Creasy, MS[1], Cara Haymaker, PhD[2], Marie-Andrée Forget, PhD[2], Gopal Singh, PhD[2], Coya Tapia, MD, PhD[2], Chantale Bernatchez[2], Jeane Painter, PhD[2], Funda Meric-Bernstam, MD[2], Caitlin Creasy, MS[1]

[1]MD Anderson Cancer Center- UTHealth Graduate School of Biomedical Sciences, Houston, TX, USA
[2]UT MD Anderson Cancer Center, Houston, TX, USA

Background

The pervasive use of therapeutic antibodies targeting PD-1 puts it on target to become the standard of care for solid tumor malignancies. However, little is known as to how blockade of PD-1 may alter the function or phenotype of tumor-infiltrating lymphocytes (TIL). By investigating samples from pre-treatment and early on-treatment biopsies from patients with varying types of solid tumors treated with anti-PD1, we hope to elucidate drug-induced changes in TIL phenotype and function.

Methods

An ongoing Phase II clinical trial of anti-PD-1 in cohorts of patients with rare solid tumor types (NCT02721732) yielded mandatory core biopsies taken at baseline and day 15-21 after the first cycle of anti-PD-1 (Pembrolizumab, 200 mg). Upon receipt, half of the biopsy was mechanically disaggregated for TIL phenotyping, which we term “fresh” flow cytometry staining. The other half of the biopsy was used to propagate TIL ex vivo using the TIL 3.0 method, which includes IL-2, agonistic anti-4-1BB antibody (Urelumab, BMS), and anti-CD3 (clone OKT3). TIL phenotype and function were evaluated after 2 or 3 weeks of culture. Functionality was determined through sorting T cell subsets and

measuring cytokine and chemokine secretion following anti-CD3 re-stimulation using MSD and Luminex platforms.

Results
Phenotypic analysis of the freshly stained and expanded TIL demonstrated an effector memory differentiation status before and after exposure to anti-PD-1. These TIL did not differ in their expansion of the CD4+ or CD8+ subsets. This is expected within the expanded TIL, given the predisposition to expand CD8+ TIL with the addition of anti-4-1BB. Further, expanded TIL retained cytotoxic potential (perforin/granzyme B) after one dose of anti-PD-1. However, PD-1 expression on expanded CD8+ tended to be elevated after therapy ($p=0.09$). Further, TIL expanded after anti-PD-1 showed enriched CTLA-4 expression in CD4+ TIL ($p=0.003$). Functional analysis of 16 paired baseline and on-treatment expanded TIL show that CD4+ TIL with higher IL-4 secretion are accompanied by inhibited cellular growth ($p<0.05$). CD8+ TIL demonstrated an inverse relationship with growth and higher expression of PD-1, CTLA-4, and cytotoxic molecules, perforin/granzyme B ($p<0.05$). Further analysis in 12 of the 16 paired expanded CD8+ TIL samples for 65 soluble factors demonstrated an aberrant secretion profile post anti-PD1 treatment suggesting impaired function.

Conclusions
Our study assesses the ramifications of one dose of anti-PD-1 on TIL in rare solid tumors. We demonstrate that although phenotypically similar after undergoing checkpoint blockade, TIL tend to have a poorer functionality after anti-PD-1.

Ethics Approval
The study was approved by UT MD Anderson Cancer Center's IRB, approval number 2015-0948.

Consent
Written informed consent was obtained from the patient for publication of this abstract and accompanying images. A copy of the written consent is available for review by the Editor of this journal.

P543

Neoantigen heterogeneity as contributing factor for non-responders to neoantigen specific T-cell therapy in patients with metastatic gastrointestinal malignancies

Eric Groh, MD[1], Jared Gartner, MS[1], Todd Prickett, PhD[1], Yong Li, MS[1], Steven Rosenberg, MD, PhD[1], Paul Robbins, PhD[1]

[1]*NCI, Bethesda, MD, USA*

Background
In an initial pilot study, tumor infiltrating lymphocytes (TIL) that recognize neoepitopes were identified in 9 of 10 patients with metastatic gastrointestinal (GI) malignancies. These findings suggest that adoptive transfer of autologous neoepitope-reactive T cells may represent an attractive treatment strategy for patients with metastatic GI malignancies; however, objective response rates for this treatment strategy remain low. Factors that may influence therapies that target one or a relatively small number of mutations include intra- and inter-tumor mutational heterogeneity, which are evaluated in this study.

Methods
Whole exome sequencing (WES) was carried out on resected flash-frozen metastatic tumor samples and matched normal cellular DNA to identify somatically mutated gene products, and TIL cultures initiated from adjacent tumor regions. Co-culture of antigen presenting cells expressing individual tumor mutations and TIL allowed identification of neoepitope-reactive TIL which were then used for

adoptive cell therapy. Additionally, FFPE tumor samples were obtained for each patient from which WES was performed to characterize tumor mutations.

Results

WES data was analyzed from 39 unique tumors from 12 patients with metastatic GI malignancy treated with neoepitope-reactive TIL. A mean of 3 tumors per patient were analyzed (range 2-6 tumors), and the mean number of mutations per sample was 101 (range 22-156 mutations). Inter-tumor heterogeneity was present in all 12 patients (Figure 1). The percent of mutations ubiquitously expressed in all samples from an individual patient ranged from 12.9% (Patient 4071) to 67.9% (Patient 3737). Mutation reactive TIL therapy resulted in an objective response in 2 of the 12 patients. The single neoantigen targeted by TIL administered to the 2 patients with objective responses was present in all additional FFPE samples studied. In contrast, for 7 of the 10 non-responders, targeted mutations that could not be detected 1 or more of the analyzed FFPE samples were identified (Table 1). These findings raised the concern that the lack of response seen in some patients receiving adoptive TIL transfer could be due to the absence of the targeted mutations in individual tumor lesions.

Conclusions

Inter-tumor heterogeneity of targeted mutations is presents in non-responders to neoepitope-reactive TIL therapy. This suggested one mechanism limiting the effectiveness of TIL therapy targeting a limited number of mutations. WES of primary and metastatic tumors from primary and metastatic tumors from individual patients may facilitate identification of ubiquitously expressed tumor mutations that, if successfully targeted by adoptively transferred TIL, may lead to improved object response rates.

Figure 1.

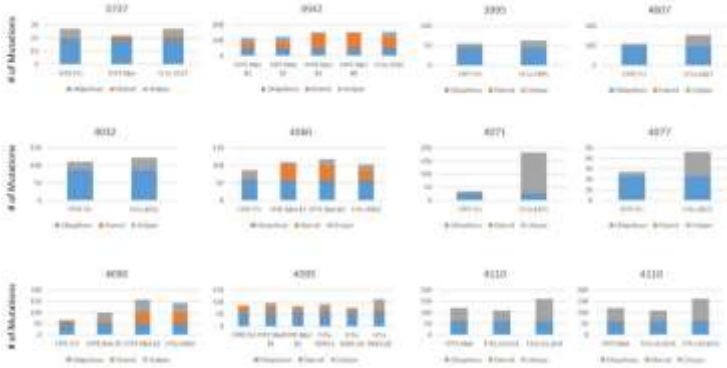

Table 1.

Patient	Targeted Antigen(s)	Response	FFPE Primary Tumor	FFPE Met #1	FFPE Met #2	FFPE Met #3	FFPE Met #4
3737	ERBB2IP	OR	Yes	Yes	-	-	-
3942	NUP98, KARS, GPD2, CHD6	NR	-	No	No	Yes	Yes
3995	KRAS, TUBGCP2, RNF213	NR	Yes	-	-	-	-
4007	SRIV2L, H3F3B	NR	Yes	-	-	-	-
4032	API5, RNF10, PHLPP1	NR	Only API5 and PHLPP1	-	-	-	-
4060	SMC1A	NR	Yes	Yes	Yes	-	-
4071	QSOX2, CRLS1, HIVEP2, PDE9A, MRPS28, POR	NR	Only MRPS28 and POR	-	-	-	-
4077	CPSF6, HIST1H2BE, FLII, DENND2D, KDM6A	NR	Only FLII	-	-	-	-
4090	USP8, RPS15, MRPL39	NR	Only USP8 and PRS15	Only USP8	Yes	-	-
4095	KRAS	OR	Yes	Yes	Yes	-	-
4110	TES, HYDIN-2, CTU2, ACLY	NR	-	No	-	-	-
4141	MPI, HK1	NR	No	No	Only HK1	-	-

NR, no objective response to TIL therapy; OR, objective response to TIL therapy
Yes denotes that all targeted antigen(s) were identified in the FFPE sample; No denotes that none of the targeted antigen(s) were identified in the FFPE sample; (-) denotes that sample was not available for sequencing

P544

Interferon-γ regulates the expression of PD-L1 and NKG2D ligand families in nasopharyngeal carcinoma

Lingling Guo[1], Yu Chen, MD, PhD[2], Chuaben Chen[2]

[1]*Fujian medical university affiliated cancer hospital, Fuzhou, Peoples Republic of China*
[2]*Fujian Province Cancer Hospital, Fuzhou, Peoples Republic of China*

Background

Nasopharyngeal carcinoma (NPC) is an Epstein-Barr virus-related malignancy that is characterized by a large number of infiltrating lymphocytes in the tumor microenvironment. The CD8+ T-lymphocytes

can release interferon γ (IFN-γ), a cytokine proven to be a strong stimulant of programmed death-ligand 1(PD-L1). Hence the high expression of PD-L1 is another characteristic of NPC. It is reported that PD-1/PD-L1 inhibitors have good therapeutic effects on solid tumors with high PD-L1 expression and extensive CD8+ T-lymphocyte infiltration. However, current clinical trials only show a limited effect of PD-1 inhibitors on recurrent or metastatic NPC. To find the mechanism of resistance to PD-1/PD-L1 inhibitors in NPC, we studied the co-expression status of the NKG2D ligand family, a group of activating molecules expressing on the surface of activated CD8+ T-lymphocytes, when IFN-γ is up-regulating the expression of PD-L1 in NPC.

Methods

We downloaded the RNA-Seq data of IFN-γ, PD-L1, MICA and ULBP2-4 in head and neck squamous cancer (HNSC, except NPC) and NPC respectively from the TCGA and the GEO databases, screened for the most related molecules to IFN-γ. We also administrated exogenous IFN-γ to three types of NPC cell lines, CNE-1, CNE-2 and 5-8F, and did qPCR, flow cytometry (FC), Western-blot (WB) and RNA-Seq after 0, 4, 12, and 24 hours, to determine the expression level of above molecules at each time point.

Results

In 501 HNSC cases from the TCGA database, the expression of PD-L1 is significantly related to IFN-γ ($R=0.65$, $P<0.001$) while the correlation between MICA and IFN-γ is very weak ($R=0.12$, $P=0.004$). Among the ULBPs, ULBP3 has the most significant correlation with IFN-γ ($R=-0.18$, $P<0.001$). The 113 NPC cases from the GEO database show the similar results. All the cell experiments proved the positive correlation between PD-L1 and IFN-γ and the negative correlation between MICA and IFN-γ ($P<0.05$). All the ULBPs had a significant negative correlation with IFN-γ in WB and FC, whereas ULBP3 showed a best correlation in RNA-Seq and qPCR($P<0.05$).

Conclusions

We confirmed that IFN-γ can up-regulate the expression of PD-L1 and change the expression of NKG2D ligands. ULPB3 has a most significant and time-dependent negative correlation with both IFN-γ. Therefore, we hypothesize the down-regulation of ULBP3 mediated by IFN-γ may be a unique mechanism of immune escape and primary resistance in NPC patients. Further studies are needed to explore the deeper molecular mechanism.

Figure 1.

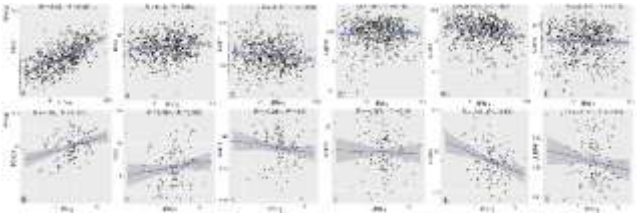

Figure 2.

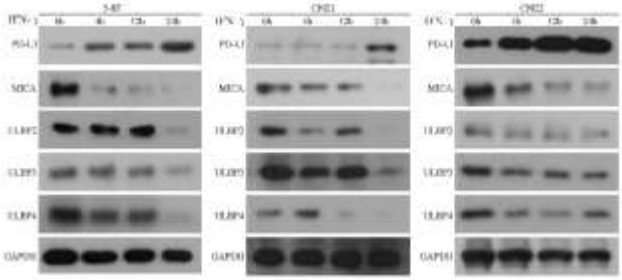

Figure 3.

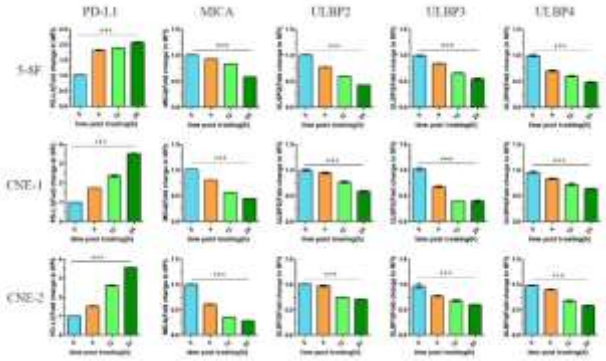

Figure 4.

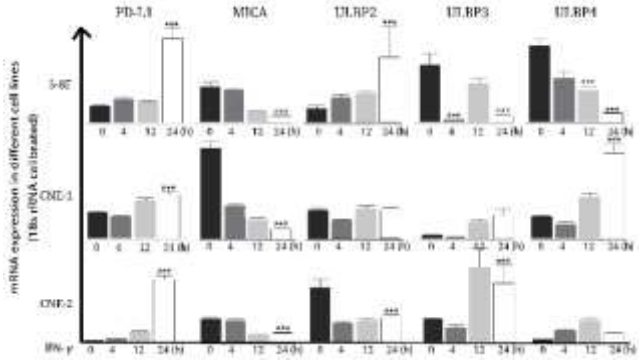

P545

The tumor inflammasome functions as a rheostat for regulating the efficacy of anti-PD-1 antibody immunotherapy by driving the recruitment of myeloid-derived suppressor cells

Brent Hanks, MD, PhD[3], Bala Thievanthiran, PhD[1], Kathy Evans, BS[1], Nicholas DeVito, MD[1], Christine Xiao, BS[1], Yubin Kang, MD[1], David Hsu, MD, PhD[1], Alisha Holtzhausen, PhD[2]

[1]*Duke University, Durham, NC, USA*
[2]*University of North Carolina, Chapel Hill, NC*
[3]*Duke University Medical Center, Durham, NC, USA*

Background
Despite the impact of anti-PD-1 antibody immunotherapy in oncology, many cancer patients do not benefit from this treatment modality. Mechanisms of resistance to checkpoint inhibitor immunotherapy in cancer remain poorly understood.

Methods
Various pre-clinical syngeneic and transgenic cancer models as well as an autologous humanized mouse model were utilized to investigate the genetic and cellular alterations of tumors escaping anti-PD-1 antibody immunotherapy based on immunohistochemistry, flow cytometry, RNAseq transcriptomic sequencing, and tandem mass spectrometry.

Results
Our studies have demonstrated that anti-PD-1 antibody immunotherapy promotes the recruitment of granulocytic myeloid-derived suppressor cells (Gr-MDSCs) to the tumor bed in a CXCR2-dependent manner. This process involves the upregulation of the CXCR2 chemokine ligand, CXCL5, which is induced by a Wnt5a-YAP non-canonical autocrine signaling pathway that, in turn, is stimulated by a HSP70-TLR4 signaling axis. Further investigation has demonstrated that this cascade of events is initiated by CD8+ T cell-dependent stimulation of the NLRP3 inflammasome in tumor cells which drives the release of HSP70 and serves to dampen the efficacy of anti-PD-1 antibody immunotherapy. This phenomenon has been observed in pre-clinical models of non-small cell lung cancer, melanoma, and pancreatic cancer, as well as an autologous humanized mouse model of renal cell carcinoma in response to anti-PD-1 antibody therapy but not anti-CTLA-4 antibody therapy or chemotherapy. Additional studies have revealed that this pathway also drives the accumulation of Gr-MDSCs in distant tissues such as the lung in a manner that is dependent upon the presence of the primary tumor. Genetic silencing of CXCL5 and pharmacological

blockade of Wnt ligand signaling suppresses Gr-MDSC recruitment in response to anti-PD-1 antibody therapy and enhances the efficacy of checkpoint inhibitor therapy. CXCR2 and CXCR2 ligand expression correlates with Wnt5a and with cytolytic T cell markers in human melanoma tissues indicating that this pathway is clinically relevant. We have determined that levels of CXCL5 and other CXCR2 ligands are increased in the plasma of transgenic tumor models escaping anti-PD-1 antibody therapy. Clinical studies are ongoing to investigate relationships between anti-PD-1 antibody response and the plasma levels of CXCR2-dependent chemokines as well as genetic inflammasome polymorphisms in advanced melanoma patients undergoing checkpoint inhibitor therapy.

Conclusions

By promoting the recruitment and accumulation of Gr-MDSCs, the tumor inflammasome functions as a rheostat that modulates the T cell response generated by anti-PD-1 antibody therapy. The elucidation of this pathway provides novel therapeutic opportunities to expand on the efficacy of checkpoint inhibitor immunotherapy for cancer patients.

Ethics Approval

This study was approved by the Institutional Animal Care and Use Committee at Duke University, registry number A249-12-09.

P546 Abstract Travel Award Recipient

Targeted hypoxia reduction restores T cell infiltration and sensitivity to immunotherapy in prostate cancer

Priyamvada Jayaprakash, PhD[1], Midan Ai, PhD[1], Arthur Liu[1], Pratha Budhani, BS, MS[1], Todd Bartkowiak[1], Jie Sheng[1], Casey Ager, BS[1], Courtney Nicholas, PhD[1], Ashvin Jaiswal[1], Yanqiu Sun[1], Krishna Shah[1], Sadhana Balasubramanyam[1], Nan Li[1], Guocan Wang, PhD[1], Jing Ning[1], Anna Zal[1], Tomasz Zal, PhD[1], Michael Curran, PhD[1]

[1]*The University of Texas MD Anderson Cancer Center, Houston, TX, USA*

Background

Checkpoint blockade using anti CTLA-4 and anti PD-1 is effective in “hot” tumors like melanoma with pre-existing immune infiltrates (1); however, “cold” tumors like prostate cancer respond poorly. Within these tumors we find prevalent zones of hypoxia from which T cells are excluded. Hypoxia impedes T cell mediated antitumor immunity by creating a hostile microenvironment through acidification of the extracellular milieu, formation of abnormal vasculature lacking in adhesion receptors needed for T cell extravasation, and recruitment of immunosuppressive stromal populations such as myeloid derived suppressor cells (MDSC) and myofibroblasts (2-5) . We hypothesized that removing these hypoxic zones would restore T cell infiltration and effector function thus sensitizing prostate tumors to checkpoint blockade.

Methods

We utilized the hypoxia-activated prodrug, TH-302 (Evofosfamide) to ablate hypoxic zones of tumors and tested its efficacy alone and in combination with immune checkpoint blockade in reducing tumor burden and enhancing anti-tumor immunity using both transplantable and spontaneous models of prostate cancer. We investigated how this therapy impacted recruitment and function of tumor-infiltrating CD8+ T cells and immune suppressive MDSC.

Results

We found that TH-302 improved survival of prostate tumor bearing mice (OS 30%) and synergized with checkpoint blockade using αCTLA-4 and αPD-1 in curing 82% of mice compared to checkpoint

blockade alone (OS 55%). This was concomitant with enhanced T cell and decreased MDSC infiltration into tumors. T cells infiltrating tumors treated with the combination of TH-302 and αCTLA-4/αPD-1 had higher proliferative capacity, improved effector cytokine production and greater mitochondrial biomass. In addition, MDSC from these tumors displayed reduced suppressive activity. Combination treatment caused a persistent defect in the ability of tumors to replenish their myeloid stroma. In addition, spontaneous prostate cancer in TRAMP transgenic mice, which is entirely checkpoint blockade resistant, responded dramatically to combination CTLA-4/PD-1 blockade when co-administered with the hypoxia-reducing agent TH-302.

Conclusions

We have shown that hypoxia reduction can sensitize otherwise resistant prostate tumors to immunotherapy. Hypoxic ablation is associated with the conversion of the immunosuppressive tumor microenvironment (TME) into an immune permissive one through improved survival, function and metabolic fitness of T cells and reduced infiltration and function of immunosuppressive MDSC. Our findings suggest that metabolic manipulation of the TME is a viable approach to enhance immunotherapy responses.

References

1. Curran MA, Montalvo W, Yagita H, and Allison JP. PD-1 and CTLA-4 combination blockade expands infiltrating T cells and reduces regulatory T and myeloid cells within B16 melanoma tumors. Proc Natl Acad Sci U S A. 2010;107(9):4275-80. 2. Corzo CA, Condamine T, Lu L, Cotter MJ, Youn JI, Cheng P, Cho HI, Celis E, Quiceno DG, Padhya T, et al. HIF-1alpha regulates function and differentiation of myeloid-derived suppressor cells in the tumor microenvironment. J Exp Med. 2010;207(11):2439-53. 3. Dang EV, Barbi J, Yang HY, Jinasena D, Yu H, Zheng Y, Bordman Z, Fu J, Kim Y, Yen HR, et al. Control of T(H)17/T(reg) balance by hypoxia-inducible factor 1. Cell. 2011;146(5):772-84. 4. Ben-Shoshan J, Maysel-Auslender S, Mor A, Keren G, and George J. Hypoxia controls CD4+CD25+ regulatory T-cell homeostasis via hypoxia-inducible factor-1alpha. Eur J Immunol. 2008;38(9):2412-8. 5. Becker JC, Andersen MH, Schrama D, and Thor Straten P. Immune-suppressive properties of the tumor microenvironment. Cancer immunology, immunotherapy : CII. 2013;62(7):1137-48.

P547 Abstract Travel Award Recipient

Adoptive cell therapy and intratumoral nanoplexed poly I:C as an effective immunotherapy in interferon-signaling deficient melanoma

Anusha Kalbasi, MD[2], Kevin Hakimi, BS[1], Sarah Kremer[1], Christine Nguyen, BS[1], Davis Torrejon, MD[1], Giulia Parisi[1], Pedro Lopez-Casas, PhD[3], Marisol Quintero, PhD, MBA[3], Antoni Ribas, MD, PhD[4]

[1]*University of California Los Angeles, Los Angeles, CA, USA*
[2]*UCLA, Los Angeles, CA, USA*
[3]*Bioncotech, Madrid, Spain*
[4]*University of California, Los Angeles, Los Angeles, CA*

Background

We examined the impact of defects in type I and/or II interferon signaling on the efficacy of adoptive cell therapy (ACT) with tumor-specific T cells in B16 murine melanoma.

Methods

Using CRISPR, we generated B16 tumor cell lines deficient in type I (Ifnar1-KO) or type II (Jak2-KO) interferon signaling, or both (Jak1-KO). ACT was performed using gp100-specific pmel T cells. Tumor cell were labeled with RFP to determine tumor-specific MHC-I expression in vivo. We also tested a nanoplexed formulation of poly I:C (BO-112) that

activates TLR3/MDA5/RIG-I.

Results

Pmel ACT was effective against B16 tumors lacking type I (Ifnar1-KO) or type II (Jak2-KO) interferon signaling, but ineffective against tumors lacking both (Jak1-KO) (Figure 1). We observed a similar phenomenon in vitro, where growth of B16 tumor cells lacking type I or II interferon signaling (but not both) were inhibited by tumor-specific pmel T cells compared to non-specific T cells, provided the alternate interferon pathway was activated ($p < 0.0001$). We then examined interferon-dependence of MHC-I expression in vivo. We observed that basal MHC-I expression by B16 in vivo is dependent on type II, but not type I, interferon signaling. After pmel ACT, tumors lacking type II interferon (Jak2-KO) signaling were able to augment MHC-I expression compared to B2m-KO tumors ($p = 0.068$). Jak1-KO tumors did not express MHC-I even after pmel ACT ($p = 0.5283$). To overcome resistance of B16 Jak1-KO tumor cells to pmel ACT, we tested intratumoral delivery of BO-112, which has direct anti-tumor efficacy against B16 and augments anti-tumor efficacy of pmel ACT against B16. Notably, the direct anti-tumor effects of BO-112 are abrogated in the B16 Jak1-KO compared to wildtype B16 tumors both in vitro and in-vivo. Regardless, in combination with BO-112, pmel ACT was effective against B16 Jak1-KO tumors compared to non-specific T cells in combination with BO-112 (Figure 2). RNA sequencing of tumors 5 days after ACT revealed 209 genes enriched (fold change > 2, adjusted p-value < 0.05) in tumors treated with pmel ACT and BO-112, which were not enriched in tumors treated with pmel ACT and vehicle or non-specific ACT and BO-112, including genes involved in T cell recruitment, antigen presentation, direct T cell cytotoxicity, and interferon signaling.

Conclusions

Our findings suggest ACT can be an effective immunotherapy in tumors lacking type I or II interferon signaling. For tumors lacking both type I and II interferon signaling, intratumoral BO-112 can resensitize tumors to ACT.

Figure 1.

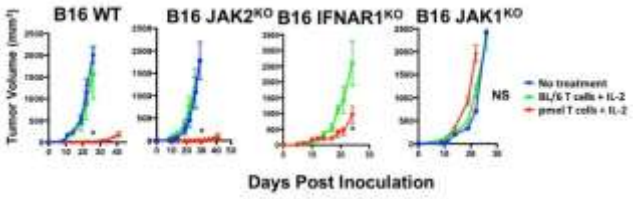

Figure 2.

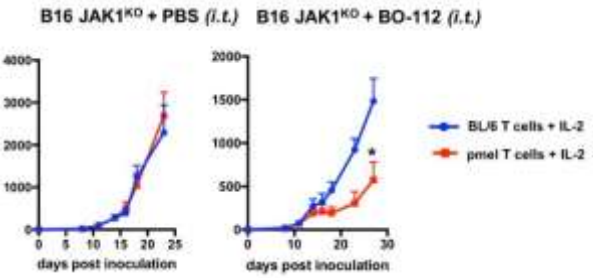

P548

Association between corticosteroid use at time of immune checkpoint inhibitor (CPI) therapy initiation and CNS disease control/survival in patients with brain metastases (BM)

William Kelly, MD[1], Neil Shah[1], Michael Serzan, MD[1], Barbara Ma[1], Matthew Blackburn[1], Sebastian Ochoa[1], Alice Knoedler[1], Jeevan Puthiamadathil[1], Ariana Santopietro[1], Subha Madhavan[2], Anas Belouali[2], Shruti Rao[2], Kellie Gardner, NP[1], Suthee Rapisuwon, MD[1], Stephen Liu, MD[1], Deepa Subramaniam[1], Michael Atkins, MD[1], Geoffrey Gibney, MD[1]

[1]*Medstar Georgetown University Hospital,*

Washington, DC, USA
[2]Georgetown University, Washington, DC, USA

Background
CPI therapy targeting CTLA-4 and PD-1 has improved clinical outcomes in patients with BM [1], including objective responses in patients (pts) with active, untreated melanoma or non-small cell lung cancer (NSCLC) BM [2-4]. Pts with newly diagnosed BM often require corticosteroids at CPI initiation and the impact of such concomitant therapy on disease control and survival remains unclear. The clinical outcomes of pts with BM receiving CPI therapy and associations with corticosteroids and other prognostic factors were analyzed.

Methods
Pts with metastatic solid tumors and BM history treated with ipilimumab (anti-CTLA-4), nivolumab or pembrolizumab (anti-PD-1), and nivolumab/ipilimumab (nivo/ipi) at 3 Medstar Hospitals were identified by pharmacy records and chart review. Pts were excluded if initial BM occurred after CPI initiation or if baseline pretreatment/follow up brain MRI/CT imaging were not available. Data collected included demographics, baseline performance status, systemic corticosteroid use within 14 days of CPI initiation, provider-assessed best disease response and overall survival (OS).

Results
71 pts were identified (40 melanoma, 25 NSCLC, 3 renal cell carcinoma, 3 other). 55% were male, 86% had ECOG PS 0-1, and 66% had ≥2 brain metastases. 82% of pts had surgery and/or stereotactic radiosurgery for BM management prior to therapy. 22% of pts received anti-CTLA-4, 54% received anti-PD-1, and 24% received nivo/ipi. 52% had neurological symptoms and 24% received corticosteroids within 14 days of CPI initiation. The response rate (extracranial) was 23% and median OS was 13.8months for all pts. Survival was superior in pts with melanoma and those treated with nivo/ipi. BM control (no new BM or progression in treated BM) was seen in 38%. Extracranial disease control was associated with intracranial disease control (p=0.001). The use of corticosteroids was associated with BM progression (but not extracranial disease progression) and worse OS (median 5.8months vs 19.8months for no corticosteroid use, P=0.011). There was a trend for worse OS in patients with greater number of BM (p=0.053). The presence of baseline neurological symptoms was not associated with OS.

Conclusions
Pts with BM can have long-term survival with CPI therapy, particularly with nivo/ipi. There is general concordance between extracranial disease control and BM control, but discordance with BM progression can occur. The use of corticosteroids at time of CPI therapy in pts with BM is associated with worse BM control and survival. Pts initially requiring corticosteroids may benefit from alternative systemic therapy options.

References
1. Sloot S, et al. Improved survival of patients with melanoma brain metastases in the era of targeted BRAF and immune checkpoint therapies. Cancer, 2018;124(2):297-305.
2. Goldberg S, et al. Pembrolizumab for patients with melanoma or non-small-cell lung cancer and untreated brain metastases: early analysis of a non-randomised, open-label, phase 2 trial. Lancet Oncol, 2016;17(7):976-983.
3. Long G, et al. Combination nivolumab and ipilimumab or nivolumab alone in melanoma brain metastases: a multicentre randomised phase 2 study. Lancet Oncol, 2018.
4. Margolin K, et al. Ipilimumab in patients with melanoma and brain metastases: an open-label, phase 2 trial. The lancet oncology, 2012.

P549

Cell proliferation defines an additional mechanism of immune escape in non-small cell lung cancer

Carl Morrison, MD, DVM[1], Sarabjot Pabla, MSc, PhD, BS[1], Mary Nesline, MS[1], Jeffrey Conroy, BS[1], Sean Glenn, PhD[1], Antonios Papanicolau-Sengos, MD[1], Paul DePietro, PhD[1], Jacob Hagen[1], Blake Burgher, BS, RN[1], Vincent Giamo, BS, MS[1], Jonathan Andreas, MS[1], Felicia Lenzo[1], Maochun Qin, MD, MS[1], Yirong Wang, MS[1], Devin Dressman, PhD[1], Konstantin Dragnev, MD[2], Laura Tafe[2], Tian Zhang, MD[3], Jeffrey Clarke, MD[3], Matthew Zibelman, MD[4], Luis de la Cruz-Merino[5], Alexander MacKinnon[6], Robin Jacob[7], Oliver Binns[8], Neel Shah[9], Mark Gardner[1], Grace Dy[10]

[1]OmniSeq, Inc., Buffalo, NY, USA
[2]Dartmouth-Hitchcock Medical Center, Hanover, NH, USA
[3]Duke University, Durham, NC, USA
[4]Fox Chase Cancer Center, Philadelphia, PA, USA
[5]Hospital Universitario Virgen Macarena, Sevilla, Spain
[6]Medical College of Wisconsin, Milwaukee, WI, USA
[7]Meharry Medical College, Nashville, TN, USA
[8]Mission Health System, Asheville, NC, USA
[9]Northwest Oncology, Munster, IN, USA
[10]Roswell Park Comprehensive Cancer Center, Buffalo, NY, USA

Background

Prior to this study, the most important mechanisms of immune escape in NSCLC include checkpoint blockade and low tumor mutational burden (TMB). In this study we have identified a third equally important mechanism of immune escape of cell proliferation in NSCLC.

Methods

169 NSCLC patients from ten institutions were evaluated for PD-L1 expression by IHC, TMB, and cell proliferation by RNA-seq of 10 immune and proliferation related genes including BUB1, CCNB2, CDK1, CDKN3, FOXM1, KIAA0101, MAD2L1, MELK, MKI67, and TOP2A, of which 46 represented historical controls and 113 had prior treatment with one more immune checkpoint inhibitors (ICIs) and for which response (RECIST v1.1) and survival were available.

Results

For all patients (n=169) the majority were non-proliferative (59.2%; 100/169), with a minority of proliferative results (40.8%; 69/169). Response rate in non-proliferative patients was 42.2% (27/64) versus 18.4% (9/49) in proliferative. Using a value of 10 mutations per megabase of DNA or greater as high the percent of TMB high cases in proliferative tumors (67%; 47/70) was higher than in non-proliferative tumors (47%; 47/99). The rate of PD-L1 IHC positive (TPS >50) was not different in proliferative (21.7%; 15/69) versus non-proliferative (26%; 26/100) supporting that PD-L1 expression is independent of proliferation status. Survival analysis using TMB high versus low did not show a survival advantage for all ICI-treated patients (p=0.7), proliferative cases (p=0.057), or non-proliferative cases (p=0.12). For 18 non-proliferative PD-L1 positive cases the response rate was 67% (12/18) and nearly double that in the corresponding proliferative group at 38% (5/14). For 46 non-proliferative PD-L1 negative cases the response rate was 35% (12/18) and more than three times that in the corresponding proliferative group at 11% (4/35). Survival for all combinations of PD-L1 and cell proliferation was greatest for PD-L1 positive non-proliferative cases, but perhaps equally if not more important was survival for PD-L1 negative non-proliferative cases was nearly equal to that for PD-L1 proliferative cases.

Conclusions

Cell proliferation, or more specifically high proliferation, is an important immune escape mechanism in NSCLC. Non-proliferation is an

emerging biomarker for response to ICIs in NSCLC.

Ethics Approval
OmniSeq's analysis utilized deidentified data that qualified as non-human subject research under IRB protocol (BDR #080316) approved by Roswell Park Comprehensive Cancer Center (Buffalo, NY).

P550

Defeating checkpoint resistance: Highly specific inhibition of latent TGFβ1 activation renders resistant solid tumors vulnerable to PD-1 blockade

Thomas Schürpf[1], Constance Martin, PhD[1], Christopher Littlefield, MSc[1], Christopher Chapron, MS[1], Stefan Wawersik, PhD[1], Ashish Kalra, PhD[1], Kevin Dagbay, PhD[1], Allison Simpson, BS[1], Francis Danehy, BS[1], Christopher Boston[1], Anastasia Nikiforov, MS[1], Susan Lin, BS[1], Justin Jackson, BS[1], Pichai Raman, PhD[2], Elizabeth Rainbolt, BS[3], Laurie Comfort, BS[3], David Harris[3], Madelyn Cecil-Taylor[3], Lorne Celentano[3], Danielle Meadows[3], gregory carven, PhD[1], Alan Buckler, PhD[1], Allan Capili, PhD[1], Abhishek Datta, PhD[1], Thomas Schürpf[1]

[1]Scholar Rock, Cambridge, MA, USA
[2]Pichai Raman Consulting, Bryn Mawr, PA, USA
[3]Charles River Discovery Services, Morrisville, NC, USA

Background
Despite the clinical breakthroughs achieved by cancer immunotherapy, a majority of patients fail to respond to PD-(L)1 inhibition due to primary or acquired resistance. Profiling of human urothelial cancer and melanoma tumors has recently implicated TGFβ activation as a potential mechanism of primary resistance to checkpoint therapies. However, therapeutic targeting of the TGFβ pathway has been hindered by dose-limiting cardiotoxicities, most likely due to inhibition of signaling from multiple TGFβ isoforms. Upon secretion, TGFβ growth factor is held in a latent complex with its non-covalently associated prodomain. TGFβ activation is induced by extracellular events that release the growth factor from this latent complex. We previously demonstrated that isoform-specific inhibition of TGFβ activation can be achieved by targeting the latent TGFβ complex. We hypothesized that the identification and inhibition of the predominant TGFβ isoform in tumors would enable a more targeted and potentially safer approach to TGFβ inhibition.

Methods
The Cancer Genome Atlas (TCGA) database was interrogated to assess mRNA levels of TGFβ isoforms. Antibody-mediated inhibition of TGFβ1 activation was tested using luciferase-based reporter cells. Efficacy of TGFβ1-selective inhibition in combination with anti-PD-1 was assessed in the MBT-2 bladder cancer and CloudmanS91 melanoma models.

Results
Bioinformatic analysis of TCGA data identified TGFβ1 as the predominant isoform in many human tumors. We generated high affinity, fully-human antibodies against latent TGFβ1. They inhibit the activation of latent TGFβ1 with no detectable binding to or inhibition of latent TGFβ2 or latent TGFβ3. Efficacy was tested in MBT-2 and CloudmanS91, two syngeneic mouse models that recapitulate key aspects of the primary PD-1 resistance phenotype of human disease. Inhibition of TGFβ1 activation is sufficient to completely block TGFβ signaling in MBT-2 tumors. Both models are largely resistant to anti-PD-1 or anti-TGFβ1 alone. However, the combination of anti-PD-1 with blockade of TGFβ1 activation leads to tumor growth delay, a substantial number of complete responses, and prolonged survival coupled with increased effector CD8+ T cell infiltration.

Conclusions
We show here that in many human tumor types, especially those for which checkpoint inhibitors are

approved as therapies, TGFβ1 is the predominant isoform. Pharmacologic blockade of TGFβ1 activation is sufficient to sensitize TGFβ1-predominant tumors to PD-1 inhibition. These encouraging efficacy data and the potentially favorable safety profile of TGFβ1 isoform-selective inhibition establish a strong rationale for exploring therapeutic application of combining PD-(L)1 blockade with latent TGFβ1 inhibition in treatment of multiple cancer types.

Ethics Approval

Animal studies were conducted in compliance with CR Disovery Services IACUC ASAP # 980701 & #980702, and AAALAC Certification

P551

Suppression of immune response by tumor cell-induced XIAP-NFκB signaling and targeting strategies to overcome immunotherapy resistance in breast cancer

Michael Morse[1], Scott Sauer, PhD[2], Myron Evans[3], Mohamed Ibrahim, MD[2], Xuhui Bao, MD[2], Pranalee Patel[2], Gayathri Devi, MSc, PhD[2]

[1]Duke University Medical Center, Durham, NC, USA
[2]Duke University School of Medicine, Durham, USA
[3]St. Jude's, Memphis, USA

Background

Locally advanced breast cancers (LABC) that display lymphovascular invasion (LVI), such as inflammatory breast cancer (IBC), rapidly acquire therapeutic resistance and are highly lethal. A critical question is how, despite trafficking through lymphatics where they encounter immune effectors and inflammatory stress, do the tumor cells evade immune-mediated cell death. IBC expresses high levels of the anti-apoptotic protein, X-linked inhibitor of apoptosis protein (XIAP). We previously identified that, in addition to its canonical function as a potent caspase inhibitor in both the extrinsic and intrinsic apoptosis pathways, XIAP activates nuclear transcription factor (NFκB) in suppression of two mechanisms of cell death caused by anti-tumor immune effectors (antibodies and T cells), granzyme-mediated cell death and accumulation of reactive oxygen species. Further, we identified a mechanism of stress-induced protein translational upregulation of XIAP in promoting tumor cell survival in models of IBC. Therefore, we hypothesized that stress-mediated XIAP-NFκB signaling can lead to a tumor cell-promoted immunosuppressive environment and targeting this signaling axis can enhance the efficacy of immunotherapy.

Methods

Using multiple cell models of aggressive breast cancer, we observed that increased XIAP expression caused decreased immune-mediated caspase activation, lower ROS induction/increased antioxidant protein, and NFκB target gene transcripts in the immune/inflammatory network. To directly test if increased XIAP-NFκB survival signaling can suppress efficacy of immunotherapy, we tested the FDA approved EGFR-specific monoclonal antibody (cetuximab), widely used in cancer therapy, in in vitro antibody-dependent cellular cytotoxicity (ADCC) assays and in in vivo tumor growth kinetic analysis of IBC cells with differential apoptotic capability when implanted orthotopically in the mammary fat pad of mice with functional NK activity.

Results

IBC cells with XIAP overexpression and resultant increases in NFκB target genes regulating antioxidant and immune factors were insensitive to cetuximab-mediated ADCC and resistant to cetuximab-mediated inhibition of in vivo tumor growth when compared to the ADCC-sensitive cell lines. In order to re-sensitize these XIAP overexpressing cells towards ADCC, we tested two strategies- 1. targeting XIAP-NFkB signaling using NRAGE peptide that blocks the XIAP-Tab1-Tak1 complex; 2. SMAC mimetics/birinapant, a synthetic small molecule and peptidomimetic of

second mitochondrial-derived activator of caspases (SMAC) and inhibitor of IAP family proteins. Our results reveal enhanced immune-mediated cell death/sensitivity to immunotherapy.

Conclusions
Our in vitro and in vivo preclinical studies identify the cellular stress-mediated induction of the XIAP-NFκB signaling axis as a novel mechanism of immune evasion and reveal the potential of targeting this signaling pathway to improve breast cancer immunotherapy.

Acknowledgements
Supported in part by Department of Defense Partnership Idea grant awards [W81XWH-13-1-0046 (GRD); W81XWH-13-1-0046 (MAM)]; Duke School of Medicine Bridge Funds (GRD); Duke University Diversity Enhancement Fellowship (MKE) and the National Cancer Institute T32CA009111 (SJS).

Ethics Approval
The animal research was approved by the Duke University IACUC

P552

Analysis of TIL from human carcinoma combined with tissue imaging and in vitro models uncovers tumor-inflicted T cell deviations related to immune escape and strategies of intervention

Elfriede Noessner, PhD[1], Elfriede Noessner, PhD[1], Petra Prinz[2], Ilias Masouris[3], Anna Mendler[2]

[1]Helmholtz Zentrum Munchen, Munich, Germany
[2]Helmholtz Zentrum München, Munich, Germany
[3]Klinikum LMU München, München, Germany

Background
Many tumors are infiltrated with CD8 lymphocytes. Yet, tumors are not rejected suggesting that the tumor environment limits effector cell efficacy to control tumor growth.

Methods
Using human renal cell carcinoma, multiparameter fluorescence staining and confocal microscopy was performed to determine the status of lymphocytes in direct physical contact with malignant cells under the control of the local microenvironment. Ex vivo TIL analysis was used to identify TCR signaling alterations in CD8-TILs compared to CD8 T cells of non-tumor kidney.

Results
A special image analysis, modeled on the process of lytic granule exocytosis, was applied to identify CD8-TILs with active tumor recognition. The cytotoxic status of CD8-TILs, determined in relation to the TILs' spatial distribution within the tumor, revealed a pivotal role of the tumor microenvironment in restraining lytic function of CD8-TILs. Some TILs appeared actively engaged in tumor recognition; however, there was no evidence that any CD8 cell was stimulated to produce IFNg. Application of in vitro models, which mimic conditions of solid tumors, identified tumor lactic acidosis as one potent factor abrogating TCR-stimulated IFNg production by inhibition of p38 and JNK/c-Jun activation. Ex vivo analyses of TILs identified TCR signaling alterations in CD8-TILs compared to CD8 T cells of non-tumor kidney, which were associated with failure to degranulate. These deviations were reversible concomitantly with gain in perforin and function.

Conclusions
The results reveal mechanisms of inhibition of CD8- and NK-TIL function imparted by the tumor environment which are related to immune escape in RCC. Based on identified alterations strategies to engineer T cells (i.e chimeric costimulatory proteins) and to modulate the tumor environment are designed to empower T cells for higher efficacy in adoptive therapy.

Acknowledgements
We acknowledge the patients and their families for donating tissue for analysis, and the clinicians and pathologists for the sample collection.

Ethics Approval
The ethics board of the Ludwig Maximilians University has approved the tissue collection

P553

Targeting mechanisms of immune suppression via CXCR2 inhibition to enhance checkpoint blockade

Elaine Pinheiro, PhD[1], Sarah Javaid, PhD[1], Ruban Mangadu[1], Marlene Hinton[1], Yun Wang[1], Sonia Feau[1], Amanda Watkins, PhD[1], Andrey Loboda, PhD[1], Xue Liang[1], Dario Gutierrez[1], Rebecca Ruck[1], Michael Rosenzweig, DVM, PhD[1], Vincent Giranda, MD, PhD[1]

[1]*Merck Research Laboratories, Boston, MA, USA*

Background
Myeloid-derived suppressor cells (MDSCs) are an adverse cancer-wide prognostic population of immune infiltrating cells that contribute to tumor immune evasion by suppressing local T-cell activation and viability and influencing tumor progression by promoting tumor metastases, angiogenesis and tumor cell invasion [1]. PMN-MDSC cell signatures have emerged as a significant predictor of poor survival across solid tumors [2]. Here we explore the role of the CXCR2 pathway on PMN-MDSCs in the tumor microenvironment and the mechanisms of CXCR2-driven enhancement of checkpoint blockade.

Methods
Chemotaxis assays were performed. Anti-tumor activity was assessed in the B16-F10 syngeneic tumor model utilizing a small molecule antagonist of CXCR2, MK-7123 (Navarixin) and an anti-mouse PD-1 blocking antibody, muDX400. Molecular and cellular responses associated with anti-tumor activity were evaluated by RNA-Sequencing analysis, flow cytometry, and functional assays.

Results
Here we show that cancer patient PMN-MDSCs highly express the CXC G protein-coupled receptor, CXCR2, and that its chemokine ligand, IL-8, can influence the migration of this myeloid population. In addition, CXCR2 expression significantly correlates with poor survival across solid tumor types. In mouse tumor models, CXCR2 blockade disrupts the trafficking of CD11b(+)Ly6C(-)Ly6G(+) PMN-MDSCs/neutrophils in the tumor microenvironment and enhances the anti-tumor effect of checkpoint blockade. Preclinical studies to further explore the molecular and cellular mechanisms behind these combination effects will be presented, utilizing a small molecule antagonist of CXCR2, MK-7123 (Navarixin), and an anti-mouse PD-1 blocking antibody, muDX400. Tumor transcriptome and network analyses by RNA-sequencing reveal that MK-7123 + muDX400 combination treatment result in the enrichment of immune and tumor-related pathways. Moreover, changes to chemokine profiles favor enhanced T cell infiltration into the tumor. In addition, the effects of commensal microbiota on response to monotherapy and combination treatment will be explored.

Conclusions
Taken together, these preclinical oncology studies support the concept of targeting CXCR2 to increase the therapeutic efficacy of PD-1 blockade. Clinical investigation of Navarixin in combination with pembrolizumab/Keytruda is ongoing for the treatment of multiple cancers.

References
1. Veglia F, Perego M, Gabrilovich D. Myeloid-derived suppressor cells coming of age. Nat Immunol. 2018;19:108–119 2. Gentles AJ, Newman AM, Liu CL, Bratman SV, Feng W, Kim D, Nair VS, Xu Y, Khuong A,

Hoang CD, Diehn M, West RB, Plevritis SK, Alizadeh AA. The prognostic landscape of genes and infiltrating immune cells across human cancers.Nat Med. 2015; 21(8):938-945

P554

Role of immune escape for resistance to cancer (immuno) therapy and its strategies targeting these mechanisms

Barbara Seliger, MD, PhD[1], Jurgen Bukur, PhD, MD[1]

[1]*Martin Luther University Halle-Wittenber, Halle, Germany*

Background
Despite impressive durable clinical responses in tumor patients with distinct subtypes of cancer employing cancer immunotherapies, a high frequency of patients does not respond or develop resistances during treatment overtime. Therefore, identification of the underlying molecular mechanisms of these resistances as well as identification of novel therapeutic approaches to overcome them might significantly improve the clinical outcome and survival of patients.

Methods
A number of both tumor intrinsic as well as tumor extrinsic factors have been identified by us, which are involved in the escape of immune surveillance of different tumors.

Results
These include downregulation of MHC class I antigen processing and interferon signaling components, upregulation of co-inhibitory molecules, such as HLA-G and PD-L1, as well as downregulation of extracellular matrix proteins. These different alterations could occur either at the transcriptional, epigenetic or posttranscriptional level, while structural alterations leading to loss of expression of these immune modulatory molecules appear to be a rare event. Interestingly, impaired HLA class I APM component expression has been demonstrated to be directly associated with disease progression after adoptive T cell therapy. Next to these tumor intrinsic factors, the tumor microenvironment also plays an important role in immune escape. In particular, the immune cell compositions in peripheral blood as well as the spatial distribution of immune cells in the tumor microenvironment are key factors of immune suppression. This was directly associated with a worse prognosis, reduced survival and/ or lack of response to cancer (immuno)therapies.
Furthermore, treatment of cells with cytokines, like interferons, as well as recombinant proteoglycans anti-oxidant substances, e.g. methyl selenic acid, and epigenetic drugs were able to enhance HLA class I surface expression thereby resulting in an enhanced immune response.

Conclusions
Thus, overcoming the acquired an intrinsic therapy resistance of tumors is an important tool for improving (immuno)therapeutic strategies.

P555

A role for mutant p53 in mediating T cell immune evasion in pancreatic adenocarcinoma and other solid tumors

Deborah Silverman, BS[1], Emily Ashkin[1], Simone Punt, PhD[1], Minying Zhang[1], Leila Williams, MSc[1], Anil Korkut[1], Jason Roszik, PhD[1], Anirban Maitra, MBBS[1], Patrick Hwu, MD[1]

[1]*MD Anderson Cancer Center, Houston, TX, USA*

Background
Harnessing the immune system by altering the ability of T-cells to attack cancer has led to long-lasting cures in some tumors. Nonetheless, pancreatic ductal adenocarcinoma (PDAC), one of the most

lethal malignancies, remains resistant to immunotherapy. To design effective therapies, it is critical to learn how PDAC evades the immune system.

Methods

We hypothesize that p53 mutations mediate tumor escape from T-cells in PDAC, and test whether subsets of p53 mutations in PDAC tumors impact T-cell migration and killing, using novel in vitro and inducible in vivo models, to characterize a new role for p53's regulation in cancer.

Results

Here we present results suggesting that a subset of p53 missense mutants impact T-cell infiltration into and autologous T-cell killing in PDAC tumors, in a possible dominant gain-of-function mechanism.

Conclusions

These findings begin to elucidate the role of p53 activating mutations in tumorigenesis,and providing rationale to investigate mutant p53 immune-regulation in PDAC and other tumor types.

Acknowledgements

The authors thank and acknowledge Eran Kotler and Moshe Oren for generously providing H1299-p53-mutant lines; Gigi Lozano, Florencia McAllister, Russell Broaddus, Stephanie Watowich, and Katy Rezvani for their valuable advice and insight; Sara Leahey, Soraya Zorro Manrique, Elien Doordjuin, and Weiyi Peng for their advice and support; and the University of Texas MD Anderson Cancer Center Pancreatic Cancer Moon Shot Program for their generous financial support of this project.

References

1. Carter S L, Cibulskis K, Helman E, McKenna A, Shen H, Zack T, Beroukhim R. Absolute quantification of somatic DNA alterations in human cancer. Nat biotechnology. 2012; 30(5): 413-421.
2. Hingorani S R, Wang L, Multani A S, Combs C, Deramaudt T B, Hruban R H, Tuveson D A. Trp53R172H and KrasG12D cooperate to promote chromosomal instability and widely metastatic pancreatic ductal adenocarcinoma in mice. Cancer cell. 2005; 7(5), 469-483.
3. Morton J P, Timpson P, Karim S A, Ridgway R A, Athineos D, Doyle B, Frame M C. Mutant p53 drives metastasis and overcomes growth arrest/senescence in pancreatic cancer. PNAS. 2010; 107(1), 246-251.
4. Aschauer L, Muller P A. Novel targets and interaction partners of mutant p53 Gain-Of-Function. Biochem Soc Transactions. 2016; 44(2), 460-466.
5. Joerger,A C, Fersht A R. Structure–function–rescue: the diverse nature of common p53 cancer mutants. Oncogene. 2007; 26(15), 2226-2242.
6. McKenzie, J A, Mbofung, R M ., Malu, S, Zhang, M, Ashkin, E, Devi, S, & Xu, C. The Effect of Topoisomerase I Inhibitors on the Efficacy of T-Cell-Based Cancer Immunotherapy. J Natl Cancer Inst. 2018;110(7):777-786.

P556 Abstract Travel Award Recipientb

STAT3-related cytokines drive IR-specific immune suppression of effector, memory and naïve, peripheral blood CD8+ T cells in cancer patients

Ashwin Somasundaram, MD[1], Dario A. Vignali, PhD[1], Anthony Cillo, PhD[1], James Herman[1], John Kirkwood, MD[1], Robert Ferris, MD, PhD[1], Tullia Bruno, PhD[1]

[1]*University of Pittsburgh, Pittsburgh, PA, USA*

Background

Cancer patients that do not respond to PD1 blockade have increased inhibitory receptor (IR) expression in peripheral blood lymphocytes (PBL) and increased cytokine concentrations in the plasma. Cancer patients off therapy and with normal white blood cell counts are often at greater risk for infections, immune dysregulation, progressive disease or reactivation of viral infections. However, the exact

mechanism of this systemic immunosuppression in cancer patients is not fully understood. We performed flow cytometric assays to assess both phenotype and function of peripheral CD8+ T cells in cancer patient samples and healthy donor controls. We hypothesize that cancer patients may have systemic immune suppression via cytokine-driven IR expression in all CD8+ T cells subsets, including naïve cells.

Methods

PBL were obtained from healthy donors and treatment-naïve NSCLC, HNSCC, and melanoma patients. IR (i.e. LAG3, PD1, CTLA4, etc) expression was assessed on CD8+ T cells, CD4+ T cells, and regulatory T cells. Cytokine concentrations were compared by Luminex between plasma from healthy donors and plasma from cancer patients with high and low IR expression on peripheral CD8+ T cells. Autologous micro-stimulation assays were performed on peripheral CD8+ or CD4+ T cells with antigen presenting cells plus or minus IR blockade.

Results

CD8+ T cells, including CD45RA+CCR7+CD62L+CD8+ T cells, from cancer patient PBL contain elevated total LAG3 expression which correlated with stage and elevated expression of other IRs. Further, CD8+ T cells from these patients had decreased proliferation, which was rescued with the addition of anti-LAG3 or anti-PD1. Plasma from these patients had significantly elevated levels of cytokines that can signal via STAT3 (i.e. IL-6, IL-8, IL-9), which were independently found to increase total IR expression in healthy donor, naïve CD8+ T cells.

Conclusions

The current understanding of PD1 blockade resistance has been limited to the tumor microenvironment (TME) and our findings support the growing body of literature that tumor-related systemic immune suppression is a potent mechanism of cancer progression. Patients with cancer have systemic elevations of cytokines that signal via STAT3 leading to increased IR expression in naïve, peripheral CD8+ T cells making them poised for exhaustion even before TCR binding. These findings suggest that IR blockade also plays a significant role in reversing immune tolerance outside of the TME and cytokine blockade may play a role in reversing PD1 blockade resistance.

Ethics Approval

The study was approved by the University of Pittsburgh's IRB and Ethics Board, approval number: PRO16070383.

P557 Abstract Travel Award Recipient

Overcoming genetically-based resistance mechanisms to PD-1 blockade

Davis Torrejon, MD[1], Gabriel Abril-Rodriguez, MS[2], Jennifer Tsoi[2], Ameya Champhekar[2], Giulia Parisi[2], Gardenia Cheung-Lau[2], Tom Wohlwender[2], Mykola Onyshchenko[2], Beata Berent-maoz[2], Catherine Grasso[2], Begoña Comin-Anduix, PhD[2], Siwen Hu-Lieskovan, MD, PhD[2], Antoni Ribas, MD, PhD[2]

[1]UCLA Hematology-Oncology, Los Angeles, CA, USA
[2]UCLA, Los Angeles, CA, USA

Background

We studied loss of function (LOF) mutations within the interferon (IFN) pathway (JAK1 or JAK2) and in the antigen presentation pathway (beta-2-microglobulin-B2M) found in biopsies from patients who are resistance to anti-PD-1 therapy, and tested strategies to overcome the resistance.

Methods

Using CRISPR/Cas9 genome editing we generated JAK1, JAK2 and B2M knockout (KO) sublines of the murine MC38 carcinoma, a model of high mutational load cancer that responds well to anti-PD-1, as well

as of human MART-1-positive melanoma cell lines, tested using in-vitro T cell co-culture systems. We analyzed signaling changes in human cell lines (parental and KOs) exposed to IFN-gamma using RNAseq. In addition, we performed in-vivo antitumor activity in the MC38 variants using mass cytometry (CyTOF) to characterize the tumor microenvironment. Finally, we tested strategies to overcome resistance mechanisms with SD-101 (TLR-9-agonist) and NKTR-214 (CD-122 biased agonist).

Results

The JAK1-KO sublines lost sensitivity to IFN-alpha, IFN-beta and IFN-gamma, while the JAK2-KO cell line was insensitive only to IFN-gamma induced signaling (PD-L1, MHC class I) and growth arrest ($p<0.001$ compared with IFN-alpha or beta). There was no difference in the in-vitro cytotoxicity by MART-1 specific T-cells against JAK1/2-KO-MART-1+ melanoma cells compared to the parental (94%, 95% vs 90% cytotoxicity at 10:1 E:T ratio, pNS). However, B2M-KO was resistant to killing by MART-1 specific T-cells (2% vs 90% cytotoxicity at 10:1 E:T ratio, $p<0.0001$). RNAseq differential gene expression analysis showed that the IFN-gamma-induced increased expression of antigen presenting machinery, IFN-gamma signaling and chemokines (CXCL9, CXCL10) were not expressed by JAK1/2-KOs. In the MC38 model, the significant antitumor activity of anti-PD-1 against the parental was lost in JAK1/2 and B2M KOs (Table1); in these KO sublines, CyTOF analysis revealed that anti-PD-1 therapy was unable to change tumor CD8 T-cell infiltration. Using JAK1/2-KOs cell lines we showed that intratumoral administration of the TLR-9 agonist SD-101 was able to overcome local resistance to anti-PD-1 even in abscopal sites, and the NKTR-214 overcame resistance to anti-PD-1 in the B2M-KO tumor growth and significantly increased survival.

Conclusions

JAK1/2 LOF mutant tumors result in loss of sensitivity to IFN induced antitumor effects but do not impair T cell recognition and cytotoxicity, while B2M LOF results in lack of antigen presentation to T cells and loss of antitumor activity. Both lead to in-vivo resistance to anti-PD-1 therapy, and JAK1/2 KO resistance can be overcome by a TLR9 agonist, and B2M-KO resistance can be overcome by a new generation IL-2.

Table 1.

P558

Secondary resistance to immunotherapy associated with β-catenin pathway activation or genetic loss of phosphatase and tensin homolog (PTEN) in metastatic melanoma

Jonathan Trujillo, MD, PhD[2], Jason Luke, MD, FACP[1], Stefani Spranger, PhD[3], Yuanyuan Zha, PhD[1], Karen Matijevich, RN, BSN[2], Thomas Gajewski, MD, PhD[1]

[1]*University of Chicago, Chicago, IL, USA*
[2]*Univeristy of Chicago, Chicago, IL, USA*
[3]*MIT, Cambridge, MA, USA*

Background

While immune checkpoint blockade therapy and even some vaccines have given rise to durable responses in many cases of advanced melanoma, a large fraction of patients subsequently develop

secondary resistance to therapy. Mechanisms of immune-resistant cancer progression in this context are incompletely understood. Our lab previously showed tumor-intrinsic WNT/β-catenin activation can mediate T cell exclusion from tumor and primary resistance to anti-CTLA-4 + ant-PD-L1 therapy [1,2]. In addition, genetic loss of the tumor suppressor PTEN has been associated with defective T cell infiltration and primary resistance to PD-1 blockade [3]. However, whether secondary resistance might occur upon acquired oncogenic pathway alterations following initial response to immunotherapy is not known. We describe two metastatic melanoma patients who had a durable response to immunotherapy, but subsequently developed secondary resistance characterized by a phenotypic shift from a T cell-inflamed to non-T cell-inflamed tumor microenvironment, associated with oncogenic pathway alterations.

Methods

Case 1: A patient with metastatic melanoma was treated on a peptide/interleukin-12 vaccine protocol every 3 weeks for one year and achieved a partial response. Three years later a new metastatic lesion developed. Tumor gene expression profiling and histologic analysis for CD8 T cell infiltration and β-catenin expression were performed at baseline and at recurrence. Case 2: A patient with metastatic melanoma was treated with anti-CTLA-4 + PD-1 therapy and achieved a major partial response for a total of nineteen months. Baseline and treatment-resistant tumors underwent next-generation sequencing comprising a panel of commonly altered cancer genes for mutational and copy number analysis. Tumor biopsies were examined for CD8 T cell infiltration.

Results

Case 1: The baseline tumor prior to peptide vaccination demonstrated a T cell-inflamed gene signature and a robust intratumoral CD8 T cell infiltrate. In contrast, the recurrent treatment-resistant metastasis had a non-T cell inflamed phenotype and no infiltrating CD8 T cells. The new metastasis also acquired extensive expression of β-catenin, which was undetectable in the baseline lesion. Target antigens and circulating tumor-reactive T cells were detectable at the time of progression. Case 2: The on-treatment biopsy during anti-CTLA-4 + PD-1 therapy showed intratumoral CD8 T cells, while the recurrent metastasis lacked infiltrating CD8 T cells. The treatment-resistant metastasis uniquely harbored biallelic PTEN loss with no detectable PTEN protein present.

Conclusions

Our findings suggest that secondary resistance to immunotherapy may arise when tumor up-regulates β-catenin expression or undergoes genetic loss of PTEN, oncogenic events capable of driving T cell exclusion from the tumor microenvironment.

References

1. Spranger S, Bao R, Gajewski TF. Melanoma-intrinsic beta-catenin signalling prevents anti-tumour immunity. Nature 2015; 523:231-5.
2. Spranger S, Dai D, Horton B, Gajewski TF. Tumor-residing Batf3 dendritic cells are required for effector T cell trafficking and adoptive T cell therapy. Cancer Cell. 31:711-23.e4.
3. Peng W, Chen JQ, Liu C, et al. Loss of PTEN promotes resistance to T cell-mediated immunotherapy. Cancer Discovery. 2016; 6:202-16.

Ethics Approval

The study was approved by University of Chicago's Ethics board.

Consent

Consent was received

P559

Co-expression of TNF receptor 1 and 2 on human BRAF V600E+ melanomas is required for TNF-induced resistance to MAPK pathway inhibitors

Lazar Vujanovic, PhD[1], Cindy Sander, BS[1], Jian Shi, MD[1], John Kirkwood, MD[1], Lisa Butterfield, PhD[1]

[1]*University of Pittsburgh, Pittsburgh, PA, USA*

Background

The effectiveness of MAPK cascade-targeting therapies to treat patients with BRAF-V600E-mutant melanomas has been limited by a range of resistance mechanisms that may be driven by the tumor necrosis factor (TNF). TNF signaling is mediated through TNF receptor type-1 (TNFR1) and TNF receptor type-2 (TNFR2). TNFR1 signaling mediates apoptosis or cell survival/cytokine secretion, while TNFR2 selectively mediates cell survival/cytokine secretion. Although TNFR1 and TNFR2 are preferentially activated by soluble (sol)TNF and transmembrane (tm)TNF, respectively, they can crosstalk via shared signaling molecules. While TNF receptor 1 (TNFR1) is ubiquitously expressed, little is known about the expression patterns and functional roles of TNFR2 on melanomas. The primary goals of this study are to evaluate whether TNFR2 is expressed on melanoma, to determine which TNFR mediates TNF- mediated resistance reprogramming to MAPK inhibitors (MAPKi) and to decipher whether INB03, a dominant-negative TNF biologic and specific antagonist of solTNF, can antagonize this therapeutic resistance pathway.

Methods

TNFR1/2 expression patterns on BRAF-mutant melanomas were evaluated by multi-color flow cytometry. Recombinant TNF was used to induce MAPKi resistance in melanomas. Activated human macrophages were used in transwell co-culture systems to induce MAPKi resistance in melanomas. The effectiveness of INB03 to antagonize this therapeutic resistance pathway was compared to an anti-TNF antibody and a selective NF-kB inhibitor. CRISPR/Cas9 system was utilized to edit out TNFR1 and TNFR2 on a melanoma cell line, and these knockout variants were used to test the intrinsic roles of these receptors in TNF-induced resistance to MAPKi. MTT viability assay was used as the readout for melanoma sensitivity to MAPKi.

Results

TNFR1 and TNFR2 were co-expressed by 48% of BRAF-V600E-mutant melanoma cell lines and primary melanomas. Interestingly, only cell lines that co-expressed TNFR1 and TNFR2 could acquire MAPKi resistance in response to recombinant and macrophage-derived TNF. Functional studies of TNFR1 and TNFR2 knockout cell lines indicated that both TNFR1 and TNFR2 signaling were necessary for the TNF-mediated induction of resistance to MAPKi. Finally, selective sequestration of both recombinant and macrophage-derived TNF using INB03 effectively prevented acquisition of resistance to MAPKi by BRAF-V600E mutant melanoma cell lines in vitro.

Conclusions

solTNF-mediated induction of MAPKi resistance in BRAF-V600E-mutant melanomas is predicated on the co-expression of TNFR1 and TNFR2. Our data indicate that almost half of BRAF-V600E-mutant melanomas express TNFR2. These results indicate that TNFR2 could be a biomarker that could be used to select for melanoma patients that could benefit from TNF-targeting therapies.

Acknowledgements

The authors thank David E. Szymkowski, Ph.D. of Xencor Inc. for providing the dominant-negative TNF biologic. This study was supported by the UPCI SPORE in melanoma and skin cancer (P50 CA121973) Developmental Research Project (DRP) award.We thank the following UPCI shared resources (supported in part by NIH P30CA047904): Flow

Cytometry Facility and the Immunologic Monitoring Laboratory (Luminex).

Ethics Approval
Specimens collection was performed under IRB-approved protcol UPCI-96-099

P560

Resistance of CD44+ subpopulation to CTL though high production a protease inhibitor in colorectal cancer

Tomonori Yaguchi, MD, PhD[1], Tsubasa Miyauchi[1], Kenji Morii, MS[1], Yutaka Kawakami, MD PhD[1]

[1]*Keio University School of Medicine, Tokyo, Japan*

Background
Colorectal carcinoma (CRC) is generally resistant to immunotherapies, suggesting possible CRC-specific immunosuppressive mechanisms. In this study, we have identified markers which could define particular subpopulation harboring immuno-resistant properties and investigated the underlying mechanisms of the immunosuppression.

Methods
We analyzed the expression pattern of 30 CD (cluster of differentiation) antigens on 10 human CRC cell lines. We sorted a CRC cell line into the CD44-positive fraction and the CD44-negative fraction, and evaluated their sensitivity to CTL lysis. Gene expression profiles of the CD44-positive CRC fraction which showed resistance to CTL lysis were compared with those of the CD44-negative CRC fraction using the cDNA micro array. For the functional analysis of protease inhibitor X (PI-X) which was preferentially expressed in CD44-positive fraction, we evaluated the effect of PI-X knockdown by siRNA or PI-X overexpression in CRC cell lines on the sensitivity to CTL lysis in vitro and the effect of PI-X overexpression in murine CRC cells on the therapeutic efficacy of anti PD-1 therapies in vivo. We also evaluated the correlation of the PI-X expression in human CRC and T cell infiltration and the patients' prognoses by the analyses of immunohistochemistry and TCGA RNA-seq data.

Results
10 out of 30 tested CD antigens were heterogeneously expressed on the human CRC cell lines. Among these 10 CD antigens, we found that the CD44-positive fraction in human CRC cell lines were more resistant to tumor specific CTL-mediated killing compared to the CD44-negative fraction. cDNA microarray analysis revealed the CD44-positive fractions more highly expressed protease inhibitor X (PI-X) than the CD44-negative fractions. The expression level of PI-X was also positively correlated with that of CD44 in TCGA RNA-seq database. PI-X showed the highest expression in CRC among 17 human cancer tissues in meta-analysis using open-access gene expression data. The experiments of PI-X overexpression or PI-X knockdown in CRC cell liens showed PI-X could suppressed CTL-mediated killing. TCGA RNA-seq data showed the negative correlation between PI-X expression and CD8 expression. Moreover, analyses of immunohistochemistry and TCGA RNA-seq data revealed the best prognosis of the patients with low PI-X expression and high CD8+ T cell infiltration. In tumor-bearing mouse models, over expression of PI-X in a murine cancer cell line induced the resistance to anti PD-1 Ab therapies.

Conclusions
CD44 and PI-X may be potential biomarkers for prognosis and responses of CRC patients to cancer therapies including PD-1 blockade, and also be attractive therapeutic targets for combination immunotherapies.

Ethics Approval
The study was approved by Keio Univ. school of medicine Institutution's Ethics Board, approval number 20P16

P561

A new mechanism of ADCC resistance

David Zahavi, MS, BS[1], Dalal Aldeghaither[1], Louis Weiner, MD[1], Joseph Murray, MD, PhD[2], Elana Fertig[2], Garrett Graham[1], Yong-Wei Zhang[1], Allison O'Connell, MD/PhD Candidate[1], Junfeng Ma[1], Sandra Jablonski, PhD[1]

[1]*Georgetown University, Washington, DC, USA*
[2]*Johns Hopkins University, Ellicott City, MD, USA*

Background
Antibody-dependent cell-mediated cytotoxicity (ADCC) is an important mechanism underlying targeted monoclonal antibody (mAb) therapy in cancer. The majority of patients develop resistance to mAb therapy; however the resistance mechanisms are not well characterized. In vitro modeling of ADCC provides an experimental system for uncovering tumor cell immune resistance mechanisms.

Methods
We continuously exposed epidermal growth factor receptor (EGFR) positive A431 cells to KIR-deficient NK92-CD16V effector cells and the anti-EGFR mAb Cetuximab.

Results
Persistent ADCC exposure yielded ADCC-resistant cells, that when compared with control ADCC-sensitive cells, exhibited reduced EGFR expression, overexpression of histone- and interferon-related genes, failure to activate NK cells, and no evidence of epithelial to mesenchymal transition. These properties gradually reversed following withdrawal of ADCC selection pressure. Remarkably, ADCC-resistant cells possessed lower expression of multiple cell surface molecules that contribute to intercellular interactions and immune synapse formation. Classic immune checkpoints did not modulate ADCC in this unique model system of immune resistance.

Conclusions
We show that the induction of ADCC resistance involves genetic and epigenetic changes that lead to a general loss of target cell adhesion properties required for the establishment of an immune synapse, killer cell activation, and target cell cytotoxicity.

Acknowledgements
We would like to thank Dr. Kerry Campbell for providing the NK92-CD16V cells.

Mechanisms of Toxicity

P562

Delayed immune-related events after discontinuation of immunotherapy – DIRE syndrome?

Marcus Couey, MD, DDS[1], Bell, MD, DDS, FACS[1], Ashish Patel, MD[2], Marka Crittenden, MD, PhD[1], Brendan Curti, MD[1], Rom Leidner, MD[1]

[1]*Earle A. Chiles Research Institute, Portland, OR, USA*
[2]*Providence Cancer Center, Portland, OR, USA*

Background
Although the temporality of immune-related adverse events (irAE) is well-recognized during immunotherapy to be highly variable and often delayed,[1] post-immunotherapy irAE are rarely described and potentially under-recognized. In 2013, two cases were reported in abstract form in Deutschen Dermatologischen Gesellschaft.[2] In July 2018 a case of autoimmune hepatitis eight months post-immunotherapy was reported in The Oncologist[3] and a dermatologic series appeared online in JAMA Dermatology.[4] With expanding indications for IO and an increasing number of

clinical trials in the curative-neoadjuvant setting, larger numbers of patients are being treated in earlier stages of disease and often for short courses. Given this trend, under-recognition of delayed immune-related events (DIRE) after completion of immunotherapy could pose a growing clinical hazard.

Methods

We performed a literature review in PubMed and Google Scholar (search terms included in Table 1); DIRE syndrome was defined as immune-related events post-immunotherapy, newly incident beyond two elimination half-lives (t 1/2) of drug.

Results

We identified 10 cases, 6 by literature review (5 melanoma, 1 cutaneous SCC) and an additional 4 cases at our institution (4 HNSCC). Median cumulative immunotherapy exposure was 4 doses (range: 2 to 22 doses). Median interval from last immunotherapy dose to DIRE onset was 5 months (range: 2 to 28 months). All literature cases were in the recurrent/metastatic context; we report four cases in the curative-neoadjuvant context (italicized) with one recurrence.

Conclusions

An influx of neoadjuvant clinical trial design over the last 2-3 years, incorporating brief IO exposure (typically checkpoint blockade) followed by surgical resection and/or adjuvant therapy, is attracting interest in multiple tumor types in the curative setting.[5–9] In this context, it will be necessary to recognize an emerging phenomenon, which we have termed DIRE syndrome (delayed immune-related events). Clinical vigilance has the potential to reduce morbidity from delayed diagnosis, as these conditions are generally manageable with prompt initiation of treatment; or from misdiagnosis, to avert unnecessary/harmful interventions (in the autoimmune meningitis case we report, an Omaya reservoir was placed at an out-of-state hospital based on erroneous diagnosis of leptomeningeal carcinomatosis). Several factors confound diagnosis in the neoadjuvant-IO context: 1) intervening treatments with potentially overlapping toxicities; 2) brief and remote IO exposure; 3) reduced vigilance during NED surveillance, in contrast to active disease follow-up; 4) protracted process of diagnosis-by-exclusion. DIRE syndrome should therefore figure prominently in the differential diagnosis of patients presenting with diseases of unclear etiology, irrespective of elapsed post-immunotherapy interval.

References

1. Champiat S, et al. Management of immune checkpoint blockade dysimmune toxicities: a collaborative position paper. Ann. Oncol. Off. J. Eur. Soc. Med. Oncol. 2016;27:559–574.
2. Abstracts of the 8th World Congress of Melanoma, the 9th Congress of the European Association of Dermatology (EADO), the 7th Interdisciplinary Melanoma/Skin Cancer Meeting, and the 3rd European Post-Chicago Melanoma Meeting. July 17-20, 2013. Hamburg, Germany. J. Dtsch. Dermatol. Ges. J. Ger. Soc. Dermatol. 2013;JDDG 11 Suppl 7:1–119.
3. Parakh S, Cebon J, Klein O. Delayed autoimmune toxicity occurring several months after cessation of anti-PD-1 therapy. The Oncologist. 2018;23:849–851.
4. Wang L, et al. Timing of onset of adverse cutaneous reactions associated with programmed cell death protein 1 inhibitor therapy. JAMA Dermatol. 2018; doi:10.1001/jamadermatol.2018.1912
5. Forde P, et al. Neoadjuvant PD-1 blockade in resectable lung cancer. N. Engl. J. Med. 2018;378:1976–1986.
6. Uppaluri R, et al. Neoadjuvant pembrolizumab in surgically resectable, locally advanced HPV negative head and neck squamous cell carcinoma (HNSCC). J. Clin. Oncol. 2017;35:6012–6012.
7. Ferris R, et al. LBA46An open-label, multicohort, phase 1/2 study in patients with virus-associated cancers (CheckMate 358): Safety and efficacy of neoadjuvant nivolumab in squamous cell carcinoma

of the head and neck (SCCHN). Ann. Oncol. 2017;28.
8. Necchi, A. et al. Interim results from PURE-01: A phase 2, open-label study of neoadjuvant pembrolizumab (pembro) before radical cystectomy for muscle-invasive urothelial bladder carcinoma (MIUC). J. Clin. Oncol. 2018;36:TPS533-TPS533.
9. Powles, T. et al. A phase II study investigating the safety and efficacy of neoadjuvant atezolizumab in muscle invasive bladder cancer (ABACUS). J. Clin. Oncol. 2018;36: 4506–4506.

Table 1.

Malignancy Age / Gender	Disease Setting	irAE	Months post-ICI	Drug	Doses (total)	Interim Rx
[1]Melanoma / 70 / M	Metastatic	Vitiligo	11	Pembro	4	NR
[1]Melanoma / 52 / M	Metastatic	Neuropathy	"some months"	Pembro	3	NR
[1]Melanoma / ?? / ?	Metastatic	Hepatitis	8	Nivo	22	RT 60Gy x6 adrenal met
[1]Melanoma / 60's / M	Metastatic	Sarcoidosis	5	Pembro	10	NR
[1]Melanoma / 80's / ?	Metastatic	Dermatitis lichenoid	1	Pembro	4	NR
[1]SCC [redacted] / 80's / ?	Metastatic	Pemphigoid bullous	6	Pembro	4	NR
Oropharynx SCC HPV+ 62 / M	*Neoadjuvant*	*Meningitis (autoimmune)*	*28*	*MEDI6469 (OX40)*	*3*	*Surgery + adj. RT 2Gy x33*
Oropharynx SCC HPV+ 62 / M	*Neoadjuvant*	*Encephalopathy (sepsis) Adrenal Crisis*	*4*	*Nivo*	*2*	*Surgery + adj. RT 2Gy x27*
Larynx SCC 68 / F	*Neo / adjuvant*	*Adrenal crisis Hypothyroidism*	*3*	*Nivo*	*3*	*Surgery*
Oral SCC 46 / M	*Neo / recurrent*	*Psoriasis*	*3*	*Nivo*	*12*	*Chemo: Carb/5FU/Cetx*

P563

Characterizing immune-mediated adverse events of anti-PD-1 and anti-CTLA-4 monotherapies and combinations using a quantitative model based meta-analysis

Gabriel Helmlinger, PhD[1], Boris Shulgin, PhD[2], Yuri Kosinsky, PhD[2], Andrey Omelchenko, PhD[2], Lulu Chu, PhD[1], Ganesh Mugundu, PhD[1], Garrett DeYulia, PhD[1], Rodrigo Pimentel, MD[1], Kirill Peskov, PhD[2]

[1]*AstraZeneca, Waltham, MA, USA*
[2]*M&S-Decisions LLC, Moscow, Russian Federation*

Background
Immune checkpoint inhibitors (ICIs) may be associated with treatment-mediated and immune-mediated adverse events (trAEs and imAEs, respectively), in particular when used in combination. The objective of this model-based meta-analysis (MBMA was to characterize immune mediated AEs of anti-PD-1 and anti-CTLA-4 monotherapies and combinations, normalized by drug exposure and drug potency.

Methods
We performed an exhaustive search of clinical ICI safety data in PubMed-Medline, the ASCO Abstracts, TrialTrove, and other sources. To quantitatively compare safety across monotherapy and combination studies, we normalized the data by drug exposure, as derived from pharmacokinetic models for anti-PD-1 and anti-CTLA-4 agents, and by drug potency. A cross-study model-based meta-analysis (MBMA) of safety was then performed for Grade 3&4 trAEs and imAEs, for five organ classes: gastrointestinal (GI), skin, pulmonary, hepatic, and endocrine. Exposure vs. safety meta-regression and subgroup analyses were implemented with the R software metafor package.

Results
Safety data from 133 cohorts out of 82 publications on 65 clinical trials were built into the study-level database for ICI trAEs and imAEs. Performing the corresponding MBMA, we determined: (a) no significant dependence on dose, for both Grade 3&4 total AEs and imAEs, under anti-PD-1 monotherapies, except for rare GI imAEs; (b) significant dose dependence, for both Grade 3&4 total AEs (increase from 23% [low] to 40% [high dose]) and hepatic AEs (increase 1% to 7%), under anti-CTLA-4 monotherapies, (c) significant anti-CTLA-4 dose dependence, for both Grade 3&4 total AEs (increase from 35% to 52%) and hepatic (increase 6.5% to 19%), GI, skin and endocrine AEs, under anti-CTLA-4 and anti-PD-1 combination treatments. AE rates for anti-PD-1 and anti-CTLA-4 combinations were supra additive vs. AE rates in the respective monotherapy, with an increase of ~10% for Grade

3&4 AES and ~15% for Hepatic AEs. Furthermore, under combination treatments, AE rates were from 5% (monotherapy) up to 20% (combination) higher in 1L patients (vs. other lines of treatment) and also about 15% higher in patients with positive PD-L1 status (vs. PD-L1 negative). Higher AE rates, generally, were also associated with higher efficacy responses to ICI therapies (Figure 1).

Conclusions

A comprehensive database combined with an exposure/potency-normalized MBMA of ICI-related imAEs enabled a quantitative comparison of AEs across anti-PD-1 / CTLA-4 mono- and combination therapies, and in relation to key patient characteristics (PD-L1 status, line of treatment) and efficacy measures. This analysis may support rational dose selection and can be applied to other ICI agents, in mono- and combination treatment settings.

Figure 1. Dependence of Grade 3&4 AEs upon ICI drug exposure

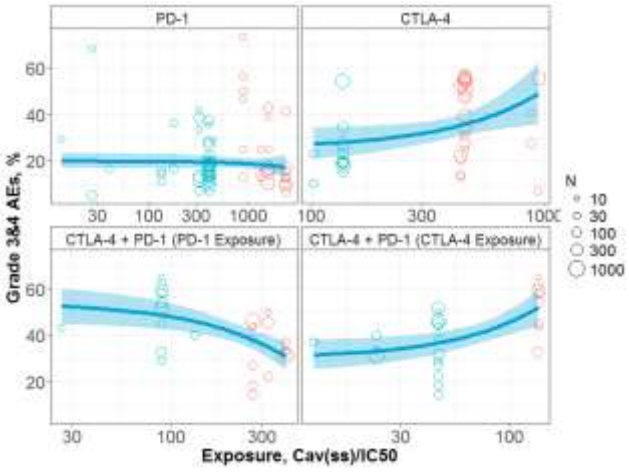

P564 Abstract Travel Award Recipient

Interleukin-6 gene expression is highly upregulated in immune checkpoint mediated enterocolitis

Daniel Johnson, MD[1], Cara Haymaker, PhD[1], Khalida Wani, PhD[1], Wai Chin Foo, MD[1], Salah Eddine Bentebibel[1], Yinghong Wang, MD, PhD[1], Jonathan Curry, MD[1], Adi Diab, MD[1], Jennifer Wargo, MD, MMSc[2], Alexandre Reuben[2], Elizabeth Burton[2]

[1]MD Anderson Cancer Center, Houston, TX, USA
[2]MD Anderson, Houston, TX, USA

Background

A deep understanding of the immunobiology of checkpoint inhibitor (CPI) induced immune related toxicities (irAEs) could lead to development of strategies that uncouple autoimmunity from anti-tumor immunity. Immune-related enterocolitis (irEC) is the most common serious complication from CPIs. Interleukin-6 (IL-6) is a key cytokine in autoimmunity (rheumatoid-arthritis, inflammatory-bowel disease) contributing to acute and chronic inflammation and is an essential differentiating cytokine committing naïve CD4+T-cells into T-helper17 (Th17) lineage. The role of Th17 cells in irAEs is not fully explored, and their tumor immunity function is controversial. Through RNA gene-expression profiling, we sought to identify the critical immune pathways in irEC and how these compare to the immune signatures in CPI-responding tumor samples.

Methods

Total RNA from patient-matched irEC and normal colon FFPE tissue from patients [n=12] receiving CPIs (aPD-1 = 3, aCTLA-4= 7, aCTLA-4 + aPD-1 = 2) were profiled with the NanoString nCounter PanCancer Immune Profiling Panel (NanoPCIP). Of the 770 NanoPCIP-panel genes, fold change in gene expression were compared between the normal and inflamed colonic tissue using two-sample T tests. P-

values were corrected using Benjamin-Yekutieli adjusted false discovery rate, and an adjusted p-value < 0.05 were considered significant. We also summarized fold-changes in gene-expression in CPI-responding melanoma tumors from a longitudinal NanoPCIP panel immune signature analysis previously performed at our institution.

Results

Significantly upregulated differentially expressed genes (DEGs) in the inflamed irEC tissue was observed in 52 genes compared to the normal colon control (adjusted p<0.05; figure 1). The highest up-regulated DEG encoded for IL6 (Fold change of +24.1). Other genes highly upregulated included IL-11 (a member of the IL-6-type cytokine-family) and genes that encode chemotactic molecules (Table-1).In our melanoma historical control, 173 DEGs significantly upregulated with a-CTLA-4 treatment (pre vs. on-treatment tumors) had a significant interaction with treatment-response. Only one gene was concordantly in our highest up-regulated DEGs in colitis (CXCL2). Most of our 10 highest colitis DEGs were not significantly up-regulated in tumors of CPI-responders compared to non-responders (Table-1). None of the 10 genes significantly and highest up-regulated in responding tumors were significantly upregulated in irEC (Table-2).

Conclusions

IL6 was the most significantly upregulated gene within inflamed-irEC samples compared to matched controls; the majority were not upregulated in association with tumor-response to CPIs. Our data suggest that IL-6 is important in irEC. IL-6-mediated inflammation may be more prevalent in irEC than in the responding tumors; targeting IL-6 may ameliorate irEC without hindering anti-tumor immunity.

Table 1.

Gene	Rank	Fold change (irEC v Normal Colon)	Adjusted P-value	Gene	Rank	Fold change in tumors (IL vs NR)	Adjusted P-value
CD45RA	1	24.1	**0.0042**	CD45RA	N/A	Not tested	N/A
CHIT1	2	9.5	**0.0109**	CHIT1	602	0.901	**1.00**
CD200R1	3	9.24	**0.0089**	CD200R1	N/A	Not tested	N/A
C3	4	7.61	**0.0369**	C3	192	1.50	**0.346**
CCL19	5	7.4	**0.0080**	CCL19	117	1.77	**0.521**
PDCD1	6	7.02	**0.0040**	PDCD1	140	1.65	**0.9**
NLRC3	7	6.86	**0.0048**	NLRC3	N/A	Not tested	N/A
CD3G	8	6.04	**0.0026**	CD3G	270	1.35	**1.00**
GZMA	9	5.83	**0.0024**	GZMA	261	1.37	**0.919**
GZMK	10	5.4	**0.0019**	GZMK	153	1.60	**0.174**

Table 2.

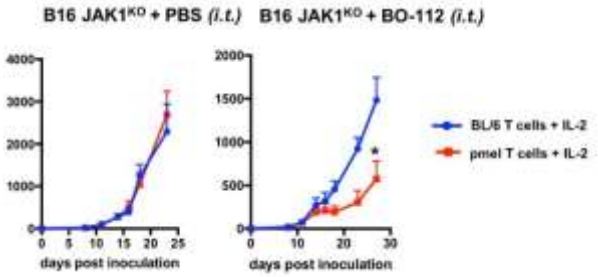

Figure 1.

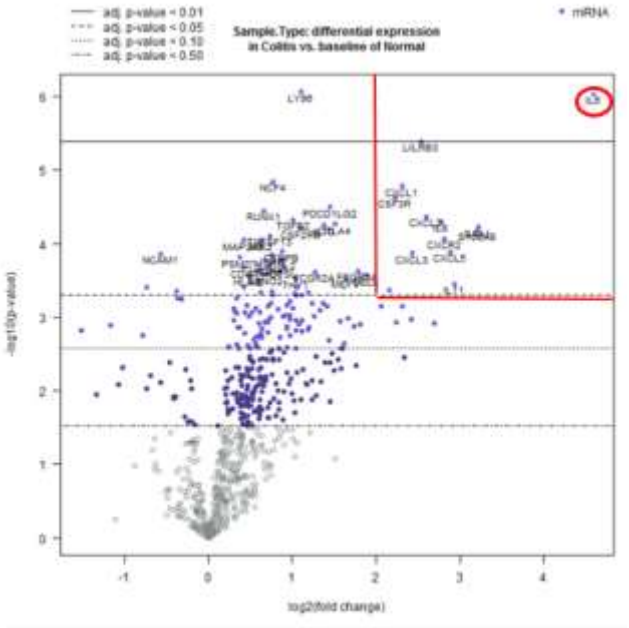

P565

Characterization of lymphoid cells in synovial fluid from cancer patients with immunotherapy-associated arthritis

Sang Kim, MD, PhD[1], Roza Nurieva, PhD[1], Jean Tayar, MD[1], Huifang Lu, MD, PhD[1], Jennifer Wang, MD[1], Don Gibbons, MD[1], Guillermo Garcia-Manero, MD[1], Maria Suarez-Almazor, MD, PhD[1], Patrick Hwu, MD[1], Adi Diab, MD[1]

[1]*MD Anderson Cancer Center, Houston, TX, USA*

Background

Immune related arthritis (ir-arthritis) is well documented Checkpoint inhibitors (ICIs) toxicity [1]. Ir AR occur in ~2% of cancer patients who receive ICI [2,3,4]. Although it is not life-threatening toxicity, it is clinically symptomatic toxicity and can severely impact the patients' quality of life and can lead to disconsolation of ICI treatment. Usually, ir-arthritis requires a substantially prolonged period of immune suppression compared to other irAEs, which we may negatively impact and compromise the clinical anti-cancer benefit. A deeper understanding of the immunobiology of ir-arthritis and detailed immune-characterization of the inflamed tissues will possibly allow us to develop treatment strategies that lead to uncoupling autoimmunity from anti-tumor immunity. Here, we characterize synovial immune cells isolated from five patients who developed ir-arthritis post-ICI.

Methods

We analyzed synovial fluid from five symptomatic patients, who developed ir-arthritis (joint pain and swelling) after ICI treatment. Using flow cytometry, we stained lymphoid immune cells with lineage-specific markers and measured effector cytokines in the CD4+ T cell populations.

Results

Median time of joint aspiration from the first ICI-infusion was 34 weeks (Range [4,166]). Arthritis was initially treated with systemic or local injection of prednisone. Two patients achieved complete resolution of arthritis ("steroid responders") while three patients remained refractory with partial relief/response to prednisone requiring additional/alternative treatment ("steroid refractory"). Immune analysis demonstrated that CD4+ T cells (53.1±13.2%) most abundant lymphoid immune-cells followed by CD8+ T cells, NK cells, NK T cells, and B cells. Most CD4+ and CD8+ T cells were effector memory phenotype. Several relevant CD4+ T-cell subsets were identified in the synovial fluid, including regulatory T cells (Treg), naïve T cells, Th1 (CXCR3hi CCR6lo), Th17.1 (CXCR3hi CCR6hi), Th17 (CXCR3lo CCR6hi), and follicular helper T cells (CXCR5+). Effector CD4+ T cell cytokines, including interferon gamma, IL-4, IL-17, and IL-21, were produced by both Tregs and non-Tregs. Interestingly, IL-17 producing non-Tregs were expanded in synovial fluid from steroid –refractory patients compared to synovial fluid from steroid-responders, suggesting that Th17 cells might play a role in persistent ir-arthritis and steroid resistance.

Conclusions

Although our preliminary data is very limited and descriptive in nature, we find the observed expansion of IL-17 producing non-Tregs in synovial fluid from steroid- refractory very intriguing and consistent with our prior recent publication of a successfully treated patients with steroid resistant ir-arthritis with IL-6 blockade [5]. Larger and prospective studies with longitudinal collection of tissue and blood are planned.

References

1. Suarez-Almazor ME, Kim ST, Abdel-Wahab N, et al. Review: Immune-Related Adverse Events With Use of Checkpoint Inhibitors for Immunotherapy of Cancer. Arthritis Rheumatol 2017;69(4):687-99.

2. Cappelli LC, Gutierrez AK, Baer AN, et al. Inflammatory arthritis and sicca syndrome induced by nivolumab and ipilimumab. Annals of the rheumatic diseases 2017;76(1):43-50.
3. Robert C, Schachter J, Long GV, et al. Pembrolizumab versus Ipilimumab in Advanced Melanoma. The New England journal of medicine 2015;372(26):2521-32.
4. Prieto PA, Yang JC, Sherry RM, et al. CTLA-4 blockade with ipilimumab: long-term follow-up of 177 patients with metastatic melanoma. Clin Cancer Res 2012;18(7):2039-47.
5. Kim ST, Tayar J, Trinh VA, et al. Successful treatment of arthritis induced by checkpoint inhibitors with tocilizumab: a case series. Annals of the rheumatic diseases 2017;76(12):2061-64.

Ethics Approval
The study was approved by MD Anderson Cancer Center's ethic board (Protocol number: PA16-0935)

P566

Hypoalbuminemia as a predictor factor for immune related adverse events (irAEs) in advanced melanoma patients treated with immune checkpoint inhibitors (ICIs)

E Rahma, MD[2], Steven Blum, MD[2], Jeffrey Ishizuka, MD,DPhil[2], Taha Qazi, MD[3], Rawad Elias, MD[4], Kruti Vora, BA[5], Alex Ruan[5], Anita Giobbie-Hurder, MS[2], Shilpa Grover, MD, MPH[3], Rizwan Haq, MD, PhD[2], Meredith Davis[2], Maria Gargano, PA-C[2], Elizabeth Buchbinder, MD[2], Patrick Ott, MD, PhD[2], F. Stephen Hodi, MD[2]

[1]*Dana-Farber Cancer Institute, Boston, MA, USA*
[2]*Dana Farber Cancer Institute, Boston, MA, USA*
[3]*Brigham and Women Hospital, Boston, MA, USA*
[4]*Boston Medical Center, Hartford, CT, USA*
[5]*Harvard Medical School, Boston, MA, USA*

Background
Despite the expansion of Immune checkpoint inhibitors (ICIs) indications there is limited data to date on predictors of ICIs' immune related adverse events (irAEs).

Methods
Melanoma patients (pts) who received anti-CTLA-4 (ipilimumab), anti-PD-1 (pembrolizumab or nivolumab), or the combination at the Center for Immuno-Oncology and Melanoma at DFCI in the past 5 years (up to December 31-2016) were included. Patients with irAEs were divided into 2 groups based on the severity of AEs: Grade (G) 1-2 and ≥ G 3. We analyzed the following patient characteristics and their prediction for irAE grade: Gender, age, BMI, ECOG, smoking and alcohol history, Flu or pneumonia vaccine administered within 6 months of starting ICIs, infections while on ICIs, history of autoimmune disease, asthma, and seasonal allergies. The following lab values were collected prior to starting ICIs: Albumin, LDH, neutrophil/lymphocyte ratio, and eosinophil count. We also analyzed the following: Prior chemo, targeted or radiation therapy, the presence of Kit, BRAF, or NRAS mutation, the number of metastatic sites, and concomitant medications (ACE and ARB inhibitors, NSAID, PPI, statins, antibiotics and vitamin D). Multivariable logistic regression of grade 3-4 vs. grade 1-2 irAEs was fit using the preceding characteristics as candidate predictors.

Results
We identified 213 patients who received a total of 246 ICIs (44 pts had 2 and 5 pts had 3 ICIs). The maximum grade irAEs reported were: G1 or 2 (92 pts, 43%), G 3 or 4 (121 pts, 57%). Table 1 summarizes the type of ICI the patient was taking at the time of the worst grade irAE. Patients who received combination of ICIs had significantly increased risk of grade 3-4 irAEs compared with patients who received single ICI. Patients with albumin levels above 4.2 had significantly reduced

risks of G 3-4 irAEs compared with patients who had lower albumin level (table 2).

Conclusions

This is the first report to identify hypoalbuminemia as a predicting factor for the development of grade 3-4 irAEs while on ICIs. Hypoalbuminemia could represent poor nutritional status that may predispose patients to irAEs. We are in the process of performing correlative analyses using cytokine Luminex to identify inflammatory markers that could predict toxicity, and this will be correlated with the observation of an association between hypoalbuminemia and higher incidence of grade 3-4 irAE.

Acknowledgements

Parker Institute for Cancer Immunotherapy for providing funding for this project

Ethics Approval

The study was approved by Dana-Farber Institutional Review Board (IRB)

Table 1. Type of ICI received at time of worst irAEs grade

	Maximum irAE grade	
	1-2	*3-4*
	N	*N*
Checkpoint class		
Combination with Ipilimumab	30	63
Ipilimumab	33	33
Nivolumab	12	5
Pembrolizumab	59	32

Table 2. Prediction Model for irAEs

P-values			
Predictor	DF	Wald Chi-Square	P-value
Checkpoint class	3	20.97	0.0001
Albumin	1	4.25	0.04

Odds Ratio Estimates			
Predictor	Point Estimate	95% Wald Confidence Limits	
Checkpoint class			
Combination vs. Pembrolizumab	3.89	2.09	7.21
Ipilimumab vs. Pembrolizumab	1.93	1.02	3.66
Nivolumab vs. Pembrolizumab	0.68	0.20	2.27
Combination vs. Ipilimumab	2.01	1.04	3.88
Albumin (> 4.2 vs. ≤ 4.2)	0.57	0.34	0.97

P567

A meta-analysis of immune checkpoint inhibitors tumor type and dose-toxicity correlation

E Rahma, MD[1], E Rahma, MD[1], E Rahma, MD[1], E Rahma, MD[1], Joshua Reuss, MD[2], Ghazaleh Shoja E Razavi, MD[3], Rawad Elias, MD[4], Anita Giobbie-Hurder, MS[1], Samir Khleif, MD[5*]

[1]Dana-Farber Cancer Institute, Boston, MA, USA
[2]Sidney Kimmel Cancer Center, Baltimore, MD, USA
[3]Tom Baker Cancer Centre, Alberta, Canada
[4]Boston Medical Center, Hartford, CT, USA
[5]Georgetown University, Washington, DC, USA

Background

The relationship between ICIs dose-escalation and toxicity has not been established. We performed a meta-analysis of clinical trials investigating ICIs to understand whether there is a correlation between dose or disease type and toxicity.

Methods

We searched PubMed and abstracts presented at national and international meetings for trials (T) using FDA-approved ICIs including Ipilimumab, Atezolizumab, Nivolumab, and Pembrolizumab. The

rates of treatment-related grade 3-5 adverse events (G3/4 AEs) were collected and the overall incidence rates for each dose cohort (DC) were estimated using exact binomial methods. Generalized linear models with GEE were fit to assess important predictors of G3/4 AEs.

Results

A total of 52 T published between January 2010 and December 2017 were reviewed. The overall incidence rate of G3/4 AEs was 34% in melanoma T using Ipilimumab. Patients (Pts) treated at 3 mg/kg q3w (3 T) had 27% reduced risk of G3/4 AEs compared to 10 mg/kg q3w (3 T) (Figure 1, Table 1). There was no difference in the incidence of G3/4 AEs for urothelial cancer (2 T) vs. NSCLC (3 T) using Atezolizumab (1200mg q3w) (Figure 2, Table 2). The investigation of Nivolumab included 39 DC within 24 different T. We compared the following DC: 2mg/kg q3w (2 DC), 3 mg/kg q2w (20), ≤ 1mg/kg q2w (8), ≤ 1mg/kg q3w (2), 10 mg/kg q2w (4), 10 mg/kg q3w (3). The overall incidence rate of G3/4 AEs was 22% which was significantly lower for pts with NSCLC than any of the other tumor types (26-40% reductions). No relationships between dose and incidence of AEs were noted (Figure 3, Table 3). The Pembrolizumab analysis consisted of 23 DC from 17 reported T. Frequencies of DC: 2 mg/kg q3w (3), 200 mg q3w (8), 10 mg/kg q3w (5), 10 mg/kg q2w (7). The incidence of G3/4 AEs was significantly lower in melanoma compared to any of the other tumor types (20% risk reduction). Pts receiving flat dose of 200mg had significantly lower odds of G3/4 AEs compared to 2 mg/kg q3 (P= 0.04) or 10 mg/kg q2 or 3w (P= 0.01) (Figure 4, Table 4).

Conclusions

This is the largest meta-analysis to date investigating dose-toxicity relationship of ICIs. There is a clear correlation between increased dose and toxicity using CTLA-4 antibodies (Ipilimumab). However, there is no evidence of dose-toxicity correlation using Nivolumab, while a flat dose of Pembrolizumab was associated with lower toxicity compared to weight-based dose.

Figure 1. Incidence of Grade 3-5 Adverse Events Ipilimumab

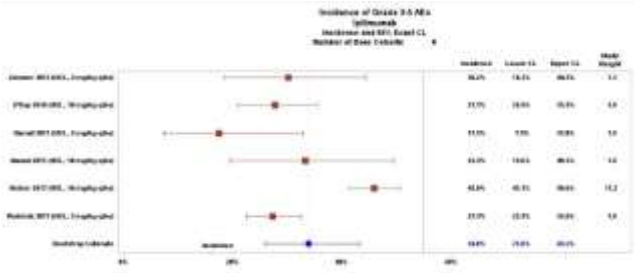

Figure 2. Incidence of Grade 3-5 Adverse Events Atezolizumab

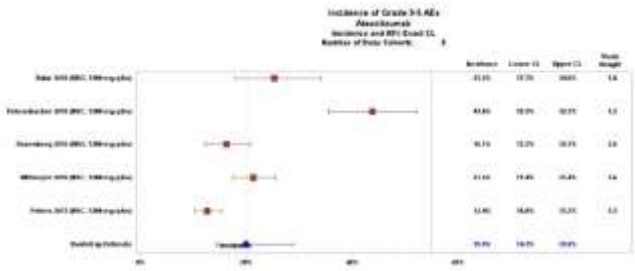

Figure 3. Incidence of Grade 3-5 Adverse Events Nivolumab

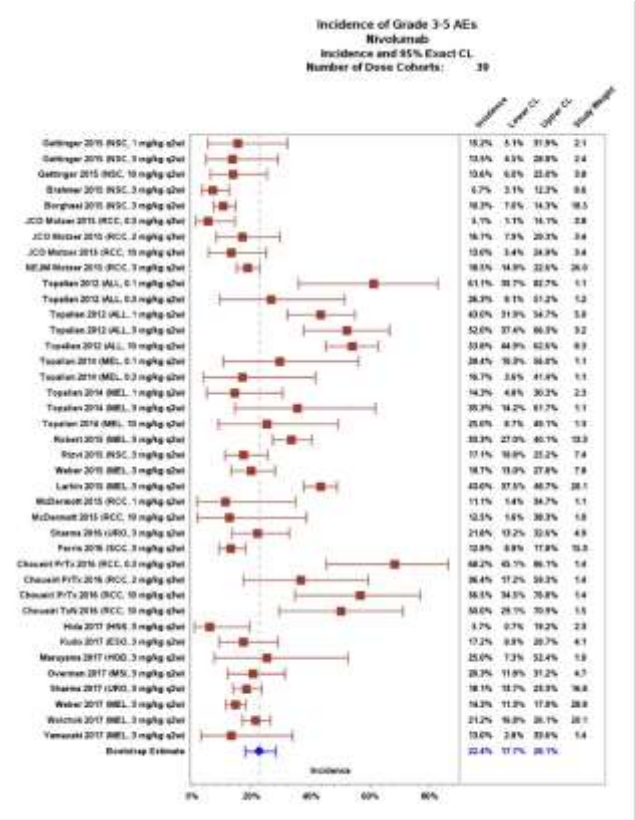

Figure 4.Incidence of Grade 3-5 Adverse Events Pembrolizumab

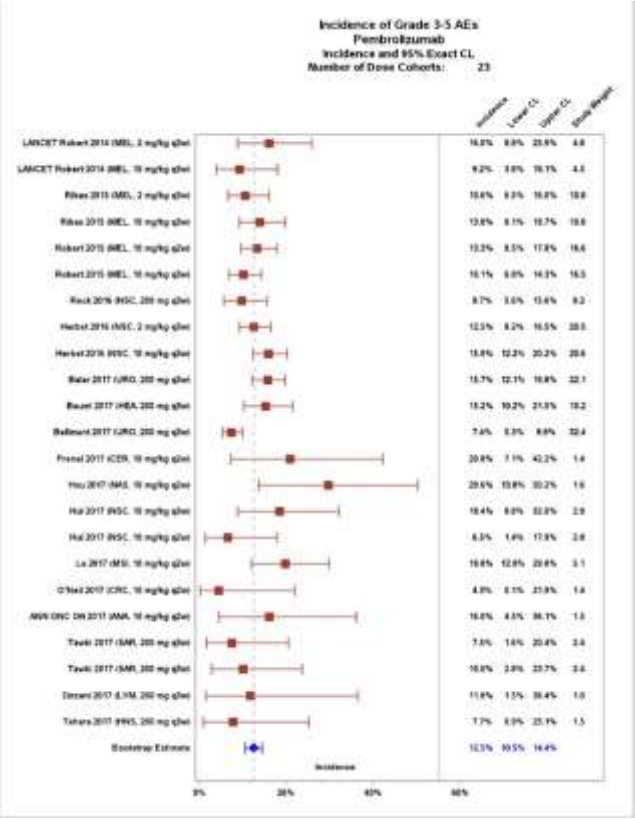

Table 1. Dose-Toxicity Correlation of Ipilimumab

Comparison	Odds ratio	95% CI			p-value
3 mg/kg q3w vs 10 mg/kg q3w	0.73	0.28	1.89		0.503

Table 2. Tumor Type-Toxicity Correlation of Atezolizumab

Comparison		Odds ratio	95% CI		p-value
Urothelial vs NSCLC		0.89	0.71	1.39	0.89

Table 3A. Tumor Type-Toxicity Correlation of Nivolumab

Comparison		Odds ratio	95% CI		P
NSCLC	RCC/MRCC	0.74	0.57	0.95	
NSCLC	MULTIPLE	0.64	0.47	0.88	
NSCLC	MELANOMA	0.60	0.39	0.90	
RCC/MRCC	MULTIPLE	0.87	0.66	1.16	
RCC/MRCC	MELANOMA	0.81	0.55	1.19	
MULTIPLE	MELANOMA	0.93	0.61	1.41	

Table 3B. Dose-Toxicity Correlation of Nivolumab

Comparison		Odds ratio	95% CI		
≤ 1 mg/kg q2w	≤ 1 mg/kg q3w	1.21	0.21	7.19	
10 mg/kg q2w	10 mg/kg q3w	1.12	0.39	3.20	
≤ 1 mg/kg	2 or 3 mg/kg	1.15	0.34	3.91	
≤ 1 mg/kg	10 mg/kg	0.56	0.14	2.19	
2 or 3 mg/kg	10 mg/kg	0.49	0.23	1.15	

Table 4A. Tumor Type-Toxicity Correlation of Pembrolizumab

Comparison		Odds ratio	95% CI		P
MELANOMA	NSCLC	0.90	0.78	1.03	
MELANOMA	MULTIPLE	0.80	0.66	0.98	
NSCLC	MULTIPLE	0.89	0.72	1.11	

Table 4B. Dose-Toxicity Correlation of Pembrolizumab

Comparison		Odds ratio	95% CI		
2 mg/kg q3w	200 mg q3w	1.24	0.99	1.57	
10 mg/kg q3w	200 mg q3w	1.31	1.04	1.66	
10 mg/kg q2w	200 mg q3w	1.32	0.99	1.75	
10 mg/kg q3w	10 mg/kg q2w	1.00	0.81	1.22	

P568

Pembrolizumab induced multiple immune related adverse events including myasthenia gravis, hepatitis and thyroiditis in a patient with thymoma

Kyunghoon Rhee, MD[1], Taeyeong ko, MD[1], Sangmin Chang, MD[1], Ji Hyun Rhee, MD[2], Lee Chun Park, MD[1], Young Kwang Chae, MD[1]

[1]Northwestern Univ, Feinberg School Med, Towson, MD, USA
[2]Greater Baltimore Medical Center, Towson, MD, USA

Background

The rapidly developing field of cancer immunotherapy has shown remarkable progress in its utilization as a treatment option of various tumors in recent years. Although it is currently not recommended as a first line treatment for thymoma, pembrolizumab, which blocks the PD-1 pathway thereby enhancing the immune system, is used as an alternative option in treatment. However, it was shown to also induce rare immune-related adverse events (irAEs) in multiple organs [1, 2], which have been reported in limited cases.

Methods

Here we report a case of possible pembrolizumab induced myasthenia gravis (MG), hepatitis and thyroiditis.

Results

A 60-year-old female with metastatic thymoma on her second cycle of pembrolizumab presented with worsening SOB for two weeks, left ptosis, limited extra-ocular movement, lower bifacial, upper and lower extremity weakness. She was thought to have either pembrolizumab induced MG or unmasking of occult thymoma related MG, supported by elevated acetylcholine receptor binding antibodies. She was treated with pyridostigmine, IVIG, and

plasmapheresis. On labs, TSH was found to be increased and free T4 decreased. Considering her normal thyroid functions before immunotherapy and the rapid development of hyperthyroidism within 2 weeks after the second cycle, pembrolizumab induced thyroiditis was suspected.In addition, she had gradually increasing Alk-P, AST, ALT and total bilirubin. Liver biopsy demonstrated marked portal and lobular T-cell infiltration with bile duct injury, consistent with immune modulator drug effect. She was treated with steroids and Cellcept with improvement in her LFTs. However, she developed septic shock and died.

Conclusions

This is a patient with stage IV thymoma on pembrolizumab who developed multiple irAEs. It is important to have a high clinical suspicion of such irAEs, and not only to discontinue the culprit PD-1 inhibitor but also to start early treatment for each involved organ. Since pembrolizumab is not a standard treatment of stage IV thymoma, there are only few reports of irAEs in thymoma. We do not know if pembrolizumab induced a new onset MG or exacerbated underlying MG. It is also unclear if simultaneous development of MG, hepatitis and thyroiditis is only unique in thymoma. Further investigation of irAEs in thymoma patients on pembrolizumab is therefore warranted.

References

1. Hofmann L et al. Cutaneous, gastrointestinal, hepatic, endocrine, and renal side-effects of anti-PD-1 therapy. Eur J Cancer. 2016 Jun;60:190-209
2. Zimmer L et al. Neurological, respiratory, musculoskeletal, cardiac and ocular side-effects of anti-PD-1 therapy. Eur J Cancer. 2016 Jun;60:210-25.

Consent

Consent top publish was received.

Microbiome and Anti-Tumor Immunity or I-O Agent Toxicity

P569

Novel Pharmacobiotic approach to enhance the tamoxifen efficacy using bacterial extracellular vesicles as the immunotherapy in breast cancer

Jeongshin An, MD,PhD[1], Yeun-yeoul Yang[1], Won-Hee Lee[2], Jinho Yang[2], Jong-kyu Kim[1], HyunGoo Kim[1], Se Hyun Paek[1], Jun Woo Lee[1], Joohyun Woo[1], Jong Bin Kim[1], Hyungju Kwon[1], Woosung Lim[1], Nam Sun Paik[1], Yoon-Keun Kim[2]

[1]Ewha Womans University, Seoul, Republic of Korea
[2]MD healthcare company, Seoul, Republic of Korea

Background

The anti-cancer effect of bacteria has a long history. According to Bierman et al., spontaneous remission of cancer has been observed in patients with severe bacteremia[1]. The reason was not revealed at that time, but we studied that in breast cancer. There are four main ways in which microbiota affects cancer: probiotics, prebiotics, drugs that target microbial enzymes and microbial products that have anticancer properties[2]. Among them, bacterial extracellular vesicles(EVs) are one of microbial products. In this study, we investigated the effects of bacterial EVs on the growth of breast cancer cells and tamoxifen efficacy.

Methods

Here, we analized microbiota of urine samples by NGS to select the target EVs that were expected to affect the growth of breast cancer cells. A total of 347 female urine samples – from 127 breast cancer patients (cancer group) and 220 normal individuals (control group) – were collected and analyzed by NGS using a universal bacterial primer of 16S rDNA. Human breast cancer cells were cultured, and the cells were treated with EVs of S. aureus and

K.pneumoniae for 72 h. Real-time polymerase chain reaction (PCR) and Western blotting for signalling molecule analysis were performed after treatment of EVs in each breast cancer cell.

Results

There was a significant difference in the distribution of bacterial EVs between the urine samples from breast cancer patients and from normal controls. Especially, S.aureus EVs were predominant in the normal group, and K.pneumoniae was abundant in the breast cancer group. Therefore, we selected these two bacterial EVs that may have an effect on breast cancer cell growth. We found that S.aureus and K.pneumoniae EVs down-regulated cell growth in MDA-MB-231 cells. We also found that S.aureus or K.pneumoniae EVs had a synergic effect on growth inhibition of while co-treated with tamoxifen. S.aureus EVs down-regulated mRNA expression of cyclin E2 and up-regulated that of TNF-alpha which was related ERK pathway while co-treated with tamoxifen.

Conclusions

The anti-cancer effect of S.aureus and K.pneumoniae was initiated by its bacterial EVs and consequently inhibited the growth of breast cancer cells in triple negative breast cancer cells and improved the efficacy of tamoxifen in ER-positive cells. In the near future, we plan to conduct animal studies which are expected to further clarify the effect of bacterial EV on breast cancer.

References

1 Bierman, H. R. et al. Remissions in leukemia of childhood following acute infectious disease. Staphylococcus and streptococcus, varicella, and feline panleukopenias. Cancer 6, 591-605 (1953).2 Zitvogel, L., Daillère, R., Roberti, M. P., Routy, B. & Kroemer, G. Anticancer effects of the microbiome and its products. Nature Reviews Microbiology 15, 465 (2017).

Ethics Approval

The study was approved by Ewha Womans University Medical Center's Ethics Board.

Consent

Written informed consent was obtained from the patient for publication of this abstract and any accompanying images. A copy of the written consent is available for review by the Editor of this journal.

Figure 1.

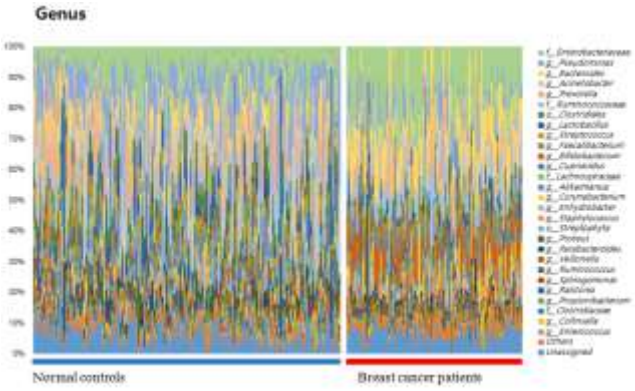

Figure 2.

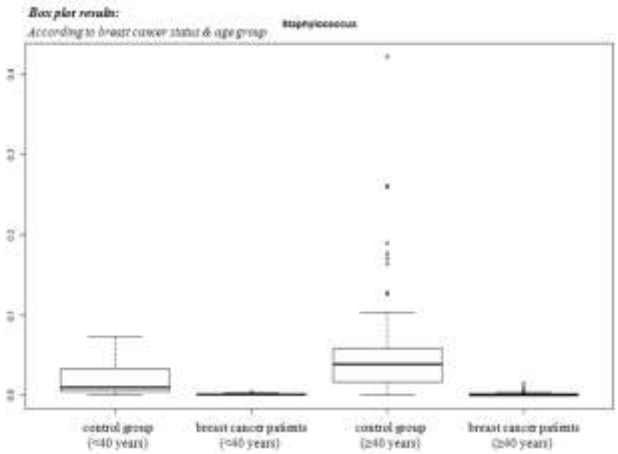

Figure 3.

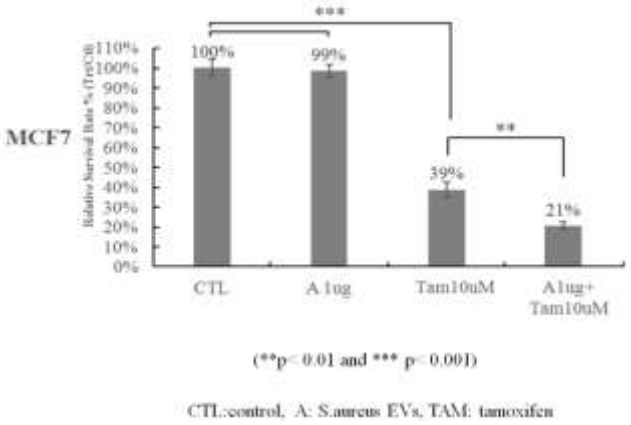

Figure 4.

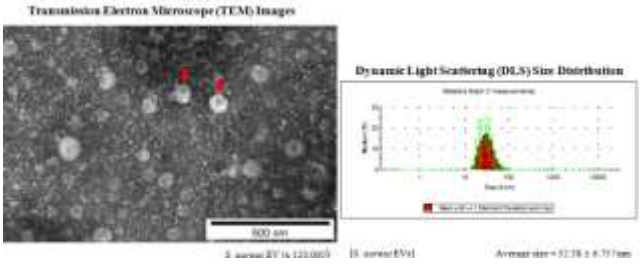

Figure 5.

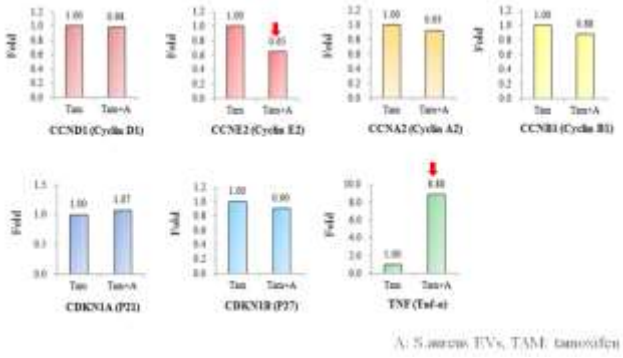

Figure 6.

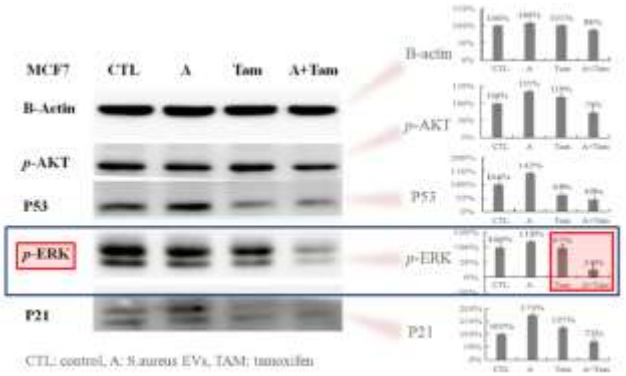

Figure 7.

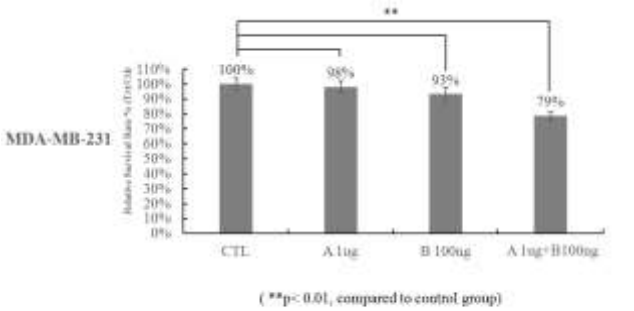

P570

Commensal bacteria Bifidobacterium stimulates an anti-tumor response via cross-reactivity.

Catherine Bessell, BA[1], Catherine Bessell, BA[1], Ariel Isser[1], Jonathan Havel, PhD[2], Sangyun Lee, PhD[3], Ruhong Zhou, PhD[4], Jonathan Schneck, MD, PhD[1], David Bell, PhD[3]

[1]*Johns Hopkins University, Baltimore, MD, USA*
[2]*Memorial Sloan Kettering Cancer Center, New York, NY, USA*
[3]*IBM Thomas J. Watson Research Center, New York, NY, USA*
[4]*Columbia University, New York, NY, USA*

Background
While recent studies have shown an important role of the microbiome in modulating anti-tumor immune responses, its mechanism remains unclear. One proposed mechanism is due to cross-reactivity between antigens expressed in commensal bacteria and neoepitopes found in tumors. We have identified a cross-reactive antigen expressed in commensal bacteria Bifidobacterium (Bifido) "SVYRYYGL" (henceforth called SVY) and show that it conveys a neoantigen-specific cross-reactivity to the classic neoantigen "SIY."

Methods
The SVY-specific response was analyzed through biophysical experiments and molecular dynamics simulations to determine antigen processing and MHC binding. T cell expansion studies from SIY and SVY T cell populations along with cross specificity studies reveals the cross-reactive T cell populations. B6 mice housed from Jackson, Bifido colonized mice, and Taconic, Bifido lacking, mice were used for examine Bifido colonization on T cell expansion. Sorting cross-reactive T cell populations from Bifido positive or negative mice based on antigen specificity and T cell receptor (TCR) beta sequencing allows to examine the effect of colonization on TCR repertoire composition. Finally the anti-tumor activity of the commensal bacteria population against the cross-reactive tumor antigen was tested by adoptive transfer studies with B16-SIY melanoma model.

Results
The SVY-specific response results from SVY peptide binding the H2-Kb MHC and can be processed from whole bacteria. The commensal bacteria SVY-specific T cells population has a cross-reactive SIY-specific T cell response and can recognize tumors expressing the "SIY" antigen. Mice lacking Bifido have a decreased SVY-specific T cell response and an altered (TCR) repertoire compared to Bifido. colonized animals. Bifido. colonization not only shapes the SVY-specific TCR repertoire but selects for clones that are represented in the SIY TCR repertoire. Cross-reactive SVY-specific T cells recognize tumors bearing SIY in vivo in an adoptive T cell transfer model of murine melanoma and leads to decreased tumor growth and extended survival.

Conclusions
Our work demonstrates that commensal bacteria can directly stimulate anti-tumor immune responses via T cell cross-reactivity and provides a proof of principle for how bacterial antigens can shape the T-cell landscape.

P571

Targeted sequencing of 16s rRNA Gene to understand the diversity and composition of the gut microbiome

Rajesh Gottimukkala, MS[1], Jianping Zheng[2], Karen Clyde, PhD[2], Fiona Hyland[2], Janice Au-Young, PhD[2]

[1]ThermoFisher Scientific, Fremont, CA, USA
[2]Thermo Fisher Scientific, south san francisco, CA, USA

Background
Recent studies in humans and experiments in mouse models demonstrated the key role of the gut microbiota in modulating the tumor response to check point blockade immunotherapy. One study showed an association between negative outcome using CTLA-4 blockade therapy and the absence of a specific gut microbiome. So, the gut microbiota has emerged as a promising biomarker to assess the efficacy of immune-modulatory drugs. Next generation sequencing of the 16S rRNA Gene is widely used as standard for understanding the composition of the gut microbiome.

Methods
The AmpliSeq pan-Bacterial Research panel that contains 24 primer pairs targeting the 16S rRNA gene

provides a cost-effective approach to identify the bacterial species present in the sample. Due to highly homologous nature of 16S sequences, it is challenging to correctly identify organisms at the Genus/Species level using short reads. We have developed a new algorithm that can identify all the organisms in the 16S database at Genus level and a majority at Species level. For every sequence in the database, we construct a coverage pattern using the aligned reads across the multiple amplicons. By matching the observed pattern per sequence with an expected pattern that is pre-computed we can identify the organisms present in the sample. The algorithm reports the identified microbes with Genus/Species level taxonomic classifications and the relative abundance of the organisms in the sample.

Results

We sequenced DNA from 12 fecal samples with the assay using Ion GeneStudio S5 System and detected the 25 frequently observed Genera across all the samples including Bifidobacterium, Lactobacillus, Clostridium, Ruminococcus and Bacteroides etc. We sequenced a metagenomics mock community sample comprising of 20 different strains and identified all the 20 species including few organisms relevant to cancer microbiome studies like H.pylori, E.Faecalis, B.vulgatus etc. We did an in-silico analysis using the primers in the assay and demonstrated that using the assay we can identify the frequent bacterial microbes in Gut microbiome resolved to Genus and/or Species level.

Conclusions

The AmpliSeq Pan-Bacterial Research panel with the described Bioinformatics pipeline will enable usage of 16s rRNA sequencing to assess the Gut microbiome as a biomarker for immunotherapy.

P572 **Abstract Travel Award Recipient**

Variation of the gut microbiome of complete responders to immune checkpoint blockade and healthy individuals – implications for clinical trial design

Beth Helmink, MD PhD[1], Vancheswaran Gopalakrishnan, MPH, PhD[1], Abdul Wadud Khan, MD[1], Pierre-Olivier Gaudreau[1], Elizabeth Sirmans[1], Elizabeth Burton[1], Vanessa Jensen, DVM[1], Adrienne Duran, BAS[1], Linsey Martin[1], Angela Harris[1], Miles Andrews, MD, PhD[1], Jennifer McQuade, MD[1], Alexandria Cogdill, MEng[1], Christine Spencer, PhD[1], Reetakshi Arora[1], Nadim Ajami, PhD[1], Joseph Petrosino, PhD[2], Jamal Mohamed[1], Sapna Patel, MD[1], Michael Wong, MD PhD FRCPC[1], Rodabe Amaria, MD[1], Jeffrey Gershenwald, MD[1], Patrick Hwu, MD[1], Wen-Jen Hwu, MD, PhD[1], Michael Davies, MD, PhD[1], Isabella Glitza, MD, PhD[1], Hussein Tawbi, MD, PhD[1], George Marnellos[3], Jaclyn Sceneay[3], Jennifer Wortman[3], Lata Jayaraman[3], David Cook[3], Theresa LaVallee[4], Robert Jenq, MD[1], Timothy Heffernan, PhD[1], Jennifer Wargo, MD, MMSc[1]

[1]MD Anderson Cancer Center, Houston, TX, USA
[2]Baylor College of Medicine, Houston, TX, USA
[3]Seres Therapeutics, Cambridge, MA, USA
[4]Parker Institute Cancer Immunotherapy, San Francisco, CA, USA

Background

The gut microbiome has been shown to have profound influences on host and anti-tumor immunity, and pre-clinical studies suggest that gut microbiota may be modulated to enhance responses to immune checkpoint blockade [1-4]. Recent studies demonstrate differences in the gut microbiome of responders (Rs) versus non-responders (NRs) to anti-PD-1 therapy in patients [5-8], with identification of a microbiome signature associated with a 100% response rate (Type-1 signature) [5]. Several clinical

trials are in development/underway that aim to modulate the microbiome to augment responses to immune checkpoint blockade. These are, in part, based on foundational evidence that treatment with fecal microbiota transplant (FMT) from healthy donors is associated with clinical responses in other diseases (*C. difficile* infection and inflammatory bowel disease, CDI and IBD)[9]; however, the optimal donors for FMT to enhance responses to immune checkpoint blockade remain incompletely understood.

Methods

To address this critical question, we performed profiling of the gut microbiota (via 16s and metagenomic sequencing) in a cohort of patients with complete responses (CRs) to anti-PD-1 therapy (n=11) versus healthy controls[10] (n=116). Importantly, immune profiling was also performed in available baseline tumor biopsies from CRs. Diversity (inverse Simpson) and composition of the gut microbiota was assessed in each of these cohorts, and FMT of selected CR donors versus a known NR (n=3 and 1, respectively) was then performed into gnotobiotic mice and melanoma tumors were implanted. Mice were then treated with immune checkpoint blockade. Tumor outgrowth was assessed and longitudinal microbiome analyses and immune profiling of tumor and the periphery in FMT-treated mice were also performed.

Results

Characterization of gut microbiota revealed wide variation in the diversity and composition of the gut microbiota, with preliminary work demonstrating a trend towards higher diversity in CR donors versus healthy controls (p=0.2); validation in a larger cohort of CRs is ongoing. Interestingly, not all CRs demonstrated a Type-1-like signature (with higher relative abundance of Clostridiales versus Bacteroidales) (27%, n=3/11) nor did healthy controls 28% (n=33/116). This has critical implications for FMT donor selection in immune checkpoint blockade trials (versus those for CDI or IBD). Murine studies demonstrated reduced tumor growth in CR-FMT mice vs. NR-FMT mice, with variability noted between donors. Immune profiling in available patient tumor samples and in murine studies and comparisons to gut microbiota are currently being performed.

Conclusions

Together, these studies provide important information about potential donor selection in FMT trials in immunotherapy, warranting additional studies and translational research.

References

1. Borody TJ, Khoruts A. Fecal microbiota transplantation and emerging applications. Nat Rev Gastroenterol Hepatol. 2011;9:88-96.
2. Frankel AE, Coughlin LA, Kim J, Froehlich TW, Xie Y, Frenkel EP, Koh AY. Metagenomic shotgun sequencing and unbiased metabolomic profiling identify specific human gut microbiota and metabolites associated with immune checkpoint therapy efficacy in melanoma patients(). Neoplasia (New York, NY). 2017;19,848-855.
3. Garrett WS. Cancer and the microbiota. Science. 2015; 348, 80-86.
4. Gopalakrishnan V, Spencer CN, Nezi L, Reuben A, Andrews MC, Karpinets TV, Prieto PA, Vicente D, Hoffman K, Wei SC, et al. Gut microbiome modulates response to anti-PD-1 immunotherapy in melanoma patients. Science. 2017.
5. Matson V, Fessler J, Bao R, Chongsuwat T, Zha Y, Alegre ML, Luke JJ, and Gajewski TF. The commensal microbiome is associated with anti-PD-1 efficacy in metastatic melanoma patients. Science. 2018; 359, 104-108.
6. McDonald D, Hyde E, Debelius JW, Morton JT, Gonzalez A, Ackermann G, Aksenov AA, Behsaz B, Brennan C, Chen Y, et al. American gut: an open platform for citizen science microbiome research. mSystems 3. 2018.
7. Routy B, Le Chatelier E, Derosa L, Duong CPM,

Alou MT, Daillere R, Fluckiger A, Messaoudene M, Rauber C, Roberti MP, et al. Gut microbiome influences efficacy of PD-1-based immunotherapy against epithelial tumors. Science. 2017.
8. Segre JA. Microbiome. Microbial growth dynamics and human disease. Science. 2015; 349, 1058-1059.
9. Sivan A, Corrales L, Hubert N, Williams JB, Aquino-Michaels K, Earley ZM, Benyamin FW, Lei YM, Jabri B, Alegre ML, et al. Commensal Bifidobacterium promotes antitumor immunity and facilitates anti-PD-L1 efficacy. Science. 2015; 350, 1084-1089.
10. Vetizou M, Pitt JM, Daillere R, Lepage P, Waldschmitt N, Flament C, Rusakiewicz S, Routy B, Roberti MP, Duong CP, et al. Anticancer immunotherapy by CTLA-4 blockade relies on the gut microbiota. Science. 2015; 350,1079-1084.

Ethics Approval
The study was approved by MD Anderson Cancer Center Institutution's Ethics Board, approval numbers LAB00-063, PA15-0232, and RN00001344-RN01.

P573

Antibiotic use and clinical outcomes of PD-1 antagonists in advanced non-small cell lung cancers

Amit Kulkarni, MD[1], Manish Patel, DO[1], Ying Wang, MD, PhD[1], Todd Defor, MS[1]

[1]*University of Minnesota, Minneapolis, MN, USA*

Background
Pre-clinical evidence in mice suggests that antibiotics induced dysbiosis can negatively influence efficacy of immune check-point inhibitors (ICI). The effects of antibiotic use on clinical outcomes of ICI are limited and has yielded inconsistent results. We evaluated whether antibiotic use impacts efficacy of PD-1 inhibitors in patients with advanced non-small-cell lung cancer (NSCLC)

Methods
We retrospectively reviewed clinical outcomes of advanced NSCLC patients treated with nivolumab or pembrolizumab at our institution between 5/2015 to 5/2018. Patients who received antibiotics 3 months prior to initiating ICI were considered to be in the Antibiotic exposure (ATB+) group. The remainder of patients were included in antibiotic naïve (ATB-) group. The primary outcome was clinical benefit rate (CBR) defined as proportion of patients with complete response (CR), partial response (PR) or stable disease (SD) per RECIST 1.1 among patients eligible for response assessment. Secondary outcomes of interest included progression-free survival (PFS) and overall survival (OS) across the entire patient population. Logistic regression and Cox proportional hazards model were used to compare outcomes between ATB+ and ATB- groups.

Results
111 patients were included in the analysis. The median age was 66 years (range 36-87 years). The majority of patients were female (55%), Caucasian (94%) and had adenocarcinoma (61%) histology. Most patients received Nivolumab (91%) in the second or subsequent line. 30% patients had brain metastasis prior to receiving ICI. 44 (39%) patients received antibiotics up to 3 months prior to ICI initiation, most received fluoroquinolones for respiratory infections. 96 patients were eligible for response assessment (>3 doses before restaging). Antibiotics exposure did not impact CBR, 63% in ATB+ and 53% in ATB- group (OR=1.5; p=0.36). Similarly, no statistically significant difference was seen in median PFS and OS between the two groups (PFS 4.1 months vs 2.8 months, p=0.66 and OS of 12 months vs 10 months, p=0.4 in ATB+ and ATB- group respectively). HR for association of antibiotic use with PFS and OS was 0.8 (p=0.36) and 0.8 (p=0.25) respectively. No significant difference was noted when controlling for age, sex, ECOG status, prior lines of therapy, brain metastasis and steroid use.

Conclusions
To our knowledge, this is the largest study showing clinical outcomes are not affected by prior antibiotic use in NSCLC patients receiving ICI. While our study has limitations, more studies are needed to establish an association. Data analysis of more patients is currently underway that will be reported in the final analysis prior to meeting.

P574

A rationally-designed consortium of human gut commensals induces CD8 T cells and modulates host anti-cancer immunity

Bruce Roberts, PhD[6], Takeshi Tanoue[1], Satoru Morita[1], Koji Atarashi[1], Wataru Suda[2], Damian Plichta[3], Seiko Narushima[4], Ashwin Skelly[1], Atsushi Shiota[5], Jason Norman[6], Vanni Bucci[7], Yutaka Kawakami, MD PhD[1], Masahira Hattori[2], Ramnik Xavier[3], Bernat Olle[6], Bruce Roberts, PhD[6], Kenya Honda, MD, PhD[8]

[1]Keio University School of Medicine, Tokyo, Japan
[2]Waseda University, Tokyo, Japan
[3]Broad Institute of MIT and Harvard, Cambridge, MA, USA
[4]Riken Center for Integrative Medical Science, Kanagawa, Japan
[5]JSR-Keio University Innovation Center, Tokyo, Japan
[6]Vedanta Biosciences, Cambridge, MA, USA
[7]University of Massachusetts, North Dartmouth, MA, USA
[8]Keio University School of Medicine and JSR-Keio University Innovation Center, Tokyo, Japan

Background
Clinical data suggests the gut microbiome influences response to checkpoint inhibitor therapy however the precise identity and mode of action of commensals associated with clinical response has not been elucidated. We report the generation of a consortium of human gut derived commensals capable of inducing CD8 T cells and augmenting anti-cancer immunity.

Methods
The microbiota of healthy humans was used to inoculate germ-free mice and assess the level of CD8 T cell induction. Human derived commensals were isolated from inoculated mice exhibiting high levels of CD8 T cell induction and sequenced. Consortia consisting of isolated human commensals were tested for the ability to induce CD8 T cells in germ-free and SPF mice. A minimal consortium capable of inducing CD8 T cells was administered with checkpoint inhibitor antibodies to tumor-bearing mice to assess anti-cancer activity and the level of accumulation of tumor infiltrating lymphocytes.

Results
Interferon-gamma producing CD8 T are abundant in the intestines of SPF but not germ-free mice. A consortium of human-derived commensals dubbed VE800 which robustly induces CD8 T cells in germ-free mice was identified. VE800 administration promotes activation of intestinal dendritic cells and stimulation of interferon-gamma producing CD8 T cells is dependent on the transcription factor BATF3. Comparative gene pathway analysis revealed several of the VE800 strains are related to strains associated with favorable clinical response in metastatic melanoma patients treated with immunotherapy. Administration of the VE800 cocktail with anti-CTLA4 enhanced anti-tumor activity and survival in the MC38 tumor model. VE800 also enhanced the anti-tumor activity of anti-PD1 in the MC38 and B-raf Pten melanoma tumor models. VE800 treatment alone is sufficient to enhance the level of tumor infiltrating CD8 T cells in the MC38 model to a level comparable to anti-PD1 alone however the combination of VE800 and anti-PD1 promoted the highest level of tumor infiltrating CD8 T cells in the MC38 model as well as in the more aggressive B-raf Pten model. VE800 administration promoted enhanced accumulation of interferon-gamma

producing CD8 T cells in the spleens of tumor-bearing mice indicating the consortium promotes systemic cellular immune cell activation.

Conclusions
A rationally-designed consortium of human gut-derived commensals induces CD8 T cells in vivo and potentiates anti-cancer immunity when administered with checkpoint inhibitors. Given the consortium can be produced via cGMP manufacturing and administered orally on a repeated basis, VE800 constitutes a safe agent for alteration of the microbiome of cancer patients to enhance anti-cancer immunity.

P575

Classification of the human gut microbiome using a validated 16S rRNA next generation sequencing method

Janet Doolittle-Hall[1], Melissa Howard[1], Jennifer Sims[1], Scott Yourstone[1], Jason Powers[1], Patrick Hurban, PhD[1], Victor Weigman[1]

[1]Q2 Lab Solutions, Morrisville, NC, USA

Background
Analysis of the gut microbiome composition is becoming increasingly important given its influence on a wide variety of human diseases including cancer. Numerous studies have indicated that the gut microbiome can influence cancer susceptibility, tumorigenesis and cancer progression at least in part through its profound impact on the immune cell function and its inherent metabolic capacity. Emerging evidence suggest that gut microbiome can be manipulated for improving the effects of cancer therapies. Microbiome composition and relative abundance of different microbial taxa can be measured by combining DNA sequencing of hypervariable regions of the 16S ribosomal RNA gene or a whole-genome shotgun sequencing with computational analysis. The scientific and clinical utility of microbial analysis by NGS strongly depends on the accuracy and precision of identifying and quantitating the microbial taxa. Here we report on the development and validation of a new assay and bioinformatics analysis pipeline for accurate taxonomic classification of complex microbial samples such as stool using 16S rRNA sequencing.

Methods
DNA isolation from stool was performed using a validated MoBio Power Soil method. Illumina 16S rRNA targeted sequencing was performed using custom PCR amplification primers for the bacterial 16S V3 and V4 regions and a 2x300 bp paired-end strategy. A bioinformatic sequence alignment and classification pipeline was developed to enable accurate taxonomic identification of constituent bacteria based on genetic differences in the hypervariable regions of the 16S rRNA gene. Output includes taxonomic classification and relative abundance of the identified taxa.

Results
Assay analytical performance was determined using admixtures of 4 bacterial strains, at varying levels, into human reference DNA. Correct bacterial species present at or above 0.01% relative abundance were detected with >99.9% accuracy and 100% detection sensitivity. Clinical feasibility with human stool samples is ongoing. In addition, feasibility of recovering microbial communities from formalin-fixed paraffin-embedded (FFPE) tumor tissues was demonstrated using short amplicon/ multiple primer Ion Torrent 16S rRNA sequencing method. Composition and structure of the recovered microbial communities were affected by the FFPE preparation methods, highlighting the need for standardization of the pre-processing procedures.

Conclusions
Analytically validated 16S rRNA sequencing assay, with our computational pipeline, offers an option for

accurate identification and classification of constituent microbiome components from complex mixtures at a lower coverage and cost option than would be required for shotgun metagenomic approaches. In addition, analysis of microbial communities is feasible from the FFPE tumor tissue.

Micro-RNA, Epigenetics and Tumor/Immune-cell Signaling Pathways in Anti-Tumor Immunity

P576

Evaluating the importance of inhibiting HDAC6 in metastatic breast cancer to enhance the efficacy of immunotherapy

Debarati Banik, PhD[2], Erica Palmer, BS[2], Melissa Beaty, MS[2], Satish Noonepalle, PhD[2], Maria Hernendez, BS[2], Prathima Vembu, MS[2], Alejandro Villagra, PhD[2]

[1]George Washington University, Washington DC, USA
[2]The George Washington University, Washington DC, USA

Background
Histone deacetylases (HDAC) are recognized to perform diverse functionalities beyond their conventional roles in remodeling the chromatin landscape. These functionalities may range from regulating the outcomes of cellular-health to local or systemic immune-diseases including autoimmunity and cancer, positioning the HDAC inhibitors (HDACi) at a crucial junction of immunotherapy. The excessive toxicity and variability among broad-spectrum HDACi have led to the development of more selective inhibitors, which helped to understand the individual roles of HDACs in shaping anti-tumor immune responses. One such member HDAC6 is reported to promote the pro-tumorigenic STAT3 pathway. By using ultra-selective HDAC6i, the downstream immune-modulatory pathways of STAT3, e.g. co-stimulatory pathways of PD-L1, PD-L2 and B7-H4 could be targeted. HDAC6 has been also involved in a number of structural functions related to cellular motility, shape and intracellular transport through the regulation of the acetylation of numerous targets, including tubulin and cortactin. This function is strongly suggestive of HDAC6 being a key player in metastatic cancer progression. We further hypothesize that by means of modulating PDL1 pathway, the TME and cytoskeletal molecules, HDAC6i may enhance the efficacy of anti-PD1 therapy in Triple Megative Breast Cancer (TNBC).

Methods
4T1 was used as a model for murine TNBC implanted orthotopically. Both in vitro and in vivo methods were used to investigate the HDAC6i NexturastatA, with or without combining with anti-PD1 antibody in vivo.

Results
NexturastatA was able to reduce primary tumor growth, as well as inhibit tumor invasion and modify the expression of EMT-specific gene signature, even in presence of metastasis-promoting cytokine IL6. Additionally, the size and number of secondary tumor nodules in the lungs were significantly diminished after the HDAC6i treatment. NexturastatA was also able to inhibit anti-PD1 antibody mediated enhancement in PDL1 expression in vitro, suggesting the utility of combining it with checkpoint inhibitor in vivo. While both anti-PD1 and CTLA4 treatments showed certain degrees of success in reducing tumor growth, we demonstrated that in a pre-treatment setting, HDAC6i improves anti-tumor responses when combined with anti-PD1. This was measured in terms of the primary and secondary tumor growth, composition of infiltrating immune cells in the primary tumor, EMT gene signature, and expression of co-stimulatory molecules as well as intra-tumoral interferon gamma expression, indicative of intra-tumoral effector T cell functionality.

Conclusions
NexturastatA alone and in combination with anti-PD1 antibody was able to modify some of the critical features of invasion and metastasis as well as properties of tumor microenvironment in TNBC.

Ethics Approval
The study containing animals was approved by the IACUC of the George Washington University under protocol number A385.

P577

Activation of GSK3-beta in the melanoma tumor microenvironment renders dendritic cells refractory to immune suppression and induces T cell activation and oncolysis

Marta Lopez Gonzalez, Msc[1], Rieneke van de Ven, PhD[1], Anita Stam[1], Wen Dong[1], Victor van Beusechem[1], Tanja de Gruijl, PhD[1]

[1]CCA Amsterdam UMC, Amsterdam, Netherlands

Background
Immune checkpoint blockade results in durable clinical responses in only a fraction of treated patients. There is a growing awareness that for immune checkpoint inhibitors to be effective, sufficient tumor infiltration by effector T cells is an absolute requirement. However, a crippled myeloid compartment in the tumor microenvironment (TME) will stand in the way of T cell activation and recruitment, due to the absence of properly developed and activated dendritic cells (DC), which, as a result, won't be able to cross-prime antitumor cytotoxic effector T cells and will fail to attract an effector T cell infiltrate through the release of key chemokines. It is therefore vital to develop methodologies to normalize DC differentiation and activation in the melanoma TME.

Methods
N/A

Results
We have recently uncovered a key role for GSK3β, a known repressor of Wnt signaling, in the control of DC maturation, both at the level of melanoma cells and at the level of DC and their precursors. Employing lysates from IL-10 modulated DC precursors on a peptide kinase substrate microarray, we identified putative signaling networks at play in melanoma-associated DC suppression. GSK3β came out on top of a list of modulated kinases and STRING network analysis revealed links to JAK/STAT, MAPK and Wnt signaling pathways, all previously implicated in cancer-mediated immune suppression. Using melanoma cell line supernatants and co-cultures (employing a set of 5 melanoma cell lines encompassing various oncogenic mutations, including BRAFv600, PTEN, and NRAS), we found that enforced overexpression of constitutively active GKS3β (CA.GSK3β) rendered DC differentiation and maturation refractory to the suppressive effects of melanoma, which appeared to involve both soluble mediators and cell-cell contact. This immune stimulatory effect was accompanied by decreased levels of both phosphorylated and non-phosphorylated β-Catenin in tumor cells, consistent with its reported degradation by activated GSK3β. Of note, virally enforced over-expression of CA.GSK3β in melanoma cells also reduced their DC-suppressive effects and at later time points reduced their proliferative ability and viability. As ex-vivo proof of concept of the therapeutic modulation of GKS3β in the melanoma TME, single-cell suspensions from melanoma metastases (n=4) were transduced with CA.GSK3β. As a result, we observed activation of DC subsets and of infiltrating T cells, reduced IL-10 levels, and specific tumor cell lysis.

Conclusions
We conclude that activation of GSK3β in the melanoma TME may simultaneously induce oncolysis

and alleviate DC immune suppression, thereby enabling T cell activation and effective immune checkpoint blockade.

P578

Application of multiplexed immunofluorescence and multispectral imaging to investigate TGFβ pathway activation of immune cell populations in human lung cancer

Sebastian Marwitz[1], Carmen Ballesteros Merino, PhD[2], Shawn Jensen, PhD[1], Bernard Fox, PhD[2]

[1]Robert W Franz Cancer Center, Borstel, Germany
[2]Robert W Franc Cancer Center, Portland, OR, USA

Background
Non-Small Cell Lung Cancer (NSCLC) is the leading cause of cancer-related death worldwide and is usually diagnosed in an already locally or systemically advanced state. Depending on the stage of the tumor, surgical therapy is limited and systemic therapy required. Recent developments with targeted therapies and immune checkpoint blockade resulted in improved survival for a limited number of patients but the magnitude of patients will still progress. The transforming growth factor beta signaling pathway (TGFβ) is frequently activated in lung cancer, involved in malignant progression and a possible target for therapy [1]. TGFβ signaling is known to inhibit immune responses, immune cell proliferation and to dampen effector functions in various immune cells [2]. Therefore we set out to investigate the activation of the TGFβ signaling pathway in different immune cell populations in human lung cancer to better define the cells that are affected by TGFβ.

Methods
Multiplexed immuno-fluorescence staining and multi-spectral imaging was used to investigate a cohort of > 200 early stage NSCLC specimens assembled on TMAs for activation of the TGFB signaling pathway by targeting phosphorylated SMAD3 and different immune cell markers. Image analyses were conducted to analyze spatial relationships and local abundances in the tumor as well as stroma in tissue samples from the tumor center or margin

Results
Overall, a significantly increased number of CD3, proliferating CD3 ($p < 0.001$) and CD3-phospho SMAD3 ($p < 0.05$) cells were observed in the stroma compared to tumor tissues, however the overall percentage of CD3pS3 remained unaltered between tumor and stroma, suggesting an equal impact on both compartments. In addition, adenocarcinomas exhibited a significantly increased abundance of CD3 in the tumor and stroma in both, the invasive margin or the central region of the tumor compared to squamous cell carcinomas.

Conclusions
Using multi-parameter tissue analyses to investigate the abundance of specific immune cell populations and pathway activation in the tumor-microenvironment of lung cancer tissues enables detailed analysis of immune signaling phenotypes. Somewhat surprisingly, these studies suggest that TGFβ impacts an equal percentage of CD3 T cells in both the stroma and tumor center.

Acknowledgements
Sebastian Marwitz is funded by the Deutsche Forschungsgemeinschaft (DFG) via MA 7800/1-1.

References
1. Marwitz S, Depner S, Dvornikov D, Merkle R, Szczygiel M, Müller-Decker K, et al. Downregulation of the TGF-β pseudoreceptor BAMBI in non-small cell lung cancer enhances TGF-β signaling and invasion. Cancer Research. http://doi.org/10.1158/0008-5472.CAN-15-1326.
2. Li MO, Wan YY, Sanjabi S, Robertson A-KL, Flavell

RA. TRANSFORMING GROWTH FACTOR-β REGULATION OF IMMUNE RESPONSES. Annual Review of Immunology. 2006; 24(1): 99–146.

Ethics Approval
This study was approved by University of Lübeck´s institutional review board number (Az. 18-026).

P579

The leukocyte chemoattractant chemerin modulates PTEN and PD-L1 expression and activity via CMKLR1 in human tumors

Keith Rennier, PhD[1], Gurpal Virdi, BS[1], Woo Jae Shin, BA[1], Russell Pachynski, MD[1]

[1]*Washington University School of Medicine, St. Louis, MO, USA*

Background
Chemerin (RARRES2) is an endogenous innate leukocyte chemoattractant previously shown to recruit immune cells via its receptor CMKLR1 into the tumor microenvironment and thereby suppresses tumor growth. RARRES2 has been shown to be downregulated in many tumor types, suggesting a mechanism of immune escape. The loss of the key tumor suppressor PTEN has been shown to promote resistance to T cell-mediated immunotherapy and correlates with decreased T cell tumor infiltration in humans, while restored PTEN functions to repress PD-L1 expression. Importantly, chemerin was recently shown to suppress metastatic hepatocellular carcinoma in a mouse model by upregulating the expression and activity of PTEN. Here, we evaluate the effects of chemerin on human tumor lines in vitro and elucidate its relationship with tumor PD-L1 expression and response to T cell anti-tumor immunity.

Methods
We utilized human tumor cell lines in vitro and exposed them to exogenous recombinant human chemerin. PTEN and PD-L1 expression in tumor lines was evaluated by RT-qPCR, flow cytometry, and/or western blot analysis. In vitro matrigel invasion assays were performed to investigate the impact of chemerin exposure on tumor intrinsic activity. T cell-mediated cytotoxicity assays explored the downstream effect of chemerin-mediated PD-L1 modulation. Knockdown of CMKLR1, PTEN or PD-L1 using siRNA was performed to demonstrate their mechanistic role in the chemerin-PTEN-PDL1 pathway.

Results
We show that recombinant chemerin significantly upregulates PTEN expression in multiple tumor cell lines. Concomitantly, chemerin exposure significantly decreased PD-L1 expression in DU145 tumor cells (Figure 1). Consistent with these data, chemerin treatment results in attenuated tumor cell migration/invasion and increased T cell mediated cytotoxicity in DU145 cells (Figures 2 and 3, respectively). Using siRNA, we found that CMKLR1 knockdown diminished the modulated PTEN activity and PD-L1 expression levels. Similarly, CMKLR1 knockdown completely mitigated chemerin's effect on tumor invasion and T cell mediated cytotoxicity, suggesting the functional significance of the chemerin/PTEN/PD-L1 axis in human tumor cells. Importantly, T cell cytotoxicity assays showed chemerin-mediated increases were comparable to direct knockdown of PD-L1 and an anti-PD-L1 antibody (atezolizumab) (Figure 4).

Conclusions
Here, we characterize for the first time a novel chemerin-PTEN-PDL1 interaction in human tumor cells. We have shown treatment with exogenous chemerin, through induction of PTEN, significantly reduces tumor migration and increases T cell mediated cytotoxicity via its impact on tumor PD-L1

expression. Ongoing experiments are focused on in vivo mechanisms of action and will serve as the basis for translational studies.

Figure 1. Chemerin upregulates PTEN decreases PD-L1 via CMKLR1

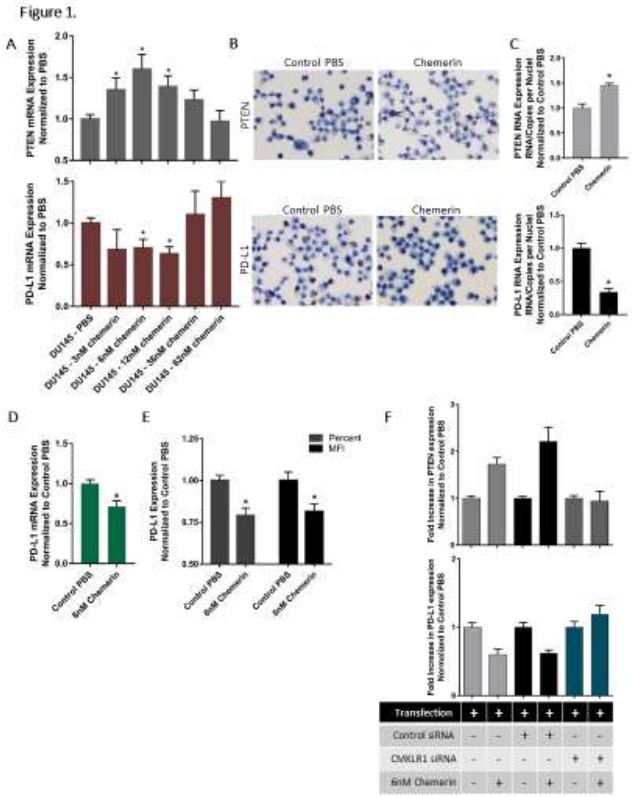

Figure 2. Chemerin diminishes tumor cell invasion via CMKLR1

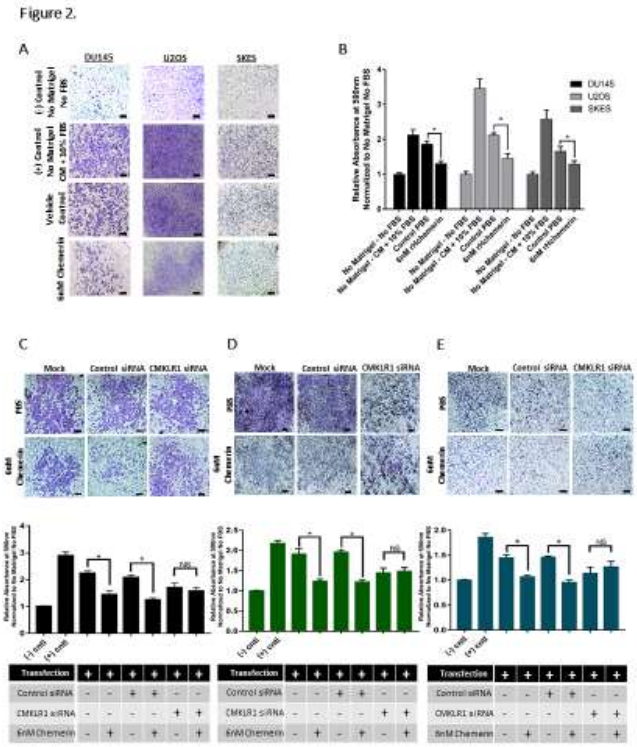

Figure 3. Cytotoxicity increased chemerin-treated tumor cells

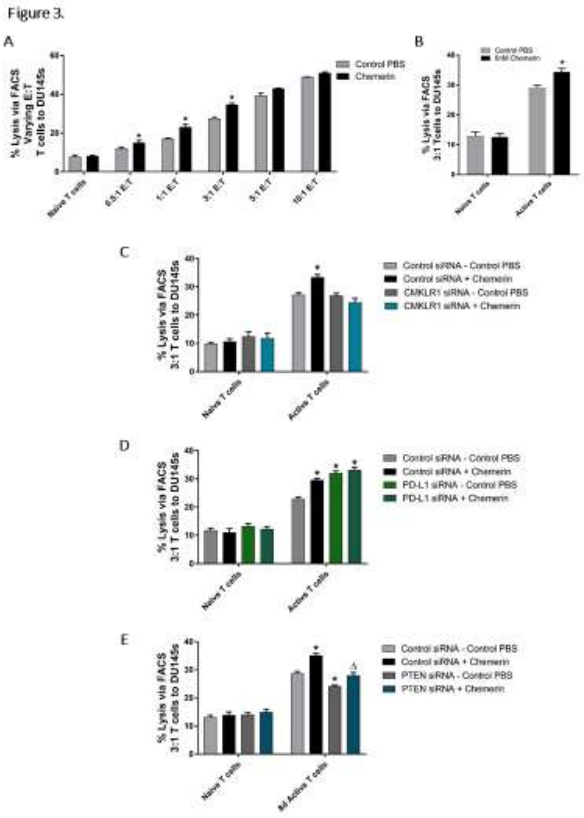

Figure 4. Chemerin treatment comp PD-L1 siRNA & atezolizumab

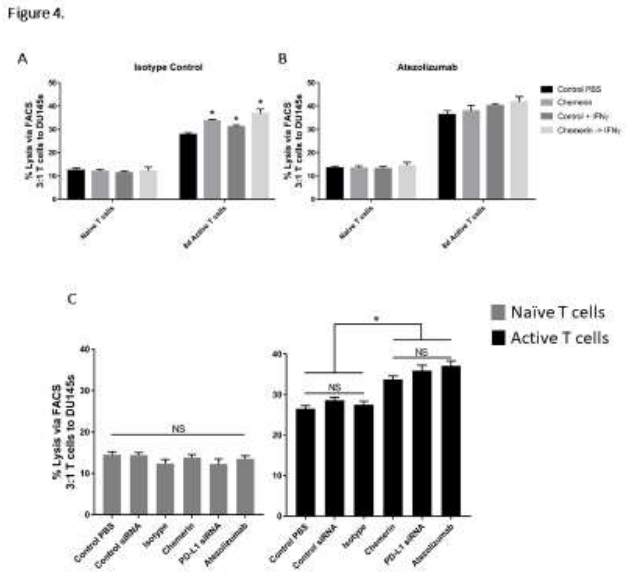

Oncogenetics and Immunogenomics

P580

Genomic portraits of immune escape mechanism in cold tumours

Venkateswar Addala, PhD[1], Futoshi Kawamata[1], Stephen Kazakoff, PhD[1], Pamela Mukhopadhyay[1], Catherine Bond[1], Katia Nones[1], Felicity Newell[1], Jennifer Borowsky[1], Scott Wood[1], Conrad Leonard[1], Qinying Xu[1], Matthew E Burge[2], Akinobu Taketomi[3], Toshiya Kamiyama[1], Barbara Leggett, MD FRACP[1], John Pearson[1], Vicki Whitehall[1], Ann-Marie Patch[3], Nic Waddell[3]

[1]QIMR Berghofer Medical Research Institute, Brisbane, QLD, Australia
[2]Royal Brisbane and Women's Hospital, Brisbane, Australia
[3]Hokkaido University, Sapporo, Japan

Background

Immunotherapy promises to revolutionise cancer treatment. 'Hot' tumors are responsive to immune checkpoint blockade that 'releases the breaks' of immune system to target tumor cells. High mutation/neoantigen burden with active tumor microenvironment markers predicts response to immunotherapy in tumors associated with UV damage in melanoma and microsatellite instability in colorectal cancer (CRC). However 'cold' tumours remain a major research challenge as they exist in an immune suppressed environment. In this study, we investigated the immune escape mechanism of microsatellite stable primary CRC and matched liver metastasis samples.

Methods

Whole genome sequencing and RNA sequencing of 15 matched primary CRC and matched liver metastases patients was performed. DNA and RNA Sequence analysis was performed using previously described methods [1] [2]. Four digit HLA class I allele types were determined by Polysolver [3] and Optitype [4] and loss of heterozygosity in the HLA loci was identified from tumor and normal samples using LOHHLA [5]. The pVAC-Seq neoantigen prediction framework [6] was applied to identify the neoantigens using NetMHCpan algorithm. Deconvolution of Immune cells were estimated using CIBERSORT [7] and TCR repertoire diversity predicted through MixCR [8] approach in all paired samples.

Results

Frequently shared neoantigens with IC50<500nM were identified in both primary tumor and liver metastasis but did not identify any mutations in antigen processing machinery genes. HLA allele specific loss of heterozygosity occurs in the majority of primary and metastatic samples whereas one metastatic sample showed inconsistency in HLA genotype from germline and primary tumor. The tumor micro-environment is dominated by lymphocytes in the primary tumor and macrophages in liver metastasis. TCR repertoire diversity found to be decreased at metastatic stage in few patients.

Conclusions

We found several potential immune escape mechanisms in these cold tumors. This included loss of heterozygosity of the HLA alleles which may lead to a decreased ability to present strong binding neoantigens to the tumor cell surface and so fail to activate immune system. Another mechanism is the loss in TCR diversity in a 10 patients which may result in the T cells being unable to recognise the diverse neoantigens present. In addition the tumor micro-environment in the metastases has become immunologically quiet with enrichment of macrophages and depletion of lymphocytes compared to the primary tumor micro-environment. Our findings highlight the mechanisms that may predict response to immunotherapies and also those that can be targeted in the future in order to convert cold tumours into hot tumours.

References

1. Waddell N, Pajic M, Patch AM et al. Whole genomes redefine the mutational landscape of pancreatic cancer. Nature. 2015;518:495.
2. Bailey P, Chang DK, Nones K et al. Genomic analyses identify molecular subtypes of pancreatic cancer. Nature. 2016;531:47.
3. Shukla SA, Rooney MS, Rajasagi M et al. Comprehensive analysis of cancer-associated somatic mutations in class I HLA genes. Nature biotechnology. 2015;33:1152.
4. Szolek A, Schubert B, Mohr C et al. OptiType: precision HLA typing from next-generation sequencing data. Bioinformatics. 2014;30:3310-6.
5. McGranahan N, Rosenthal R, Hiley CT et al. Allele-specific HLA loss and immune escape in lung cancer evolution. Cell. 2017;171:1259-71.
6. Hundal J, Carreno BM, Petti AA et al. pVAC-Seq: A genome-guided in silico approach to identifying tumor neoantigens. Genome medicine. 2016;8:11.
7. Newman AM, Liu CL, Green MR, Gentles AJ et al.

Robust enumeration of cell subsets from tissue expression profiles. Nature methods. 2015;12:453.
8. Bolotin DA, Poslavsky S, Mitrophanov I et al. MiXCR: software for comprehensive adaptive immunity profiling. Nature methods. 2015;12:380.

Ethics Approval
The study was approved by the QIMR Berghofer Medical Research Institute's Ethis Committee HREC (P2139) and the Hokkaido University Human Research Ethics Committee (HREC) (14-005)

P581

Whole-genome sequencing and multi-omic analysis of immuno-oncology biomarkers using formalin-fixed, paraffin-embedded samples

Shannon Bailey, PhD[1], Wanfeng Yu, PhD[1], Jim Lund, PhD[1], Richard Williams[1], Jeffrey Gulcher[1]

[1]*WuXi NextCODE Genomics, Arlington, MA, USA*

Background
Next-generation sequencing analysis of archival formalin-fixed, paraffin-embedded (FFPE) tumor samples has the potential to lead to significant insights in immuno-oncology when analyzed with their accompanying rich phenotypic and pathologic data. Analysis of tumor mutation burden (TMB) using FFPE tissues has previously been restricted to estimates from exome or gene panel sequencing approaches, which provide narrow views of mutation burden. Analysis of whole-genome sequencing (WGS) data derived from FFPE samples has been limited due to challenges in isolating quality DNA from these samples and the ability to distinguish true variant calls from artifacts. Despite these challenges, WGS approaches are optimal when applied to quality tumor specimens as they provide whole-genome coverage of all regions including untranslated regions, regulatory regions, human leukocyte antigen (HLA) loci, and microsatellite regions allowing complete microsatellite instability (MSI) analysis, direct TMB calculations, and overall higher quality data for neoantigen prediction.

Methods
We have developed an efficient DNA extraction method (SeqPlus) that produces abundant quantities of high-quality DNA and permits robust WGS sequencing of FFPE samples. This method additionally provides improved depth and evenness of coverage for WES sequencing. SeqPlus was used to sequence primary and relapsed tumor FFPE samples from several different cancer types to perform MSI, TMB, and related analyses. Using the same tissue, we also measured mRNA expression by RNA-Seq and DNA methylation by array analysis.

Results
Similar to previous studies, we found that, for the majority of samples, low MSI status and low TMB correlate. We also found that, while high MSI and elevated TMB often correlate, samples with high TMB with a low or stable MSI status are more common. A majority of samples without MMR mutations have alterations in one or more genes in other DNA repair pathways. Further analysis will examine correlations between repair gene expression and mutation burden status to investigate discrepancies e.g., samples with elevated TMB and high MSI without MMR mutations. The impact of MSI and the TMB status on DNA methylation will also be examined for key genes in a global measure of genome disruption in samples

Conclusions
Our data demonstrate the feasibility of using WGS of FFPE samples to enable patient selection strategies for immune checkpoint inhibitor therapies. Our approach may be useful in standard clinical care or trials in the future and facilitate retrospective analysis of archival FFPE cancer tissues. This method will enhance our understanding of genomic features that respond to immuno-oncology, targeted, or

conventional therapies.

P582

Implications of ARID1A deficiency on tumor microenvironment and immune landscape in non-small cell lung cancer (NSCLC)

Young Kwang Chae, MD[1], Pedro Viveiros, MD[1], Bhoomika Sukhadia, MD[1], Lee Chun Park, MD[1], Muhammad Mubbashir Sheikh, MBBS / MD[1], Jeffrey Chuang[2]

[1]*Northwestern University Feinberg School of Medicine, Chicago, IL, USA*
[2]*The Jackson Laboratory for Genomic Medicine, Farmington, CT, USA*

Background
AT-rich interactive domain-containing gene 1A (*ARID1A*) is the most frequently mutated gene in the SWI/SNF chromatin remodeling family [1, 2], involved in transcription regulation and DNA repair. Loss of function of *ARID1A* is associated with disruption of mismatch repair [2] and poor prognosis in many solid tumors, especially gastrointestinal [3,4] and gynecological cancers [5]. Due to its tumor suppressor nature, it was believed to be a poor therapeutic target [2]. Recently, *ARID1A* deficiency was shown to be associated with increased CD8 T-cell infiltration and expression of programmed death-ligand 1 (PD-L1) in ovarian cancer [2], implying the potential of *ARID1A* as a predictor of response to immune checkpoint inhibitors (ICIs). Since the role of *ARID1A* has not been explored in NSCLC, we investigated how *ARID1A* deficiency affected tumor microenvironment and immune landscape in these patients.

Methods
We obtained *ARID1A* mRNA levels for NSCLC samples [Adenocarcinoma (ADC), n=517; Squamous cell carcinoma (SqCC), n= 501] from TCGA. The data was arranged into 4 quartiles based on *ARID1A* expression derived from mRNA-seq z-scores, defining the lowest quartile (Q1) as low *ARID1A* and highest quartile (Q4) as high *ARID1A*. We examined how *ARID1A* expression levels correlated with a) PD-L1 expression and b) microsatellite analysis for normal-tumor instability (MANTIS) score [6]. We also evaluated tumor mutational burden (TMB), neoantigen burden and immune landscape [7] among low and high quartiles.

Results
In both ADC and SqCC, analysis of immune landscape demonstrated higher infiltration of activated CD8 T-cells in the low quartile (each $p<0.01$, Figure 1). Lower *ARID1A* expression was associated with higher PD-L1 expression in both ADC and SqCC (each $p<0.05$, Figure 2A and 2B). There was a significant difference in MANTIS score between the low and high *ARID1A* quartiles in both ADC and SqCC ($p<0.05$, $p<0.01$ respectively). One sample in the low quartile of each ADC and SqCC had microsatellite instability (MANTIS>0.4), while the rest of the samples had MANTIS score in the microsatellite stable range. No correlation was found between *ARID1A* expression and TMB or neoantigen burden.

Conclusions
In both lung ADC and SqCC, *ARID1A* deficiency appears to influence the tumoral immune landscape. This suggests that *ARID1A* deficiency could be harnessed to select patients who may derive benefit from immunotherapy even in microsatellite stable NSCLC patients.

References
1. Trizzino M, Barbieri E, Petracovici A, Wu S, Welsh SA, Owens TA, Licciulli S, Zhang R, Gardini A. The tumor suppressor ARID1A controls global transcription via pausing of RNA polymerase II. Cell Rep. 2018;23(13):3933-3945.
2. Shen J, Ju Z, Zhao W, Wang L, Peng Y, Ge Z, Nagel ZD, Zou J, Wang C, Kapoor P, Ma X, Ma D, Liang J,

Song S, Liu J, Samson LD, Ajani JA, Li GM1, Liang H, Shen X, Mills GB, Peng G. ARID1A deficiency promotes mutability and potentiates therapeutic antitumor immunity unleashed by immune checkpoint blockade. Nat Med. 2018;24(5):556-562.
3. Simbolo M, Vicentini C, Ruzzenente A, Brunelli M, Conci S, Fassan M, Mafficini A, Rusev B, Corbo V, Capelli P, Bria E, Pedron S, Turri G, Lawlor RT, Tortora G, Bassi C, Guglielmi A, Scarpa A. Genetic alterations analysis in prognostic stratified groups identified TP53 and ARID1A as poor clinical performance markers in intrahepatic cholangiocarcinoma. Sci Rep. 2018;8(1):7119.
4. Kim YS, Jeong H, Choi JW, Oh HE, Lee JH. Unique characteristics of ARID1A mutation and protein level in gastric and colorectal cancer: A meta-analysis. Saudi J Gastroenterol. 2017;23(5):268-274.
5. Itamochi H, Oumi N, Oishi T, Shoji T, Fujiwara H, Sugiyama T, Suzuki M, Kigawa J, Harada T. Loss of ARID1A expression is associated with poor prognosis in patients with stage I/II clear cellcarcinoma of the ovary. Int J Clin Oncol. 2015;20(5):967-973.
6. Kautto EA, Bonneville R, Miya J, Yu L, Krook MA, Reeser JW, Roychowdhury S. Performance evaluation for rapid detection of pan-cancer microsatellite instability with MANTIS. Oncotarget. 2017;8(5):7452-7463.
7. Angelova M, Charoentong P, Hackl H, Fischer ML, Snajder R, Krogsdam AM, Waldner MJ, Bindea G, Mlecnik B, Galon J, Trajanoski Z. Characterization of the immunophenotypes and antigenomes of colorectal cancers reveals distinct tumor escape mechanisms and novel targets for immunotherapy. Genome Biology 2015;16(1):64.

Figure 1.

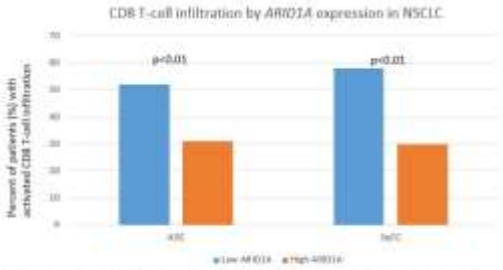

Figure 1. Activated CD8 T-cell infiltration by *ARID1A* expression in NSCLC samples from TCGA*
*Chi-square
NSCLC, non-small cell lung carcinoma; TCGA, The Cancer Genome Atlas; ADC, adenocarcinoma; SqCC, squamous cell carcinoma

Figure 2.

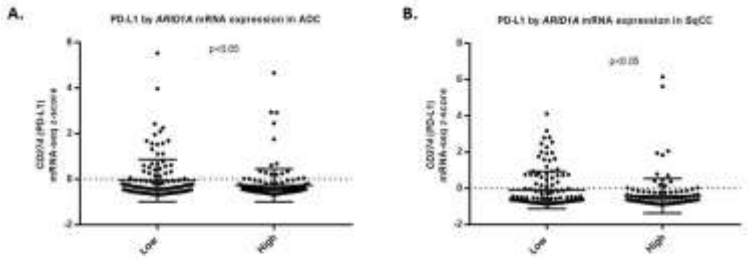

Figure 2. mRNA expression of *CD274* (PD-L1) by *ARID1A* expression in NSCLC samples from TCGA*
A. mRNA expression of *CD274* (PD-L1) by *ARID1A* expression in Low (Q1) vs High (Q4) in ADC ($p<0.05$)
B. mRNA expression of *CD274* (PD-L1) by *ARID1A* expression in Low (Q1) vs High (Q4) in SqCC ($p<0.05$)
*unpaired T-test with Welch's correction
NSCLC, non-small cell lung carcinoma; TCGA, The Cancer Genome Atlas; ADC, adenocarcinoma; SqCC, squamous cell carcinoma

P583

Single cell transcriptional immune landscape of human papilloma virus positive and negative head and neck squamous cell carcinoma

Anthony Cillo, PhD[1], Tullia Bruno, PhD[1], Tracy Tabib[1], Zengbiao Qi[1], Ting Wang[1], Umamaheswar Duvvuri[1], Ryan Soose, MD[1], Wei Chen[1], Robert Lafyatis[1], Robert Ferris[1], Dario Vignali, PhD[1]

[1]*University of Pittsburgh, Pittsburgh, PA, USA*

Background

Head and neck squamous cell carcinoma (HNSCC) develops through either exposure to environmental carcinogens (HPV— HNSCC), or through malignant transformation following infection with human

papillomavirus (HPV+ HNSCC) [1]. Patients with HPV+ HNSCC have longer overall survival compared to patients with HPV— HNSCC [2]. We hypothesize that these differences in etiology will contribute to a spectrum of immune transcriptional signatures ranging from similar to highly divergent between these two tumor microenvironments (TMEs).

Methods

Paired peripheral blood mononuclear cells (PBMC) and tumor specimens were obtained from immunotherapy treatment naïve HNSCC patients. PBMC and normal tonsils were obtained from healthy donors and patients undergoing tonsillectomy as treatment for sleep apnea. Viable CD45+ cells were isolated by fluorescence based cell sorting from PBMC, tumors, and tonsils. Single-cell RNA sequencing (scRNAseq) libraries were generated using a 3' droplet-based approach (10X Genomics). Filtered gene/barcode matrices were generated by CellRanger, and analysis was performed using the R packages SCRAN (library size deconvolution), Seurat (clustering and t-distributed stochastic neighbor embedding [tSNE]) and Destiny (diffusion-based pseudotime modeling).

Results

Single-cell RNAseq analysis identified a total of 57,891 single cells from 4 healthy donor PBMC, 2 tonsils, 6 paired PBMC and tumor infiltrating leukocytes (TIL) from HPV— HNSCC patients, and 5 paired PBMC/TIL from HPV+ HNSCC patients. Unbiased transcriptional analysis of TIL revealed that B cells and conventional CD4+ T cells (Tconv) had the greatest transcriptional differences between HPV+ and HPV— disease, while CD4+ regulatory T cells (Treg) were the most similar. B cells were more frequently detected in HPV+ versus HPV— disease, and B cells found in HPV+ tumors had transcriptional signatures consistent with germinal center B cells while those from HPV— tumors had memory B cell signatures. Tconv cells from HPV— HNSCC had type 1 helper signatures, while Tconv from HPV+ HNSCC expressed predominantly a T follicular helper cell signature. CD8+ T cells from HPV— HNSCC expressed higher levels of inhibitory receptors and were more terminally differentiated by diffusion pseudotime analysis. Treg cells from TIL expressed a signature associated with effector Treg cells, and this signature was consistent between HPV— and HPV+ HNSCC.

Conclusions

The transcriptional landscape of immune cells in HPV— versus HPV+ HNSCC differs by cell type, with B cells and CD4+ Tconv being the most divergent and CD4+ Treg the most consistent. These findings suggest that different immunotherapies may be required to achieve optimal clinical responses in these two types of HNSCC.

References

1. Marur S, et al. HPV-associated head and neck cancer: a virus-related cancer epidemic. Lancet Oncology. 2010 Aug;11(8):781-9.2. Fakhry C, et al. Improved survival of patients with human papillomavirus-positive head and neck squamous cell carcinoma in a prospective clinical trial. JNCI: Journal of the National Cancer Institute. 2008 Feb;100(4):261-9.

Ethics Approval

This study was approved by the local Institutional Review Board under protocol UPCI 99-069, and patients provided informed consent.

P584

High DNA repair activity is associated with immune exclusion in pediatric kidney cancers

Emily Higgs, BA[1], Ami Desai, MD[1], Riyue Bao, PhD[1], Thomas Gajewski, MD, PhD[1]

[1]*University of Chicago, Chicago, IL, USA*

Background

A T-cell rich tumor microenvironment has been associated with improved clinical outcome and better response to immune checkpoint blockade therapies in several adult cancers. Our group and others have discovered mechanisms, such as β-catenin activation and PTEN loss, that drive a lack of T cell infiltration in tumor. However, much less is known about the tumor microenvironment in pediatric cancers, which harbor a lower tumor mutational burden (TMB) than most adult cancers, as well as the molecular mechanisms responsible for driving T cell exclusion in these patients. Thus, we analyzed pediatric kidney cancer data from the Therapeutically Applicable Research to Generate Effective Treatments (TARGET) database.

Methods

RNAseq, somatic mutations, and clinical data were obtained for Wilms tumor (WT), rhabdoid tumor (RT), osteosarcoma (OS), and neuroblastoma (NBL) from TARGET, and adult kidney cancers from TCGA. After normalization and log2-transformation, we used a 26-gene activated CD8 T cell signature [1] and identified anti-correlated genes at Pearson's correlation r<-0.20 and FDR-adjusted P<0.05. Differentially expressed genes were detected by ANOVA at FDR-adjusted P<0.05 and fold change >2.0. Association with progression-free survival (PFS) and overall survival (OS) was assessed using Mantel-Cox test.

Results

Among the four pediatric cancers, we observed the lowest activated CD8 scores in WT, only detected in tumor and not in matched normal. We identified 2,128 significant genes negatively correlated with the score, 1,553 genes higher in WT compared to the adult kidney cancers, and 1,952 genes higher in WT than matched normals. There were 502 overlapping genes between these methods. Pathway analysis revealed the most activated pathways involve DNA repair. This was validated in RT. We then calculated a DNA repair expression score consisting of 4 genes (BRCA1, BRCA2, MSH2, MSH6). Within the FHWT histology where > 90% of the patients progressed, higher DNA repair score is associated with worse PFS (P=0.02), but not OS.

Conclusions

Our results showed that a higher DNA repair expression score is associated with lower activated T cell gene expression in childhood kidney cancers such as WT and RT, and is associated with worse survival. While loss of DNA repair pathways has previously been associated with increased neoantigens and greater response to checkpoint blockade immunotherapy, our current data suggest that upregulated DNA repair pathways may generate the opposite phenotype. Strategies targeting DNA repair pathways could be considered as new therapeutic interventions to transform non-T cell-inflamed pediatric tumors into clinically favorable tumors despite the low presence of somatic mutations.

References

1. Charoentong, Pornpimol, Finotello F, Angelova M, Mayer C, Efremova M, Rieder D, Hackl H, Trajanoski Z. Pan-cancer immunogenomic analyses reveal genotype-immunophenotype relationships and predictors of response to checkpoint blockade. Cell Reports. 2017; 18:248–62.

P585

Structured literature review and meta-analyses of the prevalence of microsatellite instability high (MSI-H) and deficient mismatch repair (dMMR) in endometrial and ovarian cancers

Maria Lorenzi[1], Mayur Amonkar, PhD[2], Jacky Zhang[1], Shivani Mehta[1], Kai-Li Liaw[2]

[1]*Precision Xtract, Oakland, CA, USA*
[2]*Merck and Co., Inc., North Wales, PA, USA*

Background
Pembrolizumab has been approved in the US for the treatment of patients with unresectable or metastatic MSI-H/dMMR solid tumors that have progressed after prior treatment. There is limited and inconsistent data on the prevalence of MSI-H and dMMR across solid tumors.

Methods
A structured literature review covering all solid tumor types identified English language publications that used immunohistochemistry (IHC) for all four MMR proteins or polymerase chain reaction (PCR) techniques using specified NCI or Promega marker panels. MEDLINE, EMBASE, Cochrane databases and key cancer congresses were searched for relevant publications. Data were extracted on the study population, sample size, MSI-H and dMMR prevalence. For this report, we summarized the studies and performed meta-analysis (random effects model) on the prevalence of MSI-H and dMMR among endometrial and ovarian cancers. If sufficient data were available, prevalence estimates were also obtained by geography, disease stage, and histology.

Results
Of 1,176 citations retrieved in the larger review across all tumor types, 53 and 23 studies reported prevalence of MSI-H or dMMR in endometrial and ovarian cancers, respectively. Among endometrial cancers, MSI-H pooled prevalence (with 95% CI) from 27 studies (6,813 patents) was estimated at 26% (23-29%) and dMMR pooled prevalence from 26 studies (5,248 patients) was estimated at 25% (22-28%). In ovarian cancers, MSI-H pooled prevalence from 17 studies (4,150 patients) was estimated at 11% (6-18%) and dMMR pooled prevalence from 5 studies (356 patients) was estimated at 8% (6-11%). Based on histology, the highest MSI-H pooled prevalence was observed for endometrioid subtype for each tumor with 30% (25-35%) based on 6 studies (1,204 patients) for endometrial cancers and 17% (25-35%) based on 3 studies (211 patients) for ovarian cancers. In both cancer types, pooled prevalence was further explored by geography and disease stage.

Conclusions
This comprehensive literature review provides pooled prevalence estimates of MSI-H and dMMR across two key gynecological tumors based on published data. The pooled prevalence estimates of MSI-H among endometrial and ovarian cancers were similar to the corresponding pooled prevalence estimates for dMMR for these tumors.

P586

Frameshift indel selectively correlates with immunotherapy outcome for advanced NSCLC

Wungki Park, MD[1], Lee Chun Park, MD[2], Vaia Florou, MD[3], Diana Saravia, MD[3], Sangmin Chang, MD[2], Si Wang, MD[2], Lauren Chiec[2], Ashkon Rahbari[2], Pedro Viveiros, MD[2], Bhoomika Sukhadia, MD[2], Muhammad Mubbashir Sheikh, MBBS / MD[2], Nisha Mohindra[2], Victoria Villaflor, MD[2], Gilberto Lopes, MD, MBA[3], Young Kwang Chae, MD[2], Wungki Park, MD[1]

[1]Memorial Sloan Kettering Cancer Center, New York, NY, USA
[2]Northwestern University, Chicago, IL, USA
[3]University of Miami, Miami, FL, USA

Background
Frameshift insertion-deletion (fsindel) was suggested as more immunogenic type of mutation associating with higher tumor-specific neoantigens which also correlated with clinical outcome of immunotherapy in melanoma and renal cell carcinoma patients[1]. Our group recently demonstrated that the presence of fsindel is also relevant in NSCLC patients treated with PD-1/L1 inhibitors-based immune checkpoint inhibitors (ICIs) independently from their Tumor Mutational Burden (TMB) [2]. Also, we showed

higher fsindel burden was associated with higher activated CD4 and CD8 T cell RNA signatures and antigen presentation signature from The Cancer Genome Atlas (TCGA) database. Yet, whether this favorable outcome association in fsindel-present NSCLC patients is specifically for immunotherapy only or other treatments is still unknown.

Methods

A retrospective analysis was performed from 122 advanced NSCLC patients treated with ICIs from Northwestern University (N=62) and the University of Miami (N=60). The presence or absence of fsindel and tumor mutation burden (TMB) were determined from 324-gene sequencing by FoundationOneTM (F1). Progression free survivals (PFS) of fsindel-present and -absent patients during ICIs and during their first-line chemotherapy (1L Chemo, n=89) were compared.

Results

Fsindel-present advanced NSCLC patients treated with ICIs had significantly more favorable outcome with median PFS of 6.2 months vs. 2.7 months (Hazard Ratio [HR], 0.59; 95% Confidence Interval [CI], 0.38 to 0.90 (Figure 1). Importantly, this finding was specific to ICIs and there was no difference observed in 1L Chemo (HR, 1.02; 95% CI, 0.67 to 1.54 (Figure 2).

Conclusions

Fsindel may serve as a novel predictive biomarker strategy specifically for immunotherapy independent of TMB, but not for chemotherapy. Future prospective clinical data analysis and immune monitoring assays may validate this hypothesis further. Further exploration on pancancer landscape of TMB and fsindel is underway.

References

1. Turajlic S, Litchfield K, Rosenthal R. Insertion-and-deletion-derived tumour-specific neoantigens and the immunogenic phenotype: a pan-cancer analysis. Lancet Oncol, 2017; 8:1009-1021.
2. Hellmann M, Ciuleanu T, Pluzanski A. Nivolumab plus ipilimumab in lung cancer with a high tumor mutational burden. N Engl J Med, 2018; 22: 2093-2104.

Ethics Approval

The study was approved by Institution's Ethics Board at University of Miami, approval number ePROST# 20170427.

Figure 1.

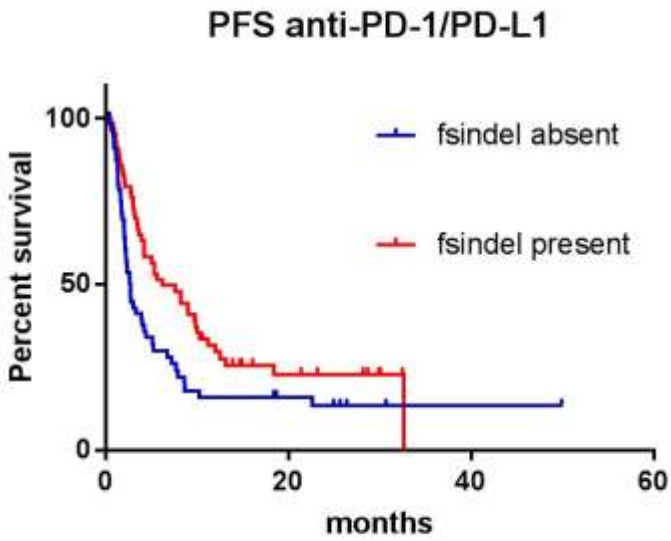

Figure 2.

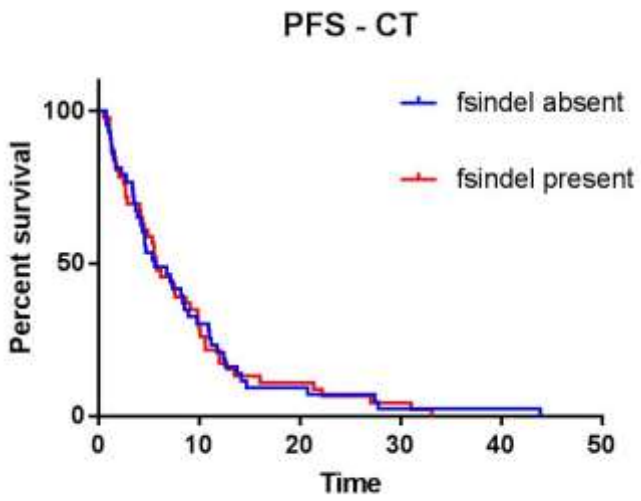

P587

Conditional activation of immune-related pathways and prognostic significance: a pan cancer analysis

Jessica Roelands, Master[1], Michele Ceccarelli[2], Darawan Rinchai, PhD[3], Sara Pai, MD, PhD[4], Francesco Marincola, MD[5], Lance Miller, MS, PhD[6], Peter Kuppen[7], Davide Bedognetti, MD, PhD[3], Wouter Hendrickx, PhD[3]

[1]1. Sidra Medicine; 2. Leiden University Medical Center, Doha, Qatar
[2]AbbVie Inc., Benevento, Italy
[3]Sidra Medicine, Doha, Qatar
[4]Massachusetts General Hospital, Boston, MA, USA
[5]Refuge Biotechnologies, Half Moon Bay, CA, USA
[6]Wake Forest School of Medicine, Winston-Salem, NC, USA
[7]Leiden University Medical Center, Leiden, Zuid-Holland, Netherlands

Background

It has been proposed that cancers can be divided in opposite phenotypes according to their immune orientation. This immune orientation influences response to therapy and clinical prognosis. The previously described Immunologic Constant of Rejection (ICR) signature is used here to define two opposite immune phenotypes (i.e., immune-active and immune-silent) across 31 different histologies. The relationship between tumor genetic makeup and immune orientation only recently began to be elucidated. In this pan-cancer study, we systematically analyzed the interconnection between tumoral genetic programs and immune orientation, and the prognostic impact of this interplay.

Methods

RNA-seq data of samples from a total of 9282 patients across 31 cancer types were obtained from TCGA. Additionally, RNA and DNA was isolated from fresh frozen tissue samples of an internal cohort of 366 colon cancer patients from LUMC. Exome and RNA sequencing was performed at Sidra. TCGA- and internal RNA-seq (HiSeq4000) data were normalized. Exome sequencing for our internal cohort is currently ongoing. We performed unsupervised consensus clustering for each cancer type separately based on the expression of the ICR gene signature (Figure 1A-E)[2,3]. Oncogenic pathway gene set enrichment and mutational status were analyzed in relation to ICR phenotypes. To explore whether tumor intrinsic attributes associate with the prognostic value of ICR across cancers, we compared mutational load, oncogenic alterations and expression of oncogenic pathways between cancer types.

Results

Our analysis identified a distinct prognostic connotation of ICR depending on cancer type. We confirmed a positive impact of ICR gene expression in our colon cancer cohort (Figure 1D). We identified several oncogenic pathways whose enrichment inversely correlated with ICR (Figure 2) in multiple tumor types. Such alterations include novel pathways as well as pathways previously described to influence immune disposition in specific tumor

types. In addition, mutations in specific genes were associated with ICR (Figure 3). Interestingly, we found various pathways associated with cancer-cell intrinsic features that were differentially enriched between tumors in which ICR had a prognostic impact versus the ones in which ICR did not bear any prognostic connotation.

Conclusions

We identified tumor-intrinsic attributes that correlated with immune phenotypes and potentially influence their development. In addition, a relation was observed between the enrichment of oncogenic pathways and the prognostic significance of the ICR. Such information can be used to prioritize potential candidates for immunogenic conversion and to refine stratification algorithms. A validation of the TCGA results is ongoing through the analysis of the aforementioned internal cohort.

Acknowledgements

The authors would like to acknowledge the support from Qatar Foundation, Qatar National Research Fund (grant number: JSREP07-010-3-005).

References

1. Turan T, Kannan D, Patel M, Matthew Barnes J, Tanlimco SG, Lu R, et al. Immune oncology, immune responsiveness and the theory of everything. Journal for ImmunoTherapy of Cancer. 2018 Jun 5;6(1):50.
2. Hendrickx W, Simeone I, Anjum S, Mokrab Y, Bertucci F, Finetti P, et al. Identification of genetic determinants of breast cancer immune phenotypes by integrative genome-scale analysis. OncoImmunology. 2017 Feb 6;0.
3. Bedognetti D, Hendrickx W, Ceccarelli M, Miller LD, Seliger B. Disentangling the relationship between tumor genetic programs and immune responsiveness. Current Opinion in Immunology. 2016 Apr;39:150–8.

Ethics Approval

Samples were used for research according to the code of good conduct regarding secondary use of human tissue as described in “Human Tissue and Medical Research: Code of Conduct for responsible use (2011)” Drawn up by the FEDERA (Netherlands).

Figure 1.

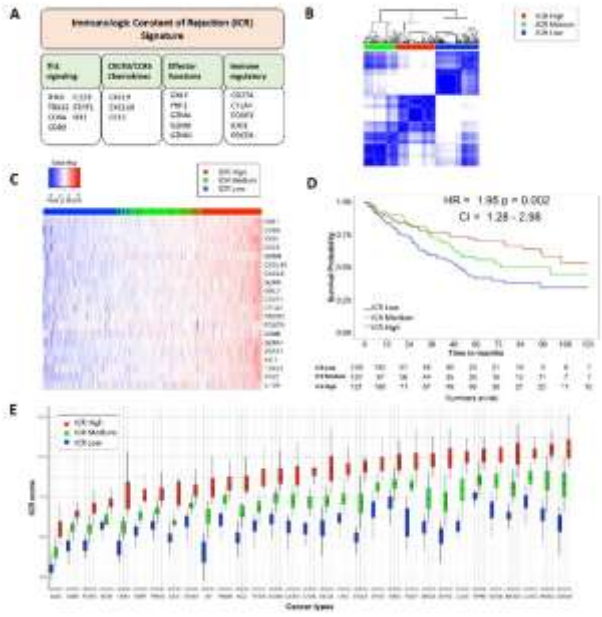

Figure 2.

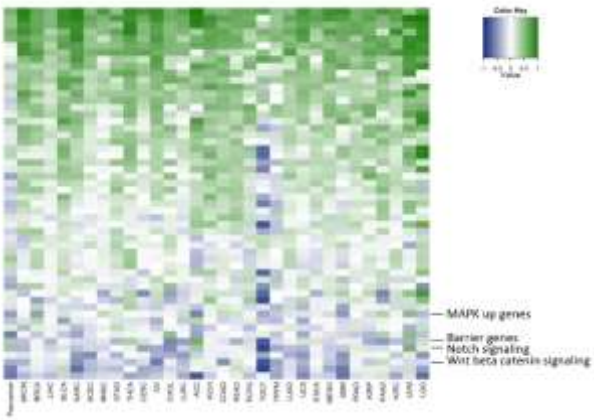

Figure 3.

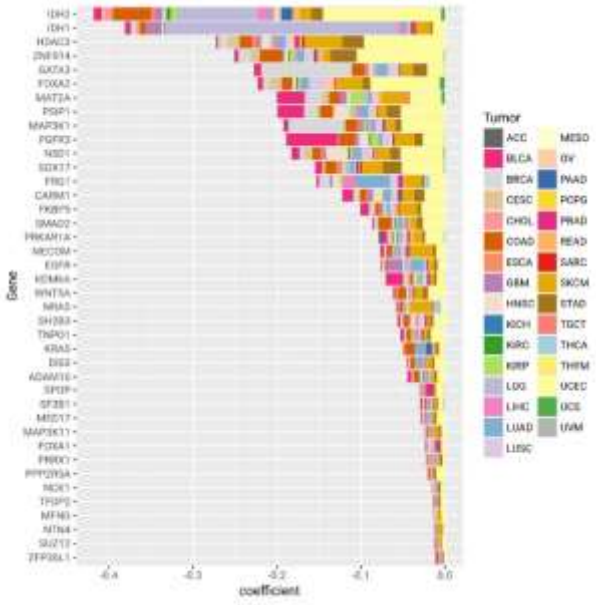

P588 **Abstract Travel Award Recipient**

Deep learning of the immune synapse

John-William Sidhom, MSE[1], Drew Pardoll, MD, PhD[1], Alexander Baras[1]

[1]*Johns Hopkins University, Baltimore, MD, USA*

Background

Artificial intelligence is poised to revolutionize every aspect of human life, finding applications in everything from self-driving cars to diagnosing cancer. In fact, almost any task that involves pattern recognition can be formulated in a way that modern AI algorithms can be used to achieve super-human performance. The immune synapse is a highly complex interaction between several proteins and peptides that allows for a constant surveillance of foreign invaders. However, modeling these interactions is extremely difficult as the combinations of interactions is simply intractable. In immuno-oncology, the study of this interaction is crucial as anti-tumor responses rely on sensitive and specific recognition of tumor-specific antigens. Implications of accurately predicting and modeling these interactions in immune-oncology range from improved and potent vaccine design to biomarkers for predicting response to immunotherapy.

Methods

Our group has developed a variety of deep learning models to model the signal transmission within the immune synapse. At the core of all architectures designed, convolutional layers, similar to ones used to learn features in images, are used to learn motifs within the sequencing data for a predictive or descriptive purpose.

Results

We first present AI-MHC, an applied deep convolutional neural network for class-specific MHC

binding algorithm that achieves state-of-the-art performance in both Class and Class II predictions. By incorporating 'meaning' of the allele within the network, we are able to model the interaction of allele and peptide within the context of a neural network (Figure 1)[1]. We take these concepts further in the development of DeepMANA, a deep learning framework which combines sequence-specific information about an allele/peptide pairing to not only predict binding affinity for any allele with a known protein sequence but also provide an antigen 'quality' score, based on the "non-self/foreign-ness" of a neoantigen. We observe in three previously published immunotherapy clinical trials, these quality neoantigens are enriched in long-term survivors or responders (Figure 2)[2]. Finally, we present DeepTCR, a collection of unsupervised and supervised deep learning algorithms capable of revealing structure in T-cell receptor repertoire. We demonstrate that DeepTCR achieves state-of-the-art performance in clustering antigen-specific TCR's (Figure 3A). and is capable of learning a predictive signature in TIL repertoire of mice treated with various immunotherapies (Figure 3B)[3,4].

Conclusions

These types of AI technologies could yield an entire new area of biomarker discovery as well as improve our understanding of the complex interaction occurring at the immune synapse that is ultimately required for a successful anti-tumor response.

References

1. Sidhom, J.-W., Pardoll, D. & Baras, A. AI-MHC: an allele-integrated deep learning framework for improving Class I & Class II HLA-binding predictions. bioRxiv 318881 (2018). doi:10.1101/318881
2. Łuksza, M. et al. A neoantigen fitness model predicts tumour response to checkpoint blockade immunotherapy. Nature (2017). doi:10.1038/nature24473
3. Glanville, J., Huang, H., Nau, A., Hatton, O. & Nature, W. L. Identifying specificity groups in the T cell receptor repertoire. (2017). 4. Rudqvist, N., Pilones, K. & Immunol …, L. C. Radiotherapy and CTLA-4 blockade shape the TCR repertoire of tumor-infiltrating T cells. (2018).

Figure 1. AI-MHC

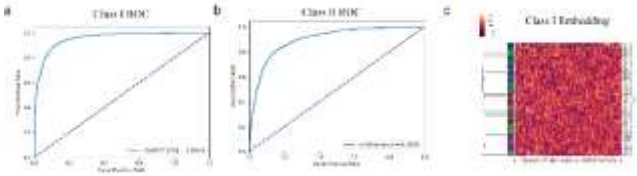

Figure 2. DeepMANA

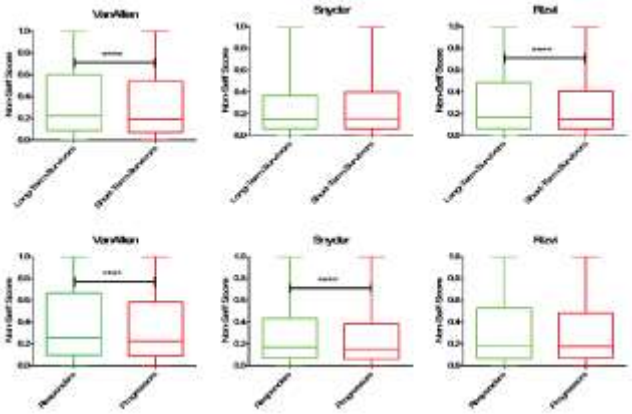

Figure 3. DeepTCR

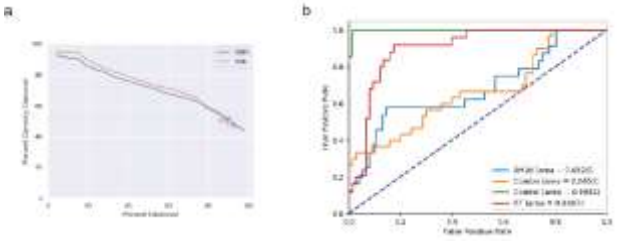

P589 **Abstract Travel Award Recipient**

Endogenous oncogene mutation-specific T cell responses in patients with clinical response to PD-1 blockade

Kellie Smith, PhD[1], Nicolas Llosa, MD[1], Valsamo Anagnostou, MD PhD[1], Hok Yee Chan, MS[1], Jiajia Zhang, MD, MPH[1], Haidan Guo, BS, and BA[1], Tricia Cottrell, MD, PhD[1], Jarushka Naidoo, MD[1], Kristen Marrone, MD[1], Janis Taube, MD, MSC[1], Victor Velculescu, MD, PhD[1], Julie Brahmer, MD[1], Patrick Forde, MD[1], Drew Pardoll, MD, PhD[1], Franck Housseau, PhD[1]

[1]*Johns Hopkins School of Medicine, Baltimore, MD, USA*

Background

High tumor mutational burden (TMB) is associated with objective clinical response to checkpoint blockade. We and others have shown that in patients with high TMB, negatively-regulated T cells specific for mutation-associated neoantigens are unleashed upon treatment and may facilitate tumor regression [1-3]. However, some cancers without high mutational burden do respond to anti-PD-1. Understanding the basis for these responses in the absence of high TMB and, consequently, immunogenic neoantigens, will provide potential biomarkers for therapeutic guidance and may provide insights into improving immunotherapy outcomes in patients with low TMB.

Methods

Whole exome sequencing was performed on matched tumor/normal tissue from patients receiving checkpoint blockade. The patients spanned multiple tumor types. Putative neoantigens, including those derived from oncogenic driver mutations, were selected for experimental testing based on predicted MHC class I affinity and expression of the mutated gene as reported by TCGA. Neoantigen recognition was evaluated using MANAFEST [4], followed by tracking of neoantigen-specific T-cells in tumor and serial blood using quantitative sequencing of the T cell receptor V-beta CDR3 (TCRseq). When fresh tumor was available, TCRseq was performed on tumor infiltrating lymphocytes pre-sorted based on PD-1 expression.

Results

Three patients with low TMB tumors who derived durable clinical benefit demonstrated broad endogenous neoantigen-specific T cell responses. Two of these patients, one with NSCLC and one with a neuroendocrine tumor, exhibited persistent memory T cell responses to neoantigens derived from mutations in the oncogenic BRAF and tumor-suppressor PTCH1 genes, respectively. Additionally, while not considered low TMB, a patient with mismatch repair proficient CRC demonstrated recognition of a neoantigen derived from the hotspot AKT1 E17K mutation. These neoantigens were validated using in vitro binding and stability assays. Analyses of the peripheral dynamics of T-cell clonotypes sorted by differential PD-1 expression are ongoing.

Conclusions

These findings suggest that oncogenic driver mutations are recognized by T-cells more often than previously appreciated. Responses to these neoantigens may be particularly efficacious in low TMB tumors owing to the likelihood that oncogenic mutations are required for tumor survival and are less likely to be eliminated. Sensitive bioassays, such as the MANAFEST assay used here, may identify patients that would not otherwise be predicted to respond to checkpoint blockade based on current biomarkers, such as high mutational burden or mismatch repair status. In patients without endogenous T cell recognition, identifying T cell clonotypes specific for these mutations provides the foundation for vaccines or T cell therapies targeting

oncogene mutation-derived neoantigens.

References

1. Forde PM, Chaft JE, Smith KN, Anagnostou V, Cottrell TR, Hellmann MD, Zahurak M, Yang SC, Jones DR, Broderick S, Battafarano RJ, Velez MJ, Rekhtman N, Olah Z, Naidoo J, Marrone KA, Verde F, Guo H, Zhang J, Caushi JX, Chan HY, Sidhom J, Scharpf RB, White J, Gabrielson E, Wang H, Rosner GL, Rusch V, Wolchok JD, Merghoub T, Taube JM, Velculescu VE, Topalian SL, Brahmer JR, Pardoll DM. Neoadjuvant PD-1 blockade in resectable lung cancer. NEJM. 2018; 378(21): 1976-1986.
2. Le DT, Durham JN, Smith KN, Wang H, Barlett BR, Aulakh LK, Lu S, Kemberling H, Wilt C, Luber BS, Wong F, Azad NS, Rucki AA, Laheru D, Donehower R, Zaheer A, Fisher GA, Crocenzi TS, Lee JJ, Greten TF, Duffy AG, Ciombor KK, Eyring AD, Lam BH, Joe A, Kang SP, Holdhoff M, Danilova L, Cope L, Meyer C, Zhou S, Goldberg RM, Armstrong DK, Bever KM, Fader AN, Taube J, Housseau F, Spetzler D, Xiao N, Pardoll DM, Papadoploulos N, Kinzler KW, Eshleman JR, Vogelstein B, Anders RA, Diaz LA Jr. Mismatch repair deficiency predicts response of solid tumors to PD-1 blockade. Science. 2017; 357(6349):409-413.
3. Rizvi NA, Hellmann MD, Snyder A, Kvistborg P, Makarov V, Havel JJ, Lee W, Yuan J, Wong P, Ho TS, Miller ML, Rekhtman N, Moreira AL, Ibrahim F, Bruggeman C, Gasmi B, Zappasodi R, Maeda Y, Sander C, Garon EB, Merghoub T, Wolchok JD, Schumacher TN, Chan TA. Mutational landscape determines sensitivity to PD-1 blockade in non-small cell lung cancer. Science. 2015; 348(6230): 124-8.
4. Danilova L, Anagnostou V, Caushi JX, Sidhom J, Guo H, Chan HY, Suri P, Tam A, Zhang J, El Asmar M, Marrone KA, Naidoo J, Brahmer JR, Forde PM, Baras AS, Cope L, Velculescu VE, Pardoll DM, Housseau F, Smith KN. The mutation associated neoantigen functional expansion of specific T cell receptor clonotypes (MANAFEST) assay: a sensitive platform for monitoring anti-tumor immunity. Cancer Immunol Res. 2018; 6(8): 1-12.

Ethics Approval

This study was approved by the Johns Hopkins University Institutional Review Board, approval numbers IRB00100653 and NA_00090257.

P590

Evaluation of whole exome sequencing for quantitative immune cell type deconvolution in tumor for clinical application in oncology

Alex So, PhD[1], Joyee Yao, BA[1], Aaron Wise, PhD[1], Kevin Wu[1], Kristina Kruglyak, PhD[1], Sven Biike[1], Traci Pawlowski, PhD[1], Shile Zhang, PhD[1]

[1]*Illumina, San Diego, CA, USA*

Background

The rise of cancer immunotherapy has led to increasing interest in detecting the presence of immune cells in the tumor microenvironment. Along with tumor mutation burden (TMB) and microsatellite instability (MSI) status, recent studies have also demonstrated that the level of immune cells in the tumor microenvironment correlates with patient responsiveness to immunotherapy. Here, we present our work demonstrating the feasibility of quantifying immune cells in analytical titration samples and real dissociated tumors from bulk RNA sequencing using an in-house developed immune cell deconvolution algorithm (FRICTION).

Methods

Libraries were generated using Illumina's TruSeq™ RNA Exome. The samples were paired-end sequenced (2x75bp) using the Illumina HiSeq™ 2500 Rapid Run mode. RNA purified from immune cells (CD4+, CD8+, and CD19+ cells) were titrated into RNA from various tissue backgrounds and subjected to RNA sequencing and FRICTION analysis. The fraction of immune cells present in cryopreserved dissociated melanoma tumors were quantified through flow cytometry or RNA sequencing and

analyzed with FRICTION.

Results

In preliminary testing, immune cell line titration experiments with various percentages of immune cell mixtures added into different tissue backgrounds demonstrated our method's linearity in quantifying these cells (median R2 > 0.98). The titration experiments were performed by spiking in immune cell RNA into various tissues background at the RNA level. Then, we analyzed cryopreserved dissociated melanoma tumors (n=38) with flow cytometry to determine the percentage of immune cells present and TruSeq™ RNA Exome for immune cell signatures by FRICTION. Our data demonstrated that we can quantify the fractions of CD4+ T cells, CD8+ T cells, and CD19+ B cells presence corresponding to flow cytometry data on each subset of immune cells. Finally, we correlated inflamed tumors, or those with high immune cell content, by FRICTION to CD45+ immune cells from flow cytometry with a linearity of R2 > 0.82.

Conclusions

In summary, we demonstrate that the TruSeq™ RNA Exome next-generation sequencing workflow combined with FRICTION, an immune cell deconvolution algorithm, can predict the presence of CD4+ T cells, CD8+ T cells, and CD19+ B cells within tumor microenvironment in a quantitative manner and accurately determine the inflammation of the tumor microenvironment.

P591

Somatic alterations in PD-L1 predict response to platinum-based chemotherapy in patients with advanced prostate cancer

Panagiotis Vlachostergios, MD, PhD[1], Aileen Lee[1], Charlene Thomas[1], Priyanka Patel[1], Amy Hackett[1], Naureen Rashid[1], Ana Molina, MD[1], David Nanus, MD[1], Himisha Beltran, MD[1], Scott Tawaga, MD[1]

[1]*Weill Cornell Medicine, New York, NY, USA*

Background

The interplay between malignant tumors and the immune system is becoming increasingly understood. Immune checkpoint inhibitors are approved for treatment of several cancer types, with PD-L1 immunohistochemical expression as a companion test in many cases. Immune checkpoint blockade is not an established therapy for advanced prostate cancer (PC) patients (castration-resistant or neuroendocrine PC); however platinum agents are active and in clinical use. This study aimed to assess the impact of somatic alterations in PD-L1 on clinical responses to platinum chemotherapy in patients with advanced PC.

Methods

We reviewed records of advanced PC patients enrolled in our Precision Medicine cohort, who received platinum-based chemotherapy with available tumor tissue specimens and clinical information of known prognostic factors. We used whole exome sequencing (WES) to assess for mutations and copy number alterations in the CD274 gene (encoding PD-L1). We used Kaplan Meier curves, univariable and multivariable Cox regression analyses to predict time to PSA progression-free survival (PSA-PFS), radiographic progression-free (rPFS) and overall survival (OS) after initiation of platinum-based chemotherapy.

Results

Our cohort included 31 men, median age 69 years (range 50-85). Based on histological features 8 patients (26%) were NEPC. Twenty five patients had bone metastases and 19 had visceral metastases (16 liver, 11 lung, 1 brain). The majority or patients (26/31) received carboplatin, 8 received cisplatin and 4 received both sequentially, with initial platinum used for data analysis. Most patients received chemotherapy doublets, and platinum was most

frequently combined with paclitaxel (N=11) and etoposide (N=12). Somatic alterations (mutations or/and copy number changes) in CD274 (encoding for PD-L1) were associated with a significantly longer rPFS compared to men with wild-type PD-L1 (median rPFS: (median rPFS: 8 versus 4 months, P=0.022). PD-L1 alterations were less frequent observed in men with bone metastases (2/22 vs 4/9, P=0.043). No significant correlations were identified between CD274 status (wild-type versus mutations/copy number alterations) and PSA-PFS or OS. On multivariate analysis (adjusted for Gleason score, PSA, alkaline phosphatase, lactate dehydrogenase, hemoglobin, visceral metastases, performance status, use of opioids), PSA (P=0.049) and the presence of visceral metastases (P=0.048) were independent prognosticators of OS.

Conclusions
Our study suggests that somatic alterations in PD-L1 may predict radiologic responses in patients with advanced PC treated with platinum-based chemotherapy. Validation of these findings in larger prospective studies are warranted.

Ethics Approval
The patient consented to participate in the Precision Medicine protocol at Weill-Cornell Medicine (WCM). The study was approved by our Institutional Review Board and Ethics Committee (WCM / New York-Presbyterian IRB protocol #: 1305013903).

P592

Clonality of tumor infiltrating and peri-tumoral lymphocytes in colorectal cancers with high-microsatellite instability

Pamela Ward, PhD[1], Mihaela Campan, PhD[1], Katherine Scribner, DO[1], Ashley Hagiya, MD[1], Cristina Costales, MD[1], Michael Bask, BS[1], Tiffany Long, BS[1], Afsaneh Barzi, MD[1], Jonas Pettersson, PhD[1], Louis Dubeau, MD PhD[1]

[1]*University of Southern California, Los Angeles, CA, USA*

Background
Immune checkpoint inhibitor therapy is approved for colorectal cancers that show high microsatellite instability. These cancers typically show increased mutational burden associated with increased T cell infiltration correlating with higher Immunoscores. Not all these tumors respond to immunotherapy, hence a need for additional predictors of responsiveness. We sought to quantitate tumor infiltrating and peritumoral lymphocytes in patients with colorectal cancers displaying high-microsatellite instability and examine the clonality of their expression profiles based on the hypothesis that these parameters are predictors of such responsiveness.

Methods
T cells of interest were identified by immunostains against CD3 and CD8 in 4-micron thick formalin-fixed, paraffin-embedded tissue sections from 4 colorectal cancers with high microsatellite instability including 2 from patients with Lynch syndrome and 2 from sporadic cancers. The average number of immunopositive tumor infiltrating and peritumoral lymphocytes and the ratio of CD8 over CD3 positive cells in 10 high power fields (totaling approximately 3 square millimeters) were scored independently by two pathologists. Areas of at least 5 square millimeters containing representative tumor infiltrating and peritumoral lymphocytes were macrodissected and subjected to RNA extraction using a Promega Maxwell instrument. The Archer Immunoverse NGS TCR assay and an Illumina Miseq instrument were used to sequence 400ng RNA from each sample. Results were analyzed using Archer's analysis pipeline.

Results
All tumors had over 100 tumor infiltrating lymphocytes per high power field, 63% showing CD8 positivity. There was a range of 10-100 peritumoral lymphocytes per high power field, 75% with CD8 positivity. The two cases associated with sporadic cancer had 234 and 338 unique TCR-beta sequences respectively, with a single dominant clone (44% of total sequences) in one case and two dominant clones (15% and 16% of total sequences) in the other. The two Lynch syndrome cases had 665 and 1442 unique receptor sequences respectively in infiltrating lymphocytes, none above background frequency. Peritumoral lymphocytes in 3 cases showed from 1394 to 2986 unique T cell receptor beta sequences, none of which were dominant. The remaining case, from a patient with sporadic cancer, had 438 unique sequences, one representing 21% of all sequences, but the selected region contained a small number of admixed tumor cells.

Conclusions
T-cell clonality in tumor infiltrating lymphocytes was detectable and associated with sporadic tumors in this small cohort of colorectal cancers with high microsatellite instability. Whether or not this can predict responsiveness to immunotherapy merits investigation.

Ethics Approval
This study was approved by USC Institutional Review Board; approval number HS-18-00285.

P593

Robust TMB values calculated from tumor-only material show correlation and precision with paired results

Victor Weigman[1], Natalie Mola, MS[1]

[1]*EA Genomics, Q Squared Solutions*

Background
Tumor mutational burden (TMB), a measure of the number of somatic mutations per Mb of the assay target region, is becoming a common biomarker in prediction of immunotherapy response. As the tumor evolves, mutations are accumulated, leading to growth advantages and opportunities for presentation of new neoantigens. Immunotherapies designed to antagonize common checkpoint inhibitors like PD1/PD-L1 and CTLA4 correct for this immune evasion and mutational burden provides a continuous variable that's prognostic to this attainment. This is also showing promise in 2nd and 3rd line inhibitory compounds (TIM-3, LAG3, IDO1) and co-stimulatory antibodies (OX40, GITR, CD40).Calculation of TMB is dependent on calling tumor-derived (somatic) mutations that are derived from identifying variants in the tumor cells and contrasting them against variants in a matched normal/germline sample. However, this approach increases costs of testing and in many cases, may not be possible if a normal sample cannot be obtained, consented or absent from a clinical trial protocol for TMB testing.

Methods
Our tumor-only TMB pipeline uses somatic classifications determined using a random forest model. Utilizing TCGA samples, the model was trained across multiple indications using variant classifications (somatic/germline) produced by our original paired TMB analysis pipeline. The pan-cancer model consists of 236 TCGA samples from 5 separate indications that have been shown to have a range of median TMB values. This model has 17 significant predictors (like variant allele frequency, ExAC frequency, SIFT score, etc) derived from variant call metrics and database annotations pulled from GoldenHelix Varseq.

Results
Utilizing data from TCGA samples from indications not included in our model we looked to compare

tumor-only TMB using correlation to known values, precision in biological replicates, preservation of dynamic range and linearity. Using indications outside of our original model,, we observed slopes ranging from 0.72-1.1 and R2 values consistently above 0.92 against our paired values. We observed similarly high correlation (slope 0.92/R2 0.87) in paired values generated from TCGA. Utilizing procured case-matched fresh frozen and FFPE samples and showed TMB from FFPE ranging within 30% of the frozen values. When testing replicates for both frozen and FFPE, we consistently observed TMB scores under 10% in frozen and ranging from 1-21% in FFPE.

Conclusions
To increase applicability of TMB to the volume of retrospective studies, calculation must be able to be performed by using only the tumor specimen and we feel our approach provides robust calculation across use cases.

P594

Dynamic analysis and visualization of the interactions between tumor and the immune cell infiltration by integrating TCGA genomic- and transcriptional- data

Mingchao Xie, PhD[1], Bolan Linghu[1], Pei Zhang, PhD[1], Zhongwu Lai, PhD[1], Jonathan Dry[1], Benjamin Sidders[1]

[1]*Astrazeneca, Waltham, MA, USA*

Background
Investigation of the interactions between the tumor genomic landscape and immune cell infiltration is critical for immune-oncology (IO) projects. Such analysis facilitates the discovery of novel prognostic biomarkers, identification of new drug targets, and understanding of drug resistance mechanisms. However, due to a lack easily available datasets and proper analysis tools, systematically exploring the tumor–immune interaction is a big challenge.

Methods
Here, we deconvoluted the immune cell compositions of 9,721 primary tumor samples from 33 TCGA cancer types using transcriptomic data, and developed a web-based application, IO Browser.

Results
The browser allows the user to visualize the immune composition of a sample or cohort, and to define disease segments or “immuno-types” based on the presence of single or multiple immune cell types. Users can then perform survival comparisons, explore gene expression of key cancer and IO genes as well as generate oncoprints in the different segments. The browser also provides statistical analysis to identify the gene or mutations enriched in the immuno-typed disease segment, and correlate gene expression or mutations with specific immune cell types in tumor microenvironment (TME).

Conclusions
In summary, IO Browser enables comprehensive analysis and visualization of the dynamic interactions between tumor and immune landscape, and will aid our understanding of the interplay between tumor genomics and immune biology to facilitate line of sight and disease segmentation.

P595

Smoking and KRAS mutation status in lung adenocarcinomas are associated with distinct favorable immune cell contexture in the tumor microenvironment

Yuanquan Yang, MD, PhD[1], Qiang Hu, MD, PhD[1], Song Liu[1], Maya Khalil, MD[1], Grace Dy[1]

[1]*Roswell Park Comprehensive Cancer Center, Buffalo, NY, USA*

Background

EGFR mutated- NSCLC or NSCLC among never-smokers (regardless of EGFR or ALK mutation status) have inferior responses to anti-PD-1 antibody therapies compared to NSCLC with KRAS mutation or smoking-associated NSCLC.[1,2] We hypothesized that tumor immune microenvironment (IME) differences between smokers vs non-smokers, KRAS mutants vs EGFR mutants may explain this clinical association.

Methods

Using the Cancer Genome Atlas (TCGA) lung adenocarcinoma provisional database, genomic profiles and clinically annotated data were obtained. Patients without RNA-seq data were excluded. 22 different IME cell proportions were estimated using The Cancer Immunome Atlas (TCIA) and CIBERSORT gene expression deconvolutional algorithm LM22.[3,4] Relative IME cell proportions were compared using t-test. Holm-Bonferroni method was applied to control for type I error at alpha=0.05.

Results

75 lifelong non-smokers and 426 current/former smokers with lung adenocarcinomas were identified. 58 and 160 patients had putative driver mutations in EGFR and KRAS, respectively. Compared to non-smokers, smokers had significantly higher percentage of activated memory CD4 T cells (5.1% vs 2.6%, p=0.002), and plasma cells (10.1% vs 7.3%, p=0.003). In contrast, non-smokers had higher proportion of resting dendritic cells (9.7% vs 6%, p=0.003) (Figure 1). KRAS mutants had higher fractions of cytotoxic CD8 T cells (1.4% vs 0.5%, p=0.002), activated memory CD4 T cells (4.5% vs 2%, p=0.002) and plasma cells (9.9% vs 6.4%, p=0.003) compared to EGFR mutants (Figure 2). The rest of comparisons did not reach statistical significance.

Conclusions

There are distinct phenotypes of immune cell contexture of lung adenocarcinomas in association with smoking status and genotype. Smokers and KRAS mutants have a more favorable immune microenvironment compared to non-smokers and EGFR mutants. It may play a role in determining immunotherapy responsiveness.

References

1. Borghaei H, Paz-Ares L, Horn L, et al. Nivolumab versus docetaxel in advanced nonsquamous non–small-cell lung cancer. New England Journal of Medicine 2015;373:1627-39.
2. Reck M, Rodriguez-Abreu D, Robinson AG, et al. Pembrolizumab versus chemotherapy for PD-L1-positive non-small-cell lung cancer. N Engl J Med 2016;375:1823-33.
3. Charoentong P, Finotello F, Angelova M, et al. Pan-cancer immunogenomic analyses reveal genotype-immunophenotype relationships and predictors of response to checkpoint blockade. Cell Reports 2017;18:248-62.
4. Newman AM, Liu CL, Green MR, et al. Robust enumeration of cell subsets from tissue expression profiles. Nature Methods 2015;12:453.

Figure 1.

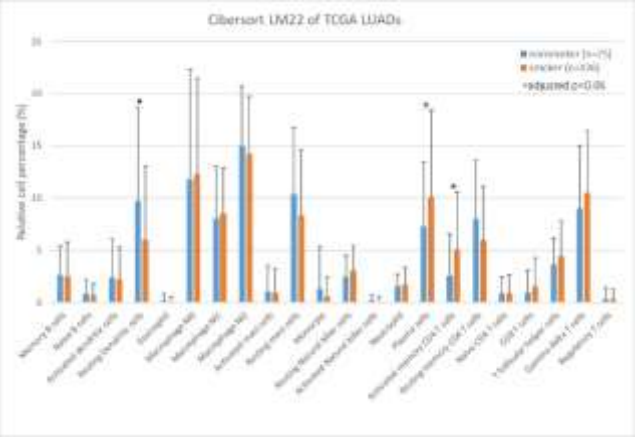

Figure 2.

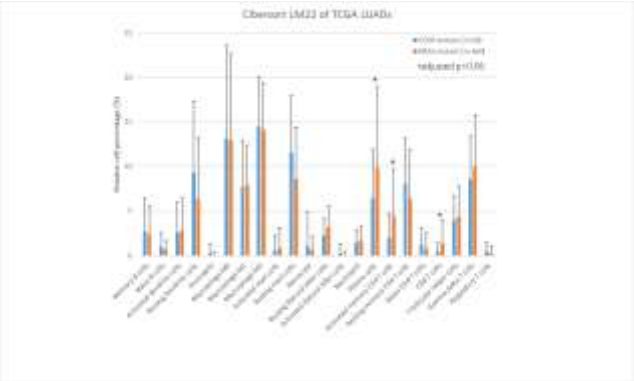

P596

Immune gene expression characterization of genomic subsets of metastatic non-squamous non-small cell lung cancer

Edwin Yau, MD, PhD[1], Sarabjot Pabla, MSc, PhD, BS[2], Sean Glenn, PhD[2], Antonios Papanicolau-Sengos, MD[2], Jason Zhu, MD[3], Matthew Labriola, MD[3], Tian Zhang, MD[3], Jeffrey Clarke, MD[3], Carl Morrison, MD, DVM[4], Grace Dy[1]

[1]Roswell Park Comprehensive Cancer Center, Buffalo, NY, USA
[2]Omniseq Inc., Buffalo, NY, USA
[3]Duke Cancer Institute, Durham, NC, USA
[4]Omniseq Inc, Buffalo, NY, USA

Background

The use of PD-1/PD-L1 checkpoint inhibitors (CPI) has dramatically altered the treatment of metastatic Non-Small Cell Lung Cancer (NSCLC). However, a large proportion of patients with NSCLC do not derive clinical benefit from CPI treatment resulting in efforts aimed at improving patient selection. Molecular profiling of NSCLC has identified genomic subsets of NSCLC such as EGFR mutant NSCLC and KRAS mutant NSCLC with co-occurring mutations in the Nrf2 axis (STK11, KEAP1, and NFE2L2) that appear resistant to CPI monotherapy [1-3]. Using a cohort of patients whose tumors underwent comprehensive genomic and targeted immune transcriptomic analysis, we characterized the immune gene expression profile of EGFR mutant and Nrf2 altered NSCLC tumor samples.

Methods

We performed comprehensive analysis of the genomic and immunological landscape of 134 formalin-fixed, paraffin-embedded tumor samples from metastatic non-squamous NSCLC patients at eight institutions using a CLIA-certified laboratory test that included whole-exon DNA-seq and abundance of 394 immune transcripts by RNA-seq. Differential gene expression analyses of immune transcripts for various mutant subtypes was performed using Wilcoxon rank sum test on gene expression ranks (normalized gene expression values ranked against a large tumor reference population). Benjamini-Hochberg adjusted p-values are reported.

Results

Among the cohort of 134 cases, 8 were EGFR mutant, 28 were KRAS mutant (6 KRAS/TP53 and 4 KRAS/Nrf2 axis co-mutants), and 11 had Nrf2 axis mutations. In EGFR mutant cases, there was a trend towards enrichment of an IFN-g gene expression signature [4] and significant enrichment for a T-cell exhaustion gene expression signature [5] (p=0.043) (Fig. 1) including elevated expression of PD-L2 (p=0.031) and LAG3 (Fig. 2A). Nrf2 axis altered cases showed decreased PD-L1 expression (p=0.036) (Fig. 3) consistent with previous studies [2-3]. Nrf2 altered cases also demonstrated an increase in suppressive Treg genes and an immunosuppressive environment (Fig. 2B). Potential therapeutic targets of interest that were significantly increased in the Nrf2 altered cohort include NOTCH3 (p=0.048), TBP (p=0.033), HGF (p=0.043), and BCL2L11 (p=0.034). Similar trends were observed comparing the smaller subsets of KRAS and TP53 co-mutants compared to KRAS and Nrf2 altered subsets (Fig. 2C).

Conclusions

Using NSCLC patient tumor samples from multiple institutions, we characterized the immune gene expression signatures of CPI resistant EGFR and Nrf2 altered NSCLC genomic subsets and identified different potential mechanisms of CPI resistance in these genomic subsets. Alternative checkpoints resulting in T-cell exhaustion was observed in EGFR mutant NSCLC and an immunosuppressive Treg dominated signature was seen in Nrf2 altered NSCLC.

References

1. Lee CK, Man J, Lord S, Links M, Gebski V, Mok T, Yang JC. Checkpoint inhibitors in metastatic EGFR-mutated non-small cell lung cancer – a meta-analysis. J Thorac Oncol. 2017; 12:403-407. 2. Skoulidis F, Goldberg ME, Greenawalt DM, Hellmann MD, Awad MM, et al. STK11/LKB1 mutations and PD-1 inhibitor resistance in KRAS-mutant lung adenocarcinoma. Cancer Discov. 2018; 8:822-835. 3. Arbour KC, Jordan E, Kim HR, Dienstag J, Yu HA, et al. Effects of co-occurring genomic alterations on outcomes in patients with KRAS-mutant non-small cell lung cancer. Clin Cancer Res. 2018; 24:334-340. 4. Ayers M, Lunceford J, Nebozhyn M, Murphy E, Loboda A, et al. IFN-g-related mRNA profile predicts clinical response to PD-1 blockade. J Clin Invest. 2017; 127:2930-2940. 5. Guo X, Zhang Y, Zheng L, Zheng C, Song J, et al. Global characterization of T cells in non-small cell lung cancer by single-cell sequencing. Nat Med. 2018; 24:978-985.

Ethics Approval

OmniSeq's analysis utilized deidentified data that qualified as non-human subject research under IRB-approved protocols, approved by both Roswell Park Comprehensive Cancer Center (Buffalo, NY, BDR #080316) and Duke Cancer Institute (Durham, NC, PRO00088762).

Figure 1. Gene Expression Signature

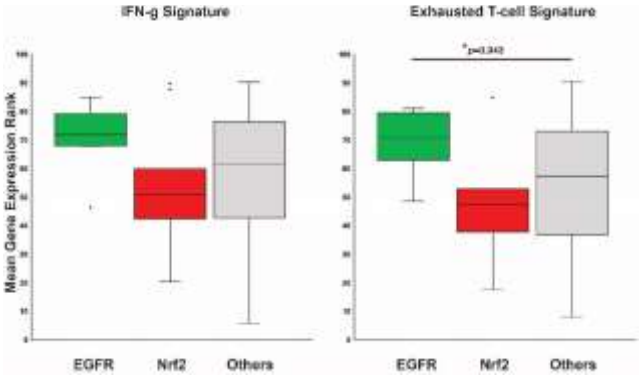

Figure 2. Gene Rank Score comparisons

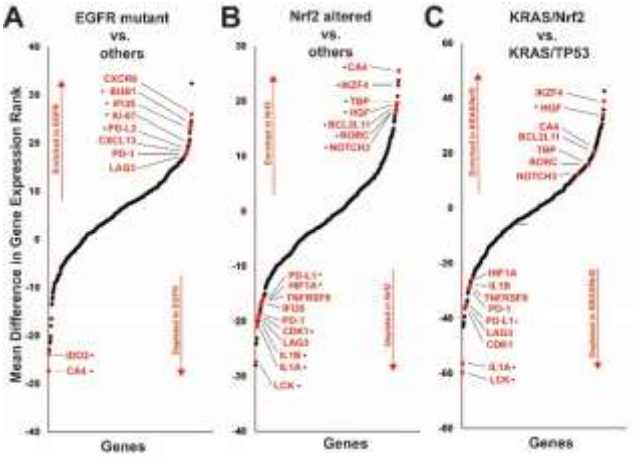

Figure 3. PD-L1 gene expression

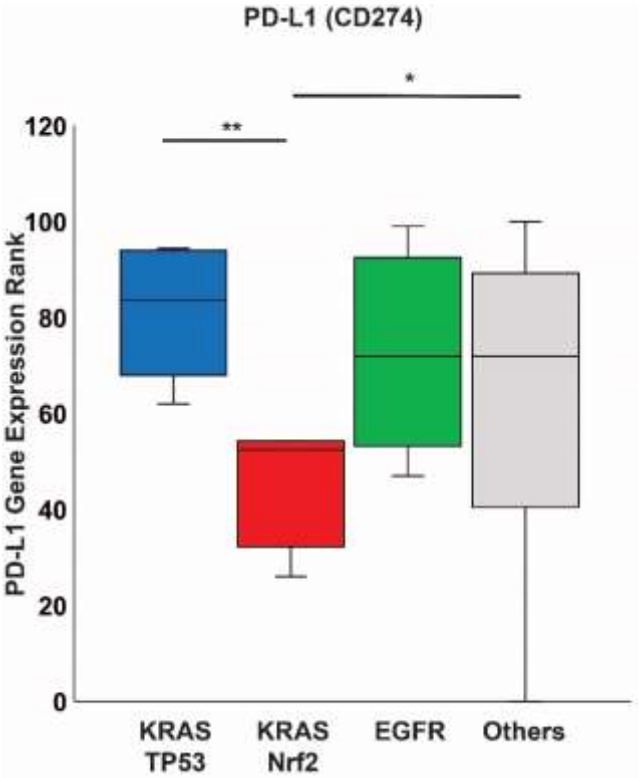

Oncolytic Viruses and Intratumoral Therapies

P597

Reovirus infection of prostate cancer induces upregulation of the negative regulators PD-L1 and BTLA

Nicola Annels, PhD[1], Guy Simpson[1], Hardev Pandha, PhD, FRCP, FRACP, FR[1], Mehreen Arif[1], Kevin Harrington, MD[1], Alan Melcher[1], Richard Vile, PhD[1]

[1]*The University of Surrey, Guildford, UK*

Background

Prostate cancers are generally considered to be a 'cold' tumour with this non-inflamed phenotype thought to be largely responsible for the disappointing lack of sensitivity of prostate cancer patients to immune checkpoint blockade (ICB) therapy. However, the use of oncolytic viruses can overcome pre-existing mechanisms of resistance to ICB in prostate cancers by transforming these cold tumours into 'hot', immune cell infiltrated, tumours. Such biological therapy can be further enhanced with the use of relevant immune checkpoint blockade that can overcome any constitutive or compensatory inhibitory resistance mechanisms. In this study, we investigated whether the effectiveness of oncolytic viral therapy for prostate cancer could be improved with targeted blockade of PD-1 and/or CD73.

Methods

The susceptibility of prostate cancer cell-lines to reovirus infection was tested in-vitro using MTS assays. The immunogenic cell death profile of reovirus-infected TRAMP-C2 cells was determined by analysing the cell-surface expressed ICD determinants, calreticulin and HSP70, by FACS and the secreted determinants by ELISA (HMGB1) or ATP assay. The capacity of reovirus to target TRAMP-C2 tumours in-vivo were evaluated using immunocompetent C57BL/6. Anti-PD-1 and/or anti-CD73 blockade in the TRAMP-C2 prostate cancer murine model was tested as a monotherapy and in combination with reovirus infection. Nanostring's PanCancer Immune Profiling RNA Panel was used to investigate the impact of reovirus therapy on the tumour microenvironment.

Results

Prostate cancer cell-lines were highly susceptible to reovirus infection and displayed significant increases in the immunogenic cell death determinants, calreticulin and HMGB1, post-infection. Using the TRAMP-C2 immunocompetent C57BL/6 murine model, reovirus but not PBS-treated tumours resulted in significant tumour control but did not

induce complete regression of tumours. Blockade with either anti-CD73 or anti-PD-1 as a monotherapy did not significantly control tumour growth. However, the addition of these antibodies after reovirus infection significantly controlled tumour growth resulting in complete tumour regressions in some mice who subsequently displayed protective immunity to tumour rechallenge. Whilst Nanostring analysis revealed the expected increase in immune infiltration within the virus-treated TRAMP-C2 tumours, even more interesting was the finding of significant upregulation of the negative regulators, BTLA and PD-L1 in the reovirus-treated TRAMP-C2 tumours compared to untreated tumours.

Conclusions

Whilst blockade of the PD-L1 signal with an anti-PD-1 antibody clearly sensitized TRAMP-C2 tumours to cytotoxic T lymphocyte (CTL) killing in the current study, results will be presented to show whether blockade of BTLA can synergise with anti-PD-1 at reversing tumour-specific T cell inhibition.

P598

Discovery and preclinical development of E7766, a novel STING agonist for cancer immunotherapy with a superior profile over a leading reference compound

Xingfeng Bao, PhD[1], Kuan-Chun Huang, PhD[1], Atsushi Endo[1], Dinesh Chandra, PhD[1], Jiayi Wu[1], Dae-Shik Kim[1], Diana Albu[1], Karen Tendyke[1], Kara Loiacono[1], Thomas Noland, PhD[1], Christy Ingersoll[1], David Verbel, MPH[1], Rongrong Jiang[1], Donna Kolber-Simonds[1], Chi Zhang[1], Muzaffar Akram, MSc, MA[1], Minghong Hao[1], HyeongWook Choi[1], Vaishali Dixit[1], Janna Hutz, PhD[1], John Wang[1], Frank Fang[1]

[1]Eisai Inc., Andover, MA, USA

Background

Activation of Stimulator of Interferon Genes (STING) in tumor microenvironment is considered to be a novel and promising approach to cancer immunotherapy via turning immune cold tumors into immune hot tumors. Here, we present for the first time E7766, a novel and proprietary STING agonist, and its preclinical profile in comparison with clinical stage reference compound X

Methods

E7766 was designed and synthesized to optimize the potency of binding to dimerized STING proteins of different genetic isoforms. Co-crystalization of E7766 with recombinant STING proteins were performed. E7766 was comparatively characterized with 2'3'-cGAMP and compound X in a variety of biochemical, molecular and cell biological, and in vivo pharmacological assays including human primary cells and tumor tissues. ADME and pharmacokinetics were determined.

Results

E7766, a representative of a novel class of compounds, was found to be a highly specific agonist. In primary human cells, E7766 was consistently active across all seven tested STING genetic isoforms and one to three orders of magnitude depending on the isoforms more potent than compound X. The broader target specificity and superior potency of E7766 were explained by advantageous molecular interactions in its co-crystal structures with various STING genetic isoforms. E7766 had no direct anti-proliferative activity in vitro, but when E7766 was administrated as single intratumoral (I.T.) injection to twelve subcutaneous syngeneic tumor models, all tumors responded by either complete regression or significant tumor growth delay without serious adverse effects. Single I.T. administration of E7766 eradicated anti-PD1 refractory large CT26 tumors or anti-PD1 resistant

MC-38T1 tumors. Furthermore, single administration of E7766 to subcutaneous tumor in mice bearing dual CT26 tumors in liver and under skin cured 90% of animals without recurrence for over 8 months. In contrast, compound X had 30% cure rate in the same treatment condition. The effective abscopal antitumor activity by E7766 was mediated by type I IFN signaling, CD8 T cells, and TNFα, and the tumor free mice completely rejected rechallenges of the same tumor in the absence of CD8 T cells or NK cells. Treatment with E7766 induced expression of signature innate genes, accumulation of active T cells, and tumor cell death. Finally, E7766 was metabolically stable and had a short half-life in plasma with moderate to high plasma clearance through a hepatic transporter-mediated mechanism.

Conclusions

We have developed a novel STING agonist E7766 that has an excellent and structurally-supported superior preclinical profile over compound X, supporting further clinical investigation for cancer immunotherapy.

P599

OncoVEXmGM-CSF in combination with checkpoint inhibition leads to tumor-specific systemic immunity and increased tumor antigen response in a murine syngeneic melanoma model

Keegan Cooke, BS[1], Juan Estrada[1], Petia Mitchell[1], Jinghui Zhan[1], Jing Qing[1], Jude Canon[1], Pedro Beltran[2]

[1]Amgen, MS: 15-2-A, CA, USA
[2]Unity Biotechnology, Brisbane, CA, USA

Background

Talimogene laherparepvec (T-VEC) is a first-in-class oncolytic immunotherapy derived from herpes simplex virus type 1 (HSV-1). T-VEC was designed to selectively replicate in neoplastic cells, lyse tumor cells, produce GM-CSF and stimulate anti-tumor immune responses. To study T-VEC-induced systemic immunity and T-cell responses against tumor antigens, we developed a mouse model of melanoma. We have previously shown that the combination of OncoVEXmGM-CSF (a virus modified similarly to talimogene laherparepvec, except that it contains mGM-CSF instead of hGM-CSF) and an anti-CTLA-4 antibody results in enhanced efficacy in both primary and metastatic B16F10 tumors. Here we set out to 1) determine whether OncoVEXmGM-CSF and anti-CTLA-4 combination treatment elicits a durable anti-tumor memory response and 2) to identify tumor-specific MHC-I epitopes generated by the treatment.

Methods

Experimental lung metastases were established by delivering B16F10-GFP cells intravenously (IV) to C57Bl/6 mice. Subcutaneous (SC) tumors were established by implanting B16F10-mNectin1 cells. When SC tumors reached ~100mm3, mice were administered intratumoral injections of OncoVEXmGM-CSF every third day (3 doses). Anti-CTLA-4 antibody was dosed on the same schedule (4 doses). Naïve control mice and treated mice whose SC tumors had resolved were rested for 60 days and then re-challenged with B16F10 tumor cells either on the SC flank or IV. Lungs were collected from IV challenged mice on day 28 for enumeration of lung metastasis. B16F10 tumor antigen epitopes were identified using exome sequencing and MHC/HLA-binding prediction algorithms. Antigen-specific T cell response was measured using an IFN-γ ELISPOT assay.

Results

OncoVEXmGM-CSF in combination with an anti-CTLA-4 antibody led to complete SC tumor regression in 60% of mice. These mice rejected a re-challenge with B16F10 either on the SC flank (10/10 tumor-free vs. 0/10 in age-matched naïve mice) or when delivered IV (10/10 tumor-free lungs at day 28

vs. 0/10 in controls). Splenocytes from OncoVEXmGM-CSF treated mice were activated by the tumor antigen-specific peptide P15E and two neoantigen peptides. T cell responses to P15E were associated with efficacy in SC tumors in the combination group, suggesting that it may be a tumor-rejection antigen.

Conclusions

The combination of OncoVEXmGM-CSF and anti-CTLA-4 antibody treatment elicited a durable effector memory response against B16F10 tumors. Moreover, OncoVEXmGM-CSF induces both neo-antigen- and tumor antigen-specific T-cell responses. The response to P15E was augmented by anti-CTLA-4 and associated with efficacy of the combination treatment.

Ethics Approval

All in vivo work was conducted under an IACUC approved protocol and in an AAALAC accredited facility.

P600

IL12/IL15 and PD-L1 blocker co-expressing oncolytic herpes virus VG161 significantly alters tumor microenvironment and eliminates prostate tumors in animal models

Zahid Delwar, PhD[1], Neetu Saxena, PhD[2], Erica Lee, PhD[3], Morgan Roberts, PhD[2], Luke Bu, MSc[3], Guoyu Liu, MD[3], Yanal Murad, PhD[4], Jun Ding, PhD[3], Dmitry Chouljenko, PhD[3], Igor Moskalev[2], Syam Somasekharan, PhD[2], Ronghua Zhao, MD[3], Paul Rennie, PhD[1], William Jia, PhD[3]

[1]*University of British Columbia, Vancouver, Canada*
[2]*Vancouver Prostate Centre, Vancouver, Canada*
[3]*Virogin Biotech Ltd, Vancouver, BC, Canada*
[4]*Virogin Biotech Ltd., Vancouver, BC, Canada*

Background

Oncolytic virotherapy has recently emerged as a promising anti-cancer therapeutic approach. A herpes virus-based oncolytic virus (oHSV-1), T-VEC, an oncolytic HSV-1 virus carrying GM-CSF, is the first oncolytic virus (OV) that has been approved by FDA in 2015 for treating melanoma. However, GM-CSF also stimulates myeloid derived suppressive cells (MDSCs) and therefore may not be the best immune stimulating factor to be expressed by OVs. To explore other immune regulatory factors that may better arm oHSV, we developed an oncolytic virus VG161 that expresses IL-12, IL-15 with its receptor alpha subunit and PD-L1 blocking peptide. VG161 has demonstrated to have a very strong antitumor effect in prostate cancer (PCa) mouse models.

Methods

Two expression cassettes that express IL-12 and IL-15 with its alpha receptor subunit, and PD-L1 blocking peptide (TF-Fc), respectively, were constructed into an oHSV backbone to generate VG161. Anti-tumor effect of VG161 virus was evaluated using MTT cell viability assay in a panel of prostate cancer cells in vitro. Viral replication in prostate tumor cells were determined by single step viral growth assay. In vivo anti-tumor efficacy was evaluated with a subcutaneously implanted human prostate cancer cell line (LNCaP), as well as the immunocompetent TRAMPC2 murine model of prostate cancer. Immune cell infiltration into the tumor microenvironment was determined by flow cytometry.

Results

Cell viability assay demonstrated that viability of PCa cells was reduced following VG161 infection in a dose dependent manner. Additionally, growth assay of VG161 in LNCaP cells showed the replication competency of the virus in PCacells. In vivo treatment of the LNCaP tumours with VG161 led to a dramatic reduction in tumor size compared to treatment with vehicle or replication deficient

control virus. Antitumor efficacy by VG161 was also observed in the TRAMPC2 syngeneic prostate cancer model. Our data demonstrated that immunostimulatory transgene expression by VG161 virus, dramatically enhanced NK cell infiltration into LNCaP tumours in Nude mice. Moreover, VG161 intratumoral injections significantly increased cytotoxic CD8+ T cells in TRAMPC2 tumors in both subcutaneous and orthotopic models. More interestingly, immunosuppressive immune cells such as T regulatory cells and MDSC populations were significantly decreased after VG161 treatment.

Conclusions

Our study indicates that IL-12/IL-15 and PD-L1 blocker delivering oHSV-1 vector (VG161) alters the prostate tumor microenvironment and thereby significantly inhibits tumor growth.

P601

STING signaling can enhance melanoma antigenicity

Rana Falahat, PhD[1], Adam Mailloux, PhD[1], Patricio Perez-Villarroel[1], Genyuan Zhu, PhD[1], Shari Pilon-Thomas, PhD[1], Glen Barber, PhD[2] , James Mulé, PhD[1]

[1]Moffitt Cancer Center, Tampa, FL, USA
[2]University of Miami Miller School of Med, Miami, FL, USA

Background

Among different gene-targeted mouse models deficient in specific innate immune pathways, only mice lacking STING or its downstream transcription factor IRF3 fail to reject immunogenic tumors [1]. Based on this finding, activation of STING by intratumoral injection of pharmacologic agonists has been investigated as a cancer therapy. While these studies have mainly focused on STING signaling in antigen presenting cells, its functional impact on tumor cells has not been well characterized. Here, we studied the impact of STING signaling activation on antigenicity of human melanoma cell lines following exposure to an agonist.

Methods

We examined STING and cGAS expression in a panel of human melanoma cell lines by immunoblot. Functional STING signaling activation was examined in STING-positive melanoma cell lines upon stimulation with the agonist 2'3'-cGAMP by measuring the induction of CXCL-10 and IFN-beta. To determine if hypermethylation was involved in the suppression of STING expression and signaling where gene mutations were absent, we treated melanoma cells lacking STING expression with 5-aza-2'-deoxycytidine (5AZADC). To study the role of STING signaling on antigenicity of melanoma, we co-cultured expanded human tumor infiltrating lymphocytes (TIL) with their HLA-matched melanoma cell lines in the presence or absence of 2'3'-cGAMP agonist. We assessed TIL production of IFN-γ and ^{51}Cr release for cytotoxicity.

Results

Immunoblot analysis revealed a diverse STING/cGAS expression status in human melanoma cell lines. STING expression was not detected in 11 of 18 of them. Induction of STING expression in 5AZADC-treated melanoma cell lines lacking STING and production of CXCL-10 following their stimulation with the STING agonist suggested DNA hypermethylation involvement in cases where STING gene mutations were absent. Among STING-positive cell lines, two responded strongly to STING signaling activation with 2'3'-cGAMP. Activation of the STING pathway in these cell lines when cultured with their HLA-matched TILs resulted in up to a 15-fold increase in IFN-γ secretion ($p < 0.01$) as well as augmentation of TIL cytotoxicity by >2-fold ($p < 0.05$). In addition, STING activation could induce enhanced surface expression of MHC class I in human melanoma cell lines leading to more effective tumor antigen recognition by TIL.

Conclusions
Direct activation of the STING pathway in human melanoma cell lines can result in improved antigenicity. Further understanding of the regulation and function of STING in melanomas may lead to the development of new strategies using STING agonists to improve TIL-based immunotherapies.

Acknowledgements
Funding: Dr. Miriam and Sheldon G. Adelson Medical Research Foundation.

References
1. Woo, Seng-Ryong, et al. STING-dependent cytosolic DNA sensing mediates innate immune recognition of immunogenic tumors. Immunity. 2014;41(5): 830-842.

P602

Generation and characterization of a CTLA-4 antibody with improved FcgammaR-dependent Treg deletion for tumor microenvironment-targeted oncolytic virotherapy of cancer

Bjorn Frendeus, PhD[1], Monika Semmrich, PHD[1], Jean-Baptiste Marchand, pHD[2], Petra Holmkvist[1], Linda Mårtensson[1], Ulla-Carin Tornberg[1], Ingrid Teige[1], Andres McAllister[1], Eric Quemeneur, PharmD, PhD[2], Nathalie Silvestre[2]

[1]*BioInvent, Lund, Sweden*
[2]*Transgene S.A., Illkirch Graffenstaden, France*

Background
Treatment with checkpoint inhibitor antibodies results in long-lasting antitumor responses in a variety of cancers [1]. However, a great unmet need remains since only a small fraction of patients responds. Reasons for lack of efficacy of checkpoint inhibition are believed to include lack of or inadequate tumor infiltrating immune cells (TIL), a notion supported by improved efficacy observed following combined checkpoint blockade with tumor microenvironment-modulating oncolytic virotherapy [2]. While combination therapy with anti-CTLA-4 and anti-PD-1 antibodies significantly improve efficacy, concerns with tolerability following systemic administration has limited wide-spread clinical use [3]. Here we present a potentially safe and more efficacious strategy to combine anti-CTLA-4 and anti-PD-1/PDL1 checkpoint inhibition in the context of oncolytic virotherapy. A Vaccinia virus (VV)-based oncolytic vector will be armed with herein described full-length human recombinant anti-CTLA-4 antibody, selected and characterized for its improved FcγR-dependent Treg depleting efficacy [4]. FcgammaR-dependent Treg depletion was recently found to underly human anti-CTLA-4 antibody efficacy in vivo, and FcgammaR-polymorphisms were associated with clinical responses to ipilimumab [4]. The Vaccinia virus vector was chosen based on its ability to achieve high intratumoral but low systemic exposure of encoded antibodies following intratumoral injection, and for its ability to induce intratumoral innate immune and effector T cell infiltration in conjunction with checkpoint inhibition in immunocompetent mouse tumor models [5-8].

Methods
The n-CoDeR® F.I.R.S.T™ human antibody and target discovery platform [9-12] was screened for antibodies with specificity for CTLA-4. Full-length antibody clones were characterized for efficacy and potency of binding human, cynomolgus and mouse CTLA-4 and for blocking CTLA-4 binding to B7 ligands. Functional activity was assessed in vitro monitoring CTLA-4-mediated T cell suppression and FcγR-dependent T cell depletion. Antibody-mediated deletion of human Treg in vivo was assessed using a human PBMC-based NOG/SCID-transfer model. Ipilimumab was used as benchmarking control.

Results
Biopanning, biochemical-, in vitro-, ex vivo- and in vivo-functional characterization of multiple antibody

clones identified a lead human anti-CTLA-4 antibody candidate with improved Treg-depleting activity compared with ipilimumab. Its selective improved Treg deleting efficacy contrasted by near identical efficacy and potency compared with ipilimumab in overcoming CTLA-4-mediated effector T cell suppression.

Conclusions

A human CTLA-4 antibody optimized for FcgammaR-dependent Treg deletion has been generated for arming of a Vaccinia-based oncolytic viral vector. Oncoviral tumor-localized delivery of this mAb may improve the therapeutic window for CTLA-4 targeted checkpoint intervention, allowing better tolerated and more effective combination therapy with approved antibodies targeting the PD-1/PDL1 axis.

References

1. Sharma P, Allison J P. The future of immune checkpoint therapy. Science, 2015; 348(6230): 56-61.
2. Ribas, A., et al., Oncolytic Virotherapy Promotes Intratumoral T Cell Infiltration and Improves Anti-PD-1 Immunotherapy. Cell, 2017; 170(6): 1109-1119 e10.
3. Postow, M.A., et al., Nivolumab and ipilimumab versus ipilimumab in untreated melanoma. N Engl J Med, 2015; 372(21): 2006-17.
4. Arce Vargas F, et al. Fc Effector Function Contributes to the Activity of Human Anti-CTLA-4 Antibodies. Cancer Cell, 2018.
5. Kleinpeter P, et al. Vectorization in an oncolytic vaccinia virus of an antibody, a Fab and a scFv against programmed cell death -1 (PD-1) allows their intratumoral delivery and an improved tumor-growth inhibition. Oncoimmunology, 2016; 5(10): e1220467.
6. Fend, L., et al., Immune Checkpoint Blockade, Immunogenic Chemotherapy or IFN-alpha Blockade Boost the Local and Abscopal Effects of Oncolytic Virotherapy. Cancer Res, 2017; 77(15): 4146-4157.
7. Liu, Z., et al., Rational combination of oncolytic vaccinia virus and PD-L1 blockade works synergistically to enhance therapeutic efficacy. Nat Commun, 2017; 8: 14754.
8. Marchand, J.-B., et al., Antibody-armed oncolytic Vaccinia virus to block immunosuppressive pathways in the tumor microenvironment, in Society of Immunotherapy 33rd Annual meeting. 2018, Journal of Cancer Therapy: National Harbour, MD.
9. Soderlind, E., et al., Recombining germline-derived CDR sequences for creating diverse single-framework antibody libraries. Nat Biotechnol, 2000; 18(8): 852-6.
10. Roghanian A, et al. Antagonistic human FcgammaRIIB (CD32B) antibodies have anti-tumor activity and overcome resistance to antibody therapy in vivo. Cancer Cell, 2015; 27(4): 473-88.
11. Frendeus B., Function-first antibody discovery: Embracing the unpredictable biology of antibodies. Oncoimmunology, 2013; 2(8): e25047.
12. Ljungars, A., et al., A platform for phenotypic discovery of therapeutic antibodies and targets applied on Chronic Lymphocytic Leukemia. Precision Oncology, 2018. In press.

Ethics Approval

Ethical approvals for human cells were obtained by the Ethics Committee of Skåne University Hospital and written informed consent was provided in accordance with the declaration of Helsinki. Mouse experiments were performed in agreement with ethical permissions from Malmö Lund Animal Ethics Committee.

Consent

Ethical approvals for human cells were obtained by the Ethics Committee of Skåne University Hospital and written informed consent was provided in accordance with the declaration of Helsinki. Mouse experiments were performed in agreement with ethical permissions from Malmö Lund Animal Ethics Committee.

P603

Novel treatment strategy for peritoneal carcinomatosis: adoptive cell transfer of tumor-specific lymphocytes after dual therapy with oncolytic virus and PD-1 blockade

Esther Giehl, MD[1], David Bartlett, MD[2], Zong Sheng Guo, PhD[2], Mathilde Feist, MD[3]

[1]*University of Pittsburgh Medical Center, Pittsburgh, USA*
[2]*UPMC, Pittsburgh, PA, USA*
[3]*Charite, Berlin, Germany*

Background
Current treatment strategies for peritoneal carcinomatosis (PC), the most frequent metastatic spread of primary gastrointestinal tract cancers, are associated with high recurrence rates and poor long-term survival. Preclinical evidence demonstrates that oncolytic viruses (OV) can be delivered intraperitoneally and augment the immune response within the peritoneal cavity. vvDD and its IL15-IL15-Rα-fusion protein-expressing version (vvDD-IL15-Rα) stimulate a highly CD8 T cell dependent antitumor immunity in colon or ovarian murine cancers in vivo. OV's ability to induce a T cell population with potent tumor-specific reactivity might present a novel strategy to overcome the immunosuppressive tumor microenvironment of solid organ malignancies and thereby augmenting their response to adoptive cell transfer (ACT).

Methods
Female C57BL/6 mice were inoculated intraperitoneally (i.p.) with colon adenocarcinoma cells (MC38). Tumor bearing mice underwent regional i.p. treatment with parental vvDD, vvDD-IL15-Rα or PBS. At different post treatment days, i.p. lavage was performed and T cells were isolated with magnetic beads. Virally induced ascites fluid lymphocytes have been tested for tumor cell recognition ex vivo via coculture assay, ELISA, ELISPOT and flow cytometry and applied for ACT.

Results
OV i.p. therapy stimulates a strong immune response with a 100-fold increase of the amount of T cells ($p<0.005$). Ten days post treatment, T cells isolated from vvDD-IL15-Rα-treated mice exibit a more potent adaptive MC38-specific immunity in comparison to those isolated from control mice as measured by elevated IFNγ release ($p<0.005$) or 4-1BB expression ($p<0.005$) on CD8 T cells. CD8 T cells isolated from ascites fluid 10 days after i.p. vvDD-IL15-Rα injection also exert an increased expression of PD-1 ($p<0.005$) and coexpression of PD-1 and TIGIT ($p<0.5$). The transfer of these T cells in combination with anti-PD-1 antibody to MC38 tumor bearing mice in the absence of OV therapy cures 80% of animals and extends survival ($p<0.005$).

Conclusions
Regional OV therapy of PC stimulates the i.p. T cell population and induces an adaptiv tumor-specific immune response. When applied in ACT in combination with an anti-PD-1 antibody, these OV induced T cells exert potent therapeutic efficacy as depicted by a high complete response rate and prolonged overall survival. The results demonstrate that the combination of OV and PD-1 blockade possesses great therapeutic potential to enhance efficacy of ACT as treatment strategy of solid cancers as highlighted in this preclinical study.

Acknowledgements
I thank Dr. Udai S. Kammula and Dr. Abhishek K. Srivastava for their guidance with regard to their expertise in T cell immunology.

P604

DNA-based delivery of immunomodulatory antibodies is effective both in muscle and tumor despite distinct pharmacokinetics

Liesl Jacobs, MPharm[1], Elien De Smidt[1], Nick Geukens[1], Paul Declerck[1], Kevin Hollevoet, PhD[1]

[1]*KU Leuven - University of Leuven, Leuven, Belgium*

Background

Many cancer patients fail to optimally benefit from monoclonal antibody (mAb) immunotherapy because of the high costs, limited single-agent efficacy and toxicity following systemic infusion. DNA-based antibody gene transfer administers the mAb-encoding nucleotides, rather than the protein, allowing the site of delivery to produce the therapeutic in a cost-effective manner[1]. Recently, we achieved preclinical proof of concept for intramuscular gene transfer of tumor-targeting mAbs using plasmid DNA (pDNA) electroporation, a well-established clinical approach[2]. In the current study, we aimed to extend our DNA platform to immunomodulatory mAb combinations and explore the tumor as site of pDNA delivery. We hypothesized that intratumoral mAb production can lead to local and systemic anti-tumor responses, while avoiding high systemic mAb exposure and associated toxicity. We thereto compared the efficacy and pharmacokinetics of intramuscular and intratumoral antibody gene transfer.

Methods

Plasmids were designed to express an optimized anti-CTLA-4 mAb (p(aCTLA-4)) or anti-PD-1 mAb (p(aPD-1)), and were evaluated in a subcutaneous MC38 mouse tumor model. An empty plasmid (pNull) served as a control. Intramuscular and intratumoral pDNA electroporation were applied using tweezer electrodes and the NEPA21 Electroporator.

Results

Intramuscular p(aCTLA-4) and p(aPD-1) electrotransfer significantly improved survival, with the former resulting in 10% complete responders (CRs). The combination of both DNA-based mAbs further increased response, up to 30% CRs. pNull had no impact on tumor growth. Intratumoral delivery improved the efficacy of p(aPD-1) (33% CRs), while response rates of the other treatment arms were maintained (p(aCTLA-4): 9-17% CRs; combination: 33% CRs). Similar to the literature, intratumoral pNull electroporation resulted in a dose-dependent anti-tumor effect. The survival benefit, however, was less pronounced than when expressing the mAbs. In cured mice rechallenged with MC38 cells, tumor growth was absent or delayed, suggesting long-term anti-tumor immunity. Plasma mAb concentrations resulting from intratumoral mAb expression were up to 20-fold lower and more transient compared to intramuscular pDNA electrotransfer, and correlated with response. For both pDNA delivery sites, plasma mAb levels were similar in the single- and combination-treatment arms, demonstrating our ability to properly express mAb combinations.

Conclusions

Intramuscular and intratumoral DNA-based gene transfer of immunomodulatory mAbs enable significant anti-tumor responses, despite the distinct mAb pharmacokinetics. Combining a high efficacy with limited systemic mAb exposure, the tumor emerges as an appealing delivery site for DNA-based therapeutics.

References

1. Hollevoet K, Declerck PJ. J Transl Med. 2017; 15:131-150.2. Hollevoet K, et al. Oncotarget. 2018; 9:13623–13636.

Ethics Approval

This study was approved by the KU Leuven Animal Ethics Committee, approval number P130/2017.

P605

Localized treatment with oncolytic adenovirus Delta-24-RGDOX elicits efficacious abscopal

immunity against disseminated melanomas

Hong Jiang, PhD[1], Dong Ho Shin[2], Caroline Carrillo, BS[2], Verlene Henry, BS[2], Teresa Nguyen, BS[2], Yisel Rivera-Molina, PhD[2], Frederick Lang, MD[2], Candelaria Gomez-Manzano, MD[2], Juan Fueyo[2]

[1]University of Texas MD Anderson Cancer Center, Houston, TX, USA
[2]MD Anderson Cancer Center, Houston, TX, USA

Background
We have reported that Delta-24-RGDOX, an oncolytic adenovirus expressing immune co-stimulator OX40 ligand (OX40L), induces efficacious anti-glioma immunity in syngeneic intracranial glioma models of immune competent mice. It is unknown if the virus could be used to treat metastatic melanomas.

Methods
Flow cytometry was used to determine the expression of OX40L on tumor cells, cell lysis, immunophenotyping of the lymphocyte populations. To study the abscopal immunity against metastatic melanomas induced by intratumoral injection of the virus in primary melanomas, we established subcutaneous/subcutaneous (s.c./s.c.) and subcutaneous/intracranial (s.c./i.c.) melanoma models with B16-Red-FLuc cells, a derivative of B16F10, in C57BL/6 mice to evaluate the effect of Delta-24-RGDOX on tumor-bearing mice survival, and the lymphocyte populations and their distribution in the mice. The tumor growth was monitored with bioluminescence imaging.

Results
Delta-24-RGDOX expressed mouse OX40L and induced cell lysis in both human and mouse melanoma cells. It replicated efficiently in human melanoma cells and also showed a moderate replication activity in B16-Red-FLuc cells. In the s.c./s.c. model, compared to treatment with PBS, Delta-24-RGDOX significantly inhibited the growth of both the injected and the untreated distant tumors, resulting in prolonged survival of the mice with 50% long-term survival (P = 0.001). The surviving mice is resistant to rechallenging with the same tumor cells but is susceptible to lung cancer cells, suggesting the development of immune memory specific to the virus-injected tumor type. The virus treatment increased the presence of CD3+ T lymphocytes, CD3+CD4+ helper T cells, CD3+CD8+ cytotoxic T cells and the effector T cell frequency, and decreased the amount of T regulatory cells in the tumor. In addition, analysis of T cells in the blood and spleen demonstrated that the virus mediated an abscopal effect which was indicated by the increment of effector CD4+ and CD8+ T cells frequency, and PD-1 expression on these cells. In the s.c./i.c. model, viral injection into the s.c. tumor induced anti-melanoma activity in the brain, resulting in growth inhibition of both the s.c. and i.c. tumors and an improved survival of the animals. The viral injections in the s.c. tumor increased the presence of T cells and the frequency of the effector cells in the hemispheres with the tumor implant.

Conclusions
Localized intratumoral injection of Delta-24-RGDOX induces an in situ antovaccination of the treated melanoma, of which the effect changes the immune landscape of the treated mice, resulting in the immunity against the disseminated s.c. or i.c. tumors.

Ethics Approval
The study was approved by the MD Anderson Cancer Center's Ethics Board, approval number 00000977-RN01.

P606

IFN gamma-independent upregulation of PD-L1 in oHSV-1 infected tumour cells

Erica Lee, PhD[1], Jun Ding, PhD[2], Sheng Yu[2], Yanal

Murad, PhD[2], Dmitry Chouljenko, PhD[2], Guoyu Liu, MSc, MD[2], Zahid Delwar, PhD[3], Luke Bu, MSc[2], Will Liu, PhD[2], Ronghua Zhao, MD[2], William Jia, PhD[2]

[1]*Virogin Biotech Ltd., Vancouver, BC, Canada*
[2]*Virogin Biotech Inc., Vancouver, BC, Canada*
[3]*University of British Columbia, Vancouver, Canada*

Background

Oncolytic viruses (OVs) are capable of direct tumour lysis along with recruitment of anti-tumour immune response. Notably, a systemic effect can be mediated through the induction of systemic anti-tumour immunity, especially when OVs are armed with immunomodulators [1,2]. Recently, an approved oncolytic virus T-VEC shows dramatic improvement in clinical efficacy when combined with PD-1 antibody pembrolizumab [3]. This enhanced efficacy has been implicated through increasing T cell infiltration in tumor microenvironment. In the present study, we attempt to demonstrate that OV/PD-1 antibody combination might be necessary for the anti-tumour function of infiltrating T cells through restricting tumour resistance induced by oncolytic herpes simplex virus-1 (oHSV-1).

Methods

We constructed a novel oHSV-1 (VG161) encoding human IL-12 and IL-15/IL-15Ralpha to synergistically stimulate the function of immune cells, and a PD-1 mimic peptide to block PD-1/PD-L1 interaction. Liver and colon cancer cells were infected with VG161 in vitro or intratumorally injected with VG161 in vivo and the PD-L1 expression was evaluated. In experiment investigating which virus-related signaling pathways regulated PD-L1 expression, inhibitors specifically targeting JAK/STAT, STING, or MyD88 pathway were co-treated in VG161-infected cancer cells. To examine the anti-tumour efficacy of oHSV and PD-L1 blockade combination, VG161 was compared with parental oHSV only encoding human IL-12 and IL-15/IL-15Ralpha on stimulation of immune cell functions against cancer cells.

Results

Our results demonstrate that VG161 induces PD-L1 expression on liver and colon cancer cell surfaces immediately following infection. In addition, in vivo colon cancer model shows that tumours received VG161 injection intratumorally up-regulate PD-L1 protein level. The upregulation of PD-L1 expression by oHSV infection was mediated by IFN-beta but not IFN-alpha nor IFN-gamma. Furthermore, using inhibitors on different virus-related signaling pathways, we have shown that VG161-induced PD-L1 expression involves activation of STING and STAT that was independent of JAK signal. Finally, we show that an oHSV-1 expressing PD-L1 blocking peptide (VG161) induced stronger anti-tumor effect by immune cells than its parental oHSV-1 without PD-L1 blocker.

Conclusions

Our results suggest there is a reciprocal effect between oHSV and PD-1/PD-L1 blocker. oHSV delivery in tumour site increases T cell infiltration, but meanwhile also upregulates PD-L1 expression on tumour, which renders increased resistance to T-cell mediated cytotoxicity. Combing with PD-1/PD-L1 blocker might be necessary for better clinical efficacy of oHSV-1 virotherapy by suppressing virally induced PD-L1 inhibitory effect.

References

1. Bartlett DL, Liu Z, Sathaiah M, Ravindranathan R, Guo Z, He Y, Guo ZS. Oncolytic viruses as therapeutic cancer vaccines. Mol. Cancer. 2013; 12:103-118.
2. Lichty BD, Breitbach CJ, Stojdl DF, Bell JC. Going viral with cancer immunotherapy. Nat. Rev. Cancer. 2014; 14:559–567.
3. Ribas A, Dummer R, Puzanov I, VanderWalde A, Andtbacka RHI, Michielin O, Olszanski AJ, Malvehy J, Cebon J, Fernandez E, Kirkwood JM, Gajewski TF, Chen L, Gorski KS, Anderson AA, Diede SJ, Lassman ME, Gansert J, Hodi FS, Long GV. Oncolytic virotherapy promotes intratumoral T cell infiltration

and improves anti-PD-1 immunotherapy. Cell. 2017; 170:1109-1119.

P607

The TLR4 agonist G100 enhances the efficacy of adoptive T-cell therapy

Jardin Leleux, PhD[1], Tina Albershardt, PhD[1], Peter Berglund, PhD[1], Jan Ter Meulen, MD, PhD[1],

[1]*Immune Design, Seattle, WA, USA*

Background
Immunosuppression in the tumor microenvironment (TME) and immune escape mechanisms of tumor cells may impede the effectiveness of adoptive cell therapies (ACT). To this end, strategies to reverse these mechanisms by enhancing T-cell trafficking and immune exposure of the tumor are needed. G100 is a synthetic TLR4 agonist formulated for intratumoral treatment, which has been shown preclinically and clinically to inflame the TME, stimulate local draining lymph nodes, enhance antigen presentation and induce systemic CD4 and CD8 T cell responses that result in antitumor efficacy. G100 also improves infiltration of vaccine-induced T-cells into murine tumors. In this study, we investigated whether the efficacy of ACT is enhanced when combined with intratumoral G100.

Methods
Female C57BL/6 recipient mice were inoculated with B16F10 or ovalbumin-expressing-B16F10 (B16-OVA) melanoma tumors. Once tumors were palpable, biweekly treatments of G100 were initiated. Splenic CD8+ T cells from OT-I and pmel mice, which carry a rearranged TCR transgene specific for an OVA or gp100 epitope, respectively, were magnetically isolated and transferred into the tumor-bearing mice. Tumor growth was monitored 2-3 times per week by caliper measurement until tumors either completely regressed or mice were euthanized due to tumor growth. In some experiments, tumors and tumor-draining lymph nodes were isolated from animals and analyzed by flow cytometry for infiltration of transferred CD8+ T cells.

Results
Mice that received both ACT and G100 treatments ("transfer-pull") experienced significantly enhanced tumor protection compared to mice that received ACT or biweekly intratumoral G100 alone. Treatment of B16-OVA tumor-bearing mice using the transfer-pull regimen resulted in complete tumor regression in 70% of the animals, whereas no tumor regression was observed for animals receiving either monotherapy. Consistent with the proposed mechanism of action, actively proliferating transferred T-cells were present in tumors as well as tumor-draining lymph nodes of transfer-pull treated mice. When targeting the less immunogenic gp100 melanoma antigen, median survival was significantly extended and complete regression observed in up to 28% of animals.

Conclusions
These data collectively demonstrate that intratumoral G100 can be effectively used in combination with adoptive cell therapy to enhance tumor rejection and survival, warranting further preclinical and clinical evaluation.

P608

ProTriTAC: a protease-activatable T cell engager platform that links half-life extension to functional masking and expands therapeutic window to enable targeting of broadly expressed tumor antigens

S. Jack Lin, PhD[1], Maria Rosalyn Dayao[1], Kendrick Kim[1], Sony Rocha[1], Kathryn Kwant, PhD[1], Timothy Yu[1], Thomas Evans[1], Stephen Yu[1], Michael Cremin[1], Wade Aaron, BS[1], Maria Gamez-Guerrero[1], Evan Callihan[1], Golzar Hemmati[1], Kevin Wright, PhD[1],

Yinghua Xiao, Master Degree[1], Manasi Barath[1], Che-Leung Law, PhD[1], Bryan Lemon, PhD[1], Richard Austin, PhD[1], Holger Wesche, PhD[1]

[1]*Harpoon Therapeutics, Inc., South San Francisco, CA, USA*

Background

T cell engagers, such as blinatumomab, have demonstrated clinical activity in several hematological malignancies, but their use in solid tumors is limited by the low number of antigens that are expressed in tumors but not in normal tissues. Conditionally active T cell engagers that function preferentially in the tumor microenvironment offer a path to expanding the therapeutic window by reducing their on-target but off-tumor activity. Here, we describe a prodrug version of our T cell engager platform, termed ProTriTAC, that is activated by proteases in the tumor microenvironment and enables the safe targeting of broadly expressed solid tumor antigens.

Methods

ProTriTACs were engineered with three binding domains on a single polypeptide: anti-albumin for half-life extension, anti-CD3e for T cell engagement, and anti-tumor-associated antigen. They have an anti-albumin domain, comprising a masking moiety and a protease-cleavable linker, to keep the molecules inert outside the tumor microenvironment. Activation by tumor-associated proteases removes the anti-albumin domain along with the masking moiety to reveal the active drug. The masking moieties were identified using phage display. Binding studies to recombinant CD3e protein were determined using ELISA assays and to primary T cells using flow cytometry assays. T cell engager function was assessed using T cell-dependent cellular cytotoxicity (TDCC) assays with resting human T cells. In vivo efficacy studies were performed using a subcutaneous tumor xenograft model in immunodeficient NCG mice.

Results

Proof-of-concept experiments were carried out in vitro and in vivo. The protease-activated ProTriTAC had markedly increased binding to recombinant CD3e protein and to human primary T cells as well as increased T cell-redirected killing activity in TDCC assays when compared to the prodrug. Consistent with tumor-dependent activation of ProTriTACs in vivo, ProTriTACs have comparable anti-tumor activity to the unmasked molecule but significantly more anti-tumor activity than the masked non-cleavable molecule.

Conclusions

ProTriTACs are designed as long-lived inert prodrugs when in circulation and become short-lived active drugs for T cell-redirected tumor killing when activated in the tumor microenvironment. This half-life differential between the prodrug and the active drug is desirable as any aberrant activation of prodrug outside the tumor will be cleared rapidly, thereby further expanding the therapeutic window. This technology enables more T cell engager targets for solid tumors, and we are building a pipeline of ProTriTACs against these targets.

Ethics Approval

In vivo studies were reviewed and approved by Harpoon's Institutional Animal Care and Use Committee.

P609

First in man study of TK positive oncolytic vaccinia virus delivered by adipose stromal vascular fraction cells

Boris Minev, MD[1], Elliot Lander, MD[3], John Feller, MD[4], Mark Berman, MD[5], Stuart May, MD[4], Bernadette Greenwood[4], Ivelina Minev, MSc[6], Duong Nguyen, PhD[6], Antonio Santidrian[6], Dobrin Draganov, PhD[6], Mehmet Kilinc, PhD[6], Santosh Kesari, MD,

PhD[7], Edward McClay, MD[8], Gabriel Carabulea, MD[9], Aladar Szalay, PhD[6]

[1]*Moores University of California San Dieg, San Diego, CA, USA*
[2]*Moores UCSD Cancer Center, San Diego, CA, USA*
[3]*California Stem Cell Treatment Center, Rancho Mirage, CA, USA*
[4]*Desert Medical Imaging, Indian Wells, CA, USA*
[5]*Cell Surgical Network, Beverly Hills, CA, USA*
[6]*Calidi Biotherapeutics, San Diego, CA, USA*
[7]*John Wayne Cancer Institute, Santa Monica, CA, USA*
[8]*cCare, Encinitas, CA, USA*
[9]*Ocean View Hematology and Oncology Group, San Clemente, CA, USA*

Background
Recent oncolytic virus clinical studies have shown safety and implied anti-tumor activity. However, a major obstacle to this approach has been the rapid oncolytic virus elimination by patient's immune system. We hypothesized that oncolytic viruses would be protected and delivered efficiently to tumor sites by autologous adipose stromal vascular fraction (SVF) cells. Effective virus protection by adipose derived cells has been confirmed in preclinical studies. Here, we report the results of a first-in-man trial to determine the safety and feasibility of this approach in patients with advanced solid tumors and AML.

Methods
In this single-arm, open-label safety study, 24 patients with advanced solid tumors and 2 patients with AML were treated with a single administration of the oncolytic virus ACAM2000 (vaccinia) delivered by SVF cells. Patients received ACAM2000/SVF by intravenous application, or by a combination of intravenous and intratumoral or intra-peritoneal injections. The dose for ACAM2000 was between 1.4 x 106 pfu to 1.8 x 107 pfu incubated with same number of SVF cells. The primary endpoint was safety/tolerability by incidence of dose-limiting toxicity. Secondary endpoints included evaluations of overall survival and induction of anti-tumor and anti-vaccinia immune responses. Blood samples were collected at multiple time points for quantifying vaccinia virus DNA in peripheral blood by qPCR. In addition, levels of 30 plasma cytokines and the effects on activated T cells, Tregs, memory T cells, NK cells, and MDSC were analyzed.

Results
No serious toxicities (> grade 2) were reported. Eight of the 26 subjects reported an AE: self-limiting skin lesions, lasting 7 to 18 days – an expected reaction to ACAM2000. No infusion-related AEs were reported. No AEs leading to study discontinuation were reported. Viral DNA was detected in all patients immediately following treatment. Interestingly, in 8 patients viral DNA disappeared 1 day and re-appeared 1 week post treatment, suggesting active viral replication, possibly at tumor sites. This viral DNA reappearance correlated with longer survival of these patients. No major increase in cytokine levels was observed in any of the patients. No correlation between cytokine levels and pox lesions was noted. Flow cytometry showed gradual changes suggesting improved immune cell activation status. Tumor size reduction was documented in several patients.

Conclusions
Treatment with ACAM2000/SVF in patients with advanced solid tumors and AML is safe and well tolerated, with clear antitumor effects in several patients. These promising initial clinical results merit further investigation of therapeutic utility.

Acknowledgements
Boris Minev, MD and Elliot Lander, MD contributed equally to this work.

Ethics Approval
The study was approved by International Cell Surgical Society's Ethics Board, approval number ICSS-2017-004

P610

Transcriptome analysis of CT26 tumors treated with HSV-1 oncolytic virus expressing multiple immune factors

Yanal Murad, PhD[1], Jun Ding, PhD[1], Erica Lee, PhD[1], Dmitry Chouljenko, PhD[1], Luke Bu, MSc[1], Guoyu Liu, MSc, MD[1], Zahid Delwar, PhD[2], Will Liu, PhD[1], Ronghua Zhao, MD[1], William Jia, PhD[2]

[1]Virogin Biotech. Inc., Vancouver, BC, Canada
[2]University of British Columbia, Vancouver, Canada

Background
Oncolytic HSV-1 (oHSV-1) treatment induces a potent immune response against tumor antigens, which can be augmented once combined with other immune stimulatory factors. Previously, we have generated an oncolytic HSV-1 virus (VG161) which carries 2 immunomodulator cytokines, IL12 and IL15/IL15RA1, along with a PD-L1 mimic peptide capable of blocking PD-1/PD-L1 interaction. These factors work synergistically to trigger and maintain an efficient anti-tumor immune response in the tumor microenvironment. In this work, we demonstrate the superior activity of the VG161 virus, compared to the back-bone virus (with no payloads) using a mouse colon cancer tumor model. We also perform a transcriptome analysis to determine the differential gene expression in the treated tumors and compare the two treatments.

Methods
We tested the efficacy of VG161 treatment in CT26 mouse model and examined the differential expression of transcriptome in these tumors collected 5 days post treatment with VG161 or the corresponding backbone virus. After extracting the RNA from the tumor samples, we performed RNA sequencing and analyzed differential expression of genes and compared them between the 2 treatments. qRT-PCR was used to validate targets identified by RNA sequencing.

Results
In the CT26 model, tumors regressed to undetectable limits upon intra-tumoral injection with VG161. When the treated mice were challenged with the same tumor, the tumor cells did not grow. Tumor treated with VG161 has demonstrated a higher number of tumor-infiltrating CD8 T cells, which activity against the tumor cells was also demonstrated by ELISpot assay. Differential expression of 24342 genes was performed and 18 differentially expressed genes with q-Value <0.05 were identified. These genes included chemokines and interferon response elements associated with inflammatory response, along with acute phase proteins. Some of the overexpressed genes, especially those related IFN response elements genes were also validated by qRT-PCR.

Conclusions
We have demonstrated by transcriptome analysis that VG161, a novel oncolytic virus which can induce a strong anti-tumor immunity and oncolytic activity, can induce multiple genes which result in efficacy against tumors. The efficacy of VG161 can be partially attributed to the immune response generated by the modified virus, which is likely induced by the change in the tumor microenvironment triggered by the VG161 payload. Further work is needed to dissect the function of each of the differentially expressed genes to understand the role they play in the regression of cancer upon VG161 treatment.

P612

Overcoming oncolytic poliovirus-mediated adaptive immune resistance by combining with anti-PD1/-PDL1 therapy in cancer.

Smita Nair, PhD[1], Eda Holl, PhD, RAC[1], Michael

Brown, PhD[1], Victoria Frazier[1], David Boczkowski, BS, MSc[1], Vidyalakshmi Chandramohan, PhD[1], Darell Bigner, MD, PhD[1], Shelley Hwang[1], Matthias Gromeier, MD[1]

[1]*Duke University School of Medicine, Durham, NC, USA*

Background

Oncolytic poliovirus (OncPV) PVSRIPO is a recombinant, non-pathogenic polio:rhinovirus chimera that targets cancer cells via CD155. PVSRIPO also targets antigen-presenting cells (APCs), including dendritic cells (DCs) and macrophages. PVSRIPO infection of APCs induces sustained type I interferon and APC activation (1). In a phase-1 clinical trial of intratumor PVSRIPO in 61 patients with recurrent glioblastoma (GBM), the survival rate at 24-months and 36-months was 21% (2). This study examines the following hypotheses: 1] Intratumor OncPV administration causes oncolysis and inflammation, which stimulates innate and adaptive immunity; 2] Immune cell activation in tumor triggers adaptive immune resistance via the PD1/PDL1 axis; 3] Blocking PD1/PDL1 in conjunction with OncPV will eliminate adaptive resistance and potentiate durable antitumor immunity.

Methods

OncPV-mediated immune activation was analyzed in: 1] immunocompetent murine models of orthotopic E0771 breast cancer and subcutaneous B16 melanoma; 2] human tumor cell lines and primary human tumor tissue from patients with breast cancer, melanoma and GBM; 3] human DCs and macrophages. To investigate combination PVSRIPO and PD1/PDL1 blockade, C57BL6-CD155 transgenic mice were orthotopically implanted with E0771-CD155 tumor cells. Mouse PVSRIPO (mRIPO) was injected intratumorally once in 50-100 mm3 tumors. Checkpoint antibodies were injected intraperitoneally 1-day post-mRIPO, 4-6 times every 3 days. Tumor growth was monitored.

Results

Intratumor mRIPO induced recruitment of immune cells (Figure 1), a classical acute inflammatory response and systemic antitumor cytotoxic T cell responses (1). Tumor infiltrating CD8/CD4 T cells demonstrated an effector phenotype and expressed PD1 (Figure 2). Infection of primary human tumors with PVSRIPO induced Stat1-p, IFIT1 and PDL1 expression and production of pro-inflammatory cytokines (Figure 2). Infection of human tumor cell lines with PVSRIPO induced PDL1 expression (Figure 2). PVSRIPO-infected primary human DCs and macrophages demonstrated sustained activation and PDL1 expression.Based on these data we investigated combination PVSRIPO with PD1/PDL1 blockade in murine breast cancer model. mRIPO, anti-PD1/-PDL1, and mRIPO+anti-PD1/-PDL1 significantly inhibited tumor growth compared to PBS. There were no significant differences in tumor growth inhibition between mRIPO and anti-PD1/-PDL1 monotherapies. Combination mRIPO+PD1/PDL1 blockade was significantly more effective than the monotherapies alone at controlling tumor growth.

Conclusions

We demonstrate that OncPV-mediated adaptive immune resistance involves the PD1/PDL1 axis and is mitigated by combining OncPV with anti-PD1/-PDL1 in murine breast cancer model. We are currently investigating PVSRIPO-mediated local and systemic immune bioactivity in women with triple-negative breast cancer and planning a trial of PVSRIPO with anti-PDL1 in women with breast cancer.

Acknowledgements

This study is funded by the Department of Defense Breast Cancer Research Program award (PI, Smita Nair).

Trial Registration

ClinicalTrials.gov Identifier: NCT03564782

References

1. Brown MC, Holl EK, Boczkowski D, Dobrikova E, Mosaheb M, Chandramohan V, Bigner DD, Gromeier M, Nair SK. Cancer immunotherapy with recombinant poliovirus induces IFN-dominant activation of dendritic cells and tumor antigen-specific CTLs. Sci Transl Med. 2017 Sep 20;9(408).
2. Desjardins A, Gromeier M, Herndon JE 2nd, Beaubier N, Bolognesi DP, Friedman AH, Friedman HS, McSherry F, Muscat AM, Nair S, Peters KB, Randazzo D, Sampson JH, Vlahovic G, Harrison WT, McLendon RE, Ashley D, Bigner DD. Recurrent Glioblastoma Treated with Recombinant Poliovirus. N Engl J Med. 2018; 379(2):150-161.

Ethics Approval

All studies are conducted under Duke University IACUC- and IRB-approved protocols. The human samples used in the study were conducted under IRB-exempt protocols.

Figure 1.

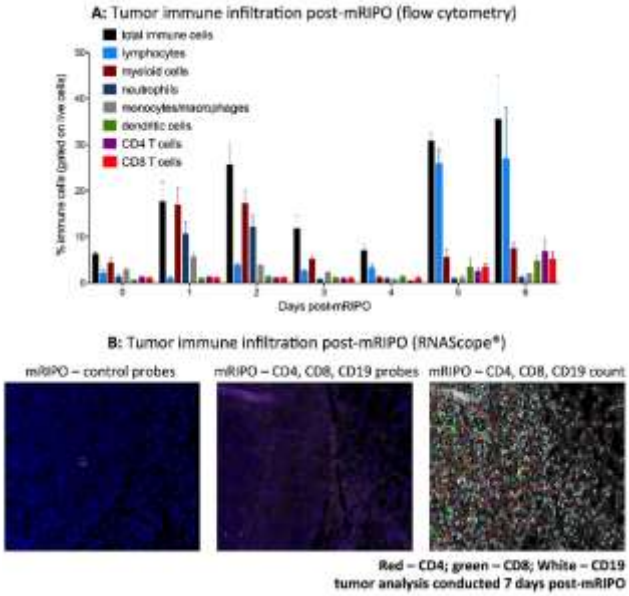

Figure 2.

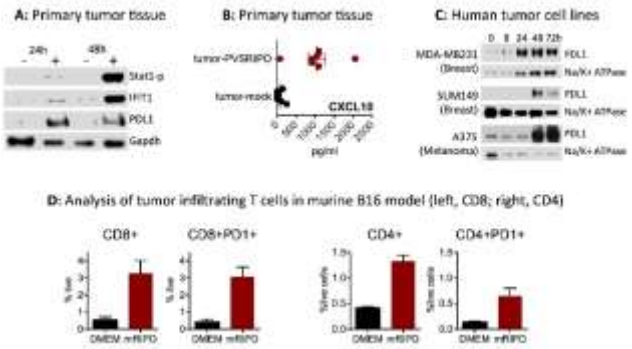

P613

Non-oncolytic viral infection reduces tumor burden and promotes anti-tumor immunity in synergy with checkpoint blockade

Jenna Newman[1], Charles Chesson, PhD[2], Andrew Zolza[1]

[1]*Rutgers Cancer Institute of New Jersey, Colonia, NJ, USA*
[2]*MD Anderson Cancer Center, Houston, TX, USA*

Background

Immunotherapy for cancer has had clinical success in recent years, with adoptive cell therapies and checkpoint blockade inducing long-term regression in an unprecedented subset of patients. Despite success, a significant fraction of patients are resistant to immunotherapy, prompting investigation into alternative strategies to initiate anti-tumor immunity. One approach that has had clinical impact is the intratumoral administration of oncolytic viruses, such as the recently FDA-approved T-VEC. While oncolytic viruses have shown efficacy in promoting cell lysis, tumor cell antigen release, and ultimately initiating an anti-tumor CD8+ T cell response, little is known regarding the impact of non-oncogenic, non-oncolytic viruses on tumor growth and immunity. Therefore, we sought to characterize the impact of influenza, a non-oncolytic

virus, on tumor growth and initiation of anti-tumor immune responses in a B16 murine melanoma model.

Methods

C57BL/6 mice were challenged with 120,000 cells B16 F10 intravenously to allow for development of melanoma foci in the lungs. Five days following tumor challenge, mice were administered 1 × 106 pfu of A/PR8/H1N1 influenza intranasally. Body weight was recorded every 2-3 days to assess the health of influenza-infected mice. Tumor size was monitored every 2-3 days via caliper measurement. Mice receiving PD-1 blockade were treated with 250 µg α-PD-1, or isotype control antibody, every 3 days. Mice were sacrificed at days 7 and 14 after tumor challenge; tissues were harvested for flow cytometry and LEGENDPlex™ analysis.

Results

Mice concomitantly challenged with influenza and melanoma in the lungs exhibited a decrease in the number of melanoma foci in the lungs, relative to that observed in influenza-naïve counterparts ($p<0.05$). Synergy between influenza infection and checkpoint blockade was observed; influenza-infected tumor-bearing mice treated with PD-1 blockade exhibited the lowest tumor burden of all groups. Influenza-infected, melanoma-bearing mice exhibited a significantly higher proportion of gp100-reactive (anti-tumor) CD8+ T cells in the lungs, than that observed in uninfected controls ($p<0.05$). PD-1 blockade-treated influenza-infected mice exhibited an elevated proportion of anti-tumor CD8+ T cells relative to counterparts administered an isotype control antibody. Furthermore, LEGENDPlex™ analysis revealed an elevation in the pro-inflammatory cytokine IL-12 (p40) in the lungs of infected mice, compared to that observed in influenza-naïve, tumor-bearing mice, and that of influenza-infected mice without tumors.

Conclusions

Our results suggest that a non-oncogenic, non-oncolytic viral infection, influenza, can induce reduction of tumor growth and generation of anti-tumor immunity when administered at the site of a tumor. Further research will address potential therapeutic impact in humans.

P614

Nano-Pulse Stimulation™ of murine melanoma and mammary carcinoma is a physical modality that eliminates the treated tumor by regulated cell death and induces innate and adaptive immune responses

Richard Nuccitelli, MS, PhD[1], Amanda McDaniel, BA[2], Bruce Freimark, PhD[2], Joel Benjamin, PhD[2], Jessica Sood, BS[2], Darrin Uecker, MS[2]

[1]Pulse Biosciences Inc., Hayward, CA, USA
[2]Pulse Biosciences, Burlingame, CA, USA

Background

Nano-Pulse Stimulation (NPS™) is a non-thermal, precise, focal tissue treatment technology comprised of nanosecond (billionth of second)-range pulsed electric energy that directly affects the cell membrane and intracellular structures, and initiates regulated cell death in treated cells. NPS has been shown in preclinical models to induce immunogenic cell death (ICD) which exposes the unique antigens of the treated cells to the immune system and recruits immune system cells to mount an adaptive immune response [1, 2, 3].

Methods

Two syngeneic murine tumor models (B16-F10 melanoma and 4T1 mammary carcinoma) were used to investigate NPS effects on murine tumors. Tumor cells were injected intradermally on the left flank

and when tumors reached 4-5 mm in diameter, we treated with NPS. Tumor volume measurements were conducted twice per week and tumors were excised at predetermined timepoints for immunophenotyping of tumor-infiltrating immune cells by flow cytometry and gene expression profiling using NanoString. Splenocytes were also evaluated for responses to tumor cell stimulation by IFN-gamma ELISpot.

Results

NPS-treated tumors undergo regulated cell death and are eliminated within 2 weeks providing complete local control. In addition, ELISpot analysis of splenocytes indicates that NPS initiates an immune response to the treated tumor by 4 weeks after treatment. Gene expression profiling of NPS-treated tumors revealed that transcripts for specific intrinsic apoptotic pathways, damage-associated molecular patterns (DAMPs) and immune mediators increase 24 h after NPS treatment. Splenocytes from tumor-bearing animals treated with NPS have greater IFN-gamma-secreting cells compared to naive or resected animals in response to co-culture with tumor cells. Studies to determine the optimal conditions for NPS treatment are underway.

Conclusions

NPS is a physical modality that targets intracellular structures to trigger regulated cell death in the treated tumor cells. Our studies indicate that this treatment initiates endoplasmic reticulum stress and immunogenic cell death (ICD) that leads to a tumor-specific immune response.

References

1. Nuccitelli R, Berridge JC, Mallon Z, Kreis M, Athos B, Nuccitelli P. Nanoelectroablation of murine tumors triggers a CD8-dependent inhibition of secondary tumor growth. PLoS ONE. 2015; 10(7): e0134364 1-17.
2. Nuccitelli R, McDaniel A, Anand S, Mallon Z, Berridge JC, Uecker D. Nano-Pulse Stimulation is a physical modality that can trigger immunogenic tumor cell death. J Immunotherapy Cancer. 2017; 5:32 DOI 10.1186/s40425-017-0234-5.
3. Skeate JG, DaSilva DM, Chavez-Juan E, Anand S, Nuccitelli R, Kast W.M. Nano-Pulse Stimulation induces immunogenic cell death in human papillomavirus-transformed tumors and initiates an adaptive immune response. 2018; PLoS ONE. 13(1): e0191311.

P615

Antibody-armed oncolytic Vaccinia virus to block immunosuppressive pathways in the tumor microenvironment

Eric Quemeneur, PharmD, PhD[1], Jean-Baptiste Marchand, pHD[1]

[1]*Transgene S.A., Illkirch-Graffenstaden, France*

Background

Vaccinia virus (VV) has proven to be a powerful oncolytic vector thanks to its large spectrum of tumor cell targets, large genome capacity, good safety properties, and strong immunogenic properties. We have developed an improved VV-based platform in the Copenhagen strain, with a double deletion in the J2R/TK, and I4L/RR genes, that displays a very high therapeutic index (over 104), compatible with the intravenous route. VVTK-RR- can be genetically modified to express full-length monoclonal antibodies, and additional cytokines, at the site of active viral replication and accumulation, i.e. directly in the tumor. Thus, checkpoint blockers can be targeted to boost the immune response locally initiated by the oncolytic activity. Moreover, the benefit of vectorizing a mAb would be to diminish the severe side effects reported for some systemic administration, and to increase the intratumoral antibody concentration to maximize the probability of efficacy. Our first products addressed the two major inhibitory pathways : a VV-anti-PD-1

to restore the activity of infiltrated effector T cells, and a VV-anti-CTLA-4 to selectively deplete intratumoral regulatory T cells via ADCC.

Methods
Mice bearing syngeneic tumors were treated with oncolytic VV either alone or in combination with immune checkpoint inhibitors (anti-mCTLA4, and anti-mPD1). In the POC experiment, the anti-mPD1 was vectorized in VVTK-RR- as two independent cassettes at the J2R locus expressing the light and the heavy chains under strong viral promoters. The level of expression of the vectorized mAb was monitored over time after intra-tumoral injection and in blood stream of tumor-bearing mice.

Results
Combination experiments in immunocompetent preclinical models demonstrated that oncolytic VV and ICI can have at least additive anti-tumoral activities if administrated sequentially (i.e. VV first and ICI several days later). The vectorization of a mAb allowed its intratumoral expression with a kinetics that mimicked the schedule of administration of the combination (peak of tumor accumulation at days 3-5). The expression lasted for several days after administration of the virus, allowing for a similar anti-tumoral activity as repeated administrations of the reference mAb. Finally, unlike the combination, the vectorization resulted in a minimal systemic exposure to the ICI.

Conclusions
Vectorization in an oncolytic VV allows the intratumoral delivery of an active doses of therapeutic antibody. This recombinant platform is particularly relevant for ICIs with unfavorable toxic profiles such as anti-CTLA4 mAb. BioInvent and Transgene are currently developing the next generation of oncolytic viruses by arming VV with Fc–optimized anti-CTLA4 mAbs.

P616 **Abstract Travel Award Recipient**

Fueling antitumor immunity using oncolytic viruses encoding metabolic modulators

Dayana Rivadeneira, PhD[1], Kristin DePeaux[1], Nicole Scharping, BS[1], Padmavathi Sampath, PhD1, Saumendra Sarkar, PhD[1], Stephen Thorne, PhD[1], Greg Delgoffe, PhD[1]

[1]*University of Pittsburgh, Pittsburgh, PA, USA*

Background
Immunotherapy has shown impressive clinical responses, but many patients do not respond to single modality immunotherapy due to a number of non-redundant resistance mechanisms. Our lab and others have proposed that tumor cells compromise T cell function by generating a metabolically inhospitable microenvironment, suggesting that immune or tumor metabolism can be differentially modified to improve T cell responses and thus immunotherapy.

Methods
We identified the adipokine leptin as a means to remodel the metabolic state of tumor infiltrating T cells. To assess the effects of leptin in the tumor microenvironment, we generated an aggressive PTEN/BRAF melanoma line overexpressing leptin, as well as an oncolytic strain of Vaccinia virus engineered to induce tumor-specific secretion of leptin.

Results
Treatment of T cells with leptin in vitro resulted in dramatic metabolic reprogramming. In vivo, intratumoral administration of leptin resulted in enhanced T cell metabolic and effector function. We then engineered melanoma cell lines to locally secrete leptin. While there was no proliferation difference between wild-type and leptin-expressing

tumor cells in vitro, these cells are controlled in vivo in a CD8+ T cell specific manner. Leptin overexpressing tumors have increased T cell infiltration compared to control tumors, and these TIL are metabolically and functionally superior. In order to translate out findings to a therapeutic setting we utilized an oncolytic virus model. Oncolytic viruses are an attractive therapeutic modality promoting tumor specific killing as well as inducing an anti-tumor immune response. While wild-type oncolytic Vaccinia resulted in some tumor regression, leptin-engineered Vaccinia had superior therapeutic efficacy inducing complete regressions in 30% of mice. TIL from these tumors have improved T cell infiltration and function. We profiled immune infiltrates by single cell RNAseq and TCR sequencing. Data revealed the influx of new T cells by vaccinia which was characterized by a polyclonal repertoire. On the other hand, T cells from tumors treated with leptin-expressing virus showed a reduced polyclonal phenotype indicative of specific clonal expansion. This clonal expansion is associated with a more memory like state, and indeed leptin-engineered VV induced a greater percentage of CD127hi memory precursors than the oncolytic VV alone.

Conclusions

Taken together, these data suggest metabolic modulators like leptin can be therapeutically exploited to bolster intratumoral T cell function using the oncolytic virus platform. Our goal is to further design novel therapeutic strategies using oncolytic viruses.

P617

A cell-based platform to protect and enhance oncolytic virus therapies

Antonio Santidrian[1], Dobrin Draganov, PhD[1], Duong Nguyen, PhD[1], Okyay Kilinc[1], Ivelina Minev, MSc[1], Boris Minev, MD[1], Aladar Szalay, PhD[1]

[1]*Calidi Biotherapeutics*

Background

Different types of viruses, including vaccinia virus (VACV), can selectively replicate in cancer cells and trigger antitumor immunity. Oncolytic virotherapies, as a monotherapy or in combination with other immunotherapeutics, have shown safety and exciting proof-of-concept results in pre-clinical studies as well as in different clinical trials. The therapeutic potential of oncolytic viruses, however, can be severely restricted by multiple innate and adaptive immune barriers that can be overcome using cell-based delivery approaches. Mesenchymal stem cells are particularly attractive carriers of oncolytic viruses due to their unique immunosuppressive properties allowing protection of the virus from complement/antibodies-mediated neutralization and to overcome anti-viral cellular immunity in both autologous and allogeneic settings

Methods

As carriers of oncolytic VACV, we used cells a) freshly isolated from adipose tissue stromal vascular fraction (SVF), and b) SVF-derived cultured Adipose-Derived Mesenchymal Stromal/stem Cells (AD-MSC). We analyzed the ability of those carrier cells to take up, protect, amplify the virus as well as to overcome innate and adaptive immune barriers by flow cytometry, microscopy and virus plaque assays of ex vivo co-cultures of cells infected with VACV in the presence of human serum or peripheral blood mononuclear cells from healthy donors. Comparative analyses were performed to establish statistically significant correlations.

Results

We have demonstrated that autologous SVF cells did protect VACV against serum-inactivation. Cell sorting demonstrated that supra adventitial-adipose stromal cells (SA-ASC; CD235a-/CD45-/CD34+/CD146-/CD31-), and pericytes (CD235a-/CD45-/CD34-/CD146+/CD31-) were the two cell populations of

SVF cells that were efficient facilitating the delivering of VACV to the tumor cells, validating their clinical use as a tool to potentiate oncolytic virus therapies in autologous settings. We further analyzed the potential of using cultured AD-MSC (derived from CD34+ SA-ASC) as a delivery vehicle in allogeneic settings. AD-MSCs demonstrated ability to protect against serum-inactivation as well as to amplify the virus in the presence of human PBMCs in both autologous and allogeneic settings. This activity can be linked to their intrinsic immunosuppressive properties and the evasion of allogeneic rejection. Moreover, these cells demonstrated ability to provide transient immunosuppression by inhibiting antiviral responses originating from both innate (NK)- and adaptive (T)-immune cells, thus augmenting viral oncolysis and the generation of anti-tumor immunity.

Conclusions

Overall, our findings indicate the feasibility to significantly potentiate oncolytic virotherapy by using either a simple autologous or a more scalable off-the-shelf allogeneic cell-based delivery technology allowing rational design of virus-based therapies that are not dramatically eliminated by immune barriers.

Ethics Approval

The study was approved by International Cell Surgical Society Ethics Board; IRB# ICSS-2016-024

P618

Selective delivery of exosome-mediated STING agonist to antigen presenting cells results in significantly improved potency and reduced toxicity

Su Chul Jang, PhD[1], Raymond Moniz[1], Christine Sia[1], Joyoti Dey, PhD, MPH[2], Rane Harrison[1], NIKKI ROSS, PhD[1], Ke Xu[1], Kevin Dooley[1], Nuruddeen Lewis[1], Christine McCoy[1], Agata Villiger-Oberbek[1], Scott Estes[1], Jorge Sanchez-Salazar[1], Kyriakos Economides[1], Sriram Sathyanarayanan[1]

[1]Codiak Biosciences, Cambridge, MA, USA
[2]Presage Biosciences, Seattle, WA, USA
[3]Codiak, Cambridge, MA, USA

Background

Emerging research has established the role of exosomes as an efficient natural messenger system to deliver macromolecules between cells. We have leveraged this capacity to develop a novel, engineered exosome therapeutic, to selectively deliver agonists of the Stimulator of Interferon Gene (STING) pathway to tumor resident antigen presenting cells (APC).

Methods

ExoSTING is composed of exosomes, which are molecularly engineered to over-express an exosomal membrane glycoprotein, and which are loaded ex vivo with a STING agonist (SA).

Results

In vitro assays with human PBMCs showed ExoSTING enhanced the potency of dendritic cell and monocyte activation and IFN_beta production by 100-fold compared to comparable amounts of free SA. Although liposomal formulated SA also improved potency, it resulted in dose-dependent loss of viability in APC. Intra-tumoral micro-dosing of ExoSTING with the CIVO® platform demonstrated selective activation of pTBK1 and pIRF3 in APC resulting in superior IFN_beta production compared to free SA. Anti-tumor activity of Exo-STING and free SA was compared in a checkpoint therapy refractory B16F10 tumor model. Intra-tumoral (IT) administration of ExoSTING resulted in 500-fold enhancement in potency versus free SA, with dose-dependent anti-tumor activity resulting in tumor cures in 50% of the mice in the highest (0.2µg) ExoSTING dose cohort. ExoSTING treated mice were

refractory to re-challenge with B16F10 demonstrating the presence of an immune memory response. IT administration of efficacious doses of ExoSTING stimulated robust IFN_gamma but did not result in systemic induction of inflammatory cytokines as seen with an efficacious dose of free SA. ExoSTING IT treatment induced IFNγ regulated genes, PD-L1 and chemokines responsible for T-cell recruitment in the tumor, resulting in significant systemic induction of tumor antigen-specific T cell response.

Conclusions

ExoSTING affords selective agonism of the STING pathway in tumor resident APC that results in improved potency, reduced systemic toxicity and enhanced T-cell responses, and highlight the potential of our exosome engineering technology as an impactful therapeutic platform.

P619

Image-guided intratumoral delivery of immunotherapeutics: interventional radiology perspective

Rahul Sheth, MD[1], Ravi Murthy, MD[1], Funda Meric-Bernstam, MD[1], David Hong, MD[1], Sapna Patel, MD[1], Alda Tam[1*]

[1]*MD Anderson Cancer Center, Houston, TX, USA*

Background

There has been an exponential proliferation in the direct intratumoral (IT) delivery of a range of immunotherapies (IMT), ranging from cell-based therapies to viruses, bacteria, cytokines, and monoclonal antibodies. In this study, we report our single institutional experience with IT injections in the investigational, off-label, and standard-of-care settings in patients with solid tumors.

Methods

All patients who underwent image-guided IT delivery of IMT agents by Interventional Radiology over a 2 year period (Jan 2016 –18) were included in this single institution retrospective analysis. Lesion characteristics (size, location, concomitant biopsy) were recorded. Injection technique and adverse events related to needle insertion vs. drug delivery were identified by chart review.

Results

66 patients underwent 429 image-guided IT investigational agent injections; malignancies included melanoma (50%), sarcoma (21%), ovarian cancer (4.5%), breast cancer (3%) and colon cancer (3%), and other (18.5%). Additionally, 18 patients (9 cutaneous melanoma patients as standard-of-care, 9 uveal melanoma patients as off-label use) underwent 113 image-guided IT injections of TVEC. A tracer and fanning methodology was employed to optimize distribution within the lesion when using a single end-hole beveled needle. The median number of encounters per patient was 6 (range: 1-20) in the investigational setting and 5 (range: 1-17) for TVEC. Subcutaneous lesions represented 62% and 100% of injected tumors in the investigational and TVEC patients, respectively. Visceral lesions in deeper locations and solid organs were also injected: pelvic (6.7%), abdominal (6.2%), intramuscular (6.2%), adrenal (4.3%), liver (3.7%), and lung (2.4%) (Figure 1). The median target lesion tumor volume was 6.4cc (range: 0.1 – 984cc) in investigational patients and 3.5cc (range: 0.2 – 250cc) in TVEC patients. There were no adverse events related to needle insertion. However, serious adverse events NCI CTC >3 including dyspnea and rigors developing within 90 minutes of the injection and requiring hospitalization occurred following 2.4% of investigational agent and 3.5% of TVEC injections. NCI CTC AE<3 including allergic reactions that did not require an escalation of care occurred in 3.4% of clinical trial patients and 0.9% of TVEC patients.

Conclusions
Initial observations indicate that image guided IT injections of a variety of IMT agents are feasible for both subcutaneous as well as deeper, visceral organ-based lesions. Immediate post delivery anticipated adverse events occur in a small minority of instances. Performing physicians should have the necessary safeguards in place to respond as needed. Moreover, efforts to standardize drug delivery techniques may also be required.

Ethics Approval
This study was approved by our institution's Ethics Board; approval number PA18-0650.

Figure 1. Intratumoral injection site

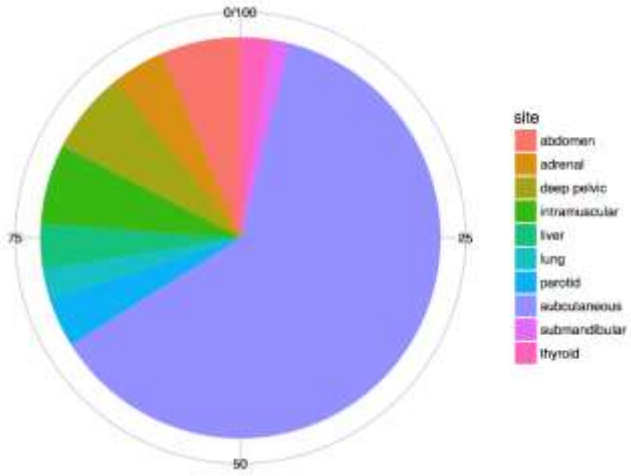

P620

Enhanced efficacy and combinability of low dose toca 511 and 5-FC with metronomic chemotherapy in preclinical models

Sophie Viaud[1], Derek Ostertag[1]

[1]*Tocagen, San Diego, CA, USA*

Background
Toca 511 (vocimagene amiretrorepvec) is an investigational, conditionally lytic, retroviral replicating vector that selectively infects cancer cells due to specificity for dividing cells combined with the immune-suppressed tumor microenvironment. Toca 511 spreads and stably delivers optimized yeast cytosine deaminase (CD) that converts subsequent Toca FC (an investigational, extended-release version of 5-fluorocytosine [5-FC]) into 5-fluorouracil (5-FU). 5-FU kills infected dividing cancer cells and, in preclinical models, local immunosuppressive myeloid cells leading to therapeutically active anti-tumor immunity. A similarly derived antitumor response may occur in cancer patients, as local injection of recurrent high grade gliomas with Toca 511 followed by treatment with Toca FC has been associated with prolonged survival and durable complete responses (median duration of follow-up for response: 37.4+ months); responses were delayed in onset, consistent with an immunological mechanism. Not all patients responded and, clinically, only portions of the tumors were infected. These data led to the currently enrolling phase III trial (NCT02414165). To model submaximal infections, and look for clinically-compatible synergistic treatments, we implemented a novel preclinical model. We used this model system to test the immuno-stimulatory and antiangiogenic properties of cyclophosphamide following a metronomic/low dose regimen and its previously reported ability to cross the blood-brain-barrier, in a combination therapy.

Methods
Naive B6C3F1 mice were implanted in the right flank with a mouse glioma cell line Tu-2449SQ that has been adapted to grow subcutaneously. Tu-2449SQ cells were first 100% infected in vitro with Toca 511 or a sister vector that expresses GFP (Green Fluorescent Protein) instead of CD. In order to control Toca 511 spread, these cells were then admixed at various percentages as Toca 511 does not readily infect cells already infected with the GFP virus. Controlling the percent of Toca 511-infected tumor cells allows the screening of potential drugs combinations for efficacy.

Results
We show a significant survival benefit with metronomic cyclophosphamide compared to controls with only 10% of tumor cells infected with Toca 511. This survival benefit is associated with a significant depletion of peripheral Tregs and increase in CD8+ T cells.

Conclusions
These data demonstrate that Toca 511 and 5-FC therapy can be combined with metronomic chemotherapeutics like cyclophosphamide to enhance efficacy in preclinical models when the percent of Toca 511-infected tumor cells is manipulated to be submaximal. Data from this study will inform future clinical development of Toca 511 & Toca FC in combination with other therapies.

P621

Local immunotherapy with a mixture of mRNAs encoding pro-inflammatory cytokines promotes potent anti-tumor immunity and tumor eradication across multiple preclinical tumor models.

Timothy Wagenaar[1], Christian Hotz[2], Friederike Gieseke[2], Hui Cao[1], Jan Diekmann[2], Mustafa Diken[2], Christian Grunwitz[2], Andrew Hebert[1], Karl Hsu[1], Marie Bernardo[1], Katalin Kariko, PhD[2], Sebastian Kreiter[2], Andreas Kuhn[2], Mikhail Levit[1], Natalia Malkova[1], Serena Masciari, MD, MSc[1], Jack Pollard[1], Hui Qu[1], Abderaouf Selmi[3], Julia Schlereth[2], Fangxian Sun[1], Bodo Tillmann[3], Tatiana Tolstykh[1], Lena Wicke[2], Sonja Witzel[3], Qunyan Yu[1], Yu-An Zhang[1], Gang Zheng[1], Gary Nabel[1], Joanne Lager[1], Ugur Sahin, MD[2], Dmitri Wiederschain

[1]Sanofi, Cambridge, MA, USA
[2]BioNTech, Mainz, Germany
[3]TRON, Mainz, Germany

Background
Local administration of immunotherapies to the tumor microenvironment provides the opportunity to stimulate innate and adaptive immune responses against tumors, while avoiding toxicities related to systemic administration of immuno-modulatory therapeutics. Current strategies for tumor-targeted, gene-based delivery of immune therapies face limitations in the clinic due to suboptimal target expression, anti-vector immunity, or the potential for unwanted genomic rearrangements.

Methods
We examined the intratumoral administration of synthetic mRNA encoding immunomodulatory cytokines to provide sustained in vivo protein translation localized to the tumor microenvironment and limiting adverse effects associated with systemic administration of recombinant cytokines. Using iterative rounds of in vivo screening in murine syngeneic tumor models, a mixture of four synthetic mRNAs encoding bioactive versions of interleukin-12, interferon alpha, GM-CSF and interleukin-15 was identified which mediated complete tumor regression across multiple different tumor models.

Results
Mechanistically, maximal anti-tumor activity of cytokine mRNAs was associated with multiple immune populations including CD4+ and CD8+ T cells as well as NK cells. Localized administration of cytokine mRNA was accompanied by robust intratumoral induction of interferon gamma, systemic expansion of antigen-specific T cells and increased granzyme B positive CD8+ T cell infiltration. Immunological memory to both dominant and subdominant antigens was formed that protected long-term survivors from re-challenge with autologous tumors. Importantly, although cytokine mRNAs were administered locally, anti-tumor activity extended beyond the injected tumor to effectively control the growth of distant tumors in both a dual-tumor model and in an experimental

lung metastasis model. Finally, the combination of mRNAs encoding interleukin-12, interferon alpha, GM-CSF and interleukin-15 cytokines with immunomodulatory antibodies enhanced the anti-tumor response in both injected and uninjected tumors leading to improved overall survival and higher incidence of complete tumor regressions across several preclinical models.

Conclusions

In summary, the robust and versatile synthetic mRNA platform reported herein was used to identify multi-modal localized cancer immunotherapy with broad anti-tumor activity against treated and untreated tumors.

P622

Phase 1/2 evaluation of intratumoral INT230-6 for the treatment of solid tumors

Anthony Olszanski, MD, RPh[1], Nilofer Azad, MD[2], Lewis Bender, MS, MA, MBA[3], Ian Walters, MD[3], Diana Hanna, MD[4], Jacob Thomas, MD[5], Lillian Siu, MD[6], Anthony El-Khoueiry, MD[5]

[1]*Fox Chase Cancer Center, Phildelphia, PA, USA*
[2]*Johns Hopkins, Chevy Chase, MA, USA*
[3]*Intensity Therapeutics, Westport, CT, USA*
[4]*University of Southern California, Hoag, Los Angeles, CA, USA*
[5]*University of Southern California, Norris, Los Angeles, CA, USA*
[6]*Princess Margaret Cancer Center, UHN, Toronto, Canada*

Background

INT230-6 is a novel formulation of cisplatin and vinblastine with an amphiphilic cell penetration enhancer designed specifically for intratumoral administration. It is designed to improve dispersion throughout tumors and facilitate diffusion specifically in cancer cells while sparing healthy cells. In colon 26 animal models, injection into large primary lesions led to substantial tumor necrosis, recruitment of dendritic cells, and engagement of CD4 and CD8 T-cells. Injected tumors experienced high rates of complete response (up to 80%). Importantly, untreated lesions, distal to the injection site, responded and CR animals developed protection from re-challenge. Tumor growth control in injected and bystander tumors and survival improved significantly when INT230-6 was combined with checkpoint inhibitors.

Methods

This study is a phase 1/2 evaluation of multiple doses of INT230-6 injected into ≥ 1 superficial or deep tumor(s). The initial cohort treated superficial lesions at low dose once a month x 5. Upon establishing safety, subsequent sequential cohorts opened including a deep tumor cohort of once monthly injections, a superficial cohort of every 2 week dosing, and a cohort treating both deep and superficial tumors every 2 weeks utilizing a higher drug volume and dose load. A multiprong needle was utilized for injecting large tumors. Pharmacokinetic (PK) and pharmacodynamics (PD) samples (for flow cytometry and circulating cytokines) were collected.

Results

Fifteen heavily pretreated subjects have been dosed. Median age was 59 (46-72), ECOG 0:1 2:13, 87% Caucasian, 67% Female. 7/15 Subjects had received prior checkpoint antibodies. Cancer types include melanoma, SCC, ovarian, chordoma, cholangiocarcinoma, sarcoma, rectal, thyroid and H&N. Dosing has been into single or multiple lesions. PK analysis reveals negligible amounts of cisplatin and vinblastine in blood, suggesting the majority of INT230-6's active agents are retained in the tumor (consistent with no observable systemic AE's). No DLTs or drug-related SAEs were reported. The most frequent adverse events were low grade pain (26% of patients) and swelling/edema (20%). Many injected tumors showed visible necrosis or

decreased contrast uptake. Patients dosed every two weeks remained on treatment longer than those treated once a month. 5 out of 11(45%) evaluable patients had increases in circulating CD8+ T-cells, of these 60% also had increases in circulating CD4+ T-cells.

Conclusions
INT230-6 is safe when administered intratumorally at doses given to date. Updated results will be presented, including biomarker and response data. Additional planned cohorts include higher drug concentrations and combination with an anti-PD1 antibody.

Trial Registration
NCT: 03058289

Ethics Approval
The study was approved by Fox Chase Cancer Center, USC, John's Hopkins, and Princess Margaret Cancer Centers Institutution's Ethics Boards

Consent
Written informed consent was obtained from the patient for publication of this abstract and any accompanying images. A copy of the written consent is available for review by the Editor of this journal.

P623

The oncolytic peptide LTX-315 promotes natural killer cell recruitment and reduces lung metastatic burden in combination with local radiation therapy

Erik Wennerberg, PhD[1], Takahiro Yamazaki, PhD[1], Baldur Sveinbjornsson, PhD[2], Oystein Rekdal, PhD[2], Lorenzo Galluzzi, PhD[1], Sandra Demaria, MD[1]

[1]*Weill Cornell Medicine, New York, NY, USA*
[2]*Lytix Biopharma, Tromso, Norway*

Background
Cancer patients who lack tumor infiltration by T cells are poorly responsive to immune checkpoint blockade (ICB), prompting efforts to identify immunomodulating strategies to convert T cell-poor into T cell-rich tumors. The oncolytic peptide LTX-315 perturbs the mitochondrial membrane of cancer cells, culminating in the induction of immunogenic cell death (ICD) [1]. Recruitment of XCR1+ dendritic cells (DCs) to the tumor is critical for priming of anti-tumor CD8+ T cells following induction of ICD, and this process can be regulated by natural killer (NK) cells [2]. Here, we tested the interaction of focal radiotherapy (RT) with LTX-315 and their ability to trigger local and systemic anti-tumor immune responses.

Methods
BALB/c mice were injected subcutaneously with syngeneic 4T1 tumor cells, a mouse model of triple-negative breast cancer that spontaneously metastasizes to the lung. When average tumor volume reached 70 mm3, mice were randomized and treated on three consecutive days with: [1] LTX-315 (0.3 µg) or [2] saline (both intratumorally), [3] 8 Gy focal RT, [4] LTX-315+RT. Some mice were sacrificed 6 days after treatment for analysis of lymphocytes and DCs in primary tumors and lungs. Remaining mice were followed for tumor growth, and lung metastases were evaluated 23 days after treatment initiation.

Results
Monotherapy with LTX-315 significantly inhibited tumor growth ($p<0.001$) and there was a trend towards improved tumor growth inhibition achieved by RT. Lung metastasis were significantly reduced only in mice treated with the combination of RT+LTX-315 (17±12.8 in mock-treated v. 1.5±1.2 in mice treated with LTX-315+RT, $p<0.05$). The percentage of XCR1+ DCs was increased in the tumor of mice treated with LTX-315+RT compared to mice treated with saline, LTX-315 alone or RT alone (8.4±2.4% in

LTX-315+RT ($p<0.05$) v. 4.2±0.4% in RT v. 5.7±0.8% in LTX-315 v. 4.1±0.7% in mock-treated). Interestingly, LTX-315 enriched NK cells among leukocytes in both primary tumors and whole lung (tumor: 1.1±0.3% in mock-treated v. 3.5±1.2% in LTX-315 ($p<0.01$), lung: 2.1±0.3% in mock-treated v. 5.1±0.4% in LTX-315 treated ($p<0.0001$).

Conclusions

In conclusion, our data show that local LTX-315 therapy delays tumor growth and potentiates systemic anti-tumor effects in combination with RT. Importantly, LTX-315 cooperates with RT to promote tumor infiltration by XCR1+ DCs, which are essential for induction of anti-tumor immunity. LTX-315-driven enrichment of NK cells in tumors and lungs from tumor-bearing mice may play an important role in systemic tumor control. LTX-315 represents a promising agent for the treatment of patients with poorly immunogenic and metastatic cancers.

References

1. Zhou H, Forveille S, Sauvat A, Yamazaki T, Senovilla L, Ma Y, Liu P, Yang H, Bezu L, Muller K, Zitvogel L, Rekdal O, Kepp O, Kroemer G. The oncolytic peptide LTX-315 triggers immunogenic cell death. Cell Death Dis, 2016; 7: e2134.

2. Barry KC, Hsu J, Broz ML, Cueto FJ, Binnewies M, Combes AJ, Nelson AE, Loo K, Kumar R, Rosenblum MD, Alvarado MD, Wolf DM, Bogunovic D, Bhardwaj N, Daud AL, Ha PK, Ryan WR, Pollack JL, Samad B, Asthana S, Chan V, Krummel MF. A natural killer-dendritic cell axis defines checkpoint therapy-responsive tumor microenvironments. Nat Med. 2018; [Epub ahead of print]

P624

Development of a STING agonist-producing synthetic Biotic™ medicine to activate innate and adaptive immunity and drive antitumor immune responses

Kip West, PhD[1], Kip West, PhD[1], DANIEL LEVENTHAL, PHD[1], Ning Li, PhD[1], Christopher Plescia, MS[1], Starsha Kolodziej, BS[1], Rudy Christmas, BS[1], Carey Gallant, BS[1], Michael James, BS[1], Adam Fisher, PhD[1], Anna Sokolovska, PhD[1], Paul Miller, PhD[1], Jose Lora, PhD[1]

[1]*Synlogic, Cambridge, MA, USA*

Background

Engagement of both the innate and adaptive arms of the immune system has been shown to be critical in generating an efficacious anti-tumor immune response. Recent studies demonstrate that activation of the stimulator of interferon genes (STING) pathway plays an essential role in initiating anti-tumor immunity through activation of antigen presenting cells (APCs), production of type I interferon and subsequent T cell priming and tumor-specific T-cell-responses. Bacteria may provide an ideal mechanism for STING activation as they can be deployed within the tumor microenvironment (TME), are engulfed by APCs and activate parallel pathways of innate immunity that may potentiate the interferon response.

Methods

Using synthetic biology we introduced an anaerobically inducible di-nucleotide cyclase gene into our probiotic chassis, E. coli Nissle (EcN), to generate a bacterial strain capable of efficient production of the STING agonist cyclic-di-AMP (CDA) in response to the hypoxic TME, which we refer to as SYN-STING. We then employed a suite of cell-based assays and mouse tumor models to evaluate the activity of SYN-STING in vitro and in vivo.

Results

In in vitro assays, SYN-STING generated high levels of CDA and triggered expression of IFN-beta when co-cultured with both mouse and human APCs. In syngeneic tumor-bearing mice, intra-tumoral administration of SYN-STING resulted in an early rise of innate cytokines which later shifted towards molecules indicative of an effector-T-cell response. These pharmacodynamic changes correlated with increased immune infiltrate, robust anti-tumor responses and complete tumor regressions. We also observed increased tumoral innate cytokine levels and anti-tumor activity in response to treatment with the un-engineered EcN, supporting that our bacterial chassis itself is able to stimulate innate immunity in the TME, and this feature is further potentiated by arming it with STING agonist. Additionally, mice that exhibited complete regressions in response to SYN-STING treatment demonstrated long-term immunological memory when re-challenged with tumor cells >40 days post tumor eradication. Finally, administration of SYN-STING, singly or in combination with antibodies targeting co-stimulatory molecules, led to abscopal effects with significant anti-tumor activity observed in both injected and non-injected lesions.

Conclusions

Taken together, these results demonstrate that a Synthetic Biotic medicine designed to specifically deliver STING agonist locally within the TME leads to significant anti-tumor activity, systemic immunity and long-term immunological memory in mouse tumor models. Moreover, the ability of our platform to engage multiple innate immune pathways simultaneously further supports the development of Synthetic Biotic medicines for cancer-immunotherapy in humans.

Other

P625

Outcomes with first-line PD-1/PD-L1 inhibition in advanced urothelial cancer (UC): A single institution experience

Arjun Balar, MD[1], Miles Hsu, BS[2], Yuhe Xia[3], Andrea Troxel, PhD[3], Daniela Delbeau, RN[3], Kaitlyn Francese, RN[3], Dayna Leis, RN[3], Deneuve Shepherd[3]

[1]*Perlmutter Cancer Center - New York Univ, New York, NY, USA*
[2]*NYU School of Medicine, New York, NY, USA*
[3]*NYU Langone Health, New York, NY, USA*

Background

First-line PD-1 checkpoint inhibition (CI) in cisplatin-ineligible advanced UC represents a new treatment standard based on single arm trials [1,2], leaving uncertainty regarding role of chemotherapy. Describing utilization and corresponding outcomes with second-line treatment will provide guidance in this new sequence. We present the outcomes of these patients treated at our institution.

Methods

43 patients with advanced UC received 1st-line CI from 6/2014 – 6/2018 on or off protocol. Clinical, laboratory and imaging data within 30 days of 1st-line initiation were gathered and clinical outcomes were analyzed including response by RECIST v1.1 and survival (OS). Disposition and treatment post- CI were also analyzed. Clinical outcomes were analyzed for the entire study population as well as known prognostic subgroups. A multivariable analysis was used to determine the prognostic value of baseline factors, and a log rank test was used to compare outcomes in prognostic subgroups.

Results
43 patients were treated with 1st-line CI (atezolizumab or pembrolizumab) from 6/2014 until 6/2018. Median age was 77 (range 34 - 89), (74% male) (26% prior BCG), (60% visceral metastases, 19% liver), (reason for cisplatin ineligibility: ECOG PS =2 30%, Impaired renal function 44%, both 21%). ORR to first-line CI was 30.2% (95% CI 28% – 32%), CR 14%. Median OS and PFS was 11.7 mos (95% CI 7.6 – 19.8) and 3.0 mos (95% CI 2 - 11.2), respectively (median follow up 11.7 mos). OS was negatively correlated with visceral metastases at baseline. Of 29 patients who progressed, 17 received 2nd-line treatment (71% chemotherapy (most commonly Gem/Carbo (10 pts)) or 29% immunotherapy). Patients on chemotherapy had an RR of 38.46% while those on immunotherapy had an RR of 20.0%. Combined, 2nd-line treatment resulted in a median OS of 6.2 months (95% CI of 2.9-12.66), an ORR of 11.1% (95% CI of 8.0% to 15.0%) and an RR of 33.3% (95% CI of 28% - 39%).

Conclusions
In our single institution experience, OS and ORR with 1st-line CI are similar to outcomes reported in single arm trials. RR to 2nd-line chemotherapy is comparable to historical rates with gem/carbo in the first-line, however 12 of 29 progressing patients did not receive 2nd-line treatment, highlighting the importance of patient selection for first-line CI. Outcomes by PD-L1 status will be presented.

References
1. Balar AV, Galsky MD, Rosenberg JE, Powles T, Petrylak DP, Bellmunt J, et al. Atezolizumab as first-line treatment in cisplatin-ineligible patients with locally advanced and metastatic urothelial carcinoma: a single-arm, multicentre, phase 2 trial. Lancet. 2017 Jan 7;389(10064):67-76. doi: 10.1016/S0140-6736(16)32455-2. PMID: 27939400
2. Balar AV, Castellano D, O'Donnell PH, Grivas P, Vuky J, Powles T, Plimack ER, Hahn NM, de Wit R, Pang L, Savage MJ, Perini RF, Keefe SM, Bajorin DF, Bellmunt J. First-line Pembrolizumab in cisplatin-ineligible advanced urothelial cancer: results of the Phase 2 KEYNOTE-052 study. Lancet Oncol. 2017 Nov; 18(11):1483-1492. doi: 10.1016/S1470-2045(17)30616-2. Epub 2017 Sep 26.

P626

Overcoming target-driven fratricide for CAR-T cell therapy

Eytan Breman, MSc[1], Benjamin Demoulin[1], Sophie AGAUGUE, PhD[1], Sebastien Mauen, PhD[1], Alexandre Michaux, PhD[1], Lorraine Springuel[1], Fanny Huberty[1], Céline Jacques-Hespel[1], Celine Marchand, Laboratory Technician[1], Jérôme Marijsse, master[1], Peter DeWaele[1], David Gilham, PhD[1], Valérie Steenwinckel, PhD[1]

[1]*Celyad, Mont-St-Guibert, Belgium*

Background
Chimeric Antigen Receptor (CAR) T cells expressing the fusion of the NKG2D protein with CD3ζ (termed CYAD-0 cells) acquire a specificity for eight ligands, the UL16 Binding Protein 1-6 (ULBP1-6) and MHC class I chain-related A and B (MICA and MICB). These stress-induced ligands are expressed on multiple cancers, while they are absent from most normal tissues, rendering them an interesting target for cancer therapy. However, these stress ligands are also transiently expressed by activated T cells, implying that CYAD-01 cells may undergo self-killing (fratricide) during production. Since NKG2D potentially targets eight individual ligands, genetic editing to avoid T cell fratricide is currently challenging. Therefore, alternative strategies are required to enable the production of CYAD-01 CAR-T cells.

Methods
CYAD-01 cells were manufactured by isolating PBMCs from healthy donors and activating the T cells

with IL-2 and OKT3 for 2 days. Cells were then transduced with the CAR construct (or control truncated CD19) for two days and expanded for an additional 4-6 days. The broad Phosphoinositol-3-Kinase inhibitor (LY294002) was added following the two-day transduction. Alternatively, or in combination, blocking anti-CD314 antibody was added at the expansion phase.

Results

The first approach to inhibit NKG2D-mediated fratricide focused upon the inclusion of LY294002 into the production process. A second strategy involved the inclusion of antibody blockade of NKG2D itself. Both processes impacted T cell fratricide, albeit at different levels. The antibody process was the most effective in terms of cell yield, with a T cell phenotype closely resembling the control condition, while the LY294002 process impacted both T cell proliferation and T cell phenotype. Nonetheless, both approaches generated highly potent CYAD-01 cells. Interestingly, the differing T cell populations could be tweaked through the phased combination of LY294002 and blocking antibody into a single process. The combined approach led to a high yield of potent CYAD-01 CAR T cells. CYAD-01 CAR T cells are currently part of the phase I THINK clinical trial (NCT03018405) where clinical objective responses have been observed.

Conclusions

These results indicate that target-driven fratricide can be overcome using clinically relevant approaches where technologies such as gene-editing may be more challenging.

P627

From staining to analysis: fully automated workflow for multiplexed immuno-profiling in FFPE tumor samples using UltiMapper™ reagent kits

Amanda Bares, PhD[1], Michael Murphy[1], Heike Boisvert, PhD[1], Katir Patel, PhD[1], Bonnie Phillips, PhD[1], Sean Downing, PhD[1], Mael Manesse, PhD[1]
[1]*Ultivue, Cambridge, MA, USA*

Background

The success of personalized medicine hinges on translating the biological complexity of a disease into actionable information. To achieve this goal, high-content data generation and analysis is required, covering both the detection of biomarkers as well as understanding their spatial interaction. In the case of oncology, understanding the protein expression profile in the tumor microenvironment is the basis for the development of new and improved translational research and future companion diagnostic tools. To enable this effort, multiplex immunohistochemistry (mIHC) methods have been established to provide insights into a wide number of markers of interest and their spatial context in a single sample. We have developed a fully automated approach to enable high-multiplexing detection of protein markers in tumor samples using an integrated workflow compatible with a range of autostainers and fluorescence whole slide scanners.

Methods

UltiMapper reagent kits were used to stain formalin-fixed, paraffin-embedded (FFPE) samples from human tonsil and primary tumor biopsies on automated staining platforms such as the Leica BondRX autostainer. The kits contain a cocktail of primary antibodies of interest, modified with unique, addressable DNA barcodes, applied to tissue samples in a single staining step. A cocktail of fluorescently labeled oligonucleotides is then used to tag the targets of interest for multiplexed imaging. Images

were acquired using commercially available fluorescence whole slide scanners and analyzed using the Indica Labs HALO software.

Results

The UltiMapper kits alleviate lengthy assay development efforts by offering a convenient, optimized assay kit with a simplified workflow. The staining workflow includes a single staining step for all targets which eliminates the need to optimize staining order and solves issues of tissue damage during cyclical staining steps. Fully automated staining protocols were developed on autostainers to enable high throughput and highly reproducible results. The optimized protocols were used to stain a series of FFPE tumor sections and perform multiplexed quantification analysis of immune cell phenotypes in tumor samples.

Conclusions

The workflow of the InSituPlex technology enables multiplexed immune-profiling in tumor FFPE sections though a highly streamlined, automated workflow with existing high-throughput staining and imaging instrumentation.

P628

High dimensional immune cell profiling with data-independent acquisition mass spectrometry

Jakob Vowinckel, PhD1, Tobias Treiber[1], Nicholas Dupuis, PhD[1], Kristina Beeler[1], Claudia Escher[1]

[1]*Biognosys, Zurich, Switzerland*

Background

Recent successes with therapies directed at the immune system have demonstrated the utility of targeting the immune response for control of multiple cancers. These successes have also spurred interest in characterizing immune cell sub-populations to understand mechanisms of activation and suppression, and their relationship to therapeutic response. Currently, antibody-based approaches are commonly used to characterize immune cells, however these methods are limited to 30-40 markers from previous hypotheses, limiting new discovery. In this context, determination of the surface and cellular proteome of responsive populations will provide a powerful tool for insight into response mechanisms, so far hampered by low sample availability and limited sensitivity of proteomic methodology. Here, we demonstrate how data-independent acquisition mass spectrometry can be used for high-dimensional characterization of immune cell sub-populations, even with limited cell numbers. These studies open the way for further understanding sub-populations contained within those defined by classical cell markers.

Methods

Primary human Cytotoxic CD8+ T cells, CD4+ T cells, CD14+ monocytes and natural killer (NK) cells, isolated from peripheral blood mononuclear cells, were prepared for mass spectrometry using standard sample preparation workflows. All samples were analyzed using 4 hour gradients on a C18 column coupled to a Thermo Scientific Q Exactive HF mass spectrometer in data-independent acquisition (DIA-MS) mode. DIA data was extracted using Spectronaut Pulsar X (Biognosys) with directDIA data searching.

Results

Cytotoxic CD8+ T cells were evaluated using 100,000 cells of input material, which resulted in >3500 proteins quantified in the primary cells. Serial dilutions revealed that >2750 proteins (~73% of all proteins detected) were quantified even with lower numbers of cells (30k). In the current experimental setup, 30k cells also represents the lower limit of detection of CD8A and CD8B. Among other previously characterized proteins associated with CD8+ T cells, KLRG1, CCL5, TBX21, GZMH, PRF1, GNLY, CST7 were all detected at 30k cell input, except KLRG1 which was detected at 50k cell input.

Additionally, Granzyme A and B were also quantified which have classically been used, along with PRF1, as markers of lymphocyte infiltration. Data will be presented for the additional cell types (CD4+ T cells, CD14+ monocytes, and NK cells) to further map the immune cell phenotypic landscapes.

Conclusions
Our DIA-MS platform enables deep proteomic phenotyping of sorted immune cell samples, even with limited numbers of cells. These new data sets make available broad and un-constrained biomarker investigation for deconvolution of the processes driving immune cell activation and suppression.

P629

Addressing immunotherapy educational needs: esults from an educational program on immunotherapy for cancer patients and caregivers

Maria Gonzalo[1], Liliana Zigo, BA[1], Claire Saxton, MBA[1], Heather Hollen, BS, MS[1], Julie Olson, PhD[2], Kevin Stein, PhD, FAPOS[2]

[1]Cancer Support Community, Washington, DC, USA
[2]Cancer Support Community, Philadelphia, PA, USA

Background
As cancer treatment becomes more personalized and the use of immunotherapy expands, it's important that patients and caregivers have access to educational tools to make informed decisions, reduce cancer-related distress, and get optimal benefit across the continuum of care. This analysis explores participants' experiences with the Cancer Support Community's national evidence-based educational program, Frankly Speaking about Cancer: Immunotherapy. This comprehensive psychosocial program was created for people diagnosed with cancer and their families to provide information about immunotherapy as a treatment option, including how immunotherapy works, how to cope with the delayed response to treatment that is characteristic of some immunotherapy drugs, and the different side effects that people encounter while taking these treatments.

Methods
593 patients and 213 caregivers attending in-person Frankly Speaking about Cancer: Immunotherapy workshops across the country between 2014 and 2017 completed post-workshop evaluations. Survey questions focused on how cancer patients and their caregivers met their informational and assistance needs in regard to immunotherapy and whether participating in the workshop was associated with positive gains. Descriptive analyses and ANOVAs were used to assess workshop outcomes.

Results
73% of participants were cancer patients and post-treatment survivors; the remainder were caregivers who included spouses/partners (14%), family members (7%), and friends (6%). The average age of participants was 62 years old (s.d.= 11.4 years). While 39% of patients listed their primary diagnosis as 'breast cancer,' 31 other cancer diagnoses were represented in the survey. At the time of the workshops, 49% of patients had received the diagnosis within the last two years and 10% reported to have received immunotherapy treatment. Comparing retrospective pre-post workshop self-assessment means, participating in the workshops was associated with positive gains in knowledge about immunotherapy ($F=265.8$, $p<.05$). At the same time, 85% of patients and 67% of caregivers indicated that after the workshop they felt more confident to talk to their healthcare team about immunotherapy. The majority (78% of patients and 94% of caregivers) reported feeling better prepared to ask questions about side effects of immunotherapy. Finally, 95% of all participants said that they would recommend the program to their loved ones.

Conclusions

Results suggest that the program successfully improves self-rated knowledge about immunotherapy and boosts confidence in discussing this treatment modality and its side effects with healthcare providers. Furthermore, we found this program to be effective with both patients and caregivers, as over two-thirds in both groups indicated gaining confidence in talking to their providers.

P630

Patient-reported toxicities in lung cancer patients receiving immune checkpoint blockade

Heather Jim, PhD[1], Sandra Shaw, BS, MBA[2], Sarah Eisel, PhD[1], Aasha Hoogland, PhD[1], David LeDuc, CFRE[2], Adam Dicker, MD, PhD[3]

[1]*Moffitt Cancer Center, Tampa, FL, USA*
[2]*Addario Lung Cancer Foundation, Harleysville, PA, USA*
[3]*Thomas Jefferson University, Philadelphia, PA, USA*

Background

Background: There is increasing clinical and research interest in patient-reported outcomes (PROs) which provide unique and complementary information to provider-rated adverse events. While several studies have been published of PROs in lung cancer patients receiving immune checkpoint blockade, to our knowledge all have focused on PROs collected as part of a clinical trial. Clinical trial participants tend to be younger and healthier than patients who receive standard of care. The goal of the current observational study is to describe PROs outside the context of a clinical trial in lung cancer patients treated with immune checkpoint inhibitors.

Methods

Method: The Addario Lung Cancer Foundation (ALCF) international patient registry was used to collect patient-reported clinical information. English-speaking patients who reported current or past treatment with an FDA-approved immune checkpoint inhibitor (i.e., atezolizumab, durvalumab, ipilumumab, nivolumab, pembrolizumab) were asked to complete a second survey of symptomatic toxicities of these therapies. Patients rated 40 symptoms (e.g., fatigue, rash) on a five-point scale (0=none, 4=very much). The Charlson Comorbidity Index and Functional Assessment of Cancer Therapy General (FACT-G) were administered to assess comorbidities and quality of life, respectively.

Results

Results: A total of 90 patients (mean age 62, 72% female, 87% White, 92% from the USA) who reported treatment with nivolumab (48%) or pembrolizumab (52%) were included in analyses. Patients reported 3 comorbidities on average (range 2-17). The majority of patients (53%) had been treated for 6 months or less. The most commonly reported symptoms were fatigue (89%), aching joints (72%), itching (65%), aching muscles (63%) skin dryness (62%), and insomnia (62%). A total of 25% of patients had experienced a treatment delay, 10% had been to the emergency room, and 8% had been hospitalized due to toxicity. Participants reported a mean score of 76.65 (SD=18.30) on the FACT-G, significantly lower than previously-published normative data for cancer patients [1].

Conclusions

Conclusions: This study is among the first to our knowledge to evaluate symptomatic toxicities of immune checkpoint inhibitors outside the context of a clinical trial. Results indicate that symptomatic toxicities of immune checkpoint inhibitors are common in lung cancer patients. Additional research is needed to better understand the longitudinal course of symptomatic toxicities and evaluate

whether supportive care interventions to ameliorate symptoms are efficacious.

Acknowledgements
Addario Lung Cancer Foundation, Society for Immunotherapy in Cancer

References
1. Pearman T, Yanez B, Peipert J, Wortman K, Beaumont J, Cella D. Ambulatory cancer and US general population reference values and cutoff scores for the functional assessment of cancer therapy. Cancer. 2014; 120: 2902-2909.

Ethics Approval
This study was determined to be non-human subjects research because it uses anonymous data.

P631

A novel CD137/PD-L1 bispecific antibody modulates the tumour microenvironment by activating CD8⁺ T cells and results in tumour growth inhibition

Matthew Lakins, PhD[1], Jose Munoz-Olaya[1], Daniel Jones[1], Raffaella Giambalvo[1], Clinton Hall[1], Anne Knudsen[1], Neus Masque Soler, Dr[1], Sarka Pechouckova[1], Emma Goodman, BSc[1], Cristian Gradinaru[1], Alexander Koers, PhD[1], Sylwia Marshall[1], Mateusz Wydro, PhD[1], Francisca Wollerton[1], Sarah Batey[1], Dan Gliddon[1], Jacqueline Doody, PhD[1], Michael Davies[1], Michelle Morrow, PhD[1], Mihriban Tuna, PhD[1], Neil Brewis, PhD[1]

[1]F-star Biotechnology Ltd, Cambridge, UK

Background
Blockade of the PD-1/L1 axis has shown durable responses and extended overall survival in multiple cancer types. However, there is still a significant unmet need for patients who relapse and activation of the Tumour Necrosis Factor Receptor (TNFR) superfamily embodies the next stage of cancer immunotherapy. CD137-mediated costimulation directs the fate of antigen-stimulated T and NK cells. Upon interaction with its ligand, CD137 signalling supports cell activation, survival and proliferation. Current agonist therapeutic interventions aimed at CD137 hold great promise for cancer immunotherapy with the caveat of being associated with safety concerns. Here, we show how a novel bispecific antibody (mAb² ™) directed to CD137 and PD-L1 induces potent in vitro T cell activity in a PD-L1-dependent manner, and results in significant tumour control across three syngeneic tumour models without toxicity.

Methods
An anti-CD137/PD-L1 mAb² was generated by introducing a CD137-binding specificity into the Fc-region of a human IgG1 targeting PD-L1. FcγR binding was abrogated by introducing the LALA mutation. Binding characterisation was carried out via SPR and in vitro activity was assessed using functional assays employing engineered overexpressing T cell lines, and a mouse primary OT-1 CD8⁺ T cell assay. The anti-tumour activity of the anti-CD137/PD-L1 mAb² was tested in CT26, MC38 and B16-F10 tumour-bearing mice.

Results
An anti-CD137/PD-L1 bispecific antibody was developed, which binds mouse PD-L1 and which, upon binding to mouse CD137, elicits potent T cell stimulation in vitro (EC50: 3 pM in primary antigen-specific OT-1 assay). The mAb² significantly reduced tumour growth in MC38 and CT26 syngeneic colon carcinoma models, as well as in the B16-F10 syngeneic melanoma model. In CT26 this activity was dose-dependent resulting in a significant survival benefit at concentrations of 0.3 mg/kg or above and liver pharmacology was minimal as defined by histopathology.

Conclusions
We report potent in vitro CD137-mediated activation

only upon engagement of PD-L1 using the anti-CD137/PD-L1 bispecific mAb² which outperforms monospecific antibodies on their own and in combination in multiple syngeneic mouse tumour models in a dose-dependent manner. None of the liver pharmacology and resultant toxicity reported with other CD137 agonist mAbs are observed with the anti-CD137/PD-L1 mAb². This warrants the development of a first-in-class anti-human CD137/PD-L1 bispecific antibody with a novel mode of action and improved therapeutic index for the treatment of human cancer.

Ethics Approval
The murine syngeneic tumour studies were approved by the Home Office, project license number 70/7991.

P632

A multi-omics approach to understanding the tumor microenvironment

Deepali Malhotra, PhD[1], Gordon Moody[1], Michael Surace, PhD[1], Jaime Rodriguez-Canales, MD[1], Ronald Herbst, PhD[1], John Mumm, PhD[1]

[1]*MedImmune, Gaithersburg, MD, USA*

Background
Human tumors contain highly variable immune and stromal cell infiltrates. Tumor heterogeneity, classically defined by tumor intrinsic variation in morphology and metabolism, is also observed at the level of infiltrating immune cell localization and activation within these tissues. Understanding the composition and functional consequences of different tumor microenvironments (TMEs) is critical to identifying correlates that inform our development and use of IO therapies in patients. Therefore, it is essential that tumor-targeted IO therapies be tested within the relevant context of the human TME. To this end, we developed a multi-omics work flow to characterize primary human tumors and to assess the functional consequences of intervention with immunotherapeutics that target different cell types and pathways within the TME.

Methods
Within 24 hours of surgical resection, tumors are enzymatically processed using a protocol optimized for cellular viability and maximal cellular yield. Additional tumor tissue is processed for FFPE to enable multi-parameter IHC analysis of the composition and structure of the TME. Flow cytometry panels were developed to define the immune, tumor, and stromal cell makeup of each disaggregated tumor and to provide insight into the nature and activation state of infiltrating lymphocytes and myeloid cells. Disaggregated tumors were treated in vitro with IO therapeutics that target different pathways and cell types, such as: co-stimulation, checkpoint blockade, and myeloid activation. Tumor disaggregates and supernatants are collected at various timepoints to assess the ability of these compounds to modulate transcriptional activity and cytokine outputs.

Results
Tumors representative of colon, lung, renal, and pancreatic cancers were assessed using the aforementioned workflow. The TMEs defined by each of these metrics highlighted the diversity of these samples, some samples were enriched for lymphocytes, other myeloid cells, while some had similar contributions of lymphocytes and myeloid cells. Infiltrating T cells also demonstrated various degrees of activation and exhaustion, likely affecting the ability of these disaggregates to respond to different classes of IO therapies.

Conclusions
We have developed a multi-omics workflow to allow evaluation of how the TME influences responses to different preclinical IO assets. This project represents an ongoing functional and phenotypic

characterization effort to enable the development and implementation of novel tumor-targeted IO therapies. Preliminary results suggest that multi-omics approaches are required to understand the IO context within the TME. Further refinements of this methodology may include alternative approaches that better reproduce more complex aspects of the TME such as structure and localization of immune cells within the tumor.

Ethics Approval
All tumor samples were received in agreement with the IRB of the University of Maryland and processed in agreement with the ethical guidelines of MedImmune.

P633

Generation of a modular landing pad cell line for T cell receptor exchange and screening

Ethan Patterson[1], Stacey Ward, PhD[1], Jason Gustin[1]

[1]*Milliporesigma, St. Louis, MO, USA*

Background
T cell biology is integral to the study of normal immune regulation as well as cancer biology, CAR-T cells, epitope specificity and antigen presentation. However, primary T cells can be difficult to propagate in culture for the length of time necessary for functional assays. In addition, populations of primary T cells express variant T cell receptor (TCR) heterodimers that can be challenging to identify and may not be optimal for downstream studies.

Methods
We sought to simplify this system using transformed T cells which can be grown in culture for extended periods of time. We engineered a floxed landing pad sequence into the safe harbor AAVS1 locus using CompoZr® zinc finger nucleases. Both the promoter and landing pad expression cassette are flanked by unique lox sites, allowing swapping of the promoter and/or expression cassette as needed. We ensured that only one copy of this sequence was found within the genome to avoid any complications associated with random insertion events.

Results
We also generated a landing pad cell line null for the endogenous TCR using targeted nucleases. Both the TCR alpha and beta loci were rendered null due to non-homologous end joining and the presence of insertions and deletions culminating in premature stop codons were genotyped using next generation sequencing. The absence of a functional TCR was validated using flow cytometry staining for surface TCR and CD3. This cell line was then used to generate a knock-in of the desired exogenous TCR heterodimer to the landing pad locus, verified using flow cytometry staining.

Conclusions
These lines will be very useful for a multitude of studies where a researcher needs to express a gene of interest in a discrete genetic locus or wants to generate a panel of TCR expressing cell lines.

P634

Precision genome editing in macrophage and CD8+ human primary T cells for immuno-therapeutics applications

Laura Daley[1], Ethan Patterson[1]

[1]*Milliporesigma, St. Louis, MO, USA*

Background
Innate immune cells play a critical role in cell-mediated immunity and have the potential to serve as cell-based therapies to treat a broad spectrum of immune diseases such as cancer and autoimmune disorders. Modified immune cells, such as genetically engineered CAR-T cells, have proven to be critical in

developing new cell-based therapies for these diseases. However, immune cell biology creates challenges during the gene-editing process that lead to hyper-regulated RNA and DNA sensing pathways and enhanced cell death upon introduction of exogenous ribonucleotides. Further, engineering in primary immune cells is often restricted due to their limited expansion capacity.

Methods
Genetic engineering in immune cells has traditionally relied on random integration of gene-editing components using viral delivery systems. In contrast, genome editing mediated by nucleases, such as CRISPR/Cas9-single guide RNA ribonucleoproteins (RNPs), provide a platform for precision editing, and alleviate the potential side effects caused by randomly integrated viral DNA. While RNP gene editing in immune cells is just beginning to be considered by the immune-therapeutics field, our recent advances demonstrate that this approach can be used to create targeted modifications in two key cell types, the macrophage and the CD8+ primary T-cell.

Results
In an effort to circumvent challenges with the finite lifespan of primary T-cells, we targeted genes to edit that rendered this cell type “pseudo-immortalized”, thus allowing additional passages for further downstream genome editing and propagation. In addition, we demonstrated that precision editing can be used to introduce disease relevant single-nucleotide-polymorphisms (SNPs) into the macrophage genome, which resist introduction of exogenous ribonucleotides due to the induction of apoptotic pathways.

Conclusions
Advances such as these overcome many of the obstacles currently faced with immune cell editing and offer improved gene stability and expression in immune cells and, in doing so, will transform the Immuno-Oncology and Gene Therapy fields.

P635

Effectiveness and tolerance of immune checkpoint blockade in a real-world lung cancer patient population

Daniel Pease, MD[1], Michael Shyne[2], Shilvi Joshi[2], Allison Lee[2], Manish Patel, DO[2]

[1]*Hennepin Healthcare, Minneapolis, MN, USA*
[2]*University of Minnesota, Minneapolis, MN, USA*

Background
The PD-1 inhibitors nivolumab and pembrolizumab are approved for treatment of non-small cell lung cancer in the second line setting, based on superior outcomes compared to chemotherapy. The study populations generally were composed of younger patients with excellent performance status (ECOG 0-1) and a minimal number of prior lines of therapy. In our study we evaluated outcomes with these agents in older, less fit, and more heavily pretreated lung cancer patients that are reflective of real-word practice.

Methods
A single-institution retrospective analysis of all lung cancer patients treated with nivolumab or pembrolizumab at the University of Minnesota from 2015 to 2016. Outcomes were compared by age, performance status (PS), prior lines of therapy, presence of brain metastases, history of autoimmune disease, and immune-related adverse events (irAE). Overall survival (OS) data was calculated using two-sample log-rank testing.

Results
111 patients received at least two doses of nivolumab or pembrolizumab, with median age 65 years. Overall the complete response rate was 2.7%, partial response 27.9%, and stable disease 19.8%, for

a clinical benefit rate of 50.4%. The median duration of response was 12.5 months and median OS 11 months. The clinical benefit rate was not significantly different by age (52.8% for ≤65 versus 59.6% for >65 and 55.4% for ≤75 versus 58.8% for >75), PS (55.1% for ECOG 0-1 versus 62.5% for >1), or prior lines of therapy (53.6% for 0-1 versus 59.1% for >1). Median OS was 5 months for patients with ECOG PS >1 compared to 13 months for PS 0-1 (p-value 0.00042). Survival by age and prior lines of therapy was not significantly different. The incidence of irAE requiring steroids was 19.8%, with no treatment-related deaths. The median OS for patients experiencing an irAE was 23.9 months versus 9 months for patients without an irAE. Of 9 patients with a history of autoimmune disease, only 1 experienced disease flair. In patients with no history of brain metastases, only 5 (6.3%) developed CNS progression. Of those with previously treated brain metastases, 29.6% had CNS progression.

Conclusions

The clinical benefit of immune checkpoint blockade persists in older or heavily pretreated patients. Survival for patients with PS >1 is very limited, suggesting these agents should be used judiciously in this group. Therapy was well tolerated, with a low risk for flare of previous autoimmune disease, and appears to be effective for CNS disease. Incident irAE predicted for improved OS.

Ethics Approval

This study was approved by the University of Minnesota's institutional review board; approval number 1606M88925.

P636

Evaluating the occurrence of early tumor progression (ETP) in patients with gastric cancer treated with nivolumab versus placebo

Yan Feng[1], Paul Nghiem, MD, PhD[2], Ricardo Zwirtes, MD[1], Dan Reshef[1], Greg Plautz[1], Narikazu Boku[3], Li-Tzong Chen[4], Yoon-Koo Kang[5], Akintunde Bello, PhD[1], Amit Roy[1], Jennifer Sheng[1]

[1]*Bristol-Myers Squibb, Princeton, NJ, USA*
[2]*University of Washington, Seattle, WA, USA*
[3]*National Cancer Center Hospital, Tokyo, Japan*
[4]*National Institute of Cancer Research, Tainan, Taiwan, Province of China*
[5]*Asan Medical Center, Seoul, Korea, Republic of*

Background

Early tumor growth has been documented as a feature of natural disease progression in some patients [1,2]. However, without consideration of the natural history of disease progression, there have been recent reports of "hyperprogression" (using various definitions of the term) to suggest accelerated tumor growth in some patients receiving anti–programmed death 1/programmed death ligand 1 therapies [3-5]. Additionally, these reports do not account for the necessity for randomization and suitable control groups [5]. The reported phenomenon of "hyperprogression" was assessed with data from a randomized controlled phase 3 trial of nivolumab versus placebo (as a surrogate for the natural history of disease progression) in patients with unresectable, advanced, or recurrent gastric cancer who had received at least 2 prior lines of treatment (NCT02267343, ATTRACTION-2). Tumor growth of all patients was retrospectively evaluated at the first on-treatment scan, relative to baseline, using a tumor growth dynamics (TGD) model, with a focus on patients experiencing ETP at the first tumor assessment.

Methods

Patients from Japan, Korea, and Taiwan with unresectable, advanced, or recurrent gastric cancer, refractory or intolerant to standard therapy, were randomized 2:1 to nivolumab or placebo (N = 493). A TGD model was developed to characterize change of tumor size using longitudinal data from 358 patients who had baseline and at least 1 post treatment tumor measurement available. An increase of ≥20% in the sum of longest diameter (SLD) of target lesions at 8 weeks post baseline was considered ETP.

Results

A high variability of change in tumor size was observed among both placebo- and nivolumab-treated patients, consistent with the variable nature of cancer progression and response. The percentage of ETP was lower in patients receiving nivolumab compared with placebo, across cutoffs up to 100% increase in SLD relative to baseline (Table 1). Pseudoprogression was reported in 2 patients receiving nivolumab (~1%) and in none of the patients receiving placebo. Furthermore, the maximum observed SLD increases in nivolumab and placebo arms were 260% and 130%, respectively. A small fraction of patients in both nivolumab and placebo arms (~1%) experienced ETP >100% of observed SLD at the first assessment.

Conclusions

This study does not support any association between nivolumab therapy and early tumor progression. However, this study focused on patients with gastric cancer; the potential of hyperprogression following immuno-oncology therapy should be investigated in other randomized trials with a placebo arm, focusing on different tumor types.

Acknowledgements

Medical writing assistance was provided by Katerina Pipili, PhD, of Spark Medica Inc. (US), funded by Bristol-Myers Squibb. This study was funded by Bristol-Myers Squibb. Mitsunobo Tanimoto contributed as the NCT02267343 Study Director.

Trial Registration

ClinicalTrials.gov: NCT02267343

References

1. Detterbeck FC, Gibson CJ. Turning gray: the natural history of lung cancer over time. J Thorac Oncol. 2008;3:781-792.
2. Wang J, Mahasittiwat P, Wong KK, Quint LE, Kong FM. Natural growth and disease progression of non-small cell lung cancer evaluated with 18F-fluorodeoxyglucose PET/CT. Lung Cancer. 2012;78:51-56.
3. Champiat S, Dercle L, Ammari S, Massard C, Hollebecque A, Postel-Vinay S, Chaput N, Eggermont A, Marabelle A, Soria JC, Ferté C. Hyperprogressive disease is a new pattern of progression in cancer patients treated by anti-PD-1/PD-L1. Clin Cancer Res. 2017;23:1920 1928.
4. Kato S, Goodman A, Walavalkar V, Barkauskas DA, Sharabi A, Kurzrock R. Hyperprogressors after immunotherapy: analysis of genomic alterations associated with accelerated growth rate. Clin Cancer Res. 2017;23:4242-4250.
5. Sharon E. Can an immune checkpoint inhibitor (sometimes) make things worse? Clin Cancer Res. 2017;23:1879-1881.

Ethics Approval

The protocol and all amendments were approved by the institutional review board or independent ethics committee for each study center.

Table 1.

Treatment	Nivolumab (n = 243)	Placebo (n = 115)
Observed mean increase from baseline at first assessment (%)	10.1	21.2
% ≥20% increase from baseline	27.6	43.5
% ≥50% increase from baseline	5.4	7.8
% ≥100% increase from baseline	1.2	0.9

P637

Fibroblast activation protein (FAP)-selective delivery of CD40 agonistic DARPin® molecule for tumor-restricted immune activation

Nicolo Rigamonti, PhD[1], Anja Schlegel[1], Sophie Barsin, Master of Science[1], Jonas Schwestermann[1], Jennifer Krieg[1], Susanne Mangold[1], Maria Paladino[1], Valérie Calabro, PhD[1], Victor Levitsky, MD PhD[1], Simon Plyte, PhD[1], Michael Stumpp, PhD[1], Clara Metz, PhD[1]

[1]*Molecular Partners AG, Schlieren - Zurich, Switzerland*

Background

CD40 is a co-stimulatory molecule belonging to the tumor necrosis factor receptor superfamily which can activate both innate and adaptive immune system, making it an interesting target for tumor immunotherapy. Systemic activation of CD40 receptor, induced by administration of agonistic CD40 antibodies, has shown signs of activity in cancer patients, but dose-limiting toxicities have impaired the efficacy. New therapeutic approaches are therefore needed to increase the therapeutic index of CD40-targeting molecules and achieve better clinical outcomes. Here, we report a novel approach based on systemic administration of a tumor-restricted CD40 agonistic DARPin® molecule targeting human CD40 and fibroblast activation protein (FAP) alpha, a tumor antigen (TA) abundantly expressed in many solid tumors, enabling CD40 pathway activation exclusively in the presence of TA-expressing cells.

Methods

Using ribosome display technology, we generated a panel of bispecific CD40/FAP DARPin® molecules able to trigger specifically CD40 receptor and activate the NF-κB pathway in a reporter cell assay, in the presence of FAP-transfected Chinese hamster ovary (CHO) cells, but not in the presence of parental CHO cells. Selected bispecific DARPin® clones were then tested in more meaningful cell assays using human 1) primary B cells, 2) monocyte-derived dendritic cells and 3) monocyte-derived macrophages from whole blood, in the presence of FAP-positive or FAP-negative cells.

Results

In these immune cell populations, bispecific CD40/FAP DARPin® molecules confirmed a FAP-dependent activation of CD40 pathway inducing an upregulation of costimulatory molecules and proinflammatory cytokines, such as CD86 and IL12, only in the presence of FAP-expressing cells. In order to properly address the in vivo activity, a surrogate mouse-specific CD40/FAP DARPin® molecule was also generated and tested in different in vitro assays showing a FAP-dependent activation and similar results as the human counterpart. Experiments are ongoing to assess the efficacy and mechanism of action of this tumor-restricted CD40 agonistic DARPin® molecule.

Conclusions

In conclusion, we have generated bispecific agonist CD40/FAP DARPin® molecules able to activate the CD40 pathway in cellular assays in a targeting-dependent manner, supporting the hypothesis that these DARPin® molecules could lead to a tumor-localized immune activation in vivo. Data of the ongoing in vivo experiments in mouse tumor models to test this hypothesis will be shown at the meeting.

Ethics Approval

In vivo studies were approved by Veterinary Authorities of the Canton Zurich, approval number ZH102/16.

P638

Comparison of immunoprofiling from whole tumor versus pathologist-selected regions of interest in

tissues: a study using multiplex immunofluorescence and multispectral analysis on lung cancer

Michael Surace, PhD[1], Matthew Gates[1], Clifford Hoyt, MS[2], Jennifer Cann, PhD[1], Jaime Rodriguez-Canales, MD[1]

[1]*MedImmune, Gaithersburg, MD, USA*
[2]*PerkinElmer, Hopkinton, MA, USA*

Background
Multiplex immunofluorescence (mIF) and multispectral analysis has become an important tool for cancer immunoprofiling. An investigator, usually pathologist, selects regions of interest (ROI) within the tumor area for multispectral scanning and immunophenotyping analysis. However, tumor heterogeneity and human sample bias may affect the representation of the immunoprofiling in the whole tumor area. Our goal was to compare the tumor immunoprofiling data using ROI analysis versus whole tumor region scanned in multispectral mode.

Methods
20 non-small cell lung carcinomas (9 adenocarcinomas (ADC), 11 squamous cell carcinomas (SCC) were stained with a 6-marker mIF panel (PD-L1, CD8, Ki-67, CD68, pancytokeratins, and PD-1) and imaged using a multispectral scanner. Two pathologists (A and B) independently selected 5 ROI (0.64 mm2 each) within the tumor area for each case. Additionally, to assess the human sampling bias, two sets of 5 ROI where generated randomly within the tumor by a computer (C and D). The immunoprofiling data was generated using HALO software from all ROI sets (A-D) and independently compared to the whole tumor region.

Results
Cell densities and percentages of 8 cell subpopulations [CD8+; CD68+; PD-1+; (PD-1+/CD8+); (CK+/Ki67+); (CK+/PDL1+); (CD68+/PD-L1+), and (CD8+/Ki67+)] were evaluated in tumor epithelium and stroma compartments. These data were assessed in each set of 5 ROI (A-D) and compared with the data from the whole tumor. Pearson's correlation coefficients (PCC) between the whole tumor and ROI data ranged from 0.65 to 0.99. The endpoints for which ROI were least representative of whole tumor were percent of CD8+/Ki67+ cells in the stroma (PCC 0.65), and PD-1+/CD8+ cell density in the epithelial compartment (PCC 0.70). The endpoints for which ROI were most representative of whole tumor were PD-1+ cell density in tumor stroma (0.98) and percent CD68+ macrophages in stroma (0.99). The average PCC for randomly-assigned ROI (computer) was 0.96 vs 0.90 for pathologist-assigned ROI. ADC were more robustly assessed by ROI (PCC 0.97) as compared to SCC (0.88). As compared to the whole tumor, and across all reportable metrics, pathologist-placed ROI undercounted by an average of 18.36% and computer-placed ROI undercounted by 7.02%.

Conclusions
Overall, our results suggests that immunoprofiling using 5 ROI is comparable to the data from whole tumor region. However, the assessment of cell densities in ROI for certain populations showed a lower correlation, suggesting an advantage of the analysis of either more than five ROI or the whole tumor region for the evaluation of cell densities.

Ethics Approval
Tissues were commercially available and obtained according the Declaration of Helsinki

P639

Tumor-associated B cells promote melanoma cell dedifferentiation and invasiveness

Anastasia Samarkina, MSc[1], Rajasekharan Somasundaram, PhD[1], Meenhard Herlyn, DVM PhD[1*]

[1]*The Wistar Institute, Philadelphia, PA, USA*

Background
Tumor heterogeneity and dedifferentiation of cancer cells have been shown to hamper the effective response to the targeted- and immune-therapies. This ultimately leaves two-thirds of metastatic melanoma patients with a limited number of treatment options. The role of the tumor microenvironment and specifically tumor-associated stromal cells on the induction of dedifferentiation and on the presence of heterogenous tumor subpopulations is not fully understood.

Methods
In the present work, we have dissected the functional interplay between tumor-associated B cells (TABs) and melanoma cells through the integration of a humanized mouse model, computational transcriptome analysis, and organotypic 3D culture assays.

Results
We first found that immunotherapy-resistant tumors from humanized mice showed a dramatic influx of CD19+ B cells and exhibited the focal loss of melanoma-specific antigens intratumorally. Of note, both of these trends are not seen in immunotherapy-responding tumors. We then performed a gene microarray and detected that in a stark contrast to the normal B cells (NBs) derived from healthy donors, TABs' transcriptome had enriched signature of inflammatory and angiogenic factors, as well as numerous molecules involved in invasion and matrix degradation. In concordance with our mouse studies, we also found that TABs induced a robust upregulation of migration-associated, neural crest and early neural progenitor markers across different melanoma cell lines as determined by microarray and RT-qPCR. The enhanced invasive phenotype was further functionally validated in a 3D organotypic culture, where melanoma spheroids cultured in the presence of TABs showed an average two-fold increase in invasive potential when compared to spheroids co-cultured with NBs.

Conclusions
Ultimately, our results reveal a novel role of TABs in mediating the invasiveness and dedifferentiation of human melanoma cells.

Ethics Approval
All mouse studies were performed at the Wistar Institute (AAALAC accredited) and approved by the Institutional Animal Care and Use Committee.

P640

hMENA is a key regulator of tumor cell-cancer associated fibroblasts dialogue via Gas6/Axl paracrine axis

sheila spada, PhD[1], Roberta Melchionna[2], Francesca Di Modugno, PhD[2], Mariangela Panetta[2], Anna Di Carlo[2], Anna Maria Mileo[2], Isabella Sperduti[2], Barbara Antoniani[2], Rita Teresa Lawlor[3], Lorenzo Piemonti[4], Maria Grazia Diodoro[2], Daniel D'Andrea, PhD[5], Paolo Visca[2], Michele Milella[2], Gian Luca Grazi[2], Francesco Facciolo[2], Emily Chen[6], Aldo Scarpa[3], Paola Nistico', MD[7]

[1]*Weill Cornell Medicine, new york, NY, USA*
[2]*IRCCS - Regina Elena National Cancer Institute, Rome, Italy*
[3]*ARC-NET Research Centre, Univ. of Verona, Verona, Italy*
[4]*IRCCS - San Raffaele Scientific Inst., Verona, Italy*
[5]*Centre for Cell Signaling and Inflammation, Imperial*

College, London, UK
[6]Herbert Irving Comprehensive Cancer Center, Columbia University Medical Centre, New York, USA
[7]Regina Elena National Cancer Institute, Rome, Italy

Background

Cancer-associated fibroblasts (CAFs) play a critical role in the complex process of tumor-stroma interaction, and may either favor or hinder tumor initiation, progression and drug resistance.The identification of phenotypical and functional subtypes is of great relevance for the development of microenvironment-related anti-tumor treatment.Pancreatic ductal adenocarcinoma (PDAC) and non-small cell lung cancer (NSCLC) are tumours with an abundant fibrotic stroma, and we have demonstrated that the tissue-specific alternative splicing of the actin regulator hMENA, generates hMENA11a and hMENAΔv6 isoforms that represent powerful diagnostic and prognostic factors in early stage NSCLC and PDAC [1-3]. hMENA/hMENAΔv6 influence intracellular signaling pathways involved in invasion and epithelial mesenchymal transition (EMT)[4-6] and [3].Here we aimed at investigating the role of hMENA isoforms in CAF functions and cancer cell-CAF crosstalk.

Methods

We have analyzed the expression of hMENA isoforms in normal fibroblasts and in CAFs isolated from pancreatic and lung cancer tissues, by IF and WB. The role of hMENA isoforms in CAF activity were analyzed by loss and gain of function experiments. hMENAΔv6-driven secreted factors were identified by LC-MS/MS proteomic analysis.

Results

CAFs express hMENA and hMENAΔv6 isoforms but not hMENA11a. hMENAΔv6 is overexpressed in CAFs compared to normal pancreatic fibroblasts and lung fibroblasts isolated from tissue distant from the tumor. The downregulation of hMENA/hMENAΔv6 isoforms, by siRNA, reduced the contractile activity of CAFs and MMP2 activity. Conversely, hMENAΔv6 overexpression in CAFs promoted their ability to invade, to activate the MMP2 and increase CAF-mediated cancer cell invasiveness. Notably, tumor cells over-expressing hMENA/hMENAΔv6 secrete factors essential for hMENAΔv6 overexpression and CAF activation, indicating hMena as crucial in tumor/CAF co-evolution. LC-MS/MS analysis revealed that CAFs over-expressing hMENAΔv6 secret the Axl ligand Gas6, favoring the invasiveness of Axl-expressing NSCLC and PDAC cells. Of relevance we demonstrated that hMENA regulate Axl expression in tumor cells and sustain the paracrine Gas6-Axl axis. Clinically, we found that a high hMENA/Gas6/Axl gene expression signature is associated with a poor prognosis in PDAC patients.

Conclusions

We demonstrated that hMENA/hMENAΔv6 identify a subset of CAFs with pro-tumoral functions and defined a novel function of hMENA in regulating tumour/stroma cross-talk via paracrine Gas6-Axl signaling, described as crucial in EMT, drug resistance and immune evasion [7]. We indicate that the network-based on hMENA/Gas6/Axl expression may represent novel prognostic and therapeutic targets and the pattern of hMENA isoform expression in both tumor cells and CAFs may reveal tumor mesenchymal traits identifying cancer subtypes for tailored therapies.

Acknowledgements

* S.S. and R.M. contributed equallyThe project is supported by the Italian Association for Cancer Research AIRC: 5×1000, 12182, and IG 15224.

References

1. Bria E, Di Modugno F, Sperduti I, Iapicca P, Visca P, Alessandrini G, Antoniani B, Pilotto S, Ludovini V, Vannucci J, Bellezza G, Sidoni A, Tortora G, Radisky DC, Crinò L, Cognetti F, Facciolo F, Mottolese M, Milella M, Nisticò P. Prognostic impact of alternative splicing-derived hMENA isoforms in resected, node-

negative, non-small-cell lung cancer. Oncotarget. 2014; 30;5(22):11054-63.
2. Di Modugno F, Spada S, Palermo B, Visca P, Iapicca P, Di Carlo A, Antoniani B, Sperduti I, Di Benedetto A, Terrenato I, Mottolese M, Gandolfi F, Facciolo F, Chen EI, Schwartz MA, Santoni A, Bissell MJ, Nisticò P. hMENA isoforms impact NSCLC patient outcome through fibronectin/β1 integrin axis. Oncogene. 2018 Jun 15.
3. Melchionna R, Iapicca P, Di Modugno F, Trono P, Sperduti I, Fassan M, Cataldo I, Rusev BC, Lawlor RT, Diodoro MG, Milella M, Grazi GL, Bissell MJ, Scarpa A, Nisticò P. The pattern of hMENA isoforms is regulated by TGF-β1 in pancreatic cancer and may predict patient outcome. Oncoimmunology. 2016 ; 12;5(12).
4. Di Modugno F, Iapicca P, Boudreau A, Mottolese M, Terrenato I, Perracchio L, Carstens RP, Santoni A, Bissell MJ, Nisticò P. Splicing program of human MENA produces a previously undescribed isoform associated with invasive, mesenchymal-like breast tumors. Proc Natl Acad Sci U S A. 2012 Nov 20; 19280-5.
5. Di Modugno F, Caprara V, Chellini L, Tocci P, Spadaro F, Ferrandina G, Sacconi A, Blandino G, Nisticò P, Bagnato A, Rosanò L. hMENA is a key regulator in endothelin-1/β-arrestin1-induced invadopodial function and metastatic process. Proc Natl Acad Sci U S A. 2018 20; 3132-3137.
6. Sistigu A, Di Modugno F, Manic G, Nisticò P. Deciphering the loop of epithelial-mesenchymal transition, inflammatory cytokines and cancer immunoediting. Cytokine Growth Factor Rev. 2017 Aug;36:67-77.
7. Aguilera TA, Giaccia AJ. Molecular pathways: oncologic pathways and their role in T-cell exclusion and immune evasion-a new role for the AXL receptor tyrosine kinase. Clin Cancer Res. 2017;15;23(12):2928-2933.

Ethics Approval

The Study was approved by Regina Elena National Cancer Institute's Ethics Board, approval number 1008/17

P641

Development of automated protocols for OPAL, SMIFT and ESIFT 4-color lymphocyte kits

Joe Vargas[1], Julio Masabanda, PhD[1], David Tacha, PhD[1*]

[1]*Biocare Medical, Martinez, CA, USA*

Background

We have compared the staining of the OPAL 4-color lymphocyte kit for manual use with the staining of the same kit adapted for the ONCORE automatic stainer. This kit is composed of primary antibodies against CD4, CD8 and CD20, and they are detected using a TSA-based fluorescence reaction. Additionally, we had developed in-house two additional kits with the same components as the OPAL 4 color kit, e.g. containing CD4, CD8 and CD20 antibodies. These kits we designated as SMIFT- (Sequential Multiplex Immunofluorescence Technology) and ESIFT- (Enhanced Sequential Immunofluorescence Technology) - 4-color lymphocyte kits, respectively. The goal was to develop an effective fluorescence-based assay that can be fully automated and used to assess the numbers of immune cells within the tumor microenvironment.

Methods

SMIFT is based on the indirect detection of antibody binding to hapten using secondary antibodies labeled with fluorescence. ESIFT is based on the use of primary antibodies directly labeled with HRP and detection with fluorescence. Additionally, we had compared the staining of the manual protocols for OPAL with SMIFT 4-color lymphocyte kits.

Results

Microscope observations show that the staining

intensities are comparable for both OPAL and ESIFT on the ONCORE. The intensity of the staining for SMIFT 4-color kit is the lowest of the compared systems. This is expected because SMIFT is not a TSA-based detection technology. Noteworthy, the fluorescence from the 3 antibodies of all kits systems is clearly visible directly under the fluorescence microscope and this is also valid for the SMIFT system.On the tissues in general the fluorescence from all the kits components was brighter for the Melanoma tissue compared to the tonsil control. For running the OPAL kit on the ONCORE, the manufacturer suggested protocol had to be adjusted in order to get a satisfactory staining on the tested tissues. The SMIFT protocol compared to OPAL required less optimization during the conversion of the manual to the ONCORE version. The ESIFT kit required the least efforts for protocol optimization for the ONCORE. Protocol run time on the ONCORE was the shortest for ESIFT (about 5.5 hours) and for SMIFT and OPAL the run times on the ONCORE were comparable (about 7 hours).

Conclusions

The manual performance is more labor intensive for the OPAL compared to the SMIFT kit. Obviously, the availability of automatic stainers has enabled the consistent performance without major human intervention of involved technologies such as OPAL 4-color kit.

P643

Oncology Nursing Society's patient immunotherapy wallet cards improve communication and immune-related adverse event management

Kathleen Wiley, RN, MSN, AOCNS[1], Michele Galioto, RN, MSN[1], Kathleen Wiley, RN, MSN, AOCNS[1], Nicole Lininger[1], Lisa Sheldon, PhD, ANP-BC, PhD APRN[1]

[1]*Oncology Nursing Society, Woolwich, NJ, USA*

Background

As the number of patients receiving immunotherapy agents continue to grow, so too does the potential for non-oncology clinicians to need to manage immune related toxicities. The similarities in the side effect profile of chemotherapy and immunotherapy agents are striking, yet their mechanism of action and evidence-based management strategies differ greatly. Oncology Nursing Society (ONS) members recognized the need to facilitate communication between oncology and non-oncology providers to improve outcomes of patients receiving immunotherapy.

Methods

ONS developed immunotherapy wallet cards to improve communication between oncology providers and non-oncology healthcare teams. The card enables patients to carry information about their treatment and side effects with them to appointments with non-oncology providers. The goal is to help inform providers who may not be involved with a patient's cancer treatment that he/she is receiving immunotherapy, and this will greatly impact their care. On the card, the oncology provider indicates whether the patient is receiving checkpoint inhibitors, monoclonal antibodies, adoptive cell therapy, vaccines or oncolytic viral therapy. Wallet cards include information about expected side effects associated with these agents and cautions them to be aware that these side effects, while they may mimic those of chemotherapy, require vastly different management. The cards include a prompt to contact the oncology care team before altering immunotherapy treatment regimens.

Results

Immunotherapy wallet cards were finalized and marketed to the public starting in January 2018. Since that time, 90,000 wallet cards have been ordered by oncology providers, nurses, pharmacists and patients and families, both within the USA and

internationally. Those who have ordered cards from ONS have been contacted for feedback on utilization and outcomes observed as a result of using wallet cards.

Conclusions

Immunotherapy as a form of cancer treatment is growing at an exponential rate. This increase in treatment options is met with many questions about adverse event management, and the speed at which approvals are seen mean clinicians outside the immediate oncology arena may not be fully aware of the intricacies of immunotherapy that set it apart from other antineoplastic strategies. The ONS Immunotherapy Wallet Card offers a strategy to help mitigate the unanticipated effects of such rapid growth of this class of treatment, and ensure patients have a way to communicate their treatment status and side effects likely to affect this patient population.

T-cell Checkpoints and Checkpoint Inhibitors

P644

Checkpoint inhibitor therapy in solid organ and allogeneic stem cell transplantation: data mining of The Truven Health Marketscan Research Database

Noha Abdel-Wahab, MD, PhD[1], Ala Abudayyeh[1], Xiudong Lei[1], Gheath Alatrash, DO, PhD[1], Hui Zhao[1], Sharon Giordano[1], Houssein Safa, MD[1], Daniel Johnson, MD[1], Van Trinh, DPharm[1], Maen Abdelrahim, MD, PhD[2], Ahmed Gaber, MD[2], Maria Suarez-Almazor, MD, PhD[1], Adi Diab, MD[1]

[1]UT MD Anderson Cancer Center, Houston, TX, USA
[2]Houston Methodist, Houston, TX, USA

Background

There are paucity of data on the safety of checkpoint-inhibitors (CPI) in patients (pts) with solid-organ transplant (SOT) and allogeneic stem-cell transplant (ASCT), primarily from case reports and small series. As the use of CPI expands to many new indications, stratifying the risk-benefit ratio in this population is needed. To estimate the magnitude of this oncological challenge, we used a health insurance-based database to identify the rate of rejection among transplant recipients treated with CPI.

Methods

We identified cancer pts with SOT/ASCT receiving CPI from the Truven Health MarketScan Research Database between 2011 and 2016. Only pts who had CPI claims post-transplant were considered. Validated ICD9&10 diagnostic codes were used to identify definite graft rejection or graft versus host disease (GVHD) occurred at any time after the first CPI.

Results

A total of 50 pts were identified. The SOT cohort included 22 pts; median age was 53 (12-70) years; 73% were male; 40.9% had melanoma. Most received PD1 inhibitors (59.1%). Kidney transplant was reported in 77.3%. Other SOT included liver, lung, heart, and pancreas. Median time from SOT till CPI initiation was 3.7 (0.2-11.6) years. Median duration of follow-up since CPI initiation was 3.2 (0.1-17.8) months. Four pts (36.4%) had graft rejection after a median of 0.7 (0-3) months post CPI initiation (3 kidney, and 1 heart); 3 after receiving ipilimumab. Seven pts (63.6%) with at least four months follow-up had no rejection. Additionally, 11 pts had shorter follow-up (0.4-3.8 months) and no rejection at last claim. The ASCT cohort included 28 pts; median age was 46 (14-64) years; 53.6% were male; 46.4% had lymphoma. Most received PD1 inhibitors (75.0%). Median time from ASCT till CPI initiation was 3.6 (1.1 -8.6) years. Median duration of follow-up since CPI initiation was 6.5 (0.1-24.3) months. Nine pts (52.9%) had GVHD after a median of 1.7 (0-6.6) months post CPI initiation; 8 after receiving PD1 inhibitors. Eight pts (47.1%) with at

least six months follow-up had no GVHD. Additionally, 11 pts had shorter follow-up (0.1-5.2 months) and no GVHD at last claim.

Conclusions

Acute rejection and GVHD were reported as a claim in over a third and over a half of SOT and ASCT recipients, respectively, after CPI initiation. Organ rejection tend to occur earlier than GVHD. Pre-clinical studies, and multi-institutional prospective studies in transplant recipients are needed to evaluate potential risk factors and management strategies that maintain graft tolerance without compromising antitumor benefits.

P645

Clinical characteristics and outcomes of immune checkpoint inhibitor-induced pancreatic injury

Hamzah Abu-Sbeih, MD[1], Tenglong Tang, MD[1], Yinghong Wang, MD, PhD[1]

[1]*MD Anderson Cancer Center, Houston, TX, USA*

Background

Lipase elevation is one of the reported immune checkpoint inhibitor (ICI)-induced adverse events.[1-3] The incidence and clinical characteristics of immune-mediated pancreatitis with clinical symptoms and suggestive imaging findings are not well studied in the literature. Therefore, we aimed to describe the clinical characteristics and outcomes of patients who developed immune mediated pancreatic injury (IMPI).

Methods

We studied consecutive patients that received ICI and developed IMPI from 1/2010 through 3/2018. IMPI was defined as CTCAE grade ≥3 lipase elevation. Comprehensive chart review was then conducted to confirm the diagnosis of IMPI, based on the clinical judgement of the treating oncologist or gastroenterologist, and to exclude other etiologies. Chi-square test, Fisher exact test, and Wilcoxon rank-sum test were used to compare clinical characteristics. Kaplan-Meier curves and log-rank test were used to estimate and compare unadjusted survival time distributions.

Results

Eighty-two (3.5%) out of the 2279 patients who received ICI and had lipase follow-up values had IMPI; most were white (77%), males (66%) with a mean age of 57 years (Table 1). Seven patients (9%) had a history of pancreatitis, and 11 (13%) had pancreatic metastasis at the time of ICI initiation. Overall, 65% of patients received inhibitors of programmed death protein-1 or its ligand-1. The median duration from ICI initiation to IMPI onset was 5 months (SD, 7 months), and it was the shortest for patients who received cytotoxic T-lymphocyte-associated protein-4 (P=0.033; Table 2). Patients who had clinical symptoms of pancreatitis (n=24 [1%]) had higher levels of lipase (P=0.006) and amylase (P=0.029), more frequent imaging findings of pancreatitis (P=0.030), more frequent hospitalization (P<0.001) with treatment with intravenous fluids (P=0.004) and steroids (P=0.016; Table 3). We observed no differences of clinical characteristics between patients that had pancreatic metastasis and those that did not. Patients who developed long-term consequences of IMPI (chronic pancreatitis on imaging studies (n=3), recurrence of IMPI (n=3), and subsequent diabetes (n=6)) received ICI treatment for longer duration (P=0.006), had more frequently past history of smoking (P=0.048) or hyperlipidemia (P=0.021), received less intravenous fluids treatment (P=0.031), and resumed ICI treatment more frequently (P=0.017; Table 4). Patients who resumed ICI treatment had a trend for better survival rates (P=0.0559; Figure 1).

Conclusions

IMPI can present as a typical clinical scenario of acute pancreatitis, with the risk of pseudocyst,

diabetes and chronic pancreatitis. ICI resumption in patients who had IMPI resulted in more long-term IMPI consequences, however, was associated with longer survival durations.

References

1. Cramer P, Bresalier R.S. Gastrointestinal and hepatic complications of immune checkpoint inhibitors. Curr Gastroenterol Rep, 2017. 19(1):3.2. 2. Wolchok, J.D., et al. Nivolumab plus ipilimumab in advanced melanoma. New England Journal of Medicine, 2013. 369(2):122-33.3. 3. Hofmann L, et al. Cutaneous, gastrointestinal, hepatic, endocrine, and renal side-effects of anti-PD-1 therapy. European Journal of Cancer, 2016. 60: 190-209.

Ethics Approval

This retrospective, single-center study was approved by the Institutional Review Board at The University of Texas MD Anderson Cancer Center (IRB No. PA18-0472).

Consent

This study was granted waiver for consent.

Table 1.

Table 1. Baseline clinical characteristics.

Characteristics	No. of patients (%)
Mean age (years, SD)	57 (14)
Male sex	54 (66)
Race	
White	63 (77)
Black	7 (9)
Hispanic	9 (11)
Other	3 (4)
Baseline risk factors	
History of smoking	35 (43)
Alcohol consumption	35 (43)
Diabetes mellitus type II	21 (26)
Hyperlipidemia	39 (48)
Drug allergy	51 (62)
Prior history for pancreatitis	7 (9)
Pancreatic metastasis	11 (13)
Cancer type	
Melanoma	30 (37)
Genitourinary	24 (29)
Lung, Head & Neck	11 (13)
Gastrointestinal	5 (6)
Other solid tumors	5 (6)
Hematological malignancies	7 (9)
Cancer Stage*	
Stage III	3 (4)
Stage IV	72 (88)
Median duration from ICI to injury (months, SD)	5 (7)
ICI type	
CTLA-4 monotherapy	12 (15)
PD-1/L1 monotherapy	53 (65)
Combination therapy	17 (21)
Other immune mediated adverse events	
Skin	13 (16)
Endocrine	7 (9)
Gastrointestinal tract	27 (33)
Liver	17 (21)
Lung	5 (6)
Other	6 (7)

Abbreviations: SD, standard deviation; ICI, immune checkpoint inhibitors; IQR, interquartile range; CTLA-4, cytotoxic T-lymphocytes associated protein-4; PD-1/L-1, programmed death protein and ligand.
*Cancer stage was recorded for 75 patients.

Table 2.

Table 2. Clinical characteristics stratified by ICI regimen.

Characteristics	CTLA-4 N = 12	PD-1/L1 N = 53	Combination N = 17	P
Clinical presentation, n (%)				
Fever	1 (8)	5 (9)	0 (0)	0.425
Nausea & vomiting	3 (25)	14 (26)	2 (12)	0.544
Epigastric pain	5 (42)	15 (28)	4 (24)	0.599
Dyspnea	2 (17)	11 (21)	4 (24)	1.000
Hemodynamic instability	3 (25)	12 (23)	4 (24)	0.984
Mean duration from ICI initiation to onset (days, SD)	89 (80)	189 (156)	123 (79)	0.033
Reason to stop ICI, n (%)				0.052
Pancreatitis	1 (8)	10 (19)	2 (12)	
Cancer progression	6 (50)	18 (34)	6 (35)	
Other adverse events	5 (42)	8 (15)	7 (41)	
Other reasons	0 (0)	17 (32)	2 (12)	

Abbreviations: SD, standard deviation; ICI, immune checkpoint inhibitors; CTLA-4, cytotoxic T-lymphocytes associated protein-4; PD-1/L-1, programmed death protein and ligand.

Table 3.

Table 3. Characteristics of patients who had clinical symptoms diagnostic of pancreatitis.

Characteristics	Clinical symptoms N = 24	NO clinical symptoms N = 58	P
Mean duration from ICI to onset (SD)	156 (136)	163 (141)	0.838
Baseline risk factors			
History of smoking	13 (54)	22 (38)	0.222
Alcohol consumption	11 (46)	24 (41)	0.808
Diabetes mellitus type II	4 (17)	17 (29)	0.278
Drug allergy	16 (67)	35 (60)	0.627
Prior history for pancreatitis	5 (21)	2 (3)	0.021
Pancreas metastasis	5 (21)	6 (10)	0.285
Biochemistry-peak value (mean, SD)			
Lipase (U/L)	3654 (3965)	1984 (1462)	0.006
Amylase (U/L)	415 (377)	270 (205)	0.029
CT findings of pancreatitis, n (%)	7 (29)	4 (7)	0.030
Pancreatitis treatment, n (%)			
Intravenous fluid	22 (92)	34 (59)	0.004
Antibiotic	17 (71)	31 (52)	0.218
Steroids	6 (25)	3 (5)	0.016
Duration from injury to improvement (SD)	52 (50)	54 (50)	0.885
Outcomes, n (%)			
Pancreatic pseudocyst	2 (8)	1 (2)	0.204
Hospitalization	16 (67)	2 (3)	< 0.001
Duration of hospitalization	6 (4)	6 (1)	0.926
Diabetes	0 (0)	6 (10)	0.173
Chronic pancreatitis features	1 (4)	2 (3)	1.000
Recurrence lipase elevation	1 (4)	2 (3)	1.000

Abbreviations: SD, standard deviation; ICI, immune checkpoint inhibitors; CT, computed tomography.

Table 4.

Table 4. Clinical characteristics of patients who had long-term consequences of pancreatitis (chronic pancreatitis, diabetes, and recurrence).

Characteristics	Long-term consequences N = 11	No long-term consequences N = 71	P
Age, years (SD)	62 (10)	56 (14)	0.232
Male sex, n (%)	9 (82)	45 (63)	0.316
Race, n (%)			0.116
White	6 (55)	57 (80)	
Other	5 (46)	14 (20)	
Duration of ICPI treatment, days (SD)	412 (361)	200 (197)	0.006
ICI type			1.000
CTLA-4 monotherapy	1 (9)	11 (16)	
PD-1/L1 monotherapy	8 (73)	45 (63)	
Combination therapy	2 (18)	15 (21)	
Baseline risk factors			
History of smoking	8 (73)	27 (38)	0.048
Alcohol consumption	6 (55)	29 (41)	0.516
Hyperlipidemia	9 (82)	30 (42)	0.021
Diabetes mellitus type II	5 (55)	16 (23)	0.139
Drug allergy	8 (73)	43 (61)	0.521
Prior history for pancreatitis	0 (0)	7 (10)	0.586
Pancreas metastasis	1 (9)	10 (14)	1.000
Clinical presentation, n (%)			
Fever	1 (9)	5 (7)	1.000
Nausea & vomiting	2 (18)	17 (24)	1.000
Epigastric pain	2 (18)	22 (31)	0.495
Dyspnea	0 (0)	17 (24)	0.109
Hemodynamic instability	0 (0)	19 (27)	0.060
Biochemistry-peak value (mean, SD)			
Lipase (U/L)	1700 (636)	2592 (2723)	0.285
Amylase (U/L)	248 (208)	323 (282)	0.403
CT findings of pancreatitis, n (%)	1 (10)	10 (19)	1.000
Duration from injury to improvement (SD)	59 (33)	53 (53)	0.695
ICI resumption, n (%)	8 (73)	23 (32)	0.017
Pancreatitis treatment, n (%)			
Intravenous fluids	4 (36)	52 (73)	0.031
Antibiotic	7 (64)	41 (58)	1.000
Steroids	1 (9)	8 (11)	1.000

Abbreviations: SD, standard deviation; ICI, immune checkpoint inhibitors; CT, computed tomography; CTLA-4, cytotoxic T-lymphocytes associated protein-4; PD-1/L-1, programmed death protein and ligand.

P646

Discovery and characterization of therapeutic human monoclonal antibodies against 17 immuno-oncology targets using microfluidics and molecular genomics

Adam Adler, PhD[1], Rena Mizrahi, PhD[1], Carter Keller, MBA[1], David Johnson, PhD[1]

[1]*GigaGen, South San Francisco, CA, USA*

Background

Monoclonal antibodies (mAbs) have proven to be extremely effective immuno-oncology therapeutics that lead to previously unseen durable responses in melanoma, bladder cancer, RCC, lung cancer, and other malignancies. Most mAb therapeutics, including current anti-PD-1 drugs, were discovered by mouse immunization followed by hybridoma isolation, a highly inefficient process that leads to few high affinity, developable antibodies. We recently developed a novel method for human mAb discovery that leverages humanized mice, microfluidics, multiplex PCR, yeast single chain variable fragment (scFv) display, and fluorescence activated cell sorting (FACS). Using this technology we have discovered thousands of high affinity antibodies against 17 immuno-oncology targets in less than 6 months.

Methods

We embarked on a discovery campaign for 17 immuno-oncology targets, including the antagonist targets PD-1, PD-L1, CTLA-4, LAG-3, TIM-3, B7-H3, B7-H4, TIGIT, CSF1R, VISTA, & CD47, and the agonist targets OX40, GITR, CD27, ICOS, TLR2, and TLR4. We immunized chimeric humanized mice (Trianni) with antigen twice weekly for four weeks. B cells were isolated from lymph nodes, spleen, and bone marrow, and >4 million single cells per target were processed through our microfluidic platform, generating DNA libraries that maintain proper heavy:light chain pairing. We built yeast scFv libraries for each of the 17 antigen-specific B cell repertoires and performed multiple rounds of FACS sorting to enrich for antigen-specific binders.

Results

We deep sequenced the libraries of enriched, high-affinity scFvs, which yielded the sequences for >2,800 candidate scFv binders. More than 400 of these candidate scFvs were engineered into full-length mAb constructs and expressed transiently in Chinese hamster ovary (CHO) cells. The affinity of individual mAbs ranged from 26 pM to 530 nM, with a median KD of 12.3 nM and ~10% with KD <1 nM. More than 55% of full-length antibodies were validated as specific binders to cell surface expressed target protein, and cell-based reporter assays for T cell activation revealed that ~60% of verified binders were functional. Epitope cross binning revealed extensive epitope diversity among the binders.

Conclusions

Candidates mAbs that are high affinity, bind cell surface antigen, and induce immune cell activation are now being tested in combinations or bispecific molecules for in vitro and in vivo efficacy. Combinations or bispecifics that show improved in vitro and in vivo efficacy over currently available checkpoint inhibitors will be moved forward into clinical studies.

P647

DuoBody-PD-L1x4-1BB combines checkpoint blockade and 4-1BB co-stimulation to promote antigen-specific T-cell stimulation and proliferation

Isil Altintas, PhD[1], Alexander Muik, PhD[2], Friederike Gieseke[2], Theodora Salcedo[1], Saskia Burm[1], Mustafa Diken, PhD[2], Christian Grunwitz[2], Sebastian Kreiter, MD[2], David Satijn, PhD[1], Danita Schuurhuis[1], Ozlem Tureci[2], Esther Breij, PhD[1], Ugur Sahin, MD[2]

[1]Genmab, Utrecht, Netherlands
[2]BioNTech, Mainz, Germany

Background

Currently pursued approaches in immuno-oncology involve either inhibition of immune checkpoints or activation of T cell co-stimulatory pathways. The concept of combining both modes-of-action within a single molecule, however, is so far not being clinically explored. Here, we introduce DuoBody-PD-L1x4-1BB (GEN1046), a first-in-class bispecific antibody for conditional engagement of T-cell co-stimulatory receptor 4-1BB in concert with PD-L1 checkpoint blockade.

Methods

DuoBody-PD-L1x4-1BB is an Fc-silenced IgG1 bispecific antibody that was obtained by controlled Fab-arm exchange of human(ized) PD-L1 and 4-1BB monoclonal antibodies. The binding characteristics of DuoBody-PD-L1-x4-1BB were assessed by flow cytometry, and functional characterization was performed using reporter assays and primary human T-cell assays. The effect on tumor-infiltrating lymphocytes (TIL) and their TCR repertoire was analyzed ex vivo in human primary tumor tissue cultures. In vivo activity of a surrogate mouse-reactive bispecific antibody was evaluated in both an OT-1 adoptive-cell-transfer model with ovalbumin vaccination and a CT26 mouse tumor model. The non-clinical safety profile of DuoBody-PD-L1x4-1BB was assessed in cynomolgus macaques.

Results

DuoBody-PD-L1x4-1BB showed dose-dependent binding to 4-1BB and PD-L1, with the PD-L1-specific arm being able to effectively antagonize PD-1:PD-L1 interactions. In T-cell stimulation assays with and without an active PD-1:PD-L1 axis, DuoBody-PD-L1x4-1BB enhanced T cell proliferation and pro-inflammatory cytokine secretion. DuoBody-PD-L1x4-1BB showed superior potency when compared to PD-1:PD-L1 checkpoint blockade alone. The 4-1BB agonist activity of DuoBody-PD-L1x4-1BB was shown to be strictly conditional, depending on simultaneous binding of both targets. In fresh human tumor tissue cultures, DuoBody-PD-L1x4-1BB increased TIL expansion ex vivo. In vivo, the mouse surrogate PD-L1x4-1BB bispecific antibody, led to massive expansion of adoptively transferred ovalbumin specific T-cells upon ovalbumin vaccination. In a subcutaneous CT26 tumor model >80% of tumor-bearing mice experienced long-term tumor remission when treated with the surrogate bispecific antibody. Finally, DuoBody-PD-L1x4-1BB showed a favorable safety profile in cynomolgus macaque at doses up to 30 mg/kg.

Conclusions

This data supports that DuoBody-PD-L1x4-1BB induces conditional stimulation of T cells by blocking the inhibitory PD-1:PD-L1 axis and simultaneously inducing a co-stimulatory signal via 4-1BB. This unique and distinctive mechanism of action may result in potent anti-tumor immunity with an improved safety profile compared to using single PD-1/PD-L1 and 4-1BB antibodies as a combination. The clinical safety of DuoBody-PD-L1x4-1BB in patients with solid cancers will be assessed in a first-in-human clinical trial.

Ethics Approval

Cynomolgus macaque studies were performed at Charles River Laboratories, Tranent, UK, in accordance with the EU legislations described in Directive 2010/63/EU. This study was licensed by UK Home Office under the Animals (Scientific Procedures) Act 1986 (approval number PBAD559F8, Toxicology of Pharmaceuticals, Protocol 15) and overseen by Genmab B.V. The use of tumor tissue resections was approved by BioNTech AG's Ethics Board, approval number 837.309.12 (8410-F).

P648

Different exhausted t-cell subsets exhibit different degrees of dysfunction in follicular lymphoma

Theodora Anagnostou, MD[1], Zhi Zhang Yang, MD[1], Hyo Jin Kim, PhD[1], Jose Villasboas, MD[1], Tammy Price-Troska[1], Shahrzad Jalali, PhD[1], Anne Novak, PhD[1], Stephen M. Ansell, MD, PhD[1]

[1]*Mayo Clinic, Rochester, MN, USA*

Background

Although PD1 inhibitors represent a breakthrough in classical Hodgkin lymphoma, responses are substantially lower in follicular lymphoma (FL) (1). T-cell exhaustion plays an important role in the tumor microenvironment (TME) of FL and expression of exhaustion markers, such as PD1, TIM3 and LAG3, correlates with poor outcomes (2, 3). The reactivation potentials of different exhausted T-cell subsets in FL remain unknown. In this study we sought to determine different degrees of dysfunction in FL.

Methods

We developed a model to induce T-cell exhaustion in healthy donor T-cells isolated from peripheral blood and activated using IL-12, which allows us to manipulate the exhaustion phenotypes over time and mimics the exhaustion state present in FL. We assessed expression of exhaustion markers, cytokines and proliferation by flow cytometry. We compared these results to 6 samples from FL lymph nodes. To assess different degrees of dysfunction, we blocked PD1, TIM3 and LAG3 signaling alone and in combination.

Results

The ability of T-cells activated and treated with IL-12 to proliferate and produce perforin was lower compared to that of cells not treated with IL-12, confirming that IL-12 induces exhaustion (Figure 1a). IL-12 led to expression of PD1 ligands on the majority of PD1-expressing cells whereas TIM3 ligands were predominantly expressed on TIM3- cells. Of note, activation did not lead to co-expression of PD1/PD-L1 suggesting a possible autocrine mechanism of exhaustion (Figure 1b). Prolonged exposure to IL-12 led to increased expression of TIM3 over time, whereas PD1 expression occurred early and plateaued after day 6 of treatment (Figure 1c). LAG3 was mainly expressed on PD1+ cells and most were also TIM3+ (Figure 1d). Cells expressing PD1 had a higher degree of dysfunction compared to PD1-TIM3+ cells (Figure 2a) and TIM3 blockade led to better reversal of function compared to PD1 or LAG3 blockade (Figure 2b). Since PD1-TIM3+ cells appeared more functional, we tested the effect of blocking antibodies on them. TIM3 or LAG3 blockade were able to restore both proliferation and IFN-g production, but dual TIM3/LAG3 blockade did not have better effects than either blockade alone (Figure 3a). PD1-TIM3+ cells had the highest reactivation potential amongst other subsets (Figure 3b).

Conclusions

Different exhausted T-cell subsets exhibit different degrees of dysfunction in FL. Future studies should focus on identifying targets for immunotherapy on T-cell subsets with high reactivation potential.

References

1. Ding W, et al. PD-1 blockade with Pembrolizumab in relapsed low grade non-hodgkin lymphoma, blood. 2017; 130: 4055-55.
2. Yang, ZZ,et al. PD-1 expression defines two distinct T-cell sub-populations in follicular lymphoma that differentially impact patient survival., Blood Cancer J. 2015 5:e281.
3. Yang, ZZ, et al. 2017. Expression of LAG-3 defines exhaustion of intratumoral PD-1(+) T cells and correlates with poor outcome in follicular lymphoma., Oncotarget. 2015; 8:61425-39.

Figure 1. Effects of IL-12 on healthy T-cells

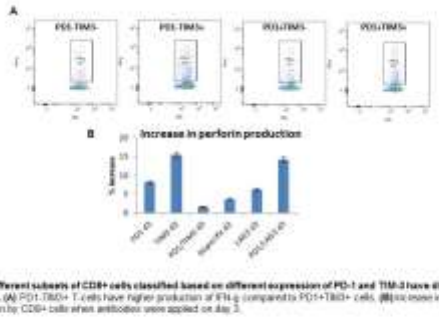

Figure 2. Different subsets of CD8+ cells classified

Table 2. Clinical characteristics stratified by ICI regimen.

Characteristics	CTLA-4 N = 12	PD-1/L1 N = 53	Combination N = 17	P
Clinical presentation, n (%)				
Fever	1 (8)	5 (9)	0 (0)	0.425
Nausea & vomiting	3 (25)	14 (26)	2 (12)	0.544
Epigastric pain	5 (42)	15 (28)	4 (24)	0.599
Dyspnea	2 (17)	11 (21)	4 (24)	1.000
Hemodynamic instability	3 (25)	12 (23)	4 (24)	0.984
Mean duration from ICI initiation to onset (days, SD)	89 (80)	189 (156)	123 (79)	0.033
Reason to stop ICI, n (%)				0.052
Pancreatitis	1 (8)	10 (19)	2 (12)	
Cancer progression	6 (50)	18 (34)	6 (35)	
Other adverse events	5 (42)	8 (15)	7 (41)	
Other reasons	0 (0)	17 (32)	2 (12)	

Abbreviations: SD, standard deviation; ICI, immune checkpoint inhibitors; CTLA-4, cytotoxic T-lymphocytes associated protein-4; PD-1/L-1, programmed death protein and ligand.

Figure 3. Effects of antibodies blocking different inhibitor

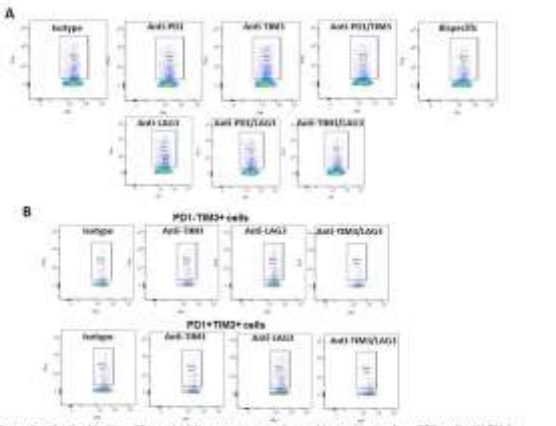

P649 **Abstract Travel Award Recipient**

Resistance to PD1 blockade in the absence of metalloprotease-mediated LAG3 shedding

Lawrence Andrews, PhD[1], Ashwin Somasundaram, MD[1], Jessica Moskovitz, MD[1], Andrea Szymczak-workman[1], Chang Liu, PhD[1], Anthony Cillo, PhD[1], Brenda Kurland[1], Huang Lin[1], Kelly Moynihan, PhD[2], Darrell Irvine, PhD[2], Robert Ferris, MD, PhD[1], Tullia Bruno, PhD[1], Creg Workman, PhD[1], Dario Vignali, PhD[1]

[1]*University of Pittsburgh, Pittsburgh, PA, USA*
[2]*Massachusetts Institute of Technology, Cambridge, MA, USA*

Background

Inhibitory receptors (IRs) prevent exacerbated T cell activation, yet can be hijacked by tumors for protection from immune attack. LAG3 co-expression with PD1 defines functionally exhausted T cells, with combinatorial blockade against these IRs in clinical trial. However, LAG3 expression and function is itself regulated by ADAM10/17-mediated cell surface cleavage at the connecting peptide. Our previous studies have shown that non-cleavable LAG3 (LAG3.NC) mutant T cells exhibit reduced cytokine production and proliferation in vitro, prompting us to examine whether LAG3 shedding from the surface of T cells is necessary to mount an effective antitumor immune response in vivo [1].

Methods

A conditional knock-in mouse was generated to restrict LAG3.NC to all T cells (CD4Cre) or specifically CD8+ (E8ICre.GFP), CD4+ (ThPOKCreERT2) or CD4+Foxp3+ populations (Foxp3CreERT2), by Cre-LoxP-mediated replacement of the connecting peptide with a mutant form. Moreover, LAG3 and ADAM10 expression was assessed to understand the translational relevance of LAG3 shedding in a cohort of patients with head and neck squamous cell

carcinoma (HNSCC).

Results

LAG3.NC-CD4Cre and LAG3.NC-ThPOKCreERT2 mice resist anti-PD1 therapy and succumb to MC38 tumor growth, compared to ~40% of controls and LAG3.NC-E8ICre.GFP mice becoming tumor-free. This phenotype is effector CD4+ T cell-mediated, and not Treg-mediated, as LAG3.NC-Foxp3CreERT2 mice clear tumors. Intrinsically, CD4+Foxp3– TIL isolated from LAG3.NC-CD4Cre mice show reduced proliferation and IFN-g/TNF-a compared with controls. CD8+ TIL also show reduced cytokine release, extrinsically affecting CD8+ pmel-1 T cells in an adoptive transfer model into B16-gp100-bearing LAG3.NC-CD4Cre hosts. Selective ADAM10 inhibition in vivo, also reduces IFN-g/TNF-a proposing that metalloproteinase-mediated LAG3 cleavage limits an antitumor immune response. This is clinically relevant as HNSCC patients show reciprocal expression of LAG3 and ADAM10 that is particularly evident on CD4+ T cells. This inverse correlation shown in patients with high LAG3 and low ADAM10 expression on CD4+Foxp3– T cells in peripheral blood is associated with higher HNSCC disease stage and reduced patient survival.

Conclusions

Overall, these data suggest that failure of LAG3.NC-CD4Cre/ThPOKCreERT2, but not LAG3.NC-E8ICre/Foxp3CreERT2, mice to clear MC38 tumors suggests that LAG3 shedding on CD4+Foxp3– T cells is necessary for CD8+ TIL to mediate an effective antitumor immune response. Indeed, HNSCC patients with higher LAG3 expression on CD4+Foxp3– T cells, due to lower ADAM10 expression, have poorer prognosis. Understanding the role of LAG3 shedding on T cells is thus clinically relevant, and may be useful as a potential biomarker for patient responsiveness to anti-PD1 immunotherapy.

References

1. Li N, Wang Y, Forbes K, Vignali KM, Heale BS, Saftig P, Hartmann D, Black RA, Rossi JJ, Blobel CP, Dempsey PJ, Workman CJ, Vignali DAA. Metalloproteases regulate T-cell proliferation and effector function via LAG-3. EMBO J. 2007; 26, 494-504..

P650

Selective CD47 immune checkpoint targeting on tumor cells modulates the tumor microenvironment to enhance macrophage tumoricidal function

Vanessa Buatois, PhD[1], Xavier Chauchet, PhD[1], Laura Cons[1], Laurence Chatel[1], Limin Shang, PhD[1], Marie Kosco-Vilbois[1], Krzysztof Masternak, PhD[1], Nicolas Fischer, PhD[1], Walter Ferlin, PhD[1]

[1]*Novimmune SA, Geneva, Switzerland*

Background

CD47 is a membrane protein overexpressed on tumor cells and considered as an innate immune checkpoint. CD47 interacts with SIRPα on myeloid cells and induces a “don’t eat me” signal that allows healthy cells to limit elimination by immune cells, in particular macrophages. CD47 upregulation in solid and hematological cancers is correlated with poor clinical prognosis, almost certainly by allowing tumor cells to escape immune surveillance. Blocking the CD47-SIRPα axis is thus an attractive approach to foster tumor cell killing by tumor-associated macrophages (TAMs) and boost cross-priming of anti-tumor T cells by dendritic cells (DC). However, CD47 targeting is hindered by haematological toxicity due to its ubiquitous expression. To focus CD47 blockade on tumor cells, we generated two bispecific antibodies (biAbs) pairing a high affinity arm targeting a tumor associated antigen (TAA), i.e., CD19 or mesothelin (MSLN), to an optimized lower affinity arm targeting CD47 and investigated their efficacy in xenograft tumor models.

Methods
BiAbs targeting CD47xCD19 or CD47xMSLN were tested in immunodeficient mice implanted with the following human tumor cell lines: Raji (CD19+, lymphoma), OVCAR-3 (MSLN+, ovarian) or MSLN-transfected HepG2 (hepatic). Analysis by flow cytometry and Nanostring technology was used to evaluate the impact of the biAbs on the tumor microenvironment. The contribution of macrophages to tumor growth inhibition was addressed by clodronate-mediated depletion. Finally, biAbs-stimulated cross-priming of anti-tumor T-cells by DC was assessed in vitro.

Results
BiAbs controlled the growth of CD19+ lymphomas and MSLN+ tumors. In the Raji xenograft model, treatment with the CD47xCD19 biAb did not increase the number of TAMs, but enhanced their tumoricidal activity (i.e., more macrophages engulfing tumor cells). The treatment also reduced the proportion of CD11b+Ly6g+ granulocytic myeloid-derived suppressor cells. In contrast, in the MSLN-transfected HepG2 xenograft model, treatment with the CD47xMSLN biAb induced a significant increase of macrophages in the tumor. Depletion of phagocytic cells with clodronate impaired the anti-tumor activity of the biAbs, highlighting the role of macrophages. Finally, the biAbs promoted cross-priming of tumor antigen-specific T-cells, suggesting the potential of CD47xTAA biAbs to enhance anti-tumor T cell responses.

Conclusions
CD47 targeting biAbs, tethered to cancer cells by their TAA binding arm, remodel the tumor microenvironment enhancing macrophage tumoricidal function. Furthermore, the ability for the biAbs to amplify DC-induced cross-priming of tumor antigen to T-cells further augments the antitumor efficacy potential of such molecules.

P651

First-in-human study of FAZ053, an anti-PD-L1 mAb, alone and in combination with spartalizumab, an anti-PD-1 mAb, in patients with advanced malignancies

Janis Callister1, Filip Janku, MD, PhD[2], David Tan[3], Juan Martin-Liberal[4], Shunji Takahashi[5], Ravit Geva, MD[6], Ayca Gucalp[7], Xueying Chen[8], Kulandayan Subramanian[9], Jennifer Mataraza[9], Jennifer Wheler[9], Philippe Bedard, MD[10]

[1]*Articulate Science, Manchester, UK*
[2]*MD Anderson Cancer Center, Houston, TX, USA*
[3]*National University Cancer Institute, Singapore, Singapore*
[4]*Vall d'Hebron Institute of Oncology, Barcelona, Spain*
[5]*The Cancer Institute Hospital of JFCR, Tokyo, Japan*
[6]*Tel Aviv Sourasky Medical Center, Tel-Aviv, Israel*
[7]*Memorial Sloan Kettering Cancer Center, New York, NY, USA*
[8]*Novartis Pharmaceuticals Corporation, East Hanover, NJ, USA*
[9]*Novartis Institutes for BioMedical Resea, Cambridge, MA, USA*
[10]*Princess Margaret Cancer Centre, Toronto, ON, Canada*

Background
FAZ053 and spartalizumab are humanized immunoglobulin G4 monoclonal antibodies (mAbs) that bind anti-programmed death ligand-1 (PD-L1) and programmed death-1 (PD-1), respectively. We report the dose-escalation results from an ongoing Phase I study of FAZ053 ± spartalizumab in patients with advanced malignancies, enriched for patients with chordoma, a rare subtype of sarcoma.

Methods
Patients received escalating doses of single-agent (SA) FAZ053 intravenously once every 3 weeks (Q3W) or 6 weeks (Q6W), or FAZ053 + spartalizumab Q3W. The primary objective was to assess the safety and tolerability of FAZ053 ± spartalizumab, and determine recommended doses for expansion (RDEs). Dose escalation was guided by an adaptive Bayesian logistic regression model following the escalation with overdose control principle.

Results
As of the data cutoff of March 30, 2018, 61 patients received SA FAZ053 at doses 80–1600 mg Q3W or 800–1600 mg Q6W. Most patients (n=54; 89%) received prior treatment; 1 (2%) received prior anti-PD-1. FAZ053 exposure was generally dose proportional, with terminal half-life of ~16–18 days. A dose-limiting toxicity occurred in 1 patient (Grade 4 renal failure; FAZ053 1600 mg Q6W). RDE was determined to be 1200 mg Q3W or 1600 mg Q4W. Adverse events (AEs) of all grades assessed as possibly related to treatment were reported for 33 patients (54%); most commonly (≥10%) fatigue (n=11; 18%) and pruritus (n=8; 13%); 4 patients (7%) had Grade 3/4 treatment-related AEs, including elevated amylase (3%), renal failure, elevated lipase, elevated AST, and elevated blood CPK (each 2%). For these patients treated with SA FAZ053, partial responses (PRs) were demonstrated in 4 patients (7%) with chordoma, alveolar soft part sarcoma (ASPS), poorly differentiated carcinoma of scalp, and penile squamous cell carcinoma (duration of treatment 5.5–12.5 months; all with treatment ongoing). Among 5 patients with chordoma treated with SA FAZ053, 1 patient has a PR, treatment ongoing >12 months, and 4 patients have stable disease ongoing (+4% to –29%). Data for 57 patients treated with combination FAZ053 (20–1200 mg) + spartalizumab 300 mg Q3W are preliminary. Updated results and biomarker data for patients receiving SA and combination treatment, including additional patients with chordoma, will be presented.

Conclusions
SA FAZ053 was well tolerated and the RDE was determined to be 1200 mg Q3W. Clinical activity was observed in a range of indications including chordoma, a rare tumor without standard therapy options.

Trial Registration
www.clinicaltrials.gov; NCT02936102

Ethics Approval
This study was approved by an independent ethics committee or institutional review board at each site.

P652

Cytokine-mediated induction of PD-L1 expression on tumor and immune cells

Shuming Chen, PhD[1], George Crabill, MS[1], Theresa Pritchard, MS[1], Tracee McMiller, MS[1], Drew Pardoll, MD, PhD[1], Fan Pan[1], Suzanne Topalian, MD[1]

[1]Johns Hopkins University School of Medicine, Sidney Kimmel Comprehensive Cancer Center, and Bloomberg~Kimmel Institute for Cancer Immunotherapy, Baltimore, MD, Canada

Background
The PD-1/PD-L1 checkpoint is a central mediator of immunosuppression in the tumor immune microenvironment (TME). To characterize factors regulating PD-L1 expression on tumor and/or immune cells, we investigated the effects of TME-resident cytokines and the role of transcription factors in constitutive and cytokine-induced PD-L1 expression.

Methods
Thirty-four cultured human tumor lines derived from 18 melanomas (MEL), 12 renal cell carcinomas (RCC),

and 4 squamous cell carcinomas of the head and neck (SCCHN), and normal donor peripheral blood monocytes (Monos), were treated with cytokines that we found expressed in the PD-L1+ TME by gene expression profiling (GEP), including IFN-g, IL-1a, IL-10, IL-27 and IL-32g. PD-L1 cell surface protein expression was detected by flow cytometry, and mRNA by quantitative RT-PCR. Total and phosphorylated STAT1, STAT3, p65 and c-jun proteins were detected by Western blotting. STAT1, STAT3, p65 and c-jun were knocked down with siRNAs. The proximal promoter region of CD274 (PD-L1) was sequenced in all cultured tumor lines.

Results

PD-L1 protein was not constitutively expressed on cultured MELs, but was found on some RCCs (n=6) and SCCHNs (n=3). Brief IFN-g exposure induced PD-L1 on MELs, and induced or upregulated PD-L1 on RCCs and SCCHNs. Among other TME-resident cytokines detected in human PD-L1+ tumor biopsies by GEP, IL-27 and IL-1a increased PD-L1 expression on cultured tumor lines, alone or in combination with IFN-g. In short-term cultured Monos, PD-L1 expression was induced by these and additional cytokines, including IL-10 and IL-32g. Changes in PD-L1 protein expression (FACS) correlated with mRNA levels, suggesting cytokine regulation primarily via mRNA transcription and not via protein translocation. siRNA knockdown of STAT1 but not STAT3 reduced IFN-g- and IL-27-induced PD-L1 protein expression on tumor lines and Monos. In contrast, STAT3 knockdown in Monos reduced IL-10-induced PD-L1 protein expression, and p65 knockdown in tumor lines reduced IL-1a-induced PD-L1 expression. Notably, constitutive PD-L1 expression was not affected by knocking down STAT1, STAT3, p65 or c-jun. Differential effects of IFN-g, IL-1a, and IL-27 were not due to CD274 promoter polymorphisms or mutations.

Conclusions

Multiple cytokines play important and cell type-selective roles in promoting PD-L1 expression in the TME. Activation of STAT1, STAT3 or p65 was associated with PD-L1 expression in response to distinct cytokines. Factors driving constitutive tumor cell PD-L1 expression were not identified in this study. However, in many cancers, adaptive expression of PD-L1 on tumor and/or stromal cells reflects an immune-reactive TME that can be unleashed by anti-PD-1/PD-L1 therapy.

Acknowledgements

Supported by NCI R01 CA142779 and the Johns Hopkins Bloomberg~Kimmel Institute for Cancer Immunotherapy.

P653

Discovery of a novel TIGIT therapeutic antibody with strong efficacy in tumor xenografts as monotherapy

Feifei Cui, PhD[1], Lei Fang[1], Zhengyi Wang[1], Taylor Guo[1], Jingwu Zhang[1], Feifei Cui, PhD[1]

[1]I-Mab Biopharma, Shanghai, China

Background

The immune checkpoint co-inhibitory receptor TIGIT (T cell immunoglobulin and immunoreceptor tyrosine-based inhibitory motif) is expressed on activated CD4+ T, CD8+ T and NK cells and on regulatory T cells (Tregs). Blocking TIGIT interaction with its ligand CD155 can re-energize tumor antigen-specific CD8+ T cells, unleash NK cells and inhibit Treg-mediated immunosuppression in the tumor microenvironment. Previous reports showed strong efficacy of anti-TIGIT antibodies in combination with anti-PD(L)1 agents in multiple tumor models, indicating a potential for TIGIT blocking antibodies as a combination partner for cancer treatment. Here we report discovery of a novel, humanized, Fc-

enabled, subnanomolar anti-TIGIT antibody with significantly enhanced tumor inhibition as a monotherapy, thus differentiating it from current anti-TIGIT molecules.

Methods
TJT6 was generated by traditional hybridoma technology using extracellular domain (ECD) of human TIGIT as immunogen and then humanized through complementarity determining region (CDR) grafting. The TIGIT antigen binding and CD155 receptor blocking activities of TJT6 were evaluated for through both protein-based and cell-based assays. The immunological function of TJT6 was further studied in a TIGIT- and its counterreceptor CD226-overexpressed Jurkat cell activation assay. The in vivo efficacy of TJT6 was investigated in MC38 tumor model using human TIGIT knock-in mice. Percentages of tumor infiltrating CD4+ T and CD8+ T cells and the production of interferon gamma (IFN-gamma) were analyzed by flow cytometer.

Results
TJT6, an Fc-enabled human IgG1 antibody, binds human and cynomolgus TIGIT with similar sub-nanomolar binding. It blocked the interaction of TIGIT to its ligand CD155, leading to increased production of interleukin 2 (IL-2) in a Jurkat cell line which overexpressed TIGIT and CD226. Mono-treatment of TJT6 significantly suppressed tumor growth in a dose-dependent manner in a syngeneic MC38 tumor model compared to vehicle, achieving maximal 80% tumor growth inhibition at 10 mg/kg. Percentages of tumor infiltrating CD4+ and CD8+ T cells and the production of IFN-gamma in CD8+ T cells were significantly enhanced after anti-TIGIT antibody treatment.

Conclusions
We have successfully discovered a TIGIT-blocking therapeutic antibody with strong efficacy in the inhibition of tumor growth and reinvigoration of tumor-infiltrating CD8+ T cells. TJT6 represents potentially a best-in-class molecule with superior potency as a single agent and is undergoing preclinical development with an aim to enter clinical studies in 2019.

P654

T-cell profiling in cancer tissue with multiplexed IHC using UltiMapper™ I/O assays

Alexis Wong, PhD[1], Alexis Wong, PhD[1], Amy Zhang, MS[1], Max Rubinstein[1], Laura Sciarra, PhD[1], Chakib Boussahmain, BS[1], Bonnie Phillips, PhD[1], Katir Patel, PhD[1], Sean Downing, PhD[1], Stephanie Hennek, PhD[1]

[1]*Ultivue, Cambridge, MA, USA*

Background
With high spatial heterogeneity and biological complexity, resected tumor samples present a significant characterization challenge, particularly when samples are scarce. Multiplexing in a single, intact tissue sample is required to identify cell types, understand biological pathways, and map cellular interactions. Ultivue has developed a portfolio of multiplexed immunofluorescence tissue imaging assays (UltiMapper assays) that simultaneously enable whole-slide imaging and integrate seamlessly with existing instrumentation to address key questions in immuno-oncology. This work highlights the application of UltiMapper assays in human tumor samples to profile and phenotype T-cells – including regulatory T-cells, activated T-cells, exhausted T-cells, and memory T-cells. Each T-cell subtype plays an important role in the immune response to cancer and determining the presence and interactions of each T-cell population drives a deeper understanding of the biological mechanisms at work.

Methods
UltiMapper assays were used to perform multiplexed IHC on deidentified FFPE tissue samples using control tissues (tonsil) and on multiple tumor types (lung,

melanoma, colon, or breast). Three separate panels were run on serial sections. The UltiMapper I/O T-Reg panel included the markers CD4, CD25, and FoxP3, as well as a tumor markers pan-cytokeratin (CK) for carcinomas and Sox10 for melanomas. The UltiMapper I/O T-Act panel included markers CD3, Granzyme B, Ki67, CK, and SOX10. The UltiMapper I/O PD-1 panel included markers CD3, CD45RO, PD-1, CK, and SOX10. Staining was performed manually or using the Leica Bond Rx™ autostainer. Imaging was performed on various tissue scanners including the Zeiss Axio Scan.Z1, and image analysis was performed using HALO from Indica Labs.

Results

Each marker in the UltiMapper panels was individually compared at the singleplex level to reference IHC assays to confirm staining specificity. Serial tissue sections stained with the UltiMapper panels were found to have good reproducibility. In tumor samples, a range of abundance and expression of infiltrating T-cells was observed. Cell counts for all possible phenotypes were obtained for each panel to identify regulatory T-cells, activated T-cells, exhausted T-cells, and memory T-cells. Spatial analysis was employed to map the degree of T-cell infiltration between tissue samples.

Conclusions

Target specificity was confirmed for the UltiMapper I/O T-Reg, T-Act, and PD-1 panels. UltiMapper assays are proficient in maintaining tissue integrity and identifying several subsets of T-cells within and surrounding tumor sections. The UltiMapper assay can be implemented by any lab possessing a standard fluorescent microscope and does not rely on the purchase of, nor access to, more expensive platforms.

P656

ATOR-1017, a tumor directed Fcγ-receptor cross linking dependent 4-1BB agonistic antibody

Karin Enell Smith, PhD[1], Anna Rosén[1], Karin Barchan[1], Ida Aberg[1], Doreen Werchau, BS[1], Mia Thagesson[1], Anna Dahlman[1], Niina Veitonmaki[1], Christina Furebring, PhD[1], Peter Ellmark, PhD[1]

[1]*Alligator Bioscience, Lund, Sweden*

Background

4-1BB is an inducible costimulatory receptor expressed on activated T and natural killer (NK) cells. Activation of 4-1BB results in improved survival, proliferation and enhanced effector functions of the T and NK cells. Treatment with 4-1BB antibodies in preclinical mouse tumor models leads to tumor eradication and induction of long-term immunity. 4-1BB is a promising candidate for immunotherapy, however 4-1BB antibodies in clinical development, have either been suffering from poor efficacy or toxicity. ATOR-1017 is a 4-1BB ligand-blocking IgG4 antibody, designed for improved safety and enhanced efficacy. The functional activity is dependent on engagement with Fcγ receptors (FcγRs), directing the immune activation to the tumor area where 4-1BB as well as certain FcγRs are highly expressed.

Methods

ATOR-1017 was characterized using human primary cells isolated from leukocyte concentrates from healthy donors or 4-1BB reporter assays co-cultured with FcγR-expressing cells. The in vitro effects were measured using either ELISA or FACS. Co-expression of 4-1BB, FcγRI and FcγRIIb was assessed on human tumor tissue samples by immunohistochemistry (IHC).

Results

ATOR-1017 blocks the 4-1BBL binding to the 4-1BB

receptor and binds to a unique epitope compared to the 4-1BB antibodies currently in clinical development. Co-stimulation of human primary CD8+ T cells with ATOR-1017 induces a potent CD8+ T cell activation only after cross-linking by FcγRI or FcγRIIb. Similarly, ATOR-1017 induces an FcγR-dependent cytotoxic phenotype in NK cells. The importance of the improved cytotoxic profile of NK cells is further supported by combining ATOR-1017 with a tumor targeting antibody, which synergistically enhances the induction of antibody-dependent cell-mediated cytotoxicity (ADCC).Co-expression of FcγRs and 4-1BB is required for induction of a tumor-directed immune response. This was demonstrated in solid tumors as well as lymphomas, using IHC multiplex staining of 4-1BB, FcγRI and FcγRIIb. Tumor tissue from several tumor indications demonstrated a high and co-localized expression of the targets, supporting a tumor-directed immune response of ATOR-1017.

Conclusions

ATOR-1017 is a FcγR crosslinking dependent 4-1BB agonistic antibody with an activation profile that minimize the risk for inducing systemic immune activation and toxicity. ATOR-1017 was designed for an optimal efficacy and improved safety, by combining the IgG4-format that mediates a potent FcγR cross-linking with a unique binding epitope on 4-1BB. The immune activation will be directed to tumors co-expressing both specific FcγRs and 4-1BB, which are potential biomarkers for patients as well as tumor indication selection. ATOR-1017 is currently in preclinical development phase and clinical studies are planned for 2019

Ethics Approval

This study was approved by Lund/Malmö Ethics Board approval number M142-15.

P657

Agonist redirected checkpoint platform (ARC), engineering bi-functional fusion proteins (PD1-Fc-OX40L), for cancer immunotherapy

George Fromm, PhD[1], Suresh de Silva, PhD[2], Taylor Schreiber, MD, PhD[2]

[1]*Shattuck Labs, Inc, Apex, NC, USA*
[2]*Shattuck Labs, Inc., Durham, NC, USA*

Background

Current combination immunotherapy with bispecific antibodies, linked scFv's or T cell engagers have not been able to both block checkpoints and agonize TNF receptors; likely because these molecules lose target avidity when engineered to bind multiple targets with monovalent antigen binding arms. Fusion proteins incorporating the extracellular domain (ECD) of type I membrane proteins (e.g., Enbrel, Orencia) or type II membrane proteins (e.g., OX40L-Fc, GITRL-Fc), linked to the hinge-CH2-CH3 domain of antibodies are both functional, despite the fact that their ECDs are in opposite orientations. Here we report the generation of a two-sided fusion protein platform linking type I ECDs to type II ECDs by a central domain (Agonist Redirected Checkpoint, ARC), and present preclinical findings on one of the PD1-containing molecules in our pipeline; PD1-Fc-OX40L.

Methods

Human and mouse PD1-Fc-OX40L were produced and characterized using a range of biochemical assays to determine molecular weight, subunit composition & binding affinity; molecular assays to characterize in vitro/ex vivo binding & functional activity; and anti-tumor efficacy in multiple syngeneic tumor models. Human PD1-Fc-OX40L completed GMP manufacturing and GLP NHP toxicity studies, with anticipated IND filing in Q4 2018.

Results

The PD-1 end of the ARC binds immobilized PD-L1 and PD-L2 at 2.08 and 1.76 nM affinity, respectively, and binds PD-L1 on human tumor cells in vitro and in vivo. The OX40L end of the ARC binds immobilized OX40 at 246 pM affinity and binds OX40 on primary T cells. High binding affinity on both sides of the construct translated to potent stimulation of OX40 signaling and PD1:PD-L1/L2 blockade, in multiple in vitro assays, including improved potency as compared to pembrolizumab, nivolumab, tavolixizumab and combinations of those antibodies. Furthermore, when activated human T cells were co-cultured with PD-L1 positive human tumor cells, PD1-Fc-OX40L was observed to concentrate within the immune synapse, which enhanced proliferation of T cells and production of IL-2, IFNγ and TNFα; leading to efficient killing of tumor cells. The therapeutic activity of PD1-Fc-OX40L in established murine tumors was superior to PD1 blocking, OX40 agonist, or combination antibody therapy. Importantly, all agonist functions of PD1-Fc-OX40L are independent of Fc receptor cross-linking.

Conclusions

These data demonstrate feasibility and function of a novel chimeric fusion protein platform, providing checkpoint blockade and TNF superfamily costimulation in a single molecule, which is uniquely advantageous because the construct links those two signals in the same microenvironment, at the time in which T cells are engaging cognate tumor antigens.

P658

Agonist redirected checkpoint platform (ARC), engineering bi-functional fusion proteins (TIM3-Fc-OX40L and TIM3-Fc-CD40L), for cancer immunotherapy

George Fromm, PhD[1], Suresh de Silva, PhD[2], Taylor Schreiber, MD, PhD[2]

[1]*Shattuck Labs, Inc, Apex, NC, USA*
[2]*Shattuck Labs, Inc., Durham, NC, USA*

Background

Current combination immunotherapies with bispecific antibodies, linked scFv's or T cell engagers have not been able to both block checkpoints and agonize TNF receptors. This is likely because these molecules lose target avidity when engineered to bind multiple targets with monovalent antigen binding arms. Fusion proteins incorporating the extracellular domain (ECD) of type I membrane proteins (e.g., Enbrel, Orencia) or type II membrane proteins (e.g., OX40L-Fc, GITRL-Fc), linked to the hinge-CH2-CH3 domain of antibodies are both functional, despite the fact that their ECDs are in opposite orientations. Here we report the generation of a two-sided fusion protein platform that links type I ECDs to type II ECDs by a central domain (Agonist Redirected Checkpoint, ARC), and present preclinical findings on two molecules in our pipeline; TIM3-Fc-OX40L and TIM3-Fc-CD40L.

Methods

Shattuck synthesizes both murine and human versions of ARCs, and assesses them using biochemical assays to determine molecular weight, subunit composition & binding affinity; molecular assays to characterize in vitro/ex vivo binding, in vitro functional activity; and anti-tumor efficacy in multiple syngeneic tumor model systems. TIM3-Fc-OX40L & TIM3-Fc-CD40L have advanced into cell line development and early manufacturing.

Results

The TIM3 end of the fusion protein binds GAL9 and phosphtidylserine (PS) on human tumor cells. The OX40L/CD40L ends bind OX40 and CD40, respectively, on the surface of primary PBMCs. Both TIM3-Fc-OX40L & TIM3-Fc-CD40L activate NF B signaling in cells engineered to overexpress OX40 or CD40 and an NF B-luciferase reporter, and also in NIK signaling reporter cells. Each TIM3-containing ARC induces a unique cytokine signature in PBMCs incubated with the super-antigen Staphylococcal enterotoxin B, or when cultured in AIMV media. In vivo, the therapeutic activity of TIM3-Fc-OX40L and TIM3-Fc-CD40L in established murine MC38 and CT26 tumors was superior to TIM3-blocking antibody, OX40-/CD40-agonist antibody monotherapies, and the respective correlating combination antibody therapy. Importantly, a pharmacodynamic biomarker of tumor rejection was identified by coordinated elevations in serum IFNγ, IL-2, IL-4, IL-5, IL-6 and IL-17A. Interestingly, therapeutic activity (anti-tumor in mice or human cytokine secretion in the SEB assay) was enhanced when ARCs were combined with antibody blockade of PD1.

Conclusions

These data demonstrate feasibility and functional activity of a novel chimeric fusion protein platform, providing checkpoint blockade and TNF superfamily costimulation in a single molecule, which is uniquely advantageous because the construct links those two signals in the same microenvironment, at the time in which T cells are engaging cognate tumor antigens.

P659

AGEN2373 is a conditionally-active agonist antibody targeting the co-stimulatory receptor CD137 for the treatment of human malignancies

Claire Galand, PhD[1], David Savitsky[1], Vignesh Venkatraman[1], Min Lim[1], Rebecca Ward, MSc[1], Nicholas Wilson[1], Christina Riordan[1], Matthew Costa[1], Randi Gombos, PhD[1], Benjamin Morin, PhD[1], Dhan Chand, PhD[1], Claire Galand, PhD[1]

[1]*Agenus, Lexington, MA, USA*

Background

CD137 is a co-stimulatory member of the tumor necrosis factor receptor superfamily (TNFRSF) that is expressed by discrete populations of T and natural killer (NK) cells. Agonist antibodies targeting CD137 are potent inducers of tumor-reactive T cell proliferation, cytokine production and cytotoxicity, and have been explored clinically for their ability to enhance immune cell-mediated destruction of tumor cells. Despite early signs of clinical activity, the development of first generation anti-CD137 antibody has been hampered by on-target dose-limiting hepatotoxicity. Next-generation CD137 therapies have therefore sought to localize CD137 agonism to the tumor microenvironment (TME) to potentially improve tolerability in patients. However, these approaches may also limit the potential benefit of CD137 signaling outside the TME that contributes to anti-tumor immunity, such as T cell priming in tumor draining lymph nodes. Here we describe the pharmacologic and non-clinical safety profile of AGEN2373, a novel anti-CD137 antibody designed to provide potent CD137 co-stimulation in the presence of CD137 ligand and Fc gamma receptor-expressing antigen presenting cells. Importantly, AGEN2373 was well-tolerated in non-human primates, therefore supporting the potential for a therapeutic window in patients either as a monotherapy, or in combination with immune checkpoint blockade.

Methods
Binding assay; Pharmacologic and non-clinical safety study in non human primates; Signaling reporter assay; Cytokine secretion assay

Ethics Approval
Non human primate and rodent studies were approved by Agenus Institutional Animal Care and Use Committee (IACUC).

P660

A novel bispecific agent targeting PD-L1 and IL-15/IL-15Ralpha promotes potent anti-tumor efficacy in multiple models of human solid carcinomas

Karin Knudson, PhD[1], Kristin Hicks, PhD[1], Yohei Ozawa, MD, PhD[1], Jeffrey Schlom, PhD[1], John Lee, MD[2], Shahrooz Rabizadeh, PhD[3], Patrick Soon-Shiong, MD, FRCS, FACS[4], Sofia Gameiro, PharmD, PhD[1]

[1]National Cancer Institute, NIH, Bethesda, MD
[2]NantKwest LLC, Culver City, CA
[3]NantOmics, LLC, Culver City, CA
[4]NantWorks, LLC, Culver City, CA

Background
The PD-1/PD-L1 checkpoint axis is a negative regulator of CD8+ T and NK cell function. Immunotherapy targeting this axis has failed to provide significant and durable clinical benefit in the majority of patients with solid carcinomas. In a recent clinical study, patients with NSCLC refractory to PD-1 blockade showed signs of clinical responses to the PD-1 targeting antibody nivolumab when given in combination with the IL-15 superagonist N-IL15 (previous known as ALT803). N-IL15 has been shown to promote significant expansion of circulating NK and CD8+ T cells in cancer patients and has displayed anti-tumor efficacy in murine models of solid carcinomas. Current studies are investigating the combination of N-IL15 with other immunotherapies, especially those that decrease immune suppression in the tumor microenvironment (TME). Thus, it may be possible to improve anti-tumor efficacy through the generation of a molecule that targets IL-15 activity to the TME and potentially reduces immunosuppression and immune-related adverse events.

Methods
Using multiple murine models of human solid carcinomas, we examined the immunomodulatory effects and anti-tumor efficacy of N-IL15/PDL1, a novel bifunctional immune-oncology agent comprising N-IL15 fused to two single chain anti-PD-L1 variable region domains.

Results
Similar to N-IL15, N-IL15/PDL1 expanded splenic NK and CD8+ T cells. N-IL15/PDL1 promoted a 3.5- and 3.8-fold increase in NK and CD8+ T cell numbers, respectively, as compared to PBS treatment. Both NK and CD8+ T cell populations displayed a more active phenotype, characterized by significant upregulation of numerous activation- and effector function-associated proteins including NKG2D, Ki67, and Granzyme B. Additionally, N-IL15/PDL1 was able to partially block PD-L1 expression in the spleen and tumor. Importantly, N-IL15/PDL1 promoted significant reduction in the growth of MC38-CEA+ colon carcinoma tumors, with 70% of mice undergoing complete tumor rejection. In addition, N-IL15/PDL1 was able to drastically reduce spontaneous metastasis of 4T1 triple-negative breast tumors to the lung by 82% as compared to PBS treatment. In both murine carcinoma models, N-IL15/PDL1 was well-tolerated and displayed comparable or improved anti-tumor efficacy versus previous studies with N-IL15 or PD-L1 monotherapy or N-IL15 plus PD-L1 combination therapy.

Conclusions
Together, these findings offer a preclinical proof of concept for the clinical use of the novel bifunctional immune-oncology agent N-IL15/PDL1 to promote tumor control given either as a monotherapy or in combination with additional immunotherapies or standards of care.

P661

Quantitative cell-based reporter gene bioassays to advance individual or combination cancer immunotherapy

Jamison Grailer, PhD[1], Jun Wang[1], Julia Gilden, PhD[1], Pete Stecha[1], Denise Garvin[1], Michael Beck[1], Jim Hartnett[1], Frank Fan, PhD[1], Mei Cong, PhD[1], Zhi-jie Cheng, PhD[1]

[1]*Promega, Madison, WI, USA*

Background
Targeting immune checkpoint receptors (e.g., PD-1, CTLA-4) has emerged as a promising new approach to enhance anti-tumor immune responses. While cancer immunotherapies directed against PD-1 and CTLA-4 are showing unprecedented efficacy, some patients and tumor types remain refractory to these therapies. This has resulted in a broadening of immunotherapy research and development to include additional inhibitory (e.g., LAG-3, TIGIT) or stimulatory (e.g., 4-1BB, ICOS) co-receptors targeted individually or in combination with other immune co-receptors.A major challenge in the development of biologics is access to quantitative and reproducible functional bioassays. Existing methods rely on primary cells and measurement of complex functional endpoints. These assays are cumbersome, highly variable, and fail to yield the data quality required for drug development. To address this need, we have developed a suite of cell-based reporter gene bioassays for drug candidates of immune checkpoint targets (PD-1 CTLA-4, LAG-3, TIGIT, BLTA), drug candidates of immune co-stimulatory targets (ICOS, 4-1BB, OX40, GITR, CD27, HVEM (LIGHT), CD40), as well as bispecific antibody drugs targeting two immune checkpoint receptors simultaneously (PD-1+LAG-3, PD-1+TIGIT, PD-1+CTLA-4, PD-1+4-1BB).

Methods
These reporter-based bioassays were rationally designed to reflect the mechanism of action (MOA) of drug candidates targeting immune receptors. For each assay, an engineered cell line in an immune cell background was generated which stably expresses an immune target receptor and a luciferase reporter driven by a promoter responding to TCR signaling or activation of a specific immune receptor. These cell lines were further developed into a Thaw-and-Use format that can be used in assays without the need for cell culture.

Results
These cell-based bioassays reflect the MOA of each drug target and demonstrate specificity for research-grade antibodies as well as FDA-approved drugs (e.g., nivolumab, ipilimumab). The assay signals are robust and highly reproducible. The assays have been pre-qualified according to ICH guidelines and demonstrate the performance required for use in antibody screening, QC lot release and stability studies.

Conclusions
We have developed a suite of MOA-based bioassays for immune checkpoint and co-stimulatory T cell receptors. These assays are easy to use, demonstrate high assay specificity, sensitivity and reproducibility, and are suitable for drug development in a quality-controlled environment.

P662

A phase 1a/b study investigating novel anti-PD-L1 antibody (LY3300054): interim safety and clinical activity in patients with advanced cancers.

Antoine Hollebecque, MD[2], Hyun Cheol Chung, MD, PhD[3], Marcus Butler, MD[4], Antoine Italiano, MD[5], Chia-Chi Lin, MD, PhD[6], Jean-Pascal Machiels, MD, PhD[7], Wu-Chou Su, MD[8], Marc Peeters, MD, PhD[9], Leijun Hu, PhD[1], Anna Szpurka, PhD[1], Danni Yu, PhD[1], Anindya Chatterjee, PhD[1], Burkhard Vangerow, MD[10], Shivani Nanda, MS[1], Yumin Zhao, PhD[1], Mythili Koneru, MD[1], Yung-Jue Bang, MD PhD[11]

[1]*Eli Lilly and Company, Indianapolis, IN, USA*
[2]*Institut de Cancerologie Gustave Roussy, Villejuif, France*
[3]*Yonsei University College of Medicine, Seoul, Korea, Republic of*
[4]*UHN/Princess Margaret Cancer Centre, Toronto, ON, Canada*
[5]*Institut Bergonie, Bordeaux, France*
[6]*National Taiwan University Hospital, Taipei, Taiwan, Province of China*
[7]*Cliniques Universitaires Sain-Luc, Brussels, Belgium*
[8]*National Cheng Kung University, Tainan, Taiwan, Province of China*
[9]*Antwerp University, Antwerp, Belgium*
[10]*Lilly Deutschland GmbH, Bad Homburg, Germany*
[11]*Seoul National University Hospital, Seoul, Korea*

Background

LY3300054 is a novel human monoclonal antibody (IgG1, lambda, Fc-null) targeting PD-L1 expressed on tumor cells and tumor-infiltrating immune cells, preventing binding to its T-cell receptors (PD-1 and CD-80). Here we report phase 1b safety and preliminary efficacy results from LY3300054 monotherapy in patients (pts) with MSI-high (MSI-H) solid tumors and metastatic melanoma (M).

Methods

This ongoing, phase 1a/b, multicenter, dose escalation and expansion study enrolled patients with histologically or cytologically confirmed advanced cancer having ECOG PS 0-1, measurable disease (assessable by RECIST v1.1), and no prior treatment with PD-1/PD-L1 agents. The primary objectives for this study were to assess safety and tolerability, secondary objectives included efficacy and pharmacokinetics, and exploratory objectives were biomarker analysis and overall survival. All patients received intravenous infusions of LY3300054 Q2W at 700 mg. Adverse events (AEs) were assessed per NCI CTCAE v4.0; tumor assessment per RECIST v1.1. Recruitment in the M cohort was closed early as eligible melanoma patients were not able to be identified.

Results

As of 8 December 2017, 30 patients (MSI-H: n=22, M: n=8) were treated. There were no deaths due to adverse events. Two patients in MSI-H cohort experienced grade 3 treatment-related AEs (TRAEs): diarrhea (n=1, 4.5%), blood creatinine phosphokinase increased (n=1, 4.5%), and hyponatraemia (n=1, 4.5%). No grade 3 events were reported in M cohort, and no grade 4/5 TRAEs were reported in either cohorts. There were no TRAEs leading to discontinuation of study treatment. Preliminary efficacy data in MSI-H cohort showed ORR of 36% [CR in 1 pt (5%) (ovarian), PR in 7 pts (32%) (small intestine adenocarcinoma [1 pt], endometrial [3 pts], colon [3 pts])], DCR in 64% [SD in 6 pts (27%)]; mPFS was 7.39 months (95% CI 1.7, NR). In the M cohort, DCR was 63% [PR in 1 pt (13%), SD in 4 pts (50%)]. As of data cut-off, 16 pts (53%) remain on treatment. Preliminary biomarker analysis, including but not limited to, PD-L1 and CD8 expression and circulating markers will be presented.

Conclusions

LY3300054 was well-tolerated and demonstrated antitumor activity in patients with MSI-H solid

tumors; combination expansions are ongoing.

Trial Registration
NCT02791334

Ethics Approval
The study included multiple investigator sites, and some of these had approval dates instead of approval numbers. The following are listed showing approving committee followed by approval date or approval # (if available): IntegReview, 15Jun2016; IntegReview, 21June2016; MD Anderson Office of Protocol Approval IRB, 26May2016; Princess Margaret Cancer Centre, University Health Network Research Ethics Board, 16-5824 (initial approval date 01Feb2017); Comite de protection des Personnes (CPP), EudraCT number 2016-000440-33

P663

Successful monitoring of checkpoint inhibitors by flow cytometry

Laila-Aicha Hanafi[1], Valerie Hebert[1], Delphine Labit[1], Vicky Sgouroudis, PhD[1], Jean-Francpos Poulin, PhD, MBA[1], Philippe Pouliot, PhD[1]

[1]*Caprion Bioscienes, Montreal, Canada*

Background
Cancer immunotherapies represent more than half of treatments approved for oncology, as well as those currently in development. Among the key targets of these therapies are immune-checkpoint molecules (i.e. PD-1, LAG3, PD-L1, CTLA-4). Novel immunotherapies targeting these molecules are designed to impact tumor microenvironment immune-suppression. The characterization and monitoring of circulating and tumor infiltrating immune cells by flow cytometry is a critical aspect of drug development. In order to generated robust data to support drug development, flow cytometric methods must be fully optimized. This poster will discuss the critical aspects of assay optimization for flow cytometric methods with an emphasis on screening monoclonal antibody clones for PD-1, PD-L1, and LAG-3. The importance of the data is illustrated in the differences in assay performance when the correct clones are identified.

Methods
Four different anti-PD-1 obtained from different providers were screened on activated PBMC. Additionally, four PD-L1 and five LAG-3 monoclonal antibody clones were screened on activated or rested PBMC spiked in whole blood. All antibodies were all titrated to obtain saturating concentration and optimal titers were compared.

Results
On CD4+ T cells from thawed cryopreserved peripheral blood mononuclear cells (PBMC), the best performance was observed with EH12.2H7 or EH12.1 clones which identified 30-33% of CD4+ T cells as PD-1 positive and up to 55-60% of CD8+ T cells as PD-1 positive. Clone eBioJ105 staining of the same samples on the same day identified 14% PD-1 positive in CD4+ T cell and around 40% PD-1 positive in CD8+ T cell, while clone MIH4 staining revealed low level of PD-1 expression on CD4+ T cells and CD8+ T cells. After ex vivo stimulation with staphylococcus enterotoxin B (SEB), EH12.2H7, EH12.1 and eBioJ105 clones all yielded similar results with 76-85% PD-1 positive on both CD4+ T cells and CD8+ T cells but fewer positive cells were identified with MIH4 clone. Out of the four PD-L1 antibodies tested, only two were able to distinguish a clear PD-L1 population on PBMC rested for 4 days and spiked in whole blood used as positive control for PD-L1 induction. For LAG-3 antibodies, all five were able to reveal the induction of this checkpoint molecule on cells activated by SEB and spiked in whole blood with % of LAG3+ cells in lymphocytes ranging from 13% to 25%.

Conclusions
These results illustrate the importance of thorough reagent evaluation in order to achieve a sensitivity coherent with the information-rich promises of flow cytometry.

P664

Simultaneous checkpoint - checkpoint or checkpoint - costimulatory receptor targeting with bispecific antibodies promotes enhanced human T cell activation

Michael Hedvat, PhD[1], Gregory Moore, PhD[1], Matthew Bernett, PhD[1], Christine Bonzon, PhD[1], Kendra Avery, PhD[1], Rumana Rashid, PhD[1], Alex Nisthal, PhD[1], Umesh Muchhal, PhD[1], John Desjarlais PhD[1]

[1]*Xencor, Inc., Monrovia, CA, USA*

Background
Combination checkpoint blockade promotes productive anti-tumor clinical responses that are often associated with an increase in immune-related adverse events. Because tumor infiltrating lymphocytes (TILs) typically express multiple immune checkpoints and costimulatory receptors [1, 2, 3], we hypothesized that bispecific antibodies will enable targeting of tumor-reactive TILs, leading to safer and more cost-effective combination checkpoint blockade.

Methods
We developed optimized bispecific antibody candidates that simultaneously engage PD1 and CTLA4 (XmAb20717), CTLA4 and LAG3 (XmAb22841), and PD1 and ICOS (XmAb23104). These antibodies contain substitutions in the Fc domain to eliminate effector function. These candidate bispecific antibodies preferentially bind cells co-expressing the targeted receptors using transfected cell lines. The in vitro activity of these antibodies were evaluated by measuring cytokine release from Staphylococcal Enterotoxin B (SEB) stimulated PBMC or mixed lymphocyte reactions (MLR). The in vivo activity of the candidate antibodies were evaluated using a model in which human PBMC are engrafted into NSG mice (huPBMC-NSG). Anti-tumor activity was assessed in huPBMC-NSG mice engrafted with established human cancer cell lines.

Results
XmAb20717 selectively binds cells expressing both PD1 and CTLA4. Treatment with XmAb20717 enhanced engraftment of hCD45+ cells and the release of IFNγ in NSG mice to levels equivalent to a combination of anti-CTLA4 and anti-PD1 antibodies. XmAb20717 enhanced allogeneic anti-tumor activity of huPBMCs against KG1a cancer cells in vivo. XmAb22841 selectively binds cells expressing both CTLA4 and LAG3. XmAb22841 combined productively with an anti-PD1 antibody enhancing the engraftment of hCD45+ cells and the release of IFNγ in NSG mice via triple-checkpoint blockade. XmAb22841 combined productively with an anti-PD1 antibody, enhancing allogeneic anti-tumor activity of huPBMCs against established MCF7 solid tumors.A bispecific antibody pairing PD1 blockade with engagement of the T cell co-stimulatory receptor ICOS resulted in superior IL-2 release from SEB-stimulated PBMC, warranting preclinical development of XmAb23104. XmAb23104 promoted significant IFNγ release in vitro from a MLR in contrast to a combination of anti-PD1 and anti-ICOS antibodies that lacked activity, illustrating the unique biological properties of XmAb23104. XmAb23104 enhanced engraftment of hCD45+ cells and IFNγ release in NSG mice to levels higher than anti-PD1 antibody alone. XmAb23104 enhanced allogeneic anti-tumor activity of huPBMCs against established MCF-7 tumors in vivo.

Conclusions
Compelling ex vivo and in vivo data support the development of XmAb20717, XmAb23104 and

XmAb22841 for the treatment of human malignancies. XmAb20717 is currently in a phase 1 study, and IND filings for XmAb23104 and XmAb22841 are anticipated in 2018.

References

1. Fourcade J, Sun Z, Pagliano O, et al. CD8(+) T cells specific for tumor antigens can be rendered dysfunctional by the tumor microenvironment through upregulation of the inhibitory receptors BTLA and PD-1. Cancer Res. 2012 ;72(4):887-96
2. Gross A, Robbins PF, Yao X, et al. PD-1 identifies the patient-specific CD8+ tumor-reactive repertoire infiltrating human tumors. J Clin Invest. 2014;124(5):2246-2259.
3. Matsuzaki J, Gnjatic S, Mhawech-Fauceglia P. Tumor-infiltrating NY-ESO-1–specific CD8+ T cells are negatively regulated by LAG-3 and PD-1 in human ovarian cancer. PNAS. 2010;107(17):7875-7880

P665

Anti-tumor synergy evaluation of an AZD4635/ anti-PD-L1 combination therapy using a quantitative systems model

Veronika Voronova, MSc[2], Lulu Chu, PhD[1], Yuri Kosinsky, PhD[2], Alexandra Borodovsky, PhD[1], Richard Woessner, PhD[1], Kris Sachsenmeier, PhD[1], Ganesh Mugundu, PhD[1], Melinda Merchant, MD, PhD[1], Wenlin Shao, PhD[1], Kirill Peskov, PhD[2], Gabriel Helmlinger, PhD[1]

[1]*AstraZeneca, Waltham, MA, USA*
[2]*M&S-Decisions LLC, Moscow, Russian Federation*

Background

Adenosine accumulation in the tumor microenvironment (TME) has been shown to limit anti-tumor immune responses [1]. We developed a model which provides a mechanistic understanding of interactions between the A2AR inhibitor AZD4635 and an anti-PD-L1 antibody (Ab), as observed in four studies in CT26, MC38 and MCA205 syngeneic mice. The model also helped identify factors underlying inter-individual and inter-study variabilities (IIV and ISV), through non-linear mixed effects (NLME) modeling.

Methods

A system of differential equations was used to describe antigen presenting cell (APC)-dependent T cell influx into the tumor, T cell proliferation and activation into cytotoxic lymphocytes (CTL), tumor cell death, as well as corresponding PD-L1 expression and related immune response modulation. APC and CTL activation are both regulated by adenosine-dependent A2AR occupancy. Mechanisms of AZD4635 and anti PD-L1 Ab were characterized in the model: while AZD4635 prevents adenosine binding to A2AR, diminishing its immunosuppressive effects, anti-PD-L1 Ab blocks the negative PD-L1 effects on CTL (Fig 1A). Model parameters were taken from literature and estimated using NLME modeling of individual longitudinal tumor size data pooled from the studies. The following treatment regimens were used for calibration: (1) vehicle; (2) AZD4635 10-50 mg/kg BID; (3) anti-PD-L1 Ab 10 mg/kg BIW; (4) combination of (2) and (3). Treatments were initiated when tumors reached a volume of 50-90mm2.

Results

The model adequately described individual and population tumor size patterns, for all treatment regimens and studies. IIV and ISV were explained by differences in T cell infiltration and adenosine effect on antigen presentation efficiency. Model simulations showed that AZD4635 increased T cell influx and anti-tumor cytotoxic ability in a dose-dependent manner, by stimulation of antigen presentation efficacy and a direct effect on T cell activation in the TME. However, monotherapy efficacy with AZD4635 was limited by PD-L1 negative feedback, providing a mechanistic explanation of synergistic effect observed in combination

treatment. The model also revealed that animals with stabilized tumor size dynamics ("non-progressors") are characterized by more efficient antigen presentation, thereby maintaining high CTL infiltration during treatment (Fig 1B).

Conclusions

A quantitative model was developed to provide mechanistic insights into potentially synergistic effects between AZD4635 and anti-PD-L1. Model-based simulations showed that inhibition of intra-tumor adenosine effects can lead to an increase in antigen presentation efficiency and CTL infiltration – important considerations for further dose and sequencing studies of combination therapies.

References

1. Borodovsky A, et al. Inhibition of A2AR by AZD4635 induces anti-tumor immunity alone and in combination with anti-PD-L1 in preclinical models. AACR annual meeting 2018.

Figure 1.

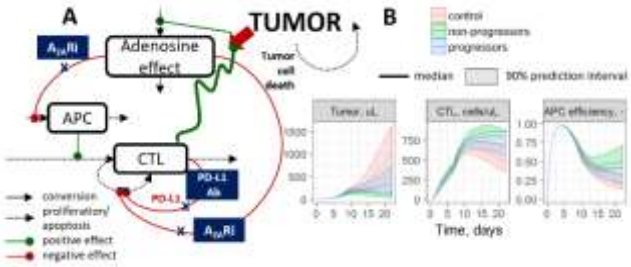

P666

Antitumor efficacy of anti-TIGIT antagonist antibody EOS884448 is mediated by a dual mechanism of action involving restoration of T cell effector functions and preferential depletion of Tregs.

Chaterine Hoofd[1], Julia Cuende, PhD[1], Virginie Rabolli, PhD[1], Julie Preillon, MSc[1], Noemie Wald, PhD[1], Lucile Garnero[1], Florence Lambolez, PhD[1], Marjorie Mercier[1], Shruthi Prasad, PhD[1], Florence Nyawame[1], Sofie Denies, PhD[1], Margreet Brouwer, MSc[1], Erica Houthuys, PhD[1], Veronique Bodo, PhD[1], Xavier Leroy, PhD[1], Scott Chappel[1], Michel Detheux, PhD[1], Gregory Driessens, PhD[1], Chaterine Hoofd[1], Olivier de Henau[1]

[1]*iTeos Therapeutics, Gosselies, Belgium*

Background

T cell Immunoreceptor with Ig and ITIM domains (TIGIT) is a co-inhibitory receptor expressed by lymphocytes, preferentially CD8+ T cells, NK, as well as by regulatory T cells (Tregs). TIGIT ligands belong to the PVR/nectin family, among which PVR (CD155) shows the highest affinity and is commonly expressed on myeloid and upregulated on tumor cells. TIGIT costimulatory counterreceptor CD226 (DNAM-1) competes with TIGIT for PVR binding but with a lower affinity. Co-expression of TIGIT and CD226 receptors on T and NK effector cells suggests a role of these molecules in the fine control of cell activation. TIGIT expression is upregulated in cancer patients, especially on Tregs within the tumor microenvironment that are almost all positive for TIGIT and are described to be highly suppressive 1 [1]. Frequent co-expression with exhaustion markers such as PD-1 is an extra argument to develop anti-TIGIT blocking antibodies as a therapeutic approach to reverse T or NK cell dysfunction associated with tumor immune escape.

Methods
Antagonist anti-TIGIT antibodies were selected using a synthetic yeast display library of fully human antibodies and characterized for their binding and antitumor properties.

Results
EOS884448 anti-TIGIT mAb displays a strong affinity for recombinant and native human TIGIT. It competes with PVR for binding to TIGIT and the blockade of the TIGIT/PVR axis restores cytokine production in human primary T cells. To further explore its potency, EOS884448 was produced in a mammalian system with different human isotypes that exhibit different Fc effector functions. When PBMC from healthy volunteers were incubated with its hIgG1 format, EOS884448 demonstrated preferential depletion of Treg cells in vitro. In vivo, two different isotypes of a surrogate mouse anti-TIGIT mAb were used to evaluate the anti-tumor efficacy in the colon carcinoma CT26 syngeneic murine model. Interestingly, only the ADCC enabling mIgG2a isotype was able to induce strong antitumor efficacy in monotherapy and in combination with an anti-PD1, resulting in a complete regression of pre-established tumors in the majority of animals. Antitumor efficacy was associated with an increased activity of conventional T cells but also with Treg depletion within the tumor microenvironment, reaffirming the in vitro data generated on human PBMCs.

Conclusions
In summary, in vitro and in vivo data demonstrate the potential for anti-TIGIT mAb EOS884448 to promote antitumor immunity by preferential depletion of Treg cells and activation of conventional T cells, which supports the rationale for its clinical evaluation.

References
1. Joller et al., Treg cells expressing the coinhibitory molecule TIGIT selectively inhibit proinflammatory Th1 and Th17 cell responses. Immunity. 2014 Apr 17;40(4):569-81.

P667

EOS100850, an insurmountable and non-brain penetrant A2A receptor antagonist, inhibits adenosine-mediated T cell suppression, demonstrates anti-tumor activity and shows best-in class characteristics.

Erica Houthuys, PhD[1*], Stefano Crosignani, PhD[1], Reece Marillier, PhD[1], Theo Deregnaucourt, MSc[1], Margreet Brouwer, MSc[1], Romain Pirson, MSc[1], Joao Marchante, MSc[1], Annelise Hermant, MSc[1], Florence Nyawouame, MSc[1], Julie Preillon, MSc[1], Kim Frederix, PhD[1], Anne-Catherine Michaux, MSc[1], Jakub Swiercz, PhD[1], Noemie Wald, PhD[1], Chiara Martinoli, PhD[1], Veronique Bodo, PhD[1], Michel Detheux, PhD[1], Xavier Leroy, PhD[1]

[1]*iTeos Therapeutics, Gosselies, Belgium*

Background
High levels of extracellular adenosine in the tumor microenvironment promote tumor immune evasion. We and others have shown that adenosine, predominantly through the A2A receptor (A2AR), suppresses the Th1 cytokine production of T cells and monocytes and cytolytic activity of T cells.

Methods
Human CD3 T cells were isolated from healthy donor PBMC using Dynabeads. T cells in whole blood or isolated T cells were activated using aCD3/aCD28 stimulation. pCREB assays were performed using freshly collected mouse whole blood.

Results
We demonstrated that A2AR antagonists initially designed for Parkinson's disease but repurposed for immuno-oncology dramatically lost potency in a high adenosine environment. We therefore developed

EOS100850, a novel, non-brain penetrant and highly selective inhibitor of A2AR with sub-nanomolar Ki. Using experimental conditions that mimic tumor environment, we have shown that EOS100850 potently inhibited A2AR signalling in human T lymphocytes independently of adenosine concentrations, and rescued cytokine production, even in the presence of high concentrations of A2AR agonists. iTeos A2AR antagonist potently rescued Th1 cytokine production in human whole blood treated by A2AR agonists, and increased CD8+ T cell cytotoxicity in a co-culture assay of effector CD8+ T cells and target cancer cells. An in vivo pharmacodynamic assay based on phosphorylation of CREB (pCREB) in mouse peripheral CD8+ and CD4+ T cells was developed and validated as a readout for A2AR activation. EOS100850, 30 minutes after oral gavage at doses ranging from 0,03 to 1mg/kg demonstrated 80 to 100% inhibition of pCREB induced by the ex vivo addition of A2AR agonist. Remarkably, 12 hours after gavage at 1 and 3mg/kg, when the EOS100850 antagonist was no longer detectable in the plasma, more than 50% of inhibition of pCREB was still observed. These results demonstrate that EOS100850 has a PD activity that extends well beyond its PK based on a long residence time. iTeos's A2AR antagonist, uniquely designed to address the challenge of counteracting elevated adenosine concentrations in tumors, was tested for the first time in a mouse A20 lymphoma model. iTeos's A2AR antagonist in combination with anti-PD-L1 demonstrated significant tumor growth suppression compared with anti-PD-L1 alone, with a decrease in tumor volume compared to anti-PD-L1 alone.

Conclusions

EOS100850 represents a novel, potent, insurmountable and best-in-class A2AR antagonist, specifically optimized for immuno-oncology indications, that deserves studies in Human.

P668

Selection of optimized drug candidates, dosing regimen, pharmacodynamic endpoints, tumor types, and biomarkers for translating inhibition of the adenosine pathway into effective anti-tumor activity

Juan Jaen, PhD[1], Jay Powers, PhD[1], Ulrike Schindler, PhD[1], Steve Young, PhD[1], Matthew Walters, PhD[1], Joanne Tan, PhD[1], Lisa Seitz, MSc[1]

[1]*Arcus Biosciences, Inc., Hayward, CA, USA*

Background

High intra-tumoral adenosine concentrations are prevalent and highly suppressive of the ability to mount an effective anti-tumor immune response. This presents multiple therapeutic opportunities, either by preventing extracellular adenosine generation from nucleotide precursors or by blocking adenosine receptor activation. Translating these therapeutic hypotheses into clinical benefit requires careful selection of tumor types and individual patients most likely to respond to a particular mechanism of action. Equally important is identification of drug candidates with optimal activity profiles and dosing regimens that allow for maximal interference with the selected targets.

Methods

The ability of small-molecule adenosine receptor antagonists AB928 – dual A2aR/A2bR – and AB745 (selective A2aR) and CD73 inhibitors (AB680) to inhibit their respective targets was evaluated using recombinant biochemical/cell-based assays, human blood T cells, and immune function assays (e.g., CD3/CD8; MLR). Potency under physiological conditions was assessed using blood or serum-based assays. Blood-based pharmacodynamic assays were used to bridge plasma levels effective in mouse tumor models with those expected to achieve maximal biological effects in humans. Gene

expression data from TCGA were used to select tumor types most likely to respond to adenosine receptor or CD73 inhibition. Immunohistochemistry was used to confirm this selection. Various tumor and blood-based biomarkers were developed to assess levels of adenosine-producing enzymes in individual patients receiving one of these drug candidates.

Results

AB928: hA2aR KB: 1.5 nM (buffer) & hA2bR KB: 2.0 nM (buffer); hA2aR KD: 1.9 nM (20% serum); reversal of adenosine-mediated inhibition of polyclonal T-cell activation, IC50: 1-3 nM; inhibition of pCREB activation (human whole blood), IC50: 88 nM; healthy volunteer receptor coverage (blood CD8 T cells), 90% inhibition at trough, 150 mg QD. Tumor types selected: NSCLC, CRC, GE, RCC, TNBC, Ovarian.AB680: hCD73 IC50 (CD8 T cells): 0.008 nM; Ki (soluble CD73): 0.005 nM; reversal of AMP-mediated inhibition of T-cell activation in MLR, IC50 ~ 3 nM; inhibition of soluble CD73 (human serum), IC50 ~16 nM; projected human half-life: ≥ 4 days; projected clinical dosing to maintain >90% CD73 inhibition: ≤ 15 mg q2w. Tumor types selected: CRC, NSCLC, GE, SCCHN.

Conclusions

The totality of the data for AB928 and AB680 (both of which are in clinical development) indicate that 100-150 mg once-daily oral doses of AB928 and 10-20 mg intravenous AB680 every ~2 weeks should be explored in tumor types that either rely on multiple pathways for adenosine generation (AB928) or those that primarily utilize CD73 for that purpose (AB680).

P669

First-in-human Phase 1 study of INCMGA00012 in patients with advanced solid tumors: Interim results of the cohort expansion phase

Janice Mehnert, MD[1], Anthony Joshua, MD[2], Nehal Lakhani, MD, PhD[3], Udai Banerji[4], Drew Rasco[5], Iwona Lugowska[6], Monika Tomaszewska-Kiecana[7], Elena Garralda[8], Deanna Kornacki, PhD[9], Bradley Sumrow[10], Mark Cornfeld, MD, MPH[9], Chuan Tian[9], John Powderly, MD, CPI[11]

[1]*Rutgers Cancer Institute of New Jersey, New Brunswick, NJ, USA*
[2]*Kinghorn Cancer Centre, St Vincents Hospital, Syndey, Australia*
[3]*START Midwest – South Texas Accelerated, Grand Rapids, MI, USA*
[4]*The Royal Marsden, Sutton, UK*
[5]*START – South Texas Accelerated Research, San Antonio, TX, USA*
[6]*Maria Sklodowska-Curie Institute – Oncol, Warsaw, Poland*
[7]*BioVirtus Research Site, Otwock, Poland*
[8]*Vall D'Hebron Institute of Oncology (VHIO), Barcelona, Spain*
[9]*Incyte Corporation, Wilmington, DE, USA*
[10]*MacroGenics, Inc, Rockville, MD, USA*
[11]*Carolina BioOncology Institute, Huntersville, NC, USA*

Background

INCMGA00012 (or MGA012) is a humanized, hinge-stabilized IgG4 monoclonal antibody that binds to PD-1, inhibits the interaction of PD-1 with PD-L1/PD-L2, and disrupts the negative signaling axis to restore T-cell function. At doses up to 10 mg/kg twice weekly (Q2W), INCMGA00012 has an acceptable tolerability profile with no DLTs or MTD. A dose of 3 mg/kg Q2W was selected as the recommended phase 2 dose (RP2D) for the tumor-specific cohorts.

Methods
The expansion contained 4 tumor-specific cohorts (endometrial, cervical, soft tissue sarcoma, and non-small cell lung [NSCLC]) and 2 tumor-agnostic flat dose cohorts (500 and 750 mg Q4W). All patients were ≥18 years old; and had disease progression during or following 1–5 prior treatments, measurable disease per RECIST v1.1, and no prior immune checkpoint inhibitors. The primary endpoint was safety. Adverse events were graded via CTCAE v4.03. Response was evaluated by RECIST v1.1 with treatment past progression allowed at the discretion of the investigator.

Results
As of July 10, 2018, 127 patients have been treated with INCMGA00012 in the tumor-specific cohorts (29 endometrial, 33 cervical, 32 sarcoma, 33 NSCLC), and 15 each in the tumor-agnostic flat-dose cohorts. Median (range) age was 59 (18–86) years. The majority of patients were female (66.9%), white (85.4%), and had ECOG performance status of 1 (67.5%). Of the 127 patients treated at the RP2D, 59 (46.5%) had treatment-related adverse events (TRAEs), with rash occurring most frequently (n=7 [5.5%]). Eleven patients (8.7%) had immune-related AEs; the only immune-related AE occurring in >1 patient was colitis (n=3). Five patients discontinued treatment due to TRAEs (colitis [n=3], transaminases increased, and iritis [n=1 each]). There were no treatment-related deaths. RECIST responses (confirmed and unconfirmed) were observed in all 4 tumor types (6/25 evaluable patients with cervical cancer, 6/26 with NSCLC, 3/29 with endometrial cancer, and 1/22 with sarcoma). Pharmacokinetics, receptor occupancy, and safety for the 500 mg Q4W flat dose compared favorably to weight-based dosing at 3 mg/kg Q2W.

Conclusions
In the cohort expansion portion of this Phase 1 study, INCMGA00012 has been generally well tolerated with evidence of antitumor activity, particularly in the refractory cervical cancer and NSCLC cohorts. Pharmacologic properties with flat dosing are favorable for further development. This study will be further expanded to evaluate the 500-mg Q4W dose in a larger cohort of MSI-h or dMMR endometrial cancer patients as well as a Q3W flat dosing regimen in a tumor-agnostic population.

Trial Registration
NCT03059823

Ethics Approval
The study was approved by institutional review boards or independent ethics committees of participating institutions.

P671

Discovery of a novel anti-LAG3 antagonist antibody

Wenqing Jiang, PhD[1], Lei Fang[1], Zhengyi Wang[1], Taylor Guo[1], Jingwu Zang[1]

[1]*I-Mab Biopharma, Shanghai, China*

Background
LAG3 (CD223) is an inhibitory checkpoint expressed on activated T cells (CD4 and CD8), NK cells and Treg cells. Persistent T-cell activation in a chronic inflammatory environment, such as in a tumor, results in sustained LAG3 expression, contributing to a state of exhaustion manifest in impaired proliferation and cytokine production. In addition, LAG3 is also found to be expressed on Treg cells and play a role in Treg mediated immune suppression. Co-expression of LAG3 and PD-1 on tumor-infiltrating T cells is found in many human cancers including ovarian cancer, melanoma, hepatocellular carcinoma (HCC) and colon cancer. Dual blockade of LAG3 and PD-1 pathway demonstrated significant therapeutic synergy for the treatment of melanoma patients from the latest clinical studies. Here we report the discovery of a novel LAG3 antibody, which showed a

strong potency in the T cell activation and tumor growth inhibition in combination with anti-PD-L1 antibodies, indicating a potential therapeutic value of this antibody as a combination partner with PD-1 or PD-L1 agent.

Methods

A mouse lead clone, termed mu147H was generated by traditional hybridoma library using human LAG3-extracellular domain as antigen. After humanization and affinity maturation, the candidate antibody (TJA3) was selected based on a series of in vitro assays, including affinity measurement, receptor blocking and T cell activation assay. In vivo efficacy of TJA3 was evaluated in combination with anti-PD-L1 antibody (Tecentriq) using a syngeneic tumor model.

Results

TJA3 is an antagonist antibody against LAG3 with sub-nanomolar affinity. Upon binding, it blocks the interaction of LAG3 to its receptor MHCII, leading to the increased production of IL-2 in Jurkat cells overexpressing LAG3 and in activated human primary T cells. Under the same T cell activation system, TJA3 showed strong synergistic effects on the T cell activation in combo with anti-PDL1 antibody. Consistently, when combined with PD-L1 antibody, TJA3 can significantly inhibit tumor growth in a syngeneic MC38 tumor model using LAG3-humanized mice. Developability assessment of the TJA3 sequence indicates that it is a reasonably developable molecule to be taken forward. CMC-wise, a cell line with decent titer have been developed.

Conclusions

We have successfully discovered a LAG3-blocking therapeutic antibody with high binding affinity and strong potency in the T cell re-invigoration and anti-tumor efficacy. The observed synergy of our LAG3 antibody with anti-PD-L1 agent indicated a great potential of this asset in the treatment of PD-1/PD-L1 refractory or resistant cancer patients.

P672

Discovery and development of a humanized monoclonal antibody targeting the CD73 immune checkpoint for cancer immunotherapy

H. Toni Jun, PhD[1], Fen Pei, PhD[1], Hui Zou, PhD[1], Ming Wang, PhD[1]

[1]Phanes Therapeutics, Inc., San Diego, CA, USA

Background

Extracellular adenosine in the tumor microenvironment can create an immunosuppressive milieu that can act on multiple immune cell types, including effector T cells [1]. CD73 plays a key role in the generation of extracellular adenosine. It is highly overexpressed on multiple tumor types and is expressed on endothelial cells as well as lymphoid and myeloid subsets [reviewed in 2]. CD73 is normally tethered to the cell surface via a GPI linkage but can also be shed from the surface of cells [3] which may result in the presence of a soluble CD73 enzyme in the tumor microenvironment. Combined, soluble and cell expressed CD73 may generate high adenosine levels in the tumor microenvironment. Therefore, inhibition of CD73 should reduce adenosine levels in the tumor environment, thereby relieving immune suppression and preventing tumor evasion from the host immune system. This inhibition, either alone or in combination with immune checkpoint inhibitors such as anti-PD-1 or anti-CTLA4, may consequently be an attractive therapeutic strategy.

Methods

Mice were immunized with soluble CD73 to generate a panel of monoclonal antibodies. Antibodies were selected for ability to bind cellular CD73 and inhibit the enzymatic activity of CD73. Select candidates showing desirable activity profiles were humanized prior to further characterization.

Results

We have discovered PT199, a humanized antibody that can potently inhibit CD73 catalytic activity in both soluble and cell based enzymatic assays. When compared to other anti-CD73 benchmark molecules, we demonstrate equivalent or improved activity, and we do not observe a "hook" effect common to other anti-CD73 antibodies. This is likely due to the distinct binding epitope of our antibody. Interestingly, PT199 binding to cellular CD73 is affected by the addition of AMPCP, suggesting that the CD73 catalytic site is important to the PT199/CD73 interaction. We are currently characterizing the antibody in a PBMC T-cell suppression assay and the mixed lymphocyte reaction (MLR) assay to confirm activity in cell based functional assays as well as investigating the in vivo activity of PT199 in a mouse A375 xenograft model. These data will be presented.

Conclusions

We have generated a potent inhibitory antibody to CD73 that demonstrates activity against cell surface and soluble forms of the enzyme. Based on its expression on tumor and stromal cells as well as its role in immunosuppression, this antibody may represent an important tool as an immunooncology therapy.

References

1. Ohta A, Gorelik E, Prasad SJ, Ronchese F, Lukashev D, Wong MK, Huang X, Caldwell S, Liu K, Smith P, et al. 2006. A2A adenosine receptor protects tumors from antitumor T cells. Proc. Natl. Acad. Sci. USA 103: 13132–13137.
2. Ghiringhelli F, Bruchard M, Chalmin F, Reb´e C. Production of adenosine by ectonucleotidases: a key factor in tumor immunoescape. Journal of Biomedicine and Biotechnology. 2012; 473712-47321.
3. Airas L, Niemelä J, Salmi M, Puurunen T, Smith DJ, Jalkanen S. Differential regulation and function of CD73, a glycosyl-phosphatidylinositol–linked 70-kD adhesion molecule, on lymphocytes and endothelial cells. JCB 1997; 136 (2): 421–431.

P673

Preliminary results from an ongoing phase 1 study of AB122, an anti-programmed cell death-1 (PD-1) monoclonal antibody, in patients with advanced solid tumors

Paul de Souza, MBBS, MPH, PHD, FRACP[1], Chee Khoon Lee[2], Katrin Sjoquist[2], Shu Pan[2], Amanda Idan[2], Aimee Rieger, BS[3], Wade Berry, BA[3], Lixia Jin[3], Lisa Seitz, MSc[3], Devika Ashok, PhD[3], Matthew Walters, PhD[3], Dana Piovesan, MSc[3], Joanne Tan, PhD[3], Susan Lee, PhD[3], Adam Park, BS[3], Daniel DiRenzo, PhD[3], Joyson Karakunnel, MD, MSc[3]

[1]University of Western Sydney, Sydney, Australia
[2]St George Public Hospital, Kogarah, Australia
[3]Arcus Biosciences, Inc., Hayward, CA, USA

Background

AB122, a fully human monoclonal antibody targeting PD-1, has shown preclinically to be similar to currently approved anti-PD-1/programmed cell death ligand 1 agents, but it may offer some unique characteristics. Based on preclinical models, the binding affinity of AB122 for PD-1 appears to be greater than that of nivolumab, which may be due to a difference in epitopes for AB122 versus nivolumab, allowing for tighter target engagement.

Methods

We present preliminary data from a phase 1, open-label, dose-escalation (3+3 design) study evaluating AB122 monotherapy in select advanced solid tumors. AB122 is administered intravenously every 2 weeks (Q2W) at escalating doses (80, 240, 720 mg). Intermediate Q2W doses and other schedules are also being evaluated. Treatment continues until progressive disease, unacceptable toxicity, withdrawal of consent, or other reasons for study drug discontinuation occurs. The primary endpoint is

safety/tolerability, and secondary endpoints are immunogenicity, pharmacokinetics, pharmacodynamics, and clinical activity.

Results

As of 15Jun2018, 15 patients have been treated: 3 at 80 mg, 6 at 240 mg, and 1 at 360 mg Q2W, 2 at 360 mg every 3 weeks, and 3 at 480 mg every 4 weeks. The number of doses received ranged from 1 to 14. The most common adverse events (AEs; regardless of grade or relationship to study drug) were fatigue (40%), diarrhea (27%), nausea (20%), and constipation, insomnia, anemia, and pain (13% each). Five patients (2 each in 80 and 240 mg Q2W cohorts and 1 in 360 mg Q2W cohort) had treatment-related AEs (fatigue in 2 patients, vision blurred and tremor in 1 patient, rash in 1 patient, and rash macular in 1 patient); all were Grade 1. There were no treatment-related grade ≥3 AEs, dose limiting toxicities, serious AEs, or discontinuations due to AEs. Data from patients in the 80 and 240 mg Q2W cohorts showed that AB122 serum concentrations ≥1.5 µg/mL (equivalent to 10 nM) are associated with full receptor occupancy. In 9 of 15 efficacy-evaluable patients, the best overall response was stable disease in 4 patients (44%) and progressive disease in 5 patients (56%). For those with stable disease, tumor sites were colorectal (n=2), ovarian (n=1), and head and neck (n=1), and time on study ranged from 1.9 to 5.8 months. The patients with head and neck and ovarian cancer each experienced a reduction in tumor lesion size.

Conclusions

AB122 demonstrated a manageable safety profile and evidence of clinical activity in several solid tumor types.

Ethics Approval

The study was approved by Bellberry Human Research Ethics committee (HREC), 129 Glen Osmond Road Eastwood South Australia 5063; Institutional Review Board approval number 2017-10-748.

P674

Defining Tim-3 signaling and localization during T cell activation

Shunsuke Kataoka, PhD[1], Lawrence Kane, PhD[1]

[1]*University of Pittsburgh, Pittsburgh, PA, USA*

Background

The transmembrane protein Tim-3 is thought to have inhibitory effects on immune responses and its expression is increased on exhausted T cells during chronic infection or in tumors. Despite containing tyrosine residues, the C-terminal cytoplasmic domain of Tim-3 does not have any known inhibitory motifs. On the other hand, Tim-3 has been shown to have stimulatory effects under acute stimulation conditions. We previously found that the Tim-3 has an ability to enhance TCR signaling, as read-out by phosphorylation of S6 (pS6) and other markers of T cell activation. Other studies suggest that extension of acute T cell activation may contribute to T cell exhaustion. However, it is still unclear how Tim-3 expression enhances TCR signaling and where Tim-3 is localized relative to the immune synapse.

Methods

Jurkat T cells transfected with WT or truncated Tim-3, or naïve T cells from CD8-specific Tim-3-induced mice, were pretreated with mitogen-activated protein kinase kinase (MEK) or/and protein kinase B (AKT) inhibitors before being stimulated through the TCR; pS6 was then assessed by flow cytometry. Jurkat cells were also conjugated with superantigen-pulsed antigen presenting cells (APCs) to track the localization of Tim-3 during immunological synapse (IS) formation. These samples were analyzed by ImageStream.

Results

As we reported previously, Tim-3 expression enhanced TCR-induced pS6 in both Jurkat and primary cells, and either MEK or AKT inhibitors significantly inhibited pS6 induction. Furthermore, combined treatment with both inhibitors reduced pS6 more than either inhibitor alone and blocked the enhancement of pS6 by Tim-3 expression. We also found that Tim-3 was recruited to the IS by conjugation with superantigen-pulsed APCs from early time points, although the extent of polarization of Tim-3 into the synapse was not as robust as that of CD3. Using various deletion mutants of Tim-3, we observed that neither the extracellular IgV domain nor the intracellular cytoplasmic tail of Tim-3 was required for recruitment to the IS.

Conclusions

These results suggest that the MEK/ERK MAPK and PI3K-AKT pathways both play key roles in the enhancement of TCR signaling by Tim-3. In addition, Tim-3 may interact with TCR signaling components by its recruitment proximal to the TCRCD3 complex, although our results suggest that such recruitment is not sufficient to co-stimulate T cells. Nonetheless, this localization may help promote more sustained T cell activation. These findings could aid further the study of Tim-3 effects on immune regulation.

P675

Mechanisms of primary resistance to immune checkpoint blockade

Duane Moogk, PhD[2], Michelle Krogsgaard, PhD[2], Kaitao Li, PhD[3], Zhou Yuan, PhD[3], Shi Zhong, PhD[2], Zhiya Yu[4], Ivan Liadi[5], William Rittase, PhD[3], Victoria Fang, BS[2], Janna Dougherty, BS[2], Arianne Perez-Garcia, PhD[2], Iman Osman[2], Jeffrey Weber, MD, PhD[2], Navin Varadarajan, PhD[5], Nicholas Restifo, MD[4], Alan Frey, PhD[2], Cheng Zhu, PhD[3]

[1]New York University School of Medicine, New York, NY, USA
[2]NYU School of Medicne, New York, NY, USA
[3]Georgia Institute of Technology, Atlanta, GA, USA
[4]NCI, NIH, Bethesda, MD
[5]University of Houston, Houston, TX

Background

Although much clinical progress has been made in harnessing the immune system to recognize and target cancer, there is still a significant lack of an understanding of how tumors evade immune recognition and the mechanisms that drive tumor resistance to both T cell and checkpoint blockade immunotherapy. Our objective is to understand how tumor-mediated signaling through inhibitory receptors, including PD-1, combine to affect the process of T cell recognition of tumor antigen and activation signaling. This with the goal of understanding the basis of resistance to PD-1 blockade and potentially identify new molecular targets to enable T cells to overcome dysfunction mediated by multiple inhibitory receptors.

Methods

Methods and results are combined.

Results

We show that Lck activity affects T cell sensitivity and influences the probability of inducing effector function[1]. Further, we showed that Shp-1 directly influences Lck activity under non-activating conditions, as inhibition of Shp-1 leads to increased Lck activity. Importantly, inhibition of Shp-1/2, a major mediator of PD-1 signaling, targeting CD28 and Lck[2], prior to activation leads to increased T cell cytotoxic effector function. Our proteomics-based analysis of patient T cells identified additional mediators of PD-1 signaling and signaling components and pathways associated with blockade resistance. It has generally been thought that TCR and CD8 binding depend mainly on their ectodomain interactions with pMHC. We have shown, however, that Lck-CD8 binding[3] and Lck activity[4] are

required for upregulated CD8 binding to pre-bound TCR-pMHC complex. Therefore, the cytoplasmic associations of Lck with CD8 and Zap-70, as well as CD3 with Zap-70 may influence formation and stability of the TCR-pMHC-CD8 complex. To determine the mechanistic basis of PD-1 inhibition of TCR-pMHC-CD8 binding we utilized 2D affinity combined with Biomembrane Force Probe (BFP) measurements[5, 6] and showed that PD-1 directly suppresses TCR-pMHC-CD8 binding. Our data also revealed that TCR-pMHC binding was independent of PD-1-PD-L1, but TCR-pMHC-CD8 binding was suppressed by PD-1-PD-L1 binding demonstrating negative cooperativity, as fewer bonds formed than the sum of bonds formed by each interaction alone.

Conclusions

Together, our results show that the activities of TCR-proximal signaling components affect T cell mechanosensing and sensitivity at the earliest stages of antigen recognition and are influenced by PD-1. Targeting these interactions may enhance tumor-specific T cell sensitivity and provide an understanding the basis of resistance to PD-1 blockade to potentially allow identification of new molecular targets to enable T cells to overcome dysfunction mediated by multiple inhibitory receptor.

Acknowledgements

This work was supported by research grants from National Institute of Health U01 CA214354 (to M.K. and C.Z.) and Merck OTSP grant 58166 (to M.K.) and 57570 (to M.K.).

References

1. D. Moogk et al. Constitutive Lck activity drives sensitivity differences between CD8+ memory T cell subsets. J. Immunol.. July 2016; 15; 197(2):644-54.
2. Hui E, et al. T cell costimulatory receptor CD28 is a primary target for PD-1-mediated inhibition. Science. Mar 31 2017; 355(6332):1428-1433.
3. Casas J, et al. Ligand-engaged TCR is triggered by Lck not associated with CD8 coreceptor. Nat Commun. 2014; 5:5624.
4. Jiang N, et al. Two-stage cooperative T cell receptor-peptide major histocompatibility complex-CD8 trimolecular interactions amplify antigen discrimination. Immunity. 2011; 34(1):13-23.
5. Evans E, Ritchie K, Merkel R. Sensitive force technique to probe molecular adhesion and structural linkages at biological interfaces. Biophys J.Jun 1995; 68(6):2580-7.
6. Huang J, et al. The kinetics of two-dimensional TCR and pMHC interactions determine T-cell responsiveness (in eng). Nature. Apr 8 2010; 464(7290):932-6.

Ethics Approval

The study was approved NYU School of Medicine Institutions Ethics Board, approval numbers 170302-02 (IACUC) and i10362 (IRB).

P676

Targeting the sialoglycan/Siglec pathway in combination with checkpoint inhibitors for cancer immunotherapy

Michal Stanczak[1], Natalia Rodrigues Mantuano[1], Adam Petrone[2], Melissa Anne Gray[3], Carolyn Bertozzi[3], Li Peng, PhD[2], Alfred Zippelius, MD[4], Heinz Läubli, MD PhD[4]

[1]University of Basel, Switzerland, Switzerland
[2]Palleon Pharmaceuticals, Waltham, MA, USA
[3]Stanford University, Stanford, USA
[4]University Hospital Basel, Basel, Switzerland

Background

Immunotherapy with immune checkpoint inhibitors (ICI) targeting PD-(L)1 and CTLA-4 has been successfully introduced into routine oncological practice. Despite the success of ICI, most patients derive no benefit from ICI therapy and new approaches are needed including combinations of ICI

with new immunotherapeutics. Emerging evidence demonstrated a critical role for the sialoglycan/Siglec axis in cancer immune escape.

Methods
In order to further investigate the potential of targeting the sialoglycan/Siglex axis, we used genetic mouse models, tumor cell lines deficient for sialylation and tumor-targeted sialidases. Tumor growth in preclinical mouse models was analysed after targeted desialylation of tumors combined with checkpoint inhibitors including anti-PD-1 and anti-CTLA-4 antibodies.

Results
We discovered that hypersialylation on tumor cells and the extracellular tumor matrix results in an immunesuppressive tumor microenvironment through engagement of sialic acid-binding Siglec receptors on immune cells including CD8 T cells. We also found that various Siglecs were upregulated on tumor-infiltrating T cells from cancer patients, and such expression in NSCLC patients correlated with a reduced survival. Siglec-expressing T cells co-expressed several inhibitory receptors including PD-1, suggesting potential for combination therapies by targeting the sialoglycan/Siglec pathway and PD-1 or CTLA-4 inhibition. Here, our work shows that the combination therapy targeting the sialoglycan/Siglec pathway and PD-1 or CTLA-4 inhibition induces tumor control in different preclinical mouse models and increases T cell activation in primary patient tumor samples. Therapeutic intervention of the pathway using EAGLE-301, a Herceptin-sialidase antibody-enzyme conjugate let to targeted desialylation of the tumor microenvironment and resulted in intratumoral T cell activation and T cell-dependent tumor rejection, which was non-redundant to PD-1 or CTLA-4 inhibition. The efficacy was dependent on inhibitory Siglecs. Accordingly, ICI therapies in Siglec-deficient animals were more effective and priming of T cells Siglec-dependent.

Conclusions
We demonstrate that targeting the sialoglycan/Siglec pathway is a new immunotherapeutic strategy and can be combined with PD-(L)1 and/or CTLA-4 inhibition for further clinical development.

Ethics Approval
Mouse experiments were approved by the local committee of Basel Stadt, Switzerland (approval number 2747).

P677

The antitumor efficacy of TIM-3 blockade in a murine model of sarcoma

Kristen McEachern, PhD[1], Geeta Sharma[1], Srimoyee Ghosh, PhD[1], Sridhar Ramaswamy, MD[1], David Jenkins, PhD[1]

[1]*TESARO, Inc., Waltham, MA, USA*

Background
TSR-022 is an anti-TIM-3 antibody that is currently undergoing clinical development in combination with anti-PD-1 (NCT02817633). TIM-3 is an immune checkpoint receptor that negatively regulates T-cell activity and is implicated in resistance to PD-1 blockade. In addition, TIM-3 is also expressed on myeloid cells and has been shown to regulate dendritic cell activity. We previously reported a case study of a patient with leiomyosarcoma who had a partial response to TSR-022 monotherapy. Here we explore the mechanism of the antitumor effect of TIM-3 blockade in a preclinical mouse model of fibrosarcoma.

Methods
A/JCr mice were inoculated with murine fibrosarcoma SaL/N cells. Mice were randomized into 4 groups of 8 mice each at tumor volumes of 80-120 mm^3 and treated with isotype control, anti-mouse PD-1, anti-mouse TIM-3, or a combination of

both. A total of 5 doses were administered in a twice-weekly schedule. Mice with complete tumor regression were re-challenged with SaL/N cells along with a fresh cohort of 5 mice to serve as control group. The mice were monitored for tumor regrowth until all the mice in the control group were euthanized due to tumor burden. In a follow-up study to understand the mechanism of efficacy, the mice were randomized at tumor volumes of 200-300 mm^3, treatment initiated, and tumors collected for immunoprofiling using flow cytometry.

Results

Both anti-PD-1 and anti-TIM-3 treatment resulted in antitumor efficacy with 73% and 53% tumor growth inhibition, respectively, which improved to 98% in the combination group. In addition, 2 mice in the anti-PD-1 group and 6 in the combination group showed complete tumor regression. The mice with complete regression were re-challenged and monitored for tumor growth. The tumors in the fresh cohort of mice grew normally; however, no tumor growth was observed in the re-challenged mice, consistent with the induction of immune memory. Tumor immune contexture correlated with the antitumor efficacy seen.

Conclusions

In the preclinical setting, TIM-3 blockade alone and in combination with PD-1 resulted in a robust antitumor response associated with durable immunologic memory, further supporting the development of anti-TIM-3 agents, such as TSR-022, in the clinic.

P678

Targeting Siglec-15 with NC318, a novel therapeutic antibody to enhance anti-tumor immunity

Linda Liu, PhD[1], Jun Wang, PhD[2], Jingwei Sun, PhD[2], Dallas Flies, PhD[1], Chang Song, PhD[1], Melissa Zarr, PhD[1], Kristina Archer, PhD[1], Alison McGuire, BS[1], Tom O'Neill, MS[1], Karla Maloveste, MS[1], Xinxin Nie, PhD[2], Agedi Boto, MD/PhD[2], Ron Copeland, PhD[1], Sathya Janardhanan, MS[1], Tete Obot, BS[1], Jim Bingham, PhD[1], Kevin Heller, MD[1], Sol Langermann, PhD[1], Lieping Chen, MD, PhD[2]

[1]NextCure, Inc., Beltsville, MD, USA
[2]Yale School of Medicine, New Haven, CT, USA

Background

Siglec-15 (S15), a member of sialic acid-binding immunoglobulin-type lectins, is a highly conserved Type I cell surface protein, which was previously reported to play a role in osteoclast differentiation and bone remodeling [1,2]. Here we describe S15 as a novel co-inhibitory ligand expressed on tumors and myeloid cells that suppresses T cell function and promotes cancer growth. Blocking S15 by antibody enhances anti-tumor immunity in preclinical models.

Methods

S15 KO mice were generated and challenged with syngeneic tumors to study its role in tumor immunology. S15 specific hybridomas were generated by immunizing the KO mice with human S15 fusion protein. Recombinant S15 antibodies that cross react with murine S15 were generated and assessed for their functionality in vitro and in vivo. Top candidate was humanized and characterized.

Results

Mice with S15 KO or a conditional KO in myeloid cells have decreased tumor growth and enhanced T cell responses. Additional studies revealed that S15 expression was limited in normal tissues but expressed in tumor cells and tumor-associated myeloid cells. S15 was inducible on myeloid cells by M-CSF and downregulated by IFN-γ, demonstrating that S15 expression was associated with suppressive macrophages. Anti-S15 clone 5G12, bound to S15 with sub-nanomolar affinity, cross reacted with murine and cynomolgus monkey S15, and demonstrated an ability to block S15 Fc fusion

protein mediated suppression of human and mouse T cells in vitro. This immunomodulatory property was further demonstrated in several in vivo tumor models, where 5G12 showed monotherapy activity. An increase of tumor antigen-specific effector CD8+ T cell and reduced myeloid cell infiltration were demonstrated within the tumors of 5G12 treated mice. 5G12 also demonstrated anti-tumor synergy with PD-1 blockade. Based on these data, clone 5G12 was humanized and the selected variant, which maintained high affinity and activity, was named NC318. In follow up experiments, NC318 increased IL-2 production in human PBMC assays in a dose dependent manner.

Conclusions

S15 immunosuppressive properties in the TME make it a rational target for immunotherapy. NC318 is a high affinity humanized IgG1 mAb specific for S15 developed to reverse tumor immune suppression and promote an effective anti-tumor immune response. NextCure has completed IND-enabling studies and is planning to begin evaluations of NC318 in patients with advanced malignancies in Q4/2018.

References

1. Macauley MS, Crocker PR, Paulson JC. Siglec-mediated regulation of immune cell function in disease. Nat Rev Immunol. 2014 Oct;14(10):653-66.
2. Hiruma Y, Tsuda E, Maeda N, Okada A, Kabasawa N, Miyamoto M, Hattori H, Fukuda C. Impaired osteoclast differentiation and function and mild osteopetrosis development in Siglec-15-deficient mice Bone. 2013 Mar;53(1):87-93.

P679 **Abstract Travel Award Recipient**

Neuropilin-1 is a T cell memory checkpoint limiting long-term tumor immunity

Chang Liu, PhD[1], Ashwin Somasundaram, MD[2], Tullia Bruno, PhD[2], Creg Workman, PhD[1], Dario Vagnali[1]

[1]*University of Pittsburgh, Pittsburgh, PA, USA*
[2]*UPMC Hillman Cancer Center, Pittsburgh, PA, USA*

Background

Memory CD8+ T cells are pivotal for conferring long-term protective immunity against tumors, and the promotion of their generation and survival is key to achieving effective immunotherapy. At the conclusion of a primary response, a long-lived memory T cell pool is generated from a small fraction of effector CD8+ T cells deviated from terminal differentiation, a process which is thought to be corrupted in tumor-bearing patients and mouse models, resulting in diminished long-term tumor immune surveillance [1]. However, the cell-intrinsic mechanisms limiting this process remain unclear. We found that Neuropilin-1 (NRP1), a receptor constitutively expressed by thymically-derived regulatory T cells (Tregs) and crucial for their suppression of anti-tumor immunity [2], is transiently induced in effector CD8+ T cells in mouse tumor models and in patients with advanced head and neck cancer.We are interested in understanding the impact of CD8+ T cell-expressing NRP1 on both the short- and long-term tumor surveillance and the implication in cancer immunotherapy.

Methods

The B16F10 tumor growth in the CD8-restrictive Nrp1-deficient mice (Nrp1L/LE8ICre) was assessed upon initial inoculation, as well as re-challenge after surgical removal of the primary tumors. In a competitive setting, we investigated the long-term persistence and recall activity of Nrp1–/– and Nrp1+/+ pMel-T cells (transgenic CD8+ T cells expressing TCR specific for gp100 melanoma antigen) in response to gp100-B16 tumors, after co-transferred into the same host. Transcriptome analysis was performed in these pMel-T cells (Nrp1–/– vs. Nrp1+/+) recovered from both effector and memory phase to gain insight into the downstream pathways that are modulated by NRP1.

Results
Surprisingly, CD8+ T cell-restricted Nrp1-deficient mice showed significantly enhanced protection following B16.F10 tumor challenge, despite unchanged primary tumor growth prior to resection. Constitutive NRP1 expression by CD8+ T cells is sufficient to drive resistance to tumor vaccine-induced secondary tumor protection. Moreover, Nrp1–/– gp100-specific pMel-T cells outcompeted their wildtype counterparts to persist longer in vivo.

Conclusions
These data revealed NRP1 as a unique "immune checkpoint" limiting the memory maturation of tumor-reactive CD8+ T cells in a cell-intrinsic manner, which is distinct from the mechanism of action of well-known immune checkpoints (PD1, CTLA4, LAG3) that primarily suppress effector CD8+ T cell function. Importantly, blockade of checkpoint inhibitors of T cell memory may be necessary to achieve durable anti-tumor immunity.

References
1. Klebanoff CA, Gattinoni L, Restifo NP. CD8+ T-cell memory in tumor immunology and immunotherapy. Immunol Rev. 2006;211:214-24. Epub 2006/07/11. doi: 10.1111/j.0105-2896.2006.00391.x. PubMed PMID: 16824130; PubMed Central PMCID: PMCPMC1501075.
2. Delgoffe GM, Woo SR, Turnis ME, Gravano DM, Guy C, Overacre AE, et al. Stability and function of regulatory T cells is maintained by a neuropilin-1-semaphorin-4a axis. Nature. 2013;501(7466):252-6. Epub 2013/08/06. doi: 10.1038/nature12428. PubMed PMID: 23913274; PubMed Central PMCID: PMCPMC3867145.

P681

A translational platform using primary human immune cells in vitro, syngeneic and humanized models in vivo to support and advance immune-oncology drug discovery

Shilina Roman[1], Gary Salmon[1], Julie Hawkins[1], Jonathan White, PhD[1], Julia Lloyd[1], Ria Goodwin[1], Arunima Ganguli, PhD[1], Omar Aziz[1], Julia Schueler[1], Martin O'Rourke1, Ian Waddell[1], Edgar Wood, PhD[1]

[1]Charles River, Cambridge, UK

Background
Charles River Laboratories (CRL) are establishing a powerful translational immuno-oncology platform with the capability of progressing biologics or small molecule modulators of immune response from in vitro to in vivo assays using human and mouse variants of current check-point inhibitors and small molecules.The platform is supported by an internal blood donor panel which ensures highly reproducible data and high-quality immune cells which are prepared immediately once sampled.

Methods
Our in vitro platform includes primary human immune cell assays which profile T cell activation, cytokine release, T cell mediated cancer cell kill, expansion of T cell populations, T cell invasion and macrophage mediated T cell phagocytosis.The platform is currently being expanded to determine the effect of activated immune cell populations on tumour cell spheroid cultures. We are in the process of developing a range of GFP expressing cell lines which will be used to support co-culture experiments. The platform has been validated with standard of care chemotherapeutics, including anti-CTLA4, anti-PD1 and a selection of small molecule inhibitors of targets known to modulate immune responses including IDO inhibitors. Ex-vivo analysis of activated mouse splenocytes response to check-point inhibitors measured as cytokine release and modulation of immune cell populations, as measured by flow cytometry supports the translation of important compounds from the bench to pre-clinical models. Syngeneic mouse tumour models have frequently been used to profile immune responses in tumours, CRL have optimized and profiled existing

check-point inhibitors to support immuno-oncology drug discovery using mouse and rat antibody variants of anti-CTLA4 and anti-PD1. To confirm the translational development of our platform CRL have developed and optimized humanized mouse models using sub-cutaneous implanted patient derived xenografts (PDX) with human engraftment via CD34+ haematopoeitic stem cells in NOG mice which were treated with anti-CTLA4 and anti-PD1. Infiltration of human immune cells and PDL-1 expression was detected by flow cytometry (FC) and immunohistochemistry (IHC) in hematopoietic organs and tumor tissue, supporting the initial in vitro response in primary immune cells.

Results
We present a screening platform which will support translation of compounds from in vitro primary immune cell assays, to modulation of mouse immune cell population in spleen and tumours, resulting in efficacy and tumour immune cell activation in humanized mouse models.

Conclusions
N/A

P682

Treatment-naïve HPV+ head and neck cancers display a T-cell-inflamed phenotype distinct from their HPV- counterparts that has implications for immunotherapy

Saman Maleki Vareki[1], Steven Gameiro[1], Farhad Ghasemi[1], John Barrett[1], James Koropatnick[1], Anthony Nichols[1], Joe Mymryk[1]

[1]*University of Western Ontario, London, Canada*

Background
Head and neck squamous cell carcinomas (HNSCC) are often characterized by aggressive local invasion and overall poor prognosis. HPV status is a strong predictor of positive clinical outcome in HNSCC. Expression of viral antigens by HPV+, but not HPV-, HNSCC allows direct comparison of the immune status (immune cell presence and characteristics) between these two otherwise anatomically-similar tumors. Currently, the FDA has approved two anti-programmed death 1 antibodies for the treatment of HNSCC, regardless of the HPV status of the disease. A detailed comparison of the immunological differences between HPV+ and HPV- HNSCC provides an opportunity to identify immunological determinants that contribute to successful treatment in HNSCC that may be broadly applicable to cancer treatment in general.

Methods
Patient data from The Cancer Genome Atlas, including Merged Clinical data and Level 3 RSEM normalized Illumina HiSeq RNA expression data for the HNSCC cohort, was downloaded from the Broad Genome Data Analysis Centers Firehose server. RSEM-normalized expression data was extracted and HPV status was manually curated. Primary patient samples with known HPV status were grouped as HPV+, HPV-, or normal. Patient samples with unknown HPV status were omitted from our calculations. This resulted in 73 HPV+, 442 HPV-, and 43 normal control samples with data available for the HNSCC gene expression analysis. Boxplot comparison of gene expression was performed using GraphPad Prism v7.0.

Results
We determined that HPV+ HNSCC tumors exhibit a strong Th1 response, characterized by increased infiltration with dendritic cells, CD4+ and CD8+ T-cells, and increased expression of interferon-γ, but not tumor necrosis factor-α. HPV+ HNSCC also expressed higher levels of multiple T-cell exhaustion markers compared to HPV- HNSCC. This gene expression profile is consistent with a “T-cell-inflamed” phenotype, one that is dominated by T-cell markers and chemokines associated with

effector T-cell recruitment. Importantly, higher expression of these T-cell inhibitory genes correlated with markedly improved patient survival in HPV+, but not HPV-, HNSCC.

Conclusions

The presence of high expression levels of multiple immune inhibitory genes in HPV+ HNSCC suggests that these patients have an existing antitumor immunity and may exhibit strong beneficial responses to immunotherapy, providing a strong rationale for using ICIs as single or combination therapies in first-line treatment of HPV+ HNSCC. This would save patients from disfiguring surgery, or the toxicities associated with conventional chemotherapy or radiation treatment. Finally, expression of immune checkpoint molecules could serve as a predictive biomarker of patient outcome in HPV+ HNSCC.

P683

The CTLA-4 x OX40 bispecific antibody ATOR-1015 induces anti-tumor effects through tumor-directed immune activation

Anne Mansson Kvarnhammar, PhD[1], Niina Veitonmäki[1], Karin Hagerbrand, PhD[1], Mia Thagesson[1], Doreen Werchau, BS[1], Kristine Smedenfors[1], Anna Dahlman[1], Anna Rosen, MSc[1], Maria Johansson[1], Ida Åberg[1], Per Norlen, MD, PhD[1], Christina Furebring, PhD[1], Peter Ellmark, PhD[1]

[1]*Alligator Bioscience, Lund, Sweden*

Background

ATOR-1015 is a human IgG1 CTLA-4 x OX40 bispecific antibody, designed as a next generation CTLA-4 antibody with improved benefit-risk profile. Dual targeting of CTLA-4 and OX40, both overexpressed on tumor-infiltrating regulatory T cells (Tregs), directs the effect to the tumor area. This allows ATOR-1015 to induce enhanced anti-tumor effects with lower systemic toxicity compared to CTLA-4 monotherapy. Mode of action is a combination of effector T-cell (Teff) activation and Treg depletion.

Methods

Human cells were isolated from leukocyte concentrates from healthy donors. T-cell activation induced by ATOR-1015 upon CTLA-4 or Fcy receptor crosslinking was measured as IL-2 and IFN-y release. Treg depletion was studied using FcyRIIa (H131) and FcyRIIIa (V158) reporter assays and ADCC assays with NK cells measuring LDH release. The effect of ATOR-1015 on Treg function was studied in terms of suppressive activity and IL-10 release.Human OX40 transgenic (knock-in) mice (hOX40KI) with syngeneic tumors were used, enabling studies of both targets as ATOR-1015 binds to murine CTLA-4. Tumor growth and survival were studied after administration of ATOR-1015, monotargeting antibodies to CTLA-4, OX40 and/or PD-1. Tumors and spleens from treated mice were analyzed for Treg and Teff numbers and activation markers by flow cytometry. Tumor localization was assessed by flow cytometry and near infrared (NIR) live imaging of tumor-bearing mice.

Results

ATOR-1015 binds CTLA-4 and OX40 simultaneously, promoting cell-cell interactions for enhanced immune stimulating effects. In vitro, ATOR-1015 induces a superior T-cell activation and depletion of Tregs compared to the combination of monotargeting antibodies to CTLA-4 and OX40. ATOR-1015 slightly inhibits the suppressive effect of Tregs and reduces their IL-10 production.ATOR-1015 administered to hOX40KI mice with colon cancer localizes specifically to the tumor via binding to OX40. Similarly, ATOR-1015 increases the intratumoral CD8+ Teff/Treg ratio by depleting Tregs and increasing the infiltration/expansion and cytotoxic activity of Teffs without affecting systemic T cells.Treatment with ATOR-1015 reduces tumor growth and prolongs survival in several tumor

models. Re-exposure of mice that responded to ATOR-1015 treatment with the same and an irrelevant tumor, demonstrates that the response is tumor-specific and induces long-lasting immunological memory. Lastly, ATOR-1015 improves the anti-tumor responses of anti-PD-1 treatment.

Conclusions

ATOR-1015 is a next generation CTLA-4 antibody with tumor-directed activity for enhanced efficacy and reduced toxicity. ATOR-1015 increases the anti-tumor responses of anti-PD-1 treatment in mice, supporting the combination with PD-1/PD-L1 in the clinic. ATOR-1015 is planned to enter clinical phase I in H2 2018.

Ethics Approval

The studies were approved by Malmö/Lund Ethics Board approval number M142-15.

P684

Preclinical studies of TIM-3 blockade supporting clinical development of BMS-986258, an anti–TIM-3 monoclonal antibody

Xiao Min Schebye, PhD[1], Minhua Han[1], Hong-An Truong[1], Andy Deng[1], Alan Korman, PhD[1], Mark Selby, PhD[1], Christine Bee[2]

[1]Bristol-Myers Squibb, Redwood City, CA, USA
[2]Bristol Myers Squibb, x, USA

Background

T-cell immunoglobulin- and mucin-domain-containing-3 (TIM-3) is among the next generation of checkpoint inhibitors whose role in human cancer therapy is being explored. TIM-3 is often co-expressed with PD-1 in $CD8^+$ T cells and is a marker of $CD8^+$ T-cell dysfunction or exhaustion in several cancers [1-3]. TIM-3 is also expressed on natural killer cells, regulatory T cells, and antigen-presenting cells (APCs), where its role in mediating tumor immunity is not well understood. To this end, we have developed a TIM-3 antagonist for evaluation in human trials. Here we describe the preclinical characterization of BMS-986258, a fully human immunoglobulin (Ig)G1 anti–TIM-3 monoclonal antibody that was engineered to eliminate Fc-gamma receptor binding.

Methods

BMS-986258 binding activity was evaluated by fluorescence-activated cell sorting (FACS) and Scatchard analysis. An artificial APC:Th1 co-culture assay, in which CHO cells expressing a single-chain anti-CD3 (CHO-OKT3) were irradiated, was developed to assess BMS-986258 functions. In addition, CHO-OKT3 cells expressing PD-L1 were cultured with Th1 cells to evaluate co-blockade of TIM-3 and PD-1. Single-cell suspension of human tumor-infiltrating leukocytes (TIL) derived from surgically resected tumor tissues of a variety of tumor types was co-cultured with the irradiated CHO-OKT3 cells. Interferon (IFN)-gamma production was evaluated by enzyme-linked immunosorbent assay (ELISA), and the percentage of IFN-gamma$^+$CD8$^+$ T cells was determined using FACS.

Results

BMS-986258 bound with high affinity and selectivity to TIM-3 expressed on activated human T cells (EC_{50}: 0.1 nM; K_D: 0.16 nM). The antibody bound to the phosphatidylserine (PS) binding site of TIM-3 as revealed by a crystal structure of TIM-3 IgV domain complexed with the Fab of BMS-986258 resolved to 1.5Å, consistent with the observation that BMS-986258 blocks TIM-3 from binding to PS in an in vitro TIM-3:PS blocking assay. BMS-986258 and its monovalent Fab fragments promoted Th1-cell proliferation in a concentration-dependent manner, indicating that BMS-986258 acts as an antagonistic antibody in promoting T-cell function. When using the irradiated CHO-OKT3 cells expressing PD-L1, BMS-986258 and nivolumab (anti–PD-1) promoted Th1-cell proliferation as single agents, and co-

blockade of TIM-3 and PD-1 showed an additive effect. In the human TIL assay, BMS-986258 increased both IFN-gamma production and IFN-gamma$^+$CD8$^+$ T cells. The EC_{50} value for a human tumor TIL assay was 1.2 nM.

Conclusions

These results support the notion that TIM-3 blockade promotes CD8$^+$ T-cell functions in tumors. Preclinical characterization of BMS-986258 supports its evaluation alone and in combination with nivolumab in patients with advanced cancers (NCT03446040).

References

1. Fourcade J, Sun Z, Benallaoua M, et al. Upregulation of Tim-3 and PD-1 expression is associated with tumor antigen-specific CD8+ T cell dysfunction in melanoma patients. *J Exp Med*. 2010;207:2175-2186.
2. Gao X, Zhu Y, Li G, et al. TIM-3 expression characterizes regulatory T cells in tumor tissues and is associated with lung cancer progression. *PLoS One*. 2012;7:e30676.
3. Yang ZZ, Grote DM, Ziesmer SC, et al. IL-12 upregulates TIM-3 expression and induces T cell exhaustion in patients with follicular B cell non-Hodgkin lymphoma. *J Clin Invest*. 2012;122:1271-1282.

Ethics Approval

This preclinical study was conducted in accordance with ethical principles and local laws/regulations. The use of samples were reviewed and approved by an institutional review board or independent ethics committee.

P685

CD226 impact on TIGIT blockade in T-cell rejuvenation

Katherine (Kate) MacDonald, PhD[1], Yoon Park[1], Padma Perkins[1], Eric Boyer[1], Salvatore Santino[1], Michael Hamilton[1], Ishita Barman[1], Pavel Strop[1], Alan Korman, PhD[1], Bryan Barnhart, PhD[1]

[1]*Bristol-Myers Squibb, Redwood City, CA, USA*

Background

T-cell immunoreceptor with Ig and ITIM domains (TIGIT) is a checkpoint molecule that interacts with poliovirus receptor (PVR) and plays a key role in maintaining immune homeostasis. TIGIT counterbalances CD226-mediated T-cell activation by competing with CD226 for binding to PVR, a receptor that is expressed in multiple tumor types. Signaling through TIGIT contributes to T-cell exhaustion, resulting in inhibition of antitumor T-cell responses. Importantly, antibody blockade of TIGIT has shown antitumor activity in preclinical mouse models, highlighting the potential utility of this pathway for tumor immunotherapy. Previous work has demonstrated an interdependence between TIGIT and CD226 for maximal activity of TIGIT blockade; however, the precise mechanism of T-cell rejuvenation by TIGIT blockade remains elusive. Here we present data describing the relationship between TIGIT and CD226 in T-cell activation.

Methods

Tumor-infiltrating lymphocytes (TILs) from a variety of human tumors, including non-small cell lung cancer, renal cell carcinoma, and colorectal cancer, were analyzed for coexpression of TIGIT and CD226. *In vitro* functional assays were established to test the impact of TIGIT blockade on antigen-specific T cells from healthy donors, exploring the relationship between CD226 expression and its impact on TIGIT-mediated T-cell suppression. This relationship was further analyzed in various subsets of CD8$^+$ T cells, focusing on those with phenotypic characteristics representative of exhausted T cells.

Results

CD8$^+$ TILs expressed higher levels of TIGIT together with other checkpoint receptors, including PD-1, but

lower levels of CD226 than T cells from patient-matched peripheral blood. Stimulation of TILs with anti-CD3 restored CD226 expression in some samples but correlated with an increase in expression of TIGIT and other exhaustion markers. In analyses of healthy donor peripheral blood, $CD226^{low}$ $CD8^+$ T cells displayed phenotypic characteristics of exhausted T cells and impaired effector function compared with $CD226^{high}$ $CD8^+$ T cells. In contrast to $CD226^{low}$ $CD8^+$ T cells, the antigen-specific T-cell response of $CD226^{high}$ $CD8^+$ T cells was greatly enhanced by TIGIT blockade alone or combined TIGIT and PD-1 blockade.

Conclusions

These findings highlight the importance of the relative expression of CD226 and TIGIT required for T-cell function and suggest that these pathways play a role in governing optimal T-cell activity. Together, these observations suggest that TIGIT and CD226 potentially regulate antitumor T-cell responses and warrant further investigation of these molecules in human cancers.

Ethics Approval

This preclinical study was conducted in accordance with ethical principles and local laws/regulations. The use of samples were reviewed and approved by an institutional review board or independent ethics committee.

Tumor-infiltrating lymphocytes (TILs) from a variety of human tumors, including non-small cell lung cancer, renal cell carcinoma, and colorectal cancer, were analyzed for coexpression of TIGIT and CD226. *In vitro* functional assays were established to test the impact of TIGIT blockade on antigen-specific T cells from healthy donors, exploring the relationship between CD226 expression and its impact on TIGIT-mediated T-cell suppression. This relationship was further analyzed in various subsets of $CD8^+$ T cells, focusing on those with phenotypic characteristics representative of exhausted T cells.

Results

$CD8^+$ TILs expressed higher levels of TIGIT together with other checkpoint receptors, including PD-1, but lower levels of CD226 than T cells from patient-matched peripheral blood. Stimulation of TILs with anti-CD3 restored CD226 expression in some samples but correlated with an increase in expression of TIGIT and other exhaustion markers. In analyses of healthy donor peripheral blood, $CD226^{low}$ $CD8^+$ T cells displayed phenotypic characteristics of exhausted T cells and impaired effector function compared with $CD226^{high}$ $CD8^+$ T cells. In contrast to $CD226^{low}$ $CD8^+$ T cells, the antigen-specific T-cell response of $CD226^{high}$ $CD8^+$ T cells was greatly enhanced by TIGIT blockade alone or combined TIGIT and PD-1 blockade.

Conclusions

These findings highlight the importance of the relative expression of CD226 and TIGIT required for T-cell function and suggest that these pathways play a role in governing optimal T-cell activity. Together, these observations suggest that TIGIT and CD226 potentially regulate antitumor T-cell responses and warrant further investigation of these molecules in human cancers.

Ethics Approval

This preclinical study was conducted in accordance with ethical principles and local laws/regulations. The use of samples were reviewed and approved by an institutional review board or independent ethics committee.

P686

The number of metastatic compartments involved at immunotherapy initiation may influence survival in stage-IV non-small cell lung cancer.

Abdul Rafeh Naqash, MD[1], Mahvish Muzaffar, MD[1], Paul Walker, MD[1], Li Yang, PhD[1]

[1]*East Carolina University, Greenville, NC, USA*

Background
In recent years immune checkpoint blockade (ICB) has revolutionized the management of non-small cell lung cancer (NSCLC). However, outside of clinical trials, the lack of uniform responses suggests clinical heterogeneity. Often patients with high tumor burden tend to do poorly with ICB. Even in non-bulky disease, due to organ-specific tumor microenvironments (TME), metastasis to >1 organ may suggest distinct tumor biology that may in turn influence outcomes. Hence, we sought to investigate if the number of metastatic compartments involved at ICB initiation could impact survival.

Methods
We retrospectively identified 100 stage-IV NSCLC patients treated with ICB from April 2015 to February 2018. Follow up cutoff for survival analysis was set on July 1, 2018. A single metastasis to >1 organ was categorized as >1 metastatic compartment involvement (MCI) which was independent of the number of lesions in the organ or total tumor bulk. Overall survival after immunotherapy (OSI) was defined as the time from ICB initiation to last follow up or death. Cox regression was used to assess survival correlations.

Results
The median age was 63 years with predominant histology being adenocarcinoma (65.0 %). A majority of patients were of Caucasian ethnicity (66.0 %) and male gender (59.0 %). Nivolumab (72.0%), Carboplatin/Alimta/Pembrolizumab (17.0%), Pembrolizumab (6.0%), and Atezolizumab (5.0%) were used for ICB. The median number of cycles for ICB was 4.0. Skeletal involvement (45.0 %), brain (35.0 %) and liver (20.0 %) were the most common metastatic compartments. 47.0 % of patients had > 1 MCI at ICB initiation. No differences in baseline medians for C-reactive protein, albumin or neutrophil-lymphocyte ratio were seen based on MCI. The median OSI for our NSCLC cohort was 7.5 months. Brain or liver involvement did not show inferior OSI. >1 MCI at ICB initiation was noted to be independently associated with inferior OSI both in the univariate [p= 0.02, HR 1.68, CI(1.06-2.65)] and multivariate Cox regression [p=0.02, HR 1.85, CI(1.09-3.13)].

Conclusions
Involvement of >1 metastatic compartment which may or may not be synonymous with the total tumor bulk, appears to be an important factor in survival stratification of NSCLC treated with ICB. This suggests that patients with >1 MCI may have baseline aggressive tumor biology that adapts to different TME and does not respond well to ICB. Hence improving outcomes in such subgroups will require exploring strategies that involve combining different immunotherapies or other novel agents with ICB to overcome this resistant biology.

Ethics Approval
Study was approved by ECU UMCIRB 15-001400

P687

Single-cell analysis of human T cells in the bladder tumor microenvironment reveals novel cytotoxic CD4s that are modulated by anti-PD-L1 therapy

David Oh, MD, PhD[1], Serena Kwek[1], Siddharth Raju, BS[1], Tony Li, BS[1], Eric Chow, PhD[1], Arun Burra, BS[1], Chien-Chun Pai, PhD[1], Chiara Rancan, PhD[1], Yang Sun, PhD[1], Jacky Li, BS[1], Dvir Aran, PhD[1], Matthew Spitzer, PhD[1], Serghei Mangul, PhD[2], Sima Porten, MD[1], Maxwell Meng, MD[1], Terence Friedlander, MD[1], Chun Jimmie Ye, PhD[1], Lawrence Fong, MD[1]

[1]University of California, San Francisco, San Francisco, CA, USA
[2]University of California, Los Angeles, Los Angeles, CA, USA

Background
Bladder cancer can be responsive to immunotherapies such as PD-1 checkpoint inhibitors, but overall response rates are low. While tumor-resident T cells may demonstrate considerable heterogeneity in their antigenic repertoire and functional phenotype, the genotypic and phenotypic features of T cells in the bladder tumor environment and how both are modulated by systemic therapies remains unclear.

Methods
We performed droplet single-cell RNA and paired T cell receptor (TCR) sequencing of CD4+ and CD8+ T cells isolated from localized bladder tumors and paired adjacent non-malignant tissue including patients who received anti-PD-L1 antibody prior to surgery.

Results
Bladder tumors possess both known and novel CD4+ T cell populations, including multiple populations of regulatory (CD4reg) and central memory (CD4cm) cells, as well as novel populations of cytotoxic (CD4cyto) CD4+ T cells expressing cytolytic effectors and granule-associated proteins. Moreover, CD4cyto cells are functionally competent and capable of killing autologous tumor cell. While CD4reg populations are consistently enriched in tumor compared to adjacent non-malignant tissue, anti-PD-L1 therapy results in enrichment of a specific CD4cyto population in treated tumor compared to treated non-malignant tissue, which is not enriched in untreated bladder tumors. Anti-PD-L1 therapy also elicits a more oligoclonal TCR repertoire in intratumoral CD4cyto1 as well as CD4reg populations compared to non-malignant tissue. Individual CD8+ populations are not detectably enriched in tumor across all samples, and anti-PD-L1 therapy does not specifically enrich CD8+ populations or restrict their repertoire in tumors.

Conclusions
These findings reveal the importance of CD4+ T cell heterogeneity in the bladder tumor environment, and underscores that cancer immunotherapies may elicit both quantitative enrichment and focusing of the antigenic repertoire of novel intratumoral cytotoxic CD4+ populations in lieu of effects on cytotoxic CD8+ cells.

Ethics Approval
The study was approved by the Institutional Review Board of the University of California, San Francisco (approval # 14-15423).

P688

Peripheral blood profiling to identify predictors of sensitivity to anti–PD-1 blockade in non-small cell lung cancer

Akio Osa, Student[1], Yujiro Naito[1], Takeshi Uenami[2], Masahide Mori[2], Atsushi Kumanogoh[1]

[1]*Osaka University Graduate School of Medicine, Suita city, Japan*
[2]*National Hospital Organization Toneyama National Hospital, Suita City, Japan*

Background
Recent clinical trials have demonstrated that a specific subset of patients with non–small cell lung cancer (NSCLC) exhibits a clear response to PD-1 blockade. Although selecting for patients with high PD-L1 expression enriches the response to anti–PD-1 therapy, more than 50% of selected patients do not demonstrate a durable response to PD-1 blockade. Several studies have reported that the neutrophil-to-lymphocyte ratio (NLR) at the initiation of anti–PD-1 blockade is potentially a marker of therapeutic outcomes in cancer patients; however, a definitive predictive biomarker in peripheral blood has not been found. Therefore, we performed immune cell analysis on peripheral blood from patients with

NSCLC receiving nivolumab.

Methods
This study enrolled 96 patients with NSCLC who began nivolumab as second-line or further-line therapy at Osaka University Hospital and Toneyama Hospital between January 2016 and May 2018. After excluding patients who were driver mutation positive (n=15), discontinued treatment due to immune-related adverse events (n=11), or recently received treatment for another malignancy (n=2), 68 patients were in the analysis. The distribution of immune cell populations in freshly collected blood samples before nivolumab administration were examined using flow cytometry including differentiation and proliferation markers. We also examined plasma humoral factors and serum interferon-inducing activity using THP-1-ISG reporter cells.

Results
We divided patients into two groups: the durable response (DR) group, who received 6 or more doses of nivolumab (n=38), and the early progression (EP) group, who received less than 6 doses (n=30). The percentage of neutrophils among all CD45-positive cells was significantly lower in the DR group, whereas the percentages of CD56+ T cells and CD141+ dendritic cells were significantly higher in the DR group. Regarding differentiation and proliferation markers, the percentage of effector memory T cells and Ki-67–positive T cells were significantly higher in the DR group. We will present humoral factor and interferon-inducing activity findings at the presentation.

Conclusions
Immune analysis using fresh peripheral whole blood might be useful in identifying NSCLC patients who are nivolumab sensitive or resistant. Profiling results suggest that neutrophil-rich status is possibly linked to suppression of effector T cell count and function. Future studies will focus on the detailed mechanisms in the immunosuppressive role of neutrophils in patients with NSCLC resistant to anti PD-1 therapy.

Ethics Approval
The study was approved by Osaka University and Toneyama National Hospital Institutution's Ethics Board, approval number 15383 and 1545.

Consent
Written informed consent was obtained from the patient for publication of this abstract and any accompanying images. A copy of the written consent is available for review by the Editor of this journal.

P690

Pharmacokinetics (PK) and dosing regimen selection of the PD-1 Inhibitor ABBV-181 in patients with advanced solid tumors: Preliminary Phase 1 results from study M15-891

Apurvasena Parikh, PhD[1], Sreeneeranj Kasichayanula, PHD[1], Rajeev Menon[1], Daniel Afar, PhD[1], Stacie Lambert[1], Benjamin Engelhardt[1], Sven Mensing[1]

[1]*AbbVie Inc., Redwood City, CA, USA*

Background
ABBV-181 is a humanized, recombinant, IgG1 monoclonal antibody targeting programmed cell death 1 (PD-1). ABBV-181 is currently being evaluated in a phase 1 clinical trial (NCT03000257) in patients with solid tumors. Preliminary ABBV-181 pharmacokinetic (PK) data, population PK modeling and PK-pharmacodynamic (PD) simulations supporting a flat dose and alternate regimens are described herein.

Methods
Patients with previously treated advanced solid tumors received ABBV-181 at 1, 3, or 10 mg/kg IV Q2W in dose escalation. The ongoing expansion cohorts include patients with multi-histology, non-

small cell lung cancer and head and neck squamous cell cancer. Intensive PK samples for ABBV-181 were collected in Cycle 1 and Cycle 3, along with pre-dose concentrations for other Cycles, for all subjects. PD assessments included circulating T-cell PD-1 receptor saturation by flow cytometry. Serum concentration-time data were summarized using non-compartmental PK analysis (Phoenix WinNonlin 7.0) and modeled using nonlinear mixed effects modeling (NONMEM 7.3) using a two compartment PK model. PK/PK-PD simulations for flat doses and varying regimens were conducted utilizing a distribution of wide range of body-weight values (47-128 kg) to compare exposures and corresponding PD between weight-based, and flat dosing.

Results

Preliminary PK data were available for 62 patients (N=24 for 1-10 mg/kg Q2W in dose escalation and N=38 for 250 mg Q2W in dose expansion). ABBV-181 PK were approximately dose-proportional across the dose range studied with Cmax values ranging from 19.5-277 µg/mL (%CV 26-43%), AUCinf values of 214-3129 µg*day/mL (%CV 31-59%), and 2-3 fold accumulation with Q2W dosing in Cycle 3 compared to Cycle 1. Population PK modeling and simulation analyses indicated that a 250 mg fixed dose would result in similar overall exposures achieved with a 3 mg/kg dose, which was consistent with the observed data. PK predictions indicated the exposures achieved with alternate dosing regimens, i.e., 375 mg Q3W and 500 mg Q4W will result in PD-1 positive CD4 T central memory cell saturation and significant PD-1 blockade, with likely no impact on safety based on the available safety data.

Conclusions

The 3 mg/kg and 250 mg Q2W doses were safe, well-tolerated and indicated complete receptor saturation at clinical concentrations. Flat alternate dosing regimens of 375 mg Q3W and 500 mg Q4W were predicted to achieve comparable efficacious exposures as the 250 mg Q2W regimen. PK data and simulations support flat dosing and less frequent dosing regimen for ABBV-181 in expansion, with likely no impact on safety events.

Acknowledgements

AbbVie and the authors thank the patients participating in this clinical trial and all study investigators for their contributions

Ethics Approval

This study was approved by an institutional review board or ethics committee at each participating center.

P691

Correlating skin toxicity and steroid treatment with outcomes of Anti-PD-1 therapy

Henry Quach, BS[1], Anna Dewan, MD[2], Douglas Johnson, MD, MSCI[2]

[1]*Vanderbilt University School of Medicine, Nashville, TN, USA*
[2]*Vanderbilt University Medical Center, Nashville, TN, USA*

Background

Immune checkpoint inhibitors (ICI) such as anti-programmed death protein 1 (anti-PD-1) antibodies produce durable responses in a subset of cancer patients. ICI can produce immune-related adverse events (irAEs). Among the earliest and most common irAEs are skin toxicities [1]. Several studies have associated the development of irAEs with increased treatment efficacy, though it remains unclear whether steroid treatment for irAEs interferes with the antitumor effects of ICI [2-4]. We sought to evaluate the effect of cutaneous irAEs on treatment outcomes.

Methods

We retrospectively assessed whether skin toxicity

with anti-PD-1 correlated with clinical response in patients with metastatic melanoma. Skin toxicity was defined as new rash or pruritus arising on therapy. Subjects at one center that received treatment with anti-PD-1 therapy were included (n = 318). Presence and timing of skin toxicity, and steroid treatment (topical vs. systemic) were correlated with response rate (RR), progression-free survival (PFS), and overall survival (OS).

Results

38% of patients on anti-PD-1 therapy (n = 121) developed skin toxicity. Skin toxicity was correlated with higher RR (60.3% vs. 28.4%, p<0.0001), clinical benefit rate (response + stable disease; 73.6% vs. 41.6%, p<0.0001), median PFS (743 days vs. 112 days, p<0.0001), and median OS (1691 days vs. 517 days, p<0.0001). Late skin toxicity (after 3 months on therapy) was associated with superior clinical outcomes than early skin toxicity. Not developing cutaneous toxicity was associated with the worst outcomes both in terms of median PFS (not reached vs. 383 days vs. 112 days, p<0.0001 for late, early, and no skin toxicity, respectively) and OS (median not reached vs. 1065 days vs. 526 days p<0.0001). There was no difference in PFS or OS for patients who received topical steroids, systemic steroids, or no steroids. Interestingly, patients who experienced pruritus without rash had inferior PFS compared with other skin toxicities (p=0.0008), which was comparable to patients without skin toxicity.

Conclusions

The development of cutaneous toxicity is correlated with clinical response to anti-PD-1 therapy. Late toxicity is associated most strongly with response, and illustrates that time on therapy can confound toxicity-efficacy correlations. The development of pruritis alone does not correlate with beneficial outcomes, suggesting that distinct mechanisms may be responsible for pruritus. The use of steroids to treat these skin toxicities did not affect treatment outcomes.

Acknowledgements

We would like to acknowledge the Vanderbilt Medical Scholars Program and UL1 RR 024975 (NIH CTSA grant).

References

1. Postow M, Sidlow R, Hellmann M. Immune-Related Adverse Events Associated with Immune Checkpoint Blockade. N Engl J Med. 2018; 378(2):158-168.
2. Hua C, Boussemart L, Mateus C, Routier E, Boutros C, Cazenave H, Viollet R, Thomas M, Roy S, Benannoune N, Tomasic G, Soria JC, Champiat S, Texier M, Lanoy E, Robert C. Association of Vitiligo With Tumor Response in Patients With Metastatic Melanoma Treated With Pembrolizumab. JAMA Dermatol. 2016; 152(1):45-51.
3. Teulings H, Limpens J, Jansen S, Zwinderman A, Reitsma J, Spuls P, Luiten R. Vitiligo-like depigmentation in patients with stage III-IV melanoma receiving immunotherapy and its association with survival: a systematic review and meta-analysis. J Clin Oncol. 2015; 33(7):773-81.
4. Sanlorenzo M, Vujic I, Daud A, Algazi A, Gubens M, Luna SA, Lin K, Quaglino P, Rappersberger K, Ortiz-Urda S. Pembrolizumab Cutaneous Adverse Events and Their Association With Disease Progression. JAMA Dermatol. 2015; 151(11):1206-1212.

Ethics Approval

This study was approved by Vanderbilt University Medical Center's Ethics Board; approval number 150625.

P692

Effect of steroids in metastatic non-small cell lung cancer (mNSCLC) patients treated with nivolumab after initial platinum therapy in community practices in the USA

Jenine Sanzari, PhD[1], Jay Rathi, Marc Monté[2], David

Smith[3], Mark Danese[4], Michelle Gleeson[4], Deborah Lubeck[4], James White[1], Pranav Abraham[1], Beata Korytowsky[1], Brian Ulrich[5]

[1]*Bristol-Myers Squibb, Lawrence, NJ, USA*
[2]*St. Bernards Medical Group, Jonesboro, AR, USA*
[3]*Compass Oncology, Vancouver, WA, USA*
[4]*Outcomes Insights, Inc, Westlake Village, CA, USA*
[5]*Texas Oncology, Houston, TX, USA*

Background

Limited data are available on mNSCLC patients treated with nivolumab and steroids. Recent presentations suggest that mNSCLC patients who received concomitant steroids and anti–programmed death-1 (PD-1) receptor or anti–PD-ligand 1 (PD-L1) treatment have worse survival when compared to patients who received anti–PD(L)1 alone [1,2]. However, these analyses were not adjusted to account for residual confounding by variables associated with mortality. Here, we present analyses exploring the effect of confounding variables on the efficacy of concomitant steroid and nivolumab treatment in mNSCLC patients in a real-world setting, using data from CA209-118, a prospective observational study of 70 community practices in the USA.

Methods

Only mNSCLC patients who received initial platinum-based therapy and were enrolled before initiating second-line treatment between April 2014 and January 2018 were included in this analysis. Patients were followed until death, initiation of subsequent immunotherapy, end of follow-up, or study withdrawal. Study sites reported therapy start and end dates, sites of metastases, and outcomes. Inverse probability of treatment weighting was used to account for possible residual confounding between factors associated with using steroids and mortality [3].

Results

174 patients received nivolumab after initial platinum therapy. Of these, 24 (14%) received systemic steroids at a dose of ≥10 mg, and 17 (10%), 30 (17%), 68 (39%), 28 (16%), and 24 (14%) had liver, brain, lymph node, adrenal, and pleural effusion metastases, respectively.In this analysis, confounding variables included age, sex, ECOG score, duration of first-line therapy, and liver, brain, lymph node, adrenal and pleural effusion metastases. Taking into account the confounding variables, the adjusted Kaplan-Meier curve suggests that concomitant steroid and nivolumab treatment does not negatively impact overall survival (Figure 1).

Conclusions

These analyses demonstrate that variables that could result in residual confounding should be considered when evaluating the effects of concomitant steroid and nivolumab treatment. Additional validation in larger cohorts of patients receiving immune checkpoint inhibitors is warranted.

References

1. Scott and Pennell. Poster presented at: International Association for the Study of Lung Cancer (IASLC) 2017. Poster number: PS02.09.
2. Arbour KC, Mezquita L, Long N, et al. Poster presented at: 2018 American Society of Clinical Oncology (ASCO) Annual Meeting. Abstract number: 9003.
3. Brookhart MA, Stürmer T, RJ Glynn, et al. Confounding control in healthcare database research: challenges and potential approaches. Med Care. 2010;48(6 Suppl):S114-20.

Ethics Approval

This multi-site study was approved by the Western Institutional Review Board (IRB) (December 2013), approval number 20132144; US Oncology IRB (January 2014), approval number 13172; Cone Health IRB (March 2014), approval number 1790; St. Charles Health System IRB (May 2014), approval

number not applicable; and the UCLA IRB (May 2015), approval number 14-000865.

Figure 1.

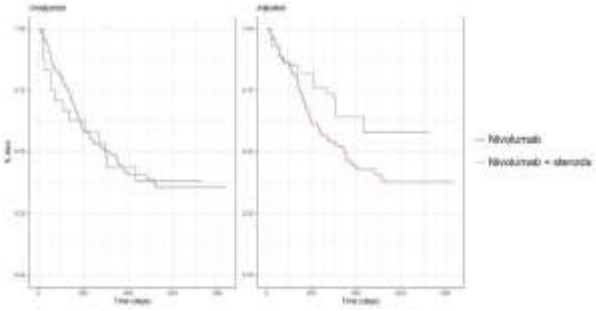

P693

Efficacy of ex-vivo PD-1 blockade in cervical tumor draining lymph nodes is related to a CD8+FoxP3+ T-cell subset with high levels of multiple immune checkpoints and superior effector functions

Jossie Rotman, MD[1], Marijne Heeren, MSc[2], Anita Stam[1], Noëlle Pocorni, MsC[1], Awa Gassama[1], Sanne Samuels, MD, PhD[2], Maaike Bleeker[1], Stijn Mom, MD PhD[2], Henry Zijlmans, MD PhD[3], Gemma Kenter, MD,PhD[2], Ekaterina Jordanova, PhD[1], Tanja de Gruijl, PhD[1]

[1]Amsterdam UMC, Cancer Center Amsterdam, Amsterdam, Netherlands
[2]Amsterdam UMC, Amsterdam, Netherlands
[3]Netherlands Cancer Institute, Amsterdam, Netherlands

Background

An important prognostic factor in cervical cancer (CxCa) is lymph node metastasis. Our previous findings of PD-L1 expression in primary tumors and high and interrelated rates of Tregs and PD-L1-positive macrophages in metastatic tumor-draining lymph nodes (TDLN) point to the possible applicability of PD-(L)1 blockade to halt metastatic spread (Heeren et al, 2015). Here, through extensive flowcytometric profiling and ex-vivo functional analyses, we confirm the validity of PD-1 blockade in early-stage CxCa and relate its efficacy to the presence of a specific CD8+ effector T-cell subset.

Methods

Multicolor flow cytometric analysis of T-cells in TDLN (n=23) and PT (n=10) was performed. In addition, the effect of PD-1 blockade on T-cell reactivity against the HPV16 E6 oncoprotein in TDLN (n=12) and PT (n=7) single cell suspensions was assessed by IFNγ Elispot read-out after 10 days in-vitro culture. Cytokine and Granzyme-B production was analyzed after anti-CD3 stimulation of metastatic TDLN (n=4) and PT samples (n=3). Moreover, multicolor immunofluorescence histochemistry was performed on FFPE sections from metastatic TDLN (n=4) and PT (n=4) to study T-cell localization.

Results

Extensive flow cytometric analysis revealed progressively elevated levels of activated regulatory T-cells (aTregs) and central and effector memory T-cells, from tumor negative to tumor positive TDLN, to PT. Similarly, significantly and progressively increasing levels of multiple immune checkpoints were observed on both CD4+ and CD8+ T-cells. High levels of PD-1 supported further exploration of PD-1 blockade. Ex-vivo PD-1 blockade consistently enhanced measurable T-cell responses to HPV16 E6 in TDLN with HPV-16+ metastases (4/4), but, remarkably, only in 1/4 HPV16+ PT. Whereas activated Treg (aTreg) rates were significantly higher in PD-1 non-responders, in responders elevated levels of CD8+ CD25+ FoxP3+ T-cells were observed, which correlated significantly with the efficacy of PD-1 blockade (p=0.018). This subset, mainly found in the peritumoral compartment in the tumor microenvironment, was characterized by an activated effector phenotype with elevated expression levels of PD-1, CTLA-4, Tim-3 and Lag-3 checkpoints, but, rather than exhausted, was shown

upon ex-vivo polyclonal activation to express higher levels of Granzyme B and effector cytokines as compared to its CD8+FoxP3- counterparts.

Conclusions

These data support earlier reports of a "poised" HPV-specific T-cell repertoire in metastatic TDLN and PT and show it to be an actionable target for PD-1 blockade, which may benefit from additional depletion of aTregs. Moreover, they specifically point to a CD8+CD25+FoxP3+ T-cell subset as likely therapeutic target for PD-1 blockade.

References

1. Heeren AM, Koster BD, Samuels S, Ferns DM, Chondronasiou D, Kenter GG, et al. High and interrelated rates of PD-L1+CD14+ antigen-presenting cells and regulatory T cells mark the microenvironment of metastatic lymph nodes from patients with cervical cancer. Cancer Immunol Res. 2015;3:48–58.

Ethics Approval

The study was approved by the local Institutional Review Boards of the Antoni van Leeuwenhoek (AVL) Hospital and the Academic Medical Center (AMC), both in Amsterdam.

P694

An orally bioavailable small molecule dual antagonist of TIGIT and PD-L1 pathways shows immune-mediated anti-tumor activity

Murali Ramachandra, PhD[2], Pottayil Sasikumar, PhD[1], Sudarshan Naremaddepalli, PhD[2], Sandeep Patil, PhD[2], Chennakrishnareddy Gundala[2], Raghuveer Ramachandra, PhD[2], Nagesh Gowda, PhD[2], Saikrishna Tangela[2], Sreenivas Adurthi, PhD[2], Amit Dhudashia, MSc[2], Dodheri Samiulla, PhD[2], Nagaraj Gowda, PhD[2], Kavitha Nellore[2]

[1]*Aurigene Discovery Technologies, Bangalore, India*

[2]*Aurigene Discovery Technologies Limited, Bangalore, India*

Background

Immune checkpoint inhibition using antibodies targeting CTLA4 and PD-1/PD-L1 is considered as a major breakthrough in cancer therapy in recent years. Apart from PD-1 and CTLA-4, there are several other checkpoint proteins in tumor microenvironment that play a role in dampening the anti-tumor immune response. Interestingly, these immune checkpoint pathways are non-redundant thus providing an opportunity for simultaneous targeting more than one checkpoint protein to overcome the immune tolerance in the tumor. T cell Ig and ITIM domain (TIGIT) is a recently identified co-inhibitory receptor expressed by activated T cells, Tregs, and NK cells. TIGIT binds two ligands, CD112 (PVRL2, nectin-2) and CD155 (PVR), and these ligands are expressed by T cells, APCs, and tumor cells. TIGIT is upregulated on tumor antigen-specific $CD8^+$ T cells and $CD8^+$ tumor-infiltrating lymphocytes in various cancer types and TIGIT receptor/poliovirus receptor (PVR) ligand interaction signaling inhibits cytotoxicity mediated by NK and CD8+ T cells. Interestingly, TIGIT-expressing $CD8^+$ T cells often co-express the inhibitory receptor PD-1 providing a strong rationale for simultaneously targeting TIGIT and PD-L1 for optimal anti-tumor activity.

Methods

We sought to discover and develop small molecule immune checkpoint antagonists capable of simultaneously targeting TIGIT and PD-L1 pathways. We reasoned that such agents will be amenable for oral dosing, likely show greater response rate due to dual antagonism and allow better management of irAEs due to shorter pharmacokinetic profile. In order to develop an oral agent, we took the approach of identifying a minimal pharmacophore from the interface of TIGIT/PVR interactions via truncating the interfacial sequences. Considering the pockets of sequence similarity of PDL1 and TIGIT

proteins a focused library of small molecule compounds, based on minimal pharmacophore, mimicking the interaction of checkpoint proteins was designed and synthesized to achieve compounds exhibiting dual antagonism towards TIGIT and PD-1 pathways.

Results

The dual antagonism of these agents have been inferred through potent rescue of PVR-mediated inhibition of IL-2 production from T cells and PD-L1 mediated IFN-γ production. The SAR optimized lead compounds exhibits desirable invitro ADME and DMPK profile including oral bioavailability and better tumor distribution. The lead compounds exhibit significant anti-tumor activity in a syngeneic tumor model and demonstrated profound immune PD in vivo on both T and NK cells.

Conclusions

Preclinical data demonstrate a proof-of-concept showing that a dual antagonism of oral small molecules antagonizing TIGIT and PD-L1 pathways significantly enhance anti-tumor efficacy. Efficacy studies and biomarker characterization in additional tumor models are ongoing.

P695

Differential expression of microRNAs in immune cell subpopulations during checkpoint inhibitor treatment

Barbara Seliger, MD, PhD[1], Rolf Kiessling, MD, PhD[1]

[1]Martin Luther University Halle-Wittenber, Halle, Germany
[2]Karolinska Institutet, Stockholm, Sweden

Background

Checkpoint blockade has revolutionized the treatment of metastatic melanoma, with significant increases in overall survival, and a dramatic improvement in patient quality of life. Ipilimumab, a fully human antibody that blocks CTLA-4, was the first checkpoint inhibitor that received FDA approval in 2011. Despite the success of this therapeutic approach, the number of responding patients is limited and there is a need for predictive, prognostic and pharmacodynamic biomarkers. Non-coding RNAs have recently been shown to have important clinical implications in cancer therapeutics and could be used as targets or as the aforementioned biomarkers for diagnosis, prognosis and prediction of responses to ipilimumab treatment. This study aims (i) to determine the expression of miR-155, known to be a potent regulator of immune cell activity, in untreated and ipilimumab treated melanoma patients and (ii) to correlate miR-155 expression pattern with clinical response to treatment.

Methods

30 metastatic melanoma receiving ipilimumab treatment at Karolinska Hospital were enrolled in this study. 6/30 patients had a long-term survival of > 182 weeks. 2/6 responders were Braf V600E mutated, 4/6 expressed wt Braf. CD4+, CD8+ as well as CD14+ cells were sorted from PBMCs purified before, during and at the end of treatment. Expression of miR-155 in each of the purified cellular populations was measured by qPCR.

Results

Interestingly, data show a constitutive and stable expression of miR-155 in CD14+ monocytes prior and during the whole course of ipilimumab treatment. In contrast, an induction of miR-155 was found in the different T cell subpopulations. In 7/30 patients an upregulation of miR-155 expression in CD8+ T cells was found with a frequency ranging between 3.6 to 70.3 fold, while in 9/30 patients miR-155 was upregulated in CD4+ T cells in a range between 3.5 to 96 fold. A coordinated upregulation of miR-155 in both T cell subpopulations was only found in 2 patients demonstrating distinct effects of ipilimumab on miR-155 expression in the distinct immune cell

subpopulations. In order to determine whether the distinct miR-155 expression pattern had clinical relevance, the miR-155 expression pattern was correlated to the response to ipilimumab. 1/6 responders showed a dramatic 96-fold increase of miR-155 expression in CD4+ T cells over time. In contrast, an upregulation of miR-155 expression was only seen in non-responders.

Conclusions
Currently, samples are analyzed for general miR expression pattern in order to identify other differentially expressed miRs, which might serve as markers for monitoring of therapy response and resistance.

P696

Combined anti-PD-1 and anti-LAG-3 checkpoint blockade enhances CD8+ TIL effector function while reducing Tregs leading to reduced immune suppression and improved overall survival

Elizabeth Sturgill, PhD[1], Courtney Mick, BS[1], David Jenkins, PhD[2], Johanna Kaufmann, PhD, MSc[2], William Redmond, PhD[1]

[1]*Earle A. Chiles Research Institute, Portland, OR, USA*
[2]*Tesaro, Waltham, MA, USA*

Background
Checkpoint inhibition is a potent strategy to reinvigorate T cells. However, aCTLA-4 or aPD-1 monotherapy has not been effective for the majority of patients, resulting in the exploration of combinatorial approaches to improve treatment efficacy. One such target is LAG-3, which is upregulated on T cells that have experienced repeated antigen exposure, such as in the tumor microenvironment (TME), and is associated with reduced T cell effector function. In addition, high LAG-3 expression on regulatory T cells (Tregs) has been reported for patients with varying cancer types, providing an additional rationale for targeting LAG-3 with the aim of reducing immune suppression within the TME. We hypothesized that the combination of aPD-1 and aLAG-3 would synergize to promote tumor regression and increase survival via a reduction in tumor-induced immune suppression and enhanced CD8+ T cell effector function.

Methods
CT26 (colon carcinoma) tumor-bearing BALB/c mice received aPD-1 and/or aLAG-3 (200 µg/dose; ip) 3x/week on days 7, 10, and 13 post-tumor implant. Tumor growth (area) was assessed 2-3x/week and mice were sacrificed when tumors exceeded 150 mm2. In additional cohorts, tumors were harvested 7 days post-treatment (d17) and tumor-infiltrating lymphocytes (TIL) were analyzed by flow cytometry. Responders to combined aPD-1/aLAG3 therapy were designated as those exhibiting decreased tumor size on the day of harvest (d17) compared to maximum tumor growth post-implant.

Results
Combined aPD-1/aLAG-3 immunotherapy significantly improved the survival of CT26 tumor-bearing mice compared to monotherapy ($p<0.05$). Further analysis revealed that aPD-1/aLAG-3 therapy significantly increased the percentage of CD8+ TIL compared to aPD-1 ($p<0.01$) or aLAG-3 ($p<0.05$) alone. Additionally, we observed increased effector function in CD8+ TIL from aPD-1/aLAG-3-treated mice, as evidenced by increased cytotoxicity (granzyme A; $p<0.05$) and cytokine production (TNF-a; $p<0.05$ and IFN-g; $p<0.01$). Interestingly, responders to aPD-1/aLAG-3 therapy were enriched for CD8+ TIL with higher cytolytic activity and effector cytokine production, which correlated with a reduction in PD-1 MFI amongst the PD-1+/CD8+ TIL. Lastly, aPD-1/aLAG-3 treatment significantly increased the frequency of effector CD4+ T cells (Teff) compared to FoxP3+CD4+ Tregs ($p<0.05$).

Conclusions

In summary, these data suggest that aPD-1/aLAG-3 immunotherapy increased recruitment of CD8+ TIL exhibiting enhanced effector function, increased CD4+ Teff/Treg ratios, which likely mitigated Treg-mediated immune suppression. Together, these positive immunological changes led to a more immune stimulatory TME capable of supporting tumor regression and significantly improved tumor-free survival.

P697

Preclinical characterization of AB154, a fully humanized anti-TIGIT antibody, for use in combination therapies

Joanne Tan, PhD[1], Amy Anderson, PhD[1], Daniel DiRenzo, PhD[1], Annette Becker, PhD[1], Susan Lee, PhD[1], Lisa Seitz, MSc[1], Rick Stanton, MSEE[2], Hema Singh[1], Sharon Zhao[1], Nigel Walker, PhD[1], Matthew Walters, PhD[1]

[1]*Arcus Biosciences, Inc., Hayward, CA, USA*
[2]*Stanton Biosciences, Newbury Park, CA, USA*

Background

TIGIT (T-cell immunoreceptor with Ig and ITIM domains) is an inhibitory receptor expressed on natural killer (NK) cells, CD8+ T cells, CD4+ T cells and regulatory T cells (Treg). CD226 (DNAX Accessory Molecule-) is an activating receptor found on NK cells, monocytes and a subset of T cells. TIGIT and CD226 are paired receptors that compete for shared ligands CD155 (PVR) and CD112 (Nectin-2) expressed by cancer and antigen-presenting cells. TIGIT binding to CD155 results in immune suppression, whereas binding of CD226 to the same ligand promotes immune activation. AB154 is a fully humanized antibody that binds and blocks human TIGIT with sub-nanomolar affinity.

Methods

TIGIT and CD226 expression in healthy and cancer patient PBMCs were assessed by flow cytometry. TIGIT and CD226 expression in various tumor types and normal tissues was derived from TCGA (The Cancer Genome Atlas), GTEX (Genotype-Tissue Expression Project), and immunohistochemistry. Binding affinity of AB154 was determined using CHO.hTIGIT and human T cells. Functional consequences of TIGIT blockade were determined using a TIGIT-expressing reporter gene cell line and a mixed lymphocyte reaction assay. Receptor occupancy (RO) analyses were quantified using a competing anti-TIGIT antibody.

Results

Data assembled from TCGA identified tumor types in which expression of TIGIT is greater than PD-1, equivalent to PD-1, or expressed at low levels. TIGIT and PD-1 marked primary tumor samples containing T cells. In these tumors, TIGIT and PD-1 expression were higher compared to normal adjacent tissue. Immunophenotyping performed on dissociated human tumor cells demonstrated strong correlation between TIGIT and PD-1 expression on immune cells. The intensity of TIGIT staining was lowest on conventional CD4+ T cells while its intensity in Treg and CD8+ T cells was 1.5 to 3-fold higher on average. Consistent with a high degree of PD-1 and TIGIT co-expression, combination of AB154 with anti-PD-1 (AB122) significantly increased IFN-gamma secretion relative to anti-PD-1 alone. Using flow cytometry, we demonstrated target engagement by AB154 in T cells and NK cells in the low nanomolar range in both healthy and cancer patient whole blood.

Conclusions

Blockade of multiple immune checkpoint proteins can confer effective and durable responses in the treatment of cancer. The data presented here provide: 1) selection of tumor types based on TIGIT RNA and protein expression profile, 2) rationale for combining AB154 with AB122 in upcoming clinical

trials, and 3) methodology to evaluate TIGIT receptor occupancy in AB154 Phase 1 studies.

P698

Outcomes of advanced triple negative breast cancer patients enrolled in immune oncology clinical trials

Tira Tan, MBBS[1], Lisa Wang[1], David Cescon[1], Eitan Amir[1], David Warr[1], Christine Elser[1], Marcus Butler, MD[1], Albiruni Razak[1], Aaron Hansen[1], Anna Spreafico, MD PhD[1], Lillian Siu, MD[1], Philippe Bedard, MD[1]

[1]*Princess Margaret Cancer Centre, Toronto, Canada*

Background

Advanced triple negative breast cancer (aTNBC) is an aggressive disease with poor prognosis. Immune-oncology (IO) agents are under investigation for this disease. We evaluated the outcomes of aTNBC patients (pts) enrolled on IO clinical trials at a large academic medical center and explored factors associated with IO treatment outcomes.

Methods

We retrospectively reviewed the medical records of aTNBC patients who consented for IO monotherapy or combination clinical trials at Princess Margaret Cancer Centre between June 2013 and June 2018. Demographics data, medical history, details of trial enrolment and response to study treatment according to RECIST 1.1 were recorded. Univariable logistic regression was used to identify factors associated with poor outcomes defined as screen failure due to rapidly progressive disease (PD) or central nervous system metastases (CNS) and/or duration of treatment of 21 days or less.

Results

A total of 99 pts with aTNBC consented for 15 IO clinical trials, 60% IO monotherapy, 22% chemotherapy-IO combination and 18% IO combinations. Median age at time of trial enrolment was 52 (range 25-78) and median number of lines of prior systemic therapy for advanced disease was 1 (range 0-8). ECOG performance status, was 0 (39%), 1(58%) and 2/unknown (3%). 15% had de-novo metastatic disease, 58% recurred after a distant disease free interval (DDFI) of less than 3 years and 25% after a DDFI of more than 3 years. 61% had fewer than 3 metastatic disease sites, and 71% had metastases involving the viscera. Of patients consented, 67% started trial treatment and 33% were screen failures, including 19 due to rapid PD and/or CNS metastases. Median progression free survival (mPFS) and overall survival (mOS) in all treated pts were 1.9 months (95% CI 1.7-3.4) and 10.6 months (95% CI 7.7-17.2). In pts who achieved partial response (PR), the mPFS was 7.6 months [3.75-not reached (NR)] and mOS NR. 32% of pts had poor outcomes. In univariate analysis, higher Royal Marsden Index (RMI) (p=0.01), higher Princess Margaret IO prognostic index (PM-IPI) (p=0.01), elevated LDH (p=0.002), higher number of metastatic sites (p=0.03) and presence of visceral metastases (p=0.01) were associated with disease related screen failures and/or duration on IO trial treatment of 21 days or less. (Table 1, 2)

Conclusions

The overall prognosis of aTNBC pts enrolled in IO clinical trials is poor with heterogeneous treatment outcomes. Pts with poor prognostic indices, elevated LDH, higher number of metastatic sites and visceral metastases should be reconsidered for IO trials.

Ethics Approval

The study was approved by UHN Research Ethics Board, approval number 15-9269.

Table 1.

Demographics	Group	All	%	Screen fail (disease)	%	Trial Subjects	%
N		99	100	19	100	80	100
Age, median (range)	-	58 (24.8, 77.8)		49 (25,73)		52.5 (28.7, 77.8)	
CCI	0-1	73	74	16	84	48	73
	>/= 2	26	26	3	16	18	27
ECOG PS	0	39	39	6	32	25	38
	1	57	58	10	53	41	62
	2	2	2	2	11	0	0
	Unk	1	1	1	5	0	0
RMI	0-1	58	60	7	37	46	70
	2-3	31	31	10	53	20	30
	Unk	9	9	2	11	0	0
PM-IPI	0-1	65	63	9	47	48	73
	2-3	29	29	9	47	12	18
	Unk	8	9	1	5	0	0
GRIm	0-1	75	76	13	45	55	83
	2-3	16	16	6	26	11	17
	Unk	8	8	1	5	0	0
Discordant histology	Yes	22	22	5	26	14	21
	No	76	77	14	74	52	79
	NA	1	1	0	0	0	0
Advanced disease status	Denovo metastatic	15	15	1	5	12	18
	DDFI < 3 yrs	57	58	15	79	36	55
	DDFI > 3 yrs	25	25	3	16	17	0
	Locally advanced	1	1	0	0	1	2
	NA	1	1	0	0	0	0
No. metastatic sites	<3	60	61	9	47	41	62
	>/=3	39	39	10	53	25	38
Visceral disease	Yes	70	71	18	95	43	65
	No	29	29	1	5	23	35
Germline status	NM / Unknown	83	84	16	84	55	83
	Pathogenic mutation	9	9	2	11	6	9
	VUS	7	7	1	5	5	8
Prior therapies in advanced setting, median (range)		1 (0,5)		2 (0,5)		1 (0,5)	

Abbreviations: aTNBC, advanced triple negative breast cancer; CCI, Charlson co-morbidity index; ECOG PS, Eastern Cooperative Oncology Group performance status; RMI, Royal Marsden Hospital Index; PM-IPI, Princess Margaret Immune Oncology prognostic index; GRIm, Gustave Roussy immune score; DDFI, distant disease free interval; VUS, Variant of unknown significance

Table 2.

Variable	Estimated effect , OR (95% CI)	P
Age		0.53
CCI 1 2 ≥3 0		0.41
RMI 1 ≥2 0 (ref)	1.27(0.30,5.41) 4.67(1.16,18.78)	0.03
PM-IPI 1 2 3 0 (ref)	3.10(0.77, 12.55) 12.57(2.74, 57.74) 7.33(1.30, 41.35)	0.03
GRIm 1 ≥2 0		0.15
ECOG PS		0.46
NLR		0.35
LDH (10 units)	1.04(1.02, 1.07)	0.002
Discordant histology		>0.90
Advanced disease status		0.08
No. of metastatic sites 2 3 >=4 <=1 (ref)	2.75(0.78, 9.66) 4.65(1.43, 15.20) 6.29(1.65, 23.92)	0.03
Visceral disease	6.13(1.69, 22.19)	0.01
Germline mutation status		>0.90
Prior therapies in advanced setting		0.52
Phase of study		0.15

Abbreviations: OR, odds ratio; CI, confidence interval; CCI, Charlson co-morbidity index; RMI, Royal Marsden Hospital Index; PM-IPI, Princess Margaret Immune Oncology prognostic index; GRIm, Gustave Roussy immune score; ECOG PS, Eastern Cooperative Oncology Group performance status; NLR, neutrophil lymphocyte ratio; LDH, lactate dehydrogenase

P699

MEDI0562, a humanized OX40 agonist monoclonal antibody (mAb), increases T cell effector function and depletes regulatory T cells in blood and tumor

Katie Streicher, PhD[2], Roger Wild[1], Keith Steele, DVM, PhD[2], Steven Eck, PhD[2], Yanan Zheng, PhD[2], Farzad Sekhavati, PhD[3], Han Si[2], Fernanda Pilataxi[2], Song Wu, PhD[2], Brandon Higgs, PhD[2], Danielle Townsley[2], Rakesh Kumar, PhD[2], Mike Sheehan, PhD[2], Scott Hammond, PhD[2], Matthew Gribbin[2], Victoria Chiou, MD[2], Maria Jure-Kunkel[2], Sandip Patel, MD[4], John Powderly, MD, CPI[5], Bonnie Glisson, MD[6], Koustubh Ranade, PhD[2]

[1]*Ashfield Healthcare*

[2]MedImmune, Gaithersburg, MD, USA
[3]Definiens, Munich, Germany
[4]University of California San Diego, La Jolla, CA, USA
[5]Carolina BioOncology Institute, Huntersville, NC, USA
[6]MD Anderson Cancer Center, Houston, TX, USA

Background

In preclinical models, OX40 agonists display a dual mechanism of action (MOA) that leads to antitumor activity: stimulating effector/memory T cell function and depleting regulatory T cells. To determine if these pharmacodynamic changes are measurable in patients with advanced solid tumors, we evaluated blood and tumor samples pre/post treatment in a Phase 1 trial of MEDI0562, a humanized OX40 agonist mAb (NCT02318394).

Methods

Patients received 1 of 6 escalating doses of MEDI0562 (0.03, 0.1, 0.3, 1.0, 3.0, and 10 mg/kg) Q2W until confirmed disease progression or unacceptable toxicity. Tumor response was assessed using irRECIST and RECIST. Selected patients with head and neck squamous cell carcinoma, bladder or cervical cancer had mandatory pre- and on-treatment tumor biopsies to evaluate pharmacodynamic changes. Tumor samples were evaluated pretreatment and at day 29 from a subset of 14 patients by quantitative digital analysis of immunohistochemistry images and gene expression. Peripheral blood from all patients with evaluable samples (n = 36) was monitored using gene expression and flow cytometry.

Results

A total of 55 patients received MEDI0562 across 6 dose cohorts where 10 mg/kg Q2W was the maximum administered dose. Serum exposure increased approximately dose proportionally. Post-treatment antidrug antibodies (ADAs) were detected in 51% of patients, with an impact on MEDI0562 PK at all doses below 3 mg/kg. The activity of MEDI0562 was evaluated in both blood and tumor. In blood, a 1.5- to 3.0-fold increase in mean maximum percentage of Ki67+CD4+ and Ki67+CD8+ memory T cells was observed across doses. Ratios of T effector/T regulatory gene expression signatures increased 3.5- to 8-fold in blood ($p < 0.05$) at all doses at 2 days post-treatment. In tumor, paired biopsies showed ≥ 2-fold increased expression of PD-L1 and/or CD8+ T cell infiltration in 7/14 patients, with a 60% median reduction in OX40+FOXP3+ cells at doses of 1 and 3 mg/kg compared with doses <1 mg/kg. Ratio of T effector/T regulatory gene expression signatures increased intratumorally as seen peripherally. Intratumoral pharmacodynamic changes were more prominent in patients with high OX40 expression (> median) regardless of MEDI0562 dose or presence of ADAs.

Conclusions

MEDI0562-treated patients exhibited increased Ki67+CD4+ and CD8+ memory T cells in the periphery and decreased intratumoral OX40+FOXP3+ cells, consistent with the hypothesized dual MOA of this agonist mAb. The enhancement of these pharmacodynamic effects in patients with high OX40 levels at baseline may help identify patients or indications where MEDI0562 could provide clinical benefit.

Trial Registration

ClinicalTrials.gov [NCT02318394]

Ethics Approval

Multicenter study conducted at 3 sites:(1) MD Anderson Cancer Center, 7007 Bertner Avenue, Unit 1637, Houston, TX 77030, USA [PI: Bonnie Glisson; IRB Registration No. IRB00000121](2) University of California San Diego Moores Cancer Center, 9444 Medical Center Drive, 3rd Floor, Room 3-030, La Jolla, CA 92093, USA [PI: Sandip Patel; IRB Registration No. Committee O: 00009940](3) Carolina BioOncology Institute, PLLC, 1019 39th Avenue South East, Suite 120, Puyallup, WA 98374-

2115, USA [PI: John Powderly II; IRB Registration No. IRB00000533]

P700

Immune checkpoint inhibitors induce differential anti-tumor response and immune cell infiltration across syngeneic models

Brandy Wilkinson, PhD[2], Patrick Allison, PhD[2], Hua-Chen Chang[2], Lauren Ursic, BA[2], Paul Trampont, PhD[2], Lindsey Standarski[2], Jennifer Rusk, NA[2]

[1]*Integrated Oncology & Covance (LabCorp), Greenfield, IN, USA*
[2]*Covance, Greenfield, IN, USA*

Background
Clinical success of immune checkpoint inhibitors has accelerated the evaluation of immune-related targets for novel anti-cancer therapies. Preclinical testing of immune-targeted oncology agents requires preclinical models with functional immune systems. Utilization of murine syngeneic tumor models provides a robust system to evaluate both anti-tumor activity and mechanism of action of novel therapeutics. This study evaluates the efficacy and anti-tumor immune response of different IO therapies across a panel of syngeneic murine models.

Methods
Cohorts of mice were inoculated with six different murine derived cancer cell lines (MC38, CT-26, LL/2, EMT-6, 4T1, B16F10). Tumor bearing mice were administered anti-CTLA-4, anti-PD-1, anti-PD-L1, anti-OX40 or anti-LAG3 twice weekly for 3 weeks. Tumor volume was used to assess anti-tumor activity. Subsets of tumors from treated mice were analyzed two weeks following dosing initiation for tumor-infiltrating lymphocytes (TILs) and myeloid cell populations.

Results
Following 3 weeks of dose administration: anti-CTLA4, anti-PD-1, anti-PD-L1, anti-OX40, and anti-LAG3 conferred significant antitumor activity on some of the xenograft models surveyed, while other models were resistant. Phenotypes of TILs resident in tumors were profiled across the xenograft models. CD45+ lymphocytes were analyzed for populations of cytotoxic lymphocytes (CTLs, CD8+ cells), T-helper cells (CD4+ cells), regulatory T-cells (T-regs, CD4+/CD25+/FoxP3+ cells), and myeloid populations including B-Cells, neutrophils and monocytes. The immune cell response to checkpoint inhibitors were distinct, but varied across xenograft models.

Conclusions
In this study, we demonstrate differential responses between immune-checkpoint inhibitors across several syngeneic xenograft models with respect to anti-tumor activity and lymphocyte tumor infiltration responses. These models constitute a highly-relevant tool to evaluate efficacy and mechanism of action for novel immune-targeted therapies for oncology.

P701

Off-label use of immunotherapy in advanced malignancies

David Xu[1], Kathryn Gold, MD[1], Lyudmila Bazhenova, MD[1], Sandip Patel, MD[1]

[1]*UCSD Moores Cancer Center, San Diego, CA, USA*

Background
Immunotherapy with checkpoint inhibitors (CI) has become a standard treatment in an increasing number of cancers. Off-label use of these agents is common but their efficacy is not known.

Methods
We performed a retrospective review of 98 consecutive patients treated at a single institution

using CI through a patient assistance program with start dates between 5/2015 to 11/2016. Patients were excluded from further analysis if they received treatment for an FDA-approved indication.

Results

Sixty-one patients were included in our analysis: 41% male; 75% white, 3% black, 7% Asian, 11% Hispanic, and 3% other. Median age at diagnosis was 59; median age at start of CI was 62. Median time between diagnosis and start of CI was 23 months. Most patients had good performance status at the time of CI initiation (69% ECOG 0 or 1). Most patients had metastatic disease (87%) at the start of CI. All but 3 patients had received prior chemotherapy; most had prior surgery (70%) and prior radiation (69%). Twenty patients received nivolumab (33%), and 41 patients received pembrolizumab (67%). Two patients had received prior immunotherapy (anti-CD40, tremilumumab). Most common tumor types were breast (11), sarcoma (7), thyroid (5), glioblastoma, hepatocellular carcinoma, and ovarian cancer (four each). Time on therapy ranged between 0 and 21+ months (median 2 months). Eight patients remained on therapy at the time of analysis (9.6 to 21.6 months). Ten patients were on therapy for 1 year or more (esophageal SCC, triple negative breast cancer [2], nasopharyngeal carcinoma, pleomorphic sarcoma, adrenal cortical carcinoma, cutaneous SCC, uterine sarcoma, basal cell carcinoma). Median number of cycles of CI was 5. 20% of the patients had some evidence of response, 21% stable disease, 7% mixed response, and 38% progression of disease as their best treatment response per clinician assessment. Restaging was not available for 15% of patients. Median PFS defined as time from first dose of CI to date of progression was 2 months. Median overall survival was 9 months.

Conclusions

In this study, we observed activity in a wide variety of malignancies with off label use of CIs. Several patients with uncommon cancers have remained on therapy for an extended period of time. For rare cancers for which clinical trials are not feasible, retrospective analyses such as this can suggest some evidence of efficacy.

P702

Acute liver injury in the context of immune checkpoint inhibitor-related colitis treated with infliximab

Hao Chi Zhang, MD[1], Wenyi Luo, MD[2], Yinghong Wang, MD, PhD[2]

[1]*UT Health Science Center at Houston, Houston, TX, USA*
[2]*University of Texas MD Anderson Cancer Center, Houston, TX, USA*

Background

Immune checkpoint inhibitors (ICPI) are commonly used in the treatment of several advanced cancers. ICPI can also be associated with immune-related adverse events (irAEs) including enterocolitis and hepatitis. Infliximab has been used successfully in treating steroid-refractory gastrointestinal irAE [1], but it carries the risk for liver injury. We describe a challenging case of a patient with a new diagnosis of acute hepatitis after infliximab treatment for gastrointestinal irAE.

Methods

A 79-year-old man with a history of metastatic prostate adenocarcinoma, treated with ipilimumab and nivolumab, was evaluated for new elevation in liver enzymes and bilirubin. He had no known risk factors for acute or chronic liver disease. After three cycles of ipilimumab and nivolumab, he had developed grade 3 diarrhea/colitis, and ICPI was discontinued. His diarrhea was steroid-refractory and required a one-time treatment with infliximab (5 mg/kg) which led to prompt resolution of diarrhea. Three weeks later, the patient developed jaundice

with elevated liver enzymes and total bilirubin (Figures 1-2). Physical examination did not reveal stigmata of advanced liver disease. A liver biopsy showed cholestatic hepatitis with predominantly microvesicular steatosis, and mild portal and peri-portal fibrosis (Figure 3). A short course of steroid treatment did not improve the hepatitis condition. By exclusion of other etiologies, acute drug-induced liver injury secondary to infliximab was deemed to be the most likely cause of his liver condition, rather than an adverse effect of ICPI. By fourteen weeks post-infliximab administration, liver enzymes and total bilirubin eventually returned close to normal baseline levels (Figures 1-2).

Results

N/A

Conclusions

Ipilimumab- and nivolumab-related irAEs have been reported; high-grade liver irAE in particular occur with an incidence of <10% [2-5]. In the context of gastrointestinal irAE management, concern was raised about liver toxicity from infliximab, a previously described effective rescue therapy. In our patient's case, the clinical history and data supported infliximab-associated hepatotoxicity, rather than an irAE. Lack of pathognomonic histologic features from hepatic irAE [6-7] limited the value of liver biopsy in this situation. With the increasing application of ICPI for different cancers and the understanding of potential risks for irAE, liver function and liver biochemical tests should be closely monitored during treatment using ICPI and during treatment using anti-TNF-α agents in this patient population.

References

1. Pagès C, Gornet JM, Monsel G, et al. Ipilimumab-induced acute severe colitis treated by infliximab. Melanoma Res. 2013;23(3):227-30.
2. National Institutes of Health. LiverTox: Clinical and Research Information on Drug-Induced Liver Injury. Ipilimumab. [online] Available at: https://livertox.nlm.nih.gov/Ipilimumab.htm [Accessed 28 Jul 2018].
3. National Institutes of Health. LiverTox: Clinical and Research Information on Drug-Induced Liver Injury. Nivolumab. [online] Available at: https://livertox.nlm.nih.gov/Nivolumab.htm [Accessed 28 Jul 2018].
4. DeSouza K, Savva C. Management of Immunotherapy Related Adverse Effects. J Cancer Prev Curr Res. 2016;6(1):00187.
5. Ibrahim RA, Berman DM, DePril V, et al. Ipilimumab safety profile: Summary of findings from completed trials in advanced melanoma. J Clin Oncol 2011;29(15):8583-8583.
6. Kleiner DE, Berman D. Pathologic changes in ipilimumab-related hepatitis in patients with metastatic melanoma. Dig Dis Sci. 2012;57(8):2233-40.
7. Zen Y, Yeh MM. Hepatotoxicity of immune checkpoint inhibitors: a histology study of seven cases in comparison with autoimmune hepatitis and idiosyncratic drug-induced liver injury. Mod Pathol. 2018;31(6):965-973.

Figure 1. Trends in liver enzymes

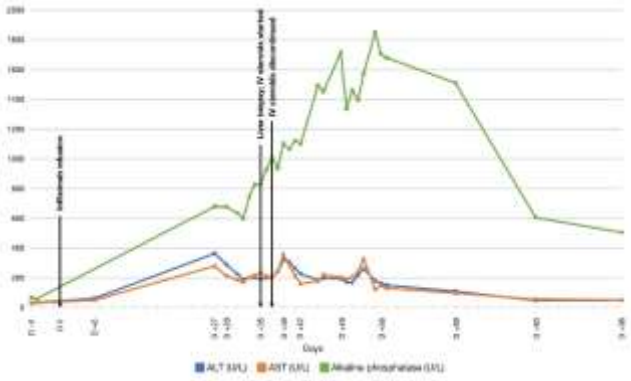

Figure 2. Trends in additional liver biochemical tests

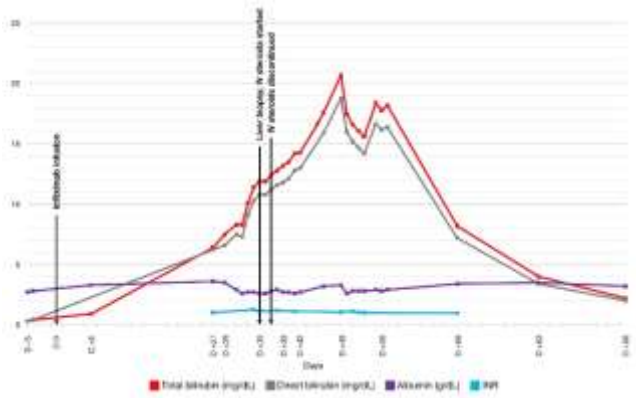

Figure 3. Liver biopsy histology

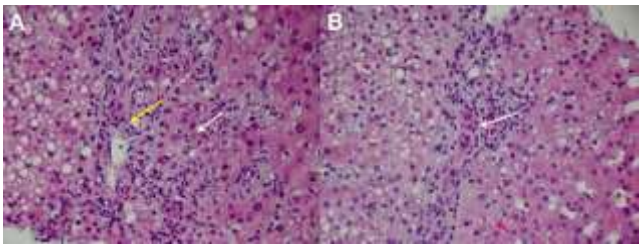

P703

Exploration of PD-1/PD-L1 spatial interaction and T cells functionality to predict anti-PD-1 treatment outcome in GI tract tumors using automated quantitative fluorescence multiplexed IHC

Xiangxue Wang, BS[1], Shizen Moh, BS[1], José L. Muñoz-Rodríguez, PhD[1], Antony Hubbard, BS[1], Mehrnoush Khojasteh, PhD[1], Qingfeng Zhu, PhD[2], Robert A. Anders, MD, PhD[2], Luis A. Diaz, MD[2], Lidija Pestic-Dragovich[1], Lei Tang, PhD[1], Wenjun Zhang, MD, PhD[1]

[1]Roche Tissue Diagnostics, Tucson, AZ, USA
[2]John Hopkins Univeristy Hospital, Balitmore, MD, USA

Background

Blockade of the PD-1/L1 axis is the effective immunotherapy in a proportion of cancer patients. Identification of predictive biomarkers for patient selection represents a major challenge. The predictive value of PD-L1 IHC, tumor mutational load and mismatch repair (MMR) status are limited for the variable strength of association among studies and tumor types. This study aims to quantitatively assess the content and spatial interaction of key immune suppression components (e.g. PD-1 & LAG3 for T cell exhaustion, PD-1/L1 interaction) in tumor micro-environment, and their predictive values to anti-PD-1 treatment.

Methods

Multiplex IHC for PD-L1, PD-1, CD8, LAG3, and pan-cytokeratin (panCK) stained 50 pre-pembrolizumab treatment patient specimens including pancreatic, colorectal and cholangio carcinoma, among which 17 are MMR proficient (13PD, 3SD, and 1CR) and 33 deficient (3PD, 12SD, 3NE, 4CR, and 11PR). Whole slides were scanned with ZEISS Axio Scan.Z1 scanner, on which pathologists annotated tumor area. HALO® Hi-Plex software was used for image analysis. Epithelial tumor (panCK+), stroma (panCK-), artifacts, and no-tissue areas were annotated with Halo's random forest classifiers. X/y coordinates, number, intensity and density of PD-1+, PD-L1+, LAG3+, and CD8+ cells were identified. CD8+ cells co-expressing PD-1, PD-L1, and/or LAG3 phenotypes and their fraction over CD8+ cells were extracted. Spatial relationships including the number of PD-1+ cells within 10/20um of PD-L1+ cells and the average distance between them were computed. MATLAB® was used for feature selection, reduction, ranking and prediction of the responses to anti-PD-1 treatment.

Results

Responders versus non-responders classes were defined as PR and CR versus SD, PD, and NE. From ~190 features analyzed, both Relieff and random forest rank the following feature in the top two features in predicting response to treatment: "Maximum number of CD8+/low-intensity-PD-1+ cells within 20um of PD-L1+ cells in epithelial tumor". Quadrant Discriminant Analysis (QDA) with five-fold cross validation yields a prediction accuracy of 85%.

When combined with the “average number of PD-1+ cells within 20um radius of PD-L1+” and the "max value of CD8+ cell Lag3+ intensity", the accuracy reaches 90.2%, regardless of the MMR status. Other features have lower accuracy (e.g. 60-70%). Independent cross-validation was not performed due to small sample size.

Conclusions

Deep immune characterization of tumor microenvironment on high dimensional image features from multiplexed IHC staining may provide insightful directions on finding and validating predictive markers for PD-1/PD-L1 blockage and other immunotherapies.

Acknowledgements
We acknowledge Sriravali Kamthamraju for her technical assistance on image analysis, John Hurley, Jorge Lozano and Nick Cummins for their technical assistance on assay development.

P704

Batf3 dendritic cells within the tumor microenvironment are necessary during the effector phase of the immune response for anti-PD-L1 efficacy through a mechanism involving the 4-1BB/4-1BB ligand axis

Andrea Ziblat, PhD[1], Brendan L. Horton[2], Philip C. He, BA[1], Thomas F. Gajewski, MD, PhD[1]

[1]University of Chicago, Chicago, IL, USA
[2]MIT, Boston, MA, USA

Background
Spontaneous CD8+ T cell responses against tumor antigens can be detected in both cancer patients and in murine models. However, immunosuppressive mechanisms arise within the tumor microenvironment that blunt T cell functions and enable tumor escape. Immunotherapy that targets the interaction between the T cell inhibitory receptor PD-1 and its ligand PD-L1 can generate durable tumor regressions that translate into clinical benefit across many cancer types. However, many patients fail to respond to immune checkpoint blockade and many others acquire resistance. Therefore, understanding the mechanisms involved in anti-PD-L1 immunotherapy efficacy may enable new strategies for improving efficacy. We and others previously demonstrated that Batf3-lineage dendritic cells (DCs), which express the markers CD8α or CD103, act in at least two steps in anti-tumor immunity: 1) spontaneous T cell priming in the tumor-draining lymph node, and 2) recruitment of effector CD8+ T cells to the tumor [1-3]. In the current work, we examined whether Batf3+ DCs are also required at a third level, during the effector phase of the anti-tumor immune response upon treatment with PD-1/PD-L1 blockade.

Methods
We utilized the B16-SIY melanoma model, CD11c-DTR-GFP bone marrow chimeras and CD11c-DTR-GFP/Batf3 KO mixed bone marrow chimeras to study the role Batf3-DCs play during anti-PD-L1 immunotherapy. To focus on the effector phase of the immune response we depleted CD11c+ cells with diphtheria toxin from day seven of tumor injection while simultaneously blocking T cell entry into the tumor with FTY720. In other experiments anti-4-1BBL blocking antibody was administered alone or in combination with anti-PD-L1 simultaneously with FTY720. Also, wild type or 4-1BB-deficient splenocytes were transferred into Rag KO mice and anti-PD-L1 efficacy was evaluated. Tumor growth and phenotypic analysis of the tumor infiltrate was evaluated in all of the experiments.

Results
Interestingly, we found that CD11c+ cells, and specifically Batf3-CD11c+ cells, must be present in the tumor before the beginning of anti-PD-L1 treatment for therapeutic efficacy of anti-PD-L1. Phenotypic analysis of the tumor infiltrate showed high expression of 4-1BBL on CD11c+CD103+ DCs

compared to other antigen-presenting cell subsets. Unexpectedly, when anti-4-1BBL blocking antibody was co-administered with anti-PD-L1, therapeutic efficacy was lost. In addition, transfer of 4-1BB-deficient splenocytes into Rag KO hosts revealed a requirement of 4-1BB expression on T cells for anti-PD-L1 efficacy.

Conclusions

Overall, these results suggest that Batf3-DCs are necessary during the effector phase of the immune response for anti-PD-L1 efficacy, at least in part through the co-stimulation of 4-1BB signaling on CD8+ TILs.

References

1. Fuertes MB, Kacha AK, Kline J, Woo SR, Kranz DM, Murphy KM, Gajewski TF. Host type I IFN signals are required for antitumor CD8+ T cell responses through CD8α+ dendritic cells. J Exp Med. 2011; 208(10):2005-2016.

2. Roberts EW, Broz ML, Binnewies M, Headley MB, Nelson AE, Wolf DM, Kaisho T, Bogunovic D, Bhardwaj N, Krummel MF. Critical role for CD103(+)/CD141(+) dendritic cells bearing CCR7 for tumor antigen trafficking and priming of T Cell immunity in melanoma. Cancer Cell. 2016; 30(2): 324-336.

3. Spranger S, Dai D, Horton B, Gajewski TF. Tumor-residing Batf3 dendritic cells are required for effector T cell trafficking and adoptive T cell therapy. Cancer Cell. 2017; 31(5):711-723.

P705

Time to GoInVivo(TM), validated checkpoint functional antibodies for cancer research

Miguel Tam, PhD[1], Josh Croteau[1]

[1]*BioLegend*

Background

Immune checkpoint molecules control the fate of an immune response. Well- studied combinations of molecules include PD-1/PD-L1, CTLA-4/CD80 and CD86, LAG-3/MHC II, and Tim-3/Galectin 9. Our GoInVivo™ antibodies, against some of these immune checkpoint molecules, offer several advantages. They have been tested by flow cytometry and in vitro bioassays, are pathogen-free as tested by qPCR, and have excellent price for large sizes, among others. Here we present our results on the use of anti-mouse PD-L1 in the treatment of a mouse cancer model, melanoma. We characterize the phenotype and localization of T cells, in the tumor microenvironment and draining lymph nodes. We also study the cytokine profile in serum, as well as the antigen-specific T cell response.

Methods

Balb/cJ or C57BL/6J mice were injected with 106 B16F10 melanoma cells in the flank and treated with 100 or 200 µg of anti-PD-L1 at the time points indicated. Tissue samples and serum were collected and analyzed by flow cytometry, microscopy, or screened for cytokine content with LEGENDplex™.

Results

CD4 and CD8 T cells redistribute in the spleen (Figure 1). Animals were implanted for 14 days with B16 melanoma cells, after receiving 3 doses of anti-PD-L1 the CD8/CD4 T cell ratio increases. Splenic CD4 T cells show an activated phenotype (Figure 2). After tumor implant and antibody treatment, CD4 T cells show increased expression of CD25, CD69, CD278, and CD279. Similar results were observed in CD8 T cells. CD8+ cells infiltrate the tumor and co-localize with CD11c+ cells (Figure 3). After tumor implant and antibody treatment, the tumors were excised and analyzed by fluorescent microscopy. Pictures were taken with a 40X objective. Cytokine and chemokine profile in serum. After tumor implant and antibody treatment, the analysis of the samples with LEGENDplex™ show A) Increased Th Cytokines. B) Decreased pro-inflammatory cytokines. C) Increased

chemokine production. (Figure 4)A) Tumor-specific infiltrating CD8+ T cells increase 24 days after treatment. Animals were implanted with SIYRYYGL-expressing B16 cells and 24 days after treatment the tumor was collected and analyzed. B) Anti-PD-L1 treatment reduces tumor growth. (Figure 5)

Conclusions

Injection of anti-mouse PD-L1 in mice implanted with B16 melanoma cells:1. Redistributes CD4 and CD8 T cell content in spleen and tumor, and induce activation of T cells2. Stimulates production of Th cytokines and chemokines, while suppressing pro-inflammatory cytokine production 3. Increases tumor-specific T cells, as well as IFN-g-producing cells (not shown) 4. Reduces tumor growth

Figure 1.

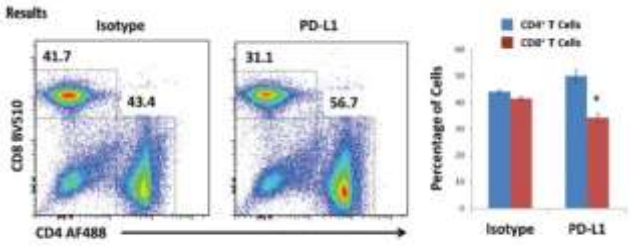

Figure 1. CD4 and CD8 T cells redistribute in the spleen. Animals were implanted for 14 days with B16 melanoma cells, after receiving 3 doses of anti-PD-L1 the CD8/CD4 T cell ratio increases.

Figure 2.

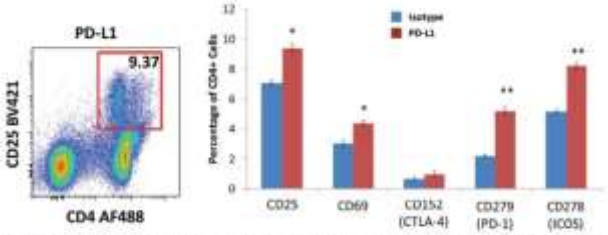

Figure 2. Splenic CD4 T cells show an activated phenotype. After tumor implant and antibody treatment, CD4 T cells show increased expression of CD25, CD69, CD278, and CD279. Similar results were observed in CD8 T cells (not shown).

Figure 3.

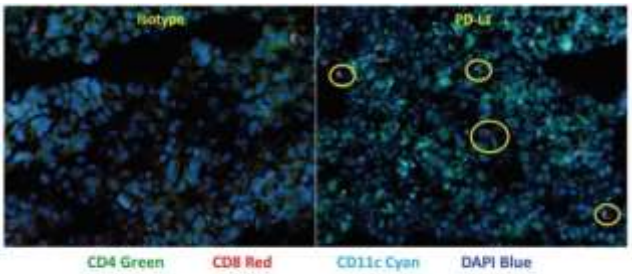

Figure 3. CD8+ cells infiltrate the tumor and co-localize with CD11c+ cells. After tumor implant and antibody treatment, the tumors were excised and analyzed by fluorescent microscopy. Pictures were taken with a 40X objective.

Figure 4.

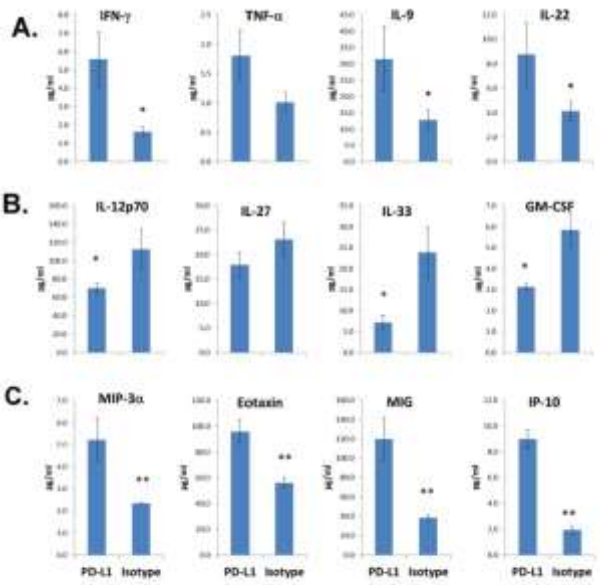

Figure 4. Cytokine and chemokine profile in serum. After tumor implant and antibody treatment, the analysis of the samples with LEGENDplex™ show A) Increased Th Cytokines. B) Decreased pro-inflammatory cytokines. C) Increased chemokine production.

Figure 5.

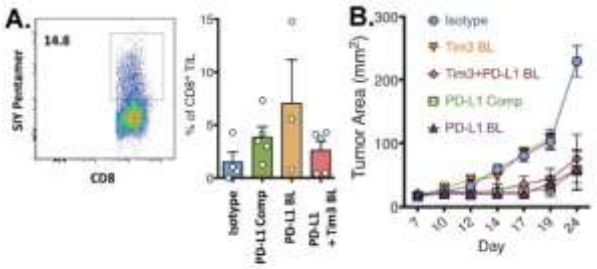

Figure 5. A) Tumor-specific infiltrating CD8+ T cells increase 24 days after treatment. Animals were implanted with SIYRYYGL-expressing B16 cells and 24 days after treatment the tumor was collected and analyzed. B) Anti-PD-L1 treatment reduces tumor growth.

Late-Breaking Abstract Oral Presentation

Biomarkers and Immune Monitoring

O48

In silico assessment of variation in TMB quantification across diagnostic platforms: Phase 1 of the Friends of Cancer Research Harmonization Project

David Fabrizio, PhD[1], Shu-Jen Chen, PhD[2], Mingchao Xie, PhD[3], Wangjuh (Sting) Chen, PhD[4], Katie J. Quinn, PhD[5], Chen Zhao, PhD[6], Ahmet Zehir, PhD[7], Vincent Funari, PhD (CGMBS)[8], Jennifer S. Dickey, PhD[9], Vikas Gupta, PhD[10], Dinesh Cyanam, PhD[11], Lisa M. McShane, PhD[12], Naiyer A. Rizvi, MD[13], Matthew Hellmann, MD[7], Mark Stewart, PhD[14], Diana M. Merino, PhD[14], Jeff Allen, PhD[14], Friends of Cancer Research TMB Harmonization Team[14]

[1]Foundation Medicine, Cambridge, MA, USA
[2]ACT Genomics, Taipei City, Taiwan
[3]AstraZeneca, Waltham, MA, USA
[4]Caris Life Sciences, Phoenix, AZ, USA
[5]Guardant Health, Redwood City, CA, USA
[6]Illumina, San Diego, CA, USA
[7]Memorial Sloan Kettering Cancer Center, New York, NY, USA
[8]NeoGenomics Laboratories, Inc., Aliso Viego, CA, USA
[9]Personal Genome Diagnotics, Baltimore, MD, USA
[10]Qiagen, Aarhus, Denmark
[11]Thermo Fisher Scientific, Ann Arbor, MI, USA
[12]National Cancer Institute, Bethesda, MD, USA
[13]Columbia University Medical Center, New York, NY, USA
[14]Friends of Cancer Research, Washington, DC, USA

Background
Tumor mutational burden (TMB) is a measure of the number of somatic mutations and a predictive biomarker of response to immune checkpoint inhibitors (ICI) across several cancers. TMB can be estimated using targeted next-generation sequencing (NGS), but differences in quantification can arise based on platform differences, testing panel size and composition, and bioinformatic algorithms. Harmonization of methods to quantify TMB will facilitate biomarker development and optimize clinical utilization and treatment decision-making. Friends of Cancer Research (Friends) convened a group of leading diagnostic partners to assess and identify sources of TMB variability and determine best practices for harmonizing TMB estimation to ensure consistent clinical interpretation in the future.

Method
Eleven diagnostic members of the Friends TMB Harmonization Team used whole exome sequencing (WES) data from The Cancer Genome Atlas (TCGA) MC3 samples, comprising 32 cancer types. Each diagnostic partner calculated TMB from the subset of the exome restricted to the genes covered by their targeted panel and using their own bioinformatics pipeline (panel-derived TMB). A “gold-standard” TMB estimate was calculated from the entire exome using a uniform bioinformatics pipeline that all members agreed upon (WES-derived TMB). Linear regression analyses were performed to investigate relationship between WES-derived TMB and each panel-derived TMB. Exploratory analyses by cancer type were also performed. Bias and variability in TMB estimates across panel-derived TMB values were assessed.

Results
In silico quantification of TMB is relatively consistent between panels across a wide range of TMB values (0-40 mut/Mb). Panel-derived TMB strongly correlated with WES-derived TMB (regression R2 values range across panels 0.85-0.93, with slopes ranging from 0.82-1.37). Variation in TMB quantification was attributable to unique composition and technical specifications of each panel, as well as differences in the underlying algorithms used to estimate TMB from observed somatic mutations. Exploratory analyses suggested

possible cancer type dependence for the relationship of panel vs WES-derived TMB, meriting further investigation.

Conclusions

In this in silico analysis, panel-derived TMB was strongly correlated with WES-derived TMB. Some variation in TMB quantification across panel-based diagnostic platforms exists. Identifying factors that contribute to variation will facilitate harmonization and help ensure appropriate use and implementation of tests results in the clinic. Subsequent steps will assess the effect of biologic factors (e.g. specimen type, cancer type, treatment setting), the impact of variation on clinical outcomes, align standards, and define best practices for quantification of TMB.

O49

Imaging of tumor infiltrating T cells with an anti-CD8 minibody 89Zr-IAB22M2C in advanced solid tumors: a phase I first-in-human study

Michael S. Gordon, MD[1], Frank Tsai[1], Michael Postow, MD[2], Matthew Hellmann, MD[2], James J. Harding, MD[2], Ronald L. Korn, MD[3], Michael D. Farwell, MD[4], Tara C. Mitchell[4], Lynn M. Schuchter, MD[4], Martha Ziolkowska[2], Joseph O'Donoghue[2], Jason S. Lewis, [2] Anna M. Wu, PhD[5], William Le[6], Ian Wilson[6], Wolfgang A. Weber[2], Jedd D. Wolchok, MD, PhD[2], Deepak Behera, MD[6], Neeta Pandit-Taskar[2]

[1]HonorHealth Research Institute, Scottsdale, AZ, USA
[2]Memorial Sloan Kettering Cancer Center, New York, NY, USA
[3]Imaging Endpoints, Scottsdale, AZ, USA
[4]University of Pennsylvania, Philadelphia, PA, UA
[5]City of Hope, Duarte, CA, USA
[6]ImaginAb Inc, Inglewood, CA, USA

Background

The degree and character of tumor infiltration by CD8 T-cells is associated with favorable outcomes to immunotherapy. Biopsies to assess T-cell infiltration are invasive, and one biopsy may not capture the immunologic heterogeneity that exists among various tumors in an individual patient. Non-invasive CD8 T-cell imaging could provide a more comprehensive view of T-cell infiltration and potentially correlate with patient outcomes.

Method

We conducted a phase 1 first-in-human study assessing the ability of positron emission tomography (PET) scans using anti-CD8 radiolabeled minibody, 89Zr-IAB22M2C (CD8-tracer), to detect whole body and tumor CD8 distribution, in patients with metastatic solid tumors. All patients received 3mCi 89Zr-IAB22M2C once intravenously followed by serial PET scans over a 5-7 day period. The study was conducted in two stages. During stage 1, 6 patients received increasing protein doses, 0.2 mg through 10 mg (dose escalation), to establish safety and determine appropriate scanning parameters. In Stage 2 (dose expansion) an additional 9 subjects were scanned to better delineate our recommended phase 2 dose. All patients were monitored for drug-related adverse events and evaluated with blood chemistry, hematology, cytokine assay and anti-drug antibodies (ADA). Biodistribution, radiodosimetry and semi-quantitative evaluation of CD8-tracer uptake were performed in all patients.

Results

15 Subjects with metastatic cancer were enrolled (31-82 years, M/F = 9/6). Primary cancer types were melanoma (n=8), non-small cell lung carcinoma (n=6), and hepatocellular carcinoma (n=1). Two subjects were treatment naïve, 3 had discontinued prior treatment, and 10 were on immunotherapy for 2 weeks to >2 years. There were no drug-related adverse reactions, cytokine release or blood test abnormalities. Transient increase in ADA was noted in 1/15 subject. The CD8-tracer rapidly cleared from the blood and accumulated in CD8 rich tissues (e.g. spleen, bone marrow and lymph nodes), which were saturable as demonstrated by decreasing activity

with increasing protein dose (Figure 1). Tracer uptake in tumors was variable and noted in 10/15 subjects as early as 1-2hr post-infusion (Figure 2, Figure 3). Tracer excretion was primarily hepato-biliary. Low background was seen in non-T cell rich tissues such as muscle, brain and heart. Biodistribution and pharmacokinetics were favorable between 0.5-1.5 mg protein doses. The estimated mean effective radiation dose was 24 rem/mCi.

Conclusions

Our first-in-human study demonstrated the safety of the CD8-tracer 89Zr-IAB22M2C and provided detailed whole-body information demonstrating the biodistribution of CD8 T-cells in tumors and reference tissues with the possibility of same-day imaging.

Acknowledgements

Research Support: ImaginAb, Inc., Parker Institute for Cancer Immunotherapy

Ethics Approval

The study was approved by Institutional Review Boards of MSKCC (IRB #16-1109), Honor Health (West IRB #1179278) and University of Pennsylvania (IRB # 828992).

Consent

Written informed consent was obtained from the patient for publication of this abstract and any accompanying images. A copy of the written consent is available for review by the Editor of this journal.

Trial Registration

ClinicalTrials.gov Identifier: NCT03107663

Figure 1: 89Zr-IAB22M2C PET images in dose escalation stage

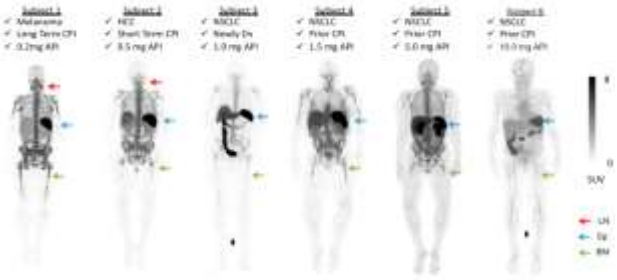

Figure 2: Stable 89Zr-IAB22M2C uptake over time

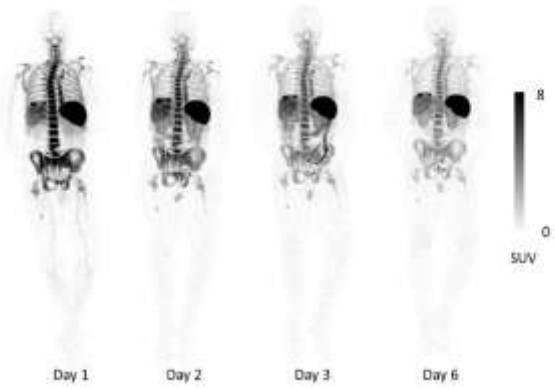

Clinical Trials (Completed)

O50

Pembrolizumab in combination with chemoradiotherapy (CRT) in human papilloma virus (HPV)-associated head and neck squamous cell carcinoma (HNSCC)

Steven F. Powell, MD[1], Mark Gitau, MD[2], John Reynolds, MD[1], Andrew Terrell, MD[2], Michele M. Lohr, MD, MS[1], Steven McGraw, MD[1], Ryan K. Nowak, MD[1], Ash Jensen, MD[2], Miran Blanchard, MD[2], Christopher D. Fischer, MD[3], Christie Ellison, RN[4], Lora Black, MPH[4], Paul A. Thompson, PhD[4], Kathryn Gold, MD[5], Ezra Cohen, MD[5], Julie Bykowski, MD[5], John Lee, MD[6], William C. Spanos, MD[1]

[1]Sanford Cancer Center, Sioux Falls, SD, USA
[2]Roger Maris Cancer Center, Fargo, ND, USA
[3]Sanford Clinic Molecular Imaging, Sioux Falls, SD, USA
[4]Sanford Research, Sioux Falls, SD, USA
[5]Moores Cancer Center UCSD, San Diego, CA, USA
[6]Chan Soon-Shiong Institute for Medicine, Culver City, CA, USA

Background

Inhibitors of the programmed death receptor-1 (PD-1) and its ligand (PD-L1) have activity in recurrent and metastatic HNSCC. Now these agents are moving rapidly into curative-intent treatment approaches. Our group has previously reported the safety of adding the PD-1 inhibitor, pembrolizumab, to concurrent cisplatin-based CRT [1]. Here we will report the efficacy of this approach in HPV-associated HNSCC.

Method

Patients (pts) with stage III-IVB HPV-associated (based on p16 immunohistochemistry) HNSCC eligible for definitive CRT were enrolled as part of an expansion cohort. The treatment regimen is outlined in Figure 1. Efficacy was the primary endpoint defined as complete response (CR) rate on imaging or with salvage surgery (pathologic CR) at 100 days post-CRT completion. Imaging CR was determined by RECIST 1.1 criteria for computed tomography (CT) and/or Hopkins Criteria (Score 1, 2 or 3) [2] for positron emission tomography (PET). Progression-free survival (PFS), overall survival (OS), and locoregional control (LRC) rate were key secondary endpoints.

Results

From November 2015 to February 2018, 34 pts with HPV-associated HNSCC were enrolled and assessable for the primary endpoint with median follow-up of 21 months (range 8-26 months). Demographic and disease characteristics are outlined in Table 1. 29 (85%) of pts achieved a CR based on imaging and/or surgical criteria. An additional 2 pts were felt to have no clinical evidence of disease despite imaging findings and did not undergo salvage surgery. 1 (2.9%) patient developed progressive disease with distant metastases. PFS at 1 year was 97.1% (95% CI 80.9% - 99.6%). Treatment compliance is outlined in Table 2. Acute CRT-associated grade ≥3 toxicities included mucositis (n=12, 35%), dysphagia (n=21, 62%), and radiation dermatitis (n=2, 6%).

Conclusions

The addition of pembrolizumab to low-dose cisplatin-based CRT in a predominantly intermediate-risk HPV+ population displayed promising response and early PFS data. No new immune-related safety signals were seen in this expansion cohort. Several phase III trials further evaluating the efficacy of this approach are underway.

Acknowledgements

We would like to acknowledge the Merck Investigator Studies Program for providing grant support for this study.

Ethics Approval

The study was approved by the WIRB Institutional Review Board, approval number 20152167.

Trial Registration

NCT02586207

References

1. Powell SF, Gitau MM, Sumey CJ, Reynolds JT, Lohr M, McGraw S, Nowak RK, Terrell AM, Jensen AW, Blanchard MJ, Ellison C, Black LJ, Thompson PA, Gold KA, Cohen EEW, Lee JH, Spanos WC. Safety of pembrolizumab with chemoradiation (CRT) in locally advanced squamous cell carcinoma of the head and neck (LA-SCCHN). J Clin Oncol 35, 2017 (suppl, abstr 6011)

Figure 1: Study Treatment

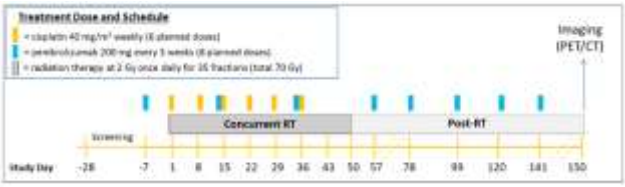

Table 1: Demographics and Disease Characteristics

Age (median, range)	59 yrs (36-81 yrs)
Sex	
Male	32 (94%)
Female	2 (6%)
Race	
White, non-Hispanic	33 (97%)
White, Hispanic	1 (3%)
Primary Tumor Site	
Oropharynx	31 (91.2%)
Larynx	2 (5.9%)
Hypopharynx	1 (2.9%)
Stage (AJCC 7th Edition)	
III	3 (8.8%)
IVA	31 (91.2%)
T Stage	
T0-3	23 (68%)
T4	11 (32%)
N Stage	
N0-1	7 (21%)
N2	27 (79%)
Intermediate Risk Disease*	27 (79%)

Table 2: Treatment Compliance

Pembrolizumab (8 planned doses)	**N (%)**
<3 doses (CRT)	1 (3%)
>3 but <8 doses (post-CRT)	3 (9%)
All 8 doses	30 (88%)
Cisplatin (40 mg/m2 x 6 weekly doses)	**N (%)**
Dose reduction (N,%)	4 (12%)
Dose omission (N,%)	9 (26%)
Completed ≥ 200 mg/m2 (N,%)	30 (88%)
Median Cumulative Dose (SD)	227 mg/m2
Radiation Therapy (70 Gy planned)	**N (%)**
Treatment Delay > 5 days (N,%)	0 (0%)
Treatment Delay ≤ 5 days (N,%)	2 (7.4%)
Mean Days Duration (SD)	49.5 (2.4)
70 Gy RT Completed (N,%)	34 (100%)

Combination Therapy

O51

Monalizumab in combination with cetuximab in recurrent or metastatic squamous cell carcinoma of the head and neck (R/M SCCHN): clinical and translational biomarker results.

Roger Cohen[1], Jerome Fayette[2], Marshall Posner, MD[3], Gautier Lefebvre[4], Jessica Bauman, MD[5], Sebastien Salas[6], Caroline Even[7], Dimitrios Colevas[8], Antonio Jimeno, MD, PhD[9], Esma Saada-Bouzid, MD, PhD[10], Barbara A. Burtness, MD[11], Franceline Calmels[12], Robert Zerbib, MSc[12], Agnès Boyer-Chammard, MD[12], Pascale André, PhD[12], Tanguy Seiwert, MD[13]

[1]Abramson Cancer Center, Philadelphia, PA, USA
[2]Centre Leon Berard, Lyon, France
[3]Mount Sinai Medical Center, New York, NY, USA
[4]Oscar Lambret Institute, Lille, France
[5]Fox Case Cancer Center, Philadelphia, PA, USA
[6]AP-HM, Marseille, France
[7]Institut Gustave Roussy, Villejuif, France
[8]Stanford University Medial Center, Stanford, CA, USA
[9]University of Colorado, Denver, CO, USA
[10]Centre Antoine Lacassagne, Nice, France
[11]Yale University, New Haven, CT, USA
[12]Innate Pharma, Marseille, France
[13]University of Chicago, Chicago, IL, USA

Background

Monalizumab is a novel immune checkpoint inhibitor targeting NKG2A (Natural Killer Group 2A), which is expressed as a heterodimer with CD94 on subsets of NK (Natural Killer) cells, T cells and tumor-infiltrating CD8+ T cells. The NKG2A ligand, HLA-E, is upregulated in cancer, including SCCHN. NKG2A blockade promotes innate anti-tumor immunity mediated by NK and CD8+ T cells and enhances human NK cell antibody-dependent cell-mediated cytotoxicity (ADCC) induced by cetuximab.

Cetuximab is approved for SCCHN patients (pts) progressing after platinum-based chemotherapy, with a response rate of 13%.

Method

This is a multicenter phase I/II trial testing the combination of monalizumab and cetuximab in pts with advanced SCCHN. The phase I part was previously reported showing a favorable safety profile for the combination. In the phase II part, pts received monalizumab at the recommended phase 2 dose of 10 mg/kg q2weeks and cetuximab according to the label (loading dose 400 then 250 mg/m2 q1week). Pts were required to be progressing after platinum-based chemotherapy and to have received <2 prior lines of therapy in the R/M setting. The primary endpoint was ORR per RECIST assessed every 8 weeks. Pts were treated until disease progression or unacceptable toxicity. Various biomarkers were assessed in tumor biopsies and peripheral blood.

Results

As of August 31, 2018, 40 pts have been enrolled and are evaluable for safety and efficacy. All pts received prior platinum-based chemotherapy, 17 (43%) prior anti-PD-(L)1 and 5 (13%), prior cetuximab. The most frequent related adverse events (AEs) were fatigue (18%), rash (15%) and hypophosphatemia (15%). Most AEs were Grade 1-2, 18% of pts had treatment-related grade 3-4 AEs. ORR was 27.5% [16.1-42.8], with 11 confirmed responses (1 complete and 10 partial responses). With a median follow-up of 8 months, median duration of response, PFS and OS were 5.0 months [3.7-6.9] and 10.3 months [7.3-NR], respectively. Data show a trend towards an increase in infiltrating NKp46+ and CD8+ cells in available biopsies of responders after first administration. Additional biomarker analyses will be presented (including tumor mutation burden, HLA-E and NKG2A expression on peripheral and tumor infiltrating lymphocytes).

Conclusions

These data confirm the activity and safety of monalizumab in combination with cetuximab in R/M SCCHN, with deep and durable responses. This study continues to enroll additional R/M SCCHN patients who received both platinum-based chemotherapy and PD-(L) 1 inhibitors.

Trial Registration

NCT02643550

Oncolytic Viruses and Intratumoral Therapies

O52

Intratumoral injection of a novel oncolytic virus, Voyager V1 (VV1): completed phase 1 monotherapy in patients with refractory solid tumors

Steven F. Powell, MD[1], Jaime Merchan[2], Manish R. Patel, DO[3], Timothy P. Cripe, MD, PhD[4], James Strauss, MD[5], Matthew Old, MD[6], Rosa M. Diaz, PhD[7], Kah Whye Peng, PhD[7], Stephen J. Russell, MD, PhD[7], Alice S. Bexon[7], Steven F. Powell, MD[1]

[1]Sanford Health, Sioux Falls, SD, USA
[2]U Miami, Miami, FL, USA
[3]U Minnesota, Minneapolis, MD, USA
[4]Nationwide Children's, Columbus, OH, USA
[5]Mary Crowley Cancer Center, Dallas, TX, USA
[6]Ohio State University, Columbus, OH, USA
[7]Vyriad, Rochester, MN, USA

Background

VV1 is derived from VSV, an RNA virus with low human seroprevalence, engineered to replicate selectively in and kill human cancer cells. VV1 encodes hIFNβ gene to boost antitumoral immune response, plus the thyroidal sodium iodide symporter NIS gene to allow noninvasive imaging of virus spread. VV1 is synergistic with different anti-PD-(L)1 antibodies in preclinical models. Here we report first-in-human data from the completed IT monotherapy dose escalation.

Method

This was an open label phase 1 dose escalation study with a classical 3+3 design. Single VV1 doses from 3 x 106 to 3 x I09 TCID50 were injected IT into one target lesion. Dose increments were ½ log. Objectives include identifying the monotherapy MTD and RP2D, preliminary efficacy, PK by RT-PCR for viral genomes, serum IFNβ levels, and Tc-99m SPECT/CT imaging.

Results

The study is ongoing at dose level 6 (n=20). No DLTs have been observed. Most pts were male (55%), white (85%), with ECOG PS median 1 (range 0-1) and median 5 lines of prior systemic therapy for head & neck (SCCHN, 30%), colon (25%), rectal (5%), pancreas (15%), breast (10%), lung (5%) or other (10%) cancers. AEs (in 80% pts) related to VV1 were mild-moderate, short-lived clinical AEs or transient G2-4 neutro- or lymphopenia at higher doses. More pts had related AEs at higher doses, including a G2 cytokine release syndrome and G1 hypotension (both SAEs). Ten pts had mild biopsy-or injection-related AEs (pain, swelling, bruising, subclinical pneumothorax), and two had an SAE related to procedure (pneumothorax). There were no deaths related to treatment or procedure. Seven pts at higher doses had positive SPECT/CTs to date, showing viral replication in tumor +/- concomitant lymphocyte/neutrophil trafficking. Most pts at higher dose levels had IFNß in serum indicative of viral replication in tumor, but no positive viral titers or shedding. IFNβ levels show a dose response relationship. One pancreas cancer pt had tumor cavitation with cystic fluid positive for viral RNA and IFNß. Five pts had stable disease on CT at D43, two with decrease in sum of target lesions.

Conclusions

IT Voyager-V1 is well-tolerated as a single agent. Injection reactions are manageable with few serious AEs or toxicity >G2. There are indications of antitumor efficacy, and evidence of viral replication based on observed disease stability with positive SPECT and detectable IFNß at higher doses. Data from the highest planned dose level will be reported at presentation.

Late-Breaking Abstract Poster Presentations

Biomarkers and Immune Monitoring

P706

Effects of indoximod plus gemcitabine/nab-paclitaxel on tumor microenvironment of patients with metastatic pancreas cancer

Jiayi Yu, PhD[1], Gabriela R. Rossi, PhD[1], Devora Delman[2], Joey Li, BS[2], Ravindra Kolhe, MD, PhD[3], David H. Munn, MD[3], Nathan Bahary, MD, PhD[4], Nicholas Vahanian, MD[1], Eugene P. Kennedy, MD, FACS[1], Gregory L. Beatty, MD, PhD[2], Charles Link, Jr., MD[1]

[1]NewLink Genetics, Ankeny, IA, USA
[2]University of Pennsylvania, Philadelphia, PA, USA
[3]Medical College of Georgia, Augusta Univ, Augusta, GA, USA
[4]Hillman Cancer Center, Pittsburgh, PA, USA

Background

The indoleamine 2,3-dioxygenase (IDO) pathway mediates immunosuppressive effects through the metabolism of tryptophan (Trp) to kynurenine (Kyn). This metabolic pathway triggers downstream signaling through the Trp sensors GCN2 and mTOR and the Kyn sensor AHR [1-4]. Indoximod is an orally administered, small-molecule IDO pathway inhibitor that reverses the immunosuppressive effects of low Trp and high Kyn that result from IDO activity. The mechanism of action (MOA) of indoximod targets four main cell types: CD8+ T cells, CD4+ helper and regulatory T cells, and DCs. Indoximod has immunostimulatory effects by increasing proliferation of effector T cells, reprograming Treg into helper T cells, and downregulation of IDO expression in DCs. These effects are observed in both the presence and absence of IDO activity [5].

Method

Treatment-naïve metastatic pancreas cancer patients were treated with combination of indoximod and gemcitabine/nab-paclitaxel (SOC) in Phase 2 trial (NCT02077881). Patients underwent pre-treatment tumor biopsy with a repeat biopsy on week 8. Sixteen pairs of tumor specimens (8 patients with objective response, and 8 non-responders) underwent RNA sequencing analysis and multiplex immunohistochemistry (IHC) staining to assess the phenotype and functional status of multiple immune populations in the TME.

Results

Upon treatment, significantly higher intratumoral CD3+ ($p = 0.04$) and CD8+ T ($p = 0.003$) cells density were observed in clinical-responding patients compared to non-responding patients. For these tumor-infiltrated CD3+ cells, higher T cell proliferation (Ki67+) and T cell function (GzmB+) were observed in responding patients. Higher GzmB in CD3- cells (most likely NK cells) was also detected in responding patients. Additionally, CD4+ T cells, NK cells, macrophages and neutrophils were induced in these patients upon treatment. Importantly, consistent with indoximod MOA, both Tregs (Foxp3+) population ($p = 0.05$) and IDO1 expression ($p = 0.04$) were significantly reduced after treatment. Moreover, the CD8: Foxp3 T-cell ratio ($p = 0.0008$) was significantly increased. These findings provided strong evidences to support the hypothesized MOA for indoximod [5] including the upregulation of both innate and adaptive immune responses in TME.

Conclusions

The treatment with indoximod plus SOC induced increased density and activity of intratumoral T cells, increased activity of innate immune cells (NK cells) in responding patients. This treatment also significantly downregulated Treg population and IDO expression in the TME. The combination of indoximod and SOC increased both innate and adaptive immune responses in TME of patients with metastatic pancreas cancer in strong support with the proposed MOA for indoximod.

Trial Registration
ClinicalTrials.gov Identifier NCT02077881

References
1. McGaha TL, et al. Immunol Rev. 2012,249(1):135-157.
2. Munn DH, et al. Immunity. 2005,22(5):633-642.
3. Metz R, et al. OncoImmunology. 2012,1(9):1460-1468.
4. Opitz CA, et al. Nature. 2011,478(7368):197-203.
5. Brincks EL, et al. Presented at: Annual Meeting of the American Association for Cancer Research (AACR), April 14-18, 2018, Chicago, IL. Abstract 3753.

P707

Tumor mutational burden (TMB) ring study: Comparison of multiple targeted next-generation sequencing (NGS) sequencing platforms

Jeffrey Conroy, BS[1], Sarabjot Pabla, MSc, PhD, BS[1], Yirong Wang, MS[1], Sean T. Glenn, PhD[1], Razelle Kurzrock, MD[2], Shumei Kato, MD[2], Ryosuke Okamura[2], Denis A. Smirnov[3], Brad Foulk[3], Traci Pawlowski, PhD[4], Dinesh Cyanam, PhD[5], Geoffrey M. Lowman, PhD[5], Blake Burgher, BS, RN[1], Jacob Hagen[1], Mary Nesline, MS[1], Antonios Papanicolau-Sengos, MD[1], Felicia L. Lenzo[1], Mark Gardner[1], Carl D. Morrison, MD, DVM[1]

[1]OmniSeq, Inc., Buffalo, NY, USA
[2]UC San Diego Moores Cancer Center, San Diego, CA, USA
[3]Janssen Research and Development, Sping Hous, PA, USA
[4]Illumina, Inc., San Diego, CA, USA
[5]ThermoFisherScientific, Carlsbad, CA, USA

Background
Tumor mutational burden (TMB), a measurement of the frequency of mutations in tumor cells, is currently being evaluated as a biomarker to predict response to immune checkpoint inhibitors. Whole exome sequencing is considered the gold standard assay, but is inefficient and too costly to run routinely. Consequently, several targeted NGS assays have been designed to measure TMB. In this study, we compared TMB measurements from four targeted NGS assays using a common source of specimens. Concordance and accuracy of TMB values, cutoffs and clinical interpretations were assessed.

Method
Genomic DNA from 161 FFPE specimens representing 24 tumor types was extracted following anatomical pathologist review. TMB testing was completed or first attempted by Foundation Medicine (FoundationOne®), followed by on-site analysis by OmniSeq (Immune Report Card®), Illumina (TruSight Oncology 500™), and ThermoFisher (Oncomine™ Tumor Mutation Load) from a subsequent central DNA isolation. Each laboratory followed its own protocol for reporting TMB values (mutations/Mb). Pairwise Pearson product-moment correlations (R) were performed to estimate concordance of TMB values between platforms. 150 gold standards were established (7 TMB-high, 143 TMB-low) for which at least three of four platforms were concordant when using a TMB-high cutoff of ≥10. Each platform was assessed for TMB interpretation accuracy at this threshold.

Results
TMB values were successfully reported for >90% of samples and were concordant across platforms (R = 0.74 - 0.91). TMB distribution for each platform demonstrated a value of 10 mutations/Mb within the 84th-91st percentiles and captured all consensus TMB-high gold standard samples at >90% accuracy. Where results were available, the seven TMB-high gold standard samples were identified across all platforms resulting in 100% sensitivity. For the 143 TMB-low, the number of false positives ranged from 2-11, resulting in 89.6-98.6% specificity. PPV ranged from 31.3-77.8% across all tumor types, but improved to ≥75% across platforms when restricted to NSCLC samples (n=14). Pair-wise linear regression

model fits did not significantly improve concordance between platforms ($p>0.05$).

Conclusions

The TMB assays evaluated were robust across a wide range of solid tumor specimens. There is general concordance between the platforms despite considerable variability in TMB calling parameters and the genes targeted. Nevertheless, each platform is highly accurate when using a TMB-high cutoff of ≥10, which improves when restricted to NSCLC. This study suggests that TMB can be measured accurately across multiple platforms, but further studies utilizing additional NGS platforms and samples are required to validate these findings.

Ethics Approval

OmniSeq's analysis utilized deidentified data that qualified as non-human subject research under IRB protocol (BDR #080316) approved by Roswell Park Comprehensive Cancer Center (Buffalo, NY).

P708

Immunopharmacodynamic responses of Imprime PGG combined with Pembrolizumab in chemotherapy-resistant metastatic triple negative breast cancer subjects in a Phase 2 trial: Analyses of Stage 1 patients

Nadine Ottoson, BS[1], Adria B. Jonas, MS[2], Anissa S. Chan, PhD[2], Xiaohong Qiu, BS[2], Blaine Rathmann, BS[2], Richard Walsh, BS[1], Ben Harrison, MS[2], Mike Danielson, PhD[2], Kyle S. Michel, BA[2], Michaela Finley[2], Mark Uhlik, PhD[2], Jamie Lowe, BA[2], Paulette Mattson, BFA[2], Michele A. Gargano, MS[2], Michael J. Chisamore, PhD[3], Joanna Cox, MD[2], Bruno Osterwalder, MD[4], Jeremy R. Graff, PhD[2], Nandita Bose, PhD, Nadine Ottoson, BS[1]

[1]Biothera Pharmaceuticals, Inc., Eagan, MN, USA
[2]Biothera, Eagan, MN, USA
[3]Merck & Co, Rahway, NJ, USA
[4]B.O. Consulting GmbH, Riehen, Switzerland

Background

Though efficacious, checkpoint inhibitor (CPI) monotherapy fails to elicit response in the majority of patients. TNBC is one such cancer type where CPI antibodies (pembrolizumab, avelumab, atezolizumab), have demonstrated only a ~5-10% response rate, irrespective of PD-L1 expression. We are developing Imprime PGG (Imprime), a novel yeast derived β-glucan PAMP in combination with pembrolizumab, to enhance the benefit that TNBC patients derive from CPI-based therapy.

Method

In this analysis, we present the serum and cellular IPD responses elicited by Imprime and pembrolizumab in the peripheral blood of 12 TNBC subjects who previously failed front-line chemotherapy, enrolled as part of a Phase 2 study (NCT02981303). Subjects received Imprime (4 mg/kg qw) + Pembro IV (200 mg q3w) in 3 week cycles. Anti-beta glucan antibodies (ABA), circulating immune complexes (CIC), complement activation, cytokine production, gene expression changes, and phenotypic changes on immune cells were evaluated.

Results

As Imprime is known to complex with serum IgG ABA, a drop in the free ABA levels and a concomitant increase in the CIC was observed at the end of infusion (EOI) of every Imprime dose. Interestingly, 11 of 12 subjects showed increased ABA levels between cycles 1 and 2, with peak levels increasing ~1.5 to 35-fold over baseline. In line with this ABA increase, peak levels in serum CIC levels (range ~3 to 22-fold) and complement protein SC5b-9 (~1.4 to 41-fold) were also observed at cycle 2 EOI. In a subset of patients, a maximum increase of ~10-1000-fold in several chemokines was detected at cycle 2 EOI. Gene expression analyses of whole blood indicated peak activation of several genes at cycle 2 associated with activation of innate immune cells and T-cells. In 8 of 12 subjects, an increased frequency up to 11-fold in the CD16+ monocytes, cells known for their

enhanced cytotoxicity as well as M1-polarizing functions, was observed between cycles 1 and 2. We also observed an increase, up to 2-fold, in CD16+ inflammatory DC in 8 of 12 subjects. The maximal increase (~4 to 20-fold) in newly proliferating (Ki67+), activated CD8 T cells (PD-1+ CD38+ HLADR+) was observed at cycle 2 in 4 subjects. Of all these immunological responses, robust cytokine production together with an increased frequency of activated CD8 T cells, correlated with objective tumor responses.

Conclusions

These data provide the first evidence in cancer patients that Imprime can drive the critical IPD changes known to be associated with efficacy in preclinical cancer models.

Ethics Approval

The study was approved by central IRB (Western Institutional Review Board) under approval number 20162506 for sites that are able to use a central IRB, for sites with local IRBs, approval was obtained for each site by their respective IRB for this study.

Consent

Written informed consent was obtained from the patient for publication of this abstract and accompanying images. A copy of the written consent is available for review

Trial Registration

NCT02981303

P709

Peripheral Blood TCRB Chain Convergence Predicts Response to Dendritic Cell-Based Immunotherapy in Advanced-Stage Melanoma Patients

Walter J. Storkus, PhD[1], Yan Lin[1], Lauren Miller, BS[2], Denise S. Topacio-Hall, BS, MA[2], Geoffrey M. Lowman, PhD[2], Timothy Looney, PhD[2], Lisa H. Butterfield, PhD[1], Jennifer L. Taylor, PhD[1], Ahmad A. Tarhini, MD, PhD[3], Hussein A. Tawbi, MD, PhD[4], John M. Kirkwood, MD[1]

[1]University of Pittsburgh, Pittsburgh, PA, USA
[2]ThermoFisher, Carlsbad, CA, USA
[3]Cleveland Clinic Foundation, Cleveland, OH, USA
[4]MD Anderson Cancer Center, Houston, TX, USA

Background

T cell receptor (TCR) convergence refers to the phenomenon whereby antigen-driven selection enriches for TCRs having a shared antigen specificity but different nucleotide sequences. TCR convergence may be indicative of tumor immunogenicity and thus the sensitivity of a cancer to immunotherapy. Here we used next-generation sequencing of peripheral blood TCRB chain repertoires to evaluate TCR convergence as a predictive biomarker for response to dendritic cell-based immunotherapy for advanced melanoma. We further evaluated the relationship between TCR convergence and response biomarkers derived from targeted gene expression profiling of pre-treatment tumor biopsies.

Method

Total RNA was extracted from peripheral blood leukocytes (PBL) isolated from 13 evaluable HLA-A2+ patients with advanced-stage melanoma treated with dasatinib plus an autologous dendritic cell/peptide-based vaccine targeting 6 tumor-associated vascular antigens (UPCI 12-048, NCT01876212), which included 6 responders (4 PR, 2 SD) and 7 non-responders (PD). TCRB chain repertoire libraries were constructed by multiplex PCR utilizing FR1 and constant gene targeting primers via the Oncomine TCRB-LR assay, then sequenced using the Ion Torrent S5 to a target depth of 1.5M raw reads per library. To evaluate T cell repertoire convergence we searched for instances where TCRB chains were identical in amino acid space but had distinct nucleotide sequences owing to N-addition and exonucleotide chewback within the V-D and D-J junctions of the CDR3. Targeted gene expression profiling of pre- and post-treatment tumor biopsies was performed via the Oncomine Immune Response Research Assay using total RNA input.

Results
Sequencing of TCRB libraries yielded on average 20k clonotypes per individual with mean evenness (normalized Shannon entropy) of .84. TCR convergence was elevated in pretreatment PBL of responders compared to non-responders (mean frequency .012 vs .006, p=.01, Wilcoxon), discriminated responders from non-responders with high accuracy (AUROC = .90), and closely correlated with time to progression following treatment (Spearman correlation = .78). Targeted gene expression profiling of tumor revealed elevated PD-L1 expression in pre-treatment responders compared to non-responders and reduced PTP1B and HIF1A in post-treatment biopsies from responders compared to non-responders. Combining pre-treatment PBL TCR convergence values with tumor PD-L1 expression values improved the prediction of response.

Conclusions
These data suggest that peripheral blood TCRB convergence may serve as a biomarker for response to dendritic cell-based immunotherapy, to be used alone or in combination with established biomarkers derived from profiling of the tumor microenvironment. Ongoing and future studies will further clarify the prognostic and/or predictive utility of this immune repertoire biomarker.

Acknowledgements
This work was supported by NIH R01 CA168118 (WJS).

Ethics Approval
This study was approved by the University of Pittsburgh's IRB, approval PRO12060479.

Clinical Trials (In Progress)

P710

Phase 1/2 study of image guided intratumoral CD40 agonistic monoclonal antibody (APX005M) in combination with systemic pembrolizumab for treatment-naïve metastatic melanoma

Salah Eddine Bentebibel[1], Daniel H. Johnson, MD[1], Srisuda Lecagoonporn, PhD DPharm[1], Cara Haymaker, PhD[1], Houssein Safa, MD[1], Cassian Yee, MD[1], Rodabe N. Amaria, MD[1], Sapna Patel, MD[1], Hussein A. Tawbi, MD, PhD[1], Isabella C. Glitza, MD, PhD[1], Michael Davies, MD, PhD[1], Michael K. Wong, MD PhD FRCPC[1], Wen-Jen Hwu, MD, PhD[1], Patrick Hwu, MD[1], Willem W. Overwijk, PhD[1], Ovid C. Trifan, MD, PhD[2], Chantale Bernatchez[1], Adi Diab, MD[1]

[1]MD Anderson Cancer Center, Houston, TX, USA
[2]Apexigen Inc., San Carlos, CA, USA

Background
Immune-checkpoint blockade has become a major modality in the treatment of metastatic melanoma. However, long-term survival and durable remission rates remain low and new treatment options are needed to improve clinical outcome. CD40 activation on antigen presenting cells (APCs) initiates their ability to prime and activate CD8+ T cells through upregulation of co-stimulatory molecules as well as expression of effector cytokines. APX005M is a humanized IgG1 CD40 agonistic antibody that binds with high affinity to human CD40 expressed on APCs. Our pre-clinical studies have demonstrated that intratumoral (IT) CD40 activation induced systemic anti-tumor effects and augmented the activity of anti-PD-1. We hypothesized that this combination will stimulate local APCs resulting in activation of tumor-specific CD8+ T cells and distant responses

Method
This is an ongoing dose escalation and expansion study of image guided IT CD40 agonistic monoclonal

antibody (APX005M) in combination with standard systemic pembrolizumab in metastatic melanoma with an accelerated 3+3 design. Approximately 36 participants will be enrolled, all patients (pts) will receive IT APX005M every 3 weeks for a total of 4 doses. The primary objectives of the study are to evaluate safety and tolerability, determine the recommended phase 2 dose (RP2D), and assess the overall response rate (ORR) 12 weeks after treatment initiation by RECIST 1.1 at RP2D. The dose escalation portion of the trial has enrolled 10 pts in 5 dose escalating cohorts of APX005M at 0.1, 0.5, 1, 3 and 10 mg in combination with standard pembrolizumab at 2 mg/Kg. 26 pts will have 75% power to detect an improvement from a null ORR of 33% to 55%, using a one group chi-square test and assuming a one-sided α level of 5%. Biomarker analyses of blood and tumor biopsies both in injected and non-injected tumors are being performed to measure immune activation using immunophenotyping including Mass Cytometry (CyTOF), Multiplexed ion beam imaging analysis (MIBI), TCR sequencing and gene expression analyses.

Results

9 pts treated across all five dosing cohorts have had disease evaluations (as of September 13, 2018 data cut), 3 partial responses were observed (34%). 4/9 (45%) pts had stable disease (SD), 2 of SD patients are experiencing tumor reduction (>20%). No Grade ≥3 treatment-related adverse events (TRAEs) were reported.

Conclusions

APX005M in combination with pembrolizumab is well tolerated and has clinical activity. Updated safety, biomarker and response data will be presented.

Trial Registration

NCT: 02706353

P711

HepaVac-101 first-in-man therapeutic cancer vaccine Phase I/II clinical trial for hepatocellular carcinoma patients

Luigi Buonaguro, MD[1], Andrea Mayer-Mokler[2], Roberto Accolla[2], Yuk T. Ma[4], Regina Heidenreich[5], Antonio Avallone[1], Ester Simeone[1], Alfred Koenigsrainer[6], Markus Loeffler[6], Cecile Gouttefangeas, PhD[6], Christian Flohr[2], Jörg Ludwig[2], Diego D. Alcoba, MSc, PhD[2], Sarah Kutscher[2], Maria Tagliamonte[1], Paolo A. Ascierto[1], Hans-Georg Rammensee, PhD[6], Bruno Sangro[7], Mercedes Iñarrairaegui Bastarrica[7], Sven Francque, MD, PhD[8], Luisa Vonghia[8], Danila Valmori[9], Tanguy Chaumette[9], Toni Weinschenk, PhD[2], Carsten Reinhardt, MD, PhD[2], Ulrike Gnad-Vogt, MD[5], Luigi Buonaguro, MD[1], Harpreet Singh-Jasuja[2]

[1]National Cancer Institute 'Pascale', Napoli, Italy
[2]IMMATICS Biotechnologies GmbH, Tuebingen, Germany
[2]University of Insubria, Varese, Italy
[4]University of Birmingham, Birmingham, UK
[5]CUREVAC AG, Tuebingen, Germany
[6]Univ. Hospital Tuebingen, Tuebingen, Germany
[7]University of Navarra, Pamplona, Spain
[8]Antwerp Univ. Hospital, Antwerp, Belgium
[9]University of Nantes, Nantes, France

Background

Hepatocellular carcinoma (HCC) is the third leading cause of death from cancer globally with an extremely variable 5-year survival rate. Immunotherapy strategies for HCC may represent a key therapeutic tool to improve clinical outcome in HCC patients. The HepaVac-101 phase I/II, first-in-man, single-arm clinical trial is performed as part of the HepaVac project, funded by the European Commission's 7th Framework Program under the Grant Agreement Nr. 602893 (www.hepavac.eu). The HepaVac-101 trial identification numbers are NCT03203005 (Clinical trials.gov) and 2015-003389-10 (EudraCT).

Method

The therapeutic cancer vaccine IMA970A is a multi-peptide-based HCC vaccine composed of 16 newly discovered and overexpressed tumor-associated peptides (TUMAPs) directly identified from resected HCC tissues. Of these TUMAPs, 7 are restricted to HLA-A*02, 5 to HLA-A*24 and 4 to HLA class II. CV8102 is a novel ribonucleic acid (RNA) based immunostimulatory agent inducing a balanced Th1/Th2 immune response. Patients with very early, early and intermediate stage of HCC are enrolled to be treated with a single pre-vaccination infusion of low-dose cyclophosphamide, followed by 9 intradermal vaccinations consisting of IMA970A plus CV8102. The study drugs are applied without concomitant anti-tumor therapy, in order to reduce risk of tumor recurrence/progression in patients having received all indicated standard treatments and without evidence of active disease. The primary endpoints of the HepaVac-101 clinical trial are safety, tolerability, and immunogenicity. Secondary/exploratory endpoints are additional immunological parameters in circulation (e.g. regulatory T-cells, myeloid-derived suppressor cells, impact of the standard therapy on the natural immune response), infiltrating T-lymphocytes in tumor tissue, biomarkers in blood and tissue, disease-free survival/progression-free survival and overall survival. Overall, it is planned to enroll about 20 to 40 patients. Suitable patients enrolled at Tuebingen are invited to participate in a trial extension investigating an actively personalized vaccine (APVAC). The HepaVac-101 trial is conducted in 6 centers located in 5 European countries. Five centers are actively recruiting patients and one additional site will start enrollment in Q3 2018. As of the time of abstract submission, 42 HCC patients have been screened for HLA haplotype. Two patients are engaged in the vaccination protocol and one patient has completed the study treatment (currently on follow-up phase).

P712

Early phase 2 clinical results of IL-15RαFc superagonist N-803 with BCG in BCG-unresponsive non-muscle invasive bladder cancer (NMIBC) patients demonstrating 86% CR of carcinoma in situ (CIS)

John Lee, MD[1], Patrick Soon-Shiong, MD[1], FRCS, FACS, Karim Chamie, MD[2], Amy Rock, PhD[1], Peter Rhode, PhD[3]

[1]NANT Cancer Immunotherapy Inc., Culver City, CA, USA
[2]Ronal Reagan UCLA Medical Center, Los Angeles, CA, USA
[3]NantCell, Culver City, CA, USA

Background

Patients with BCG-unresponsive non-muscle-invasive bladder cancer (NMIBC) have limited treatment options and the standard of care is radical cystectomy. N-803 is an IL-15-based immunostimulatory protein complex (IL-15RαFc) that promotes proliferation and activation of natural killer (NK) cells, effector and memory CD8+ T cells, but not Treg cells. Preclinical data have shown that when combined with BCG, N-803 activates natural killer cells and reduces tumor burden [1]. Phase Ib data in BCG-naïve patients with NMIBC demonstrate that intravesical administration of N-803 with BCG induced complete response in all patients, without recurrences for more than 24 months [2]. A patient with high-risk NMIBC who had failed multiple intravesical therapies remained disease-free for over 19 months when treated with N-803 and BCG [3].

Method

Based on these studies fast track designation was obtained and an open label single arm multicenter Phase 2 study of intravesical BCG plus N-803 in patients with BCG unresponsive high grade NMIBC (NCT03022825) was opened. Two study groups: group A patients with BCG-unresponsive carcinoma in situ (CIS) [with or without Ta or T1 disease] and

group B patients with BCG-unresponsive high-grade Ta or T1 disease [no CIS]. All patients treated received intravesical N-803 plus BCG, weekly for 6 consecutive weeks during the induction treatment period. First response assessment at Week 12. Patients with no disease or low-grade Ta disease at months 6, 9, 12, and 18 are eligible for continued maintenance treatment. The primary endpoint is incidence of complete response of CIS at any time.

Results

To date, twenty-two patients have enrolled in the phase 2 trial (Group A (CIS), n=11, Group B (Papillary), n=11). Seven of the eleven patients in Group A with BCG-unresponsive CIS have reached at least the 12 week response assessment timepoint. Of these seven patients, six patients (86%) have a reported complete response. Eight of the eleven patients with BCG-unresponsive high-grade Ta or T1 disease have evaluable data. None of the eight have experienced recurrence of disease. Two serious adverse events (AEs) have been reported (E coli infection, anemia), with no immune related AEs. In Group B, not a single patient out of eleven has recurred on study to date (3-12 months since resection).

Conclusions

Early objective response in patients with NMIBC unresponsive to BCG with CIS demonstrated a complete response in 6 out of the first 7 patients (86%). Furthermore, these patients demonstrated no immune related AEs. In patients with papillary, no recurrences to date.

Trial Registration

NCT03022825

References

1. Gomes-Giacoia E, Miyake M, Goodison S, Sriharan A, Zhang G, You L, Egan JO, Rhode PR, Parker AS, Chai KX, Wong HC, Rosser CJ. Intravesical ALT-803 and BCG treatment reduces tumor burden in a carcinogen induced bladder cancer rat model, a role for cytokine production and NK cell expansion. PLoS One. 2014 Jun 4,9(6):e96705.
2. MP-15-12: Phase 1b trial of ALT-803, an IL-15 superagonist, plus BCG for the treatment of BCG-naïve patients with non-muscle invasive bladder cancer. Rosser CJ, Nix J, Ferguson L, Wong HC, The Journal of Urology, Vol. 197, Issue 4, e175 Published in issue: April 2017.
3. Huang J, Schisler J, Wong HC, Rosser CJ, Sterbis J. Intravesical ALT-803 for BCG-unresponsive Bladder Cancer - A Case Report. Urol Case Rep. 2017 Jun 8,14:15-17.

P713

NANT Cancer Vaccine an orchestration of immunogenic cell death by overcoming immune suppression and activating NK and T cell therapy in patients with third line or greater metastatic pancreatic cancer

Patrick Soon-Shiong, MD, FRCS, FACS[1], John Lee, MD[1], Tara Seery, MD[2], Mira Kistler, MD[2], Arvind Shinde[2], Anand Annamalai[2], Leonard Sender[2], Frank Jones, PhD[3], Omid Jafari, MD[4]

[1]Nantkwest, Culver City, CA, USA
[2]Chan Soon-Shiong Institute for Medicine, el Segundo, CA, USA
[3]NantCell, Culver City, CA, USA
[4]Medical Imaging Center of SoCal, Los Angeles, CA, USA

Background

Pancreatic cancer has multiple mechanisms to prevent immune recognition that lead to the creation of an immune suppressive tumor microenvironment. We hypothesize that effective and sustained response against tumors requires a coordinated approach that: 1. reverses the immune-suppressive tumor microenvironment, 2. induces immunogenic tumor cell death and 3. reengages NK and T-cell tumor response against a 4. cascade of tumor antigens. To test this hypothesis, we have developed the NANT Cancer Vaccine: a temporospatial approach that combines:

metronomic low dose chemotherapy, SBRT, off-the-shelf cryopreserved allogeneic NK cells, yeast and adenoviral tumor associated antigen vaccines, IL-15RαFc superagonist N-803 immunostimulatory cytokine, with checkpoint inhibitor.

Method

A phase 1b, single-arm, open-label trial of the NANT Cancer Vaccine in patients with recurrent metastatic pancreatic cancer was initiated. Treatment occurred in 3-week cycles of low-dose chemotherapy (aldoxorubicin, cyclophosphamide, oxaliplatin, nab-paclitaxel, 5-FU/L), antiangiogenic therapy (bevacizumab), SBRT, engineered allogeneic high affinity CD-16 NK-92 cells (haNK), IL-15RαFc (N-803), adenoviral vector-based CEA vaccine (Ad-CEA), yeast vector-based RAS vaccine (Ye-RAS), and an IgG1 PD-L1 inhibitor, avelumab. The primary endpoint is incidence of treatment-related adverse events. Secondary endpoints include ORR, DCR, PFS, and OS.

Results

To date, 10 patients with 3rd-line or greater metastatic pancreatic cancer have initiated treatment with response evaluated past 10 weeks. All therapies were safely administered in an outpatient setting. AEs were primarily hematologic which were managed by appropriate planned dose chemo reduction. No dose-limiting, immune-related AE's (irAE's) have been observed to date. Eight out of ten patients (80%) have had a best response of stable disease with a 100% disease control of target lesions to date. Median progression-free survival is 5.8 months (3.3 – 8.8) and median overall survival is 9.5 months (5.0 – NR) with patients continuing treatment.

Conclusions

This preliminary data suggests that the NANT Cancer Vaccine of low-dose chemo-radiation combined with innate and adaptive immunotherapy can be administered safely in an outpatient setting. Preliminary efficacy results are encouraging and the overall survival of 9.5 months currently exceeds all standards of care for patients at this advanced stage of disease.

Trial Registration

NCT03387098

P714

Phase 2 trial of CA-170, a novel oral small molecule dual inhibitor of immune checkpoints VISTA and PD-1, in patients (pts) with advanced solid tumor and Hodgkin lymphoma.

Vivek S. Radhakrishnan, MD, DM[1], Sameer Bakhshi, MD[2], Kumar Prabhash, MD[3], Chetan Deshmukh, MD[4], Shona Nag, MD[5], KC Lakshmaiah, MD[6], M Gopichand, MCh[7], Murali Ramachandra, PhD[8], Sudeep Gupta, MD[9], Shripad D. Banavali, MD[3], Divyesh Mandavia[8], Akhil Kumar, MD[10]

[1]TMC Kolkata, Kolkata, India
[2]AIIMS, New Delhi, India
[3]TMH Mumbai, Mumbai, India
[4]Deenanath Mangeshkar Hospital, Pune, India
[5]Jehangir Hospital, Pune, India
[6]Sreenivasam Cancer Care Hospitals, Bengaluru, India
[7]City Cancer Centre, Vijayawada, India
[8]Aurigene Discover Technologies Limited, Bangalore, India
[9]ACTREC, Navi Mumbia, India
[10]Advisor-Aurigene, Bengaluru, India

Background

V-domain Ig suppressor of T-cell activation (VISTA) and Programmed-death 1 (PD-1) are independent immune checkpoints that negatively regulate T-cell function and are implicated in various malignancies. Preclinical studies have demonstrated that dual blockade of these pathways is synergistic. CA-170 is a first-in-class oral small molecule that directly targets both VISTA and PD-1/PD-L1 pathways and has shown anti-tumor activity in multiple preclinical models. A Phase 1 dose escalation study (Clinicaltrials.gov NCT02812875) has shown acceptable safety of CA-170 with dose escalated up to 2400mg daily.

Method
The Phase II study is a multi-tumor (Head & Neck Cancer, Squamous-NSCLC, Non-Squamous-NSCLC, MSI-H positive solid tumors and Hodgkin Lymphoma) Simon Two Stage design, investigating two dosages (400mg versus 800mg) of CA-170. The total sample size, if all tumor types go into Simon Stage 2, is 130. Key eligibility criteria include: age ≥ 18 years, ECOG ≤1, adequate organ function, no previous exposure to immuno-oncology agents, and 1-3 prior lines of systemic therapy. Primary objective is efficacy, as measured by response rates. Secondary endpoints include additional efficacy measures, as well as safety and PK/PD endpoints.

Results
As of September 13, 2018, 58 patients (18 Head & Neck Cancer, 5 Squamous-NSCLC, 18 Non-Squamous NSCLC, 5 MSI-H positive Solid Tumors and 12 Hodgkin Lymphoma) have been enrolled. Out of these 22 patients have had at least one follow up scan. Among the patients who have had follow up scans, significant anti-tumor activity is seen in three patients – two Hodgkin lymphoma patients showing partial response by Lugano criterion and a Head and Neck Cancer patient showing 48.1% reduction in SPD by irRC criterion. The Clinical Benefit Rate (SD or better) is 68.18%. The AEs and SAEs have been as expected in this population, without any concerns. With respect to immune related adverse events, two patients developed skin rash, one patient developed hypothyroidism, and one patient developed Grade 3 neutropenia and anemia. Both anemia and neutropenia resolved upon drug interruption, however, neutropenia re-appeared after re-exposure, confirming causality. CA-170 was permanently discontinued without any sequalae, suggesting that smaller half life (6-8 hours) of CA-170 provides an advantage over longer lasting antibodies, from safety perspective.

Conclusions
To our knowledge, this is the first Phase 2 study of an oral immuno-oncology (IO) agent, showing activity in cancer patients. Updated efficacy and safety data will be presented at the meeting.

Acknowledgements
All the patients and institutes which participated in the study

Ethics Approval
The study was approved by the respective Ethics Committee of each of the 15 participating institutions.

Trial Registration
Clinical Trials Registry - India (CTRI/2017/12/011026)

P715

A Phase II study of bemcentinib (BGB324), a first-in-class selective AXL inhibitor, in combination with pembrolizumab in patients with advanced NSCLC: Analysis of the first stage

Matthew G. Krebs, MD PhD[1], Paal F. Brunsvig, MD, PhD[2], Nuria Vinolas Segarra[3], Luis Paz-ares[4], Enric Carcereny[5], Enriqueta Felip, MD PhD[6], Manuel Dómine Gómez, MD PhD[7], José Trigo, MD[8], Edume Arriola, MD PhD[9], Maria Rosario Garcia Campelo, MD PhD[10], James Spicer, MD, PhD[11], Jonathan Thompson, MD MS[12], Konstantin Dragnev, MD[13], David Micklem, PhD[14], Robert Holt, PhD[14], Anthony Brown[14], James Lorens, PhD[15], Michael J. Chisamore, PhD[16], Matthew G. Krebs, MD PhD[1]

[1]The Christie NHS Foundation Trust, Manchester, UK
[2]Oslo University University Hospital, Oslo, Norway
[3]Hospital Clinic de Barcelona, Barcelona, Spain
[4] Hospital Universitario Virgen del Rocio, Sevilla, Spain
[5]Hospital Universitari Germans Trias, Barcelona, Spain
[6]Hospital Unviersitario Val d'Hebron, Barcelona, Spain
[7] Hospital Unviersitario Fundacion Jimenez, Madrid, Spain
[8]Hospital Universitartio Virgen de la Victoria, Malaga, Spain

[9]Hospital del Mar, Barcelona, Spain
[10]Hospital Teres Herrera/CHUAC, A Coruña, Spain
[11]Guy's and St Thomas' NHS Foundation, London, UK
[12]Medical College of Wisconsin, Milwaukee, WI
[13]Dartmouth-Hitchcock Medical Center, Hanover, NH, USA
[14]BerGenBio ASA, Bergen, Norway
[15]University of Bergen, Bergen, Norway
[16]Merck & Co, Inc., Rahway, NJ, USA

Background

AXL kinase suppresses innate immune response and its over-expression has been observed in patients failing anti-PD-1 therapy. Bemcentinib (BGB324) is a first-in-class, oral, highly selective AXL inhibitor in phase II clinical development. We evaluated the safety and preliminary efficacy of bemcentinib in combination with the anti-PD-1 pembrolizumab in NSCLC patients.

Method

Patients with stage IV lung adenocarcinoma, unselected for PD-L1, who progressed following 1L platinum doublet chemotherapy were eligible. Bemcentinib (200mg) was administered daily with 3-weekly pembrolizumab (200mg) until disease progression, unacceptable toxicity, or withdrawal.The primary endpoint was ORR (RECIST v1.1), additional objectives included DCR, PFS, OS and safety of the combination.A two-stage Simon-like design was employed (48 patients for a H0 of RR≤0.15, p=0.1, 80% power) with an interim futility analysis after the first 22 patients had had the potential for 24 weeks of follow-up.Fresh pre-treatment tumour biopsies were mandatory for PD-L1 (22C3 pharmDx assay, Agilent) and AXL analysis by IHC (Indivumed).

Results

As of 3 Sep 2018, enrolment into the first stage was complete. Twenty-four patients were recruited (PD-L1 negative: 11 (46%), weak positive (TPS: 1 - 49%): 7 (29%), strong positive (TPS: >50%): 2 (8%)) and had completed an average of 4.2 cycles of treatment (range 0 – ongoing), five patients remained on treatment.In the total (intention-to-treat) population, ORR was 21% (5/24) with DCR of 54% (PR+SD = 13/24) (Table 1). Median PFS was 4.0 months (95% CI 2.0 – NR). Among 21 patients evaluable for AXL status, 10 had AXL positive tumour tissue by IHC. Efficacy was higher in AXL positive patients with ORR 40% (4/10) and DCR 70% (7/10). Of note, 4 (40%) of these patients were PD-L1 negative. This compared with an ORR of 9% (1/11) and DCR 45% (5/11) in AXL negative patients of whom 6 (55%) were PD-L1 negative. Median PFS was 5.9 months (1.7 – NR) in AXL positive patients versus 3.3 months (1.2 - NR) in AXL negative. Treatment was generally well tolerated with no grade 4 or 5 treatment related adverse events (TRAEs). Most common TRAEs were diarrhea (25%) and elevated alanine aminotransferase (25%).

Conclusions

Promising clinical activity was seen particularly in patients with AXL positive disease including those with weak or no PD-L1 expression. The combination treatment of bemcentinib and pembrolizumab was overall well tolerated. Efficacy, safety and putative biomarker data will be further explored in stage 2 of the study.

Acknowledgements

The authors would like to thank all patients and their caretakers for participating in this trial.

Ethics Approval

All relevant approvals have been obtained.

Trial Registration

NCT03184571

Table 1: Stage 1 Efficacy Results Overall and by AXL Status

	Overall (N = 24)	AXL positive (N = 10)	AXL negative (N = 11)
Antitumour activity by RECIST v1.1			
ORR, %	21	40	9
Best overall response, n (%)			
PR	5 (21)	4 (40)	1 (9)
SD	8 (33)	3 (30)	4 (36)
PD	10 (42)	3 (30)	5 (45)
Disease control, n (%)	13 (54)	7 (70)	5 (45)
Median PFS, months (95% CI)	**4.0 (2.0 – NR)**	**5.9 (1.7 – NR)**	**3.3 (1.2 – NR)**

Combination Therapy

P716

The first clinical/translational data from the expansion cohorts of a Ph1/1b Study of IPI-549, a tumor macrophage-reprogramming small molecule, in combination with nivolumab in advanced solid tumors

Bartosz Chmielowski, MD, PhD, Ryan J. Sullivan, MD, Michael Postow, MD, Amita Patnaik, MD FRCP(C), Geoffrey Shapiro, MD, PhD, Ezra Cohen, MD, Martin Gutierrez, MD, Conor Steuer, MD, Antoni Ribas, MD, PhD, Lucy Lee, PHARMD, DABCP, FCP, Brenda O'Connell, PhD, Jeffery Kutok, MD, PhD, Jennifer Roberts, Suresh Mahabhashyam, MBBS, Marie-Louise Fjallskog, MD, Jedd D. Wolchok, MD, PhD, David Hong, MD,

Background

IPI-549 is a first-in-class, oral, selective PI3K-γ inhibitor. In preclinical studies IPI-549 reprograms macrophages/myeloid derived suppressor cells (MDSCs) from an immune-suppressive to an immune-activating phenotype and overcomes resistance to checkpoint inhibitors.

Method

Study IPI-549-01 (NCT02637531) is evaluating the safety, tolerability, pharmacokinetics/pharmacodynamic, immunomodulatory activity and efficacy of IPI-549 in advanced solid tumor patients, as monotherapy and in combination with nivolumab. The recommended dose for expansion was IPI-549 40 mg QD PO + nivolumab 240 mg Q2W IV. The trial is currently enrolling 6 disease-specific combination expansion cohorts including patients with intrinsic and acquired resistance to anti-PD(L)1 therapy, and a 7th combination expansion cohort with patients prospectively selected for high blood MDSC levels (>20.5%). Pre- and on-treatment blood samples for flow cytometry, gene expression, and serum analysis, and paired biopsies for gene expression and immunohistology are mandated.

Results

As of 22 Aug 2018, 57 patients have been enrolled in the combination expansion cohorts: triple-negative breast cancer (TNBC) (n=13), mesothelioma (11), melanoma (11), head and neck squamous cell carcinoma (9), high MDSCs (7), adrenocortical carcinoma (4), and non-small cell lung cancer (2). Clinical activity data is available in 27 evaluable (>1 scan) patients and include two PRs: 1/7 patients in the anti-PD(L)-1 therapy refractory melanoma cohort and 1/6 patients in the anti-PD(L)1 therapy naïve TNBC cohort. Most adverse events (AEs) were Grade 1-2 in severity. The most common treatment-related adverse events (TRAEs) included rash (24%), fatigue (17%), AST increased (17%), ALT increased (14%), pyrexia (14%), and ALP increased (12%), and the most common Grade 3-4 TRAEs included rash (11%) and increased AST (9%), ALP (7%) and ALT (5%). There were no treatment-related deaths.Translational data is being evaluated for alterations in MDSCs, interferon-gamma-induced proteins and proliferation of previously exhausted CD8 memory T-cells in blood, as well as changes in immune infiltrates from paired tumor biopsies Currently, translational data is available in the anti-PD1 therapy refractory melanoma patient showing an 86% reduction in MDSCs at C2D1 by flow cytometry and a 68% increase in the proliferative fraction of previously exhausted T-cells at C3D1 relative to baseline.Updated clinical and translational

data from the combination expansion cohorts will be presented.

Conclusions
The combination of IPI-549 + nivolumab demonstrates an acceptable safety profile and clinical activity associated with on-mechanism immunomodulation in patients not expected to respond to PD1 inhibition alone, including a PR in a melanoma patient progressing on immediate prior nivolumab.

P717

Initial report of intratumoral tavokinogene telseplasmid with pembrolizumab in advanced melanoma: an approach designed to convert PD-1 antibody progressors into responders. (NCT 03132675)

Sharron E. Gargosky, PhD[1], Victoria Atkinson, MD[2], Andrew Haydon, MBBS PhD[3], Phillip Parente[4], Tom Van Hagen[5], Gregory A. Daniels, MD, PhD[6], Pablo Fernandez-Penas, MD, PhD[7], Mecker Moller[8], Igor Puzanov, MD, MSCI, FACP[9], Sajeve Thomas[10], Robert H. Andtbacka, MD, CM, FACS, FRCSC[11], Clemens Krepler, MD[13], David A. Canton, PhD[1], Christopher Twitty, PhD[1], Sharron E. Gargosky, PhD[1]

[1]Oncosec Medical Incorporated, San Diego, CA, USA
[2]Princess Alexandra Hospital, Woolloongabba, Australia
[3]The Alfred Hospital, Melbourne, Australia
[4]Eastern Health Monash University, Box Hill, Australia
[5]4St. John of God Hospital, Subiaco, Australia
[6]University of California San Diego, San Diego, CA, USA
[7]Westmead Hospital, Westmead, Australia
[8]University of Miami, Miami, FL, USA
[9]Roswell Park Comprehensive Cancer Center, Buffalo, NY, USA
[10]UF Health Cancer Center at Orlando Health, Orlando, FL, USA
[11]University of Utah, Salt Lake City, UT, USA
[13]Merck & Co. Inc., Kenilworth, NJ, USA

Background
Anti-PD-1 antibodies are the mainstay of treatment for advanced melanoma, but PD-1 resistance has emerged as a major mechanism that limits clinical benefit in a majority of treated patients. Absence of T cell-inflamed lesions have emerged as a key determinant of this poor response. Delivery of tavokinogene telseplasmid (tavo) intratumorally by electroporation (IT-tavo-EP) produces expression of the proinflammatory cytokine IL-12, which can convert treated and non-treated, weakly immunogenic/poorly T cell-inflamed tumors into highly inflamed, immunologically active lesions. The current trial examines whether IT-tavo-EP can reverse resistance to anti-PD-1 therapies (NCT 01313267).

Method
PISCES is a multicenter phase 2, open-label trial of IT-tavo-EP with pembrolizumab in patients with stage III/IV melanoma who have progressed on either pembrolizumab or nivolumab mono- or combination therapy. The primary endpoint is ORR by RECIST v1.1 at 24 weeks as determined by central review. 48 eligible patients will be treated with IT-tavo-EP to accessible lesions on Days 1, 5 and 8 every 6 weeks combined with IV pembrolizumab (200 mg) on Day 1 of each 3-week cycle for 24 weeks. Longitudinal blood, tissue and fecal samples are being collected and will be used to explore immunological mechanism via transcriptional analyses, multispectral IHC, immune phenotypic analysis, and TCR sequencing.

Results
The current data comprises 21 patients with the first 9 patients having completed 12 weeks of treatment. Of the 21 patients, the average age is 63 +/- 12 years with 62% (13/21) males. All patients have previously been treated and progressed on anti-PD-1 therapies with 36% (7/19) having had more than one prior line of therapy. Immunologically, all enrolled patients

had exceedingly low frequencies of intratumoral peCTL (PD-1+/CTLA-4+CD8+ T cells) at screening with a notable increase in TIL density with treatment. Tavo dosing ranged 0.1-12.5mL per lesion. AEs were predominantly grade 1 associated with injection site or procedural pain. One expected SAE of cellulitis (grade 3) has been reported and two unrelated SAEs (grade3) of respiratory tract infection and elective surgery, all resolved. Of the first 9 patients who had completed 12 weeks of treatment, Tumor responses (RECIST v1.1) were noted in both treated and non-treated lesions with 2 partial responses and 1 stable disease being observed per investigator assessment. These responses were associated with treatment-related upregulation of immune-based transcripts in the tumor microenvironment as well as increased intratumoral T cells within 3 weeks of therapy.

Conclusions
The trial is showing early signs of reversing resistance and continues enrolling.

Ethics Approval
WIRB protocol #20171064

Emerging Models and Imaging

P718

Profiling PD-1 blockade pharmacodynamics using a live tissue explant model of head and neck squamous cell carcinoma.

Munisha Smalley[1], PharmD, Steven B. Maron, MD[2], Manjusha Biswas, MD[1], Mark Lawson, BA, HTL(ACSP)[1], Biswanath Majumder[1], Basavaraja Uddajjara Shanthappa[1], Saravanan Thiyagaragan[1], Kodaganur S. Gopinath[3], K.S. Sabitha[4], Joseph F. Grosso, PhD[5], Tanguy Seiwert, MD[2], Aaron Goldman[6]

[1]Mitra Biotech, Woburn, MA, USA
[2]University of Chicago, Chicago, IL, USA
[3]HCG Oncology Centre, Bangalore, India
[4]Kidwai Memorial Insitute of Oncology, Bangalore, India
[5]Bristol Myers Squibb, Lawrenceville, NJ, USA
[6]Brigham and Women's Hospital, Boston, MA, USA

Background
Immune checkpoint inhibitors revolutionized cancer immunotherapy, yet clinical success remains highly variable and often patient-specific. Therefore, a method to study the mode-of-action of checkpoint blockade at the individual patient level is a critical step towards effectively personalizing immuno-oncology.

Method
Here, we characterized the immune fidelity of CANscript, a live tissue explant model that harnesses a clinically-trained algorithm to predict tumor response to therapy (a.k.a M-Score). We profiled spatio-temporal immune cell heterogeneity using multi-spectral imaging and gene expression analysis. In addition, we examined how well functional tumor-immune biology was preserved across the lymphoid and myeloid compartments during ex-vivo culture using multiple different platforms including cytokine multiplex analysis, flow cytometry, gene expression quantification and multispectral immunohistochemistry. In this platform, we interrogated clinically-approved PD-1 inhibitors (e.g. Nivolumab and Pembrolizumab) using tumor biopsies from patients (N=50) with head and neck squamous cell carcinoma (HNSCC). To buttress these data, and provide a clinical translation, we profiled 12 patient samples in the explant model in which we also obtained the matched clinical response.

Results
We show that in vivo spatial T-cell heterogeneity, including CD4 and CD8 T-cell distributions, tumor-immune pathways and lymphocyte lineage differentiation were recapitulated by CANscript. We identified robust retention of the tumor-immune contexture during the ex-vivo tumor culture (72 hours), and found a statistically significant correlation between the baseline heterogeneity of

the tumor microenvironment (when the tissue arrived at the lab) across gene and protein expression as well as preservation of immune cell signaling networks. Furthermore, we determined that spatial heterogeneity of immune cells within the tumor was unique to each patient, which was also retained after culture. Following treatment with PD-1 inhibitors, we identified high inter-patient gene and protein expression variability is induced by drug pressure, which was predominated by a shift in T-helper and activated T-cell activity particularly Th1 and Th2. Using a clinically-trained algorithm that predicts clinical response, we stratified samples further to study pharmacodynamics of PD-1 blockade, identifying a subset of patient samples that induce adaptive immune response and inflammatory cytokines, which associated to drug efficacy vs. resistance. Induction of T-helper cell gene signatures, particularly a Th1-Hi phenotype from the ex-vivo model were validated using tumor samples from patients ON-TREATMENT.

Conclusions

These findings highlight the now-obvious need to profile efficacy of immunotherapy at the individual patient level, and the utility of ex-vivo tumor models with high immune-fidelity to advance the goals of personalized immuno-oncology.

Ethics Approval

The study was approved by IRB at Kidwai and HCG Oncology Hospitals, Bangalore India.

Other

P719

A SITC-sponsored randomized clinical trial to determine criteria to guide clinicians on when to stop immunotherapy through a community-driven data repository, leveraging the SITC community

Jennifer L. Guerriero, PhD[1], Jessica Thaxton, PhD, MSCR[2], Todd Bartkowiak[3], Esha Sachdev, MD[4], Jiajia Zhang, MD, MPH[5], Abdul Rafeh Naqash, MD[6], Rania H. Younis, BDS, MDS, PhD[7], Sarah E. Church[8], Maria E. Rodriguez-Ruiz, MD, PhD[9], Rosa Nguyen[10], Kit Fuhrman, PhD[8], Sabrina Kaczanowska[11], Abigail E. Overacre-Delgoffe, PhD[12], Dipti Thakkar, PhD[13], Yinghong Wang, MD, PhD[14], Aideen E. Ryan, PhD[15], Claire A. Margolis, MS[1], Rachel Howard[16], Daniel J. Olson, MD[17], Michal Sheffer, PhD[1], Kristin G. Anderson, PhD[18], Yuanquan Yang, MD, PhD[19], Namrata S. Chandhok[20], Vaia Florou, MD[21], Sangeetha M. Reddy, MD, MSci[14], David H. Aggen, MD, PhD[22], Ravi Patel, MD, PhD[23], Thomas U. Marron, MD PhD[24]

[1]Dana-Farber Cancer Institute, Boston, MA, USA
[2]Medical University of South Carolina, Columbia, SC, USA
[3]Vanderbilt University, Nashville, TN, USA
[4]University of California, Los Angeles, Los Angeles, CA, USA
[5]John Hopkins School of Medicine, Baltimore, MD, USA
[6]East Carolina University, Greenville, NC, USA
[7]University of Maryland Baltimore, Baltimore, MD, USA
[8]Nanostring Technologies, Inc., Seattle, WA, USA
[9]Clinica Universidad de Navarra, Pamplona, Spain
[10]St. Judes' Children's Research Hospital, Memphis, TN, USA
[11]National Cancer Institute, Bethesda, MD, USA
[12]Children's Hospital of Pittsburgh, Pittsburgh, PA, USA
[13]Hummingbird Bioscience, Singapore, Singapore
[14]MD Anderson Cancer Center, Houston, TX, USA
[15]NUI Galway, Galway, Ireland
[16]H. Lee Moffitt Cancer Center & Research, Tampa, FL, USA
[17]Univeristy of Chicago, Chicago, IL, USA
[18]Fred Hutchinson Cancer Research Center, Seattle, WA, USA
[19]Roswell Park Cancer Institute, Buffalo, NY, USA
[20]Yale Univeristy, New Haven, CT, USA
[21]University of Miami, Miami, FL, USA

[22]Columbia Univeristy Medical Center, New York, NY, USA
[23]University of Wisconsin – Madison, Madison, WI, USA
[24]Icahn School of Medicine at Mount Sinai, New York, NY, USA

Background
SITCure: Sparkathon 2018: When is it safe to stop immunotherapy?

Metastatic melanoma patients have received immense clinical benefit from checkpoint blockade therapies that have extended long-term survival rates. This advance in cancer treatment has left clinicians and patients in uncharted territory, questioning when it is safe to stop treatment. While many patients achieve maximal response within 6-8 months from the start of treatment, most clinical trials have treated patients for 24 months or indefinitely until progression. Continued treatment beyond best response may provide little additional clinical benefit, result in late-onset immune-related adverse events, and pose excessive personal and societal financial burden. While some physicians opt to stop therapy at or before 24 months of treatment, there are currently no available data-driven guidelines to inform these decisions, therefore, a standardized guideline is critical.

Method
To improve quality of care for patients and financial burden on the health care system, we have designed a clinical trial to guide when to stop immunotherapy through a community driven data resource, leveraging the SITC community.

Clinical trial design: This study will challenge the standard-of-care for anti-PD-1 treatment with a non-inferiority multi-institutional trial. The trial will enroll patients with metastatic melanoma that have received 1-year of standard anti-PD-1 therapy and have stable disease for at least 3 months—having achieved complete response, partial response, or stable disease. Patients will be randomized to a 2-year observational arm or will continue anti-PD-1 for one additional year, after which therapy will be discontinued. Retrospective medical history and imaging will be obtained, and prospective blood, serum, and stool will be collected every 3 months (Figure 1). The primary endpoint will be time to progression following randomization. Secondary endpoints will be 3-year overall and progression-free survival.

Data Analysis: Steering Committees spearheaded by SITC Sparkathon Class of 2018 will be formed and will drive development of standard operating procedures for collection, processing and storage. The Steering Committees encompassing a broad range of scientific expertise (Figure 2), will determine metrics used to analyze specimens, identify biomarkers of remission or risk of recurrence upon discontinuation of anti-PD-1, and test hypotheses to determine safety guidelines for termination of therapy. All data obtained from sample analysis will be deposited into an open-access data repository available to the larger SITC community. Steering Committees will design and test hypotheses to identify discrete markers or signatures that determines when/if it is safe for clinicians to discontinue immunotherapy.

Results
N/A

Conclusions
N/A

Acknowledgements
We would like to thank our business leader, David A. Rosen, for his time and patience in helping us create this proposal and the SITC Sparkathon staff for their support.

Figure 1.

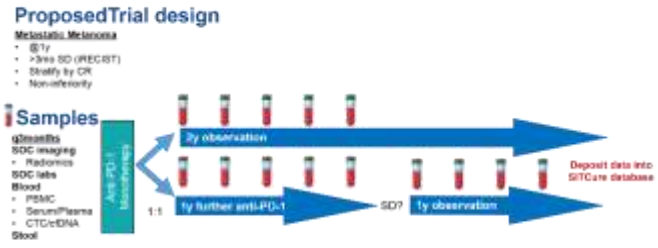

Figure 2.

T-cell Checkpoints and Checkpoint Inhibitors

P720

Regional delivery of anti-CTLA-4 to induce systemic anti-tumor immunity with limited autoimmune toxicity

Airi Harui, PhD[1], Michael D. Roth, MD[1], Sandra M. McLachlan, PhD[2]

[1]UCLA, Los Angeles, CA, USA
[2]Cedars-Sinai Medical Center, Los Angeles, CA, USA

Background

Recent advances in immunotherapy targeting checkpoint inhibitors such as PD-1 and CTLA-4 has begun to out-perform conventional chemotherapy for melanoma, renal, lung cancer and other malignancies. While combining anti-CTLA-4 mAb (α-CTLA-4) with α-PD-1 demonstrates superior efficacy over either agent alone, this combination also magnifies the extent of inflammatory and autoimmune toxicity and can limit clinical utility. The delicate balance that exists between unleashing tumor killing and promoting autoimmune toxicity represents a major obstacle when targeting multiple immune checkpoint inhibitors. We hypothesize that regional administration of low-dose α-CTLA-4 that targets tumor-draining lymph nodes, rather than high-dose systemic therapy, may be particularly important in controlling this risk/benefit ratio.

Method

In order to facilitate regional administration of α-CTLA-4 we formulated a proprietary biocompatible hydrogel that: (a) rapidly polymerizes in situ so that it can be delivered by either subcutaneous or standard image-guided needle injection, (b) protects incorporated biologic agents from degradation, (c) is optimized for the controlled delivery of mAbs over a period of 3-5 days, (d) facilitates trafficking to draining lymph nodes and (e) can be customized to self-resorb to enable repeated administration.Anti-tumor effects of regionally administered low-dose α-CTLA-4 were assessed in an MC-38 mouse model. C57BL/6 mice bearing subcutaneous tumors were treated with either hydrogel encapsulated low dose α-CTLA-4 (α-CTLA-4/hydrogel) by injection into the subcutaneous peri-tumoral tissue or conventional systemic dosing with α-CTLA-4 in PBS by intraperitoneal injection. Anti-tumor efficacy was also evaluated when regional administration of α-CTLA-4 was combined with systemic α-PD-1. The impact of treatment route on the induction of autoimmune toxicity was evaluated in a NOD-H2H4 mouse model in which administration of iodine-containing water enhances autoimmune thyroiditis. Thyroid-specific autoimmunity was assessed as the change in serum levels of anti-thyroglobulin antibody.

Results

Our results demonstrated 1) regional delivery of α-

CTLA-4/hydrogel produced anti-tumor responses that were equal/better than systemic dosing while requiring only 1/6th of the total dosing, 2) Serum exposure to α-CTLA-4 (AUC) averaged only 1/16th of that measured following systemic dosing, 3) Regional α-CTLA-4/hydrogel synergized with systemic α-PD-1 and complete responders were immune to a secondary tumor challenge at a distant site, 4) while systemic therapy with α-CTLA-4 markedly enhanced the generation of anti-thyroglobulin antibodies in iodide-exposed NOD-H2H4 mice, regional low-dose α-CTLA-4/hydrogel had a significantly lesser effect.

Conclusions

Controlled regional delivery of α-CTLA-4/hydrogel has significant potential to improve the risk/benefit ratio associated with neutralizing checkpoint inhibitor therapy.

P721

Single-cell PSI of CD8+ TILs in melanoma shows uniquely sensitive correlation with response to anti-PD-1 therapy, where histology and serum cytokines were unable to detect significant associations

Sean G. Mackay, MBA[1], Brianna Flynn, MS[1], Kevin Morse[1], Patrick Paczkowski[1], Jonathan Chen, MS[1], Antonella Bacchiocchi[2], James R. Heath[3], Rong Fan, PhD[2], Mario Sznol, MD[2], Ruth Halaban, PhD[2], Jing Zhou, MD, PhD[1]

[1]IsoPlexis, Branford, CT, USA
[2]Yale Univeristy, New Haven, CT, USA
[3]Insitute for Systems Biology, Seattle, WA, USA

Background

Functional alteration of tumor-infiltrating T lymphocytes (TILs) may serve as a predictor for clinical outcome in cancer patients receiving immunotherapy. However, due to great heterogeneity and small sample size of TILs in primary tumor tissues from cancer patients, it requires single-cell highly-multiplexed analysis for precise yet comprehensive evaluation of TILs function kinetics. In addition, increasing evidence has shown a positive correlation of polyfunctional T cells (co-secretion of 2+ proteins per single cell) with improved clinical outcome in patients after CAR-T cell therapy and vaccination. Herein, we employed a single-cell 17-plex proteomics to profile the full spectrum of TILs functionality in patients with metastatic melanoma after anti-PD-1 therapy.

Method

Biopsied melanoma tissues were dissociated with Collagenase I (1 mg/ml) and DNase (20 µg/ml). CD8+ TILs from the digest were enriched by CD8 microbeads, stimulated with immobilized anti-CD3 antibody (10 µg/ml) at 37°C, 5% CO2 for 24 hours and loaded into an IsoCode chip containing ~12000 microchambers pre-patterned with a complete copy of a 17-plex antibody array. After 16-hour-on-chip incubation at 37°C, 5% CO2, cytokine signals from ~2000 single cells were captured. The polyfunctional CD8+ TILs were evaluated across 4 functional groups: The polyfunctionality was evaluated across 4 functional groups: Effector (Granzyme B, IFN-gamma, MIP-1alpha, Perforin, TNF-alpha), Stimulatory (GM-CSF, IL-2, IL-5, IL-8, IL-9), Regulatory (IL-4, IL-10, IL-13, IL-22), and Inflammatory (IL-6, IL-17A, MCP-1). Melanoma tissues were also sectioned for histopathological assessment. Serum cytokines were measured with human CD8+ T cell magnetic bead panel using bead-based technology.

Results

The single-cell analysis of CD8+ TILs revealed a statistically significant upregulation of polyfunctional strength index (PSI) in patients who responded to anti-PD-1 antibody therapy (n=7), compared to nonresponding patients (n=4, P=0.0294, Figure 1). The enhanced PSI in responding patients was driven by antitumor associated effector proteins, including Granzyme B, IFN-gamma, TNF-alpha, MIP-1alpha and Perforin. However, cytokines in serum and histopathological metrics including TILs percentage, mitotic rate, tumor size, and necrosis, fibrosis and

apoptosis measurements were unable to show any significant associations with patient outcome.

Conclusions

Single-cell PSI of CD8+ TILs was able to uniquely dissect the functional kinetics of CD8+ TILs from patients with metastatic melanoma and significantly distinguishes responders from nonresponders to anti-PD-1 therapy. Our study indicates the potential of PSI as an integral clinical biomarker for evaluating the efficacy of the therapy on a per-patient basis, and enables understanding of the checkpoint mechanism and its application to drug development.
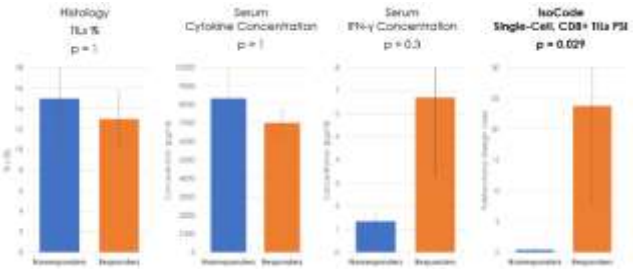
Figure 1. CD8+ TILs PSI Associates with Anti-PD-1 Therapy Response